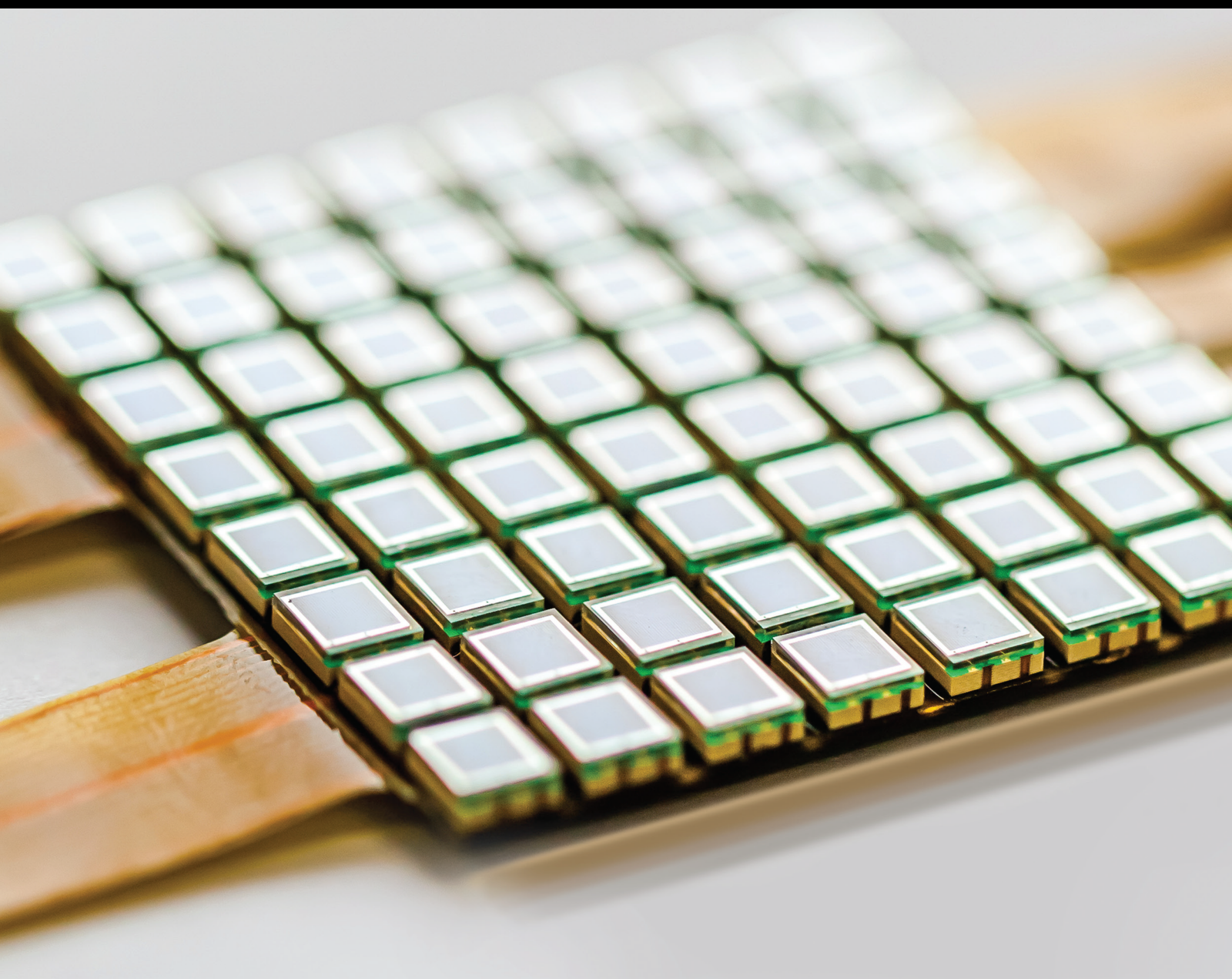


Multi Sensors and Reliable Smart Technologies for Developing Intelligent Environments

Lead Guest Editor: C. Venkatesan

Guest Editors: Imran Shafique Ansari and Danilo Pelusi





**Multi Sensors and Reliable Smart Technologies
for Developing Intelligent Environments**

Journal of Sensors

**Multi Sensors and Reliable Smart
Technologies for Developing Intelligent
Environments**

Lead Guest Editor: C. Venkatesan

Guest Editors: Imran Shafique Ansari and Danilo
Pelusi






Copyright © 2023 Hindawi Limited. All rights reserved.

This is a special issue published in "Journal of Sensors." All articles are open access articles distributed under the Creative Commons Attribution License, which permits unrestricted use, distribution, and reproduction in any medium, provided the original work is properly cited.

Chief Editor

Harith Ahmad , Malaysia

Associate Editors

Duo Lin , China
Fanli Meng , China
Pietro Siciliano , Italy
Guiyun Tian, United Kingdom

Academic Editors

Ghufran Ahmed , Pakistan
Constantin Apetrei, Romania
Shonak Bansal , India
Fernando Benito-Lopez , Spain
Romeo Bernini , Italy
Shekhar Bhansali, USA
Matthew Brodie, Australia
Ravikumar CV, India
Belén Calvo, Spain
Stefania Campopiano , Italy
Binghua Cao , China
Domenico Caputo, Italy
Sara Casciati, Italy
Gabriele Cazzulani , Italy
Chi Chiu Chan, Singapore
Sushank Chaudhary , Thailand
Edmon Chehura , United Kingdom
Marvin H Cheng , USA
Lei Chu , USA
Mario Collotta , Italy
Marco Consales , Italy
Jesus Corres , Spain
Andrea Cusano, Italy
Egidio De Benedetto , Italy
Luca De Stefano , Italy
Manel Del Valle , Spain
Franz L. Dickert, Austria
Giovanni Diraco, Italy
Maria de Fátima Domingues , Portugal
Nicola Donato , Italy
Sheng Du , China
Amir Elzawawy, Egypt
Mauro Epifani , Italy
Congbin Fan , China
Lihang Feng, China
Vittorio Ferrari , Italy
Luca Francioso, Italy

Libo Gao , China
Carmine Granata , Italy
Pramod Kumar Gupta , USA
Mohammad Haider , USA
Agustin Herrera-May , Mexico
María del Carmen Horrillo, Spain
Evangelos Hristoforou , Greece
Grazia Iadarola , Italy
Syed K. Islam , USA
Stephen James , United Kingdom
Sana Ullah Jan, United Kingdom
Bruno C. Janegitz , Brazil
Hai-Feng Ji , USA
Shouyong Jiang, United Kingdom
Roshan Prakash Joseph, USA
Niravkumar Joshi, USA
Rajesh Kaluri , India
Sang Sub Kim , Republic of Korea
Dr. Rajkishor Kumar, India
Rahul Kumar , India
Nageswara Lalam , USA
Antonio Lazaro , Spain
Chengkuo Lee , Singapore
Chenzong Li , USA
Zhi Lian , Australia
Rosalba Liguori , Italy
Sangsoon Lim , Republic of Korea
Huan Liu , China
Jin Liu , China
Eduard Llobet , Spain
Jaime Lloret , Spain
Mohamed Louzazni, Morocco
Jesús Lozano , Spain
Oleg Lupan , Moldova
Leandro Maio , Italy
Pawel Malinowski , Poland
Carlos Marques , Portugal
Eugenio Martinelli , Italy
Antonio Martinez-Olmos , Spain
Giuseppe Maruccio , Italy
Yasuko Y. Maruo, Japan
Zahid Mehmood , Pakistan
Carlos Michel , Mexico
Stephen. J. Mihailov , Canada
Bikash Nakarmi, China

Ehsan Namaziandost , Iran
Heinz C. Neitzert , Italy
Sing Kiong Nguang , New Zealand
Calogero M. Oddo , Italy
Tinghui Ouyang, Japan
SANDEEP KUMAR PALANISWAMY ,
India
Alberto J. Palma , Spain
Davide Palumbo , Italy
Abinash Panda , India
Roberto Paolesse , Italy
Akhilesh Pathak , Thailand
Giovanni Pau , Italy
Giorgio Pennazza , Italy
Michele Penza , Italy
Sivakumar Poruran, India
Stelios Potirakis , Greece
Biswajeet Pradhan , Malaysia
Giuseppe Quero , Italy
Linesh Raja , India
Maheswar Rajagopal , India
Valerie Renaudin , France
Armando Ricciardi , Italy
Christos Riziotis , Greece
Ruthber Rodriguez Serrezuela , Colombia
Maria Luz Rodriguez-Mendez , Spain
Jerome Rossignol , France
Maheswaran S, India
Ylias Sabri , Australia
Sourabh Sahu , India
José P. Santos , Spain
Sina Sareh, United Kingdom
Isabel Sayago , Spain
Andreas Schütze , Germany
Praveen K. Sekhar , USA
Sandra Sendra, Spain
Sandeep Sharma, India
Sunil Kumar Singh Singh , India
Yadvendra Singh , USA
Afaque Manzoor Soomro , Pakistan
Vincenzo Spagnolo, Italy
Kathiravan Srinivasan , India
Sachin K. Srivastava , India
Stefano Stassi , Italy

Danfeng Sun, China
Ashok Sundramoorthy, India
Salvatore Surdo , Italy
Roshan Thotagamuge , Sri Lanka
Guiyun Tian , United Kingdom
Sri Ramulu Torati , USA
Abdellah Touhafi , Belgium
Hoang Vinh Tran , Vietnam
Aitor Urrutia , Spain
Hana Vaisocherova - Lislalova , Czech
Republic
Everardo Vargas-Rodriguez , Mexico
Xavier Vilanova , Spain
Stanislav Vitek , Czech Republic
Luca Vollero , Italy
Tomasz Wandowski , Poland
Bohui Wang, China
Qihao Weng, USA
Penghai Wu , China
Qiang Wu, United Kingdom
Yuedong Xie , China
Chen Yang , China
Jiachen Yang , China
Nitesh Yelve , India
Aijun Yin, China
Chouki Zerrouki , France

Contents

Retracted: Internet of Things Remote Piano Information Teaching System and Its Control Method

Journal of Sensors

Retraction (1 page), Article ID 9891317, Volume 2023 (2023)

Retracted: Motion Control System of IoT Intelligent Robot Based on Improved ResNet Model

Journal of Sensors

Retraction (1 page), Article ID 9876579, Volume 2023 (2023)

Retracted: Complex Structure of Braid in Fiber Art Creation with Multisensor IoT Technology

Journal of Sensors

Retraction (1 page), Article ID 9872602, Volume 2023 (2023)

Retracted: Interior Design of Aging Housing Based on Smart Home System of IOT Sensor

Journal of Sensors

Retraction (1 page), Article ID 9870703, Volume 2023 (2023)

Retracted: Deconstruction of Urban Public Space Art Design Using Intelligent Sensor and Information Fusion

Journal of Sensors

Retraction (1 page), Article ID 9870298, Volume 2023 (2023)

Retracted: Deep Learning-Based Leaf Region Segmentation Using High-Resolution Super HAD CCD and ISOCELL GW1 Sensors

Journal of Sensors

Retraction (1 page), Article ID 9862849, Volume 2023 (2023)

Retracted: Advances in Hyperspectral Image Classification with a Bottleneck Attention Mechanism Based on 3D-FCNN Model and Imaging Spectrometer Sensor

Journal of Sensors

Retraction (1 page), Article ID 9854512, Volume 2023 (2023)

Retracted: Slope Shape and Edge Intelligent Recognition Technology Based on Deep Neural Sensing Network

Journal of Sensors

Retraction (1 page), Article ID 9850154, Volume 2023 (2023)

Retracted: 3D Simulation Landscape Design Based on Image Sensor

Journal of Sensors

Retraction (1 page), Article ID 9846710, Volume 2023 (2023)

Retracted: Key Technologies of Face Sensor Recognition Entry System for New Energy Vehicles Based on Particle Swarm Neural Network

Journal of Sensors

Retraction (1 page), Article ID 9843931, Volume 2023 (2023)

Retracted: Information Steganography Technology of Optical Communication Sensor Network Based on Virtual Reality Technology

Journal of Sensors

Retraction (1 page), Article ID 9836764, Volume 2023 (2023)

Retracted: A Voice Recognition Sensor and Voice Control System in an Intelligent Toy Robot System

Journal of Sensors

Retraction (1 page), Article ID 9836050, Volume 2023 (2023)

Retracted: Design and Implementation of College Students' Physical Fitness Test Management System Using IoT Smart Sensors

Journal of Sensors

Retraction (1 page), Article ID 9827071, Volume 2023 (2023)

Retracted: Smart Grid Security Based on Blockchain with Industrial Fault Detection Using Wireless Sensor Network and Deep Learning Techniques

Journal of Sensors

Retraction (1 page), Article ID 9824038, Volume 2023 (2023)

Retracted: Application of Internet of Things Based on Wireless Sensor in Tunnel Construction Monitoring

Journal of Sensors

Retraction (1 page), Article ID 9823845, Volume 2023 (2023)

Retracted: The Application Effect of Remote Sensing Technology in Hydrogeological Investigation under Big Data Environment

Journal of Sensors

Retraction (1 page), Article ID 9815031, Volume 2023 (2023)

Retracted: Online Fault Detection of Dry Reactor Based on Improved Kalman Filter

Journal of Sensors

Retraction (1 page), Article ID 9812198, Volume 2023 (2023)

Retracted: Numerical Sensing and Simulation Analysis of Three-Dimensional Flow Field and Temperature Field of Submersible Motor

Journal of Sensors

Retraction (1 page), Article ID 9798769, Volume 2023 (2023)

Retracted: Gymnastics Action Recognition and Training Posture Analysis Based on Artificial Intelligence Sensor

Journal of Sensors

Retraction (1 page), Article ID 9790106, Volume 2023 (2023)

Contents

Retracted: Wearable Sensor-Based Edge Computing Framework for Cardiac Arrhythmia Detection and Acute Stroke Prediction

Journal of Sensors

Retraction (1 page), Article ID 9785363, Volume 2023 (2023)

Retracted: Application of Artificial Intelligence-Based Sensor Technology in the Recommendation Model of Cultural Tourism Resources

Journal of Sensors

Retraction (1 page), Article ID 9782491, Volume 2023 (2023)

Retracted: Accurate Detection of Intelligent Running Posture Based on Artificial Intelligence Sensor

Journal of Sensors

Retraction (1 page), Article ID 9780459, Volume 2023 (2023)

Retracted: Intelligent Campus Resource Sharing System Based on Data Fusion Sensor

Journal of Sensors

Retraction (1 page), Article ID 9758081, Volume 2023 (2023)

Retracted: Convolution-LSTM-Based Mechanical Hard Disk Failure Prediction by Sensoring S.M.A.R.T. Indicators

Journal of Sensors

Retraction (1 page), Article ID 9756794, Volume 2023 (2023)

Retracted: Integrated Sensory Throughput and Traffic-Aware Arbiter for High Productive Multicore Architectures

Journal of Sensors

Retraction (1 page), Article ID 9753534, Volume 2023 (2023)

Retracted: Application of Symmetric Encryption Algorithm Sensor in the Research of College Student Security Management System

Journal of Sensors

Retraction (1 page), Article ID 9865418, Volume 2023 (2023)

Retracted: Application of Internet of Things Technology in Mobile Education of Smart Campus Culture and Etiquette

Journal of Sensors

Retraction (1 page), Article ID 9865068, Volume 2023 (2023)

Retracted: Application of Image Processing Sensor and Pattern Recognition in Detection of Bearing Surface Defects

Journal of Sensors

Retraction (1 page), Article ID 9861989, Volume 2023 (2023)

Retracted: Energy Efficiency Improvement of Composite Energy Building Energy Supply System Based on Multiobjective Network Sensor Optimization

Journal of Sensors

Retraction (1 page), Article ID 9861937, Volume 2023 (2023)

Retracted: Tennis Technology Recognition and Training Attitude Analysis Based on Artificial Intelligence Sensor

Journal of Sensors

Retraction (1 page), Article ID 9843919, Volume 2023 (2023)

Retracted: Software for Mapping and Extraction of Building Land Remote Sensing Data Based on BIM and Sensor Technology

Journal of Sensors

Retraction (1 page), Article ID 9842860, Volume 2023 (2023)

Retracted: Data Management Platform of Forest Ecological Station Based on Internet of Things and Big Data Sensor

Journal of Sensors

Retraction (1 page), Article ID 9836484, Volume 2023 (2023)

Retracted: Application of Sensor and Fuzzy Clustering Algorithm in Hybrid Recommender System

Journal of Sensors

Retraction (1 page), Article ID 9836067, Volume 2023 (2023)

Retracted: Signal Optimization of Electronic Communication Network Based on Internet of Things

Journal of Sensors

Retraction (1 page), Article ID 9829451, Volume 2023 (2023)

Retracted: PKPM Architectural Engineering Software System Based on Architectural BIM Technology

Journal of Sensors

Retraction (1 page), Article ID 9817909, Volume 2023 (2023)

Retracted: Analysis of People Flow Image Detection System Based on Computer Vision Sensor

Journal of Sensors

Retraction (1 page), Article ID 9812538, Volume 2023 (2023)

Retracted: Interactive Knowledge Visualization Based on IoT and Augmented Reality

Journal of Sensors

Retraction (1 page), Article ID 9806940, Volume 2023 (2023)

Retracted: Application of Industrial Big Data Cloud Control Platform Based on Fusion Transmission Sensor

Journal of Sensors

Retraction (1 page), Article ID 9804852, Volume 2023 (2023)

Retracted: Optical Hybrid Network Structure Based on Cloud Computing and Big Data Technology

Journal of Sensors

Retraction (1 page), Article ID 9798048, Volume 2023 (2023)

Contents

Retracted: Digital Library Information Integration System Based on Big Data and Deep Learning

Journal of Sensors

Retraction (1 page), Article ID 9796318, Volume 2023 (2023)

Retracted: The Study of Virtual Reality Sensing Technology in the Form Design and Perception of Public Buildings

Journal of Sensors

Retraction (1 page), Article ID 9793180, Volume 2023 (2023)

Retracted: Data Transmission and Processing Analysis of Power Economic Management Terminal Based on the Internet of Things

Journal of Sensors

Retraction (1 page), Article ID 9787212, Volume 2023 (2023)

Retracted: Active Vibration Control of Robot Gear System Based on Adaptive Control Algorithm

Journal of Sensors

Retraction (1 page), Article ID 9786982, Volume 2023 (2023)

Retracted: Information Extraction and Data Planning of Smart City Based on Internet of Things

Journal of Sensors

Retraction (1 page), Article ID 9786743, Volume 2023 (2023)

Retracted: Intelligent Evaluation Method of Engineering Cost Feasibility Model Based on Internet of Things

Journal of Sensors

Retraction (1 page), Article ID 9786479, Volume 2023 (2023)

Retracted: Life Prediction of Dry Reactor Sensor Based on Deep Neural Network

Journal of Sensors

Retraction (1 page), Article ID 9785854, Volume 2023 (2023)

Retracted: Test of Ultimate Bearing Capacity of Building Concrete Structures in Earthquake Area Based on Virtual Reality

Journal of Sensors

Retraction (1 page), Article ID 9783121, Volume 2023 (2023)

Retracted: Online English Teaching System Based on Internet of Things Technology

Journal of Sensors

Retraction (1 page), Article ID 9765848, Volume 2023 (2023)

Retracted: Optimization of Distribution Automation System Based on Artificial Intelligence Wireless Network Technology

Journal of Sensors

Retraction (1 page), Article ID 9896306, Volume 2023 (2023)

Retracted: Fractal Art Pattern Information System Based on Genetic Algorithm

Journal of Sensors

Retraction (1 page), Article ID 9879306, Volume 2023 (2023)

Retracted: Abnormal Data Monitoring and Analysis Based on Data Mining and Neural Network

Journal of Sensors

Retraction (1 page), Article ID 9865161, Volume 2023 (2023)

Retracted: Spatial and Temporal Evolution of Urban Green Space Pattern Based on GIS Sensors and Remote Sensing Information: Taking Xi'an as an Example

Journal of Sensors

Retraction (1 page), Article ID 9827253, Volume 2023 (2023)

Retracted: Research on Data Mining Algorithm of Associated User Network Based on Multi-Information Fusion

Journal of Sensors

Retraction (1 page), Article ID 9807043, Volume 2023 (2023)

Retracted: A Monitoring System for Air Quality and Soil Environment in Mining Areas Based on the Internet of Things

Journal of Sensors

Retraction (1 page), Article ID 9792129, Volume 2023 (2023)

Retracted: Application of 3D Virtual Reality Sensor in Tourist Scenic Navigation System

Journal of Sensors

Retraction (1 page), Article ID 9896501, Volume 2023 (2023)

Retracted: A Wood Quality Defect Detection System Based on Deep Learning and Multicriterion Framework

Journal of Sensors


Retraction (1 page), Article ID 9850214, Volume 2023 (2023)

[Retracted] Deep Learning-Based Leaf Region Segmentation Using High-Resolution Super HAD CCD and ISOCELL GW1 Sensors

Srinivas Talasila , Kirti Rawal , and Gaurav Sethi


Research Article (20 pages), Article ID 1085735, Volume 2023 (2023)

[Retracted] Smart Grid Security Based on Blockchain with Industrial Fault Detection Using Wireless Sensor Network and Deep Learning Techniques

Manivel Kandasamy, S. Anto, K. Baranitharan, Ravi Rastogi, Gunda Satwik, and A. Sampathkumar 

Research Article (13 pages), Article ID 3806121, Volume 2023 (2023)


[Retracted] Key Technologies of Face Sensor Recognition Entry System for New Energy Vehicles Based on Particle Swarm Neural Network

Fusong Li, Xin Su , Haibin Zhao, Ruixue Hu, and Bingzhen Shen

Research Article (6 pages), Article ID 3375744, Volume 2023 (2023)

Contents

[Retracted] Motion Control System of IoT Intelligent Robot Based on Improved ResNet Model

Zeyad Farisi 






Research Article (7 pages), Article ID 6229162, Volume 2023 (2023)

[Retracted] Numerical Sensing and Simulation Analysis of Three-Dimensional Flow Field and Temperature Field of Submersible Motor

Dongxin Wang  and Yabin Pan

Research Article (7 pages), Article ID 6523818, Volume 2023 (2023)



[Retracted] Wearable Sensor-Based Edge Computing Framework for Cardiac Arrhythmia Detection and Acute Stroke Prediction

R. Lavanya , D. Vidyabharathi , S. Selva Kumar , Manisha Mali , M. Arunkumar , S. S.

Aravindh , Md. Zainabuddin , K. Jose Triny , J. Sathyendra Bhat , and Miretab Tesfayohanis 

Research Article (9 pages), Article ID 3082870, Volume 2023 (2023)

[Retracted] Interior Design of Aging Housing Based on Smart Home System of IOT Sensor

Xiao Dong Cui  and Wonjun Chung 


Research Article (7 pages), Article ID 9281248, Volume 2023 (2023)

[Retracted] A Voice Recognition Sensor and Voice Control System in an Intelligent Toy Robot System

Cong Luo 


Research Article (8 pages), Article ID 4311745, Volume 2023 (2023)

[Retracted] The Application Effect of Remote Sensing Technology in Hydrogeological Investigation under Big Data Environment

Honglei Wang, Ronghang Yang , Li Zhao, Feng Tian, and Shizhong Yu



Research Article (12 pages), Article ID 5162864, Volume 2022 (2022)

[Retracted] Deconstruction of Urban Public Space Art Design Using Intelligent Sensor and Information Fusion

He Meng and Yanming Sun 

Research Article (9 pages), Article ID 9360982, Volume 2022 (2022)

[Retracted] Intelligent Evaluation Method of Engineering Cost Feasibility Model Based on Internet of Things

Liangqiong Chen , Hao Zhang , and Fang Wang 


Research Article (8 pages), Article ID 3420723, Volume 2022 (2022)

[Retracted] Convolution-LSTM-Based Mechanical Hard Disk Failure Prediction by Sensoring S.M.A.R.T. Indicators

Junjie Shi, Jing Du, Yingwen Ren, Boyu Li, Jinwei Zou, and Anyi Zhang 


Research Article (15 pages), Article ID 7832117, Volume 2022 (2022)

[Retracted] Information Extraction and Data Planning of Smart City Based on Internet of Things

Zeyad Farisi 



Research Article (8 pages), Article ID 2893702, Volume 2022 (2022)

[Retracted] Interactive Knowledge Visualization Based on IoT and Augmented Reality

Hanjie Sun 

Research Article (8 pages), Article ID 7921550, Volume 2022 (2022)

[Retracted] Application of Artificial Intelligence-Based Sensor Technology in the Recommendation Model of Cultural Tourism Resources

Shuang Hou  and Shihui Zhang 

Research Article (8 pages), Article ID 3948298, Volume 2022 (2022)

[Retracted] Signal Optimization of Electronic Communication Network Based on Internet of Things

Bo Feng , Wei Li , and Lina Wang 

Research Article (8 pages), Article ID 3711776, Volume 2022 (2022)

[Retracted] Optimization of Distribution Automation System Based on Artificial Intelligence Wireless Network Technology

Weihua Tian , Xiangbin Meng , Jianing Wang , and Hongkui Yan 

Research Article (8 pages), Article ID 1646667, Volume 2022 (2022)

[Retracted] Integrated Sensory Throughput and Traffic-Aware Arbiter for High Productive Multicore Architectures

T. Venkata Sridhar  and G. Chenchu Krishnaiah 





Research Article (14 pages), Article ID 2911777, Volume 2022 (2022)

[Retracted] A Monitoring System for Air Quality and Soil Environment in Mining Areas Based on the Internet of Things

Hongjing Dai , Dena Huang , and Haili Mao 


Research Article (7 pages), Article ID 5419167, Volume 2022 (2022)

[Retracted] 3D Simulation Landscape Design Based on Image Sensor

Yao Lu , Bingyan Chen , Yan Xing , and Yang Geon Seok 

Research Article (7 pages), Article ID 1577945, Volume 2022 (2022)

[Retracted] Data Transmission and Processing Analysis of Power Economic Management Terminal Based on the Internet of Things

Hao Tang 


Research Article (8 pages), Article ID 2649993, Volume 2022 (2022)

[Retracted] Advances in Hyperspectral Image Classification with a Bottleneck Attention Mechanism Based on 3D-FCNN Model and Imaging Spectrometer Sensor

Deren Yuan, Xiaochun Xie , Gao Gao, and Ju Xiao

Research Article (16 pages), Article ID 7587157, Volume 2022 (2022)


[Retracted] Online English Teaching System Based on Internet of Things Technology

Hui Tao 

Research Article (8 pages), Article ID 7748067, Volume 2022 (2022)


Contents

[Retracted] Optical Hybrid Network Structure Based on Cloud Computing and Big Data Technology

Huiting Wei 







Research Article (6 pages), Article ID 3936876, Volume 2022 (2022)

[Retracted] Internet of Things Remote Piano Information Teaching System and Its Control Method

Yangjie Fan 


Research Article (6 pages), Article ID 4730550, Volume 2022 (2022)

[Retracted] Online Fault Detection of Dry Reactor Based on Improved Kalman Filter

Lu Zheng , Xuan Liu , Qi Kang , Yue Yang , Hua Xun , and Jianying Zhang 



Research Article (6 pages), Article ID 3947025, Volume 2022 (2022)

[Retracted] Fractal Art Pattern Information System Based on Genetic Algorithm

MengLin Chen 

Research Article (8 pages), Article ID 9350301, Volume 2022 (2022)

[Retracted] The Study of Virtual Reality Sensing Technology in the Form Design and Perception of Public Buildings

Leili Li  and Xinyu Zheng 

Research Article (9 pages), Article ID 7903386, Volume 2022 (2022)

[Retracted] Design and Implementation of College Students' Physical Fitness Test Management System Using IoT Smart Sensors

Jin Xu, Qing Chen , and Xinwen Li

Research Article (13 pages), Article ID 1481930, Volume 2022 (2022)

[Retracted] Accurate Detection of Intelligent Running Posture Based on Artificial Intelligence Sensor

Chenguang Zhang  and Kun Cheng 



Research Article (7 pages), Article ID 6561159, Volume 2022 (2022)

[Retracted] Application of Internet of Things Technology in Mobile Education of Smart Campus Culture and Etiquette

Yanhui Guo 

Research Article (10 pages), Article ID 6321784, Volume 2022 (2022)

[Retracted] Research on Data Mining Algorithm of Associated User Network Based on Multi-Information Fusion

Xiancai Kang  and Chuangli Hua 



Research Article (8 pages), Article ID 2417826, Volume 2022 (2022)

[Retracted] Software for Mapping and Extraction of Building Land Remote Sensing Data Based on BIM and Sensor Technology

Shaoping Zhang  and Yaqin Wan 





Research Article (7 pages), Article ID 1026361, Volume 2022 (2022)

[Retracted] Application of Symmetric Encryption Algorithm Sensor in the Research of College Student Security Management System

Kexu Wu  and Chaolin Li 


Research Article (7 pages), Article ID 3323547, Volume 2022 (2022)

[Retracted] Slope Shape and Edge Intelligent Recognition Technology Based on Deep Neural Sensing Network

Yansen Huang , Ke Yu , Ningbo Wu , and Juanjuan Chang 




Research Article (7 pages), Article ID 5901803, Volume 2022 (2022)

[Retracted] Complex Structure of Braid in Fiber Art Creation with Multisensor IoT Technology

Jingyu Wang, Pengpeng Li, and Mengyao Wang 

Research Article (13 pages), Article ID 6358247, Volume 2022 (2022)

[Retracted] Analysis of People Flow Image Detection System Based on Computer Vision Sensor

Bing Ou , Jingjing Yang , and Wei Wang 


Research Article (7 pages), Article ID 8099876, Volume 2022 (2022)

[Retracted] Spatial and Temporal Evolution of Urban Green Space Pattern Based on GIS Sensors and Remote Sensing Information: Taking Xi'an as an Example

Wei Li , Hui Wang , Shaowei Zhang , Bingshen Jiang , and Shi-Young Lee 


Research Article (8 pages), Article ID 3648880, Volume 2022 (2022)

[Retracted] PKPM Architectural Engineering Software System Based on Architectural BIM Technology

Ying Fu 




Research Article (7 pages), Article ID 5382026, Volume 2022 (2022)

[Retracted] Intelligent Campus Resource Sharing System Based on Data Fusion Sensor

Guangshun Huang 



Research Article (7 pages), Article ID 4814727, Volume 2022 (2022)

[Retracted] Information Steganography Technology of Optical Communication Sensor Network Based on Virtual Reality Technology

ZhongBao Wang , WenMing Li , and GuoQing Wang 



Research Article (7 pages), Article ID 4827306, Volume 2022 (2022)

[Retracted] Active Vibration Control of Robot Gear System Based on Adaptive Control Algorithm

Dayu Zhang  and Cong Guan 

Research Article (8 pages), Article ID 4481296, Volume 2022 (2022)

[Retracted] Application of Sensor and Fuzzy Clustering Algorithm in Hybrid Recommender System

Zihang Xu  and Jiawei Zhu 

Research Article (8 pages), Article ID 4294777, Volume 2022 (2022)


Contents

[Retracted] Application of 3D Virtual Reality Sensor in Tourist Scenic Navigation System

Fei Deng 

Research Article (7 pages), Article ID 1112261, Volume 2022 (2022)

[Retracted] Digital Library Information Integration System Based on Big Data and Deep Learning

Xiao Lin , Ying Zhang, and Jiangong Wang




Research Article (8 pages), Article ID 9953787, Volume 2022 (2022)

[Retracted] Energy Efficiency Improvement of Composite Energy Building Energy Supply System Based on Multiobjective Network Sensor Optimization

Jingyun Huang 



Research Article (11 pages), Article ID 6935830, Volume 2022 (2022)

[Retracted] Test of Ultimate Bearing Capacity of Building Concrete Structures in Earthquake Area Based on Virtual Reality

Hui Liu , Xintian Yang , and Lijun Dou 


Research Article (7 pages), Article ID 6049308, Volume 2022 (2022)

[Retracted] Application of Image Processing Sensor and Pattern Recognition in Detection of Bearing Surface Defects

Qinghong Wu  and Minghui Zhu 

Research Article (7 pages), Article ID 7924982, Volume 2022 (2022)

[Retracted] A Wood Quality Defect Detection System Based on Deep Learning and Multicriterion Framework

Pingan Sun 


Research Article (8 pages), Article ID 3234148, Volume 2022 (2022)

[Retracted] Gymnastics Action Recognition and Training Posture Analysis Based on Artificial Intelligence Sensor

Yuanxiang Chen  and Qiao Chen 






Research Article (7 pages), Article ID 1605529, Volume 2022 (2022)

[Retracted] Data Management Platform of Forest Ecological Station Based on Internet of Things and Big Data Sensor

Ping'an Sun 

Research Article (8 pages), Article ID 1207745, Volume 2022 (2022)

[Retracted] Application of Internet of Things Based on Wireless Sensor in Tunnel Construction Monitoring

Jianfeng Cao , Ruichuan Zhao , Liqiang Hu , Qing Liang , and Zhenhua Tang 

Research Article (8 pages), Article ID 5302754, Volume 2022 (2022)

[Retracted] Application of Industrial Big Data Cloud Control Platform Based on Fusion Transmission Sensor

Weiping Meng  and Wenxin Shao 


Research Article (8 pages), Article ID 6955028, Volume 2022 (2022)

[Retracted] Life Prediction of Dry Reactor Sensor Based on Deep Neural Network

Hongbing Guo , Jianying Meng , Yue Yang , Lu Zheng , Xuan Liu , and Ming Tan 

Research Article (7 pages), Article ID 6982950, Volume 2022 (2022)

[Retracted] Tennis Technology Recognition and Training Attitude Analysis Based on Artificial Intelligence Sensor

Ke Li 

Research Article (7 pages), Article ID 6594701, Volume 2022 (2022)

[Retracted] Abnormal Data Monitoring and Analysis Based on Data Mining and Neural Network

Yanyan Chen 

Research Article (7 pages), Article ID 2635819, Volume 2022 (2022)

Retraction

Retracted: Internet of Things Remote Piano Information Teaching System and Its Control Method

Journal of Sensors

Received 12 December 2023; Accepted 12 December 2023; Published 13 December 2023

Copyright © 2023 Journal of Sensors. This is an open access article distributed under the Creative Commons Attribution License, which permits unrestricted use, distribution, and reproduction in any medium, provided the original work is properly cited.

This article has been retracted by Hindawi, as publisher, following an investigation undertaken by the publisher [1]. This investigation has uncovered evidence of systematic manipulation of the publication and peer-review process. We cannot, therefore, vouch for the reliability or integrity of this article.

Please note that this notice is intended solely to alert readers that the peer-review process of this article has been compromised.

Wiley and Hindawi regret that the usual quality checks did not identify these issues before publication and have since put additional measures in place to safeguard research integrity.

We wish to credit our Research Integrity and Research Publishing teams and anonymous and named external researchers and research integrity experts for contributing to this investigation.

The corresponding author, as the representative of all authors, has been given the opportunity to register their agreement or disagreement to this retraction. We have kept a record of any response received.

References

- [1] Y. Fan, "Internet of Things Remote Piano Information Teaching System and Its Control Method," *Journal of Sensors*, vol. 2022, Article ID 4730550, 6 pages, 2022.

Retraction

Retracted: Motion Control System of IoT Intelligent Robot Based on Improved ResNet Model

Journal of Sensors

Received 12 December 2023; Accepted 12 December 2023; Published 13 December 2023

Copyright © 2023 Journal of Sensors. This is an open access article distributed under the Creative Commons Attribution License, which permits unrestricted use, distribution, and reproduction in any medium, provided the original work is properly cited.

This article has been retracted by Hindawi, as publisher, following an investigation undertaken by the publisher [1]. This investigation has uncovered evidence of systematic manipulation of the publication and peer-review process. We cannot, therefore, vouch for the reliability or integrity of this article.

Please note that this notice is intended solely to alert readers that the peer-review process of this article has been compromised.

Wiley and Hindawi regret that the usual quality checks did not identify these issues before publication and have since put additional measures in place to safeguard research integrity.

We wish to credit our Research Integrity and Research Publishing teams and anonymous and named external researchers and research integrity experts for contributing to this investigation.

The corresponding author, as the representative of all authors, has been given the opportunity to register their agreement or disagreement to this retraction. We have kept a record of any response received.

References

- [1] Z. Farisi, "Motion Control System of IoT Intelligent Robot Based on Improved ResNet Model," *Journal of Sensors*, vol. 2023, Article ID 6229162, 7 pages, 2023.

Retraction

Retracted: Complex Structure of Braid in Fiber Art Creation with Multisensor IoT Technology

Journal of Sensors

Received 12 December 2023; Accepted 12 December 2023; Published 13 December 2023

Copyright © 2023 Journal of Sensors. This is an open access article distributed under the Creative Commons Attribution License, which permits unrestricted use, distribution, and reproduction in any medium, provided the original work is properly cited.

This article has been retracted by Hindawi, as publisher, following an investigation undertaken by the publisher [1]. This investigation has uncovered evidence of systematic manipulation of the publication and peer-review process. We cannot, therefore, vouch for the reliability or integrity of this article.

Please note that this notice is intended solely to alert readers that the peer-review process of this article has been compromised.

Wiley and Hindawi regret that the usual quality checks did not identify these issues before publication and have since put additional measures in place to safeguard research integrity.

We wish to credit our Research Integrity and Research Publishing teams and anonymous and named external researchers and research integrity experts for contributing to this investigation.

The corresponding author, as the representative of all authors, has been given the opportunity to register their agreement or disagreement to this retraction. We have kept a record of any response received.

References

- [1] J. Wang, P. Li, and M. Wang, "Complex Structure of Braid in Fiber Art Creation with Multisensor IoT Technology," *Journal of Sensors*, vol. 2022, Article ID 6358247, 13 pages, 2022.

Retraction

Retracted: Interior Design of Aging Housing Based on Smart Home System of IOT Sensor

Journal of Sensors

Received 12 December 2023; Accepted 12 December 2023; Published 13 December 2023

Copyright © 2023 Journal of Sensors. This is an open access article distributed under the Creative Commons Attribution License, which permits unrestricted use, distribution, and reproduction in any medium, provided the original work is properly cited.

This article has been retracted by Hindawi, as publisher, following an investigation undertaken by the publisher [1]. This investigation has uncovered evidence of systematic manipulation of the publication and peer-review process. We cannot, therefore, vouch for the reliability or integrity of this article.

Please note that this notice is intended solely to alert readers that the peer-review process of this article has been compromised.

Wiley and Hindawi regret that the usual quality checks did not identify these issues before publication and have since put additional measures in place to safeguard research integrity.

We wish to credit our Research Integrity and Research Publishing teams and anonymous and named external researchers and research integrity experts for contributing to this investigation.

The corresponding author, as the representative of all authors, has been given the opportunity to register their agreement or disagreement to this retraction. We have kept a record of any response received.

References

- [1] X. D. Cui and W. Chung, "Interior Design of Aging Housing Based on Smart Home System of IOT Sensor," *Journal of Sensors*, vol. 2023, Article ID 9281248, 7 pages, 2023.

Retraction

Retracted: Deconstruction of Urban Public Space Art Design Using Intelligent Sensor and Information Fusion

Journal of Sensors

Received 12 December 2023; Accepted 12 December 2023; Published 13 December 2023

Copyright © 2023 Journal of Sensors. This is an open access article distributed under the Creative Commons Attribution License, which permits unrestricted use, distribution, and reproduction in any medium, provided the original work is properly cited.

This article has been retracted by Hindawi, as publisher, following an investigation undertaken by the publisher [1]. This investigation has uncovered evidence of systematic manipulation of the publication and peer-review process. We cannot, therefore, vouch for the reliability or integrity of this article.

Please note that this notice is intended solely to alert readers that the peer-review process of this article has been compromised.

Wiley and Hindawi regret that the usual quality checks did not identify these issues before publication and have since put additional measures in place to safeguard research integrity.

We wish to credit our Research Integrity and Research Publishing teams and anonymous and named external researchers and research integrity experts for contributing to this investigation.

The corresponding author, as the representative of all authors, has been given the opportunity to register their agreement or disagreement to this retraction. We have kept a record of any response received.

References

- [1] H. Meng and Y. Sun, "Deconstruction of Urban Public Space Art Design Using Intelligent Sensor and Information Fusion," *Journal of Sensors*, vol. 2022, Article ID 9360982, 9 pages, 2022.

Retraction

Retracted: Deep Learning-Based Leaf Region Segmentation Using High-Resolution Super HAD CCD and ISOCELL GW1 Sensors

Journal of Sensors

Received 12 December 2023; Accepted 12 December 2023; Published 13 December 2023

Copyright © 2023 Journal of Sensors. This is an open access article distributed under the Creative Commons Attribution License, which permits unrestricted use, distribution, and reproduction in any medium, provided the original work is properly cited.

This article has been retracted by Hindawi, as publisher, following an investigation undertaken by the publisher [1]. This investigation has uncovered evidence of systematic manipulation of the publication and peer-review process. We cannot, therefore, vouch for the reliability or integrity of this article.

Please note that this notice is intended solely to alert readers that the peer-review process of this article has been compromised.

Wiley and Hindawi regret that the usual quality checks did not identify these issues before publication and have since put additional measures in place to safeguard research integrity.

We wish to credit our Research Integrity and Research Publishing teams and anonymous and named external researchers and research integrity experts for contributing to this investigation.

The corresponding author, as the representative of all authors, has been given the opportunity to register their agreement or disagreement to this retraction. We have kept a record of any response received.

References

- [1] S. Talasila, K. Rawal, and G. Sethi, "Deep Learning-Based Leaf Region Segmentation Using High-Resolution Super HAD CCD and ISOCELL GW1 Sensors," *Journal of Sensors*, vol. 2023, Article ID 1085735, 20 pages, 2023.

Retraction

Retracted: Advances in Hyperspectral Image Classification with a Bottleneck Attention Mechanism Based on 3D-FCNN Model and Imaging Spectrometer Sensor

Journal of Sensors

Received 12 December 2023; Accepted 12 December 2023; Published 13 December 2023

Copyright © 2023 Journal of Sensors. This is an open access article distributed under the Creative Commons Attribution License, which permits unrestricted use, distribution, and reproduction in any medium, provided the original work is properly cited.

This article has been retracted by Hindawi, as publisher, following an investigation undertaken by the publisher [1]. This investigation has uncovered evidence of systematic manipulation of the publication and peer-review process. We cannot, therefore, vouch for the reliability or integrity of this article.

Please note that this notice is intended solely to alert readers that the peer-review process of this article has been compromised.

Wiley and Hindawi regret that the usual quality checks did not identify these issues before publication and have since put additional measures in place to safeguard research integrity.

We wish to credit our Research Integrity and Research Publishing teams and anonymous and named external researchers and research integrity experts for contributing to this investigation.

The corresponding author, as the representative of all authors, has been given the opportunity to register their agreement or disagreement to this retraction. We have kept a record of any response received.

References

- [1] D. Yuan, X. Xie, G. Gao, and J. Xiao, "Advances in Hyperspectral Image Classification with a Bottleneck Attention Mechanism Based on 3D-FCNN Model and Imaging Spectrometer Sensor," *Journal of Sensors*, vol. 2022, Article ID 7587157, 16 pages, 2022.

Retraction

Retracted: Slope Shape and Edge Intelligent Recognition Technology Based on Deep Neural Sensing Network

Journal of Sensors

Received 12 December 2023; Accepted 12 December 2023; Published 13 December 2023

Copyright © 2023 Journal of Sensors. This is an open access article distributed under the Creative Commons Attribution License, which permits unrestricted use, distribution, and reproduction in any medium, provided the original work is properly cited.

This article has been retracted by Hindawi, as publisher, following an investigation undertaken by the publisher [1]. This investigation has uncovered evidence of systematic manipulation of the publication and peer-review process. We cannot, therefore, vouch for the reliability or integrity of this article.

Please note that this notice is intended solely to alert readers that the peer-review process of this article has been compromised.

Wiley and Hindawi regret that the usual quality checks did not identify these issues before publication and have since put additional measures in place to safeguard research integrity.

We wish to credit our Research Integrity and Research Publishing teams and anonymous and named external researchers and research integrity experts for contributing to this investigation.

The corresponding author, as the representative of all authors, has been given the opportunity to register their agreement or disagreement to this retraction. We have kept a record of any response received.

References

- [1] Y. Huang, K. Yu, N. Wu, and J. Chang, "Slope Shape and Edge Intelligent Recognition Technology Based on Deep Neural Sensing Network," *Journal of Sensors*, vol. 2022, Article ID 5901803, 7 pages, 2022.

Retraction

Retracted: 3D Simulation Landscape Design Based on Image Sensor

Journal of Sensors

Received 12 December 2023; Accepted 12 December 2023; Published 13 December 2023

Copyright © 2023 Journal of Sensors. This is an open access article distributed under the Creative Commons Attribution License, which permits unrestricted use, distribution, and reproduction in any medium, provided the original work is properly cited.

This article has been retracted by Hindawi, as publisher, following an investigation undertaken by the publisher [1]. This investigation has uncovered evidence of systematic manipulation of the publication and peer-review process. We cannot, therefore, vouch for the reliability or integrity of this article.

Please note that this notice is intended solely to alert readers that the peer-review process of this article has been compromised.

Wiley and Hindawi regret that the usual quality checks did not identify these issues before publication and have since put additional measures in place to safeguard research integrity.

We wish to credit our Research Integrity and Research Publishing teams and anonymous and named external researchers and research integrity experts for contributing to this investigation.

The corresponding author, as the representative of all authors, has been given the opportunity to register their agreement or disagreement to this retraction. We have kept a record of any response received.

References

- [1] Y. Lu, B. Chen, Y. Xing, and Y. G. Seok, "3D Simulation Landscape Design Based on Image Sensor," *Journal of Sensors*, vol. 2022, Article ID 1577945, 7 pages, 2022.

Retraction

Retracted: Key Technologies of Face Sensor Recognition Entry System for New Energy Vehicles Based on Particle Swarm Neural Network

Journal of Sensors

Received 12 December 2023; Accepted 12 December 2023; Published 13 December 2023

Copyright © 2023 Journal of Sensors. This is an open access article distributed under the Creative Commons Attribution License, which permits unrestricted use, distribution, and reproduction in any medium, provided the original work is properly cited.

This article has been retracted by Hindawi, as publisher, following an investigation undertaken by the publisher [1]. This investigation has uncovered evidence of systematic manipulation of the publication and peer-review process. We cannot, therefore, vouch for the reliability or integrity of this article.

Please note that this notice is intended solely to alert readers that the peer-review process of this article has been compromised.

Wiley and Hindawi regret that the usual quality checks did not identify these issues before publication and have since put additional measures in place to safeguard research integrity.

We wish to credit our Research Integrity and Research Publishing teams and anonymous and named external researchers and research integrity experts for contributing to this investigation.

The corresponding author, as the representative of all authors, has been given the opportunity to register their agreement or disagreement to this retraction. We have kept a record of any response received.

References

- [1] F. Li, X. Su, H. Zhao, R. Hu, and B. Shen, "Key Technologies of Face Sensor Recognition Entry System for New Energy Vehicles Based on Particle Swarm Neural Network," *Journal of Sensors*, vol. 2023, Article ID 3375744, 6 pages, 2023.

Retraction

Retracted: Information Steganography Technology of Optical Communication Sensor Network Based on Virtual Reality Technology

Journal of Sensors

Received 12 December 2023; Accepted 12 December 2023; Published 13 December 2023

Copyright © 2023 Journal of Sensors. This is an open access article distributed under the Creative Commons Attribution License, which permits unrestricted use, distribution, and reproduction in any medium, provided the original work is properly cited.

This article has been retracted by Hindawi, as publisher, following an investigation undertaken by the publisher [1]. This investigation has uncovered evidence of systematic manipulation of the publication and peer-review process. We cannot, therefore, vouch for the reliability or integrity of this article.

Please note that this notice is intended solely to alert readers that the peer-review process of this article has been compromised.

Wiley and Hindawi regret that the usual quality checks did not identify these issues before publication and have since put additional measures in place to safeguard research integrity.

We wish to credit our Research Integrity and Research Publishing teams and anonymous and named external researchers and research integrity experts for contributing to this investigation.

The corresponding author, as the representative of all authors, has been given the opportunity to register their agreement or disagreement to this retraction. We have kept a record of any response received.

References

- [1] Z. Wang, W. Li, and G. Wang, "Information Steganography Technology of Optical Communication Sensor Network Based on Virtual Reality Technology," *Journal of Sensors*, vol. 2022, Article ID 4827306, 7 pages, 2022.

Retraction

Retracted: A Voice Recognition Sensor and Voice Control System in an Intelligent Toy Robot System

Journal of Sensors

Received 12 December 2023; Accepted 12 December 2023; Published 13 December 2023

Copyright © 2023 Journal of Sensors. This is an open access article distributed under the Creative Commons Attribution License, which permits unrestricted use, distribution, and reproduction in any medium, provided the original work is properly cited.

This article has been retracted by Hindawi, as publisher, following an investigation undertaken by the publisher [1]. This investigation has uncovered evidence of systematic manipulation of the publication and peer-review process. We cannot, therefore, vouch for the reliability or integrity of this article.

Please note that this notice is intended solely to alert readers that the peer-review process of this article has been compromised.

Wiley and Hindawi regret that the usual quality checks did not identify these issues before publication and have since put additional measures in place to safeguard research integrity.

We wish to credit our Research Integrity and Research Publishing teams and anonymous and named external researchers and research integrity experts for contributing to this investigation.

The corresponding author, as the representative of all authors, has been given the opportunity to register their agreement or disagreement to this retraction. We have kept a record of any response received.

References

- [1] C. Luo, "A Voice Recognition Sensor and Voice Control System in an Intelligent Toy Robot System," *Journal of Sensors*, vol. 2023, Article ID 4311745, 8 pages, 2023.

Retraction

Retracted: Design and Implementation of College Students' Physical Fitness Test Management System Using IoT Smart Sensors

Journal of Sensors

Received 12 December 2023; Accepted 12 December 2023; Published 13 December 2023

Copyright © 2023 Journal of Sensors. This is an open access article distributed under the Creative Commons Attribution License, which permits unrestricted use, distribution, and reproduction in any medium, provided the original work is properly cited.

This article has been retracted by Hindawi, as publisher, following an investigation undertaken by the publisher [1]. This investigation has uncovered evidence of systematic manipulation of the publication and peer-review process. We cannot, therefore, vouch for the reliability or integrity of this article.

Please note that this notice is intended solely to alert readers that the peer-review process of this article has been compromised.

Wiley and Hindawi regret that the usual quality checks did not identify these issues before publication and have since put additional measures in place to safeguard research integrity.

We wish to credit our Research Integrity and Research Publishing teams and anonymous and named external researchers and research integrity experts for contributing to this investigation.

The corresponding author, as the representative of all authors, has been given the opportunity to register their agreement or disagreement to this retraction. We have kept a record of any response received.

References

- [1] J. Xu, Q. Chen, and X. Li, "Design and Implementation of College Students' Physical Fitness Test Management System Using IoT Smart Sensors," *Journal of Sensors*, vol. 2022, Article ID 1481930, 13 pages, 2022.

Retraction

Retracted: Smart Grid Security Based on Blockchain with Industrial Fault Detection Using Wireless Sensor Network and Deep Learning Techniques

Journal of Sensors

Received 12 December 2023; Accepted 12 December 2023; Published 13 December 2023

Copyright © 2023 Journal of Sensors. This is an open access article distributed under the Creative Commons Attribution License, which permits unrestricted use, distribution, and reproduction in any medium, provided the original work is properly cited.

This article has been retracted by Hindawi, as publisher, following an investigation undertaken by the publisher [1]. This investigation has uncovered evidence of systematic manipulation of the publication and peer-review process. We cannot, therefore, vouch for the reliability or integrity of this article.

Please note that this notice is intended solely to alert readers that the peer-review process of this article has been compromised.

Wiley and Hindawi regret that the usual quality checks did not identify these issues before publication and have since put additional measures in place to safeguard research integrity.

We wish to credit our Research Integrity and Research Publishing teams and anonymous and named external researchers and research integrity experts for contributing to this investigation.

The corresponding author, as the representative of all authors, has been given the opportunity to register their agreement or disagreement to this retraction. We have kept a record of any response received.

References

- [1] M. Kandasamy, S. Anto, K. Baranitharan, R. Rastogi, G. Satwik, and A. Sampathkumar, "Smart Grid Security Based on Blockchain with Industrial Fault Detection Using Wireless Sensor Network and Deep Learning Techniques," *Journal of Sensors*, vol. 2023, Article ID 3806121, 13 pages, 2023.

Retraction

Retracted: Application of Internet of Things Based on Wireless Sensor in Tunnel Construction Monitoring

Journal of Sensors

Received 12 December 2023; Accepted 12 December 2023; Published 13 December 2023

Copyright © 2023 Journal of Sensors. This is an open access article distributed under the Creative Commons Attribution License, which permits unrestricted use, distribution, and reproduction in any medium, provided the original work is properly cited.

This article has been retracted by Hindawi, as publisher, following an investigation undertaken by the publisher [1]. This investigation has uncovered evidence of systematic manipulation of the publication and peer-review process. We cannot, therefore, vouch for the reliability or integrity of this article.

Please note that this notice is intended solely to alert readers that the peer-review process of this article has been compromised.

Wiley and Hindawi regret that the usual quality checks did not identify these issues before publication and have since put additional measures in place to safeguard research integrity.

We wish to credit our Research Integrity and Research Publishing teams and anonymous and named external researchers and research integrity experts for contributing to this investigation.

The corresponding author, as the representative of all authors, has been given the opportunity to register their agreement or disagreement to this retraction. We have kept a record of any response received.

References

- [1] J. Cao, R. Zhao, L. Hu, Q. Liang, and Z. Tang, "Application of Internet of Things Based on Wireless Sensor in Tunnel Construction Monitoring," *Journal of Sensors*, vol. 2022, Article ID 5302754, 8 pages, 2022.

Retraction

Retracted: The Application Effect of Remote Sensing Technology in Hydrogeological Investigation under Big Data Environment

Journal of Sensors

Received 12 December 2023; Accepted 12 December 2023; Published 13 December 2023

Copyright © 2023 Journal of Sensors. This is an open access article distributed under the Creative Commons Attribution License, which permits unrestricted use, distribution, and reproduction in any medium, provided the original work is properly cited.

This article has been retracted by Hindawi, as publisher, following an investigation undertaken by the publisher [1]. This investigation has uncovered evidence of systematic manipulation of the publication and peer-review process. We cannot, therefore, vouch for the reliability or integrity of this article.

Please note that this notice is intended solely to alert readers that the peer-review process of this article has been compromised.

Wiley and Hindawi regret that the usual quality checks did not identify these issues before publication and have since put additional measures in place to safeguard research integrity.

We wish to credit our Research Integrity and Research Publishing teams and anonymous and named external researchers and research integrity experts for contributing to this investigation.

The corresponding author, as the representative of all authors, has been given the opportunity to register their agreement or disagreement to this retraction. We have kept a record of any response received.

References

- [1] H. Wang, R. Yang, L. Zhao, F. Tian, and S. Yu, “The Application Effect of Remote Sensing Technology in Hydrogeological Investigation under Big Data Environment,” *Journal of Sensors*, vol. 2022, Article ID 5162864, 12 pages, 2022.

Retraction

Retracted: Online Fault Detection of Dry Reactor Based on Improved Kalman Filter

Journal of Sensors

Received 12 December 2023; Accepted 12 December 2023; Published 13 December 2023

Copyright © 2023 Journal of Sensors. This is an open access article distributed under the Creative Commons Attribution License, which permits unrestricted use, distribution, and reproduction in any medium, provided the original work is properly cited.

This article has been retracted by Hindawi, as publisher, following an investigation undertaken by the publisher [1]. This investigation has uncovered evidence of systematic manipulation of the publication and peer-review process. We cannot, therefore, vouch for the reliability or integrity of this article.

Please note that this notice is intended solely to alert readers that the peer-review process of this article has been compromised.

Wiley and Hindawi regret that the usual quality checks did not identify these issues before publication and have since put additional measures in place to safeguard research integrity.

We wish to credit our Research Integrity and Research Publishing teams and anonymous and named external researchers and research integrity experts for contributing to this investigation.

The corresponding author, as the representative of all authors, has been given the opportunity to register their agreement or disagreement to this retraction. We have kept a record of any response received.

References

- [1] L. Zheng, X. Liu, Q. Kang, Y. Yang, H. Xun, and J. Zhang, "Online Fault Detection of Dry Reactor Based on Improved Kalman Filter," *Journal of Sensors*, vol. 2022, Article ID 3947025, 6 pages, 2022.

Retraction

Retracted: Numerical Sensing and Simulation Analysis of Three-Dimensional Flow Field and Temperature Field of Submersible Motor

Journal of Sensors

Received 12 December 2023; Accepted 12 December 2023; Published 13 December 2023

Copyright © 2023 Journal of Sensors. This is an open access article distributed under the Creative Commons Attribution License, which permits unrestricted use, distribution, and reproduction in any medium, provided the original work is properly cited.

This article has been retracted by Hindawi, as publisher, following an investigation undertaken by the publisher [1]. This investigation has uncovered evidence of systematic manipulation of the publication and peer-review process. We cannot, therefore, vouch for the reliability or integrity of this article.

Please note that this notice is intended solely to alert readers that the peer-review process of this article has been compromised.

Wiley and Hindawi regret that the usual quality checks did not identify these issues before publication and have since put additional measures in place to safeguard research integrity.

We wish to credit our Research Integrity and Research Publishing teams and anonymous and named external researchers and research integrity experts for contributing to this investigation.

The corresponding author, as the representative of all authors, has been given the opportunity to register their agreement or disagreement to this retraction. We have kept a record of any response received.

References

- [1] D. Wang and Y. Pan, “Numerical Sensing and Simulation Analysis of Three-Dimensional Flow Field and Temperature Field of Submersible Motor,” *Journal of Sensors*, vol. 2023, Article ID 6523818, 7 pages, 2023.

Retraction

Retracted: Gymnastics Action Recognition and Training Posture Analysis Based on Artificial Intelligence Sensor

Journal of Sensors

Received 12 December 2023; Accepted 12 December 2023; Published 13 December 2023

Copyright © 2023 Journal of Sensors. This is an open access article distributed under the Creative Commons Attribution License, which permits unrestricted use, distribution, and reproduction in any medium, provided the original work is properly cited.

This article has been retracted by Hindawi, as publisher, following an investigation undertaken by the publisher [1]. This investigation has uncovered evidence of systematic manipulation of the publication and peer-review process. We cannot, therefore, vouch for the reliability or integrity of this article.

Please note that this notice is intended solely to alert readers that the peer-review process of this article has been compromised.

Wiley and Hindawi regret that the usual quality checks did not identify these issues before publication and have since put additional measures in place to safeguard research integrity.

We wish to credit our Research Integrity and Research Publishing teams and anonymous and named external researchers and research integrity experts for contributing to this investigation.

The corresponding author, as the representative of all authors, has been given the opportunity to register their agreement or disagreement to this retraction. We have kept a record of any response received.

References

- [1] Y. Chen and Q. Chen, "Gymnastics Action Recognition and Training Posture Analysis Based on Artificial Intelligence Sensor," *Journal of Sensors*, vol. 2022, Article ID 1605529, 7 pages, 2022.

Retraction

Retracted: Wearable Sensor-Based Edge Computing Framework for Cardiac Arrhythmia Detection and Acute Stroke Prediction

Journal of Sensors

Received 12 December 2023; Accepted 12 December 2023; Published 13 December 2023

Copyright © 2023 Journal of Sensors. This is an open access article distributed under the Creative Commons Attribution License, which permits unrestricted use, distribution, and reproduction in any medium, provided the original work is properly cited.

This article has been retracted by Hindawi, as publisher, following an investigation undertaken by the publisher [1]. This investigation has uncovered evidence of systematic manipulation of the publication and peer-review process. We cannot, therefore, vouch for the reliability or integrity of this article.

Please note that this notice is intended solely to alert readers that the peer-review process of this article has been compromised.

Wiley and Hindawi regret that the usual quality checks did not identify these issues before publication and have since put additional measures in place to safeguard research integrity.

We wish to credit our Research Integrity and Research Publishing teams and anonymous and named external researchers and research integrity experts for contributing to this investigation.

The corresponding author, as the representative of all authors, has been given the opportunity to register their agreement or disagreement to this retraction. We have kept a record of any response received.

References

- [1] R. Lavanya, D. Vidyabharathi, S. S. Kumar et al., “Wearable Sensor-Based Edge Computing Framework for Cardiac Arrhythmia Detection and Acute Stroke Prediction,” *Journal of Sensors*, vol. 2023, Article ID 3082870, 9 pages, 2023.

Retraction

Retracted: Application of Artificial Intelligence-Based Sensor Technology in the Recommendation Model of Cultural Tourism Resources

Journal of Sensors

Received 12 December 2023; Accepted 12 December 2023; Published 13 December 2023

Copyright © 2023 Journal of Sensors. This is an open access article distributed under the Creative Commons Attribution License, which permits unrestricted use, distribution, and reproduction in any medium, provided the original work is properly cited.

This article has been retracted by Hindawi, as publisher, following an investigation undertaken by the publisher [1]. This investigation has uncovered evidence of systematic manipulation of the publication and peer-review process. We cannot, therefore, vouch for the reliability or integrity of this article.

Please note that this notice is intended solely to alert readers that the peer-review process of this article has been compromised.

Wiley and Hindawi regret that the usual quality checks did not identify these issues before publication and have since put additional measures in place to safeguard research integrity.

We wish to credit our Research Integrity and Research Publishing teams and anonymous and named external researchers and research integrity experts for contributing to this investigation.

The corresponding author, as the representative of all authors, has been given the opportunity to register their agreement or disagreement to this retraction. We have kept a record of any response received.

References

- [1] S. Hou and S. Zhang, "Application of Artificial Intelligence-Based Sensor Technology in the Recommendation Model of Cultural Tourism Resources," *Journal of Sensors*, vol. 2022, Article ID 3948298, 8 pages, 2022.

Retraction

Retracted: Accurate Detection of Intelligent Running Posture Based on Artificial Intelligence Sensor

Journal of Sensors

Received 12 December 2023; Accepted 12 December 2023; Published 13 December 2023

Copyright © 2023 Journal of Sensors. This is an open access article distributed under the Creative Commons Attribution License, which permits unrestricted use, distribution, and reproduction in any medium, provided the original work is properly cited.

This article has been retracted by Hindawi, as publisher, following an investigation undertaken by the publisher [1]. This investigation has uncovered evidence of systematic manipulation of the publication and peer-review process. We cannot, therefore, vouch for the reliability or integrity of this article.

Please note that this notice is intended solely to alert readers that the peer-review process of this article has been compromised.

Wiley and Hindawi regret that the usual quality checks did not identify these issues before publication and have since put additional measures in place to safeguard research integrity.

We wish to credit our Research Integrity and Research Publishing teams and anonymous and named external researchers and research integrity experts for contributing to this investigation.

The corresponding author, as the representative of all authors, has been given the opportunity to register their agreement or disagreement to this retraction. We have kept a record of any response received.

References

- [1] C. Zhang and K. Cheng, "Accurate Detection of Intelligent Running Posture Based on Artificial Intelligence Sensor," *Journal of Sensors*, vol. 2022, Article ID 6561159, 7 pages, 2022.

Retraction

Retracted: Intelligent Campus Resource Sharing System Based on Data Fusion Sensor

Journal of Sensors

Received 12 December 2023; Accepted 12 December 2023; Published 13 December 2023

Copyright © 2023 Journal of Sensors. This is an open access article distributed under the Creative Commons Attribution License, which permits unrestricted use, distribution, and reproduction in any medium, provided the original work is properly cited.

This article has been retracted by Hindawi, as publisher, following an investigation undertaken by the publisher [1]. This investigation has uncovered evidence of systematic manipulation of the publication and peer-review process. We cannot, therefore, vouch for the reliability or integrity of this article.

Please note that this notice is intended solely to alert readers that the peer-review process of this article has been compromised.

Wiley and Hindawi regret that the usual quality checks did not identify these issues before publication and have since put additional measures in place to safeguard research integrity.

We wish to credit our Research Integrity and Research Publishing teams and anonymous and named external researchers and research integrity experts for contributing to this investigation.

The corresponding author, as the representative of all authors, has been given the opportunity to register their agreement or disagreement to this retraction. We have kept a record of any response received.

References

- [1] G. Huang, "Intelligent Campus Resource Sharing System Based on Data Fusion Sensor," *Journal of Sensors*, vol. 2022, Article ID 4814727, 7 pages, 2022.

Retraction

Retracted: Convolution-LSTM-Based Mechanical Hard Disk Failure Prediction by Sensoring S.M.A.R.T. Indicators

Journal of Sensors

Received 12 December 2023; Accepted 12 December 2023; Published 13 December 2023

Copyright © 2023 Journal of Sensors. This is an open access article distributed under the Creative Commons Attribution License, which permits unrestricted use, distribution, and reproduction in any medium, provided the original work is properly cited.

This article has been retracted by Hindawi, as publisher, following an investigation undertaken by the publisher [1]. This investigation has uncovered evidence of systematic manipulation of the publication and peer-review process. We cannot, therefore, vouch for the reliability or integrity of this article.

Please note that this notice is intended solely to alert readers that the peer-review process of this article has been compromised.

Wiley and Hindawi regret that the usual quality checks did not identify these issues before publication and have since put additional measures in place to safeguard research integrity.

We wish to credit our Research Integrity and Research Publishing teams and anonymous and named external researchers and research integrity experts for contributing to this investigation.

The corresponding author, as the representative of all authors, has been given the opportunity to register their agreement or disagreement to this retraction. We have kept a record of any response received.

References

- [1] J. Shi, J. Du, Y. Ren, B. Li, J. Zou, and A. Zhang, "Convolution-LSTM-Based Mechanical Hard Disk Failure Prediction by Sensoring S.M.A.R.T. Indicators," *Journal of Sensors*, vol. 2022, Article ID 7832117, 15 pages, 2022.

Retraction

Retracted: Integrated Sensory Throughput and Traffic-Aware Arbiter for High Productive Multicore Architectures

Journal of Sensors

Received 12 December 2023; Accepted 12 December 2023; Published 13 December 2023

Copyright © 2023 Journal of Sensors. This is an open access article distributed under the Creative Commons Attribution License, which permits unrestricted use, distribution, and reproduction in any medium, provided the original work is properly cited.

This article has been retracted by Hindawi, as publisher, following an investigation undertaken by the publisher [1]. This investigation has uncovered evidence of systematic manipulation of the publication and peer-review process. We cannot, therefore, vouch for the reliability or integrity of this article.

Please note that this notice is intended solely to alert readers that the peer-review process of this article has been compromised.

Wiley and Hindawi regret that the usual quality checks did not identify these issues before publication and have since put additional measures in place to safeguard research integrity.

We wish to credit our Research Integrity and Research Publishing teams and anonymous and named external researchers and research integrity experts for contributing to this investigation.

The corresponding author, as the representative of all authors, has been given the opportunity to register their agreement or disagreement to this retraction. We have kept a record of any response received.

References

- [1] T. Venkata Sridhar and G. C. Krishnaiah, "Integrated Sensory Throughput and Traffic-Aware Arbiter for High Productive Multicore Architectures," *Journal of Sensors*, vol. 2022, Article ID 2911777, 14 pages, 2022.

Retraction

Retracted: Application of Symmetric Encryption Algorithm Sensor in the Research of College Student Security Management System

Journal of Sensors

Received 17 October 2023; Accepted 17 October 2023; Published 18 October 2023

Copyright © 2023 Journal of Sensors. This is an open access article distributed under the Creative Commons Attribution License, which permits unrestricted use, distribution, and reproduction in any medium, provided the original work is properly cited.

This article has been retracted by Hindawi following an investigation undertaken by the publisher [1]. This investigation has uncovered evidence of one or more of the following indicators of systematic manipulation of the publication process:

- (1) Discrepancies in scope
- (2) Discrepancies in the description of the research reported
- (3) Discrepancies between the availability of data and the research described
- (4) Inappropriate citations
- (5) Incoherent, meaningless and/or irrelevant content included in the article
- (6) Peer-review manipulation

The presence of these indicators undermines our confidence in the integrity of the article's content and we cannot, therefore, vouch for its reliability. Please note that this notice is intended solely to alert readers that the content of this article is unreliable. We have not investigated whether authors were aware of or involved in the systematic manipulation of the publication process.

Wiley and Hindawi regrets that the usual quality checks did not identify these issues before publication and have since put additional measures in place to safeguard research integrity.

We wish to credit our own Research Integrity and Research Publishing teams and anonymous and named external researchers and research integrity experts for contributing to this investigation.

The corresponding author, as the representative of all authors, has been given the opportunity to register their agreement or disagreement to this retraction. We have kept a record of any response received.

References

- [1] K. Wu and C. Li, "Application of Symmetric Encryption Algorithm Sensor in the Research of College Student Security Management System," *Journal of Sensors*, vol. 2022, Article ID 3323547, 7 pages, 2022.

Retraction

Retracted: Application of Internet of Things Technology in Mobile Education of Smart Campus Culture and Etiquette

Journal of Sensors

Received 17 October 2023; Accepted 17 October 2023; Published 18 October 2023

Copyright © 2023 Journal of Sensors. This is an open access article distributed under the Creative Commons Attribution License, which permits unrestricted use, distribution, and reproduction in any medium, provided the original work is properly cited.

This article has been retracted by Hindawi following an investigation undertaken by the publisher [1]. This investigation has uncovered evidence of one or more of the following indicators of systematic manipulation of the publication process:

- (1) Discrepancies in scope
- (2) Discrepancies in the description of the research reported
- (3) Discrepancies between the availability of data and the research described
- (4) Inappropriate citations
- (5) Incoherent, meaningless and/or irrelevant content included in the article
- (6) Peer-review manipulation

The presence of these indicators undermines our confidence in the integrity of the article's content and we cannot, therefore, vouch for its reliability. Please note that this notice is intended solely to alert readers that the content of this article is unreliable. We have not investigated whether authors were aware of or involved in the systematic manipulation of the publication process.

In addition, our investigation has also shown that one or more of the following human-subject reporting requirements has not been met in this article: ethical approval by an Institutional Review Board (IRB) committee or equivalent, patient/participant consent to participate, and/or agreement to publish patient/participant details (where relevant).

Wiley and Hindawi regrets that the usual quality checks did not identify these issues before publication and have since put additional measures in place to safeguard research integrity.

We wish to credit our own Research Integrity and Research Publishing teams and anonymous and named external researchers and research integrity experts for contributing to this investigation.

The corresponding author, as the representative of all authors, has been given the opportunity to register their agreement or disagreement to this retraction. We have kept a record of any response received.

References

- [1] Y. Guo, "Application of Internet of Things Technology in Mobile Education of Smart Campus Culture and Etiquette," *Journal of Sensors*, vol. 2022, Article ID 6321784, 10 pages, 2022.

Retraction

Retracted: Application of Image Processing Sensor and Pattern Recognition in Detection of Bearing Surface Defects

Journal of Sensors

Received 17 October 2023; Accepted 17 October 2023; Published 18 October 2023

Copyright © 2023 Journal of Sensors. This is an open access article distributed under the Creative Commons Attribution License, which permits unrestricted use, distribution, and reproduction in any medium, provided the original work is properly cited.

This article has been retracted by Hindawi following an investigation undertaken by the publisher [1]. This investigation has uncovered evidence of one or more of the following indicators of systematic manipulation of the publication process:

- (1) Discrepancies in scope
- (2) Discrepancies in the description of the research reported
- (3) Discrepancies between the availability of data and the research described
- (4) Inappropriate citations
- (5) Incoherent, meaningless and/or irrelevant content included in the article
- (6) Peer-review manipulation

The presence of these indicators undermines our confidence in the integrity of the article's content and we cannot, therefore, vouch for its reliability. Please note that this notice is intended solely to alert readers that the content of this article is unreliable. We have not investigated whether authors were aware of or involved in the systematic manipulation of the publication process.

Wiley and Hindawi regrets that the usual quality checks did not identify these issues before publication and have since put additional measures in place to safeguard research integrity.

We wish to credit our own Research Integrity and Research Publishing teams and anonymous and named external researchers and research integrity experts for contributing to this investigation.

The corresponding author, as the representative of all authors, has been given the opportunity to register their agreement or disagreement to this retraction. We have kept a record of any response received.

References

- [1] Q. Wu and M. Zhu, "Application of Image Processing Sensor and Pattern Recognition in Detection of Bearing Surface Defects," *Journal of Sensors*, vol. 2022, Article ID 7924982, 7 pages, 2022.

Retraction

Retracted: Energy Efficiency Improvement of Composite Energy Building Energy Supply System Based on Multiobjective Network Sensor Optimization

Journal of Sensors

Received 17 October 2023; Accepted 17 October 2023; Published 18 October 2023

Copyright © 2023 Journal of Sensors. This is an open access article distributed under the Creative Commons Attribution License, which permits unrestricted use, distribution, and reproduction in any medium, provided the original work is properly cited.

This article has been retracted by Hindawi following an investigation undertaken by the publisher [1]. This investigation has uncovered evidence of one or more of the following indicators of systematic manipulation of the publication process:

- (1) Discrepancies in scope
- (2) Discrepancies in the description of the research reported
- (3) Discrepancies between the availability of data and the research described
- (4) Inappropriate citations
- (5) Incoherent, meaningless and/or irrelevant content included in the article
- (6) Peer-review manipulation

The presence of these indicators undermines our confidence in the integrity of the article's content and we cannot, therefore, vouch for its reliability. Please note that this notice is intended solely to alert readers that the content of this article is unreliable. We have not investigated whether authors were aware of or involved in the systematic manipulation of the publication process.

Wiley and Hindawi regrets that the usual quality checks did not identify these issues before publication and have since put additional measures in place to safeguard research integrity.

We wish to credit our own Research Integrity and Research Publishing teams and anonymous and named external researchers and research integrity experts for contributing to this investigation.

The corresponding author, as the representative of all authors, has been given the opportunity to register their agreement or disagreement to this retraction. We have kept a record of any response received.

References

- [1] J. Huang, "Energy Efficiency Improvement of Composite Energy Building Energy Supply System Based on Multiobjective Network Sensor Optimization," *Journal of Sensors*, vol. 2022, Article ID 6935830, 11 pages, 2022.

Retraction

Retracted: Tennis Technology Recognition and Training Attitude Analysis Based on Artificial Intelligence Sensor

Journal of Sensors

Received 17 October 2023; Accepted 17 October 2023; Published 18 October 2023

Copyright © 2023 Journal of Sensors. This is an open access article distributed under the Creative Commons Attribution License, which permits unrestricted use, distribution, and reproduction in any medium, provided the original work is properly cited.

This article has been retracted by Hindawi following an investigation undertaken by the publisher [1]. This investigation has uncovered evidence of one or more of the following indicators of systematic manipulation of the publication process:

- (1) Discrepancies in scope
- (2) Discrepancies in the description of the research reported
- (3) Discrepancies between the availability of data and the research described
- (4) Inappropriate citations
- (5) Incoherent, meaningless and/or irrelevant content included in the article
- (6) Peer-review manipulation

The presence of these indicators undermines our confidence in the integrity of the article's content and we cannot, therefore, vouch for its reliability. Please note that this notice is intended solely to alert readers that the content of this article is unreliable. We have not investigated whether authors were aware of or involved in the systematic manipulation of the publication process.

In addition, our investigation has also shown that one or more of the following human-subject reporting requirements has not been met in this article: ethical approval by an Institutional Review Board (IRB) committee or equivalent, patient/participant consent to participate, and/or agreement to publish patient/participant details (where relevant).

Wiley and Hindawi regrets that the usual quality checks did not identify these issues before publication and have since put additional measures in place to safeguard research integrity.

We wish to credit our own Research Integrity and Research Publishing teams and anonymous and named external researchers and research integrity experts for contributing to this investigation.

The corresponding author, as the representative of all authors, has been given the opportunity to register their agreement or disagreement to this retraction. We have kept a record of any response received.

References

- [1] K. Li, "Tennis Technology Recognition and Training Attitude Analysis Based on Artificial Intelligence Sensor," *Journal of Sensors*, vol. 2022, Article ID 6594701, 7 pages, 2022.

Retraction

Retracted: Software for Mapping and Extraction of Building Land Remote Sensing Data Based on BIM and Sensor Technology

Journal of Sensors

Received 17 October 2023; Accepted 17 October 2023; Published 18 October 2023

Copyright © 2023 Journal of Sensors. This is an open access article distributed under the Creative Commons Attribution License, which permits unrestricted use, distribution, and reproduction in any medium, provided the original work is properly cited.

This article has been retracted by Hindawi following an investigation undertaken by the publisher [1]. This investigation has uncovered evidence of one or more of the following indicators of systematic manipulation of the publication process:

- (1) Discrepancies in scope
- (2) Discrepancies in the description of the research reported
- (3) Discrepancies between the availability of data and the research described
- (4) Inappropriate citations
- (5) Incoherent, meaningless and/or irrelevant content included in the article
- (6) Peer-review manipulation

The presence of these indicators undermines our confidence in the integrity of the article's content and we cannot, therefore, vouch for its reliability. Please note that this notice is intended solely to alert readers that the content of this article is unreliable. We have not investigated whether authors were aware of or involved in the systematic manipulation of the publication process.

Wiley and Hindawi regrets that the usual quality checks did not identify these issues before publication and have since put additional measures in place to safeguard research integrity.

We wish to credit our own Research Integrity and Research Publishing teams and anonymous and named external researchers and research integrity experts for contributing to this investigation.

The corresponding author, as the representative of all authors, has been given the opportunity to register their agreement or disagreement to this retraction. We have kept a record of any response received.

References

- [1] S. Zhang and Y. Wan, "Software for Mapping and Extraction of Building Land Remote Sensing Data Based on BIM and Sensor Technology," *Journal of Sensors*, vol. 2022, Article ID 1026361, 7 pages, 2022.

Retraction

Retracted: Data Management Platform of Forest Ecological Station Based on Internet of Things and Big Data Sensor

Journal of Sensors

Received 17 October 2023; Accepted 17 October 2023; Published 18 October 2023

Copyright © 2023 Journal of Sensors. This is an open access article distributed under the Creative Commons Attribution License, which permits unrestricted use, distribution, and reproduction in any medium, provided the original work is properly cited.

This article has been retracted by Hindawi following an investigation undertaken by the publisher [1]. This investigation has uncovered evidence of one or more of the following indicators of systematic manipulation of the publication process:

- (1) Discrepancies in scope
- (2) Discrepancies in the description of the research reported
- (3) Discrepancies between the availability of data and the research described
- (4) Inappropriate citations
- (5) Incoherent, meaningless and/or irrelevant content included in the article
- (6) Peer-review manipulation

The presence of these indicators undermines our confidence in the integrity of the article's content and we cannot, therefore, vouch for its reliability. Please note that this notice is intended solely to alert readers that the content of this article is unreliable. We have not investigated whether authors were aware of or involved in the systematic manipulation of the publication process.

Wiley and Hindawi regrets that the usual quality checks did not identify these issues before publication and have since put additional measures in place to safeguard research integrity.

We wish to credit our own Research Integrity and Research Publishing teams and anonymous and named external researchers and research integrity experts for contributing to this investigation.

The corresponding author, as the representative of all authors, has been given the opportunity to register their agreement or disagreement to this retraction. We have kept a record of any response received.

References

- [1] P. Sun, "Data Management Platform of Forest Ecological Station Based on Internet of Things and Big Data Sensor," *Journal of Sensors*, vol. 2022, Article ID 1207745, 8 pages, 2022.

Retraction

Retracted: Application of Sensor and Fuzzy Clustering Algorithm in Hybrid Recommender System

Journal of Sensors

Received 17 October 2023; Accepted 17 October 2023; Published 18 October 2023

Copyright © 2023 Journal of Sensors. This is an open access article distributed under the Creative Commons Attribution License, which permits unrestricted use, distribution, and reproduction in any medium, provided the original work is properly cited.

This article has been retracted by Hindawi following an investigation undertaken by the publisher [1]. This investigation has uncovered evidence of one or more of the following indicators of systematic manipulation of the publication process:

- (1) Discrepancies in scope
- (2) Discrepancies in the description of the research reported
- (3) Discrepancies between the availability of data and the research described
- (4) Inappropriate citations
- (5) Incoherent, meaningless and/or irrelevant content included in the article
- (6) Peer-review manipulation

The presence of these indicators undermines our confidence in the integrity of the article's content and we cannot, therefore, vouch for its reliability. Please note that this notice is intended solely to alert readers that the content of this article is unreliable. We have not investigated whether authors were aware of or involved in the systematic manipulation of the publication process.

Wiley and Hindawi regrets that the usual quality checks did not identify these issues before publication and have since put additional measures in place to safeguard research integrity.

We wish to credit our own Research Integrity and Research Publishing teams and anonymous and named external researchers and research integrity experts for contributing to this investigation.

The corresponding author, as the representative of all authors, has been given the opportunity to register their agreement or disagreement to this retraction. We have kept a record of any response received.

References

- [1] Z. Xu and J. Zhu, "Application of Sensor and Fuzzy Clustering Algorithm in Hybrid Recommender System," *Journal of Sensors*, vol. 2022, Article ID 4294777, 8 pages, 2022.

Retraction

Retracted: Signal Optimization of Electronic Communication Network Based on Internet of Things

Journal of Sensors

Received 17 October 2023; Accepted 17 October 2023; Published 18 October 2023

Copyright © 2023 Journal of Sensors. This is an open access article distributed under the Creative Commons Attribution License, which permits unrestricted use, distribution, and reproduction in any medium, provided the original work is properly cited.

This article has been retracted by Hindawi following an investigation undertaken by the publisher [1]. This investigation has uncovered evidence of one or more of the following indicators of systematic manipulation of the publication process:

- (1) Discrepancies in scope
- (2) Discrepancies in the description of the research reported
- (3) Discrepancies between the availability of data and the research described
- (4) Inappropriate citations
- (5) Incoherent, meaningless and/or irrelevant content included in the article
- (6) Peer-review manipulation

The presence of these indicators undermines our confidence in the integrity of the article's content and we cannot, therefore, vouch for its reliability. Please note that this notice is intended solely to alert readers that the content of this article is unreliable. We have not investigated whether authors were aware of or involved in the systematic manipulation of the publication process.

Wiley and Hindawi regrets that the usual quality checks did not identify these issues before publication and have since put additional measures in place to safeguard research integrity.

We wish to credit our own Research Integrity and Research Publishing teams and anonymous and named external researchers and research integrity experts for contributing to this investigation.

The corresponding author, as the representative of all authors, has been given the opportunity to register their agreement or disagreement to this retraction. We have kept a record of any response received.

References

- [1] B. Feng, W. Li, and L. Wang, "Signal Optimization of Electronic Communication Network Based on Internet of Things," *Journal of Sensors*, vol. 2022, Article ID 3711776, 8 pages, 2022.

Retraction

Retracted: PKPM Architectural Engineering Software System Based on Architectural BIM Technology

Journal of Sensors

Received 17 October 2023; Accepted 17 October 2023; Published 18 October 2023

Copyright © 2023 Journal of Sensors. This is an open access article distributed under the Creative Commons Attribution License, which permits unrestricted use, distribution, and reproduction in any medium, provided the original work is properly cited.

This article has been retracted by Hindawi following an investigation undertaken by the publisher [1]. This investigation has uncovered evidence of one or more of the following indicators of systematic manipulation of the publication process:

- (1) Discrepancies in scope
- (2) Discrepancies in the description of the research reported
- (3) Discrepancies between the availability of data and the research described
- (4) Inappropriate citations
- (5) Incoherent, meaningless and/or irrelevant content included in the article
- (6) Peer-review manipulation

The presence of these indicators undermines our confidence in the integrity of the article's content and we cannot, therefore, vouch for its reliability. Please note that this notice is intended solely to alert readers that the content of this article is unreliable. We have not investigated whether authors were aware of or involved in the systematic manipulation of the publication process.

Wiley and Hindawi regrets that the usual quality checks did not identify these issues before publication and have since put additional measures in place to safeguard research integrity.

We wish to credit our own Research Integrity and Research Publishing teams and anonymous and named external researchers and research integrity experts for contributing to this investigation.

The corresponding author, as the representative of all authors, has been given the opportunity to register their agreement or disagreement to this retraction. We have kept a record of any response received.

References

- [1] Y. Fu, "PKPM Architectural Engineering Software System Based on Architectural BIM Technology," *Journal of Sensors*, vol. 2022, Article ID 5382026, 7 pages, 2022.

Retraction

Retracted: Analysis of People Flow Image Detection System Based on Computer Vision Sensor

Journal of Sensors

Received 17 October 2023; Accepted 17 October 2023; Published 18 October 2023

Copyright © 2023 Journal of Sensors. This is an open access article distributed under the Creative Commons Attribution License, which permits unrestricted use, distribution, and reproduction in any medium, provided the original work is properly cited.

This article has been retracted by Hindawi following an investigation undertaken by the publisher [1]. This investigation has uncovered evidence of one or more of the following indicators of systematic manipulation of the publication process:

- (1) Discrepancies in scope
- (2) Discrepancies in the description of the research reported
- (3) Discrepancies between the availability of data and the research described
- (4) Inappropriate citations
- (5) Incoherent, meaningless and/or irrelevant content included in the article
- (6) Peer-review manipulation

The presence of these indicators undermines our confidence in the integrity of the article's content and we cannot, therefore, vouch for its reliability. Please note that this notice is intended solely to alert readers that the content of this article is unreliable. We have not investigated whether authors were aware of or involved in the systematic manipulation of the publication process.

Wiley and Hindawi regrets that the usual quality checks did not identify these issues before publication and have since put additional measures in place to safeguard research integrity.

We wish to credit our own Research Integrity and Research Publishing teams and anonymous and named external researchers and research integrity experts for contributing to this investigation.

The corresponding author, as the representative of all authors, has been given the opportunity to register their agreement or disagreement to this retraction. We have kept a record of any response received.

References

- [1] B. Ou, J. Yang, and W. Wang, "Analysis of People Flow Image Detection System Based on Computer Vision Sensor," *Journal of Sensors*, vol. 2022, Article ID 8099876, 7 pages, 2022.

Retraction

Retracted: Interactive Knowledge Visualization Based on IoT and Augmented Reality

Journal of Sensors

Received 17 October 2023; Accepted 17 October 2023; Published 18 October 2023

Copyright © 2023 Journal of Sensors. This is an open access article distributed under the Creative Commons Attribution License, which permits unrestricted use, distribution, and reproduction in any medium, provided the original work is properly cited.

This article has been retracted by Hindawi following an investigation undertaken by the publisher [1]. This investigation has uncovered evidence of one or more of the following indicators of systematic manipulation of the publication process:

- (1) Discrepancies in scope
- (2) Discrepancies in the description of the research reported
- (3) Discrepancies between the availability of data and the research described
- (4) Inappropriate citations
- (5) Incoherent, meaningless and/or irrelevant content included in the article
- (6) Peer-review manipulation

The presence of these indicators undermines our confidence in the integrity of the article's content and we cannot, therefore, vouch for its reliability. Please note that this notice is intended solely to alert readers that the content of this article is unreliable. We have not investigated whether authors were aware of or involved in the systematic manipulation of the publication process.

Wiley and Hindawi regrets that the usual quality checks did not identify these issues before publication and have since put additional measures in place to safeguard research integrity.

We wish to credit our own Research Integrity and Research Publishing teams and anonymous and named external researchers and research integrity experts for contributing to this investigation.

The corresponding author, as the representative of all authors, has been given the opportunity to register their agreement or disagreement to this retraction. We have kept a record of any response received.

References

- [1] H. Sun, "Interactive Knowledge Visualization Based on IoT and Augmented Reality," *Journal of Sensors*, vol. 2022, Article ID 7921550, 8 pages, 2022.

Retraction

Retracted: Application of Industrial Big Data Cloud Control Platform Based on Fusion Transmission Sensor

Journal of Sensors

Received 17 October 2023; Accepted 17 October 2023; Published 18 October 2023

Copyright © 2023 Journal of Sensors. This is an open access article distributed under the Creative Commons Attribution License, which permits unrestricted use, distribution, and reproduction in any medium, provided the original work is properly cited.

This article has been retracted by Hindawi following an investigation undertaken by the publisher [1]. This investigation has uncovered evidence of one or more of the following indicators of systematic manipulation of the publication process:

- (1) Discrepancies in scope
- (2) Discrepancies in the description of the research reported
- (3) Discrepancies between the availability of data and the research described
- (4) Inappropriate citations
- (5) Incoherent, meaningless and/or irrelevant content included in the article
- (6) Peer-review manipulation

The presence of these indicators undermines our confidence in the integrity of the article's content and we cannot, therefore, vouch for its reliability. Please note that this notice is intended solely to alert readers that the content of this article is unreliable. We have not investigated whether authors were aware of or involved in the systematic manipulation of the publication process.

Wiley and Hindawi regrets that the usual quality checks did not identify these issues before publication and have since put additional measures in place to safeguard research integrity.

We wish to credit our own Research Integrity and Research Publishing teams and anonymous and named external researchers and research integrity experts for contributing to this investigation.

The corresponding author, as the representative of all authors, has been given the opportunity to register their agreement or disagreement to this retraction. We have kept a record of any response received.

References

- [1] W. Meng and W. Shao, "Application of Industrial Big Data Cloud Control Platform Based on Fusion Transmission Sensor," *Journal of Sensors*, vol. 2022, Article ID 6955028, 8 pages, 2022.

Retraction

Retracted: Optical Hybrid Network Structure Based on Cloud Computing and Big Data Technology

Journal of Sensors

Received 17 October 2023; Accepted 17 October 2023; Published 18 October 2023

Copyright © 2023 Journal of Sensors. This is an open access article distributed under the Creative Commons Attribution License, which permits unrestricted use, distribution, and reproduction in any medium, provided the original work is properly cited.

This article has been retracted by Hindawi following an investigation undertaken by the publisher [1]. This investigation has uncovered evidence of one or more of the following indicators of systematic manipulation of the publication process:

- (1) Discrepancies in scope
- (2) Discrepancies in the description of the research reported
- (3) Discrepancies between the availability of data and the research described
- (4) Inappropriate citations
- (5) Incoherent, meaningless and/or irrelevant content included in the article
- (6) Peer-review manipulation

The presence of these indicators undermines our confidence in the integrity of the article's content and we cannot, therefore, vouch for its reliability. Please note that this notice is intended solely to alert readers that the content of this article is unreliable. We have not investigated whether authors were aware of or involved in the systematic manipulation of the publication process.

Wiley and Hindawi regrets that the usual quality checks did not identify these issues before publication and have since put additional measures in place to safeguard research integrity.

We wish to credit our own Research Integrity and Research Publishing teams and anonymous and named external researchers and research integrity experts for contributing to this investigation.

The corresponding author, as the representative of all authors, has been given the opportunity to register their agreement or disagreement to this retraction. We have kept a record of any response received.

References

- [1] H. Wei, "Optical Hybrid Network Structure Based on Cloud Computing and Big Data Technology," *Journal of Sensors*, vol. 2022, Article ID 3936876, 6 pages, 2022.

Retraction

Retracted: Digital Library Information Integration System Based on Big Data and Deep Learning

Journal of Sensors

Received 17 October 2023; Accepted 17 October 2023; Published 18 October 2023

Copyright © 2023 Journal of Sensors. This is an open access article distributed under the Creative Commons Attribution License, which permits unrestricted use, distribution, and reproduction in any medium, provided the original work is properly cited.

This article has been retracted by Hindawi following an investigation undertaken by the publisher [1]. This investigation has uncovered evidence of one or more of the following indicators of systematic manipulation of the publication process:

- (1) Discrepancies in scope
- (2) Discrepancies in the description of the research reported
- (3) Discrepancies between the availability of data and the research described
- (4) Inappropriate citations
- (5) Incoherent, meaningless and/or irrelevant content included in the article
- (6) Peer-review manipulation

The presence of these indicators undermines our confidence in the integrity of the article's content and we cannot, therefore, vouch for its reliability. Please note that this notice is intended solely to alert readers that the content of this article is unreliable. We have not investigated whether authors were aware of or involved in the systematic manipulation of the publication process.

Wiley and Hindawi regrets that the usual quality checks did not identify these issues before publication and have since put additional measures in place to safeguard research integrity.

We wish to credit our own Research Integrity and Research Publishing teams and anonymous and named external researchers and research integrity experts for contributing to this investigation.

The corresponding author, as the representative of all authors, has been given the opportunity to register their agreement or disagreement to this retraction. We have kept a record of any response received.

References

- [1] X. Lin, Y. Zhang, and J. Wang, "Digital Library Information Integration System Based on Big Data and Deep Learning," *Journal of Sensors*, vol. 2022, Article ID 9953787, 8 pages, 2022.

Retraction

Retracted: The Study of Virtual Reality Sensing Technology in the Form Design and Perception of Public Buildings

Journal of Sensors

Received 17 October 2023; Accepted 17 October 2023; Published 18 October 2023

Copyright © 2023 Journal of Sensors. This is an open access article distributed under the Creative Commons Attribution License, which permits unrestricted use, distribution, and reproduction in any medium, provided the original work is properly cited.

This article has been retracted by Hindawi following an investigation undertaken by the publisher [1]. This investigation has uncovered evidence of one or more of the following indicators of systematic manipulation of the publication process:

- (1) Discrepancies in scope
- (2) Discrepancies in the description of the research reported
- (3) Discrepancies between the availability of data and the research described
- (4) Inappropriate citations
- (5) Incoherent, meaningless and/or irrelevant content included in the article
- (6) Peer-review manipulation

The presence of these indicators undermines our confidence in the integrity of the article's content and we cannot, therefore, vouch for its reliability. Please note that this notice is intended solely to alert readers that the content of this article is unreliable. We have not investigated whether authors were aware of or involved in the systematic manipulation of the publication process.

Wiley and Hindawi regrets that the usual quality checks did not identify these issues before publication and have since put additional measures in place to safeguard research integrity.

We wish to credit our own Research Integrity and Research Publishing teams and anonymous and named external researchers and research integrity experts for contributing to this investigation.

The corresponding author, as the representative of all authors, has been given the opportunity to register their agreement or disagreement to this retraction. We have kept a record of any response received.

References

- [1] L. Li and X. Zheng, "The Study of Virtual Reality Sensing Technology in the Form Design and Perception of Public Buildings," *Journal of Sensors*, vol. 2022, Article ID 7903386, 9 pages, 2022.

Retraction

Retracted: Data Transmission and Processing Analysis of Power Economic Management Terminal Based on the Internet of Things

Journal of Sensors

Received 17 October 2023; Accepted 17 October 2023; Published 18 October 2023

Copyright © 2023 Journal of Sensors. This is an open access article distributed under the Creative Commons Attribution License, which permits unrestricted use, distribution, and reproduction in any medium, provided the original work is properly cited.

This article has been retracted by Hindawi following an investigation undertaken by the publisher [1]. This investigation has uncovered evidence of one or more of the following indicators of systematic manipulation of the publication process:

- (1) Discrepancies in scope
- (2) Discrepancies in the description of the research reported
- (3) Discrepancies between the availability of data and the research described
- (4) Inappropriate citations
- (5) Incoherent, meaningless and/or irrelevant content included in the article
- (6) Peer-review manipulation

The presence of these indicators undermines our confidence in the integrity of the article's content and we cannot, therefore, vouch for its reliability. Please note that this notice is intended solely to alert readers that the content of this article is unreliable. We have not investigated whether authors were aware of or involved in the systematic manipulation of the publication process.

Wiley and Hindawi regrets that the usual quality checks did not identify these issues before publication and have since put additional measures in place to safeguard research integrity.

We wish to credit our own Research Integrity and Research Publishing teams and anonymous and named external researchers and research integrity experts for contributing to this investigation.

The corresponding author, as the representative of all authors, has been given the opportunity to register their agreement or disagreement to this retraction. We have kept a record of any response received.

References

- [1] H. Tang, "Data Transmission and Processing Analysis of Power Economic Management Terminal Based on the Internet of Things," *Journal of Sensors*, vol. 2022, Article ID 2649993, 8 pages, 2022.

Retraction

Retracted: Active Vibration Control of Robot Gear System Based on Adaptive Control Algorithm

Journal of Sensors

Received 17 October 2023; Accepted 17 October 2023; Published 18 October 2023

Copyright © 2023 Journal of Sensors. This is an open access article distributed under the Creative Commons Attribution License, which permits unrestricted use, distribution, and reproduction in any medium, provided the original work is properly cited.

This article has been retracted by Hindawi following an investigation undertaken by the publisher [1]. This investigation has uncovered evidence of one or more of the following indicators of systematic manipulation of the publication process:

- (1) Discrepancies in scope
- (2) Discrepancies in the description of the research reported
- (3) Discrepancies between the availability of data and the research described
- (4) Inappropriate citations
- (5) Incoherent, meaningless and/or irrelevant content included in the article
- (6) Peer-review manipulation

The presence of these indicators undermines our confidence in the integrity of the article's content and we cannot, therefore, vouch for its reliability. Please note that this notice is intended solely to alert readers that the content of this article is unreliable. We have not investigated whether authors were aware of or involved in the systematic manipulation of the publication process.

Wiley and Hindawi regrets that the usual quality checks did not identify these issues before publication and have since put additional measures in place to safeguard research integrity.

We wish to credit our own Research Integrity and Research Publishing teams and anonymous and named external researchers and research integrity experts for contributing to this investigation.

The corresponding author, as the representative of all authors, has been given the opportunity to register their agreement or disagreement to this retraction. We have kept a record of any response received.

References

- [1] D. Zhang and C. Guan, "Active Vibration Control of Robot Gear System Based on Adaptive Control Algorithm," *Journal of Sensors*, vol. 2022, Article ID 4481296, 8 pages, 2022.

Retraction

Retracted: Information Extraction and Data Planning of Smart City Based on Internet of Things

Journal of Sensors

Received 17 October 2023; Accepted 17 October 2023; Published 18 October 2023

Copyright © 2023 Journal of Sensors. This is an open access article distributed under the Creative Commons Attribution License, which permits unrestricted use, distribution, and reproduction in any medium, provided the original work is properly cited.

This article has been retracted by Hindawi following an investigation undertaken by the publisher [1]. This investigation has uncovered evidence of one or more of the following indicators of systematic manipulation of the publication process:

- (1) Discrepancies in scope
- (2) Discrepancies in the description of the research reported
- (3) Discrepancies between the availability of data and the research described
- (4) Inappropriate citations
- (5) Incoherent, meaningless and/or irrelevant content included in the article
- (6) Peer-review manipulation

The presence of these indicators undermines our confidence in the integrity of the article's content and we cannot, therefore, vouch for its reliability. Please note that this notice is intended solely to alert readers that the content of this article is unreliable. We have not investigated whether authors were aware of or involved in the systematic manipulation of the publication process.

Wiley and Hindawi regrets that the usual quality checks did not identify these issues before publication and have since put additional measures in place to safeguard research integrity.

We wish to credit our own Research Integrity and Research Publishing teams and anonymous and named external researchers and research integrity experts for contributing to this investigation.

The corresponding author, as the representative of all authors, has been given the opportunity to register their agreement or disagreement to this retraction. We have kept a record of any response received.

References

- [1] Z. Farisi, "Information Extraction and Data Planning of Smart City Based on Internet of Things," *Journal of Sensors*, vol. 2022, Article ID 2893702, 8 pages, 2022.

Retraction

Retracted: Intelligent Evaluation Method of Engineering Cost Feasibility Model Based on Internet of Things

Journal of Sensors

Received 17 October 2023; Accepted 17 October 2023; Published 18 October 2023

Copyright © 2023 Journal of Sensors. This is an open access article distributed under the Creative Commons Attribution License, which permits unrestricted use, distribution, and reproduction in any medium, provided the original work is properly cited.

This article has been retracted by Hindawi following an investigation undertaken by the publisher [1]. This investigation has uncovered evidence of one or more of the following indicators of systematic manipulation of the publication process:

- (1) Discrepancies in scope
- (2) Discrepancies in the description of the research reported
- (3) Discrepancies between the availability of data and the research described
- (4) Inappropriate citations
- (5) Incoherent, meaningless and/or irrelevant content included in the article
- (6) Peer-review manipulation

The presence of these indicators undermines our confidence in the integrity of the article's content and we cannot, therefore, vouch for its reliability. Please note that this notice is intended solely to alert readers that the content of this article is unreliable. We have not investigated whether authors were aware of or involved in the systematic manipulation of the publication process.

Wiley and Hindawi regrets that the usual quality checks did not identify these issues before publication and have since put additional measures in place to safeguard research integrity.

We wish to credit our own Research Integrity and Research Publishing teams and anonymous and named external researchers and research integrity experts for contributing to this investigation.

The corresponding author, as the representative of all authors, has been given the opportunity to register their agreement or disagreement to this retraction. We have kept a record of any response received.

References

- [1] L. Chen, H. Zhang, and F. Wang, "Intelligent Evaluation Method of Engineering Cost Feasibility Model Based on Internet of Things," *Journal of Sensors*, vol. 2022, Article ID 3420723, 8 pages, 2022.

Retraction

Retracted: Life Prediction of Dry Reactor Sensor Based on Deep Neural Network

Journal of Sensors

Received 17 October 2023; Accepted 17 October 2023; Published 18 October 2023

Copyright © 2023 Journal of Sensors. This is an open access article distributed under the Creative Commons Attribution License, which permits unrestricted use, distribution, and reproduction in any medium, provided the original work is properly cited.

This article has been retracted by Hindawi following an investigation undertaken by the publisher [1]. This investigation has uncovered evidence of one or more of the following indicators of systematic manipulation of the publication process:

- (1) Discrepancies in scope
- (2) Discrepancies in the description of the research reported
- (3) Discrepancies between the availability of data and the research described
- (4) Inappropriate citations
- (5) Incoherent, meaningless and/or irrelevant content included in the article
- (6) Peer-review manipulation

The presence of these indicators undermines our confidence in the integrity of the article's content and we cannot, therefore, vouch for its reliability. Please note that this notice is intended solely to alert readers that the content of this article is unreliable. We have not investigated whether authors were aware of or involved in the systematic manipulation of the publication process.

Wiley and Hindawi regrets that the usual quality checks did not identify these issues before publication and have since put additional measures in place to safeguard research integrity.

We wish to credit our own Research Integrity and Research Publishing teams and anonymous and named external researchers and research integrity experts for contributing to this investigation.

The corresponding author, as the representative of all authors, has been given the opportunity to register their agreement or disagreement to this retraction. We have kept a record of any response received.

References

- [1] H. Guo, J. Meng, Y. Yang, L. Zheng, X. Liu, and M. Tan, "Life Prediction of Dry Reactor Sensor Based on Deep Neural Network," *Journal of Sensors*, vol. 2022, Article ID 6982950, 7 pages, 2022.

Retraction

Retracted: Test of Ultimate Bearing Capacity of Building Concrete Structures in Earthquake Area Based on Virtual Reality

Journal of Sensors

Received 17 October 2023; Accepted 17 October 2023; Published 18 October 2023

Copyright © 2023 Journal of Sensors. This is an open access article distributed under the Creative Commons Attribution License, which permits unrestricted use, distribution, and reproduction in any medium, provided the original work is properly cited.

This article has been retracted by Hindawi following an investigation undertaken by the publisher [1]. This investigation has uncovered evidence of one or more of the following indicators of systematic manipulation of the publication process:

- (1) Discrepancies in scope
- (2) Discrepancies in the description of the research reported
- (3) Discrepancies between the availability of data and the research described
- (4) Inappropriate citations
- (5) Incoherent, meaningless and/or irrelevant content included in the article
- (6) Peer-review manipulation

The presence of these indicators undermines our confidence in the integrity of the article's content and we cannot, therefore, vouch for its reliability. Please note that this notice is intended solely to alert readers that the content of this article is unreliable. We have not investigated whether authors were aware of or involved in the systematic manipulation of the publication process.

Wiley and Hindawi regrets that the usual quality checks did not identify these issues before publication and have since put additional measures in place to safeguard research integrity.

We wish to credit our own Research Integrity and Research Publishing teams and anonymous and named external researchers and research integrity experts for contributing to this investigation.

The corresponding author, as the representative of all authors, has been given the opportunity to register their agreement or disagreement to this retraction. We have kept a record of any response received.

References

- [1] H. Liu, X. Yang, and L. Dou, "Test of Ultimate Bearing Capacity of Building Concrete Structures in Earthquake Area Based on Virtual Reality," *Journal of Sensors*, vol. 2022, Article ID 6049308, 7 pages, 2022.

Retraction

Retracted: Online English Teaching System Based on Internet of Things Technology

Journal of Sensors

Received 17 October 2023; Accepted 17 October 2023; Published 18 October 2023

Copyright © 2023 Journal of Sensors. This is an open access article distributed under the Creative Commons Attribution License, which permits unrestricted use, distribution, and reproduction in any medium, provided the original work is properly cited.

This article has been retracted by Hindawi following an investigation undertaken by the publisher [1]. This investigation has uncovered evidence of one or more of the following indicators of systematic manipulation of the publication process:

- (1) Discrepancies in scope
- (2) Discrepancies in the description of the research reported
- (3) Discrepancies between the availability of data and the research described
- (4) Inappropriate citations
- (5) Incoherent, meaningless and/or irrelevant content included in the article
- (6) Peer-review manipulation

The presence of these indicators undermines our confidence in the integrity of the article's content and we cannot, therefore, vouch for its reliability. Please note that this notice is intended solely to alert readers that the content of this article is unreliable. We have not investigated whether authors were aware of or involved in the systematic manipulation of the publication process.

Wiley and Hindawi regrets that the usual quality checks did not identify these issues before publication and have since put additional measures in place to safeguard research integrity.

We wish to credit our own Research Integrity and Research Publishing teams and anonymous and named external researchers and research integrity experts for contributing to this investigation.

The corresponding author, as the representative of all authors, has been given the opportunity to register their agreement or disagreement to this retraction. We have kept a record of any response received.

References

- [1] H. Tao, "Online English Teaching System Based on Internet of Things Technology," *Journal of Sensors*, vol. 2022, Article ID 7748067, 8 pages, 2022.

Retraction

Retracted: Optimization of Distribution Automation System Based on Artificial Intelligence Wireless Network Technology

Journal of Sensors

Received 13 September 2023; Accepted 13 September 2023; Published 14 September 2023

Copyright © 2023 Journal of Sensors. This is an open access article distributed under the Creative Commons Attribution License, which permits unrestricted use, distribution, and reproduction in any medium, provided the original work is properly cited.

This article has been retracted by Hindawi following an investigation undertaken by the publisher [1]. This investigation has uncovered evidence of one or more of the following indicators of systematic manipulation of the publication process:

- (1) Discrepancies in scope
- (2) Discrepancies in the description of the research reported
- (3) Discrepancies between the availability of data and the research described
- (4) Inappropriate citations
- (5) Incoherent, meaningless and/or irrelevant content included in the article
- (6) Peer-review manipulation

The presence of these indicators undermines our confidence in the integrity of the article's content and we cannot, therefore, vouch for its reliability. Please note that this notice is intended solely to alert readers that the content of this article is unreliable. We have not investigated whether authors were aware of or involved in the systematic manipulation of the publication process.

Wiley and Hindawi regrets that the usual quality checks did not identify these issues before publication and have since put additional measures in place to safeguard research integrity.

We wish to credit our own Research Integrity and Research Publishing teams and anonymous and named external researchers and research integrity experts for contributing to this investigation.

The corresponding author, as the representative of all authors, has been given the opportunity to register their agreement or disagreement to this retraction. We have kept a record of any response received.

References

- [1] W. Tian, X. Meng, J. Wang, and H. Yan, "Optimization of Distribution Automation System Based on Artificial Intelligence Wireless Network Technology," *Journal of Sensors*, vol. 2022, Article ID 1646667, 8 pages, 2022.

Retraction

Retracted: Fractal Art Pattern Information System Based on Genetic Algorithm

Journal of Sensors

Received 13 September 2023; Accepted 13 September 2023; Published 14 September 2023

Copyright © 2023 Journal of Sensors. This is an open access article distributed under the Creative Commons Attribution License, which permits unrestricted use, distribution, and reproduction in any medium, provided the original work is properly cited.

This article has been retracted by Hindawi following an investigation undertaken by the publisher [1]. This investigation has uncovered evidence of one or more of the following indicators of systematic manipulation of the publication process:

- (1) Discrepancies in scope
- (2) Discrepancies in the description of the research reported
- (3) Discrepancies between the availability of data and the research described
- (4) Inappropriate citations
- (5) Incoherent, meaningless and/or irrelevant content included in the article
- (6) Peer-review manipulation

The presence of these indicators undermines our confidence in the integrity of the article's content and we cannot, therefore, vouch for its reliability. Please note that this notice is intended solely to alert readers that the content of this article is unreliable. We have not investigated whether authors were aware of or involved in the systematic manipulation of the publication process.

Wiley and Hindawi regrets that the usual quality checks did not identify these issues before publication and have since put additional measures in place to safeguard research integrity.

We wish to credit our own Research Integrity and Research Publishing teams and anonymous and named external researchers and research integrity experts for contributing to this investigation.

The corresponding author, as the representative of all authors, has been given the opportunity to register their agreement or disagreement to this retraction. We have kept a record of any response received.

References

- [1] M. Chen, "Fractal Art Pattern Information System Based on Genetic Algorithm," *Journal of Sensors*, vol. 2022, Article ID 9350301, 8 pages, 2022.

Retraction

Retracted: Abnormal Data Monitoring and Analysis Based on Data Mining and Neural Network

Journal of Sensors

Received 13 September 2023; Accepted 13 September 2023; Published 14 September 2023

Copyright © 2023 Journal of Sensors. This is an open access article distributed under the Creative Commons Attribution License, which permits unrestricted use, distribution, and reproduction in any medium, provided the original work is properly cited.

This article has been retracted by Hindawi following an investigation undertaken by the publisher [1]. This investigation has uncovered evidence of one or more of the following indicators of systematic manipulation of the publication process:

- (1) Discrepancies in scope
- (2) Discrepancies in the description of the research reported
- (3) Discrepancies between the availability of data and the research described
- (4) Inappropriate citations
- (5) Incoherent, meaningless and/or irrelevant content included in the article
- (6) Peer-review manipulation

The presence of these indicators undermines our confidence in the integrity of the article's content and we cannot, therefore, vouch for its reliability. Please note that this notice is intended solely to alert readers that the content of this article is unreliable. We have not investigated whether authors were aware of or involved in the systematic manipulation of the publication process.

Wiley and Hindawi regrets that the usual quality checks did not identify these issues before publication and have since put additional measures in place to safeguard research integrity.

We wish to credit our own Research Integrity and Research Publishing teams and anonymous and named external researchers and research integrity experts for contributing to this investigation.

The corresponding author, as the representative of all authors, has been given the opportunity to register their agreement or disagreement to this retraction. We have kept a record of any response received.

References

- [1] Y. Chen, "Abnormal Data Monitoring and Analysis Based on Data Mining and Neural Network," *Journal of Sensors*, vol. 2022, Article ID 2635819, 7 pages, 2022.

Retraction

Retracted: Spatial and Temporal Evolution of Urban Green Space Pattern Based on GIS Sensors and Remote Sensing Information: Taking Xi'an as an Example

Journal of Sensors

Received 13 September 2023; Accepted 13 September 2023; Published 14 September 2023

Copyright © 2023 Journal of Sensors. This is an open access article distributed under the Creative Commons Attribution License, which permits unrestricted use, distribution, and reproduction in any medium, provided the original work is properly cited.

This article has been retracted by Hindawi following an investigation undertaken by the publisher [1]. This investigation has uncovered evidence of one or more of the following indicators of systematic manipulation of the publication process:

- (1) Discrepancies in scope
- (2) Discrepancies in the description of the research reported
- (3) Discrepancies between the availability of data and the research described
- (4) Inappropriate citations
- (5) Incoherent, meaningless and/or irrelevant content included in the article
- (6) Peer-review manipulation

The presence of these indicators undermines our confidence in the integrity of the article's content and we cannot, therefore, vouch for its reliability. Please note that this notice is intended solely to alert readers that the content of this article is unreliable. We have not investigated whether authors were aware of or involved in the systematic manipulation of the publication process.

Wiley and Hindawi regrets that the usual quality checks did not identify these issues before publication and have since put additional measures in place to safeguard research integrity.

We wish to credit our own Research Integrity and Research Publishing teams and anonymous and named external researchers and research integrity experts for contributing to this investigation.

The corresponding author, as the representative of all authors, has been given the opportunity to register their agreement or disagreement to this retraction. We have kept a record of any response received.

References

- [1] W. Li, H. Wang, S. Zhang, B. Jiang, and S. Lee, "Spatial and Temporal Evolution of Urban Green Space Pattern Based on GIS Sensors and Remote Sensing Information: Taking Xi'an as an Example," *Journal of Sensors*, vol. 2022, Article ID 3648880, 8 pages, 2022.

Retraction

Retracted: Research on Data Mining Algorithm of Associated User Network Based on Multi-Information Fusion

Journal of Sensors

Received 13 September 2023; Accepted 13 September 2023; Published 14 September 2023

Copyright © 2023 Journal of Sensors. This is an open access article distributed under the Creative Commons Attribution License, which permits unrestricted use, distribution, and reproduction in any medium, provided the original work is properly cited.

This article has been retracted by Hindawi following an investigation undertaken by the publisher [1]. This investigation has uncovered evidence of one or more of the following indicators of systematic manipulation of the publication process:

- (1) Discrepancies in scope
- (2) Discrepancies in the description of the research reported
- (3) Discrepancies between the availability of data and the research described
- (4) Inappropriate citations
- (5) Incoherent, meaningless and/or irrelevant content included in the article
- (6) Peer-review manipulation

The presence of these indicators undermines our confidence in the integrity of the article's content and we cannot, therefore, vouch for its reliability. Please note that this notice is intended solely to alert readers that the content of this article is unreliable. We have not investigated whether authors were aware of or involved in the systematic manipulation of the publication process.

Wiley and Hindawi regrets that the usual quality checks did not identify these issues before publication and have since put additional measures in place to safeguard research integrity.

We wish to credit our own Research Integrity and Research Publishing teams and anonymous and named external researchers and research integrity experts for contributing to this investigation.

The corresponding author, as the representative of all authors, has been given the opportunity to register their agreement or disagreement to this retraction. We have kept a record of any response received.

References

- [1] X. Kang and C. Hua, "Research on Data Mining Algorithm of Associated User Network Based on Multi-Information Fusion," *Journal of Sensors*, vol. 2022, Article ID 2417826, 8 pages, 2022.

Retraction

Retracted: A Monitoring System for Air Quality and Soil Environment in Mining Areas Based on the Internet of Things

Journal of Sensors

Received 13 September 2023; Accepted 13 September 2023; Published 14 September 2023

Copyright © 2023 Journal of Sensors. This is an open access article distributed under the Creative Commons Attribution License, which permits unrestricted use, distribution, and reproduction in any medium, provided the original work is properly cited.

This article has been retracted by Hindawi following an investigation undertaken by the publisher [1]. This investigation has uncovered evidence of one or more of the following indicators of systematic manipulation of the publication process:

- (1) Discrepancies in scope
- (2) Discrepancies in the description of the research reported
- (3) Discrepancies between the availability of data and the research described
- (4) Inappropriate citations
- (5) Incoherent, meaningless and/or irrelevant content included in the article
- (6) Peer-review manipulation

The presence of these indicators undermines our confidence in the integrity of the article's content and we cannot, therefore, vouch for its reliability. Please note that this notice is intended solely to alert readers that the content of this article is unreliable. We have not investigated whether authors were aware of or involved in the systematic manipulation of the publication process.

Wiley and Hindawi regrets that the usual quality checks did not identify these issues before publication and have since put additional measures in place to safeguard research integrity.

We wish to credit our own Research Integrity and Research Publishing teams and anonymous and named external researchers and research integrity experts for contributing to this investigation.

The corresponding author, as the representative of all authors, has been given the opportunity to register their agreement or disagreement to this retraction. We have kept a record of any response received.

References

- [1] H. Dai, D. Huang, and H. Mao, "A Monitoring System for Air Quality and Soil Environment in Mining Areas Based on the Internet of Things," *Journal of Sensors*, vol. 2022, Article ID 5419167, 7 pages, 2022.

Retraction

Retracted: Application of 3D Virtual Reality Sensor in Tourist Scenic Navigation System

Journal of Sensors

Received 22 August 2023; Accepted 22 August 2023; Published 23 August 2023

Copyright © 2023 Journal of Sensors. This is an open access article distributed under the Creative Commons Attribution License, which permits unrestricted use, distribution, and reproduction in any medium, provided the original work is properly cited.

This article has been retracted by Hindawi following an investigation undertaken by the publisher [1]. This investigation has uncovered evidence of one or more of the following indicators of systematic manipulation of the publication process:

- (1) Discrepancies in scope
- (2) Discrepancies in the description of the research reported
- (3) Discrepancies between the availability of data and the research described
- (4) Inappropriate citations
- (5) Incoherent, meaningless and/or irrelevant content included in the article
- (6) Peer-review manipulation

The presence of these indicators undermines our confidence in the integrity of the article's content and we cannot, therefore, vouch for its reliability. Please note that this notice is intended solely to alert readers that the content of this article is unreliable. We have not investigated whether authors were aware of or involved in the systematic manipulation of the publication process.

Wiley and Hindawi regrets that the usual quality checks did not identify these issues before publication and have since put additional measures in place to safeguard research integrity.

We wish to credit our own Research Integrity and Research Publishing teams and anonymous and named external researchers and research integrity experts for contributing to this investigation.

The corresponding author, as the representative of all authors, has been given the opportunity to register their agreement or disagreement to this retraction. We have kept a record of any response received.

References

- [1] F. Deng, "Application of 3D Virtual Reality Sensor in Tourist Scenic Navigation System," *Journal of Sensors*, vol. 2022, Article ID 1112261, 7 pages, 2022.

Retraction

Retracted: A Wood Quality Defect Detection System Based on Deep Learning and Multicriterion Framework

Journal of Sensors

Received 22 August 2023; Accepted 22 August 2023; Published 23 August 2023

Copyright © 2023 Journal of Sensors. This is an open access article distributed under the Creative Commons Attribution License, which permits unrestricted use, distribution, and reproduction in any medium, provided the original work is properly cited.

This article has been retracted by Hindawi following an investigation undertaken by the publisher [1]. This investigation has uncovered evidence of one or more of the following indicators of systematic manipulation of the publication process:

- (1) Discrepancies in scope
- (2) Discrepancies in the description of the research reported
- (3) Discrepancies between the availability of data and the research described
- (4) Inappropriate citations
- (5) Incoherent, meaningless and/or irrelevant content included in the article
- (6) Peer-review manipulation

The presence of these indicators undermines our confidence in the integrity of the article's content and we cannot, therefore, vouch for its reliability. Please note that this notice is intended solely to alert readers that the content of this article is unreliable. We have not investigated whether authors were aware of or involved in the systematic manipulation of the publication process.

Wiley and Hindawi regrets that the usual quality checks did not identify these issues before publication and have since put additional measures in place to safeguard research integrity.

We wish to credit our own Research Integrity and Research Publishing teams and anonymous and named external researchers and research integrity experts for contributing to this investigation.

The corresponding author, as the representative of all authors, has been given the opportunity to register their agreement or disagreement to this retraction. We have kept a record of any response received.

References

- [1] P. Sun, "A Wood Quality Defect Detection System Based on Deep Learning and Multicriterion Framework," *Journal of Sensors*, vol. 2022, Article ID 3234148, 8 pages, 2022.

Retraction

Retracted: Deep Learning-Based Leaf Region Segmentation Using High-Resolution Super HAD CCD and ISOCELL GW1 Sensors

Journal of Sensors

Received 12 December 2023; Accepted 12 December 2023; Published 13 December 2023

Copyright © 2023 Journal of Sensors. This is an open access article distributed under the Creative Commons Attribution License, which permits unrestricted use, distribution, and reproduction in any medium, provided the original work is properly cited.

This article has been retracted by Hindawi, as publisher, following an investigation undertaken by the publisher [1]. This investigation has uncovered evidence of systematic manipulation of the publication and peer-review process. We cannot, therefore, vouch for the reliability or integrity of this article.

Please note that this notice is intended solely to alert readers that the peer-review process of this article has been compromised.

Wiley and Hindawi regret that the usual quality checks did not identify these issues before publication and have since put additional measures in place to safeguard research integrity.

We wish to credit our Research Integrity and Research Publishing teams and anonymous and named external researchers and research integrity experts for contributing to this investigation.

The corresponding author, as the representative of all authors, has been given the opportunity to register their agreement or disagreement to this retraction. We have kept a record of any response received.

References

- [1] S. Talasila, K. Rawal, and G. Sethi, "Deep Learning-Based Leaf Region Segmentation Using High-Resolution Super HAD CCD and ISOCELL GW1 Sensors," *Journal of Sensors*, vol. 2023, Article ID 1085735, 20 pages, 2023.

Research Article

Deep Learning-Based Leaf Region Segmentation Using High-Resolution Super HAD CCD and ISOCELL GW1 Sensors

Srinivas Talasila ^{1,2}, Kirti Rawal ¹ and Gaurav Sethi¹

¹School of Electronics and Electrical Engineering, Lovely Professional University, Phagwara, Punjab, India

²VNR Vignana Jyothi Institute of Engineering and Technology, Hyderabad, Telangana, India

Correspondence should be addressed to Srinivas Talasila; srinivas.41900454@lpu.in and Kirti Rawal; kirti.20248@lpu.co.in

Received 17 October 2022; Revised 14 December 2022; Accepted 5 April 2023; Published 4 July 2023

Academic Editor: C. Venkatesan

Copyright © 2023 Srinivas Talasila et al. This is an open access article distributed under the Creative Commons Attribution License, which permits unrestricted use, distribution, and reproduction in any medium, provided the original work is properly cited.

Super HAD CCD and ISOCELL GW1 imaging sensors are used for capturing images in high-resolution cameras nowadays. These high-resolution camera sensors were used in this work to acquire black gram plant leaf diseased images in natural cultivation fields. Segmenting plant leaf regions from the black gram cultivation field images is a preliminary step for disease identification and classification. It is also helpful for the farmers to assess the plants' health and identify the diseases in their early stages. Even though plant leaf region segmentation has been effectively handled in many contributions, no universally applicable solution exists to solve all issues. Therefore, an approach for extracting leaf region from black gram plant leaf images is presented in this article. The novelty of the proposed method is that MobileNetV2 has been utilized as a backbone network for DeepLabv3+ layers to segment plant leaf regions. The DeepLabv3+ with MobileNetV2 segmentation model exhibited superior performance compared to the other models (SegNet, U-Net, DeepLabv3+ with ResNet18, ResNet50, Xception, and InceptionResNetV2) in terms of accuracy of 99.71%, Dice of 98.72%, and Jaccard/IoU of 97.47% when data augmentation was applied. The algorithms were developed and trained using MATLAB software. Each of the experimental trials reported in this article surpasses the prior findings.

1. Introduction

Agriculture is one of the most effective tool to end extreme poverty, enhance economic prosperity, and feed 9.7 billion people, expected by 2050. It contributed 4% of the global GDP in 2018 and may account for more than 25% of GDP in certain developing nations, playing a crucial role in economic growth [1]. According to 2016 studies, agriculture provided a livelihood for 65% of impoverished working people. One of the leading global issues that humankind confronts nowadays in the agriculture sector is food insecurity, a significant source of plant diseases. In rural areas, experts have often detected and identified plant diseases through their naked eyes. However, to identify diseases in the early stages, specialists must always be present, which is time-consuming and expensive for the farmers. An automatic method would be effective for determining the measures taken to improve the quality and productivity of the plant/crop.

Most currently available professional RGB cameras capture high-resolution images using a CCD image sensor with a colour filter. There is a significant need for high-resolution image data in various research areas such as medical, military, and agriculture. CCD image sensors are widely used in digital cameras and are found in these areas for image acquisition. To capture high-quality images using their CCD image sensors, Sony introduced a technology called HAD CCD. Through the use of this technology, sensitivity has increased significantly compared to the previous versions. ISOCELL GW1 is a high-resolution 64 MP image sensor introduced by Samsung. This imaging sensor supports a real-time high dynamic range of up to 100 dB. GW1 sensor adopts DCG (dual conversion gain) to convert captured light into an electrical signal and super P.D. for quick autofocus. The devices that are utilized these two imaging sensors were used in this work for image acquisition. During the COVID-19 pandemic, A.I. was extensively used in

biomedical and agricultural image processing applications [2–4]. In artificial intelligence, convolutional neural networks (CNNs) proved their effectiveness in various computer vision applications. Semantic segmentation using deep, fully convolutional networks is one of the critical computer vision tasks that has been effectively used in multiple domains, including medicine, agriculture, and autonomous driving [5–7]. In this work, we aimed to employ semantic segmentation techniques to extract plant leaf regions from the black gram plant leaf images having complex backgrounds.

Black gram is a highly prized pulse crop grown in the Indian subcontinent. The essential amino acids in most grains are complemented by the black gram, making it a necessary part of the Indian diet. It offers many health benefits to humankind, including maintaining heart rate, decreasing inflammation, assisting in skin maintenance, increasing bone strength, boosting the nervous system, and improving the digestive system. The black gram crop can withstand adverse weather conditions and fixes atmospheric nitrogen in the soil, improving soil fertility. The black gram crop has recorded a whopping 22.10 kg of nitrogen per hectare, equating to an annual urea supplement of 59 thousand tonnes. The productivity of the black gram crop decreases because of the most common diseases such as leaf crinkle, yellow mosaic, powdery mildew, and anthracnose. Higher crop yield demands an accurate and prompt identification and classification of such diseases.

Segmenting plant leaf regions from the images is critical for disease identification and classification. Numerous authors made significant contributions to this area of study in the early stages of its development, introducing a slew of methods based on edges, regions, clustering, threshold, and watershed techniques [8–10], all of which are still in use today. But these methods have numerous limitations; they do not work correctly with too many edges, are sensitive to noise, and are expensive in terms of time, memory, and computations. Even though plant leaf region segmentation has been effectively handled in many contributions, no universally applicable solution exists to solve all issues. A comprehensive method for extracting leaf region from the plant leaf images is therefore presented in this article. The novelty of the proposed method is that MobileNetV2 has been utilized as a backbone network for DeepLabv3+ layers to segment plant leaf regions. Compared with the other adopted semantic segmentation networks, this combination is more effective in terms of time, computation, and size.

The significant contributions of this article are as follows:

- (i) Black gram Plant Leaf Disease (BPLD) dataset was collected with images taken from the cultivation fields using the devices having high-resolution super HAD CCD and ISOCELL GW1 imaging sensors
- (a) Data were collected using two different imaging sensor devices. The first device is the Sony Cyber-shot DSC-H300 camera which uses a super HAD CCD imaging sensor with a powerful 35x optical zoom and a resolution of 20.1

megapixels. The second device is a Samsung Galaxy F41 smartphone which uses an ISOCELL GW1 imaging sensor: 64 megapixels and an aperture of $f/1.89$. Nagayalanka, Andhra Pradesh, India, with latitude and longitude of 15.9455° N, 80.9180° E is the data source location. The original RGB images have different dimensions due to the usage of various devices, which were then reduced to 512×512 in the preprocessing stage using MATLAB Software [11]

- (ii) Ground truth labels were generated for all the images in the dataset with the help of an agricultural expert using the image segmenter tool in MATLAB
- (iii) SegNet, U-Net, and DeepLabv3+ semantic segmentation architectures were implemented to extract the leaf regions from the images with complicated backgrounds. While implementing DeepLabv3+ architecture, the weights were initialized using ResNet18, ResNet50, MobileNetV2, Xception, and InceptionResNetV2 models
- (iv) All the experiments were conducted with and without data augmentation techniques to know the strength of the limited available data

2. Related Works

Researchers conducted several studies in plant phenotyping over the past few years to address the issues like plant species identification, abnormality detection, leaf region segmentation, counting leaves, and disease severity estimation. Segmentation, feature extraction, and classification are essential in automated plant leaf disease detection computer vision algorithms. Segmentation is a crucial and necessary step in disease classification as it highly impacts the classification accuracy of the algorithms. Several approaches for extracting leaf regions from the background have been reported in the literature. These techniques succeeded well when the targeted leaf region has a homogeneous environment and suffers from varied experiences. Only a few authors developed segmentation algorithms on complex scenes reported in the literature. However, only a few successfully discriminate leaf regions and must improve further.

Minervini et al. [12] developed a technique that automatically segments and analyzes plant specimens from the Arabidopsis plant images acquired from laboratory circumstances. The method mainly relies on the combination of level-set and learning-based segmentation. The authors achieved a Dice similarity coefficient (DSC) of 96.7%, and the technique can segment images even in the unseen background. Öztürk and Akdemir [13] proposed an automatic segmentation method based on a grey wolf optimizer used to optimize neural networks and achieved 99.31% accuracy on plain background plant leaf images. Yin et al. [14] proposed a multileaf segmentation, alignment, and tracking system for fluorescence plant video of Arabidopsis thaliana. The authors evaluated their algorithm with the metrics

SAT accuracy (based on leaf counting (F), alignment (E), and tracking (T)) and SBD (symmetric best dice). The proposed framework was tested on the Leaf Segmentation Challenge (LSC) dataset and achieved an accuracy of 78% of SBD. Kumar and Domnic [15] proposed a three-step leaf region extraction and leave counting method in digital plant images. In this work, the authors adopted a graph-based approach for leaf region segmentation and Circular Hough Transform (CHT) for leave counting. Khan and Debnath [16] proposed a novel segmentation method to segment single or overlapping leaves by obtaining the contours of every individual leaf. The model achieved a 95.34% segmentation rate on single leaves and 86.73% on overlapping leaves. Jeyalakshmi and Radha [17] developed an enhanced GrabCut algorithm that does not require human intervention to extract leaf regions from the healthy and unhealthy plant leaf images.

Patil and Amarapur [18] proposed a novel leaf extraction technique based on modified factorization-based active contour (MFACM). Tomato leaf disease images with complicated backgrounds were utilized by Ngugi et al. [19] to propose KijaniNet that could effectively remove complex environments. Results make it clear that the suggested CNN model performs better than the current approaches, with mean weighted intersection over union of 0.9766 and an *F1* score of 0.9493, respectively. Yang et al. [20] proposed a 15-class species classification model that combines Mask R-CNN and VGG16 for segmentation and classification, respectively. The effectiveness of the segmentation model was measured using misclassification error (M.A.), and the proposed Mask R-CNN achieved a low MA of 1.15% against GrabCut and Otsu segmentation algorithms. Xiong et al. [21] developed the automatic image segmentation algorithm (AISA) using the GrabCut technique to design a crop disease classification model on the expanded PlantVillage dataset. The proposed segmentation model achieved a 95% correct rate against 87% with GrabCut. An instance segmentation method, ISC-MRCNN, was developed by Yang et al. [22] to address the complicated background issues that influence the classification performance of plant leaf images. Finally, the outcomes of ISC-MRCNN were given as input to the APS-DCCNN for classification. The suggested ISC-MRCNN increases the average precision by 1.89% against the state-of-the-art Mask R-CNN method. A U-Net-based semantic segmentation was employed by Trivedi and Gupta [23] on an LSC dataset to monitor a plant's growth.

Hou et al. [24] developed an automated graph cut algorithm to segment leaf regions from the potato leaf images gathered from the A.I. Challenger Global A.I. Contest (<http://www.challenger.ai>). In this work, the authors considered the Otsu thresholding method for segregating foreground pixels and colour statistical thresholding for segregating background pixels. The superpixel technique was used to differentiate if background pixels matched with the foreground leaf-infected patches. Jibrin et al. [25] developed a dynamic, iterative model for segmenting single leaves from the overlapping leaves, called DCV-SO based on CV-SO (Chan-Vese-Sobel Operator) model, which reduces the mean error rate by 1.23% against the original CV-SO model.

Triki et al. [26] developed a deep leaf to assess the morphological characteristics of the herbarium leaf. These characteristics include length, width, area, perimeter, and petiole length. In this work, the authors used segmentation as the preliminary step to extract leaf regions from the images using Mask R-CNN.

Similarly, numerous approaches have been developed for leaf segmentation [8–10, 27]. However, most of these approaches were employed to segment leaf regions on a simple/plain background or images containing leaf regions at their centre. But in real-life applications, a leaf may appear anywhere in the picture. Segmentation of leaf regions from real-world images is challenging, as these images may have stems, occluded leaves, human parts, and nonleaf objects. Thus, prior findings may not sufficiently segment the leaf region from the complex environment and other overlapping leaf images. Hence, developing new models for segmenting leaf regions from real-time field images is necessary to overcome the limitation of poor segmentation accuracy and similarity index (Dice) of leaf region segmentation algorithms presented in the literature. In this article, we propose using semantic segmentation networks based on deep convolutional neural networks such as SegNet, U-Net, and DeepLabv3+. To create the DeepLabv3+ network, we used ResNet18, ResNet50, MobileNetV2, Xception, and InceptionResNetV2 as base networks.

3. Materials and Methods

The designed approach's primary goal is to automatically segment plant leaf regions from images with complex backgrounds. Figure 1 is a flowchart representation of the proposed method. Various imaging sensor devices are initially utilized to collect the diseased plant leaf images directly from the fields. After image acquisition, preprocessing techniques are applied to enhance the image's quality. Later, divide the dataset into a training set and testing set, where a few data augmentation techniques are used to the training set to avoid overfitting. At the same time, training with the deep network extracted the leaf regions from the images and evaluated the performance of the adopted networks.

3.1. Image Dataset. Nagayalanka, Andhra Pradesh, India, is the data source location where the images were acquired from the black gram fields using two different imaging sensor devices. The first device is the Sony Cyber-shot DSC-H300 camera having a super HAD CCD imaging sensor with a powerful 35x optical zoom and a resolution of 20.1 megapixels. The second device is a Samsung Galaxy F41 smartphone with having ISOCELL GW1 imaging sensor with 64 megapixels and an aperture of *f*/1.89. Because of utilizing different devices, the original RGB images in the dataset had varying dimensions, which were resized to 512 × 512 using MATLAB software during the preprocessing stage [28]. The BPLD dataset consists of 1000 images of four diseased and healthy categories. The dataset is freely available at [doi:10.17632/zfcv9fmrqv.3](https://doi.org/10.17632/zfcv9fmrqv.3). The aim of creating this BPLD dataset is to develop an effective and automated black gram plant leaf disease detection and classification system to help

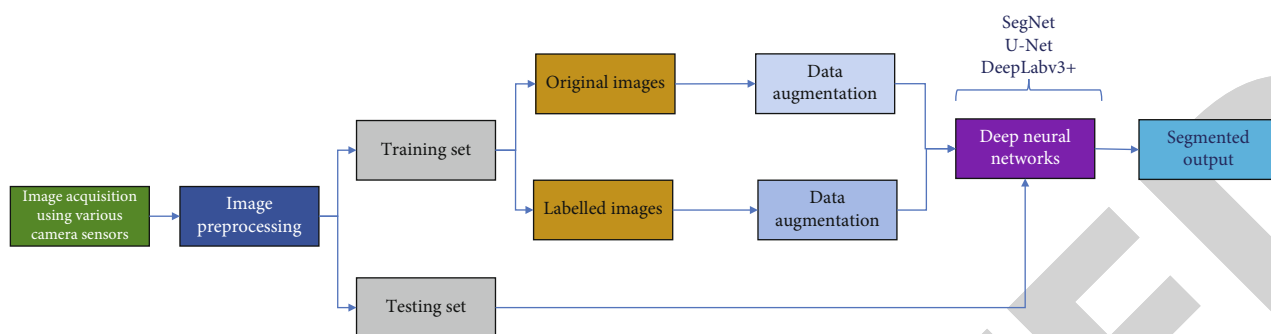


FIGURE 1: Flow of the proposed research work.

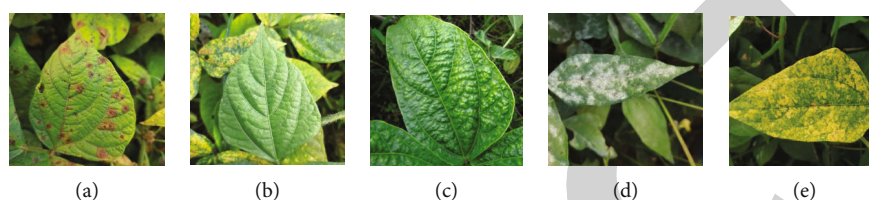


FIGURE 2: Sample images in dataset: (a) anthracnose; (b) healthy; (c) leaf crinkle; (d) powdery mildew; (e) yellow mosaic disease.

the farmers for recognizing the most prevalent black gram leaf diseases (leaf crinkle, yellow mosaic, powdery mildew, and anthracnose) [11]. However, the present work is aimed at developing an automatic leaf region segmentation from the cultivation field images, which have complex greenery/plain backgrounds and different illumination conditions. Some sample black gram plant leaf images in the dataset are shown in Figure 2. Moreover, each shot in Figure 2 represents each disease category in the dataset.

3.2. Preprocessing. In the preprocessing stage, data was cleaned, and then, the images' size was reduced to 256×256 and 300×300 dimensions. Since deep learning algorithms require all input images to be of the same size and they have their own input size requirements (256×256 for SegNet, U-Net, ResNet 18, ResNet50, and MobileNetV2 and 300×300 for Xception and InceptionResNetV2). Ground truth binary masks for all the images in the dataset were generated using the image segmenter app (MathWorks Inc., n.d.). Now the 1000 image pairs (original images and their corresponding binary masks) were split into training pair and testing pair such that 80% of images were in the training set and 20% of images were in the testing set. So, there were 800 images in the training set and 200 in the testing set. We split the dataset such that both the training and testing sets contained images of all the disease categories and ensured no repetition of instances.

3.3. Data Augmentation. Data augmentation refers to generating a considerable amount of data from limited available data. This work employed rotation augmentation (45° , 90° , 135° , 180° , 225° , 270° , and 315°) and mirror symmetry augmentation (horizontal symmetry and vertical symmetry) (shown in Figure 3) [29]. Eight thousand images increased the training set pair with the mentioned augmentation techniques. The number of samples available in the dataset for

each disease category before and after the data augmentation techniques is tabulated in Table 1.

3.4. Deep Learning for Semantic Segmentation. Deep learning has proven to be very effective when dealing with image data, and it is now at a point where it outperforms humans in several applications. Image classification, object detection, and segmentation are the most significant issues that humanity has been particularly interested in solving with computer vision. Image segmentation is a more complicated task since it requires both object recognition and localization, where each pixel is assigned to a particular class. Nowadays, semantic segmentation is used widely for segmentation as it is a heavily influenced method for deep learning and aids computer vision to analyze the images quickly. The general semantic segmentation network consists of an encoder network followed by a decoder network. An encoder is a pretrained classification network, whereas a decoder is responsible for discriminative features learned by the encoder for dense classification. Several semantic segmentation models have been reported in the literature. To exploit the best segmentation model for leaf region extraction under a complicated background, we examined SegNet, U-Net, and DeepLabv3+ layers in the proposed research work.

3.4.1. U-Net. Ronneberger et al. [30] developed the U-Net architecture (Figure 4) for biomedical image segmentation. Its architecture has two main paths. The contraction path is known as the encoder, which is responsible for capturing the context of an image using convolutional and max-pooling layers. Another is the expansion path known as the decoder, which is responsible for object detection and localization using transposed convolutions. Typically, the encoder path reduces the spatial resolution of an input image, and the decoder recovers spatial resolution gradually

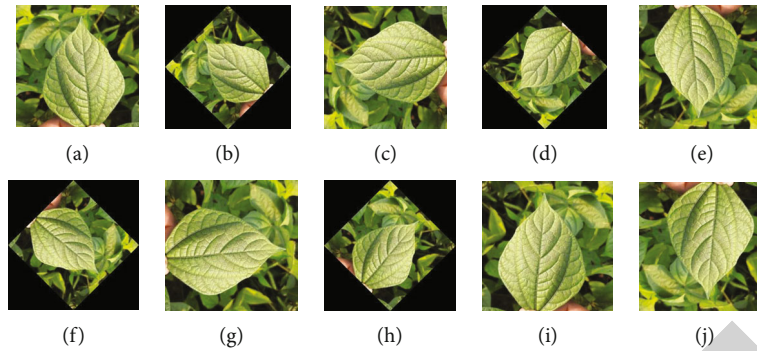


FIGURE 3: Data augmentation: (a–h) rotation augmentation, (i) horizontal symmetry, and (j) vertical symmetry.

TABLE 1: Number of samples available in the dataset on each disease category before and after the data augmentation.

Disease	Images	Training images	Testing images	Training images after augmentation
Anthraco nose	230	184	46	1840
Healthy	220	176	44	1760
Leaf crinkle	150	120	30	1500
Powdery mildew	180	144	36	1440
Yellow mosaic	220	176	44	1760
Total	1000	800	200	8000

using upsampling layers. U-Net can handle images of any size because of not having dense layers. It only depends on convolutional layers to be an end-to-end fully convolutional network. The grey arrows in Figure 4 illustrate the skip connections used to connect encoder block outputs to corresponding decoder blocks. This phase attempts to retrieve the fine details learned by the encoder stage to restore the spatial resolution of the original input image. For 2D biomedical segmentation, U-Net has shown exceptional performance, and still, it continues to be utilized as a baseline for research in this area.

The basic architecture of the U-Net model is illustrated in Figure 4. The contracting path performed a downsampling operation, consisting of two 3×3 convolutions repeatedly, followed by a ReLU activation function and a 2×2 max pooling with stride 2. The number of feature channels is increased by a factor of two for each downsampling, whereas the expansive path performed the upsampling operation, having a 2×2 convolution which reduces the number of feature channels by half, a concatenation with corresponding features from the contracting path and two 3×3 convolutions, each followed by a ReLU. At the final layer, a 1×1 convolution is used to map each 64-component feature vector to the desired number of classes. Mathematically, convolution is accomplished using equation (1), which performs as a kind of transformation [31].

$$Z(x_k(ii, jj)) = f\left(\sum_{k=1}^k x_k(ii, jj) \cdot w_k + b_k\right) \leftrightarrow Z = f(X \cdot W + b), \quad (1)$$

where w is the weight vector, b is the bias vector, and $x_k(ii, jj)$ is the activation function's input and the convolu-

tion operation's output. After the convolution operation, U-Net utilized ReLU as an activation function represented in equation (2).

$$A(x_k(ii, jj)) = \max(0, Z(x_k(ii, jj))). \quad (2)$$

3.4.2. *SegNet*. SegNet architecture has been put forth by Badrinarayanan et al. [32] with 13 convolutional layers in each encoder and decoder network, followed by a softmax layer responsible for probabilities for every class per pixel. Finally, the segmented output is formed by the class with the most excellent chance of being present at each pixel. The network architecture of the SegNet is illustrated in Figure 5. In SegNet, max-pooling indices (instead of using skip connections in U-Net) of the feature map in the encoder network are stored and utilized in its decoder network for better performance, making it more efficient. SegNet has significant advantages like compactness in size, needing less memory, and being more accessible to train than other semantic segmentation networks.

$$s(x_i) = \frac{e^{x_i}}{\sum_{j=1}^n e^{x_j}}, \quad (3)$$

where n is the number of classes, x is the output vector of the model, and i is in the range of 0 to $n - 1$.

If an image with a size of $M \times N$ is fed into the encoder's first layer, then the activation map of $(m + 1)^{\text{th}}$ layer of the encoder is given in equation (4), and an activation map of $(m + 1)^{\text{th}}$ decoder layer is given in equation (5) [33].

$$x_{m+1} = \{\text{MAX}[\text{ReLU}(\text{conv}_m\{x_m\} + b_m)]\}, \quad (4)$$

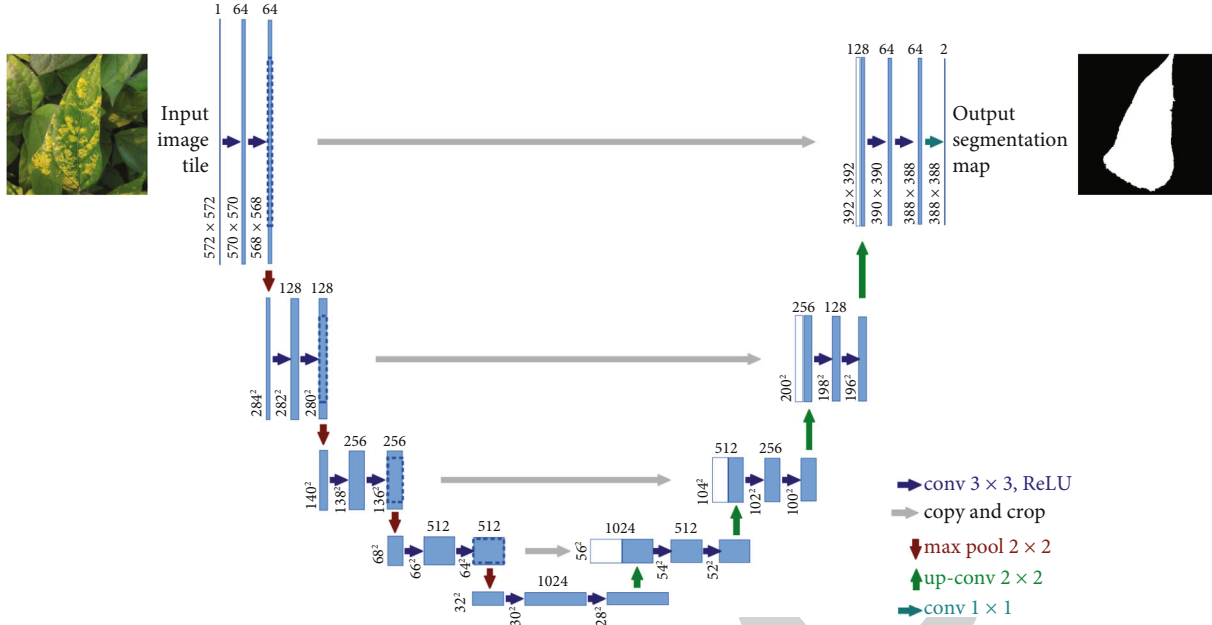


FIGURE 4: Architecture of U-Net proposed by Ronneberger et al. [30].

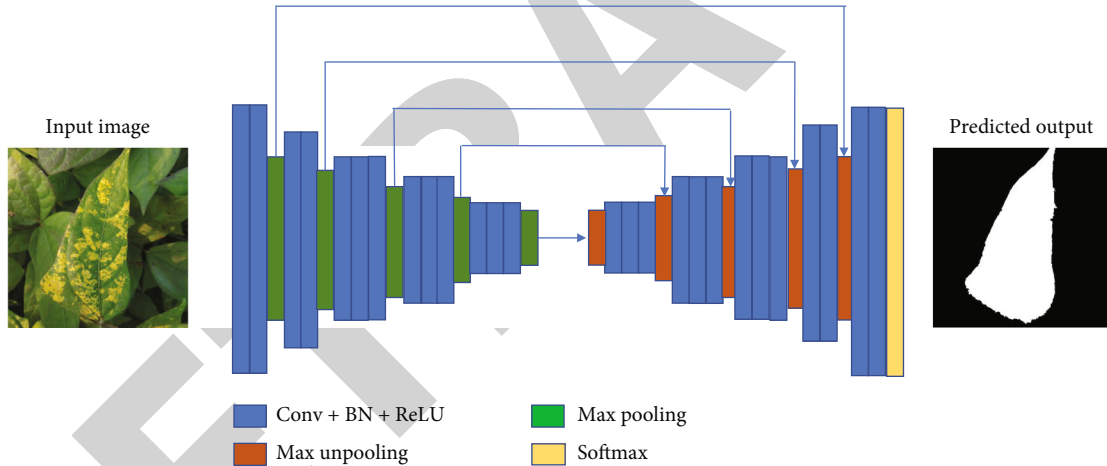


FIGURE 5: Architecture of SegNet.

$$y_{m+1} = \text{NORM}[\text{conv}_m\{\text{US}(y_m) + b_m\}], \quad (5)$$

where x_m is the activation map of m^{th} encoder layer, b_m is the learned bias of m^{th} layer, y_m is the activation map of m^{th} decoder layer, $\text{conv}\{\cdot\}$ is the convolution operation, $\text{ReLU}(\cdot)$ is the ReLU activation function, $\text{MAX}[\cdot]$ is the max-pooling operation, $\text{NORM}[\cdot]$ is the batch normalization, and $\text{US}(\cdot)$ is the upsampling.

3.4.3. DeepLabv3+. DeepLabv3+ was developed by Chen et al. [34], who works at Google Inc., to overcome the issues present in the existing DeepLab series. It is the extended version of DeepLabv3. A simple but effective decoder module has been added to DeepLabv3 to improve the segmentation results, particularly along object boundaries, by gradually recovering the spatial information. To regain the spatial resolution, the authors recommended atrous convolution,

designed for efficient computing and presented in equation (6). DeepLabv3+ extensively uses an aligned Xception network as its principal feature extractor and replaced max-pooling layers with depthwise separable convolutions. It is important to note that the depthwise separable convolutions introduced in DeepLabv3 were carried over to DeepLabv3+. Depthwise separable convolution is the opposite of standard convolution as it performs both depthwise and pointwise convolutions separately. With the convolutional filter, depthwise convolution carries out spatial convolution per each input channel, and pointwise convolution combines the outputs of depthwise convolutions. The authors improved the encoder-decoder network by applying depthwise separable convolution to atrous spatial pyramid pooling (ASPP) and decoder modules (shown in Figure 6), making it quicker and more robust. DeepLabv3+ utilizes pretrained CNNs in the encoder stage for feature extraction. In this

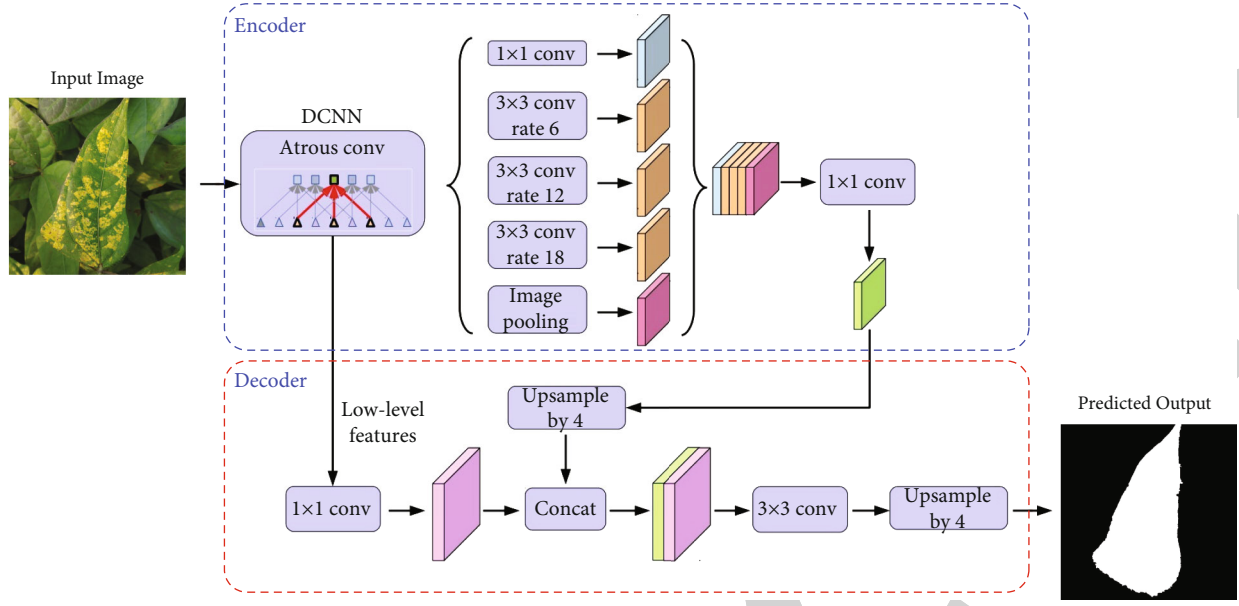


FIGURE 6: Architecture of DeepLabv3+ proposed by Chen et al. [34].

TABLE 2: Summary of hyperparameters.

Hyperparameters		
Input size	300 × 300	Xception and InceptionResNetV2
	256 × 256	Remaining networks
Batch size	12	—
Learning rate	0.001	—
Optimizer	SGDM	—
Loss function	Binary cross-entropy	—
Epochs	50	Case I
	15	Case II

work, ResNet18, ResNet50, MobileNetV2, Xception, and InceptionResNetV2 were used as backbone networks for the DeepLabv3+.

$$y(i) = \sum_k x[i + r.k]w[k], \quad (6)$$

where i , w , x , and y are the location, filter, input feature map, and output feature map of 2D signals, respectively, and r is the atrous rate [35].

4. Experimental Results and Discussion

The experiments were conducted on MATLAB 2021 environment with the system specifications as Intel® Core™ i5-8250U CPU @ 1.60GHz 1.80GHz, 8GB RAM, and with 64-bit Windows 10 operating systems.

4.1. Evaluation of Semantic Segmentation. Evaluation metrics such as global accuracy, mean accuracy, Jaccard/IoU,

Dice, weighted IoU, and mean score will be calculated to validate semantic segmentation networks. In this work, “leaf” and “background” are the two classes in the dataset. Let us consider that K is the no. of classes in the image and N is the total number of testing images in the dataset.

4.1.1. Global Accuracy (G.A.). Global accuracy is the ratio of accurately categorized pixels to the total number of pixels in the image, irrespective of the class.

$$\text{Acc} = \frac{\text{TP} + \text{TN}}{\text{TP} + \text{TN} + \text{FP} + \text{FN}}, \quad (7)$$

where TP is true positive, TN is true negative, FP is false positive, and FN is false negative.

$$\text{GA} = \frac{1}{N} \sum_{n=1}^N \text{Acc}_n, \quad (8)$$

where Acc_n is the accuracy of a particular image n .

4.1.2. Mean Accuracy. Mean accuracy is the average accuracy of all classes of all images in the dataset.

$$\text{MA} = \frac{1}{KN} \sum_{k=1}^K \sum_{n=1}^N \text{Acc}_{kn}, \quad (9)$$

where Acc_{kn} is the accuracy measured using equation (1) for a specified class k in an image n .

4.1.3. Mean IoU/Jaccard. Mean IoU/Jaccard is the ratio of accurately categorized pixels to the total number of ground truth and predicted pixels in that class.

TABLE 3: Algorithms for training and testing the networks.

Algorithm for training the networks	Algorithm for testing the networks
Load training data	Load the trained network
Create an image datastore for the training images	Load the test data
Define class names and their associated label IDs	Create image datastore for the testing images
Create a pixel label datastore holding the ground truth pixel labels for the training images	Define class names and their associated label IDs
Create SegNet or U-Net or DeepLabv3+ layers	Create a pixel label datastore holding the ground truth pixel labels for the testing images
Combine image and pixel label data for training	Run the trained network on the test images
Set up training options	Evaluate the prediction results against the ground truth
Initial learning rate	Global accuracy
Minibatch size	Mean accuracy
Optimizer	Mean IoU
Epochs	Dice similarity index
Train the network	Mean weighted IoU
Save the network	Mean BFScore
	Display confusion metrics

TABLE 4: Comparison results for each object category, when no data augmentation is applied.

S. no.	Model	Accuracy		IOU		BFScore	
		Background	Leaf	Background	Leaf	Background	Leaf
1	SegNet	0.90766	0.98012	0.85052	0.84438	0.78024	0.72435
2	U-Net	0.55684	0.98417	0.49013	0.61486	0.5356	0.53883
3	DeepLabv3+-ResNet18	0.98279	0.98469	0.95368	0.93497	0.9177	0.87159
4	DeepLabv3+-ResNet50	0.98044	0.97501	0.94332	0.92449	0.89813	0.85699
5	DeepLabv3+-Xception	0.98723	0.98961	0.96236	0.95166	0.92509	0.89564
6	DeepLabv3+-InceptionResNetV2	0.99235	0.99401	0.97236	0.96423	0.9542	0.93509
7	DeepLabv3+-MobileNetV2 (proposed model)	0.98155	0.94971	0.93202	0.8883	0.85183	0.72799

TABLE 5: Performance evaluation of the networks without data augmentation.

S. no.	Model	Global accuracy	Mean accuracy	Mean IoU/ Jaccard	Dice/ similarity index	Mean weighted IoU	Mean BFScore	Size of the trained network (MB)
1	SegNet	0.93771	0.94389	0.84745	0.91743	0.84797	0.75229	0.831
2	U-Net	0.74189	0.77051	0.55249	0.71175	0.54414	0.53721	110
3	DeepLabv3+-ResNet18	0.98355	0.98373	0.94432	0.97136	0.94605	0.89464	58.4
4	DeepLabv3+-ResNet50	0.97822	0.97773	0.9339	0.96582	0.93563	0.87756	141
5	DeepLabv3+-Xception	0.98821	0.98842	0.95701	0.97803	0.95799	0.91036	83.4
6	DeepLabv3+-InceptionResNetV2	0.99303	0.99318	0.96829	0.98389	0.96904	0.94465	238
7	DeepLabv3+-MobileNetV2 (proposed model)	0.96868	0.96563	0.91016	0.95297	0.91435	0.78991	9.5

$$\text{IoU}_{kn} = \frac{\text{TP}}{\text{TP} + \text{FN} + \text{FP}}, \quad (10)$$

where IoU_{kn} is the IoU of a particular class k in an image n .

Mean IoU is the average of the IoU of all the classes of all the images in the dataset.

$$\text{meanIoU} = \frac{1}{KN} \sum_{k=1}^K \sum_{n=1}^N \text{IoU}_{kn}. \quad (11)$$

4.1.4. Dice/Similarity Index. Dice is used to determining how well the predicted segmented output correlates with the

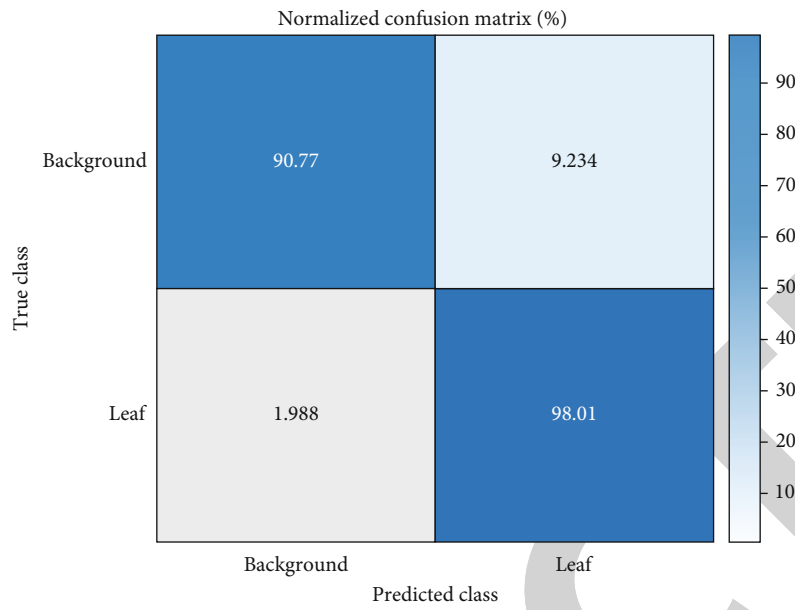
ground truth. It can be calculated using Jaccard/IoU (if already known).

$$\text{Dice} = \frac{2 * \text{Jaccard}}{1 + \text{Jaccard}}. \quad (12)$$

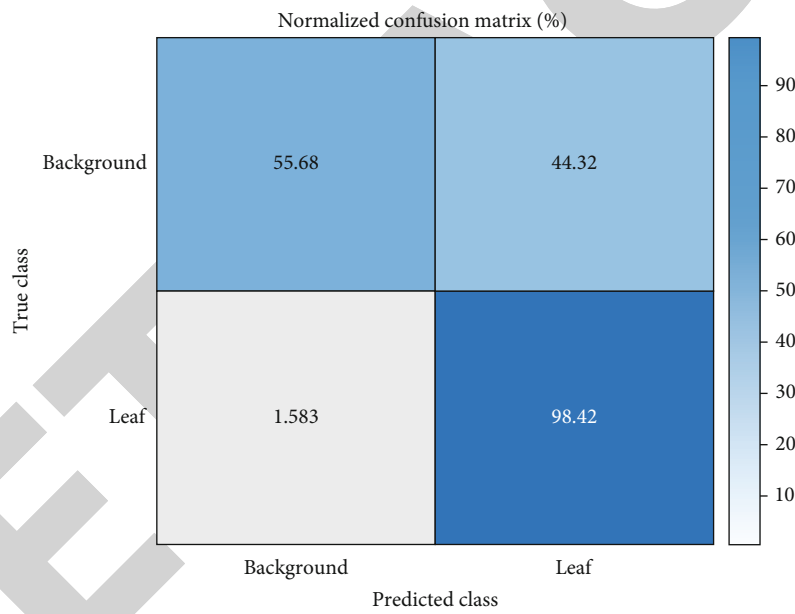
4.1.5. Mean Weighted IoU (mwIoU). It is the average IoU of each class weighted by the total number of pixels in that class.

$$\text{mwIoU} = \frac{1}{KN} \sum_{k=1}^K p_k^{-1} \sum_{n=1}^N \text{IoU}_{kn}, \quad (13)$$

where p_k is the total number of pixels in the class k .

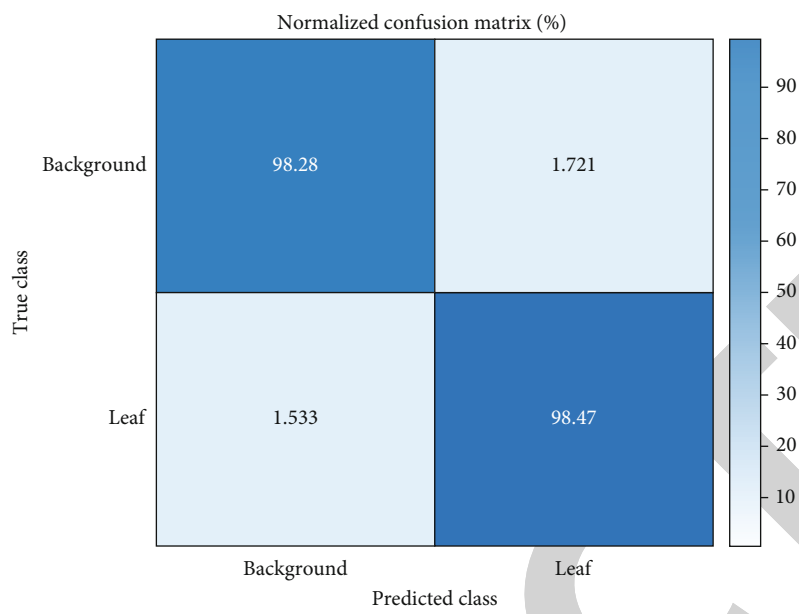


(a)

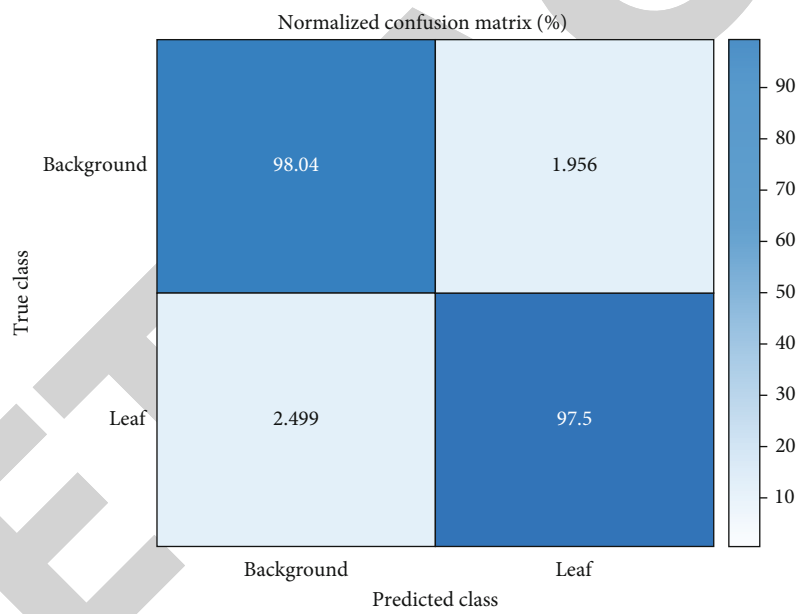


(b)

FIGURE 7: Continued.

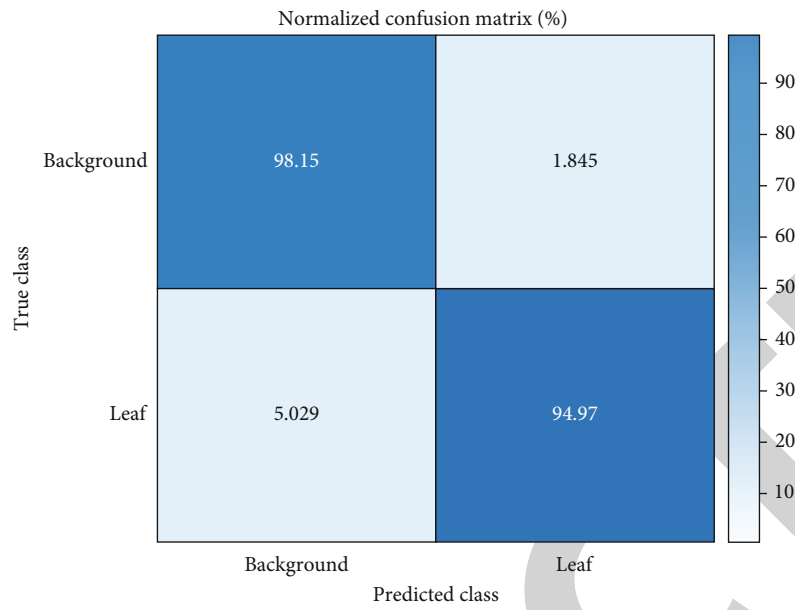


(c)

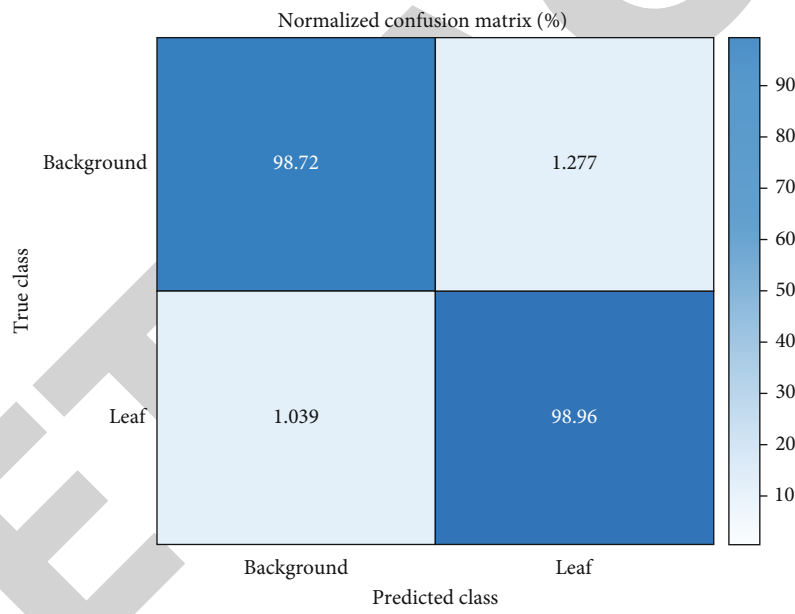


(d)

FIGURE 7: Continued.



(e)



(f)

FIGURE 7: Continued.

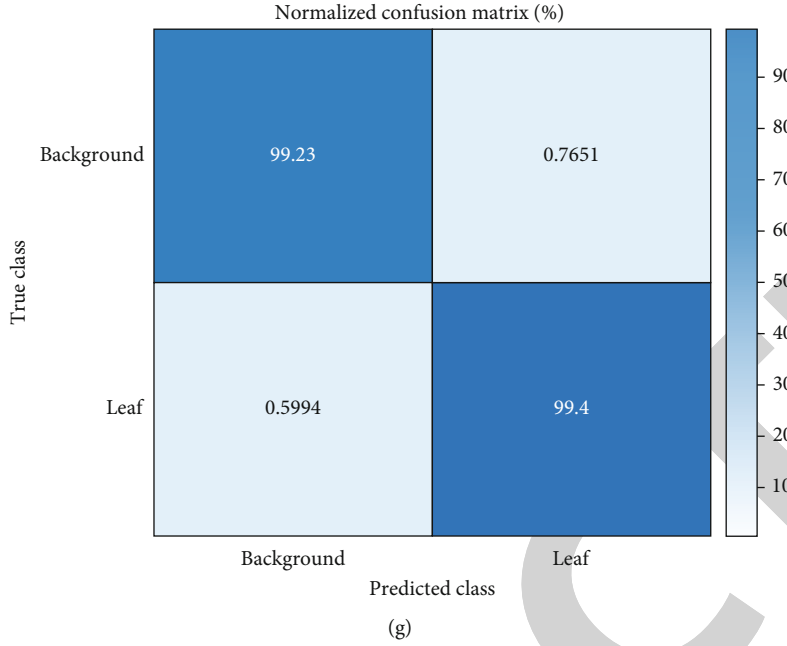


FIGURE 7: Confusion matrices of (a) SegNet, (b) U-Net, and DeepLabv3+ with (c) ResNet18, (d) ResNet50, (e) MobileNetV2, (f) Xception, and (g) InceptionResNetV2 models on the test set when no data augmentation applied on the training set.

4.1.6. *Mean BFScore*. The mean BFScore is mathematically defined as follows:

$$\text{BFScore} = \frac{2 * \text{precision} * \text{recall}}{\text{precision} + \text{recall}}, \quad (14)$$

where $\text{precision} = \text{TP}/(\text{TP} + \text{FP})$ and $\text{recall} = \text{TP}/(\text{TP} + \text{FN})$.

$$\text{mean BFScore} = \frac{1}{KN} \sum_{k=1}^K \sum_{n=1}^N \text{BFScore}_{kn}, \quad (15)$$

where BFScore_{kn} is the boundary F1 score of a particular class k of an image n .

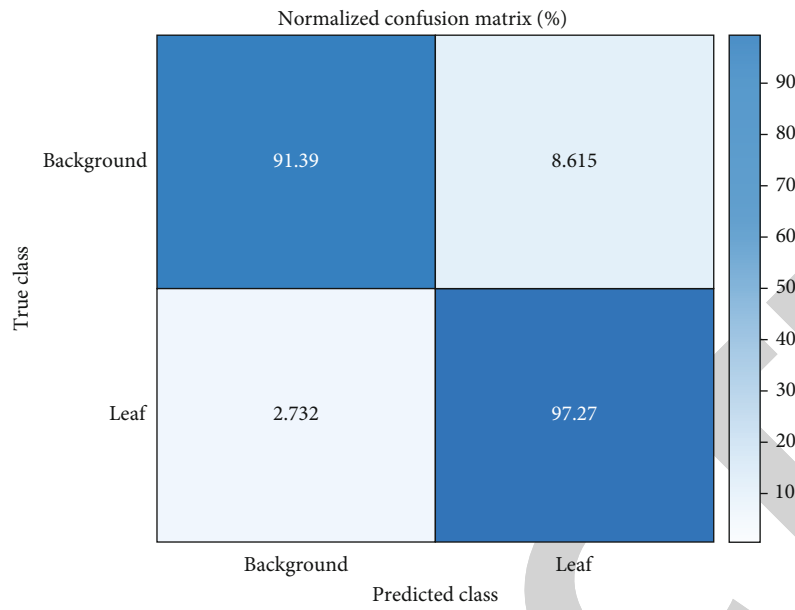
4.2. *Performance Evaluation of the Adopted Networks*. All the images in the dataset and their corresponding ground truth labels were rescaled to 256×256 and 300×300 dimensions to meet the training need of deep network models. Rotation and mirror symmetry augmentation techniques were utilized to enhance the dataset. We adopted SegNet, U-Net, and DeepLabv3+ network models for the segmentation. Moreover, ResNet18, ResNet50, MobileNetV2, Xception, and InceptionResNetV2 networks were utilized as backbone networks for DeepLabV3+ layers. Initially, the dataset is divided into training and testing sets. In the data, 80% (800) of images were used to train the models, and the other 20% (200) images were used to test the trained model's reliability. The robustness of the trained model was evaluated by comparing segmented results with the ground truth images generated by the image segmenter tool in MATLAB. To assess the generalizability of the models, we have done experiments in two cases: with and without the use of data augmentation techniques on the training set. As a result, in

the case without using data augmentation, the training set has 800 images, while in the case of using data augmentation, the training set has 8000 images.

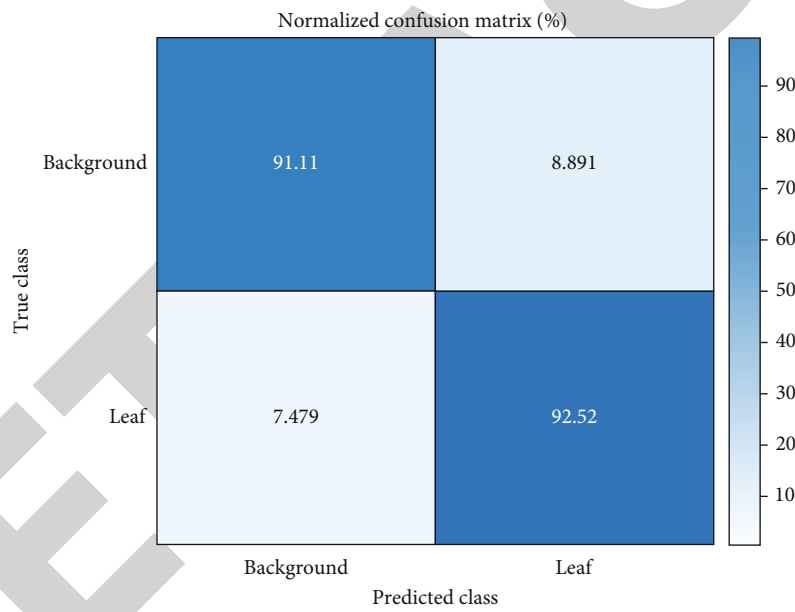
Parameter selection, commonly called hyperparameter tuning, is a necessary step before training the CNN architectures to find the correct equilibrium among the bias and variance, to prevent the vanishing/exploding gradient problem, and to speed up the learning process. It is essential, as these selected parameter values determine the behaviour of the training algorithm. Several approaches are available to choose the parameter values. Manual search, grid search, random search, and Bayesian search methods are commonly used. In this article, we have employed a manual search method to tune the hyperparameters for all experimentation. One does not need a dedicated library for the manual tuning of hyperparameters. Instead, one needs to try the different combinations of hyperparameters for the model and select the combination that performs the best. In the manual search method, we have utilized different varieties such as optimizers (SGDM, Adam, and RMSProp), initial learning rate (0.01, 0.001, and 0.0001), minibatch size (12, 24, and 32), and epochs (15, 30, 50, and 100). Through extensive experimentation, we have set the hyperparameters as an initial learning rate of 0.001, optimizer SGD with 0.9 momentum, minibatch size of 12, and 50 epochs without data augmentation and 15 for with data augmentation. Table 2 represents the hyperparameters employed for training the adopted segmentation models.

The algorithm for training and testing the networks is shown in Table 3.

4.2.1. *Case I: Without the Use of Data Augmentation on the Training Set*. In this case, the training set has 800 images, and the testing set has 200 images. Results for each object

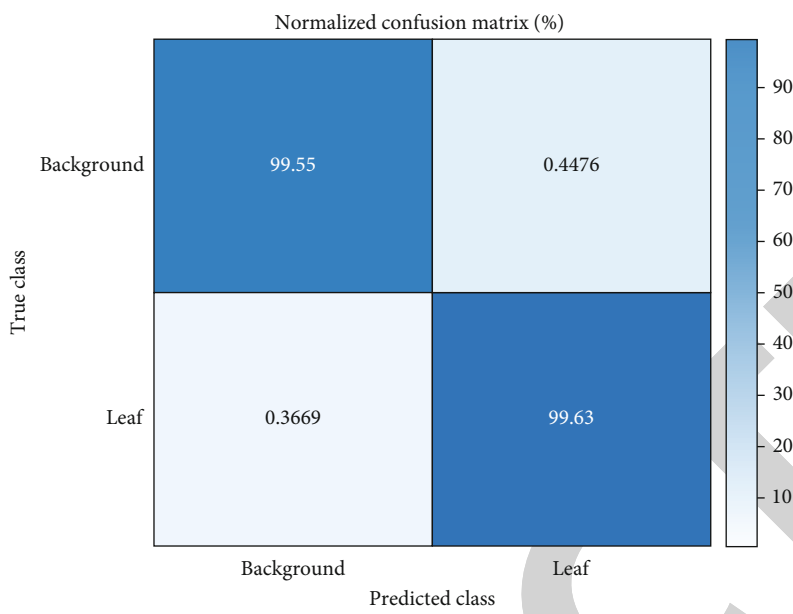


(a)

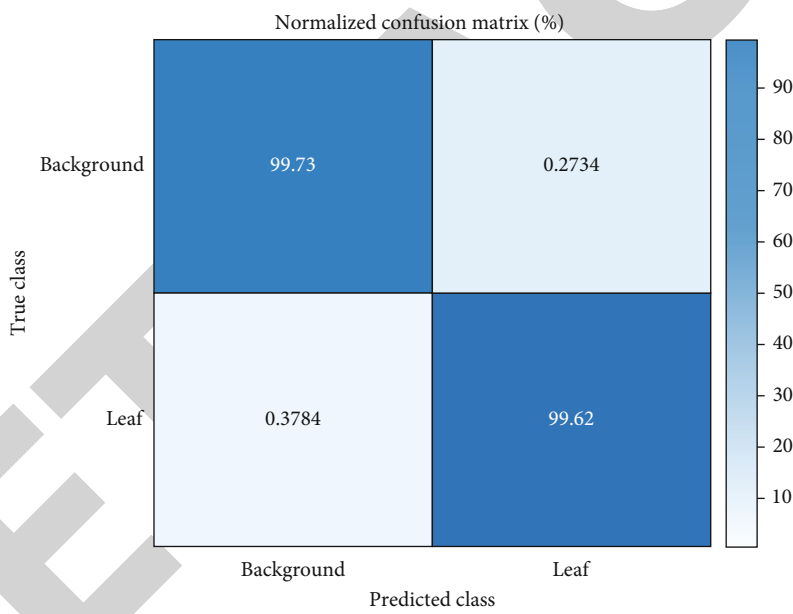


(b)

FIGURE 8: Continued.

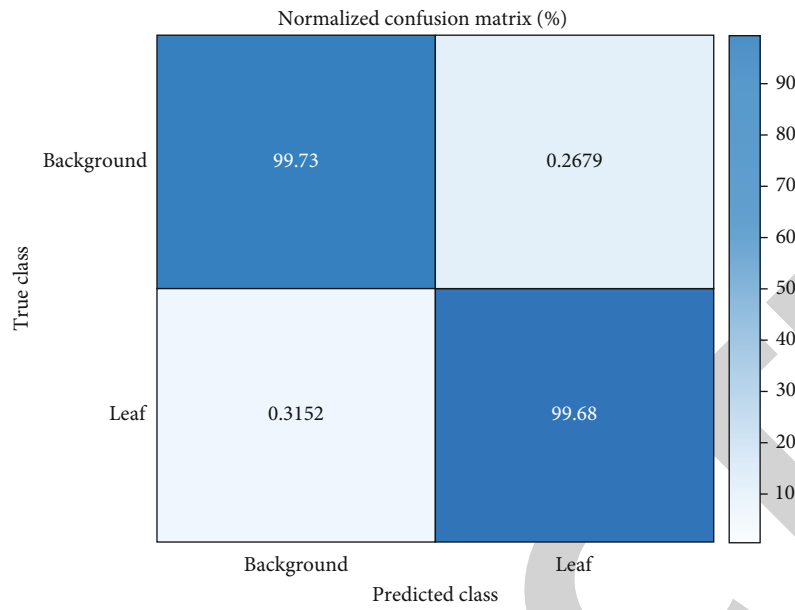


(c)

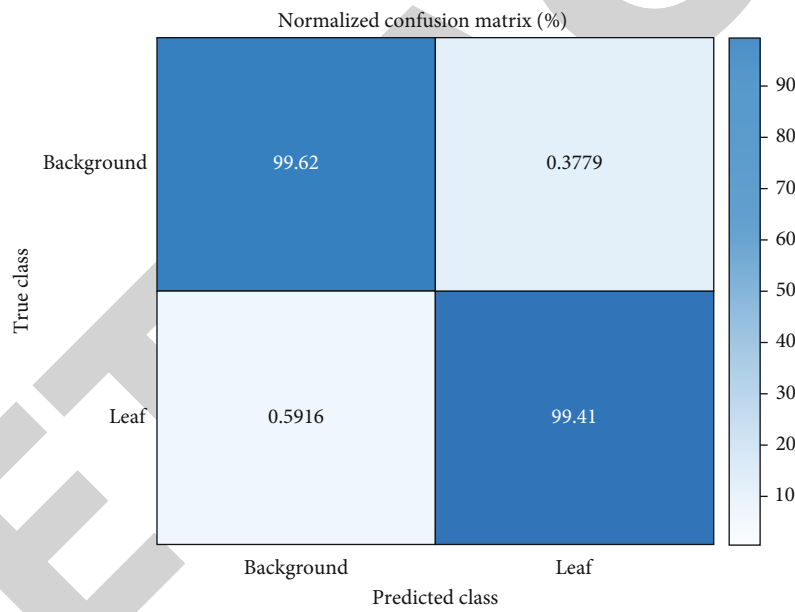


(d)

FIGURE 8: Continued.



(e)



(f)

FIGURE 8: Continued.

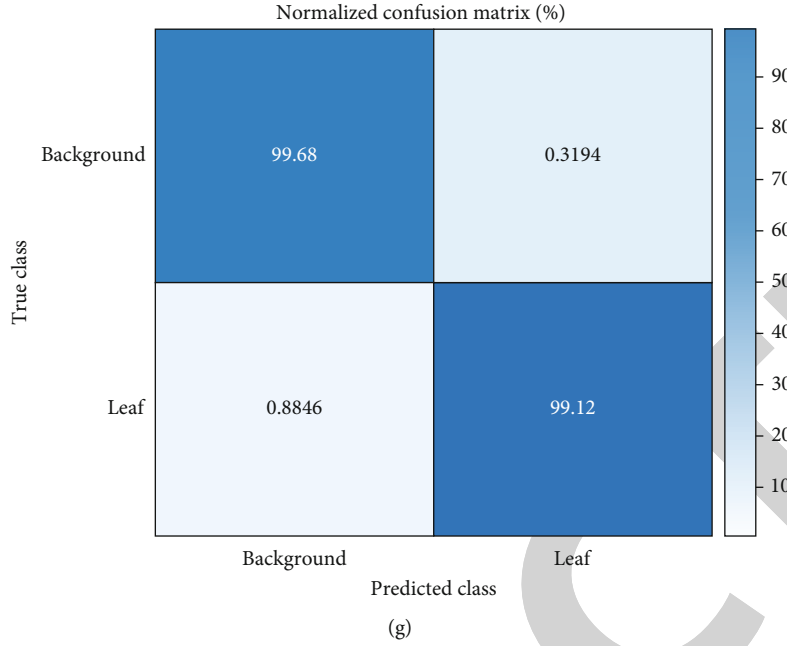


FIGURE 8: Confusion matrices of (a) SegNet, (b) U-Net, and DeepLabv3+ with (c) ResNet18, (d) ResNet50, (e) MobileNetV2, (f) Xception, and (g) InceptionResNetV2 models on a test set when data augmentation applied on the training set.

TABLE 6: Comparison results for each object category when data augmentation is applied.

S. no.	Model	Accuracy		IOU		BFScore	
		Background	Leaf	Background	Leaf	Background	Leaf
1	SegNet	0.91385	0.97268	0.85024	0.84061	0.75634	0.6839
2	U-Net	0.91109	0.92521	0.82538	0.78383	0.68544	0.54375
3	DeepLabv3+-ResNet18	0.99552	0.99633	0.97673	0.96713	0.97328	0.95758
4	DeepLabv3+-ResNet50	0.99727	0.99662	0.97904	0.96966	0.97823	0.96355
5	DeepLabv3+-Xception	0.99622	0.99408	0.97826	0.96841	0.97346	0.95671
6	DeepLabv3+-InceptionResNetV2	0.9984	0.98881	0.97771	0.96759	0.98487	0.9675
7	DeepLabv3+-MobileNetV2 (proposed model)	0.99732	0.99685	0.97874	0.97065	0.97576	0.96222

category (leaf and background) in Table 4 and mean values of performance metrics in Table 5 are outlined. The results show that DeepLabv3+ exhibited superior performance compared to SegNet and U-Net segmentation models. DeepLabv3+ with InceptionResNetV2 achieved an accuracy of 99.401% for the leaf class, slightly higher than the background class accuracy of 99.235%. The same model reached an Intersection over Union (IoU) of 97.236% for the background class and 96.423% for the leaf class. At the same time, considering the BFScore, 95.42% for the background class and 93.509% for the leaf class are achieved. Coming to the mean values presented in Table 5, the DeepLabv3+-InceptionResNetV2 achieved global accuracy of 99.303%, mean accuracy of 99.318%, mean IoU of 96.829, Dice similarity index of 98.389%, mean weighted IoU of 96.904%, and mean BFScore of 94.465%. The results show that the accuracy and the similarity indexes are good, but boundary $F1$ or mean BFScore is not up to the mark. To increase the boundary $F1$ score, we applied rotation and mirror symmetry augmentation techniques on the training set and performed the same experiments similar manner.

The confusion matrices for all trained models in terms of individual class accuracies without and with data augmentation techniques are presented in Figures 7 and 8.

4.2.2. Case II: With the Use of Data Augmentation on the Training Set. In this case, we applied rotation and mirror symmetry augmentation techniques on the training set to have a total of 8000 images, and the testing set had 200 images. Results for each object category (leaf and background) in Table 6 and mean values of performance metrics in Table 7 are outlined. In this case, the proposed model achieved an accuracy of 99.685% for the leaf class compared with the background class accuracy of 99.732%. The same model reached an Intersection over Union (IoU) of 97.874% for the background class and 97.065% for the leaf class. Considering the BFScore, DeepLabv3+-InceptionResNetV2 achieved 98.487% for the background class and 96.75% for the leaf class. Coming to the mean values presented in Table 7, the proposed DeepLabv3+-MobileNetV2 achieved higher performance in terms of global accuracy of 99.713%, mean accuracy of 99.708%, mean IoU of 97.47, Dice similarity

TABLE 7: Performance evaluation of the networks with data augmentation.

S. no.	Model	Global accuracy	Mean accuracy	Mean IoU/ Jaccard	Dice/ similarity index	Mean weighted IoU	Mean BFScore	Size of the trained network (MB)
1	SegNet	0.93822	0.94327	0.84542	0.91624	0.84625	0.72012	0.831
2	U-Net	0.91687	0.91815	0.8046	0.89172	0.80837	0.61459	110
3	DeepLabv3+-ResNet18	0.99585	0.99593	0.97193	0.98577	0.97282	0.96543	58.4
4	DeepLabv3+-ResNet50	0.99684	0.99674	0.97435	0.98701	0.97522	0.97089	141
5	DeepLabv3+-Xception	0.99535	0.99515	0.97333	0.98648	0.97424	0.96508	83.4
6	DeepLabv3+-InceptionResNetV2	0.99449	0.99361	0.97265	0.98614	0.97358	0.97619	238
7	DeepLabv3+-MobileNetV2 (proposed model)	0.99713	0.99708	0.9747	0.98719	0.97544	0.96899	9.5

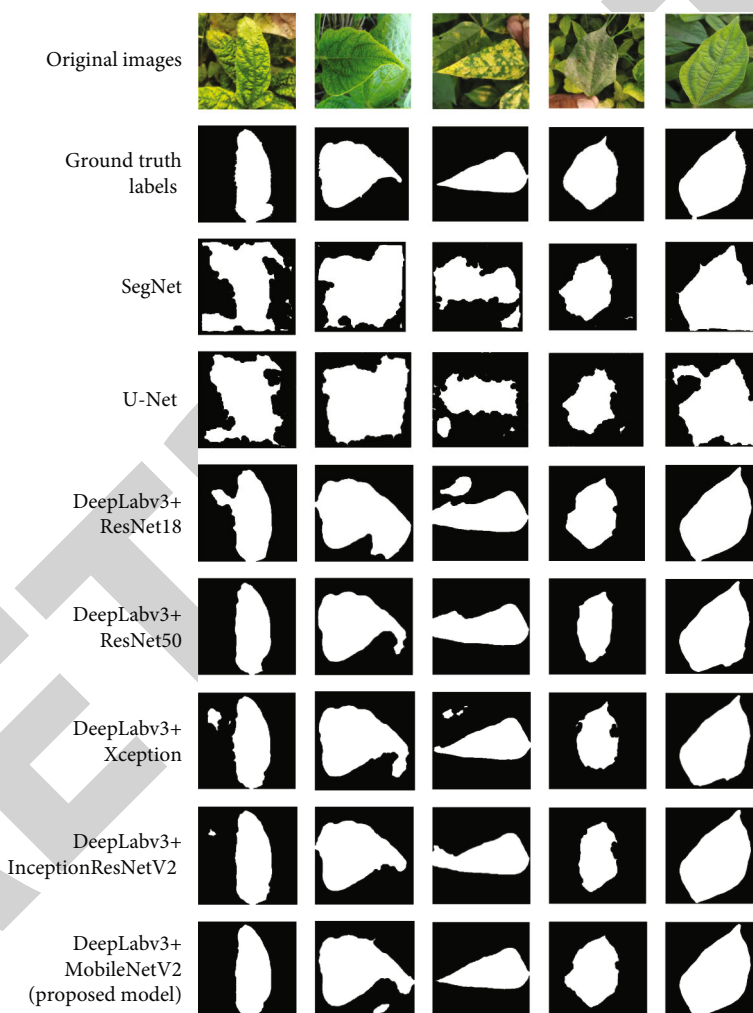


FIGURE 9: Segmented outputs of adopted networks.

index of 98.719%, mean weighted IoU of 97.544%, and mean BFScore of 96.899%. The results show that DeepLabv3+ with MobileNetV2 outperforms the remaining models when data augmentation is applied to the training set.

In both cases, U-Net stood last; mainly when, in case 2, it stayed 7.9%, 17.01%, 9.55%, and 35.44% behind DeepLabv3+-MobileNetV2 in terms of MA, IoU, Dice, and mean BFScore, respectively.

Figure 9 shows the segmented outcomes of all trained models for five sample images of the testing set in our dataset. Original images are shown in the first row, followed by respective ground truth labels in the second. The following seven rows, i.e., row three to row nine, correspond to the segmented outputs produced by each network.

The leaf region segmentation is challenging when the plant images have overlapping/occluded leaves and complex

TABLE 8: Comparison of computational complexity between the adopted networks.

Network	Training time (H.H.:MM:S.S.)		No. of epochs		Size of the trained network	Initial learning rate
	Case I	Case II	Case I	Case II		
SegNet	08:39:30	24:12:20	50	15	0.831	0.001
U-Net	15:27:32	61:20:16	50	15	110	0.00001
DeepLabv3+-ResNet18	05:55:50	18:09:10	50	15	58.4	0.001
DeepLabv3+-ResNet50	10:56:29	36:59:07	50	15	141	0.001
DeepLabv3+-Xception	26:12:08	66:24:36	25	15	83.4	0.001
DeepLabv3+-InceptionResNetV2	25:24:57	78:27:47	25	15	238	0.001
DeepLabv3+-MobileNetV2 (proposed method)	07:29:15	22:28:37	50	15	9.5	0.001

backgrounds. Most presently available leaf segmentation methods [12, 15, 17, 24, 26, 36, 37] were designed to work specifically with certain acquisition circumstances. As a consequence, these techniques are not able to give good results in field conditions. Even though some other authors [18–20, 22, 25] developed the segmentation models based on field conditions, they have to be improved further due to the lack of performance. [13] pointed out that their model’s process load increases as the number of features increases for better results. When more than 23% overlap between the leaves, the algorithm [14] treats two leaves as one. When the resolution of the input images is inferior and on blurred images, the authors [16] found that their model fails to recognize leaves. Due to the lack of training images, which is crucial for deep learning, the model could not remember the shape and textures of the region of interest [38]. Because pixels in the backdrop resemble leaves [39], the segmentation technique still has certain flaws and cannot assure that their model’s processing time will be competitive. The model proposed by [23] is not performed well in certain situations, like the images with numerous plants and leaves of the plant that are not green. The demand for high computational time, the enormous datasets required for training, and low performance due to under/over segmentation are all significant drawbacks of the methods discussed in the literature. The proposed method provides a solution to the issues that have been addressed so far.

Our proposed segmentation algorithm was developed using DeepLabv3+ layers with the MobileNetV2 model as a backbone. DeepLabv3+ is a state-of-the-art semantic segmentation model combining encoder-decoder architecture and atrous spatial pyramid pooling. From the experimental findings, the proposed DeepLabv3+-MobileNetV2 model has the potential and can be employed for successfully segmenting leaf regions from complex backgrounds. It is a fully automatic segmentation algorithm and outperforms other networks with considerable accuracy and similarity index. We have developed and evaluated the proposed segmentation model on the BPLD dataset, which has five disease categories of images. A primary emphasis of our future research work is to design leaf disease identification systems tailored to mobile phone applications and expand the proposed model’s effectiveness to extract the leaf regions from the images of other crops/plants.

The computational complexity of any computer vision-based segmentation algorithm is the number of resources needed to execute it. Special attention is given to the time and memory required to complete the task. Table 8 depicts the computational complexity comparison between the proposed network with the other networks. The training time of DeepLabv3+-Xception and DeepLabv3+-InceptionResNetV2 is higher in both training cases because they are deeper networks than others, whereas DeepLabv3+-ResNet18 was relatively faster in training in both cases but exhibited lower performance than DeepLabv3+-MobileNetV2. However, despite its depth, the proposed DeepLabv3+-MobileNetV2 network trained very fast because of its limited number of parameters. The table shows that the proposed DeepLabv3+-MobileNetV2 model achieved a remarkable segmentation accuracy with less training time (7 h 23 min for case I and 22 h 28 min for case II) and no. of epochs (50 for point I and 15 for case II). And also, the size of the network is 9.5 MB, which is significantly less in comparison with the other models and can quickly implement and run on mobile devices.

5. Conclusion

This work proposed and evaluated the use of deep fully convolutional neural networks to segment plant leaf regions under complex backgrounds. The images in the dataset were collected using the devices having super HAD CCD and ISOCELL GW1 imaging sensors from the black gram crop cultivation fields. Seven FCN models were adopted for the proposed work: SegNet, U-Net, and five DeepLabv3+ variants, such as ResNet18, ResNet50, MobileNetV2, Xception, and InceptionResNetV2. In comparison to other FCN models, the segmentation results show that DeepLabv3+ architecture is more efficient in working with plant leaf images that have complex backgrounds. Significantly, the proposed DeepLabv3+-MobileNetV2 segmentation model exhibited higher global accuracy of 99.713%, mean accuracy of 99.708%, mean IoU of 97.47%, Dice similarity index of 98.719%, mean weighted IoU of 97.544%, and mean BFScore of 96.899%. The results show that the proposed DeepLabv3+-MobileNetV2 model outperforms the remaining FCN models in case 2, i.e., using data augmentation on the training set.

Under realistic conditions like variable illumination and overlapping and occluded leaves, extracting leaf region will become more complicated, and the proposed method is one of the solutions to this problem. MobileNetV2 is a lightweight network with less computational complexity, so the proposed semantic segmentation network (DeepLabv3+-MobileNetV2) can be easily implemented and run on mobile devices. Our future goal is to use these segmented leaf outcomes for disease detection and classification algorithms, designed using deep learning techniques. Combining this leaf segmentation step for disease recognition algorithms may lead to less training time and greater accuracy.

Data Availability

The data used to support the findings of this study are available from the corresponding author upon request.

Conflicts of Interest

The authors declare that they have no conflict of interest.

References

- [1] J. Ranganathan, R. Waite, T. Searchinger, and C. Hanson, "How to sustainably feed 10 billion people by 2050, in 21 charts," 2018, <https://www.wri.org/insights/how-sustainably-feed-10-billion-people-2050-21-charts>.
- [2] A. S. Panayides, A. Amini, N. D. Filipovic et al., "AI in medical imaging informatics: current challenges and future directions," *IEEE Journal of Biomedical and Health Informatics*, vol. 24, no. 7, pp. 1837–1857, 2020.
- [3] F. Isensee, P. F. Jaeger, S. A. A. Kohl, J. Petersen, and K. H. Maier-Hein, "nnU-Net: a self-configuring method for deep learning-based biomedical image segmentation," *Nature Methods*, vol. 18, no. 2, pp. 203–211, 2021.
- [4] N. Ortega-Sánchez, E. Rodríguez-Esparza, D. Oliva et al., "Identification of apple diseases in digital images by using the gaining-sharing knowledge-based algorithm for multilevel thresholding," *Soft Computing*, vol. 26, no. 5, pp. 2587–2623, 2022.
- [5] A. Inés, C. Domínguez, J. Heras, E. Mata, and V. Pascual, "Biomedical image classification made easier thanks to transfer and semi-supervised learning," *Computer Methods and Programs in Biomedicine*, vol. 198, article 105782, 2021.
- [6] N. S. Chandel, S. K. Chakraborty, Y. A. Rajwade, K. Dubey, M. K. Tiwari, and D. Jat, "Identifying crop water stress using deep learning models," *Neural Computing and Applications*, vol. 33, no. 10, pp. 5353–5367, 2021.
- [7] S. Grigorescu, B. Trasnea, T. Cocias, and G. Macesanu, "A survey of deep learning techniques for autonomous driving," *Journal of Field Robotics*, vol. 37, no. 3, pp. 362–386, 2020.
- [8] G. Cerutti, L. Tougne, A. Vacavant, and D. Coquin, "A parametric active polygon for leaf segmentation and shape estimation," *Advances in Visual Computing*, vol. 6938, pp. 202–213, 2011.
- [9] J. C. Neto, G. E. Meyer, and D. D. Jones, "Individual leaf extractions from young canopy images using Gustafson-Kessel clustering and a genetic algorithm," *Computers and Electronics in Agriculture*, vol. 51, no. 1–2, pp. 66–85, 2006.
- [10] X.-F. Wang, D.-S. Huang, X. Du, H. Xu, and L. Heutte, "Classification of plant leaf images with complicated background," *Applied Mathematics and Computation*, vol. 205, no. 2, pp. 916–926, 2008.
- [11] S. Talasila, K. Rawal, G. Sethi, and M. S. S. Sanjay, "Black gram plant leaf disease (BPLD) dataset for recognition and classification of diseases using computer-vision algorithms," *Data in Brief*, vol. 45, article 108725, 2022.
- [12] M. Minervini, M. M. Abdelsamea, and S. A. Tsafaris, "Image-based plant phenotyping with incremental learning and active contours," *Ecological Informatics*, vol. 23, pp. 35–48, 2014.
- [13] Ş. Öztürk and B. Akdemir, "Automatic leaf segmentation using grey wolf optimizer-based neural network," in *2017 Electronics*, pp. 1–6, Palanga, Lithuania, 2017.
- [14] X. Yin, X. Liu, J. Chen, and D. M. Kramer, "Joint multi-leaf segmentation, alignment, and tracking for fluorescence plant videos," *IEEE Transactions on Pattern Analysis and Machine Intelligence*, vol. 40, no. 6, pp. 1411–1423, 2018.
- [15] J. P. Kumar and S. Domnic, "Image based leaf segmentation and counting in rosette plants," *Information Processing in Agriculture*, vol. 6, no. 2, pp. 233–246, 2019.
- [16] R. Khan and R. Debnath, "Segmentation of single and overlapping leaves by extracting appropriate contours," in *Proceedings of the 6th International Conference on Computer Science, Engineering and Information Technology (CSEIT-2019)*, Zurich, Switzerland, 2019.
- [17] S. Jeyalakshmi and R. Radha, "A novel approach to segment leaf region from plant leaf image using automatic enhanced grab cut algorithm," *CompuSoft: An International Journal of Advanced Computer Technology*, vol. 8, no. 11, 2019.
- [18] B. M. Patil and B. Amarapur, "Cotton leaf image segmentation using modified factorization-based active contour method," *International Journal of Advanced Computer Science and Applications (IJACSA)*, vol. 11, no. 9, 2020.
- [19] L. Ngugi, M. Abdelwahab, and M. Abo-Zahhad, "Tomato leaf segmentation algorithms for mobile phone applications using deep learning," *Computers and Electronics in Agriculture*, vol. 178, article 105788, 2020.
- [20] K. Yang, W. Zhong, and F. Li, "Leaf segmentation and classification with a complicated background using deep learning," *Agronomy*, vol. 10, no. 11, p. 1721, 2020.
- [21] Y. Xiong, L. Liang, L. Wang, J. She, and M. Wu, "Identification of cash crop diseases using automatic image segmentation algorithm and deep learning with expanded dataset," *Computers and Electronics in Agriculture*, vol. 177, article 105712, 2020.
- [22] X. Yang, A. Chen, G. Zhou et al., "Instance segmentation and classification method for plant leaf images based on ISCMRCNN and APS-DCCNN," *IEEE Access*, vol. 8, pp. 151555–151573, 2020.
- [23] M. Trivedi and A. Gupta, "Automatic monitoring of the growth of plants using deep learning-based leaf segmentation," *International Journal of Applied Science and Engineering*, vol. 18, article 2020281, 2021.
- [24] C. Hou, J. Zhuang, Y. Tang et al., "Recognition of early blight and late blight diseases on potato leaves based on graph cut segmentation," *Journal of Agriculture and Food Research*, vol. 5, article 100154, 2021.
- [25] B. Jibrin, H. Bello-Salau, I. J. Umoh, A. J. Onumanyi, A. T. Salawudeen, and B. Yahaya, "Development of hybrid automatic segmentation technique of a single leaf from overlapping

Retraction

Retracted: Smart Grid Security Based on Blockchain with Industrial Fault Detection Using Wireless Sensor Network and Deep Learning Techniques

Journal of Sensors

Received 12 December 2023; Accepted 12 December 2023; Published 13 December 2023

Copyright © 2023 Journal of Sensors. This is an open access article distributed under the Creative Commons Attribution License, which permits unrestricted use, distribution, and reproduction in any medium, provided the original work is properly cited.

This article has been retracted by Hindawi, as publisher, following an investigation undertaken by the publisher [1]. This investigation has uncovered evidence of systematic manipulation of the publication and peer-review process. We cannot, therefore, vouch for the reliability or integrity of this article.

Please note that this notice is intended solely to alert readers that the peer-review process of this article has been compromised.

Wiley and Hindawi regret that the usual quality checks did not identify these issues before publication and have since put additional measures in place to safeguard research integrity.

We wish to credit our Research Integrity and Research Publishing teams and anonymous and named external researchers and research integrity experts for contributing to this investigation.

The corresponding author, as the representative of all authors, has been given the opportunity to register their agreement or disagreement to this retraction. We have kept a record of any response received.

References

- [1] M. Kandasamy, S. Anto, K. Baranitharan, R. Rastogi, G. Satwik, and A. Sampathkumar, "Smart Grid Security Based on Blockchain with Industrial Fault Detection Using Wireless Sensor Network and Deep Learning Techniques," *Journal of Sensors*, vol. 2023, Article ID 3806121, 13 pages, 2023.

Research Article

Smart Grid Security Based on Blockchain with Industrial Fault Detection Using Wireless Sensor Network and Deep Learning Techniques

Manivel Kandasamy,¹ S. Anto,² K. Baranitharan,³ Ravi Rastogi,⁴ Gunda Satwik,⁵
and A. Sampathkumar ⁶

¹UnitedWorld School of Computational Intelligence, Karnavati University, Gandhinagar, Gujarat 382422, India

²School of Computer Science and Engineering, Vellore Institute of Technology, Vellore, India

³Department of ECE, Alva's institute of Engineering & Technology, Mangalore, Karnataka, Affiliated to VTU, India

⁴Department of CSE, Koneru Lakshmaiah Education Foundation, Vaddeswaram, AP, India

⁵Department of Computer Science and Engineering, Graphic Era Deemed to Be University, Dehradun, India

⁶Department of Computer Science and Engineering, Dambi Dollo University, Dambi Dollo, Ethiopia

Correspondence should be addressed to A. Sampathkumar; dr.sampathkumar@dadu.edu.et

Received 19 September 2022; Revised 12 December 2022; Accepted 20 April 2023; Published 9 May 2023

Academic Editor: C. Venkatesan

Copyright © 2023 Manivel Kandasamy et al. This is an open access article distributed under the Creative Commons Attribution License, which permits unrestricted use, distribution, and reproduction in any medium, provided the original work is properly cited.

Low-cost monitoring and automation solutions for smart grids have been made viable by recent advancements in embedded systems and wireless sensor networks (W.S.N.s). A well-designed smart network of subsystems and metasystems known as a “smart grid” is aimed at enhancing the conventional power grid’s efficiency and guaranteeing dependable energy delivery. A smart grid (S.G.) requires two-way communication between utility providers and end users in order to accomplish its aims. This research proposes a novel technique in enhancing the smart grid security and industry fault detection using a wireless sensor network with deep learning architectures. The smart grid network security has been enhanced using a blockchain-based smart grid node routing protocol with IoT module. The industrial analysis has been carried out based on monitoring for fault detection in a network using Q-learning-based transfer convolutional network. The experimental analysis has been carried out in terms of bit error rate, end-end delay, throughput rate, spectral efficiency, accuracy, M.A.P., and RMSE. The proposed technique attained bit error rate of 65%, end-end delay of 57%, throughput rate of 97%, spectral efficiency of 93%, accuracy of 95%, M.A.P. of 55%, and RMSE of 75%. This proposed paradigm is advantageous for the operation of smart grids for increased security and industrial fault detection across the network because security is the biggest barrier in smart grid implementation.

1. Introduction

Due to its portability, affordability, and ease of deployment, WSN is one of the best approaches for many real-time applications. Monitoring the area of interest, gathering data, and sending it to BS for postprocessing and analysis are the duties of the WSN [1]. Some WSN implementations make use of a lot of sensor nodes. Additionally, the battery life and memory of these wireless nodes are constrained. Therefore, in order to maximise the benefits of these WSNs, these

WSN nodes must have a management system capable of controlling both their interactions with one another and with the access point. For instance, the Internet Engineering Team (IETF) established the ZigBee and 6LoWPAN protocols for common transmission over IEEE 802.15.4 [2] to allow administration of WSNs. These protocols allow for the usage of IEEE 802.15.4 in 2.4 GHz band and the support of brief transmissions by contemporary management systems. For instance, based on IP addresses on various tiers, 6LoWPAN IPv6 offers a connection between WSNs. The

network architecture is also mapped using the 6LoWPAN Low Power and Loss Network (RPL) standard, and WSN connection is secured using the AES encryption technique [3]. These networks' dynamic topologies, however, will affect network routing tactics, delay, multilayer design, coverage, QoS, and fault detection. As part of the smart grid revolution, the electrical grid is being changed. An automated and widely dispersed energy generating, transmission, and distribution network is known as a "smart grid." It is distinguished by a full duplex network with a two-way flow of information and electricity. It is a closed-loop monitoring and reaction system [4]. Many organisations around world, including NIST (National Institute of Standards and Technology), IEEE (Institute of Electrical and Electronics Engineers), ETP (European Technology Platform), IEC (International Electro technical Commission), and EPRI (Electric Power Research Institute), are developing and conceptualising the smart grid. These organisations are also diligently researching the harmonisation of numerous standards and a wide range of standards. It is defined in a variety of ways depending on how useful, technological, or functional it is. As per definition represented by U.S. Department of Energy, "A smart grid uses digital technology to improve reliability, security, and efficiency (both economic and energy) of the electric system from large generation, through the delivery systems to electricity consumers and a growing number of distributed-generation and storage resources" [5]. The power grid (PG) can be made more dependable, adaptable, efficient, and durable through the use of smart grid technology, which integrates electrical, informational, and communication technologies. It is an intelligent PG that incorporates a variety of renewable and alternative energy sources. Key components of a SG implementation include automated monitoring, data collecting, control, and developing communication methods. Utilizing a wide range of communication standards necessitates analysis and optimization based on requirements and limits. These specifications are chosen based on factors including bandwidth needs, application kind, and coverage area. According to applications of communication methods at different levels of SG deployment, the hierarchical communication network for SG may be divided into 3 methods: HAN (home area network), NAN (neighbourhood area network), and WAN (wide area network). Global effect of ML and DL methods is growing and looking positive. The original use of ML and DL was in the condition monitoring of electric machinery. Emerging models offer reliable and precise measurements for fault prediction in rolling bearings and electric machinery. Applications can also be found in supply chains and logistics. A supply chain that is connected will change and accommodate new information as it is supplied. A linked method can proactively respond to that reality and shift manufacturing priorities if a shipment is associated to a weather delay. Another industry where ML and DL methods are used is transportation. Secure IoT methods are also being developed to store and handle massive data from scalable sensors for health care applications. Another platform for applying ML and DL models is smart grids [6].

Contribution of this research is as follows:

- (1) To propose novel method in enhancing the smart grid security and industry fault detection using wireless sensor network with deep learning architectures
- (2) The smart grid network security has been enhanced using blockchain-based smart grid node routing protocol with IoT module
- (3) The industrial analysis has been carried out based on monitoring for fault detection in network using Q-learning-based transfer convolutional network

The organisation of this article is as follows: Section 2 gives the related works, the proposed technique is described in Section 3, Section 4 explains the performance analysis, and the conclusion is given in Section 5.

2. Related Works

The following are the main issues in a smart city: smart grids in smart buildings, smart classrooms, traffic monitoring, education and classrooms, waste management, governance, environment monitoring, health care in hospitals, agriculture, industrial IoT, etc. We will now map each smart city issue with solution offered by WSN-IoT ML methods. In field of machine learning, WSN node localization issue is regarded as a classification or multivariate regression problem. To address node localization issues in WSN-IoT, SVM classification [7] or SVM regression method [8] methods are used. Correlation techniques and the Bayesian learning methodology are used to address security challenges, as shown in [9]. In the ML domain, clustering tasks in the WSN-IoT are referred to as cluster head selection tasks. For clustering, k-NN, PCA, and ANN have all been employed. In the ML field, WSN node energy management is seen as a prediction issue. Energy difficulties have been predicted using Q-learning [10]. Similar to this, energy harvesting-based WSN (EH-WSN) uses reinforcement learning methods like Q-learning, SARSA, and deep Q-learning to forecast future energy availability [11]. Problems with fault detection and event monitoring are regarded as classification models. SVM [12] and rule-based learning [13] techniques are used to resolve this. The approach proposed by work [14] employs RSSI to forecast the link quality. Author [15] uses RSSI calibration to enhance measurement quality; however, because this method may increase computational complexity, it is not appropriate for low-cost WSNs. LQI can, however, be utilized to find high-quality links when it is very high [16]. Otherwise, LQI has trouble determining if a link is of good quality or not. A Kalman filter-based LQP approach is proposed by the author in [17]. To gather smooth value of SNR, they filter RSSI and eliminate noise floor. ANNs are used in several manufacturing processes, such as process control and the production of semiconductors. Additionally, ANNs were used in [18–20] to predict as well as evaluate machine specification data, such as machine geometry and design, motor performance, range, and cost. Exhaustiveness, comparable incentive structure

with an untraceability characteristic, exhaustiveness, and the compact outcomes of a different neural network technique are measured empirically to determine the success of the suggested model [21, 22]. The processing and data transfer of physical processes is known as the cyberphysical system (CPS) [23]. Advancement in artificial neural networks (ANNs) was also utilized to predict and estimate jet engine component manufacturing costs during the early design phase [24]. Last but not least, ANNs were employed to monitor machine tools in real time [25].

More expensive nodes want greater rewards for accomplishing transactions in a business which work with the code of demand and supply [26]. Smaller ledger: this could affect the security and the immutability of the blockchain and all the data stored in it. Slower transactions: transactions could be slower than usual process even with the absence of third parties. Transaction expenses and speed of network: the transaction charge of the blockchain technology is rather high after being advertised as “nearly free” during the first few years. Analysis of variance (ANOVA) and back propagation neural networks (BPNN) with feed-forward architecture are two techniques for locating approximations and the optimum fit for optimization and search issues [27]. To evenly distribute traffic across these sensor nodes, several routing protocols must be developed [28]. The purpose of this review is to give readers a greater understanding of the function and application of security-based architecture in various approach. It will therefore help us assess the size of our problem.

3. System Model

This section discusses novel technique in enhancing the smart grid security and industry fault detection using wireless sensor network with deep learning architectures. The smart grid network security has been enhanced using blockchain-based smart grid node routing protocol with IoT module. The industrial analysis has been carried out based on monitoring for fault detection in network using Q-learning-based transfer convolutional network. The proposed blockchain-based smart grid sensor network architecture is shown in Figure 1.

3.1. Blockchain-Based Smart Grid Node Routing Protocol with IoT Module. Figure 2 displays the network model taken into consideration in this study. In this paradigm, a smart metre (SM_i) is connected to a number of consumers, and a service provider (SP_j) is connected to a number of smart metres. Peer-to-peer (P2P) service provider networks, often known as P2P SP networks, are created by a collection of service providers. All installed smart metres SM_i and service providers SP_j must be registered with a trustworthy registration authority (RA) in offline mode. The RA conducts the registration procedure in a secure manner. Smart metres SM_i and service providers SP_j interact securely using a session key they establish among themselves with the use of an access control mechanism, whereas users and smart metres SM_i communicate via secure communication. The SP network’s service providers additionally create private

pairwise keys among themselves for their secure connections. In accordance with this network paradigm, SM_i surreptitiously collects data from its affiliated users before bringing it to the service provider SP_j , with whom the smart metres SM_i are registered. Using the information gathered, SP_j then builds a block of transactions. Once the service providers in the SP network have reached consensus, the newly produced block can be added to the blockchain that already exists.

When estimating IoT device energy usage, we need take into account both receiving and delivering energy. Let $E_{Trans}(n, d)$ represent the price of sending n bits of data over d metres, and let $E_{Rev}(n)$ represent the price of receiving n bits of data over d metres. For sending n bits using

$$E_{Trans}(n, d) = \begin{cases} E_{Embwo} * n + E_{Amp} * n * d^2, & d \leq d_0, \\ E_{Embwo} * n + E_{Amp} * n * d^4, & d > d_0. \end{cases} \quad (1)$$

For receiving n bits by

$$E_{Rev}(n) = E_{Embb} * d. \quad (2)$$

IoT device energy consumption is calculated using

$$E_{sleep}(t) = E_{low} * t, \quad (3)$$

where flow represents the power used by any device during a single second of sleep. T seconds are spent in sleep mode in total. Each IoT device in the network uses up equivalent to

$$E_{Total} = E_{Trans}(n, d) + E_{Rece}(n) + E_{sleep}(t). \quad (4)$$

The distance formula uses the space taken up by data as it travels from the CH to the sink and distance covered by data packets as they go from sink to the cluster node. Distance should fall between 0 and 1. The normalisation is finished as a result. The distance metric is normalised using the denominator $\sum_{k=1}^m \sum_{i=1}^n |N_k^n - N_i^h|$. When the distance between the CH and normal node is great, as illustrated in equation (5), the distance parameter receives a substantial value. Route discovery of packets in the networks is represented in Algorithm 1.

$$F_i^d = \frac{\sum_{k=1}^m \sum_{l=1}^n |N_k^n - N_l^h| + |N_i^h - N^s|}{\sum_{k=1}^m \sum_{i=1}^n |N_k^n - N_i^h|}, \quad (5)$$

where m represents all of the network’s nodes and h represents total number of CHs. The symbols for sink node, normal node, and CH node are N^s , N^n , and N^h . Maximise problem becomes a minimising problem by eliminating the cumulative energies from one, as shown in (9). Energy is the most important measure, and it may be estimated by figuring out how much energy each node still has. By calculating cumulative cluster energy as well as total

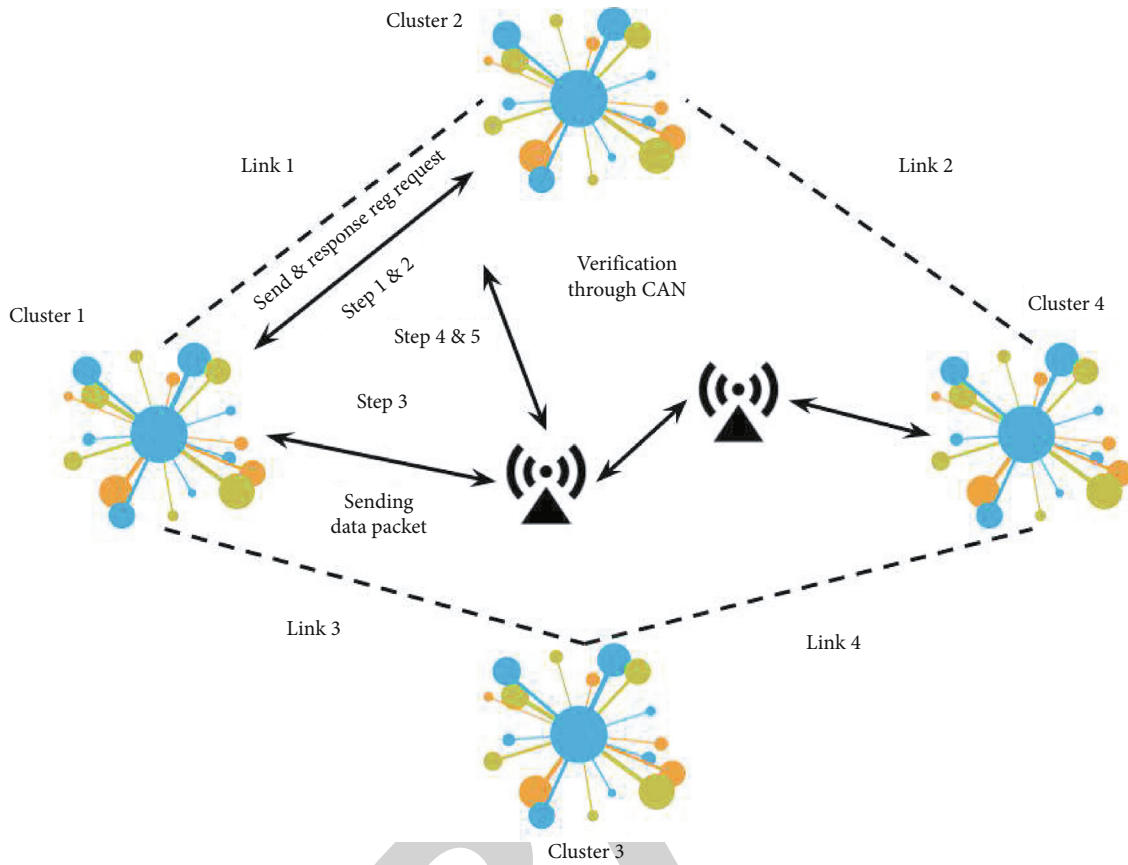


FIGURE 1: Blockchain-based smart grid sensor network architecture.

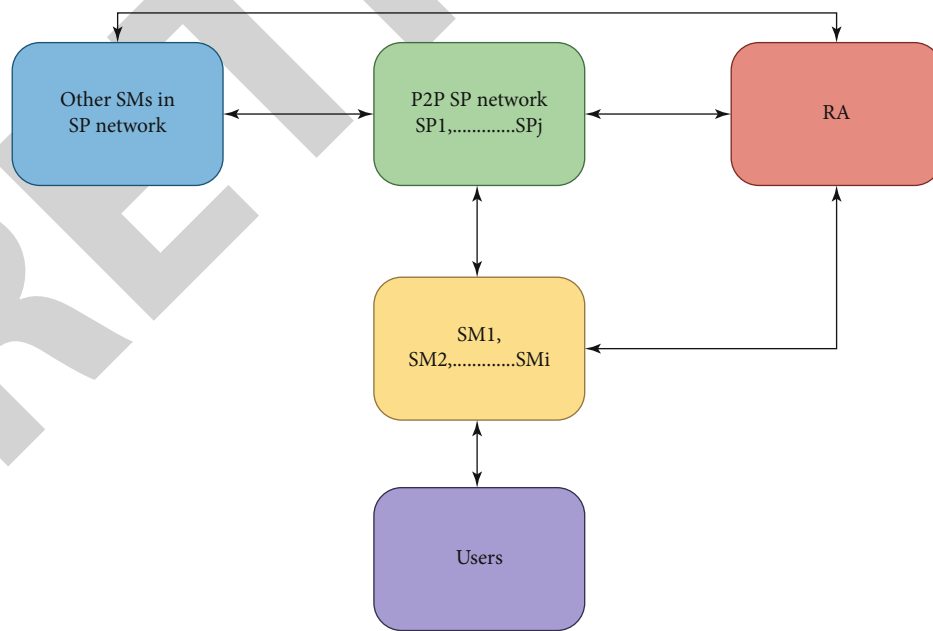


FIGURE 2: Blockchain-based IoT-enabled smart grid flow chart.

energy from all clusters, remaining energy is determined. The modelled energy metric is displayed in

$$F_i^* = \frac{\sum_{c=1}^h N_c^E(t)}{h \times \text{Max}_{l=1}^h [\varepsilon(N_l^n)] \times \text{Max}_{l=1}^h [\varepsilon(N_l^H)]}, \quad (6)$$

$$N_c^E(l) = \sum_{k=1}^m [1 - \varepsilon(N_k^n) * \varepsilon(N_l^H)], \quad (1 \leq l \leq h).$$

The node with the highest energy will be regarded as the ideal CH. The symbol for the total energy associated with CH is $\sum_{l=1}^h N_c^E(t)$. Maximum energy represented by CH and other nodes plus sum of all CHs is expressed as $h \text{Max}_{l=1}^h [\varepsilon(N_l^n)] \times \text{Max}_{l=1}^h [\varepsilon(N_l^H)]$. The denominator can only show a maximum value of 1. When choosing the best CH, the network delay must be minimised, and all cluster members are immediately affected. The network delay increases by equation (7) if the number of cluster members rises.

$$F_i^\delta = \frac{\text{Max}_{l=1}^h (C_{ml}^H)}{m}. \quad (7)$$

The network's i^{th} CH is represented by the letters C , H , m , and l . The delay value might range between 0 and 1. A minimum level of traffic density must be maintained to ensure an efficient network. The key factors affecting traffic density are packet loss, channel load, and buffer usage. The

traffic density by equation (8) is determined by the average of these three metrics.

$$F_i^l = \frac{1}{3} [B_{ut} + P_{dr} + C_l]. \quad (8)$$

The best CH is believed to be the node with the most energy, shortest distance to the sink node, lowest traffic density, and shortest delay. Following the manta rays that came before it, each one swims in the direction of the best plankton. Each person updates their position based on the best answer found. In equation (9), the charging foraging model is illustrated.

$$x_i^d(t+1) = \begin{cases} x_i^d(t) + r \cdot (x_{\text{best}}^d(t) - x_i^d(t)) + \alpha \cdot (x_{\text{bett}}^d(t) - x_i^d(t)), & i = 1, \\ x_i^d(t) + r \cdot (x_{i-1}^d(t) - x_i^d(t)) + \alpha \cdot (x_{\text{best}}^d(t) - x_i^d(t)), & i = 2, \dots, N, \end{cases} \quad (9)$$

where d and t stand for dimension and iteration number, and $\alpha = 2 \cdot r \cdot p \cdot |\log(r)|$. Random vector whose value ranges from $[0, 1]$ is r , while position of i^{th} individual is $x_i^d(t)$. denotes weight coefficient. The cluster formations are represented in Algorithm 2.

Area with a higher concentration of plankton is shown as $x_{\text{best}}^d(t)$. $x_i^d(t)$ is used to denote the updated position of individual i . Then, the participants are engaged in a spiral path, which is modelled in

$$\begin{cases} X_i(t+1) = X_{\text{best}} + r \cdot (X_{i-1}(t) - X_i(t)) + e^{h\omega} \cdot \cos(2\pi\omega) \cdot (X_{\text{best}} - X_i(t)), \\ Y_i(t+1) = Y_{\text{best}} + r \cdot (Y_{i-1}(t) - Y_i(t)) + e^{\phi\omega} \cdot \sin(2\pi\omega) \cdot (Y_{\text{best}} - Y_i(t)), \end{cases} \quad (10)$$

where the random number in equation (10) is denoted by the symbol, whose value can fall anywhere between $[0, 1]$. The definition of mathematical expression for cyclone foraging in the $n - D$ dimension is as follows:

$$\beta = 2e^r \frac{Z_{\text{lngy}} - t_{+1}}{r} \cdot \sin(2\pi r_1), \quad (11)$$

where r_1 is a random number with a value that can be between 0 and 1. Each person conducts a random search using reference position. Cyclone foraging improves the exploratory capability while also achieving good exploitation. Each person must adjust their position rather than remain in the same one in order to arrive at the best answer. A new reference position is assigned to each person in order to accomplish this position change in

$$x_{\text{namd}}^d = Lb^d + r \cdot (Ub^d - Lb^d). \quad (12)$$

Equation (13) represents the RBM 1 mathematical model

$$N^2 = \{N_1^2, N_2^2, \dots, N_g^2, \dots, N_r^2\}, \quad (13)$$

$$G^2 = \{G_1^2, G_2^2, \dots, G_z^2, \dots, G_h^2\},$$

where hidden neuron g of RBM 1 is G_n^1 and N_m^1 denotes j^{th} input neuron. Both visible and hidden levels receive bias. The total number of neurons in hidden and input layers is denoted in RBM 1 by letters r and v in

$$G_n^1 = \kappa \left[\sigma_n^1 + \sum_m N_m^1 \times w_{mn}^1 \right], \quad (14)$$

where weight corresponding to hidden neuron n and input neuron m is w_{mn}^1 and bias supplied to n^{th} hidden layer of RBM 1 is N_r^2 . RBM 1 output is based on the DBN classifier's

```

Produce a Random Connected Graph
Start  $Ec_i$ 
Start maximum energy capacity value  $\max E_{caj}$ 
Start energy harvesting value  $E_H$ 
Start Activated Services Sact so
Start Objective Function to reduncum Periods = 0
node donumPeriods= numperiods +1
Solve Paths = MathematicalModel( $E_{ci}$ , Sact* $\theta$ , F)
for every  $i$ -node in Paths do
  Update  $E_{cc_i}$ 
end for
for every  $i$ -node in network do  $E_{c_i} = E_{c_i} - E_H$ 
end for
for every origin node do
  Determine a path  $P$  in Paths to transmit
  if  $P = \theta$  then
    Sect $^{\infty} = 0$ 
  end if
end for
end while
return numPeriods

```

ALGORITHM 1: Route discovery algorithm.

```

INPUT: CH sends  $CH_{info}$  packet packet to the CMs.
OUTPUT: CH sends Cluster member (CH) to the hub and TDMA slots to each CM.
Device  $a$  receives the  $CH_{info}$  packet from the Device  $\beta$ , where  $\beta \in CH$ 
 $CH_{info}f_0 : \langle CH_{info}f_0, ID_{\beta} \rangle$ 
Device  $a$  selects the CH with the maximum received signal intensity as its CH after receiving
all  $CH_{info}$  packets.
Device  $a$  sends the  $CH_{join}$  packet to the selected CH.
Device  $a$  receives the  $CH_{join}$  packet from the Device  $\beta$ , where  $\alpha \in CH$ 
 $CH_{join} : \langle CH_{join}, ID_{\beta}, ID_{CH} \rangle$ 
if ( $ID_{\alpha} = ID_{CH}$ ) then
  Device  $a$  sends the Cluster momier ( $\alpha$ ) to the hub after receiving all the  $CH_{join}$  packets.
  Device  $a$  sends the TDMA slots to each CM.
Else
  Discard the packet.
end if

```

ALGORITHM 2: Cluster formation algorithm.

input features. Then, RBM 2, which is specified in, receives the produced output as an input in

$$N^2 = \{N_1^2, N_2^2, \dots, N_g^2, \dots, N_r^2\}, \quad (15)$$

$$G^2 = \{G_1^2, G_2^2, \dots, G_z^2, \dots, g_h^2\},$$

where RBM 1 and RBM 2 layers' input and hidden neurons, respectively, are represented by A and G . The weight value derived from subsequent layers is denoted as equation (16) in RBM 2.

$$w^2 = \{w_{8R}^2\}. \quad (16)$$

In RBM 2, hidden neuron n and visible neuron n_0 are combined as $w_{mN'}^2$. The output of RBM 2 is given by

$$G_n^2 = \omega \left[\omega_n^2 + \sum_m N_m^2 \times w_{mN'}^2 \right] \forall N_m^2 \approx G_n^1. \quad (17)$$

3.2. Q-Learning-Based Transfer Convolutional Network Based on Monitoring for Fault Detection. Each batch of data, comprising action, reward, and state, is utilized to update Q table in Q-learning method. Entry $Q_k (S_k, a_k)$ in Q table is desirability of actions in finite sequence $A_{j \in J+}$ in relation to states in the finite sequence $(S_i)_{i \in I+}$. The central component of reinforcement learning consists of a system and an agent, as shown in Figure 1. The agent examines the current

state s_k at time step k before choosing action a_k from a list of possible actions (A). Based on an acceptable reward, the results of the chosen action a_k are scored (r_{k+1}, R). The agent determines whether the previous action was “good” or “poor” based on the reward’s worth. Utilizing the Q-learning method, the agent finds the best possible course of action to maximise expected value $E[]$ of discounted reward, which is determined by

$$J(r_k) = \mathbb{E} \left[\sum_{k=1}^{\infty} \theta^{k-1} r_k \right]. \quad (18)$$

When $\theta = 0$, the agent just examines the current reward; however, when approaches 1, the agent considers both the current and future rewards. This is represented by $\theta \in [0, 1]$ in equation (18). In this regard, the Q table will be updated based on the Q-learning method, which is given by equation (19), when the agent calculates action a_k and reward r_{k+1} with respect to state transition s_{k+1}

$$Q_k(s_k, a_k) = Q_{k-1}(s_k, a_k) + \eta_k(s_k, a_k) \times [r_{k+1} + \max_{\Delta_{k+1}} Q_{k-1}(s_{k+1}, a_{k+1}) - Q_{k-1}(s_k, a_k)]. \quad (19)$$

Notably, Q-learning method starts with a Q1 initialization (s_1, a_1). The Q table will then be modified in light of the observations. It is usual to employ a tolerance parameter with the condition $|Q_k - Q_{k-1}| \leq \delta$ to determine the minimal threshold for convergence. Actually, the agent’s decision-making is supported by this knowledge. The controller will select the action a_k as equation (20) at each time step.

$$a_k = (A_j)_{j \in J+j} j = \operatorname{argmax}(Q_k(s_{k+c})). \quad (20)$$

Equation (21) is the function that is used to determine the agent’s reward for moving from state s_k to state s_{k+1} .

$$r_{k+1} = \begin{cases} \frac{e(kT) - c(k+1)T}{e(kT)}, & |e((k+1)T)| < |e(kT)|, \\ -\xi, & |e((k+1)T)| < |c(kT)|. \end{cases} \quad (21)$$

The algorithm is able to reach the ideal Q table when $k \rightarrow \infty$. Additionally, systems often converge to their optimal solution with an acceptable tolerance δ for a limited value of k . For each agent I , dynamic of local neighbourhood tracking error is defined as

$$\varepsilon_i(k+1) = \sum_{j \in \mathcal{N}_i} e_{ij}(x_j(k+1) - x_i(k+1)) + b_i(x_0(k+1) - x_i(k+1)). \quad (22)$$

It can be further rewritten as

$$\varepsilon_i(k+1) = A\varepsilon_i(k) - (d_i + b_i)B_i u_i(k) + \sum_{j \in \mathcal{N}_i} e_{ij} B_j u_j(k). \quad (23)$$

The definition of local performance index for each agent I is

$$J_i(\varepsilon_i(k), u_i(k), u_j(k)) = \sum_{k=0}^{\infty} \gamma^k U_i(\varepsilon_i(k), u_i(k), u_j(k)). \quad (24)$$

With the utilitarian purpose, U_i is expressed as equation (25) for each agent I .

$$U_i(\varepsilon_i(k), u_i(k), u_j(k)) = \varepsilon_i^T(k) Q_{ii} \varepsilon_i(k) + u_i^T(k) R_{ii} u_i(k) + \sum_{j \in \mathcal{N}_i} u_j^T(k) R_{ij} u_j(k), \quad (25)$$

where $Q_{ii} \geq 0 \leq \mathbb{R}^{n \times n}$, $R_{ii} > 0 \in \mathbb{R}^{m_i \times m_i}$ and $R_{ij} > 0 \in \mathbb{R}^{m_i \times m_j}$ are all positive symmetric weighting matrices and $0 < \gamma \leq 1$ is a discount factor. Value function of every agent I is therefore described as equation (26) given fixed control ($u_i(l), u_j(l)$) of agent I and its neighbours.

$$V_i(\bar{\varepsilon}_i(k)) = \sum_{l=k}^{\infty} \gamma^{l-k} U_i(\varepsilon_i(l), u_i(l), u_j(l)),$$

$$\bar{\varepsilon}_i(k) = \begin{bmatrix} \varepsilon_i(k)^T & \varepsilon_{j_1}(k)^T & \varepsilon_{j_2}(k)^T & \cdots & \varepsilon_{j_p}(k)^T \end{bmatrix}^T$$

$$\in \mathbb{R}^{n \times (p+1)}; j_1, j_2, \dots, j_p \in \mathcal{N}_i, \quad (26)$$

where p is number of neighbours of agent I . Each agent’s performance is rated by local performance index (9). Local information is captured by value function for each agent I (11). As a result, value function’s solution structure is expressed in terms of local vector $i(k)$. We can derive by equation using equations (25) and (26) and

$$V_i(\bar{\varepsilon}_i(k)) = \sum_{l=k}^{\infty} \gamma^{l-k} U_i(\varepsilon_i(l), u_i(l), u_j(l))$$

$$= \sum_{l=k}^{\infty} \gamma^{l-k} \left(\varepsilon_i^T(l) Q_{ii} \varepsilon_i(l) + u_i^T(l) R_{ii} u_i(l) + \sum_{j \in \mathcal{N}_i} u_j^T(l) R_{ij} u_j(l) \right)$$

$$= \sum_{l=k}^{\infty} \gamma^{l-k} (\varepsilon_i^T(l) Q_{ii} \varepsilon_i(l) + \bar{u}_i^T(l) R_i \bar{u}_i(l)), \quad (27)$$

where control law of agent I ($u_i(l)$) and neighbouring agents’ control laws are included in the vector $u_j(l)$, i.e., $u_j(l)$ and $\bar{u}_i(l) [u_i(l)^T \ u_{j_1}(l)^T \ u_{j_2}(l)^T \ \cdots \ u_{j_p}(l)^T]^T$; $j_1, j_2, \dots, j_p \in \mathcal{N}_i$, R_i ,

Each agent's diagonal matrix, R_i , contains the diagonal entries R_{ii} and R_{ij} . We may find equation (14) and control law $\bar{u}_i(k) = -K_i \varepsilon_i(k)$ by using the following two equations:

$$\begin{aligned} V_i(\bar{\varepsilon}_i(k)) &= \sum_{l=k}^{\infty} \gamma^{l-k} (\varepsilon_i^T(l) Q_{ii} \varepsilon_i(l) + \bar{u}_i^T(l) R_i \bar{u}_i(l)) \\ &= \sum_{l=0}^{\infty} \gamma^l (\varepsilon_i^T(l+k) Q_{ii} \varepsilon_i(l+k) + \bar{u}_i^T(l+k) R_i \bar{u}_i(l+k)) \\ &= \sum_{l=0}^{\infty} \gamma^l \varepsilon_i^T(l+k) (Q_{ii} + K^T R_i K) \varepsilon_i(l+k). \end{aligned} \quad (28)$$

Dynamic of neighbourhood tracking error in a local setting can be rewritten as

$$\begin{aligned} \varepsilon_i(k+1) &= A \varepsilon_i(k) - (d_i + b_i) B_i u_i(k) + \sum_{j \in \mathcal{N}_i} e_{ij} B_j u_j(k) \\ &= A \varepsilon_i(k) + [-(d_i + b_i) B_i \quad e_{ij_1} B_{j_1} \quad e_{ij_2} B_{j_2} \quad \cdots \quad e_{ij_p} B_{j_p}] \\ &\quad \times [u_i(k) \quad u_{j_1}(k) \quad u_{j_2}(k) \quad \cdots \quad u_{j_p}(k)]^T \\ &= A \varepsilon_i(k) + B \bar{u}_i(k), \end{aligned} \quad (29)$$

where $j_1, j_2, \dots, j_p \in \mathcal{N}_i$. Substituting $\bar{u}_i(k) = -K_i \varepsilon_i(k)$ into equation (16), next equation is deduced by

$$\varepsilon_i(k+1) = (A - BK_i) \varepsilon_i(k) = K_{1i} \varepsilon_i(k), \quad (30)$$

where $K_{1i} = A - BK_i$.

The suggested approach should be conditional on features having similar distributions across domains to transfer knowledge from source domain to target domain. Using back propagation computation of the pretrained CNNs, an error minimization optimization method is used to overcome feature distribution mismatch. Maximum mean discrepancy, or MMD, was a widely used distance metric for comparing probability distributions between two domains in earlier literature. That is, $DS = \{X_S, X_T\}$ and $DT = \{X_T, P(X_T)\}$, respectively, represent datasets in source domain and target domain. In the meantime, $X_S = \prod_{nsi=1} \{X_{T_i}\}$ and $X_T = \prod_{nti=1} \{x_{T_i}\}$ with n_t samples. Equation (31) determines their MMDs:

$$\begin{aligned} \text{Mean}_H(X_S) &= \frac{1}{n_s} \sum_{i=1}^{n_s} H(x_s^i), \\ \text{Mean}_H(X_T) &= \frac{1}{n_t} \sum_{j=1}^{n_t} H(x_T^j), \end{aligned} \quad (31)$$

where $H(\cdot)$ is an RKHS and $\sup(\cdot)$ is supremum of aggregate (reproducing kernel Hilbert space). For evaluating

feature distribution difference of domain invariant features in this study, MMD is used. MMD (X_S, X_T) is taken into consideration as optimization objective to regularise weights of CNNs in order to attain similar distributions from two domains. A linear-time approximation of MMD is utilized by equation (32) in place of MMD due to computational expense of doing MMD calculation on feature embeddings. The transfer of cluster process by utilizing CL is represented in Algorithm 3.

$$\text{MMD}_1^2(X_S, X_T) = \frac{2}{M} \sum_{i=1}^{M/2} h_1(\mathbf{z}_i), \quad (32)$$

where $\mathbf{z}_i = (\mathbf{x}_{2i-1}^s, \mathbf{x}_{2i}^s, \mathbf{x}_{2j-1}^t, \mathbf{x}_{2j}^t)$ and $h_1(\mathbf{z}_i)$ is a kernel operator described on quad-tuple as follows by

$$h_1(\mathbf{z}_i) = k(x_{2i-1}^s, x_{2i}^s) + k(x_{2j-1}^t, x_{2j}^t) - k(x_{2i-1}^s, x_{2j}^t) - k(x_{2i}^s, x_{2j-1}^t). \quad (33)$$

While CNNs are being reweighted, the prediction error should also be kept to a minimum. Therefore, another optimization goal is the prediction error. $\text{MMDH}(X_S, X_T)$ and MSE can therefore be used to compute the overall loss. Normalisation is necessary since the value ranges of MSE and $\text{MMDH}(X_S, X_T)$ vary. Nadir and utopia points are used in this study to normalise the aforementioned goals. Lower bound of no. I goal, as determined by minimising objective as given by equation (34), is provided by the utopia point z_i^u :

$$z_i^u = \min f(i). \quad (34)$$

By maximising the objectives according to equation (35), nadir point z_i^N gives upper bound of objective number I :

$$z_i^N = \max_{1 \leq j < I} f(j), \quad (35)$$

where I represents how many objective functions there are in total. Equation (36) can be used to calculate the normalised MMD and MSE in accordance with equations (34) and (35):

$$\begin{aligned} \text{NMMD}_H &= \frac{(\text{MMD}_{H1}(X_S, X_T) - z_1^u)}{(z_1^N - z_1^u)}, \\ \text{NMSE} &= \frac{(\text{MSE} - z_2^u)}{(z_2^N - z_2^u)}, \end{aligned} \quad (36)$$

where NMMDH and NMSE are, respectively, normalised $\text{MMDH}(X_S, X_T)$ and MSE . Total loss function is the last.

```

Initialize  $X_i^s, X_i^t; Y_i^s \leftarrow 0$ ,
Evaluate initial kernel parameter list  $\sigma \sim [2^u], -1 \leq n \leq 12$ 
iteration = 0;
while training do
iteration = iteration + 1;
Evaluate  $i$  forward mini-batch predictions utilizing CNNs layers on target data
 $\varphi_i^t = \mathbf{W}_{CNN}(X_i^t) + \mathbf{B}_{CNN}$ 
Evaluate  $i$  forward feature embeddings for source and target domain batch:
 $\varphi_{s,l}(X_i^s) \leftarrow f(X_i^s, l)$ 
 $\varphi_{t,l}(X_i^t) \leftarrow f(X_i^t, l)$ 
Project feature embeddings  $\varphi(X_s)$  and  $\varphi(X_t)$  into RKHS with chosen Gaussian kernels  $N \sim (0, \sigma)$ 
 $h_l(\mathbf{z}_i) = k(\mathbf{x}_{2i-1}^s, \mathbf{x}_{2i}^s) + k(\mathbf{x}_{2j-1}^t, \mathbf{x}_{2j}^t) - k(\mathbf{x}_{2i-1}^s, \mathbf{x}_{2j}^t) - k(\mathbf{x}_{2i}^s, \mathbf{x}_{2j-1}^t)$ 
Select optimal kernel parameter  $\sigma \in \sigma$  to enhance distribution difference between embeddings
Evaluate layer-wise MMD as
 $MMD_i^2(s, t) = 2/M \sum_{i=1}^{M/2} h_l(\mathbf{z}_i)$ 
Evaluate mini-batch loss on  $i$  examples:
 $\mathcal{L}_{total}(X_s, X_t, Y^s, Y^t) = w_1 \text{MSE}(Y, Y^s) + (w_2/R) \sum_{r=1}^R MMD_i^2(X_s, X_t)_r$ 
End while

```

ALGORITHM 3: Algorithm of transfer CL.

TABLE 1: Comparative analysis of bit error rate.

Number of grids	EH_WSN	6LoWPAN	SMS_IFD_WSN_DL
50	56	52	45
100	59	55	48
150	63	59	51
200	66	62	53
250	68	63	55
300	71	65	56
350	75	69	59
400	79	71	61
450	81	73	63
500	83	75	65

The weighted sum of the two normalised targets by equation (37) can be used to determine loss.

$$\mathcal{L}_{total}(X_s, X_t, \hat{Y}, Y) = w_1 \cdot \text{NMMD}_H + w_2 \cdot \text{NMSE}, \quad (37)$$

where w_1 and w_2 are weights of two objectives and $\sum w_i = 1$. Weighting is used to compromise between task loss objective and MMD minimization. In light of this, these are set to $w_1, w_2 = [0.9, 0.1]$.

4. Experimental Analysis

A sample distribution grid made up of a 15 kV 485 MV grid and 400 V LV grids is simulated in order to test the planned services. Used grid is made up of buses on MV side, one of which is main HV/MV substation, 9 nodes connected to MV/LV 488 substations feeding residential loads. Radial operation of grid is constrained in experiments that follow. A reference case for tests is one of the branches that is

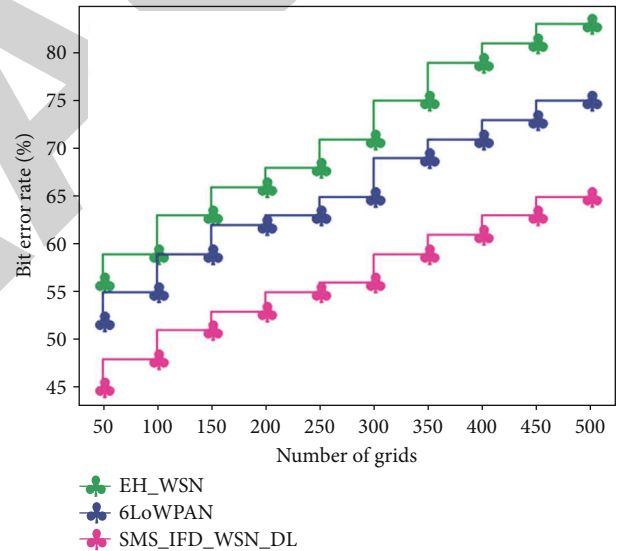


FIGURE 3: Comparative analysis of bit error rate.

regarded as normally open. However, potential to open or close any of the MV lines is taken into consideration while rating the Network Topology Reconfiguration service.

Table 1 and Figure 3 show comparative analysis between proposed and existing techniques in terms of BER. BER, which is typically stated as ten to a negative power, is the proportion of bits that are incorrect to the total amount of bits received during a transmission. The bit error ratio is evaluated by dividing total number of bits transferred over time period under consideration by number of bit mistakes. BER is a performance metric that has no units and is frequently stated as a percentage. Expected value of BER is known as the bit error probability. The proposed technique obtained BER of 65%, while existing technique EH_WSN attained 83% and 6LoWPAN attained 75%.

TABLE 2: Comparison of end-to-end delay.

Number of grids	EH_WSN	6LoWPAN	SMS_IFD_WSN_DL
50	45	42	38
100	48	45	39
150	51	48	42
200	53	51	43
250	55	55	45
300	59	58	49
350	63	62	51
400	66	64	53
450	69	65	55
500	75	72	57

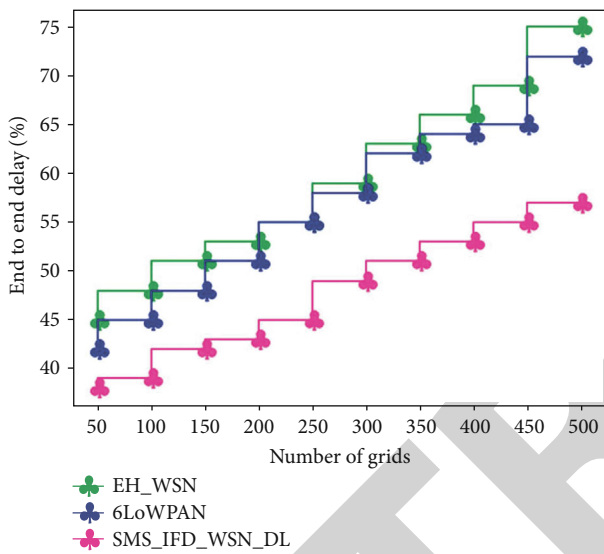


FIGURE 4: Comparison of end-to-end delay.

TABLE 3: Comparison of throughput rate.

Number of grids	EH_WSN	6LoWPAN	SMS_IFD_WSN_DL
50	70	75	79
100	72	77	81
150	75	79	83
200	77	81	85
250	79	83	88
300	81	85	90
350	83	88	92
400	85	89	94
450	88	91	96
500	89	93	97

From Table 2 and Figure 4, the comparison of end-end delay has been analysed between proposed and existing techniques. One-way delay (OWD), often known as end-to-end delay, is the amount of time it takes a packet to travel from source to destination across a network. This term, which is frequently used in IP network monitoring, varies from RTT in that it only measures the journey from source to

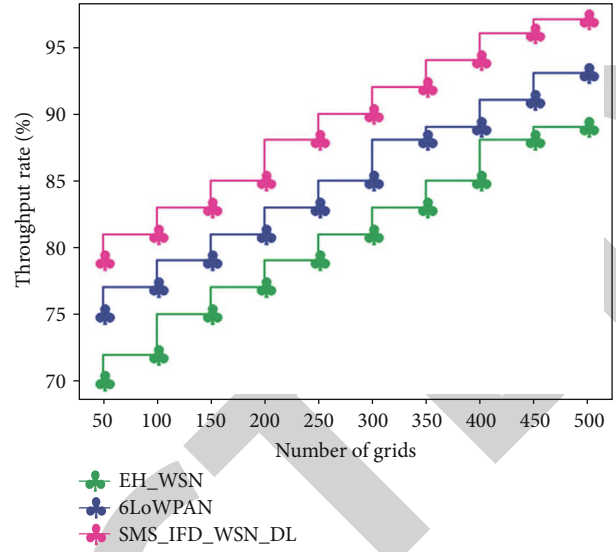


FIGURE 5: Comparison of throughput rate.

TABLE 4: Comparative analysis of spectral efficiency.

Number of grids	EH_WSN	6LoWPAN	SMS_IFD_WSN_DL
50	61	66	72
100	63	71	75
150	65	73	77
200	68	75	79
250	71	79	82
300	73	81	85
350	75	82	88
400	79	84	89
450	81	85	92
500	83	88	93

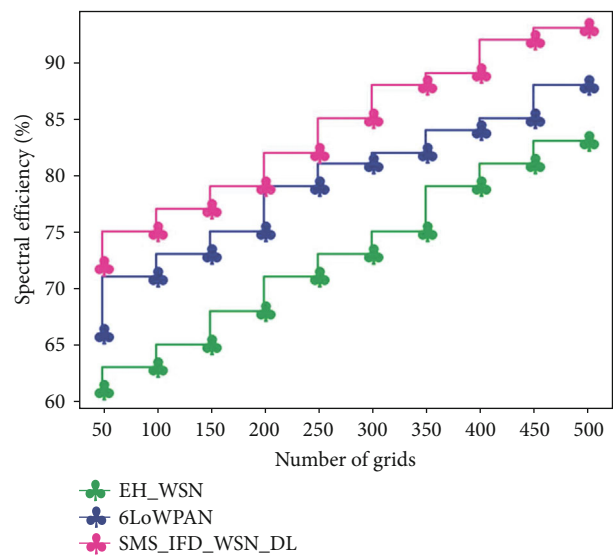


FIGURE 6: Comparative analysis of spectral efficiency.

TABLE 5: Comparison of accuracy.

Number of grids	EH_WSN	6LoWPAN	SMS_IFD_WSN_DL
50	60	65	72
100	63	66	75
150	65	69	79
200	66	72	81
250	71	74	83
300	73	78	85
350	75	79	88
400	79	81	91
450	81	83	92
500	83	85	95

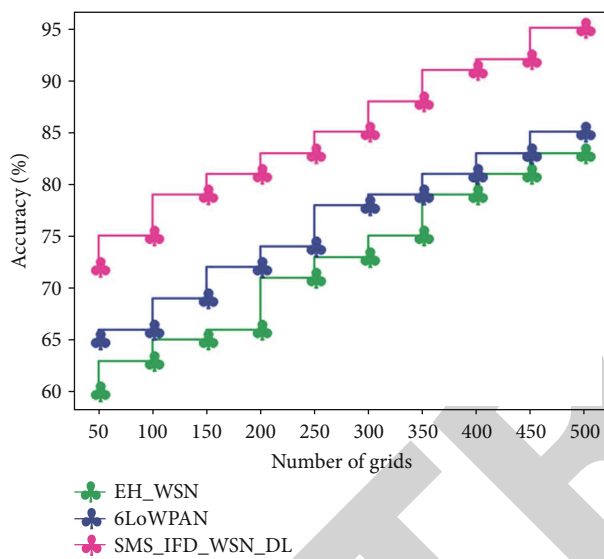


FIGURE 7: Comparison of accuracy.

TABLE 6: Comparison of RMSE.

Number of grids	EH_WSN	6LoWPAN	SMS_IFD_WSN_DL
50	65	62	55
100	68	65	56
150	71	66	58
200	73	72	59
250	77	75	62
300	80	79	63
350	82	81	65
400	84	83	71
450	86	85	73
500	89	88	75

destination in a single direction. The proposed technique obtained end-to-end delay of 57%, while existing technique EH_WSN attained 75% and 6LoWPAN attained 72%.

Table 3 and Figure 5 show comparative analysis between proposed and existing techniques in terms of throughput rate. There are several ways to calculate the throughput efficiency formula, but the fundamental formula is $I = R * T$. In

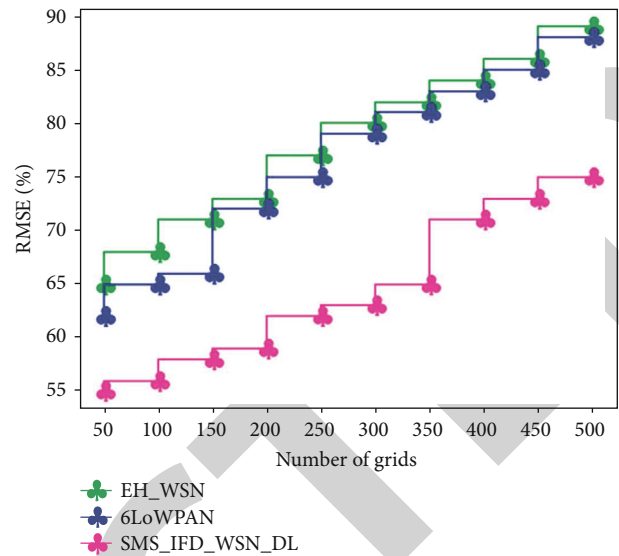


FIGURE 8: Comparison of RMSE.

TABLE 7: Comparative analysis of MAP.

Number of grids	EH_WSN	6LoWPAN	SMS_IFD_WSN_DL
50	45	42	36
100	48	44	38
150	49	46	39
200	52	49	41
250	54	51	43
300	58	53	45
350	61	55	49
400	63	57	51
450	66	61	53
500	69	63	55

other terms, when “rate” refers to the throughput, inventory is equal to rate times time. Throughput rate attained by proposed technique is 97%; existing EH_WSN obtained 89%, and 6LoWPAN obtained 93%.

Table 4 and Figure 6 show comparative analysis of spectral efficiency between proposed and existing techniques. The maximum amount of data that may be sent over a cellular network to a given number of users per second while preserving a reasonable level of service is referred to as spectral efficiency. When we talk about spectral efficiency, we often refer to the total spectral efficiency of all transmissions within a cellular network cell. It is expressed as bit/s/Hz. Bits/s/Hz (b/s/Hz) is the unit of measurement for spectral efficiency, which is a measure of how quickly data can be delivered within a designated bandwidth. There is a maximum theoretical spectral efficiency value for each type of modulation. Another significant element that affects spectral efficiency is SNR. Spectral efficiency attained by proposed technique is 93%; existing EH_WSN obtained 83%, and 6LoWPAN obtained 88%.

From Table 5 and Figure 7, the comparative analysis has been carried out in terms of accuracy between proposed

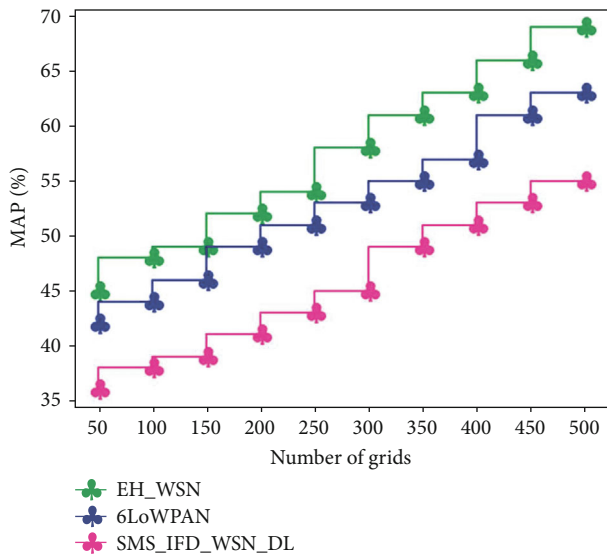


FIGURE 9: Comparative analysis of MAP.

and existing techniques. One parameter for assessing classification models is accuracy. Percentage of predictions that our method correctly predicted is called accuracy. It is one way to evaluate a model's performance, but by no means the only one. The proposed technique attained accuracy of 95%, existing EH_WSN obtained 83%, and 6LoWPAN obtained 85%.

Table 6 and Figure 8 show comparative analysis of RMSE between proposed and existing techniques. One of the methods most frequently utilized assess accuracy of forecasts is RMSE (root-mean-square deviation). It illustrates the Euclidean distance between measured true values and forecasts. The model can be deemed to be reasonably accurate in predicting the data if the RMSE values are between 0.2 and 0.5. Proposed method attained RMSE of 75%, existing EH_WSN obtained 89%, and 6LoWPAN obtained 88%.

Table 7 and Figure 9 show comparative analysis of MAP between proposed and existing techniques. Using a model and a prior probability or belief about the model, MAP entails computing a conditional probability of observing the data. For machine learning, MAP offers an alternative probability framework to maximum likelihood estimation. It uses the mean average precision (mAP). mAP evaluates a score by comparing detected box to ground-truth bounding box. Method detections are more precise in higher score. MAP attained by proposed technique is 55%; existing EH_WSN obtained 69%, and 6LoWPAN obtained 63%.

5. Conclusion

In this research, the proposed model is designed for improving the security of smart grid based on blockchain and routing. Here, the aim is to enhance the smart security using blockchain-based smart grid node routing protocol with IoT module. Then, the industrial analysis based on monitoring for fault detection using Q-learning-based transfer convolutional network is carried out. The seamless operation of energy management is ensured by smart grids, which

respond to home and industrial requests from the cloud server and send the precise amount of energy. Each demand is filtered out by a cloud server, which reports on any unusual energy requests made by customers. Additionally, it stores energy projection data that can be used for more thorough research. This paper outlines an infrastructure for deploying resource-limited controlled devices at various consumer locations. These devices will be connected to a cloud monitoring server using an IoT network to upload their current demands and alert them of future needs. The experimental analysis has been carried out in terms of bit error rate of 65%, end-end delay of 57%, throughput rate of 97%, spectral efficiency of 93%, accuracy of 95%, MAP of 55%, and RMSE of 75%. For future work, we will consider an edge computing enabled blockchain network in the smart grid, where energy nodes can access and utilize computing services from an edge computing service provider. This integration may help the energy nodes achieve optimal energy management policy.

Data Availability

The data used to support the findings of this study are available from the corresponding author upon request.

Conflicts of Interest

The authors declare that they have no conflict of interest

References

- [1] M. Marei, S. El Zaatari, and W. Li, "Transfer learning enabled convolutional neural networks for estimating health state of cutting tools," *Robotics and Computer-Integrated Manufacturing*, vol. 71, article 102145, 2021.
- [2] G. Arya, A. Bagwari, and D. S. Chauhan, "Performance analysis of deep learning-based routing protocol for an efficient data transmission in 5G WSN communication," *IEEE Access*, vol. 10, pp. 9340–9356, 2022.
- [3] R. K. Lenka, M. Kolhar, H. Mohapatra, F. Al-Turjman, and C. Altrjman, "Cluster-based routing protocol with static hub (CRPSH) for WSN-assisted IoT networks," *Sustainability*, vol. 14, no. 12, p. 7304, 2022.
- [4] C. Mu, Q. Zhao, Z. Gao, and C. Sun, "Q-learning solution for optimal consensus control of discrete-time multiagent systems using reinforcement learning," *Journal of the Franklin Institute*, vol. 356, no. 13, pp. 6946–6967, 2019.
- [5] S. Sengan, V. Subramaniaswamy, V. Indragandhi, P. Velayutham, and L. Ravi, "Detection of false data cyberattacks for the assessment of security in smart grid using deep learning," *Computers and Electrical Engineering*, vol. 93, article 107211, 2021.
- [6] T. Kotsiopoulos, P. Sarigiannidis, D. Ioannidis, and D. Tzovaras, "Machine learning and deep learning in smart manufacturing: the smart grid paradigm," *Computer Science Review*, vol. 40, article 100341, 2021.
- [7] S. Sivarajan and S. S. Jebaseelan, "Efficient adaptive deep neural network model for securing demand side management in IoT enabled smart grid," *Renewable Energy Focus*, vol. 42, pp. 277–284, 2022.

Retraction

Retracted: Key Technologies of Face Sensor Recognition Entry System for New Energy Vehicles Based on Particle Swarm Neural Network

Journal of Sensors

Received 12 December 2023; Accepted 12 December 2023; Published 13 December 2023

Copyright © 2023 Journal of Sensors. This is an open access article distributed under the Creative Commons Attribution License, which permits unrestricted use, distribution, and reproduction in any medium, provided the original work is properly cited.

This article has been retracted by Hindawi, as publisher, following an investigation undertaken by the publisher [1]. This investigation has uncovered evidence of systematic manipulation of the publication and peer-review process. We cannot, therefore, vouch for the reliability or integrity of this article.

Please note that this notice is intended solely to alert readers that the peer-review process of this article has been compromised.

Wiley and Hindawi regret that the usual quality checks did not identify these issues before publication and have since put additional measures in place to safeguard research integrity.

We wish to credit our Research Integrity and Research Publishing teams and anonymous and named external researchers and research integrity experts for contributing to this investigation.

The corresponding author, as the representative of all authors, has been given the opportunity to register their agreement or disagreement to this retraction. We have kept a record of any response received.

References

- [1] F. Li, X. Su, H. Zhao, R. Hu, and B. Shen, "Key Technologies of Face Sensor Recognition Entry System for New Energy Vehicles Based on Particle Swarm Neural Network," *Journal of Sensors*, vol. 2023, Article ID 3375744, 6 pages, 2023.

Research Article

Key Technologies of Face Sensor Recognition Entry System for New Energy Vehicles Based on Particle Swarm Neural Network

Fusong Li,¹ Xin Su ,² Haibin Zhao,¹ Ruixue Hu,¹ and Bingzhen Shen¹

¹Department of Automotive Engineering, Hebei Jiaotong Vocational and Technical College, Shijiazhuang, Hebei 050035, China

²Department of Computer & Information Engineering, Hebei Petroleum University of Technology, China

Correspondence should be addressed to Xin Su; 2018213205@mail.chzu.edu.cn

Received 23 September 2022; Revised 15 October 2022; Accepted 24 November 2022; Published 12 April 2023

Academic Editor: C. Venkatesan

Copyright © 2023 Fusong Li et al. This is an open access article distributed under the Creative Commons Attribution License, which permits unrestricted use, distribution, and reproduction in any medium, provided the original work is properly cited.

In order to solve the problem of high dimensionality and low recognition rate caused by complex calculation in face recognition, the author proposes a face recognition algorithm based on weighted DWT and DCT based on particle swarm neural network applied to new energy vehicles. The algorithm first decomposes the face image with wavelet transform, removes the influence of the diagonal component, the weighted low-frequency and high-frequency discrete cosine transform coefficients are extracted as feature vectors, and finally, the particle swarm optimization BP neural network is used for classification and identification. Experimental results show that when the wavelet weights take $a_0 = 0.9$, $a_1 = 0.05$, and $a_2 = 0.05$, the recognition rate reaches the highest. Regardless of whether the low-frequency component continues to increase or decrease, and the high-frequency component continues to decrease or increase, the recognition rate will decrease. When the eigenvector dimension is around 60, the recognition rate difference between the weighted wavelet algorithm and the general low-frequency wavelet algorithm reaches the maximum. The recognition rate of the proposed algorithm is much higher than the other two traditional algorithms. *Conclusion.* The effectiveness and feasibility of the algorithm are verified on the ORL face database.

1. Introduction

People's living standards have been steadily improved in the rhythm of faster social development, and the improvement of living standards has prompted people to have more and more needs for material functions. In today's society, almost every household has a car, which has become one of the necessities of life. In China, people's concept of cars has changed from "possible to own" to the pursuit of technology, comfort, and safety of cars. In the face of the huge demand for automobiles, many automobile companies have increased the research on these aspects; among which, the automobile antitheft technology that meets the scientific and technological requirements is one of the key research topics. Keyless entry (PKE, Passive Keyless Enter) is a mainstream car antitheft technology today, but the actual key is not completely removed and there is still a risk of vehicle theft if the car key is lost. In the development of the automobile industry, the number of electronic control systems on automobiles increases exponentially, which leads to a gradual

increase in the consumption of power loads by these electronic devices. Under the current social background, the biggest application challenge of the electronic control system in the car is that under the same battery power supply conditions, find ways to balance power load consumption with the ever-increasing number and functionality of automotive electronics. Among all the methods, reducing power consumption is the most effective method, so it is necessary to reduce the power consumption of the electronic control system as much as possible in practical automotive applications. As a hot research field in the 21st century, image recognition technology, it has always attracted the attention of all walks of life and has great potential for application value in the fields of natural disaster prediction, military target detection, biomedical diagnosis, pattern recognition research and development, etc. [1]. As a type of image recognition technology, face recognition technology is the most widely used in daily life; at present, technologies such as unlocking through face collection and catching fugitives through target detection are becoming more and more mature. It is precisely

because of the wide application of face recognition technology; as a result, it has gained more and more “plays” in people’s daily life, and the connection with the general public has become more and more close, as shown in Figure 1.

2. Literature Review

Le et al. proposed a face segmentation method (mainly applying the region growth method), which uses the Hough transform and edge detection and template matching techniques to obtain the segmented face; the features of facial organs, such as the eyebrows, eyes, and nose, are quickly and effectively extracted [2]. A. Kadum and J. Kadum proposed a face detection method that locates the facial features of grayscale images [3]. Gunawan and Halimawan used the self-organizing mapping algorithm to compress the large-scale face and nonface images into a small number of images for face detection. Learning these pictures, the multilayer perceptron is used to classify the faces and nonface parts [4]. In order to detect the frontal face image, the eyebrows, eyes, nose, and mouth are used as subtemplates, and the line segmentation is used as the basis to build a model. The lines of the input image are compared with the subtemplate using the maximum gradient change extraction. Detecting the candidate area of the face is done by using the correlation between the subcontour template and the image and comparing other subtemplates in the candidate area [5]. Guo et al. searched using a combination of multilayer perceptrons and intelligent algorithms, so as to locate the face [6]. This face localization method needs to use MLP to directly perceive the image and use the intelligent algorithm as the theoretical basis for agile search. Sun et al. proposed to select only three face images for each person, and the lighting conditions of these three face images are different, and use this image to calculate the matrix; using this method can eliminate the influence of illumination on the image [7].

In order to solve the shortcomings of traditional face recognition methods, the author proposes a particle swarm neural network algorithm based on weighted DWT and DCT for new energy vehicles. The weighted wavelet transform and discrete cosine transform are used for feature extraction, and then, the particle swarm optimization BP neural network is used for classification and identification. Experiments show that the method proposed by the author not only has fast operation speed but also has high recognition efficiency.

3. Research Methods

3.1. Weighted Wavelet Transform. Wavelet analysis is one of the important applications in the field of image processing, which is similar to Fourier analysis but better than Fourier analysis. Its essence is to decompose the mixed signal into different frequency bands with a set of high and low-pass filter families of different scales, which has the ability of multi-resolution and multiscale decomposition and is known as “mathematical microscope.” A two-dimensional face image is subjected to a wavelet transform, which can be decomposed to obtain 4 subimages whose size is 1/4 of the original

image size, as shown in Figure 2. The LL subband is the low-frequency component, the HL and LH subbands are the horizontal and vertical components, and the HH subband is the high frequency component. Its low-frequency components can also undergo two-dimensional wavelet transformation again and can be decomposed into four frequency band components, as shown in Figure 3—the image after a wavelet transform. Most of its energy information is concentrated in the low-frequency part, and the high frequency part contains a small amount of texture and edge information [8].

In order to distinguish the traditional wavelet algorithm, a weighted wavelet transform is proposed, which assigns different weights to each frequency band and then weights them for fusion. Since the HH band contains less information, more noise, poor stability, and does not use classification and identification, this is discarded, that is, the following:

$$F = a_0LL + a_1LH + a_2HL. \quad (1)$$

Among them, F is the weighted image after fusion, a_0 , a_1 , and a_2 are weighting coefficients, and $a_0 + a_1 + a_2 = 1$.

3.2. Discrete Cosine Transform. The discrete cosine transform DCT was developed from Fast Fourier. Its transform kernel is a real number, and its compression performance is second only to K-L transform; it has unique advantages in image compression and calculation speed. It is a commonly used orthogonal transform image compression method [9, 10].

For an $M \times N$ grayscale image $f(x, y)$, the discrete cosine transform is defined as the following:

$$g(u, v) = \& \frac{2}{\sqrt{MN}} c(u)c(v) \sum_{x=0}^{M-1} \sum_{y=0}^{N-1} f(x, y) \cos \frac{(2x+1)u\pi}{2M} \cos \frac{(2y+1)v\pi}{2N}. \quad (2)$$

Among them, $x, u = 0, 1, 2, \dots, M-1$; $y, v = 0, 1, 2, \dots, N-1$ is the frequency domain transform factor and $g(u, v)$ is the transformation result, that is, the DCT coefficient. $c(u)$ and $c(v)$ are defined as the following:

$$c(u) = \begin{cases} \frac{1}{\sqrt{2}}, & u = 0, \\ 1, & u = 1, 2, \dots, M-1, \end{cases} \quad (3)$$

$$c(v) = \begin{cases} \frac{1}{\sqrt{2}}, & v = 0, \\ 1, & v = 1, 2, \dots, N-1. \end{cases} \quad (4)$$

Its inverse discrete cosine transform (IDCT) is the following:

$$f(x, y) = \& \frac{2}{\sqrt{MN}} c(u)c(v) \sum_{u=0}^{M-1} \sum_{v=0}^{N-1} F(u, v) \cos \frac{(2x+1)u\pi}{2M} \cos \frac{(2y+1)v\pi}{2N}. \quad (5)$$



FIGURE 1: Particle swarm neural network for face sensing recognition of new energy vehicles.

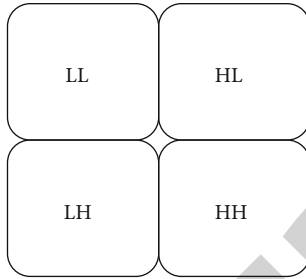
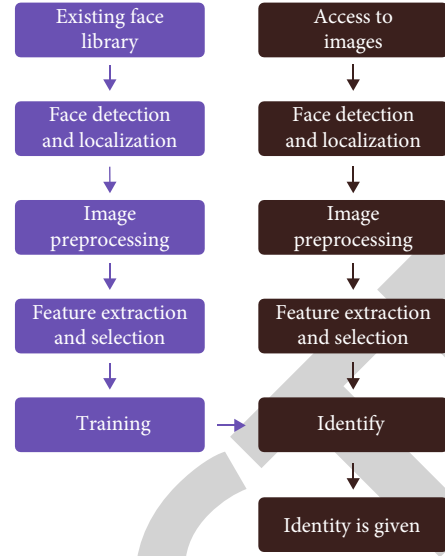


FIGURE 2: Schematic diagram of wavelet first-order decomposition.

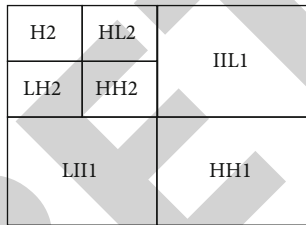


FIGURE 3: Schematic diagram of wavelet secondary decomposition.

It can be known from equations (1)–(5) that after DCT transformation, the obtained coefficient matrix is equal to the size of the original image. When the frequency domain transform factors u and v are large, the value of the DCT coefficient $g(u, v)$ is small; when u and v are small, the value of DCT coefficient $g(u, v)$ is large, and most of its energy is concentrated in the low-frequency part. The energy of the image transformed by DCT is mainly concentrated in the low-frequency part of the upper left of the image, which contains the main feature information of the image. Therefore, a new image similar to the original image can be reconstructed only by retaining part of the low-frequency information;

although there is a certain error between the two, the main information is retained after all [11].

3.3. Particle Swarm Optimization Neural Network Model

3.3.1. Particle Swarm Optimization Algorithm. Particle swarm optimization algorithm PSO (Particle Swarm Optimization) uses real numbers to solve; there is no crossover mutation in genetic algorithm, and fewer parameters need to be adjusted. It is an iterative optimization algorithm with strong global optimization ability and relatively simple calculation. The mathematical description of the PSO algorithm is as follows: in a D -dimensional search space, a population $x = (x_1, x_2, \dots, x_m)$ is composed of m particles. Assuming that the current number of iterations is t , the position of the i -th particle is $X_i^t = (x_{i1}^t, x_{i2}^t, \dots, x_{iD}^t)$, its velocity is $V_i^t = (v_{i1}^t, v_{i2}^t, \dots, v_{iD}^t)$, the individual optimal value is $p_i^t = (p_{i1}^t, p_{i2}^t, \dots, p_{iD}^t)$, and the group global optimal value is $p_g^t = (p_{g1}^t, p_{g2}^t, \dots, p_{gD}^t)$. Where $i = 1, 2, \dots, m$, t is the number of iterations.

Determine the current optimal value of the individual particle and the current optimal value of the group by evaluating the fitness of the particle individual and then update its own speed and position according to the following:

$$v_{id}^{t+1} = \omega v_{id}^t + c_1 r_1 (p_{id}^t - x_{id}^t) + c_2 r_2 (p_{gd}^t - x_{id}^t), \quad (6)$$

$$x_{id}^{t+1} = x_{id}^t + v_{id}^t. \quad (7)$$

In the formula, ω represents the inertia weight; c_1 and c_2 are learning factors; and r_1 and r_2 are random numbers between (0, 1). v_{id}^t and x_{id}^t are the velocity and position of particle i in the d -th dimension in the t -th iteration, respectively; p_{id}^t is the position of the individual extreme value of particle i in the d -th dimension; p_{gd}^t is the position of the

TABLE 1: The recognition rate of the author's algorithm under different weights.

Wavelet weights (a_0, a_1, a_2)	(0.7, 0.15, 0.15)	(0.75, 0.125, 0.125)	(0.8, 0.1, 0.1)	(0.85, 0.075, 0.075)	(0.9, 0.05, 0.05)	(0.95, 0.025, 0.025)
Recognition rate%	89.18	89.29	89.94	90.91	91.77	89.51

TABLE 2: Comparison of recognition rates of different algorithms.

Algorithm	Recognition rate%	Time (s)
Wavelet+DCT+BP	81.9	266.03
Weighted wavelet+DCT+BP	84.4	271.37
Author algorithm	91.8	132.49

global optimal extreme value of the population in the d -th dimension [12].

In addition, it is suggested that the value of ω should decrease linearly with the increase of the number of iterations, where the calculation formula of ω is the following:

$$\omega = \omega_{\max} - \frac{t}{t_{\max}} (\omega_{\max} - \omega_{\min}). \quad (8)$$

Among them, ω_{\max} and ω_{\min} are the maximum and minimum inertia weights, respectively, and t and t_{\max} are the current iteration number and the maximum iteration number, respectively.

3.3.2. Particle Swarm Optimization BP Neural Network. BP neural network is a multilayer forward neural network that adopts forward propagation and error back propagation and has good adaptability and classification and recognition capabilities. It mainly uses the steepest descent learning algorithm and continuously adjusts the weights and thresholds through error backpropagation to minimize the sum of squares of errors in the network, thereby improving the accuracy of the input mode. It mainly includes input layer, hidden layer, and output layer; the hidden layer can be one layer or multiple layers. The author adopts a three-layer network with only one hidden layer for classification and recognition.

The gradient descent algorithm of BP neural network requires the function to be differentiable and differentiable, and through the error backpropagation, it is prone to problems such as long training time, slow convergence speed, and easy to fall into local minima. The PSO algorithm can better avoid these problems; therefore, using PSO to optimize the BP neural network can further improve the generalization ability and recognition ability of the network [13].

The process of particle swarm optimization BP neural network is as follows:

- (1) First, initialize the parameters of the BP neural network and determine its topological structure, including the determination of the number of nodes in the input layer, the number of hidden layer nodes, and the number of nodes in the output layer. Then, initialize the particle swarm parameters, including particle population size, dimension, maximum number of iterations, learning factor, inertia weight, maximum velocity, maximum position, and the initial

velocity and position of randomly generated particles within the allowable range [14]

- (2) Calculate the particle fitness and take the mean square error between the actual output value and the expected output value of the neural network as the fitness J , as shown in the following

$$J = \frac{1}{2M} \sum_{i=1}^M \sum_{j=1}^N (y_{ji}^d - y_{ji})^2. \quad (9)$$

In the formula, M is the number of training samples, y_{ji}^d and y_{ji} are the ideal output value and actual output value of the j th network output node of the i th sample, respectively, and N is the number of output layer nodes.

- (3) For each particle individual, compare the fitness of the individual extreme value (pBest) with the current fitness of the individual. If the current fitness is good, then pBest is replaced, and similarly, the global extreme value (gBest) is also updated with the same judgment
- (4) According to formulas (6) and (7), update the speed and position of the particle within the allowable range to generate the next generation of particles
- (5) Increase the number of iterations by 1, go to step (2), until the maximum number of iterations is satisfied; the algorithm ends and the global optimal solution gBest is obtained, and the optimal solution is mapped to the initial weight and threshold of the BP neural network [15, 16].

4. Analysis of Results

The author uses the standard ORL face database provided by the University of Cambridge, UK. The database contains 400 images of 40 individuals, 10 images each, 112×92 pixels each, 256 grayscales. These images were taken at different times and contained different facial expressions, different lighting expressions, and different pose changes. According to the experimental design scheme mentioned above, the author adopts i5 processor with 4 GB of memory and 2 main frequency, the computer with 53 GHz; 32-bit operating system is used as a hardware device; and the software is compiled and simulated in the MATLAB R2009a environment, to mainly study the effectiveness of the algorithm proposed by the author and the relationship between the recognition rate and the training sample set [17].

In the experiment, the formula $S_2 = S_1 + 0.618 \times (S_1 - S_3)$ defined by the number of nodes in the hidden layer of the BP neural network is determined. Among them, $S_1, S_2,$

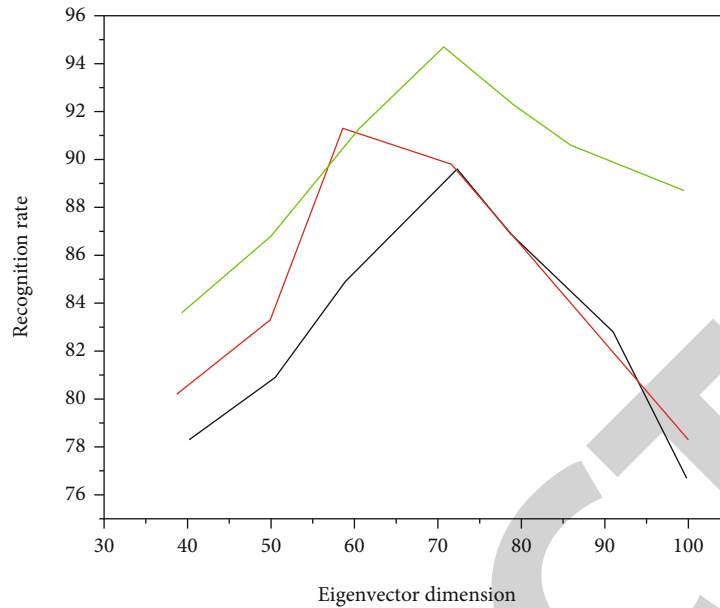


FIGURE 4: Comparison of recognition rates of three algorithms under different eigenvector dimensions.

and S_3 are the number of nodes in the input layer, hidden layer, and output layer, respectively; here, we take 80. The number of output layer nodes is determined by the number of face categories and has nothing to do with the number of pictures. Since the ORL face library used in the experiment contains 400 pictures of 40 different people, the number of output layer nodes is taken here as 40. During the experiment, firstly, the sample images of 40 people in the ORL face database are divided into training sample set and test sample set without overlapping. Then, it is subjected to weighted wavelet transform, and the fused image is subjected to discrete cosine transform, and then, the zigzag scanning method is used to extract its main components as the input of the neural network. Then, the feature components are sent to the particle swarm optimized BP neural network for training. Finally, the same feature extraction as above is performed on the test sample, and the extracted feature vector is sent to the trained network for classification and identification.

Experiment 1 is shown in Table 1, which is the experiment performed by the algorithm proposed in this paper under the condition that the number of training samples and testing numbers of each type is 5, and the feature dimension is 64. For the assignment of wavelet weights, since the low-frequency band contains most of the information of the original image, a larger weight is assigned to it, while the high-frequency part is assigned a smaller weight (generally, the vertical and horizontal components divide the rest of the weights equally) [18].

It can be seen from Table 1 that when the wavelet weights take $a_0 = 0.9$, $a_1 = 0.05$, and $a_2 = 0.05$, the recognition rate reaches the highest. Regardless of whether the low-frequency component continues to increase or decrease and the high-frequency component continues to decrease or increase, the recognition rate will decrease.

Experiment 2 set is the parameters of the simulation experiment; let the wavelet weight be $a_0 = 0.9$, $a_1 = 0.05$,

and $a_2 = 0.05$, and the feature dimension is 64. As shown in Table 2, when the number of training samples and test samples for each type of face is 5, the recognition rate and time between two traditional algorithms and the algorithm proposed by the author are compared.

It can be seen from Table 2 that when the experimental conditions are exactly the same, when the number of training samples and the number of test samples are both 200, the recognition rate of the algorithm proposed by the author is much higher than that of the other two traditional algorithms, and the time used is also much lower than the other two traditional algorithms. This is mainly because the algorithm proposed by the author uses the particle swarm algorithm to optimize the initial weights and thresholds of the BP neural network, thereby avoiding the neural network from falling into local minima, and the convergence speed is accelerated; on the one hand, the training time is saved, and on the other hand, the recognition rate is improved.

Experiment 3 set is the experimental simulation parameters; take the weighted wavelet weights as $a_0 = 0.9$, $a_1 = 0.05$, and $a_2 = 0.05$, the number of training samples for each type of face is 6, and the number of test samples is 4. As shown in Figure 4, it mainly studies that when the dimension of each type of face is different, the recognition rate accuracy of the proposed algorithm and two traditional algorithms is compared [19, 20].

As can be seen from Figure 4, with the increase of the dimension of each type of face feature vector, the recognition rate of the weighted wavelet algorithm is slightly higher than that of the general low-frequency wavelet algorithm. This is mainly because the weighted wavelet algorithm adds high-frequency components, but its main information is still stored in the low-frequency part, and the high-frequency part accounts for a small proportion, so the difference is not too large; when the eigenvector dimension is around 60, the recognition rate difference between the weighted

Retraction

Retracted: Motion Control System of IoT Intelligent Robot Based on Improved ResNet Model

Journal of Sensors

Received 12 December 2023; Accepted 12 December 2023; Published 13 December 2023

Copyright © 2023 Journal of Sensors. This is an open access article distributed under the Creative Commons Attribution License, which permits unrestricted use, distribution, and reproduction in any medium, provided the original work is properly cited.

This article has been retracted by Hindawi, as publisher, following an investigation undertaken by the publisher [1]. This investigation has uncovered evidence of systematic manipulation of the publication and peer-review process. We cannot, therefore, vouch for the reliability or integrity of this article.

Please note that this notice is intended solely to alert readers that the peer-review process of this article has been compromised.

Wiley and Hindawi regret that the usual quality checks did not identify these issues before publication and have since put additional measures in place to safeguard research integrity.

We wish to credit our Research Integrity and Research Publishing teams and anonymous and named external researchers and research integrity experts for contributing to this investigation.

The corresponding author, as the representative of all authors, has been given the opportunity to register their agreement or disagreement to this retraction. We have kept a record of any response received.

References

- [1] Z. Farisi, "Motion Control System of IoT Intelligent Robot Based on Improved ResNet Model," *Journal of Sensors*, vol. 2023, Article ID 6229162, 7 pages, 2023.

Research Article

Motion Control System of IoT Intelligent Robot Based on Improved ResNet Model

Zeyad Farisi 

Applied College, Taibah University, Medina City, Saudi Arabia

Correspondence should be addressed to Zeyad Farisi; 1520190132@st.usst.edu.cn

Received 19 August 2022; Revised 15 September 2022; Accepted 27 September 2022; Published 4 April 2023

Academic Editor: C. Venkatesan

Copyright © 2023 Zeyad Farisi. This is an open access article distributed under the Creative Commons Attribution License, which permits unrestricted use, distribution, and reproduction in any medium, provided the original work is properly cited.

In order to further optimize the precision and efficiency of intelligent robot navigation system control, an IoT intelligent robot motion control system based on the improved ResNet model is proposed. Based on the deep learning method, using the Faster R-CNN target detection architecture and the ResNet50 convolutional neural network, the network is trained according to the characteristics of the operation target of the distribution line maintenance robot system. On this basis, combined with the binocular vision ranging principle, the coordinates of the job target in the camera coordinate system are measured, and the coordinates are converted into the robot base coordinate system through hand-eye calibration, so as to complete the spatial positioning of the job target. The results showed that the errors of the binocular measurement methods adopted by the system are all within 1%. *Conclusion.* The method can well adapt to the complex background of the operation scene, the change of illumination, and the partial occlusion of the target and can meet the requirements of the distribution line maintenance robot for the measurement and positioning of the target space.

1. Introduction

With the continuous improvement of people's quality of life, the pace of their life is also accelerated [1]. Now there are robots in smart homes and industrial intelligent manufacturing, the functions of their products are also diverse, their performance is constantly improving, and they are widely used in intelligent manufacturing and other fields, providing a shortcut for human convenience [2]. Intelligent robot is a product integrating kinematics, bionics, motion control, image recognition and analysis, and other disciplines; its high technology content has been greatly applied in the fields of industry, smart home, and chemical production [3]. Coupled with the fact that the economy is moving forward significantly, and the demographic dividend is continuously decreasing, which makes the labor force relatively reduced, which leads to the increase of labor costs, and the cost of products produced has also increased invisibly, the introduction of intelligent robots not only completes the assembly line production of products but also improves the production efficiency and quality of products, realizes rapid, continuous, and high-efficiency production of different

products, and reduces labor intensity and labor, this makes industrial intelligent robots widely used in spraying, handling, welding, and other fields [4].

With the development of intelligent manufacturing and industrialization, the demand for automatic control and intelligent control systems in every field is also increasing, and industrial intelligent robots are no exception, with the continuous expansion of application fields, it puts forward strict requirements on the performance and functions of industrial robots, at the same time, it also promotes the rapid development of motion simulation, intelligent control, and other fields [5]. When the intelligent robot is in motion, it can adjust and control its posture by controlling each joint, so as to realize the function of the end operation of the robot [6]. This control method is quite different from single-step control, but it also has certain connections. Single-step control is the basis of continuous control, that is to say, the realization of single-step control can realize continuous control, so as to realize the control of the end operation of the robot [7].

With the continuous development of economy, national defense, and science and technology, the application of

robots has become more and more popular, and the application of robots not only greatly improves the efficiency of industrial production but also improves the production quality of products [8]. Through the use of robotics, industrial manufacturing, industrial production, and smart home can be improved to a new level, and the motion control system of the robot can be designed [9]. Mainly analyze the motion of the robot from the perspective of motion, and solve the faults in the motion of the robot in time, so that the development of the robot is in line with the development of international electrical engineering [10]. In recent years, in the academic and robotic application technology research at home and abroad, the technology research of robots has become the focus of discussion, as a way to improve the overall level of industrial manufacturing and production, through the characteristics of robot automation technology, for improve the negative effects of traditional industrial production and construction, and to find and solve the problems in robot motion control at the first time, is the significance of promoting the widespread use of robots [11].

2. Literature Review

Robots have a wide range of applications, from agriculture and forestry, environmental protection, mineral exploration, and military reconnaissance to outer space planet surface detection and can play the role of “human” in various application fields [12]. According to different tasks and environments, the requirements for the intelligence level of mobile robots are also different [13]. The intelligent design of the mobile robot mainly includes the function and structure design of the control system. Functional design mainly completes the software design of control functions and algorithms, while structural design is the realization of functions in hardware [14]. As an emerging technology with strong interdisciplinarity, robotics brings great convenience to human life [15]. Due to its advantages of simple operation and simple structure, intelligent detection robots are widely used in detection in various fields, which can effectively reduce the risk of manual detection and have high application value [16]. The emergence of intelligent detection robots has promoted the development of socialization, accelerated the rate of productivity, and effectively solved the drawbacks of manual detection [17]. However, at present, there are problems such as low control accuracy and control trajectory offset in the motion control of intelligent detection robots, a large number of researchers in this field design control systems based on motion trajectory data [18].

At present, in the maintenance of distribution lines, operators still need to climb high-voltage iron towers or work with insulated bucket trucks, which is dangerous [19]. With the development of robotics and computer vision technology, it is possible to develop a vision-guided distribution line maintenance robot [20]. The use of robots to replace manual work with live power can free operators from dangerous working environments, ensure the safety of operators to the greatest extent, and improve the efficiency of power maintenance and inspection.

The distribution line maintenance robot needs to automatically identify the operation target, but because it works in an unstructured environment, the collected images have a complex background and are easily disturbed by light, noise, etc., at the same time, the texture of the job target is relatively simple and the features are not obvious, which poses a great challenge to the design of the robot’s vision system. Target detection methods are divided into template matching methods, methods based on statistical machine learning, and methods based on deep learning, among them, template matching methods are easily affected by illumination, etc., and are not suitable for distribution line maintenance robot systems. Methods based on statistical machine learning usually need to design different features and classification algorithms for the detection of different objects, at the same time, they are easily affected by environmental noise and light, so it is difficult to meet the requirements of distribution line maintenance systems. With the development of deep learning technology in the field of image recognition, the application of deep learning to image target detection has also achieved good detection results. Taking the most common task of replacing surge arresters for distribution line maintenance robots as an example, the author designs Faster R-CNN based on ResNet50 to detect high-voltage lead terminals and the upper end of surge arresters, at the same time, the hand-eye calibration is completed based on Tsai’s two-step method, and finally combined with the principle of binocular ranging, complete the spatial positioning of the job target. The experimental results show that the adopted method can meet the requirements of the distribution line maintenance robot.

3. Methods

3.1. Visual System Design. The experimental system of the distribution line maintenance robot designed by the author is shown in Figure 1, and the system consists of a binocular camera, a six-degree-of-freedom robotic arm, and a liftable platform. The binocular camera is composed of two industrial cameras placed in parallel, the binocular camera is fixedly installed on the bracket outside the robotic arm, forming an eye-to-hand (eye outside the hand) hand-eye system with the robotic arm.

During the operation, the robot first moves the liftable platform to the vicinity of the cross arm installed with the arrester, adjusts the platform position, and makes the arrester and the high-voltage lead terminal connected to the upper end of the arrester completely appear in the field of vision of the binocular camera. The binocular camera transmits the collected images to the computer, the computer completes the detection and spatial positioning of the job target, and the position information is then converted into motion information of the manipulator and sent to the manipulator control cabinet to drive the motion of the manipulator to complete the task. During the replacement of the arrester, the robot is required to independently place the bolt holes of the upper high-voltage lead terminals into the new upper bolts of the arrester that have been fixed to the crossarm through the end clamping tool, therefore, it is

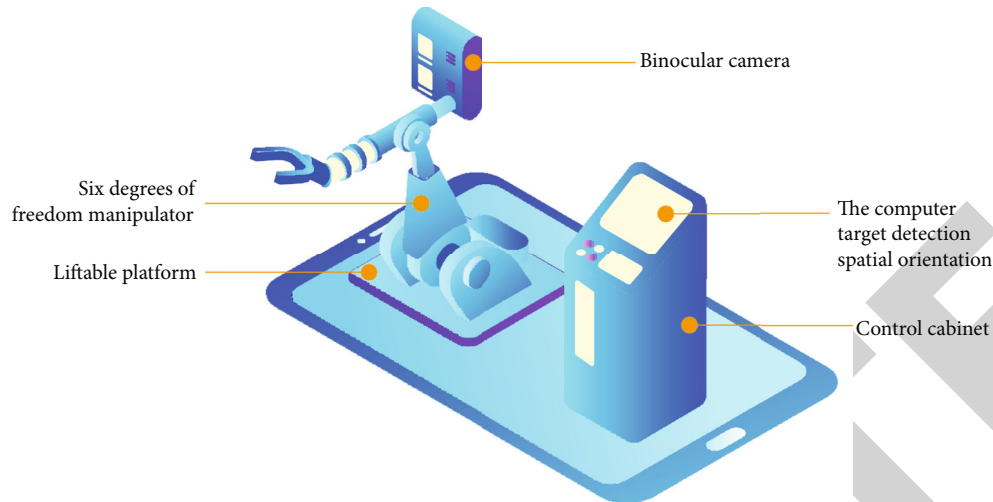


FIGURE 1: Experimental system structure diagram.

necessary to complete the detection and positioning of the upper high-voltage lead terminal and the upper end of the arrester. At the same time, considering that in the distribution line maintenance operation scene, due to the complex and changeable operation background and lighting, therefore, the robustness of robot target detection and the spatial positioning accuracy of the target are required to be high.

3.2. Object Detection. The use of convolutional neural networks for target detection is divided into two levels and one level. The drag phase is represented by a series of R-CNNs, such as R-CNN, Fast R-CNN, and Faster R-CNN. This method first extracts candidate regions that will be the target and then uses a neural network. For these candidates to detect areas, bounding box regression is used to fine-tune the target boundaries, and finally, outliers are used to limit the targets in the output image with a bounding box. The performance speed of R-CNN, fast R-CNN, and faster R-CNN is increasing, and the accuracy is also increasing.

The one-step method includes YOLO and SSD and does not need to decompress the target region compared to the two-step method, and the speed is faster, but the actual detection is not as good as the above this hill. Because Faster R-CNN and Faster R-CNN can perform real-time detection in GPU acceleration, the author finally chooses Faster R-CNN as the target model for robot detection.

Figure 2 shows the basic network of Faster R-CNN based on ResNet50. The basic convolutional neural network can choose different models such as ZFNet, VGG-16, or ResNet with different performance and processing time. Among them, ResNet won the first place in the task division of the ImageNet competition and has been widely used in search, segmentation, recognition, and other tasks due to its high performance. The corresponding models of ResNet are ResNet50 and ResNet101, which 50 and 101 correspond to the structure of the network, the depth of the layers, the higher the accuracy, and the lower the speed and accuracy. The author chose ResNet50 as the base convolutional neural network model for Faster R-CNN detection model.

ResNet50 network model is divided into 5 parts: conv1, conv2_x, conv3_x, conv4_x, and conv5_x. conv1 is a 1-layer convolution layer, while conv2_x, conv3_x, conv4_x, and conv5_x have 3, 4, 6, and 3 building blocks, respectively, and each building block has 3 convolution layers.

After the feature map is output from the central convolutional neural network, RPN (Region Proposal Networks) is added to generate candidate region maps, and then feature maps and regions candidates are fed into the ROI fusion layer. The corresponding regions of the target candidates in the feature map are combined into a long-distance feature vector, and then the softmax distribution method and the bounding box regression method.

The RPN model is shown in Figure 3, the sliding window is used to rotate the feature map, each position in the feature map corresponds to the output n -dimensional feature vector, and each position corresponds to 9 competing windows. These competing windows are called anchors because they have three locations, 1282, 2562, and 5122, each with three ratios of 1:1, 1:2, and 2:1. The n -dimensional output feature vector is fed to the classification process and the regression window process, respectively, and the classification process outputs the probability that 9 anchors of each position are in the front and back, while the window regression layer outputs the parameters of the window regression layer. Define and measure the corresponding 9 anchors for each position.

In practice, the transfer learning method is used to train deep convolutional neural networks, that is, the network is started with learning models first from other large data, and then fine-tuned with new images. The Faster R-CNN used by the author is started with the prelearning model of ImageNet, and the training steps are as follows.

- (a) Plan the training process and testing process and adapt the model to the PASCAL VOC2007 target detection data
- (b) Initialization of RPN network parameters with pre-training ResNet50 network of ImageNet, optimization

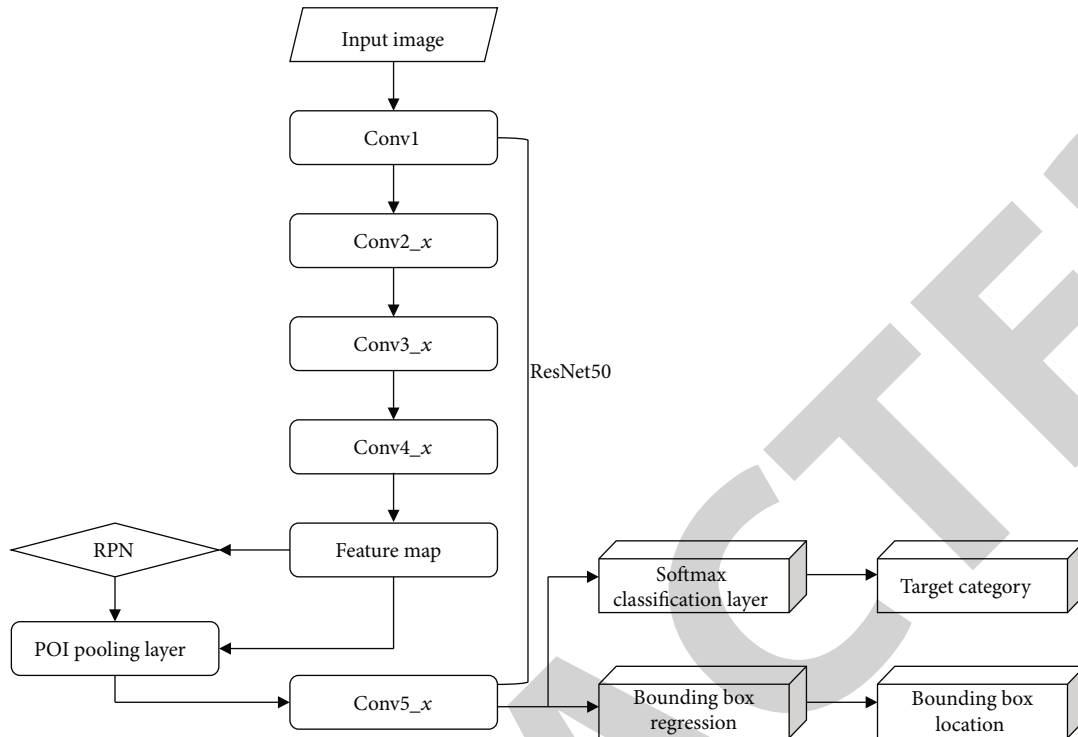


FIGURE 2: Faster R-CNN network frame diagram based on ResNet50.

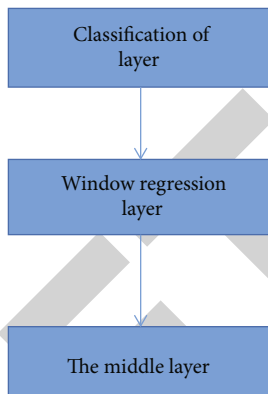


FIGURE 3: RPN structure.

of RPN network using back propagation method, and stochastic gradient descent

- (c) Initialize Faster-R-CNN target detection network parameters with ResNet50 network before training on ImageNet, extract regional candidates using RPN network, and train target detection network
- (d) Restart the RPN network without the plan to find the network, fine-tune the RPN network separately
- (e) Use the fine-tuned RPN network in step d to extract candidate regions and fine-tune the target detection network
- (f) Repeat steps d~e until the network is connected or reaches the learning limit and ends

3.3. Target Space Positioning

3.3.1. Hand-Eye Calibration. Hand-eye calibration is an important prerequisite for using robotic vision servos. Hand-eye calibration aims to integrate the camera coordinate system and the robot coordinate system, so that the spatial target position determined by the vision system can be converted into the robot control system controls the robot arm and completes the task purpose. The hand eye calibration should be done with a calibration object such as a floorboard, and the calibration plate is attached to the end of the robot arm by controlling the robot arm, calibration plate, and people metal movement. The camera moves to each other, the camera receives the relative information of the adjustment plate and integrates the angle information of the robot arm to determine the relative to the camera and the central robot, that is, hand-eye changes matrix. Solving the hand-eye transformation matrix using a two-step approach, that is, the rotation and translation matrix is divided into two parts: rotation and translation to solve. First, the rotation matrix is solved, and then the rotation matrix is converted into the definition vector of the solution.

Consider the manipulator base coordinate system, the manipulator end coordinate system, the camera coordinate system, the calibration board coordinate system, and the translation from the manipulator coordinate system camera to the manipulator base coordinate system, from the manipulator end coordinate system to the manipulator base coordinate system, and from the adjustment plate coordinate system to the coordinate system. In the equation, T_e^b is the transformation from calibration plate coordinate system to

the end coordinate system of the manipulator, and T_c^b is the transformation from calibration plate coordinate system to camera coordinate system. When adjusting the hand eye, the adjustment plate and the end of the manipulator are relatively fixed, that is, fixed. What needs to be solved is the conversion from the camera coordinate system to the coordinate system of the manipulator base, that is, T_r^c . The coordinate system position transformation relationship (1) is obtained.

$$T_r^e T_e^b = T_r^c T_c^b. \quad (1)$$

Control the manipulator to move the calibration plate so that the calibration plate completely appears in the left and right camera images, and perform N ($N \geq 20$) image acquisitions, at the same time, the angle values of each joint of the manipulator at N positions are recorded. Then, the i -th coordinate system position transformation relationship is the following formula:

$$T_{r(i)}^e T_e^b = T_r^c T_{c(i)}^b. \quad (2)$$

In the formula, $T_{r(i)}^e$ is the i -th transformation from the coordinate system of the end of the manipulator to the coordinate system of the base of the manipulator, through each joint angle of the manipulator at the corresponding position, it can be obtained by combining the D-H parameter method and the forward kinematics equation of the manipulator; $T_{c(i)}^b$ is the transformation from the i th calibration plate coordinate system to the camera coordinate system, which can be obtained by calibrating the camera. Combining the i -th and $i+1$ -th coordinate system position transformation relationship, equations (3) and (4) can be obtained

$$T_{r(i)}^e T_{r(i+1)}^e T_r^c = T_r^c T_{c(i)}^b T_{c(i+1)}^b. \quad (3)$$

$$\text{Make } A = T_{r(i)}^e T_{r(i+1)}^e, B = T_{c(i)}^b T_{c(i+1)}^b, X = T_r^c.$$

$$AX = XB. \quad (4)$$

That is, the solution of T_r^c is transformed into the solution of X in formula (4).

3.3.2. Target Space Coordinate Measurement. Before using the camera to measure the spatial position of the target, first, the camera imaging model must be modeled, the pinhole camera model is the simplest ideal linear model among many camera models, and it is derived from the principle of lens imaging without considering lens distortion and is the most common because of its simplicity and intuitiveness in imaging models, as shown in Figure 4.

Let the coordinate of a point p_1 in the space in the camera coordinate system $O_C X_C Y_C Z_C$ be (x_{c1}, y_{c1}, z_{c1}) , the coordinate of the corresponding image point p_2 in the image pixel coordinate system $O_f uv$ is (u_1, v_1) , and then there is a coordinate conversion relationship (5) as shown in the following formula:

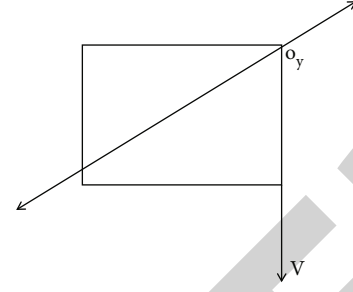


FIGURE 4: Pinhole camera model.

$$\begin{bmatrix} u_1 \\ v_1 \\ 1 \end{bmatrix} = \begin{bmatrix} \alpha_x f & 0 & u_0 \\ 0 & \alpha_y f & v_0 \\ 0 & 0 & 1 \end{bmatrix} \begin{bmatrix} \frac{x_{c1}}{z_{c1}} \\ \frac{y_{c1}}{z_{c1}} \\ 1 \end{bmatrix} = M_{in} \begin{bmatrix} \frac{x_{c1}}{z_{c1}} \\ \frac{y_{c1}}{z_{c1}} \\ 1 \end{bmatrix}. \quad (5)$$

In the formula, α_x and α_y are the magnification coefficients from the imaging plane to the image plane in the u -axis and v -axis, respectively; f is the focal length of the camera; M_{in} is the internal parameter matrix of the camera, which can be calibrated by Zhang's plane method. Equation (6) can be obtained from the principle of similar triangles:

$$z_{c1} = \frac{B \cdot f}{u_{left} - u_{right}} = \frac{B \cdot f}{d}. \quad (6)$$

In the formula, B is the baseline distance between the binocular cameras, which can be obtained by camera calibration; d is the parallax. The in-camera parameters of the two parallel cameras after stereo correction are mathematically the same. Substitute equation (6) into equation (5) to obtain the coordinate (x_{c1}, y_{c1}, z_{c1}) of the target point in the left-eye camera coordinate system. Using the results of the aforementioned hand-eye calibration, the corresponding coordinate (x, y, z) of the target point in the coordinate system of the robot arm base can be obtained as the following formula

$$[x, y, z, 1]^T = T_r^c [x_{c1}, y_{c1}, z_{c1}, 1]^T. \quad (7)$$

4. Results and Discussion

The experiment is divided into two parts: target detection and target space positioning, in the laboratory, a working environment for replacing surge arresters was built to simulate the outdoor scene. By moving the liftable platform shown in Figure 4, a binocular camera was used to collect 2,705 images including the high-voltage lead terminals and the upper end of the surge arrester from different angles, the image set is made into a standard PASCAL VOC2007 target detection set, of which 2000 are used as a training set for model training, and the remaining 705 are used for testing, the Faster R-CNN model is built under the Ubuntu system through the TensorFlow deep learning framework.

TABLE 1: Comparison of Z coordinate measurement results.

Serial number	Reference/mm	Measurements/mm	Relative error/%
1	582.82	581.37	0.249
2	544.55	544.87	0.006
3	557.47	558.97	0.269
4	554.37	554.69	0.006
5	525.43	526.02	0.112
6	569.32	572.55	0.567

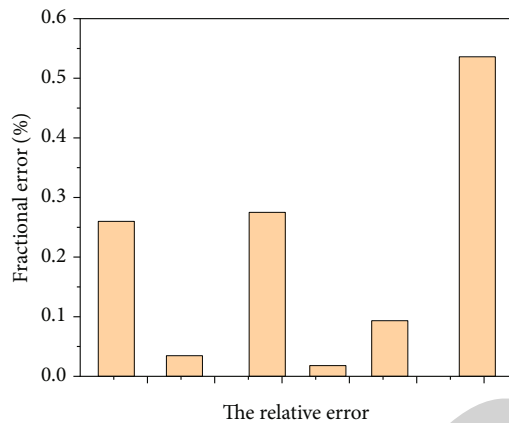


FIGURE 5: Comparative analysis of relative errors.

The model is trained using the momentum gradient descent method, and some hyperparameters are set as follows: the initial learning rate is 0.0003, the maximum number of iterations is 2×10^4 , and the momentum is 0.8999. Apply the trained Faster R-CNN to the test set for testing. After training, the network model can obtain better detection results in different backgrounds, and at the same time, it can overcome the influence of illumination and can be detected even when the target is partially occluded.

The target space positioning experiment is realized by calling the trained Faster R-CNN model in the background through Qt combined with OpenCV. On the robot teach pendant, the coordinates of the robot end center point in the robot base coordinate system can be directly read, and the robot motion can be controlled so that the robot end center point coincides with the upper end point of the arrester and takes the coordinates of the end center point displayed on the teach pendant as the reference value for measurement. In the experiment, because the center point of the end and the upper end of the arrester cannot be guaranteed to be completely coincident, only the accuracy of the reference value in the z-axis direction can be guaranteed, therefore, only the Z coordinate is measured and analyzed in the experiment.

Measure the Z coordinate of the upper end point of the arrester for many times from different positions and randomly select 6 groups of measurement results as shown in Table 1 and Figure 5.

It can be seen from the Z coordinate measurement results in Table 1 that the error of the binocular measurement method used is all within 1%, which meets the measurement accuracy requirements of the distribution line maintenance robot operation, at the same time, the accuracy of the hand-eye calibration algorithm used is also verified from the side.

5. Conclusion

The author proposes an IoT intelligent robot motion control system based on the improved ResNet model, the author applied the Faster R-CNN model based on ResNet50 to the target detection of the replacement arrester operation of the distribution line maintenance robot, on this basis, combined with the binocular vision ranging principle, the coordinates of the high-voltage lead terminal and the upper end of the arrester in the camera coordinate system are measured, finally, the coordinates are converted into the robot base coordinate system through the hand-eye calibration result, so as to complete the spatial positioning of the job target.

All in all, driven by the steady development of social economy and science and technology, people's living standards are constantly improving, their dependence on robots is also increasing, and their requirements are increasing in the process of practical application. Therefore, the positioning of mobile robots in the control technology needs to be connected to the Internet of Things for optimization, and the technology should be innovated on the existing basis. The application status ensures that it can be optimized on the existing basis, maximize the technical application effect, and meet people's various needs for mobile robots.

Data Availability

The data used to support the findings of this study are available from the corresponding author upon request.

Conflicts of Interest

The author declares no conflicts of interest.

References

- [1] S. K. Nataraj, P. M. Pandiyan, S. B. Yaacob, and A. Adom, "Intelligent robot chair with communication aid using text responses and higher order spectra band features," *Informat-ics*, vol. 17, no. 4, pp. 92–103, 2021.
- [2] G. Li, "Clue mining based on the online gambling intelligent robot customer service platform," *International Journal of System Assurance Engineering and Management*, vol. 3, pp. 1–11, 2021.
- [3] S. Stalljann, L. Whle, J. Schfer, and M. Gebhard, "Performance analysis of a head and eye motion-based control interface for assistive robots," *Sensors*, vol. 20, no. 24, p. 7162, 2020.
- [4] J. Zhao and F. Feng, "Optimization technology of passenger service system based on railway intelligent robot," *Journal of Physics Conference Series*, vol. 1746, no. 1, article 012065, 2021.

Retraction

Retracted: Numerical Sensing and Simulation Analysis of Three-Dimensional Flow Field and Temperature Field of Submersible Motor

Journal of Sensors

Received 12 December 2023; Accepted 12 December 2023; Published 13 December 2023

Copyright © 2023 Journal of Sensors. This is an open access article distributed under the Creative Commons Attribution License, which permits unrestricted use, distribution, and reproduction in any medium, provided the original work is properly cited.

This article has been retracted by Hindawi, as publisher, following an investigation undertaken by the publisher [1]. This investigation has uncovered evidence of systematic manipulation of the publication and peer-review process. We cannot, therefore, vouch for the reliability or integrity of this article.

Please note that this notice is intended solely to alert readers that the peer-review process of this article has been compromised.

Wiley and Hindawi regret that the usual quality checks did not identify these issues before publication and have since put additional measures in place to safeguard research integrity.

We wish to credit our Research Integrity and Research Publishing teams and anonymous and named external researchers and research integrity experts for contributing to this investigation.

The corresponding author, as the representative of all authors, has been given the opportunity to register their agreement or disagreement to this retraction. We have kept a record of any response received.

References

- [1] D. Wang and Y. Pan, “Numerical Sensing and Simulation Analysis of Three-Dimensional Flow Field and Temperature Field of Submersible Motor,” *Journal of Sensors*, vol. 2023, Article ID 6523818, 7 pages, 2023.

Research Article

Numerical Sensing and Simulation Analysis of Three-Dimensional Flow Field and Temperature Field of Submersible Motor

Dongxin Wang¹ and Yabin Pan²

¹College of Information and Electrical Engineering, Heilongjiang Bayi Agricultural University, Daqing, Heilongjiang 163000, China

²Daqing Oilfield Powerlift Pump Industry Co., Ltd., Daqing, Heilongjiang 163000, China

Correspondence should be addressed to Dongxin Wang; 20141380@stu.sicau.edu.cn

Received 5 September 2022; Revised 1 October 2022; Accepted 10 October 2022; Published 31 March 2023

Academic Editor: C. Venkatesan

Copyright © 2023 Dongxin Wang and Yabin Pan. This is an open access article distributed under the Creative Commons Attribution License, which permits unrestricted use, distribution, and reproduction in any medium, provided the original work is properly cited.

In order to accurately study the temperature field distribution of the submersible motor, the author proposes the numerical sensing and simulation analysis of the three-dimensional flow field and temperature field of the submersible motor. For a marine air gap water-cooled internal submersible permanent magnet motor, based on the principle of computational fluid dynamics (CFD), numerical simulation analysis and geometric structure improvement of the three-dimensional flow field and temperature field of the motor were carried out, eliminate the reverse flow phenomenon in the internal flow field of the motor, improve the heat dissipation efficiency of the whole machine, and optimize the flow field and temperature rise of the motor. Experimental results show that after the motor geometry is optimized, the flow rate of the cooling water in the air gap channel is 36.7 L/min, which is 7.9 L/min higher than the original model, it means that the heat in the motor can be better carried away by the water flow in the air gap channel. It is proved that the results obtained in this study have certain reference significance for the geometric structure design of the submersible motor.

1. Introduction

Due to the frequent occurrence of natural disasters and mining accidents in recent years, more and more attention has been paid to the efficient, safe, and stable operation of submersible pumps for main drainage [1]. As the core component of the submersible pump, the submersible motor is the most concerned component. Because the high-pressure wet submersible motor is more adaptable to the harsh working environment than the high-pressure dry submersible motor, this makes the high-pressure wet submersible motor the first choice for flood control and drainage in the country in the future, therefore, it is particularly important to study high-pressure wet submersible motors [2].

Submersible motors are important equipment for urban sewage discharge, sewage treatment, road and bridge engineering drainage, and irrigation and waterlogging drainage in water conservancy projects [3]. With the improvement

of national environmental protection regulations and the enhancement of people's awareness of environmental protection, submersible pumps for sewage treatment have received more and more needs and applications [4]. The submersible motor is matched with various types of submersible motors and is integrated with the motor; it runs in sewage of various water quality for a long time, and the working environment is harsh. Therefore, the development of submersible motors with excellent performance, safety, and reliability has broad market prospects.

Since the submersible motor is submerged and operated in the water, the working conditions are complicated; therefore, the structural design must be strictly sealed to prevent water from entering, at the same time, do a good job of monitoring and keep abreast of the operation of the motor, this is the main difference between the submersible motor and the three-phase asynchronous motor [5]. The main problem of the current submersible motor is that the online measurement technology

of the internal pressure and humidity in the motor operation has not been well solved, which affects the safe operation of the motor to a certain extent, these problems still need to be further studied and solved [6]. The submersible motor is the key equipment in the mine drainage system and the disaster relief drainage system; its development has successfully broadened the application scope of the mine submersible motor and enriched the types of high-power submersible pumps provided equipment support for the construction of mine disaster-resistant drainage system [7]. A large number of engineering practices have proved that, high-power submersible motors have a broad application space and can not only obtain economic benefits but also produce good social benefits in engineering applications.

2. Literature Review

Submersible motors are generally divided into oil-filled submersible motors, water-filled submersible motors, inflatable submersible motors, and shielded submersible motors [8]. The shielded motor and the pump together form a shielded electric pump, which is used to transport flammable, toxic, precious, corrosive, and radioactive media without solid particles, absolutely leak-free, and low-noise operation when transferring liquids [9]. Shielded motors have the advantages of small size, light weight, easy installation and use, high reliability, and high performance and are widely used in water extraction from underground or lakes, industrial and mining enterprise drainage, urban and rural building drainage, residential water, and sewage treatment [10]. With the development of high-efficiency and miniaturized motors, the heating problem of motors has become the main obstacle to the growth of single-machine capacity and is one of the key technical problems that needs to be solved in motor design [11]. The submersible motor has high power density, and the heat dissipation problem is more prominent. If the temperature inside the motor is too high, it will affect the life of the insulating material, in severe cases, it may also cause irreversible demagnetization of the permanent magnet, which is directly related to the service life and operational reliability of the motor; therefore, the temperature rise of the motor is one of the key indicators of the motor performance assessment; it is of great significance to study the motor cooling method and the optimal design of the temperature rise for the safety assessment of the motor [12].

In recent years, there have been many studies on the motor flow field and temperature rise of different cooling types. Hofmann designed an oil-spray cooling scheme for an oil-cooled motor and analyzed the temperature distribution of the motor [13]. Kopyrin, et al. numerically simulated the flow field of the outer air path of the motor and studied the effect of the stator axial ventilation holes on the temperature rise of the windings [14]. Based on a permanent magnet motor for an electric vehicle, Chen et al. conducted a comparative analysis of the flow field and temperature field of the motor under the spiral and Z-shaped water channel structures [15]. Different from conventional natural heat dissipation and casing water-cooled motors, submersible motors directly use water to cool the inside of the motor, so the problem of tem-

perature rise is less significant than that of closed motors, and there are fewer related temperature rise studies [16].

The author's research object is a certain marine submersible permanent magnet motor, which is a new type of motor with air gap water cooling; the cooling water enters the motor through the gap between the bearing and the rotating shaft [17]. Since the thermal circuit method cannot reflect the influence of the amount of water absorbed by the motor on the heat dissipation of the motor, and in order to obtain the fine flow field and temperature field results of each part of the motor, the author uses the CFD program Fluent to simulate the three-dimensional flow field and temperature field of the motor; through theoretical analysis and geometric structure improvement, the reverse flow phenomenon in the flow field inside the motor is eliminated, the heat dissipation efficiency of the whole machine is improved, and the flow field and temperature rise of the motor are optimized [18].

3. Methods

3.1. Physical Model. The installation diagram of a marine submersible motor (hereinafter referred to as "motor") is shown in Figure 1; driven by the propeller, the water flows through the hollow shaft of the motor, and a part of the water will enter the motor through the bearing gap to cool the motor [19]. The water flow driven by the hollow shaft propeller is 200 L/min, the basic performance parameters of the motor are shown in Table 1, the material of the motor bearing is a composite material, and its temperature is limited to 60°C.

Due to the cycle symmetry of the motor geometry, in order to maximize the saving of computing resources and shorten the computing cycle, the author takes the minimum periodic unit 1/36 model for simulation calculation [20]. The simulation calculation grid adopts the combination of hexahedral structured grid and unstructured tetrahedral grid to divide the overall calculation domain; the total number of grids is 11264193, and the maximum skewness of the grid is about 0.756, the mesh quality meets the engineering calculation requirements.

3.2. Mathematical Model. Fluent is a CFD software based on the finite volume method, its basic principle is to describe a series of partial differential equations for flow and heat transfer; the problem of algebraic equations defined on a finite number of discrete points of the control volume is transformed by the discrete method; finally, the approximate solution of the partial differential equation can be obtained by solving the algebraic equation numerically. The author's research object is a fluid-solid conjugate heat transfer problem; for all solid regions such as casings and end caps, Fluent uses a three-dimensional heat conduction model to solve the problem, and its energy equation is

$$\nabla \lambda_s \nabla T_s + Q_s - Q_h = 0, \quad (1)$$

where λ_s , T_s , and Q_s are the thermal conductivity, temperature, and internal heat source of the solid material, respectively.

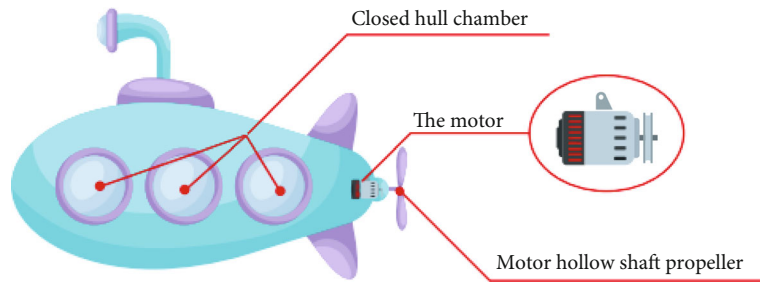


FIGURE 1: Schematic diagram of motor installation.

TABLE 1: Basic parameters of the motor.

Parameter name	Parameter value
Motor rated power /kW	140
Number of stator slots	216
Number of motor poles	36
Rated speed /($r^* \text{ min}^{-1}$)	300
Hollow shaft water flow /($L^{-1} \cdot \text{min}^{-1}$)	200
Cooling water inlet temperature / $^{\circ}\text{C}$	45
Bearing temperature limits / $^{\circ}\text{C}$	60

For nonheating solids such as casings and end caps, the value of the internal heat source Q_s is 0. Q_h is the heat exchange between the fluid and the solid wall, which can be expressed as

$$Q_h = h(T_s - T_h), \quad (2)$$

where h is the convective heat transfer coefficient between the fluid and the solid.

The cooling water of the calculation model can be considered as an incompressible fluid, and the flow state is turbulent flow; therefore, the author uses a three-dimensional incompressible turbulence model to solve the problem. For an incompressible fluid, the density ρ is considered to be a constant, then the fluid connection equation, momentum equation, and energy equation, as well as the equations of turbulent kinetic energy k and dissipation rate ε can be expressed as

$$\begin{aligned} \nabla \cdot \mathbf{u} &= 0, \\ \nabla \cdot (\mathbf{u}\mathbf{u}) &= -\nabla \cdot \left(p\mathbf{I} + \frac{2}{3}k\mathbf{I} \right) + \nabla \cdot \left\{ (\nu + \nu_t) [\nabla \mathbf{u} + (\nabla \mathbf{u})^T] \right\}, \\ \nabla \cdot (\mathbf{u}T_f) &= \nabla \cdot \left[\left(\frac{\nu}{Pr} + \frac{\nu_t}{Pr_t} \right) \nabla T_f \right] + \frac{Q_h}{\rho C_p}, \\ \mathbf{u} \cdot \nabla k &= \nabla \cdot \left[\left(\nu + \frac{\nu_t}{\sigma_k} \right) \nabla k \right] + G - \varepsilon, \\ \mathbf{u} \cdot \nabla \varepsilon &= \nabla \cdot \left[\left(\nu + \frac{\nu_t}{\sigma_k} \right) \nabla \varepsilon \right] + C_{\varepsilon 1} \frac{\varepsilon}{k} G - C_{\varepsilon 2} \frac{\varepsilon^2}{k}. \end{aligned} \quad (3)$$

Among

$$\begin{aligned} \nu_t &= C_\mu \frac{k^2}{\varepsilon}, \\ G &= \frac{1}{2} \nu_t [\nabla \mathbf{u} + (\nabla \mathbf{u})^T]^2, \\ C_\mu &= 0.09, \\ \sigma_k &= 1.0, \\ \sigma_\varepsilon &= 13, \\ C_{\varepsilon 1} &= 1.44, \\ C_{\varepsilon 2} &= 1.92, \end{aligned} \quad (4)$$

where \mathbf{u} is the fluid velocity vector; p is the pressure after dividing by the fluid density; \mathbf{I} is the identity matrix; ν is the kinematic viscosity coefficient of the fluid; T_f is the fluid temperature; Pr is the laminar Prandtl number of the fluid; Pr_t is the turbulent Prandtl number of the fluid; C_p is the specific heat of the fluid [21].

3.3. Loss Loading and Boundary Conditions. The thermo-physical properties of the materials of each component of the motor are shown in Table 2, for the heat-generating components, a heat source needs to be loaded during the calculation. The heat source loaded by the temperature field calculation is the result of the loss value calculated based on the electromagnetic scheme; Table 3 shows the load loss of each heating component of the motor.

The boundary condition settings of the author's simulation calculation are shown in Table 4. For the periodic surface of the established 1/36 motor model, set the periodic boundary condition in the Fluent program. The motor is installed in the closed chamber of the hull, and the heat dissipation conditions are very poor; in the simulation calculation, the author ignores the natural heat dissipation of the outer surface such as the casing in the closed chamber of the hull and believes that the heat of the motor is only carried out by the water flow in the air gap, so the boundary condition of the outer surface of the motor is set as adiabatic. The amount of water entering and leaving the bearing clearance is automatically calculated by the program, so the author only needs to specify the boundary conditions of the hollow shaft inlet during simulation [22].

TABLE 2: Material properties of motor components.

Part	Thermal conductivity/ ($W \cdot m^{-1} \cdot K^{-1}$)	Constant pressure specific heat / ($J \cdot kg^{-1} \cdot K^{-1}$)	Density/($kg \cdot m^{-3}$)
Bearing	025	1500	1160
Chassis/end cover/shaft	30	460	7650
Stator and rotor shield	20	520	4500
Permanent magnets	76	460	7500
Stator and rotor core	Radial/tangential 30 Tangential 30 axial 1128	460	7650
Stator winding	401	385	8933
Potting glue	022	1500	1200
Stator wedge insulation	0.14	1450	1500

TABLE 3: Motor loss loading scheme.

Heating parts	Loss value	1/36 model loss value
Stator winding	309450	85958
Stator core	2352.75	65354
Rotor core	373.75	10382
Stator shield	373.75	10382

4. Results and Discussion

4.1. Analysis of Motor Temperature Field Results. According to the hollow shaft inlet flow rate of 200 L/min (corresponding to 1/36 model flow rate of about 5.56 L/min), the simulation calculation is carried out, the obtained 1/36 model bearing clearance water inlet flow rate is 0.8 L/min (converted to 28.8 L/min for the whole machine), and the temperature statistics of key components are shown in Table 5. The research results show that under the rated operating conditions, the maximum temperature in the motor is 72.2°C, the maximum temperature in the bearing is 53.3°C, and the temperature rise meets the design requirements. However, the difference between the maximum temperature of the bearing and its temperature limit (60°C) is only 6.7 K; considering the simulation error and special working conditions, the bearing safety margin is not enough [23].

Combined with the results in Table 5, it can be seen that the highest temperature position of the motor is mainly distributed on the stator winding; the temperature of the motor near the inlet end of the hollow shaft (hereinafter referred to as “front end”) is higher than that at the outlet end of the hollow shaft (hereinafter referred to as “rear end”); the reason is that the velocity vector diagram of the cooling water shows that the overall trend of water flow enters from the rear bearing gap and flows out from the front bearing gap; and the flow direction of the water in the air gap is from the rear end to the front end. When the cooling water flows, the heat is absorbed and the temperature rises, and the cooling capacity decreases, so the rear end temperature of the motor parts is lower and the front end temperature is high.

The temperature distribution of the motor is that the front end temperature is lower and the rear end temperature is higher, indicating that the flow direction of the cooling

water in the air gap channel is from the front end to the rear end. Therefore, the reverse flow phenomenon in the air gap water channel of the motor is related to the rotation of the motor.

4.2. Analysis and Optimization of Backflow Phenomenon in Air Gap Channel. When the motor rotates, there is a linear velocity in the circumferential direction of the rotating part, and the water in the driving hollow shaft flows into the air gap water channel through the bearing gap at the front and rear ends, and the air gap water channel presents the phenomenon of “water absorption.” The overall trend of cooling water entering from the rear bearing clearance when the motor rotates, it flows out from the front end bearing clearance, indicating that the rear end bearing clearance has a stronger water absorption capacity than the front end.

In order to analyze this phenomenon, the author firstly verifies the boundary conditions that may affect the calculation results. Modify the relevant boundary conditions of the simulation calculation (such as changing the outlet boundary condition from outflow to pressure outlet and changing the rotation direction from clockwise to counterclockwise), it is found that the numerical simulation result is still that the temperature of the front end of the motor is high, the temperature of the rear end is low, and the water flow trend in the air gap channel is still from the rear end to the front end, this shows that the backflow phenomenon of the air gap water channel is independent of the boundary condition settings.

By excluding boundary conditions, calculation grids and other factors that may affect the calculation results, it can be preliminarily inferred that the backflow phenomenon of the air gap water channel is caused by the geometric structure of the model itself. The pressure in the cavity at the back end of the air gap channel is higher than that at the front end. Careful observation of the calculated geometric model shows that the front-end cavity of the air gap channel is wide and long, the rear-end cavity is narrow and short, and the volume of the front-end cavity is larger than that of the back end. In the case where the bearing gaps at the front and rear ends absorb water at the same time, the volume of the rear cavity is smaller than that of the front end, therefore, the pressure is higher than that of the front end, which eventually causes the cooling water to flow from the side with the higher

TABLE 4: Boundary conditions for simulation calculation.

Hollow shaft inlet flow rate / ($L \cdot \text{min}^{-1}$)	Inlet water temperature / $^{\circ}\text{C}$	Motor outer surface	Periodic surface
200	45	Adiabatic	Period boundary

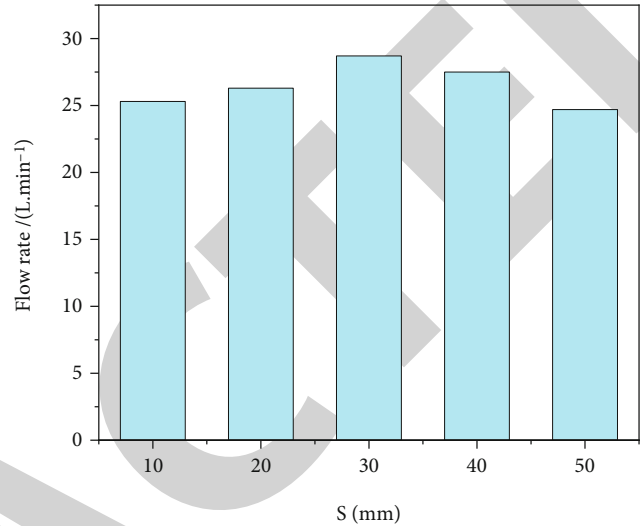
TABLE 5: Temperature results of key components of the motor ($^{\circ}\text{C}$).

Part name	Average temperature	Maximum temperature
Winding	69.6	722
Stator core	61.1	699
Stator shield	52.1	620
Rotor shield	49.9	530
Magnetic steel	49.1	514
Front bearing	50.4	533
Rear bearing	47.8	514

pressure (the rear end) to the side with the lower pressure (the front end), resulting in a reverse flow phenomenon [24].

In order to eliminate the reverse flow phenomenon in the air gap channel, the author optimizes the calculated geometric model. On the basis of the original geometric model, the front cavity of the air gap water channel is filled with potting glue, at the same time, the length of the front end of the rotating shaft is lengthened to further reduce the volume of the cavity at the front end of the air gap water channel. In the optimized structure, the length of the front end of the rotating shaft is elongated, and the remaining axial length of the front end cavity is S . In order to discuss in detail the influence of front-end cavity changes on the motor air gap water flow and temperature rise, the author established five different fluid region calculation models with different front-end cavity axial lengths, the water flow in the air gap is discussed when S is 10, 20, 30, 40, and 50 mm, respectively. Figure 2 shows the flow rate of the air gap water channel with different S lengths, the air gap water flow rate increases first and then decreases with the increase of the axial length of the front end cavity. The reason is that when the front-end cavity is very small, the axial length S is increased, and the volume of the front-end cavity is increased, which is convenient for the water flow in the air gap, but at the same time, the pressure of the front-end cavity also decreases; therefore, when the volume of the front-end cavity of the air gap channel is large to a certain extent, the flow rate of the air gap channel will not increase but decrease due to the greater pressure of the rear-end cavity. It can be seen from Figure 2 that when the axial length S of the cavity at the front end of the air gap is about 30 mm, the maximum flow rate can be obtained in the air gap water channel.

The greater the air gap channel flow rate, the more heat is removed from the motor. After the above analysis, the author's final optimized geometric model takes $S = 32$ mm (this value aligns the elongated plane of the rotating shaft with the end of the winding, which is easy to divide the

FIGURE 2: Variation curve of air gap channel flow rate with different S lengths.

structured mesh). The motor presents the result that the front-end temperature is low and the rear end temperature is high. After the geometric structure is optimized, the overall average pressure of the cavity at the front end of the air gap channel is stronger than that at the rear end, the reverse flow phenomenon is suppressed, and the cooling water in the air gap channel will flow from the front end to the rear end. The above results show that the author reduces the cavity volume at the front end of the air gap water channel by optimizing the geometric structure of the air gap water channel, which can eliminate the backflow phenomenon of cooling water in the air gap water channel. After the motor geometry is optimized, the flow rate of the cooling water in the air gap channel is 36.7 L/min, which is 7.9 L/min higher than the original model, it means that the heat in the motor can be better carried away by the water flow in the air gap channel. Table 6 shows the statistics of the temperature results of the key components of the motor after the model optimization, it can be seen that compared with the original model, the overall temperature rise of the motor has been reduced, and the safety margin of the bearing temperature rise has been improved. After the model is optimized, the cooling water flow direction of the air gap channel changes from back to front to front to back, so the temperature rise of the front end bearing decreases most obviously, and the maximum temperature can be reduced by 6.3 K. Although the average temperature of the rear bearing increased slightly, its maximum temperature still decreased [25]. The above results show that, the temperature rise of the motor in this paper can be optimized by reducing the volume of

TABLE 6: Comparison of motor temperature results before and after model optimization.

Part name	Average temperature/ $^{\circ}\text{C}$	Compare with original model/ K	Max temperature/ $^{\circ}\text{C}$	Compare with original model/ K
Winding	681	-15	696	-26
Stator core	594	-1.7	671	-28
Stator shield	508	-13	594	-26
Rotor shield	478	-2.1	506	-24
Magnetic steel	473	-18	493	-21
Front bearing	459	-45	470	-63
Rear bearing	500	22	506	-08

the front-end cavity in the air gap channel. In the design of the motor geometry, the cavity structure at the front and rear ends of the air gap water channel should be fully considered, avoid the backflow phenomenon that the pressure in the rear cavity is stronger than the front end.

5. Conclusion

The author proposes the numerical sensing and simulation analysis of the three-dimensional flow field and temperature field of the submersible motor, based on the CFD software Fluent, the author conducted a three-dimensional flow field and temperature field simulation analysis of a submersible motor; the study found that the reverse flow phenomenon occurred in the air gap water channel of the motor, which caused the temperature of the front end of the motor to be higher than that of the back end. The author made a systematic and in-depth analysis of the reverse flow phenomenon in the air gap water channel of the motor and found that the reverse flow was caused by the pressure of the back cavity of the air gap water channel being stronger than that of the front cavity. In order to eliminate the reverse flow phenomenon, the author optimizes the model geometry, improves the safety margin of bearing temperature rise, and further improves the motor temperature rise. Studies have shown that when designing the motor geometry, the cavity structure at the front and rear ends of the air gap channel should be fully considered, avoid the phenomenon of reverse flow and reduce the cooling efficiency of the system.

Data Availability

The data used to support the findings of this study are available from the corresponding author upon request.

Conflicts of Interest

The authors declare that they have no conflicts of interest.

Acknowledgments

This study was supported by the University Nursing Program for Young Scholars with Creative Talents in Heilongjiang Province, Project No:UNPYSCT-2020040.

References

- [1] M. G. ZVolkov and Y. V. Zeigman, "Application of the virtual temperature sensor algorithm for electric submersible motor in bringing the oil-producing well on to stable production," *Petroleum Engineer*, vol. 19, no. 3, p. 43, 2021.
- [2] Q. Zhang, Z. L. Li, X. W. Dong, Y. X. Liu, and R. Yu, "Comparative analysis of temperature field model and design of cooling system structure parameters of submersible motor," *Journal of Thermal Science and Engineering Applications*, vol. 13, no. 5, 2021 Transactions of the ASME (13-5).
- [3] D. Wang, "Design and temperature field analysis of submersible motor," in *2020 5th International Conference on Electromechanical Control Technology and Transportation (ICECTT)*, Nanchang, China, 2020.
- [4] K. Raveendran, S. R. Sai, A. Christy, A. G. Pillai, and T. S. Angel, "Intelligent monitoring system for submersible motor protection," in *2020 Fourth World Conference on Smart Trends in Systems Security and Sustainability (WorldS4)*, London, UK, 2020.
- [5] A. A. Markova, V. A. Kopyrin, M. V. Deneko, R. N. Khamitov, and A. V. Logunov, "Investigation of transients in a submersible electric motor with a downhole compensator," *Journal of Physics: Conference Series*, vol. 1901, no. 1, article 012074, 2021.
- [6] J. Cui, W. Xiao, W. Zou, S. Liu, and Q. Liu, "Design optimization of submersible permanent magnet synchronous motor by combined doe and taguchi approach," *IET Electric Power Applications*, vol. 14, no. 6, pp. 1060–1066, 2020.
- [7] L. G. Janger, R. B. Ashbaugh, D. L. Self, J. W. Nowitzki, and D. C. Beck, "Dynamic power optimization system and method for electric submersible motors," US20210140289A1, 2021.
- [8] N. H. Hatsey and S. E. Birkie, "Total cost optimization of submersible irrigation pump maintenance using simulation," *Journal of Quality in Maintenance Engineering*, vol. 27, no. 1, pp. 187–202, 2020.
- [9] Y. Wang and Y. Du, *Discussion on Long Distance Low Voltage Distribution Design*, Electrical Technology of Intelligent Buildings, 2020.
- [10] V. A. Trushkin, O. N. Churlyayeva, and R. V. Kozichev, "Effect of submersible motor temperature on diagnostic insulation parameters," *Machinery and Equipment for Rural Area*, no. 6, pp. 36–39, 2020.
- [11] D. Duan, Z. Wang, Q. Wang, and J. Li, "Research on integrated optimization design method of high-efficiency motor propeller system for uavs with multi-states," *Access*, vol. 8, pp. 165432–165443, 2020.

Retraction

Retracted: Wearable Sensor-Based Edge Computing Framework for Cardiac Arrhythmia Detection and Acute Stroke Prediction

Journal of Sensors

Received 12 December 2023; Accepted 12 December 2023; Published 13 December 2023

Copyright © 2023 Journal of Sensors. This is an open access article distributed under the Creative Commons Attribution License, which permits unrestricted use, distribution, and reproduction in any medium, provided the original work is properly cited.

This article has been retracted by Hindawi, as publisher, following an investigation undertaken by the publisher [1]. This investigation has uncovered evidence of systematic manipulation of the publication and peer-review process. We cannot, therefore, vouch for the reliability or integrity of this article.

Please note that this notice is intended solely to alert readers that the peer-review process of this article has been compromised.

Wiley and Hindawi regret that the usual quality checks did not identify these issues before publication and have since put additional measures in place to safeguard research integrity.

We wish to credit our Research Integrity and Research Publishing teams and anonymous and named external researchers and research integrity experts for contributing to this investigation.











The corresponding author, as the representative of all authors, has been given the opportunity to register their agreement or disagreement to this retraction. We have kept a record of any response received.

References

- [1] R. Lavanya, D. Vidyabharathi, S. S. Kumar et al., “Wearable Sensor-Based Edge Computing Framework for Cardiac Arrhythmia Detection and Acute Stroke Prediction,” *Journal of Sensors*, vol. 2023, Article ID 3082870, 9 pages, 2023.

Research Article

Wearable Sensor-Based Edge Computing Framework for Cardiac Arrhythmia Detection and Acute Stroke Prediction

R. Lavanya ¹, **D. Vidyabharathi** ², **S. Selva Kumar** ³, **Manisha Mali** ⁴,
M. Arunkumar ⁵, **S. S. Aravinth** ⁶, **Md. Zainlabuddin** ⁷, **K. Jose Triny** ⁸,
J. Sathyendra Bhat ⁹ and **Miretab Tesfayohanis** ¹⁰

¹Department of Computing Technologies, SRM Institute of Science and Technology, India

²Department of Computer Science and Engineering, Sona College of Technology, India

³School of Computer Science and Engineering, Vellore Institute of Technology, Andhra Pradesh, India

⁴Department of Computer Engineering, Vishwakarma Institute of Information Technology, India

⁵Department of Biomedical Engineering, Karpagam Academy of Higher Education, India

⁶Department of Computer Science and Engineering Honours, Koneru Lakshmiah Education Foundation, India

⁷Department of Computer Science and Engineering, Khader Memorial College of Engineering and Technology, India

⁸Department of Computer Science and Engineering, M.Kumarasamy College of Engineering, India

⁹MCA Department, St Joseph Engineering College, India

¹⁰Department of Information Technology, College of Engineering and Technology, Dambi Dollo University, Ethiopia

Correspondence should be addressed to Miretab Tesfayohanis; miretab@dadu.edu.et

Received 19 September 2022; Revised 13 October 2022; Accepted 24 November 2022; Published 23 February 2023

Academic Editor: C. Venkatesan

Copyright © 2023 R. Lavanya et al. This is an open access article distributed under the Creative Commons Attribution License, which permits unrestricted use, distribution, and reproduction in any medium, provided the original work is properly cited.

Internet of Things-based smart healthcare systems have gained attention in recent years for improving healthcare services and reducing data management costs. However, there is a requirement for improving the smart healthcare system in terms of speed, accuracy, and cost. An intelligent and secure edge-computing framework with wearable devices and sensors is proposed for cardiac arrhythmia detection and acute stroke prediction. Latency reduction is highly essential in real-time continuous assessment, and classification accuracy has to be improved for acute stroke prediction. In this paper, preprocessing and deep learning-based assessment is performed in the edge-computing layer, and decisions are communicated instantly to the individuals. In this work, acute stroke prediction is performed by a deep learning model using heart rate variability features and physiological data. Classification accuracy is improved in this approach when compared to other machine learning approaches. Cloud servers are utilized for storing the healthcare data of individuals for further analysis. Analyzed data from these servers are shared with hospitals, healthcare centers, family members, and physicians. The proposed edge computing with wearable sensors approach outperforms existing smart healthcare-based approaches in terms of execution speed, latency time, and power consumption. The deep learning method combined with DWT performs better than other similar approaches in the assessment of cardiac arrhythmia and acute stroke prediction. The proposed classifier achieves a sensitivity of 99.4%, specificity of 99.1%, and accuracy of 99.3% when compared with other similar approaches.

1. Introduction

Edge of Things- (EoT-) based healthcare gained huge attention in the past few years due to the wide usage of wearable devices, 5G communication, and edge computing framework.

Wireless healthcare monitoring systems have gained huge attention recently in almost all biomedical applications. Internet of Things- (IoT-) based wearable computing devices generate a huge volume of data that has to be stored and analyzed to get important information in many real-world

applications [1]. Though IoT-based healthcare applications are highly essential for accurate and timely medical diagnosis, there are many challenges in the appropriate data collection, required computing facility, and data storage [2].

In most modern data analytics applications, machine learning algorithms are applied to improve the accuracy and efficiency of the systems. In a few applications, these intelligent algorithms even perform the detection of errors and system output. Machine learning algorithms are widely popular in the classification of data into different categories that are highly essential in analyzing biomedical data [3]. Biomedical signal monitoring and processing are highly essential in almost all medical devices and advanced equipment. In recent years, wearable devices are preferred in many healthcare monitoring to provide continuous monitoring, ease of access, flexibility, and disease detection. Wearable devices and sensors are popular recently in the wireless monitoring of infants, elderly persons, differently abled persons, and athletes. Moreover, the increase in the aging population needs special attention and continuous monitoring of elderly people in the age group above 60 [4]. These devices generate a large amount of data that have to be stored and processed. However, mobile devices are not able to store a huge volume of data, and they are not capable of performing complex computations involved in signal processing. To overcome these issues, cloud-based wireless healthcare systems gained huge attention in recent years.

IoT- and cloud computing-based healthcare systems are developed in wireless healthcare monitoring to handle huge volumes of data with variety. The main aim of IoT-based healthcare is to reduce the computing burden and storage requirements of mobile devices and to provide low-cost solutions for healthy living for users [5]. In this paper, an edge-based healthcare system is developed to assess important health parameters like blood pressure, temperature, respiratory rate, electrocardiogram (ECG), and heart rate. Healthcare ECG monitoring is useful in assessing the health condition of the heart.

IoT gained huge popularity in wireless healthcare monitoring to handle huge volumes of data with variety. The main objective of this work is to reduce the computing burden and storage requirements of mobile devices and to provide low-cost solutions with healthy life for the users [6]. In this article, an edge-based healthcare system is developed to assess important health parameters like blood pressure, temperature, respiratory rate, electrocardiogram (ECG), and heart rate. Healthcare ECG monitoring is useful in assessing the health condition of the heart.

In wireless monitoring, each patient is considered a node of the wireless sensor network, and these nodes are connected to the central node at the hospital. Wireless networking, mobile computing, and cluster computing solutions have been utilized in the performance improvement of healthcare networks. Pervasive computing and wireless sensor networks are used for different possible ways of sending data in medical applications. In that work, the authors used various wireless technologies in the biomedical domain for monitoring physiological signals. Many sensors have been utilized for signal acquisition, and signal processors are used

for preprocessing the acquired ECG signals. In this work, the healthcare system is improvised with the application of a cloud framework in healthcare monitoring.

In wireless healthcare monitoring, sensors are linked with various hardware and software components used for the effective monitoring of patients. Figure 1 shows the simple wearable computing framework with a cloud or edge computing layer. The collected data from wearable devices are preprocessed to provide relevant data to the computing layer. Preprocessed data are assessed in the computing layer using edge computing devices, and the results are sent back to the end user. To perform in-depth analysis and prediction, various machine learning and deep learning algorithms may be utilized for feature extraction and classification.

Wireless healthcare monitoring is highly essential in assessing chronic diseases such as cardiac arrhythmias, diabetes, hypertension, and cardiovascular disease. Since wireless healthcare monitoring faces some serious challenges, wearable sensors with an edge computing approach are presented in this paper. Edge computing-based smart healthcare systems are developed by researchers using wearable devices [7–9]. These approaches focus on the physiological parameters and history of patients in the assessment of individuals. A few issues in the existing works are as follows: (i) wearable sensors and devices are not capable of performing prediction tasks and critical analysis. (ii) Cloud computing frameworks are utilized in existing approaches for deep learning-based detection and prediction tasks that require intensive computing. (iii) The classification accuracy needs to be improved in life-threatening heart disease risk analysis and acute stroke prediction.

A deep learning-based CNN model is developed to assess heart disease in a fog environment [10]. However, there is a requirement for improving accuracy in cardiac arrhythmia detection and acute stroke prediction. An edge computing framework with wearable devices is presented in this paper to overcome the drawbacks of existing edge computing-based approaches and to improve the accuracy of cardiac arrhythmia detection. The simple preprocessing tasks are carried out on the user's mobile device, whereas feature extraction and deep learning-based assessment are carried out on edge devices. A cloud server is used to store and analyze a large amount of collected data. Healthcare centers, emergency services, patients, family members, and physicians are communicated through the cloud server.

In the existing works, cardiac arrhythmia detection has been carried out with different methodologies and various risk factors. A few of the risk factors are type-II diabetes, high blood pressure, tobacco use, and high cholesterol. Feature selection techniques are highly required for improving accuracy and effective utilization of computing resources in the assessment of heart diseases using machine learning approaches. An artificial neural network (ANN) with multi-layer perceptron is utilized for cardiac arrhythmia detection and acute stroke prediction. Convolutional neural network (CNN) and support vector machine (SVM) are combined with spectrogram for classifying heart sounds in the heart diseases diagnosis. It is important to segregate abnormal heart sounds and lung sounds in a phonocardiogram (PCG) based on cardiac arrhythmia analysis [11].

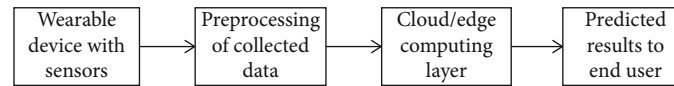


FIGURE 1: Wearable computing framework.

This paper comprises five sections. Section 2 reviews the literature related to edge computing framework, wearable computing, preprocessing of ECG signals, and machine learning-based assessment. Section 3 proposes the edge computing framework with the necessary block diagram and explanations. The obtained results are discussed in Section 4. Finally, the work is concluded in Section 5.

2. Literature Review

In wireless ECG monitoring, wearable devices and sensors collect various physiological parameters of individuals. Sensors are connected through the wireless sensor network for monitoring a greater number of patients. The high-quality signal can be observed through the microcontroller-based preprocessing circuit. ECG signal processing is performed using wavelets for better spectral feature extraction and to improve the SNR. The combination of online monitoring and high-quality processing makes this system a powerful technology for wireless monitoring systems.

CVD risk detection is performed in many works by applying machine learning approaches to identify heart abnormality detection and heartbeat classification. An artificial neural network is used for CVD risk detection in the mobile cloud approach [12]. In their work, the author used virtual machines in the cloud where ANN-based training and learning are done, and the processed data is sent back to the mobile devices. However, the training and learning are performed on the entire data which leads to numerous computations, and cloud computing devices are burdened in case of continuous monitoring of a greater number of users.

Machine learning is also used by many authors in heart disease detection. ANFIS has been used in coronary heart disease risk detection in the cloud-based monitoring system [13]. In addition, decision trees, Naïve Bayes, K -nearest neighbor (KNN), and support vectors (SVM) have been utilized in many works in developing better healthcare monitoring systems. Machine learning techniques are applied in data analysis and complex design applications where it is difficult to apply conventional algorithms and techniques [14]. In biomedical applications, many expert systems are used in smart healthcare monitoring devices, hence the huge amount of data to be processed and classified appropriately using machine learning techniques [15].

A review of ECG signal monitoring techniques indicated that there is a requirement for developing a better-quality assessment and preprocessing technique [16]. Mathematical morphology-based processing introduces distortions to the QRS waves, which cause difficulty in the extraction of R - R intervals [17]. Hence, morphology-based analysis is not effective for ECG signal preprocessing and feature extraction. To overcome the difficulties in morphology analysis, R -peak detection techniques are required. R wave slope

detection is vital in locating the QRS complex in ECG signal feature extraction applications. The low R wave slopes may mislead the physician in ECG signal diagnosis. Hence, the noise removal of ECG signals is carried out using filtering algorithms for better feature extraction [18]. In addition, while monitoring the heart rate of athletes, elderly persons and infants require some wearable devices; the conventional monitoring systems have to be improved with wireless monitoring and processing capability.

Cloud computing and edge computing are widely deployed in smart healthcare systems. In cloud-based systems, signal quality analysis is performed on the mobile device. The complex computations are transferred to the cloud server, and the results are sent back to the mobile devices with a display. Mobile and wearable devices are used for the collection of data, and a cloud server is used for storage and computation. Since mobile devices and wearable devices are connected to the hospital through the internet and router directly, the transfer of data can be accomplished easily [19]. The qualified and processed data are sent to edge devices which may be in either a healthcare center or diagnostic laboratory. The preprocessed data are sent to edge devices, and KNN-based CVD risk detection is carried out. KNN-based ECG beat classification is performed for cardiac arrhythmia detection. Many machine-learning algorithms are utilized for biomedical data analysis [20].

3. Proposed Edge Computing Framework

Cardiac arrhythmia detection and acute stroke prediction are focused on in this work using wearable sensors and an edge computing framework. Figure 2 depicts the process flow of the edge computing framework with sensors and cloud servers. In the proposed framework, preprocessing and feature extraction are performed in the edge computing layer, and decisions can be communicated instantly to the individuals. A huge amount of collected data are sent to the cloud server for storage and further analysis in improving the accuracy of acute stroke risk prediction. Since few heart arrhythmia conditions may be life-threatening, the accuracy needs to be improved in acute stroke prediction from the data acquired by wearable devices. To improve the accuracy of prediction, a deep learning-based CNN algorithm is utilized for feature extraction and classification.

A few significant contributions of the proposed work are as follows:

- (i) Time domain and frequency domain HRV features are used in cardiac arrhythmia detection
- (ii) Various physiological data and HRV features are applied to the CNN for acute stroke prediction

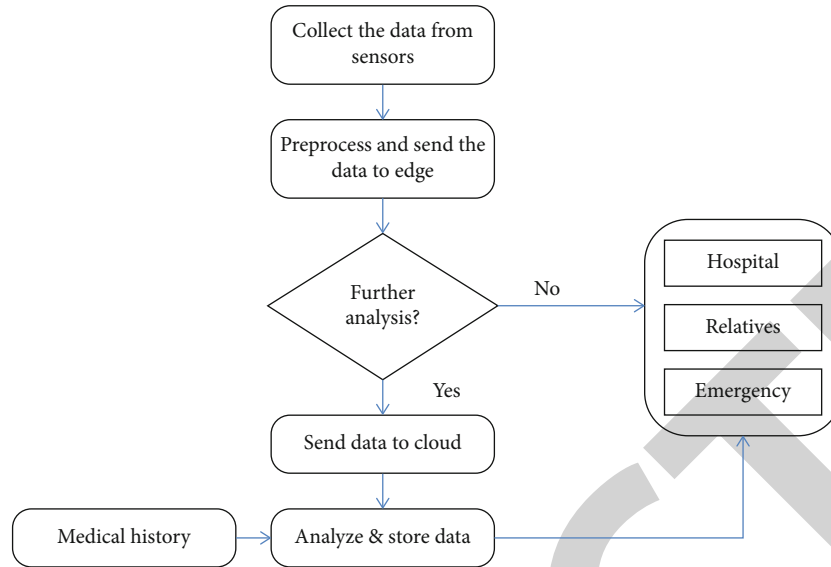


FIGURE 2: Edge computing framework with sensors and cloud.

- (iii) Both MIT-BIH and real-time recorded ECG signals are used to predict acute stroke using a deep learning model
- (iv) A deep CNN-based multiclass classification is performed in acute stroke prediction to classify the subjects into normal, less stroke-risky, and high stroke-risk

3.1. Preprocessing and Feature Extraction. The collected ECG data are preprocessed in the wearable device, and they are sent to the graphics processing unit- (GPU-) based edge computing devices for deep learning-based acute stroke prediction. Blood pressure, glucose level, and cholesterol level can be sent without any preprocessing. However, preprocessing and feature extraction play a major role in ECG signal analysis. A complete data analysis of the ECG signal is highly essential for heart rate feature extraction [21]. Wavelet transform is utilized for ECG signal preprocessing and feature extraction. Statistical and frequency domain analysis is applied to extract the heart rate variability (HRV) of the ECG signal. Statistical features and frequency domain features are utilized for obtaining experimental results. A few statistical features are the mean of RR intervals (RRmean), mean of heart rate (HRmean), the standard deviation of heart rate (HR Std), root mean square standard deviation, and frequency domain features which are VLF Power, LF Power (ms2), HF Power (ms2), and LF norm.

3.2. Assessment of Cardiac Arrhythmia and Acute Stroke Prediction. The collected data are stored as training data and testing data. Usually, 80% of the data can be trained to obtain good classification results. Cardiac arrhythmia detection is performed by preprocessing, model development, testing of the model, and prediction. CNN-based deep learning-based stroke prediction and risk classification are carried out in this stage by the following steps: (i) feature

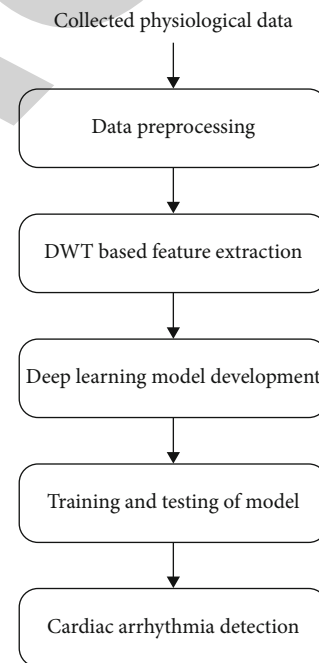


FIGURE 3: Cardiac arrhythmia detection using collected physiological data.

extraction from the quality assessed ECG signal, (ii) applying various physiological data and feature extracted ECG signals to deep learning model, and (iii) cardiac arrhythmia detection is performed by testing the developed model. Figure 3 describes the deep learning model-based cardiac arrhythmia detection.

In this work, deep CNN is utilized for the study with one input layer, two convolution layers, two pooling layers, one fully connected layer, and a classification layer. In this work, two convolution layers and two max-pooling layers are

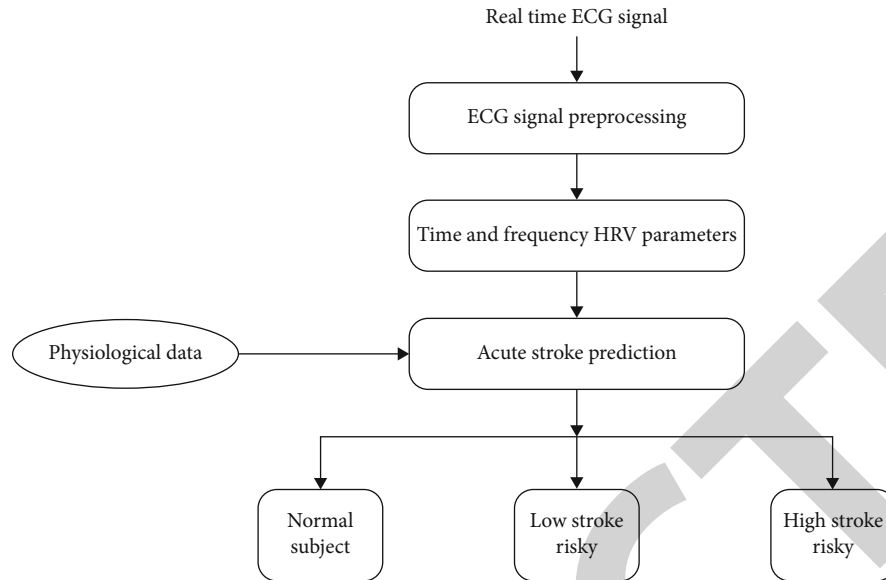


FIGURE 4: Process flow in acute stroke prediction.

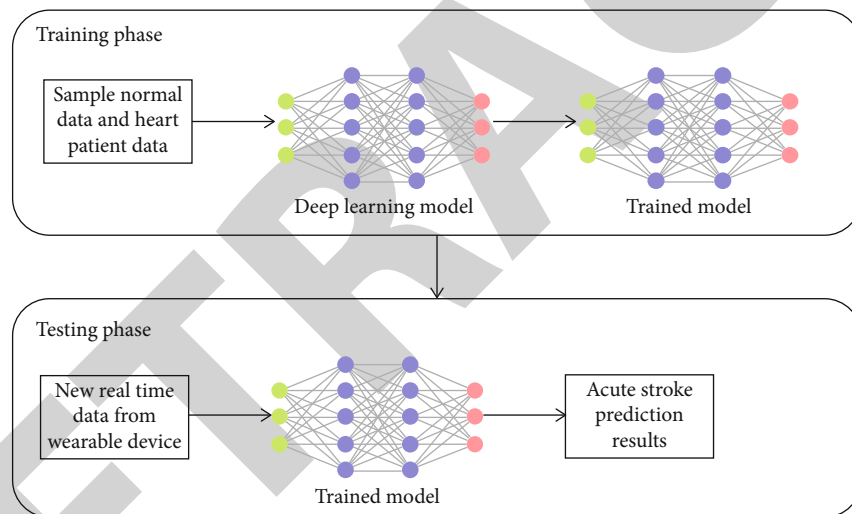


FIGURE 5: Training and testing of deep learning model.

utilized for better localization and feature mapping. Feature maps at the convolution layer are evaluated by

$$X_j^{m,l} = f \left(\sum_{i \in M_j} X_j^{m,l-1} * W_{ij}^{m,l} + b_j^{m,l} \right). \quad (1)$$

$X_j^{m,l}$ is the one-dimensional kernel to produce j^{th} feature map in the convolution layer. Bias values for the j^{th} filter are b_j and M_j .

The feature map for the pooler layer can be computed by

$$X_j^{m,l} = \max_{v \in V} \left\{ X_j^{m,l-1} (r * s + v) \right\}, \quad (2)$$

where r , s , and V are the elements of each feature map.

Acute stroke detection is also focused in the proposed edge computing framework by processing physiological signals. Heart-related chronic diseases are mainly responsible for cardiac arrest, heart attack, and sudden cardiac death. Hence, acute stroke or ischemic stroke detection is highly essential in heart-related chronic disease assessment. Real-time testing of the product enables us to make it better to use the wearable device for stroke prediction. The classification accuracy of chronic disease risk and acute stroke prediction is carried out using specificity, sensitivity, and total classification accuracy. Figure 4 depicts the procedure involved in acute stroke prediction.

A deep learning model is developed for acute stroke prediction using a multiclass CNN algorithm. The training phase and testing phase of the deep learning model is illustrated in Figure 5. The deep learning model is provided with several sample data collected from MIT-BIH and real-time

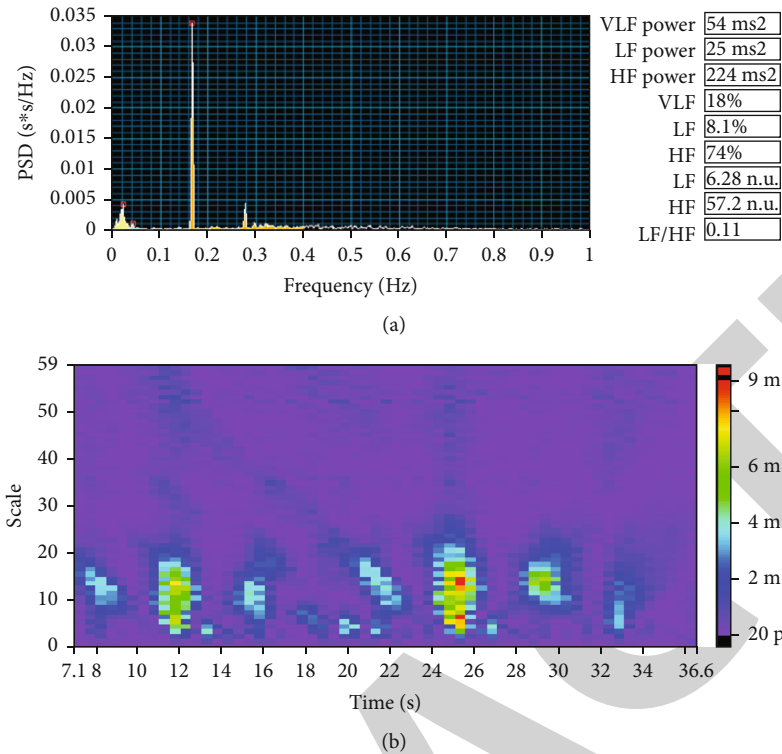


FIGURE 6: HRV feature extraction using wavelets. (a) Power spectral density. (b) Spectrogram.

data. Sample data comprises both the normal subject data and heart patient data with stroke symptoms. The input data comprises many physiological data, heart rate features, and corresponding results. Training is performed on the input data to obtain a trained deep-learning model. The obtained trained model is used to test the incoming new data from wearable devices. Predicted results from testing are communicated to physicians, healthcare centers, relatives, and emergency services. In case of high stroke risk, it is required to pay immediate attention, and information has to be sent to emergency healthcare services.

4. Results and Discussion

Experimental results are obtained using collected physiological data from wearable devices such as temperature, blood pressure, ECG, respiration rate, and cholesterol level. Heart rate variability features are extracted from both the MIT-BIH data and real-time recorded data. Simulation experiments are performed using Matlab software (version 2019a) with a laptop (8 GB DDR4 RAM and Intel i7 processor with a processor speed of up to 4.6 GHz). Feature extraction from the ECG signal is carried out using National Instruments (NI) Biomedical kit application software. The system performance and battery performance of the mobile are observed by transmitting data to edge devices and servers.

The simulation experiments were performed using both the MIT-BIH database and real-time data collected from wearable devices. From the MIT-BIH database, both the cardiac disease patient data and healthy people records have

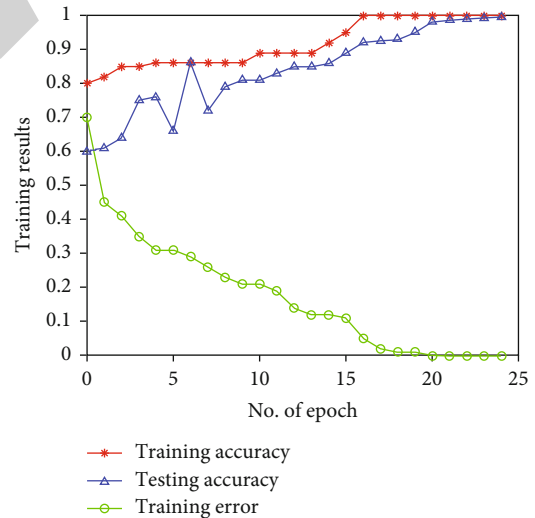


FIGURE 7: Training accuracy, testing accuracy, and error rate for several epoch.

been applied. Fifty heart patients and thirty healthy individuals were recruited for the real-time wearable computing-based data collection. Though the ECG signal amplitudes are in the mV range, the obtained amplitudes are due to the ECG amplifiers. The acquired ECG signal is processed using wavelets for measuring physiological parameters. After identifying the QRS complexes in the ECG signal using DWT, the heart rate can be measured using the interval between R peaks [22].

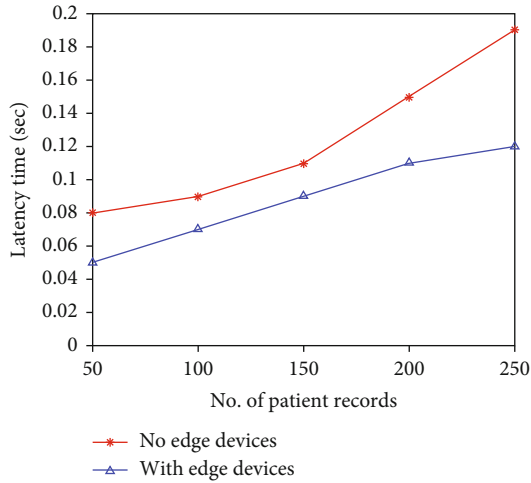


FIGURE 8: Latency analysis of edge computing framework.

TABLE 1: Comparison of execution speed while deploying different edge devices.

Data	Execution speed				Speed increase
	Without edge (sec)	Single-edge device (sec)	Two-edge devices (sec)	Three-edge devices (sec)	
MIT-BIH # 101	713	453	324	112	6.4×
MIT-BIH # 102	709	511	355	106	6.9×
MIT-BIH # 103	813	422	311	97	8.4×
MIT-BIH # 104	754	504	297	84	8.9×
MIT-BIH # 105	823	421	324	86	9.6×
MIT-BIH # 200	765	435	231	90	8.5×
MIT-BIH # 205	912	401	341	105	8.7×
NI lab #101	854	398	375	125	6.8×
NI lab 2 #102	939	431	392	132	7.1×

Heart rate variability features and physiological data such as blood pressure, respiration rate, temperature, and cholesterol level have been fed into the CNN classifier. These details are included in the first paragraph of the results and discussion section. In addition, the parameters of CNN data are discussed in Figure 6. In the existing works, machine learning algorithms

TABLE 2: Comparison of specificity, sensitivity, and accuracy.

Classifier	Specificity (%)	MIT-BIH	
		Sensitivity (%)	Accuracy (%)
ML-ECG&MIL [23]	84.7	85.4	84.9
MF-KNN [24]	86.8	87.4	87.1
EF-SVM [25]	92.2	92.4	92.2
MF-CNN [26]	94.9	95.4	95.1
Proposed (DWT + CNN)	99.1	99.4	99.3

are utilized with preprocessing and feature extraction for heart arrhythmia analysis and stroke prediction; however, they could not obtain the required classification accuracy. In this paper, the CNN classifier is used to improve classification accuracy with three output layers for providing normal, low stroke risky, and high stroke risky.

Statistical features such as the mean of *RR* intervals (*RR*mean), mean of heart rate (*HR*mean), the standard deviation of heart rate (*HR* Std), root mean square standard deviation, and frequency domain parameters such as *VLF* (*ms*²), *LF* (*ms*²), *HF* (*ms*²), frequency ratio *LF*/*HF*, *LF* norm, and *HF* norm are noted for all the subjects. Power spectral density plots with frequency domain features and spectrogram plots with wavelet coefficients are observed using NI biomedical kit. These features are highly essential to improve the accuracy of the proposed deep learning model. Figure 6(a) depicts the power spectral density plot with all the frequency domain features. Figure 6(b) shows the spectrogram plot of the ECG data to obtain the wavelet coefficients and their distribution in terms of scale values. The scale of subjects is varying from 0 to 59 from 7.1 to 36.6 sec. Assessment of the observed values is used to analyze heart arrhythmia and acute stroke prediction.

Time domain features such as mean and standard deviation of heart rate (*HR*) are considered. Threshold values are assigned to the *HR* mean and *HR* standard deviation while categorizing the considered data into normal and disease risk. A total of 512 training data (80%) with a signal length of 60 seconds have been considered which includes MIT-BIH database samples. After training, 128 testing data (20%) were used to validate the accuracy of the classifier. The *R*-peak detected signal is used to calculate beats per minute. To evaluate the performance of the proposed approach, sensitivity, specificity, and accuracy are calculated. These parameters are defined as follows:

$$\text{Sensitivity} = \frac{TP}{TP + FN} \times 100\%, \quad (3)$$

$$\text{Specificity} = \frac{TN}{TN + FP} \times 100\%, \quad (4)$$

$$\text{Accuracy} = \frac{TP + TN}{TP + FN + TN + FP} \times 100\%. \quad (5)$$

In the proposed work, a CNN classifier with a learning rate of 0.1, epochs of 25, and batch size of 640 has been selected for

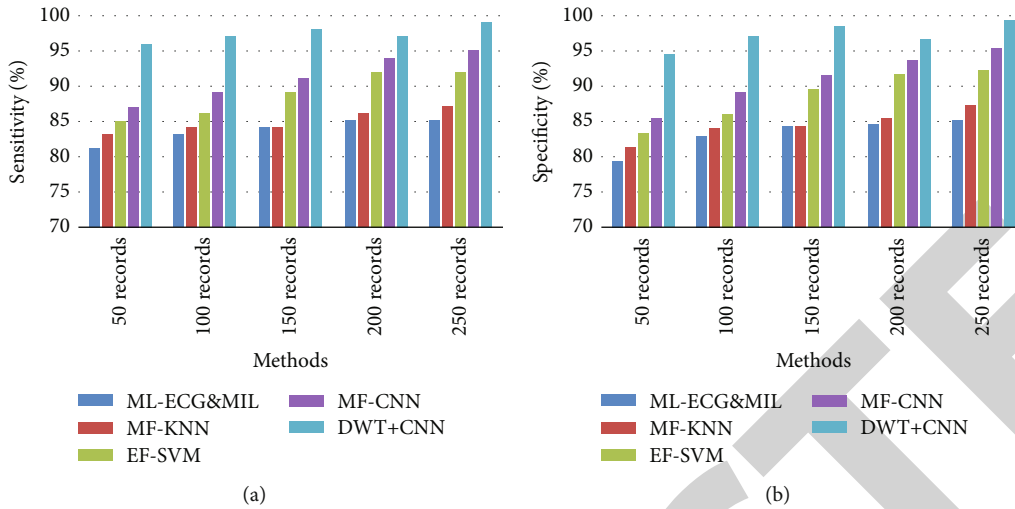


FIGURE 9: (a) Sensitivity analysis. (b) Specificity analysis.

training and learning. Training accuracy, testing accuracy, and training error are measured and depicted in Figure 7.

In the edge computing-based approach, the battery power requirement is ranging from 1 to 1.5% of the total battery power. It is worth noting that mobile approaches consume 12 to 14% of the battery. The execution speed improves by six to ten times in the proposed edge computing approach with three-edge devices when compared with single-edge devices. Latency analysis is also carried out to study the effective performance of the proposed edge framework. Figure 8 shows the latency analysis and comparison of the edge computing framework and the computing framework without any edge devices. The latency time is greatly reduced by the edge computing framework due to the less dependency on cloud services.

Execution speed and latency time are calculated to assess the performance of the proposed edge computing framework. Execution speed improves in the framework due to the local processing and analysis through edge devices. The speed is further improved by increasing the number of edge devices by minimizing the dependency on cloud-based services. Table 1 compares the execution speed of the proposed edge computing approach by deploying a different number of edge devices. In addition to performing accuracy in terms of specificity and sensitivity, the battery is not burdened much while intensive computing operations in the edge computing-based approach.

In most classification approaches, it is necessary to compare the sensitivity, specificity, and accuracy of different approaches while applying them for risk detection. In this work, extracted heart rate features using DWT and physiological parameters are applied to the deep CNN approach. Here, multilead ECG with multiple instance learning (ML-ECG&MIL), morphology features with KNN (MF-KNN), energy features with SVM (EF-SVM), and multiple feature-based CNN (MF-CNN) methods are compared to proposed DWT with deep CNN approach. Table 2 compares the obtained values of specificity, sensitivity, and accuracy while considering 250 patient records. Figures 9(a) and 9(b) depict

the comparative sensitivity analysis and comparative specificity analysis, respectively, which are performed on 50, 100, 150, 200, and 250 patient records. It is observed from these figures that there is a slight variation in the performance. However, the proposed DWT with a deep CNN approach is superior to other existing methods due to its feature extracted and well-trained data.

From Table 2, it is observed that specificity, sensitivity, and accuracy are high in the approach compared with similar methods. Sensitivity, specificity, and accuracy analyses are carried out with a different number of records.

5. Conclusion

In this work, an edge computing approach is proposed to improve the accuracy and speed of assessing cardiac arrhythmia and acute stroke prediction. A deep learning-based CNN model is developed for detecting cardiac arrhythmia and predicting acute stroke. The physiological data and heart rate features of both the MIT-BIH and real-time data are applied to the deep learning model. The proposed DWT-based feature extraction and deep CNN-based multiclass classification provide more accuracy than many existing feature extraction and classification approaches. The proposed classifier achieves a sensitivity of 99.4%, specificity of 99.1%, and accuracy of 99.3% when compared with other similar approaches. The execution speed improves by six to ten times in the proposed edge computing approach with three-edge devices when compared with the single-edge device.

Data Availability

The data used to support the findings of this study are available from the corresponding author upon request.

Conflicts of Interest

The authors declare that there are no conflicts of interest.

Retraction

Retracted: Interior Design of Aging Housing Based on Smart Home System of IOT Sensor

Journal of Sensors

Received 12 December 2023; Accepted 12 December 2023; Published 13 December 2023

Copyright © 2023 Journal of Sensors. This is an open access article distributed under the Creative Commons Attribution License, which permits unrestricted use, distribution, and reproduction in any medium, provided the original work is properly cited.

This article has been retracted by Hindawi, as publisher, following an investigation undertaken by the publisher [1]. This investigation has uncovered evidence of systematic manipulation of the publication and peer-review process. We cannot, therefore, vouch for the reliability or integrity of this article.

Please note that this notice is intended solely to alert readers that the peer-review process of this article has been compromised.

Wiley and Hindawi regret that the usual quality checks did not identify these issues before publication and have since put additional measures in place to safeguard research integrity.

We wish to credit our Research Integrity and Research Publishing teams and anonymous and named external researchers and research integrity experts for contributing to this investigation.

The corresponding author, as the representative of all authors, has been given the opportunity to register their agreement or disagreement to this retraction. We have kept a record of any response received.

References

- [1] X. D. Cui and W. Chung, "Interior Design of Aging Housing Based on Smart Home System of IOT Sensor," *Journal of Sensors*, vol. 2023, Article ID 9281248, 7 pages, 2023.

Research Article

Interior Design of Aging Housing Based on Smart Home System of IOT Sensor

Xiao Dong Cui¹ and Wonjun Chung²

¹Suzhou University, Suzhou, Anhui 234000, China

²Department of Visual Communication Design, Tongmyong University, Busan, Republic of Korea 48520

Correspondence should be addressed to Wonjun Chung; 20141189@stu.sicau.edu.cn

Received 16 September 2022; Revised 10 October 2022; Accepted 25 November 2022; Published 14 February 2023

Academic Editor: C. Venkatesan

Copyright © 2023 Xiao Dong Cui and Wonjun Chung. This is an open access article distributed under the Creative Commons Attribution License, which permits unrestricted use, distribution, and reproduction in any medium, provided the original work is properly cited.

In order to provide more comfortable living space for the elderly, this paper proposes an interior design method of aging housing based on intelligent home system of Internet of things sensors. Taking the residential area as the background environment, create the living space and environment for the elderly through intelligent means. There is a close relationship between the intelligent system in the room and the management center of the residential area and other users in the residential area. Firstly, through the theoretical research on the concepts of home-based elderly care and intelligent elderly care, the development process of intelligent elderly care is described. Finally, in the “people-oriented” concept, summarize and analyze the design methods of intelligent elderly care housing. The application results show that the interior form of the residence, the entrance of the lobby, the bedroom, and the kitchen should be designed for aging and intellectualization, respectively. For example, the clear width of the main passage of the bedroom should be greater than 900 mm, and its direction should be to the long side leading to the bed. The layout of furniture should consider leaving 1500*1500 mm wheelchair rotation space to facilitate the activities of the elderly. *Conclusion.* This method can meet the physiological and psychological needs of the elderly.

1. Introduction

In order to cope with the current severe aging situation, the report of the 19th national congress in 2017 put forward the initiative of “building a policy system and social environment for the elderly, filial piety and respect for the elderly, promoting the combination of medical care and elderly care, and accelerating the development of aging undertakings and industries,” which provides action guidelines for the issue of population aging at the national level [1]. The central urban work conference held in 2015 pointed out that “we will orderly promote the comprehensive renovation of old residential quarters, strive to basically complete the renovation of dilapidated buildings, shanty towns, and villages in the city by 2020, and finally build a harmonious, livable, dynamic, and distinctive modern city.” The government has listed the renovation of old residential quarters in urban construction as the construction focus. It can be seen that the aging transformation of residential buildings has become

one of the key issues of urban construction of the government [2]. The traditional culture of filial piety first is deeply rooted in the hearts of Chinese people. Most people tend to live at home for the elderly after they grow old. Home care is also the basis for the construction of the elderly care service system in the 13th five-year plan. In 2017, the 13th five-year plan for the development of China’s aging cause put forward the construction requirements at this stage, which improved the elderly care service system of “home-based, community-based, institutional, and medical support,” and created a social environment to support the development of the aging cause and the construction of the elderly care system by providing significantly improved quality, more reasonable structure, multilevel, and diversified elderly care services [3]. Among them, the special project to promote the livable construction of the elderly is emphasized. It is required to promote the barrier free construction and transformation of facilities and create a safe, green, and convenient living environment. It is expected that by 2020, 60% of urban

residential areas will meet the construction requirements, 40% of rural areas will meet the construction requirements, and the daily life of the vast majority of the elderly can be carried out normally relying on the community. In response to various pension policies issued by the central government and the “13th five-year plan,” various regions have carried out special planning for pension facilities, which not only carries out targeted overall planning from the urban scale but also successively issued policies for their living space/residential buildings to carry out targeted transformation from the aspect of adaptation to the elderly, in order to create a more suitable livable space for the elderly (as shown in Figure 1).

2. Literature Review

Hu et al. analyzed the light environment of the elderly when they lived and specifically studied the lighting design method in the living space of the elderly from the vision and other factors of the elderly [4]. Cox et al. made a detailed analysis on the building components, spatial scale, functional configuration in the space, common furniture and facilities in the space and the environment in the space for the elderly, put forward the interior design principles, and conducted a detailed study on the apartment for the elderly and the two generation living mode [5]. Losanno et al. mainly investigated the elderly care facilities at that time, conducted targeted research and analysis on the policies and systems at that time and the population base of the elderly, paid attention to the physical and mental conditions of the elderly, put forward a new “elderly care” model, and discussed the indoor and outdoor environment suitable for the lives of the elderly [6]. Hamada et al. summarized the design points of the main entrance space function form, furniture and facilities elements and environmental feeling through the results of investigation and information feedback on the use of the elderly, and took this as the theoretical basis for the project practice [7]. Li et al. have studied the case, design, development strategy, and other contents of elderly care facilities in Japan, thus providing a real reference for the planning, construction and operation development of elderly care facilities, and making up for some deficiencies in aging design [8]. Gong et al. tentatively put forward the landscape design strategy for the external environment of the elderly, summarized some existing problems in the landscape space, and gave the key points of landscape design with the function of health care [9]. Yi et al. drew lessons from and summarized the public space of foreign nursing homes and explored relevant issues [10]. The key points of design are given from the aspects of furniture facilities configuration and functional form in public space, and the design method is summarized from the space environment. Mamom mainly studied the aging problem of the main functional spaces in the elderly living environment and elderly care facilities and put forward the adaptive transformation design strategy [11].

From the professional perspective of architectural design, combined with environmental psychology, environmental behavior, gerontology, marketing, computer science, and other related knowledge, through the research on the

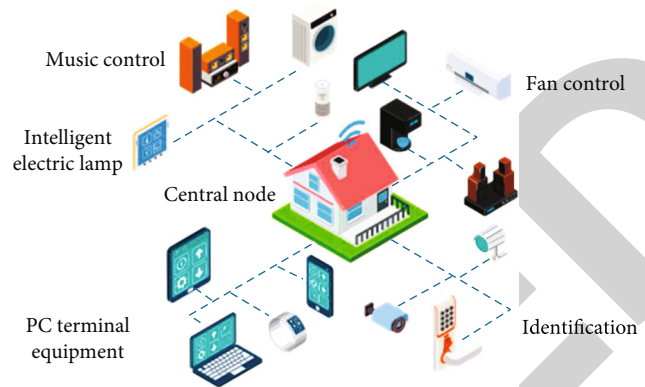


FIGURE 1: Scenario design of smart home aging housing based on IOT sensor network.

trend of social aging, national policies, and the aging market, this paper puts forward many problems about the elderly care. Through the case study, this paper makes a comprehensive analysis on the aging housing. After understanding the living characteristics of the elderly in many aspects, we should ensure that in addition to the barrier free measures that must be ensured in the design, we should combine modern intelligent technology to seek corresponding countermeasures and reasonable solutions to the problem of how to meet the special physiological and psychological needs of the elderly through high technology. This paper mainly focuses on the helping and caring elderly among the elderly.

3. Research Methods

3.1. Concept of Intelligent Home-Based Elderly Care Mode. “Smart home care,” namely, “smart elderly care”, was first proposed by the British life trust foundation and is collectively referred to as “fully intelligent elderly care system.” Intelligent home care system is based on the Internet of Things technology, which embeds intelligent chips in home devices in the house, so as to realize the remote monitoring of the life safety of the elderly. Its core idea is to apply advanced electronic information technology and management concepts, such as sensor network, cloud computing, 3G mobile communication, web services, intelligent data processing, and other related IT technology means, so as to make the government, medical community, and community cooperate closely to provide medical care, travel safety monitoring, entertainment, and other services for the daily life of the elderly. In some cities in China, such as Beijing and Yangzhou, intelligent home-based elderly care has gradually become an inevitable development trend [12].

In order to overcome the impact of the dynamic changes of the network on the transmission of various smart home sensors, the network QoS monitoring technology is introduced to lay a good foundation for intelligent transmission control with real-time monitoring. Add a timestamp at the protocol layer to monitor the network delay, add two fields to each message, and record the last received timestamp (LRT) and the currently sent timestamp (CST) [13]. After

receiving the message, the receiving end calculates the local packet delay according to the LRT and SCT of the message. At the same time, the processing delay of the message in the network can be obtained by subtracting the processing delay of the opposite end according to the last time stamp (LST) saved by the receiving end and the time when the message is currently received.

When end *B* replies *A* message,

$$\text{LRT} = \text{TB} + \Delta t_1, \quad (1)$$

$$\text{CST} = \text{TB} + \Delta t_1 + \Delta t_2. \quad (2)$$

When end *A* receives the message from end *B*, its local

$$\text{LRT} = \text{TA} + \Delta t_1. \quad (3)$$

And its current time is

$$\text{CT} = \text{TA} + \Delta t_1 + \Delta t_2 + \Delta t_3. \quad (4)$$

At this time, it can be calculated that the bidirectional delay of message sending is

$$\text{CT} - \text{LST} - (\text{CST} - \text{LRT}). \quad (5)$$

3.2. Development of Intelligent Elderly Care. The national intelligent elderly care experimental base is an intelligent elderly care demonstration project based on intelligent technology and equipment integration system and the advantages of Internet of Things and cloud computing [14]. Big data and spatial geographic information management integration is based on the principles of “fit for the old, adapt to local conditions, low-carbon environmental protection, and intelligent efficiency.” The project adheres to the policy of “government support, society participation, market-oriented, standardized construction, scientific management, and group development” and takes “platform construction, team construction, channel construction, and brand construction” as the development strategy. Through practice and exploration, the following three modes of intelligent elderly care experimental bases have been preliminarily formed (see Table 1).

The ministry of housing and urban rural development will designate a city as a pilot city for the construction of a national smart city. According to the deployment of the scheme, the smart elderly care comprehensive service platform, which is supported by the government and participated by many enterprises, is launched. The base has successfully explored a new mode of providing for the aged with a new idea of development driven by demonstration. It is realized by adopting IT technologies such as big data, Internet of Things, and mobile Internet. The base simultaneously uses five platforms to pay attention to the daily life of the elderly, and all data are finally transmitted to the children and communities of the elderly through a comprehensive platform (see Figure 2).

Academic circles have also made in-depth research and discussion on the basic theoretical issues of smart cities.

The basic characteristics of smart cities can be summarized into the following four aspects (see Table 2).

It can be seen that the practice of the actual work department in creating smart communities and smart cities and the academic discussion on the basic theoretical issues of smart cities, not only involve the theoretical and practical issues of intelligent elderly care, but also provide guidance for the innovation and development of intelligent elderly care.

4. Result Analysis

4.1. Indoor Space Form

4.1.1. Aging Design. Indoor space, according to different family structures, has different divisions of indoor space. Family population and family model elements are two basic conditions that affect family structure [15]. According to the degree of residence and separation between the elderly and their children, they can be divided into the following three types.

(1) *Sharing Type.* According to the different degree of separation of the special space for the elderly in the residential apartment type, it can be divided into the following three categories, a total of six combinations of different planes (see Table 3 and Figure 3).

(2) *Neighborhood Type.* There are mainly three forms of “living in different households on the same floor,” “living in different floors in the same building,” “living in different buildings in the same group,” and “living in different groups in the same area,” which not only facilitates the completely independent life of the two generations but also ensures the mutual care and emotional communication between the two generations in their daily life.

(3) *Split Type.* Two generations of families are highly independent, but they are still in the same community, which is in line with the living trend of “separation, proximity, long-term contact, and response” in modern life. Most of the elderly live independently [16]. At the same time, there are potential safety problems, which make the elderly unable to receive timely care in terms of physical and mental health.

4.1.2. Intelligent Design. Intellectualization will have a great impact on the division of indoor space forms. Nowadays, most rooms are divided by fixed walls with single function [17]. In the era of more and more intelligence, there are walls that can move and change, and spaces can be freely combined. With the development of science and technology, movable laminated glass, high-tech liquid crystal, or even invisible “virtual wall” may replace a single cement wall to divide the space, which will make the form of indoor space more colorful. With the application of intelligence, the division of residential indoor space will be more flexible and humanized. For example, more and more kitchen designs are changing from the corner of the house to the entrance

TABLE 1: Mode analysis of intelligent elderly care experimental base.

Base mode	Formal content
Comprehensive intelligent elderly community	Newly built intelligent residential buildings, apartments, and nursing homes for the elderly, as well as intelligent health management, life services, culture, and entertainment facilities
Intelligent elderly livable community	With the existing urban communities as the carrier, build an intelligent elderly care service platform to provide intelligent elderly care services for families, community service facilities, and community elderly service institutions
Intelligent aging service organization	Promote and apply intelligent technology and equipment in nursing homes, universities for the elderly, elderly activity centers and other institutions, train relevant family members, and establish an intelligent service network

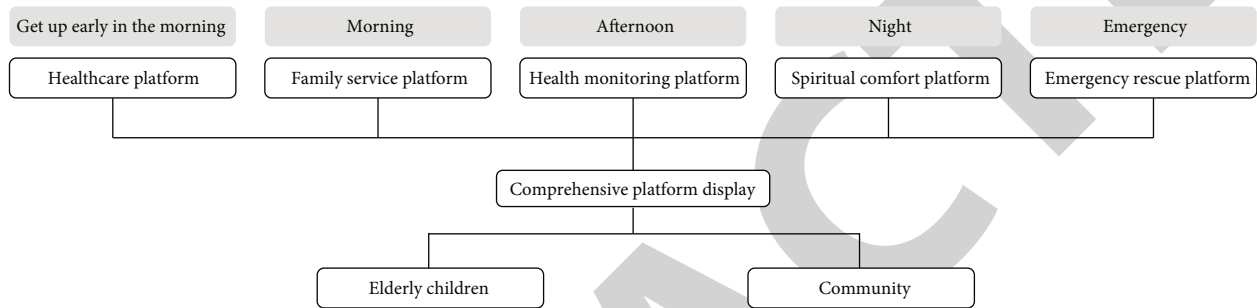


FIGURE 2: Smart community platform.

TABLE 2: Basic characteristics of smart city.

Basic feature	Content description
Comprehensive IOT	Using intelligent sensor equipment to realize the networking of all public facilities in the city
Fully integrated	Internet of Things system and Internet system are fully connected and integrated
Encourage innovation	On the basis of smart infrastructure, the government and relevant enterprises carry out innovative applications in technology and business
Collaborative operation	Each key system of the city operates efficiently and harmoniously with its participants

TABLE 3: Spatial relationship between the elderly and their children.

Cohabitation spatial relationship	
Separate bedroom (separate bedrooms, shared by other spaces)	Family shared toilet Toilet for the elderly
Separate living room and bedroom (independent living room and bedroom, shared by other spaces)	Shared toilet Toilet separation
Separate main living space (independent living room, kitchen, dining room, and bedroom, shared by other spaces)	Common in lobby Vestibule separation

of the house, connecting with the living room and dining room, or directly making an open kitchen. When the old man is alone at home, he cannot help feeling that the big room lacks a sense of security. At this time, intelligent applications come in handy. The old man can use the remote control to create a comfortable private space for himself on the movable wall of his home.

4.2. Entrance Hall

4.2.1. *Aging Design.* The entrance hall is the first place for the host to meet the guests. It is the link between inside and outside. The design of the entrance can reflect the owner's life taste and home design style. In addition to the required daily use safety, attention should also be paid to the portability of

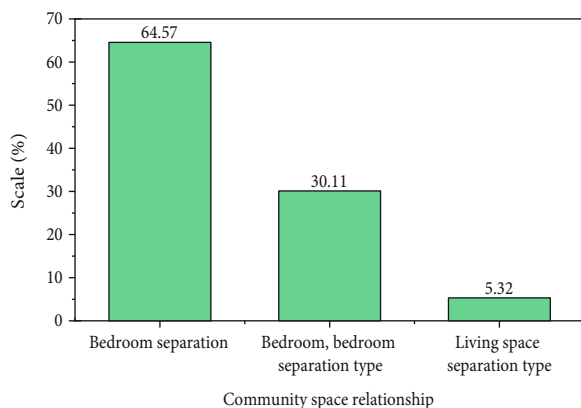


FIGURE 3: Proportion of CO habitation spatial relationship.

the elderly. It can be improved through the following specific aging measures:

- (1) The passageways inside and outside the entrance hall shall meet the smooth passage of the local ambulance stretcher to avoid that the stretcher cannot be used due to the narrow passageway
- (2) The inner side of the entrance hall should be reserved for the elderly to sit down and change shoes. Handrails and grab bars should be installed next to the seats

4.2.2. Intelligent Design. The entrance design should be comfortable, convenient, and safe. In this position, the intelligent system includes night vision waterproof camera, visual intercom function, and fingerprint door lock. A waterproof color camera with night vision function is set at the gate to facilitate the children of the owner or the elderly to observe the images at the gate through the Internet or TV touch-screen anytime and anywhere, and the records are kept for 20 days [18]. Through the visual intercom function, the elderly can easily talk with visitors to open the door in the living room, bedroom, kitchen, and bathroom. In addition, they can also contact the monitoring center and even other residents in the community. Fingerprint door lock refers to the installation of household access control equipment at one side of the house door. Generally, there are visual doorbell and electric fingerprint door lock, which can visually talk with visitors or swipe cards, input passwords, and open doors by pressing fingerprints. A set of entrance protection doors and building door electronic doors are incorporated into the community security and emergency rescue system. Emergency call buttons are installed in public places in the community and in each room of the home, ensuring that the elderly can automatically unlock when there is an emergency and get help in time. It should be noted that the height design of fingerprint door lock and emergency button should meet the ergonomics of the elderly. In addition, we only need to install a touch-screen scene panel, which has been configured with the welcome and leave modes. When visitors arrive, the welcome scene will be turned on, and

the lights will illuminate the whole living room, which is convenient for the elderly to operate, and will also reduce the loneliness of the elderly living alone at home.

4.3. Bedroom

4.3.1. Aging Design. As the elderly get older, their activity ability gradually declines, and they will spend more time indoors. Since sufficient sunshine, fresh air, and beautiful outdoor landscape will play an important role in the physical and mental health of the elderly, the bedroom design should ensure the best lighting, ventilation, and landscape line of sight requirements [19]. The bedroom where the elderly live is best equipped with an auxiliary bathroom. Good aging design of bedroom is reflected in the following points:

- (1) The design of the bedroom should consider the psychological characteristics that the elderly do not like to rest in the same bed. Because the elderly sleep less, snoring at night will interfere with each other, so most elderly people have their own beds or sleep in different rooms. Therefore, when designing the bedroom area, two single beds should be reserved for the elderly to take care of themselves. It is very convenient to provide a bed for relatives to rest when the elderly care for them
- (2) The elderly do not like to sleep in soft beds, because it is not easy to get up and turn over, and it is unhealthy. Therefore, when helping the elderly buy and select mattresses, they should pay attention. It is best to have a handle or handrail beside the bed to help the elderly get up
- (3) The layout of beds, wardrobes, dressing tables, and other furniture should conform to the living habits of the elderly, especially to avoid dead corners of space, so as to prevent the elderly from feeling at a loss or causing unexpected injuries. The bed should not be too close to the window to avoid the direct blowing of cold wind
- (4) The clear width of the main passage of the bedroom should be greater than 900 mm, and it should point to the long side leading to the bed. The layout of furniture should consider leaving 1500*1500 mm wheelchair rotation space to facilitate the activities of the elderly
- (5) The electrical control switch in the bedroom shall be set at the head of the bed for the elderly to facilitate operation

4.3.2. Intelligent Design

(1) Emergency Call System. The bedroom is equipped with an infrared detector. If the elderly do not move for a long time, the emergency call system will send an alarm signal to the community management center and the building management station.

(2) *Profile*. The intelligent control system often selects scene panel, background music panel, LCD TV, emergency button, single connected seesaw reset switch, etc. when configuring equipment. Common scene modes in the bedroom are as follows:

Home mode: it is set as normal living lighting, and the air conditioner should be adjusted to the comfortable temperature of the elderly.

Warm mode: the soft lights in the lamp pool will be turned on, and soft music will be played to create a warm atmosphere and romantic mood.

Reading mode: the illumination of the bedside lighting should be suitable for reading, and the rest should be turned off [20].

Theater mode: the curtains are automatically closed, and the lights are in place in one step, creating a visual and audio effect of being born in its environment.

Night rising mode: the wall lamp is lit slowly, and the light in the corridor leading to the bathroom is also lit, which will not disturb the rest of friends and family. When they pass by again, the light will go out naturally.

4.4. Kitchen

4.4.1. *Aging Design*. Standardized kitchen operation often brings inconvenience to the elderly. It is necessary to consider the arrangement order and position of kitchen utensils such as refrigerator, sink, stove, and storage cabinet in the cooking activities of the elderly. Considering that the elderly are relatively weak in terms of mobility and energy, the design should try to make the elderly shorten the time in the cooking process, make the operation steps smooth, simple, and convenient, and avoid wasting physical strength and overturning dishes and bowls.

- (1) *Appropriate area of the kitchen*: after the kitchen is equipped with the console, the net width shall not be less than 1500 mm to ensure that there is enough turning space for the wheelchair elderly
- (2) *The plane layout of the kitchen*: the layout form is relatively flexible. The common types are type I, II, L, H, and U. The L-shaped layout has a simple and clear operation flow line. It is reasonably arranged according to the sequence of food storage-sorting-cleaning-cutting-cooking-equipment, which is more suitable for the elderly [21]
- (3) *Kitchen cabinets*: the height from the bottom of the cabinet to the ground shall be 140~150 mm, and the height of the console shall be 750 mm. In order to facilitate the use of the elderly, the operating table with a width greater than 500 mm is more suitable, the clear height under the table should be greater than 600 mm, and the depth of the clearance under the table should be greater than 250 mm
- (4) *Pool part*: the wheelchair needs to be inserted under the console, so the pool depth should be relatively

reduced. The height of the pool table is usually as follows: the height of the knee of the person sitting in the wheelchair is 180 mm, of which the pool depth is 160 mm

4.4.2. *Intelligent Design*. The modern integrated kitchen is more fashionable and humanized than the traditional kitchen. Due to the decline of memory of the elderly, sometimes they forget to turn off the gas when cooking, and often forget to turn off the light or it is inconvenient to turn off the light. Intelligent installation provides us with great convenience.

- (1) The lighting design of the kitchen part is relatively simple, and the ordinary reset switch can be used. Connect the switch with the light control system to realize the control by the light system
- (2) Install TV in the kitchen so that residents can watch TV and listen to FM while cooking. When visitors visit, the TV in the kitchen can also be used as a visual intercom
- (3) Control the start and stop, wind speed, temperature, and mode of the kitchen air conditioner through the touch screen. If you forget to turn off the air conditioner, the elderly can turn off the air conditioner in the kitchen by pressing the "late night mode" before going to bed [22]
- (4) The elderly will inevitably forget to turn off the gas. The intelligent system will automatically cut off the gas valve and give an alarm when the CO concentration exceeds the standard. If the smoke concentration exceeds the standard, the alarm can be triggered. Finally, connect the lighting system with the alarm system. Once the alarm is given, the lights of the whole house will be bright to remind the residents more conveniently
- (5) The highly intelligent kitchen can also monitor the residents' diet and propose menus. After a dish is selected, the kitchen will search for its cooking methods through the Internet. The intelligent system can also be linked with the district supermarket to automatically order food

5. Conclusion

As a new mode of providing for the aged, intelligent home-based elderly care is still in the initial stage of exploration. With the further development of people's living standards and comprehensive national strength in the future, intelligent elderly care will become a strategic emerging industry. In addition to the characteristics and functions of ordinary houses, the residential design under the intelligent elderly care has higher requirements for comfort and personalization. In order to meet the needs of intellectualization and aging adaptation, the design is based on the principle of "aging adaptation, adaptation to local conditions, low-carbon environmental protection, intelligent, and efficient" to design the interior, appearance, landscape, and other

Retraction

Retracted: A Voice Recognition Sensor and Voice Control System in an Intelligent Toy Robot System

Journal of Sensors

Received 12 December 2023; Accepted 12 December 2023; Published 13 December 2023

Copyright © 2023 Journal of Sensors. This is an open access article distributed under the Creative Commons Attribution License, which permits unrestricted use, distribution, and reproduction in any medium, provided the original work is properly cited.

This article has been retracted by Hindawi, as publisher, following an investigation undertaken by the publisher [1]. This investigation has uncovered evidence of systematic manipulation of the publication and peer-review process. We cannot, therefore, vouch for the reliability or integrity of this article.

Please note that this notice is intended solely to alert readers that the peer-review process of this article has been compromised.

Wiley and Hindawi regret that the usual quality checks did not identify these issues before publication and have since put additional measures in place to safeguard research integrity.

We wish to credit our Research Integrity and Research Publishing teams and anonymous and named external researchers and research integrity experts for contributing to this investigation.

The corresponding author, as the representative of all authors, has been given the opportunity to register their agreement or disagreement to this retraction. We have kept a record of any response received.

References

- [1] C. Luo, "A Voice Recognition Sensor and Voice Control System in an Intelligent Toy Robot System," *Journal of Sensors*, vol. 2023, Article ID 4311745, 8 pages, 2023.

Research Article

A Voice Recognition Sensor and Voice Control System in an Intelligent Toy Robot System

Cong Luo 

School of Information Science and Engineering, Changsha Normal University, Changsha, Hunan 410100, China

Correspondence should be addressed to Cong Luo; m17201034@stu.ahu.edu.cn

Received 13 September 2022; Revised 3 October 2022; Accepted 11 October 2022; Published 14 February 2023

Academic Editor: C. Venkatesan

Copyright © 2023 Cong Luo. This is an open access article distributed under the Creative Commons Attribution License, which permits unrestricted use, distribution, and reproduction in any medium, provided the original work is properly cited.

In order to make the toy robot more entertaining, interesting, and intelligent, a voice recognition sensor and voice control system in the intelligent toy robot system are proposed. The system builds an overall system architecture including a client and a server. Through the camera calibration and data transmission module of the client, it collects images and calculates the internal and external parameters of the camera and transmits the image and external parameter data to the server. With the images and external parameter data transmitted from the terminal, a background image is constructed and the camera position and angle are updated in real time to complete the fusion of virtual and real scenes. Through the motion control part of the user interaction module, hearing-impaired children can control the movement and rotation of smart toys. The experimental results show that the system has high communication synchronization and stability and can realize high-precision control of smart toys, and the average frame rate can reach 30.97 f/s. The beneficial effect of the system is that it has various functions, has the effect of speech recognition, and is highly interesting.

1. Introduction

With the improvement of people's material and cultural living standards, people's consumption level is getting higher and higher [1]. At present, children's toys, especially smart toys, have a large market. Smart toys can not only satisfy children's curiosity and strengthen the interaction between children and toys but also stimulate children's curiosity [2]. Smart toys integrate advanced technologies in the fields of computers, electronics, and communications, breaking through the limitations of traditional toys, giving the toy the functions of "listening" and "speaking," interacting with people, and combining knowledge with pleasure, can enable children to learn and experience life in pleasure, and truly achieve the purpose of entertaining and teaching [3].

The toy industry is undergoing a technological revolution, and the future toy industry will develop in the direction of interactivity, intelligence, education, and high-tech content [4]. Traditional toys have a single function and generally only meet the requirements of entertainment. In order to develop creative and selling toys, it is necessary to emphasize the multi-

functionality of the toy, so that it can meet the needs of various functions such as entertainment, science, intelligence, and ideological education [5]. The combination of computer technology, microelectronic technology, microsensing technology, and mechanical technology makes toys more vibrant and magical [6]. The intelligent toy robot collects sound signals and performs speech recognition; the motion control of the robot is realized according to the recognized speech [7]. The system adopts a modular design scheme, which not only realizes intelligent control but also increases interactivity, and achieves the effect of entertaining toy robots.

Now most toys are developing in the direction of intelligence, and the upsurge of smart toys is unstoppable, and smart toy robots have become well-known children's playmates [8]. However, the products on the market currently have a single function, and if it is a fully functional robot, the price is very expensive. Children's robot toys mainly produced in the society for early education and companionship have strong interactive functions, which can meet the various needs of young children, and allow children to interact with robots better and increase their interest [9]. Children's intelligent toys,

with a little expansion, can replace people to perform tasks in a variety of occasions that are not suitable for human work, so this kind of intelligent children's toys have important academic research value.

2. Literature Review

Hearing-impaired children have a lack of self-awareness to varying degrees due to their physical defects; therefore, personality and psychological defects such as depression and self-enclosure are prone to occur, which will lead to hearing-impaired children form obstacles in interpersonal communication in the long run [10]. Defects in language and hearing make them more accustomed to experiencing the external life and cognition of the world through vision; therefore, smart toys designed for hearing-impaired children should pay more attention to the visual impact and interactive experience [11]. Based on this design, the intelligent toy for hearing-impaired children can arouse the emotions of hearing-impaired children and let their attention focus on the interaction with the smart toy, so that they have a deep sensory response; it can effectively stimulate their learning interest and potential, eliminate psychological barriers such as self-enclosure of hearing-impaired children, and improve their interpersonal skills [12]. In order to achieve this purpose, it is necessary to design a system that can realize the interaction between hearing-impaired children and smart toys.

The control system based on Mindstorms completes the communication between the control robot and the PC through the UDP protocol and uses PD to realize the control, the control accuracy of this system is high, but the communication synchronization and the fluency of the screen presentation are poor. The control system based on WinCE is connected with the controller through the remote debugging mode, the control of the robot under the built-in WinCE operating system of the teach pendant is completed, the fluency of the system screen presentation and the stability of communication synchronization are better, but the control accuracy is slightly worse [13]. Augmented Reality (AR) technology is a kind of real-time calculation of camera position and angle using computer vision technology, at the same time, the technology of superimposing computer-generated 3D virtual objects or 2D images into real images. It not only inherits the advantages of virtual reality technology but also makes up for the shortcomings of virtual reality technology; compared with virtual reality technology, its display effect is more realistic [14, 15].

Based on the above analysis, the author designed an intelligent toy system for hearing-impaired children based on AR technology, which belongs to a virtual intelligent toy interactive system, which can realize the accurate demonstration of the movement status and various functions of real intelligent toys and provide interactive functions at the same time [16]. The system can provide more brilliant presentation effects for hearing-impaired children through virtual intelligent toys; at the same time, it can replace the functions of real smart toys, bring fun that real toys cannot provide, and improve the interactive ability and self-cognition ability of hearing-impaired children.

3. Methods

3.1. Intelligent Toy System for Hearing Impaired Children Based on AR Technology

3.1.1. Overall System Architecture. By analyzing the requirements of the smart toy system for hearing-impaired children with AR technology, the C/S architecture is used to create an overall system architecture that protects the client and server [17]. Among them, the main tasks of the client are collecting images, calibrating cameras, and computing scene information. The key responsibilities of the server side are building and rendering virtual scenes, intelligent toy motion control, virtual-real integration of scenes, and user interface display. The overall architecture of the system is shown in Figure 1.

According to the actual application requirements of the intelligent toy system for hearing-impaired children with AR technology, the functional requirements of the system are divided into basic functional requirements and advanced functional requirements [18]. Among them, the basic functional requirements belong to the foundation of the normal operation of the system, and the camera posture is accurate by calibrating the camera, so as to achieve the purpose of virtual and real integration of the smart toy scene. The focus of advanced functional requirements is to manually control interactive functions such as virtual intelligent toy roaming and designated roaming routes for hearing-impaired children [19].

3.1.2. Division and Design of System Functional Modules

(1) Camera Calibration and Data Transmission Module. The camera is calibrated by collecting a certain amount of images with a complete identification map, and the internal parameters of the camera are calculated, and the internal parameters of the calculation are stored in an XML format file [20]. By reading the calculated internal parameters, based on each frame of image collected, the external parameters of the camera are calculated, and the calculated external parameters of the camera and the collected current frame image data are sent to the server. Continue to enter the next frame; repeat the above process to implement the frame loop. Data transmission is realized through Socket, after establishing a TCP connection with the server, each frame of data is sent in packets, and the operation is repeated until the process is completed or terminated. The process of camera calibration and data transmission module is shown in Figure 2.

(2) Scene Virtual Reality Fusion Module. This module mainly includes two parts: virtual scene construction and scene virtual-real integration. The system completes the construction of the virtual environment based on the real scene; the built virtual scene mainly includes Smart toy 3D model, virtual camera, model material, and scene light source and virtual ground. In addition, the automatic roaming function is added to the virtual intelligent toy, so that it can implement a roaming display in a virtual environment.

The camera external parameter data and image data transmitted by the client are received by the data receiving module on the server. The image data received through format

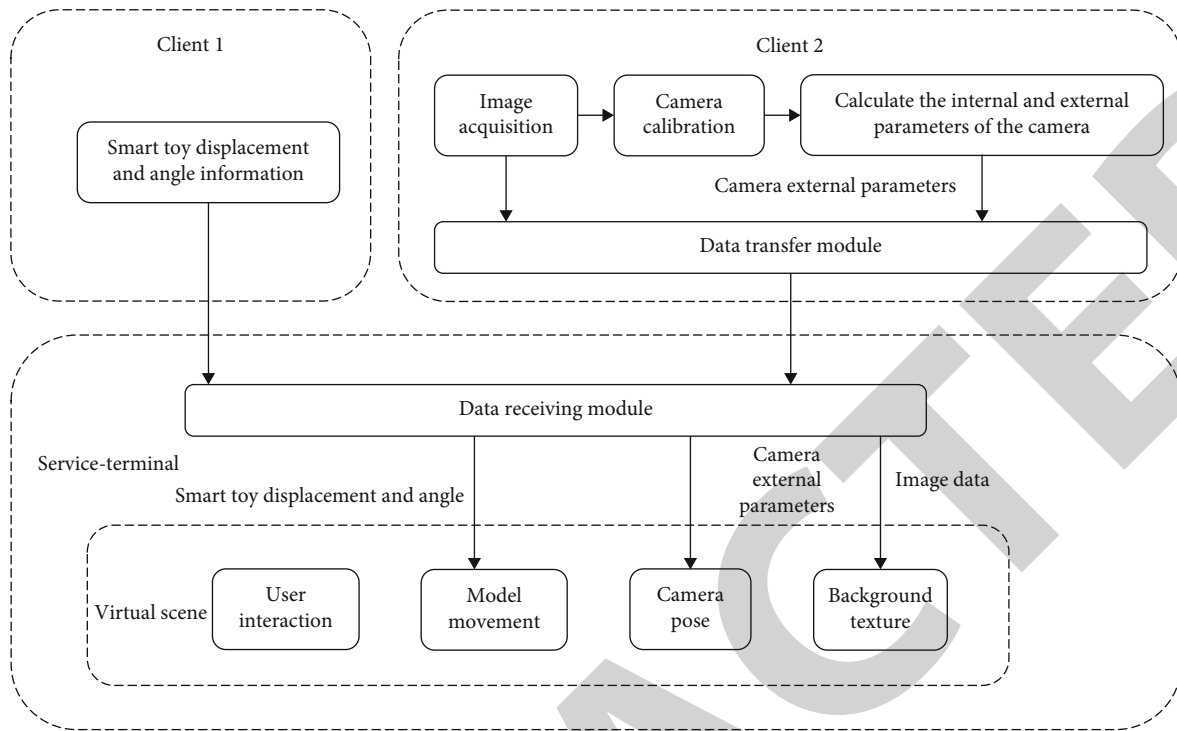


FIGURE 1: Overall architecture of the system.

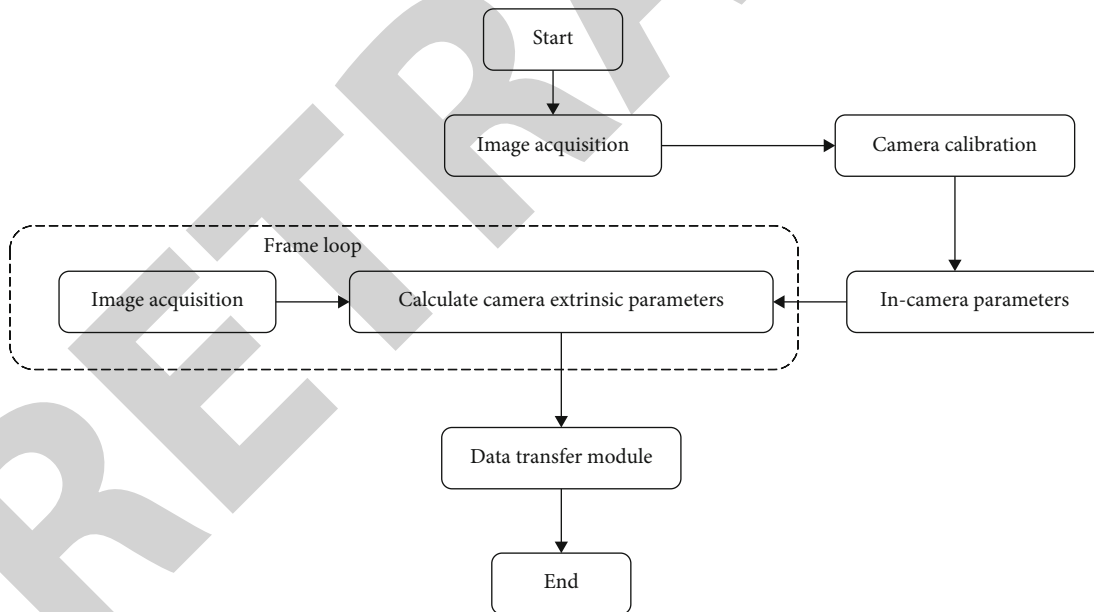


FIGURE 2: Process diagram of camera calibration and data transmission module.

transformation is regarded as the background map of the current frame. Use the received external parameters of the camera to calculate the pose and angle of the camera, and set the camera pose of the current frame according to the calculation result. Enter the next frame to perform the above process in a loop, and show the sensory effect that combines the real scene and the virtual scene to the hearing-impaired children.

(3) *User Interaction Module.* On the basis of the above two modules, a user interaction module including two parts of intelligent toy motion control and specified motion path is designed, to provide better immersion and realism to hearing-impaired children.

Through the motion control part in the user interaction module, hearing-impaired children can control the rotation

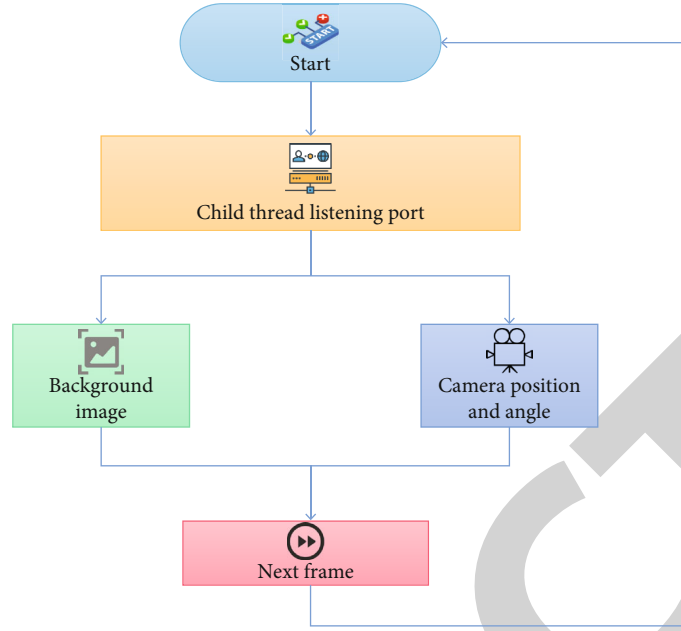


FIGURE 3: Scene update process.

and movement of smart toys with keyboard, mouse, or other input devices. The screen pick-up function can be realized through the specified motion path part in this module; for example, a hearing impaired child can specify a certain point in the virtual environment with the mouse, and the system can detect the position of the specified point and make the smart toy move according to the detected designated point position.

3.2. Calculation of Internal and External Parameters of the Camera. Suppose a point in the three-dimensional space is projected to the center of a plane, the point in the three-dimensional space is represented by $P = (X, Y, Z)^T$, and the projection center is used as the origin of the coordinates of the Euclidean space, the origin of this coordinate is the optical center of the camera, the image plane or focal plane is represented by plane $Z = f$, and f represents the camera focal length. For the pinhole camera used in the system, the intersection of the image plane and the line connecting point P and the projection center, p is the projection of point P on the image plane, based on the similarity relationship of triangles, the coordinate $(fX/Z, fY/Z, f)^T$ of the intersection point p is obtained, and the coordinate of the projection point on the projection plane is this coordinate. When the focal lengths in the x and y directions are not uniform, the coordinates can be expressed as $(f_x X/Z, f_y Y/Z, f)^T$, when the coordinates of the projection plane are converted into image coordinates, the optical center amount $(f_x X/Z + cx, f_y Y/Z + cy, f)^T$ of the optical center relative to the origin of the image coordinates should be added, and the optical center offsets in the x and y directions are represented by cx and cy , respectively. If the above projection process from three-dimensional points to the image plane is represented by a matrix, at the same time,

it is defined as a projection function π ; then, there is formula:

$$\begin{bmatrix} X \\ Y \\ Z \end{bmatrix} \mapsto \begin{bmatrix} u \\ v \\ 1 \end{bmatrix} = \pi(P) = \frac{1}{Z_p} KP = \frac{1}{Z} \begin{bmatrix} f_x & 0 & cx \\ 0 & f_y & cy \\ 0 & 0 & 1 \end{bmatrix} \begin{bmatrix} X \\ Y \\ Z \end{bmatrix}. \quad (1)$$

In the formula, K represents the camera internal parameter matrix; $(u, v, 1)$ represents a point in three-dimensional space. If the depth value $Z(p)$ of the pixel p in the image is known, the relative three-dimensional space coordinates can be obtained through the back projection function π^{-1} , which can be expressed as

$$\begin{bmatrix} u \\ v \\ 1 \end{bmatrix} \mapsto \begin{bmatrix} X \\ Y \\ Z \end{bmatrix} = \pi^{-1}(p, Z(p)) = \begin{bmatrix} \frac{Z(p)(u - cx)}{f_x} \\ \frac{Z(p)(v - cy)}{f_y} \\ Z(p) \end{bmatrix}. \quad (2)$$

The pose of the camera is represented by a 4×4 matrix, that is, the external parameter matrix of the camera, which can be expressed as

$$H_{4 \times 4} = \begin{bmatrix} R_{3 \times 3} & t_{3 \times 1} \\ 0 & 1 \end{bmatrix}. \quad (3)$$

In the formula, $R \in R^{3 \times 3}$ and $t \in R^3$ represent the rotation matrix and translation vector.

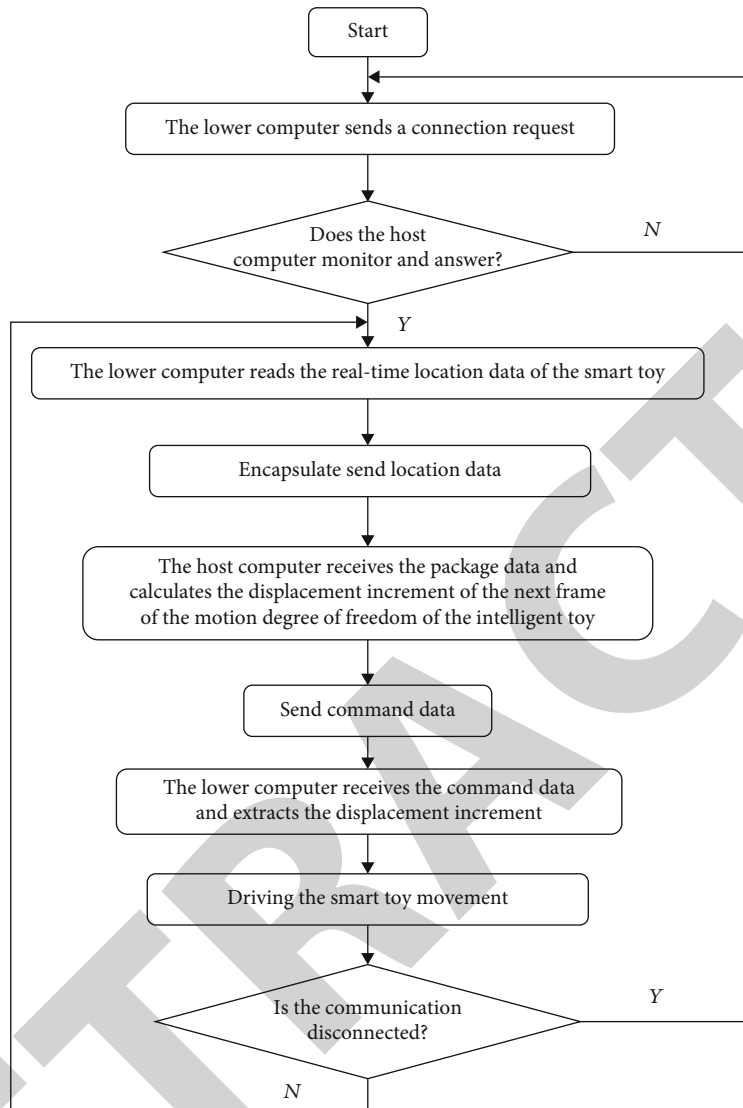


FIGURE 4: Motion control process of smart toys.

TABLE 1: System test environment.

Test environment	
Service-terminal	Microsoft SQL Server 2014 database, Windows Server 2016 server operating system, Power Builder 9.1 and IIS 6.1 Information Services Management Tools
Client	Windows 10, Power Builder 9.1, IE10 and Browser of above version

3.3. Fusion of Virtual and Real Scenes. By setting the background map and updating the camera position and angle in real time, the virtual scene and the real scene can be made close to the same, and the virtual and real scene can be merged.

3.3.1. Background Texture Structure. Fusion of virtual scenes and real scenes is the key to AR technology, so as to achieve the effect of superimposing virtual objects or images into the actual environment, so the images collected by the camera should be used as the background texture of the virtual scene. By using the depth rendering hierarchy of the auxiliary camera, constructs a background map within the scene. The objects are

rendered from high to low based on the depth value, which is the rendering order in the entire virtual scene. The depth value of the background texture is set to -1, the depth value of other scene elements is 1, the acquisition interval of the main camera in the scene is set to the depth value ≥ 1 , and the acquisition interval of the auxiliary camera is set to the depth value ≤ -1 , in this way, all other scene elements in the entire virtual scene except the background texture are imaged by the main camera, and the auxiliary camera only images the background texture. When rendering each frame of image, the part with high depth value in the entire virtual scene should be rendered first, and then the background texture with low depth value should be

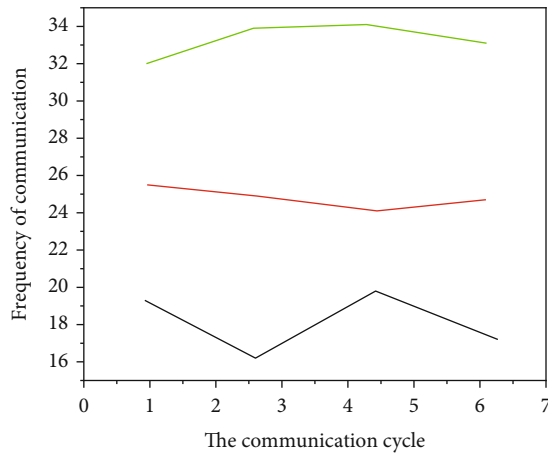


FIGURE 5: Comparison results of communication frequencies of each system.

rendered; get the final result with the background texture placed behind the entire virtual scene.

3.3.2. Data Reception and Scene Update. After the construction of the background texture is completed, each frame is rendered in the scene, the background texture is updated through the image data received by the listening port, and the position and angle of the virtual camera are adjusted in real time. The scene update process is shown in Figure 3. Use New Thread to build a child thread, and open the listening port in the child thread to implement monitoring. When the subthread listening port receives the image data, it implements the corresponding coordinate transformation. The three-channel value of the relative position pixel is set in turn by GPU operation, which avoids the problem of low operation efficiency of individually setting each pixel value. Store all the pixel values of each image in the Color array, and then set the background texture pixel values of the current frame.

3.4. Motion Control of Smart Toys. In order to realize the motion control of smart toys, it is necessary to design a feedback incremental control method based on the client/server mode and based on the TCP/IP protocol; among them, the client side and the server side are the lower computer and the upper computer, respectively. The specific control process is shown in Figure 4.

The specific control steps are as follows:

- (1) A connection request is sent by the lower computer
- (2) The upper computer monitors the connection request sent by the lower computer
- (3) When the upper computer monitors the connection request from the lower computer, if it does not give a response, it returns to step (1). If the lower computer gets the connection response from the upper computer, it will continue
- (4) The lower computer reads the current position data $\{E, A_1, A_2, \dots, A_5\}$ of the smart toy; among them, A_1

$\sim A_5$ represents the five rotational degrees of freedom of the smart toy, and E represents the overall translational degree of freedom of the smart toy, which is packaged in a data packet format and sent to the upper computer

- (5) When the upper computer receives the data packet from the lower computer, based on the set motion trajectory, the operation is performed on the displacement increment $\{\Delta E, \Delta A_1, \Delta A_2, \dots, \Delta A_5\}$ of the next frame of the motion degree of freedom of the smart toy, and it is packaged and sent to the lower computer in the instruction format
- (6) After the lower computer receives the command data from the upper computer, it extracts the displacement increment data of each degree of freedom of the smart toy and drives the smart toy to move according to the set increment
- (7) The lower computer checks whether the communication is disconnected, if not, go to step (4). Otherwise, go to step (1)

3.5. Simulation Experiment. Take the intelligent toys produced by a company as the experimental object to test the comprehensive performance of the system. Select the intelligent robot control system based on Mindstorms and the open 6R industrial robot control system based on WinCE as the system comparison system, the two comparison systems are Mindstorms' intelligent robot control system and WinCE's open 6R industrial robot control system, and experimental intelligent toys are used in the three systems to compare and analyze the comprehensive performance of each system. The system test environment is shown in Table 1.

4. Results and Discussion

When implementing the motion control of experimental smart toys in the interactive process, the communication synchronization between the upper computer and the lower computer is particularly important; the higher the synchronization, the more sensitive the smart toy is to the motion control in the interaction process, which can effectively improve the real experience of hearing-impaired children when interacting. Here, the communication synchronization of the three systems is detected and analyzed by the communication frequency, and the obtained detection results are shown in Figure 5. From Figure 5, it can be concluded that the system and WinCE system increase with the communication cycle; the communication frequency does not fluctuate significantly, while the communication frequency of the Mindstorms system fluctuates more obviously. The overall communication frequency of the system is significantly higher than the other two systems; it can be seen that the communication synchronization between the system and the WinCE system is more stable, and the communication synchronization of the system is higher.

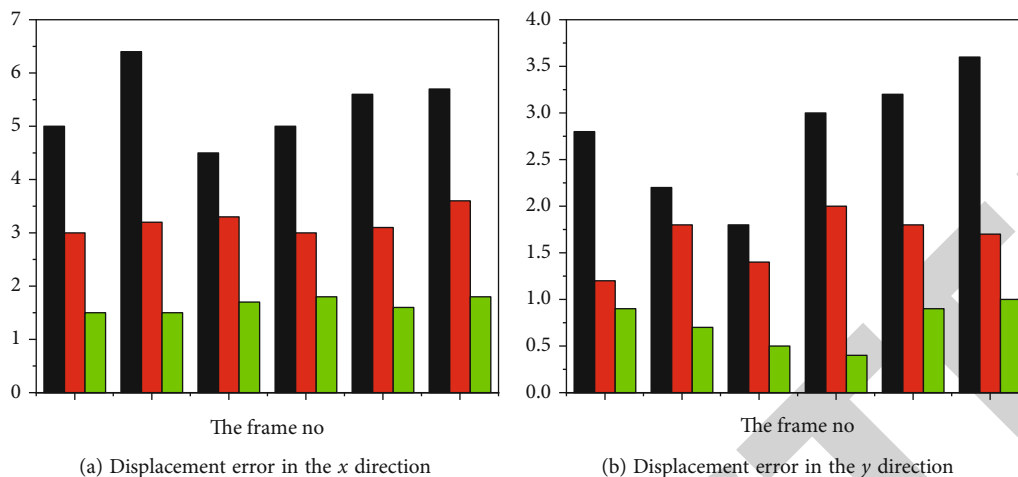


FIGURE 6: Comparison of motion errors of smart toys under the control of each system.

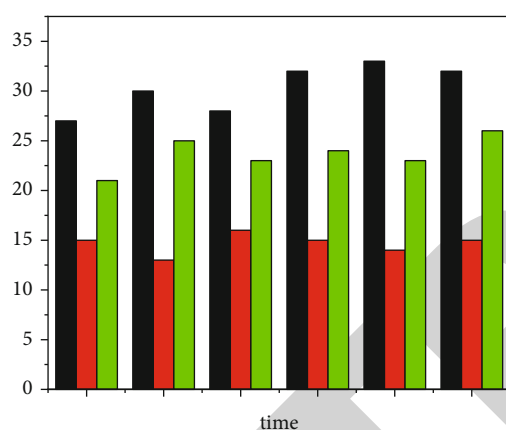


FIGURE 7: Comparison of frame rate test status of each system.

The cameras used in the three systems were installed on the experimental smart toys in turn, and the motion control errors when controlling the experimental smart toys during the interaction of each system were compared. During the motion control process of each system, the error between the actual trajectory and the designed trajectory of the experimental smart toy is calculated, this compares the motion control errors of each system. The errors in the two translation directions of x and y are compared, respectively, and the comparison results are shown in Figure 6(a) and (b). It can be seen from Figures 6(a) and 6(b) that, under the control of the system, the average displacement errors in the x , y , and two directions of the experimental smart toy are 1.96 mm and 0.69 mm and the maximum errors in the two directions are 2.41 mm and 0.98 mm in sequence. Under the control of Mindstorms system, the average displacement errors in x , y , and two directions of the experimental smart toy are 3.08 mm, 1.76 mm, respectively; the maximum errors in the two directions are 3.86 mm and 2.12 mm in turn. Under the control of the WinCE system, the average displacement errors in the x , y , and two directions of the experimental smart toy are 5.47 mm and 2.78 mm, respectively, and the maximum errors in the two directions

are 6.23 mm and 3.66 mm. This shows that the motion control error of the system for the experimental smart toy is lower; it can better realize that the actual motion trajectory of the smart toy coincides with the designed motion trajectory and has good control effect, high precision, and superior control performance.

In order to further test the smooth performance of the system for rendering dynamic images, the test statistics are now carried out on the frame rate status of the background texture update of the three systems within 30 s; the specific test statistics obtained are shown in Figure 7.

By analyzing the test results of each system in Figure 7, it can be concluded that in the process of implementing the background map update; the average frame rates of the system and WinCE system are 30.97 f/s and 25.55 f/s, respectively, which is significantly higher than the average frame rate of Mindstorms system of 15.33 f/s; it can be seen that the system and WinCE system can provide more effective guarantee for the smooth display of dynamic pictures, while the Mindstorms system is slightly weaker in the fluency of dynamic pictures.

Based on the above three sets of experimental test results, it can be seen that the comprehensive performance of the system in terms of communication synchronization, motion control performance, and smooth performance is better, and it has very good real-time interactive performance, which can effectively improve the interactive experience and interaction between hearing-impaired children and smart toys.

5. Conclusion

The author proposes a design and research on the motion control system of intelligent toy robot based on speech recognition and sensors, aiming at the defects of hearing-impaired children in interaction and interpersonal communication, and provides a system that can realize real-time interaction between hearing-impaired children and intelligent toys. Through the virtual and real fusion of AR technology, the purpose of superimposing virtual objects or images in the real environment is realized, to provide a realistic virtual interaction scene for hearing-impaired children, combine the motion

Retraction

Retracted: The Application Effect of Remote Sensing Technology in Hydrogeological Investigation under Big Data Environment

Journal of Sensors

Received 12 December 2023; Accepted 12 December 2023; Published 13 December 2023

Copyright © 2023 Journal of Sensors. This is an open access article distributed under the Creative Commons Attribution License, which permits unrestricted use, distribution, and reproduction in any medium, provided the original work is properly cited.

This article has been retracted by Hindawi, as publisher, following an investigation undertaken by the publisher [1]. This investigation has uncovered evidence of systematic manipulation of the publication and peer-review process. We cannot, therefore, vouch for the reliability or integrity of this article.

Please note that this notice is intended solely to alert readers that the peer-review process of this article has been compromised.

Wiley and Hindawi regret that the usual quality checks did not identify these issues before publication and have since put additional measures in place to safeguard research integrity.

We wish to credit our Research Integrity and Research Publishing teams and anonymous and named external researchers and research integrity experts for contributing to this investigation.

The corresponding author, as the representative of all authors, has been given the opportunity to register their agreement or disagreement to this retraction. We have kept a record of any response received.

References

- [1] H. Wang, R. Yang, L. Zhao, F. Tian, and S. Yu, “The Application Effect of Remote Sensing Technology in Hydrogeological Investigation under Big Data Environment,” *Journal of Sensors*, vol. 2022, Article ID 5162864, 12 pages, 2022.

Research Article

The Application Effect of Remote Sensing Technology in Hydrogeological Investigation under Big Data Environment

Honglei Wang,¹ Ronghang Yang ,¹ Li Zhao,² Feng Tian,² and Shizhong Yu³

¹The 7th Geological Team, Shandong Bureau of Geology and Mineral Resources Exploration and Development, Linyi, 276000 Shandong, China

²The Third Exploration Team, Shandong Coal Geology Bureau, Tai'an, 271000 Shandong, China

³Shandong Provincial Territorial Spatial Ecological Restoration Center, Jinan, 250014 Shandong, China

Correspondence should be addressed to Ronghang Yang; 201701370103@lzpcc.edu.cn

Received 19 August 2022; Revised 9 September 2022; Accepted 14 September 2022; Published 7 December 2022

Academic Editor: C. Venkatesan

Copyright © 2022 Honglei Wang et al. This is an open access article distributed under the Creative Commons Attribution License, which permits unrestricted use, distribution, and reproduction in any medium, provided the original work is properly cited.

The hydrogeological investigation is a work carried out by comprehensive utilization of various exploration methods to identify hydrogeological conditions in the target area, and develop and utilize groundwater resources. There are great differences in hydrogeological conditions in different regions. Hence, it is necessary to take exploration technology according to local conditions to master hydrogeological information as much as possible. Among them, the remote sensing (RS) technology can reflect the ground surveying and mapping results with high efficiency and precision through the analysis of satellite or aerial photographs, which is a commonly used method in the current hydrogeological investigation. According to satellite RS data, this work evaluates the distribution of groundwater levels in the study area and explores the geological and hydrogeological conditions of the groundwater system in the affected area. Firstly, the human-computer interactive interpretation method is used to analyze the topography and geomorphology conditions. Secondly, the spectral characteristic curve analysis method is used to extract the spectral characteristics of regional stratum lithology, and analyze and determine the lithology composition and structure of the aquifer. Thirdly, the single-band and multiband models of soil moisture RS estimation of groundwater level are implemented. Finally, the measured data are employed to verify and analyze the estimated value of the model. The results are in line with the actual value, and good results have been achieved.

1. Introduction

The instruments, equipments, and technical means of engineering hydrogeological investigation are developing towards automation and intelligence due to the improvement of people's understanding of the objective world and the continuous progress of science and technology [1]. On account of the traditional geological exploration industry, people continue to introduce unmanned aerial vehicles, airborne radar, laser sensors, and three-dimensional (3D) scanners. It means that the development and innovation of modern scientific and technological products are introduced into geological exploration technology [2]. With the changes of the times, the database management information system has developed rapidly. The big data processing technology

has been gradually applied to the project to improve the updating efficiency of the data volume of the surveying and mapping unit and the space for collecting the data volume to store, organize, manage, and process the hydrogeological data. The big data processing method can be adopted to comprehensively analyze and evaluate hydrogeological problems and disaster risks at the project site. Moreover, it can provide technical support for disaster prevention and reduction of hydrogeological engineering geology and environmental geology. Meanwhile, building a data system of hydrogeological engineering geology and environmental geology is also conducive to effective and full management and utilization of various information resources in the future. It can also provide real and effective data for subsequent scientific research and decision-making management [3].

The current surface water resources in most parts of northern China are relatively scarce, so most water for people's production and living comes from groundwater resources. Hence, improving groundwater resources' exploration, development, and utilization are necessary for local social development [4]. The present remote sensing (RS) technology is gradually applied to the engineering survey field. It is generally defined as the technology of detecting and perceiving things and objects from a distance. Unlike other detection technologies, the coverage of RS technology is larger, the types of detection data obtained are various, and the means are diversified. Moreover, most of the detected data information is expressed through images, and the way of acquiring the detected data information is more direct and faster, making the detection time relatively short [5]. In the hydrological survey, the specific application of RS technology attaches importance to the comprehensive analysis of environmental factors related to groundwater level and RS image's data processing methods. It can comprehensively analyze the groundwater level distribution, build a scientific and reasonable groundwater level distribution model according to the principles of soil moisture, reflectance, and pixel relationship, and conduct a professional hydrogeological investigation [6].

Through the above problems, the application effect of the RS technology in the hydrogeological investigation is studied under the background of the big data environment. In this work, the human-computer interactive interpretation system GeoFrame is used based on RS satellite image data, and the spectral characteristic curve analysis method is taken to extract the spectral characteristics of the regional stratum lithology and analyze and determine the composition and structure of water-bearing lithology in the study area. Starting from the relationship between groundwater and soil moisture, based on soil moisture of RS monitoring combined with data obtained from field experiments, the correlation equation between soil moisture and groundwater level is established, and a model for evaluating the distribution of shallow underground water level is proposed. The estimation results of the implemented multiband and single-band models are verified and analyzed, and the model with good agreement between the simulation results and the actual is determined. Furthermore, it is proved that the model can estimate the distribution of the groundwater level.

2. Literature Review

Salmivaara et al. used big data technology as a storage method to retrieve massive grid data and form a spatial database of climate and other environmental data. The structured, semistructured, and unstructured geospatial data generated by the continuous production of natural resources are collected, and a geospatial data system with an integration layer and related technical components is built [7]. Chen et al. developed and opened the online index and query system SKSO pen for large-scale geospatial data, which integrates with Terra Fly geospatial database to visualize query results and data analysis [8]. Cudennec et al. believed that, as the core of geographic information services,

the spatial analysis presented two main development trends under the big data background. The first is an accurate analysis of large-scale spatial data. Due to the progress of spatial data acquisition technology, people can obtain increasingly larger space, the scale of spatial data continues to expand, and the accuracy of spatial data analysis continues to improve. The second is the real-time demand for spatial analysis services [9].

Yao et al. proposed the possibility of thermal infrared RS to evaluate groundwater by using aerial thermal infrared images and referring to massive actually collected hydrological data, topographic and geomorphic maps, Quaternary sediment distribution maps, vegetation distribution maps, and other reference materials. They successfully measured the temperature information related to groundwater [10]. Sishodia et al. selected two typical areas in China for groundwater source research. The adjustment assumption of coordination between land use structure and groundwater source was proposed based on the analysis of the change law between land development and regional environmental factors in groundwater [11]. Mohammadi found the hydrogeological conditions closely related to landform, Quaternary Geology, and neotectonics through RS images, judged the aquifer development law and various boundary types, and more accurately evaluated groundwater resources combined with geophysical prospecting results [12]. Aasen et al. extracted relevant information on the surface water system, geological structure, and aquifer properties of Tarim Basin from Landsat-MSS images. The quality, quantity, and burial depth of groundwater in Tarim Basin were investigated using the research area's geological and geomorphologic map and the precipitation and runoff text model [13]. Muchingami et al. evaluated the groundwater resources of the crystalline basement aquifer in Zimbabwe based on the vegetation distribution map and NDVI map in the study area displayed by Landsat TM images [14]. In their work on drought in West Africa, Le Page et al. started the study of the relationship between groundwater and vegetation and explored the situation of groundwater resources through the analysis of the vegetation RS technology [15]. Suryanarayana et al. used two-band microwave remote sensors to establish radar and other microwave remote sensors on the basis of measured surface hydrological factors, soil dielectric constant, and soil reflectivity to study groundwater conditions in Visakhapatnam, India [16].

To sum up, relevant scholars have made certain theoretical achievements in the research of hydrogeological investigation under RS technology. Step-by-step exploration and research have confirmed that RS technology can monitor and collect data in hydrological work. Moreover, it can provide strong technical support for data investigation in hydrological work and prediction and treatment of hydrological problems. However, there are few studies on integrating RS technology in the big data environment. Some studies are based on spatial data structure, spatial database, map digitization, and automatic mapping technology. It suggests that scholars are exploring the application of RS technology in the hydrogeological investigation in the big data environment. This work is to study the hydrogeological

investigation's application effect by combining the characteristics of the two. It aims to apply advanced technology to future hydrogeological investigations.

3. Materials and Methods

3.1. Human-Computer Interactive Interpretation Method. RS technology interprets signs based on geology to identify ground targets or features through satellite images. The types of signs can be divided into direct interpretation and indirect interpretation. There are two types of interpretation methods: visual interpretation and human-computer interactive interpretation. This time, the human-computer interactive interpretation method is used to investigate the distribution of groundwater levels in the study area. Interactive interpretation is often translated as human-computer interactive interpretation. As the name implies, it is the work process of comprehensive interpretation of geological and geophysical data by the interpreter with the assistance of computers. The interpreter issues an instruction in the interactive interpretation workstation, and the computer displays the corresponding execution result of the instruction. Interaction means that the computer is in the working state, and the operator waits for the response of the issued instruction in front of the computer terminal. The shorter the waiting time is, the better the computer performance is. If the computer's response is inappropriate or unsatisfactory, the operator can modify the instruction at any time until it is satisfied. This process is realized by the computer and the operator in the form of dialogue. In other words, the response of the interactive system is fast, and the interpreter can immediately complete any operation within the functional scope of the interpretation system [14]. Figure 1 demonstrates the advantages of human-computer interactive interpretation over manual interpretation:

The interactive interpretation of geological data is currently in the stage of popularization and in-depth development. China's present dominant interactive interpretation system is the GeoFrame interpretation system. It is mainly adopted for comprehensive analysis and interpretation of seismic, well logging, geological, and reservoir simulation data in exploration and development [15]. After receiving an interpretation project, all kinds of data used for interactive interpretation must be collected, including the geological and geomorphic results data of the interpretation work area, the measurement curves of all water levels, and the geological stratification data. Then, the data management software of the interactive interpretation system is employed to store the above-mentioned relevant data in a specific database. The database in the interpretation system refers to a collection of interrelated data reasonably stored on the computer storage device. Usually, each work area corresponds to a database. It is equivalent to a full-time and responsible work area data keeper, who can access any data anytime. In addition to the original data, the database also reserves the position and space for the later interpreted data of reflection layer and fault and various image data. It means that the database or data management system keeps all data files

throughout the interpretation process [16]. Figure 2 details a flowchart of its startup operation:

Human-computer interactive interpretation unifies images, graphics, and data. It can be adopted to superimpose various images and graphics according to the requirements of interpreters and verifiers in the verification of the information recognition process and interpretation results. Then, the required statistical data can be obtained simultaneously after the interpretation to achieve the unification of images, graphics, and data. Now, the application scope of human-computer interactive interpretation is expanding with the rapid progress of digitalization [17]. Figure 3 is the main work steps of interactive interpretation summarized after understanding the GeoFrame interactive interpretation system:

In this work, GeoFrame is used to interpret and analyze the RS images of water bodies. Since water bodies have obvious spectral characteristics among various types of ground objects, when analyzing and extracting relevant information, selecting the most suitable synthetic band can achieve twice the result with half the effort. For example, in the visible light band, the reflectivity of relatively clear and clean water decreases rapidly as the wavelength increases (blue light-red light). In the blue-green band (0.04~0.6 μm), the reflectivity is relatively large, and the interpretation effect of the TM1 and TM2 bands is the best. For topics related to the analysis of surface vegetation, the interpretation effect of the TM4 band is better; while the reflectivity of the red-infrared band (0.06~2.5 μm) is greatly weakened, and the infrared band is basically completely absorbed. Therefore, TM3 and TM7 bands are selected to cover more comprehensive information. Here, various analysis elements and influence conditions are integrated, and TM7, 4, and 3 bands are chosen to analyze the distribution of groundwater levels [18].

3.2. RS Technology. In 1960, the American scholar E. L. Pruiet called the technology of obtaining the images or data of the detected targets by photographing and nonphotographing "RS" to comprehensively summarize the technologies and methods of detecting targets. This term was formally adopted at the Environmental Science Symposium held by the University of Michigan and other units in 1962. RS detects the target, obtains the information of the target, and then processes the acquired information to realize the positioning, qualitative, or quantitative description of the target [19]. The current remote sensing geological exploration technology has been applied to practical projects. Figure 4 displays the primary application areas. This work uses RS to investigate the hydrogeological conditions affecting the groundwater system in the study area. Then, through the RS monitoring model of groundwater level distribution, combined with Landsat5 thematic mapper (TM) RS satellite image data, the distribution of regional groundwater levels is analyzed and interpreted. For the extraction and interpretation of this information, the following exploration are carried out. By using the groundwater level data of the measured sample points in the study area, the estimation results of the single-band and multiband models are verified and analyzed, and the estimation model with good agreement between the simulation results and the actual is

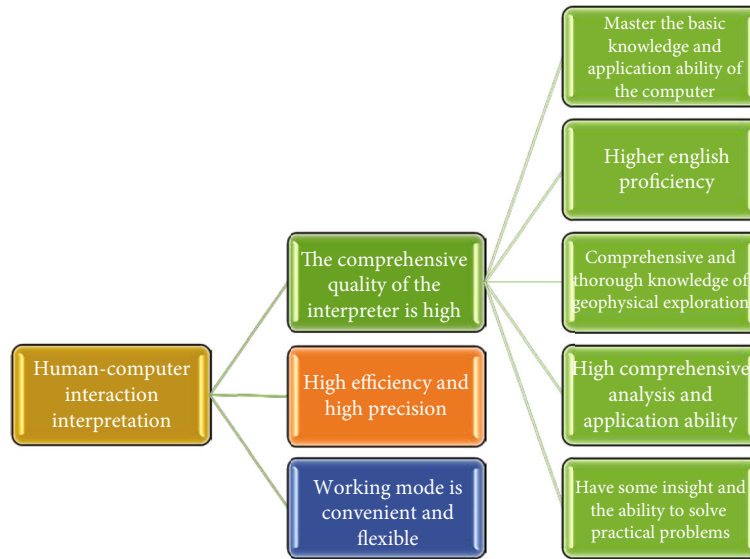


FIGURE 1: Human-computer interactive interpretation technology.

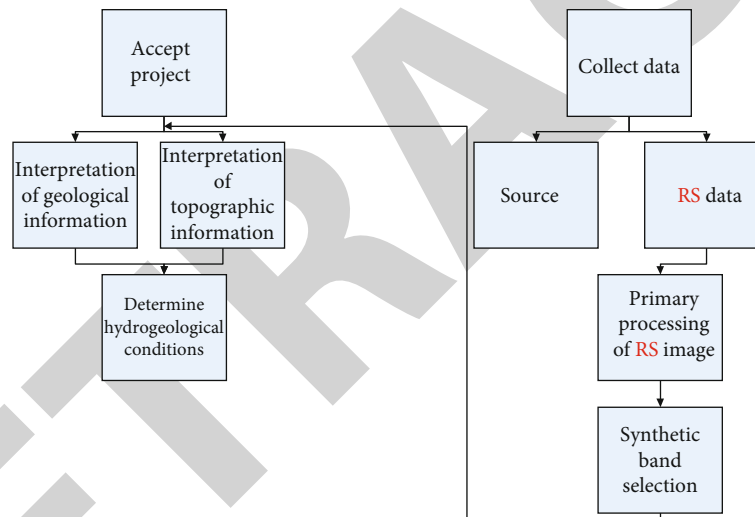


FIGURE 2: Operation flow of GeoFrame system.

determined. Furthermore, the distribution of shallow groundwater levels in the study area is estimated by this model. RS has diverse classifications from different angles [20]. Here are examples of various RS types classified by RS platform and sensor detection band. Figure 5 presents the details:

The spatial resolution and spectral resolution of RS images of optical systems are contradictory. Generally, under a certain signal-to-noise ratio, the improvement of spectral resolution is at the expense of spatial resolution. Fusing low-resolution multispectral images with high-resolution panchromatic band images can improve the multispectral data's spatial resolution. Thereby, various RS image fusion algorithms have been rapidly developed and applied [21]. Figure 6 portrays a schematic diagram of electromagnetic radiation received by the remote sensor.

Since different RS images have diverse representation capabilities of ground objects and various image characteris-

tics, it is required to select an appropriate RS data type when interpreting. After selecting the RS data type, it should also be considered to select a suitable interpretation band according to the spectral characteristic curve of the ground object. Under the premise of fully investigating the basic conditions of the study area, this work analyzes the distribution of groundwater levels in the study area based on RS data and field experimental observation data. The seven-band images of the TM of the Landsat 5 satellite launched by NASA are selected for analysis, and the applicable bands are selected according to the spectral characteristic curve of the existing.

3.3. Spectral Characteristic Curve Analysis. Gram-Schmidt (GS) transform is adopted in this work to make the fused image fidelity better and the results more practical. Orthogonalization of matrix or multidimensional images can eliminate redundant information, and the calculation process is

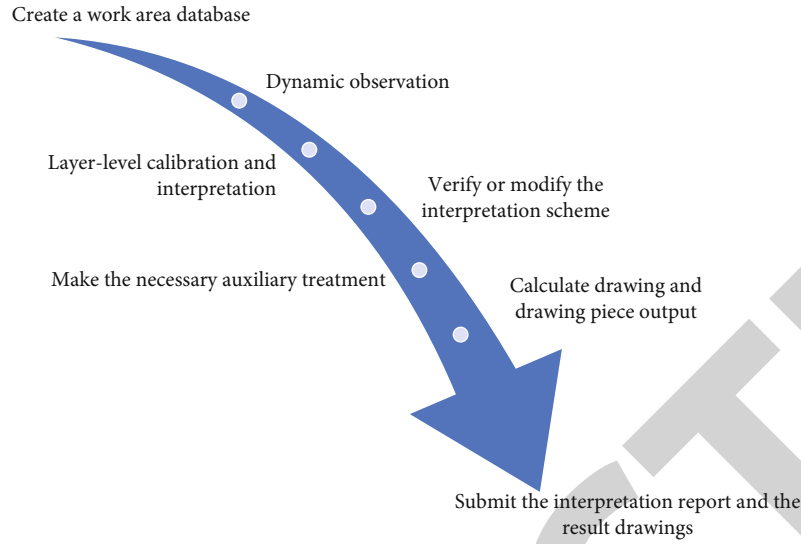


FIGURE 3: Working steps of interactive interpretation.

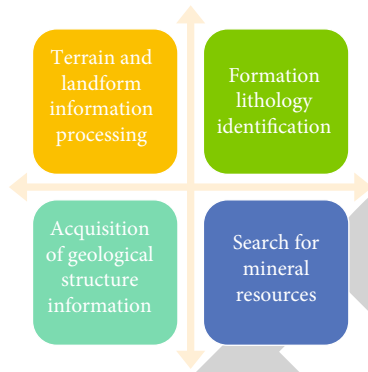


FIGURE 4: Application field of RS geological survey.

simple. Multispectral images are adopted to simulate panchromatic bands. There are two simulation methods:

- (1) The multispectral band with the low spatial resolution is simulated according to the spectral response function with a certain weight W_i . It refers to the simulated panchromatic band gray value:

$$P = \sum_{i=1}^n W_i * B_i. \quad (1)$$

In equation (1), B_i denotes the i -th band gray value of the multispectrum.

- (2) The panchromatic band image is blurred, and then a subset is taken. Next, the image is reduced to the same size as the multispectral image. The simulated panchromatic band is converted as GS_1 in the processing of the next step. The first component in the GS transform does not change after the simulated panchromatic band is adopted to exchange with the

panchromatic band. Hence, the spectral information of RS data is less distorted and has higher accuracy

The simulated panchromatic band is taken as GS_1 to perform GS transformation on the simulated panchromatic band and multispectral band. The algorithm is modified during GS transformation. The specific modification is as follows. The first $T-1$ GS component constructs the T -th GS component, that is:

$$GS_T(i, j) = [B_T(i, j) - u_T] - \sum_{i=1}^{T-1} \varphi(B_T, GS_i) * GS_i(i, j), \quad (2)$$

$$u_T = \frac{\sum_{j=1}^C \sum_{i=1}^R B_T(i, j)}{C * R}, \quad (3)$$

$$\varphi(B_T, GS_i) = \left[\frac{\sigma(B_T, GS_i)}{\sigma(GS_i, GS_i)^2} \right], \quad (4)$$

$$\sigma_T = \sqrt{\frac{\sum_{j=1}^C \sum_{i=1}^R [B_T(i, j) - u_T]^2}{C * R}}. \quad (5)$$

In equation (2), GS_T represents the T -th component generated after GS transformation. B_T is the T -th band of the original multispectral image. u_T donates the mean value of the gray value of the T -th original multispectral band image. In equation (3), B_T expresses the original multispectral T -th band. In equation (4), GS_i refers to the i -th component generated after GS transformation. In equation (5), u_T stands for the average of the grayscale values of the T -th original multispectral image.

Adjusting the statistical value of the panchromatic band to match GS_1 can generate the modified panchromatic band. This work is conducive to preserving the spectral characteristics of the original multispectral images. The modified panchromatic band is replaced with the first component after GS transform to generate a new dataset. A

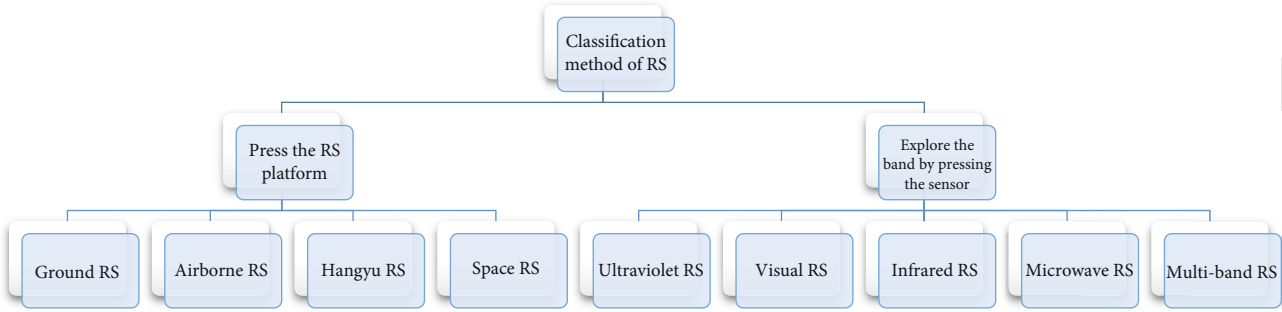


FIGURE 5: Different classifications of RS.

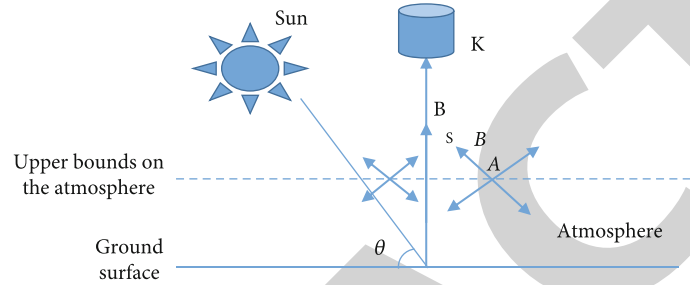


FIGURE 6: Schematic diagram of remote sensor receiving electromagnetic radiation.

multispectral image with enhanced spatial resolution can be generated by performing inverse GS inverse transform on the new dataset. The equation of GS inverse transformation is as follows:

$$\widehat{B}_T(i, j) = [GS_T(i, j) + u_T] + \sum_{i=1}^{T-1} \varphi(B_T, GS_i) * GS_i(i, j). \quad (6)$$

According to the analysis and interpretation results of the topographic and geomorphic types in the research area, the different types of areas are classified, analyzed, and interpreted to identify the stratum lithology. A lithologic spectrum library in the study area is created to facilitate the analysis and identification of the lithologic characteristics of various types of strata. According to the previous research results, the stratum lithology in the study area is mainly sandstone and mudstone, and the surface layer is mostly sandy soil and sandy loam, with a clay layer. Figures 7 and 8 are typical stratum lithologic spectral curve characteristics:

In Figures 7 and 8, the spectral characteristics of different types of rocks are quite distinct. The differences are mainly reflected in the reflectance of the spectrum and the position and depth of the characteristic absorption peak, which are also the basis for lithologic mineral identification. The waveforms of the same type of rocks are similar and the characteristic absorption peaks are consistent. However, due to different lithological purity, rocks' spectral reflectance, and characteristic absorption intensity will change accordingly. According to the difference of the reflection spectrum of the rock, it is identified that the lithology of the experimental area is dominated by sandstone and mudstone, and the surface layer is mostly sandy soil and sandy loam. Since the Quaternary stratum is mostly composed of loam, sand,

gravel, sand gravel, etc., it is easy to host groundwater. Therefore, the groundwater area in the study area generally occurs in the Quaternary strata. Moreover, half of the RS water-seeking information is close to the fault structure, and it is also easy to appear on the stratum uplift. Therefore, it is necessary to combine the specific formation conditions.

Three points are selected for the removal of the reference spectrum and pixel continuum: the absorption center and the points on both sides of the absorption center. To homogenize the noise on the continuum, several bands on both sides of the absorption center can be selected to remove the continuum by the following division:

$$L_c = \frac{L(\lambda)}{C_l(\lambda)}, \quad (7)$$

$$O_c(\lambda) = \frac{o(\lambda)}{C_0(\lambda)}. \quad (8)$$

$L(\lambda)$ denotes the spectrum as a function of wavelength λ ; O illustrates the pixel spectrum; C_l refers to continuum spectrum; C_0 means the continuous spectrum of the pixel. An additional constant K is adopted to increase the contrast of the reference spectrum:

$$L_c' = \frac{L_c + K}{1.0 + K}. \quad (9)$$

L_c' indicates the adjusted continuum removal spectrum, which best fits the observation spectrum.

3.4. RS Estimation of the Distribution of Groundwater Level. Different soils have slightly various constants due to different soil types. On account of the statistical and regression

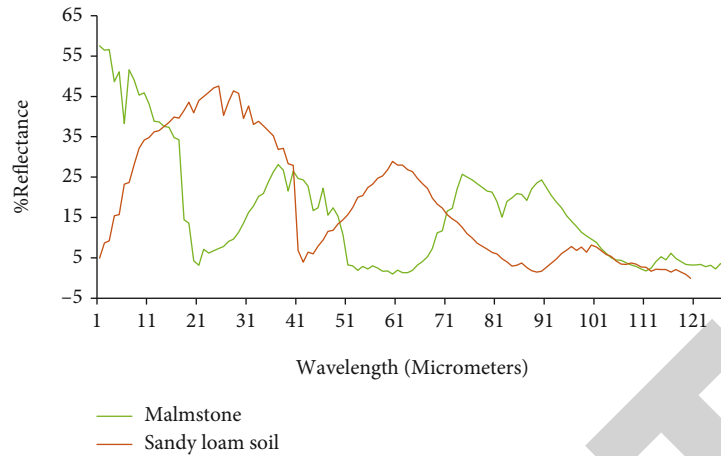


FIGURE 7: Spectral curve 1.

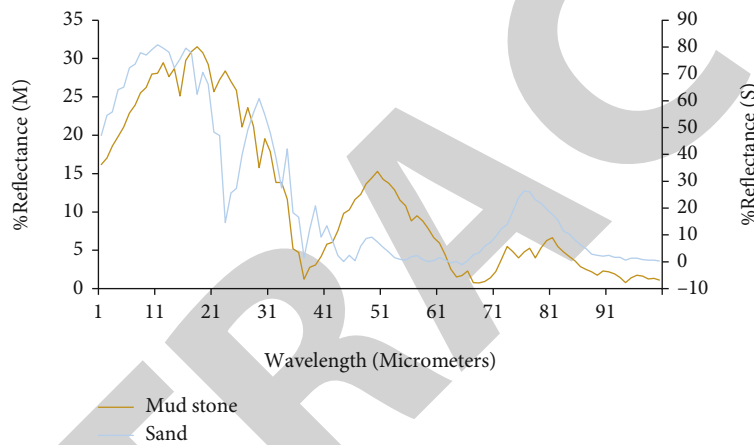


FIGURE 8: Spectral curve 2.

analysis results of the measured data in the study area, the relationship between reflectance and water content is established. The correlation coefficients of the regression analysis of various soils in the study area are generally 0.92 to 0.98 [22]. Therefore, the average value of the RS model of several types of soil moisture in this area was taken to analyze the soil moisture status:

$$W_i = 91.70 - 42.91 \cdot \log R_{i\pm} \quad (10)$$

In equation (10), W_i is the percentage of soil moisture obtained in the i -band.

The distribution of water in the capillary can be written as an equation (11):

$$W^2(y) = A + By, \max(0, H - H_m) \leq y \leq H_m. \quad (11)$$

In equation (11), H means the depth of groundwater, and H_m indicates the depth that can rise from the groundwater-soil contact surface to the capillary.

H_m is related to the physical and chemical properties of the soil. The same soil type has a similar H_m value. Different soil types have diverse heights that groundwater can rise to

the capillary. The constants A and B are determined by the following 3 boundary conditions:

- (1) At the contact surface between soil and groundwater, $y = H$, the maximum value of the soil moisture is W_{\max} ;
- (2) When the groundwater can rise to the height of the capillary, $y = H - H_m$, the minimum value of soil moisture is W_{\min} ;
- (3) At the soil-atmosphere contact surface, $y = 0$, and the soil moisture is W_0 . Boundary conditions (1) and (2) are substituted into equation (11), as follows:

$$A = W_{\max}^2 W_{\max}^2 W_{\min}^2 \frac{H}{H_m}, \quad (12)$$

$$B = \frac{W_{\max}^2 W_{\min}^2}{H_m}. \quad (13)$$

Boundary condition (2) is replaced by (3), which

transforms to:

$$A = W_0^2, B = \frac{W_{\max}^2 W_0^2}{H}. \quad (14)$$

The multiyear average precipitation in the study area is 389.34 mm, but the multiyear average evaporation is as high as 1411.49 mm. The soil in this area is mostly aeolian sandy soil developed on fixed and semifixed dunes, and the surface soil moisture is small, so the correlation between the groundwater level and the surface soil moisture is very small. Thereby, equation (14) does not need to be considered here.

When the parameters W_{\max} , W_{\min} , H_m , and the effective depth of soil moisture of RS monitoring are determined, the groundwater level in the study area can be estimated by equation (11). However, for the Landsat5 satellite, the effective depth of RS monitoring of soil moisture is limited to very shallow soil layers near the surface, and the effective

depth of monitoring is generally 0.10 m, and the relative relationship between shallow soil moisture and groundwater level is not stable. Due to the limitation of the effective depth of groundwater level monitoring by RS, this analysis is limited to areas with shallow soil and good water-richness [23].

If d is the effective depth of the monitored soil moisture, let $y = d$. W_d represents soil moisture at depth d . From equations (11), (12), and (13), the relationship equation (15) of soil moisture and groundwater level can be obtained:

$$H = d + H_m \frac{W_{\max}^2 - W_d^2}{W_{\max}^2 - W_{\min}^2}. \quad (15)$$

By using equations (10), (11), and (15), the following single-band and multiband models for RS monitoring of groundwater levels can be obtained, as denoted in equations (16) and (17):

$$H_i = d + H_m \frac{W_{\max}^2 - [76.3 - 42.91 \cdot \log(0.996B_i - 42.05)]^2}{W_{\max}^2 - W_{\min}^2}, \quad (16)$$

$$H_{432} = d + H_m \frac{W_{\max}^2 - [76.3 - 42.91 \cdot \log(0.6968B_2 + 0.5228B_3 - 0.2237B_4 + 20.26/1.089 - 0.00579B_4 + 0.003308B_2 + 0.002482B_3 - 18)]^2}{W_{\max}^2 - W_{\min}^2}. \quad (17)$$

In equations (16) and (17), H_i is the buried depth of groundwater level estimated by the i -th band of TM;

By analyzing the estimation formulas of single-band and multiband, if the hydrological constants W_{\max} , W_{\min} , H_m are known, and the effective depth d of soil moisture monitoring by RS is determined, the groundwater level can be quantitatively determined [24].

4. Results

Correlation analysis is conducted on the groundwater level estimated by the single-band and multiband groundwater level monitoring models and the measured groundwater level. Figures 9–12 present the comparison between the groundwater monitoring value and the measured data:

Figure 9 suggests that the maximum error between the monitoring value of groundwater level and the actual value in the third band is 0.8, which appears at the A10 sample point. The minimum error value is 0, which appears at sample points A3 and A4. Excluding the maximum and minimum values, the error value is basically maintained within 0.4. The error value is within the allowable error range. It suggests that the spectral characteristic curve can basically reflect the situation of groundwater. The appropriate model is chosen for future hydrogeological investigation by comparing the multiband groundwater level monitoring.

Figure 10 suggests that the maximum error between the monitoring value groundwater level and the actual value of

the fourth band is 0.8, which appears at the A10 sample point. The minimum error value is 0, which appears at A4, A5, and A8 sample points. Excluding the maximum and minimum values, the error value is basically maintained within 0.3. The error value is within the allowable error range. It proves that the spectral characteristic curve can basically reflect the groundwater situation, which is more accurate than the response of the third band. The appropriate model is selected for future hydrogeological investigation by comparing the multiband groundwater level monitoring.

Figure 11 suggests that the maximum error between the monitoring value and the actual value of the groundwater level in band 7 is 0.9, which appears at the A10 sample point. The minimum error value is 0, which appears at sample points A3, A4, and A6. Excluding the maximum and minimum values, the error value is basically kept within 0.4. The error value is within the allowable error range. It reveals that the spectral characteristic curve can basically reflect the groundwater situation. However, the prediction accuracy is slightly worse than that of the first two bands. The appropriate model is selected for future hydrogeological investigation by comparing the multiband groundwater level monitoring.

Figure 12 details that the error range between the multiband groundwater level monitoring value and the actual value is relatively stable and can be maintained within 0.4. Moreover, the error values are generally quite low, illustrating that multiband is more suitable for groundwater level monitoring than single-band. Meanwhile, the correlation

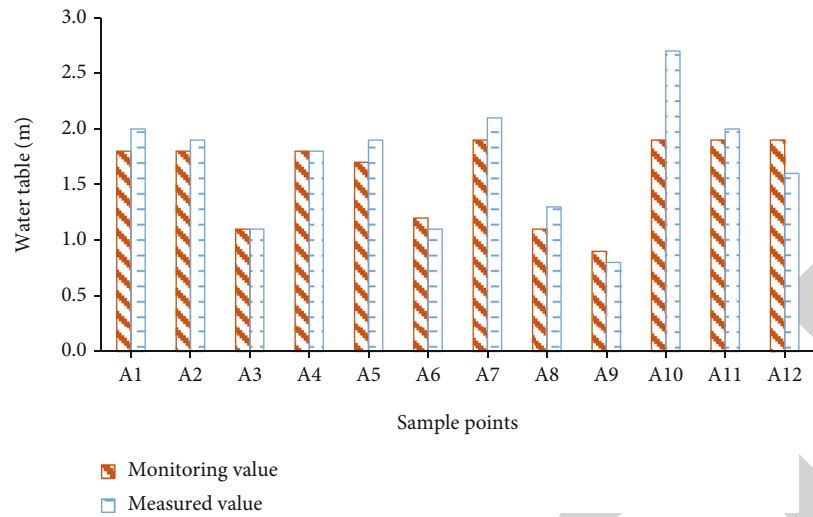


FIGURE 9: The comparison of groundwater level values in band 3.

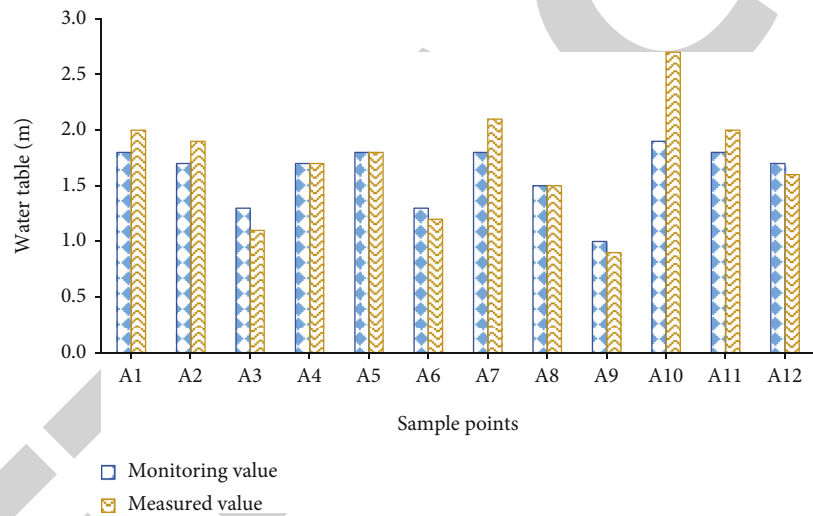


FIGURE 10: The comparison of groundwater level values in band 4.

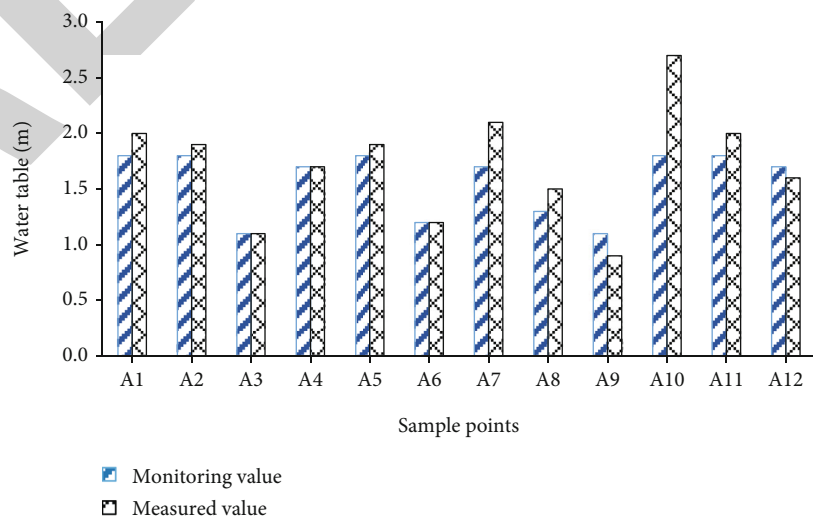


FIGURE 11: The comparison of groundwater level values in band 7.

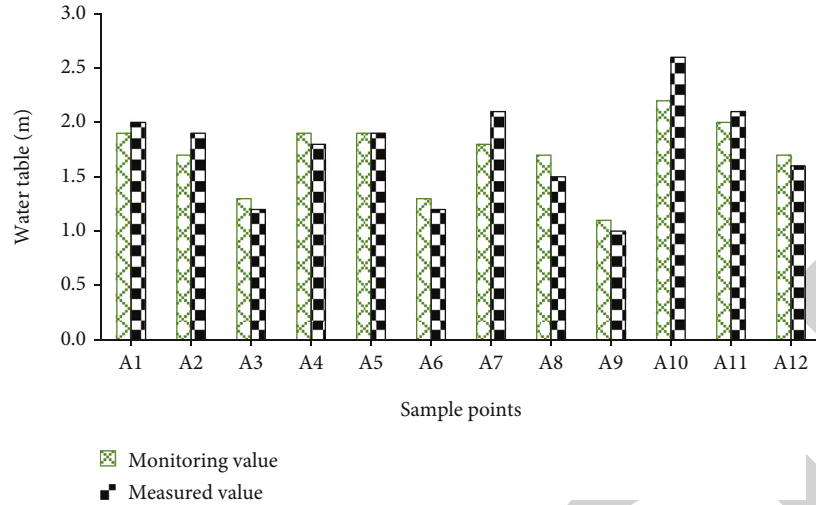


FIGURE 12: The comparison of multiband groundwater level values.

coefficient between the groundwater level estimated by the single-band groundwater level monitoring model and the measured groundwater level is generally lower than the correlation coefficient between the groundwater level estimated by the multiband groundwater level monitoring model and the measured groundwater level. It further confirms that the multiband model is better than the single-band model to be better applied to hydrogeological investigation. Table 1 exhibits the summary of the data obtained from the above histogram:

Table 1 shows that the average error values of the three single bands are 0.19, 0.18, and 0.20, respectively, and the average error value of the multiband is 0.15. In comparison, the multiband error value is the smallest, and the error values of the three single bands are equal. It illustrates that the multiband survey of groundwater levels is more accurate. Meanwhile, the correlation coefficients between the groundwater level estimated by the third, fourth, and seventh single-band groundwater level monitoring models and the measured groundwater level are 0.87, 0.83, and 0.89, respectively. The correlation coefficient between the groundwater level estimated by the second, third, and fourth multiband groundwater level monitoring models and the measured groundwater level is 0.93. In the estimation model, the multiband model is better than the single-band model, which can better reflect the groundwater level. The distribution of groundwater monitored by the model can accurately reflect the actual situation of the groundwater level, and the research results are basically in line with reality. Therefore, it is feasible to use the multiband model to monitor the groundwater level.

5. Discussion

Zhang et al. established a lithologic spectral library in the research area with the assistance of ENVI software based on the research area's interpretation and analysis of topography and geomorphology. According to different lithologic spectral characteristic curves, they analyzed the spectral

TABLE 1: The comparison of error value and correlation coefficient.

Different bands	Mean error	Correlation coefficient
Band 3	0.19	0.87
Band 4	0.18	0.83
Band 7	0.20	0.89
Multiband	0.15	0.93

characteristic differences and influence characteristics of different lithologic stratigraphic units in the research area. The lithologic and stratigraphic interpretation was conducted using the manual visual interpretation method. The strata's lithologic structure in the study area was basically mastered, and the comprehensive geological histogram of the study area was prepared [25]. Here, after extracting the characteristic spectral curve, the monitoring value of groundwater level in single-band and multiband are compared with the actual value. The single-band and multiband RS monitoring models of groundwater level distribution have been implemented, paving the way for the effective monitoring of groundwater levels through analyzing soil moisture status by RS technology. Thus, it is concluded that the spectral characteristic curve of RS technology can be employed to accurately measure the groundwater level landmark, which provides good help to the hydrogeological investigation.

Xu used human-computer interactive geomorphological interpretation technology to study submarine landslides. The results demonstrate that this technique can reduce the bias of subjective factors on interpretation. More importantly, it can fully mine the hidden information that is not easy to find in manual interpretation, improve the accuracy and scientificity of interpretation, and avoid the error caused by manual interpretation [26]. The application of human-computer interactive interpretation technology in the hydrogeological investigation suggests that the GeoFrame system used by some enterprises has certain advantages in terrain and geomorphology analysis. The 3D geological exploration

improvement will inevitably promote the rapid development of human-computer interactive interpretation technology. It is only possible to understand the structure of subtle and complex small faults when fully using the drilling and production, well logging, geological data, and imaging technology of 3D geological data, together with human experience and wisdom.

6. Conclusion

Under the background of a big data environment, RS technology is adopted to analyze the spectrum of the study area, and the information of hydrogeological factors affecting and restricting the groundwater resource system is obtained. Meanwhile, a mathematical model for effectively detecting groundwater resources by RS images is implemented through the RS - spectral fusion research method and the actual situation of the study area. The distribution of groundwater levels in this area is further analyzed, and the stratum lithology and structure of the area are basically mastered. The comprehensive geological column comparison map of the study area is made. The single-band and multi-band RS monitoring models of groundwater level distribution have been constructed. It provides a practical theory for future hydrogeological investigation and proves that the method of monitoring and evaluating groundwater distribution using a multiband model is feasible. Meanwhile, this experiment also has some shortcomings. In the process of human-computer interactive interpretation, the accuracy of interpretation results may be affected due to the lack of knowledge system and experience. There is a lack of more effective references and comparisons in lithologic information extraction due to less experimental work in the process of water information spectral extraction and the lack of a lithologic distribution map in the research area. It affects the accuracy of lithologic classification result evaluation. In the analysis of groundwater level distribution, the impact of terrain factors, air temperature, wind speed, and other factors on soil moisture is not considered, resulting in a decrease in the accuracy of the estimated value.

Data Availability

The data used to support the findings of this study are available from the corresponding author upon request.

Conflicts of Interest

The authors declare no conflicts of interest.

References

- [1] A. Bukhari, H. Hendrayana, and H. Setiawan, "Preliminary conceptual model of hydrogeological system in the Raimanuk and its surrounding area on the Timor Island," *IOP Conference Series: Earth and Environmental Science*, vol. 930, no. 1, article 012058, 2021.
- [2] F. M. D'Afonseca, M. Finkel, and O. A. Cirpka, "Combining implicit geological modeling, field surveys, and hydrogeological modeling to describe groundwater flow in a karst aquifer," *Journal*, vol. 28, no. 8, pp. 2779–2802, 2020.
- [3] M. Nursaputra, R. A. Barkey, S. Rijal, C. Anila, and M. F. Mappiasse, "The direction of land-use for hydrology balance and development of low-carbon emissions in the Jenelata catchment area," *IOP Conference Series: Earth and Environmental Science*, vol. 681, no. 1, p. 14, 2021.
- [4] Y. S. Xu, J. S. Shen, A. N. Zhou, and A. Arulrajah, "Geological and hydrogeological environment with geohazards during underground construction in Hangzhou: a review," *Arabian Journal of Geosciences*, vol. 11, no. 18, pp. 1–18, 2018.
- [5] Y. Huang, Z. X. Chen, Y. U. Tao, X. Z. Huang, and X. F. Gu, "Agricultural remote sensing big data: management and applications," *Journal of Integrative Agriculture*, vol. 17, no. 9, pp. 1915–1931, 2018.
- [6] A. Alamanos, A. Rolston, and G. Papaioannou, "Development of a decision support system for sustainable environmental management and stakeholder engagement," *Hydrology*, vol. 8, no. 1, p. 40, 2021.
- [7] A. Salmivaara, S. Launiainen, J. Perttunen et al., "Towards dynamic forest trafficability prediction using open spatial data, hydrological modelling and sensor technology," *Forestry: An International Journal of Forest Research*, vol. 93, no. 5, pp. 662–674, 2020.
- [8] L. Chen and L. Wang, "Recent advance in earth observation big data for hydrology," *Big Earth Data*, vol. 2, no. 1, pp. 86–107, 2018.
- [9] C. Cudennec, H. Lins, S. Uhlenbrook, and B. Arheimer, "Editorial – towards FAIR and SQUARE hydrological data," *Hydrological Sciences Journal*, vol. 65, no. 5, pp. 681–682, 2020.
- [10] H. Yao, R. Qin, and X. Chen, "Unmanned aerial vehicle for remote sensing applications—a review," *Remote Sensing*, vol. 11, no. 12, p. 1443, 2019.
- [11] R. P. Sishodia, R. L. Ray, and S. K. Singh, "Applications of remote sensing in precision agriculture: a review," *Remote Sensing*, vol. 12, no. 19, p. 3136, 2020.
- [12] B. Mohammadi, "Application of machine learning and remote sensing in hydrology," *Sustainability*, vol. 14, no. 13, p. 7586, 2022.
- [13] H. Aasen, E. Honkavaara, A. Lucieer, and P. Zarco-Tejada, "Quantitative remote sensing at ultra-high resolution with UAV spectroscopy: a review of sensor technology, measurement procedures, and data correction workflows," *Remote Sensing*, vol. 10, no. 7, p. 1091, 2018.
- [14] I. Muchingami, C. Chuma, M. Gumbo, D. Hlatywayo, and R. Mashingaidze, "Review: approaches to groundwater exploration and resource evaluation in the crystalline basement aquifers of Zimbabwe," *Hydrogéologie*, vol. 27, no. 3, pp. 915–928, 2019.
- [15] M. Le Page and M. Zribi, "Analysis and predictability of drought in northwest Africa using optical and microwave satellite remote sensing products," *Scientific Reports*, vol. 9, no. 1, p. 1466, 2019.
- [16] C. Suryanarayana and V. Mahmood, "Groundwater-level assessment and prediction using realistic pumping and recharge rates for semi-arid coastal regions: a case study of Visakhapatnam city, India," *Hydrogéologie*, vol. 27, no. 2, pp. 249–272, 2019.
- [17] P. Gao, "Key technologies of human-computer interaction for immersive somatosensory interactive games using VR technology," *Soft Computing*, vol. 26, pp. 10947–10956, 2022.

Retraction

Retracted: Deconstruction of Urban Public Space Art Design Using Intelligent Sensor and Information Fusion

Journal of Sensors

Received 12 December 2023; Accepted 12 December 2023; Published 13 December 2023

Copyright © 2023 Journal of Sensors. This is an open access article distributed under the Creative Commons Attribution License, which permits unrestricted use, distribution, and reproduction in any medium, provided the original work is properly cited.

This article has been retracted by Hindawi, as publisher, following an investigation undertaken by the publisher [1]. This investigation has uncovered evidence of systematic manipulation of the publication and peer-review process. We cannot, therefore, vouch for the reliability or integrity of this article.

Please note that this notice is intended solely to alert readers that the peer-review process of this article has been compromised.

Wiley and Hindawi regret that the usual quality checks did not identify these issues before publication and have since put additional measures in place to safeguard research integrity.

We wish to credit our Research Integrity and Research Publishing teams and anonymous and named external researchers and research integrity experts for contributing to this investigation.

The corresponding author, as the representative of all authors, has been given the opportunity to register their agreement or disagreement to this retraction. We have kept a record of any response received.

References

- [1] H. Meng and Y. Sun, “Deconstruction of Urban Public Space Art Design Using Intelligent Sensor and Information Fusion,” *Journal of Sensors*, vol. 2022, Article ID 9360982, 9 pages, 2022.

Research Article

Deconstruction of Urban Public Space Art Design Using Intelligent Sensor and Information Fusion

He Meng and Yanming Sun 

Academy of Fine Arts, Changchun University, Changchun 130022, China

Correspondence should be addressed to Yanming Sun; sunym@ccu.edu.cn

Received 7 July 2022; Revised 20 September 2022; Accepted 26 September 2022; Published 11 October 2022

Academic Editor: C. Venkatesan

Copyright © 2022 He Meng and Yanming Sun. This is an open access article distributed under the Creative Commons Attribution License, which permits unrestricted use, distribution, and reproduction in any medium, provided the original work is properly cited.

The main purpose of smart city is to improve the quality of life, improve the efficiency of life, and save the energy resources of life, which is in line with the current global concept of low-carbon environmental protection, energy saving and emission reduction, and ecological sustainable development. Under the process of smart city, the development of urban public space is also committed to meeting the material and spiritual needs of residents' lives. For the system hardware design, the street lamp node, and the concentrator node hardware design, the sensing node is composed of multiple sensors. Its main components are temperature sensor, infrared sensor, sound sensor, and light intensity sensor, which, respectively, realize the collection of temperature, infrared, sound, and light intensity information. The street light sensing system uses multisensor information fusion technology to detect the situation of people and vehicles in real time, so that people and vehicles can turn on the street lights and turn off the street lights of unmanned vehicles. Adjust the street light switch according to the intelligent analysis of the lighting demand scene in order to enhance the accuracy of the system to identify the lighting demand scene. This enables the system to provide safe lighting conditions for urban traffic while saving the power consumption of urban lighting. The sensor system of the street light randomly selects the detection results of temperature and humidity within a certain period of time. The error rate of the final test result is 1/2 of that of the traditional test, and the accuracy is far lower than that of the traditional measurement method. Regarding the lighting system of street lamps and public art in urban public spaces, it is worthy of extensive promotion to control street lamp lighting through sensor information fusion technology and reduce energy consumption.

1. Introduction

In the process of the Friendship Exhibition of public art, the functions and concepts of public art under the background of the development concept of the times, the social environment, and the human environment factors are different and constantly changing. Contemporary public art research mainly has two artistic levels: one is the visual plastic art as the research object, another is to take functional public facilities as the research object, and they all form an interdisciplinary, multidimensional, and multiperspective blending relationship. The new form of public art presented by means of technology shows the characteristics of technical complexity and design integration, realizes the technologicalization of urban public art, promotes the process of urban

digital development, and solves the problem of urban environmental development. The intelligent design of public art refers to the important role played by modern science and technology in the design, creation, operation, and use of public art.

Under the process of modernization, public art is constantly producing new art forms, the way of interacting with the public and the city is increasingly updated, and its own value orientation is constantly being added with new definitions. People's feelings for one another, for art, and for the city are all enhanced by the interplay of urban space. The astute provision of public art made with cognitive researchers and advanced technologies demonstrates living thing knowledge from using renewable power and the defense of the natural ecosystem, and to some degree,

understands the mystical theory of artists and dwellers to help shield this same urban environment is necessary ecosystems. Taking the intelligent art design of urban street lamps as the object, through the intelligent change of urban street lamps, the city can spread the temperature and warm every corner of the city through this street lamp.

Inductive public art refers to works of art that change the physical state of people's voice, movement, natural airflow, temperature, humidity, etc., which can trigger the original form of public art, discuss the basic types of intelligent design in public art from the perspective of intelligence, and realize the practice of humanization and human culture in urban public space from the perspectives of technological factors and sensor information fusion technology. The update and practical application of science and technology plays a key role in the intelligent design of public art. It can be said that science and technology promote the development of intelligent design of public art, and intelligent design of public art is based on science and technology.

2. Related Work

Humanities are an important concept in the construction of contemporary smart cities, and public art is the medium to reflect the unique spiritual outlook of smart cities. Yin et al. selected Nanjing Jiangbei New District Industrial Technology Research and Innovation Park as the research object based on the humanistic shaping of the smart industrial zone and discussed the effective way of its public art planning from the connotation, planning function, and planning method of public art [1]. Cayer and Bender combined participatory observations of art activists, semistructured and oral history interviews with homeless people in Tokyo, and historical analysis [2]. Crte-Real reported on a piece of public art on the limits of painting, illustrating contemporary research questions based on painting as an element or essential part of installations, public art, urban interventions, performances, nontraditional media, and materials [3]. Darivemula et al. sent the white coat to the national conference for presentation, revealing the challenges, resilience, and humanity of women's medical training to work, the ways in which women's medicine is empowered through public art [4]. While these are all about the study of public art, the scope of the study is too broad.

Currently, there are many challenges in various fields that researchers are trying to solve with sensors. Focusing on the specific application scenarios of on-board gas sensors, Yang reviewed the working principle, research progress, and application status of on-board sensors at home and abroad. The study concluded that on-board gas sensors played a huge role in power system monitoring and vehicle environment monitoring [5]. Chahine et al. combined random watershed segmentation, which provided multiple segmentation results, with the Hessian operator to obtain unique and efficient segmentations [6]. Yaghoubi et al. developed a new multiclassifier fusion method for statistical analysis of different noise levels by using Dempster-Shafer theory to measure and mitigate conflict between evidence [7]. Herrera-Quintero et al. designed an ITS (Intelligent Trans-

portation System) smart sensor prototype using a serverless and microservice architecture integrating and combined with an Internet of Things (IoT) approach to aid in a transit planning (BRT) system for bus rapid transit [8]. Chuang et al. designed a thermoelectric power generation device with a simple structure, and the designed device is expected to increase the power generation capacity without using additional energy to cool the thermoelectric power generation chip [9].

In order to keep the signal processing circuit small, low cost, simple, and robust, Morais et al. used a novel direct interface sensor-to-microcontroller circuit technique for capacitance measurement, and it was allowed to measure small capacitance deviations without a high frequency oscillator [10]. Most of these studies are about the analysis of data, and there is too little research about smart sensors in public art.

3. Public Art of Smart Sensors and Information Fusion

3.1. Application of Sensors in Smart Street Lights. A sensor is a device that detects changes in surrounding information and can convert the changes of scanned information into electronic signals or other required information output methods according to the rules of information transmission [11]. The sensory functions commonly used in today's smart public facilities are mainly realized by the sensing devices of the components, which are the main part of the automatic detection and automatic control implementation of smart public equipment. The existence of sensors enables intelligent public art design to have touch, hearing, smell, and other senses and gradually makes public art more intelligent [12]. The sensing technology based on the sensing intelligent public art is a multidisciplinary modern science and engineering technology about obtaining information from natural sources, processing, and identifying it.

With the introduction of the concept of smart city development, the development needs of modern cities are diversified. As cities grow, urban construction also needs to be sustainable and consistent with the development of urban diversification and the sharing economy. The research and development of sustainable energy applications and intelligent data processing have become a hot spot [13]. The public art needs of modern urban society have developed from pure aesthetic art to interactive experience and information exchange. Intelligent design has begun to be applied to public art. With the continuous evolution of new technological modeling and interactive intelligent functions, it has become a new art form. Based on the development of smart cities, this paper deeply analyzes and examines the main types and development of smart art in public art [14]. In order to enhance the reliability, stability, and antifailure capability of the urban street lamp intelligent monitoring and management system, and effectively improve the work efficiency of the urban street lamp intelligent monitoring and management system, most of the traditional processing solutions are based on server-centralized data processing, which is not suitable for this system. For this reason, edge computing

technology is used to realize data decentralization processing. As shown in Figure 1, the system consists of three layers: edge perception layer, transport layer, and service layer. The form of sensing technology includes optical sensing, gesture sensing, environmental sensing, infrared sensing, electromagnetic sensing, gravity sensing, and 3D sensing.

As a key carrier of urban environment and space culture, public art can be combined with urban planning and architectural design to create the overall image of the city. The size of the art work itself and the size of the open space are two important factors that affect the overall artistic effect of the work. If the scale is too large, it will make people feel depressed and heavy; if the scale is too small, it will reduce its sense of existence. If public art is placed in an indoor space, it is important to consider the distance between the viewer and the work. However, if the public art is placed in the outdoor space and it is integrated with the surrounding environment, it is necessary not only to consider the audience but also to compare and analyze the surrounding environment of the public art. It can be seen that its size determines its sense of distance and intimacy in the open space. Therefore, it is necessary to seek communication and exchange in an appropriate scale and to echo and integrate with the urban space environment.

As shown in Figure 2, the street lamp node uses multiple sensors to collect external environmental information and uses the communication module to transmit the data collected by the sensors to the concentrator node. Due to the high randomness of the flow of people and vehicles on normal roads, in order to accurately detect the flow of people and vehicles in the past, the street lamp nodes with image processing capabilities are used to identify and count the flow of people and vehicles. According to the flow rate, the controller sends corresponding control commands to realize the periodic control of street lamp brightness. Inductive intelligent public art usually sets sensors inside the work and changes the original state of the work by receiving the changes of external airflow, creature's sound, or movement through the sensor.

The realization of networked control technology for street lamps is mainly divided into wireless and wired. With the rapid development of Internet of Things technology, wireless communication networking technology has gradually become the mainstream development trend [15]. Wireless networking technology is a network of multiple independent wireless nodes that communicate with each other through radio channels. Currently, widely used wireless communication technologies include the following: ZigBee, Wi-Fi, and wireless transmission (NFC). The comparison of these several wireless communication technologies is shown in Table 1.

As can be seen from Table 1, for the comparison of commonly used ZigBee and Wi-Fi communication technologies, ZigBee has certain advantages in terms of cost and power consumption. The main problem of Wi-Fi is that the number of connected network nodes is too small, and the power consumption is high. Although the price of NFC is low, the node power consumption is high, and the communication distance is short. From the current development trend, in

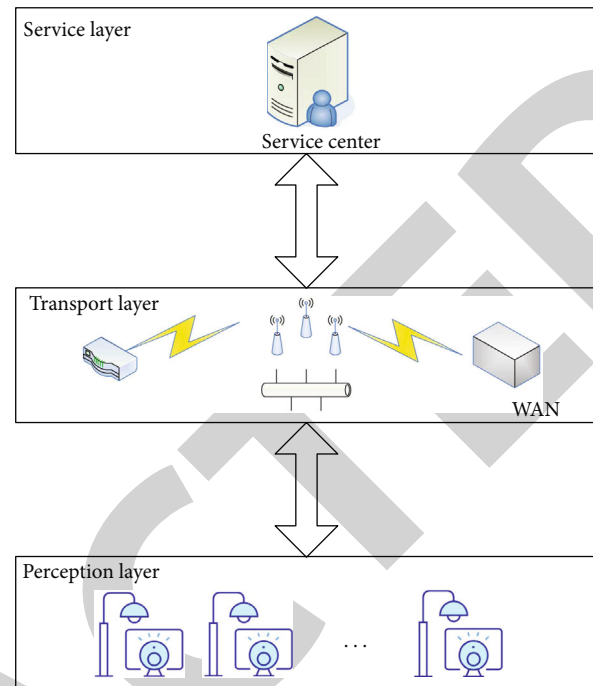


FIGURE 1: Overall frame figure of the system.

order to achieve the goals of smart lighting, smart home, and smart city, the number of nodes for networking communication should be at least more than 20; so, ZigBee has the best chance to become the mainstream of wireless communication networking technology [16]. ZigBee is divided into three frequency bands according to the channel, and the channel range is 0~20. The specific data of the center frequency, upper limit frequency, and lower limit frequency of each channel are shown in Table 2.

The comparison of the transmission rate and adjustment mode of the three frequency bands in Table 2 is shown in Table 3.

Up to now, public space is a public indoor space or outdoor environment with open space, free public participation, and experience, for example, streets, squares, outdoor venues in residential areas, parks, etc. Public art covers a rich variety of three-dimensional and dynamic art forms, based on the behavior of common presence that people communicate and share. Public art can be called public art when it echoes and integrates with its surrounding space and covers the interactive behavior of people in the space. ZigBee is a wireless communication technology, which is characterized by self-organizing network, short distance, low complexity, low power consumption, and low data rate and is mainly suitable for the field of Internet of Things and automatic control. The abovementioned street lamp control scheme has some inevitable defects, and the design scheme combining Internet technology and ZigBee technology can make up for these deficiencies [18]. Moreover, the ZigBee protocol can be used free of charge, thereby further reducing the cost of research and development [19]. In addition, the Internet technology is infiltrating all levels of social life with vigorous vitality. Therefore, using the urban public wireless network

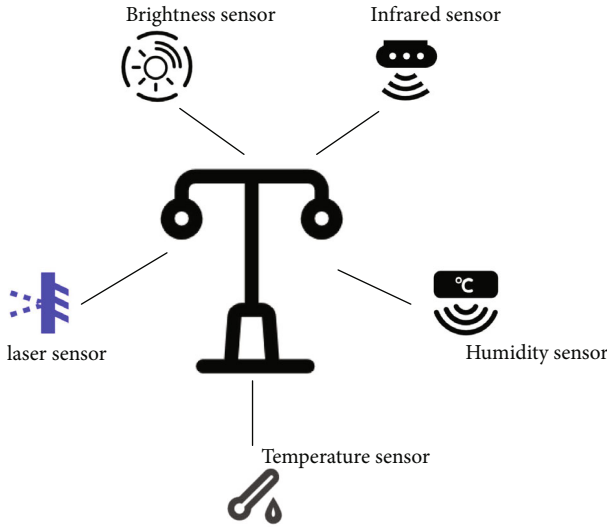


FIGURE 2: Street light node sensing design.

TABLE 1: Wireless communication technology comparison.

	ZigBee	Wi-Fi	NFC
Price	\$4	\$25	\$2-4
Communication distance	1-100 M	0-100 M	0-20 M
Transfer speed	10-250 Kbps	60 Mbps	450 Kbps
Power consumption	Minimum	Big	Larger

TABLE 2: ZigBee wireless channel composition.

Channel	Center frequency (MHz)	Upper frequency (MHz)	Lower limit frequency (MHz)
$K = 0$	850.2	850.5	850.0
$K = [1, 10]$	908	910	900
$K = [11, 17]$	2405	2408	2400

coverage, the application scheme that integrates the Internet and the Internet of Things technology can truly form complementary advantages. While avoiding the previous technical defects, it can adapt to more complex equipment communication and control scenarios in the future. It provides a comprehensive solution for the urban street lamp control system that integrates many advantages such as low power consumption, high efficiency, flexibility and autonomy, intelligence, easy maintenance, easy expansion, and remote control [20].

To accomplish the autonomous and smart administration of urban highway luminaires and to accomplish the aims of resource efficiency, sustainable pollution prevention, and individualized treatment, it is the prime goal of research street lamp controller. The intelligent street lighting system can essentially be modeled as a unique simulation environment with widely separated nodes but clear distribution principles. Its node distribution essentially matches the set-

TABLE 3: Comparison of three frequency bands.

Working frequency (MHz)	Transmission rate (Kbit/s)	Adjustment method
2405	255	O-QPSK
2408	45	BPSK
2400	25	BPSK

ting of metropolitan road traffic. The complete electronic circuit network is installed on this feature. Feedback is needed for implementing game controller for lamp posts. Consider each road like a central processing unit from such a local standpoint, where many neighboring lamppost terminals are sequentially distributed geographically, and it is easy to form a linear communication system that is related step by step. From a global perspective, multiple such linear communication systems can form a large metropolitan area network communication system [17]. Therefore, based on the above feature abstraction, the prototype of the urban street lamp control system is obtained as shown in Figure 3.

As per the conceptual model in Figure 3, a sizable broadband transceiver must be built in implementing consolidated online administration of dispersed urban lamp post nodes. The TCP/IP standard family's internetwork paradigm is the ideal option for long-distance interaction because it has an excellent long term and mature technology [21]. However, the deployment of virtualization technology by virtue of purely network designs to each lamp postcluster will be enormous for a size up city due to the numerous light pole nodes and the complicated distribution. From a variety of angles, including financial cost, implementation problems, Internet challenges, and operational battery life, it is improper. In order to enable the light pole nodes dispersed more along carriageway to build a network connection using the wireless medium, the route is employed as a legal subdivision unit. Afterward, use the entryway to surf the content using the other circuit as a sizable motherboard. This thus divides and optimizes the design methodology while still meeting the needs of protracted interaction, which lessens the total complexity of the layout. Additionally, the establishment of a small Internet of Things connecting lamp post-nodes can partially achieve the regional control of the luminaires, increasing the updated daily of the total road led lamps. The street light system may now be remotely controlled since the lamp node connection is now directly hooked up to the Internet via the portal, allowing its node intelligence to be instantly stored to a cloud host and analyzed and used by mayors via a different site [22].

3.2. Weighted Information Fusion Algorithm. In practical application, information fusion technology has huge potential and is welcomed by many industries. Among them, it shines even more in the field of Internet of Things, and a variety of smart products of the Internet of Things have appeared in the civilian market, such as sweeping robots and intelligent drones. This is all thanks to the information

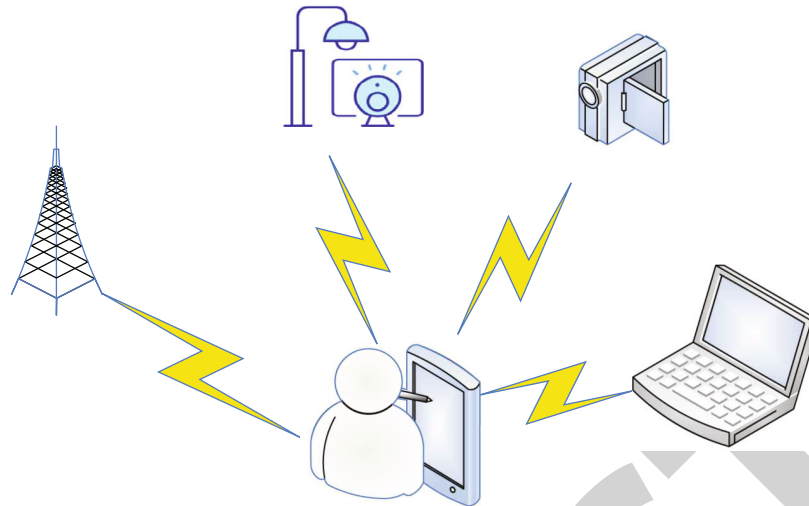


FIGURE 3: Device interaction association.

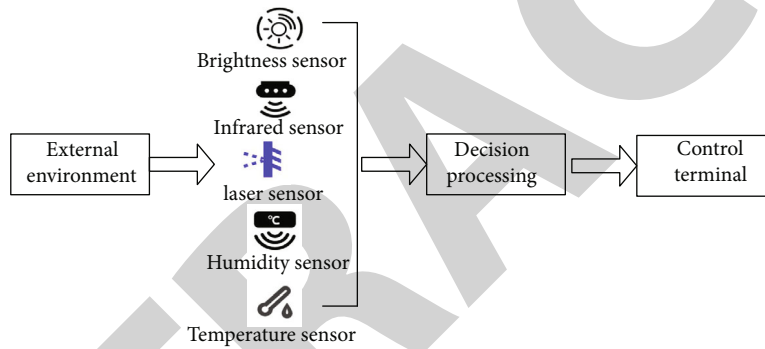


FIGURE 4: Sensor human and vehicle detection.

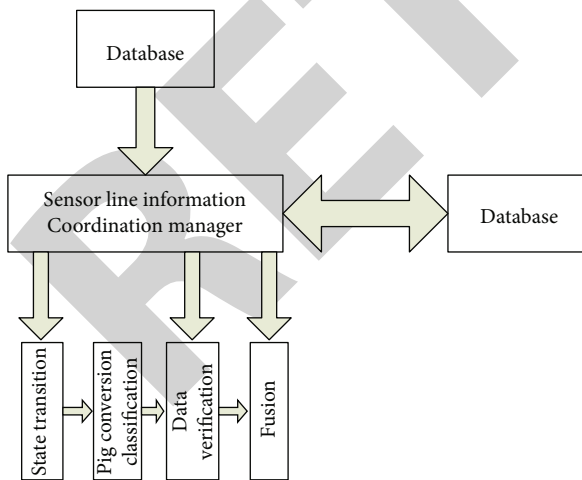


FIGURE 5: Multisensor information fusion.

fusion technology, which realizes multisource information detection of targets and improves the object recognition rate, using computer technology to automatically analyze and comprehensively process the observation information of several sensors obtained in time series under certain criteria,

so as to complete the required decision-making and estimation tasks and the information processing process. For information-related, combined and analyzed by multisensing equipment, information with higher comprehensive value can be obtained [23]. The average value fusion algorithm usually uses a mathematical average formula, which is a sensor with roughly the same weight value selected, abbreviated as MVFA. Assuming that multiple sensors in the m -sensor fusion system evaluate the state of the same target, the combined state evaluation scale satisfies the following conditions:

$${}^{\Lambda} i = \sum_{a=1}^m v_a i_a, \tag{1}$$

$$\sum_{a=1}^m v_a = 1. \tag{2}$$

The state estimate after local fusion is

$${}^{\Lambda} i = \sum_{a=1}^m v_a i_a = \frac{1}{n} \sum_{a=1}^m i_a. \tag{3}$$

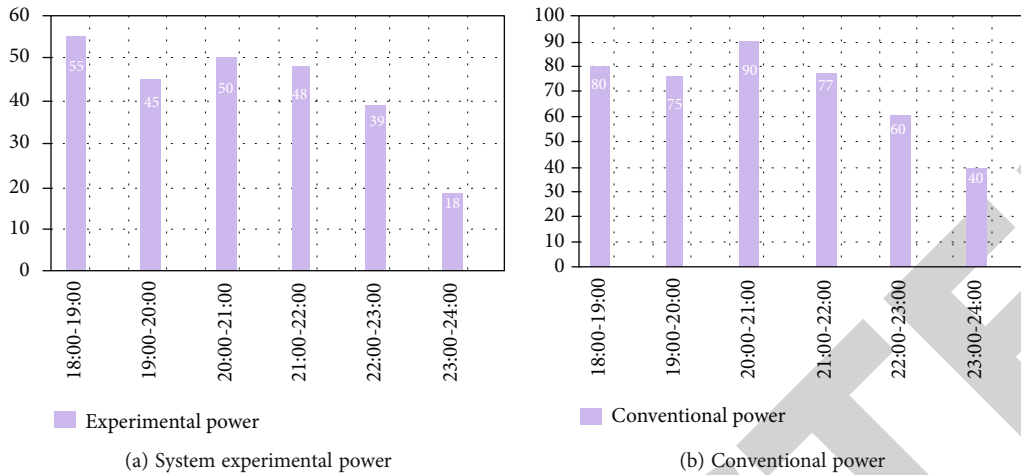


FIGURE 6: Comparison of experimental power and conventional power of smart street lamps.

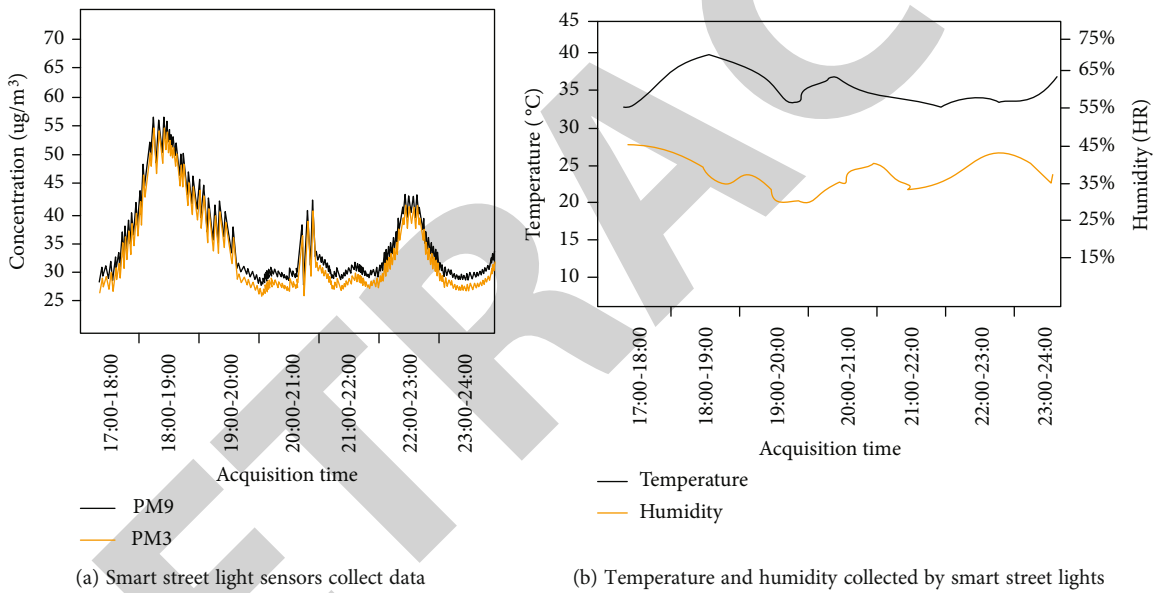


FIGURE 7: Only street light sensor data collection.

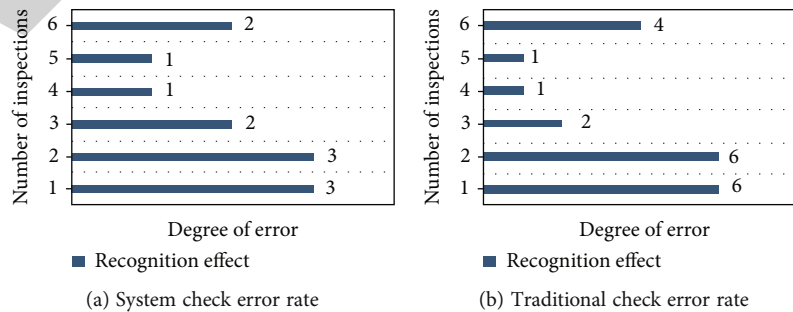


FIGURE 8: System check and traditional check error comparison.

The total mean squared error is

$$\partial^2 = A \left[\left(i - \bar{i} \right)^2 \right] = A \left[\sum_{a=1}^m v_a (i - i_a) \right]^2, \quad (4)$$

$$\partial^2 = A \sum_{a=1}^m v_a^2 (i - i_a)^2 + 2 \sum_{\substack{a=1, b=1 \\ a \neq b}}^m v_a (i - i_a) v_b (i - i_b), \quad (5)$$

$$A[(i - i_a)(i - i_b)] = 0. \quad (6)$$

So the total mean squared error is

$$\partial^2 = \left[A \sum_{a=1}^m v_a^2 (i - i_a)^2 \right] = \sum_{a=1}^m v_a^2 \partial_a^2. \quad (7)$$

For the weighted average algorithm, the total mean squared error is

$$\partial^2 = \frac{\sum_{a=1}^m v_a^2}{m^2}, \quad (8)$$

$$f(v_1, v_2, \dots, v_m, \lambda) = \sum_{a=1}^m v_a^2 \partial_a^2 - \lambda \left(\sum_{a=1}^m v_a - 1 \right). \quad (9)$$

Build a system of formulas:

$$\frac{\delta f}{\delta v_a} = 1 - \sum_{a=1}^m v_a = 0, \quad (10)$$

$$v_a = \frac{\delta_a^{-2}}{\sum_{a=1}^m \delta_a^{-2}}. \quad (11)$$

With the passage of time, the accumulation of perceptual information, the gray number measurement of each unit gradually becomes smaller, but the information of each sensor may also conflict, making the gray measurement larger. The gray fusion algorithm does the following processing. When the information is consistent, the reliability weight P is introduced:

$$x_{ab} = \min(1, x_{ab} + P), \quad (12)$$

$$x_{ab} = \max(0, x_{ab} + P). \quad (13)$$

When the information is consistent, the gray measurement adjustment weight is introduced:

$$x_{ab} = \frac{x_{ab}A + x_{ab}K}{A + K}, \quad (14)$$

$$x_{ab}^{-1} = \frac{x_{ab}(-A) + x_{ab}(-K)}{A + K}. \quad (15)$$

The process is a continuous refinement of its estimates, assessments, and evaluation of the need for additional sources of information, as well as a process of continuous

self-correction of the information processing to obtain improved results. The human-vehicle detection system based on information fusion is a complex system with strong anti-interference, high accuracy, comprehensive, and reliable measurement information [24]. Traditional street light systems mostly use single-source feature information as a control factor, which makes the measurement information often not meet the ideal system value requirements [25]. According to a variety of scene factors affecting urban traffic lighting, a multidirectional study is carried out, and a reasonable and reliable multisource information fusion street light control scheme is obtained in combination with actual needs. The scheme architecture is shown in Figure 4.

Combining information from multiple sensors combines additional or redundant information from multiple sensors in time or space according to certain criteria to obtain a consistent description or interpretation of the object being measured. Its main purpose is to obtain more information by combining information rather than the individual elements present in the input information, which is the result of optimal synergy, that is, using a combination or combination of several sensors to improve the sensor system. Figure 5 shows the multisensor information fusion process.

For the night road environment, multisensors are used to collect multisource information, and the crowd vehicles on the road are used as the information source collection objects. Due to the large demand for hardware devices such as sensors for equipment deployment, in order to reduce costs and take into account performance, the main sensors used in the system are temperature, humidity, brightness, infrared, and other sensors, which effectively reduces the error rate of system measurement information. Different sensors detect objects in the external environment and convert the physical information of different sensors into digital information and send them to the decision-making processing layer. Finally, the obtained decision-making information is sent to the street light control terminal. As the executive body of the system, the street light control terminal calculates the corresponding street light control command according to the decision information and actively regulates the street light switch.

4. Realization of Intelligent Street Lights in Urban Public Spaces

4.1. Adjustment of Street Light Data before Testing. The edge processing function of the centralized controller of smart street lamps is reflected in the analysis and processing of data. Data analysis includes power data analysis and environmental parameter analysis, and data processing refers to the processing of image data. The voltage of the smart street lamp is set to 220 v, the current is 32 A, the status of the street lamp is monitored in real time by controlling the current and voltage data, and the abnormal status is dealt with in time.

4.2. Power Test of Smart Street Light Public Art. According to the experimental results, it can be known that the core controller conveys different control commands to the street light

controller according to the real-time information of the road, and the street light controller controls the light and dark of the street light. The intelligent street lamp control system designed in this paper can realize intelligent control of street lamps without personnel management and can achieve the effect of saving energy. To this end, specific data on changes in street lights are collected. A total of six hours of monitoring from 6:00 p.m. to 12:00 p.m., with a statistical interval of 1 hour each time, calculate the approximate power consumption for six hours at night from the lighting duration at different times. The monitoring data results are shown in Figure 6:

As can be seen from the figure, the power consumption of the street lamp system designed in this paper is much lower than that of the conventional lighting system. The street lamp intelligent control system designed by the sensor and weighted information fusion algorithm can realize the purpose of saving electric energy under the premise of intelligently controlling the street lamp lighting. From the simulation point of view, the intelligent street light control system can save a lot of power compared with the conventional street light control, especially between nine o'clock and ten o'clock, it can save 44% of the power consumption, during a six-hour period a night, and the overall power saving is 40%.

4.3. Smart Street Light Sensor Data Collection. In order to more intuitively display the data collected by the smart street light centralized controller, some environmental parameters actually collected are taken as an example for specific analysis. Access to the smart street light centralized controller randomly selects the PM9 and PM3 concentration monitoring data for six hours from 6:00 pm to 12:00 pm and depicts the 6-hour period as a line figure as shown in Figure 7.

Through the analysis of environmental parameters, not only can the urban air environmental quality and climate conditions be indexed but also the equipment environment and equipment operating conditions can be analyzed in combination with power data, figures, and other data. For example, it can be seen from Figure 7 that during the 6 hours, the temperature and humidity of the external operating environment of the smart street light centralized controller at night are normal and relatively stable. If abnormal temperature and humidity are detected, the power should be cut off in time to avoid more serious damage. In addition, through the combination of illuminance and power data, it can also monitor whether the street lights are normally illuminated or support intelligent functions such as automatic dimming.

In order to further judge the error of the system algorithm, the temperature and humidity in the environment are detected by the traditional inspection method and the inspection method of the system algorithm. The detection results are shown in Figure 8.

According to the abovementioned system detection of temperature and humidity through smart street light sensors and the results of traditionally believed detection, the number of errors detected by the sensor system is controlled to

be less than three times, and the number of errors of traditional human detection is less than six times. The system test error rate is 1/2 of the traditional test error rate, and the accuracy is much lower than that of traditional measurement methods compared to traditional measurement methods. Therefore, the measurement of smart street light sensors can greatly improve the efficiency, and the test accuracy is also quite high.

5. Conclusion

The placement of public art forms a harmonious and unified whole with the surrounding landscape, architecture, and urban environment space. It is a combination of sensibility and rationality and is even more inclined to the proportional scale of the rational range. Through the intelligent system of intelligent street light sensor and weighted information fusion, the actual data of the power consumption of the lighting system and the power consumption of previous lighting in a period of time are recorded, and the results are analyzed. Finally, it is concluded that the designed system can achieve the effect of saving electric energy. Ready-made products and challenges centered on new media technologies. The public art of the future must rely on science and technology and regard art as a form of expression of technology. Through these technologies, public art is not only a work of art but also an object of emotional communication, bringing new ideas to people's boring life.

Data Availability

Data can be obtained by contacting the authors.

Conflicts of Interest

We confirmed that there is no conflict of interest.

Acknowledgments

This work was supported by the Jilin Provincial Education Department Project (No. 2021LY521W38).

References

- [1] S. Yin, B. Deng, and D. Zhao, "Public art plan of smart industrial area in China," *Arts Studies and Criticism*, vol. 3, no. 1, pp. 80–86, 2022.
- [2] A. Cayer and C. T. Bender, "Beyond public: architects, activists, and the design of akichiat Tokyo's Miyashita Park," *Architectural Research Quarterly*, vol. 23, no. 2, pp. 167–178, 2019.
- [3] E. Crte-Real, "Arachne's loom: a public art drawing for porto design biennale 2019," *Drawing Research Theory Practice*, vol. 5, no. 1, pp. 147–164, 2020.
- [4] S. Darivemula, A. Stella, F. Fahs, K. Poirier-Brode, and K. Ko, "The white coat public art project: using the white coat as a canvas for reflection for women in medicine," *Public Health*, vol. 194, no. 12, pp. 260–262, 2021.
- [5] B. Yang, "Research on application of vehicle-mounted gas sensor in the age of AI," *Transducer and Microsystem Technologies*, vol. 41, no. 9, pp. 156–160, 2022.

Retraction

Retracted: Intelligent Evaluation Method of Engineering Cost Feasibility Model Based on Internet of Things

Journal of Sensors

Received 17 October 2023; Accepted 17 October 2023; Published 18 October 2023

Copyright © 2023 Journal of Sensors. This is an open access article distributed under the Creative Commons Attribution License, which permits unrestricted use, distribution, and reproduction in any medium, provided the original work is properly cited.

This article has been retracted by Hindawi following an investigation undertaken by the publisher [1]. This investigation has uncovered evidence of one or more of the following indicators of systematic manipulation of the publication process:

- (1) Discrepancies in scope
- (2) Discrepancies in the description of the research reported
- (3) Discrepancies between the availability of data and the research described
- (4) Inappropriate citations
- (5) Incoherent, meaningless and/or irrelevant content included in the article
- (6) Peer-review manipulation

The presence of these indicators undermines our confidence in the integrity of the article's content and we cannot, therefore, vouch for its reliability. Please note that this notice is intended solely to alert readers that the content of this article is unreliable. We have not investigated whether authors were aware of or involved in the systematic manipulation of the publication process.

Wiley and Hindawi regrets that the usual quality checks did not identify these issues before publication and have since put additional measures in place to safeguard research integrity.

We wish to credit our own Research Integrity and Research Publishing teams and anonymous and named external researchers and research integrity experts for contributing to this investigation.

The corresponding author, as the representative of all authors, has been given the opportunity to register their agreement or disagreement to this retraction. We have kept a record of any response received.

References

- [1] L. Chen, H. Zhang, and F. Wang, "Intelligent Evaluation Method of Engineering Cost Feasibility Model Based on Internet of Things," *Journal of Sensors*, vol. 2022, Article ID 3420723, 8 pages, 2022.

Research Article

Intelligent Evaluation Method of Engineering Cost Feasibility Model Based on Internet of Things

Liangqiong Chen , Hao Zhang , and Fang Wang 

Xinyang Normal University, Xinyang, Henan 464 000, China

Correspondence should be addressed to Liangqiong Chen; 2020220245@mail.chzu.edu.cn

Received 12 August 2022; Revised 30 August 2022; Accepted 5 September 2022; Published 6 October 2022

Academic Editor: C. Venkatesan

Copyright © 2022 Liangqiong Chen et al. This is an open access article distributed under the Creative Commons Attribution License, which permits unrestricted use, distribution, and reproduction in any medium, provided the original work is properly cited.

In order to solve the problem of low accuracy of high-rise building cost evaluation, the author proposes an intelligent evaluation method of engineering cost feasibility model based on the Internet of Things. According to the overall investment composition of the construction project, this paper classifies the cost index, determines the overall cost correction coefficient, and uses the gray correlation analysis method to build the evaluation index system; according to the structure of BP neural network, the network error is calculated, and the error signals of output layer and hidden layer are defined by gradient descent method to obtain the network weight adjustment formula; finally, this paper uses the adaptive learning rate adjustment formula to set the network parameters, introduces the key parameters in the construction project to the input layer, and establishes the final cost evaluation model. Experimental results show that the error rate of this system is controlled within 10%, which meets the requirements of investment estimation. *Conclusion.* The proposed method can accurately and quickly evaluate the best solution for the cost of high-rise buildings with less information and has strong nonlinear information processing capabilities.

1. Introduction

At present, the world is ushering in a period of great development and change in digital transformation. The new generation of information technology has accelerated to lead the breakthrough in technology application, bringing about major changes in industrial form, organizational management, social governance, and other aspects. The development of new generation technologies such as the Internet of Things has brought new impetus and new opportunities for the development of the digital economy. The Internet of Things technology presents the characteristics of integrated development, integrated innovation, large-scale application, and ecological acceleration, and hot technologies continue to emerge. The scale deployment of networks and platforms has been accelerated to lay a foundation for the comprehensive promotion of the Internet of Things.

When we use the traditional construction project cost model to solve complex construction projects, there will be large data errors and many factors affecting the calculation results, resulting in inaccurate data, reduced credibility,

and construction difficulties [1, 2]. Based on the above deficiencies, this paper improves the design of the traditional construction project cost model. The optimized construction cost model structure adopts multilevel calculation, which replaces the single-level calculation of the original construction cost model, reduces external influencing factors, and improves the reasonable configuration of internal levels, thereby, improving the accuracy of the construction cost model and reducing the calculation influencing factors. Improve the traditional construction cost model algorithm, add refined classification, reasonable quantitative classification, multidimensional theoretical calculation, and reasonable control of result errors for complex construction projects, so that each step of the calculation is close to the final settlement, thereby, the accuracy of data calculation is improved, the calculation efficiency is improved, and the error of data processing is reduced. Through simulation experiments of different dimensions, this paper verifies the investment estimate, design estimate, revised estimate, construction drawing estimate, and near completion final account before and after improvement [3, 4].

BIM is a complete enterprise engineering information system model, which can integrate engineering information, processes, and human resources in all stages of the enterprise's entire life cycle and apply it to the same model; it is convenient for the comprehensive management and operation of enterprises, projects, and engineering parties [5, 6]. This technology uses three-dimensional digital technology to accurately analyze and simulate the real situation and construction information of a large building and provides a coordinated and internally unified information model for the design and construction of the entire construction project. It realizes the integration of architectural design and construction and optimizes the communication and collaboration between various disciplines, which can greatly reduce the cost and production cost of the entire project and ensure the smooth progress of the entire project on time and quantity.

2. Literature Review

The project cost is an investment method for enterprises and the government, and the purpose is to obtain the maximum profit, so the cost must be strictly controlled during the construction process. In recent years, the progress of China's market economy has promoted the rapid development of the construction industry, and the main body of construction investment has developed a trend of diversification [7, 8]. Under normal circumstances, the owner will do a basic preliminary assessment before investing, and accurate and rapid assessment of the project cost is the need for project bidding competition. In order to maximize profits in the process of investment and construction, we must comprehensively consider the investment cycle, amount, and other complex factors, firmly control the core elements of cost and realize scientific cost evaluation. Due to the late start of China's engineering cost management, there is no complete theoretical knowledge system and lack of effective cost control, and the complex structure of high-rise buildings requires a long construction period. Therefore, seeking an efficient and practical cost assessment method has become the focus of scholars and industry professionals.

At this stage, relevant scholars have proposed many cost assessment methods. For example, Zhan et al. and Jha et al. used WSR (Wuli-Shili-Renli, WSR for short) analytical model to evaluate the cost control of building seismic structures [9, 10]. First, they construct the hierarchical structure of price control and obtain multiple cost control schemes. Secondly, they use the QOS (quality of service) method to design the benefit control constraint equilibrium and select the best evaluation result. Finally, the simulation experiment proves that this method can effectively analyze the quality change characteristics of high-rise buildings and control the cost consumption better.

Yang proposed a project cost management method based on BIM (representing building information model, Building information model, referred to as BIM) technology [11]. They analyzed the feasibility of introducing BIM technology in combination with the problems of the existing cost evaluation methods in China. They explored the basic principles and advantages of BIM and proposed corresponding

application models for cost management of construction projects in different stages. Finally, the role of BIM technology is verified by a specific example.

Although the above two methods play a certain role in cost control, they do not take into account the dynamics of prices and have strong subjectivity, resulting in low evaluation accuracy. Based on this, the author uses the BP (representing back propagation, back propagation, referred to as BP) neural network method to establish a high-rise building project cost evaluation model. This paper debugs the neural network model through the process of determining the neural network structure, calculating the network error, adjusting the weights, designing the network parameters, etc. and introduces the important parameters in the high-rise building project into it to build the final cost evaluation model. Simulation experiments show that the BP neural network method can solve the shortcomings of slow network convergence and easy to fall into the local minimum value, effectively improve the accuracy of cost evaluation in the early decision-making stage, and achieve rapid evaluation.

3. Methods

3.1. Construction of Evaluation Index System

3.1.1. Composition of Total Investment in Construction Projects. As shown in Figure 1, the cost of construction engineering refers to the combination of known construction content, scale and standards and other related requirements, all the costs that need to be spent in the process of completing all construction contents until delivery [12, 13]. It mainly includes investment in other fixed assets such as construction equipment purchase costs, installation costs, and preparation costs.

3.1.2. Classification of Cost Index. In different stages of construction, the manifestations of engineering cost are also different, for example, in the feasibility analysis stage, the performance behavior is investment estimation, the specific manifestation of each stage is shown in Figure 2.

The cost index is an indicator that reflects price changes in a fixed period of time, it can effectively reflect the trend and magnitude of cost changes, and at the same time objectively show the supply and demand relationship between the level of productivity and the construction market. Mainly divided into the following categories:

- (1) Individual indices, such as labor and materials, by arranging the indices of different periods in chronological order to obtain the status of individual price changes and forecast the future development trend.
- (2) The price index of construction equipment and tools.
- (3) High-rise building installation cost index.
- (4) The cost index of a single project.

3.1.3. Construction of Evaluation Index System Based on Grey Correlation. The author uses the grey relational analysis method to construct the evaluation index system; the core idea is to judge the density and proximity of the cost sequence curve by combining the characteristic index sequence curve of the construction project, the smaller the

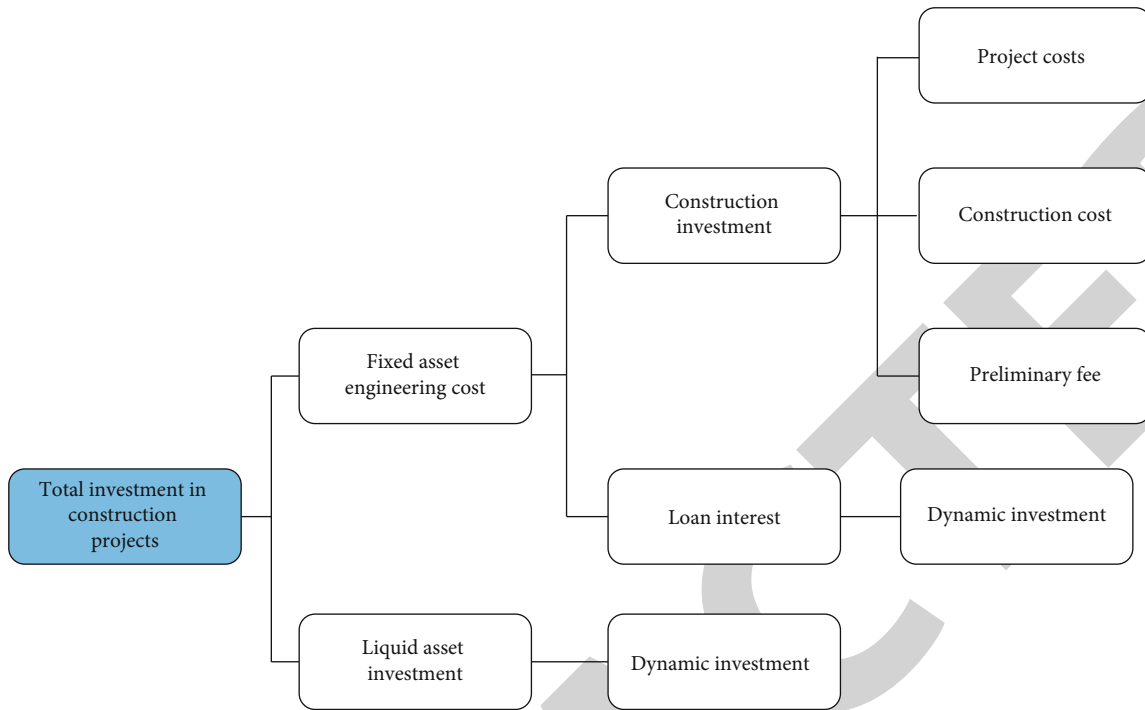


FIGURE 1: The overall investment composition of construction projects.

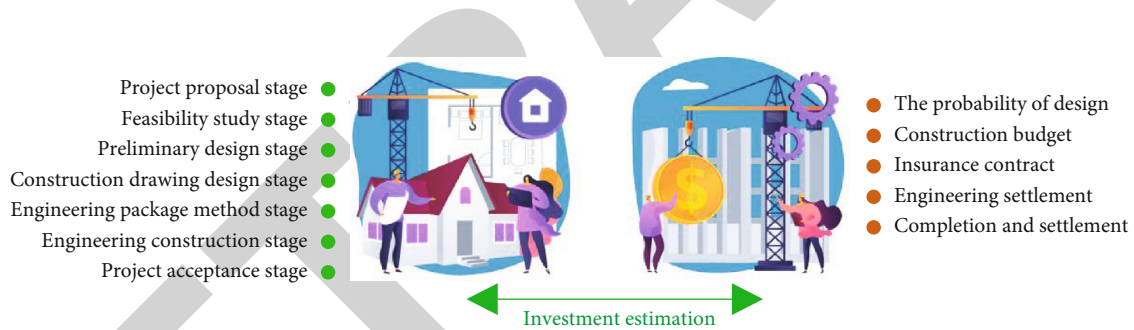


FIGURE 2: The representation of project cost at different stages.

curve gap, the higher the correlation between the series. This method is simple in data processing and convenient in calculation, and is suitable for the selection of project cost evaluation indicators [14, 15].

(1) *Compare the Selection of the Matrix and the Reference Sequence.* The comparison matrix is all the characteristic indexes that affect the project cost, suppose there are m sample projects and n index characteristics, therefore, the comparison matrix X is expressed as

$$X = \begin{bmatrix} x_{11} & x_{12} & \cdots & x_{1n} \\ x_{21} & x_{22} & \cdots & x_{2n} \\ \vdots & \vdots & \ddots & \vdots \\ x_{m1} & x_{m2} & \cdots & x_{mn} \end{bmatrix}. \quad (1)$$

When evaluating the cost, the unilateral cost is selected as the value of the reference sequence, and the correlation between different characteristic indicators and the unilateral cost is compared, the higher the degree of correlation, the closer the relationship between the eigenvalue and the unilateral cost. The formula for calculating this reference sequence value is

$$X_{i0} = [X_{i0}, X_{i20}, \dots, X_{im0}]. \quad (2)$$

In formula (2), $X_{i0}(i = 1, 2, \dots, m)$ represents the unilateral cost value.

(2) *Standardization of Index Values.* In order to improve the evaluation accuracy and ensure the equivalence between the indicators, the linearization method is used to normalize

the index values of different dimensions, and the expression is as follows:

$$X_{ij} = \frac{x_{ij}}{\max x_{ij}}. \quad (3)$$

In formula (3), $\max x_{ij}$ represents the maximum value of the k -th index in all projects.

(3) *Calculation of Correlation Coefficient.* The correlation coefficient can reflect the correlation degree of different indicators in the comparison matrix X to the reference sequence X_0 in the i -th sample. The gray correlation analysis method is used to calculate the correlation coefficient between the j -th index of the i -th project and the unilateral cost.

$$\xi_{ij} = \frac{\min_j \min_i |X_{i0} - X_{ij}| + \rho \max_j \max_i |X_{i0} - X_{ij}|}{|X_{i0} - X_{ij}| + \rho \max_j \max_i |X_{i0} - X_{ij}|}. \quad (4)$$

In formula (4), ρ represents the resolution coefficient, and its value is 0.5, and its value will affect the difference between the correlation coefficients.

(4) *Correlation Degree Calculation.* The grey correlation coefficient can only show the correlation degree of the indicators in a single sample, which is one-sided. Therefore, the author selects multiple samples and uses the mean method to determine the correlation of the j -th index.

$$\gamma_j = \frac{1}{m} \sum_{i=1}^m \xi_{ij}. \quad (5)$$

In formula (5), the obtained correlation degrees are sorted, the greater the correlation degree, the more consistent the change trend of the j -th index and the cost, that is, the higher the influence of X_j on X_0 . According to the rule of taking the larger one, the indicators with greater correlation are reserved.

3.2. Establishment of Cost Evaluation Model of BP Neural Network

3.2.1. *Features of BP Neural Network.* BP neural network is a data processing system proposed on the basis of human brain organization and activity mechanism, so it can show many human brain characteristics.

(1) *Distributed Data Storage.* The data storage method of BP neural network is quite different from traditional computer storage, the same data is not only stored in one place, but distributed in the connection structure between neural nodes.

(2) *Parallel Data Processing.* In the neural network, any neural node can receive the transmission information, can combine the information for independent processing and operation, and send the calculation result to the next neural network for parallel data processing [16, 17].

(3) *Fault Tolerance of Information Processing.* The structural characteristics of the neural network are mainly reflected in the huge structure and spatial distribution of storage, these two characteristics can make the neural network have better fault tolerance in the following two aspects: when some neural nodes are destroyed, it will not have a great impact on the network as a whole; for data input, if the data is incomplete or deformed, the neural network will repair the missing data according to some data.

(4) *Adaptability of Data Processing.* Adaptive refers to changing its own characteristics according to environmental requirements. Mainly reflected in the following aspects:

Self-Learning: during the training process, if the external environment changes, the network structure parameters can be automatically adjusted after a period of training.

Self-Organization: when stimulated by the outside world, the connection parts between neural nodes can be adjusted according to certain learning rules, and the network can be reconstructed.

3.2.2. *Basic Structure of BP Neural Network.* BP neural network belongs to a learning algorithm of forward multi-layer error back propagation. It has an input layer, an output layer and multiple hidden layers, the layers are fully interconnected, the nodes in the same layer are not connected to each other, each layer is composed of several neurons.

Suppose that the BP neural network has n input nodes, m output nodes, and the number of nodes is denoted as q . The input vector and output vector are $X = (x_1, x_2, \dots, x_n)^T$ and $Y = (y_1, y_2, \dots, y_n)$, respectively. The input vector and output vector of the hidden layer are denoted as $S = (s_1, s_2, \dots, s_n)$ and $B = (b_1, b_2, \dots, b_q)$, respectively. The input and output vectors of the output layer are described as $L = (l_1, l_2, \dots, l_m)$ and $C = (c_1, c_2, \dots, c_m)$, respectively. The neurons in the input layer and the hidden layer are i and j , respectively, and the connection weight is W_{ij} . The connection weight between the hidden layer and the output layer is V_{jt} , and the threshold of the neural node j in the hidden layer is θ_j .

3.2.3. *BP Neural Network Error Calculation.* If the output of the BP neural network is quite different from the ideal output value, the ideal output value is the instance provided by the ideal output neural network by learning the training samples, adjust the connection weight coefficient according to certain rules, continuously improve its own performance, and finally achieve the most ideal state, this state is that when the input is given externally, it can make a relatively correct output, and the output value is the ideal output value. The expression of the error output result E is as follows:

$$E = \frac{1}{2}(d - O)^2 = \frac{1}{2} \sum_{k=1}^l (d_k - o_k)^2. \quad (6)$$

In the formula, d represents the ideal state input value of BP neural network, O represents the ideal state output value of BP neural network, k represents the amount of sample data, l represents the number of hidden layer nodes, d_k represents the actual state input value of the BP neural network, and o_k represents the ideal state output value of the BP neural network.

Expanding the above error to the hidden layer, we get

$$E = \frac{1}{2} \sum_{k=1}^l [d_k - f(\text{net}_k)]^2. \quad (7)$$

In the formula, $f(\text{net}_k)$ represents the output constant value of the BP neural network.

Formula (7) is further expanded to the input layer.

$$E = \frac{1}{2} \sum_{k=1}^l \left\{ d_k - f \left[\sum_{j=0}^m \omega_{jk} f(\text{net}_j) \right] \right\}^2. \quad (8)$$

In the formula, ω_{jj} represents the number of output layer nodes.

3.2.4. Weight Adjustment Based on Gradient Descent. According to the above formula, the adjustment of the network input error is the adjustment of the weights W_{ij} and V_{ij} , so the weight adjustment can be performed by changing the error E . Using the gradient descent method to continuously reduce the network error, make sure that there is a proportional relationship between the amount of weight adjustment and the degree of error gradient descent.

$$w_{ij} = -\lambda \frac{\partial E}{\partial w_{ij}}, j = 0, 1, 2, \dots, m; k = 1, 2, \dots, l, \quad (9)$$

$$v_{ij} = -\lambda \frac{\partial E}{\partial v_{ij}}, j = 0, 1, 2, \dots, n; j = 1, 2, \dots, l. \quad (10)$$

In the formula, the negative sign represents gradient descent, and $\lambda \in (0, 1)$ belongs to a proportional coefficient, which reflects the learning rate of the neural network during the training process. Therefore, it can be seen that the BP algorithm is a kind of σ learning rule.

The above two formulas are not complete weight adjustment formulas, but only an expression of adjustment ideas. The derivation process of the adjustment formula will be described in detail below.

It is assumed that in the derivation process of the weight adjustment formula, there are, respectively, for the output and input layers, $i = 0, 1, 2, \dots, n, j = 1, 2, \dots, m$.

For the output layer, formula (9) can be rewritten as

$$\Delta w_{jk} = -\eta \frac{\partial E}{\partial w_{jk}} = -\eta \frac{\partial E}{\partial \text{net}_k} \frac{\partial \text{net}_k}{\partial w_{jk}}. \quad (11)$$

Formula (10) can be written as

$$\Delta v_{ij} = -\eta \frac{\partial E}{\partial v_{ij}} = -\eta \frac{\partial E}{\partial \text{net}_j} \frac{\partial \text{net}_j}{\partial v_{ij}}. \quad (12)$$

Define the error signals of the output layer and the hidden layer, respectively.

$$\delta_k^o = -\frac{\partial E}{\partial \text{net}_k}, \quad (13)$$

$$\delta_j^y = -\frac{\partial E}{\partial \text{net}_j}. \quad (14)$$

Combining the above two formulas, we can get

$$\Delta w_{jk} = \eta \delta_j^y. \quad (15)$$

Therefore, it can be seen that only by calculating the error signals δ_k^o and δ_j^y , the inference of the weight adjustment amount can be realized.

The expanded form of the signal error δ_k^o in the output layer is

$$\delta_k^o = -\frac{\partial E}{\partial \text{net}_k} = -\frac{\partial E}{\partial o_k} \frac{\partial o_k}{\partial \text{net}_k} = -\frac{\partial E}{\partial o_k} f'(\text{net}_k). \quad (16)$$

The expanded expression of the signal error δ_j^y in the hidden layer is

$$\delta_j^y = -\frac{\partial E}{\partial \text{net}_j} = -\frac{\partial E}{\partial y_j} \frac{\partial y_j}{\partial \text{net}_j} = -\frac{\partial E}{\partial y_j} f'(\text{net}_j). \quad (17)$$

Calculate the partial derivative of the error to the output layer and the hidden layer in the above two formulas.

$$\frac{\partial E}{\partial o_k} = -(d_k - o_k), \quad (18)$$

$$\frac{\partial E}{\partial y_j} = -\sum_{k=1}^l (d_k - o_k) f'(\text{net}_k) w_{jk}. \quad (19)$$

Bring the calculation results into formulas (15) and (16), and use formula $f'(x) = f(x)[1 - f(x)]$ to calculate

$$\delta_k^o = (d_k - o_k) o_k (1 - o_k), \quad (20)$$

$$\begin{aligned} \delta_j^y &= \left[\sum_{k=1}^l (d_k - o_k) f'(\text{net}_k) w_{jk} \right] f'(\text{net}_j) \\ &= \left(\sum_{k=1}^l \delta_k^o w_{jk} \right) y_j (1 - y_j). \end{aligned} \quad (21)$$

Through formulas (20) and (21), the calculation formula of neural network algorithm weight adjustment can be obtained as

$$\Delta w_{jk} = \eta \delta_k^o y_i = \eta (d_k - o_k) o_k (1 - o_k) y_j, \quad (22)$$

$$\Delta v_{ij} = \eta \delta_j^y x_j = \eta \left(\sum_{k=1}^l \delta_k^o w_{jk} \right) y_j (1 - y_j) x_i. \quad (23)$$

3.2.5. Network Parameter Design. This paper mainly sets the learning rate η of BP neural network. The learning rate η can also be called the step size, and its value interval is usually a constant between [0, 1] in the standard learning algorithm, but in the process of evaluating the model construction, it is very difficult to determine a learning rate that works from start to finish [18, 19]. If η is too small, the number of model training will increase, and η needs to be increased during the training process; if η is too large, training oscillation may occur. There are many ways to adjust the learning rate, the ultimate purpose of these methods is to make the learning rate play an effective role in the entire training process, therefore, the more commonly used adaptive learning rate adjustment expression is selected.

$$\eta(t+1) = \begin{cases} 1.05(t)E(t) < E(t-1), \\ 0.7\eta(t)E(t) > 1.04E(t-1), \\ \eta(t). \end{cases} \quad (24)$$

In the process of neural network training, due to the continuous reduction of errors, the learning rate will increase, when the number of training times increases to a certain extent, the learning efficiency will be higher than 1. Therefore, when using the adaptive learning rate, we must increase the threshold value of the learning rate to obtain the best learning rate.

3.2.6. Determination of BP Neural Network Evaluation Model. After the training of BP neural network is completed, we can input important project cost parameters into the learning network, and obtain the final unit cost price through evaluation. This method realizes the evaluation of numerical model based on historical data, which is easy to operate and has high accuracy. The BP neural network evaluation model is shown in Figure 3.

3.3. Experimental Test. In order to prove the effectiveness of the cost evaluation model of high-rise building projects based on BP neural network, this paper selects 10 completed high-rise building projects in a certain place, and the sample data are all from the cost information network. This can ensure the regional uniformity of sample data, and the similarity between sample data is large, so the model accuracy will not be reduced. The obtained data was preprocessed in combination with the qualitative indicators and quantitative

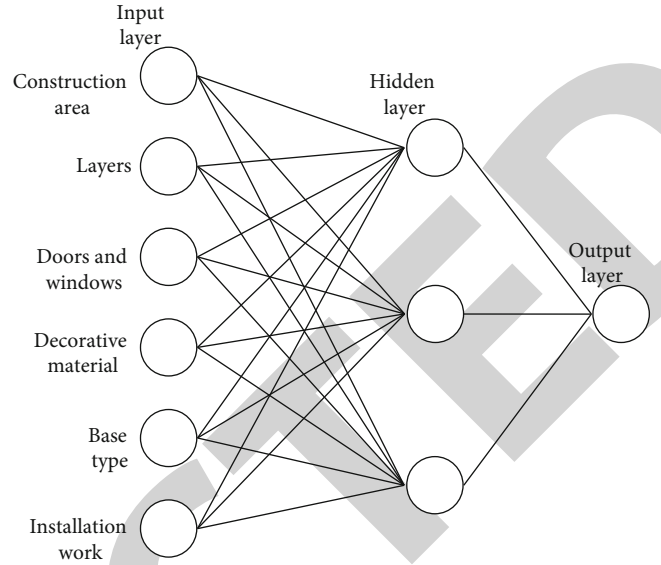


FIGURE 3: BP neural network evaluation model diagram.

standards, and the index values of the sample data after screening are shown in Table 1.

4. Results and Discussion

According to the neural network evaluation model established by the author, simulation experiments are carried out on the basis of Matlab 2016b software. The simulation results are compared with the use of WSR analysis model to control the cost of building seismic structure, the project cost management methods based on BIM technology are compared, and the comparison results are shown in Table 2.

From the results in Table 2, it can be seen that the evaluation error rates of the WSR analysis model for the cost control method of building seismic structures and the project cost management method based on BIM technology are 16.9% and 16.7%, respectively. The author compares the cost control method of building antiseismic structure and the project cost management method based on BIM technology by using WSR analysis model. The error value is small, and the error rate is controlled within 10%, meeting the requirements of investment estimation. In addition, the evaluation speed of the three methods is compared, and the results are shown in Figure 4.

When evaluating the same target, the evaluation speed of the author's method requires less time than the WSR analysis model for the cost control method of building seismic structures and the engineering cost management method based on BIM technology, and the evaluation efficiency is high [20]. The main reason is that the learning rate of the neural network in the proposed method is set more appropriately, and the BP neural network has the characteristics of distributed data storage, parallel data processing, good fault-tolerant performance of information processing, and strong adaptive ability of data processing.

TABLE 1: Engineering characteristic index values.

Serial number	Construction area	Layers	Doors and windows	Eaves high	Structure type	Installation work
1	1	18	2	54.1	1	4
2	2	20	6	59.6	1	4
3	2	24	2	87.6	1	3
4	1	19	4	92.3	2	2
5	2	25	3	89.5	2	1
6	2	23	2	87.2	1	4
7	2	19	1	74.8	1	2
8	1	18	5	94.2	3	3
9	1	24	2	84.1	1	4
10	2	25	3	87.6	1	2

TABLE 2: Model evaluation results of different methods.

Method	Actual value (yuan/m ²)	Predictive value(yuan/m ²)	Difference (yuan/m ²)	Error rate (%)
The cost control method of building seismic structure using WSR analysis model	1525.2	1835.2	310	16.9
Project cost management method based on BIM technology	1541.3	1848.2	306.9	16.7
Method	1428.6	1521.8	93.2	6.1

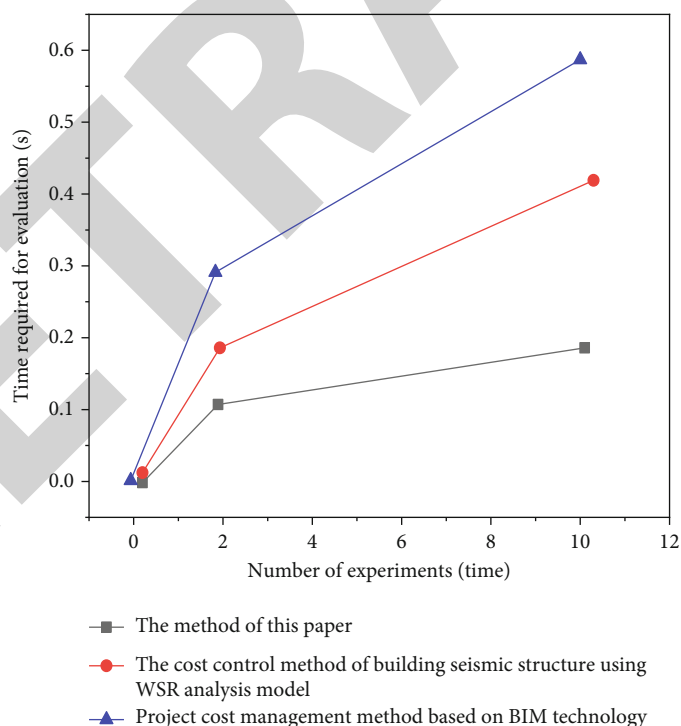


FIGURE 4: Comparison of evaluation speed of different methods.

5. Conclusion

This paper proposes an intelligent evaluation method for the feasibility model of project cost based on the Internet of Things. High-rise buildings are the key development direc-

tion of future building projects, and the cost of this project is of great significance for investment. Therefore, this paper uses BP neural network to study the cost evaluation model of high-rise buildings. First of all, this paper constructs the evaluation index system using the gray correlation analysis

Retraction

Retracted: Convolution-LSTM-Based Mechanical Hard Disk Failure Prediction by Sensoring S.M.A.R.T. Indicators

Journal of Sensors

Received 12 December 2023; Accepted 12 December 2023; Published 13 December 2023

Copyright © 2023 Journal of Sensors. This is an open access article distributed under the Creative Commons Attribution License, which permits unrestricted use, distribution, and reproduction in any medium, provided the original work is properly cited.

This article has been retracted by Hindawi, as publisher, following an investigation undertaken by the publisher [1]. This investigation has uncovered evidence of systematic manipulation of the publication and peer-review process. We cannot, therefore, vouch for the reliability or integrity of this article.

Please note that this notice is intended solely to alert readers that the peer-review process of this article has been compromised.

Wiley and Hindawi regret that the usual quality checks did not identify these issues before publication and have since put additional measures in place to safeguard research integrity.

We wish to credit our Research Integrity and Research Publishing teams and anonymous and named external researchers and research integrity experts for contributing to this investigation.

The corresponding author, as the representative of all authors, has been given the opportunity to register their agreement or disagreement to this retraction. We have kept a record of any response received.

References

- [1] J. Shi, J. Du, Y. Ren, B. Li, J. Zou, and A. Zhang, "Convolution-LSTM-Based Mechanical Hard Disk Failure Prediction by Sensoring S.M.A.R.T. Indicators," *Journal of Sensors*, vol. 2022, Article ID 7832117, 15 pages, 2022.

Research Article

Convolution-LSTM-Based Mechanical Hard Disk Failure Prediction by Sensing S.M.A.R.T. Indicators

Junjie Shi,¹ Jing Du,¹ Yingwen Ren,¹ Boyu Li,² Jinwei Zou,³ and Anyi Zhang³ 

¹State Grid Information & Telecommunication Branch, Beijing, China

²Beijing Fibrlink Communications Co., Ltd, Beijing, China

³State Key Laboratory of Networking and Switching Technology, Beijing University of Posts and Telecommunications, Xitucheng Road, Beijing, China

Correspondence should be addressed to Anyi Zhang; zhanganyi@bupt.edu.cn

Received 28 July 2022; Accepted 16 September 2022; Published 4 October 2022

Academic Editor: C. Venkatesan

Copyright © 2022 Junjie Shi et al. This is an open access article distributed under the Creative Commons Attribution License, which permits unrestricted use, distribution, and reproduction in any medium, provided the original work is properly cited.

The traditional Infrastructure as a Service (IaaS) cloud platform tends to realize high data availability by introducing dedicated storage devices. However, this heterogeneous architecture has high maintenance cost and might reduce the performance of virtual machines. In homogeneous IaaS cloud platform, servers in the platform would uniformly provide computing resources and storage resources, which effectively solve the above problems, although corresponding mechanisms need to be introduced to improve data availability. Efficient storage resource availability management is one of the key methods to improve data availability. As mechanical hard disk is the main way to realize data storage in IaaS cloud platform at present, timely and accurate prediction of mechanical hard disk failure and active data backup and migration before mechanical hard disk failure would effectively improve the data availability of IaaS cloud platform. In this paper, we propose an improved algorithm for early warning of mechanical hard disk failures. We first use the Relief feature selection algorithm to perform parameter selection. Then, we use the zero-sum game idea of Generative Adversarial Networks (GAN) to generate fewer category samples to achieve a balance of sample data. Finally, an improved Long Short-Term Memory (LSTM) model called Convolution-LSTM (C-LSTM) is used to complete accurate detection of hard disk failures and achieve fault warning. We evaluate several models using precision, recall, and Area Under Curve (AUC) value, and extensive experiments show that our proposed algorithm outperforms other algorithms for mechanical hard disk warning.

1. Introduction

At present, Infrastructure as a Service (IaaS) cloud platforms have become the main solution to provide enterprise IT infrastructure. With the development of big data technology and application, more and more enterprises begin to realize the importance of data, so they put forward higher requirements for the availability of data. The traditional IaaS cloud platform generally introduces dedicated storage devices into the platform to achieve high availability of data storage and provides virtual machines in cooperation with dedicated computing devices in Figure 1 [1]. This heterogeneous archi-

ture often leads to two problems: first, it makes the heterogeneity of platform hardware more significant and increase the operation and maintenance cost and scalability cost of the platform; second, when computing resources and storage resources come from different devices, the connection between the computing resources and the storage resource of one virtual machine have to be based on the network connection among devices, which would reduce the performance of the virtual machine. With the proposal of Hyperconverged Infrastructure (HCI), more and more IaaS cloud platforms begin to adopt the homogeneous architecture. Servers in the platform would uniformly provide

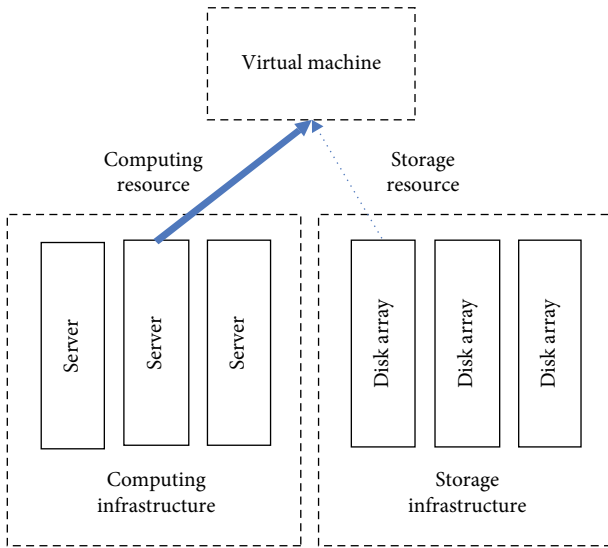


FIGURE 1: Heterogeneous architecture.

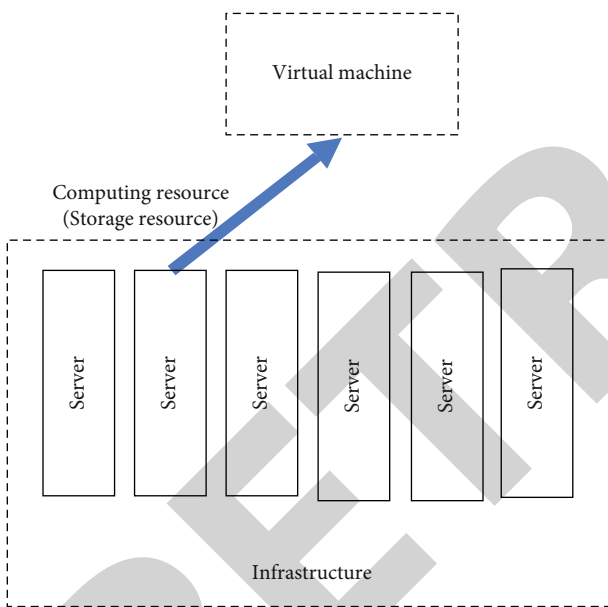


FIGURE 2: Homogeneous architecture.

computing resources and storage resources that are shown in Figure 2 [1]. This homogeneous architecture could effectively solve the problems encountered by the heterogeneous architecture.

Since there is no dedicated storage hardware for high data availability in the heterogeneous architecture, the cloud platform needs to introduce corresponding mechanisms to guarantee the data availability. Realizing high data availability of IaaS cloud platform mainly involves two aspects: one is data backup and the other is to realize the storage resources availability management. The data backup part mainly introduces backup policy management and backup data management. This part is not the focus of this paper. Furthermore, there are two main types of storage resources in the server: solid-state drive (SSD) hard disk and mechanical

hard disk. SSD hard disk could provide higher data reading and writing speed, yet the cost is high, hence it is often used to realize the virtual machine system disk with high performance requirements. The mechanical hard disk, although its data reading and writing speed is relatively low, yet its cost is low, hence the mechanical hard disk is the main way to realize the data storage capacity of IaaS cloud platform. If we can predict the life of mechanical hard disks more accurately and perform operations such as data backup in a timely manner, we can effectively reduce the risk of damage. Existing mechanical hard disks already provide Self-Monitoring Analysis and Reporting Technology (S.M.A.R.T.) that can be used to sensing the operational status of the mechanical hard disk. Furthermore, S.M.A.R.T. provides indicators of the operational status of the various components of the drive, such as heads, platters, motors, and circuits assisting in the prediction of mechanical hard disk status.

Therefore, the key issue to address is how to predict mechanical hard disk life based on S.M.A.R.T. indicators in a timely and accurate manner. In recent years, several researchers have proposed methods for mechanical hard disk failure prediction, mainly divided into mathematics-based methods [2, 3] and machine learning-based failure prediction method [4]. These methods do not adequately consider the problems of removing unnecessary S.M.A.R.T. indicators, small number of failure samples, and making full use of timing data while predicting mechanical hard disk lifetime. In addition to this, some studies [5–7] have focused on assessing the dynamic reliability and fault prediction of the whole system, while we have mainly completed fault prediction for individual component hard disk.

In details, there are three challenges for the fault prediction of hard disks:

- (1) How to filter the S.M.A.R.T. indicators that have the greatest impact on fault warning. The S.M.A.R.T. indicators of mechanical hard disks are the basis for determining faults. Nevertheless, there are also some characteristics that are not relevant to the failure result, excessive characteristics that are useless and may even affect the final analysis result
- (2) How to solve the problem of imbalanced sample size of failures. Statistically, the annual mechanical hard disk damage rate in data centers is around 2%-5%. Therefore, in the sensing data of hard disk operation status, the data related to abnormal status is far less than that related to normal status
- (3) How to make the most of the timing relationships of mechanical hard disk data. Existing warning models for faulty hard disks first use time series data compression to complete feature extraction, and then pass the extracted data into a classifier for classification. This process has the potential to result in the loss of a large number of valuable features

Therefore, the key problem to be solved in mechanical hard disk failure prediction in this paper is how to timely

and accurately predict the service life of mechanical hard disk, so as to actively carry out data backup or migration before mechanical hard disk failure, so as to improve data availability.

To address the above challenges, we first propose the Relief feature selection algorithm to filter indicators and select valuable indicators. And we propose the Generative Adversarial Networks (GAN) model to generate a small number of class samples. Then, we propose the Convolution-Long Short-Term Memory (C-LSTM) to solve the problem of long-term dependence on time-series data and accurately detects faulty hard disk data.

The outline of this paper is listed as follows: Section II Related work reviews and discusses the previous related work; Section III Algorithm presents our algorithm; the experiment setup, results, and analysis are presented in Section IV Experimental results and discussion; in the end, Section V Conclusions makes a conclusion of this paper.

2. Related Work

Mechanical hard disk failure alerts have become increasingly important with the growth of IaaS cloud platforms. The hard disk is one of the most common failed components in today's IT systems, and damage to it can lead to suspension of system services or loss of data. As more and more services run on them, the damage caused by hard disk corruption is increasing every year.

2.1. Anomaly Detection of Mechanical Hard Disks. There are already several methods for detecting anomalies on mechanical hard disks. Yang et al. [8] proposed an evaluation method for comparing feature selection methods and anomaly detection algorithms for predicting hard disks failures. Yu et al. [9] proposed an adaptive error tracking method for hard disks fault prediction. Wang et al. [10] proposed a domain adaptive method to improve fault prediction performance.

With the development of deep learning, combined with its many excellent properties, deep learning is now widely used to solve problems in the prediction domain [11–13]. How to handle time series data needs to be considered when using deep learning methods to accomplish hard disk failure prediction. Several existing studies have been considering how to handle time series data. Hu et al. [14] propose a disk failure prediction system based on a Long Short-Term Memory (LSTM) network. By replacing the input in the LSTM network with the continuous operating records of the disk, the problem of individual variation of the disk can be solved.

2.2. Self-Monitoring Analysis and Reporting Technology (S.M.A.R.T.) Indicators. Self-Monitoring Analysis and Reporting Technology (S.M.A.R.T.) is a monitoring system that collects indicator performance that can be used to infer the actual condition of a hard disk. S.M.A.R.T.-based active fault tolerance uses a threshold approach [15], but traditional S.M.A.R.T.-based fault detection has problems in terms of accuracy [16]. It is no longer sufficient to complete the analysis using S.M.A.R.T. alone. A number of

S.M.A.R.T.-based optimisation methods have been proposed. Li et al. [2] explored the ability of Decision Trees (DTs) [17] and Gradient Boosted Regression Trees (GBRT) [18] to predict hard disk faults based on S.M.A.R.T. indicators, and experimentally demonstrated that both prediction models have high fault detection rates and low false alarm rates. Chaves et al. [3] present a failure prediction method using a Bayesian network. The method calculates the deterioration of hard disks over time using S.M.A.R.T. indicators to predict eventual failures. De Santo et al. [19] propose a model based on LSTM, which combines S.M.A.R.T. indicators and temporal analysis for estimating the health of a hard disk based on its failure time.

Li et al. [20] proposed a combination of XGBoost, LSTM, and ensemble learning algorithms to effectively predict hard disk failures based on S.M.A.R.T. indicators. In conjunction with S.M.A.R.T., Shen et al. [21] propose a hard disk failure prediction model based on LSTM recurrent neural networks and a new method for assessing the degree of health. The model exploits the long-term time-dependent characteristics of hard disk health data to improve prediction efficiency and efficiently stores current health details and deterioration.

In addition to selecting all the attributes of S.M.A.R.T., some studies have also taken the approach of selecting some of the attributes. Wu et al. [4] propose the use of information entropy to optimise S.M.A.R.T. indicators to enable the selection of the most relevant attributes for prediction, combined with a Multichannel Convolutional Neural Network-Based Long Short-Term Memory (MCCNN-LSTM) model to complete the prediction of hard disk failures.

2.3. Sample Imbalance. The above study focuses on the use of S.M.A.R.T. indicators to detect anomalies and health states of hard disks. In addition, hard disks are healthy for most of their life cycle with relatively few failures, which creates a problem of sample imbalance.

GAN-based methods are often used to solve the problem of sample imbalance. Lee and Park [22] proposed a GAN-based fusion detection system for imbalanced data. Xu et al. [23] proposed a convergent Wasserstein GAN to solve the problem of class imbalance in network threat detection. Huang and Lei [24] proposed a novel Imbalanced GAN (IGAN) to deal with the problem of the class imbalance.

In addition to the GAN-based approach, a number of others have proposed solutions to the problem of imbalanced hard disk failure samples. Tomer et al. [25] propose to apply machine learning techniques to accurately and proactively predict hard disk failures. Shi et al. [26] proposed a deep generative transfer learning network (DGTL-Net) that integrates a deep generative sample for generating pseudo-failure network to generate pseudofailure samples and a deep transfer network to solve the problem of hard disk distribution discrepancy, enabling intelligent fault diagnosis of new hard disks. Ircio et al. [27] proposed an optimised classifier to solve the problem of imbalance between hard disk failure and normal hard disk height. Wang G. et al. [28] propose a multi-instance long-term data classification method

based on LSTM and attention mechanism to solve the problem of data imbalance.

3. Algorithm

We present an evaluation method for comparing feature selection methods and anomaly detection algorithms for predicting hard drive failures. It enables the rapid selection of the best algorithm for a particular model of hard disk. It includes an evaluation mechanism for assessing feature selection methods from a performance and robustness perspective and for assessing the performance, robustness, efficiency and generalisability of anomaly detection algorithms.

Hard disk failure prediction needs to deal with three important points, indicator selection, timing compression, and imbalanced sample processing. The overall process is shown in Figure 3.

First, n vectors of characteristic timing parameters are input, and the vector $A_i(a_{i1}, a_{i2}, \dots, a_{it}, \dots, a_{ik})$ is defined as the timing characteristics of parameter i input, and correlation analysis is performed using the correlation with the results, and the parameter with the higher correlation is selected. In the time series feature extraction stage, the current mainstream approach is to use single-value compression for continuous time series data over a period, it can be represented as:

$$S_t = \alpha \cdot Y_t + (1 - \alpha) \cdot S_{t-1}, \quad (1)$$

where S_t is the cumulative data, Y_t is the data of a node, and α is the coefficient.

Nevertheless, these time series feature extractions are often not enough. The main problem is that the previous data is forgotten faster and faster over time, and the sequence of values is not considered, resulting in the data not playing its due role.

On the other hand, the processing of imbalanced samples is relatively rough, often using oversampling of a few categories of data or undersampling of most categories of data. Nevertheless, oversampling of a few categories of data leads to changes in the probability of data features, which appear to have excellent performance in the training set, and decrease in the effect of the test set, resulting in a low recall rate. Using undersampling algorithms, clustering, and other methods to remove part of the samples to achieve sample balance, often resulting in loss of important features, or reduced data sample size, resulting in overfitting problems.

This algorithm is divided into offline model implementation and online data analysis. The detailed algorithm flow is shown in Figure 4.

As shown in Figure 4, this algorithm mainly includes offline model generation and online model detection. In the offline model generation stage, historical data is used for parameter selection, then time series features are extracted, samples are equalized, and finally a discriminant model is generated. In the online detection stage, parameter selection is performed, after time sequence features are extracted,

model detection is performed, and finally the prediction result is generated.

- (1) *Indicator Selection.* Relief feature selection algorithm is used to filter parameters and select valuable indicators
- (2) *Imbalanced Processing.* In view of the few samples of mechanical hard disk damage, the GAN [29] model is used to generate a small number of class samples to achieve a sample balance state model is used to generate a small number of class samples to achieve a sample balance state
- (3) *Model Generation.* Using the processed data set to train the health status of the mechanical hard disk to generate models such as C-LSTM

3.1. Relief-Based Feature Selection Algorithm Parameter Selection. The S.M.A.R.T. [30] indicators gathered by the sensors installed in the mechanical hard disks for sensing the mechanical hard disks' status usually have a fault warning characteristic, which are the basis for determining faults [31]. However, there are also some indicators that are not relevant to the failure result—excessive indicators that are useless and may even affect the final analysis result. When performing a hard disk analysis, it is necessary to consider the various complexities faced by hard disks. For instance, the capacity of a hard disk will gradually increase over time. In addition, the hard disk will slowly deteriorate, although the two are not very relevant as the capacity of a hard disk may be adjusted at any time. Therefore, it is essential to select the indicators to remove interfering features.

To address these issues, we select suitable indicators as model inputs based on the Relief feature selection algorithm [32]. The Relief algorithm focuses on the binary classification problem, which in this paper refers to whether a hard disk has been damaged. We propose the “correlation statistic” to measure the importance of a feature. The correlation statistic is a vector, each component of which is the evaluation of one of the initial features, and the importance of a subset of features is the sum of the correlation statistics for each feature in the subset. For the feature measurement problem, Relief borrows the idea of the hypothetical interval, the maximum distance that the decision surface can move while keeping the sample classification constant, which can be expressed as [33]:

$$\theta = \frac{1}{2} (\|x - M(x)\| - \|x - H(x)\|), \quad (2)$$

where $M(x)$ and $H(x)$ refer to the nearest neighbors that are of the same kind as x and those that are not of the same kind as x , respectively.

We know that when an attribute is favorable for classification, then samples of that kind are closer to that attribute, while samples of the opposite kind are further apart from that attribute.

Suppose the training set D is $(x_1, y_1), (x_2, y_2), \dots, (x_m, y_m)$, for each sample x_i , the nearest neighbour $x_{i,nh}$ of the

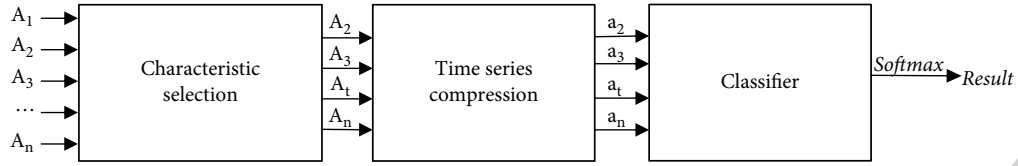


FIGURE 3: Traditional IaaS mechanical hard disk failure early warning algorithm process.

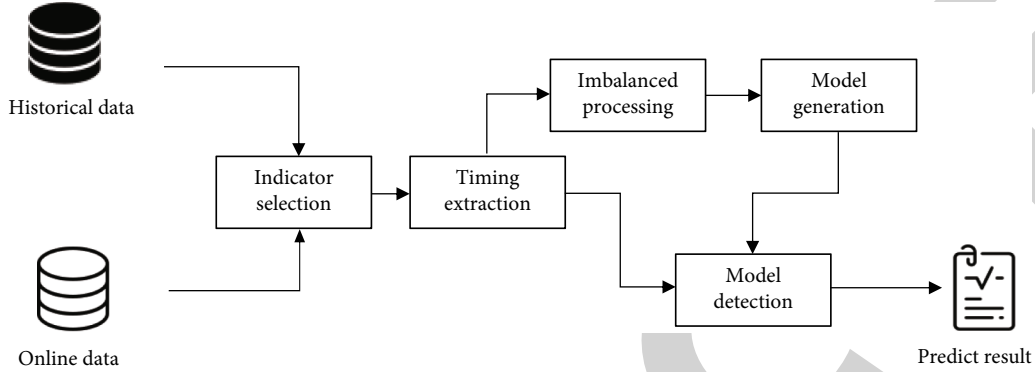


FIGURE 4: Traditional IaaS mechanical hard disk failure early warning algorithm process.

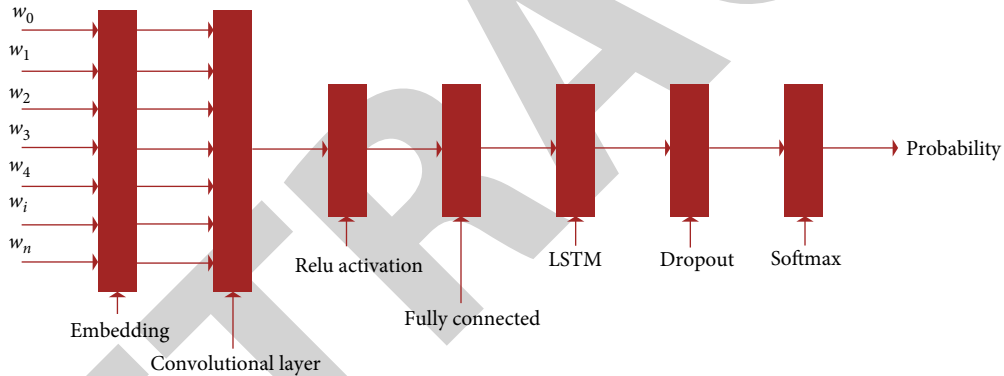


FIGURE 5: The network structure of C-LSTM.

TABLE 1: The key parameters of the neural network used for the experiments.

Name	Meaning	Value
embedding_dim	The dimension of input data	16
seq_length	The length of sequence	60
num_classes	The number of classes	2
keep_prob	The dropout rate	0.5
learning_rate	The learning rate	1e-4
batch_size	The size of batch	256
num_epochs	The number of trainings	5
lstm_size	The LSTM size	3 * 16
lstm_layers	The LSTM layer	2

same category as x_i is calculated, which is called “guessed nearest neighbor” (*near - heat*). Then the nearest neighbor $x_{i,nm}$, which is not the same as x_i , is called the “wrong nearest

neighbor” (*near - miss*), and the relevant statistic for attribute j is [33]:

$$\delta^j = \sum_i -diff(x_i^j, x_{i,nh}^j)^2 + diff(x_i^j, x_{i,nm}^j)^2, \quad (3)$$

where x_i^j represents the value of sample x_i on attribute j . The calculation of $diff(x_a^j, x_b^j)^2$ depends on the type of attribute j .

Discrete attributes:

$$diff(x_a^j, x_b^j) = \begin{cases} 0, & x_a^j = x_b^j \\ 1, & otherwise \end{cases}. \quad (4)$$

Continuous attributes:

$$diff(x_a^j, x_b^j) = |x_a^j - x_b^j|. \quad (5)$$

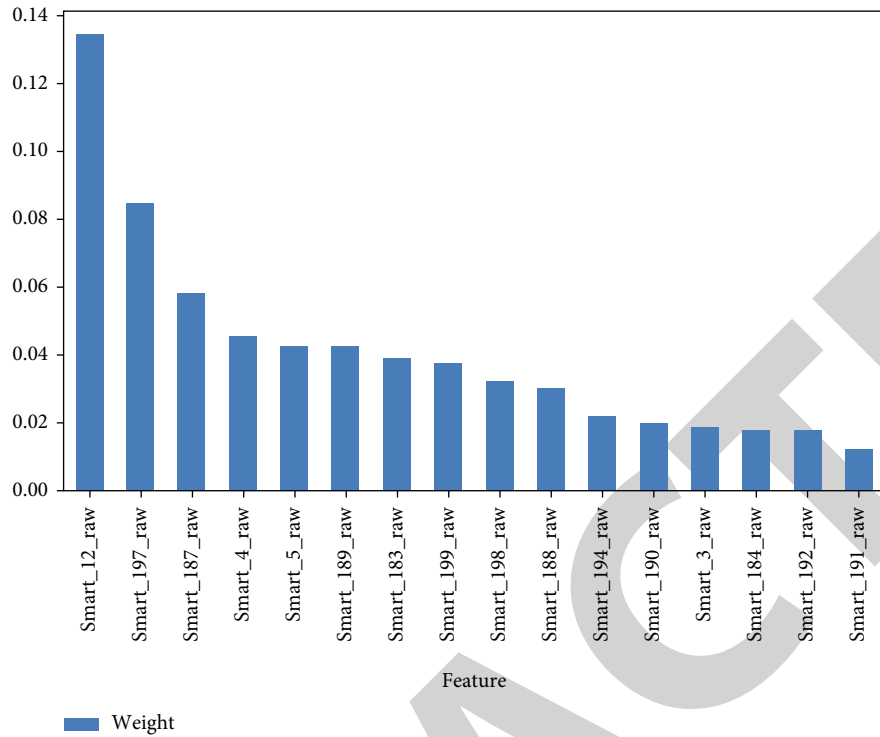


FIGURE 6: Experimental results based on Relief screening algorithm.

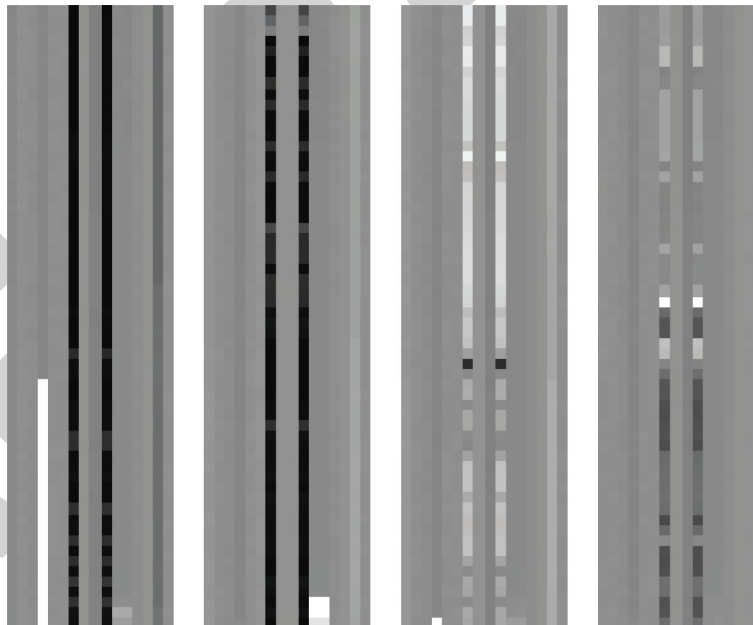


FIGURE 7: WGAN network generates samples.

3.2. GAN-Based Imbalance Data Processing. In the daily operation of an IaaS cloud platform system, the number of failed hard disks is relatively small, while the number of normal samples is always large. Statistically, the annual mechanical hard disk damage rate in data centers is around 2%-5%, and a hard disk is normal for most of the time, which results in the raw positive and negative sample data always being

imbalanced. Using machine learning methods for failure prediction on imbalanced data sets requires either oversampling a smaller number of data categories to achieve data balance or undersampling a larger portion of the data. Conventional oversampling algorithms, however, can lead to changes in the probability of data for a few classes, undersampling leading to loss of important features in most

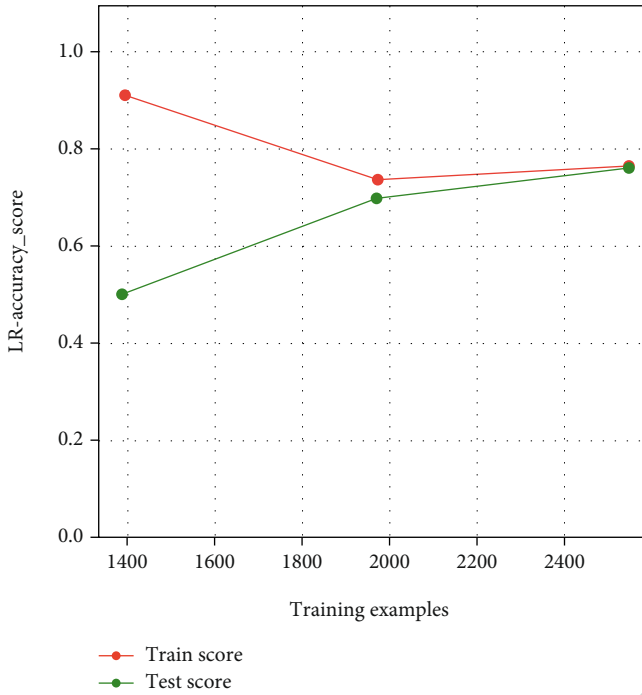


FIGURE 8: Accuracy score of LR.

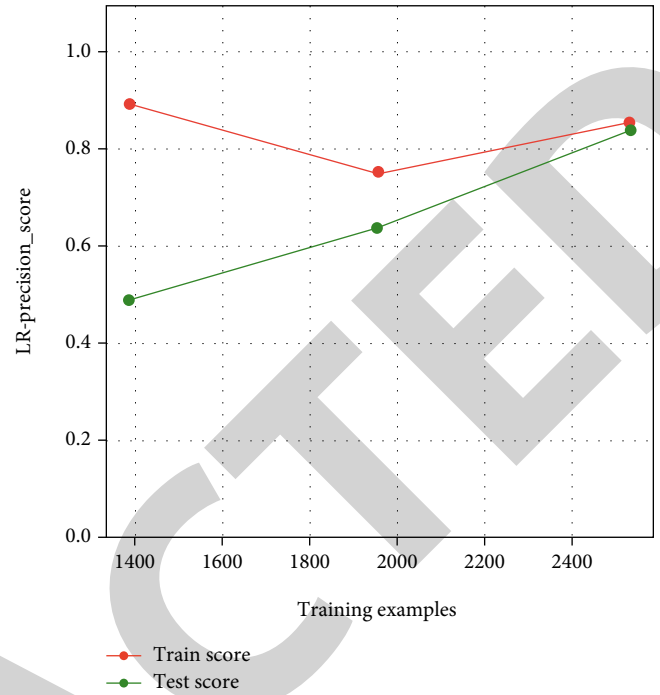


FIGURE 10: Precision score of LR.

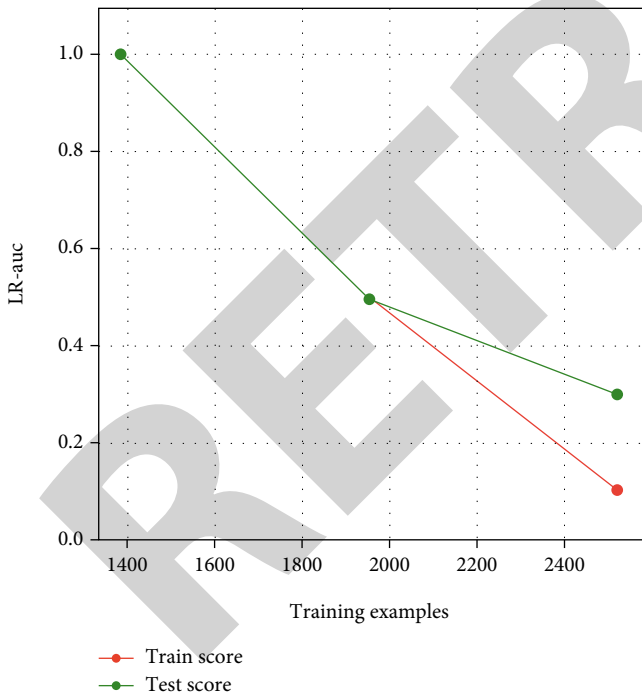


FIGURE 9: AUC of LR.

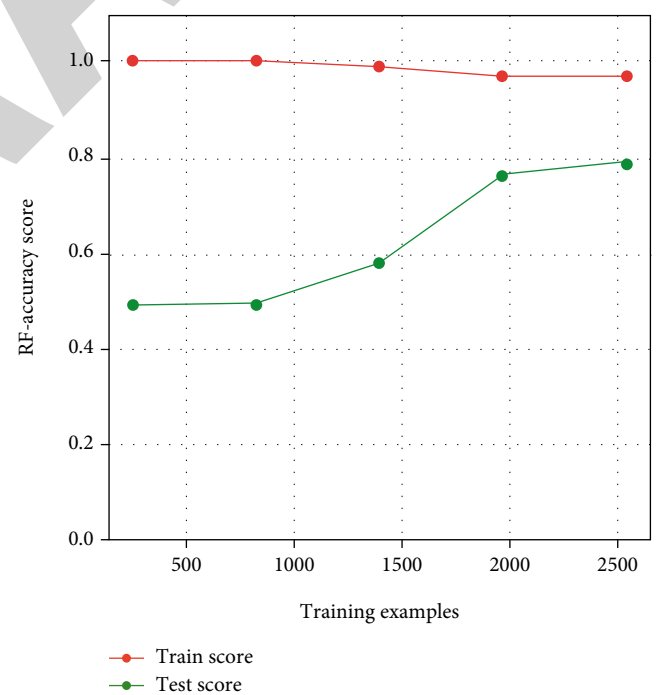


FIGURE 11: Accuracy score of RF.

classes, or overfitting problems due to insufficient training data. Examples include the use of Synthetic Minority Over-sampling Technique (SMOTE) oversampling algorithms [34], which synthesize new samples for a few classes based on interpolation, and the use of clustering algorithms to

implement undersampling and discard some samples to alleviate class imbalance.

Considering the problems of the original algorithm in dealing with imbalanced data, the innovation of this algorithm is to use the zero-sum game idea of GAN to generate less category samples. The GAN continuously plays a game through the generative network G and the discriminative

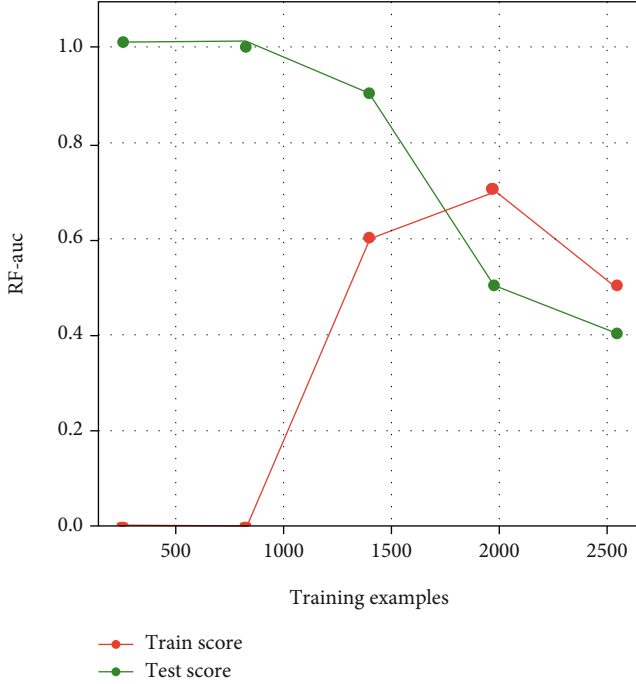


FIGURE 12: AUC of RF.

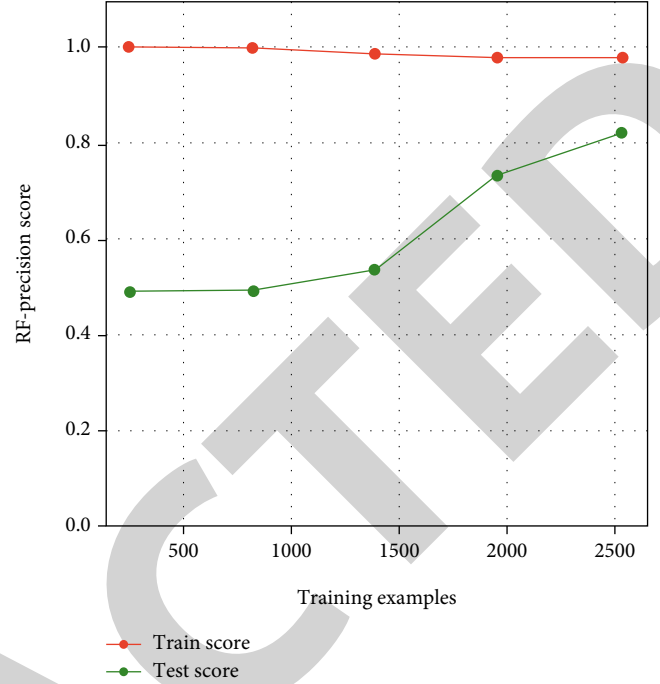


FIGURE 13: Precision score of RF.

network D , which in turn enables G to learn the distribution of the data. Using the GAN method, the generative network G and the discriminative network D are continuously played by using the zero-sum game idea in game theory, which in turn enables G to learn the distribution of the data.

Define the distribution $P_{data}(x)$ of the set of real images, x being a real image. Now it is necessary to generate some pictures that also fall within this distribution. Define the distribution generated by the generator G as $P_G(x; \theta)$, with θ being the distribution parameter. Now, compute the likelihood function in the generative model as [35]:

$$\mathcal{L} = \prod_{i=1}^m P_G(x^i; \theta). \quad (6)$$

To implement the generator G to generate the real picture maximum, the likelihood function needs to be maximized. That is, it is necessary to find a θ^* to maximize the likelihood [36]:

$$\theta^* = \arg \min_{\theta} KL(P_{data}(x) \| P_G(x; \theta)). \quad (7)$$

The generator randomly generates a vector Z and generates a picture X through the generator $G(Z) = X$ network, that is, the generator sample interval. Then the discriminator $D(X) \in [0, 1]$ is used to distinguish the samples generated by the generator from those in the original sample space. And GAN is computed as follows [36]:

$$V(G, D) = E_{x \sim P_{data}}[\log D(x)] + E_{x \sim P_G}[\log(1 - D(x))]. \quad (8)$$

The objective function is as follows [36]:

$$G^* = \arg \min_G \min_D V(G, D). \quad (9)$$

Through k rounds of training, the discriminator can accurately distinguish between the original data and the data generated by the generator G . Next, train the generator so that the generator can confuse the discriminator and make it indistinguishable. Through multiple rounds of training and adjusting the discriminator and generator network results, a better model effect can be achieved. However, the stability of GAN training is not good, and it is difficult to achieve the desired effect in this experiment. By improving GAN, there are currently better algorithms such as Deep Convolutional GAN (DCGAN) [37], Wasserstein GAN (WGAN) [38], and Wasserstein GAN with Gradient Penalty (WGAN-GP) [39].

WGAN uses the Wasserstein distance, which has superior smoothing properties compared to Jense-Shannon (JS) and solves the gradient disappearance problem [23]. In addition, WGAN addresses not only the problem of GAN training instability but also provides a reliable indicator of the training process, and the indicator is highly correlated with the quality of the generated samples. Therefore, we choose WGAN as a method to solve the data imbalance problem.

3.3. Based on LSTM Network Anomaly Detection and Recognition. Our proposed LSTM network-based model solves the problem of long-term dependence on time-series data and accurately detects faulty hard disk data. The traditional faulty hard disk early warning model uses time series data compression to first extract features, and then transfer

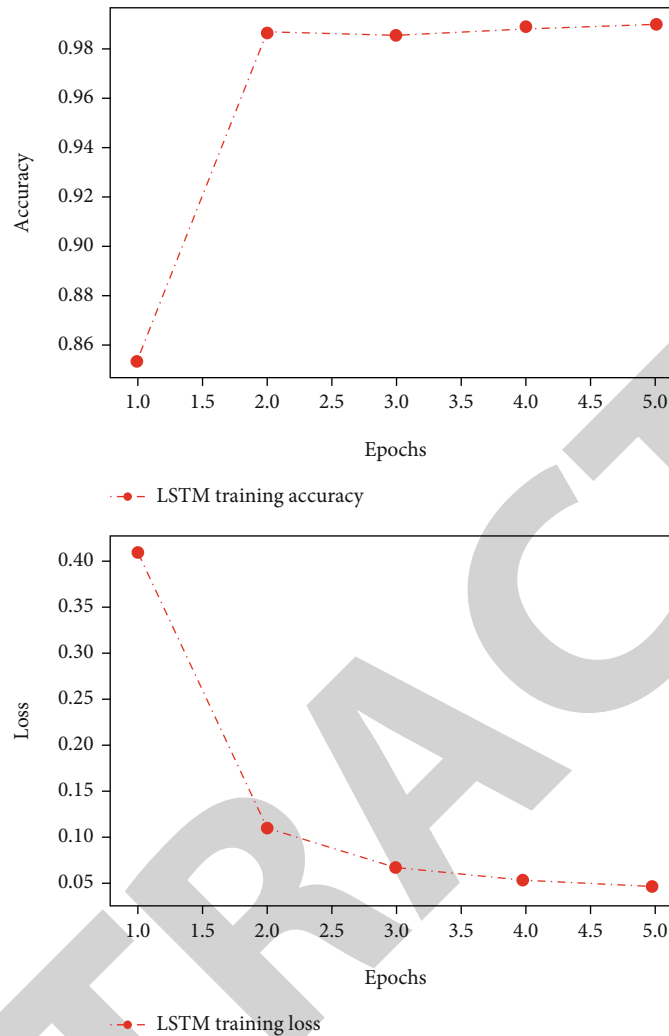


FIGURE 14: Accuracy and loss of LSTM.

the extracted data to the classifier for classification, resulting in the loss of many valuable features. To extract the temporal relationships of mechanical hard disk data, LSTM networks are added to the model training in this paper.

3.3.1. The Improved Network Structure of LSTM. The original LSTM network structure only takes into account the temporal sequence of data in time. Nevertheless, for hard disks, changes in certain parameters will affect the data of other parameters. Compared to the common LSTM structure, this algorithm borrows from the Convolutional LSTM, which means that convolutional computation is added to the input layer, local perception and pooling are introduced, spatial features are added and input to the LSTM structure together with the original data. The structure of C-LSTM is shown in Figure 5.

Considering that this model is a multcategory model, the output should be the probability of each category. The values obtained from the neural network are normalized using the Softmax function, placing the results between [0,1], with larger values corresponding to larger probabilities. The Softmax function category i probability $y_i = P(C_i|$

$x)$ is calculated as follows [40]:

$$y_i = \frac{e^{z_i}}{\sum_{j=1}^n e^{z_j}}, \quad (10)$$

where $C_i : w^i, b_i, z_i = w^i \cdot x + b_i$.

After the Softmax function has processed the results, our model uses cross entropy as the loss function. The loss function formula for Softmax is as follows [41]:

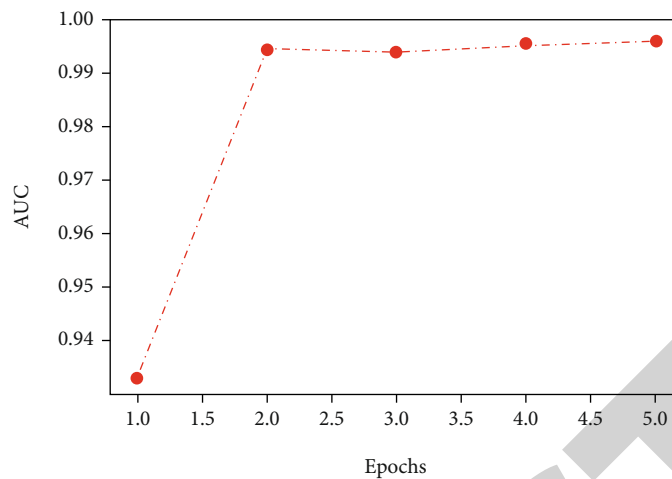
$$L = \sum -\hat{y}_i \ln y_i, \quad (11)$$

where y_i is the probability of category i .

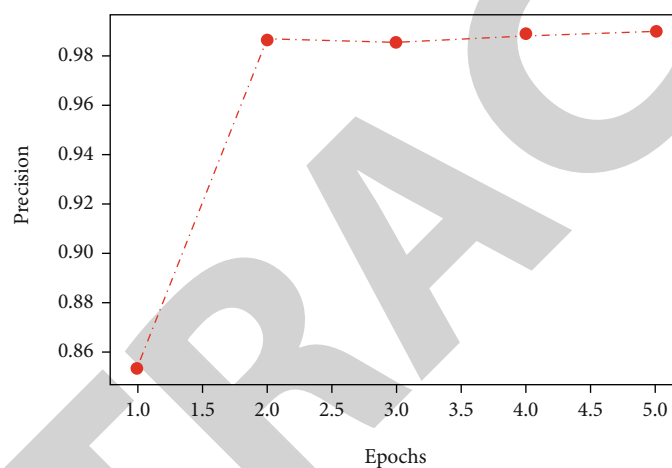
When calculating the loss function, the problem of gradient explosion arises, our model uses clip gradients method [42] to keep the weights within a certain range.

4. Experimental Results and Discussion

To verify the predictive effectiveness of the algorithm, fault warning experiments were conducted on mechanical hard

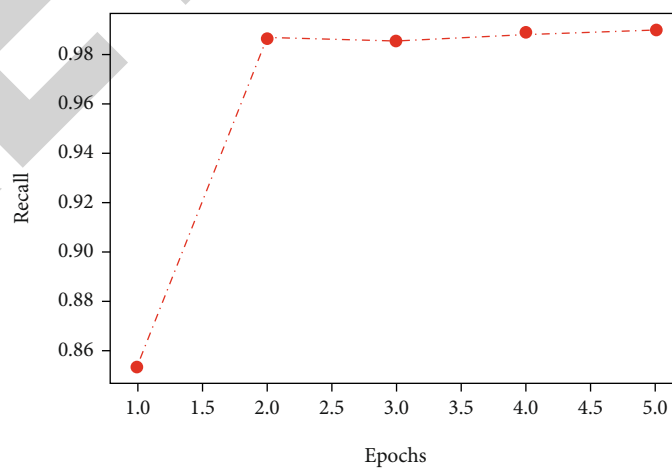


- LSTM training AUC



- LSTM training precision

FIGURE 15: AUC and precision of LSTM.



- LSTM training recall

FIGURE 16: Recall of LSTM.

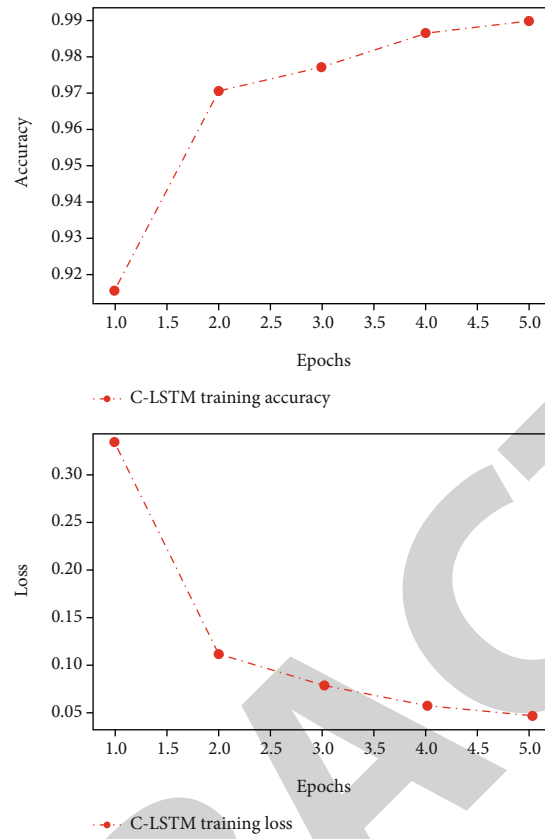


FIGURE 17: Accuracy and loss of C-LSTM.

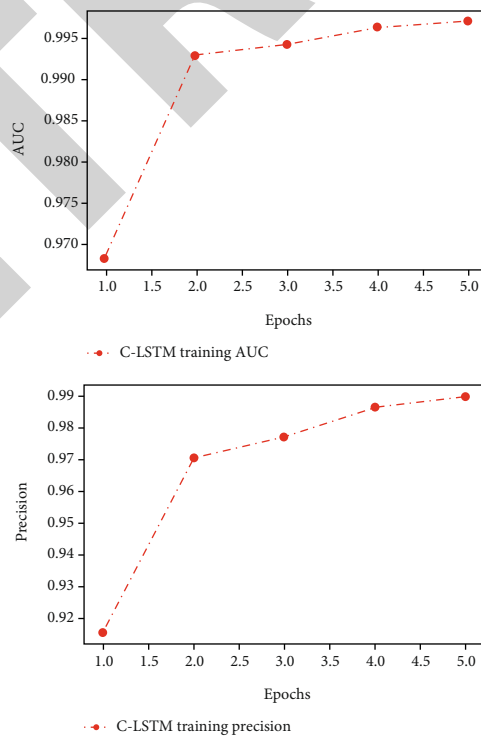


FIGURE 18: AUC and precision of C-LSTM.

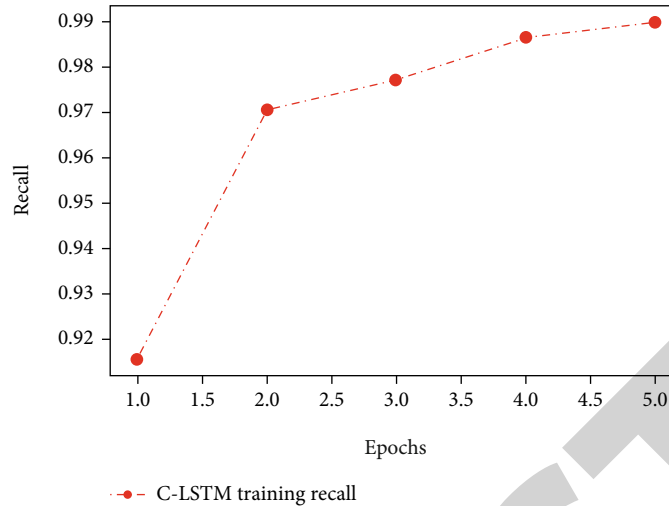


FIGURE 19: Recall of C-LSTM.

disk data from data centers and compared with traditional undersampling-based equalization and binary classification methods (the demo of experiments: <https://github.com/Eva0417/HardDisk>).

4.1. Data Description. The experimental data is from Backblaze, and it consists mainly of data which gathered by sensors from nearly 30,000,000 mechanical hard disks over a 1-year period in 2017 (the dataset: <https://github.com/1210882202/data>). The data is mainly S.M.A.R.T. indicators gathered once a day, with some of the disks not sensing S.M.A.R.T. indicators over time, indicating that the mechanical disk has been damaged. The objective of the experiment was to predict whether the disk would become damaged in the future based on the last sixty days of data for these disks. As mechanical hard disks generally deteriorate slowly as the components age, this experiment assumes that the mechanical hard disk is not damaged within fifteen days and this data is marked as healthy, and if the disk is damaged within fifteen days this data is marked as faulty. Based on the sample data, the experiment hopes to design a fault warning model with excellent performance in terms of accuracy, recall, and Area Under Curve (AUC) value.

4.2. Baseline. To evaluate the performance of C-LSTM against traditional models, traditional classifiers were added to the experiments. Details are as follows:

- (1) *Logistic Regression (LR)* [43]. LR is a supervised learning method often used in anomaly detection. For one variable or multiple independent variables, find the best fitting model to describe the set of independent variables, and complete the anomaly detection in this way
- (2) *Random Forest (RF)* [44]. RF is a common method of anomaly detection by bringing together multiple decision trees. The basic unit is a tree-structured decision tree. With this structure, normal instances can be learned and instances that are not classified as normal are considered as anomalies

4.3. Experimental Setup

4.3.1. The Settings of LSTM

- (1) *Input and Output.* For the input data, the data relevance is first judged using the Relief algorithm to obtain valid 16-dimensional data, and the data sample map is obtained based on the faulty sample generation method. The specific input is a None * Seq * 16-dimensional tensor, and the output is a None * 2-dimensional tensor
- (2) *Network Structure.* The LSTM network used in the experiments uses a network containing two layers of LSTM hidden layers, with a dropout layer added after each hidden layer, followed by a fully connected layer connecting the LSTM and the output, and finally a SoftMax layer
- (3) *Network Parameters.* The key parameters of the neural network used for the experiments were set as shown in Table 1

4.3.2. The Settings of C-LSTM

- (1) *Input and Output Settings.* The input data is the same as the original LSTM
- (2) *Network Structure.* The network used in the experiment adds a layer of Convolutional network after the input layer, which is combined with the original input data and fed into the LSTM hidden layer network

4.4. The Results of Experiment. In applying the Relief screening algorithm, attribute-related statistical components are calculated for the indicators which gathered by sensors in hard disks, the larger the score, the greater the classification power. The statistical components are ranked by size and scaled to take the key indicators needed. First, we analyzed data collected from 26,339 disks over a six-month period

TABLE 2: The analysis results of mechanical hard disk warning experiment.

Algorithm	AUC	Precision	Recall
LR	0.6983	0.9743	0.6058
RF	0.7342	0.9834	0.6253
LSTM	0.7564	0.9878	0.7054
C-LSTM	0.7613	0.9896	0.7103

in the first half of 2017. The results based on the Relief filtering algorithm are shown in Figure 6.

In Figure 6, the horizontal axis represents each dimension number, and the vertical axis represents the relevance of each dimension to the results, taking values in the range [0, 1], with closer to zero indicating less relevance to the results. Based on the results of the statistical components obtained in Figure 6, the parameters whose results are greater than the threshold are selected, and the final hard disk correlation is obtained.

According to the above analysis, we use the WGAN network to conduct experiments, and the sample generation is shown in Figure 7.

The horizontal axis of Figure 7 represents each indicator gathered by sensors of the mechanical hard disk, and the vertical axis represents time. Darker colors in Figure 7 represent lower indicator values, and lighter colors represent higher indicator values. As can be seen from Figure 7, the WGAN network uses the principles of game theory to generate samples that are relatively similar and can simulate a large amount of information, while at the same time differing from direct replication. The experimental results show that the use of WGAN for feature extraction and regeneration of the overall fault sample solves the problem of sample imbalance and expands the fault sample.

In addition to experimenting on our proposed C-LSTM model, we have also experimented on the comparison algorithms.

According to the specific experimental setup, the results of this experiment for the comparison model of LR are as shown in Figures 8–10. In these figures, we use different color to show the different scores of LR.

According to the specific experimental setup, the results of this experiment for the comparison model of RF are as shown in Figures 11–13. In these figures, we also use different color to show the different scores of RF.

According to the specific experimental setup, the results of this experiment for training the network model of LSTM are as shown in Figures 14–16.

The horizontal axis of graphs in Figures 14–16 represents the number of training epochs, the vertical axis of the first graph in Figure 14 represents the accuracy rate during training, and the vertical axis of the second graph represents the training loss data. According to the graphs in Figure 14, we can see that after 3 epochs, the training gradually leveled off (in this paper, we define that a loss reduction of no more than 0.1 after 1 epochs is considered smooth), where the loss converged at around 0.05. Based on the Figures 15 and 16, we can see that the accuracy of training is around 0.91.

The results of this experiment on the training of the C-LSTM network model are shown in Figures 17–19.

The horizontal axis of graphs in Figures 17–19 represents the number of training epochs, the first graph's vertical axis represents the accuracy rate during training in Figure 17, and the second graph's vertical axis represents the training loss data. After 4.0 epochs, the training gradually leveled off, with the loss converging at around 0.05 and the accuracy at training at around 0.93.

Comparing the training results of the LSTM in Figures 14–16 with the C-LSTM network model in Figures 17–19, we can conclude that the C-LSTM has a faster convergence speed, lower loss drop, and higher accuracy. Therefore, from a training perspective, the C-LSTM performs better.

The individual classification models were evaluated according to precision, recall and AUC value, and the results are shown in Table 2. In terms of each metric, the C-LSTM model has the best result.

5. Conclusions

Firstly, the mechanical hard disk is installed with sensors for sensing the status of the mechanical hard disk and the S.M.A.R.T. indicators gathered by these sensors on the operational status of the various components of the disk can be used to predict the life of the mechanical hard disk. Based on this, we focus on how to accurately predict mechanical hard disk failure and achieve effective improvement of data availability in the IaaS cloud platform.

The model proposed in this paper includes three parts: Relief feature selection algorithm, WGAN, and LSTM models. To remove features from the S.M.A.R.T. indicators of mechanical hard disks that are irrelevant to the failure results, we use the Relief feature selection algorithm to remove interfering features and complete the parameter screening. As the number of failed hard disks is small in the IaaS cloud platform system, we use the zero-sum game idea of WGAN to generate fewer category samples to solve the sample data imbalance problem. Finally, we use the improved C-LSTM model to complete hard disk failure detection and early warning.

Through extensive experiments, we constructed our own model and evaluated the model we designed and other methods using precision, recall, and AUC value. The experiments demonstrate that our proposed algorithm outperforms other algorithms for mechanical hard disk warning.

As our future work, we aim to extend our approach to SSD-based IaaS cloud platforms. In our proposed approach, we mainly implement mechanical hard disk S.M.A.R.T.-based fault warning through WGAN and LSTM to achieve effective improvement of data availability in IaaS cloud platforms. However, as more and more IaaS cloud platform systems gradually adopt SSD to pursue significant performance improvement. Based on this, how to better realize the automation of repair in SSD-based IaaS cloud platform and study the automatic adaptation of parameters are our future goals to achieve.

Data Availability

All data, models, and code generated or used during the study appear in the submitted article.

Conflicts of Interest

The authors declare that they have no conflicts of interests.

Acknowledgments

This work is supported by Science and Technology Project from State Grid Information and Telecommunication Branch of China: Research on Key Technologies of Operation Oriented Cloud Network Integration Platform (52993920002P).

References

- [1] S. Bhaumik, R. Bansal, R. Karmakar et al., "Netstor: Network and storage traffic management for ensuring application qos in a hyperconverged data-center," *IEEE Transactions on Cloud Computing*, vol. 10, no. 2, 2020.
- [2] J. Li, R. J. Stones, G. Wang, X. Liu, Z. Li, and M. Xu, "Hard drive failure prediction using decision trees," *Reliability Engineering and System Safety*, vol. 164, pp. 55–65, 2017.
- [3] I. C. Chaves, M. Paula, L. Leite, L. P. Queiroz, and J. C. Machado, "Banhfap: a Bayesian network based failure prediction approach for hard disk drives," in *2016 5th Brazilian Conference on Intelligent Systems (BRACIS)*, pp. 427–432, Recife, Brazil, 2017.
- [4] J. Wu, H. Yu, Z. Yang, and R. Yin, "Disk failure prediction with multiple channel convolutional neural network," in *2021 International Joint Conference on Neural Networks (IJCNN)*, pp. 1–8, Shenzhen, China, 2021.
- [5] J. Lie and E. Zio, "System dynamic reliability assessment and failure prognostics," *Reliability Engineering and System Safety*, vol. 160, pp. 21–36, 2017.
- [6] H. Khorasgani, G. Biswas, and S. Sankararaman, "Methodologies for system-level remaining useful life prediction," *Reliability Engineering and System Safety*, vol. 154, pp. 8–18, 2016.
- [7] K. L. Son, M. Fouladirad, and A. Barros, "Remaining useful lifetime estimation and noisy gamma deterioration process," *Reliability Engineering and System Safety*, vol. 149, pp. 76–87, 2016.
- [8] Q. Yang, X. Jia, X. Li, J. Feng, W. Li, and J. Lee, "Evaluating feature selection and anomaly detection methods of hard drive failure prediction," *IEEE Transactions on Reliability*, vol. 70, no. 2, pp. 749–760, 2021.
- [9] W. Yu, H. Long, J. Shan, and T. W. Chow, "Failure prediction of hard disk drives based on adaptive rao–blackwellized particle filter error tracking method," *IEEE Transactions on Industrial Informatics*, vol. 17, no. 2, pp. 913–921, 2021.
- [10] J. Wang, R. Zhang, G. Qi, and L. Hong, "A heuristicIRM method on hard disk failure prediction in out-of-distribution environments," in *2021 IEEE International Conference on Industrial Engineering and Engineering Management (IEEM)*, pp. 1661–1664, Singapore, Singapore, 2021.
- [11] W. Jiang, "Applications of deep learning in stock market prediction: recent progress," *Expert Systems with Applications*, vol. 184, article 115537, 2021.
- [12] A. Appelt, B. Elhaminia, A. Gooya, A. Gilbert, and M. Nix, "Deep learning for radiotherapy outcome prediction using dose data – a review," *Clinical Oncology*, vol. 34, no. 2, pp. e87–e96, 2021.
- [13] J. R. Jiang, J. E. Lee, and Y. M. Zeng, "Time series multiple channel convolutional neural network with attention-based long short-term memory for predicting bearing remaining useful life," *Sensors (Basel, Switzerland)*, vol. 20, no. 1, 2020.
- [14] L. Hu, L. Han, Z. Xu, T. Jiang, and H. Qi, "A disk failure prediction method based on LSTM network due to its individual specificity," *Procedia Computer Science*, vol. 176, pp. 791–799, 2020.
- [15] H. Wang and H. Zhang, "AIOPS prediction for hard drive failures based on stacking ensemble model," in *2020 10th Annual Computing and Communication Workshop and Conference (CCWC)*, pp. 0417–0423, Las Vegas, NV, USA, 2020.
- [16] J. Zhao, Y. He, H. Liu et al., "Disk failure early warning based on the characteristics of customized smart," in *2020 19th IEEE Intersociety Conference on Thermal and Thermomechanical Phenomena in Electronic Systems (ITherm)*, pp. 1282–1288, Orlando, FL, USA, 2020.
- [17] J. Guo, H. Wang, X. Li, and L. Zhang, "Stream classification algorithm based on decision tree," *Mobile Information Systems*, vol. 2021, Article ID 3103053, 11 pages, 2021.
- [18] J. H. Friedman, "Greedy function approximation: a gradient boosting machine," *Annals of Statistics*, vol. 29, no. 5, pp. 1189–1232, 2001.
- [19] A. De Santo, A. Galli, M. Gravina, V. Moscato, and G. Sperli, "Deep learning for HDD health assessment: an application based on LSTM," *IEEE Transactions on Computers*, vol. 71, no. 1, pp. 69–80, 2022.
- [20] Q. Li, H. Li, and K. Zhang, "Prediction of HDD failures by ensemble learning," in *2019 IEEE 10th International Conference on Software Engineering and Service Science (ICSESS)*, pp. 237–240, Beijing, China, 2019.
- [21] J. Shen, Y. Ren, J. Wan, and Y. Lan, "Hard disk drive failure prediction for mobile edge computing based on an LSTM recurrent neural network," *Mobile Information Systems*, vol. 2021, Article ID 8878364, 12 pages, 2021.
- [22] J. H. Lee and K. H. Park, "Gan-based imbalanced data intrusion detection system," *Personal and Ubiquitous Computing*, vol. 25, no. 1, pp. 121–128, 2019.
- [23] Y. Xu, X. Zhang, Z. Qiu, X. Zhang, J. Qiu, and Z. Hua, "Oversampling imbalanced data based on convergent WGAN for network threat detection," *Security and Communication Networks*, vol. 2021, Article ID 9206440, 19 pages, 2021.
- [24] S. Huang and K. Lei, "IGAN-IDS: an imbalanced generative adversarial network towards intrusion detection system in ad-hoc networks," *Ad Hoc Networks*, vol. 105, article 102177, 2020.
- [25] V. Tomer, V. Sharma, S. Gupta, and D. P. Singh, "Hard disk drive failure prediction using smart attribute," *Materials Today: Proceedings*, vol. 46, pp. 11258–11262, 2021.
- [26] C. Shi, Z. Wu, X. Lv, and Y. Ji, "DGTL-Net: a deep generative transfer learning network for fault diagnostics on new hard disks," *Expert Systems with Applications*, vol. 169, no. 16, article 114379, 2020.
- [27] J. Ircio, A. Lojo, J. A. Lozano, U. Mori, and J. A. Lozano, "A multivariate time series streaming classifier for predicting hard drive failures [application notes]," *IEEE Computational Intelligence Magazine*, vol. 17, no. 1, pp. 102–114, 2022.

Retraction

Retracted: Information Extraction and Data Planning of Smart City Based on Internet of Things

Journal of Sensors

Received 17 October 2023; Accepted 17 October 2023; Published 18 October 2023

Copyright © 2023 Journal of Sensors. This is an open access article distributed under the Creative Commons Attribution License, which permits unrestricted use, distribution, and reproduction in any medium, provided the original work is properly cited.

This article has been retracted by Hindawi following an investigation undertaken by the publisher [1]. This investigation has uncovered evidence of one or more of the following indicators of systematic manipulation of the publication process:

- (1) Discrepancies in scope
- (2) Discrepancies in the description of the research reported
- (3) Discrepancies between the availability of data and the research described
- (4) Inappropriate citations
- (5) Incoherent, meaningless and/or irrelevant content included in the article
- (6) Peer-review manipulation

The presence of these indicators undermines our confidence in the integrity of the article's content and we cannot, therefore, vouch for its reliability. Please note that this notice is intended solely to alert readers that the content of this article is unreliable. We have not investigated whether authors were aware of or involved in the systematic manipulation of the publication process.

Wiley and Hindawi regrets that the usual quality checks did not identify these issues before publication and have since put additional measures in place to safeguard research integrity.

We wish to credit our own Research Integrity and Research Publishing teams and anonymous and named external researchers and research integrity experts for contributing to this investigation.

The corresponding author, as the representative of all authors, has been given the opportunity to register their agreement or disagreement to this retraction. We have kept a record of any response received.

References

- [1] Z. Farisi, "Information Extraction and Data Planning of Smart City Based on Internet of Things," *Journal of Sensors*, vol. 2022, Article ID 2893702, 8 pages, 2022.

Research Article

Information Extraction and Data Planning of Smart City Based on Internet of Things

Zeyad Farisi 

Applied College, Tabah University, Medina City, Saudi Arabia

Correspondence should be addressed to Zeyad Farisi; z17301065@stu.ahu.edu.cn

Received 19 August 2022; Revised 9 September 2022; Accepted 19 September 2022; Published 30 September 2022

Academic Editor: C. Venkatesan

Copyright © 2022 Zeyad Farisi. This is an open access article distributed under the Creative Commons Attribution License, which permits unrestricted use, distribution, and reproduction in any medium, provided the original work is properly cited.

In order to solve the problem of slow resource scheduling in the process of smart city management, the author proposes a smart city information extraction and data planning system based on the Internet of Things. IoT requires different technologies for analysis for different data types. Managers use different IoT applications to analyze data from different devices and integrate relevant data for possible machine failure or emergency in smart home applications. Situation is predicted. The system includes a cloud platform intelligence center, uses the cloud management module to monitor various hardware devices, constructs the cloud computing resource scheduling objective function, uses the cultural particle swarm algorithm to solve the objective function, and obtains the cloud computing resource scheduling scheme. The experimental results show that the overall utilization rate of the system is the best, close to 100%. *Conclusion.* The system can realize the effective management of the smart city and monitor the city situation in real time. When implementing resource scheduling, the task completion time is short, the system utilization rate is high, and the resources can be maximized.

1. Introduction

In the current process of social competition, the importance of science and technology is becoming more and more obvious, and all walks of life need to develop and use new technologies, only in this way can they occupy their own position in the market. Big data is a product that emerged in the process of modern high-tech development and has strong market potential, and through relevant practical analysis, it is found that big data can play an important role in the process of urban planning. First, the government can use big data technology to understand and master the problems that arise in the process of urban spatial planning, make timely decisions, and deal with these problems [1]. Secondly, in the traditional model, the information channel is single, and the accuracy of the data obtained is limited, which can no longer match the requirements of modern urban planning; the application of big data technology can quickly expand the information and sources of urban and rural planning data. Third, the current speed of informatization is further accelerated, and the usage of the Internet is further increased, which provides great convenience for the realization of big data [2].

In the process of building a smart city, it is necessary to use the Internet of Things technology to connect with each terminal, and then realize the collection and application of data, and then it can be applied to actual production and life to realize intelligent construction [3]. In the actual process of building a smart city, terminal equipment needs to be installed in many scenarios for information collection and access, but due to the restrictions and influence of the actual environment, it is impossible to connect to external power. These results in that the power supply cannot be connected during the use of the terminal device, and only external batteries can be used for power supply, which makes the application of the terminal have power consumption problems. If the device consumes a lot of power, the battery needs to be replaced frequently, which seriously affects the effective performance of the IoT function and increases the workload of the relevant personnel [4].

Smart city refers to the full use of information technology in the process of continuous construction of the city and can be applied in various fields of social development. This is also the advanced stage of smart urbanization construction, which can not only promote a better urban

environment, at the same time, based on technologies such as cloud computing and big data, it has a certain positive significance for smart city construction, environmental protection, security protection, and other services and can respond accurately and quickly, making urbanization construction more sensitive and complete, make people's life more convenient and fast, provide people with a better living environment, and then improve the humanization and intelligence of urban construction [5]. Therefore, people's thoughts will not be limited by region and time, and the distance between urban residents will be shortened [6]. Especially under the background that the basic functions of my country's cities are becoming more and more perfect, the application of the Internet of Things can ensure the information interaction of various building equipment in the city, that is, the "Internet of Everything" in the smart city [7]. At the same time, the application of Internet of Things technology is also an important part of urban development, it can not only realize the informatization of the whole city but also achieve precise control; the relationship between the two should rely on and promote each other, specifically, it includes ecological construction, engineering construction, people's livelihood construction, road construction, public safety, logistics and transportation, and mature medical treatment through intelligent response to optimize and improve service quality, so as to meet the actual needs of our people [8].

2. Literature Review

With the continuous development of information technology, the current production and life of people are inseparable from the Internet and information technology, under this situation; people have higher requirements for the quality of the Internet and communication services [9]. At the same time, in the process of building a smart city, the number of various information collection, terminals, and smart devices used in production and life is increasing, which puts forward higher requirements for the capacity and communication quality of urban networks [10]. Therefore, in order to ensure the construction effect of smart city, in the process of practical application of IoT technology, the problem of network capacity must be solved. At present, the 5G network that China is gradually promoting and applying is an important preparation for building a smart city [11]. The comparative analysis of 5G network and 4G network is shown in Table 1.

The construction of a smart city requires the Internet of Things technology to cover a wider range as much as possible, so as to ensure a more comprehensive collection of data and information, so that the data resources in the city can be fully utilized, only in this way can the level of urban intelligence be further improved, so as to provide better services for the production and life in the city [12]. Therefore, in the process of smart city construction, it is necessary to expand the coverage of IoT technology as much as possible, however, in terms of the current technical level of various aspects in China, the promotion and application of Internet of Things technology will still be limited [13].

China's urbanization process is accelerating, and a series of social problems such as urban environment pollution, lack of public resources, lack of public safety management, rapid urban population growth, and public traffic congestion have seriously affected the normal life of urban residents [14]. Many cities focus on building smart cities and establish smart city management systems and related platforms, smart city management systems have become the focus of relevant research under the needs of the social environment [15]. Cloud computing is a product of the highly developed network information technology, all available resources are shared in the form of "cloud", and users can apply to the "cloud" to provide required services and resources through the network [16]. The resources in the cloud computing platform are heterogeneous and dynamic, when scheduling and resource allocation of large-scale data tasks, the completion time and throughput of the applied system need to be considered, and the load balancing of system resources needs to be considered, therefore, the research on resource scheduling of cloud computing platform is also a difficult problem in the current research community [17]. Taking the cloud computing platform as the basis, the smart city management system is designed to meet the development requirements of the modern city process [18].

3. Methods

3.1. Smart City Management System Based on Cloud Computing Platform

3.1.1. The Overall Structure of the System. Considering the overall positioning and management principles of the system, the business functions of the smart city system are analyzed, and the overall structure of the smart city management system based on the cloud computing platform is constructed. The results are shown in Figure 1.

The basic layer of the system is the IaaS (Basic Knowledge as a Service) resource layer, and the main construction content is the PaaS (Platform as a Service) platform layer. This layer mainly implements system management functions, and the cloud management module and business management module are designed to realize system operation and maintenance and business operation [19].

- (1) The hardware resource used in the IaaS layer is a unified resource, and its main function is to provide services to the PaaS platform layer. The IaaS layer consists of network resource pools, storage resource pools, computing resource pools, and security resource pools, which are composed of security devices, storage, networks, and servers [20]. This layer provides basic equipment resources to the SaaS layer and PaaS of the system. This layer is also responsible for the management and healthy operation of each resource pool and physical devices and allocates and controls the capacity of various resource pools
- (2) The PaaS layer provides standardized shared cloud services to each application. This layer includes business operation and application incubation

TABLE 1: Comparative analysis of 5G network and 4G network.

Network	4G	5G
Delay	10 ms	Less than 1 ms
Peak data rate	1 Gbps	20 Gbps
Number of mobile connections	8 billion (2016)	11 billion (2021)
Channel broadband	20 MHz 2200kHz(applies to Cat-NBI IoT)	100 MHz (below 6GHz) 400 MHz (above 6GHz)
Frequency band	600 MHz-5.925 GHz	600 MHz-mmWave
User terminal (UE) transmit power	+23 dBm (+26 dBm in n41 band)	+26 dBm for 2.5 GHz and above (in Sub6G band)

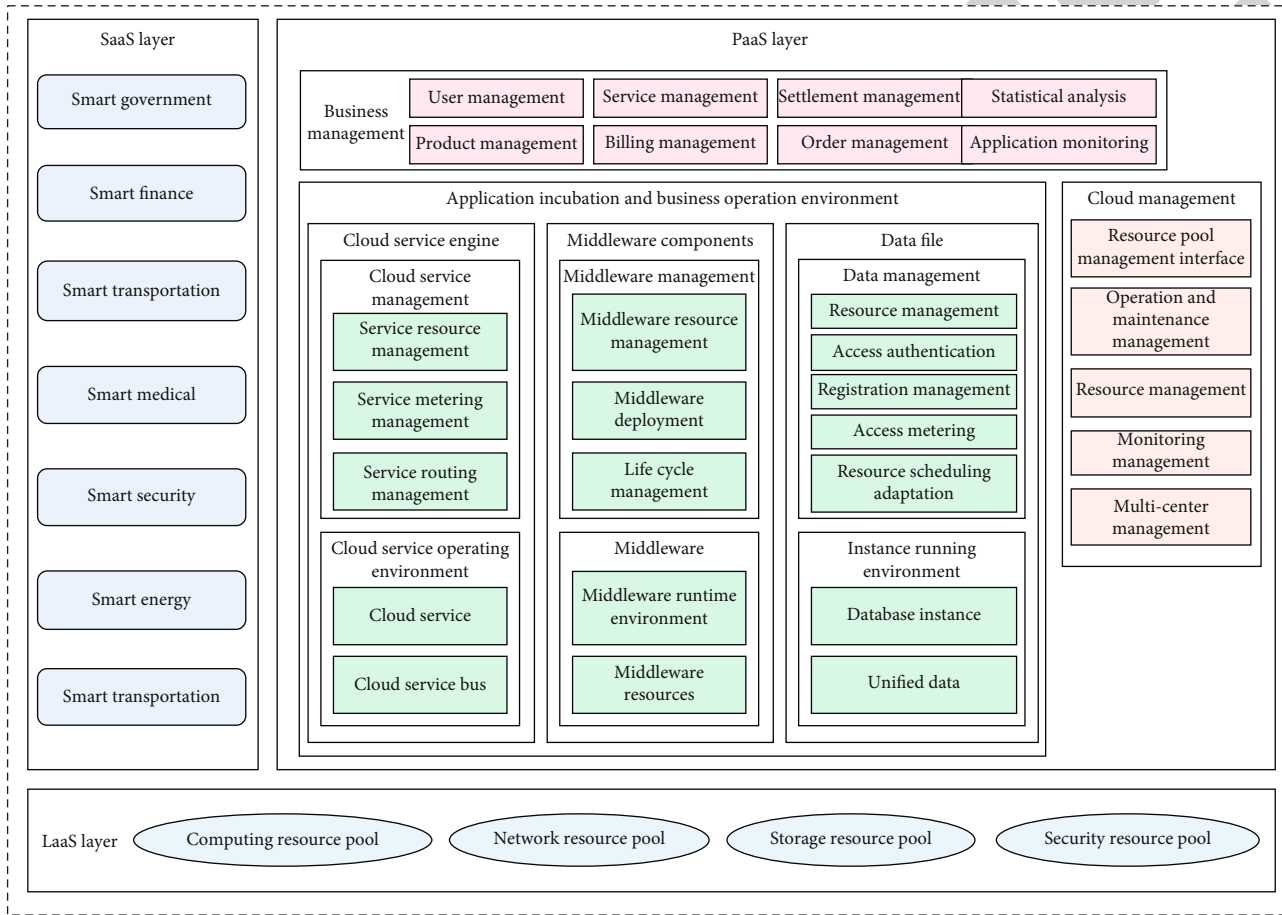


FIGURE 1: Overall structure of the system.

environment, and the three functional components are cloud service engine component, middleware component, and data component. The main functions of the cloud service engine component are scheduling and management of service measurement, service resources, service monitoring, service routing, service authentication, etc.; the middleware component is responsible for the dynamic sharing and unified management of resources; the data component completes the dynamic sharing of resources and unified management of the database. The cloud management module in this layer provides management services for the cloud management operation in the entire smart city management system and

realizes the management of submodules such as resource management; the business management module provides management services for the cloud platform business operation in the entire smart city management system and realizes the normal operation of submodules such as service management

- (3) In the SaaS (software as a service) layer, applications are deployed in detail according to the seven major areas of smart cities, mainly including national direct management applications and provincial and municipal applications; the division is based on industry division and geographical division. The way to present the application is through the cloud platform [21]



FIGURE 2: Monitoring and management submodule structure.

Monitor management submodule

- Video output function
- Electronic map display function
- Monitor the network control assignment function
- Video monitoring function
- Video surveillance function
- Video management

3.1.2. *Design of Monitoring and Management Module.* In the entire smart city management system, it is necessary to monitor the city's situation. In the cloud platform management module, the monitoring and management submodule plays an important role, the structure diagram of this submodule is shown in Figure 2. The monitoring and management submodule is mainly composed of six functions. A complete monitoring and management submodule requires audio and video acquisition equipment, transmission medium equipment, control equipment, and terminal monitoring and monitoring equipment. They are installed in the camera and jointly realize the six functions of the monitoring and control submodule. Real-time monitoring is achieved by arranging surveillance cameras in all directions in the city.

3.2. Cloud Computing Resource Scheduling Strategy

3.2.1. *Scheduling Principle.* Under the cloud computing platform, the relationship between computing resources and tasks is not one-to-one, but resources are mapped by tasks first and related physical devices are mapped to resources. Currently, the most commonly used programming model for cloud computing platforms is Map/Reduce proposed by Google. A quintuple is used to describe the resource scheduling model of cloud computing.

$$S = \{T, V, D, M_{TV}, M_{VD}\}. \quad (1)$$

In the formula, $V = \{v_1, v_2, \dots, v_m\}$, $D = \{d_1, d_2, \dots, d_m\}$, and $T = \{t_1, t_2, \dots, t_m\}$ represent the resource set, the physical device set, and the task set, respectively, and M_{VD} and M_{TV} , respectively, represent the correspondence between physical devices and resources and the mapping strategy between resources and tasks.

According to the user task computing center, the M_{TV} is allocated, and the resource utilization scheduler is scheduled to the corresponding physical device to realize the M_{VD} , therefore, resource scheduling is to realize the scheduling of resources to physical devices. Suppose that after M_{VD} mapping, a certain task t_i is mapped to the resource v_j , and the physical device d_k receives the task assigned by the resource v_j and executes it. According to the corresponding relationship between the task and the resource, after resource transfer,

the expected execution time of task t_i arriving on device d_k is expressed by $ETC(t_i, d_k)$, therefore, the entire distribution matrix of D subject to T is uniformly called the ETC matrix.

$$\begin{cases} ETC_{mn} = ETC(t_i M_{TV}, d_k), \\ 1 \leq i \leq m, 1 \leq k \leq n. \end{cases} \quad (2)$$

The essence of equation (2) is the execution time matrix, the main content is that on n physical devices, and the execution time matrix of m tasks after resource mapping $t_i M_{TV}$. The earliest completion time of task t_i on material equipment d_k is expressed by

$$\text{Finish}(t_i M_{TV}, d_k) = \text{Start}(d_k) + ETC(t_i M_{TV}, d_k). \quad (3)$$

In the formula, the earliest execution start time of physical device d_k is represented by $\text{Start}(d_k)$, which represents the total time spent by the physical device d_k to achieve task allocation and execution

$$\begin{cases} \text{Sum}(d_k) = \sum_{i=1}^m c_{ik} \text{Finish}(t_i M_{TV}, d_k), \\ c_{ik} = \begin{cases} 1 & t_i M_{TV} = d_k, \\ 0 & t_i M_{TV} \neq d_k. \end{cases} \end{cases} \quad (4)$$

In the formula, the representative physical device d_k is finally mapped and executed by the task t_i . The total execution time of all tasks $T = \{t_1, t_2, \dots, t_m\}$ is expressed by

$$\text{total}(T) = \sum_{k=1}^n \text{Sum}(d_k). \quad (5)$$

The ultimate goal of cloud computing resource scheduling is to ensure that equation (5) is a minimum value, and equation (6) is the objective function of cloud computing resource scheduling.

$$\text{Goal}(T) = \min \sum_{k=1}^n \text{Sum}(d_k). \quad (6)$$

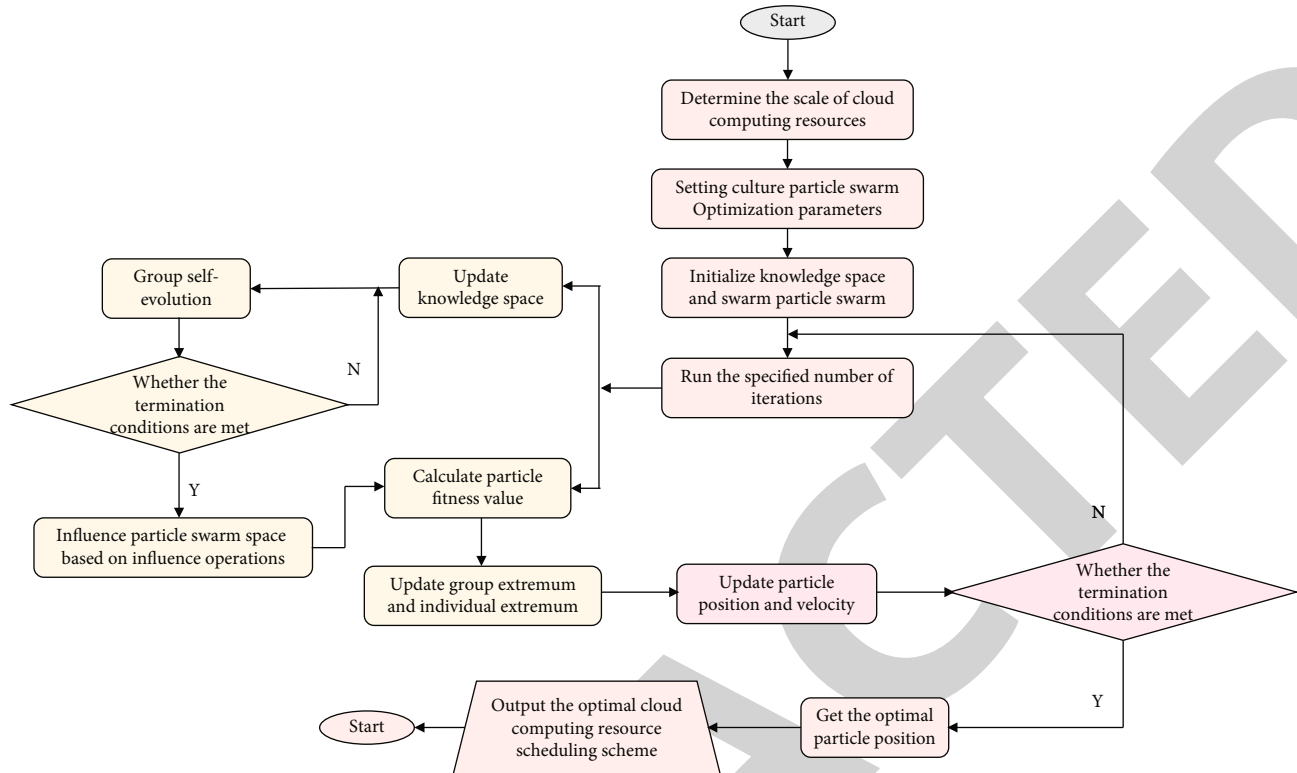


FIGURE 3: Cloud computing resource scheduling process.

3.2.2. Cloud Computing Resource Scheduling Strategy Based on Cultural Particle Swarm Algorithm. In the regular binary encoding used by the traditional particle swarm algorithm, cloud computing resource scheduling is not applicable. In order to comply with the characteristics of cloud computing resource scheduling, the author uses decimal encoding rules. $d_2, d_5, \dots, d_k \dots, d_i$ represents the particle position encoding method, d_i represents the i -th physical device, and the number of tasks determines the particle code length. If $(5, 4, 1, 7)$ is in the form of particle position encoding, then $t_1 M_{1V} \rightarrow d_2, t_2 M_{2V} \rightarrow d_5, t_3 M_{3V} \rightarrow d_1$ and $t_4 M_{4V} \rightarrow d_7$ represent four tasks corresponding to resource access physical devices [22].

Controlling the task completion goal to the shortest is the ultimate goal of cloud computing resource scheduling, if the particle quality is to be guaranteed to be high, the corresponding fitness value needs to be large, so that a better cloud computing resource scheduling scheme can be obtained. Equation (7) defines the particle fitness function.

$$\text{fit} = \frac{1}{\min \sum_{k=1}^n \text{sum}(d_k)}. \quad (7)$$

The common particle swarm algorithm generates the initial particle swarm in a random way, which is easy to cause the particles to be concentrated in a certain local area, and an uneven feasible solution will appear. In the author's study, the uniform method is used to generate the initial particle swarm, make sure that the initial particle swarm is distributed uniformly.

The cloud computing resource scheduling process based on cultural particle swarm is shown in Figure 3. First determine the scale of cloud computing resources, and then set the parameters of the cultural particles in the algorithm, initialize the knowledge space and the swarm particle swarm at the same time, determine the number of iterations, update the knowledge space, and calculate the particle fitness at the same time. After the update of the knowledge space is completed, the evolution of the group itself is carried out, and it is determined whether the evolution result satisfies the termination condition. If it cannot be satisfied, the evolution of the group itself will be reimplemented; if it can be satisfied, it will affect the particle swarm space according to the influence operation. At this time, the particle fitness is calculated, and the individual extreme values and fresh extreme values are updated according to the calculation results, at the same time, the particle position and velocity are updated, and then determine whether the termination condition is satisfied. If not, rerun the specified number of iterations, and if it can be satisfied, the optimal particle position is obtained, and finally the optimal cloud computing resource scheduling scheme is obtained [23].

3.3. Implementation and Performance Test of Smart City Management System. In order to verify the performance of the system, a city is taken as the research object. The city is a new first-tier city with 26 districts and 8 counties under its jurisdiction, with a total area of about 80,000 square kilometers and a resident population of about 31 million. According to statistics in 2019, the total regional production

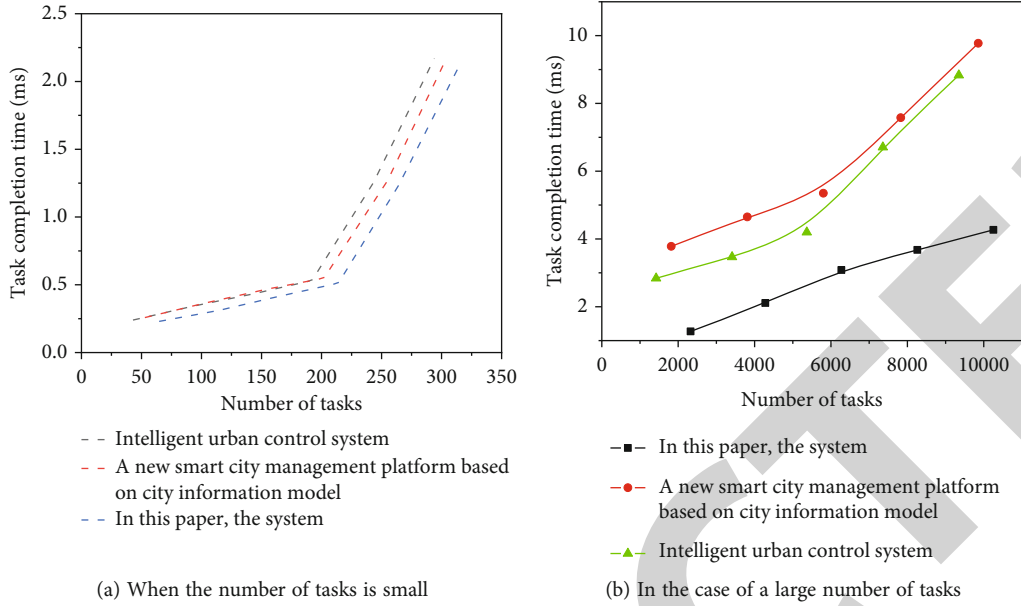


FIGURE 4: Resource scheduling completion time for different tasks.

reached 2.36 trillion yuan and the subtropical monsoon humid climate prevails in the region, with hot and sultry summers and cold and humid winters. The system includes functions such as smart government, smart finance, smart transportation, smart energy, smart security, smart medical care, and smart transportation. According to the user's needs, by clicking the corresponding button in the interface, jump to the corresponding page to expand the specific operation; the system also includes a search function and enter the keywords in the search box to find what users need.

The system displays the map of all streets and districts in the city, by dragging the mouse to browse the location-related content required by the user, and the black dots on the map are the monitoring distribution locations. If you need to check the monitoring situation of a certain location, you need to double-click the black dot at the location, that is, you can operate the monitoring equipment at this location, and you can also call the historical video of the monitoring of the location to realize the visual management of the smart city [24].

4. Results and Discussion

After the initial display of the system interface, the resource scheduling performance of the system is verified. Two types of task numbers are allocated to each cloud computing node, namely, the case of 300 tasks, which is a small number of tasks, and the case of 10,000 tasks, that is, a large number of tasks. At the same time, the use of a certain city smart management and control system is compared with the new smart city management platform and system based on the city information model, the comparison results are shown in Figure 4. It can be seen from Figure 4(a) that if the number of tasks is small, it will not affect the completion time of the resource scheduling task, the completion time of each system task is almost the same, and the task completion time is parity. In

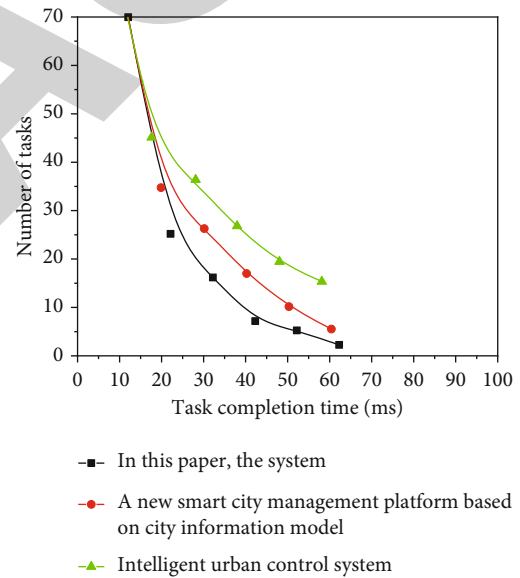


FIGURE 5: Number of nodes and task completion time.

Figure 4(b), the number of tasks is large, the number of tasks is increasing, and the time spent in resource scheduling of each system has increased. Compared with the other two systems, system resource scheduling takes the shortest time and has absolute advantages in resource scheduling.

The number of cloud computing resource nodes will also affect resource scheduling. In 60 cloud computing nodes, 5000 tasks are allocated for scheduling, and the three systems are still compared, the comparison results are shown in Figure 5.

In the smart city management system, the resource utilization rate represents the resource scheduling evaluation index in the cloud computing platform, and it is also the busy and idle degree of the resources in the system. The ultimate goal

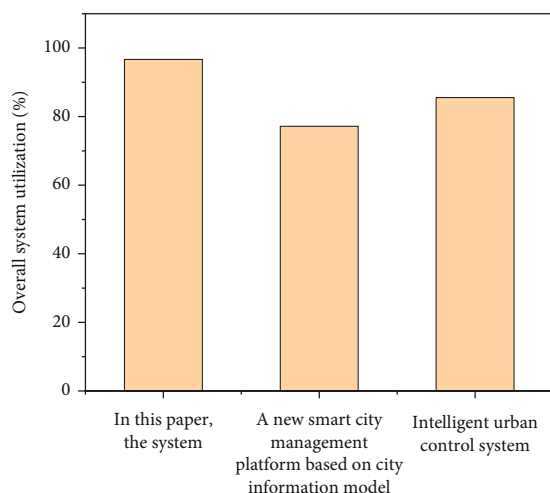


FIGURE 6: Overall utilization of the system.

of the cloud computing platform is to maximize the utilization of resources and to share resources efficiently; comparing the overall utilization of the three systems, the results are shown in Figure 6. As can be seen from Figure 6, the overall utilization of the system is the best, close to 100%, while the overall utilization of the other two systems is lower, below 90%. It can be seen that, compared with similar systems, the system has a high overall utilization rate [25].

5. Conclusion

The author proposes the information extraction and data planning of smart city based on the Internet of Things, constructs the overall structure of the system, and realizes the scheduling of cloud computing resources through the cultural particle swarm algorithm. The system can realize the effective management of smart city and monitor the city management situation in real time, and the resource scheduling effect is good. Even if the number of scheduling tasks is huge, it still maintains a relatively fast speed to complete the scheduling and has a good resource scheduling effect compared with similar systems. The design of the system lays the foundation for further research on smart city management. In future research, we can start from more detailed aspects, such as systematic research on smart medical care or smart security, in order to create better theoretical support for the healthy development of cities in the future.

Data Availability

The data used to support the findings of this study are available from the corresponding author upon request.

Conflicts of Interest

The author declares that they have no conflicts of interest.

References

- [1] L. Y. Jiang, Y. Y. Wei, H. Li, and L. F. Ma, "The central strain analytical modeling and analysis for the plate rolling process," *The International Journal of Advanced Manufacturing Technology*, vol. 118, no. 9-10, pp. 2873–2882, 2022.
- [2] K. Kane and Y. A. Kim, "Parcels, points, and proximity: can exhaustive sources of big data improve measurement in cities?," *Environment and Planning B: Urban Analytics and City Science*, vol. 47, no. 4, pp. 695–715, 2020.
- [3] M. N. Aldelaimi, M. A. Hossain, and M. F. Alhamid, "Building dynamic communities of interest for internet of things in smart cities," *Sensors*, vol. 20, no. 10, p. 2986, 2020.
- [4] S. Tori, J. Pappers, and I. Keserü, "Developing disruptive mobility scenarios for rural areas. Participatory mobility scenario building in a Belgian village for the year 2050," *European Transport Research Review*, vol. 14, no. 1, pp. 1–18, 2022.
- [5] Z. Zhao and Y. Zhang, "Impact of smart city planning and construction on economic and social benefits based on big data analysis," *Complexity*, vol. 2020, no. 4, Article ID 8879132, 11 pages, 2020.
- [6] B. F. Alghanem and J. M. Clements, "Narrowing performance gap between rural and urban hospitals for acute myocardial infarction care," *The American Journal of Emergency Medicine*, vol. 38, no. 1, pp. 89–94, 2020.
- [7] S. Madian, "Properties of neighborhood for certain classes associated with complex order and m-q-p-valent functions with higher order," *Journal of the Egyptian Mathematical Society*, vol. 30, no. 1, pp. 1–14, 2022.
- [8] J. C. Solle, S. Close, B. Koch, T. Hartley, A. Steinberg, and A. B. Emmert, "Developing an easily applicable quality improvement process to optimize and improve discrete workflows; methods for iterative change and successful scale," *Biology of Blood and Marrow Transplantation*, vol. 26, no. 3, pp. S368–S369, 2020.
- [9] S. Gao, J. Zhao, Y. Liu et al., "Research into power transformer health assessment technology based on uncertainty of information and deep architecture design," *Mathematical Problems in Engineering*, vol. 2021, no. 6, Article ID 8831872, 12 pages, 2021.
- [10] J. de Dios García-Villegas, A. García-Martínez, C. M. Arriaga-Jordán et al., "Use of information and communication technologies in small-scale dairy production systems in Central Mexico," *Experimental Agriculture*, vol. 56, no. 5, pp. 767–779, 2020.
- [11] F. L. Byk, P. V. Ilyushin, and L. S. Myshkina, "Forecast and concept for the transition to distributed generation in Russia," *Studies on Russian Economic Development*, vol. 33, no. 4, pp. 440–446, 2022.
- [12] H. Elhousseini, C. Assi, B. Moussa, R. Attallah, and A. Ghayeb, "Blockchain, ai and smart grids: the three musketeers to a decentralized ev charging infrastructure," *IEEE Internet of Things Magazine*, vol. 3, no. 2, pp. 24–29, 2020.
- [13] N. H. H. Cuong and T. C. Duy, "Information technology infrastructure for smart tourism in Da Nang city," *International Journal of Hyperconnectivity and the Internet of Things*, vol. 5, no. 1, pp. 98–108, 2021.
- [14] S. U. Khan, D. Raza, S. R. Ahmad, U. Saeed, and M. Ali, "Evaluation of foliage spread conversion into industrial land under the significance of urbanization and environment," *Fresenius Environmental Bulletin*, vol. 29, pp. 4612–4623, 2020.

Retraction

Retracted: Interactive Knowledge Visualization Based on IoT and Augmented Reality

Journal of Sensors

Received 17 October 2023; Accepted 17 October 2023; Published 18 October 2023

Copyright © 2023 Journal of Sensors. This is an open access article distributed under the Creative Commons Attribution License, which permits unrestricted use, distribution, and reproduction in any medium, provided the original work is properly cited.

This article has been retracted by Hindawi following an investigation undertaken by the publisher [1]. This investigation has uncovered evidence of one or more of the following indicators of systematic manipulation of the publication process:

- (1) Discrepancies in scope
- (2) Discrepancies in the description of the research reported
- (3) Discrepancies between the availability of data and the research described
- (4) Inappropriate citations
- (5) Incoherent, meaningless and/or irrelevant content included in the article
- (6) Peer-review manipulation

The presence of these indicators undermines our confidence in the integrity of the article's content and we cannot, therefore, vouch for its reliability. Please note that this notice is intended solely to alert readers that the content of this article is unreliable. We have not investigated whether authors were aware of or involved in the systematic manipulation of the publication process.

Wiley and Hindawi regrets that the usual quality checks did not identify these issues before publication and have since put additional measures in place to safeguard research integrity.

We wish to credit our own Research Integrity and Research Publishing teams and anonymous and named external researchers and research integrity experts for contributing to this investigation.

The corresponding author, as the representative of all authors, has been given the opportunity to register their agreement or disagreement to this retraction. We have kept a record of any response received.

References

- [1] H. Sun, "Interactive Knowledge Visualization Based on IoT and Augmented Reality," *Journal of Sensors*, vol. 2022, Article ID 7921550, 8 pages, 2022.

Research Article

Interactive Knowledge Visualization Based on IoT and Augmented Reality

Hanjie Sun 

School of Computer Science and Information Technology, Northeast Normal University, Changchun, Jilin 130117, China

Correspondence should be addressed to Hanjie Sun; 1512020122@st.usst.edu.cn

Received 26 August 2022; Revised 14 September 2022; Accepted 20 September 2022; Published 29 September 2022

Academic Editor: C. Venkatesan

Copyright © 2022 Hanjie Sun. This is an open access article distributed under the Creative Commons Attribution License, which permits unrestricted use, distribution, and reproduction in any medium, provided the original work is properly cited.

In order to solve the integration value of information technology and education, it is mainly reflected in the container for storing and disseminating information, the problem is that learners lack the proper self-learning ability, and the author proposes an interactive knowledge visualization system based on the Internet of Things and augmented reality technology. According to the applicable characteristics of augmented reality technology applied to IoT data presentation and interaction, the method can analyze and describe its application possibility. In the design of interactive electronic technology computer-aided teaching system based on NET platform, the system hardware structure consists of user interface layer, business selection layer, and data management layer. Users such as teachers and students enter their identity information at the user interface layer to log in to the system and enter the business selection layer and click the corresponding program according to their application requirements, the service selection layer transmits the user's selection instruction to the data management layer, and the data management layer selects the corresponding resources according to the user's needs and feeds it back to the user. The interaction of the system is mainly reflected in interactive teaching and information interaction, and interactive teaching is reflected in the online teaching of teachers and students. Information interaction is embodied in the information transmission of the system information interaction model. Experimental results show that after applying the system, the number of students with high self-efficacy increased from 11 to 21 and the proportion increased from 21.4% to 34.8%. The system designed by the author has strong antipressure ability, can respond to the application instructions of a large number of users in real time, and has a good interactive teaching effect, which improves the self-efficacy of students.

1. Introduction

With the development of information technology and the promotion of educational modernization, diverse learning technology tools have been applied in educational fields such as educational technology and learning design [1, 2]. In recent years, under the background of "Internet+education," Internet-related technologies and education have been continuously integrated, and the application of information technology in education has become more and more frequent. However, research shows that the current integration value of information technology and education is mostly reflected in the container for storing and disseminating information, that is, in the teacher-student dialogue structure centered on teachers, equating electronic teaching materials running on learning tools such as tablet computers,

digital collaboration software, or online concept maps to the digitization of paper teaching materials and using learning tools as auxiliary teaching aids for demonstrating content in teaching. The Internet of Things has been widely used in many industries, sensing, and collecting a large amount of data all the time. Large-scale IoT systems contain many modules, and each module is provided with diverse information by multiple IoT devices, which makes traditional data presentation methods such as LEDs, meters, and displays incapable of detecting and synthesizing outliers for a large number of devices. To support for analysis, performance evaluation, problem location, etc., it is impossible to freely switch between different fine-grained information presentations, which brings challenges to data monitoring, analysis, and equipment maintenance. It is urgent to support the Internet of Things in a user-friendly way. At the same

time, augmented reality (AR) technology has a strong ability to superimpose virtual content on reality. Under such circumstances, it is necessary to explore the use of AR technology to optimize and expand the presentation and interaction of IoT data. Augmented reality (AR) technology is an emerging technology that superimposes computer-generated virtual information into the real world and is an important branch of virtual reality technology. It improves the user's perception of the real world and provides a new way for humans to communicate with the world and has received extensive attention from researchers in recent years.

Although advanced educational technology is used to reinforce the traditional educational model, such a complex and abstract body of knowledge is thrown at students without any division, learning is only seen as the output object of the teacher's external knowledge, tools and people go their separate ways, and learners struggle with heavy low-level thinking activities, and it is difficult to intuitively perceive the essence of things from the metaphorical natural representation to construct the main cognitive schema. The construction of classroom teaching in the future should break the above situation; that is, the application of information technology should reflect the learner-centered constructivist design concept, and the external presentation of knowledge should echo the learner's internal cognitive structure [3–5]. As a new way of integrating information technology and curriculum, visual cognitive tools are used to imitate the thinking process from the aspect of information processing to reduce cognitive load and help learners to process information to build their own cognitive pattern [6]. At present, with the development of information technology, the research on cognitive tools has developed from the initial conceptual exploration stage to the empirical case application research stage based on cognitive tools [7]. As a new medium or knowledge presentation method, most of the knowledge in visualization research does not solve the problem of how to construct knowledge through visualization technology in group knowledge [8, 9]. Visual cognitive tools are the product of the combination of knowledge visualization theory and educational cognitive tools; in education and teaching, visual cognitive tools use its inherent semantic network tools, dynamic modeling tools, and information interpretation tools to realize concrete cognition and visualize the internal knowledge structure of learners; thereby, it has the effect of constructing the cognitive structure scientifically, promoting the explicitness of the invisible knowledge and reducing the cognitive conformity of the learners. However, whether it is the research on the construction of knowledge visualization model or the specific application of visual cognitive tools, researchers tend to explore the application of knowledge visualization technology.

2. Literature Review

At present, in many fields of society, the education field has a strong degree of integration and compatibility with the NET platform [10]. The integration of the NET platform and the computer teaching system has greatly improved the teaching effect of the school, solved the problem of "difficulty in

hands-on" for students, lowered the threshold for students to learn knowledge, and promoted the innovative development of the teaching system [11]. With the popularization of information technology education, there are more and more types of educational technology tools; however, some studies have shown that the integration value of information technology and education is mainly reflected in the container for storing and disseminating information, and learners lack the ability to learn independently [12]. The construction of classroom teaching in the future should reflect the learner-centered constructivist design concept, and the external presentation of knowledge should echo the learner's internal cognitive structure [13, 14]. In the past, traditional classroom teaching was mainly conducted by teachers in front of the blackboard, which not only limited the classroom time but also had poor interaction between teachers and students, and students' learning enthusiasm was low. Exploring methods to improve teaching quality through online interactive teaching and making effective educational resources play a full role are problems worth thinking about at the moment.

The essence of knowledge visualization is a graphical process for interaction and negotiation among group members and the interaction and mutual transformation of explicit knowledge and tacit knowledge, which is the aggregation of group thinking and structural cognition [15]. However, in the interpretation, construction, and development of group knowledge, knowledge visualization has not effectively solved the problem of how to better represent prior cognition through visualization for group knowledge construction; for teachers and students, knowledge visualization is only regarded as a new medium or a way of presenting knowledge, and new research needs to be carried out based on this. The role of cognitive tools is to refer to technical tools that can build contexts shared by multiple people to facilitate interactive behavior among learners; that is, with the help of the sharing and intercommunication technology of knowledge technology tools, learners can realize the linkage of self-constructed knowledge among learners through interactive behaviors such as "knowledge sharing," "conflict of opinions," "negotiating knowledge," and "reaching consensus" and construct a trinity of classroom technology learning environment of "learner group-technology tool application-classroom subject" [16, 17].

NET platform can be understood as a bridge between contacts, information, and related devices [18]. Microsoft-.NET is also known as the Microsoft XML Web service platform. This platform ensures that the system realizes communication, interaction, and information sharing based on the Internet, regardless of whether there are differences in operating systems and programming languages. XML Web services can enable applications to communicate and share data in the Internet [19]. From the user's point of view, the .NET platform is transparent. Users only need to input applications and commands, and the program will run quickly and respond to the user's operating instructions. There is no threat to the .NET platform due to time, space, or external environmental factors, the operation is simple, and the data processing performance is excellent. The author

designs an interactive electronic technology computer-aided teaching system based on .NET platform, in order to realize the interactive electronic technology computer-aided teaching.

3. Methods

3.1. Design of Interactive Electronic Technology Computer-Aided Teaching System

3.1.1. System Hardware Design. The interactive electronic technology computer-aided teaching system based on the NET platform belongs to the Web application program of Microsoft.NET, and the system structure uses the B/S mode, which can reduce the development cost [20]. The user login interface of the system is the same; through a simple login method, users with different identities can enter the system at different locations with user names that match their identities. Under normal circumstances, the client does not need to install other software, it can be used only by installing a browser, the connection between the server and the client is reduced, the danger of using program codes is reduced, and it is beneficial to the security of the system database.

The interactive electronic technology computer-aided teaching system based on the NET platform is composed of a three-layer structure system, followed by the user interface layer, the business selection layer, and the data management layer. Users such as teachers and students can enter their own identity information at the user interface layer to log in to the system and enter the business selection layer [21]. Teachers, students, and other users can click on the corresponding program in the business selection layer according to their own application requirements, and the business selection layer transmits the user's selection instructions to the data management layer. The data management layer selects the corresponding educational resources to feed back to the user according to the user's needs.

3.1.2. User Interface Layer. The user interface layer is mainly used to manage user information and provide human-computer interaction functions for users and systems [22]. Among them, the user registration module, login module, and management module are included. When a user registers, real-name authentication is required; after the user registers the information, the user information is stored in the data management layer of the system. The user login module has two units: front and back. The front unit is the user login interface; the user enters his identity information in the program of the login interface and then clicks the submit button to enter the service selection layer of the system. The back-end unit uses .NET technology to respond to user operations and verifies the correctness of the user's input identity in a timely and rapid manner according to the .NET form verification plug-in, so as to avoid theft and intrusion by illegal users. The user management module provides users with functions such as modifying and viewing user information. There are three identities of teachers, students, and system administrators in the user interface layer, among which the

system administrator has the right to manage the identity information of teachers and students.

3.1.3. Business Selection Layer. The business selection layer is set between the user interface layer and the data management layer and belongs to the middle layer of the system [23]. The business selection layer includes functions such as teaching and learning, self-assessment, questioning, assignment, and resource management. When the user enters the service selection layer from the user interface layer, the user can click the corresponding program according to their needs, and the service selection layer transmits the user's selection instruction to the data management layer. The business selection layer mainly completes the efficient access to the data management layer through .NET technology [24]. There are certain differences in the selection of services by users with different identities; taking the resource management function as an example, the schematic diagram of the teacher applying the resource management function in the service selection layer is shown in Figure 1.

In Figure 1, the teacher enters the user name and password at the user interface layer and enters the system service selection layer and enters the resource channel at the system service selection layer; in the resource channel, you can select courses or modify courseware according to your own needs, and you can also upload the courseware to the course resources for subsequent application [25].

3.1.4. Data Management Layer. The data management layer belongs to the core of the system, and the relationship between different data tables in the data management layer fully reflects the relationship between the applications in the overall system. The data in the data management layer belongs to teaching resources; after obtaining the program selection instructions of the business selection layer, the data management layer selects the corresponding educational resources according to the user's needs and feeds it back to the user. There are 12 tables in it, in the following order: user table for saving user information, department table for saving department information, course data table for saving course data, announcement of the information table used to save announcement information, courseware table used to save courseware, homework table used to save homework information, online communication table used to save the interactive information of online communication, user response information table used to save the user's response information, users select courses table used to save the user's selection of courses, user log in information table for saving user login information, operational history information table for saving user operation history information, and online exam question table for saving online exam questions.

3.2. System Interactive Design. System software design mainly revolves around interactive design, which is mainly reflected in interactive teaching and information interaction.

3.2.1. Interactive Teaching. The interactive teaching use case diagram of the interactive electronic technology computer-aided teaching system based on the NET platform is shown in Figure 2.

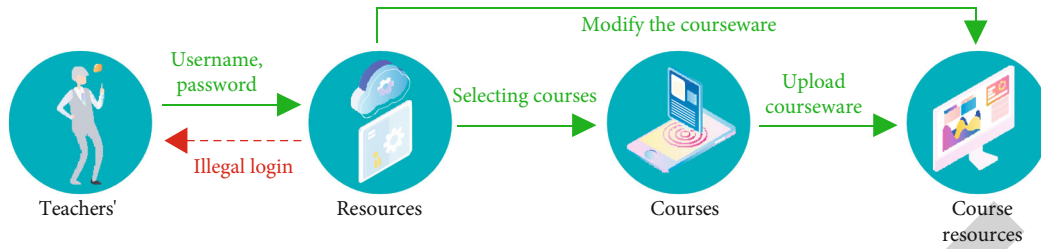


FIGURE 1: Schematic diagram of the resource management function of the service selection layer.

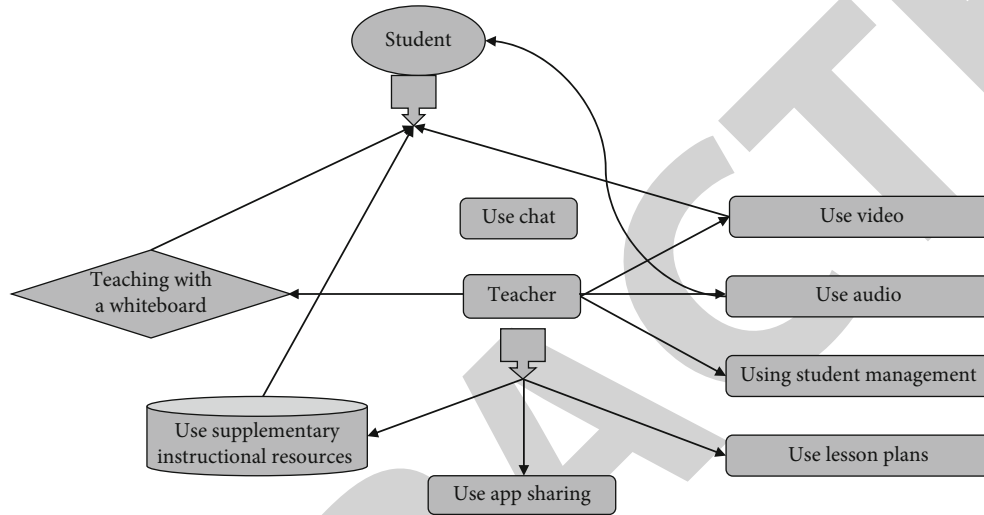


FIGURE 2: System interactive teaching use case diagram.

The interactive teaching use case diagram describes the interactive teaching function of the system. As can be seen from the use case diagram, teachers share through chat tools, video, audio, student management, lesson plans, program sharing, auxiliary teaching resources, and whiteboard teaching realizing interactive teaching with students. The most direct interactive communication method between students and teachers is the chat tool. Students are the recipients of interactive teaching.

3.2.2. Information Interaction. The data generated by IoT devices has the characteristics of real time. Combined with the support of AR technology for real-time natural interaction, it opens up new possibilities for more intuitive and panoramic data analysis and interactive behavior. Through the nature of AR superimposing virtual content in the physical space, it will be possible to realize the seamless integration of the two aspects of interaction based on the physical device and the AR device and provide real-time feedback on the results of the interaction, providing invaluable information for detection and analysis operations in complex systems or lack of support. At the same time, interaction can also provide important contextual information for IoT data presentation and provide an important basis for data screening. The interactive electronic technology computer-aided teaching system software program based on NET platform includes interactive management server, database server, Web server, and node program. The interaction management server is mainly used to assist and manage the infor-

mation interaction between members and groups in the study group; its functions mainly include the following aspects:

Course group management: for example, user login, registration, logout, and user identity management

Control information release: add and remove study group member information and stop course management

Discussion management: transfer the discussion information uploaded by each user to the clients of different group members

The functions of the node program include the following: acquisition and recovery of video and audio data, compression and decompression, and acquisition and transmission; group members apply for the transmission of learning information; group member information management; and transmission of learning information under text discussion.

Based on the above analysis, the information interaction model of the interactive electronic technology computer-aided teaching system based on the .NET platform is shown in Figure 3.

As can be seen from Figure 3, the information interaction between the interaction management server and the nodes is mainly realized through the UDP/TCP hybrid connection mode and the TCP connection mode.

3.2.3. Data Association. The AR-based IoT data presentation has spatial integration capabilities, distance-based information screening capabilities, and diverse information

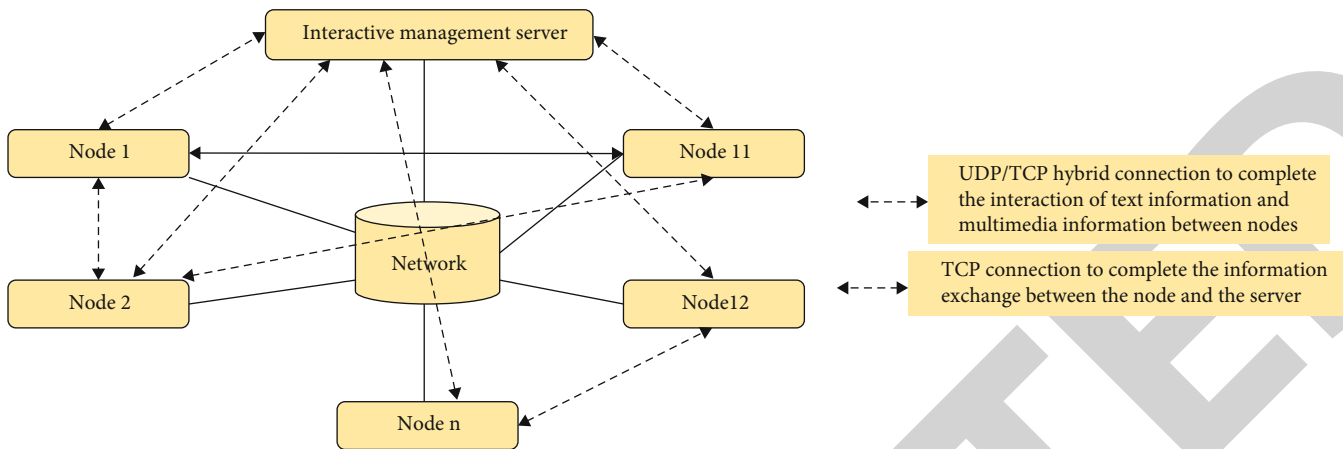


FIGURE 3: Information interaction model.

presentation methods, which can support the overlay presentation of IoT device data in complex systems with its related data, historical data, and reference data, and supports switching between different fine-grained freely, making it possible to associate data with multidimensional and multi-level of detail.

- (1) Presentation of linked data: by analyzing the correlation of data (input and output relationship, influence relationship, similar relationship, etc.), comprehensive parameter input, device connection, etc., to present the relationship between data, a single data can be placed in its environment to assist in making changes and accurate judgment
- (2) Control presentation: the historical data and indicator data are superimposed on the data presentation of the concerned equipment and its associated equipment to support on-the-spot comparative analysis of the current data
- (3) The associated presentation with global data: correlate the presentation of local data with the visualization of global data to provide context for local data analysis

3.3. Key Technologies of Augmented Reality Technology.

Augmented reality technology is developed on the basis of computer graphics, computer image processing, and machine learning. It superimposes the entity information originally in the real world into the real world through some computer technology to be perceived by human senses, so as to achieve a sensory experience beyond reality. In order to enable users to interact with virtual objects, augmented reality systems must provide high frame rate, high resolution virtual scenes, tracking and positioning devices, and interactive sensing devices.

As an immersive learning method, augmented reality technology can integrate rich resource information and other data into the real scenes that users can observe, provide teachers and students with an immersive learning envi-

ronment, stimulate students' interest in learning, and increase subjective positivity. At the same time, augmented reality technology can build and display the three-dimensional model of the target object, and students can enhance their understanding of the target object by observing the model from different perspectives and interacting with the virtual model. In addition, the real-time interaction of augmented reality system weakens the limitation of location and space. Teachers can guide students in class or remotely, which makes up for the lack of equipment in the real environment and realizes resource sharing.

3.4. System Test

3.4.1. Module Function Test. Take the students of a certain class of senior two in a university as an example, applying the system in the information technology course of this school; when students and teachers enter the system through the user login interface, set up six module functions: user management, administrator authority test, student self-learning, student courseware application, teacher course management, and teacher Q&A interaction; test whether the corresponding module functions of this system are effective. The test results are shown in Table 1. According to the test results in Table 1, the application results of the system for six different functions are consistent with the ideal effect, indicating that the module function validity test of the system has passed.

3.4.2. Interactive Test. The interactive test is mainly tested from two aspects: one is human-computer interaction, which is reflected through the user login system, and the user can access the system according to the login interface. The second is the interactive teaching between teachers and students; the author takes the students submitting the answer board and the teacher receiving the answer board and replying as an example and verifies system interactivity. When the students submit the answer board in the system, the teacher can reply to the questions raised by the students online, which shows that the system has better interactivity.

TABLE 1: System module functional test results.

System module function settings	Ideal effect	System application results
User management	If the user login information is incorrect, it will prompt	The desired effect
Admin privilege test	Editing user information for students and teachers	The desired effect
Student self-study	Select the courses you need to study, take exams, etc., and upload the exam papers independently	The desired effect
Student courseware application	Students can choose their own courseware to realize online learning	The desired effect
Teacher course management	Teachers can edit the relevant content of their own courses	The desired effect
Teacher Q&A interaction	Teachers can respond online to questions uploaded by students	The desired effect

TABLE 2: System stress test results.

Test process	Operation content	Input	Server details	Test results
1	Start the system			
2	Log in			
3	Set Stresstesting, click Start	Number of threads 110	Access is successful	No exception occurred
4	The first test, set Stresstesting	160 threads	Access is successful	No exception occurred
5	The second test, set Stresstesting	Number of threads 210	Access is successful	No exception occurred
6	The third test, set Stresstesting	Number of threads 260	Access is successful	No exception occurred
7	Stop test			

4. Results and Discussion

Since the user role of the system is not only a student, the permission settings are diversified, and the data processing volume is also huge. When students and teachers use the system to teach interactively, use Microsoft Web Application Stress Tool as a test tool, set the number of threads to 50, and the number of threads reflects the details of the amount of data processed by the system; the system was stress tested and the results are shown in Table 2.

Self-efficacy is used to describe the control effect of students on their own behavior, reflecting students' autonomous learning ability. In this subsection, the number of groups with high self-efficacy, the number of groups with general self-efficacy, and the number of groups with low self-efficacy are used to describe the application system, whether the interactive learning style of students and teachers has a positive impact on students; the results are shown in Figure 4.

As can be seen from Figure 4, after the application of the system, the number of students with high self-efficacy increased from 11 to 21, and the proportion increased from 21.4% to 34.8%; it can be understood that the application of the system has increased the number of people with high self-efficacy. The number of students with general self-efficacy and the number of students with low self-efficacy decreased slightly, indicating that after the application of the system, the interactive teaching method improved the self-efficacy of students, the students' autonomous learning ability was greatly improved, and the system application effect is better.

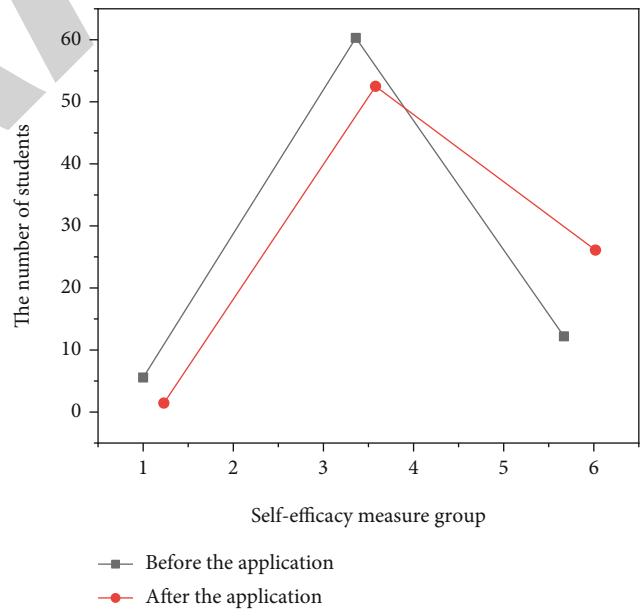


FIGURE 4: System application effect test results.

5. Conclusion

This paper proposes an interactive knowledge visualization based on the Internet of Things and augmented reality technology. With the maturity of information and communication technology and the rapid development of the Internet, the intelligent, interactive, and integrated education management is the core direction of the current education

system research and development field. This paper designs an interactive electronic technology computer-aided teaching system based on NET platform. The hardware structure of the system is composed of a user interface layer, a business selection layer, and a data management layer. Teachers, students, and other users enter their identity information at the user interface layer to log in to the system and enter the business selection layer and click the corresponding program according to their application requirements. Select the corresponding resource to feed back to the user. The interaction of the system is mainly reflected in interactive teaching and information interaction. Interactive teaching is embodied in the online teaching between teachers and students; information interaction is embodied in the information transmission of the system information interaction model.

For the environment where the Internet of Things has been widely used, AR technology can be integrated into the production, use, and maintenance process without making changes to the existing infrastructure or only adding identification marks, camera equipment, etc. and presenting data and data analysis results. This provides important assistance; by applying collaborative operation in a distributed IoT environment, it can break through the barriers in space and reduce the time and labor costs of collaboration; for hard-to-reach and high-risk environments, it can also provide intuitive and effective remote enhancements and remote operation. Augmented reality technology has broad application space in Internet of Things data presentation, data association, data interaction, data simulation, remote enhancement, collaborative operation, etc. More diverse forms of presentation and interaction help to build a more intelligent and easy-to-use IoT system.

Data Availability

The data used to support the findings of this study are available from the corresponding author upon request.

Conflicts of Interest

The author declares no conflicts of interest.

References

- [1] O. B. Onyancha, "Knowledge visualization and mapping of information literacy, 1975–2018," *IFLA Journal*, vol. 46, no. 2, pp. 107–123, 2020.
- [2] D. R. Brademan, I. J. Miller, N. W. Kwicien, D. J. Pagliarini, and E. Shishkova, "Argonaut: a web platform for collaborative multi-omic data visualization and exploration," *Patterns*, vol. 1, no. 7, article 100122, 2020.
- [3] Y. Farag, C. Horro, M. Vaudel, and H. Barsnes, "Peptidshaker online: a user-friendly web-based framework for the identification of mass spectrometry-based proteomics data," *Journal of Proteome Research*, vol. 20, no. 12, pp. 5419–5423, 2021.
- [4] M. Handzic, "Visualizations supporting knowledge-based decision making in cultural heritage management," *Culture. Society. Economy. Politics*, vol. 1, no. 2, pp. 32–40, 2021.
- [5] A. V. Makulin and M. I. Korzina, "Knowledge visualization centers and university infographics: international and domestic experience," *Vysshee Obrazovanie v Rossii = Higher Education in Russia*, vol. 29, no. 7, pp. 114–124, 2020.
- [6] A. Alper, E. S. Öztas, H. Atun, D. Çinar, and M. Moyenga, "A systematic literature review towards the research of game-based learning with augmented reality," *International Journal of Technology in Education and Science*, vol. 5, no. 2, pp. 224–244, 2021.
- [7] J. E. Rustamov, "Features and current status of the teaching of the subject "information technology in the field of services" in higher educational institutions," *Theoretical & Applied Science*, vol. 81, no. 1, pp. 112–116, 2020.
- [8] Y. Noh and S. Y. Lee, "An evaluation of the library's educational value based on the perception of public library users and librarians in Korea," *The Electronic Library*, vol. 38, no. 4, pp. 677–694, 2020.
- [9] H. Li, Z. Zhou, C. Li, and S. Zhang, "RCCM: reinforce cycle cascade model for image recognition," *IEEE Access*, vol. 8, pp. 15369–15376, 2020.
- [10] H. Zhu and Z. Wang, "Construction and research of formative evaluation system in fine art classroom teaching in rural primary schools," *Asian Agricultural Research*, vol. 12, no. 12, pp. 77–84, 2020.
- [11] R. Z. D. Cruz and R. A. O. D. Cruz, "Purposes and outcomes of information technology education towards sustainable national development," *Information Technology Education and Society*, vol. 17, no. 1, pp. 5–20, 2020.
- [12] R. Putra, A. Fauzan, and M. Habibi, "The impact of cognitive conflict based learning tools on students' mathematical problem solving ability," *International Journal of Educational Dynamics*, vol. 2, no. 1, pp. 209–218, 2020.
- [13] W. Yang, X. Wang, J. Lu, W. Dou, and S. Liu, "Interactive steering of hierarchical clustering," *IEEE Transactions on Visualization and Computer Graphics*, vol. 27, no. 10, pp. 3953–3967, 2020.
- [14] L. Ollesch, S. Heimbuch, and D. Bodemer, "Improving learning and writing outcomes: influence of cognitive and behavioral group awareness tools in wikis," *International Journal of Computer-Supported Collaborative Learning*, vol. 16, no. 2, pp. 225–259, 2021.
- [15] Z. J. Wang, A. Kale, H. Nori et al., "Gam changer: editing generalized additive models with interactive visualization," 2021, <https://arxiv.org/abs/2112.03245>.
- [16] M. S. A. Manan, X. Wang, and X. Tang, "Innovating animation teaching system: an experimental survey on the integration of design thinking and creative methods for animation education in China," *Open Journal of Social Sciences*, vol. 10, no. 3, pp. 379–388, 2022.
- [17] H. Xu, C. R. Wang, A. Berres, T. Laclair, and J. Sanyal, "Interactive web application for traffic simulation data management and visualization," *Transportation Research Record*, vol. 2676, no. 1, pp. 274–292, 2022.
- [18] R. K. Shah, "Concepts of learner-centred teaching," *Shanlax International Journal of Education*, vol. 8, no. 3, pp. 45–60, 2020.
- [19] V. Singh, G. D. Kallioliias, M. Ostaszewski, M. Veyssiere, and A. Niarakis, "Ra-map: building a state-of-the-art interactive knowledge base for rheumatoid arthritis," *Database The Journal of Biological Databases and Curation*, vol. 2020, 2020.
- [20] J. Perez, H. M. Freeman, A. P. Brown, C. Genuchten, and L. G. Benning, "Direct visualization of arsenic binding on green rust

Retraction

Retracted: Application of Artificial Intelligence-Based Sensor Technology in the Recommendation Model of Cultural Tourism Resources

Journal of Sensors

Received 12 December 2023; Accepted 12 December 2023; Published 13 December 2023

Copyright © 2023 Journal of Sensors. This is an open access article distributed under the Creative Commons Attribution License, which permits unrestricted use, distribution, and reproduction in any medium, provided the original work is properly cited.

This article has been retracted by Hindawi, as publisher, following an investigation undertaken by the publisher [1]. This investigation has uncovered evidence of systematic manipulation of the publication and peer-review process. We cannot, therefore, vouch for the reliability or integrity of this article.

Please note that this notice is intended solely to alert readers that the peer-review process of this article has been compromised.

Wiley and Hindawi regret that the usual quality checks did not identify these issues before publication and have since put additional measures in place to safeguard research integrity.

We wish to credit our Research Integrity and Research Publishing teams and anonymous and named external researchers and research integrity experts for contributing to this investigation.

The corresponding author, as the representative of all authors, has been given the opportunity to register their agreement or disagreement to this retraction. We have kept a record of any response received.

References

- [1] S. Hou and S. Zhang, "Application of Artificial Intelligence-Based Sensor Technology in the Recommendation Model of Cultural Tourism Resources," *Journal of Sensors*, vol. 2022, Article ID 3948298, 8 pages, 2022.

Research Article

Application of Artificial Intelligence-Based Sensor Technology in the Recommendation Model of Cultural Tourism Resources

Shuang Hou  and Shihui Zhang 

Shenyang University, Shenyang Liaoning 110044, China

Correspondence should be addressed to Shihui Zhang; 20150235224@mail.sdufe.edu.cn

Received 15 August 2022; Revised 3 September 2022; Accepted 8 September 2022; Published 24 September 2022

Academic Editor: C. Venkatesan

Copyright © 2022 Shuang Hou and Shihui Zhang. This is an open access article distributed under the Creative Commons Attribution License, which permits unrestricted use, distribution, and reproduction in any medium, provided the original work is properly cited.

Aiming at the lack of theoretical basis for the development of cultural tourism resources, an application method of artificial intelligence-based sensor technology in the recommendation model of cultural tourism resources is proposed. Sensor network is an application-based network. Compared with traditional wireless communication network, it has the characteristics of large node scale, self-organized multihop, unattended, and no communication infrastructure. Combined with artificial intelligence sensor technology, this paper attempts to construct an evaluation index system and evaluation model for cultural tourism resources, and uses this model to conduct a comprehensive evaluation of cultural ecotourism resources in the western region. The experimental results show that the E value of the evaluation result of cultural tourism resources in the western region is 6.346, which has a good development value. Secondly, from the specific evaluation results of each level, the western region has the highest cultural tourism standard, which has 6.605. Cultural tourism resources, landscape resources, and development conditions scored lower. Among them, cultural tourism resources and landscape resources have the highest score (7.186), and the economic and cultural field has the lowest score (6.092). Among the cultural tourism development conditions, the policy conditions are high (6.823), but the location conditions are very low, only 4.879 points. Therefore, it is found that the model takes cultural tourism landscape resources, cultural tourism environment resources, and cultural tourism development conditions as the content of cultural tourism resources evaluation, which is comprehensive and has strong hierarchy and pertinence; fuzzy comprehensive evaluation method has strong objectivity to determine the weight and the value classification; and weighting evaluation model of cultural tourism resources has rationality and generalizability and can provide a scientific basis for the classification and evaluation of cultural tourism resources and the planning and development of cultural tourism.

1. Introduction

The initial definition of resources is the original given of nature, and later expand it as natural resources and cultural resources and clarifies the utility characteristics of resources [1]. Among them, natural resources can generate economic value at a certain period of time and location to improve the natural environmental factors and conditions of humanity and future welfare; cultural resources are the material and spiritual products that condense human nondifferent labor. It includes substances and intangible cultural wealth accumulated in historical evolution [2]. Tourism resources are based on functional properties, which means that there are

certain areas that can be attractive to tourists and can use and generate a variety of things and factors that use and produce economic, social, and environmental benefits. Including the development and utilization of natural humanistic tourism resources and potential nature of tourism attractive to be developed [3]. Cultural tourism resources are the child concept of tourism resources. On the narrow sense, cultural tourism resources are a type of tourist resource for cultural and tourism organic combinations; in a broad sense, any tourism resources that can provide cultural experiences for tourists, including historical, art or scientific value cultural relics, architecture site remains and oral traditions, performing art, social customs, etiquette, festive, practical experience

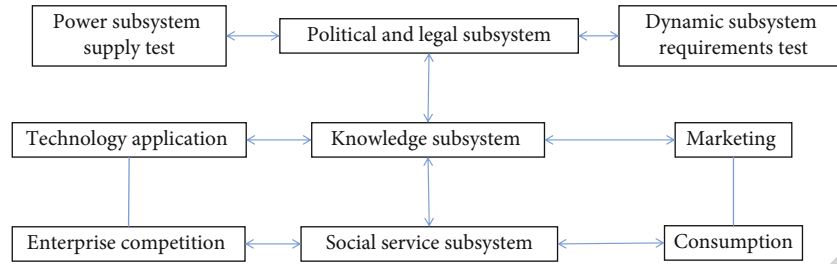


FIGURE 1: Logical model diagram of cultural industry development system.

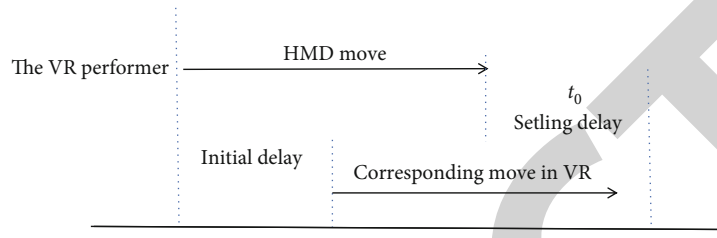


FIGURE 2: Initial delay and demystified delay.

and knowledge, and craftsmanship. It is the form of traditional cultural expressions such as cultural tourism resources [4].

In recent years, tourism is booming, and the technical cooperation between tourism and information technology (IT) has also matured [5]. In smart tourism services, IT technology such as the Internet, Artificial intelligence software, big data, wireless sensor network, and near-distance communications (NFCs) have been used to provide accurate travel information and extensive travel experiences for visitors [6]. For example, visitors can download the discipline of the leisure park and book a time slot of its play facilities or facilities. This can shorten the time of visitors waiting in line and improve the overall utilization and visitor satisfaction of the facility. In order to further improve the efficiency of tourism management and services, optimize passengers' travel experience, combine Artificial intelligence software and big data, and explore the construction of cultural tourism resources recommended models, design and efficient recommendation, and strategies. The logical model of cultural industry development system is shown in Figure 1 [7].

2. Literature Review

For this research question, Ibrahim and Adamu reviewed the spatial distribution and characteristics of national cultural tourism resources in Dounana, Nigeria [8]. The MoVR system 4 proposed by Yusuf et al. used 60GHz millimeter wave to realize wireless transmission between the rendering host and the display helmet in the separated VR system [9]. FlashBack proposed by Wisutruangdat renders the whole VR application in advance, discretizes the continuous virtual space into a large number of panoramas of different locations and stores these panoramas in a layered cache based on the design of external storage devices [10]. Bi and Wang measured the delay performance of current mainstream immersive VR systems and defined more accurate delay

indicators: initial delay and stashing delay (as shown in Figure 2) [11]. Kwiatek-Soltys and Bajgier-Kowalska used a method based on image compression: frame data of different VR scenes were compressed into JPEG format according to the same compression ratio, and the scene consuming more storage space after compression would be more complex [12]. Eunice and Mwangi used the BRISQUE value commonly used in graphics to evaluate the scene complexity [13]. Thong et al. analyzed the problems and risks of AI application in cultural industry and proposed corresponding preventive measures [14]. Palanca-Tan described the production integration, communication integration, and consumption integration of Artificial intelligence and cultural industry and carried out path optimization design for its integration innovation [15]. Iaromenko et al. proposed the use of intelligent cultural product supply chain to solve the supply-side problem of cultural industry [16]. Wang et al. deeply discussed the intelligent innovation paradigm and development boundary of cultural creative industry [17]. Based on the AI industry advantages of the Guangdong-Hong Kong-Macao Greater Bay Area, Hamad et al. proposed a new idea of promoting the cultural industry development of the Guangdong-Hong Kong-Macao Greater Bay Area with Artificial intelligence [18].

This paper is based on the existing ecotourism resource evaluation indicators: models, attempts to build a cultural tourism resource evaluation index system, evaluation model, and finally use model evaluation of western cultural tourism resources. The experimental results show that in the highest score of cultural tourism environmental resource indicators, cultural tourism is more desirable, but the environmental environment, the environmental environment, and community economy is poor, which is also the need in the development of cultural tourism development in the western region as the direction of efforts. Finally, through the simple application of cultural tourism resource evaluation model, this model is found to be evaluated by cultural tourism and

landscape resources, cultural tourism environmental resources, and cultural tourism development conditions as cultural tourism resources, more comprehensive and strong hierarchical and targeted sex, and fuzzy comprehensive evaluation method has strong objectivity for the determination of weight, which has better performance.

3. Research Methods

3.1. Introduction to Artificial Intelligence Software. Generally, artificial intelligence software refers to techniques that represent human intelligence through ordinary computer programs. In the intelligent tourism integrated system, the application of artificial intelligence software technology mainly includes machine learning, intelligent perception, intelligent reasoning, and intelligent action, but these applications are closely related to big data, mobile internet, and cloud computing technologies.

3.1.1. AI Software and Mobile Internet. The Internet is the premise of all technology. It is so ubiquitous that it is almost impossible to find a device that is not connected to the Internet. The essence of the mobile internet is still the Internet. It simply allows internet users to connect to the cloud of the Internet without geographical restrictions.

3.1.2. Artificial Intelligence Software and Big Data. They complement and promote each other. Big data mainly refers to the mass, multidimensional, multiform, etc. According to the above analysis, it can be seen that big data is one of the foundations of artificial intelligence software. It can be said that there is no so-called intelligence without big data. Data can bring a lot of information, but it is difficult to see the information and value contained in data if you just observe the disorderly data. The algorithms in artificial intelligence technology can make big data meaningful and valuable. The bridge between artificial intelligence software and big data is machine learning. The process of machine learning mainly includes data collection, algorithm design, algorithm implementation, algorithm training, and algorithm verification. It can be seen that data is the premise of machine learning, and the application of artificial intelligence software technology must be supported by relevant data. At the same time, effective information and value can be mined through the analysis of data by algorithms in machine learning.

3.1.3. AI Software and Cloud Computing. Cloud computing refers to the decomposition of huge data processing programs into countless small programs through the network "cloud", and then the results of these small programs are processed and analyzed by the system composed of multiple servers and returned to users. In simple terms, cloud computing is mainly distributed storage and distributed computing. Through the above analysis, we know that artificial intelligence software needs the vast amount of data for training and learning, the cloud is used for artificial intelligence software to calculate the force on the support, cloud computing is a powerful booster behind artificial intelligence software, while cloud computing makes your business ecosystem, and cloud computing platform resources integra-

tion requires the application of artificial intelligence software technology.

3.2. Establishment of Cultural Tourism Resources Evaluation Index. The purpose of cultural tourism resource evaluation is to identify cultural ecotourism resource type characteristics, analyze resource organization structure, determine resource value, and evaluate resources. For a long time, scholars are only studied for overall ecological tourism resources, and their corresponding evaluation indicators are also some comprehensive evaluation indicators. However, the existing evaluation index establishment basis and principles have the same reference value for this study. Follow the basic principles of concise science, systemic, representative, comparability, operability, qualitative and quantitative, combined with cultural tourism resource classification scheme, refer to the existing literature and related documents, evaluation indicators, and use frequency The degree statistics method, theoretical analysis, expert consultation law and tourist investigation method, three aspects of cultural tourism landscape resources, cultural tourism environmental resources and cultural tourism development conditions, and construct the following cultural ecotourism resource evaluation index system. Among them, cultural tourism landscape (B1) is the core constituent elements of cultural tourism, their scarcity, uniqueness, and aesthetic value directly determines the attraction of cultural tourism, and is the core and foundation of cultural tourism resource evaluation system. At the same time, the emphasis on ecological tourism has also determined the cultural tourism environment (B2) to distinguish important signs from other tourism types, and cultural landscapes can only reflect their unique aesthetic value in the corresponding cultural ecological environment. Experience the value, so the cultural tourism environment (mainly human environment) should also be an important part of cultural ecotourism resource evaluation. Furthermore, in a sense, the resources are useful to human beings, and the evaluation of resources must be inseparable from social needs, and thus combined with the source of cultural tourism, location conditions, policy conditions, etc. (B3) to analyze the value of cultural tourism resources to reflect the nature of resources and then make more objective evaluation [19].

3.3. Cultural Tourism Resource Recommended Model Construction

3.3.1. Indicator Measure and Judgment. According to the cultural tourism resource evaluation target, refer to the evaluation method of ecotourism resources in the relevant literature, using the fuzzy comprehensive evaluation method, divide the index standards into excellent, good, medium, poor, standard adoption of decimal score, full classification 10 points, and each level of fractions are: 10-8, 8-6, 6-4, 4-2. In a specific evaluation, the score of each indicator can be determined according to the actual data or expert [20].

3.3.2. Indicator Weight Calculation. Calculate the current level of analytical method (AHP method) to calculate the weight. The first step is to construct the judgment matrix.

TABLE 1: P_{ij} takes the value.

The value taken for P_{ij}	Meaning
1	Factor P_i is equally important as P_j
3	Factor P_i to P_j are slightly important
5	Factor P_i to P_j is significantly important
7	Factor P_i is much more important than P_j
9	Factor P_i to P_j is extremely important
2,4,6,8	The importance of factor P_i to P_j ranged between 1-3,3-5,5-7, and 7-9, respectively
$P_{ij} = 1/f_{ji}$	Represents the unimportance of factor P_i to P_j

According to the cultural tourism evaluation index system, the invitation experts score, determine the comparative relationship between two or two factors related to the upper layer in the same layer and construct the judgment matrix. Each matrix should be satisfied:

$$P = \begin{cases} P_{11} & P_{12} & P_{13} & P_{1n} \\ P_{21} & P_{22} & P_{23} & P_{2n} \\ \vdots & \vdots & \vdots & \vdots \\ P_{n1} & P_{n2} & P_{n3} & P_{n4} \end{cases} \quad (1)$$

$P_{ij} = 1$ and $P_{ij} = 1/f_{ji}$, P_{ij} shows the determination value of the relative importance of the element P_i pairs P_j for P_k , and the value of P_{ij} is shown in Table 1.

Use $W_i = (i = 1, 2, 3)$, $W_{ij} = (i = 1, 2, 3, j = 1, 2, \dots, 11)$ represents B and C layer indicators, and the value range is from 0 to 1 and $\sum W_i = 1$, $\sum W_{1j} = 1$, $\sum W_{2j} = 1$. The larger the value, the more important it indicates that the indicator is in its indicator layer. The smaller the value, the lower the importance. The second step is to solve the matrix feature value. According to the confirmation matrix of the constructed, the characteristic vector corresponding to the maximum feature root is obtained, which is the weight of each evaluation factor. The maximum characteristic root and feature vectors of each matrix are calculated using the accumulation method, and the specific methods are as follows:

(1) Standardize columns in the matrix P, obtained

$$P_{ij} = \frac{P_{ij}}{\sum P_{ij}} \quad (2)$$

(2) Add and count by line

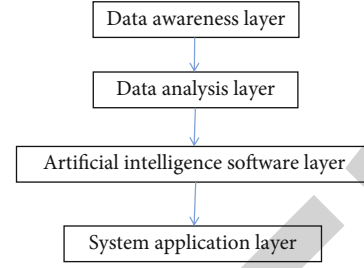


FIGURE 3: Tourism integrated system model based on artificial intelligence software.

$$W_i = \sum P_{ij} \quad (3)$$

(3) Standardization weight

$$W_i = \frac{W_i}{\sum W_{ii}} \quad (4)$$

(4) Calculate the maximum characterization of the matrix

$$\lambda = \frac{1}{\sum_{n=1}^n [(p, W_i)/W_i]} \quad (5)$$

(5) Judgment matrix consistency test

The ratio analysis method uses the ratio of the consistency index (CI) of the judge matrix and the corresponding random consistency index (RI), and the random consistency ratio (CR) is tested, and it is considered that when $CR < 0.10$, the determination matrix is satisfactory consistency in:

$$CI = \frac{(\lambda - n)}{(n - 1)} \quad (6)$$

$$CR = CI \div RI \quad (7)$$

RI can be obtained by judging the corresponding order (n) of the matrix.

3.3.3. *Evaluation Model Establishment.* Big data, Artificial intelligence software, mobile internet, cloud computing, etc. in the smart tourism integrated system, in the smart tourism system, which constructs Artificial intelligence software cultural tourism resource recommendation model, respectively. Reference Fuzzy Mathematics Medium Partition Functions and Fuzzy Comprehensive Evaluation Methods, using weighted and multi-indicators comprehensive evaluation model are used to calculate cultural tourism resource evaluation value. Construct the tourism integrated

system model based on artificial intelligence software as shown in Figure 3.

- (1) The first layer is the data perception layer, which mainly introduces how the data of tourism demand side and tourism supply side are connected with the network, mainly the application of mobile Internet technology
- (2) The second layer is the data analysis layer, namely, the big data analysis layer, which mainly contains four key steps: data collection, data cleaning, data processing and data analysis. There are two main methods to collect big data: one is through sensors and the second is the crawler that collects Internet network data information
- (3) The third layer is the artificial intelligence layer, which is mainly the application of artificial intelligence technology in the intelligent tourism integrated system, mainly including machine learning intelligent perception, intelligent reasoning and intelligent action. Machine learning should build a suitable learning model according to the actual situation of different scenic spots, regions, and each scenic spot as well as the specific goals they want to achieve
- (4) The fourth layer is the system application layer, that is, the application of tourism integrated system. The whole tourism integrated system is not a simple system but a complex one, which integrates big data, artificial intelligence mobile internet, cloud computing, and other technologies
- (5) Select the evaluation factor C layer of the evaluation index system as an evaluation factor set $C = \{C_1, C_2, \dots, C_m\}$
- (6) Determination of the indicator value. Most of the indicators in the indicator system can be obtained or calculated from the statistics of each tourism resource location. Indicators are difficult to quantify in the indicator system, and the various indicators are scored in the way of the expert to inquire and answer questions. On this basis, referring to the description and calculation of the indicators of Table 1, according to the corresponding standards and methods, the score of C_i is determined, and the results are represented by $A_i (i = 1, 2, \dots, n)$. In order to simplify the calculation, it is considered that as long as the measured value of u_i is within the standard section of the score corresponding to a certain score, the membership degree between this interval is 1, and the partition degree of other intervals is 0, so the score of u_i , that is, a score value on this scoring standard section
- (7) Take $B_i (i = 1, 2, \dots, W_m)$ as the corresponding weight value, and establish an equity set $W = \{W_1, W_2, \dots, W_m\}$

- (8) Prior to progressive, the weight value of each evaluation index and the score value are submitted to the following empowerment and multi-index evaluation model, and finally derive the value of an ecological tourism resource evaluation value

$$E = \sum_{b=1}^z \left[\sum_{i=1}^t (C_i W_i) B_b \right] \quad (8)$$

Where E is the total index score; C_i is the score of the Item 2 of the single item; W_i is the weight given by the i -th second level indicator; B_b is the weight given by the first level indicator; t is the number of second level indicators; z is the number of items in the first level.

- (9) According to the comprehensive score of cultural tourism resources (E), cultural tourism resource development value is divided into 4 grades

3.3.4. Artificial Intelligence Software Clustering Model of Tourism and Cultural Resources. On the basis of statistical analysis of artificial intelligence software of tourism cultural resources, the optimization design of artificial intelligence software model of tourism cultural resources is carried out, and a kind of artificial intelligence software model of tourism cultural resources based on big data information fusion and clustering scheduling is proposed. The feature quantity of cross frequent term rules of tourism cultural resources is extracted, and the state parameter description of artificial intelligence software of tourism cultural resources is as follows:

$$M_v = w_1 \sum_{i=1}^{m \times n} (H_i - S_i) + M_h w_2 \sum_{i=1}^{m \times n} (S_i - V_i) + w_3 \sum_{i=1}^{m \times n} (V_i - H_i). \quad (9)$$

By observing the distribution of tourism cultural resources, the grouped control model of tourism cultural resources integration is as follows:

$$x = \sum_{i=1}^N S_i \psi_i = \psi_s, \psi = [\psi_1, \psi_2, \dots, \psi_N]. \quad (10)$$

Among them, ψ_s is the initial probability distribution of tourism cultural resources, $\psi_s = \{\pi_i, i = 1, 2, \dots, N\}$ is the utilization rate of tourism cultural resources, and for tourism cultural resource information set S , the attribute relation of resource information distribution is expressed as $P \subseteq A$ according to the above functional analysis. Under the constraints of fuzzy clustering of tourism cultural resources, the constraint factors of attribute classification evaluation

TABLE 2: Evaluation results of index level (1).

	Fuzzy aggregation (C_i)				Deblurring Pc
	Excellent	Good	Centre	Poor	
Historic site landscape C1	0.144	0.402	0.423	0.030	6.315
Architecture and block views C2	0.432	0.301	0.201	0.062	7.186
Landscape of religious worship places C3	0.2333	0.331	0.222	0.211	6.157
Economic and cultural places and landscape C4	0.242	0.311	0.201	0.244	6.092
Cultural tourism landscape resources B1	0.228	0.339	0.272	0.119	6.142

Note: In the specific calculation process, each level is evaluated as a mean, Tables 3 and 4 and Figure 4.

TABLE 3: Evaluation results of the index level (2).

	Fuzzy aggregation(C_i)				Deblurring Pc
	Excellent	Good	Centre	Poor	
Ecological tourism settlement environment C5	0.512	0.311	0.100	0.076	7.513
Regional factor environment C6	0.364	0.382	0.165	0.087	7.036
Regional facilities and material environment C7	0.132	0.341	0.211	0.313	5.569
Community economic integrated environment C8	0.122	0.312	0.343	0.232	5.693
Cultural tourism environment and environmental resources B2	0.315	0.341	0.177	0.166	6.605

TABLE 4: Evaluation results of the index level (3).

	Fuzzy aggregation(C_i)				Deblurring Pc
	Excellent	Good	Good	Poor	
Customer source conditions C9	0.256	0.322	0.213	0.207	6.244
Location conditions C10	0.075	0.202	0.312	0.410	4.879
Policy conditions C11	0.334	0.323	0.265	0.077	6.823
Conditions for cultural tourism development B3	0.251	0.298	0.254	0.196	6.203

of tourism cultural resources can be obtained as follows:

$$ind(P) = \left\{ \begin{array}{l} (x, y) \in U^2 | a(x) = a(y), \\ \forall a \in P \end{array} \right\}. \quad (11)$$

The fuzzy correlation degree features of tourism cultural resources are calculated, and the c-means clustering method is adopted for big data fusion processing of the extracted correlation features of tourism cultural resources. At the significance level, the c-means clustering model is as follows:

$$L_\zeta = \begin{cases} |f(x) - y| - \zeta |f(x) - y| \geq \zeta \\ 0, |f(x) - y| < \zeta \end{cases}. \quad (12)$$

3.4. Recommended Strategy of Cultural Tourism Resources. The main goal of the recommendation strategy is to recommend a series of POIs during the process of users. The recommended strategy consists of the following three phases: (1) prefiltration: at this stage, the system first learns the user's information, which is based on social network analysis to get the relevant location and interest, and selects a tourist attraction of tourist attractions that may be interested in users; (2) sort: dynamic knowledge based on social network

behavior, allocating three different scores, namely, interest, emotion, and popularity for tourist attractions selected in the previous phase; (3) after filtration: at this stage, the three fractions are combined according to the user's location and the probability of cultural attraction and travel ontology.

3.4.1. Prefiltering Phase. The purpose of this phase is to determine a tourist attraction subset of specific users based on location, popularity, and user interest ($\hat{O} \subseteq O$). First, the user position is obtained according to the latitude and longitude, and the closer to the user's tourist attraction constitutes subset A. Then, by analyzing the user data log, you can get the subset B of the tourist attraction of the visitor, that is, a subset of the highest flush. Finally, when the user selects a tourist attraction using the machine learning technology, the last subset C is obtained by learning the user profile. The machine learning technology is a simple Bayesian classifier, which is a probability classifier based on the Bayesian theorem. The machine learning technique used calculates the association probability of each object relative to the user profile: adding a tour attraction with a given threshold λ to the subset C. The initialization set C is empty set, for any $o \in O$ existence $\lambda \geq 0$, when satisfying the relationship of the following formula $o \in O$, the tourist attraction 4 is added

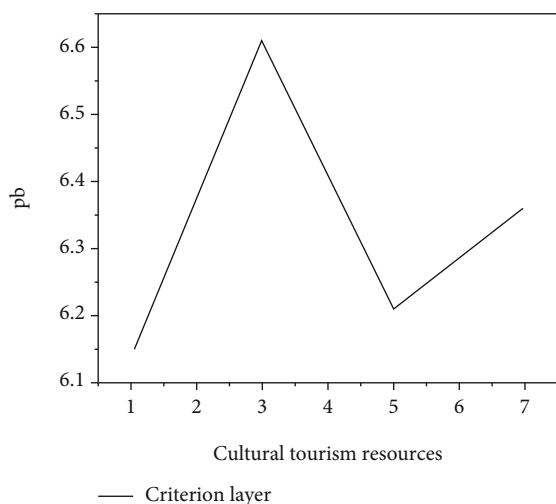


FIGURE 4: Standard layer evaluation results.

to the collection C.

$$P(x|o) = \frac{P(x|o)P(o)}{P(o)} \geq \lambda. \quad (13)$$

4. Result Analysis

4.1. Model Application: Western Cultural Tourism Resources Evaluation

4.1.1. Research Background. This item is conducted on two different scenic spots in the western part during the May 1 Golden Week. This study adopted a method of combining a field interview survey. According to the design and research questionnaire of cultural tourism resource evaluation index system, randomly extract tourists and surroundings in the scenic spot for the visit subjects, on-site filing, on-site interviews, and live recycling. 320 questionnaire were issued, 242 valid questionnaires were recovered, and the recovered efficiency was 75.62%. The surveillance include 182 men (56.88%) and 138 women (43.12%), aged from 18 to 71 (Table 2).

4.1.2. Evaluation Results. According to the previous article, the judge matrix is established, and the weight is determined, and the E value is finally obtained.

From the above evaluation results, we can see that, first, the evaluation results of cultural tourism resources in the western region have good E value 6.346, which has good development value. This result will provide an important agreement for the leading industrial status and tourism development concept of continuing to strengthen the tourism industry in the western region. Secondly, from the specific evaluation results of each level, the standards of cultural tourism in the western region is the highest, 6.605. Cultural tourism resource landscape resources and development conditions score are relatively low. Among them, cultural tourism resources landscape resources are the highest (7.186), the lowest score of the economic and cultural field (6.092). This has a high con-

sistency with the current development status and the author's research location. The cultural tourism landscape of the scenic spot is won by the ancient city building and the street, but there is a lack in the landscape development of economic and cultural places. Among cultural tourism development conditions, policy conditions are high (6.823), but the location conditions are very low, only 4.879 points. This means that the location and traffic disadvantages in the western region are still important to restrict the development of western cultural tourism, and the strong support of government policies is to promote the strong power development of cultural tourism resources in the region. Similarly, in the highest score, cultural tourism environmental resource indicators, cultural tourism gathering environment and regional elements are ideal, but the regional facilities environment, the comprehensive environment of community economy is poor, which is also working in cultural tourism development in the western region direction. Finally, through the simple application of cultural tourism resource evaluation model, this model is found to be evaluated by cultural tourism and landscape resources, cultural tourism environmental resources, and cultural tourism development conditions as cultural tourism resources, more comprehensive and strong hierarchical and targeted sex, and fuzzy comprehensive evaluation methods have strong objectivity for the determination of weight.

5. Conclusions

From the perspective of Artificial intelligence software, explore the construction of smart tourism data analysis model. A cultural tourism resource recommendation model based on Artificial intelligence software is proposed. The system is experimentally verified using a real data set. The experimental results show that the system has better performance. In a future study, the system will be implemented to real application scenarios, further verify the effectiveness of the system and make corresponding improvements in a targeted manner.

Conflicts of Interest

The authors declare that they have no conflicts of interest.

References

- [1] K. B. Tokarska, C. F. Schleussner, J. Rogelj, M. B. Stolpe, and N. P. Gillett, "Recommended temperature metrics for carbon budget estimates, model evaluation and climate policy," *Nature Geoscience*, vol. 12, no. 12, pp. 964–971, 2019.
- [2] V. P. Sriram, A. Mathur, C. J. Aarthy, B. Basumatary, and H. Pallathadka, "Model based using artificial intelligence software to overcome the human resource problem in the healthcare industry," *Annals of the Romanian Society for Cell Biology*, vol. 25, no. 4, pp. 3980–3992, 2021.
- [3] T. Mothoagae and N. Joseph, "The design of a Bayesian network model for increasing the number of graded tourism establishments," *African Journal of Hospitality Tourism and Leisure*, vol. 9(5), no. 9(5), pp. 793–809, 2020.
- [4] T. M. Ikusemiju and O. B. Osinubi, "Improving the cultural and historical tourism resources for sustainable development

Retraction

Retracted: Signal Optimization of Electronic Communication Network Based on Internet of Things

Journal of Sensors

Received 17 October 2023; Accepted 17 October 2023; Published 18 October 2023

Copyright © 2023 Journal of Sensors. This is an open access article distributed under the Creative Commons Attribution License, which permits unrestricted use, distribution, and reproduction in any medium, provided the original work is properly cited.

This article has been retracted by Hindawi following an investigation undertaken by the publisher [1]. This investigation has uncovered evidence of one or more of the following indicators of systematic manipulation of the publication process:

- (1) Discrepancies in scope
- (2) Discrepancies in the description of the research reported
- (3) Discrepancies between the availability of data and the research described
- (4) Inappropriate citations
- (5) Incoherent, meaningless and/or irrelevant content included in the article
- (6) Peer-review manipulation

The presence of these indicators undermines our confidence in the integrity of the article's content and we cannot, therefore, vouch for its reliability. Please note that this notice is intended solely to alert readers that the content of this article is unreliable. We have not investigated whether authors were aware of or involved in the systematic manipulation of the publication process.

Wiley and Hindawi regrets that the usual quality checks did not identify these issues before publication and have since put additional measures in place to safeguard research integrity.

We wish to credit our own Research Integrity and Research Publishing teams and anonymous and named external researchers and research integrity experts for contributing to this investigation.

The corresponding author, as the representative of all authors, has been given the opportunity to register their agreement or disagreement to this retraction. We have kept a record of any response received.

References

- [1] B. Feng, W. Li, and L. Wang, "Signal Optimization of Electronic Communication Network Based on Internet of Things," *Journal of Sensors*, vol. 2022, Article ID 3711776, 8 pages, 2022.

Research Article

Signal Optimization of Electronic Communication Network Based on Internet of Things

Bo Feng ¹, Wei Li ¹ and Lina Wang ²

¹Shijiazhuang Institute of Railway Technology, Shijiazhuang, Hebei 050041, China

²School of Future Information Technology, Shijiazhuang University, Shijiazhuang, Hebei 050035, China

Correspondence should be addressed to Wei Li; k17401229@stu.ahu.edu.cn

Received 7 August 2022; Revised 27 August 2022; Accepted 12 September 2022; Published 24 September 2022

Academic Editor: C. Venkatesan

Copyright © 2022 Bo Feng et al. This is an open access article distributed under the Creative Commons Attribution License, which permits unrestricted use, distribution, and reproduction in any medium, provided the original work is properly cited.

In order to solve the problem that many people communicate at the same time, there are many external interference factors, and the signal is prone to instability in the process of electronic communication, the author proposes a signal optimization method for electronic communication network based on the Internet of Things. The method takes the cloud trust mechanism as the dynamic evolution trust relationship between various Internet of Things electronic communication services, performs explicit and implicit uncertainty conversion, calculates the objective function of data communication network performance, and confirms the control strategy. The positioning information of the network nodes in the communication is added to the communication data packet, and the most stable electronic communication path in the network is obtained to form the network topology structure. The Krasovsky method is adopted, and the working state of the nodes of the communication network is divided into the congested state and the normal state, the probability of the two is calculated, and the range of the transition balance is determined, so as to realize the optimization of the stability of the network topology. Experimental results show that the transmission rate of this method has been maintained at about 180 Kb/s; although there is fluctuation, the fluctuation value is small and the transmission rate is very stable. *Conclusion.* It can improve the accuracy of electronic communication of the Internet of Things and is less affected by external interference factors, and the communication transmission rate is faster.

1. Introduction

The development of communication technology is inseparable from electronic communication technology, and the design of electronic communication technology system involves various fields of social life and production [1, 2]. The impact of big data analysis on mobile communication network optimization has two sides, it can not only provide a way to find, analyze, and solve problems for mobile communication network optimization but also has a strong complexity, which increases the complexity of fault analysis. The main goal of mobile communication network optimization is to analyze and collect relevant data, apply scientific and reasonable methods, reduce the interference of external factors, eliminate faults, and ensure the stability and security of mobile

communication networks [3, 4]. In the context of big data, the structure of the mobile communication network is more complex and the functions are more powerful, and only by fully understanding and mastering the performance of the mobile communication network, in order to improve the efficiency of troubleshooting, create a safe and stable communication environment for users.

In the era of big data, the massive generation of various data has enriched people's life activities to a large extent, and the work efficiency is getting higher and higher, which puts forward higher requirements for the operation quality and carrying capacity of mobile communication networks [5]. In the era of big data, the update speed of mobile terminals is very fast, and the cutting function is more and more powerful; if the quality of the mobile communication network does not meet

the standard, it will inevitably have a serious impact on the user experience [6]. Therefore, the design of the mobile communication network on the Internet must meet the premise of user usage and reduce the interference of external factors, so as to maximize the technical flexibility of the mobile communication network. With the continuous development of information technology, a large amount of data is generated every day; through incomplete unification, the amount of data generated is almost rising in a steep straight line [7]. Therefore, one of the most important problems faced by big data analysis in the optimization of mobile communication networks is that the data is too large.

Cloud computing technology is mainly based on resource model and information technology, which is a new computer technology [8, 9]. Because of the characteristics of cloud computing itself and its advantages in practical applications, cloud computing has become an advanced technology used in current computer networks. The characteristics of cloud computing are mainly manifested in strong reliability, versatility, low risk, and virtualization. Among them, virtualization is regarded as the most important feature. Virtualization is realized by means of various hardware facilities and networks, and there is also a very important premise, that is, a resource sharing environment needs to be created first. People can access shared resources at any time, so that they can get various services provided by cloud computing. Figure 1 shows the online monitoring of transmission lines based on IoT wireless communication [10].

2. Literature Review

If a communication company wants to achieve network optimization, it is necessary to do a good job of data acquisition optimization first, in order to further improve the acquisition quality, in order to ensure that the collected data is more authentic and accurate, and in order to meet the needs of network optimization [11, 12]. Therefore, in the actual optimization, the service base should be scientifically designed according to the specific situation of the network, and then, the entire work of data collection should be optimized, so that the relevant personnel can better complete the data sorting and analysis work. Data collection will be affected by many factors, and the location of the base is the most important factor; this requires that the most suitable location and service base should be selected according to the actual situation of the area during optimization, so as to improve the quality of data analysis and collection and provide effective guarantee for the reception of service base signals [13]. In addition, during optimization, the collection of user-related information should be further strengthened according to the actual operation of the network and data collection, and then, the collected information should be used as a basis to create a corresponding data network.

Cloud computing has an obvious feature in application, that is, by storing data in the cloud, it can expand the storage space and facilitate people to call; therefore, in order to achieve network optimization under cloud computing, it is necessary to optimize cloud applications [14, 15]. Faced with this situation, it is required that the network can be perfectly

integrated with cloud computing during actual operation, improve the network operation mode, continuously strengthen cloud applications, and further improve the storage and use of cloud resources, thereby expanding the scope of network services and increasing the types of services. After the integration of cloud technology and network, relevant staff also need to analyze cloud data, optimize the structure and procedures of the network itself, and then improve the efficiency of network operation [16].

Song et al. aimed at the communication process of in-vehicle Internet (VANET), due to the problem that the channel state becomes fast and nonstationary due to the dual motion of the transceiver. A nonstationary channel method for vehicular communication is proposed [17]. An integral term is introduced to ensure the continuity of the fading phase of the output channel, and the time-varying characteristics of the transceiver are considered to complete the accurate calculation of the Doppler frequency parameters. In order to improve the two-dimensional servo stability of laser communication, Cheng et al. used the gyroscope correction optimization method, applied the centroid optimization method, gyroscope, CCD (charge-coupled device), the dynamic performance optimization of the two-dimensional servo system is realized by introducing the method of fast convergence of small values in the same direction [18]. However, the previous research methods can only achieve normal communication; if many people communicate at the same time and there are many external interference factors, the communication stability will be poor; to this end, the author adds the location information of the communication network node into the communication data packet, and the most stable communication path is obtained to realize the optimization of communication stability.

3. Methods

3.1. Cloud Trust-Driven IoT Communication Objective Function and Dynamic Model Construction. In cloud computing, the cloud trust mechanism can realize the dynamic evolution trust relationship between IoT and communication services, as well as explicit and implicit uncertainty transformation, which is also one of the important conditions for realizing communication security [19, 20].

Assuming that the data communication network is composed of N nodes and L edges, the link sets of nodes are represented by χ, \wp , respectively, and the specific link $l_i \in \wp, i = 1, 2 \dots L$ information flow model is shown in Figure 2 [21].

Among them, $\lambda_{si}(t)$ is the input rate of external information flow of link l_i , $\lambda_{ti}(t)$ is the other link in the network, the rate at which information flow is forwarded through l_i , and μ_i represents the information service rate of l_i [22]. Set $x_i(t) \geq 0$ to be the number of packets at time t at l_i (including the number of packets received and queued); that is, $\lambda_{si}(t) = \beta_i \lambda_i(t)$ and $0 \leq \beta_i \leq 1$ are variables of l_i flow control, $\lambda_i(t)$ represents the input rate of source l_i information, $\lambda_{si}(t) = \sum_{l \in (l)} \mu_l G_l[x_l(t)]$, $\mu_l G_l[x_l(t)]$ represents the dynamic information output of link l at time t , $0 \leq G_l(\cdot) \leq 1$, $l \in \wp$ represents

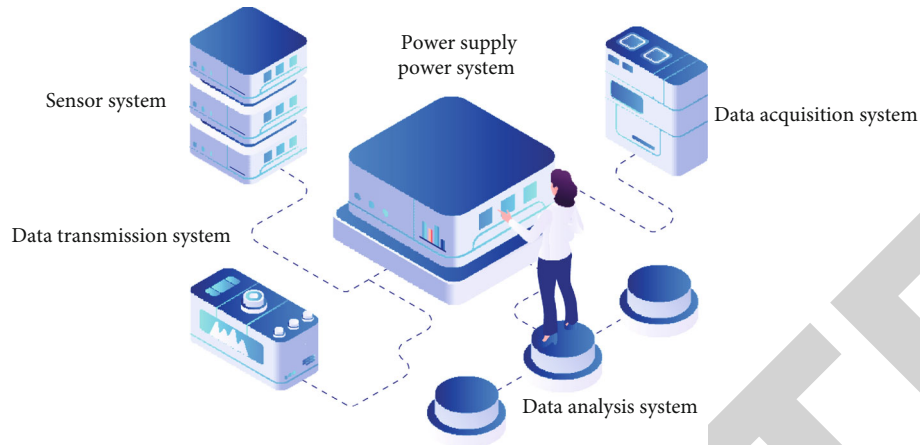


FIGURE 1: Online monitoring of transmission lines based on Internet of Things wireless communication.

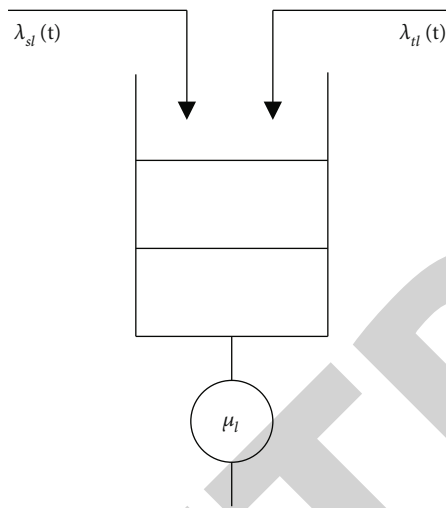


FIGURE 2: Information flow model of the overall link.

the transmission state $x_i(t)$ of link l , and as many factor functions such as link communication protocol, $I(i)$ and $O(i)$, respectively, represent the set of links that input information to link l_i and output information to link l_i [23].

If $x_i(t)$ represents the variable of the $l_i \in L$ state model, then the description formula of the $x_i(t)$ dynamic model is

$$\dot{X}_i(t) = -\mu_i G_i[X(t)] + \sum_{l(i)} \mu_l G_l[X_l(t)] + \beta_i \lambda_i(t). \quad (1)$$

In the computer network, the method of packet switching is used to shorten the average waiting time of users, and to improve the information flow in the network is the main goal of control and optimization. If the reduction in average latency is equal to the reduction in the number of users staying in each network, the number of packets on the link will also be reduced by the formula

$$\min J_1(t) = \sum_{l \in \varphi} \int_{t_0}^{t_f} x_l(t) dt, \quad (2)$$

$$\min J_2(t) = \sum_{l \in \varphi} \int_{t_0}^{t_f} (\varphi_j \beta_j \lambda_j(t)) dt. \quad (3)$$

In the formula, $\varphi_j > 0$ represents the network access income of receiving unit information, t_0 and t_f represent the start and end time of the control interval, and the performance objective function selection determines the overall performance and control strategy [24].

3.2. Electronic Communication Stability Optimization

3.2.1. Analysis of Stability Factors of Electronic Communication Network. In the process of optimizing the topology stability in the electronic communication network, at the node position, the network node positioning information in the communication process is added to the grouping of the communication data, so as to obtain the most stable communication path in the electronic communication network, the topology model of the electronic communication network is formed, so as to obtain the topology and distance relationship between the communication signals, and the main factors affecting the topological stability of the communication network are described through this relationship. The steps are as follows:

In the stability optimization process of the network topology in the electronic communication, the range of the communication signal is set to a circle with R as the radius, and the signal B of the electronic communication is within the coverage of the signal A of the communication signal; use u_1 to indicate the communication speed to A , use u_2 to indicate the speed of B communication transmission, and use (x_0, y_0) to indicate the original position of the communication signal A ; (x'_0, y'_0) represents the original position of the communication signal B , and (x_1, y_1) and (x_2, y_2) represent the real-time positions of communication signals A and B , respectively. The formula for calculating the distance between A and B is

$$d = \frac{(x_0, y_0) \times (u_1 + u_2)t}{(x'_0, y'_0) \times (x_1, y_2) * (x_2, y_2)} (A, B). \quad (4)$$

If the transmission distance of the electronic communication signal A at t is d_1 and the distance of the electronic communication signal B at t is d_2 , then the distance between the electronic communication signals A and B is S . According to formula (4), the distance between communication signals can be calculated, and the topology model of constructing electronic communication network can be obtained. The specific formula is

$$S_0 = \sqrt{\frac{(x_0 - x'_0)^2}{d_1(A, B)} + \frac{|y_0 - y'_0|^2}{d_2(A, B)}}. \quad (5)$$

In the formula, $(x_0 - x'_0)$ and $(y_0 - y'_0)$ represent constants.

By fusing formula (4) and formula (5), formula (6) can be deduced to represent the topology and distance relationship between electronic communication signals. The specific formula is

$$\omega = \frac{(x_0 - x'_0)^2 + |(x_1 - x_2)_0|^2}{d} \times S_0. \quad (6)$$

When the electronic communication signals A and B change during the transmission process, the distance is difficult to keep stable and also changes. Therefore, adding ω in formula (6), using formula (7) to describe the main factors affecting the topological stability of the communication network, the specific formula is

$$p_2 = \frac{\{t|\bar{S}_1 \geq \bar{S}_2\}}{\omega}. \quad (7)$$

In the formula, \bar{S}_1, \bar{S}_2 represents the node degree distribution sequence of the topological upper layer of the electronic communication signals A and B, and the topological stability of the network is described by formula (7), which is the basis for the optimization of communication stability [25].

3.2.2. Stability Optimization Implementation. The Krasovsky method is used to define the main factors affecting the topological stability of the electronic communication network within the stable range, and the working state of the nodes of the electronic communication network is divided into the congested state and the normal state. The range of the probabilistic transition balance between the two is calculated, thereby realizing the optimization of network topology stability. The specific process is as follows:

The state node of normal communication transmission mainly uses α to represent the probability to convert into a congested state node. In the crowded state, β is used to represent the probability of converting to a normal state node. $p_i(t)$ is used to represent the availability probability of the i th node in the network at time t , and the main factors affecting the stability of electronic communication are set in the stable range by the Krasovsky method. The specific

formula is

$$\frac{dp_i(t)}{dt} = \alpha p_i(t) \frac{[1 - p_i(t)]k_{i,\lambda} - \beta p_i(t)k}{p_2}. \quad (8)$$

In the formula, $k_{i,\lambda}$ represents the heterogeneous topological structure mode in the communication network.

Taking Equation (8) as the basis, the equilibrium point between the crowded state and the normal state is deduced. The specific formula is

$$\frac{\alpha p_i(t)}{k_{i,\lambda}} = -\beta \times p_i(t)k. \quad (9)$$

Based on formula (9), the value of the equilibrium point is calculated by formula (10). The specific formula is

$$p_0 = 1 - \frac{\beta k_i}{\alpha k_{i,\lambda}} \times \frac{dp_i(t)}{dt} \times \frac{\alpha p_i(t)}{k_{i,\lambda}}. \quad (10)$$

In the formula, k_i represents the frame structure of the communication network data.

Randomly select m transmission nodes of the network in electronic communication, add the calculation result of formula (10) to formula (11), and establish a Jacobian matrix. The specific formula is

$$F(P) = \frac{\partial f(p)}{\partial p_0} = \left[\frac{\partial f_m}{\partial p_1} \times \frac{\partial f_m}{\partial p_m} \right]. \quad (11)$$

In the formula, $\partial f(p)$ represents the in-degree value of the electronic communication network node, ∂P^T represents the out-degree value of the electronic communication network node, ∂p_1 represents the data overflow of the electronic communication network node buffer, and ∂f_m represents the highest connection degree value of the node in the network.

The above Jacobian matrix is a diagonal symmetric matrix, based on the establishment of the matrix, formula (12) is used to convert the stability optimization model of the network topology in the communication, and it is transformed into the working state balance problem of the network nodes. The specific formula is

$$\hat{F}(P) = \frac{F^T(P) + Ft(P)}{P_0} = 2 \mp [\alpha - 2\alpha p_i(t)]. \quad (12)$$

In the formula, $F^T(P)$ represents the communication link bandwidth of the network.

Using Krasovsky's method, the $\hat{F}(P)$ is brought into the set communication network stability limit, and the specific formula is

$$(\alpha - 2\alpha p_i(t))k_i - \beta k_i = \frac{F(P)}{\hat{F}(P)} \times p_i(t). \quad (13)$$

In the formula, the condition $\alpha \leq \beta$ must be satisfied.

Through the formula (13), the concept conversion balance range of the electronic communication network (congested state and normal state) can be obtained. The specific judgment formula is

$$i = \sum_{i=1}^n \frac{\alpha - \beta}{2\alpha} \otimes \frac{[\alpha - 2\alpha P_i(t)]k_i - \beta k_i}{F(P)}. \quad (14)$$

By setting a reasonable range of electronic communication network conversion balance, the stability optimization of electronic communication network can be realized.

3.3. Simulation Proof

3.3.1. Experimental Environment. In order to verify the effectiveness of the proposed method, the simulation environment is set as follows: "Pentium" (R) "Dual-Core" CPU, 2.8 GHz, 4 GB "RAM," Windows 732 bit, and "MATLAB R2013a." The simulation analysis is carried out in the simulation platform Net Logo, and the data rate of the user is set to 200 Kb/s, the bandwidth is 4 M, the communication radius is 15 m, and the network area size is 1000 * 1000. The specific experimental data are shown in Table 1.

4. Results and Discussion

4.1. Analysis of Experimental Transmission Accuracy. The communication transmission accuracy optimized by the proposed method is analyzed, and the specific results are shown in Figure 3.

By observing Figure 3, it can be seen that when the number of experiments is 10, the communication accuracy of the proposed method is 98%. Although there were slight fluctuations in the experimental results after that, the difference was not large and remained above 95%, and only when the number of experiments was 40, accuracy was greatly reduced, with an average of 88%, after a record investigation. It was found that the reason for this phenomenon was that the test user made mistakes in the transmission process, resulting in inaccurate part of the experimental data, the experimental results obtained in the end have deviations, and when the number of experiments reaches 50, the external interference disappears, and the accuracy recovers to more than 95%. Until the end of the experiment, the accuracy of the proposed method is maintained at more than 95%, indicating that the proposed method data transfer can be performed efficiently.

4.2. Comparative Analysis of Transmission Rate. Under the same conditions, the communication transmission efficiency is selected as the comparison result of this experiment, and the number of experiments is 60 times. Then, the proposed method is compared with the nonstationary channel simulation method for Internet of vehicle communication, and the dynamic performance optimization system of servo stability system for mobile laser communication equipment is used for comparison. The specific comparison results are shown in Figure 4.

TABLE 1: Experimental environment.

Experimental parameter name	Numerical settings
Experimental scene (L-W)	150 m * 100 m
Number of network nodes (N)	30~50
Maximum transmission radius	15 m
Threshold radius (r)	7.5 m
Moving speed (u)	0.5 m/s~5 m
Pause time	Os
Weight factor	$W_1 = W_2 = 1$
Starting distribution	Evenly distributed
Data transfer interval	3 s
Experimental test time	500 s

By observing Figure 4, it can be seen that the transmission rate of the proposed method has been maintained at about 180 Kb/s. Although there is fluctuation, the fluctuation value is small, and the transmission rate is very stable. The nonstationary channel simulation method for IoV communication is maintained at about 130 Kb/s, and the fluctuation is also small and relatively stable, but the transmission rate is low. However, the dynamic performance optimization system of the servo stabilization system of mobile laser communication equipment has a transmission rate of 90 Kb/s when the number of experiments is 10, and the subsequent experiments show large fluctuations, and the curve fluctuates up and down, which cannot meet the actual needs.

The load simulation is carried out in the simulation environment, by simulating the simultaneous communication state of multiple users, it is observed whether the communication process will be crowded, and the transmission efficiency will be reduced. The specific results are shown in Figure 5.

By observing Figure 5, it can be seen that when simulating the communication of 100 users at the same time, the transmission rates of the three methods are almost the same, and the difference is not large. When simulating 500 users, there is a small difference in the transmission rate among the three, while when simulating 2000 users, the transmission rates of the three methods have significant differences. At the end of the experiment, the transmission efficiency of the proposed method is reduced to 85%, the nonstationary channel simulation method for IoV communication is reduced to 65%, and the dynamic performance optimization system of the servo stabilization system of mobile laser communication equipment is reduced to 50%. Although all three methods increase with the number of communications, as a result, the transmission rate of communication is reduced, but the proposed method decreases less than the other two methods, which shows that after the proposed method optimizes the transmission stability, not only the communication accuracy is high but also the transmission rate is also obvious.

4.3. Comparative Analysis of External Interference. In order to further prove the application effect of the proposed

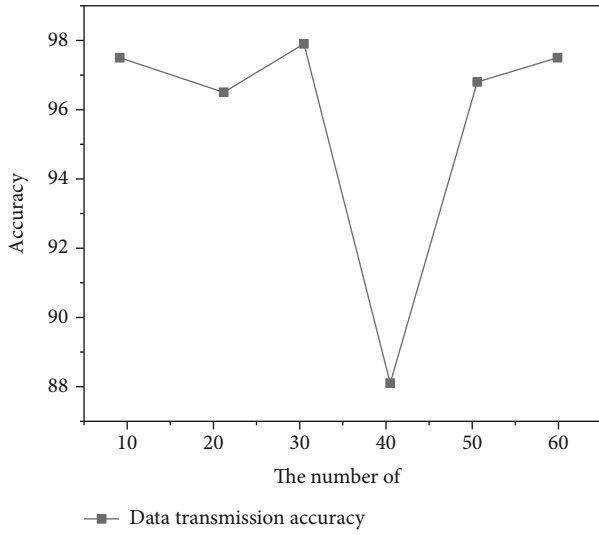


FIGURE 3: Data transmission accuracy results after stability optimization of the proposed method.

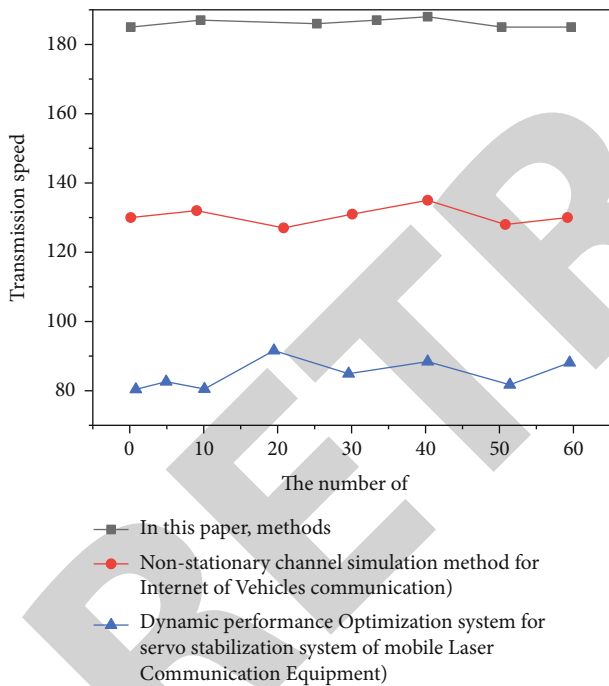


FIGURE 4: Comparison results of transmission rates of three methods.

method, the external interference signal is artificially created, at the same time, in order to avoid the communication distance being too close, and the artificially created interference signal has no effect or cannot clearly reflect the strength of the communication interference signal and increase the communication distance so that the transmission signal is in a state of weak transmission. The proposed method is compared with the nonstationary channel simulation method for IoV communication and the dynamic performance optimization system of the servo stabilization system

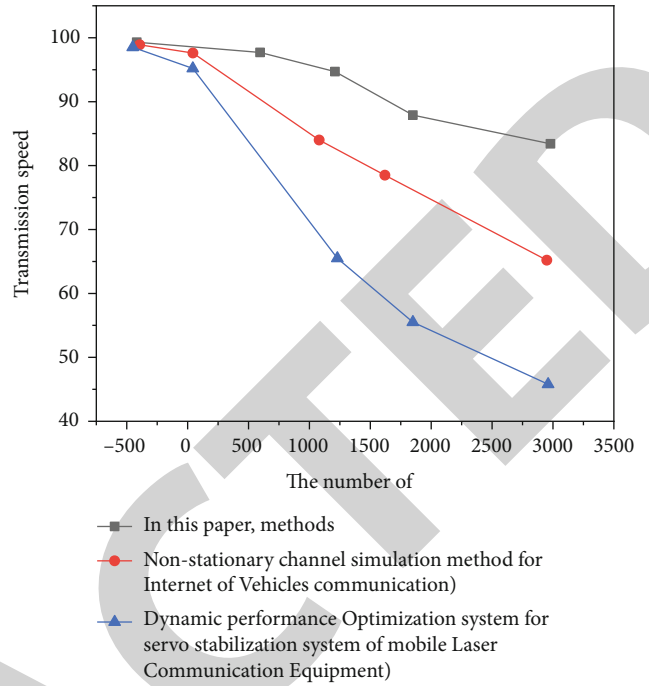


FIGURE 5: Comparison of the results of simultaneous communication with the number of individuals in the three methods.

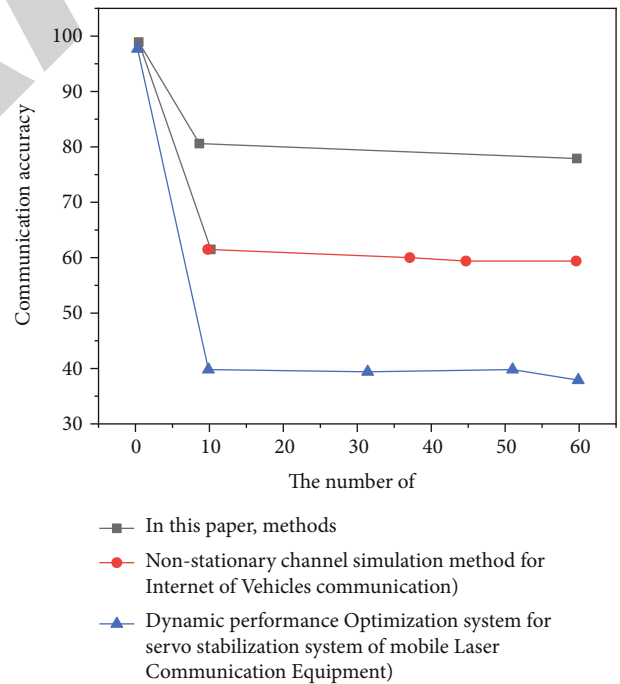


FIGURE 6: Comparison of three methods of communication signal transmission.

for mobile laser communication equipment under the same conditions. The specific results are shown in Figure 6.

By observing Figure 6, it can be seen that under the influence of external interference signals, the proposed method adopts the Krasovsky method, and the main factors affecting

the topology stability of the electronic communication network can be determined as a fixed range; therefore, although the communication signal dropped slightly, when it dropped to 80%, it almost stopped dropping, maintaining the current signal state, during data transmission, and there is no data loss, while the nonstationary channel simulation method for IoV communication shows a significant drop, and when it drops to 60%, there is a slight data loss. However, the dynamic performance optimization system of the servo stabilization system of the mobile laser communication equipment drops to 50%. During the communication process, the data is seriously lost and even cannot be transmitted.

5. Conclusion

The author proposes the optimization of electronic communication network signals based on the Internet of Things and proposes a cloud trust-driven Internet of Things electronic communication stability optimization method. When the accuracy of communication signals drops to 80%, almost no longer drops, maintaining the current signal state, and the transmission rate has been maintained at about 180 Kb/s, indicating that after stability optimization, not only the accuracy of communication transmission is high, and when multiple people transmit, the transmission rate is faster and the stability is stronger. In future research, it is not only necessary to make the communication process more stable but also to improve the speed, scope, and complexity of communication, so as to cope with the uncertainty of scientific development and communication scenarios.

Data Availability

The data used to support the findings of this study are available from the corresponding author upon request.

Conflicts of Interest

The authors declare that they have no conflicts of interest.

Acknowledgments

This work was supported by the China University Industry University Research Fund (2021BCB02005) and Ministry of Education Vocational Education Reform and Innovation Funding (HBKC217034).

References

- [1] X. Xu, L. Li, and A. Sharma, "Controlling messy errors in virtual reconstruction of random sports image capture points for complex systems," *International Journal of Systems Assurance Engineering and Management*, vol. 3, 2021.
- [2] M. Bradha, N. Balakrishnan, A. Suvitha et al., "Experimental, computational analysis of butein and lanceoletin for natural dye-sensitized solar cells and stabilizing efficiency by IoT," *Environment, Development and Sustainability*, vol. 24, no. 6, pp. 8807–8822, 2022.
- [3] J. Chen, J. Liu, X. Liu, W. Gao, J. Zhang, and F. Zhong, "Degradation of toluene in surface dielectric barrier discharge (SDBD) reactor with mesh electrode: synergistic effect of UV and TiO₂ deposited on electrode," *Chemosphere*, vol. 288, p. 132664, 2022.
- [4] R. Huang, S. Zhang, W. Zhang, and X. Yang, "Progress of zinc oxide-based nanocomposites in the textile industry," *IET Collaborative Intelligent Manufacturing*, vol. 3, no. 3, pp. 281–289, 2021.
- [5] H. Xie, Y. Wang, Z. Gao, B. Ganthia, and C. Truong, "Research on frequency parameter detection of frequency shifted track circuit based on nonlinear algorithm," *Nonlinear Engineering*, vol. 10, no. 1, pp. 592–599, 2021.
- [6] A. Qazi, G. Hardaker, I. S. Ahmad, M. Darwich, and A. D. Ahad, "The role of information & communication technology in elearning environments: a systematic review," *IEEE Access*, vol. 9, pp. 45539–45551, 2021.
- [7] I. Raça, F. Dosseville, and O. Sirost, "Analysis of the influence of individual representations on the modalities of practice in long-term towards a perception of the marine environment generating a hybrid socialization based on adventure, nomadism and awakening," *Movement & Sport Sciences - Science & Motricité*, vol. 2022, no. 115, pp. 57–67, 2022.
- [8] R. Szmytkie, A. Latocha, D. Sikorski, P. Tomczak, K. Kajdanek, and P. Miodońska, "Tourist boom and rural revival-case study of Klodzko region (SW Poland)," *Journal of Mountain Science*, vol. 19, no. 4, pp. 909–924, 2022.
- [9] C. Huang and L. Zhu, "Robust evaluation method of communication network based on the combination of complex network and big data," *Neural Computing and Applications*, vol. 33, no. 3, pp. 887–896, 2021.
- [10] T. Szul, "Application of a thermal performance-based model to prediction energy consumption for heating of single-family residential buildings," *Energies*, vol. 15, no. 1, p. 362, 2022.
- [11] W. A. Jadayil, M. Shakoob, A. Bashir, H. Selmi, and M. Qureshi, "Using serviquil to investigate the quality of provided wireless communication services in UAE," *International Journal of Quality and Service Sciences*, vol. 12, no. 1, pp. 109–132, 2020.
- [12] J. A. Neyra and G. N. Nadkarni, "Continuous kidney replacement therapy of the future: innovations in information technology, data analytics, and quality assurance systems," *Advances in Chronic Kidney Disease*, vol. 28, no. 1, pp. 13–19, 2021.
- [13] X. Lv and M. Li, "Application and research of the intelligent management system based on Internet of Things technology in the era of big data," *Mobile Information Systems*, vol. 2021, Article ID 6515792, 6 pages, 2021.
- [14] N. A. M. Said, N. E. Mustafa, and H. L. T. Ariffin, "Integrating cloud in engineering, procurement and construction contract," *Journal of Computational and Theoretical Nanoscience*, vol. 17, no. 2, pp. 893–901, 2020.
- [15] W. Wang, X. Du, D. Shan, R. Qin, and N. Wang, "Cloud intrusion detection method based on stacked contractive auto-encoder and support vector machine," *IEEE transactions on cloud computing*, vol. 6, 2020.
- [16] H. Li, G. Zhao, L. Qin, and Y. Yang, "Design and optimization of a hybrid sensor network for traffic information acquisition," *IEEE Sensors Journal*, vol. 20, no. 4, pp. 2132–2144, 2020.
- [17] J. Song, L. Meng, and J. Chang, "Delivery service optimization when the information on the consumers' time values is asymmetric," *Mathematical Problems in Engineering*, vol. 2020, Article ID 8247179, 8 pages, 2020.

Retraction

Retracted: Optimization of Distribution Automation System Based on Artificial Intelligence Wireless Network Technology

Journal of Sensors

Received 13 September 2023; Accepted 13 September 2023; Published 14 September 2023

Copyright © 2023 Journal of Sensors. This is an open access article distributed under the Creative Commons Attribution License, which permits unrestricted use, distribution, and reproduction in any medium, provided the original work is properly cited.

This article has been retracted by Hindawi following an investigation undertaken by the publisher [1]. This investigation has uncovered evidence of one or more of the following indicators of systematic manipulation of the publication process:

- (1) Discrepancies in scope
- (2) Discrepancies in the description of the research reported
- (3) Discrepancies between the availability of data and the research described
- (4) Inappropriate citations
- (5) Incoherent, meaningless and/or irrelevant content included in the article
- (6) Peer-review manipulation

The presence of these indicators undermines our confidence in the integrity of the article's content and we cannot, therefore, vouch for its reliability. Please note that this notice is intended solely to alert readers that the content of this article is unreliable. We have not investigated whether authors were aware of or involved in the systematic manipulation of the publication process.

Wiley and Hindawi regrets that the usual quality checks did not identify these issues before publication and have since put additional measures in place to safeguard research integrity.

We wish to credit our own Research Integrity and Research Publishing teams and anonymous and named external researchers and research integrity experts for contributing to this investigation.

The corresponding author, as the representative of all authors, has been given the opportunity to register their agreement or disagreement to this retraction. We have kept a record of any response received.

References

- [1] W. Tian, X. Meng, J. Wang, and H. Yan, "Optimization of Distribution Automation System Based on Artificial Intelligence Wireless Network Technology," *Journal of Sensors*, vol. 2022, Article ID 1646667, 8 pages, 2022.

Research Article

Optimization of Distribution Automation System Based on Artificial Intelligence Wireless Network Technology

Weihua Tian ¹, Xiangbin Meng ¹, Jianing Wang ², and Hongkui Yan ¹

¹School of Automation, Shenyang Institute of Engineering, Shenyang, Liaoning 110136, China

²College of Transportation Engineering, Dalian Maritime University, Dalian, Liaoning 116026, China

Correspondence should be addressed to Weihua Tian; 2020220248@mail.chzu.edu.cn

Received 7 August 2022; Revised 27 August 2022; Accepted 5 September 2022; Published 17 September 2022

Academic Editor: C. Venkatesan

Copyright © 2022 Weihua Tian et al. This is an open access article distributed under the Creative Commons Attribution License, which permits unrestricted use, distribution, and reproduction in any medium, provided the original work is properly cited.

In order to further improve the automation setting of distribution system, this paper proposes an optimization research of distribution automation system based on artificial intelligence wireless network technology. This method uses artificial intelligence wireless network technology to optimize the automation of distribution system and improve the automation ability of distribution system. The experimental results show that when the number of iterations in the training process reaches 338, the mean square error is 0.001. *Conclusion.* The optimization research method of distribution automation system based on artificial intelligence wireless network technology can more effectively improve the automation level of distribution system.

1. Introduction

Distribution automation is an important means to improve the reliability of power supply, and it is also an important part of smart grid. From the end of the twentieth century to the beginning of the twenty-first century, there was also an upsurge of pilot construction of distribution automation. However, many early built distribution automation systems did not play their due role, mainly due to two reasons: technology and management. Technical problems include immature technology in the early stage, backward communication means, and defects in the early distribution network. The management problems mainly include the lack of standards and norms to guide the planning, design, construction, operation and maintenance of distribution automation, and the pursuit of one-step “large and comprehensive” results in excessive planning and insufficient later operation and maintenance.

After nearly 10 years of exploration and practice, the distribution automation technology has matured, and the communication technology has made revolutionary progress. Power enterprises have formulated a series of standards and specifications for the design, construction, operation, and maintenance of distribution automation. With the construction of smart grid,

distribution automation system has ushered in a new round of construction climax. The State Grid Corporation of China reviewed the distribution automation project plan in three batches, completed the practical acceptance of all 4 urban distribution automation pilot projects in the first batch, and completed the project acceptance of all 19 urban distribution automation pilot projects in the second batch. This round of distribution automation system has made essential progress over the previous round in terms of automation technology, testing technology, project management, and practicality.

Industrial wireless technology is a new wireless communication technology for information interaction between devices. It is suitable for use in harsh industrial field environment. It has the characteristics of strong anti-interference ability, low-energy consumption, and good real-time communication. It is a special kind of sensor network [1]. At present, the widely used industrial wireless technologies include wireless LAN, Bluetooth, and ZigBee. Through the research of Bluetooth network communication protocol, an embedded network node with ARM9 processor and Bluetooth adapter as the core is designed, which has the functions of analog-to-digital conversion and switching input and output. In the embedded Linux system on ARM9 platform, the device driver is written, the

BlueZ protocol stack is transplanted, and the communication program is developed on the protocol stack to realize the functions of searching devices, discovering services, establishing connections, and sending and receiving data. Therefore, artificial intelligence wireless network technology is used to further optimize the distribution automation system, so as to better carry out the distribution operation and achieve the effect of high automation.

2. Literature Review

With the construction of smart grid and the development of communication technology, distribution automation technology, as an important part of smart grid, it has made great progress and has made many constructive progress in distribution automation master station, terminal, communication network, and testing technology, which has laid a solid foundation for the practical application of distribution automation system. Compared with the previous round of distribution automation research, at present, the greatest progress of the distribution automation master station lies in two aspects: the establishment of an information interaction bus in line with IEC61968 standard and the unified standard information interaction with other information systems. It has a complete and practical fault handling application module.

In practical application, the distribution automation system needs to interact with the upper level dispatching automation, production management system, power grid geographic information system, marketing management information system, and 95598. In the last round of distribution automation construction, the private protocol of “point-to-point” as shown in Figure 1 is used to realize the interconnection of distribution automation system and other application systems. Not only many interfaces need to be maintained, but also because the private protocol adopted is not standard, the interchangeability is poor, and the expansion is difficult. In the figure, EMC is an energy management system.

In the construction of smart grid, the distribution automation system adopts the information interaction bus conforming to IEC61968 standard according to the principle of “unique source data and global information sharing” and completes the information exchange and service sharing between the distribution automation system and other application systems through the bus mode based on message mechanism, as shown in Figure 2. It not only greatly reduces the number of interfaces, but also has the advantages of standardization, strong interchangeability and easy expansion. On the premise of meeting the safety protection regulations of power secondary system, the information interaction bus has the ability to realize information interaction through the forward/reverse physical isolation device through the production control area and the management information area. Follow IEC61968 standard and adopt service-oriented architecture (SOA) to realize the publishing and subscription of relevant models, graphics, and data [2].

The concept of cognitive radio was first proposed because it has good perception, reasoning, and learning ability [3]. These capabilities enable cognitive radio technology to dynamically

adjust the spectrum usage to further improve the spectrum efficiency. This undoubtedly alleviates the current shortage of spectrum resources. However, with the further development of communication technology, wireless networks that introduce the concept of cognition are changing in the direction of complexity, isomerization, and dynamics. Some traditional network management methods are no longer suitable for the complex situation faced by the current network. Therefore, in order to effectively manage the network to meet these challenges, reconfiguration technology is introduced into cognitive wireless networks. Reconfiguration technology maintains the performance of cognitive wireless networks by changing a series of wireless parameters and adjusting the corresponding network behavior. This maintenance can not only ensure the network performance, but also take into account the needs of users when the environment and system requirements change dynamically. The reconfiguration technology applied to cognitive wireless networks can provide a more flexible and adaptive network management method for the network, but correspondingly, the implementation of reconfiguration technology in cognitive networks also needs to rely on the unique perception ability, prediction ability, and learning ability of cognitive networks. The two complement each other and further improve the system performance. The decision-making of reconfiguration is the key part of the realization of reconfiguration technology. The reconfiguration decision first obtains the network parameters that need to be changed by analyzing the factors that affect the performance and then deploys the reconfiguration through calculation to map these changes to the actual network structure. This not only ensures that the system can adapt to the dynamic environment, but also saves the time of system operation.

With the mutual penetration and combination of computer network technology, wireless technology, and intelligent sensor technology, a new concept of networked intelligent sensor based on wireless technology has emerged. This networked intelligent sensor based on wireless technology enables the data of industrial sites to be directly transmitted, published, and shared on the network through wireless links. Wireless communication technology can provide high bandwidth wireless data links and flexible network topology for the communication between various intelligent field devices, mobile robots and various automation devices in the factory environment, effectively make up for the shortcomings of wired networks in some special environments, and further improve the communication performance of industrial control networks. Therefore, compared with other application fields (military, commercial, medical, etc.), wireless sensor networks are very suitable for industrial applications. The concept of micro sensing and the wireless connection of nodes make it of high theoretical and practical significance in the field of industrial measurement and control [4].

According to the above research, this paper proposes a method of distribution automation system optimization research based on artificial intelligence wireless network technology. This method uses wireless network technology to optimize the distribution system automation, and further improves the wireless network technology through reconfiguration decision, so that it

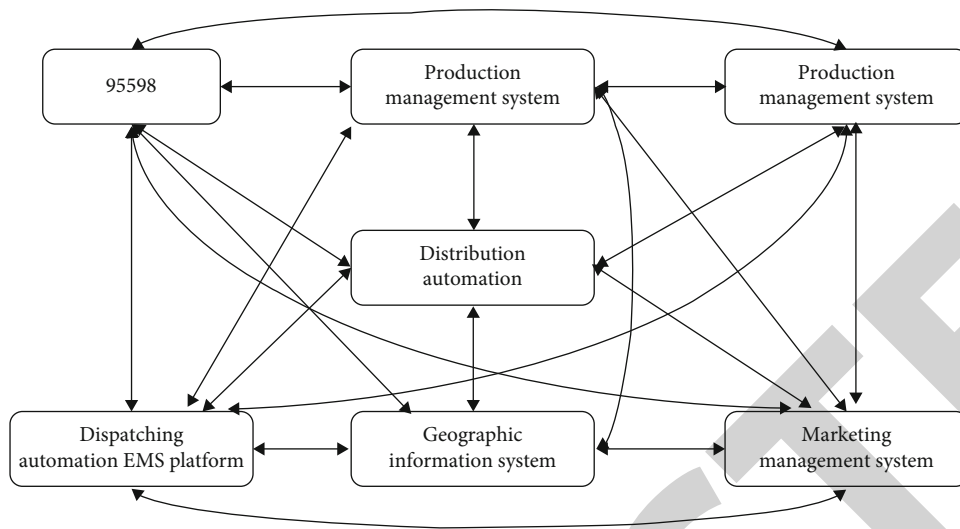


FIGURE 1: Interconnection between “point-to-point” systems.

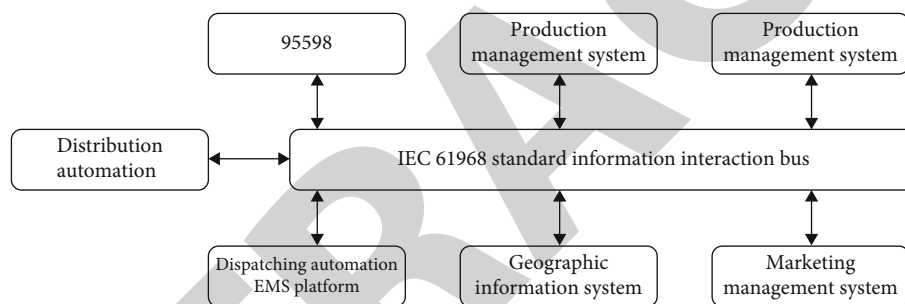


FIGURE 2: Interconnection between systems using information interaction bus conforming to IEC61968 standard.

can better improve the distribution automation system, so as to achieve the purpose of automation improvement.

3. Research Methods

3.1. Distribution Automation System

3.1.1. System Architecture. The power distribution automation system architecture of the super large data center is composed of two parts: the main workstation and the subworkstation [5]. The subworkstation is connected to the full end power equipment through RS485 bus, and the equipment is connected to the automatic control system network according to Modbus communication protocol, and uploaded to the main workstation. Based on the power data uploaded by the substation, the main workstation calculates and generates the optimal safe power supply path scheme and sends control commands to the power equipment through the subworkstation to transfer the power loss load to the safe power supply path. After the command is issued, the high-voltage switchgear executes the corresponding commands to complete the switching action based on the sampling unit, storage unit, calculation unit, comparison unit, and control unit.

3.1.2. AI Safe Power Supply Path Search Algorithm. The algorithm equates the network topology relationship to the interconnection matrix that can be recognized by the computer. When a fault occurs, identify and mark the fault area, bypass the fault area through intelligent search, and distribute the load of the fault area to other power sources [6, 7]. Based on the above principles, the search algorithm can accurately convert the electrification of the power system under different fault conditions into a mathematical model in real time and give it to the computer for overall calculation and scheduling, and then, the scheme generated by the calculation results can be dispatched by the terminal high-voltage switch through the way of communication commands, so as to meet the disaster tolerance requirements of the power system in the super large data center. After using the AI algorithm of safe power supply path, the power equipment in the whole park can be dispatched as a whole, so as to better tap the potential of equipment capacity and shorten the return period of investment. The secure path search algorithm is shown in Figure 3.

3.1.3. Load Classification Mechanism. Although the data center business is absolutely not allowed to be interrupted, different equipment and business types still have different importance, such as centralized cooling unit and core business are relatively

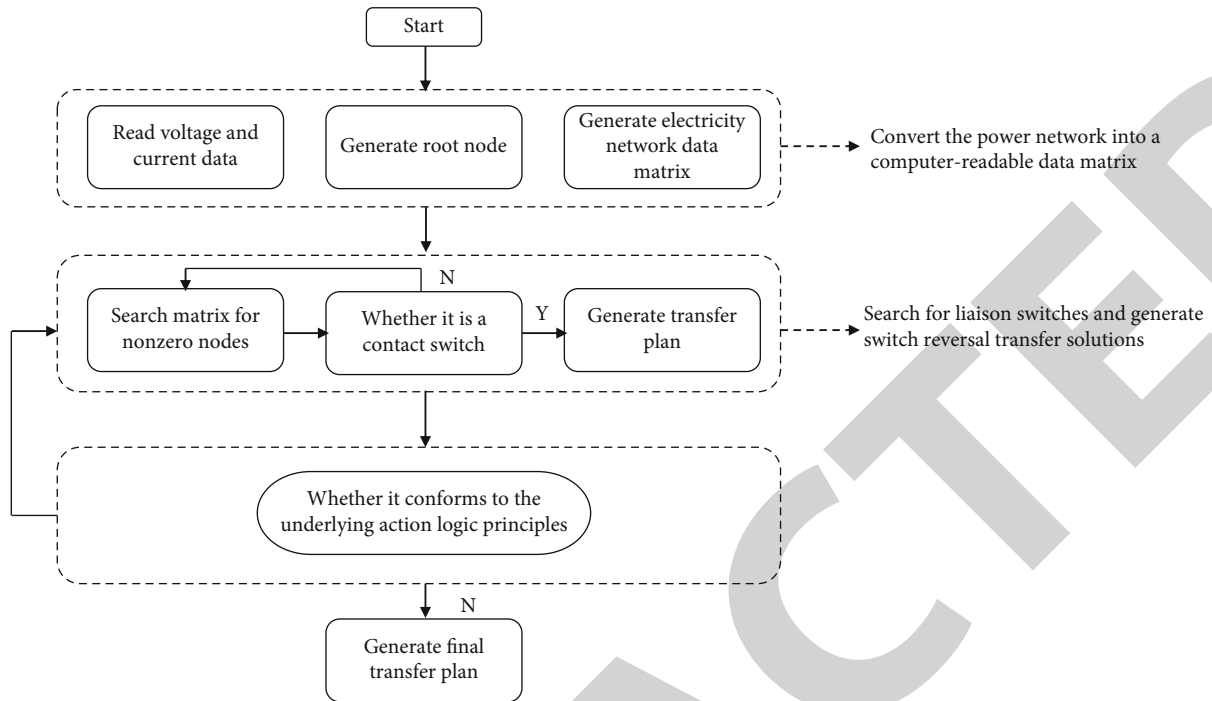


FIGURE 3: Flow chart of secure path search algorithm.

important. The priority of the system is considered from the following aspects:

(1) Priority for important power equipment: The power supply needs to be restored 4 minutes after the power failure of the centralized refrigeration station to ensure the continuity of cooling in the machine room. (2) Transmission/network export priority: After the power interruption of the transmission/network machine room in the park, a “data island” will be formed, which will disconnect the connection with the external network, and the guarantee level is also higher than that of the ordinary data machine room. (3) Priority of important business: The data room that hosts multiple regions and users also has a higher guarantee level than other ordinary data rooms.

In case of power supply interruption, the distribution automation system gives priority to the use of mains power to restore power supply to important loads. In case of insufficient load, the distribution automation system will immediately send the oil engine starting signal to the oil engine paralleling cabinet. After starting the minimum paralleling number that meets the remaining load, control the oil engine feeder cabinet to switch on, and put the generator into power supply. In this way, the safety of power supply can be guaranteed in the shortest time.

Taking a data center as an example, the differences between using ATS, standby automatic switching system, and using distribution automation system are compared. The action logic of ATS and standby automatic switching system commonly used in the traditional power industry is to start and put the oil engine into operation immediately when the load power supply loses power in two ways. If the power supply structure is multichannel incoming line, the oil engine will still be started when the municipal capacitance is sufficient [8, 9]. The distribution

automation system will give priority to judge whether the municipal capacitance can meet the requirements of power loss load. If it meets the requirements, the control switch will directly input the municipal power, and on this basis, the load grading guarantee function is realized.

3.2. Framework Basis of Reconstruction Decision

3.2.1. System Architecture. In order to reflect the unique perception process, reasoning process, learning process, decision process, and action process in cognitive wireless networks, the proposed reconfiguration decision architecture includes several modules: reasoning engine, learning engine, rule engine, decision engine, and action engine. Figure 4 shows the interconnection of each module.

In order to make reconstruction decisions, we must first know the complete external environment information and wireless control parameter information [10, 11]. This information is collected by sensing technology and stored in the wireless environment mapping (REM) database in a form that the system can understand. REM database classifies and stores these data in order to provide a data basis for reconstruction decisions and dynamically updates them throughout the operation process.

The rule engine deduces the interaction relationship between wireless parameters and system performance based on the comprehensive consideration of environmental information, wireless parameter, information and relevant policy rule information and inputs these associated information into the database. The reasoning model with predictive ability established based on these correlation information can adaptively select the appropriate configuration in the dynamic environment to meet the system performance requirements [12].

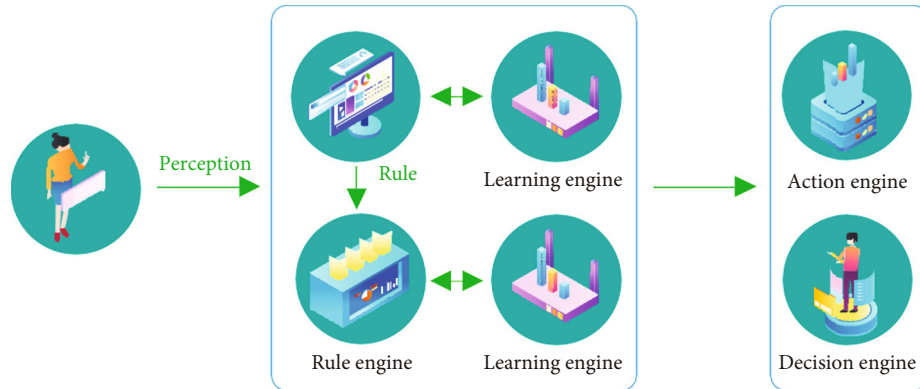


FIGURE 4: Architecture basis of reconstruction decision.

In order to realize the initiative of cognitive wireless network and save reconstruction time, the inference engine will first establish a priori analysis model with the help of a series of rules obtained by the rule engine and the expert system algorithm in artificial intelligence technology. This model can directly deduce the possible cognitive network reconstruction methods when facing the simple network structure. The learning engine optimizes the results produced by the reasoning engine by learning experience from historical information and environmental information and then stores the optimization results in the database and serves for the next decision-making. Learning engine is mainly involved in the decision-making of reconstruction in complex network structure, in order to make up for some shortcomings of reasoning engine in the face of complex data processing. The decision engine maps the calculation results of the previous reasoning engine and learning engine into reconstructed decisions and passes them to the action engine. The action engine mobilizes the system to change parameters and adjust wireless behavior according to the decisions.

3.2.2. Reconstruction Decision Algorithm Based on Artificial Intelligence Technology. In order to better use the reconfiguration decision algorithm to further improve the wireless network technology, artificial intelligence technology is introduced in this paper. Reasoning engine and learning engine are the main parts to complete the reconstruction decision in cognitive network [13]. The inference engine manages the system behavior and configuration by mapping the existing knowledge to the current environmental conditions. The learning engine optimizes the operation in the cognitive network by learning historical information and experience. In addition, the learning engine and the reasoning engine interact and promote each other: The learning process enriches the knowledge to be used in the reasoning process and optimizes the output of the reasoning engine. The inference engine provides more training data and instances for training and initializing the new learning engine.

In terms of the subtle relationship between learning and reasoning, artificial neural network (realizing the learning process) combined with rule-based expert system (realizing the reasoning process) can realize a complete reasoning learning process and complete the reconstruction decision with the sys-

tem requirements as the goal [14, 15]. Firstly, the rule expert system infers based on the rules derived from the rule engine. At the same time, these rules are used as training data input based on neural network learning engine. In this way, when the new environmental information is input into the trained learning engine, the learning engine can produce a series of new rules. With the help of these new rules, the reasoning engine can optimize the reconfiguration decision. The working condition of the reasoning engine in the reconstruction decision-making process is shown in Figure 5.

3.2.3. Reconstruction Decision Algorithm Combining Reasoning and Learning. The advantages of learning engine are reflected in three aspects [16]. Firstly, the learning engine can learn the environment information to generate new rules and update the rule storage in the database in real time. Secondly, fuzzy search can be applied to approximate reasoning in the learning process, which improves the reliability of reasoning. Finally, the learning engine can extract the objective function and optimize the reasoning results by optimizing the objective function.

3.3. Steps of Reconstructing Decision Algorithm. Step 1 Initialization.

Initialize the rule space and map the rules to the three-layer artificial neural network model. The preceding part of the rule (wireless parameter part) is mapped to layer 1 (input layer). The latter part (describing the system performance part) maps to the third layer (output layer). The hidden layer in the middle represents the mapping relationship between the input layer and the output layer.

Step 2 Set the activation function, and the function expression is shown in

$$y_k(p) = \text{sigmoid} \left[\sum_{i=1}^n x_i(p) \times \omega_{ik}(p) \right]. \quad (1)$$

Step 3 Use back propagation algorithm for training.

Step 4 Iteration.

Step 5 Apply the trained neural network model for reasoning and decision-making [17].

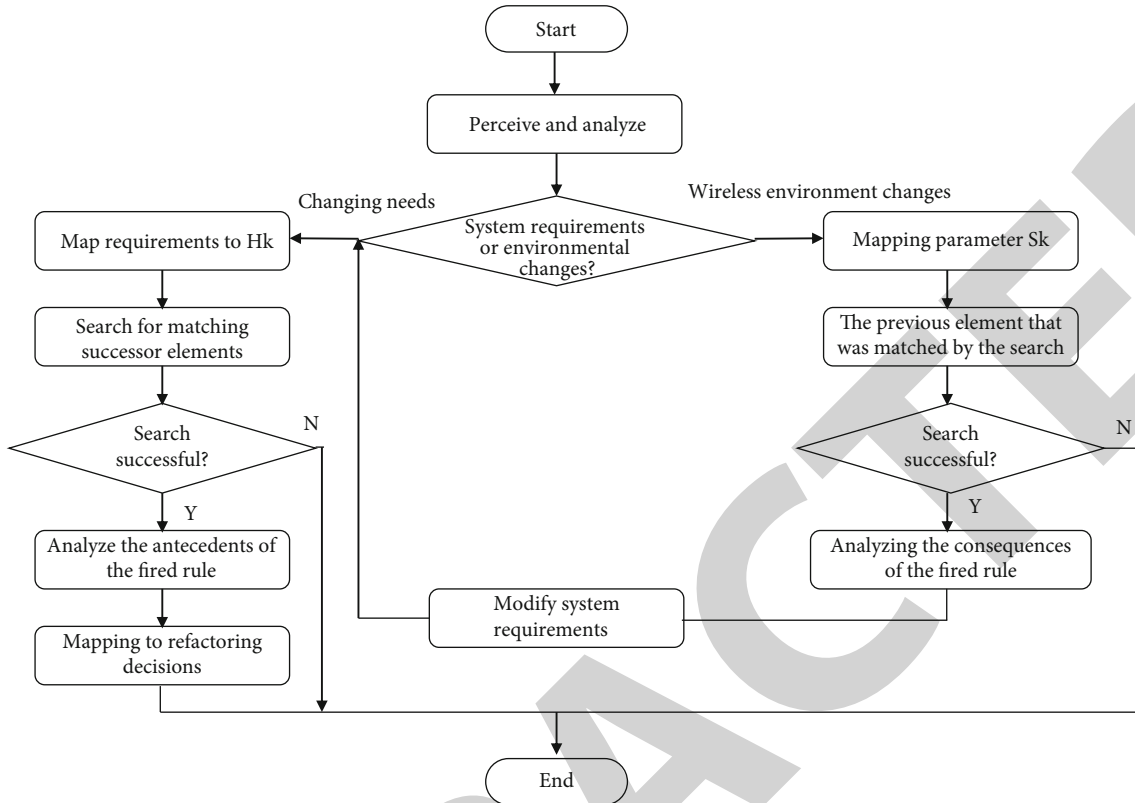


FIGURE 5: Workflow of reasoning engine in the process of reconstruction decision-making.

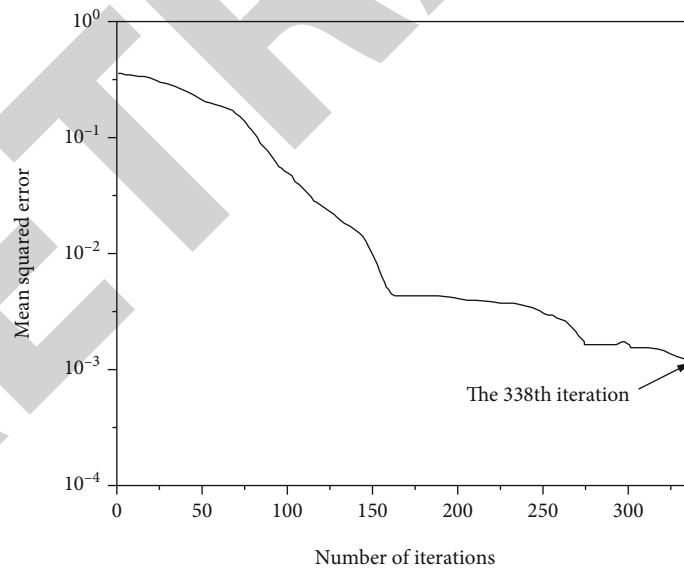


FIGURE 6: Error changes during training.

4. Results and Analysis

In the simulation process, the four parameters of data transmission rate (DR), transmission power (TP), frame length (FS), and noise level (n) represent wireless parameters, and the throughput (T) of the system is taken as the measure-

ment parameter of system performance [18]. The simulation shows the influence degree of wireless parameters on system performance in three cases: when using neural network combined with rule expert system algorithm to make reconstruction decision, when using the worst configuration, and when using the best configuration, it refers to the parameters

that can produce the best or worst system performance. The algorithm simulation of neural network combined with rule expert system starts from the most conservative configuration (equivalent to the worst configuration). Then, it adaptively adjusts parameters to meet the needs of system performance [19].

Input the parameters (data transmission rate, transmission power, frame length, and noise) that need to be reconstructed into the trained neural network system, and adjust them with the reconstruction decision algorithm based on the changes of system performance [20]. The setting scenario is as follows: the simulation duration is 180 s; the transmission rate is maintained at 10 mbit/s from 20 s to 90 s, 13 mbit/s from 90 s to 130 s, and 3 mbit/s from 130 s to 180 s; and the noise is 0.81 dbm from 40 s to 70 s, 10.3 dbm from 70 s to 110 s, 8 dbm from 110 s to 150 s, and 3.2 dbm from 150 s to 180 s. In this process, as the environment changes, the reconstruction algorithm based on artificial intelligence will adjust to maximize the throughput through the parameter performance relationship obtained above. The error is shown in Figure 6.

It can be seen that the mean square error of the method used in this paper is 0.001 when the number of iterations in the training process reaches 338, indicating that the method used in this paper can effectively reduce the error.

5. Conclusion

This paper presents a method of distribution automation system optimization research based on artificial intelligence wireless network technology. This method combines the development prospect of wireless network technology in the current era of artificial intelligence, and applies it to the distribution automation system, so as to further optimize and improve the distribution automation system. The experimental results show that the mean square error of the method used in this paper is 0.001 when the number of iterations in the training process reaches 338. It shows that the method used in this paper can effectively reduce the error. It proves that the method used in this paper can effectively improve the automation of distribution system and make it more effective in distribution work.

Data Availability

The data used to support the findings of this study are available from the corresponding author upon request.

Conflicts of Interest

The authors declare that they have no conflicts of interest.

Acknowledgments

This work was supported by Scientific Research Funds of Education Department of Liaoning Province in 2021, research on short-term wind power prediction based on attention-GRU recurrent neural network (Project No. LJKZ1099).

References

- [1] X. Feng, L. Huang, T. Dong, and D. Lv, "Application of distribution automation feeder terminal in system information acquisition technology and communication protocol," *Journal of Physics: Conference Series*, vol. 1982, no. 1, article 012140, 2021.
- [2] A. M. Shaheen, A. M. Elsayed, A. R. Ginidi, E. E. Elattar, and R. A. El-Sehiemy, "Effective automation of distribution systems with joint integration of DGs/SVCs considering reconfiguration capability by jellyfish search algorithm," *Access*, vol. 9, pp. 92053–92069, 2021.
- [3] S. Pan, Z. Ye, and J. Zhou, "Fault detection filtering for a class of nonhomogeneous markov jump systems with random sensor saturations," *International Journal of Control, Automation and Systems*, vol. 18, no. 2, pp. 439–449, 2020.
- [4] S. E. Mirsadeghi, A. Royat, and H. Rezaatofghi, "Unsupervised image segmentation by mutual information maximization and adversarial regularization," *IEEE Robotics and Automation Letters*, vol. 6, no. 4, pp. 6931–6938, 2021.
- [5] N. E. Proskuriakov, B. S. Yakovlev, N. N. Arkhangelskaia, and K. V. Dementyeva, "Automation of control the state of graphic collections and of content selection for design tasks in the printing," *Journal of Physics Conference Series*, vol. 1901, no. 1, article 012019, 2021.
- [6] X. Zhang, H. Wan, J. Ma, and Y. Huang, "Research on the application of integrated technology in power dispatching automation system," *Journal of Physics: Conference Series*, vol. 1992, no. 3, article 032123, 2021.
- [7] X. Jiang, Z. Pang, M. Luvisotto, R. Candell, and C. Fischione, "Delay optimization for industrial wireless control systems based on channel characterization," *IEEE Transactions on Industrial Informatics*, vol. 16, no. 9, pp. 5855–5865, 2020.
- [8] J. Shi and M. Sha, "Parameter self-adaptation for industrial wireless sensor-actuator networks," *ACM Transactions on Internet Technology*, vol. 20, no. 3, pp. 1–28, 2020.
- [9] M. R. Tur and H. Ogras, "Transmission of frequency balance instructions and secure data sharing based on chaos encryption in smart grid-based energy systems applications," *Access*, vol. 9, pp. 27323–27332, 2021.
- [10] A. Farao, E. Veroni, C. Ntantogian, and C. Xenakis, "P4g2go: a privacy-preserving scheme for roaming energy consumers of the smart grid-to-go," *Sensors*, vol. 21, no. 8, p. 2686, 2021.
- [11] K. M. Rafi, P. Prasad, and J. Vithal, "Coordinated control of dstatcom with switchable capacitor bank in a secondary radial distribution system for power factor improvement," *Journal of Electrical Systems and Information Technology*, vol. 9, no. 1, pp. 1–26, 2022.
- [12] J. L. Kou, M. Ding, J. Feng, Y. Q. Lu, F. Xu, and G. Brambilla, "Microfiber-based bragg gratings for sensing applications: a review," *Sensors*, vol. 12, no. 7, pp. 8861–8876, 2012.
- [13] P. Andrich, B. J. Alemán, J. C. Lee et al., "Engineered micro- and nanoscale diamonds as mobile probes for high-resolution sensing in fluid," *Nano Letters*, vol. 14, no. 9, pp. 4959–4964, 2014.
- [14] W. Wu, P. Li, B. Wang et al., "Integrated distribution management system: architecture, functions, and application in China," *Journal of Modern Power Systems and Clean Energy*, vol. 10, no. 2, pp. 245–258, 2022.

Retraction

Retracted: Integrated Sensory Throughput and Traffic-Aware Arbiter for High Productive Multicore Architectures

Journal of Sensors

Received 12 December 2023; Accepted 12 December 2023; Published 13 December 2023

Copyright © 2023 Journal of Sensors. This is an open access article distributed under the Creative Commons Attribution License, which permits unrestricted use, distribution, and reproduction in any medium, provided the original work is properly cited.

This article has been retracted by Hindawi, as publisher, following an investigation undertaken by the publisher [1]. This investigation has uncovered evidence of systematic manipulation of the publication and peer-review process. We cannot, therefore, vouch for the reliability or integrity of this article.

Please note that this notice is intended solely to alert readers that the peer-review process of this article has been compromised.

Wiley and Hindawi regret that the usual quality checks did not identify these issues before publication and have since put additional measures in place to safeguard research integrity.

We wish to credit our Research Integrity and Research Publishing teams and anonymous and named external researchers and research integrity experts for contributing to this investigation.

The corresponding author, as the representative of all authors, has been given the opportunity to register their agreement or disagreement to this retraction. We have kept a record of any response received.

References

- [1] T. Venkata Sridhar and G. C. Krishnaiah, "Integrated Sensory Throughput and Traffic-Aware Arbiter for High Productive Multicore Architectures," *Journal of Sensors*, vol. 2022, Article ID 2911777, 14 pages, 2022.

Research Article

Integrated Sensory Throughput and Traffic-Aware Arbiter for High Productive Multicore Architectures

T. Venkata Sridhar ^{1,2} and G. Chenchu Krishnaiah ³

¹Dept. of E&C, VTU, Belgaum 5900018, India

²Dept. of ETC, IIIT-BH, Bhubaneswar 751003, India

³Dept. of ECE, ASCET, Gudur 524101, India

Correspondence should be addressed to T. Venkata Sridhar; venkatasridhar@iiit-bh.ac.in

Received 27 June 2022; Accepted 11 August 2022; Published 5 September 2022

Academic Editor: C. Venkatesan

Copyright © 2022 T. Venkata Sridhar and G. Chenchu Krishnaiah. This is an open access article distributed under the Creative Commons Attribution License, which permits unrestricted use, distribution, and reproduction in any medium, provided the original work is properly cited.

The increasing demand for network and high-performance devices requires large data throughputs with minimal loss or repetition. Network on chips (NoC) provides excellent connectivity among multiple on-chip communicating devices with minimal loss compared with old bus systems. The motivation is to improve the throughput of the NoC that integrated on multicores for communication among cores by reducing the communication latency. The design of the arbiter in the crossbars switch of an NoC's router has a vital role in judging the system's speed and performance. Low latency and high-speed switching are possible with high performance and good switching equipment at the network level. One of the significant components in NoC under SoC design is the arbiter, which governs the system's performance. Proper arbitrations can avoid network or traffic congestions like livelock and buffer waiting. The proposed work in this paper is to design an efficient and high productive arbiter for multicore chips, especially SoCs and CMPs. The proposed arbiter is showing good improvement in the throughput at higher data rates; an average of more than 10% throughput improvement is noticed at higher flit injection rates independent of the VCs implemented. Further, the critical delays are reduced to 15.84% with greater throughputs.

1. Introduction

High-performance computing devices are the most regular devices at a compact level in the day-to-day lifestyle of humans in the present era. Recently, even large computing equipment becoming handy and lightweight requires the integration of larger hardware components at a large scale into compact modules resulting in an SoC (system on a chip). The design of an SoC [1, 2] is a common phenomenon in the modern manufacturing of major electronics. To meet the QoS (quality of service) of these manufacturing technologies at a scaling of nanometer level, factors like latency, power dissipation, error rate, and software error rates [3, 4] need to be appropriately managed [5]. Embedded SoC is application-oriented and requires an uncompromised communication interface for different environments on the chip, like processor(s), memory, control module, sometimes form

firmware to the software. Due to the great demand in processing speed, the manufacturers had increased the number of processors integrated on a single chip considerably, starting from dual core to many cores [6]. MPSoC [7] are the new-generation manufacturing methods from the past one and a half-decade, giving a reasonable throughput for multi-tasking. Figure 1 shows a job run of a typical application-oriented MPSoC. Smart MPSoC contains integrated hardware [8].

Before mapping the data to be handled by multiple processors, it is essential to configure and evaluate the requirements as per the specific task. To map different cores on a single chip, like processor(s), DRAM(s)/SRAM(s), DSP(s), video processors, and DMA, the established bus technology has many compromises.

NoC is a simple solution for such compromises to overcome. An NoC reduces the burden of calculation from the

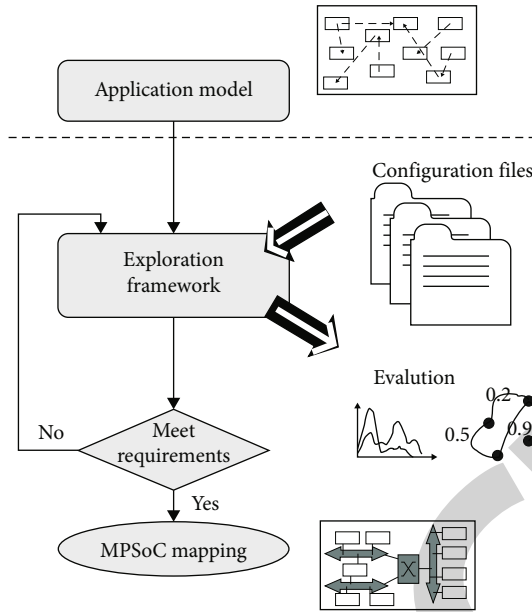


FIGURE 1: Job run of MPSoC.

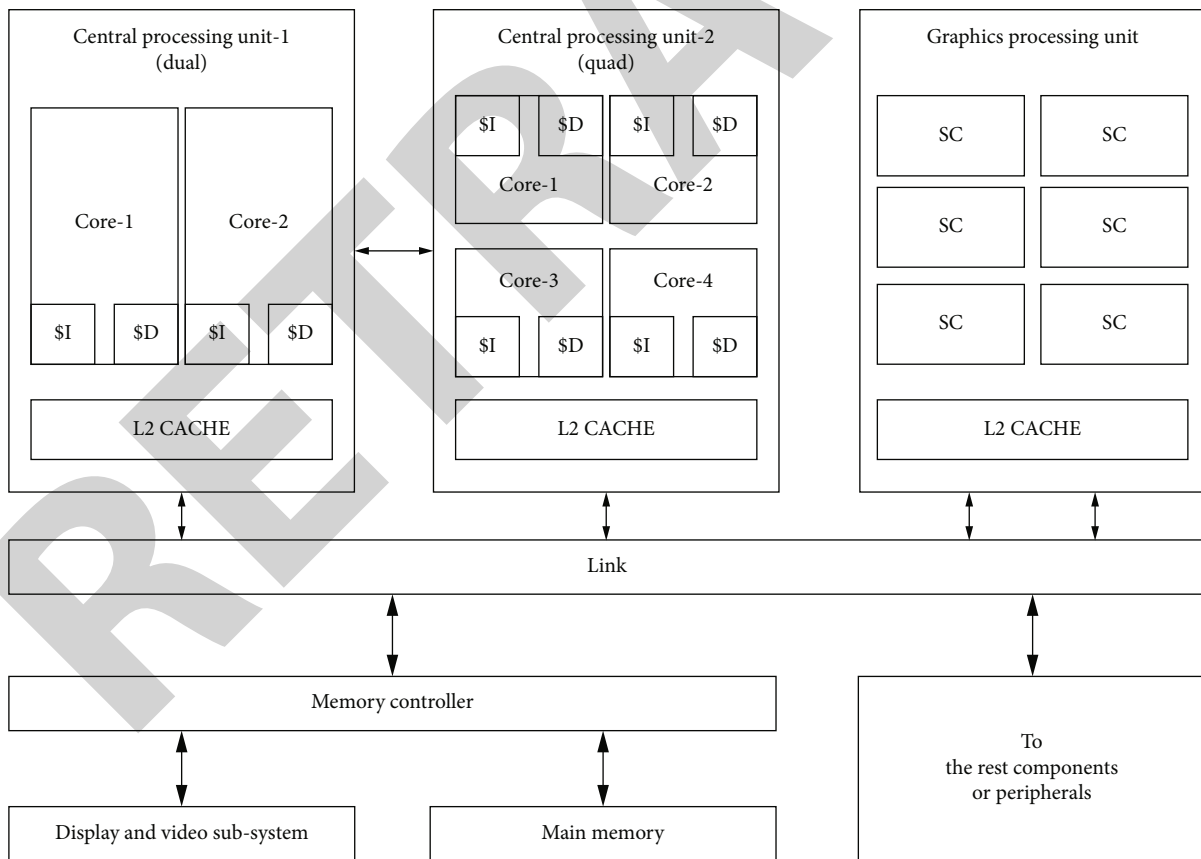


FIGURE 2: On-chip blocks of a multicore architecture.

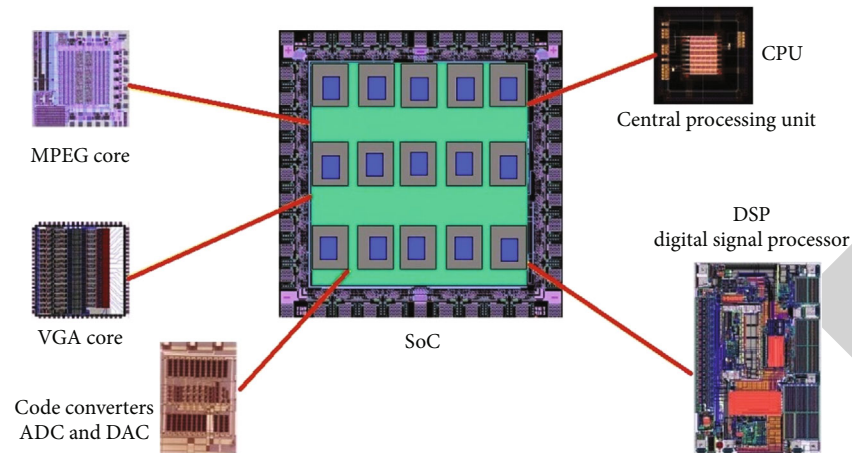


FIGURE 3: Device-level visualization of SoC.

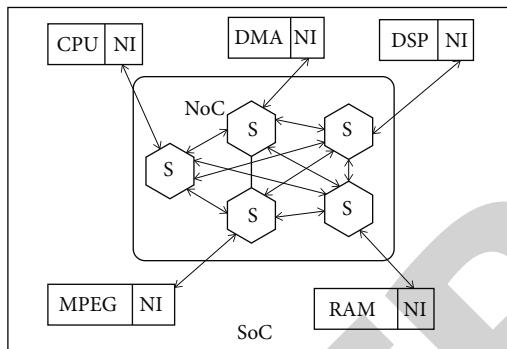


FIGURE 4: Fundamental NoC structure.

transmission. An efficient NoC requires good routing, network interfacing, and switching. A crossbar with a well-structured arbiter design is inevitable. The major contribution of the work is to improve the throughput of the arbiter in critical traffic timings that was achieved through a flexible priority resolver. The proposed arbiter is tested under synthetic traffic (ST) and uniform random traffic (URT) conditions. For both conditions, improvement in the throughput was observed. If the communication latency between the cores is reduced, then the time taken for data traversal is reduced; hence, this method can produce more throughput in a small time.

The major challenge in the existing models is handling the data when a network congestion occurs, like a deadlock or a livelock. The existing model arbiter has fixed arbitrations for all the traffic conditions and is suffering if traffic conditions are unpredictable. The proposed model has a flexible priority resolver that can adjust the arbitrations according to the traffic. The proposed arbiter is showing good improvement in the throughput at higher data rates; an average of more than 10% throughput improvement is noticed at higher flit injection rates independent of the VCs implemented. Further, the critical delays are reduced to 15.84% with greater throughputs.

The process of mapping is information exchange between multicores or processing elements in the specified architecture. An efficient routing on the NoC will execute the same without any deadlock or livelock. In the proposed model, the NoC with a flexible priority arbiter is enabling efficient information exchange between all cores in MPSoC. Many deep learning and AI platforms are in urge for high data processing systems; hence, this paper aims for such design [9–11].

Section 2 presents multicore architecture design and NoC interconnections and problems in design. Section 3 covers NoC crossbar switching with a well-organized arbiter design. Section 4 includes simulations of the proposed work and analysis. Section 5 is the conclusion containing limitations and plans of the work.

2. Multicore Systems

Multicore architectures are the best inevitable design for high-performance computers to handle large and complex data. Its architecture and design provide all the rising performance needs. Figure 2 illustrates the basic building blocks of heterogeneous SoC. And Figure 3 depicts device-level visualization.

2.1. Multiprocessor Architecture. The basic design of all multicore processors is to integrate the required data memories and instruction memories, i.e., L1 cache, secondary memories, i.e., L2 cache, on the chip itself. That is shown in Figure 2.

A proper link between different modules is required so that it should not degrade the performance of SoC. This is not achievable with the age-old bus systems. [3]. Either an SoC is general or application-specific; the NoC provides an exceptional solution for on-chip communication [12, 13].

2.2. The Communication Interface: NoC. As NoC is emerging as the leading solution to interface all on-chip devices in an SoC [14, 15], the design elements should be keenly followed. Like, choosing topology for implementation,

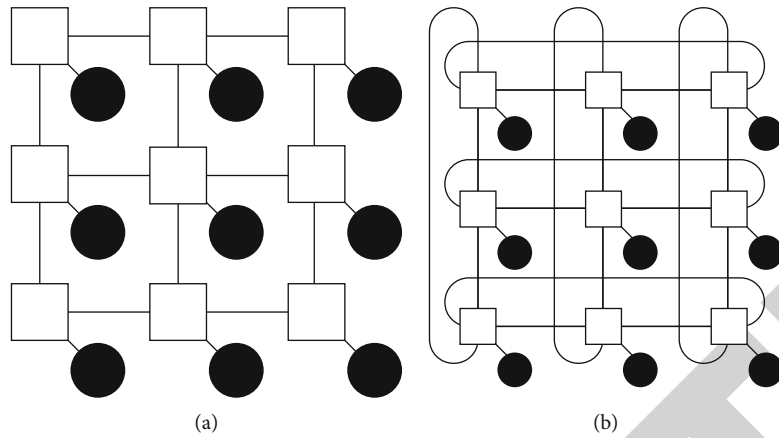


FIGURE 5: (a) A 3×3 mesh in 2D with one core connected to one router. (b) A 3×3 torus in 2D with one core connected to one router.

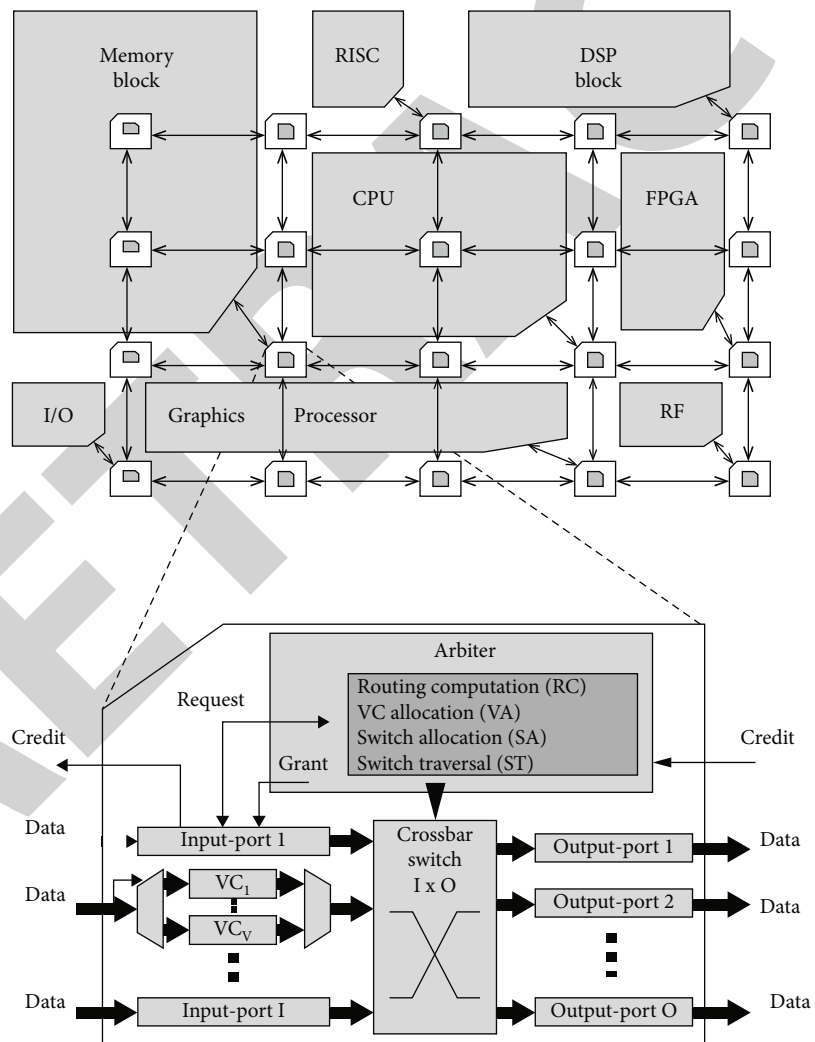


FIGURE 6: Different cores of SoC connected using NoC.

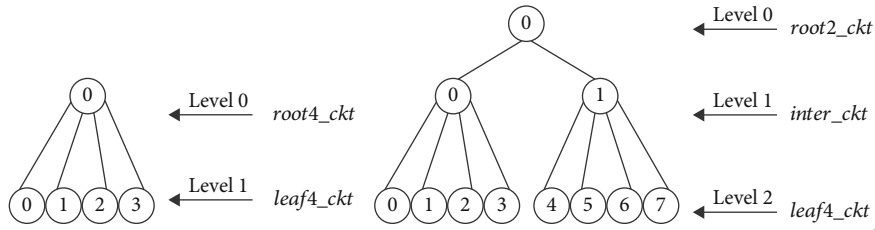


FIGURE 7: Decentralization tree of RRA.

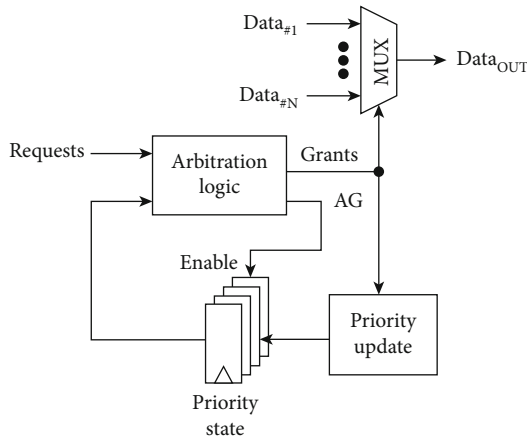


FIGURE 8: MARX structure.

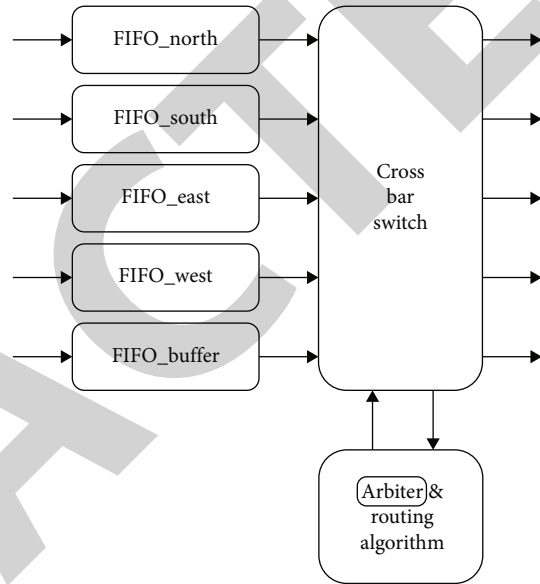


FIGURE 9: Data switching blocks.

maximum sustainable and error-free routing, and flow-control system [16, 17] are the vital elements in the design of an NoC. Figure 4 presents the basic block level understanding of the network on chip. Application-specific ONoCs (Optical NoCs) are even embedding the optics in microelectronics [18].

The aim of an NoC as the heart of SoC is to provide an efficient, mostly stand-off free, power, and throughput aware communication amidst different cores of the system on chip [19]. Modern SoC designs are coming with FinFETs, which can improve communication speed [20].

2.3. The NoC Architectonic. Network on chip architectonic contains many building blocks; among most important are *topology*, *interface*, and *routing* selection, for an efficient communication establishment.

2.3.1. Selection of Topology. The selection of the topology decides the area, power consumption, and speed of communication between the connected cores; it should be picked according to the need. That is as Application Specific (AS) or non-AS designs of SoC. Topologies like “Star,” “Mesh,” “Torus,” “Octagon,” “Spidergon,” and “Tree” in 2D and 3D [21–23]. Mesh and Torus (sometimes folded) are the regular in power considerations, shown in Figure 5. The average distance between cores should be minimum concerning a hop count.

2.3.2. Interface Design. An interface provides communication between the core and the network with an assured

throughput. An NI (network interface) will do assemble and disassemble packets and communicate them with the core. Proper choosing of network topology and routing techniques will improve the efficiency of the network interface.

2.3.3. Routing. The communication path from the source core to the destination core through NoC, without any congestions or blockages, is the aim of routing [24]. Defining a proper routing algorithm is needed to decide the latency in communication. Figure 6 illustrates a block diagram of the complete NoC architecture.

2.4. Crossbar Switch. After finalizing the routing and packing, it is required to switch the data according to the algorithm defined by NoC. Each data packet is Muxed thorough $I \times O$ crossbar (Figure 6). Per one cycle, one defined data packet can go through.

Figure 6 is a heterogeneous MPSoC architecture in which each tile contains different processing elements like memory block, DSP block, reduced instruction set computer, CPU, and graphic processor. An efficient networking architecture requires communicating data sharing among all the modules/processing elements. A single block of network interface/router is expanded in dotted line, which consists of a mechanism for data exchange in all four directions of connections. This is explained in section II-C: 2-3, D-E,

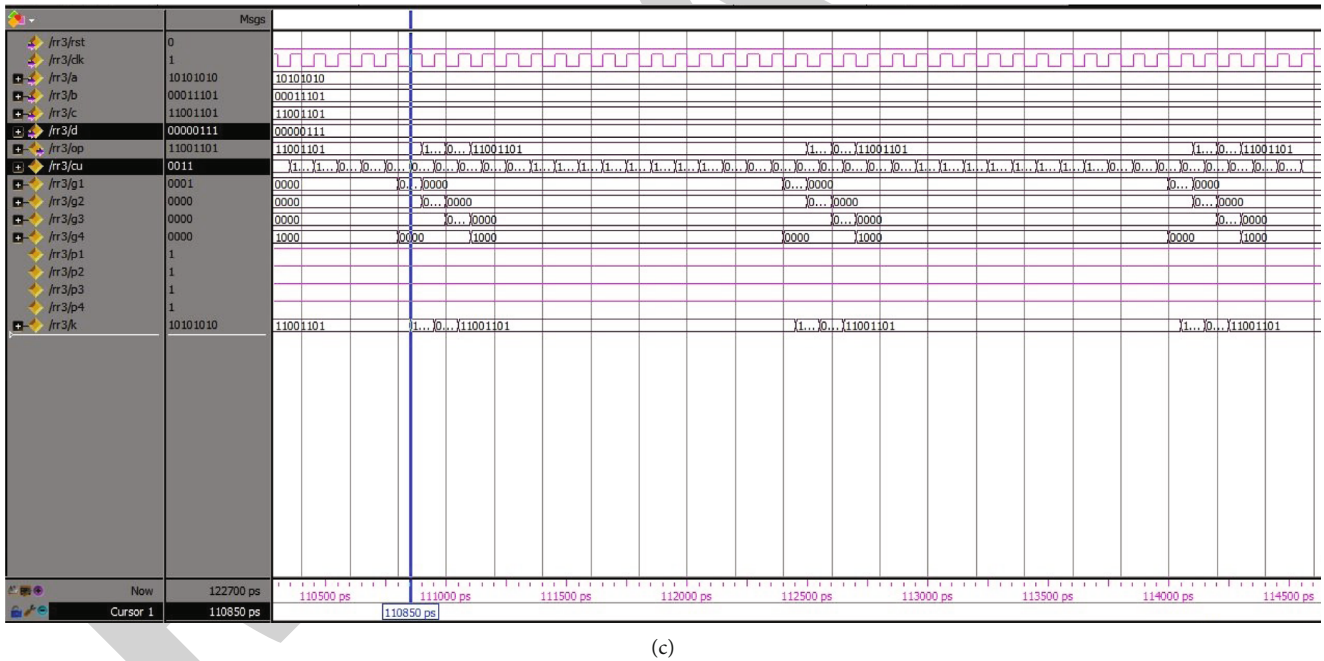
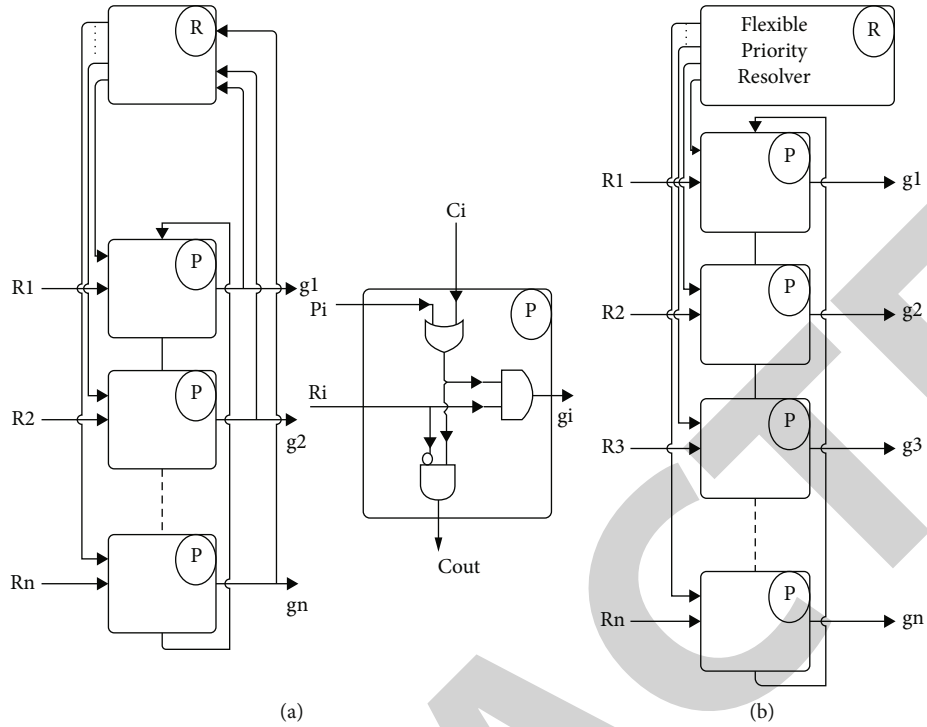


FIGURE 10: (a) Existing arbiter, (b) proposed flexible arbiter, and (c) arbitration simulation result.

respectively. The performance of the router directly depends on the efficiency of the crossbar switch and arbiter design. Hence, to achieve a low communication latency, these two are playing a very important role.

2.5. *Arbiter.* The arbitrations are dependent on the selection of virtual channels or the wormhole method. The arbiter is generally responsible for allowing the channel usage for all

the inputs according to the routing strategies. Prioritization is more vital because it decides the speed of communication. In this research, we used a flexible priority such that livelock will be mostly avoided. Once all the input data reached the crossbar, the stages of the arbiter will be terminated accordingly.

Kameda et al. [25] had proposed an SFQ design for validating the crossbar. The idea is to increase the throughput

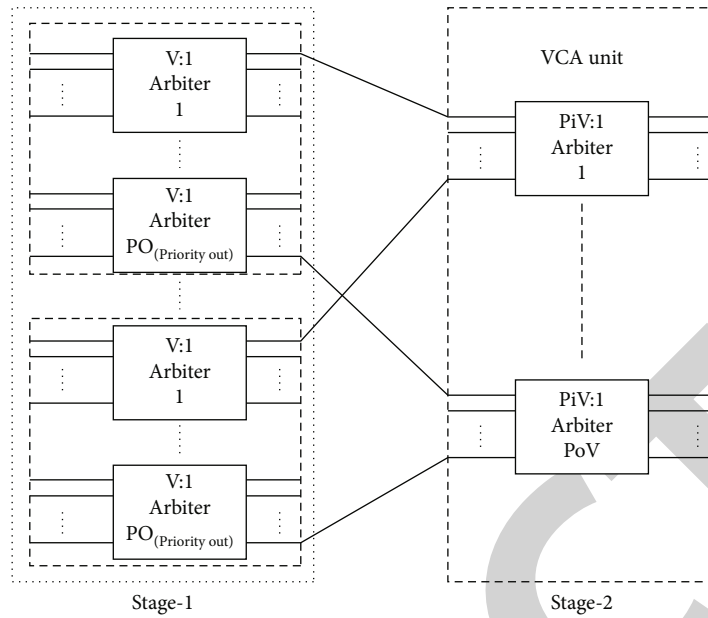


FIGURE 11: VCA arbitration.

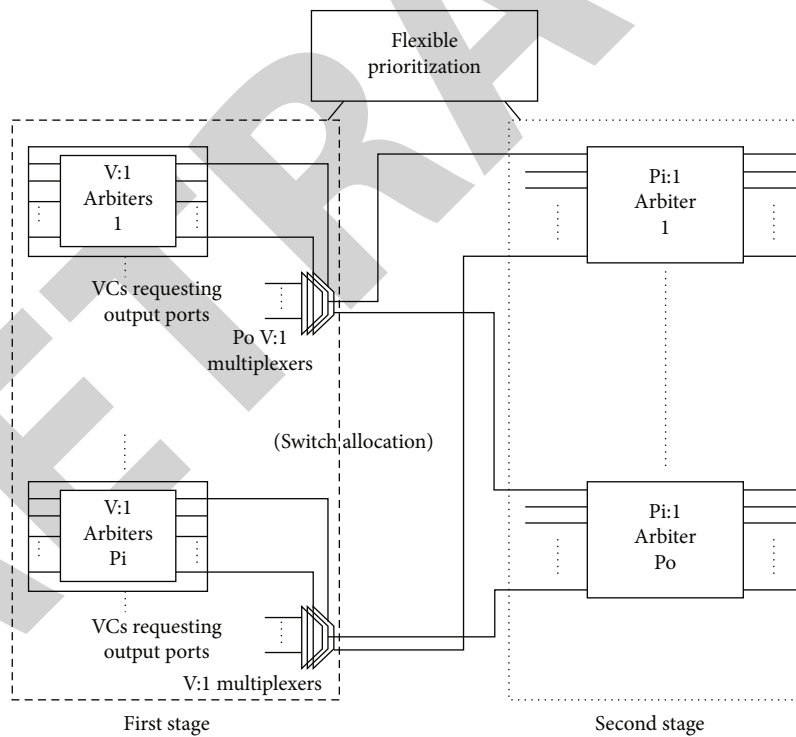


FIGURE 12: FP switch allocator.

to a considerable level by avoiding collisions. The experiment is limited to the usage of frequency and is more accurate at 40GHz. Prioritization is a parallel processing type. The RRA design leads to high speed with frequency limitation.

Lee et al. [26] had reported a decentralized arbiter with high speed (HDRA). This design is aimed only at the most

ensorious path delays to minimize the production cost. The VOQs introduced in the design will reduce the blocking of the head of the line. HRDA is a derived version of PPA ($O(\log 4 N)$ structure), PRRA, and IPRRRA as given in Figure 7.

When the integration of the cores in SoC increases, the design suffers from a large amount of complexity to find

Step 1: check all input buffer requests.
Step 2: is the load/traffic more than regular transfer with respect to previous router data.
Step 3: chose to assign priority as rotation if traffic increases else, fixed.
Step 4: map *ilp*-port to *olp*-port of arbiter for packet transfer.
Step 5: check for replication of the same packet assigned to various arbiters.
Step 6: check packets of *olp*-port mapping to *ilp*-port according to the assignment.
Step 7: verify for the multiple iterations.
Step 8: issue grant.

ALGORITHM 1

all the decentralized nodes by NoC and end assembly will become an issue.

Giorgos et al. [27] have suggested a simple design without much changes in the existing design, but with intelligent adoption. The approach is merging of the switching allocation, i.e., MARX which combines the multiplexer and arbiter as depicted in Figure 8. This design focuses majorly on the performance of the entire system, which increases the complexity in design. The Merged ARbiter and multipleXer (MARX) combines the architectures of an arbiter and multiplexer.

3. Arbiter Design

The significant component in NoC under SoC design is the arbiter, which governs the system's performance. Proper arbitrations can avoid network or traffic congestions like livelock and buffer waiting with both synchronous and asynchronous communication [28]. The proposed work in this paper is to design an efficient and high productive arbiter for multicore chips, especially SoCs and CMPs. The switching of the arbiter is shown in Figure 9. The design is a mesh topology and can communicate in four directions with a local transfer, which deserves a buffer count of five.

RR (round robin) arbiter model is the most commonly used method for NoC router design because of its ease and straightforwardness. Let us use RQ_n : request, GT_n : grant, and PR_n and PR_n^+ : priorities of current and immediate future cycle. Kin_n and $Kout_n$ decide the priorities between arbiter buffer or cells. Then, according to RRA design, the grant will be issued only when PR_n is 1 as follows:

$$GT_n = RQ_n \cdot (PR_n + Kin_n), \quad (1)$$

$$\overline{Kout}_n = RQ_n \cdot (PR_n + Kin_n), \quad (2)$$

$$PR_n^+ = GT_{n-1} + PR_n \cdot Kin_n. \quad (3)$$

Thus, the channel allocation for the next stage of traffic purely depends on the current running stage and followed by a subsequent request of existing channel using data. This is valid only if at least one present state exists. This drawback was modified with a priority resolver in our design, which estimates the density of the future traffic depending on the input requests to the router (possibly N:E:W:S direction) and load on previous router which directed the current

transfer as shown in Figure 10. It has two efficient prioritizations chosen dynamically as fixed or rotating [29–32].

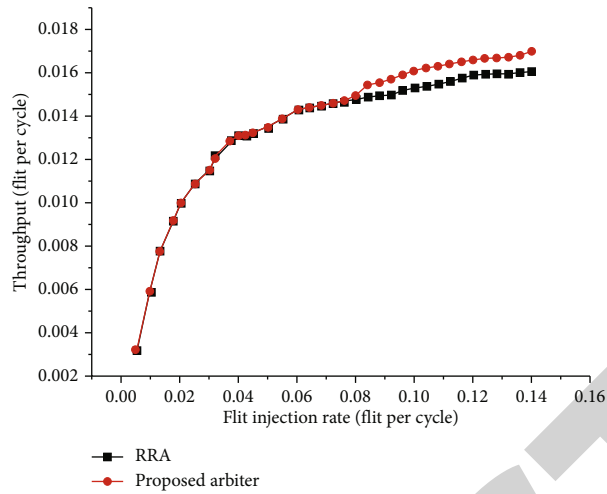
3.1. VCA Arbiter. Congestion avoidance, like a deadlock and livelock, can be handled by the arbiter. Flit bifurcation in routing is done based on the size of the data, the head flit may be one, but the body flits are packet size-dependent. The count is calculated before it reaches the VC (virtual channel). The allocation unit of the VC is done with a head flit. VCA unit allocates the channel for the data packets to travel through different routers. The mechanism of the two stages is illustrated in Figure 11.

3.2. Switching Arbiter. Once VC is allocated to the packets, the central part is to do switch allocation (SA), which leads to reaching the packet to the destination by competing with all the other VC allocated packets. Here, all the flits need to be allocated. To reduce the delay in communication to the destination, a flexible priority resolver is introduced in this proposed architecture. This reduced the computation complexity of allocation among all the VC allocations shown in Figure 12. Switch traverse (ST) and link traverse (LT) will lead the granted allocation packets to reach the specified destination.

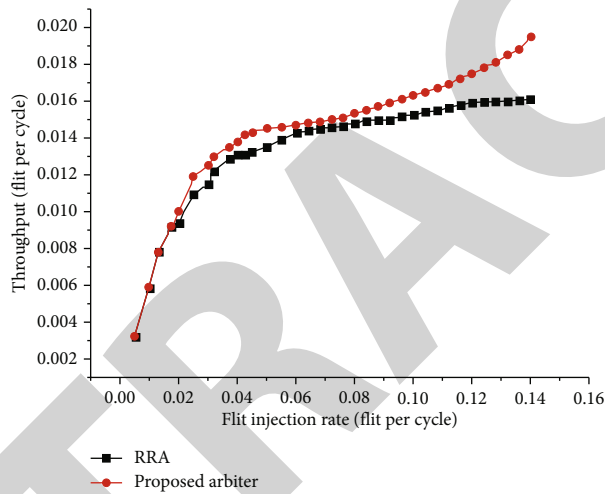
3.3. Proposed Arbiter. Most of the existing arbiter designs follow a round robin which rotates the output grants received and precedes the rest Figure 10(a). This will increase the burden on the arbiter as the flits increase for large throughputs. The proposed arbiter has a flexible priority resolver which estimates the traffic/load on the arbiter about to come Figure 10(b). Unlike normal RRA, the specific rotation or fixed orientation is predefined here; hence, the time calculation of arbitrations can reduce, and throughput will increase.

The priority resolver has flexibility depending on the traffic, like fixed, rotating. If traffic is less and the expected latency in switching is less, then fixed priority can be chosen; if not, rotating priority can be chosen to distribute equal priority to all switching flits. The structure of the algorithm is as follows.

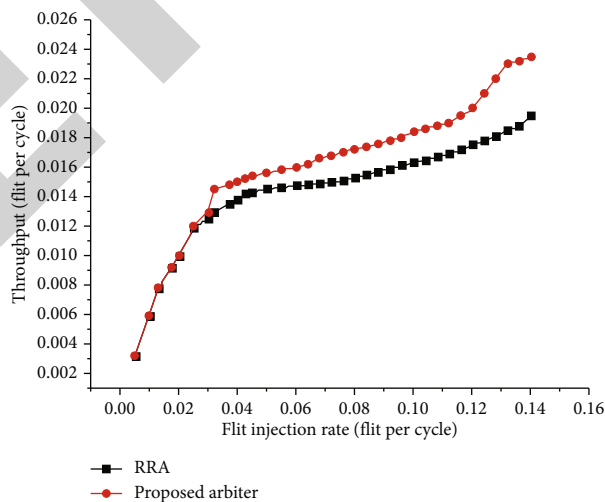
3.4. Proposed Arbiter Algorithm. The algorithm below specifies the arbiter's input request and grants according to flexible priority, depending on the load/traffic buffer channel rout calculation; VCA, SA, ST, and LT are the significant concerns in computing the travel delay. In the proposed arbiter, important computations are done in the stage of



(a)



(b)

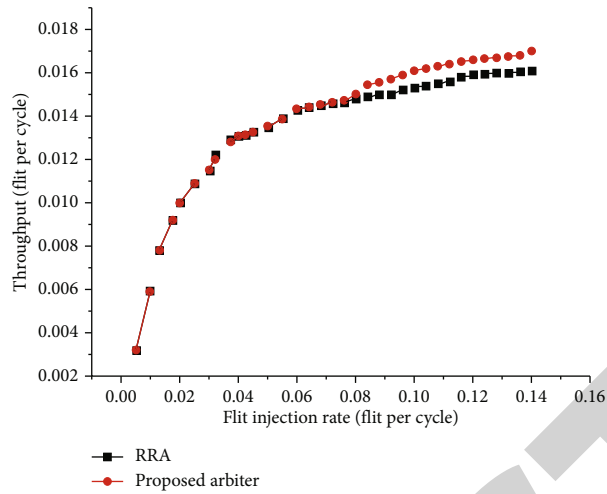


(c)

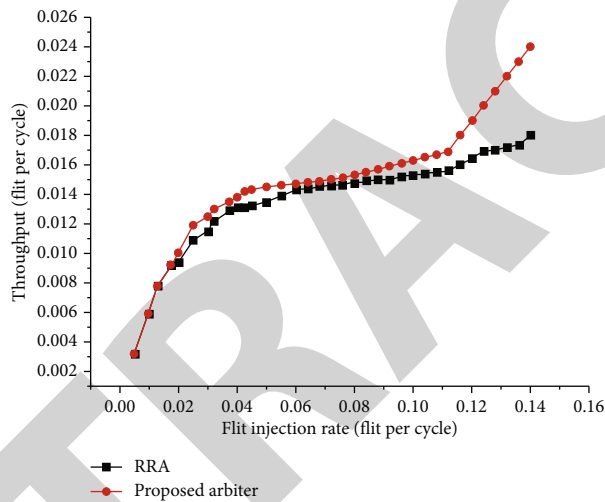
FIGURE 13: Throughput under URT. (a) FIR vs. throughput with two VCs, (b) FIR vs. throughput with four VCs, and (c) FIR vs. throughput with eight VCs, respectively.

priority resolving hence expected low latency with high throughput. First, it verifies all allocated buffers in step 1,

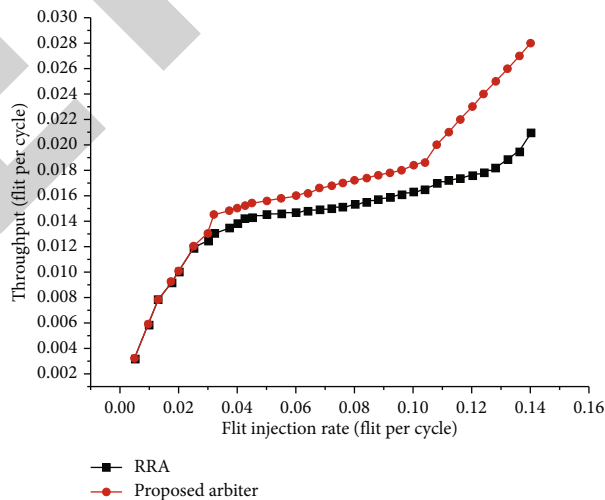
finds the density of the traffic load and enables the priority resolver if found large loads in steps 2-3, and assigns



(a)



(b)



(c)

FIGURE 14: Throughput under synthetic traffic. (a) FIR vs. throughput with two VCs, (b) FIR vs. throughput with four VCs, and (c) FIR vs. throughput with eight VCs, respectively.

mapping of source and destinations by eliminating redundant allocations in steps 4-5. Check the transfer from lower

end node to higher in the same process for finding multiple iterations; if all good, enable the transfer in steps 6-8.

TABLE 1: Flit injection ratio vs. throughput of existing model and proposed model for various test conditions (FIR and Tp are measured in flit per cycle).

			ST																			
			URT				Proposed arbiter				Existing RRA				Proposed arbiter							
			Existing RRA		2VCs		4VCs		8VCs		2VCs		4VCs		8VCs		2VCs		4VCs		8VCs	
2VCs	FIR	Tp	FIR	Tp	FIR	Tp	FIR	Tp	FIR	Tp	FIR	Tp	FIR	Tp	FIR	Tp	FIR	Tp	FIR	Tp	FIR	Tp
0.00	0.0000	0.00	0.0000	0.00	0.0000	0.00	0.0000	0.00	0.0000	0.00	0.0000	0.00	0.0000	0.00	0.0000	0.00	0.0000	0.00	0.0000	0.00	0.0000	0.00
0.01	0.0048	0.01	0.0058	0.01	0.0051	0.01	0.0061	0.01	0.0061	0.01	0.0061	0.01	0.0061	0.01	0.0059	0.01	0.0059	0.01	0.0055	0.01	0.0061	0.01
0.02	0.0089	0.02	0.0092	0.02	0.0091	0.02	0.0121	0.02	0.0121	0.02	0.0101	0.02	0.0101	0.02	0.0092	0.02	0.0092	0.02	0.0092	0.02	0.0101	0.02
0.03	0.0109	0.03	0.0115	0.03	0.0112	0.03	0.0132	0.03	0.0132	0.03	0.0130	0.03	0.0130	0.03	0.0117	0.03	0.0117	0.03	0.0113	0.03	0.0129	0.03
0.04	0.0118	0.04	0.0131	0.04	0.0138	0.04	0.0145	0.04	0.0145	0.04	0.0151	0.04	0.0151	0.04	0.0130	0.04	0.0130	0.04	0.0124	0.04	0.0140	0.04
0.05	0.0129	0.05	0.0135	0.05	0.0143	0.05	0.0137	0.05	0.0148	0.05	0.0155	0.05	0.0155	0.05	0.0137	0.05	0.0137	0.05	0.0139	0.05	0.0146	0.05
0.06	0.0142	0.06	0.0140	0.06	0.0148	0.06	0.0146	0.06	0.0150	0.06	0.0160	0.06	0.0160	0.06	0.0138	0.06	0.0138	0.06	0.0148	0.06	0.0148	0.06
0.07	0.0145	0.07	0.0144	0.07	0.0150	0.07	0.0149	0.07	0.0152	0.07	0.0167	0.07	0.0167	0.07	0.0141	0.07	0.0141	0.07	0.0150	0.07	0.0150	0.07
0.08	0.0146	0.08	0.0148	0.08	0.0152	0.08	0.0152	0.08	0.0157	0.08	0.0171	0.08	0.0171	0.08	0.0148	0.08	0.0148	0.08	0.0153	0.08	0.0155	0.08
0.09	0.0150	0.09	0.0151	0.09	0.0159	0.09	0.0159	0.09	0.0162	0.09	0.0178	0.09	0.0178	0.09	0.0150	0.09	0.0150	0.09	0.0160	0.09	0.0159	0.09
0.10	0.0152	0.10	0.0157	0.10	0.0162	0.10	0.0162	0.10	0.0171	0.10	0.0183	0.10	0.0183	0.10	0.0151	0.10	0.0151	0.10	0.0163	0.10	0.0165	0.10
0.11	0.0155	0.11	0.0161	0.11	0.0169	0.11	0.0165	0.11	0.0179	0.11	0.0190	0.11	0.0190	0.11	0.0155	0.11	0.0155	0.11	0.0167	0.11	0.0169	0.11
0.12	0.0156	0.12	0.0163	0.12	0.0175	0.12	0.0167	0.12	0.0182	0.12	0.0201	0.12	0.0201	0.12	0.0161	0.12	0.0161	0.12	0.0169	0.12	0.0189	0.12
0.13	0.0158	0.13	0.0164	0.13	0.0178	0.13	0.0169	0.13	0.0189	0.13	0.0219	0.13	0.0219	0.13	0.0170	0.13	0.0170	0.13	0.0170	0.13	0.0215	0.13
0.14	0.0160	0.14	0.0165	0.14	0.0192	0.14	0.0174	0.14	0.0195	0.14	0.0233	0.14	0.0233	0.14	0.0181	0.14	0.0181	0.14	0.0175	0.14	0.0239	0.14

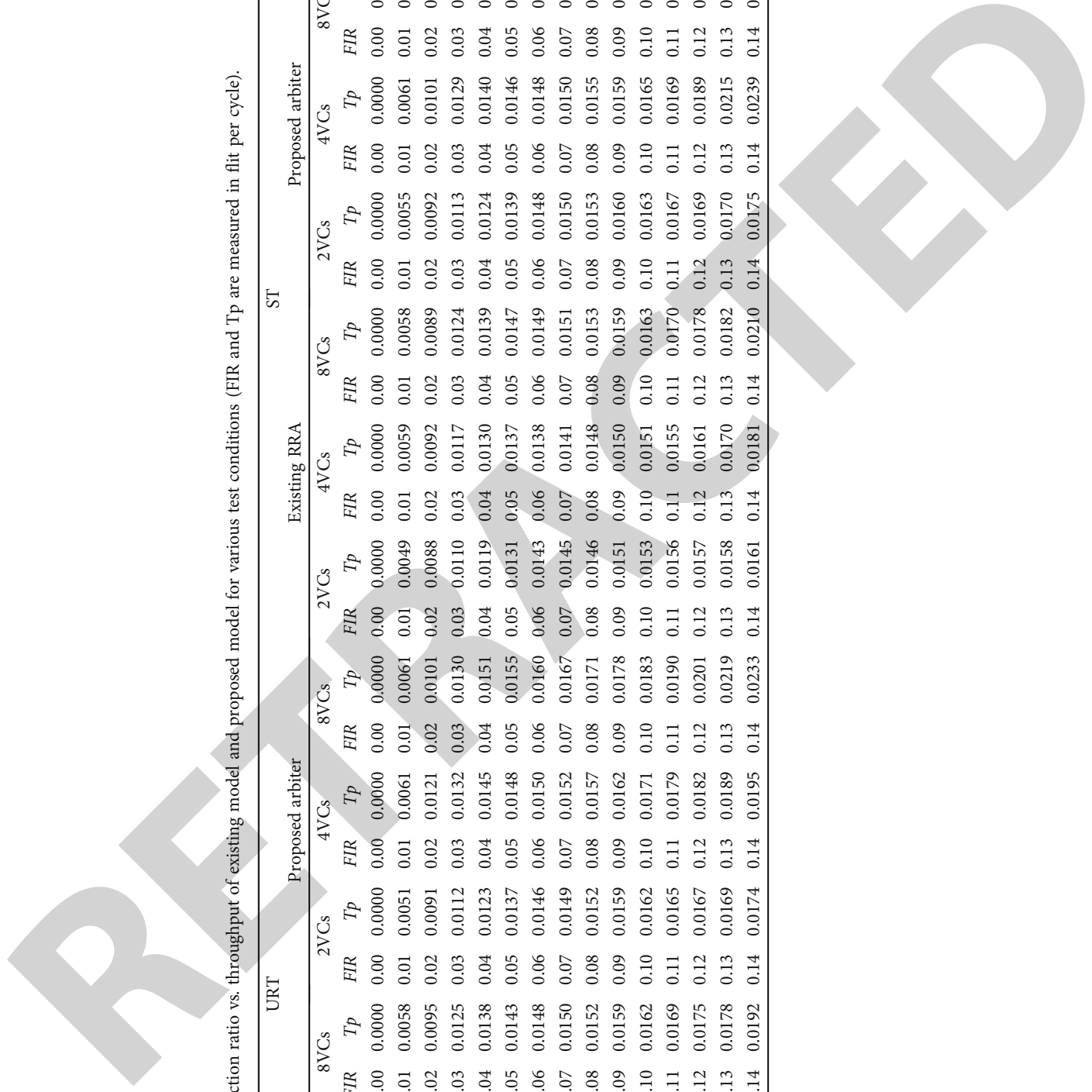


TABLE 2: Feature estimation of arbiter.

Design	Area occupation (μm^2)	Critical delay (ps)
Existing RRA	124.6	456.4
Proposed	109.5	384.2

Depending on the traffic conditions (load) of the preceding router, the flexible priority will be assigned. If a deadlock like conditions of multiple data packets path requests one channel then the priority resolver of arbiter decides the grant to which packets. So flexible priority-based dynamic arbitrations will be implemented. The initial conditions for the resolutions are to read all the requests of input ports that want grant for the same output port and then the arbiter encounters a $K \times K$ matrix developed by flexible priority resolver with bits arranged in a triangular array. The grant will be issued to the requested based on the highest priority resolved matrix to the same output port. The row in the matrix competes input requests and its priorities. The scheduling module will study the priorities of each input port request. The arbiter receives updated within the scheduling matrix when the maximum priority input is served by means of making the request which gets the earlier access. Row and column receive inversed for much less precedence for the next round of arbitration. The simulation end result for the arbitration is shown in Figure 10(c) which gives precedence with apropos to the grant generation. The arbiter is implemented using VHDL in Xilinx Vivado 2021.2.1 and simulated with Vivado-IDE.

4. Throughput Assessment

In this paper, the proposed arbiter is designed on a baseline router of NoC, where the RC, VC, and SA are not much modified. Prior prioritizations greatly reduce the burden of arbiter computation and competition for the allocations through a flexible priority resolver. To maximize the throughput, we used a 3×3 2D mesh. Input ports of all routers have four buffers of 32-bit length. The network is implemented using VHDL in Xilinx Vivado 2020.2 and simulated with Vivado-IDE. To compute the load calculations, we used a URT and synthetic traffic pattern. The throughput is VC number dependent; as the number of VCs increases, the throughput increases as illustrated in Figures 13 and 14 for URT and synthetic traffic, respectively. The prioritized circuit verifies the traffic load in all interfacing directions and preestimates the best suitable path for transmitting the flits without locking them more time at the buffer. First, the system is tested with low flit injection ratio to high flit injection ratio with uniform random traffic (URT) and then with the synthetic traffic, with more than 10% throughput improvement noticed. Table 1 shows the flit injection ratio versus throughput of existing model and the proposed model. Flexible priority resolver usage in the proposed model has larger throughput at higher flit injection ratios with various traffic conditions. It is observed that there is around 3% to 30% throughput increase with respect to low FIR to high FIR.

Table 2 shows the synthesis results of the arbiter in comparison with the existing RRA arbiters, which offers a 12% less occupation of the area and a 15.81% reduction in critical latency.

The future expansions in this model are to work for more throughputs at lower flit injection rates. Further, the area optimization techniques are expected to be implemented for better performance.

5. Conclusion

The main feature of the proposed model is to provide high throughput and efficient on-chip communications for multicore architectures. With the proposed arbiter design, it is observed that the area occupation of buffers and critical delays were considerably reduced; hence, the waiting time of the flits at the arbiter buffers will be less, and the total communication time will decrease. Further, as the priorities are resolved before the flits get granted to the arbiter, the load of the arbiter will significantly reduce, and communication will be efficient. Thus, the proposed model improves the throughput in multicore systems like SoC with an efficient arbiter at NoC. This work has a limitation, i.e., area occupation of the die and productivity (throughput) have no more remarkable improvement at low traffic/load in comparison with the existing models. The proposed arbiter is showing good improvement in the throughput at higher data rates; an average of more than 10% throughput improvement is noticed at higher flit injection rates independent of the VCs implemented. Further, the critical delays are reduced to 15.84% with greater throughputs. Besides, the design proves that at higher flit rates the throughput is increasing considerably. Hence, new hopes are increasing to do further research to accommodate more packets per cycle without compromising the system performance. The future design extensions of the proposed model are expected to handle the exceptions in data transmission over on-chip networks and reduce further latency.

Data Availability

The data used to support the findings of this study are available from the corresponding author upon request.

Conflicts of Interest

The authors declare that they have no conflicts of interest.

Acknowledgments

I thank my working place, IIIT-Bhubaneswar, which provided me with the flexibility and facilities to carry my research during my job as an Assistant Professor of the ETC department. Further, I thank my research bringing university VTU, Belgaum, for permitting me as a researcher. I specially acknowledge my guide Dr. G. Chenchu Krishnaiah and the doctoral committee for giving me timely suggestions.

References

- [1] A. Romyantsev, T. Krupkina, and V. Losev, "Development of a high-speed multi-target measurement system-on-chip," in *2019 IEEE Conference of Russian Young Researchers in Electrical and Electronic Engineering (EIConRus)*, pp. 1601–1604, Saint Petersburg and Moscow, Russia, 2019.
- [2] G. Martin and H. Chang, "System-on-chip design," in *ASICON 2001. 2001 4th International Conference on ASIC Proceedings (Cat. No.01TH8549)*, Shanghai, China, 2001.
- [3] W. Liu, W. Zhang, X. Wang, and J. Xu, "Distributed sensor network-on-chip for performance optimization of soft-error-tolerant multiprocessor system-on-chip," *IEEE Transactions on Very Large Scale Integration (VLSI) Systems*, vol. 24, no. 4, pp. 1546–1559, 2016.
- [4] U. Schlichtmann, "Tomorrow's high-quality SoCs require high-quality embedded memories today," in *Proceedings in Proc SQED*, p. 225, San Jose, CA, USA, 2002.
- [5] F. Yazıcı, A. S. Yıldız, A. Yazar, and E. G. Schmidt, "A novel scalable on-chip switch architecture with quality of service support for hardware accelerated cloud data centers," in *2020 IEEE 9th International Conference on Cloud Networking (CloudNet)*, Piscataway, NJ, USA, 2020.
- [6] W. S. Chu, C. S. Kim, H. T. Lee et al., "Hybrid manufacturing in micro/nano scale: a review," *International journal of precision engineering and manufacturing-green technology*, vol. 1, no. 1, pp. 75–92, 2014.
- [7] W. Wolf, A. A. Jerraya, and G. Martin, "Multiprocessor system-on-chip (MPSoC) technology," *IEEE Transactions on Computer-Aided Design of Integrated Circuits and Systems*, vol. 27, no. 10, pp. 1701–1713, 2008.
- [8] H. I. Gaha and M. Balti, "Novel bi-UWB on-chip antenna for wireless NoC," *Micromachines*, vol. 13, no. 2, p. 231, 2022.
- [9] K. Zou, Y. Wang, L. Cheng, S. Qu, H. Li, and X. Li, "CAP: communication-aware automated parallelization for deep learning inference on CMP architectures," *IEEE Transactions on Computers*, vol. 71, no. 7, pp. 1626–1639, 2022.
- [10] P. Chen, W. Liu, H. Chen et al., "Reduced worst-case communication latency using single-cycle multihop traversal network-on-chip," *IEEE Transactions on Computer-Aided Design of Integrated Circuits and Systems*, vol. 40, no. 7, pp. 1381–1394, 2021.
- [11] Y. You, Y. Chang, W. Wu et al., "New paradigm of FPGA-based computational intelligence from surveying the implementation of DNN accelerators," *Design Automation for Embedded Systems*, vol. 26, no. 1, pp. 1–27, 2022.
- [12] H. Li, Z. Tian, J. Xu, R. K. Maeda, Z. Wang, and Z. Wang, "Chip-specific power delivery and consumption co-management for process-variation-aware manycore systems using reinforcement learning," *IEEE Trans. on Very Large Scale Integration (VLSI) Systems*, vol. 28, no. 5, pp. 1150–1163, 2020.
- [13] B. S. Feero and P. Pande, "Networks-on-chip in a three-dimensional environment: a performance evaluation," *IEEE Transactions on Computers*, vol. 58, no. 1, pp. 32–45, 2009.
- [14] D. Bertozzi, A. Jalabert, Srinivasan Murali et al., "NoC synthesis flow for customized domain specific multiprocessor systems-on-chip," *IEEE Transactions on Parallel and Distributed Systems*, vol. 16, no. 2, pp. 113–129, 2005.
- [15] A. Psarras, S. Moisisidis, C. Nicopoulos, and G. Dimitrakopoulos, "Networks-on-chip with double-data-rate links," *IEEE Transactions on Circuits and Systems I: Regular Papers*, vol. 64, no. 12, pp. 3103–3114, 2017.
- [16] S. Kundu and S. Chattopadhyay, *Network on chip: the next generation of system-on-chip integration*, Proc CRC Press, T & F Group, 2015.
- [17] S. D. Oliveira, B. M. Carvalho, and M. E. Kreutz, "Network-on-chip irregular topology optimization for real-time and non-real-time applications," *Micromachines*, vol. 12, no. 10, p. 1196, 2021.
- [18] J. Trajkovic, S. Karimi, S. Hangsan, and W. Zhang, "Prediction modeling for application-specific communication architecture design of optical NoC," *ACM Transactions on Embedded Computing Systems*, vol. 21, no. 4, Article ID 35, pp. 1–29, 2022.
- [19] A. Chandra and K. Chakrabarty, "A unified approach to reduce SOC test data volume, scan power and testing time," *IEEE transactions on computer-aided design of integrated circuits and systems*, vol. 22, no. 3, pp. 352–362, 2003.
- [20] M. Shrivastava, R. Mehta, S. Gupta et al., "Toward system on chip (SoC) development using FinFET technology: challenges, solutions, process co-development & optimization guidelines," *IEEE Transactions on Electron Devices*, vol. 58, no. 6, pp. 1597–1607, 2011.
- [21] S. Kundu and S. Chattopadhyay, *Network on chip: the next generation of system-on-chip integration*, Proc CRC Press, T & F Group, 2015.
- [22] B. K. Joardar, R. G. Kim, J. R. Doppa, P. P. Pande, D. Marculescu, and R. Marculescu, "Learning-based application-agnostic 3D NoC design for heterogeneous manycore systems," *IEEE Transactions on Computers*, vol. 68, no. 6, pp. 852–866, 2019.
- [23] Y. Gan, H. Guo, and Z. Zhou, "3D NoC low-power mapping optimization based on improved genetic algorithm," *Micromachines*, vol. 12, no. 10, p. 1217, 2021.
- [24] S. K. Jena, S. Biswas, and J. K. Deka, "Retesting defective circuits to allow acceptable faults for yield enhancement," *Journal of Electronic Testing*, vol. 37, no. 5-6, pp. 633–652, 2021.
- [25] Y. Kameda, S. Yorozu, Y. Hashimoto, H. Terai, A. Fujimaki, and N. Yoshikawa, "Single-flux-quantum (SFQ) circuit design and test of crossbar switch scheduler," *IEEE transactions on applied superconductivity*, vol. 15, no. 2, pp. 423–426, 2005.
- [26] Y. Lee, J. M. Jou, and Y. Chen, "A high-speed and decentralized arbiter design for NoC," in *2009 IEEE/ACS International Conference on Computer Systems and Applications*, pp. 350–353, Rabat, Morocco, 2009.
- [27] G. Dimitrakopoulos, E. Kalligeros, and K. Galanopoulos, "Merged switch allocation and traversal in network-on-chip switches," *IEEE Transactions on Computers*, vol. 62, no. 10, pp. 2001–2012, 2013.
- [28] G. A. Subbarao and P. D. Häfliger, "Design and comparison of synthesizable fair asynchronous arbiter," in *2020 18th IEEE International New Circuits and Systems Conference (NEW-CAS)*, pp. 122–125, Montreal, QC, Canada, 2020.
- [29] J. Wei, J. Zhang, X. Zhang et al., "An asynchronous AER circuits with rotation priority tree arbiter for neuromorphic hardware with analog neuron," in *2019 IEEE 13th International Conference on ASIC (ASICON)*, Chongqing, China, 2019.
- [30] J. Kathuria and M. Sharma, "Data access resolver for IOT enabled SOC interconnections with dynamic programability feature," in *8th International Conference on Signal Processing and Integrated Networks (SPIN)*, pp. 333–338, Noida, India, 2021.

Retraction

Retracted: A Monitoring System for Air Quality and Soil Environment in Mining Areas Based on the Internet of Things

Journal of Sensors

Received 13 September 2023; Accepted 13 September 2023; Published 14 September 2023

Copyright © 2023 Journal of Sensors. This is an open access article distributed under the Creative Commons Attribution License, which permits unrestricted use, distribution, and reproduction in any medium, provided the original work is properly cited.

This article has been retracted by Hindawi following an investigation undertaken by the publisher [1]. This investigation has uncovered evidence of one or more of the following indicators of systematic manipulation of the publication process:

- (1) Discrepancies in scope
- (2) Discrepancies in the description of the research reported
- (3) Discrepancies between the availability of data and the research described
- (4) Inappropriate citations
- (5) Incoherent, meaningless and/or irrelevant content included in the article
- (6) Peer-review manipulation

The presence of these indicators undermines our confidence in the integrity of the article's content and we cannot, therefore, vouch for its reliability. Please note that this notice is intended solely to alert readers that the content of this article is unreliable. We have not investigated whether authors were aware of or involved in the systematic manipulation of the publication process.

Wiley and Hindawi regrets that the usual quality checks did not identify these issues before publication and have since put additional measures in place to safeguard research integrity.

We wish to credit our own Research Integrity and Research Publishing teams and anonymous and named external researchers and research integrity experts for contributing to this investigation.

The corresponding author, as the representative of all authors, has been given the opportunity to register their agreement or disagreement to this retraction. We have kept a record of any response received.

References

- [1] H. Dai, D. Huang, and H. Mao, "A Monitoring System for Air Quality and Soil Environment in Mining Areas Based on the Internet of Things," *Journal of Sensors*, vol. 2022, Article ID 5419167, 7 pages, 2022.

Research Article

A Monitoring System for Air Quality and Soil Environment in Mining Areas Based on the Internet of Things

Hongjing Dai , Dena Huang , and Haili Mao 

School of Chemistry and Chemical Engineering, Qiannan Normal University for Nationalities, Duyun, Guizhou 558000, China

Correspondence should be addressed to Haili Mao; 20160612@ayit.edu.cn

Received 24 July 2022; Revised 7 August 2022; Accepted 13 August 2022; Published 26 August 2022

Academic Editor: C. Venkatesan

Copyright © 2022 Hongjing Dai et al. This is an open access article distributed under the Creative Commons Attribution License, which permits unrestricted use, distribution, and reproduction in any medium, provided the original work is properly cited.

In order to solve the intensifying problem of heavy metal pollution of soil in mining areas, a method for monitoring air quality and soil environment in mining areas based on the Internet of Things is proposed. Using meta-analysis method and health risk assessment method, the impact of mining on soil heavy metal content in Southwest China was quantitatively analyzed, and the relationship between soil heavy metal value and its potential influencing factors was discussed, as well as the heavy metal pollution, ecological risk, and health caused by soil mining activities. Risks were assessed. The results showed that artificial and oral intake were the main modes of soil heavy metal exposure, with the highest daily intakes for noncarcinogenic risk children and the highest daily intakes for carcinogenic risk adult females. The noncarcinogenic risk ($HQ > 1$) of soil As and Pb exposure to children was 3.74 and 1.44, respectively. The carcinogenic risk values of As, Cd, Cr, and Ni in soil were all higher than 10^{-6} , indicating that the carcinogenic risk was within the tolerance range of human body. Children were exposed to the combined noncarcinogenic risk ($HI = 3.83$), and the risk values of the three types of recipients were 1.19×10^{-4} , 1.21×10^{-4} , and 1.06×10^{-4} , respectively. The correlation between heavy metal content and environmental factors was obtained. It is verified that the system in this paper can effectively monitor the meteorological environment and soil environment, and at the same time, it reveals the pollution law of heavy metals in the soil of the mining area, which provides supporting conditions for future mining and heavy metal pollution management.

1. Introduction

In recent years, the rapid exploitation of mineral resources in China has not only promoted the development of social economy, but also caused serious soil pollution. Soil pollution is a pollution caused by a kind of toxic substances produced as a result of unreasonable human activity through the way such as atmosphere, the earth surface, or underground runoff into the soil. When the soil accumulation exceeds the self-purification capacity of the soil itself, the composition, structure, and function of the soil will change, and microbial activities will be cramped, which can harm human health eventually through the food chain. Data collection is shown in Figure 1 [1]. Heavy metals refer to elements with a density greater than 5 g cm^{-3} , which gradually accumulate after entering the soil. When exceeding a certain standard, they are absorbed by soil colloid. After physical or

chemical reactions, they will form a pollutant. These pollutants cannot be degraded by microorganisms. They have great toxicity, and they are easy to enrich in the soil, resulting in serious soil heavy metal pollution. This kind of pollution has the characteristics of long-term, hidden, and irreversible, which will affect the normal agricultural production and life. It is a kind of soil pollution that is difficult to treat. Researches show that the area of soil heavy metal pollution in China has reached 50 million mu and the content of heavy metals in soil shows a rising trend, mainly Cd (cadmium), Pb (lead), Hg (mercury), and other heavy metals [2]. Heavy metal pollution not only destroys land, but also causes certain harm to human health. For example, excessive intake of Cd will lead to hypertension and cardiovascular and cerebrovascular diseases. Arsenic (As) is recognized as a carcinogenic heavy metal, which has obvious accumulation in the human body. It can cause red blood cell

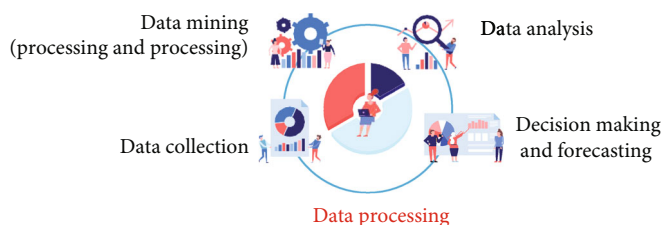


FIGURE 1: The process of big data processing environmental information.

dissolution, damage normal physiological functions, and can cause cancer and teratogenesis in serious cases. Excessive Pb in children will cause mental decline and growth retardation.

The era of big data has arrived, and big data has been involved in all walks of life. The data resources mastered by all walks of life are important wealth in the future. The government use big data thinking to solve specific problems. The big data thinking and technology are applied in environmental governance to provide data support for environmental public governance. Through data collection, real-time monitoring, the citizen participation in the form of management, and environmental governance, it can provide scientific and accurate thinking for the government decision-making in public environment monitoring and early warning [3].

2. Literature Review

At present, local provinces and cities in China are constantly developing the level of environmental protection information, and they are trying to establish information centers to coordinate environmental data resources. Ahmad et al. summarized the technologies involved in the application of environmental big data [4]. In the platform category, the local platform architecture mainly included Hadoop and Map R. The cloud architecture mainly included AWS and Azure. In the database category, the SQL category included Greenplum, No SQL category included HBase, and New SQL included Spanner. Data warehouse technology included Hive. In data processing, batch processing technologies included Map Reduce, and data flow processing technologies included Storm. Query languages included Hive QL. Machine learning included Mahout. And log processing included Splunk. Yang et al. summarized the key technologies of industrial energy and environment big data [5]. They put forward that big data was a long industrial chain. Data collection stage mainly based on industrial Internet of Things technology. Data preprocessing stage included data extraction and cleaning. Big data storage and management phase included development of distributed file system optimization storage, innovation of database technology, and maintenance of big data security. Data analysis and mining stage mainly developed various machine learning algorithms and database methods. In the parallel stage of data computation, Hadoop architecture should be adopted. FLASH and other ways were adopted to achieve data visualization. Hamidović et al. emphasized the importance of heterogeneous data sources in environmental big data. They pro-

posed that the real environmental big data should break the traditional data sources, namely the data of environmental departments themselves, and related departments included more emerging Internet data and smart facility data [6].

In the research, the process of big data technology was attempted to apply in environmental monitoring and early warning. Combining theoretical knowledge and empirical practice, the environmental big data was established in the field of public governance environment. Through specific case analysis, in view of the environmental problems, environmental public service solution and effective governance based on large data was put forward. By using big data in high efficiency value in the process of management decision, environmental big data was established, and environmental big data system and governance mechanism were formed, providing a constructive reference for the government in the construction of basic environmental public services. It helped government departments to carry out accurate regulation and optimize the government's environmental public service level [7, 8].

By using meta-analysis method and health risk assessment method, the quantitative analysis of the mining impact on soil heavy metal content in Southwest China was made, the effect of the relationship between soil heavy metals value and its potential impact factors was discussed, and the soil heavy metal pollution, the ecological risk, and the health risk caused by mining activities were evaluated. In the research, the carcinogenic risk caused by heavy metal pollution in mining area was analyzed to solve the problem of analyzing the harm caused by soil heavy metal pollution to human body.

3. Research Methods

3.1. Meta-analysis. In meta-analysis, the collected data were divided into two groups according to the treatment group and the control group, and pairwise pairing was performed. By using model calculation method, the relationship between the treatment group and the control group was expressed by a numerical value, which was the effect size (ES). In the research, the background values, sampling numbers, and standard deviations of heavy metals in soils of Southwest China recorded by China Environmental Monitoring Station (1990) were selected as the control group. The mean value, sampling quantity, and standard deviation of soil heavy metal content extracted in the literature survey were the treatment group [9, 10]. In the research,

logarithmic reaction ratio ($\ln R$) was used to measure the effect value. And its calculation formula was as follows.

$$ES = \ln R = \ln \left(\frac{X_t}{X_c} \right) = \ln (X_t) - \ln (X_c). \quad (1)$$

In Formula (1), X_t represented the average value of soil heavy metals extracted from the literature. X_c represented the background value of heavy metals in soils of provinces in Southwest China. If the effect value was higher than 0, it indicated that mining increased the content of heavy metals in soil. The intrastudy variance (v_i) corresponding to each effect value could be calculated using the following formula.

$$v_i = \frac{S_t^2}{N_t X_t^2} + \frac{S_c^2}{N_c X_c^2}. \quad (2)$$

In Formula (2), S_t and S_c were the standard deviations (SD) of the mean value and background value of soil heavy metals. N_t and N_c were the number of heavy metal groups in soil survey of the control group and the treatment group, respectively. In meta-analysis, there were two types of models: fixed effect and random effect. The former only took into account intrastudy differences, while the latter took into account both intrastudy and interstudy differences. The soil heavy metals in mining areas investigated in the research were located in different geographical locations and natural environments, and there were certain differences between studies. Therefore, the random effect model was selected to calculate its effect value [11, 12]. This model took into account not only intrastudy variance but also interstudy variance (τ^2), which was estimated by maximum likelihood function (REML). The weight w_i of each study was calculated as follows:

$$w_i = \frac{1}{v_i + \tau^2}. \quad (3)$$

The weighted w_i of each study could be used to calculate the comprehensive effect value (ES_+) after weighted average. And the calculation formula was as follows:

$$ES_+ = \frac{\sum_{i=1}^k (w_i + ES_i)}{\sum_{i=1}^k w_i}. \quad (4)$$

In Formula (4), w_i and ES_i were the weighted and unweighted effect value of the i th pair of data, respectively. k was the number of pairs between the control group and the treatment group. At the same time, the 95% confidence interval (CI) of the comprehensive effect value was calculated. If the 95% confidence interval (CI) of the comprehensive effect value was greater than 0, it was believed that the mining in Southwest China had a significant increase in the content of heavy metals in soil ($p < 0.05$). If 95% confidence intervals were all less than 0, mining in Southwest China did not significantly increase the content of heavy

metals in soil ($p < 0.05$). If the 95% confidence interval contained 0, it was believed that mining in Southwest China had no significant impact on the content of heavy metals in soil ($p < 0.05$) [13, 14]. In order to more conveniently explained the influence of mining on the content of heavy metals in soil in Southwest China, the percentage change of the content was calculated by the following formula:

$$PI = (e^{ES_+} - 1) \times 100\%. \quad (5)$$

3.2. Health Risk Assessment Method. The health risks were assessed by using a National Environmental Protection Agency health risk assessment model, which linked soil heavy metal pollution with human health and quantitatively assessed the health risks of the exposed recipients. Carcinogenic and noncarcinogenic risks were quantified based on daily heavy metal intake in children, adult women, and adult men. The calculation methods of daily intake under skin contact (ADI_{der}), hand-oral intake (ADI_{ing}), and oral-nasal respiration (ADI_{inh}) were as follows, and the specific meanings of parameters are shown in Table 1.

$$ADI_{der} = \frac{C \times SA \times ABS \times AF \times EF \times ED \times CF}{BW \times AT}, \quad (6)$$

$$ADI_{ing} = \frac{C \times IR \times EF \times ED \times CF}{BW \times AT}, \quad (7)$$

$$ADI_{inh} = \frac{C \times InhR \times EF}{PEF \times BW \times AT}. \quad (8)$$

The noncarcinogenic risk was expressed by the hazard quotient (HQ) of heavy metals, and the comprehensive noncarcinogenic risk was expressed by the total hazard index (HI) of individual heavy metals. Rfd_{der} , Rfd_{ing} , and Rfd_{inh} were the reference doses [$\text{mg} (\text{kg day})^{-1}$] of heavy metal intake in skin contact, hand-oral intake, and oral-nasal respiratory exposure, respectively. The reference values are shown in Table 2. If HQ or HI < 1 indicated that there was no noncarcinogenic risk, otherwise, heavy metal exposure presented a noncarcinogenic risk. The comprehensive noncarcinogenic risk calculation formula was as follows.

$$HI = \sum_{i=1} HQ_i = \sum \left(\frac{ADI_{der}}{Rfd_{der}} + \frac{ADI_{ing}}{Rfd_{ing}} + \frac{ADI_{inh}}{Rfd_{inh}} \right). \quad (9)$$

The carcinogenic risk (CR) was the possibility of developing cancer after exposure to soil heavy metals in the whole life cycle. SF_{der} , SF_{ing} , and SF_{inh} were soil heavy metal carcinogenic tilt factors [$\text{mg} (\text{kg day})^{-1}$] under skin contact, hand-oral ingestion, and oral-nasal respiratory exposure, respectively. See Table 2 [15, 16]. If $CR < 10^{-6}$, there was no carcinogenic health risk. Between 10^{-6} and 10^{-4} was the range of

TABLE 1: Parameter significance and selected values of daily intake of heavy metals in soil.

Parameter	Meaning	Unit	Adult		
			Child	Female	Male
C	Heavy metal content	mg kg ⁻¹			
SA	Skin surface area exposed to soil	cm ²	9310	15310	16970
ABS	Skin absorption factor	Dimensionless	0.001	0.001	0.001
AF	Adhesion coefficient of soil to skin	mg (cm ² day) ⁻¹	0.2	0.07	0.07
EF	Exposure frequency	Day year ⁻¹	345	345	345
ED	Exposed fixed number of year	Year	6	24	24
CF	Conversion factor	kg mg ⁻¹	10 ⁻⁶	10 ⁻⁶	10 ⁻⁶
InhR	Daily respiration rate	m ³ day ⁻¹	11.78	14.17	19.02
IR	Soil digestibility	mg day ⁻¹	200	100	100
BW	Weight	kg	27.7	54.4	62.7
PEF	Particulate emission factor	m ³ kg ⁻¹	1.36 × 10 ⁹	1.36 × 10 ⁹	1.36 × 10 ⁹
AT	Average non-carcinogenic time	Day	ED × 365	ED × 365	ED × 365
	Average time to carcinogenesis	Day	25550	25550	25550

TABLE 2: Reference doses and carcinogenic tilt factors of soil heavy metals exposed by different pathways [mg(kg day)⁻¹].

	Rfd _{der}	Rfd _{ing}	Rfd _{inh}	SF _{der}	SF _{ing}	SF _{inh}
As	1.23 × 10 ⁻⁴	3 × 10 ⁻⁴	3 × 10 ⁻⁴	3.66	1.5	15.1
Cd	1 × 10 ⁻⁵	1 × 10 ⁻³	1 × 10 ⁻³	6.3	6.1	6.3
Cr	6 × 10 ⁻⁵	3 × 10 ⁻³	2.86 × 10 ⁻⁵	20	0.5	42
Cu	1.2 × 10 ⁻²	4 × 10 ⁻²	4.02 × 10 ⁻²	—	—	—
Hg	2.1 × 10 ⁻⁵	3 × 10 ⁻⁴	8.57 × 10 ⁻⁵	—	—	—
Ni	5.4 × 10 ⁻³	2 × 10 ⁻²	9 × 10 ⁻⁵	42.5	1.7	0.84
Pb	5.25 × 10 ⁻⁴	3.5 × 10 ⁻³	3.52 × 10 ⁻³	—	8.5 × 10 ⁻³	—
Zn	6 × 10 ⁻²	0.3	0.3	—	—	—

Note: —: no parameter.

human tolerable cancer risk; higher than 10⁻⁴ indicated the existence of serious carcinogenic health risks, which should be paid attention to. The comprehensive carcinogenic risk calculation formula was as follows.

$$TCR = \sum_{i=1} CR_i = ADI_{der} \times SF_{der} + ADI_{ing} \times SF_{ing} + ADI_{inh} \times SF_{inh}. \quad (10)$$

4. Results Analysis

4.1. Descriptive Statistics and Spatial Distribution of Heavy Metal Content in Soil. The descriptive statistics of soil heavy metals in Southwest China are shown in Table 3. The average contents of heavy metals except Cr and Ni exceeded the national risk screening values of soil Environmental Quality Standards for corresponding agricultural lands (GB15618-2018). The average of soil As and Cd contents exceeded the national risk control value (Table 3). The overstandard rates of As, Cd, Cr, Cu, Hg, Ni, Pb, and Zn (the percentage of the number of investigation groups exceeding

the national risk screening value in the total investigation group) were 75.58%, 82.93%, 2.78%, 46.24%, 32.61%, 4.35%, 63.49%, and 50.43%, respectively. Among them, soil Cd had the highest overstandard rate, and its average overstandard multiple was 16.22. Soil As and Pb had higher overstandard rate, with overstandard multiple of 8.20 and 4.31, respectively. The exceedance rate of Cr and Ni in soil was less [17, 18]. The median of each heavy metal content was lower than the average value, and the 95th percentile value differed greatly from the maximum value, which exceeded the corresponding control value (Table 3). This indicated that the mining of mineral resources in Southwest China led to a certain accumulation of heavy metals in soil, among which Cd accumulation was the most and Cr accumulation was the least. The results showed that the distribution area of high content in soil was not only related to soil high background value, but also related to mining. Mineral resources were widely distributed in these areas, and a large number of heavy metal elements were released in the mining process, so the distribution of heavy metals showed obvious similar regional spatial distribution characteristics. As a whole, the content of heavy metals in soil around mining area in Southwest China was relatively high.

4.2. Influence of Mining on Soil Heavy Metals under Different Land Use Types in Southwest China. Table 4 shows the parameter significance of the influence factors of soil heavy metals investigated in the mining area in Southwest China. The land use types investigated in the research mainly included abandoned land soil, arable land soil, and woodland soil. On the whole, the average effect of mining on heavy metals under different land use types from high to low was as follows: wasteland soil > cultivated soil > woodland soil (Table 4). The average effect value of heavy metals in soil of abandoned mining areas was 2.59 (Table 4). Compared with soil background value, its content increased by 1232.98%. The average effect of mining on cultivated land and forest land was 1.43 (95% CI: 1.30–1.56) and 0.87

TABLE 3: Descriptive statistics of soil heavy metals in mining areas in Southwest China extracted from the literature (mg kg^{-1}).

	Minimum	25 percentile	Median	Mean	75 percentile	95 percentile	Maximum	Screening value a	Regulated value a
As	4.8	20.59	38.03	164.01	155.64	477.58	2423.57	20	100
Cd	0.19	1.03	3.46	9.73	11.15	46.53	66.17	0.6	4
Cr	18.06	50.92	82.45	101.13	125.95	186.13	683.57	250	1300
Cu	9.69	41.45	88.43	214.62	148	457.33	4480.87	100	—
Hg	0.06	0.22	0.59	3.12	1.27	18.84	35.1	1	6
Ni	12.87	36.41	57.8	74.72	74.25	164.55	656.11	190	—
Pb	9.44	72.65	250	732.14	748.39	2650.86	8816.34	170	1000
Zn	24.26	129.52	311.9	1483.57	1485.06	4924.12	36995.2	300	—

Note: Soil Environmental Quality Standard (GB15618-2018); descriptive statistics were obtained from the average of soil heavy metal content extracted from literature.

TABLE 4: Parameter significance of influencing factors of soil heavy metals in the survey location of the mining area in Southwest China.

Influencing factors	Number of observation group	Effect value	Upper limit	Lower limit	Heterogeneity
Land use type	Soil	33	0.87	0.34	1.40
	The soil	531	1.43	1.30	1.56
	Abandoned soil	38	2.59	2.10	3.09
Minerals	Non-ferrous ore	538	1.70	1.57	1.82
	Coal mine	123	0.65	0.38	0.92
	Ferrous ore	46	0.54	0.10	0.98
Geographical partition	A	323	1.83	1.66	1.99
	B	72	1.81	1.46	2.16
	C	280	0.93	0.75	1.11
	D	10	1.43	0.48	2.37
	E	22	0.94	0.31	1.58

Note: Q_m is the heterogeneity caused by this influencing factor. Df is the degree of freedom. $p < 0.05$ shows that the influence of this factor is significant. The upper limit and lower limit are the maximum and minimum value of 95% confidence interval, respectively. The number of observation group refers to the number of heavy metal groups investigated.

(95% CI: 0.34–1.40), respectively (Table 4). This showed that arable land was more affected by mining activities than forest land. Figure 2 shows the effects of mining on soil heavy metals under different land use types in Southwest China, which showed that the influence of mining on abandoned land was higher than that of arable land and woodland soil. In arable soil, Cd (2.60), Hg (2.19), and Pb (1.86) were mainly affected by mining, and the effect values of Cd (2.60), Hg (2.19), and Pb (1.86) were higher (Figure 2). Compared with the background value, the content increased by 1246.37%, 793.52%, and 542.37%, respectively.

4.3. Influence of Mining on Soil Heavy Metals in Different Provinces in Southwest China. Table 5 shows the overall heterogeneity of heavy metals in soils of mining areas in Southwest China. The p value of overall heterogeneity ($Q_t = 129330.05, p < 0.0001$) of soil heavy metals caused by mining in Southwest China was lower than 0.05. As can be seen from Table 5, the significance level (p value) of the overall heterogeneity of individual heavy metals was all less than 0.05, so it was necessary to introduce explanatory variables for analysis [19, 20]. The number of heavy metal groups in A, B, C, D, and E and Xizang were 323, 72, 280, 22 and 10, respectively. According to the survey statistics, except Cr, mining in A mine significantly increased the con-

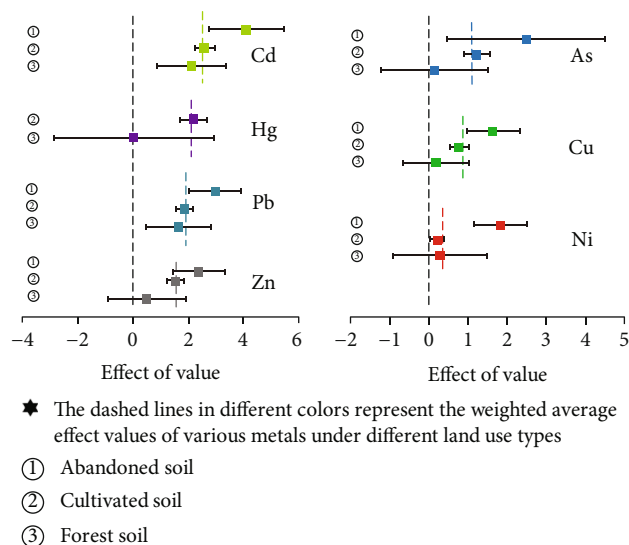


FIGURE 2: Influence of mining on heavy metals under different land use types in Southwest China.

tents of other heavy metals. The average effect values of Cd, Pb, Zn, and As in soil were 3.21, 2.33, 1.75, and 1.45, respectively. Compared with the background value, the heavy

TABLE 5: Overall heterogeneity of all heavy metals caused by mining in Southwest China.

Heavy metals	As	Cd	Cr	Cu	Hg	Ni	Pb	Zn
Q_t	8128.49	8290.86	4169.17	7437.63	4101.64	1339.61	30428.23	27456.61
p	<0.0001	<0.0001	<0.0001	<0.0001	<0.0001	<0.0001	<0.0001	<0.0001

Note: Q_t represents the overall heterogeneity of the data and p represents the level of significance.

metal content in the samples increased by 2377.91%, 927.79%, 326.31%, and 475.46%, respectively. The mining of a mine significantly increased Cd (3.78), Pb (2.96), Zn (2.27), and Hg (1.75) in soil than the other four heavy metals. Compared with soil background value, its content increased by 4281.6%, 1829.8%, 867.94%, and 475.46%, respectively. The mining of B and C both resulted in a high increase of Hg in soil. In Guizhou mining, soil Hg (2.49) had the highest effect value, while soil Cu (0.25) had the lowest. Compared with the background value, the content of Hg in soil increased by 1106.13%. Mining in Chongqing also significantly increased the content of Hg in soil, with an effect value of 2.14.

4.4. Evaluation of Ground Accumulation Index of Heavy Metal Content in Soil by Mining. The evaluation results showed that the average ground accumulation index of the eight heavy metals from high to low was Cd > Hg > Pb > Zn > As > Cu > Ni > Cr. The pollution degree of heavy metals in soil caused by mining was different. Cd was strongly polluted. Hg and Pb were moderately to strongly polluted. Zn and As were moderately polluted. Cu was slightly polluted. Ni and Cr were pollution-free. The evaluation results of potential ecological risk index showed that the average ecological risk index of 8 heavy metals from high to low was Cd/Hg > Pb/As > Cu/Zn/Ni/Cr. Soil heavy metals Cd and Hg were in extremely strong ecological risk, and the risk degree was higher than other heavy metals. The comprehensive ecological risk of soil heavy metals was extremely high, accounting for 39.72%, and Cd and Hg were the main contributing factors to the ecological risk. The results of health risk assessment showed that manual and oral intake was the main way of soil heavy metal exposure, with the highest daily intake for children under noncarcinogenic risk and the highest daily intake for adult women under carcinogenic risk. The exposure of soil As and Pb had a noncarcinogenic risk to children, with a risk value of 3.74 and 1.44, respectively. The carcinogenic risk values of As, Cd, Cr, and Ni in soil were all higher than 10^{-6} , indicating that the carcinogenic risk was within the tolerance range of human body. Children were affected by the combined non-carcinogenic risk, and the risk values of all three types of recipients were 1.19×10^{-4} , 1.21×10^{-4} , and 1.06×10^{-4} , respectively.

Based on the results, As, Cd, Hg, and Pb should be prioritized in the mining area of Southwest China. Children are a priority group of residents. Compared with the previous studies on soil heavy metals in single mining areas and a few mining areas, the above results can provide more effective decision support for soil pollution prevention and control and soil environmental quality protection in mining areas in Southwest China.

5. Conclusion

In the research, by using meta-analysis method and health risk assessment method, the quantitative analysis of the mining impact on soil heavy metal content in Southwest China was made, the effect of the relationship between soil heavy metals value and its potential impact factors was discussed, and the soil heavy metal pollution, the ecological risk, and the health risk caused by mining activities were evaluated. To a certain extent, the research results quantitatively assessed the impact of mining on soil heavy metals in Southwest China. Although some meaningful conclusions have been drawn, there are also shortcomings, mainly in the following aspects.

- (1) The fact that heavy metal content in the soil accumulates or increases is influenced by many factors, which is not just mentioned in the research. There are many other possible factors, such as pH, soil organic carbon, and mine production. The relevant data involved in the investigation is less, which is not easy to extract and need more case researches. Therefore, it has not yet been discussed in the research, and these factors should be taken into account in future research
- (2) The impact of soil heavy metal pollution on human body is not only related to the amount of heavy metal exposure, but also related to the biological availability of heavy metals ingested by human body, which should be paid attention to in future research

Mining has promoted the development of local economy, but the pollution of heavy metals in mining soil has also affected the normal production and life of human beings. And the accumulation of heavy metals in soil is also a relatively complex process. In the future further analysis, in addition to analyzing the increase of soil heavy metals caused by mining, comprehensive consideration should be given to the migration mechanism and form existence of heavy metals themselves in the soil, so as to provide more and more effective information for improving soil environmental quality and building green mines.

Data Availability

The data used to support the findings of this study are available from the corresponding author upon request.

Conflicts of Interest

The authors declare that they have no conflicts of interest.

Retraction

Retracted: 3D Simulation Landscape Design Based on Image Sensor

Journal of Sensors

Received 12 December 2023; Accepted 12 December 2023; Published 13 December 2023

Copyright © 2023 Journal of Sensors. This is an open access article distributed under the Creative Commons Attribution License, which permits unrestricted use, distribution, and reproduction in any medium, provided the original work is properly cited.

This article has been retracted by Hindawi, as publisher, following an investigation undertaken by the publisher [1]. This investigation has uncovered evidence of systematic manipulation of the publication and peer-review process. We cannot, therefore, vouch for the reliability or integrity of this article.

Please note that this notice is intended solely to alert readers that the peer-review process of this article has been compromised.

Wiley and Hindawi regret that the usual quality checks did not identify these issues before publication and have since put additional measures in place to safeguard research integrity.

We wish to credit our Research Integrity and Research Publishing teams and anonymous and named external researchers and research integrity experts for contributing to this investigation.

The corresponding author, as the representative of all authors, has been given the opportunity to register their agreement or disagreement to this retraction. We have kept a record of any response received.

References

- [1] Y. Lu, B. Chen, Y. Xing, and Y. G. Seok, "3D Simulation Landscape Design Based on Image Sensor," *Journal of Sensors*, vol. 2022, Article ID 1577945, 7 pages, 2022.

Research Article

3D Simulation Landscape Design Based on Image Sensor

Yao Lu ¹, Bingyan Chen ², Yan Xing ³, and Yang Geon Seok ⁴

¹Art Design College, Henan University of Urban Construction, Pingdingshan, Henan 467000, China

²School of Design and Art, Henan University of Technology, Zhengzhou, Henan 450000, China

³Department of Urban Planning, College of Urban Construction and Planning, Henan University of Urban Construction, Pingdingshan, Henan 467000, China

⁴School of Landscape and Architecture Landscape Discipline, Dong-a University, Busan 612-022, Republic of Korea

Correspondence should be addressed to Yao Lu; 11231419@stu.wxica.edu.cn

Received 29 June 2022; Revised 17 July 2022; Accepted 29 July 2022; Published 18 August 2022

Academic Editor: C. Venkatesan

Copyright © 2022 Yao Lu et al. This is an open access article distributed under the Creative Commons Attribution License, which permits unrestricted use, distribution, and reproduction in any medium, provided the original work is properly cited.

In order to solve the problem of heavy workload of landscape plant modeling, the lack of efficient auxiliary or automatic methods for establishing three-dimensional models for various landscape plants, and the general three-dimensional models of landscape plants which cannot reflect the natural growth of plants and the interaction between the environment, this paper proposes a method of three-dimensional simulation of landscape design based on image sensors. This method includes the construction of three-dimensional image simulation landscape feature analysis function and rationality judgment model, so as to provide theoretical support for landscape design. The experimental results show that the matching number and matching rate of landscape feature points obtained by the traditional deep evaluation method are lower than those obtained by the 3D image simulation method used in this paper, and the steps of image feature points matching are relatively simple. With the gradual expansion of the scope, the accuracy of the three-dimensional image simulation judgment method used in this paper is gradually improved, up to 89%, while the traditional method is always maintained at about 40%. *Conclusion.* The 3D simulation landscape design method based on image sensor has higher accuracy and wider application prospect.

1. Introduction

Landscape architecture planning and design plays an important role in society, economy, and ecology and is an important part of building a “beautiful China.” Good garden design helps people to live in harmony with the environment and build a good ecological and aesthetic environment. The ecological effect of garden needs the living plant environmental function to complete, and plants also have irreplaceable landscape making function and aesthetic value in garden aesthetics. The planning, design, and application of garden plants involve ecology, plant geography, plant physiology, floriculture, and other disciplines. The design shall comply with the planning requirements such as the classification standard of urban green space and consider the regional characteristics, ornamental, and other factors. In order to fully consider these factors in the design, landscape designers have already made extensive use of computer-

aided design and virtual simulation technology to carry out the planning, design, and display of plant landscape in three-dimensional landscape design software [1]. At present, three-dimensional landscape design software can realistically display the three-dimensional image form of plants, but there are still some deficiencies in simulating the growth process of plants and the dynamic effect of interaction with the environment [2]. Virtual plants can effectively improve the efficiency and quality of landscape plant configuration design [3]. Realize the dynamic visualization of landscape plants, and intuitively display the morphological appearance, growth process, and interaction with the outside world of landscape plants (including light, soil, diseases and pests, plant communities, and other elements). The virtual simulation of garden landscape plants can provide scientific basis and prediction for plant configuration, environmental protection, and plant maintenance [4]. Although many achievements have been made in the research of virtual landscape

plants, there are still some problems affecting the application of virtual landscape plants in practice. These problems mainly include the following: (1) the workload of landscape plant modeling is large, and there is a lack of efficient auxiliary or automatic methods to establish three-dimensional models for all kinds of landscape plants; (2) the general three-dimensional model of landscape plants can not reflect the natural growth of plants and the interaction between the environment.

In view of the problems existing in the above methods, the rationality of landscape design is analyzed by using the three-dimensional image simulation judgment method, which can quickly and accurately judge the rationality of landscape design and provide guarantee for environmental beauty [5].

2. Literature Review

Lb et al. combine the time series drawn modeling of the NARX neural network with mass routing protocol based on simple vector quantization and transfer of small amounts of molten data to the gravity of the suction to remove and improve the time and place and enhance data collection efficiency. However, the actual melting of this sample is not good and its efficiency is not very high [6]. Hussein modified the integration model based on the changing dimming c -application agglomeration. Adaptive clustering of the unknown C values is used for data collection. Adaptive coefficients are shown to show clusters of various shapes and sizes. The principle of Kalman filter and neural network process prediction based on multi-layer perceptrons is used in error comparison to improve melting reliability. However, the performance of these models is low, and it is difficult to meet the needs of the actual options [7]. Lin and Zhang divided the virtual plant modeling methods into four categories: plant overall shape simulation, plant organ three-dimensional modeling, plant growth process simulation, and plant structure function parallel simulation [8]. L-system is a kind of virtual plant modeling method which has been widely studied and expanded. A formal mathematical expression system L-system for plant topological structure is proposed. L-system is a string rewriting system, which can describe the morphology and growth of plants. L-system describes the topological structure of plants and expresses the topological relationship between various organs of plants in the form of symbols [9]. Mckinley et al. extended the L-system, proposed open L-system and stochastic L-system that can interact with plant growth environment, and developed l-studio system [10]. The l-studio system has been able to complete the functions from virtual plant modeling to 3D model generation and visualization and can dynamically simulate the growth of plants and the interaction with the environment [11]. In the early development of computer science, researchers began the research of automatic computer program generation and made a lot of achievements in compiler, software modeling, auxiliary program development, and so on. Recently, with the improvement of computer performance and the development of artificial intelligence, the research on the automatic generation of executable software programs by computers has also made great progress. Belloro-

bles et al. proposed a computer program automatic generation algorithm of genetic algorithm with guidance [12]. The target recognition algorithm based on 3D point cloud has made many application achievements in the research of obtaining plant point cloud and reconstructing 3D plant model by using Kinect, leap motion, and other devices [13]. Laser 3D scanning technology is widely used in plant detection, automatic driving, 3D modeling, high-precision measurement, and scene restoration [14].

Based on current research, this paper provides a way to create a triangle to identify the advantages of landscape design. The principle of using an orthophoto pair to create three-dimensional landscapes is to draw three-dimensional and three-dimensional landscapes in an orthophoto pair. The special steps are to create a harmonious orthophoto to meet the needs of the city three-dimensional landscape design, create a triangle at the same time, and bring it to create a comparison of three-dimensional images of the city. And it is regarded as the contrast image of three-dimensional urban landscape design. Depending on the location, the value of the change, the direction of the slope, the slope, and other conditions, the relative angle of the three landscapes of the different shapes should change, and all things must be accomplished. The structure of the three-dimensional landscape will be renovated, additional vegetation will be painted, and the three-dimensional landscape will be renovated according to the city plan. The results of the experiments show that this method collects data samples accurately, quickly and accurately to evaluate the quality of landscape design in difficult areas and to beautify the environment.

3. Method

3.1. Ant Colony Algorithm. The best selection of aesthetics by 3D landscape mode plays an important role in the immediate improvement and layout of the landscape [15]. During the design of a three-dimensional landscape, the choice of a path is covered by legal planning methods in a challenging environment, and practical ant colony algorithm is used to complete the model. Starting with the actual problem, the spatial scope of the selection process is defined, and the adjacent weight, representing the optimal scale of the problem, is given in a complete picture. The person of the ant is considered to be the agent in order to visualize the ants and to complete the point characteristics of each path of the whole image with the best possible resolution. At the same time, each ant in ant colony algorithm is set to have the following characteristics: traverse the complete path in the complete graph at a time, all ants left characteristic pheromones on the path they passed, and the path selected by the ants is correlated with the characteristic pheromone. The specificity of ants is related to pheromones. In order to prevent the heuristic information from being buried due to too many feature pheromones, the pheromone should be updated after the ant traverses a complete cycle, so the amount of information in the path (i, j) in the $t + n$ period can be adjusted by equation (1).

$$\tau_{ij}(t+n) = (1-\rho) \cdot \tau_{ij}(t) + \Delta\tau_{ij}(t), \quad (1)$$

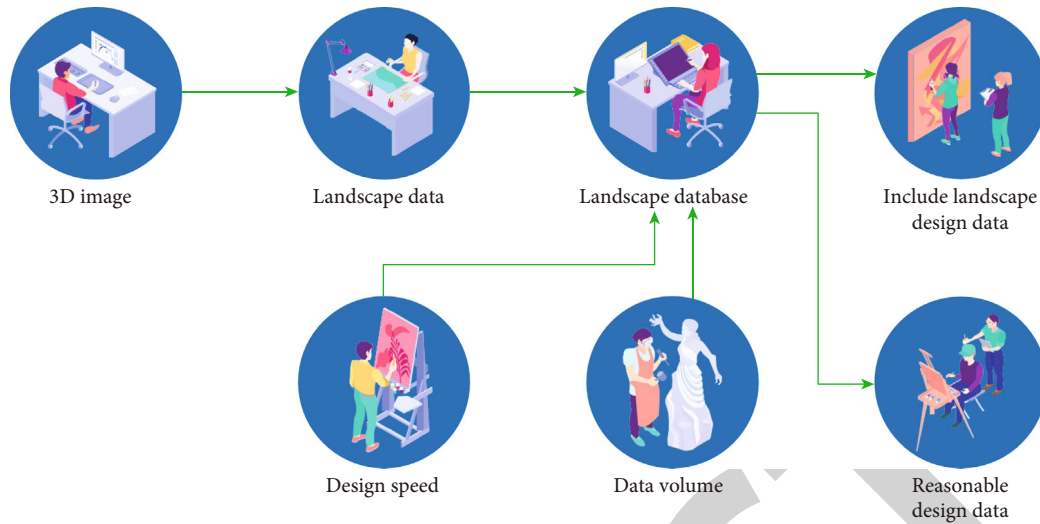


FIGURE 1: Data acquisition process of 3D image landscape.

where

$$\Delta\tau_{ij}(t) = \sum_{k=1}^m \Delta\tau_{ij}^k(t). \quad (2)$$

Among these, ρ is the volatile matter of pheromone, and M is the number of ant colony determined depending on the magnitude of the optimization problem. In general, the higher the value of m , the higher the accuracy of the optimal solution. In order to confirm the true efficacy of the ant colony algorithm, it is necessary to modify the necessary pheromone sequencing further. As each ant crosses a path with known patterns, the pheromone concentration of each edge covering along the path should be adjusted according to the length of the process. The sequence of pheromone renewal is as follows.

$$\Delta\tau_{ij}^l = \begin{cases} \frac{Q}{C^K}, \\ 0. \end{cases} \quad (3)$$

Equation (3) is a mathematical formula for pheromone renewal rates. C^K represents the entire length of the formation by K ant. Q has an uncertain value and is usually set to 1.

3.2. Research on Rationality Judgment Method of Landscape Design

3.2.1. 3D Image Data Acquisition. In daily life, due to the influence of weather factors and architectural factors, whether the landscape design is reasonably distributed cannot be guaranteed [16]. To this end, the data acquisition process of 3D image landscape is designed, as shown in Figure 1.

It can be seen from Figure 1 that the implicit data and normal data of landscape distribution are collected for the collection of 3D image garden landscape data, the data is then entered into the data for distribution, and the necessary conclusions are drawn based on the data created landscape [17].

3.2.2. 3D Image Simulation Landscape Feature Analysis Function. The three-dimensional modeling system analyzes the filtering process to see if the data meets the planning standards, including the refinement of the landscape design [18]. This analysis process is the guarantee of the data accuracy of the design rationality judgment model, and it is also the key to improve the judgment accuracy, as shown in Figure 2.

According to the analysis process in Figure 2, the overall image and local image of the landscape are represented by X and Y , respectively, the number of feature points of the landscape image set M and each image in X and Y is counted, and the pixel positions of the overall image and local image X and Y projected on image h are calculated. The camera matrix corresponding to the two-dimensional coordinate points projected on the image on the landscape image is used to mark the coordinate positions of the projection points of the three-dimensional image feature points on the landscape scene plane. Assuming that any point X_{k1} and Y_{k2} in the three-dimensional features X and y of the landscape image have been obtained, the coordinates of all feature points in X_{k1} and Y_{k2} are obtained by looking for the approximate transformation F . The transformation f is composed of the translation vector Z , the rotation matrix R , and the scaling factor s [19], and F is evaluated and converted into the minimum target function. Using the calculation flow in Figure 3, the translation vector Z , rotation matrix R , and scaling factor S of landscape image feature data are obtained.

From Figure 3, the translation vector Z , rotation matrix R , and scaling factor s can be obtained, from which the characteristic data of the whole landscape image can be obtained, and the rationality of landscape design can be judged on this basis.

3.2.3. Simulation Model Based on Rationality Judgment of 3D Image. According to the data characteristics obtained above, a three-dimensional image garden landscape design rationality judgment model is constructed, and the three-

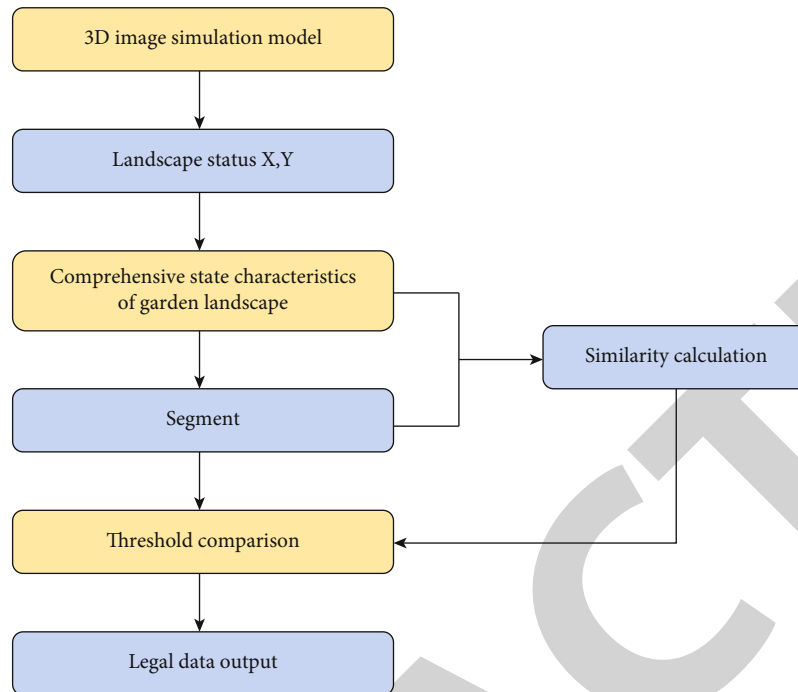


FIGURE 2: Flow chart of landscape state feature analysis.

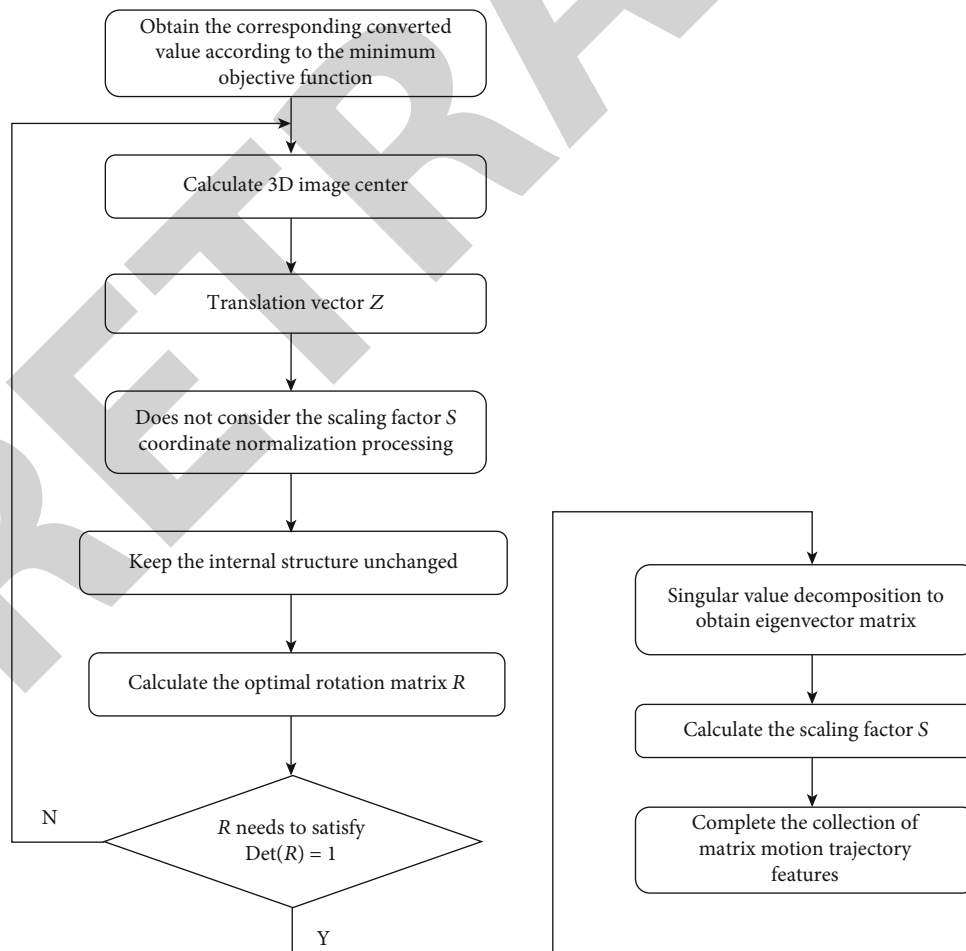


FIGURE 3: Calculation process.

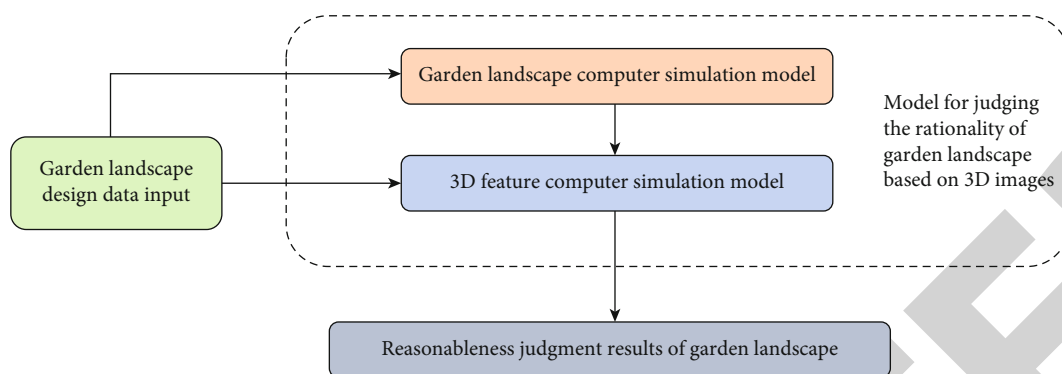


FIGURE 4: 3D image simulation judgment model.

dimensional visualization method is used to display the landscape design rationality judgment results [20]. Taking the landscape design data as input, the simulation characteristic parameters are determined, and finally, the rationality judgment results are obtained. The construction of the model is shown in Figure 4.

It can be seen from Figure 4 that the model for judging the rationality of landscape design based on 3D image simulation mainly includes two parts: one is the computer simulation model of landscape; the other part is a three-dimensional feature computer simulation model, which can be used to obtain the inertia factor of simulation judgment. Using this model, the obtained inertia factors are judged positively by introducing the dynamic forward judgment and reverse judgment methods, and then, the reverse judgment of each characteristic structure is obtained, and finally, the rationality of landscape design is judged.

3.3. Experiment. In order to measure the viability of a landscape design, it is necessary to conduct an experiment to verify the accuracy of the three-dimensional image structure. Under the environment of Windows 8, construct the analysis platform of the 12th phase image model of the three-dimensional figure 76 of garden landscape distribution rationality. The three-dimensional images are reasonably collected, identified, and analyzed, and the objective function values of different matrices are calculated. If the cost of the work is large, the determination and analysis of the garden landscape is more accurate. If the cost of the work is small, it shows that the decision of the optimal view of the landscape is not correct.

4. Results and Discussion

4.1. Result and Analysis of Matching Number and Matching Rate of Image Feature Points. The advantages of landscape design are compared with triangular models and depth measurement models. Whether or not the number of design points can filter the accuracy of the design triangle is important in how to fit the corresponding points of the landscape photos. At the same time, these two filtration methods are used to compare the necessary numbers and speeds of landscape elements. The results are shown in Table 1.

TABLE 1: Matching number and matching rate of three-dimensional image feature points by two judgment methods.

Group/ group	Traditional method		3D method	
	Matching number/ piece	Matching rate (%)	Matching number/ piece	Matching rate (%)
A	540	30.25	890	75.28
B	350	25.61	530	63.16
C	360	24.32	550	60.12
D	320	27.02	470	74.32
E	280	21.34	430	60.15
F	256	30.16	365	79.38

As can be seen from Table 1, the number and comparison of landscape images obtained by standard measurement depths is less than the three-dimensional image simulation method used in the sentence. The tuning process is also very simple. The process of simulating three-dimensional images corresponds to the height of the structural elements, which proves the total validity of the visualization. Based on the comparison results in Table 1, two methods are used to compare the simulation results of three-dimensional landscape maps. It can be seen that the classification of the garden landscape using the three-dimensional simulation method is appropriate. The main reason when determining the highlights is to adjust with high precision and the details are aggregated and distributed. The model details will be evaluated according to the characteristics of the diagram and the conclusions of the appropriateness of the garden landscape design will be based on the results of the analysis.

4.2. Comparison Results and Analysis of Judgment Rate and Accuracy. Collect data in the landscape environment, and analyze the judgment rate of the traditional method and the method in this paper, as shown in Figure 5.

As seen in Figure 5, the visual value of the process always increases gradually over time in the range of 0~10 but is always lower than that of three-dimensional simulation. During the interval between 10 and 15, the cost of the process always starts to decrease. In the next phase, the process always floats up and down, and the speed is only about 1/2

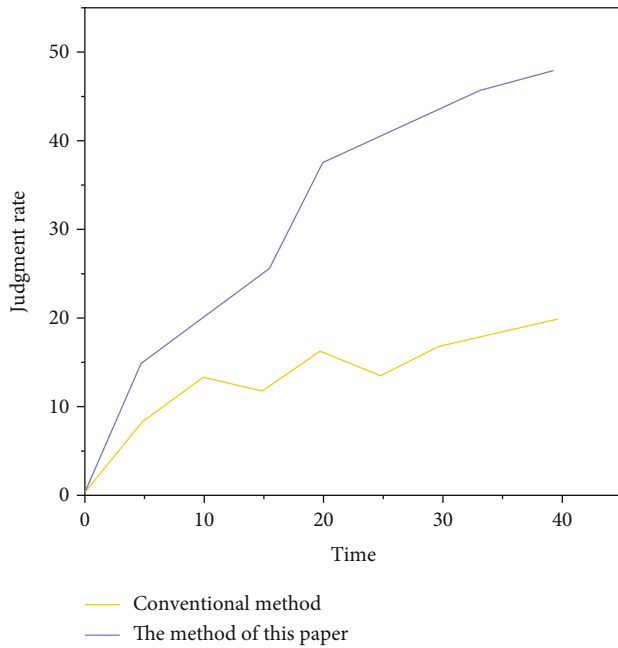


FIGURE 5: Comparison results of two methods for judging speed.

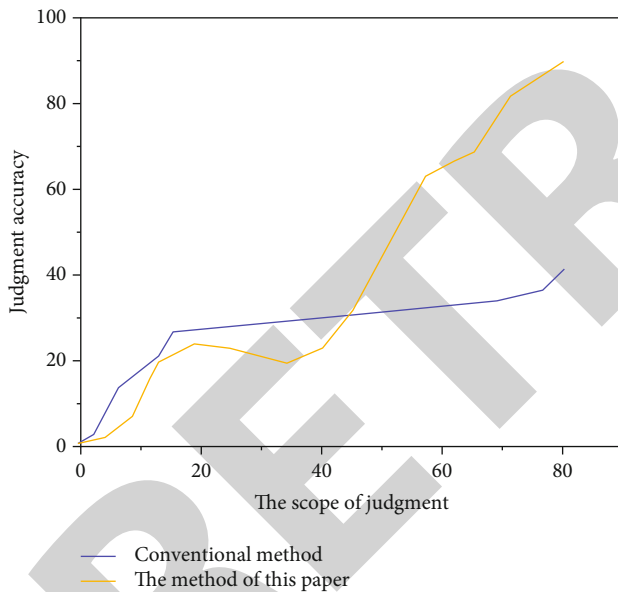


FIGURE 6: Comparison results of judgment accuracy of two methods.

of the fastest estimate for a 3D image model. This shows that the pace of use of the traditional method of assessing the optimal landscape of a garden is slow and sluggish. The speed of 3D image simulation method is faster. The comparative results of the accuracy of the conclusions are shown in Figure 6. As seen in Figure 6, there are slight differences between the conventional procedures used to measure the quality of the construction. It can be seen from Figure 6 that when the judgment range is less than 20%, there is little difference in the accuracy of the rationality judgment of landscape design between the traditional method and the

method in this paper. The truth of the judgment is always higher than in this way. When the detection range is 20%~45%, the accuracy of the standard is always higher than this model. However, as the scale has gradually expanded, the accuracy of the three-dimensional image simulation method used in this paper has gradually improved to 89%, when the process is always in place around 40%. Therefore, the process of drawing conclusions based on the modeling of 3D images is more accurate than the model of measuring the quality of landscape design.

The number and contrast of landscape data obtained by depth measurements are usually less than the three-dimensional imaging modeling method used in this paper, and the value of landscape optimization is slower and slower. The fact that the three-dimensional simulation method is faster to adjust the characteristics and filtration speed proves that this filtration method is efficient.

5. Conclusion

This article presents 3D sensor landscape model based on image sensors, which contain 3D image model to evaluate the best view of the landscape. This method can extract and analyze landscape design data, reduce the error of the conclusions, and improve the speed with simple filter steps. Attempts to identify the results of the experiment have shown that this method is effective and capable of making high decisions, which is an important theoretical basis for the application of classifications properly. In particular, there is no significant difference in the accuracy of the traditional process used to measure the efficiency of landscape design when the filtration rate is within 20%, and the accuracy of the process is always higher than in this way. When the detection range is 20%~45%, the accuracy of the standard is always higher than this model. However, as the expansion has been gradually expanded, the accuracy of the three-dimensional image simulation method used in this paper has gradually improved, and the standard has been kept around 40%.

Data Availability

The data used to support the findings of this study are available from the corresponding author upon request.

Conflicts of Interest

The authors declare that they have no conflicts of interest.

Acknowledgments

This study was supported by the Henan Province Teaching Reform Project, Innovation, and Practice of Talent Training Mode for New Construction Engineering Majors in the Digital Age, Project No. 2021SJGLX529.

Retraction

Retracted: Data Transmission and Processing Analysis of Power Economic Management Terminal Based on the Internet of Things

Journal of Sensors

Received 17 October 2023; Accepted 17 October 2023; Published 18 October 2023

Copyright © 2023 Journal of Sensors. This is an open access article distributed under the Creative Commons Attribution License, which permits unrestricted use, distribution, and reproduction in any medium, provided the original work is properly cited.

This article has been retracted by Hindawi following an investigation undertaken by the publisher [1]. This investigation has uncovered evidence of one or more of the following indicators of systematic manipulation of the publication process:

- (1) Discrepancies in scope
- (2) Discrepancies in the description of the research reported
- (3) Discrepancies between the availability of data and the research described
- (4) Inappropriate citations
- (5) Incoherent, meaningless and/or irrelevant content included in the article
- (6) Peer-review manipulation

The presence of these indicators undermines our confidence in the integrity of the article's content and we cannot, therefore, vouch for its reliability. Please note that this notice is intended solely to alert readers that the content of this article is unreliable. We have not investigated whether authors were aware of or involved in the systematic manipulation of the publication process.

Wiley and Hindawi regrets that the usual quality checks did not identify these issues before publication and have since put additional measures in place to safeguard research integrity.

We wish to credit our own Research Integrity and Research Publishing teams and anonymous and named external researchers and research integrity experts for contributing to this investigation.

The corresponding author, as the representative of all authors, has been given the opportunity to register their agreement or disagreement to this retraction. We have kept a record of any response received.

References

- [1] H. Tang, "Data Transmission and Processing Analysis of Power Economic Management Terminal Based on the Internet of Things," *Journal of Sensors*, vol. 2022, Article ID 2649993, 8 pages, 2022.

Research Article

Data Transmission and Processing Analysis of Power Economic Management Terminal Based on the Internet of Things

Hao Tang 

School of Basic Sciences, Shandong Institute of Petroleum and Chemical Technology, Dongying Shandong 250061, China

Correspondence should be addressed to Hao Tang; 202008000020@hceb.edu.cn

Received 5 July 2022; Revised 18 July 2022; Accepted 29 July 2022; Published 18 August 2022

Academic Editor: C. Venkatesan

Copyright © 2022 Hao Tang. This is an open access article distributed under the Creative Commons Attribution License, which permits unrestricted use, distribution, and reproduction in any medium, provided the original work is properly cited.

In order to explore how the power economy can realize the data transmission and processing of the management terminal, this paper presents a data transmission and processing analysis of the power economy management terminal based on the Internet of Things. This method explores the research on how to realize the data transmission and processing of management terminal in power economy through the key technical problems and solutions of information recommendation based on the Internet of Things. The research shows that the efficiency of data transmission and processing analysis of power economic management terminal based on the Internet of Things is about 65% higher than that of traditional data analysis. Improve the overall quality of employees in power enterprises and inject new vitality into the development of power economy.

1. Introduction

With the rapid development of information technology in today's society, the rapid development of massive data sharing on the Internet has promoted the rapid arrival of the big data era [1]. In recent years, with the rapid popularization of the Internet of Things technology and a large number of R&D and deployment of intelligent terminal equipment of the Internet of Things, while the types and number of intelligent Internet of Things applications are growing, the Internet of Things systems and equipment are becoming more and more popular in people's daily life. The Internet of Things devices and platforms have strong heterogeneity, closed platform architecture, high coupling, poor scalability, and a series of other problems, leading to fragmentation of the Internet of Things applications, making the development of big data platforms for intelligent Internet of Things applications costly and long cycle [2].

China Power Grid Corporation implements the new energy security strategy of "four revolutions and one cooperation," puts forward the strategic goal of "an international leading energy Internet enterprise with Chinese characteristics," and fully performs its political, economic, and social responsibilities. Put forward the strategic goal of building

an international leading energy Internet enterprise with Chinese characteristics, and it is required to carry out the digital empowerment project, implement the digital transformation, and carry out the construction of "urban energy brain" [3]. Under the above background, there is an urgent need to study "big data of energy and power economy," and it is required to dig deep into the value of energy and power data to continue to provide strong support for the steady and healthy development of economy and society [4].

As a kind of clean energy, electric energy is widely used in the world. It is a kind of energy integrated by higher technology. At present, China's power enterprises are showing a new trend of large-scale power production, which not only promotes the efficiency of power production but also increases the economic benefits of power enterprises. The expansion of power production scale has also expedited the development of new power technologies. At present, China has made certain technological breakthroughs in the field of power generation, transmission, and transformation and realized the synchronous improvement of production efficiency and economic benefits. Under the guidance of power demand and the government, the scale return of China's power enterprises has changed in three stages, from increasing to constant to decreasing. At present, most Chinese enterprises,

especially the energy industry, have gradually stabilized their demand for electric energy, and the change of electricity price will not have a significant impact on the change of enterprise production [5].

With the development of new technologies such as Internet technology, information technology, and big data technology, the energy and power industry and enterprises have invested a lot of energy and financial resources in information development and have made great achievements in big data application. However, there are still some deficiencies in the collection, management, and analysis of big data in the energy and power industry. In the era of big data, the energy and power industry has a large amount of data, so it puts forward higher requirements for data collection, storage, classification, and security management. In the past, energy and power enterprises did not make good use of and promote the massive data in the emerging stage, resulting in the fact that the collection process of more data may be different from the actual situation. At the same time, they cannot effectively distinguish the quality of the data. In the face of expired or erroneous data, they cannot timely screen and update, so the quality of the data cannot be guaranteed [6].

The data transmission middle tier platform is a bridge connecting intelligent hardware terminals and web cloud servers. The data middle tier platform is the core component of the entire Internet of Things system. The middle tier platform is closely related to the security and reliability of information and acts as a solid bridge and link between the application devices and sensing devices of the Internet of Things. The biggest advantage of the data transmission middle layer platform is that it provides the most powerful support for the data transmission of the Internet of Things applications, strengthens the application effect of the Internet of Things, and improves the economic benefits of the Internet of Things applications. The data transmission middle layer platform consists of three main parts [7]. The design of IoT data transmission and processing middle layer platform is shown in Figure 1.

2. Literature Review

Liang et al. said that from the perspective of the Internet of Things system as a whole, the world is in a high-speed development stage, including the standards and corresponding services of the Internet of Things. The continuous improvement of the Internet of Things-related technologies has accelerated the rapid establishment and growing of the Internet of Things knowledge system [8]. On this basis, the standard system of the Internet of Things urgently needs a unified standard, so as to continuously establish and improve the product system. It is expected that the IoT system market will achieve explosive growth worldwide in the next few years. Yu et al. said that it can be predicted that in the past five to ten years, the Internet of Things system will be more rapidly popularized and used worldwide [9].

To this end, the developed countries in the West and Asia quickly responded and issued many strategic policies to escort the Internet of Things industry. The United States has put forward the “smart earth” plan, which focuses on

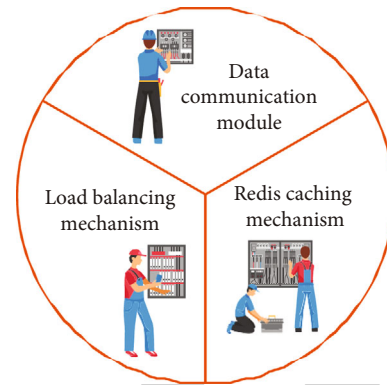


FIGURE 1: Overall design of m -server platform.

the research of the core technology of the Internet of Things applications. Yang et al. put forward a 14-point action plan on the Internet of Things industry, and Japan put forward the “u-japan plan” on the Internet of Things. These global government plans regard the Internet of Things as one of the primary strategic objectives of the current national economic construction and scientific and technological development [10].

Lin proposed that knowledge and information will be obtained from the collection and analysis of complex and huge digital data to improve the ability [11]. Jadaun et al. said that India, with the second largest population in the world, has also actively used big data in recent years, hoping to create a more convenient and people-friendly smart and civilized city [12]. As early as a few years ago, in the plans of the British government and the Japanese government, big data became one of the key decisions. The government increased its investment in the big data industry and focused on big data application technology to drive enterprises’ investment in the big data field.

Ron et al. think that the Internet of Things application development platform is quite popular at this stage. At present, it has basically disclosed its Internet of Things big data platform architecture, and some information can be queried from the Internet. There are also many technical introductions about the Internet of Things big data platform, but under its mechanism and environmental system, there are limited things that can be used for reference for traditional enterprises. Technology ultimately serves the business. There is no need to pursue progressiveness. Each enterprise should choose its own technology path according to its own actual situation [13]. Jiang et al. believed that various technologies of the existing online framework are relatively mature and have been applied in different workplaces [14]. However, these technologies are still relatively weak in terms of performance and user experience. At the same time, there is no complete set of private platform technical services in the market, so the purchase price is expensive, and there is no open source technology framework suitable for scientific research and small enterprises. However, as an important part of unstructured data, terminal data has not been well processed. The transaction record and interactive record data in unstructured data are mainly used by major enterprises

around the world for management and analysis using distributed systems, while the processing of terminal data types has not been effectively promoted. For IoT data, tens of millions of real-time data sent by terminals every day are discarded or stored without reasonable analysis and eventually become dead data. Therefore, how to use the existing distributed methods to solve the problem of the Internet of Things data is very necessary and meaningful.

Gong et al. believed that in the 21st century, electric power enterprises have ushered in rapid development. With the support of modern science and technology, the power technology upgrading of electric power enterprises has been realized. Chinese electric power enterprises have made a series of adjustments to the existing structure and made certain development achievements [15]. At present, China has built three nuclear power bases with a total installed capacity of 8.7 million KW. On the whole, the construction and operation of China's power grid are in good condition, showing an increasing trend both in terms of scale and transmission and transformation capacity. The new changes in power economic operation are mainly reflected in the following aspects: (1) the growth of power generation. With the support of Internet information technology, the interconnection of China's power grid system has been popularized. It not only increases the exchange frequency of regional power grids but also optimizes the cross regional allocation of power resources. In this process, the electricity exchange mode also presents a diversified development trend. In order to supply power to power scarce areas and regions, most power grid enterprises carry out high-power cross regional and cross provincial power transmission for a long time. This measure has improved the current situation of power supply shortage in some areas to a certain extent. (2) Electricity demand continues to grow. Electricity is closely related to economic and social development, and the change of electricity consumption is an important "barometer" of economic development. With the development of social production and enterprises, the demand for electricity is increasing, which is more prominent after the reform and opening up. (3) The economic benefits of power enterprises grew steadily. With China's attention to the development of power enterprises and the support of China's policies, the economic growth of power enterprises is in a sustained and stable state.

3. Method

3.1. Smooth Weighted Polling Algorithm. To realize software load balancing on the data transmission middle layer platform, algorithms need to be added to ensure that the load can be evenly distributed. Select one server among multiple servers as the master server of the load balancing server. The master server installed with the load balancing server (Nginx server) provides the only interface between the data transmission platform and the outside world. The main function of this interface is to distribute requests to sub-servers. The Nginx used by the platform is a reverse proxy server. A smooth weighted polling algorithm is added to the Nginx server to achieve load balancing [16].

The external requests are processed through the polling algorithm and then allocated to each subserver in turn. The polling algorithm is too weak in monitoring the performance of the subserver. After the request is allocated, there will be floating load imbalance. It is improved on the basis of the polling algorithm, and then, the smooth weighted polling algorithm is implemented [17].

The flow of the smooth weighted polling algorithm is shown as follows:

- (1) In the process of configuring files, each subserver needs to be configured with a weight C , which is fixed. Next, the current weight NC of every subserver is defined. The initial value of NC is 0, and then NC adjusts it according to polling. The value of NC will eventually become the key to the selection of subservers
- (2) After the master server receives the external request, it immediately traverses the subserver. The original subserver weight NC plus the assigned weight C refreshes the current subserver weight NC , as shown in

$$NC = C + NC \quad (1)$$

- (3) Definition: a new variable P ; P is the sum of the weights C of all subservers, as shown in

$$P = \sum_{i=0}^n C_i \quad (2)$$

- (4) After traversing and polling all the subservers once, select one of the subservers m , and the current weight NC of the subserver m is the largest among all the subservers, as shown in

$$M = \text{Max}(NC_i) \quad (3)$$

- (5) The current weight of the selected subserver m minus the sum of all subserver weights P refreshes the current weight value NC of the subserver m , as shown in [18]

$$NC = NC - P \quad (4)$$

The implementation of smooth weighted polling algorithm is now complete. Adding a smooth weighted polling algorithm to load balancing can not only distribute the load services of subservers based on the weight ratio of each

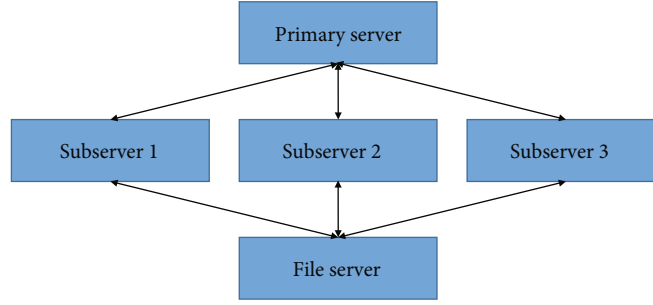


FIGURE 2: Relationship architecture between servers.

TABLE 1: Weight of four server requests.

Request number	NC (before selection)	Selected server	NC (after selection)
1st time	{4,2,2}	M1	{-4,2,2}
2nd time	{0,4,4}	M2	{0,-4,4}
3rd time	{4,-2,6}	M3	{4,-2,-2}
4th time	{8,0,0}	M1	{0,0,0}

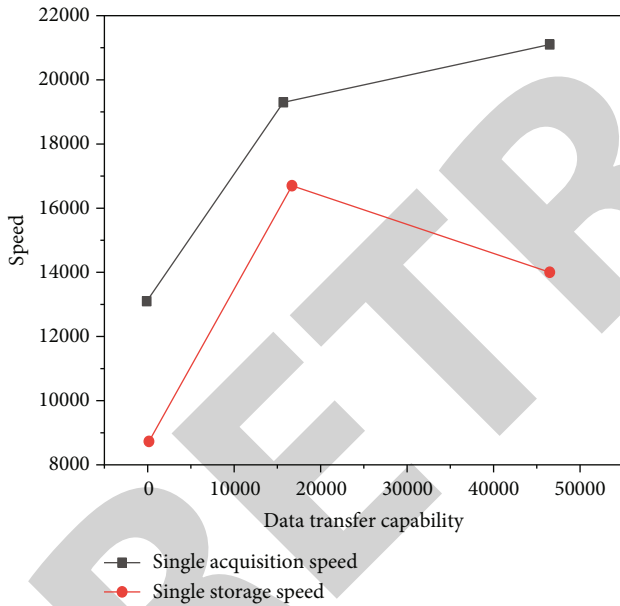


FIGURE 3: Data transmission capability for high concurrency request orders.

subserver but also maximize the average distribution of load balancing. There will be no case that connected requests are allocated to the same subserver at the same time.

The data transmission server is composed of multiple cloud servers. The server is divided into three parts: the main server, the subserver, and the file server. The servers in the three parts handle different business logic and support different functions. The server responsible for receiving external requests is the master server. The master server assigns requests to the following subservers. The subservers operate

database access and file read/write based on the same file server [19]. See Figure 2 for the relationship architecture between various parts of the server.

The weight distribution of the subserver in the four requests is shown in Table 1. According to the performance of subserver 1, subserver 2, and subserver 3, the weight of the subserver in the configuration is 2, 1, and 1, based on the smooth weighted polling algorithm.

The initial value of the current weight NC of each subserver before the first request is sent is {0,0,0}, and the current weight NC of the selected subserver for the first request is {4,2,2}[20]. It can be known that the selected subserver is 1 for the first time. After selection, the current weight NC of the subserver is refreshed to {-4,2,2}. Requests after the first request follow this rule. When the number of requests sent is accumulated to 4, the current weight NC of the subserver will be refreshed to the initial weight NC of {0,0,0}, and the current weight NC of the subsequent request subserver will repeat this process. From Table 1, it can be seen that when each request reaches 4 times, subserver 1 will be selected twice, while subserver 2 and subserver 3 will only be selected once, which is consistent with the weight C ratio of each subserver. If the number of requests is 8, the number of the selected subserver is {m1, M2, m3, M1, M1, M2, m3, m1}, and the assigned subserver is not {m1, M1, M1, M1, M2, M2, m3, m3}. The latter is assigned in a disorderly manner [21]. When the distribution is uniform according to the rules, load balancing optimizes the server performance to the greatest extent. Different requests such as files and session caches of the same client are allocated to different subservers, which will affect the operation. In this platform, the file server can be used as database step input and static file storage.

Through mathematical statistical analysis, the corresponding data distribution and probability density can be obtained, and a threshold about the reference value Z can be obtained by setting an appropriate proportional value. Since the data distribution has no obvious characteristics and influence relationship, starting from the law of central limit point, it can be considered as normal distribution as shown in formula (5), and the probability density of P is shown in

$$P \sim N(\mu, \sigma^2), \quad (5)$$

$$f(\text{Avg}(c), \mu, \sigma^2) = \frac{1}{\sqrt{2\pi\sigma}} \exp \left[-\frac{1}{2\sigma^2} (\text{Avg}(c) - \mu)^2 \right]. \quad (6)$$

Through the theoretical calculation of maximum likelihood estimation, it is obtained as shown in

$$\hat{\mu} = \bar{P}, \quad (7)$$

$$\hat{\sigma}^2 = \frac{1}{n} \sum_{i=1}^n (P_i - \bar{P})^2, \quad (8)$$

$$\hat{P} = \frac{\sum_{i=1}^n P_i}{n}. \quad (9)$$

After estimating two unknown parameters, the distribution can be calculated according to the standard normal distribution, as shown in

$$\frac{(P - \mu)}{\sigma} \sim N(0, 1). \quad (10)$$

The heartbeat data in the data transmission may be highly concurrent, and the heartbeat data format needs to be agreed between the terminal and the web server during the transmission process. This design adopts the Redis cache mechanism to ensure the cache interaction with the MySQL database during the heartbeat data transmission. The heartbeat transmission data format is consistent with that stored in Redis in the form of key value pairs. In the data format, WD001 represents the key, and the time is the corresponding time. The heartbeat data is stored in memory, which makes the data processing speed very fast. The data transmission capability for high concurrency requests is shown in Figure 3.

3.2. Multisite Configuration of uWSGI. Deploy multiple web service platforms on the same server to implement multiple sites (that is, a set of programs that can bind multiple domain names or subdomain names). Each site has independent web services, which can greatly reduce the trouble of maintaining and updating multiple Django platforms, save server resources, maximize the sharing and utilization of server resources, and reduce unnecessary expenses for enterprises. uWSGI is the most convenient component for deploying Python sites at present. It is very simple to configure a single site. Deploying multiple sites on the same server is a little more complicated. The configuration flow chart is shown in Figure 4. Multiple sites here refer to multiple sites using the same Nginx and uWSGI main process services, which are usually distinguished by domain names [22].

Big data planning for energy and power economy: based on the focus of social and economic development and the overall strategy of the state grid, with energy and power as the starting point, power data as the basis, integrating other external data, big data as the focus, and service economy as the entry point, the “energy and power economy big data” system architecture is planned for the government, enterprises, and internal [23].

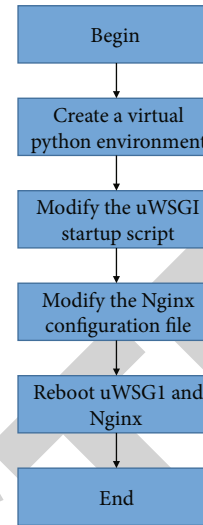


FIGURE 4: Configuration flow chart.

Technical model related to big data of energy and power economy: (1) energy and power economy big data acquisition technology. With the wide application of big data technology, the growth of energy and power big data in quantity is also huge. Through the application of energy and power economic big data collection technology, the ultimate goal is to collect data on the energy consumption characteristics of different energy and power users and then analyze and classify customers. Therefore, the data collection to be completed by this module mainly includes the user’s power consumption, power consumption characteristics, voltage level, regional characteristics, and other information, as well as the user’s regional economic conditions, climate characteristics, electricity price policies, and other relevant data information that have an impact on the power load. After data collection, the data can be extracted and input into the big data platform for later data analysis. (2) Integrated management technology for big data of energy and power economy. After the big data is collected and input into the big data platform, energy and power enterprises can classify and manage the data in the big data platform and establish a special data set targeted. The accuracy, integrity, and repeatability of the data in the data set shall be verified and checked. The wrong values shall be corrected, the missing ones shall be supplemented, and the repetitive data shall be sorted out and deleted. At the same time, the attributes and accuracy of the data shall be well managed, and the format of the data shall be standardized and unified, so as to lay a good foundation for later data analysis. (3) Analysis and processing technology for big data of energy and power economy. The analysis and processing technology for energy and power economic big data is to filter and extract the massive data information in the database, analyze and manage the useful information pertinently, and apply the analysis results to practical work, so as to provide data support and theoretical basis for the production, operation, and other activities of energy and power enterprises [24]. In the process of analysis and processing, users can be classified according to their

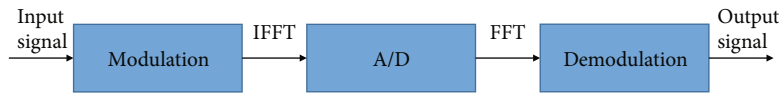


FIGURE 5: Working principle of wireless bridge.

characteristics, power consumption, and other information. At the same time, different data sets based on regions, industries, and categories can be established to provide reference for enterprise decision-making. (4) Presentation technology of big data of energy and power economy. The analysis results of power economic big data can be comprehensively displayed at different levels and different design scenarios, and more diversified data representations can be mined, so as to realize information transmission and matching between related data and provide value-added services in economic aspects for enterprises.

3.3. Wireless Bridge. Wireless bridge is the link equipment to realize the wireless network connection and to realize the wireless network bridging, that is, to establish a bridge to transmit data and information among two or more communication networks. In the link layer, LAN interconnection is realized to store and forward information, which is used for long-distance networking between digital devices.

The main working modes of the commonly used wireless bridges in practice are point-to-point (PTP) and single point-to-multipoint (PTMP). (1) Point-to-point (PTP) wireless bridge equipment is generally composed of a pair of bridges and a pair of antennas [25]. The two antennas must be placed in a relative orientation. The outdoor antenna is connected with the indoor bridge through cables, and the bridge is physically connected with the network. (2) Single point-to-multipoint (PTMP) wireless bridge equipment can interconnect the networks in multiple peripheral areas into a whole. Its structure is relatively complex. It needs to use omnidirectional antennas or a large number of wireless network cards and antennas. Point-to-multipoint communication mode is mainly used in digital oil fields.

In this system, the Breeze ACCESS VL wireless bridge of Israel ovitone company is used. It adopts OFDM orthogonal frequency division multiplexing technology and has the advantages of high throughput, long-distance transmission, high reliability, anti-interference, and multipath effect, which meets the needs [26]. It also provides 10/100 mbps Ethernet interface, which has low investment and operation cost and convenient and fast installation, and its working principle is shown in Figure 5.

4. Results and Analysis

With the continuous development of modern Internet information technology, the traditional power enterprise operation system can no longer meet the needs of modern society. It is necessary to establish a strong power grid system, and the realization of the power grid system depends on the support of information technology. As the core competitiveness of power enterprises, excellent informatization

talents are the human guarantee to realize the intelligent development of power enterprises. However, from the current development of power enterprises and the application status of informatization technology, some of them are still in a backward state, which hinders the application of artificial intelligence technology in the power economy. The lack of effective information feedback and exchange mechanism has become an urgent problem to be solved in the construction of power informatization [27].

The Breeze ACCESS VL wireless bridge adopts orthogonal frequency division technology (OFDM). When receiving data, the transmitter first modulates the data signal, transforms the frequency domain signal into time domain signal through inverse Fourier transform, and converts the time domain signal into baseband signal through digital to analog conversion. The receiver converts its fast Fourier transform into frequency domain signal of the same frequency and demodulates it into the original data signal information [28].

The remote bridge sends video data and oil well data collected by RTU module to the central bridge of the monitoring center in the station. The central network bridge is connected with the industrial control computer through the switch. The data processing and analysis software installed in the industrial control computer analyzes and processes the video data and oil well data and displays the results on the display screen of the monitoring center.

The Breeze ACCESS VL bridge consists of a base station central unit Au and a user unit SU. The central unit of the base station is connected to the backbone Ethernet through the RJ-45 connector. The user unit SU can be connected to the backbone Ethernet with RJ-45 connector, or the remote network can be connected to the central point through the central unit of the base station, so as to support multiple workstations.

The base station central unit Au is installed in the base station to communicate with the user unit (SU). Each base station central unit includes indoor and outdoor unit parts. The indoor unit is connected to the uplink equipment through a standard IEEE802.3 Ethernet 10/100basstt (RJ-45) interface and to the outdoor unit through a Cat-5 cable. The outdoor unit is connected to the sector antenna. According to the actual needs, the system uses a 120° sector directional antenna to connect to the base station center bridge, making full use of the spectrum to ensure efficient and reliable data transmission.

The development of electric power enterprises has certain particularity. The traditional ideas of enterprise employees will restrict the efficiency of electric power economic operation and management to a certain extent. In the final analysis, the competition among power enterprises is the competition of human resources. Therefore, under the background of market economy, we must innovate the form

of ideas, learn from the advanced management experience of the United States and excellent enterprises, and adjust the internal structure of enterprises to adapt to the development environment of market economy. Regularly organize enterprise employees to receive professional training, and select personnel with rich management experience and professional quality in the selection of power enterprise managers.

5. Conclusion

With the deepening of the application of Internet technology in the energy and power industry, an integrated ecosystem of energy and power applications will continue to be formed, and energy and power big data will have richer connotations. The integration and analysis of more internal and external data of the energy and power industry will make the energy and power economic big data form an important value chain effect and promote the generation of new business models and consumer service forms. At the same time, the application of big data in energy and power economy will also enter a new height with the continuous development of big data technology. Electric power economic operation is related to the national economy and the people's livelihood and is an important force for national economic growth. Electric power enterprises should strengthen the adjustment of internal management mechanism of electric power enterprises, optimize resource allocation, and promote the improvement of economic benefits of electric power from the aspects of system construction, electricity price adjustment, information construction, and so on.

Data Availability

The data used to support the findings of this study are available from the corresponding author upon request.

Conflicts of Interest

The author declares that there are no competing interests.

Acknowledgments

The study was supported by the Natural Science Fund Project in Shandong Province "Research on the Cooperative Education Mechanism of School and Enterprise Based on Modern Apprenticeship" (2013ZRE27312).

References

- [1] E. A. Hena-Garcia and R. Montoya, "Management innovation in an emerging economy: an analysis of its moderating effect on the technological innovation-performance relationship," *IEEE Transactions on Engineering Management*, vol. 2, pp. 1–14, 2021.
- [2] M. Lopez-Benitez, C. Majumdar, and S. N. Merchant, "Aggregated traffic models for real-world data in the Internet of Things," *IEEE Wireless Communication Letters*, vol. 9, no. 7, pp. 1046–1050, 2020.
- [3] G. C. Nobre and E. Tavares, "Assessing the role of big data and the Internet of Things on the transition to circular economy: part ii," *Platinum Metals Review*, vol. 64, no. 1, pp. 32–41, 2020.
- [4] J. Dan, Y. Zheng, and J. Hu, "Research on sports training model based on intelligent data aggregation processing in Internet of Things," *Cluster Computing*, vol. 25, no. 1, pp. 727–734, 2022.
- [5] Y. Luo and Y. Xiang, "Application of data mining methods in Internet of Things technology for the translation systems in traditional ethnic books," *IEEE Access*, vol. 8, pp. 93398–93407, 2020.
- [6] M. Zakharov, R. Kirichek, P. W. Khan, A. Muthanna, and A. Koucheryavy, "Analysis of traffic generated during molecular analysis based on the Internet of Things," *International Journal of Advanced Science and Technology*, vol. 29, no. 4, pp. 8572–8582, 2020.
- [7] F. Dai, "A data management strategy for property management information system based on the Internet of Things," *Ingénierie des Systèmes D Information*, vol. 25, no. 3, pp. 337–343, 2020.
- [8] W. Liang, W. Li, and L. Feng, "Information security monitoring and management method based on big data in the Internet of Things environment," *IEEE Access*, vol. 9, pp. 39798–39812, 2021.
- [9] G. Yu, X. Chen, C. Zhong, D. Ng, and Z. Zhang, "Design, analysis, and optimization of a large intelligent reflecting surface-aided B5G cellular Internet of Things," *IEEE Internet of Things Journal*, vol. 7, no. 9, pp. 8902–8916, 2020.
- [10] H. Yang, W. D. Zhong, C. Chen, A. Alphones, and X. Xie, "Deep-reinforcement-learning-based energy-efficient resource management for social and cognitive Internet of Things," *IEEE Internet of Things Journal*, vol. 7, no. 6, pp. 5677–5689, 2020.
- [11] T. Lin, "Application of feature extraction method based on support vector machine in Internet of Things," *Journal of Intelligent and Fuzzy Systems*, vol. 39, no. 6, pp. 8623–8632, 2020.
- [12] A. Jadaun, S. K. Alaria, and Y. Saini, "Comparative study and design light weight data security system for secure data transmission in Internet of Things," *International Journal on Recent and Innovation Trends in Computing and Communication*, vol. 9, no. 3, pp. 28–32, 2021.
- [13] D. Ron, C. J. Lee, K. Lee, H. H. Choi, and J. R. Lee, "Performance analysis and optimization of downlink transmission in LoRaWAN class B mode," *IEEE Internet of Things Journal*, vol. 7, no. 8, pp. 7836–7847, 2020.
- [14] W. Jiang, Z. Yang, Z. Zhou, and J. Chen, "Lightweight data security protection method for AMI in power Internet of Things," *Mathematical Problems in Engineering*, vol. 2020, no. 5, Article ID 8896783, 9 pages, 2020.
- [15] B. Gong, J. Liu, and S. Guo, "A trusted attestation scheme for data source of Internet of Things in smart city based on dynamic trust classification," *IEEE Internet of Things Journal*, vol. 8, no. 21, pp. 16121–16141, 2020.
- [16] Y. C. Yang, F. Ali, and S. Nazir, "Selection of devices based on multicriteria for mobile data in Internet of Things environment," *Mobile Information Systems*, vol. 2021, no. 8, Article ID 2117915, 7 pages, 2021.
- [17] D. Amarnath and S. Sujatha, "Internet-of-things-aided energy management in smart grid environment," *The Journal of Supercomputing*, vol. 76, no. 4, pp. 2302–2314, 2020.
- [18] C. Xie, X. Xiao, and D. K. Hassan, "Data mining and application of social e-commerce users based on big data of Internet

Retraction

Retracted: Advances in Hyperspectral Image Classification with a Bottleneck Attention Mechanism Based on 3D-FCNN Model and Imaging Spectrometer Sensor

Journal of Sensors

Received 12 December 2023; Accepted 12 December 2023; Published 13 December 2023

Copyright © 2023 Journal of Sensors. This is an open access article distributed under the Creative Commons Attribution License, which permits unrestricted use, distribution, and reproduction in any medium, provided the original work is properly cited.

This article has been retracted by Hindawi, as publisher, following an investigation undertaken by the publisher [1]. This investigation has uncovered evidence of systematic manipulation of the publication and peer-review process. We cannot, therefore, vouch for the reliability or integrity of this article.

Please note that this notice is intended solely to alert readers that the peer-review process of this article has been compromised.

Wiley and Hindawi regret that the usual quality checks did not identify these issues before publication and have since put additional measures in place to safeguard research integrity.

We wish to credit our Research Integrity and Research Publishing teams and anonymous and named external researchers and research integrity experts for contributing to this investigation.

The corresponding author, as the representative of all authors, has been given the opportunity to register their agreement or disagreement to this retraction. We have kept a record of any response received.

References

- [1] D. Yuan, X. Xie, G. Gao, and J. Xiao, "Advances in Hyperspectral Image Classification with a Bottleneck Attention Mechanism Based on 3D-FCNN Model and Imaging Spectrometer Sensor," *Journal of Sensors*, vol. 2022, Article ID 7587157, 16 pages, 2022.

Research Article

Advances in Hyperspectral Image Classification with a Bottleneck Attention Mechanism Based on 3D-FCNN Model and Imaging Spectrometer Sensor

Deren Yuan, Xiaochun Xie , Gao Gao, and Ju Xiao

School of Physics and Electronic Information, Gannan Normal University, Ganzhou 341000, China

Correspondence should be addressed to Xiaochun Xie; xiexiaochun@gnnu.edu.cn

Received 9 June 2022; Revised 22 June 2022; Accepted 29 July 2022; Published 16 August 2022

Academic Editor: C. Venkatesan

Copyright © 2022 Deren Yuan et al. This is an open access article distributed under the Creative Commons Attribution License, which permits unrestricted use, distribution, and reproduction in any medium, provided the original work is properly cited.

Deep learning approaches have significantly enhanced the classification accuracy of hyperspectral images (HSIs). However, the classification process still faces difficulties such as those posed by high data dimensions, large data volumes, and insufficient numbers of labeled samples. To enhance the classification accuracy and reduce the data dimensions and training needed for labeled samples, a 3D fully convolutional neural network (3D-FCNN) model was developed by including a bottleneck attention module. In such a model, the convolutional layer replaces the downsampling layer and the fully connected layer, and 3D full convolution is adopted to replace the commonly used 2D and 1D convolution operations. Thus, the loss of data in the dimensionality reduction process is effectively avoided. The bottleneck attention mechanism is introduced in the FCNN to reduce the redundancy of information and the number of labeled samples. The proposed method was compared to some advanced HSI classification approaches with deep networks, and five common HSI datasets were employed. The experiments showed that our network could achieve considerable classification accuracies by reducing the data dimensionality using a small number of labeled samples, thereby demonstrating its potential merits in the HSI classification process.

1. Introduction

The hyperspectral image (HSI) classification process is vital for the use of hyperspectral remote sensing data. The spectral resolution of HSI data ranges from visible light to short-wave infrared, with wavelengths reaching the order of nanometers. By exploiting the spectral characteristics of HSIs, one can effectively distinguish various objects, which has enabled the application of HSIs in a wide range of disciplines such as agriculture, early warning systems in disaster management, and national defense. Deep learning models for HSI classification are well developed. Many techniques, such as auto encoder [1], deep belief network [2], recurrent neural network [3], and convolutional neural network (CNN) models (e.g., the network described by Gu et al. [4]), are commonly used.

A convolution-related neural framework refers to a typical approach for deep learning [5–8] and HSI classification. It employs three types of models for the processing of a vari-

ety of characteristics by the CNN. The first type represents a 1D-CNN that uses only spectral data to extract the characteristics. This method requires a considerable number of training samples. The second type involves a spatial characteristics-based approach termed a 2D-CNN. Spatial characteristics are written by using a sparse representation method [9]; however, Makantasis et al. [10] developed a classification framework that uses particular scenes. The third type refers to the 3D-CNN approach that exploits spectral and spatial characteristics. It uses information on changes in local signals contained in spatial and spectral data without any pre- and postprocessing operations. The 3D convolution technique was initially employed to process videos, and it is currently used extensively in the HSI classification process [11–15]. Other methods are referred to as hybrid CNNs, and many such approaches have been developed for various uses [16, 17]. For instance, various hybrid approaches that adopt 1D-CNN and 2D-CNN were presented by Yang et al. [18] and Zhang et al. [17].

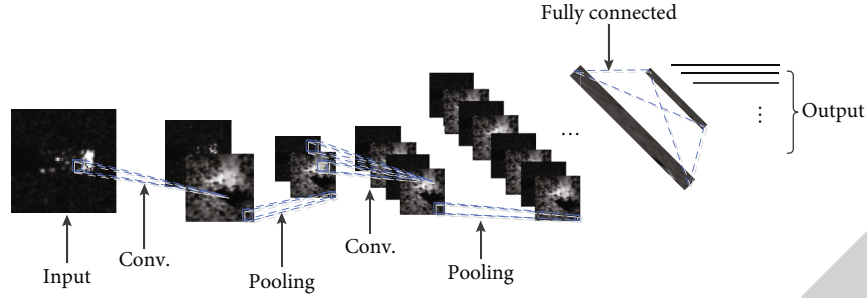


FIGURE 1: Convolutional neural network (CNN) structure.

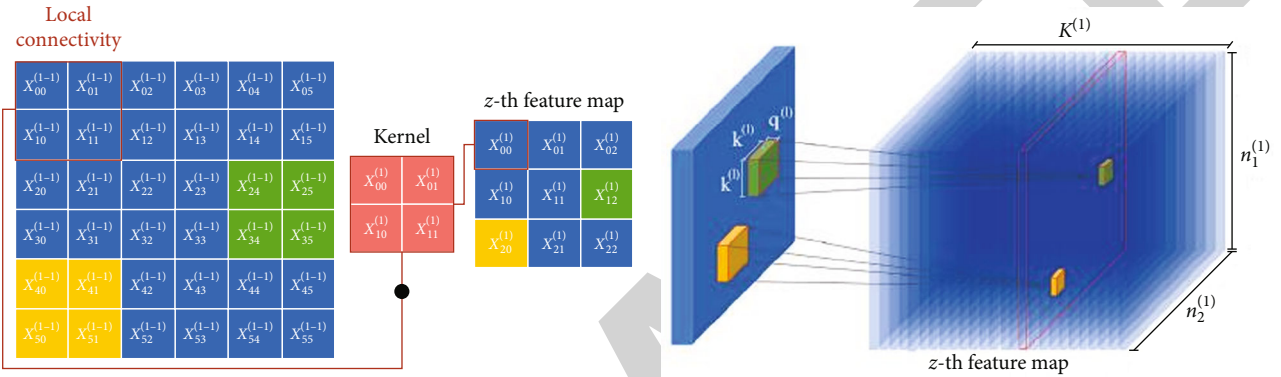


FIGURE 2: Convolutional layer working mode.

Previous studies on HSI classification based on deep learning have primarily discussed the building of deep networks to enhance accuracy. However, the number of training parameters was proportional to the complexity of the networks. For instance, approximately 360,000 training parameters were used in the classification network proposed by Zhong et al. [19]. Hamida et al. [20] proposed a 3D-1D hybrid CNN method that employs a maximum of 61,949 parameters. In the network proposed by Roy et al. [21], a 3D-2D hybrid CNN used 5,122,176 parameters. The adoption of such a high number of training parameters makes it difficult to train the network and is liable to result in overfitting. Other key issues also require attention, such as high data dimensionality, too few training-labeled samples, and spatial variability of spectral characteristics.

In this study, we present a 3D fully convolutional neural network (3D-FCNN) model with a bottleneck attention mechanism. The downsampling and fully connected layers are substituted by the convolutional layer. A 3D convolution operation is adopted to replace the commonly used 2D and 1D convolution operations, and a bottleneck attention mechanism is introduced to the FCNN to maintain end-to-end classification. A pooling layer is employed for dimension reduction and the final prediction of the classification result.

The major contributions of this study are as follows:

- (1) The downsampling layer and the fully connected layer are substituted by convolutional layers, and multiple datasets are adopted to separately alter the model and network depth. The developed network

shows improved performance in comparison with several advanced HSI classification approaches with deep networks

- (2) Network parameters are significantly reduced without adopting the fully connected layer
- (3) A bottleneck attention mechanism is added to determine the latest classification accuracy in a dataset that includes limited training data. Moreover, the time consumed by the developed network is significantly decreased

The rest of the paper is organized as follows: In Section 2, literature related to CNN is presented; in Section 3, the proposed 3D-FCNN structure following the bottleneck attention mechanism is elucidated; in Section 4, the experimental results are presented and analyzed; in Section 5, conclusions are drawn, and the direction of future research is highlighted.

2. Convolutional Neural Network (CNN)

The CNN exploits feature extraction and a weight sharing mechanism to decrease the number of network training parameters required; its structure is illustrated in Figure 1. The working mechanism involves inputting image data and passing it to the convolutional layer for image feature extraction. The downsampling layer reduces the features of the current results. After several cycles of alternating learning of the convolution and downsampling layers, the data are acquired via the rectified linear unit (ReLU) activation

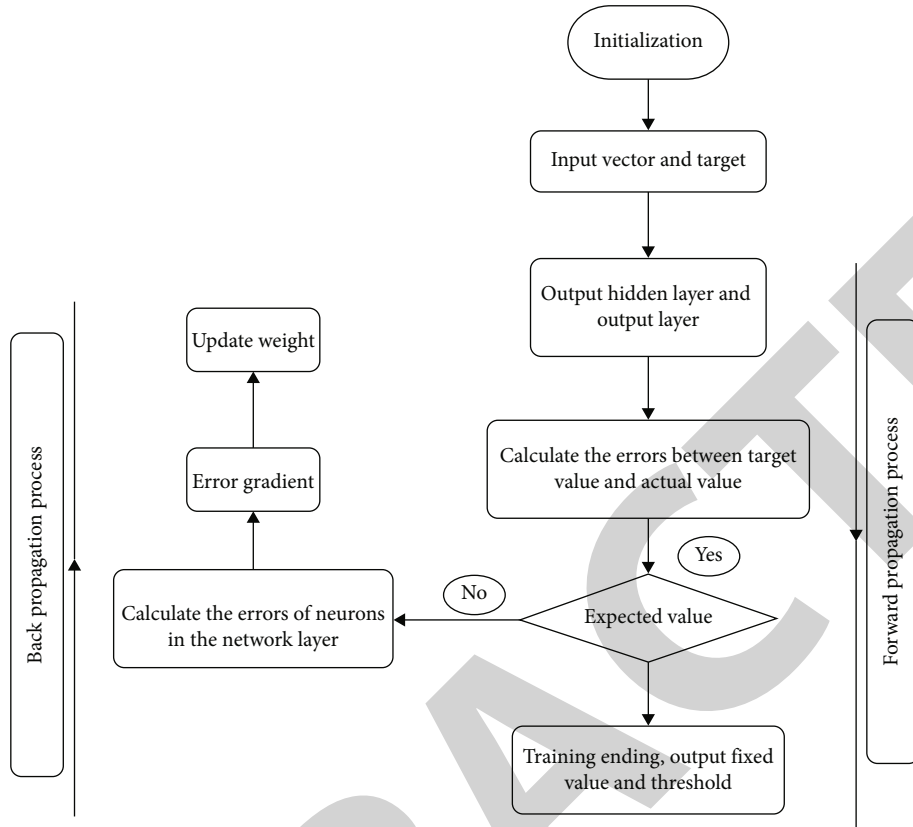


FIGURE 3: Process of CNN training.

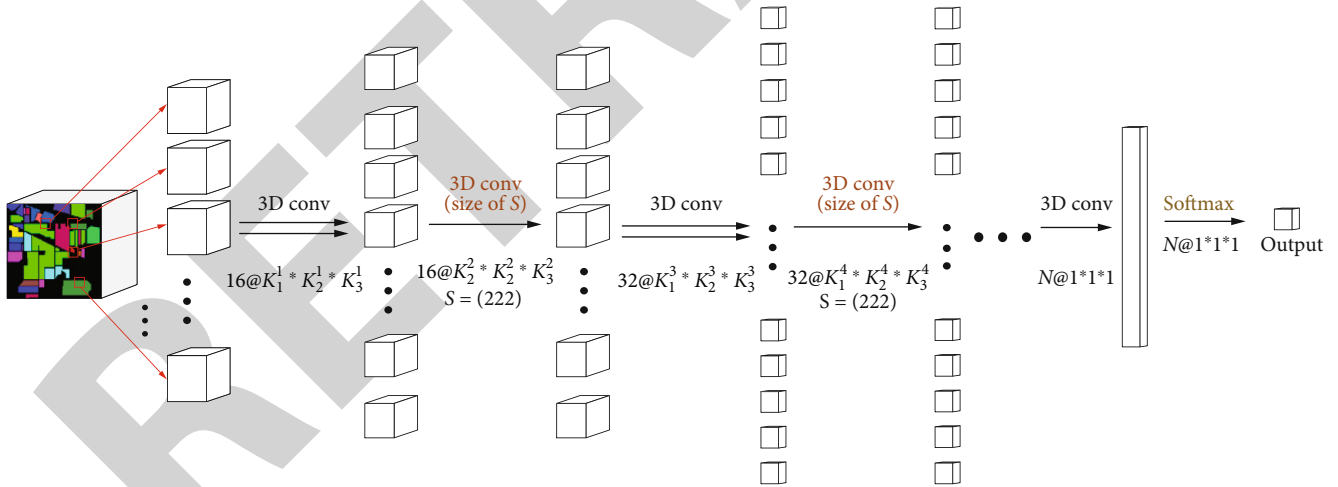


FIGURE 4: Recognition process based on the 3D-FCNN.

function with high-level abstract characteristics. The acquired abstract characteristics are introduced into a 1D vector, passed to the fully connected layer, subsequently passed to the learning of several fully connected layers, and finally outputted to the classifier to complete the entire classification of the image.

2.1. Convolutional Layer. The convolutional layer is a vital component of the CNN. The generation of multiple feature

maps is achieved by multiple learnable filters in respective convolutional layers for convolution processing of input image data. The working mode of the convolutional layer is illustrated in Figure 2. Assuming that X is the input data, its size is $m \times n \times d$, where $m \times n$ denotes the spatial pixel size of X , d is the number of channels, and x_i is the i -th feature of the X feature map. Each layer covers k filters. The parameters w_j and b_j can be employed to represent the weight and offset between the j -th filter and the feature

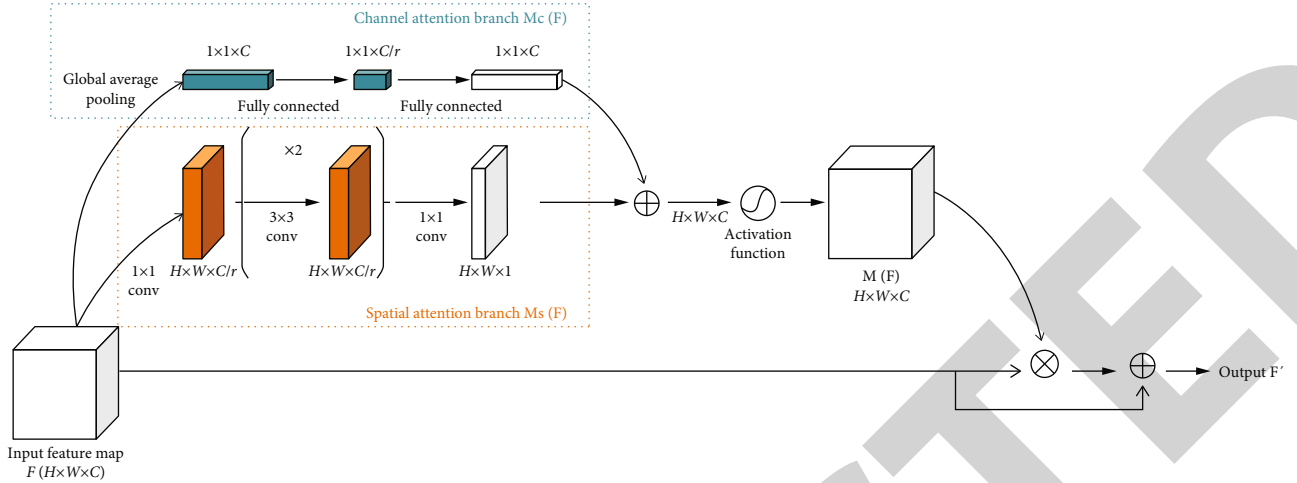


FIGURE 5: Bottleneck attention module.

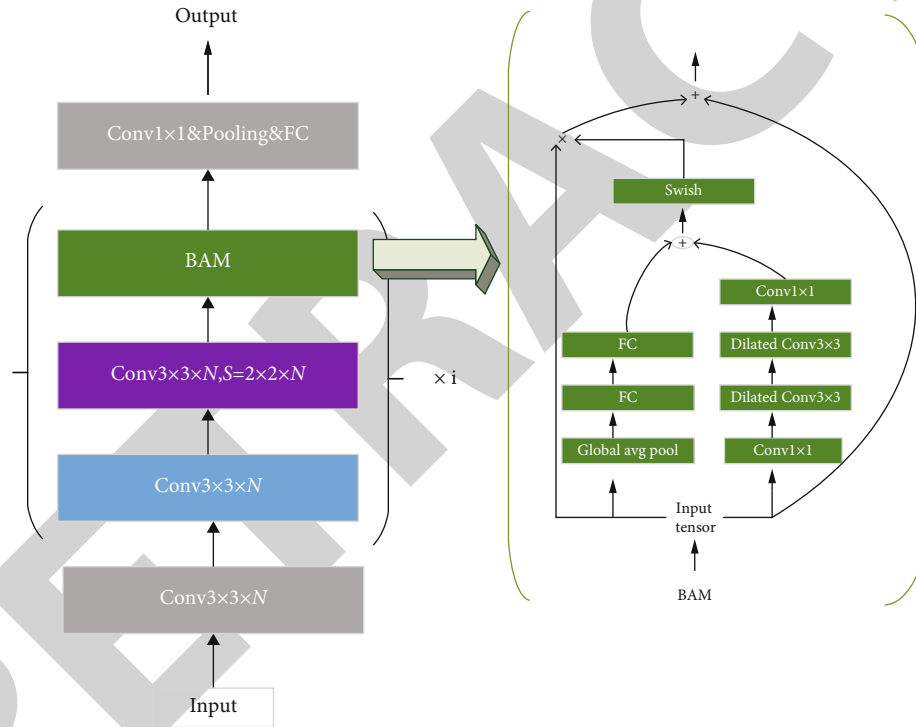


FIGURE 6: 3D-FCNN model with bottleneck attention module (BAM).

map. Subsequently, the j -th output of the convolutional layer is written as follows:

$$y_j = \sum_{i=1}^d f(x_i * w_j + b_j), \quad j = 1, 2, \dots, k, \quad (1)$$

where $*$ denotes the convolution operator and $f(\cdot)$ represents the activation function adopted to enhance the network nonlinearity.

2.2. Downsampling Layer. The downsampling layer is periodically inserted after several convolutional layers in the CNN to reduce redundant information in the image data. Net-

work training parameters and the time consumed by network training are effectively reduced through dimensionality reduction of the feature map. Moreover, if the input pixel shows a slight change in the neighborhood, the downsampling layer exerts its local translation invariance characteristics to ensure the stability of the network and exerts a certain anti-interference effect. Average pooling and max pooling are considered common. To be specific, for the $p \times p$ window size field denoted as S , the average pooling operation is written as follows:

$$z = \frac{1}{F} \sum_{(i,j) \in S} x_{ij}, \quad (2)$$

TABLE 1: Average accuracy evaluation results for the five datasets derived using different methods.

Class	SVM	1D-NN	1D-CNN	2D-CNN	3D-CNN	3D-FCNN
IP	73.03	83.89	87.68	96.69	98.66	99.32
PC	94.70	96.18	96.21	97.23	98.57	98.82
UP	90.39	91.48	91.97	96.04	97.34	99.07
BS	80.63	81.05	89.81	90.60	90.97	97.23
SV	90.36	93.38	95.87	96.66	96.90	98.59

TABLE 2: Overall accuracy evaluation results for the five datasets derived using different methods.

Class	SVM	1D-NN	1D-CNN	2D-CNN	3D-CNN	3D-FCNN
IP	81.27	84.77	86.20	95.27	99.07	99.25
PC	98.22	98.74	98.87	98.90	98.93	99.63
UP	91.54	92.60	93.44	94.07	95.72	99.60
BS	77.83	80.44	88.96	89.72	90.69	97.02
SV	87.01	89.09	92.37	93.00	94.40	96.97

TABLE 3: Kappa evaluation results for the five datasets derived using different methods.

Class	SVM	1D-NN	1D-CNN	2D-CNN	3D-CNN	3D-FCNN
IP	78.61	64.39	84.21	94.64	98.93	99.51
PC	97.50	98.22	98.40	98.51	98.48	99.47
UP	89.07	90.17	91.52	92.25	94.40	99.47
BS	75.14	78.80	88.04	88.26	89.91	96.07
SV	85.48	87.86	91.49	90.22	93.77	96.62

where F denotes the number of elements in S and x_{ij} is the activation value at position (i, j) .

2.3. Fully Connected Layer. The CNN output is acquired after the last one or two fully connected layers. Each node is connected to all the nodes in the previous layer, and the characteristics extracted after convolution downsampling are feature fused and subsequently transmitted to the classifier for classification prediction. The classifier is capable of employing logistic regression, SoftMax, support vector machine, or sigmoid [22] to be converted into probability methods. The output of the fully connected layer L is determined by the weighted summation of the input as well as the response of the activation function:

$$y_j^l = f\left(\sum w_{ji}^l * x_i^{l-1} + b_j^l\right), \quad (3)$$

where the j -th output unit y_j^l of the layer performs weighting and bias calculations and summation on all the output feature maps of x_i^{l-1} of the previous layer, which is obtained by the $f(\cdot)$ classifier; w_{ji}^l denotes the weight coefficient of the fully connected network, and b_j^l represents the bias term of the l -th fully connected layer.

2.4. Network Training. The training process of the CNN covers two stages, i.e., forward propagation with low-level propagation and high-level propagation and back propagation with high-level propagation and low-level propagation. Figure 3 presents the entire CNN training process.

The input weight parameters are first initialized to avoid gradient propagation problems, reduced training speeds, and consumption of training time. Then, the actual output is obtained after a series of forwarding propagations (e.g., a convolutional layer, downsampling layer, and fully connected layer). The error between the actual output value and the target value is calculated. If the error generated is not consistent with the expected value, the error is retransmitted to the network for training, and the backpropagation sequentially calculates the fully connected, downsampling, and convolutional layers. The weight is updated following the calculated error value, and the mentioned steps are repeated until the error is less than the expected value; then, the training is terminated.

3. 3D-FCNN Structure with a Bottleneck Attention Mechanism

In this section, a new 3D fully convolutional neural network model will be presented to overcome difficulties in the process of hyperspectral images classification. In this model,

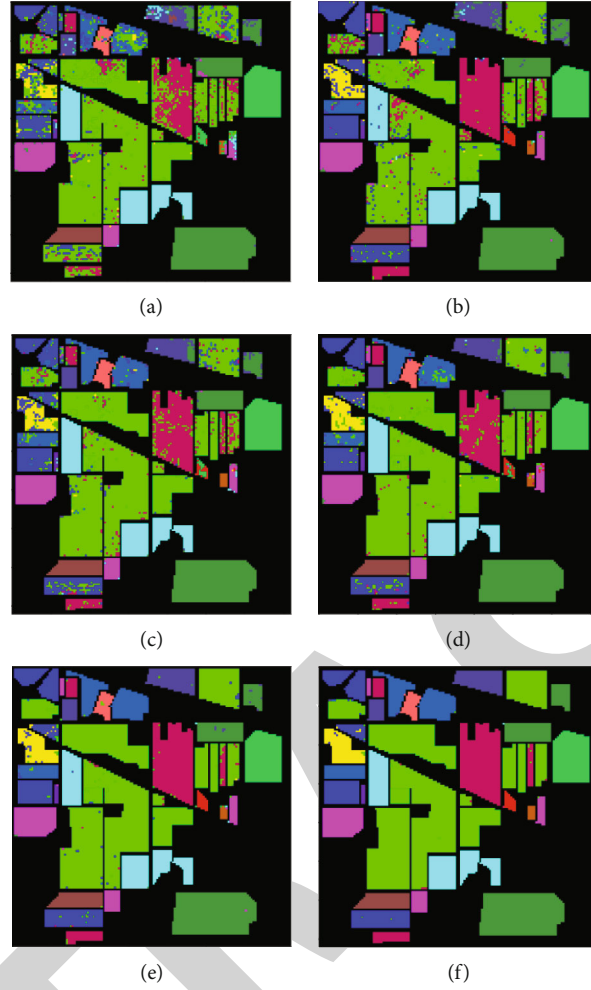


FIGURE 7: Classification effect diagrams of the IP dataset under the different models: (a) SVM; (b) 1D-NN; (c) 1D-CNN; (d) 2D-CNN; (e) 3D-CNN; and (f) 3D-FCNN.

the downsampling layer and the fully connected layer are replaced with a 3D-CNN, and a bottleneck attention mechanism is embedded. The structure of the elementary block of the developed model is first illustrated, and then the method by which the block extracts and fuses the characteristics is elucidated. Lastly, the bottleneck attention mechanism architecture is detailed.

3.1. 3D-FCNN Module. Most HSI classification models based on CNNs alternately cover multiple convolutional and downsampling layers, and several fully connected layers. Network parameters can be significantly reduced with convolutional layers instead of fully connected layers. Although the downsampling layer can increase the translation invariance of the characteristics of the CNN, it slightly improves the classification performance of the network. The downsampling of the pooling layer will give the high-level characteristics a larger receptive field while causing some loss of local characteristics. Zhang et al. [23] used a convolutional layer with a step size of 2 to replace the downsampling layer to improve the network classification performance. The 3D-FCNN proposed in the present study is used for pixel-level

HSI classification. The main components are 3D convolution and 3D convolution with a step size of S . The model is mainly composed of an input layer, a 3D convolution layer, a 3D convolution layer with a step size of S , and an output layer. Preprocessing operations during training are not required. The image cube is composed of pixels in a small spatial neighborhood (rather than in the entire image) and directly extracted as the input from the entire spectrum. The spectral-spatial characteristics are extracted through the 3D-FCNN model. Lastly, the output of the classification results from the network, that is, the specific HSI classification process based on 3D-FCNN, as shown in Figure 4. The output of the convolutional layer with step size S is represented as follows:

$$v_{(l+1)j}^{xyz} = f \left(\sum_m \sum_{h=0}^{H_{(l+1)}-1} \sum_{w=0}^{W_{(l+1)}-1} \sum_{r=0}^{R_{(l+1)}-1} k_{(l+1)jm}^{hwr} v_{lm}^{(xs+h)(ys+w)(zs+r)} + b_{(l+1)j} \right), \quad (4)$$

where l represents the l -th layer, v represents the output feature body, and H , W , and R represent the length, width, and

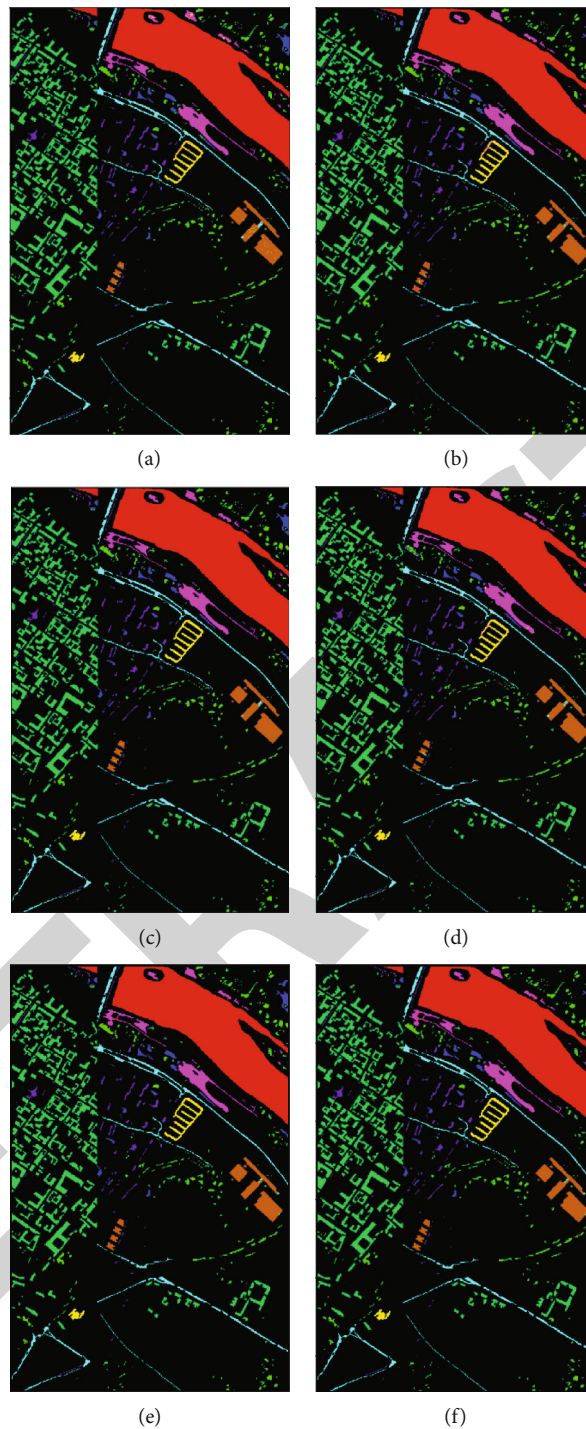


FIGURE 8: Classification effect diagrams of the PC dataset under the different models: (a) SVM; (b) 1D-NN; (c) 1D-CNN; (d) 2D-CNN; (e) 3D-CNN; and (f) 3D-FCNN.

spectral dimensions of the feature body, respectively. The number of convolution kernels in the current layer is j .

The proposed model primarily consists of three steps:

- (1) Extraction of training samples. The $N \times N \times L$ image cube is extracted from the HSI with the input size of $H \times W \times L$, where $N \times N$ denotes the size of the

neighborhood space (window size) and L represents the number of spectral bands

- (2) Spectral-spatial feature extraction based on 3D-FCNN. The model in the present study substitutes all downsampling layers with convolutional layers with a step size of S

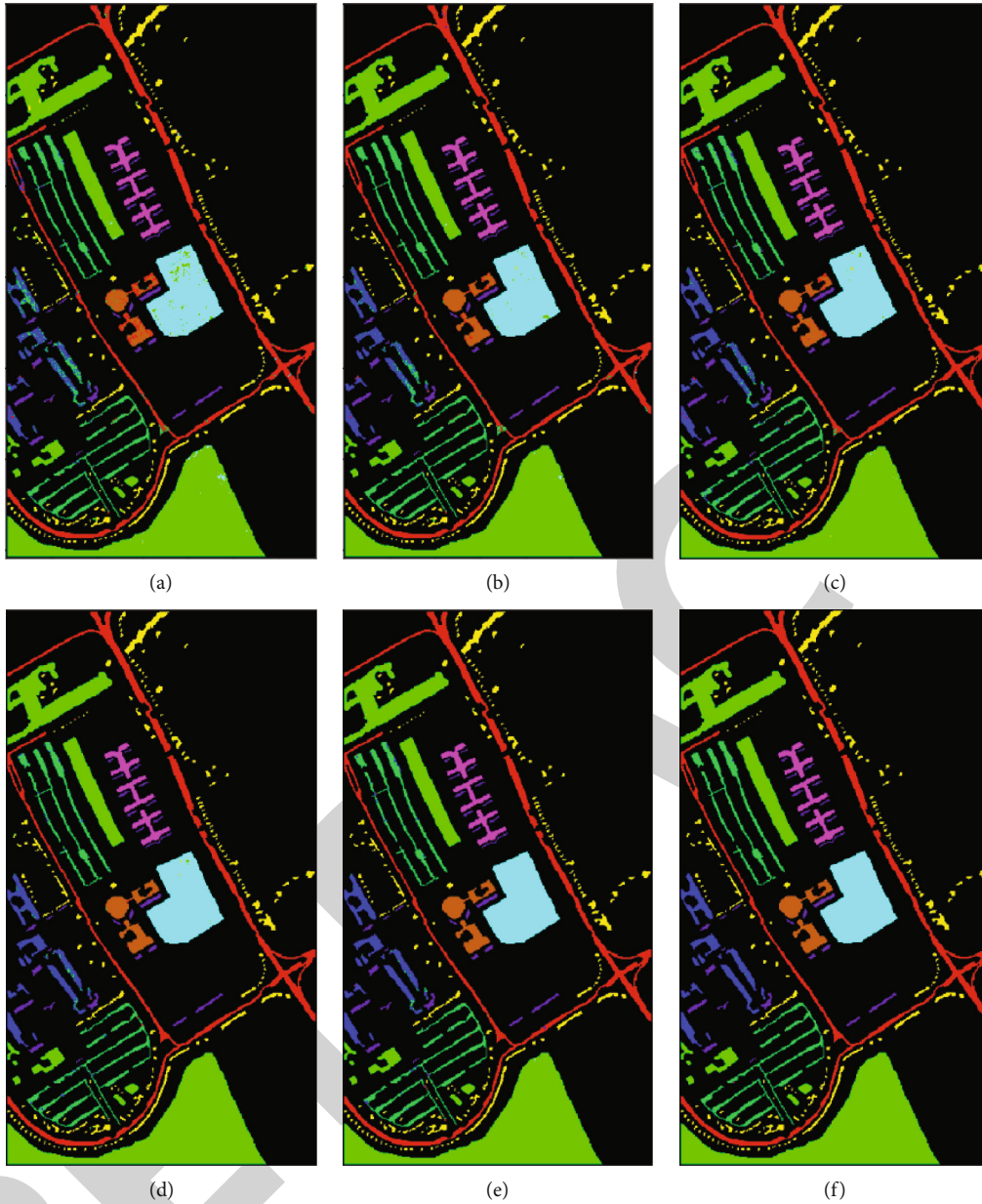


FIGURE 9: Classification effect diagrams of the UP dataset under the different models: (a) SVM; (b) 1D-NN; (c) 1D-CNN; (d) 2D-CNN; (e) 3D-CNN; and (f) 3D-FCNN.

- (3) Classification based on spatial-spectral features. The characteristics of the last layer, i.e., the $1 \times 1 \times 1 \times N$ tensor, are input into the SoftMax classifier to acquire the final classification result

3.2. Bottleneck Attention Mechanism Module. The bottleneck attention module (BAM) [20, 24] is embedded based on the 3D-FCNN classification network. The BAM extracts vital information from the spectral and spatial dimensions of the HSI through the channel and spatial attention branches, respectively, and exploits the characteristics separately without any feature engineering. The end-to-end characteristics are maintained, and the problem of information redundancy is effectively solved.

In image processing, the core of the attention mechanism refers to mask learning on the image, injecting information from each region into the algorithm, and improving the region conducive to accuracy improvement. Figure 5 illustrates the detailed structure of the BAM. For a given input feature map $F \in R^{C \times H \times W}$, the BAM derives a 3D attention feature map $M(F) \in R^{C \times H \times W}$, and the feature map F' generated after multiplying and adding the original input feature map is obtained as follows:

$$F' = F + F \otimes M(F), \quad (5)$$

where \otimes denotes multiplication by the corresponding elements, and the addition term refers to adding the

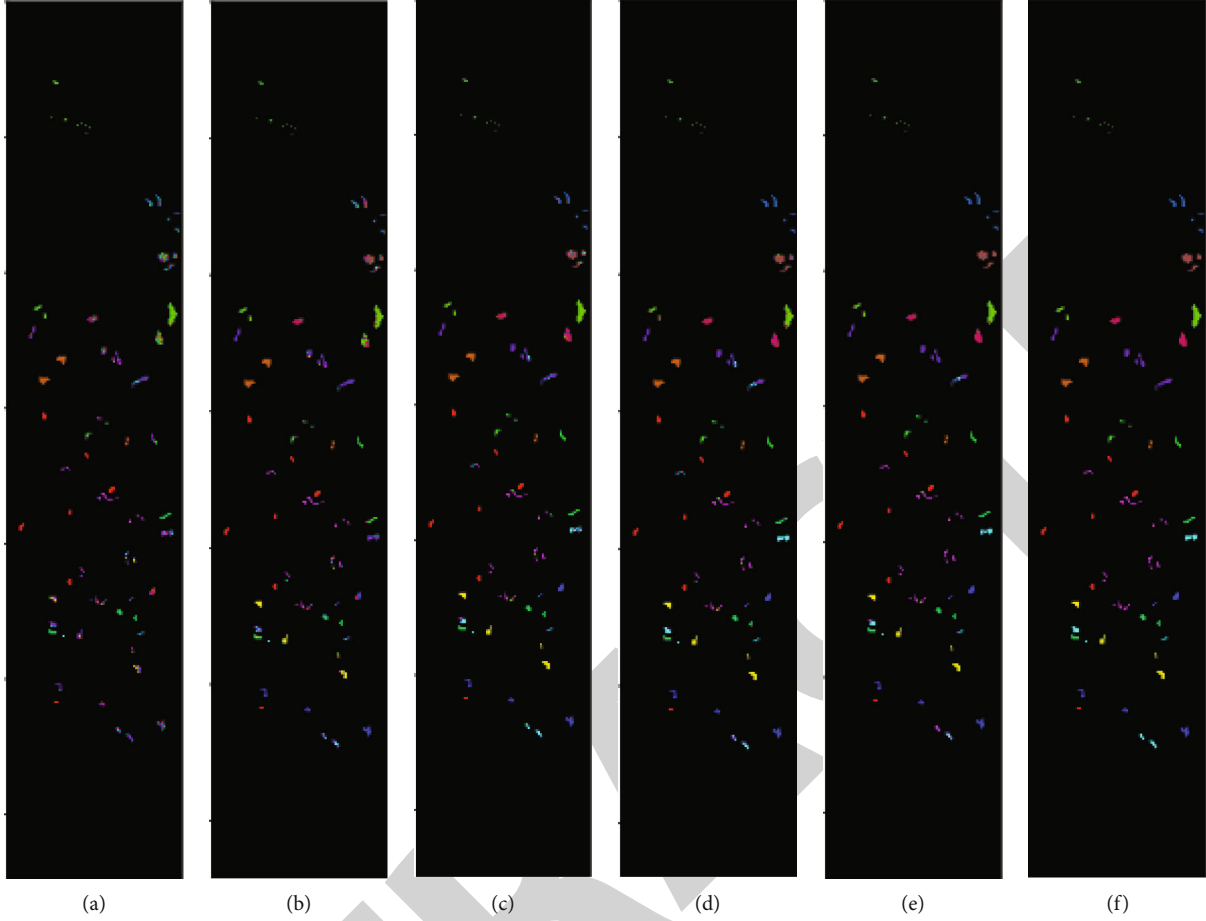


FIGURE 10: Classification effect diagrams of the BS dataset under the different models: (a) SVM; (b) 1D-NN; (c) 1D-CNN; (d) 2D-CNN; (e) 3D-CNN; and (f) 3D-FCNN.

corresponding elements. A residual structure is introduced to the BAM structure to promote gradient flow. The BAM has two attention mechanism branches, i.e., channel attention $M_c(F) \in R^C$ and spatial attention $M_s(F) \in R^{H \times W}$. The final attention mapping can be illustrated as follows:

$$M(F) = \sigma(M_c(F) + M_s(F)), \quad (6)$$

where σ denotes the sigmoid activation function, and the space size of the two branches is transformed into $R^{C \times H \times W}$ after the addition.

3.2.1. Channel Attention Branch. In the BAM proposed in this study, a channel attention branch is set to enhance or inhibit the characteristics of the band. To aggregate the characteristics in each channel, the global average pooling on the feature map F is employed to generate the channel vector $M_c(F) \in R^{C \times 1 \times 1}$. Such a vector masks global information in each channel. To estimate the cross-channel attention from the channel vector F_C , a multilayer perceptron (MLP) with a hidden layer is adopted. To save the parameter overhead, the size of the hidden layer is set to $R^{C/r \times 1 \times 1}$, where r denotes the compression ratio. After MLP inclusion, a batch normal-

ization layer is introduced to regulate the scale to match the spatial branch output. Accordingly, the channel attention calculation formula is written as follows:

$$\begin{aligned} M_C(F) &= BN(MLP(AvgPool(F))) \\ &= BN(W_1(W_0 AvgPool(F) + b_0) + b_1), \end{aligned} \quad (7)$$

where $W_0 \in R^{C/r \times C}$, $b_0 \in R^{C/r}$, $W_1 \in R^{C \times C/r}$, and $b_1 \in R^C$.

3.2.2. Spatial Attention Branch. The spatial attention branch generates a spatial attention map $M_s(F) \in R^{H \times W}$, which is adopted to enhance or inhibit characteristics in various spatial positions. The application of context-related data is critical for acquiring spatial locations that require highlighting. Accordingly, a receptive field at a large scale is required to significantly exploit context-related data. Thus, cavity convolution is adopted for expanding the receptive field and enhancing efficiency. The spatial branch employs the ‘‘bottleneck structure’’ developed by ResNet [25], thereby saving on the number of parameters required as well as computation overhead. To be specific, the feature vector $F \in R^{C \times H \times W}$ merges the feature map into a low-dimensional $R^{C/r \times H \times W}$ through 1×1 convolution, which is equated with the integration

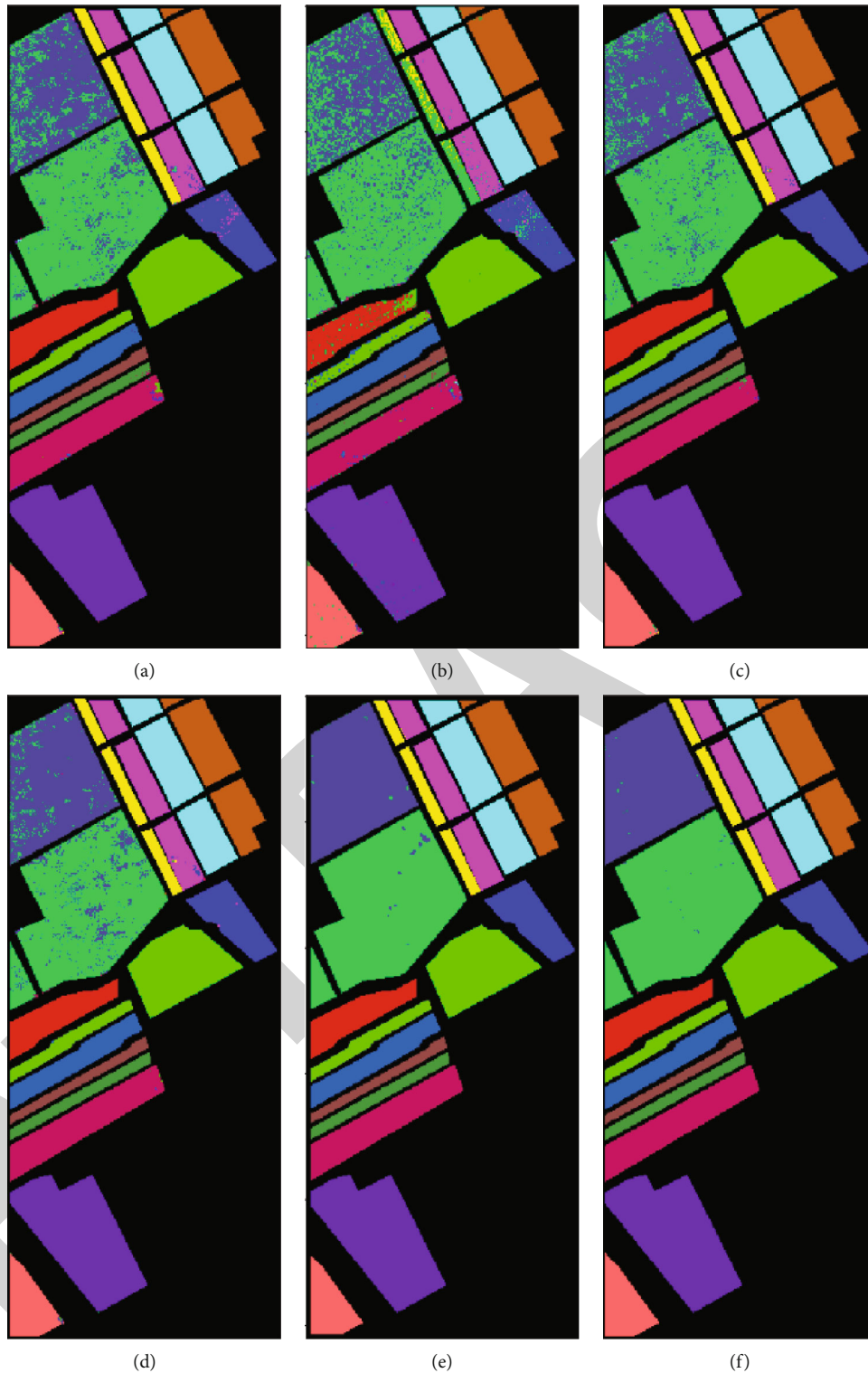


FIGURE 11: Classification effect diagrams of the SV dataset under the different models: (a) SVM; (b) 1D-NN; (c) 1D-CNN; (d) 2D-CNN; (e) 3D-CNN; and (f) 3D-FCNN.

and compression of the feature map of the channel dimension. Here, a compression rate identical to that of the channel attention branch is adopted. After dimensionality reduction, two 3×3 hole convolutions are used

to effectively utilize context information. Lastly, a 1×1 convolution is adopted for reducing the feature to the size of $R^{1 \times H \times W}$ space. For scale adjustment, a batch normalization layer is added to the end of the spatial

TABLE 4: Performances of different network depths for the 3D-CNN and 3D-FCNN models.

Model	Dataset	3	5	7	9	11
3D-CNN	IP	87.78	99.07	77.69	75.76	73.04
	PC	95.62	98.93	97.03	96.22	95.00
	UP	93.79	94.01	95.72	95.11	94.25
	BS	88.04	90.69	88.96	87.13	85.64
	SV	93.08	94.40	94.05	93.33	92.57
	IP	89.60	99.25	98.51	96.35	95.63
3D-FCNN	PC	99.33	99.63	99.68	98.72	97.77
	UP	94.80	98.25	98.49	98.55	98.41
	BS	88.44	96.13	97.02	95.45	94.28
	SV	93.76	96.38	96.97	95.87	95.44

attention branch. Accordingly, spatial attention can be expressed as follows:

$$M_s(F) = BN \left(f \int_3^{1 \times 1} \left(f \int_2^{3 \times 3} \left(f \int_0^{1 \times 1} (F) \right) \right) \right), \quad (8)$$

where f is defined as the convolution operation process, BN is a batch normalization operation, and the superscript of the convolution operation is denoted as the size of the convolution filter. Three 1×1 convolutions are adopted to compress the channel dimension, and two 3×3 dilated convolutions are used to expand the receptive field to aggregate more context-related information.

3.2.3. Merging of the Two Attention Branches. After the channel $M_C(F)$ and the spatial $M_S(F)$ attention branches are obtained, these are merged to generate the final 3D attention feature map $M(F)$. The summation maps of the attention feature maps of each branch to the size of R are obtained and are impacted by the different shapes of the attention feature maps generated by the two branches. In a range of combination methods (e.g., summation, multiplication, or maximum value operations), the corresponding elements act as the operation method. After the summation, the swish function is adopted to activate the final 3D attention feature mapping $M(F)$. The generated 3D attention feature map $M(F)$ is subsequently introduced to the original input feature map F to multiply the corresponding elements in it and generate the redefined feature map F' as expressed in the formula, i.e., to generate the BAM-processed feature map.

3.2.4. Swish Activation Function. The swish activation function refers to a novel type of activation function proposed by Ramachandran et al. [26] for Google Brain; its formula is written as follows:

$$f(x) = x * \text{sigmoid}(x). \quad (9)$$

The common activation function in deep learning is the ReLU activation function characterized by a lower bound, no upper bound, and smoothness. Swish has a lower bound and no upper bound similar to ReLU, whereas the nonmo-

tonicity of swish is inconsistent with other common activation functions. Moreover, swish exhibits both first-order derivative and second-order derivative smoothness.

3.2.5. 3D-FCNN Model with BAM. The major convolution part of the model network covers a convolutional layer and a convolutional layer with a step length of S . The $N \times N \times L$ image cube of an HSI with the size $H \times W \times L$ is extracted as a sample input of the network. $N \times N$ denotes the size of the neighborhood space (window size), and L represents the spectral band number. The type of the center pixel of the cube acts as the target label. After inputting the data samples, it first passes through a $3 \times 3 \times L$ convolutional layer. The second refers to a small-structure network covering a convolutional layer, a convolutional layer with a step size of S , and an added BAM. The number of times the small network module is superimposed is i . The last attention mechanism feature map generated undergoes a 1×1 convolution, global pooling, and fully connected operation. Then, the SoftMax function is adopted to output the final classification. The model is illustrated in Figure 6.

4. Results and Discussion

To evaluate the accuracy and efficiency of the developed model, experimental processes with respect to five datasets were created for comparison and verification with other approaches. For accurate measurements of each approach, quantitative metrics of Kappa (K), average accuracy (AA), and overall accuracy (OA) were employed. Here, OA denotes the rate of true classification of whole pixels, AA refers to the average accuracy characteristic of all types, and Kappa indicates the consistency characteristic of ground truth with the classification result. The higher these metrics are, the more effective the classification result is.

4.1. Introduction to the Dataset. Five extensively applied HSI datasets, namely, the Indian Pines (IP), Pavia Center (PC), Pavia University (UP), Salinas Valley (SV), and Botswana (BS) datasets, were applied. These datasets are briefly described below:

- (i) Indian Pines (IP): generated by the airborne visible infrared imaging spectrometer (AVIRIS) sensor in north-western Indiana, the IP dataset covers 200 spectral bands exhibiting a wavelength scope of 0.4 to $2.5 \mu\text{m}$ and 16 land cover classes. IP covers 145×145 pixels and exhibits a resolution of 20 m/pixel
- (ii) Pavia University (UP) and Pavia Center (PC): collected by the reflective optics imaging spectrometer (ROSIS-3) sensor at the University of Pavia, northern Italy, the UP dataset covers 103 spectral bands exhibiting a wavelength scope of 0.43 to $0.86 \mu\text{m}$ and 9 land cover classes. UP encompasses 610×340 pixels and exhibits a resolution of 1.3 m/pixel. The PC reaches 1096×715 pixels
- (iii) Salinas Valley (SV): collected by the AVIRIS sensor from Salinas Valley, CA, USA, the SV dataset covers

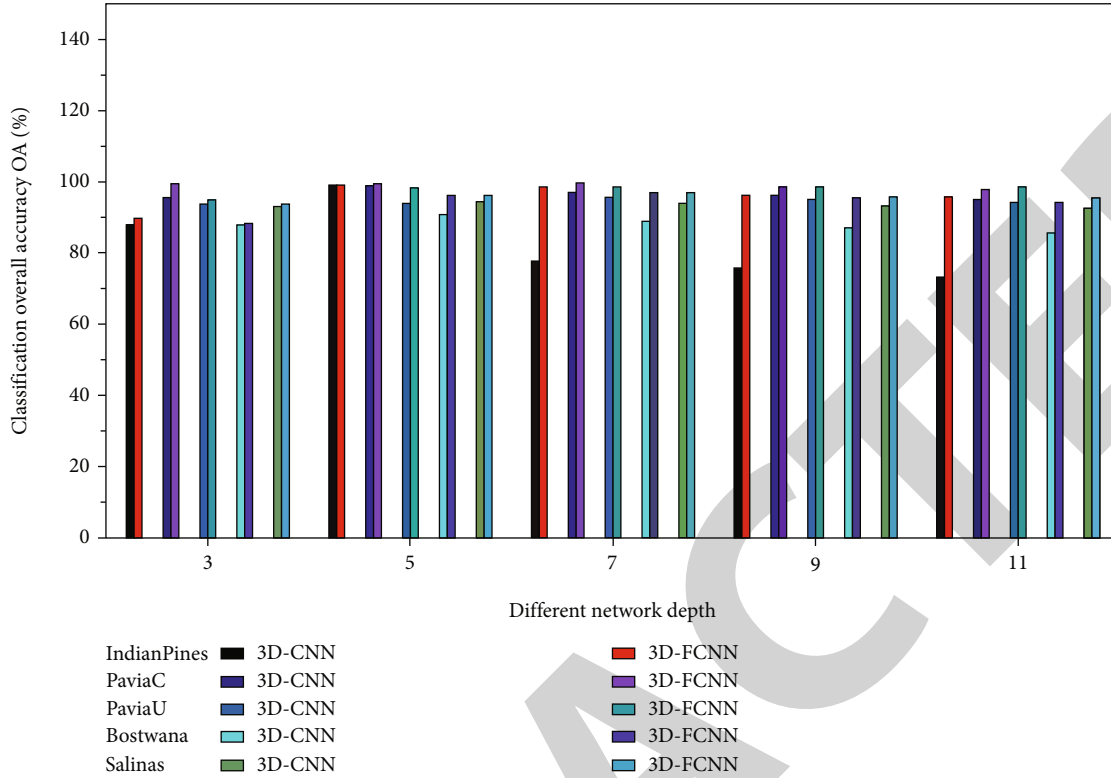


FIGURE 12: Performances of the 3D-CNN and 3D-FCNN models with each dataset at various depths.

204 spectral bands exhibiting a wavelength scope of 0.4 to 2.5 μm and 16 land cover classes. SV encompasses 512 \times 217 pixels and exhibits a resolution of 3.7 m/pixel

- (iv) Botswana (BS): captured by the NASA EO-1 satellite over the Okavango Delta, Botswana, the BS dataset covers 145 spectral bands exhibiting a wavelength scope of 0.4 to 2.5 μm and 14 land cover classes. BS encompasses 1476 \times 256 pixels and exhibits a resolution of 30 m/pixel

Deep learning algorithms are data driven and rely on large numbers of labeled training samples. As more labeled data are fed into the training, the accuracy improves. However, more data for training implies increased time consumption and higher computation complexity. The five datasets used by the 3D-FCNN are the same as those used by the other networks discussed, and we set the parameters based on experience. For the IP dataset, 50% of the samples were selected for training, and 5% were randomly selected for verification. Since the samples were sufficient for UP, PC, BS, and SV, only 10% of the samples were used for training, and the remaining 90% were used as test data. Of the 10% of samples used for training, 50% (5% of the total) were randomly selected. Accordingly, different models and different network depths were compared under identical data conditions. Notably, in the absence of training samples, the model based on the BAM was capable of maintaining excellent performance. Thus, in the experiment,

the sizes of the training and verification samples were set to the minimum level. The IP and SV datasets were employed for the experimental processes. Owing to the uneven distribution of the number of types in the IP dataset, the ratio of training-set:test-set was maintained at 1:1. As the number of labeled samples in the SV dataset is identical among different types, the ratio of training-set:test-set was maintained at 1:9.

4.2. Experimental Settings. To assess the effectiveness of the model, deep learning-based classifiers (SVM, 1D-NN, 1D-CNN, 2D-CNN, and 3D-CNN) were utilized to compare with our proposed framework. Under identical conditions, comparisons of the generalization ability and nonlinear expression ability at different network depths were conducted. The BAM added with the parameter $r=5$ was employed in the CNN model. Two other methods, SE-Net [27] (squeeze-and-excitation (SE)) and frequency band weighted module [28] (band attention module, (BandAM)), were also employed. The classification results were compared. To ensure the validity of the experiment, the same depth was maintained for all involved models, and 10 experiments were carried out to eliminate randomness.

The patch size of each classifier was set as specified in the corresponding original paper. To compare the classification performances, all experiments were performed on the same platform with 32 GB of memory and an NVIDIA GeForce RTX 2080 Ti GPU. All classifiers based on deep learning were implemented by adopting PyTorch, TensorFlow, and Keras libraries.

TABLE 5: Classification effects of different modules on the IP dataset.

Class	3D-FCNN	SE+3D-FCNN	BandAM+3D-FCNN	BAM+3D-FCNN
1	53.33	100	52.27	100
2	82.74	98.10	99.19	95.49
3	59.61	98.04	88.09	98.66
4	64.68	100	80.89	97.65
5	67.78	27.93	94.12	97.47
6	99.03	99.11	98.70	98.93
7	0	96.15	74.07	100
8	94.29	100	100	100
9	0	88.89	73.68	94.44
10	94.24	94.27	79.74	97.60
11	90.09	99.25	97.13	99.91
12	67.12	95.79	82.77	98.88
13	99.01	100	91.79	100
14	97.60	99.05	99.50	99.03
15	89.79	97.45	92.64	99.42
16	65.22	100	100	98.81
OA (%)	82.29	93.01	93.66	98.54
AA (%)	71.00	93.36	88.13	98.51
Kappa	79.64	91.98	92.75	98.33

4.3. *Experimental Results.* For SVM, 1D-NN, 1D-CNN, 2D-CNN, and 3D-CNN, the same architecture and parameter settings as in the present study were used. For those settings that are not explicitly given in the present study, we used commonly used values in the HSI classification (for example, the merge span is 2). Detailed analysis results are presented in Tables 1–3. The classification effect diagrams of various datasets under different models are presented in Figure 7 for IP, Figure 8 for PC, Figure 9 for UP, Figure 10 for BS, and Figure 11 for SV.

Our 3D-FCNN network replaces the downsampling layer and the fully connected layer with a CNN, which reduces the network training parameters, consumes less training time under identical conditions, and has a higher convergence speed, thus showing better overall performance. Furthermore, the model developed in the present study has the best classification performance with a classification accuracy of 99.63% and minimum classification error based on the three evaluation criteria. Adopting CNNs to replace the downsampling layer and the fully connected layer is suggested as a potentially feasible approach for training the deep network.

The number of network model layers (depth) is another critical parameter that should be considered. In the case of a fixed input data cube size, different network layers are employed for multiple datasets to further demonstrate the impact of the depth parameter on the classification results. The experimental processes were performed on the datasets and compared with the 3D-CNN model under identical con-

TABLE 6: Classification effects of different modules on the SV dataset.

Class	3D-FCNN	SE+3D-FCNN	BandAM+3D-FCNN	BAM+3D-FCNN
1	100	98.99	100	100
2	100	100	100	100
3	100	99.90	100	100
4	100	100	99.76	98.49
5	94.19	95.44	99.75	99.96
6	100	98.55	100	100
7	100	100	100	99.76
8	99.93	97.65	100	99.08
9	100	100	100	100
10	99.97	99.32	100	100
11	100	99.62	100	100
12	100	96.59	100	99.78
13	100	98.90	100	100
14	99.90	99.72	99.79	100
15	79.80	93.39	91.48	99.96
16	99.94	99.94	100	100
OA (%)	96.88	98.05	98.83	99.73
AA (%)	98.27	98.59	99.39	99.81
Kappa	96.52	97.83	98.70	99.70

ditions. The number of layers was 3, 5, 7, and 9. Table 4 shows the comparative results. Figure 12 presents the performances of the two models on the respective datasets at various depths.

The results show that, regardless of depth, the model developed in this study outperforms the 3D-CNN model. The 3D-FCNN model developed in the present study has better performance generalization and nonlinear expression abilities under identical conditions.

Figure 12 shows the results of different network depths. Overall, the network is better with increasing depth. Furthermore, increasing depth facilitates extraction and classification using more advanced functions. However, the results of our model are not proportional to the depth of the network, as the architecture of the developed model balances performance and cost by selecting the optimal network layer.

An optimized FCNN acts as the basic network. The network does not perform any operations and directly performs classification. The other three methods use different band weighted inputs, including the BandAM module, SE module, and the BAM proposed in the present study. Tables 5 and 6 present the specific analysis and comparison. The classification effect diagrams of various datasets under different modules (Figure 13 for IP and Figure 14 for SV) are illustrated.

In this study, we explored a novel and effective 3D-FCNN for HSI classification. On this basis, we embedded a module for the extraction of spectral and spatial features. Compared to the latest network, the most significant

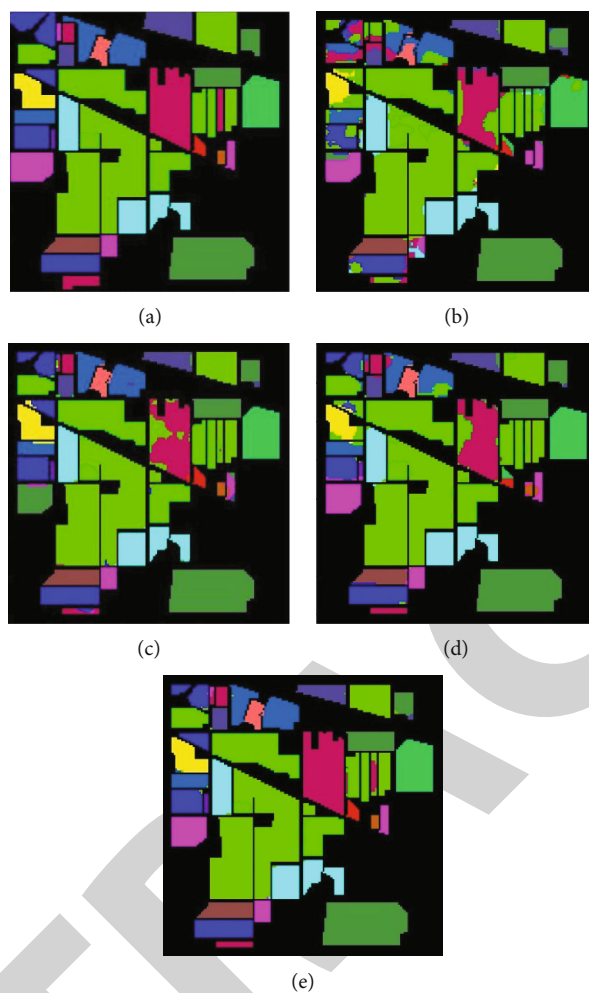


FIGURE 13: Classification effect diagrams for IP dataset of different modules: (a) ground truth; (b) 3D-FCNN; (c) SE+3D-FCNN; (d) BandAM+3D-FCNN; and (e) BAM+3D-FCNN.

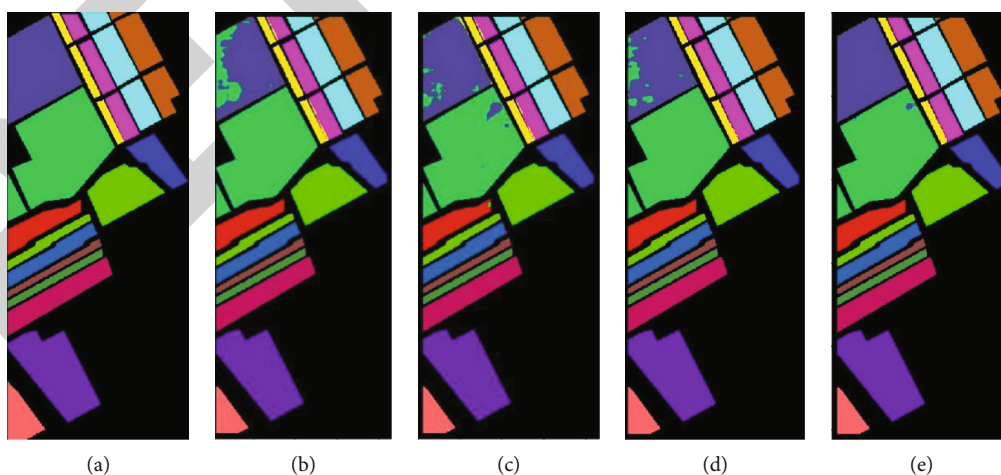


FIGURE 14: Classification effect diagrams of the SV dataset of different modules: (a) Ground truth; (b) 3D-FCNN; (c) SE+3D-FCNN; (d) BandAM+3D-FCNN; and (e) BAM+3D-FCNN. Tables 5 and 6 indicate that the proposed BAM considers spatial and spectral information, and it significantly improves classification performance. The 2–3% improvement in each standard demonstrates that the proposed BAM is effective. For HSI classification, the proposed BAM can be considered a plug-and-play supplementary module for most mainstream CNNs.

advantage of the proposed network is that it requires only a small number of network parameters to achieve considerable classification accuracy, in which an end-to-end classification mechanism is maintained. The proposed network uses various training strategies to help it converge better and faster without causing a computational burden.

5. Conclusions

The results of our study suggest the following:

- (1) Deep networks that adopt spectral and spatial characteristics achieve significantly higher classification accuracy than deep networks that adopt only spectral characteristics. The results prove that the BAM is beneficial to HSI classification
- (2) Deep learning performs well in several remote sensing fields. However, the trend to make the network more complex and deeper adds several parameters to the training process. With the inclusion of more parameters, the model can exhibit better classification capabilities. The results of the present study showed that this attempt has successfully reduced the network parameters and the loss of data information. That is, the developed method successfully replaces the downsampling layer and the fully connected layer with a convolutional layer. Furthermore, the experimental results show that the proposed network exhibits a high generalization ability and classification performance irrespective of its depth

Suggested improvements to the present study in the future are as follows:

- (1) Application of the developed framework to HSIs in specific areas, such as forest resources observation and agricultural production management, other than the open-source datasets considered here
- (2) The methods applied in the present study are all supervised. Semisupervised or unsupervised methods can be adopted using the considered limited data and achieve relatively higher performance with less labeled data
- (3) The reduction in the training time poses an attractive challenge and needs to be addressed

Data Availability

All code will be made available on request to the correspondent author's email with appropriate justification.

Conflicts of Interest

The authors declare no conflict of interest.

Acknowledgments

This research was funded by the National Natural Science Foundation of China (grant number: 61501210) and the Department of Education of Jiangxi Province (grant number: GJJ211410).

References

- [1] G. E. Hinton and R. S. Zemel, "Autoencoders, minimum description length and Helmholtz free energy," in *Advances in neural information processing systems, Proceedings of the Neural Information Processing Systems*, pp. 3–10, Denver, Colorado, November 1993.
- [2] G. E. Hinton, S. Osindero, and Y. W. Teh, "A fast learning algorithm for deep belief nets," *Neural Computation*, vol. 18, no. 7, pp. 1527–1554, 2006.
- [3] K. Gregor, I. Danihelka, A. Graves, D. J. Rezende, and D. Wierstra, "DRAW: A recurrent neural network for image generation," in *Proceedings of the 32nd International Conference on Machine Learning*, pp. 1462–1471, Lille, France, July 2015.
- [4] J. Gu, Z. Wang, J. Kuen et al., "Recent advances in convolutional neural networks," *Pattern Recognition*, vol. 77, pp. 354–377, 2018.
- [5] S. Dieleman and B. Schrauwen, "End-to-end learning for music audio," in *2014 Proceedings of the IEEE International Conference on Acoustics, Speech and Signal Processing (ICASSP)*, pp. 6964–6968, Florence, Italy, 2014.
- [6] A. R. Mohamed, T. N. Sainath, G. Dahl, B. Ramabhadran, G. E. Hinton, and M. A. Picheny, "Deep belief networks using discriminative features for phone recognition," in *2011 Proceedings of the IEEE International Conference on Acoustics, Speech and Signal Processing*, pp. 5060–5063, Prague, Czech Republic, 2011.
- [7] T. Wang, D. J. Wu, A. Coates, and A. Y. Ng, "End-to-end text recognition with convolutional neural networks," in *2012 Proceedings of the 21st International Conference on Pattern Recognition (ICPR 2012)*, pp. 3304–3308, Tsukuba Science City, Japan, November 2012.
- [8] D. Yu, L. Deng, and S. Wang, "Learning in the deep-structured conditional random fields," in *2009 Proceedings of the NIPS Workshop on Deep Learning for Speech Recognition and Related Applications*, pp. 1–8, Vancouver, Canada, December 2009.
- [9] H. Liang and Q. Li, "Hyperspectral imagery classification using sparse representations of convolutional neural network features," *Remote Sensing*, vol. 8, no. 2, p. 99, 2016.
- [10] K. Makantasis, E. Protopapadakis, A. Doulamis, N. Doulamis, and C. Loupos, "Deep convolutional neural networks for efficient vision based tunnel inspection," in *2015 Proceedings of the IEEE International Conference on Intelligent Computer Communication and Processing (ICCP)*, pp. 335–342, Cluj-Napoca, Romania, September 2015.
- [11] C. Chen, J. J. Zhang, C. H. Zheng, Q. Yan, and L. N. Xun, *Classification of hyperspectral data using a multi-channel convolutional neural network*, Intelligent computing methodologies, D. S. Huang, M. M. Gromiha, K. Han, and A. Hussain, Eds., Springer International Publishing, Berlin, 2018.
- [12] M. He, B. Li, and H. Chen, "Multi-scale 3D deep convolutional neural network for hyperspectral image classification," in *2017 Proceedings of the IEEE International Conference on Image*

Retraction

Retracted: Online English Teaching System Based on Internet of Things Technology

Journal of Sensors

Received 17 October 2023; Accepted 17 October 2023; Published 18 October 2023

Copyright © 2023 Journal of Sensors. This is an open access article distributed under the Creative Commons Attribution License, which permits unrestricted use, distribution, and reproduction in any medium, provided the original work is properly cited.

This article has been retracted by Hindawi following an investigation undertaken by the publisher [1]. This investigation has uncovered evidence of one or more of the following indicators of systematic manipulation of the publication process:

- (1) Discrepancies in scope
- (2) Discrepancies in the description of the research reported
- (3) Discrepancies between the availability of data and the research described
- (4) Inappropriate citations
- (5) Incoherent, meaningless and/or irrelevant content included in the article
- (6) Peer-review manipulation

The presence of these indicators undermines our confidence in the integrity of the article's content and we cannot, therefore, vouch for its reliability. Please note that this notice is intended solely to alert readers that the content of this article is unreliable. We have not investigated whether authors were aware of or involved in the systematic manipulation of the publication process.

Wiley and Hindawi regrets that the usual quality checks did not identify these issues before publication and have since put additional measures in place to safeguard research integrity.

We wish to credit our own Research Integrity and Research Publishing teams and anonymous and named external researchers and research integrity experts for contributing to this investigation.

The corresponding author, as the representative of all authors, has been given the opportunity to register their agreement or disagreement to this retraction. We have kept a record of any response received.

References

- [1] H. Tao, "Online English Teaching System Based on Internet of Things Technology," *Journal of Sensors*, vol. 2022, Article ID 7748067, 8 pages, 2022.

Research Article

Online English Teaching System Based on Internet of Things Technology

Hui Tao 

Inner Mongolia Vocational and Technical College of Communications, Chifeng, Inner Mongolia 024005, China

Correspondence should be addressed to Hui Tao; 202003419@stu.ncwu.edu.cn

Received 1 July 2022; Revised 17 July 2022; Accepted 28 July 2022; Published 10 August 2022

Academic Editor: C. Venkatesan

Copyright © 2022 Hui Tao. This is an open access article distributed under the Creative Commons Attribution License, which permits unrestricted use, distribution, and reproduction in any medium, provided the original work is properly cited.

In order to better improve students' English performance and adapt to the progress in the age of science and technology faster, the author proposes an online English teaching system method based on Internet of Things technology. The author studies the English SPOC teaching mode and constructs a multimedia teaching system based on the Internet of Things technology, improve the teaching system, and improve and learn the teaching mode, to achieve the improvement of the quality of English teaching. Experimental results show that under the author's method, students' scores on both the written and oral exams are about 10 points higher than those in the traditional teaching method. *Conclusion.* The online English teaching system based on Internet of Things technology can effectively improve students' English performance and allow students to better control their own progress.

1. Introduction

Online English teaching is a type of teaching and learning strategy developed with the support of network technology that has created a form of teaching English in college [1]. Now, colleges and universities can follow the schedule and practice teaching English online. However, due to the current situation of teaching English online in college, there are some issues that affect the effective use of English online at home. Therefore, in the new era, English college students are aware of the cost, advantages, and current situation of using English language training online. English language courses are used in colleges and universities, as well as online English courses to help college students learn English and increase the self-confidence of their students and instructions for colleges and universities.

The concept of the Internet of Things was first introduced in 1999 at the International Conference on Mobile Computing and Networking in the United States: "sensory networks are the development of humanity, in the coming years" [2]. Therefore, the concept of the Internet is planned: the use of wireless communication technologies such as RFID (Internet of Things) to connect everything in the

world to the Internet on the basis of the Internet, fully intelligent characters, and the exchange of information products [3]. Combining the importance of many countries and technological advances, new technology research and the Internet of Things created by various information technologies are important.

At present, the teaching of Internet of Things technology relies heavily on theoretical and informational training, which includes the characteristics of Internet of Things teaching methods [4]. The course is based on personal tools, and there is no integration of learning, which does not require students to have a good understanding of the "Internet of Things" technology. Therefore, based on IoT technology, it is possible to improve research on teaching English online, overcome the disadvantages of internet-based learning, and ultimately teach better.

2. Literature Review

Today, with the development of "Internet of Things Technology," colleges and universities have begun to develop online English language courses, and the advantages of these standards are as follows.

2.1. College Students Become Competent. Follow online English instruction in colleges and universities, encourage college students to become training centers, design online English instruction around college students, play full-time college students, follow online English instruction, and access information content, by practicing. It can be said that the use of online English courses in universities can make college students an integral part of their education. This is a creative approach to the new curriculum to make college students an integral part of classroom learning. The use of online English language training in universities can change the mindset of college students, shift college students from passive learning to informational knowledge, and enable college students to acquire English language knowledge and information.

2.2. Provide a Wealth of Educational Resources. The implementation of online teaching of English in colleges and universities provides rich educational resources for English course teaching and broadens the horizons of college students' English knowledge, so that college students can learn English courses well. For example, in response to the lack of cultural information in English language acquisition, the implementation of online English teaching provides rich culture for English teaching, including information on British and American culture and local culture. At the same time, the teaching mode of college English courses based on English online teaching and the information resources in the network platform are rich, in order to meet the diverse and personalized demands of college students in English language learning, so that college students can cultivate the core literacy of English subjects under the support of a lot of information [5]. For example, resources such as micro-courses, microvideos, and MOOCs enrich English education information and provide guarantees for the use of English teaching resources in colleges and universities.

2.3. Promoting the Study of College Students with Rules to Follow. The use of online English language programs in colleges and universities supports the learning of college students. Under the auspices of technology, "teaching English" develops online English courses for college students, such as listening to English, reading in English, listening in English, and working in English, to enhance the independence and knowledge of college students. English classes: when college students take online English courses, teachers can obtain online course materials from college students, gain a clear understanding of college students, and develop good curricula and standards for teaching English online and offline. Instructions: in addition, online education for college students has rules to follow, and these courses can be used to plan college student assessments, guide college students, and support the development of college students. However, there are still some difficulties in teaching English online, and the main problem is the inability to guarantee training. It is not possible to confirm the existence of problems affecting online English language teaching in universities and colleges, and as a result, English language programs are being used. The ability to teach

English online in colleges and colleges is weak. Teaching English online at college is one of the most technologically and computer-based courses available, and it is influenced by the personal circumstances of college students and their reluctance to teach English online. Unnecessary classrooms and game situations for college students often affect the performance of online disciplines that "slip" in performance, and the effectiveness of online English teaching in colleges and universities cannot guarantee the effectiveness of online English teaching in colleges and universities.

IoT research is not just about using the early moments of the global IoT wave. It is one of the few countries in the world that has done research before. It has similarities to its international neighbors, and after a long period of hard work, in October 2009, it announced the launch of Tangxin, Mongolia's first Chinese chip. The successful completion of the No. 1 chip is a sign that our country has overcome the vital technology of the Internet of Things and entered the international arena and that some technologies are at a critical stage. China is also one of the few countries in the world to produce one of the national leaders in the development of international standards in the field of sensor networks [6–8].

Based on this research, the author has developed an online English language course based on the Internet of Things technology [9, 10]. For example, in college, the author studies the SPOC format of English art, develops a comprehensive curriculum based on Internet of Things technology, develops measurement tools and standards, teaches English online, improves real-time online English language teaching, and improves teaching quality [11, 12].

3. Research Methods

3.1. The Deconstruction of Traditional College English Teaching by the SPOC Teaching Mode of College English. "Improving student English" and "improving student knowledge" are the main goals of college English courses. Depending on the curriculum, the required courses and electives are a key component of college-level English courses. When it comes to teaching, most colleges and universities accept the "read, write + audio-visual" mode and use computers and multimedia projection devices to teach in the classroom. However, due to the important "battle" of the education of English students in college, college English classes face many challenges. For example, a large number of students, classroom instructors, and teachers play a key role, and test-oriented instruction is the key. In the long run, the introduction of college English into CET-4 and CET-6 and the increase in CET-4 and CET-6 equivalence have become important standard for measuring the strengths and weaknesses of learning English in college. For college and university teachers, the CET-4 and CET-6 scores are the most important criteria for determining the English language proficiency of college students, interest in English, primary education, and low-value education. We use the concept of reform to reevaluate the English language teaching process in college, based on the inadequacy of traditional English language teaching in college. The word "deconstruction" comes from the philosophical thought of the postmodernist

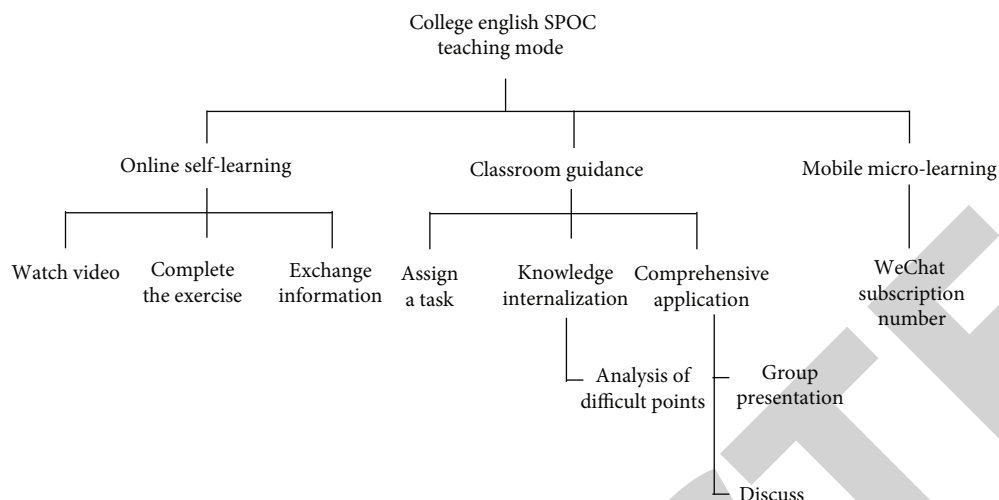


FIGURE 1: College English SPOC teaching mode.

philosopher Derrida, “deconstruction.” Dismantling is not about breaking down or disassembling, but about studying, understanding, and rebuilding the structure of the product. Unpacking the traditional teaching methods used in the SPOC curriculum of the English college will not only complete the traditional classroom training but also evaluate and reflect its concepts, procedures, and issues in order to create a new model of the English language school, teaching, supporting English language development, and improving the quality of teaching [13].

3.2. SPOC Teaching Mode of College English in the Era of “Internet +.” The purpose of the research on SPOC teaching mode of college English is to deconstruct and reconstruct college English classroom teaching, make up for the insufficiency of traditional classroom teaching, reconstruct students’ English learning process, and innovate effective English learning mode. The SPOC teaching mode of college English includes three core components: “online independent learning,” “classroom guidance,” and “mobile micro-learning”; the frame design is shown in Figure 1.

3.2.1. Online Self-Learning. “Online independent learning” means that students watch online course teaching videos before class, complete in-class quizzes and module assignments, and can post for help or communicate with classmates and teachers online in the discussion area of the online course platform. The teaching videos watched by students in online self-study are several microlecture videos about 20 minutes in length, covering background knowledge, structural analysis, article comprehension, difficult sentence analysis, vocabulary learning, and cultural introduction; learning resources are more diversified, three-dimensional, and enriched. During the video viewing process, students can pause, watch back, or watch any knowledge point repeatedly, to realize the efficient transmission of information. Online self-learning enables students to truly become the main body of learning, prepare for language input for participating in classroom guidance, and make

their learning methods more autonomous, active, and interactive. It should be noted that the content of online courses is not a simple process of digitizing paper textbooks. Teaching videos are based on the content of textbooks, combined with the advantages of classroom teaching, and based on the teaching team’s years of teaching experience, a systematic and reasonable integration of learning resources. In addition, using SPOC technology, students’ learning process and learning behavior can be recorded and supervised, which effectively guarantees the integrity of students’ learning. Students will receive appropriate feedback after completing quizzes and module assignments to maintain continuity of student learning. Online learning is not an isolated process, students and teachers can ask questions, answer questions, share learning experiences, and conduct interactive exchanges at any time. The SPOC model gives full play to and extends the teaching of language knowledge in traditional classroom teaching, expands the form and connotation of language learning, and makes the learning process more lively and interesting [14].

3.2.2. Mobile Microlearning. In the era of “Internet +,” the Internet is becoming more and more popular, and mobile intelligent terminals such as smart phones and tablet computers allow us to use the Internet to obtain and transmit information anytime, anywhere, and become a new mode of information acquisition [15]. Mobile microlearning is the continuous development of new mobile technology, a microlearning model that facilitates learning with the aid of mobile terminals. The mobile microlearning in this study is a new educational method based on WeChat software and WeChat public platform. WeChat is a multiplatform, multimedia mobile social software launched by Tencent in 2011. It is undeniable that since the launch of WeChat, it has gradually become one of the main means of communication in modern interpersonal communication due to its convenience, simplicity and ease of operation, and multidimensional interactivity. After online

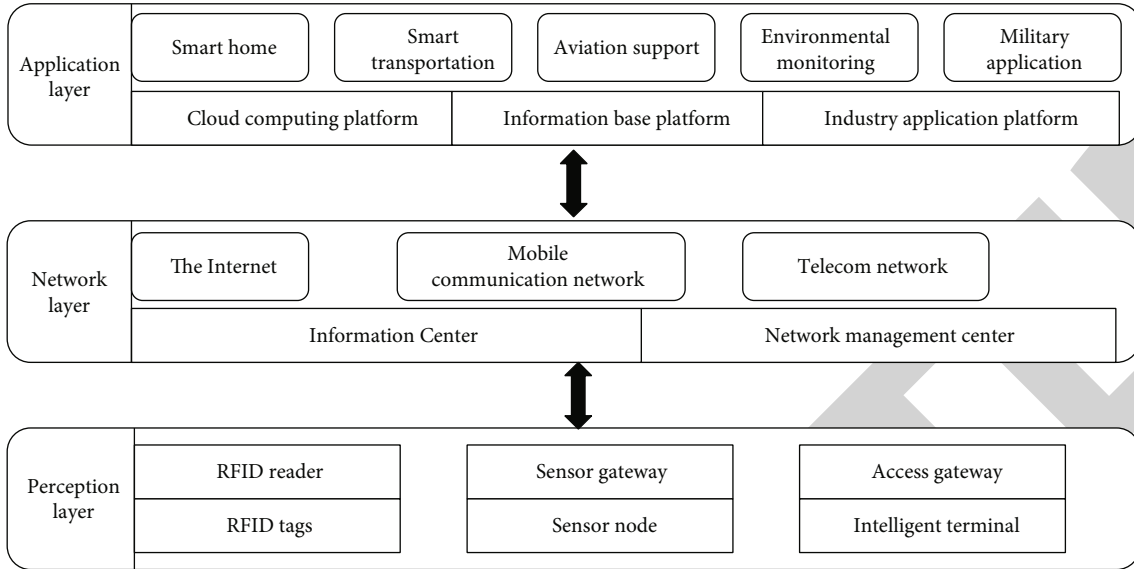


FIGURE 2: IoT architecture diagram.

self-learning and classroom guidance, teachers use WeChat personal clients and WeChat public platforms to push multimodal learning resources that integrate text, pictures, sounds, and videos to students. Before class, teachers can use the QR code generation software and generate a QR code for the course learning materials for students to download at any time. After class, teachers and students use WeChat groups to exchange learning content to achieve multiple interactions between teachers and students and between students. Teachers and students can also use the circle of friends to share learning resources. Mobile microlearning is an experience and expansion of online self-learning and classroom guidance, and it is also a useful supplement to it. Compared with the one-way knowledge transfer mode of traditional classroom teaching, mobile microlearning, with its mobility and immediacy, has created a new multidimensional interactive learning platform. In addition, rich learning resources and timely communication and feedback strengthen the breadth and depth of students' knowledge internalization, which greatly promotes students' understanding and consolidation of the knowledge they have learned. Vivid pictures, video materials, etc. bring visual and auditory multisensory experience, which helps to stimulate students' interest in learning and improve learning efficiency.

3.3. Principles of IoT Technology. The basic architecture of the Internet of Things can be represented from the bottom up as the perception layer, the network layer, and the application layer, as shown in Figure 2. The IoT formula is shown in

$$(\text{NSID} - \text{IOT}) + (\text{NB} - \text{IOT}) + (\text{OID} - \text{IOT}) = \frac{\text{IOE}}{\text{IOE}} * N = \text{IOT}. \quad (1)$$

Perception layer: it mainly completes the process of

information collection and uploading the collected information, that is, in order to collect the information of "things" anytime and anywhere through information sensing devices such as RFID, bar code, GPS, and infrared sensor, upload it to the upper end, and make preparations for information transmission [16].

Network layer: it mainly completes the all-round transmission of information, which plays a linking role in the entire Internet of Things. It is to integrate various access devices with existing networks with different transmission properties and communication protocols, such as the Internet and mobile communication networks, and upload the information collected by the perception layer to the upper layer through network nodes in real time and accurately [17].

Application layer: it mainly completes various practical applications such as intelligent identification, positioning tracking, monitoring, and management. It is to perform computational processing and scientific decision-making on the information collected by the perception layer. Accurately and intelligently realize services for customers from all walks of life [18].

3.3.1. Key Technologies of the Internet of Things. It corresponds to the basic framework of the Internet of Things. Its technical system includes perception layer technology, network layer technology, application layer technology, and public technology, as shown in Figure 3. The perception layer technology mainly includes sensor technology, automatic identification technology, wireless transmission technology, middleware technology, ad hoc network technology, and collaborative information collection technology. Network layer technologies include mobile communication network technology, Internet technology, next-generation bearer network technology, and M2M wireless access technology. The application layer technology mainly includes the support platform sublayer (public

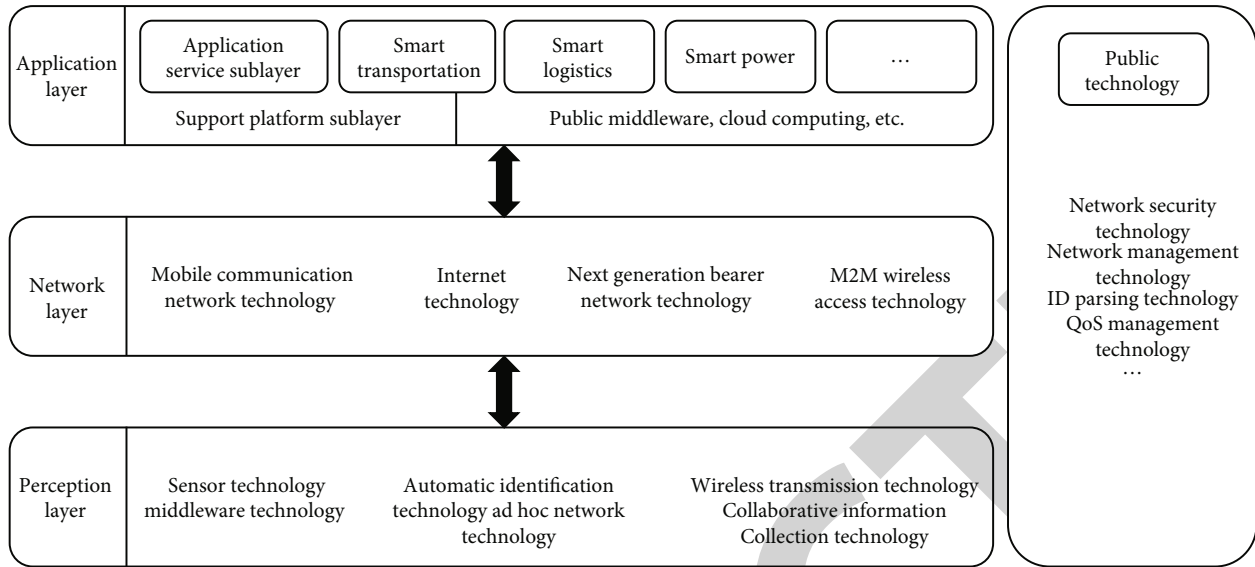


FIGURE 3: IoT technology.

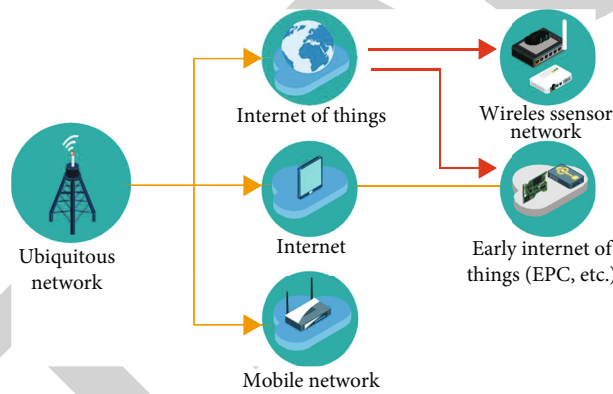


FIGURE 4: The relationship between IoT, sensor network, and ubiquitous network.

middleware, cloud computing, etc.) and the application service sublayer (industry applications such as intelligent transportation, intelligent logistics, and intelligent power). Common technologies refer to technologies related to each layer throughout the entire IoT technology architecture, including IoT security technologies, network management technologies, identification and resolution technologies, and QoS management technologies [19, 20].

3.3.2. The Relationship between the Internet of Things, Sensor Networks, and Ubiquitous Networks. As the name suggests, sensor network is a network composed of sensors, which is a narrow understanding of sensor network. This type of network uses the perception modules of various sensors to collect information on environmental factors. Transmission is carried out through self-organizing networks, but this type of network is only good at collecting signals and is weaker than identifying objects. If you want to achieve network transmission, you also need to use other network access methods and modules. With the development of science

and technology, people’s ability to understand things has improved; today, the generalized sensor network is not only the main task of information collection and processing. It can also realize the interconnection between subjects. The Internet of Things has more information collection methods than the narrow sensor network, and the access network is more flexible than the general sensor network, and the information processing capability is far stronger than the narrow and broad sensor network. It can be said that the sensor network is one of the links in the realization of the Internet of Things ubiquitous network. According to the ITU-TY2002 recommendation, it refers to a network that enables authorized individuals or devices to access services and communicate as quickly as possible when needed; in short, the ubiquitous network is the integration of various existing sensor networks, the Internet of Things, the Internet, and telecommunication networks; it integrates perception, identification, calculation, control, extensive connection, and deep communication to realize 4A (Anytime, Anywhere, Anyone, Anything) interconnected communication.

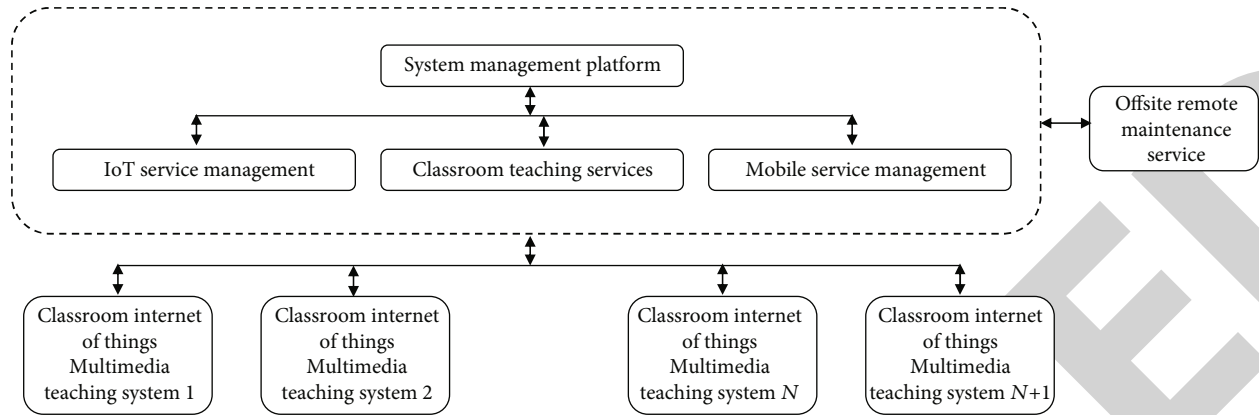


FIGURE 5: The structure of multimedia teaching system based on Internet of Things technology.

There are differences and connections among the Internet of Things, sensor networks, and ubiquitous networks, as shown in Figure 4.

3.4. Design of Multimedia Teaching System Based on Internet of Things Technology

3.4.1. System Architecture. The multimedia teaching system based on Internet of Things technology consists of two parts: hardware part and software part. As we all know, most of the current application systems are hardware systems with single-chip technology as the core. However, a system consisting only of hardware can only be a bare system or a system whose functions are not maximized and optimized for application. Therefore, the multimedia teaching system based on the Internet of Things technology is the integration of computer technology, network technology, digital signal processing technology, data sensing and acquisition technology, automatic control technology, and intelligent technology. The specific structure is shown in Figure 5.

3.4.2. Hardware System Composition

- (1) System management center: the main hardware is a computer, a display device, and a data processing server
- (2) Support system network: it is completed by the original teaching classroom network, and a wireless (WIFI) network is formed
- (3) Classroom Internet of Things multimedia teaching system
- (1) Multimedia teaching system equipment

Classroom multimedia teaching system equipment consists of computer, wired and wireless pickup equipment, audio amplification equipment, video and audio signal switching equipment, display equipment, and signal source playback equipment. Each media device is embedded with TCP/IP communication interface and protocol and device function data detection and acquisition module.

- (2) The classroom teaching recording system is mainly classroom teaching recording and broadcasting equipment, such as cameras, video and audio signal digital processors, recording and broadcasting servers, and storage devices. With the development of education, informatization, individualization, and autonomous learning have become more prominent in teaching and learning; digital teaching resources will be the key construction work of each school in the future; therefore, the Internet of Things multimedia teaching system is not only an information-based teaching system but also a teaching resource production system

- (3) Multimedia equipment network switching system

The multimedia equipment network switching system is mainly composed of two parts:

- (i) General network switching and routing equipment, and each classroom completes the internal subnet
- (ii) The internal wireless WIFI network completes the link of the system wireless access equipment, such as mobile operation control, wireless pickup, and wireless amplification and other equipment interconnection

- (4) Mobile management system

The mobile management system is mainly composed of mobile terminal devices, such as iPad, mobile tablet, portable tablet terminal, and smart phone.

The author selects the university experimental class and the control class as the experimental objects and tests the reliability of the English online teaching system by comparing the teaching results.

4. Results and Discussion

After nearly one semester of experimentation of the online English teaching system based on Internet of Things technology, under the premise that the teaching

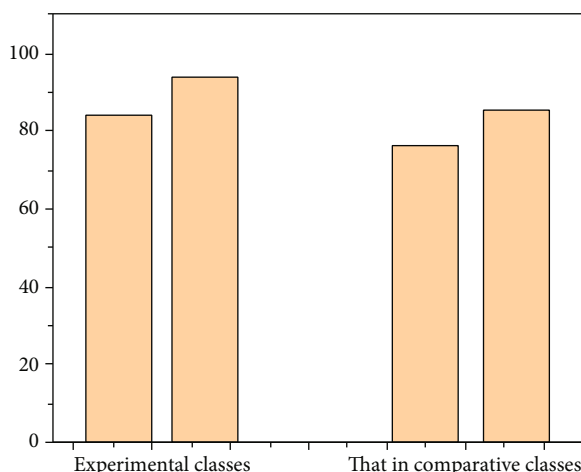


FIGURE 6: Statistical chart of the oral and written test data of the experimental class and the control class.

hours of the experimental class and the control class are equal, we conducted the same written test and oral test for the two classes at the end of the semester; the test results are shown in image 6.

From Figure 6, we can see that, under the author's method, the results of the written test and the oral test in the experimental class are about 10 points higher than the control, which shows that the use of the author's method is of great help in improving students' English performance.

5. Conclusion

In today's era, with the development of Internet of Things technology, colleges and universities have begun to develop online English teaching models; the author proposes a method of English online teaching system based on Internet of Things technology. This method analyzes the English SPOC teaching mode and constructs a multimedia teaching system based on Internet of Things technology, to improve students' awareness of Internet of Things technology, so as to improve students' English performance. The experimental results show that under the author's method, the students' scores in the written and oral tests are about 10 points higher than those in the traditional teaching method; it shows that adopting the author's method is of great help to the improvement of students' English achievement. The online English teaching system based on the Internet of Things technology has great application potential and development space.

Data Availability

The data used to support the findings of this study are available from the corresponding author upon request.

Conflicts of Interest

The author declares that there are no conflicts of interest.

References

- [1] H. Chen and J. Huang, "Research and application of the interactive English online teaching system based on the internet of things," *Scientific Programming*, vol. 2021, Article ID 3636533, 10 pages, 2021.
- [2] V. Dinu, S. P. Lazr, and I. A. Pop, "Factors that influence the adoption of the internet of things in tourism by Romanian consumers," *Amfiteatru Economic*, vol. 23, no. 57, pp. 360–375, 2021.
- [3] A. Rasyid, W. Waluyo, L. D. Mustafa, E. Kurniawati, and M. Aditya, "Aplikasi rfid sebagai pendeteksi kehadiran pada perkuliahan terkait perhitungan kompensasi bagi mahasiswa politeknik negeri malang," *Jurnal Eltek*, vol. 19, no. 1, p. 72, 2021.
- [4] X. Zhou, X. Li, and N. Su, "Design and internet of things development of network teaching resource base system for educational technology," *Journal of Physics Conference Series*, vol. 1769, no. 1, article 012005, 2021.
- [5] X. Li, "The cultivation of the core literacy of English discipline in senior high school based on "post-method" theory," *Region - Educational Research and Reviews*, vol. 2, no. 3, p. 1, 2020.
- [6] Y. Gao, P. Zhong, X. Tang, H. Hu, and P. Xu, "Feature extraction of laser welding pool image and application in welding quality identification," *Access*, vol. 9, pp. 120193–120202, 2021.
- [7] X. Nan, "Exploration of core technologies of cyber security," *Open Access Library Journal*, vol. 8, no. 9, pp. 1–11, 2021.
- [8] S. L. Sheridan, "Translating evidence updates to international standards: is more certainty needed for international standards on decision aids?," *Medical Decision Making*, vol. 42, no. 1, pp. 3–7, 2022.
- [9] A. A. Abdulmajeed, M. A. Al-Jawaherry, and T. M. Tawfeeq, "Predict the required cost to develop software engineering projects by using machine learning," *Journal of Physics: Conference Series*, vol. 1897, no. 1, article 012029, 2021.
- [10] R. Balakrishnan, M. Akdeniz, S. Dhakal, A. Anand, and N. Himayat, "Resource management and model personalization for federated learning over wireless edge networks," *Journal of Sensor and Actuator Networks*, vol. 10, no. 1, p. 17, 2021.
- [11] S. Feng, S. Lv, L. Chen, and Z. Li, "Evolution of ion-irradiated point defect concentration by cluster dynamics simulation*," *Chinese Physics B*, vol. 30, no. 5, article 056105, 2021.
- [12] P. Sanmartin, K. Avila, S. Valle, J. Gomez, and D. Jabba, "Sbr: a novel architecture of software defined network using the rpl protocol for internet of things," *Access*, vol. 9, pp. 119977–119986, 2021.
- [13] D. D. Samarasekera, B. Lieske, D. Aw, S. S. Lee, and D. R. Koh, "A new model of teaching and learning approach - collaborative learning cases activities," *The Asia Pacific Scholar*, vol. 6, no. 2, pp. 98–98, 2021.
- [14] Y. Yang, "A study on online learning behaviors of the private university students based on spoc mode—take Zhejiang Yuexiu University as an example," *Open Journal of Modern Linguistics*, vol. 11, no. 2, pp. 212–225, 2021.
- [15] A. Ampountolas, T. N. Nde, P. Date, and C. Constantinescu, "A machine learning approach for micro-credit scoring," *Risks*, vol. 9, no. 3, p. 50, 2021.
- [16] M. Fan and A. Sharma, "Design and implementation of construction cost prediction model based on svm and lssvm in

Retraction

Retracted: Optical Hybrid Network Structure Based on Cloud Computing and Big Data Technology

Journal of Sensors

Received 17 October 2023; Accepted 17 October 2023; Published 18 October 2023

Copyright © 2023 Journal of Sensors. This is an open access article distributed under the Creative Commons Attribution License, which permits unrestricted use, distribution, and reproduction in any medium, provided the original work is properly cited.

This article has been retracted by Hindawi following an investigation undertaken by the publisher [1]. This investigation has uncovered evidence of one or more of the following indicators of systematic manipulation of the publication process:

- (1) Discrepancies in scope
- (2) Discrepancies in the description of the research reported
- (3) Discrepancies between the availability of data and the research described
- (4) Inappropriate citations
- (5) Incoherent, meaningless and/or irrelevant content included in the article
- (6) Peer-review manipulation

The presence of these indicators undermines our confidence in the integrity of the article's content and we cannot, therefore, vouch for its reliability. Please note that this notice is intended solely to alert readers that the content of this article is unreliable. We have not investigated whether authors were aware of or involved in the systematic manipulation of the publication process.

Wiley and Hindawi regrets that the usual quality checks did not identify these issues before publication and have since put additional measures in place to safeguard research integrity.

We wish to credit our own Research Integrity and Research Publishing teams and anonymous and named external researchers and research integrity experts for contributing to this investigation.

The corresponding author, as the representative of all authors, has been given the opportunity to register their agreement or disagreement to this retraction. We have kept a record of any response received.

References

- [1] H. Wei, "Optical Hybrid Network Structure Based on Cloud Computing and Big Data Technology," *Journal of Sensors*, vol. 2022, Article ID 3936876, 6 pages, 2022.

Research Article

Optical Hybrid Network Structure Based on Cloud Computing and Big Data Technology

Huiting Wei 

Xuchang University, Xuchang 461000, China

Correspondence should be addressed to Huiting Wei; 11231446@stu.wxica.edu.cn

Received 5 July 2022; Revised 18 July 2022; Accepted 27 July 2022; Published 10 August 2022

Academic Editor: C. Venkatesan

Copyright © 2022 Huiting Wei. This is an open access article distributed under the Creative Commons Attribution License, which permits unrestricted use, distribution, and reproduction in any medium, provided the original work is properly cited.

In order to meet the communication requirements of photoelectric hybrid network architecture, a research based on cloud computing and big data technology is proposed. The main content of this study is based on the analysis of cloud computing and big data technology, through the study of technical characteristics, using topological optical link with bypass data structure and other methods, and finally through experiments and analysis to build the research means of cloud computing and big data technology. The experimental results show that the weights of optical links are 60, 50 and 20, respectively. When the weights of optical links become smaller, node B reaches the paths of the six destination nodes. More paths can be transmitted through optical links, and the size of the range of nearby links can be controlled, which is feasible for the photoelectric hybrid network structure. *Conclusion:* The research based on cloud computing and big data technology can meet the needs of photoelectric hybrid network structure in communication.

1. Introduction

Photoelectric hybrid network communication is a major technical support for the networking of the Internet of Things at present. The networking technology of photoelectric hybrid communication has been developed quite well [1]. Photoelectric hybrid refers to the use of optical fiber, and wire as signal transmission tools, mixed information transmission through this way of information, often has relatively high accuracy, and the efficiency of information transmission will become very fast. This is a great fit for the networking technology of the Internet of Things, which is to use all kinds of useful information to coordinate all kinds of things, and this technology is often used in the delivery industry, retail industry, and other industries that have large warehouses. Through the application of the Internet of Things technology, the deployment of all kinds of products will become very convenient. In the past, the Internet of Things was built only by electrical signals, not optical fiber and optical signals. Now, after the development of photoelectric hybrid communication Internet of things

networking technology, the current Internet of things networking can effectively apply photoelectric hybrid communication technology.

The advantages of photoelectric hybrid network lie in the high efficiency and accuracy of signal transmission. The Internet of Things networking technology of photoelectric hybrid communication uses both optical signals and electrical signals to transmit information, which is naturally more efficient than the single application of a certain signal [2]. In addition, due to mixed communication, when a certain signal transmission medium fails, another signal transmission mode can replace it well, thus having the opportunity to troubleshoot the other medium without affecting the normal use of the Internet of Things. In order to give full play to the great advantages of photoelectric hybrid communication technology, these two aspects should be the starting point and the technical professionalism should be improved. Although this kind of technology has great advantages, but because of the relatively high threshold for the application of this kind of technology, many of the Internet of Things that have been

applied this kind of technology can not meet the actual needs of professional use. Therefore, we need to further improve the professionalism.

In the application process of photoelectric hybrid network, there are several technical points that must be solved. At present, the construction of optical fiber and the construction of the Internet of things are two key points [3]. The reason why the Internet of Things networking technology of photoelectric hybrid communication is more effective is that it applies optical fiber to transmit information, while the construction of the Internet of Things is another difficult problem. Therefore, relevant personnel should focus on these two technical points to carry out the application of the Internet of Things networking technology of photoelectric hybrid communication, as shown in Figure 1.

2. Literature Review

In the current social development, in order to give full play to the advantages of photoelectric hybrid communication Internet of Things networking technology, it is necessary to improve the professionalism of this technology as much as possible. Firstly, a detailed analysis of user needs is conducted to optimize the photoelectric hybrid communication Internet of Things networking technology, so as to build a more professional Internet of things platform [4]. The Internet of Things required by Internet sales and entities is essentially the same, but surely there are some details that require more specialized technical means to ensure its actual effectiveness. Therefore, a professional Internet of Things platform should be established according to the needs of different industries. A professional Internet of Things platform can undertake more information transfer tasks and provide users with richer functions. In this way, users will have more trust in the Internet of Things networking technology, and accordingly, the reliability of the Internet of Things networking technology in China will be greatly improved, so as to play a greater advantage. 光 Electric hybrid Internet of Things networking technology is a key support technology for many industries at this stage. If there is no development of Internet of Things networking technology, the online sales industry and the physical retail industry will not be able to get rapid development, which shows the importance of Internet of Things networking technology. Therefore, we need to carry out in-depth research and discussion on photoelectric hybrid Internet of Things networking technology, in order to develop a more advantageous Internet of things platform and better serve the public. This paper mainly focuses on the development of Internet of Things networking technology advantages technical points to improve security. This paper analyzes the problems in expanding the application scope and summarizes several measures to better apply the photoelectric hybrid Internet of things networking technology, hoping to bring certain help to the relevant institutions and personnel.

Aiming at the above problems, in order to meet the communication requirements of photoelectric hybrid network structure, a research based on cloud computing and

big data technology is proposed [5]. The main content of this study is based on the analysis of cloud computing and big data technology, through the study of technical characteristics, using topological optical link with bypass data structure and other methods, and finally through experiments and analysis to build the research means of cloud computing and big data technology. The structure design of opto-electronic hybrid network and the transmission control of opto-electronic hybrid network realize the common transmission of data in optical domain and electrical domain. The performance evaluation is carried out by using simulation tools. The results show that compared with the traditional electrical domain network, the network designed in this paper has higher transmission performance, less congestion, and higher system throughput. The research based on cloud computing and big data technology can meet the needs of photoelectric hybrid network structure in communication.

3. Research Method

3.1. Cloud Computing and Big Data Technology Research

3.1.1. Technical Characteristics of Cloud Computing and Big Data Technology. Cloud computing technology breaks through previous computing concepts and fully subverts the definition of time and space. Meanwhile, it virtualizes computing resources and computing requirements. In the process of computing, its operating environment and operating platform can be migrated and expanded anytime and anywhere, and data can also be backed up [6].

The computing capacity of cloud computing is extremely powerful. With the computing function of related servers, the computing requirements can be adjusted and upgraded anytime and anywhere. Meanwhile, the virtual computing mode can be expanded to meet the demand for more computing capacity.

Capability deployment cloud computing can be created according to established requirements to meet specific requirements of directional software. It can integrate data for different databases and deploy data according to different computing requirements. It can realize multidomain integration of user requirements and platform functions with the help of cloud computing technology.

Super high flexibility in cloud computing in today's Internet application process is mostly based on software technology, hardware equipment, and other related content to calculate and comb. The relevant representatives are the network storage, software development, and data structures. Personalized management of virtual resource pools in the cloud system can not only meet the basic environment of different system configurations, but also obtain high-quality computing capabilities [7].

High safety cloud, albeit with the help of network computing resources of the cloud server data computing, but does not affect the normal operation of the cloud server, when supplying the service function of server problems at the same time, also can use virtualization technology, the computing tasks, and the requirement of the first degree

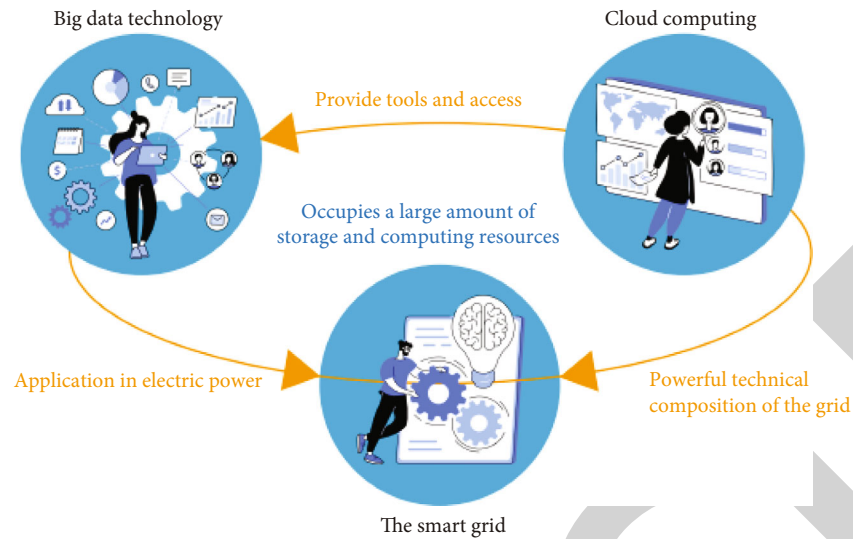


FIGURE 1: Cloud computing and big data technology.

distribution computing tasks and ensure complete corresponding computing tasks in other server. In addition, the current computing capacity can be upgraded and expanded with the help of the cloud's scalability function [8].

The characteristics of big data technology are different from those of cloud computing technology. The data groups of big data technology are not only the content provided by network data, but also include hundreds of types, involving all aspects of daily life. Meanwhile, the capacity of data packets determines the value and potential commercial space of data [9]. The core advantage of big data technology is that it can extract and capture massive data to meet users' directional needs. At the same time, the speed of acquiring target data is extremely efficient, which is the goal that traditional data application technology cannot achieve. At the same time, in the process of data processing, the corresponding results can be timely changed according to the changes of tasks. In the face of huge computing requirements and computing capacity, the authenticity and efficiency of processing data are well guaranteed. Due to the variety of types and contents of data, the process of screening is extremely complex. The degree of application and attempt in different fields is effectively reflected by the difficulty of data screening. When the data comes from a large number of data platforms and sources, the computational difficulty and application difficulty will also increase. In the field of Internet, big data technology has been applied unprecedentedly and, combined with multiple network systems, to achieve full coverage of the target group.

3.1.2. Trends in Cloud Computing and Big Data Technology. The development space of cloud computing and big data technology is very broad, and the corresponding industry content and industry types also cover a wide range, which has become the basic RESEARCH and development technology in various fields. Therefore, strengthening the computing capacity of cloud computing and the refinement degree of big data technology has become one of the

important development contents of the industry [10]. On the one hand, with the highly increase of user data, the corresponding selection criteria and extract more detailed content, such as someone stand 5 minutes in A commodity, B goods stand 50 seconds, but bought goods B, in which data is created that needs to be further mining, to understand the current affects the pain points of user needs, thereby helping to boost sales performance and related businesses. On the other hand, the continuous improvement of computing power requires that the accuracy of extracted data should be ensured in the process of sorting out and extracting user information. For example, a user's car cushion is used as a congratulatory gift for a colleague's car purchase, but the relevant platform still pushes more related products, failing to distinguish the core appeal of users, resulting in the failure of accurate marketing to users in a specific period of time. With the development of cloud computing technology, it is necessary to constantly improve the accuracy of computing content and timely excavate and refine users' various needs, so as to realize the application value of relevant technologies. Big data technology, on the other hand, needs to scientifically refine the data content and reduce the interference of invalid data, so as to ensure that the data pooling process can be more specific and clear and reduce the research and investment of invalid data.

3.2. Systematic Design

3.2.1. Topological Structure. In order to facilitate horizontal data transmission in the data center network, a two-layer multi-tree structure is adopted to add optical domain network on the basis of the existing electrical domain network of the data center to realize the common transmission of data. To facilitate system management, the control center module is configured with the flow management module and the optical switch management module. The electrical area network is used to transmit data with low traffic, while the optical area network is used to transmit data with high

traffic and some data of nearby links [11]. Switch nodes are connected to both electrical and optical domain switches. The optical switch management module is responsible for establishing and removing optical links. According to the traffic information sent by the traffic management module, the control center notifies the management module of the optical switch to set up an optical link on the link that meets the traffic requirements, controls the transmission of some data on nearby links using optical links, and instructs switch nodes to modify the routing information configured with optical links. Each cabinet houses multiple servers. Servers are connected to switches in the cabinet. Switching nodes contain one or more flow tables and a group table for data packet query and transmission. When receiving data packets, the switching node queries the flow table in sequence. If it successfully matches a flow entry, the statistical data corresponding to the flow entry is updated, including the number and length of successfully matched data packets. After performing corresponding operations, the data packets are forwarded [12]. The switching node collects statistics on the total number of successfully forwarded packets in a period of time and the number of discarded packets and other traffic information and sends the traffic information to the traffic management module, as shown in Figure 2.

3.2.2. Optical Links Carry Offline Data. After an optical link is established, the capacity of the link expands to provide more and faster data transmission services. The link with a long response time and congestion becomes unblocked. In addition, the link can also carry part of the data of adjacent links, realizing the common transmission of data in the optical and electrical domains, reducing the data backlog of nearby links and making full use of the optical link [13]. For the data carried by optical link, the distance they need to travel may be increased compared with the original path, but the original path has a slow exchange rate, limited capacity, and long waiting time, while the optical link has a large capacity and high speed, and the time it takes them to reach the destination site is shorter than the original path, as shown in Formula (1):

$$N_e \geq \frac{N_o \cdot S_e}{S_o} + (H_1 + H_2). \quad (1)$$

After the establishment of optical link, the path weight changes, and the system path cost matrix needs to be rebuilt. On the one hand, the path cost weight of optical domain changes, so the corresponding path weight should be adopted to meet the requirements of link change. On the other hand, the electrical domain link near the optical link can be equipped with optical domain for transmission, so as to provide more data for optical domain transmission, improve the transmission efficiency of optical domain, and reduce the transmission pressure of electrical domain, as shown as follows:

$$C_o = \alpha \cdot \frac{S_e}{S_o} C_e + C_u. \quad (2)$$

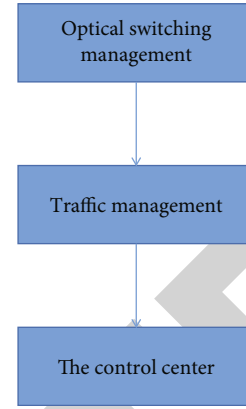


FIGURE 2: Measurement and control of flow.

3.2.3. Simulation Experiment. In this paper, network simulation tools Opnet and Matlab are used to simulate the operating environment of the network, and simulation experiments are carried out to evaluate the network performance. According to the characteristics of data center network traffic, the arrival time interval of data flow and each distribution set multiple parameters to generate data flow simulate the diversity of network flow [14]. In addition, in order to simulate the complexity and diversity of network environment, experiments under light and heavy load environments were carried out. ESM in the simulation experiment is the result of electrical domain switching mode, and HOESM is the result of photoelectric hybrid network in this paper.

The switching node is limited by its processing capability. The data packets that cannot be processed need to be cached, and the cache capacity is limited. If the number of overflows on a switching node exceeds the threshold, subsequent data packets cannot be cached. The number of overflows of nodes under heavy load environment is shown in Figure 3. Optical links are established between nodes with large flow, with fast switching rate, and some data of nearby links are loaded [15]. Therefore, the number of overflows in HOESM is significantly lower than in ESM.

In light load environment, the nodes are classified, and the overflow number of different types of nodes is examined [16]. One is the optical link node in HOESM and this part of the ESM, called class A node. The other is the nodes near the optical link in HOESM and this part of the ESM, called class B node. The overflow number of class A nodes is shown in Figure 4. As the capacity of optical links is large, HOESM carries data near optical links, and more data is transmitted on optical links, resulting in overflows. As can be seen from Figure 4, the number of overflows on optical links is much lower than that of ESM overflows of class B nodes, as shown in Figure 5. In HOESM, some data in nodes is transferred to optical links, which reduces the transmission pressure in the electrical domain. This is why the number of data overflows in HOESM is significantly reduced [17].

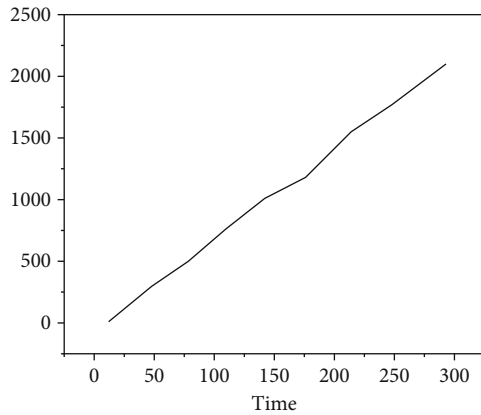


FIGURE 3: Heavy load overflow number.

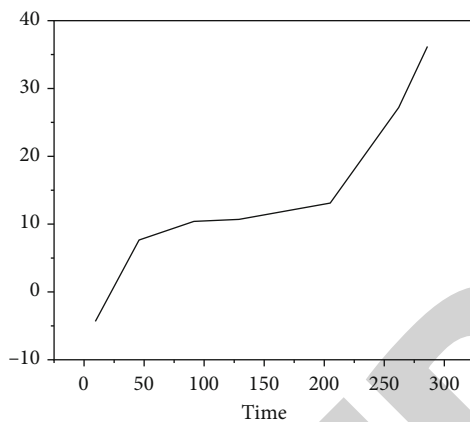


FIGURE 4: Overflow number of light load Class A nodes.

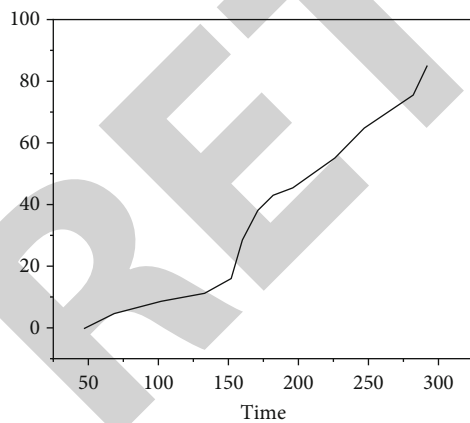


FIGURE 5: Overflow number of light load Class B nodes.

4. Interpretation of Result

The cost weight affects the transmission range of optical link. By setting parameters, the cost weight of optical link can be adjusted to control the range of optical link carrying nearby links [18]. The path c-f-i-l-o-r is an optical link, using optical switching, and the rest are electrical domain transmission. The cost weights between nodes are set as fol-

TABLE 1: Change the path.

Weight	Destination node	Path
60	r	b-f-i-l-o-r
50	q	b-f-i-l-o-q
40	n	b-f-i-l-n
40	p	b-f-i-l-n-p
20	k	b-f-i-k
20	m	b-f-i-k-m

lows: transverse paths A-D-G-J-M-P and B-E-H-K-N-Q, the weights of the longitudinal paths A-B-C, D-E-F, G-H-I, J-K-L, -M-N-O, and P-Q-R are all 70, Oblique path b - f, a - e - I, d - h - l, g - k - o, j - n - r, m - q, b, d, c - e - g, f - h - j, I - k - m, l - n - p, o - q has a weight of 90. During the experiment, when the weight is 60, only the path to R is changed among the 6 destination nodes, which is equipped with optical link F-I-L-O, and the other nodes are still electrical domain transmission [19]. When the weight value is 50, the path of destination node Q also changes. Data transmission from B to R and Q uses optical link carrying weight. When the weight value is 40, n and P are added to the destination node carrying data on optical link.

It can be seen from Table 1 that the weights of optical links are 60, 50, and 20, respectively. When the weights of optical links become smaller, more paths of node B to the six destination nodes can be transmitted through optical links, which can control the range of nearby links carried by optical links [20].

5. Conclusion

The photoelectric hybrid network structure to meet demand in the communication based on cloud computing and big data technology on the basis of the research is put forward the main contents of cloud computing and big data technology analysis, through the study of technical characteristics, using the topology and optical link with bypass method such as data structure, and finally through the experiment and analysis of the construction of cloud computing and big data technology research means. The structure design of opto-electronic hybrid network and the transmission control of opto-electronic hybrid network realize the common transmission of data in optical domain and electrical domain. The performance evaluation is carried out by using simulation tools. The results show that compared with the traditional electrical domain network, the network designed in this paper has higher transmission performance, less congestion, and higher system throughput. The research based on cloud computing and big data technology can meet the needs of photoelectric hybrid network structure in communication.

Data Availability

The data used to support the findings of this study are available from the corresponding author upon request.

Retraction

Retracted: Internet of Things Remote Piano Information Teaching System and Its Control Method

Journal of Sensors

Received 12 December 2023; Accepted 12 December 2023; Published 13 December 2023

Copyright © 2023 Journal of Sensors. This is an open access article distributed under the Creative Commons Attribution License, which permits unrestricted use, distribution, and reproduction in any medium, provided the original work is properly cited.

This article has been retracted by Hindawi, as publisher, following an investigation undertaken by the publisher [1]. This investigation has uncovered evidence of systematic manipulation of the publication and peer-review process. We cannot, therefore, vouch for the reliability or integrity of this article.

Please note that this notice is intended solely to alert readers that the peer-review process of this article has been compromised.

Wiley and Hindawi regret that the usual quality checks did not identify these issues before publication and have since put additional measures in place to safeguard research integrity.

We wish to credit our Research Integrity and Research Publishing teams and anonymous and named external researchers and research integrity experts for contributing to this investigation.

The corresponding author, as the representative of all authors, has been given the opportunity to register their agreement or disagreement to this retraction. We have kept a record of any response received.

References

- [1] Y. Fan, "Internet of Things Remote Piano Information Teaching System and Its Control Method," *Journal of Sensors*, vol. 2022, Article ID 4730550, 6 pages, 2022.

Research Article

Internet of Things Remote Piano Information Teaching System and Its Control Method

Yangjie Fan 

Department of Keyboard, Shanxi Vocational College of Art, Taiyuan, Shanxi 030000, China

Correspondence should be addressed to Yangjie Fan; 201903310@stu.ncwu.edu.cn

Received 28 June 2022; Revised 17 July 2022; Accepted 27 July 2022; Published 8 August 2022

Academic Editor: C. Venkatesan

Copyright © 2022 Yangjie Fan. This is an open access article distributed under the Creative Commons Attribution License, which permits unrestricted use, distribution, and reproduction in any medium, provided the original work is properly cited.

In order to change the current piano teaching mode and develop towards digitalization, this paper puts forward the Internet of Things remote piano information teaching system. The digital electric piano teaching system is controlled by multimedia computer. It is a kind of music teaching form composed of electric piano and other electronic keyboard instruments, music auxiliary teaching system, and music production software. It integrates viewing, listening, and practicing and changes the traditional one-to-one teaching mode. Its core structure adopts professional audio processing chip and processor to realize controllable digital audio communication channel, which solves the interference problem well, and realizes classroom simulation functions such as centralized teaching, personal guidance, personal demonstration, group demonstration, and group practice. The application results show that the average learning time of the students who pass the intelligent digital electric piano teaching system is reduced by 14%; After two months of study, 46 students still like the piano through the intelligent digital electric piano teaching system, with a retention rate of 92%, which is significantly higher than the 38 students who study the traditional piano, with a retention rate of 76%. *Conclusion.* The system makes teaching easier and more efficient.

1. Introduction

With the rapid development of computer technology and Internet technology, the wide application of computers is subverting all aspects of society and life. Computer technology is gradually infiltrating into education and teaching with its advantages of fast, efficient, convenient, and wide connection [1]. Many problems existing in traditional teaching, such as single teaching mode, lack of teaching resources, and boring teaching content, are undergoing qualitative changes with the introduction of computers. The digitalization and informatization of education and teaching will become the inevitable trend of the development of education and teaching in the future. At present, a large number of students can effectively use computers and the Internet for learning, and the development prospect of computer-assisted instruction is promising. The research and development of music classroom teaching assistant software will have the following great significance:

- (1) Expand beneficiary groups. After the informatization of music teaching resources, with the help of computer technology and the Internet, the teaching resources will spread rapidly in the network. Students will have more convenient access to music teaching resources and knowledge, and their learning will no longer be affected by region and time. More and more students will enjoy the convenience of education informatization [2].
- (2) Promote students' autonomous learning. With the help of the music teaching assistant system, students can choose the time, place, and content of learning according to their own situation. The ability of autonomous learning will be rapidly improved, and the learning efficiency will also be greatly improved
- (3) Facilitate the teaching work of music teachers. The digitalization and informatization of music classroom will provide a broad resource platform for

teachers. Teachers can easily obtain the education and teaching resources they want according to their own needs and can customize the teaching content exclusively according to the actual learning situation of students

- (4) Enrich classroom teaching content. The music classroom teaching assistant system will effectively change the traditional music classroom teaching mode in which teachers teach students to listen [3]. The music classroom teaching assistant system can provide various bathhouse teaching scenes, such as playing the piano, composing music scores, and appreciating music, and can also provide classroom tests, such as rhythm training
- (5) More comprehensive sensory experience. With the classroom teaching assistance system, students can listen to music, intuitively feel music, play music, and create their own music while listening to the music knowledge taught by teachers. Enhance students' interest in learning and improve learning quality

2. Literature Review

Yu et al. pointed out that the essence of distance education is a complex practical activity in a narrow sense and a comprehensive complex system in a broad sense [4]. Chen pointed out that ontology research is more a basic research and application research, focusing on the research and solution of practical problems [5]. In recent years, with the maturity of the educational model of "large-scale open online courses" (MOOC), many well-known foreign MOOC websites such as Coursera, EDX, and Udacity have also launched a large number of piano MOOC products, which makes the networked piano education enter a new stage of development. Under this background, many music education theorists have also begun to study the networking of piano education. Mansfield-Devine pointed out that online piano education will become the mainstream form and dominant mode of piano teaching in the future [6]. Chen et al. proposed that, based on the rapid development of information technology and the growing public demand for piano music education, the networked piano education that can provide more personalized teaching programs and educational services will gradually become the mainstream trend of the development and progress of piano education [7]. Researchers also began to shift their research perspective to the field of online piano music education. Saharkhizan et al. pointed out that the emergence of various new media and we media has brought us a new audio-visual feast era of digital and fast transmission, consumption, and education of piano music [8].

In recent years, the rapid development of Applied Electronic Technology and the continuous improvement of large-scale integrated chip technology have provided a new direction for changing the current teaching mode. At the same time, the development of information technology in colleges and universities, as a part of their own development,

has been paid more and more attention by university managers. Under this background, the combination of electronic technology and electric piano teaching has produced a digital electric piano teaching system, which has greatly improved the problems existing in the current teaching.

3. Research Methods

3.1. System Principle. Digital electric piano teaching system mainly adopts digital audio technology and FPGA large-scale logic chip technology. Verilog HDL is a hardware description language that is currently used more frequently. It expresses the structure of digital circuit in the form of text, realizes the digital logic function, and realizes the digital control and transmission of analog audio signal [3, 9]. The main working process of the system is as follows: the student terminal and the teacher terminal collect the analog signals, convert the analog signals into digital signals, and transmit them to the main control terminal through the network. The main control terminal processes the audio data of each terminal according to the operation requirements of the digital electric piano teaching software and transmits the processed audio data to the student terminal, teacher terminal, computer, and other systems.

The main components of the digital electric steel teaching system are shown in Figure 1. The main components are as follows: ① it is the teacher's piano and microphone, that is, the audio input of the teacher's terminal; ② it is a teacher's earphone for listening to the system sound; ③ ⑤ ⑦ it refers to the student piano and microphone, that is, the audio input of the student 0-62 terminal; ④ ⑥ ⑧ it refers to the 0-62 earphones for students to listen to the system sound; ⑨ it is the teacher's piano terminal, that is, the audio and other related processing at the teacher's office; ⑩ ⑪ ⑫ refers to the student 0-62 terminal, that is, the audio and other related processing at the student's office; ⑬ the main control terminal is used for the coordination and related processing of the whole system; ⑭ it refers to line input, which is used for external sound source access to the system; ⑮ it is the upper computer and the interface of human-computer interaction, which is used to operate the whole system; ⑯ it is the output of power amplifier, which is used for the system to play sound through the power amplifier; ⑰ it refers to line output, which is used to transmit signals in this system to other systems to realize mutual integration between systems [2, 10].

3.2. Functional Study. The digital electric piano teaching system broadens the teaching scope; realizes the close combination of theory and practice in the piano teaching process; organically integrates the knowledge of sight reading, music theory, harmony, improvisational accompaniment, improvisational creation, and improvisational performance in the classroom; and turns the simple skill training course into a more targeted and practical comprehensive course [11].

3.2.1. Functional Features

(1) *Full Site Guidance.* Lectures can be given to the whole class. The teacher's piano can be used to perform and give

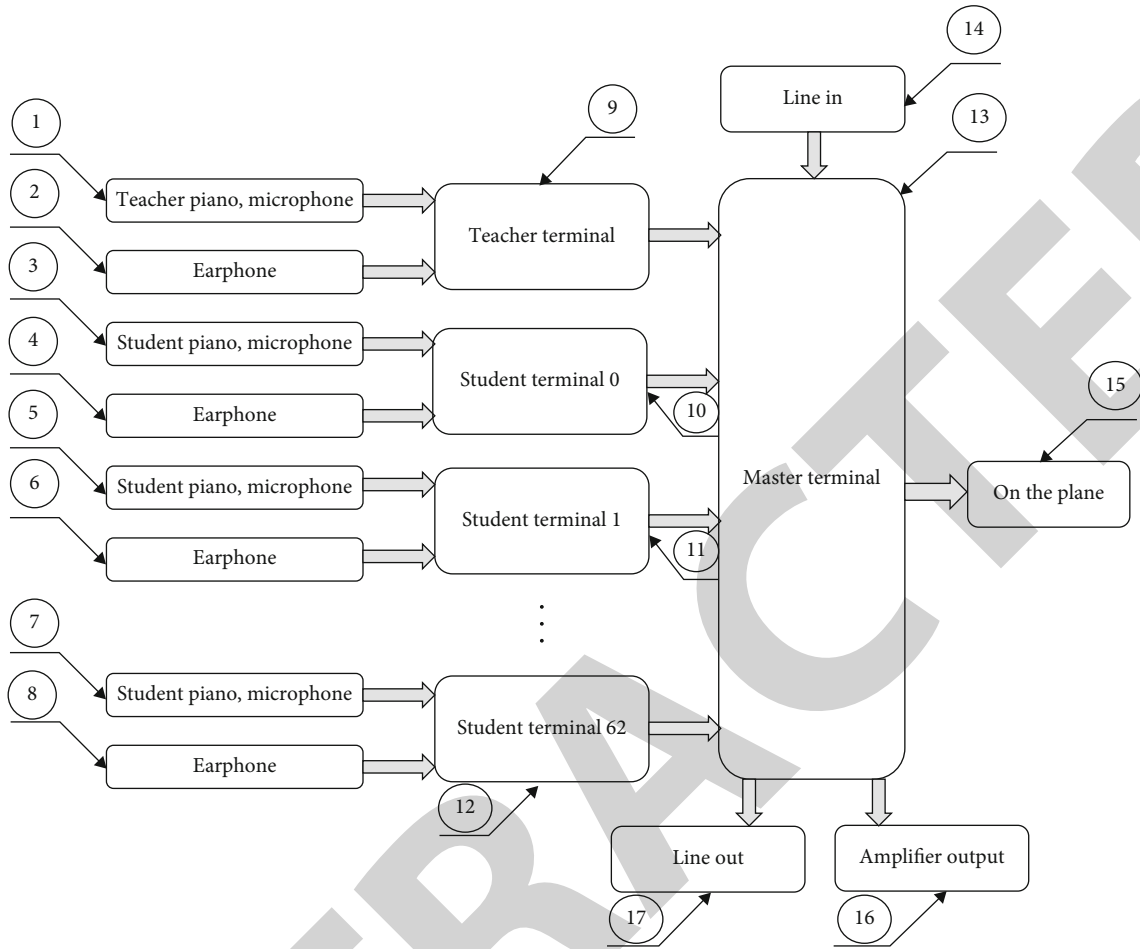


FIGURE 1: Block diagram of digital electric piano teaching system.

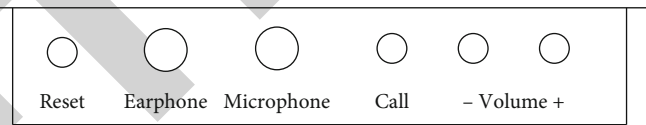


FIGURE 2: Function key diagram of student terminal.

lectures to all students. External high-quality sound sources can be introduced to play music to all students.

(2) *Personal Guidance*. Personal guidance is mainly used to simulate a class when a student has questions to ask the teacher or the teacher needs to communicate with the students. In this mode, other students in the class can practice freely according to the content assigned by the teacher. The specific operations are as follows:

The teacher can select the student terminal to be communicated, and the background color of the selected student terminal turns green. At this time, the teacher and the student can communicate through the microphone, and the student and the teacher can hear each other playing the piano, which facilitates the communication between the teacher and the student.

If students have questions to ask the teacher during free practice or class, they can press the “call” button in the student terminal. At this time, the background color of the corresponding calling students in the system interface will change, and the selected calling students can communicate with each other.

If there are multiple student terminals calling, the teacher can select one by one according to the calling sequence or arrange by himself. When students’ questions are found to be common, they can click “cancel call” and switch to the “full field guidance” mode for unified answers.

In the state of personal practice and guidance, you can also conduct personal sequential monitoring. The listening sequence can be set.

(3) *Group Exercise*. The group exercise is mainly used to simulate the class. The teacher assigns some students to form a

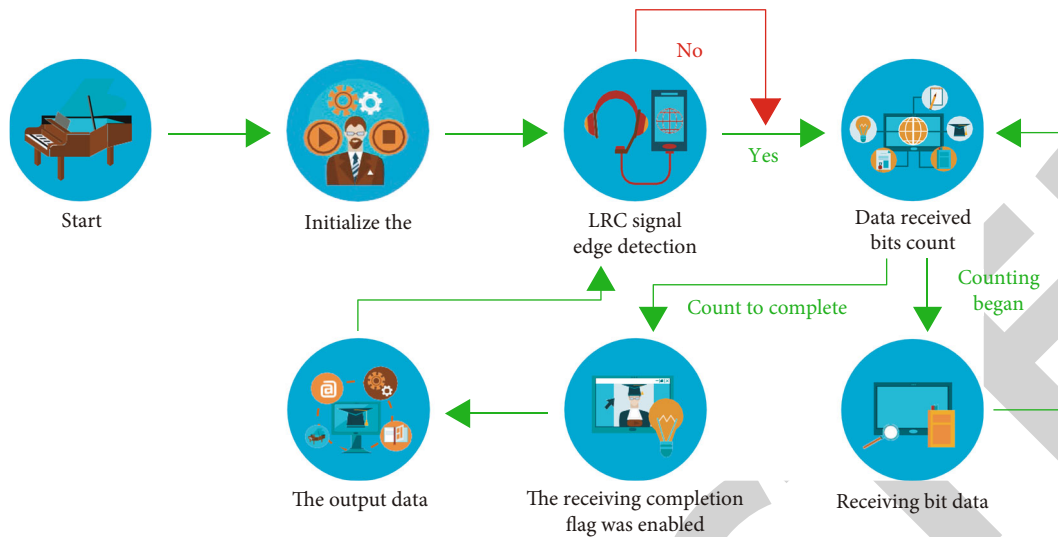


FIGURE 3: Flow chart of audio transmission data.

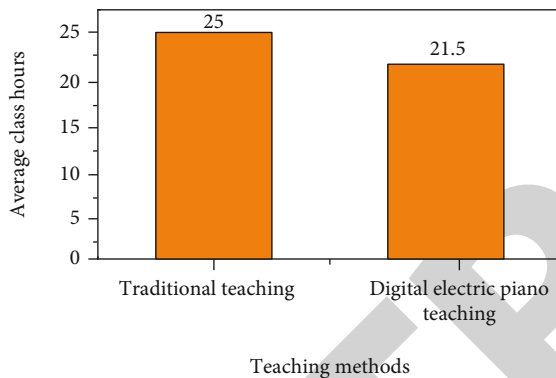


FIGURE 4: Study time of two groups of students.

group and perform the ensemble. In this mode, the specific operations are as follows: the teacher selects the students who need to join the group, the background color of the selected student terminal changes to the strobe color, the students in the group and the teacher can communicate without obstacles, and other students outside the group can practice freely according to the content assigned by the teacher.

(4) *Personal Demonstration*. The personal demonstration is mainly used to simulate the class. The teacher assigns a student to play for the whole class. In this mode, the specific operations are as follows: the teacher selects the student terminal to be demonstrated, and the background color of the selected student terminal changes to the strobe color. At this time, the selected demonstration student can communicate with the teacher, and the rest of the students can enjoy the student's performance and the teacher's comments on him.

(5) *Group Demonstration*. The group demonstration is mainly used to simulate the class. The teacher assigns some students to the whole class. In this mode, the specific operations are as follows: the teacher needs to select the student terminals demonstrated in the group, respectively, and the

background color of the student terminals selected for the group changes to the strobe color, which means that the group is selected [12]. At this time, the selected demonstration students can communicate with the teacher, and the rest of the students can enjoy the performance of the demonstration students and the teacher's comments on them.

3.2.2. *Description of the Main Control Terminal*. The main control terminal uses FPGA super large-scale logic control processing chip. It is similar to the brain of the whole system, coordinating various functional modules to complete specific tasks in different states. According to the command issued by the upper computer, FPGA will receive the data of student terminal and teacher terminal through the data transmission interface. Disassociate the received data into function data and audio data [13, 14]. Identify the function data code and make corresponding processing. After mixing the audio data according to the current status, the corresponding data will be repackaged and sent to their respective terminal devices through the data transmission interface. In the main control terminal, a variety of class modes are simulated according to the requirements to realize the communication channel between students and teachers and students and students.

3.2.3. *Student Terminal Description*. The function keys of the student terminal are shown in Figure 2.

- (1) Reset: when the student adapter cannot be gated by the teacher, press this key to restore the adapter to normal
- (2) Earphone: the socket of earphone plug of earphone microphone for students
- (3) Microphone: the socket of the microphone plug of the student's earphone microphone
- (4) Call: when a student wants to ask a teacher a question, press this key, and the "student seat number

TABLE 1: Practicing time of two groups of students.

	Traditional teaching	Digital electric piano teaching
Monthly average minutes of piano practice	530	820

TABLE 2: Number of students in the two groups who still like piano.

	Traditional teaching	Digital electric piano teaching
Students who still like the piano	38	46

TABLE 3: Average scores of two groups of students.

	Traditional teaching	Digital electric piano teaching
Average score	88	96

display” light on the teacher’s controller will flicker, and the teacher will know that the student wants to ask a question

- (5) Volume: adjust the volume of student headphones, press + to increase the volume, and press - to decrease the volume

Generally, the volume knob of the student piano should be placed at the medium position and will not change. The volume of the earphone can be adjusted by the volume knob on the student control box.

3.2.4. Flow Chart of Audio Data Transmission. The audio data transmission flow chart is divided into audio receiving data flow chart and audio sending data flow chart. The audio transmission process is shown in Figure 3, which is mainly used to convert analog signals into digital data through the audio chip and transmit them to other terminals; the audio receiving flow chart is mainly used to convert the digital data of the external terminal into analog signals through the audio chip.

4. Result Analysis

4.1. Improvement of Teaching Efficiency. The author conducted a 4-month comparative study in a cooperative institution and randomly selected 50 students participating in the traditional teaching and 50 students participating in the digital electric piano teaching system for sample comparison. The first is the comparison of teaching efficiency, which is also based on the learning of simple Thompson. After learning the second book of simple Thompson, the author compared the learning time of the two groups of students and obtained the following in Figure 4.

As can be seen from Figure 4, the learning efficiency of students who pass the intelligent digital electric piano teaching system has increased by an average of 14%, which can be said to be very obvious. With the continuous improvement

and improvement of the teaching system itself, I believe this difference will be more obvious.

4.2. Improvement of Learning Autonomy. Similarly, 50 students participating in the traditional teaching and 50 students participating in the digital electric piano teaching system are randomly selected for sample comparison. Within one month, the practicing time of the two groups of students is counted, respectively, and the following is obtained in Table 1:

It can be seen from Table 1 that the learning efficiency of students who pass the intelligent digital electric piano teaching system has increased by an average of 54.7%, which is a very significant change. Of course, this does not mean that it is entirely the improvement of students’ independent practicing time. Because the teacher can give quantitative and qualitative assignments through the intelligent digital electric piano teaching system, it is difficult for the students to be lazy. However, we can use another spot check form to see whether the students’ autonomy has been improved. We can divide them into two groups and spot check 50 students in each group for investigation and comparison. The students who are eager to learn at the beginning of school shall prevail. The anonymous survey results after two months of learning are shown in Table 2.

It can be seen from Table 2 that after two months of study, 46 students still like the piano through the intelligent digital electric piano teaching system, with a retention rate of 92%, which is significantly higher than that of 38 students in traditional learning, with a retention rate of 76% [15].

From the statistics of the survey results in the two tables, it can be seen that the students who pass the intelligent digital electric piano teaching system have significantly improved their learning autonomy, and the effect is remarkable, which is worth promoting.

4.3. Improvement of Teaching Quality. Finally, the students participating in the traditional teaching and the students participating in the digital electric piano teaching system were randomly selected for sample comparison. Two groups of sampling surveys were conducted:

The first group is subject to the students who have all completed the simple Thompson Volume II; the scores of 50 students in each group who play the same song in the error correction master performance mode are counted, and the following is obtained in Table 3.

As can be seen from Table 3 above, students who have also completed the simple Thompson Volume II, play the same song, and pass the intelligent digital electric piano teaching system can get an average score of 96 points, 8 points higher than the average score of 88 points of students in traditional teaching. Of course, some people will question that the students who pass the intelligent digital electric piano teaching system are already more skilled in this performance mode. They can play it easily. Naturally, their scores will be higher than those of the students in traditional teaching. Of course, this may also become a factor affecting their grades. Therefore, we have conducted the second group of comparative survey. For the students who also

Retraction

Retracted: Online Fault Detection of Dry Reactor Based on Improved Kalman Filter

Journal of Sensors

Received 12 December 2023; Accepted 12 December 2023; Published 13 December 2023

Copyright © 2023 Journal of Sensors. This is an open access article distributed under the Creative Commons Attribution License, which permits unrestricted use, distribution, and reproduction in any medium, provided the original work is properly cited.

This article has been retracted by Hindawi, as publisher, following an investigation undertaken by the publisher [1]. This investigation has uncovered evidence of systematic manipulation of the publication and peer-review process. We cannot, therefore, vouch for the reliability or integrity of this article.

Please note that this notice is intended solely to alert readers that the peer-review process of this article has been compromised.

Wiley and Hindawi regret that the usual quality checks did not identify these issues before publication and have since put additional measures in place to safeguard research integrity.

We wish to credit our Research Integrity and Research Publishing teams and anonymous and named external researchers and research integrity experts for contributing to this investigation.

The corresponding author, as the representative of all authors, has been given the opportunity to register their agreement or disagreement to this retraction. We have kept a record of any response received.

References

- [1] L. Zheng, X. Liu, Q. Kang, Y. Yang, H. Xun, and J. Zhang, "Online Fault Detection of Dry Reactor Based on Improved Kalman Filter," *Journal of Sensors*, vol. 2022, Article ID 3947025, 6 pages, 2022.

Research Article

Online Fault Detection of Dry Reactor Based on Improved Kalman Filter

Lu Zheng ^{1,2}, Xuan Liu ^{1,2}, Qi Kang ¹, Yue Yang ^{1,2}, Hua Xun ^{1,2}
and Jianying Zhang ^{1,2}

¹Inner Mongolia Power(Group)Co., Ltd, Inner Mongolia Power Research Institute Branch, Hohhot, Nei Monggol, 010020, China

²Inner Mongolia Enterprise Key Laboratory of High Voltage and Insulation Technology, Hohhot, Nei Monggol, 010020, China

Correspondence should be addressed to Lu Zheng; 20160670@ayit.edu.cn

Received 5 July 2022; Revised 23 July 2022; Accepted 29 July 2022; Published 4 August 2022

Academic Editor: C. Venkatesan

Copyright © 2022 Lu Zheng et al. This is an open access article distributed under the Creative Commons Attribution License, which permits unrestricted use, distribution, and reproduction in any medium, provided the original work is properly cited.

In order to meet the requirements of online fault detection for dry reactor, an online fault detection technology based on improved Kalman filter is proposed. The main content of the technology is based on the dry reactor detection technology, through the study of improved Kalman filter, the use of fault diagnosis and other methods, and finally through the experiments and analysis to build improved Kalman filter dry reactor online fault detection research means. The experimental results show that the maximum relative error of the improved Kalman filter is 6.039%, and the average relative error is 2.388%. The improved algorithm is very effective and greatly improves the prediction accuracy. The research based on improved Kalman filter can meet the demand of online fault detection of reactor.

1. Introduction

Dry reactor (hereinafter referred to as dry reactor) is widely used in substations and plays a pivotal role in improving the reliability of power system by playing the role of current limiting and reactive power compensation in the power grid [1]. At present, there is no effective means to detect the operation status of reactors in the network, and the faults cannot be found in time, and the precontrol measures cannot be taken. In order to improve the intrinsic security of equipment, it is particularly urgent for the network to accurately grasp the operating status of equipment, accurately identify anomalies in early stage, accurately locate faults, and predict and warn fault risks.

The main cause of dry resistance operation failure is coil damp, partial discharge, partial overheating insulation loss, and other reasons resulting in insulation breakdown between turns of winding coil. According to incomplete statistics, interturn short circuit faults account for more than 70% of the total failures of reactors. When the interturn short circuit fault occurs in dry resistance, the local temper-

ature at the short circuit position rises sharply, accelerating the insulation aging near the short circuit turn, resulting in the continuous development of the short circuit fault, expanding the multiturn short circuit fault and causing the reactor fire in a short time [2]. If the reactor is removed from the power grid after a fault occurs, the equipment will not only be severely burned and cannot be used for maintenance, but also bring safety risks to other electrical equipment around the station, which may further expand the accident and cause greater economic losses.

In recent years, accidents such as interturn short circuit and fire and burning occur frequently in the operation of the power grid. Special detection work is carried out to prevent accidents to a certain extent (Figure 1). However, regular offline maintenance is mainly adopted, which has many disadvantages: (1) regular outage maintenance is required, which inevitably leads to power interruption and economic losses; (2) the actual state of power equipment is not fully considered, if the excessive maintenance will cause waste of manpower and material resources, but insufficient maintenance may directly lead to the occurrence of failure; (3)

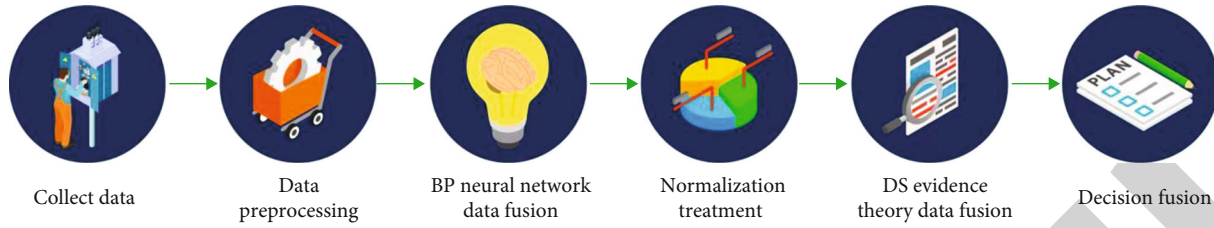


FIGURE 1: Online fault detection.

during operation, the operation state of dry reactor cannot be monitored and warned, and maintenance cannot be arranged reasonably in the early stage of failure, which may lead to the expansion of the fault range; (4) the actual test conditions cannot be completely consistent with the operating conditions of the equipment, so the reliability of the test results cannot be guaranteed. Compared with offline regular maintenance, the use of live line detection technology can not only timely warn the initial failure of equipment, but also master the development trend of dry resistance operation state. However, the limitations of existing live line detection technology are too great to be promoted and applied in the field [3].

2. Literature Review

In current social development, dry reactor is difficult to be popularized and applied mainly for the following reasons: (1) When dry resistance is charged with electricity, it is necessary to have enough safe distance, so that the detection accuracy will be reduced. At the same time, the infrared temperature measurement, whether artificial or conventional robot, can only detect the outer envelope, not the inner envelope temperature measurement. Several resistant outer layers are equipped with metal protective layer, so the live detection cannot be carried out. (2) In high altitude, high cold, high temperature, high wind, and other harsh or steep terrain areas, it is difficult to rely on personnel to conduct equipment inspection for a long time in the room, and the monitoring results are prone to error. (3) Manual inspection has problems such as high labor intensity, low work efficiency, scattered detection quality, and high management cost. Human factors are easy to lead to missed and false inspection, which will lay hidden dangers for major power accidents [4]. This research is based on multistate intelligent sensing technology of dry reactor operation state. It comprehensively uses infrared, ultraviolet, electromagnetic field dynamic imaging, acoustic positioning, local radiation, and other means to monitor the dry resistance in multiple states; to find the optimal intelligent algorithm; to realize the identification of the early warning signs of dry resistance latent fault; to judge the fault location, fault severity, and development trend; then to accurately evaluate the operating state of the equipment; and to establish the operating state sensing system. This article provides accurate decision-making basis for dry reactance equipment operation and maintenance. This article guides the maintenance team to carry out maintenance quickly, reduces the labor intensity of maintenance

staff, improves the efficiency of dry resistance maintenance, effectively extends the service life of dry resistance, ensures the reliability of power supply, improves the operation, maintenance and maintenance capacity of substation equipment, and promotes the development of nonpower failure detection technology and intelligent operation and inspection of power grid equipment.

In view of the above problems, in order to meet the requirements of online fault detection of dry reactor, a technology based on improved Kalman filter is proposed [5]. The main content of the technology is based on the dry reactor detection technology, through the study of improved Kalman filter, the use of fault diagnosis and other methods, and finally through the experiments and analysis to build improved Kalman filter dry reactor online fault detection research means. The prediction result of the improved Kalman filter algorithm is much smaller than that of the traditional Kalman filter algorithm, both the maximum relative error percentage and the average relative error percentage. The improved algorithm is very effective, and it greatly improves the prediction accuracy. In addition, the modified algorithm only calculates the correction factor at the end, so the improved algorithm also has a good convergence speed like the traditional algorithm.

3. Research Methods

3.1. Dry Reactor Detection Technology

3.1.1. Research on Encapsulation Temperature Detection Technology of Dry Air Core Reactor. In normal operation, the reactor will generate a certain amount of heat. However, with the increase of equipment operation time, the imbalance of load, and the increase of contact resistance and excessive current caused by the rust corrosion and poor contact of some contacts, the abnormal thermal state and overheating failure of the system, equipment, and line are caused [6]. These anomalies and fault spots emit more and more infrared energy than normal.

The principle of temperature measurement of infrared thermal imager is that the objective lens of infrared thermal imager receives the infrared radiation from the surface of power equipment, converging through the optical system, and the infrared energy received just falls on the focus of the system, that is, the focal plane of the infrared detector; after photoelectric conversion of the detector, the infrared energy of the power equipment is converted into electrical energy, and then a series of electrical signals are processed to obtain a thermal image of the power equipment measured

on the viewfinder of the thermal imager. The temperature anomaly in the image is found by the visual thermal image, and its temperature value is measured. Infrared thermal imager makes use of this characteristic of the power system to measure the temperature distribution field and its changes on the surface of the power equipment, to achieve contact-free temperature measurement, to carry out imaging detection, and to find out the possible thermal abnormalities and potential fault points of the power equipment, so as to realize the fault diagnosis of the equipment and the line [7].

The overheating failure of the box body, cooler, oil circuit casing, inner ring, encapsulation, and other components of the reactor due to eddy current, non-eddy current, or magnetic leakage will be detected by infrared thermal imager, which will achieve very good results [8].

In the process of partial discharge, in addition to the transfer of charge and the loss of electric energy, there will also be luminescence. The light radiation generated is mainly generated by the process of the particle returning from the excitation state to the ground state or low energy level and the recombination process of positive, negative ions, or positive ions and electrons. In view of this characteristic, it is proposed to use the light intensity of light radiation to detect the state of UV local emission, and the light intensity generated in the process of partial discharge of typical models is studied fundamentally [9]. Ultraviolet detection method is to use photodetectors to convert optical signals into electrical signals and reflect the intensity of partial discharge through the analysis and processing of electrical signals. Because the optical signal can be completely isolated from the primary loop in the detection process, it has good anti-interference ability and is favored by researchers [10]. Optical detection method can be used to detect partial discharge outside insulation. Studies show that more than 26% of electrical faults are related to external defects of insulation materials. At the same time, as the photoelectric sensor manufacturing technology tends to mature, high sensitivity, small volume, it provides the possibility for online monitoring.

3.1.2. Multistate Fault Diagnosis Method for Dry Reactor.

The fault diagnosis method needs to process different fault signals of dry reactor in order to obtain an evaluation criterion. Finally, the state of the dry reactor corresponding to the signal can be obtained by judging the characteristics of a certain field signal and the difference between it and the threshold value in the evaluation criterion [11]. There are many fault diagnosis methods, which method is suitable for the application of dry reactor and can obtain accurate criteria which will be the content of research. Evidential reasoning theory can be widely used in equipment state assessment and fault diagnosis because of its obvious advantages in redundant information processing. However, its disadvantages are also obvious; that is, it cannot be applied to events where there is conflicting evidence, as shown in Figure 2.

In view of the inherent shortcomings of D-S evidentiary reasoning theory, the D-S evidentiary reasoning theory is integrated with BP neural network to realize the comprehensive fault diagnosis of dry reactor. The diagnosis model is shown in Figure 3.

3.2. Research on Improved Kalman Filter

3.2.1. Kalman Filter Algorithm. Kalman filter algorithm can well solve the noise problem mentioned above. This algorithm describes the filter according to the state space model of the new random system composed of the state equation of the system and the observation equation [12]. Because noise and interference are inevitable in the real world, the existence of noise makes the actual value of a system have certain deviation. Thus, a system always consists of two parts; one part of the data is deterministic, and the other part of the data is noise due to interference. When these two parts are reflected in the system, the state of the system, whether past, present, or future, is not an exact value, but a statistical value. Then there is the problem of estimating the data in the future in a period of time according to the historical data of the past, which is called filtering.

3.2.2. Improve the Traditional Kalman Algorithm. Before building the model, the data will be screened to eliminate noise and interference. However, since loads will be affected by many external factors, such as temperature and date, the load changes will also be screened out, which will have a great impact on the results. After the initial prediction results are obtained, the proposed improved algorithm uses the previously screened data to perform mean calculation and divide with the mean of the screened data to obtain the correction factor [13]. Finally, the first predicted value is modified with the correction factor to obtain the final modified result and the mean value of screened data as

$$\text{mve}_k = \frac{\sum_{i=1}^l e_i}{l}. \quad (1)$$

l is the number of screened data; e_i is the screened data; mve_k represents the mean value of screened error data at the k th moment. The mean of the correct data is shown as

$$\text{mvr}_k = \frac{\sum_{i=1}^{n-l} d_i}{n-l}. \quad (2)$$

n represents the length of the total data; d_i indicates the data left after filtering. mvr_k represents the mean of the correct data at time k . Correction factor such as

$$h_k = \frac{\text{mvr}_k}{\text{mve}_k}. \quad (3)$$

In the formula, h_k represents the correction factor at moment k . The final result is expressed as

$$\vec{X}'_{ki} = h_i \vec{X}_{ki}. \quad (4)$$

3.2.3. Algorithm Analysis. The prediction results obtained by the Kalman filter load model are compared with the actual verified sample output, and the relative errors of the prediction data at each time are obtained, as shown in Figure 4 [14]. It can be seen that the prediction results of the traditional Kalman model have relatively high accuracy during 01:00~06:00, but the prediction accuracy is very poor

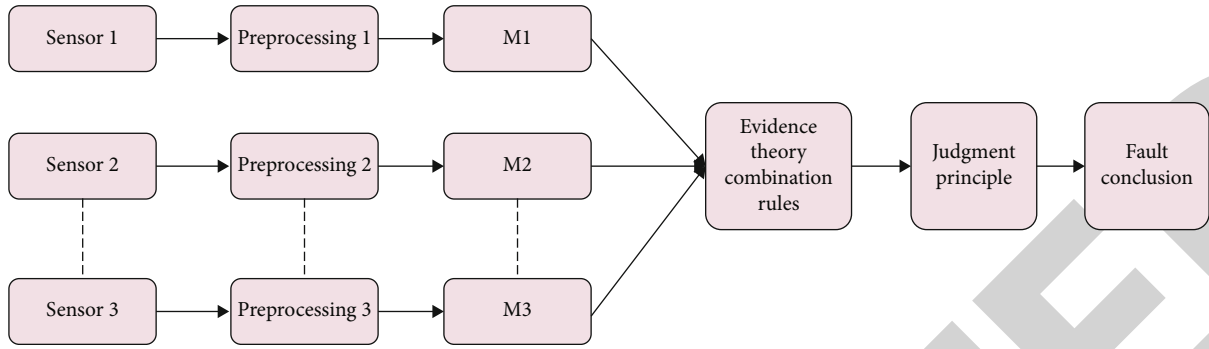


FIGURE 2: Fault diagnosis based on evidential reasoning.

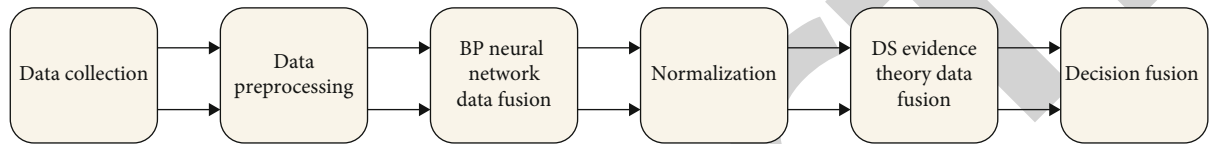


FIGURE 3: Diagnosis model of fusion of D-S evidential reasoning theory and BP neural network.

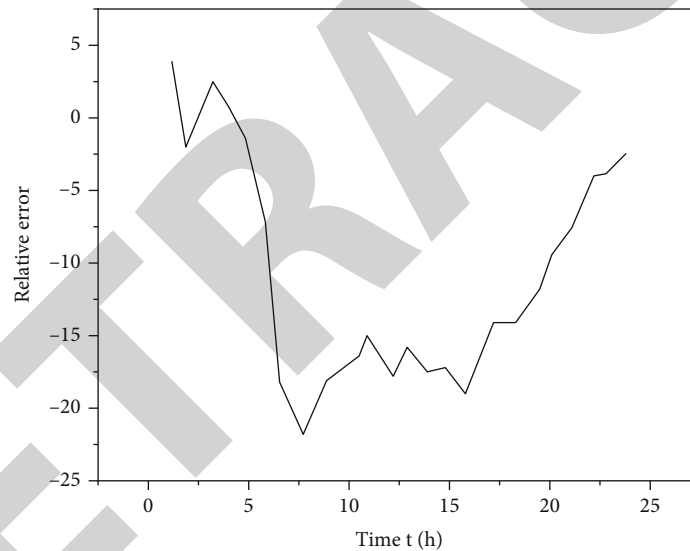


FIGURE 4: Prediction results of traditional Kalman algorithm.

during 07:00~17:00, and the maximum error can reach 21.5215%, which is unacceptable.

The screened data are used to work out the correction factor at each moment, and the correction factor is used to correct the previous results. The final prediction result is shown in Figure 5. It can be seen that the prediction result after adding the correction factor is greatly improved compared with the previous prediction result of the traditional model, and the prediction result at each moment is closer to the actual result [15].

Some popular algorithms are compared here, and the superiority of the algorithm is seen through comparison. A method of fuzzy neural network is proposed, which combines fuzzy logic with neural network to construct a prediction model. BP algorithm is used to adjust the threshold and connection weight of neural network, so that the network can

achieve the approximation of any function [16]. In this article, THE RBF neural network is used, weather conditions, temperature, wind speed, meteorological conditions and other factors are considered, and the RBF neural network model is established to realize load prediction. The superiority and feasibility of RBF network are verified by an example.

The training samples and test samples were determined by improved wheel method using data samples. The BP neural network with 56 nodes is built, and the load prediction model of BP neural network is established to predict the load. Gaussian kernel function was used as the basis function, and penalty function was used to deal with constraints, and RBF neural network was constructed as the prediction model [17]. The input and output nodes of the network are used as input and output signals of the fuzzy system,

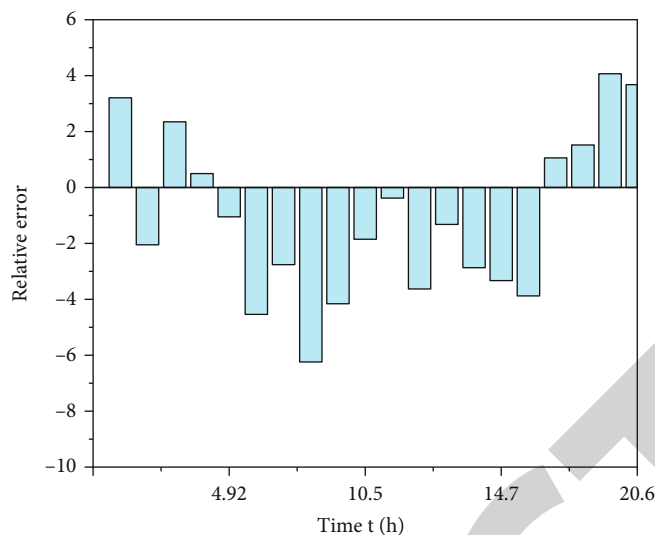


FIGURE 5: Prediction results of improved Kalman algorithm.

and the hidden nodes of the neural network are used to represent membership functions and fuzzy rules. The least square method is used to learn, and the fuzzy neural network is constructed to predict. The prediction results of various intelligent algorithms are compared with those of the algorithm proposed in this article.

Neural network algorithm needs to build neural network and needs to go through a lot of iterative process to get the optimal solution. There are also many improved algorithms for neural networks. They use other intelligent algorithms to improve the construction process of neural network model to find the optimal solution of network connection weight and threshold. However, it still cannot make up for the shortcoming of long time to build neural network. The methods of single-objective particle swarm optimization BP neural network (PSOBP) and multiobjective particle swarm optimization BP neural network (MPOS_BP) were proposed [18]. It uses the adopted data to establish the BP neural network model, the single-objective particle swarm optimization BP neural network model, and the multiobjective particle swarm optimization BP neural network model. The network hidden layer nodes of the three algorithms are all 56, and the training time of each network is analyzed.

The training time of the neural network algorithm will also increase with the increase of the number of nodes in the hidden layer, and the iteration will take a long time, and the problem of local optimization will also occur in the iterative solution process [19]. Because the improved algorithm does not need to spend a long time to solve the weights and thresholds of the neural network, the whole process of building the prediction model and solving the prediction results only takes 10s to 20s.

In conclusion, the proposed algorithm has certain advantages over today's intelligent algorithms in terms of prediction accuracy. In addition, it takes a long time to build the neural network, and the convergence may reach the local optimum. However, Kalman algorithm does not need to spend a lot of time to build the network, and there is no convergence problem [20].

TABLE 1: Maximum and average relative errors of the two methods.

	Traditional Kalman filtering algorithm	Improved Kalman filtering algorithm
Maximum relative error/%	21.521	6.039
Mean relative error/%	10.669	2.388

4. Result Analysis

As can be seen from Table 1, the prediction results of the improved Kalman filter algorithm are much smaller than those of the traditional Kalman filter algorithm, both in terms of maximum and average relative error percentage, which has greatly improved the prediction results. It can be seen that the maximum relative error of the improved Kalman filter algorithm is 6.039% and the average relative error is 2.388%. The improved algorithm is very effective and greatly improves the prediction accuracy. In addition, the modified algorithm only calculates the correction factor at the end, so the improved algorithm also has a good convergence speed like the traditional algorithm [21, 22].

5. Conclusion

In order to meet the requirements of online fault detection of dry reactor, a new technique based on improved Kalman filter is proposed. The main content of the technology is based on the dry reactor detection technology, through the study of improved Kalman filter, the use of fault diagnosis and other methods, and finally through the experiments and analysis to build improved Kalman filter dry reactor online fault detection research means. The prediction result of the improved Kalman filter algorithm is much smaller than that of the traditional Kalman filter algorithm, both the maximum relative error percentage and the average relative error percentage. The improved algorithm is very effective, and it greatly improves the prediction accuracy.

Retraction

Retracted: Fractal Art Pattern Information System Based on Genetic Algorithm

Journal of Sensors

Received 13 September 2023; Accepted 13 September 2023; Published 14 September 2023

Copyright © 2023 Journal of Sensors. This is an open access article distributed under the Creative Commons Attribution License, which permits unrestricted use, distribution, and reproduction in any medium, provided the original work is properly cited.

This article has been retracted by Hindawi following an investigation undertaken by the publisher [1]. This investigation has uncovered evidence of one or more of the following indicators of systematic manipulation of the publication process:

- (1) Discrepancies in scope
- (2) Discrepancies in the description of the research reported
- (3) Discrepancies between the availability of data and the research described
- (4) Inappropriate citations
- (5) Incoherent, meaningless and/or irrelevant content included in the article
- (6) Peer-review manipulation

The presence of these indicators undermines our confidence in the integrity of the article's content and we cannot, therefore, vouch for its reliability. Please note that this notice is intended solely to alert readers that the content of this article is unreliable. We have not investigated whether authors were aware of or involved in the systematic manipulation of the publication process.

Wiley and Hindawi regrets that the usual quality checks did not identify these issues before publication and have since put additional measures in place to safeguard research integrity.

We wish to credit our own Research Integrity and Research Publishing teams and anonymous and named external researchers and research integrity experts for contributing to this investigation.

The corresponding author, as the representative of all authors, has been given the opportunity to register their agreement or disagreement to this retraction. We have kept a record of any response received.

References

- [1] M. Chen, "Fractal Art Pattern Information System Based on Genetic Algorithm," *Journal of Sensors*, vol. 2022, Article ID 9350301, 8 pages, 2022.

Research Article

Fractal Art Pattern Information System Based on Genetic Algorithm

MengLin Chen 

Krirk University, Bangkok, Thailand

Correspondence should be addressed to MengLin Chen; 2009020137@st.btbu.edu.cn

Received 19 May 2022; Revised 7 June 2022; Accepted 18 July 2022; Published 29 July 2022

Academic Editor: C. Venkatesan

Copyright © 2022 MengLin Chen. This is an open access article distributed under the Creative Commons Attribution License, which permits unrestricted use, distribution, and reproduction in any medium, provided the original work is properly cited.

In order to solve the problem of fractal art pattern innovative design in specific fields, this paper proposes a new method of fractal technology and visualization technology based on genetic algorithm to support art pattern innovative design. In these models, the function of the fractal structure is represented by the binary structure, while the main function represented by the wooden structure is the function of creating new offspring. Provide high-quality services to meet customer needs faster and better. The experimental results show that after 14 generations, the force curve appears to be more stable, the weight scale is studied, and a new model is developed. At the same time, the pattern elements of interest to users are retained for genetic algorithm. *Conclusion.* This method can help designers quickly design fractal art patterns appreciated by users.

1. Introduction

In recent decades, major developed industrial countries have begun to pay attention to the research of design technology. For example, since the 1960s, Britain has supported the development and promotion of new design technology with national policies and financial resources; The United States has established a “Design Committee.” Germany put forward the idea of “design is science,” and the development of its design has begun to take shape. Since the 1980s, China has vigorously advocated innovative design, introduced a number of foreign advanced technologies and methods [1], and introduced computer CAD into the design field. In today’s society, with the great improvement of people’s material civilization and spiritual civilization, people’s consumption concept is gradually changing. When buying goods, people pay more and more attention to the artistry and agreeableness of the appearance of goods. As a consumer, when shopping, pay attention to the quality of the product, the price of the product, the function of the product, and the grade of the product. For example, more and more color is due to the layout of external lines, surface textures, and color matching of objects. If the quality of the product depends on the technology; then, the taste of the

product, that is, the artistry, depends on the new design of the product [2]. Therefore, for manufacturing enterprises, in order to improve the competitiveness of their products in the market, they must vigorously carry out innovative design of products, especially the innovation of appearance and plastic arts. To enhance market competitiveness, it is necessary to build a “connecting heart bridge” for customers. With good products, how to win the hearts of customers and sell the products to create benefits for the enterprise is the key. Integrity strives for the world, and high quality wins the hearts of customers. This requires the company’s sales staff to communicate well with customers, to reach a consensus and learn from each other’s strengths based on the integrity principle of “win-win interests of both parties” and to fully understand customer needs and indicators, and make products available to customers or downstream production lines. In order to help customers solve practical problems in production, we will win praise from customers, maintain a good cooperation and win-win relationship, and build a “heart-to-heart bridge” for heart-to-heart communication. Innovation and product development have become the keys to the survival and development of the industry. If designers want to be innovative, they need to express their ideas, expand their thinking, and try their best to bring creative

inspiration. In other words, how to tap creative inspiration and bring out new ideas has become the key to innovation. Fortunately, advanced computer science and technology can provide designers with a good environment to stimulate creative inspiration.

2. Literature Review

Sampath and Selvan discovered that the study of fractal theory began in 1970 and was first proposed by Benoit B. Mandelbort, a researcher in the Department of Physics and a professor in the Department of Mathematics at IBM Research Center, Harvard University 1975 [3]. Ambigapathy and Paramasivam believe that it is a geometric theory used to describe the chaotic characteristics of natural things. Since then, people have a new perspective and research method that can observe and understand natural things [4]. Al-Frady and Al-Taei said that the emergence of fractal theory is a supplement and expansion of Euclidean classical geometry. At the same time, fractal theory makes it possible to describe nature with the help of mathematical language [5]. De and others found that in the late 1970s, fashion designer Jhane Barnes began to engage in the commercial design of men's shirts [6]. When she used the old-fashioned weaving method to design the cloth on a small manual textile machine, due to the influence of fractal theory, Jhane Barnes realized that the simple rule of fractal can help her design complex clothing styles. After turning to mathematicians and computer software experts Bill Jones and Dana Cartwright, Jhane Barnes got many designs that were impossible to get by hand. Xie and others believe that she has also become the first person to apply fractal theory, thus starting the application of fractal theory in pattern design. When computer expert carpenter realized computer simulation of mountains in aircraft flight scene for Boeing, he divided a triangle into four triangles in three-dimensional space and iterated continuously to generate fractal mountains. This is the first time that fractal theory is used in the rendering of three-dimensional graphics. Since then, people began to try to use fractal theory in various places [7]. Chen and others discussed the texture features of Julia set generated based on escape time algorithm [8]; Cao and others compared the formal beauty of fractal graphics with the aesthetic law of traditional geometric patterns and believed that they were highly consistent [9]. Li and others have been committed to the generation of fractal graphics and the application of fractal graphics in silk scarf printing and dyeing for many years [10]. Peng and others applied the transformed pezley pattern with self similarity to silk scarf design through the analysis of the concept of Mandelbrot set fractal and the principle and characteristics of Mandelbrot set graphics. This paper presents a new method to support the innovative design of artistic patterns by using fractal technology and visualization technology based on genetic algorithm [11]. This method can show that it is feasible and effective to use the existing computing methods and environment to generate images to support the innovative design of artistic patterns in specific fields. Explain that in the genetic algorithm, by adding human-

computer interaction, user preferences are integrated into the genetic process to reflect the design ideas of designers. At the same time, the problem that the fitness function is difficult to express in the conceptual design is solved. The adaptive method was adopted to ensure the superiority of the genetic population.

3. Research Methods

3.1. Art Form and Theory of Fractal Pattern Composition.

The composition of the graph consists of two parts: the model structure and the composite model. In fractal art, it mainly refers to the layout and organization form of fractal pattern picture. Composition is the composition of patterns, including pattern structure and picture composition. The data included fractures as standard fractal structures, total fractal structure compositions, and incorrectly configured fractal wing compositions. In drawing, the fractal model retains the mixed plane model and uses all the computer technology in model design, color composition, composition, etc., forming a new art of simulating creative thinking and its realization. Fractal art design and development principles, in addition to the same rules and regulations as the same art form, the most important thing is to use fractal self-similarity and self-affinity, introduce recursion or iteration in the modeling or composition process and randomly affect the local process [12]. Basic procedures include:

- (1) The model is created by iterative operations and repeated application of an algorithm based on a geometric process
- (2) Using color coding technology to combine algorithms and human-computer interaction
- (3) The graphic typesetting adopts the combination of traditional and fractal algorithm, hybrid technology, etc.

3.2. *Genetic Algorithm.* Genetic algorithm is a research algorithm of natural genetics based on natural selection and biology. Its main characteristics are population search strategy and information exchange among individuals in the population. Genetic algorithm is a search algorithm that can be used for complex system optimization. Compared with traditional algorithms, it has the following four characteristics: first, it takes the coding of decision variables as the operation object; second, genetic algorithm directly uses fitness as search information, without other auxiliary information such as derivatives; third, genetic algorithm uses search information of multiple points, which has implicit parallelism; finally, it does not use nondeterministic rules, but adopts probability search technology. It uses simple coding techniques to represent a wide range of complex processes and facilitates a set of codes to represent research and research decisions for simple genetic manipulation and natural selection of the fittest. It introduces behaviors similar to genetic selection, such as cross recombination, variation, selection, and elimination, into the solution process, reflecting the evolutionary process of "natural selection and

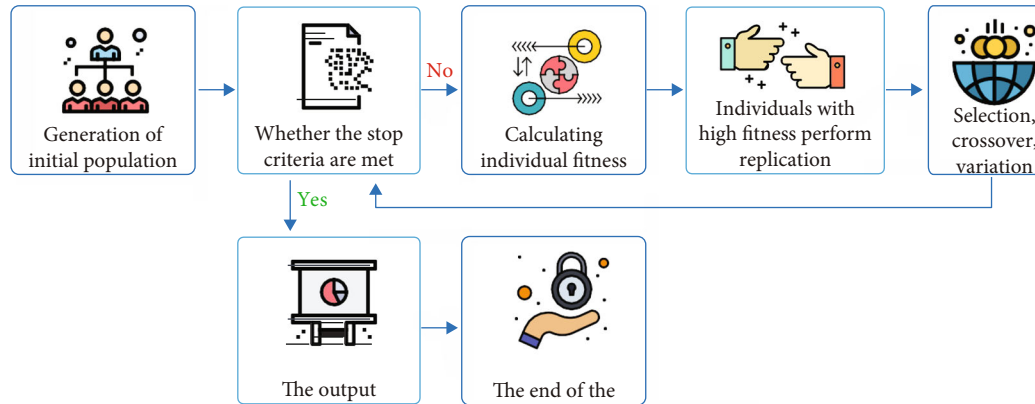


FIGURE 1: Flowchart of genetic algorithm.

survival of the fittest” in nature [13]. Genetic algorithm retains several local optimal solutions at the same time and approaches the optimal solution by multiple genetic operations on several local optimal solutions. Due to its good adaptability, the algorithm is very suitable for nonlinear solutions such as combinatorial optimization and policy discovery, so it is used in many fields.

Genetic algorithms are based on the laws of natural evolution. Initially, some people (parent 1, parent 2, ..., parent N) are created to create the first population, the function of each person is calculated, and the first generation (initial generation) is generated. If the optimization process is not met, a new generation group will be created. To produce the next generation, individuals are selected according to physical fitness, and parents need to cross to produce offspring [14]. As a result, all descendants are changed; then, the security of descendants is recalculated. Offspring are placed in the population to replace the parent to create a new generation (children 1, person 2, person 3, ...). Repeat this process until the optimization process is complete, as shown in Figure 1.

When designing genetic algorithm, the following basic steps are usually followed:

- (1) *Determine the Coding Scheme.* Genetic algorithm does not directly act on the solution space of the problem, but uses some coding representation of the solution space. The choice of encoding representation can sometimes have a positive impact on the performance and functionality of the algorithm [15]
- (2) *Determining Bodily Function.* Exercise is a measure of drug quality and depends largely on the relationship between the behavior of the solution and the environment (e.g., population). It is usually expressed in the form of an objective function or a value function. The physical value of the solution is the only basis for selection in the genetic process
- (3) *Determination of the Concept of Selection.* The selection and presentation of the survival of the fittest make the solution of human transformation have a

TABLE 1: Users' ratings of works.

Design art pattern	User personal rating	Group common score
A	1 3 3 2 3 2	14
B	2 2 3 2 3 2	14
C	1 1 3 2 1 2	10
D	1 1 1 2 1 2	8
E	3 3 3 2 3 1	15
F	1 3 1 2 2 2	11

high survival rate, which is one of the common differences between genetic algorithms and research algorithms. Different selection strategies also have a positive impact on the performance of the algorithm

- (4) *Choice of Control Parameters.* Control usually includes population size, algorithm results for different genes, and some other management services.
- (5) *Genetic Engineering.* Genetic engineering in genetic algorithms often includes advanced processes such as breeding, crossbreeding, and mutation
- (6) *Determining the Order of the Algorithm.* Since genetic computing does not use data such as the gradient of the objective function, the position of the person in the solution cannot be determined during the genetic process [16]. Therefore, the traditional method cannot be used to determine the convergence of the algorithm to terminate the algorithm. The common method is to specify a maximum genetic algebra or algorithm in advance. When there is no obvious improvement in the fitness value of the solution after several successive generations, it is terminated and can be terminated appropriately

3.3. *Generalized $M - J$ Set.* Both M sets and J sets are obtained by iterating the complex plane mapping $z \rightarrow z^2 + c$ in a region on the negative plane c . Set M uses c to get the values in this region. The j set is a pattern obtained by taking the median value of the region with a fixed c value.

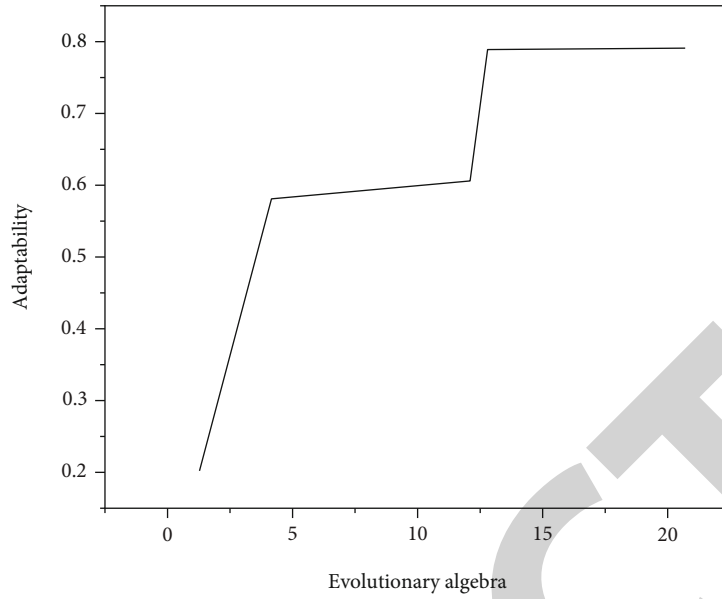


FIGURE 2: Performance tracking curve of genetic algorithm.

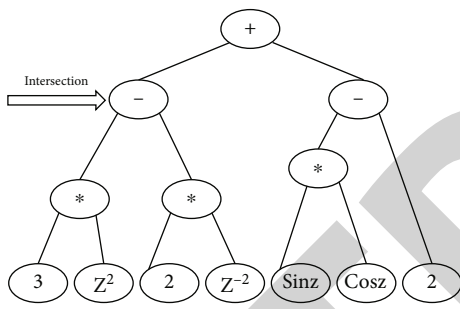


FIGURE 3: Tree A $3z^2 - 2z^{-2} + \sin z * \cos z - 2$.

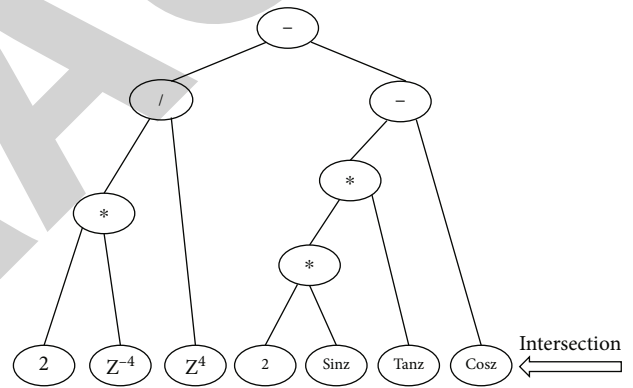


FIGURE 5: Tree C $2z^{-4}/z^4 - 2 \sin z * \tan z - \cos z$.

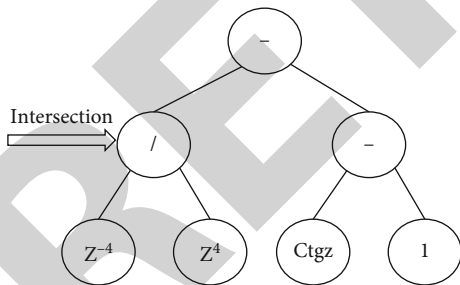


FIGURE 4: Tree B $z^{-4}/z^4 - ctgz - 1$.

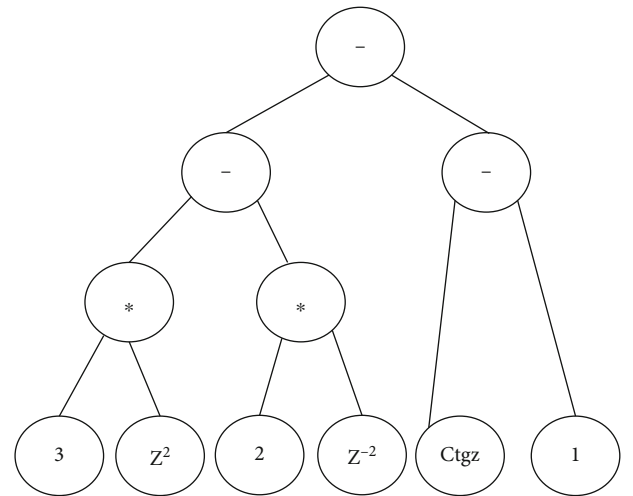


FIGURE 6: Tree D $3z^2 - 2z^{-2}ctgz - 1$.

The Julia set patterns corresponding to different c values are different, and the parameter c in a mapped M set corresponds to a connected Julia set. Because M sets and J sets are derived from the same transformation, there is a very complex correlation between them. People often combine them and study them, called $M - J$ sets [17].

The current research on M loss and J loss has been decomposed into a simple group of $z \rightarrow z2 + c$, and various equations such as $z \rightarrow \cos(z) + c$, $z \rightarrow \arctg(z8 + \sin(z)) + c$, called are generalized M sets and generalized J sets.

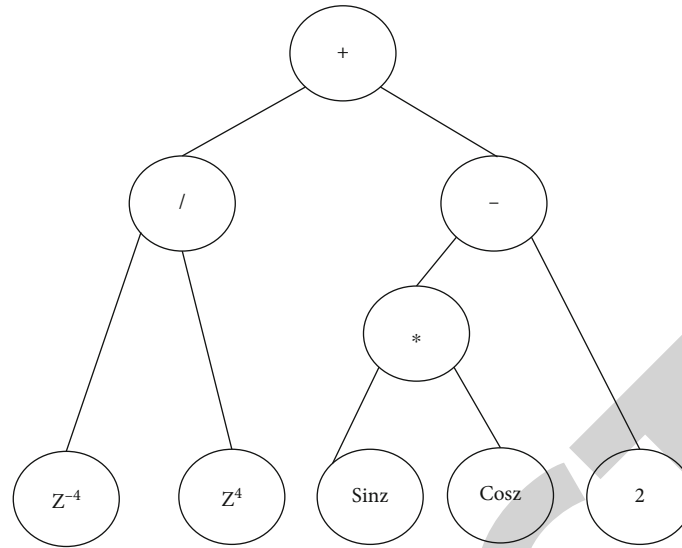


FIGURE 7: Tree B $z^{-4}/z^4 + \sin z * \cos z - 2$.

In other words, both generalized M sets and generalized J sets adopt the iterative relationship $z \rightarrow f(z) + c$ on the complex plane, where $f(z)$ is any polynomial (which can include high-order functions, trigonometric functions, and exponential functions). However, the two methods are different in construction and calculation. Given the C value of J set, search all points on the z plane to find the complex structure of attraction and its boundary, that is, draw the graph in the z plane of variable space. The M set is to select an initial Z point, track its iterative point column under different C values, record the structure of the point column on the C plane of the parameter space, and draw graphics. The generalized M set and generalized J set are called generalized $M - J$ set [18].

The composition of fractal models based on complex dynamical systems usually depends on the model number. Thus, mathematical models have an impact on the aesthetics of fractal art. The designer can design the necessary model to meet the requirements of the model. It can also be said that the designer looks at the process, and finding a suitable mathematical model is the process of finding a suitable mathematical model.

Therefore, in order to grasp this factor affecting the artistry of fractal patterns and find the mathematical formula that can generate fractal patterns with high artistic value, we propose the concept of generalized $M - J$ set [19]. The generalized fractal formula established by $J - M$ Institute is also based on the following research.

3.4. Algorithm Design

3.4.1. Chromosome Coding. Here, we regard the iterative function generating the fractal pattern of generalized $M - J$ set as an individual in the genetic algorithm population and encode its iterative function. Because the application of binary tree structure to express mathematical expression has great flexibility. Therefore, the structural coding method is adopted here to express the solution of

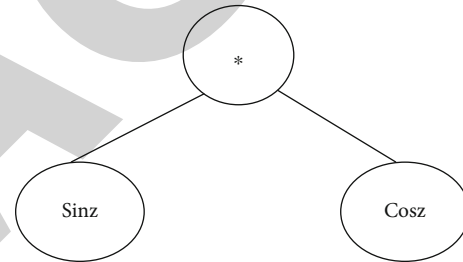


FIGURE 8: Tree F $\sin z * \cos z$.

the problem in the form of binary tree, and each tree is a chromosome [20].

The mathematical representation of a binary tree is a decision made by mathematicians and mathematicians. This encoding means that the operands of the instruction are at the end of the binary tree, the operands can be changed or rotated, and the operators are in the middle of the binary tree. An order-of-magnitude traversal sequence of a binary tree is a valid mathematical expression.

3.4.2. Establishment of Fitness Function. The fitness function in genetic operation is the basis for evaluating the advantages and disadvantages of genetic evolution chromosome individuals. Here, we use the “satisfaction” and “consensus” of users to design works as the index to measure the quality of genetic chromosomes.

The fitness function of this paper adopts the group common scoring model. The group common score adopts the third-order evaluation scale, which divides the user’s preference into three evaluation preferences: “satisfied,” “average,” and “dissatisfied.” Among them, “satisfied” corresponds to 3 points rated by the user, “general” corresponds to 2 points, and “dissatisfied” is 1 point. Accumulate the scores of each user to obtain the satisfaction score of the user. If n users participate in the scoring, the satisfaction scoring interval is $[n, 3n]$. If the satisfaction scores are the same, the fitness

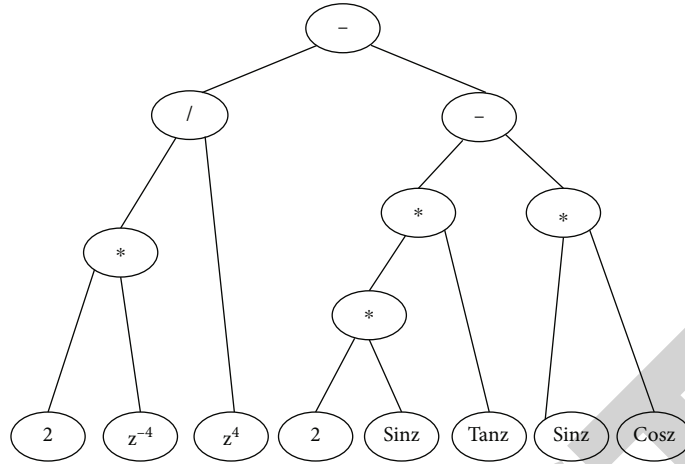


FIGURE 9: Tree G $2z^{-4}/z^4 - 2 \sin z * \tan z - \sin z * \cos z$.

function is jointly determined by calculating the consensus standard. Taking Table 1 as an example, although the common score of design work A and design work B is 14, work B does not show a “dissatisfied” attitude, and the degree of consistency of evaluation is high. Therefore, it is more in line with the actual needs of users.

Set the user evaluation score sequence $\{V_i\} (i = 1, 2, \dots, n)$ and make $V_{\max} = \{V_j; V_j \geq V_i, i = 1, 2, \dots, n\}$, $V_{\min} = \{V_k; V_k \leq V_i, i = 1, 2, \dots, n\}$, then, the value of V_i after $[0,1]$ standardization is the following formula.

$$S(V_i) = \frac{V_i - V_{\min}}{V_{\max} - V_{\min}}. \quad (1)$$

Let the degree of consensus be T , and calculate the degree of consensus by using the standard deviation of the following formula.

$$T = 1 - \frac{\sqrt{\sum_{i=1}^n (V_i - \bar{V})^2}}{n}. \quad (2)$$

The satisfaction is as follows.

$$\bar{S}(V_i) = \frac{\sum_{i=1}^n S(V_i)}{n}, \quad (3)$$

Where \bar{V} is the average value of all user evaluation results, i and n are positive integers, and $1 \leq i \leq n$.

Assuming that the proportion of consensus degree and satisfaction $\bar{S}(V_i)$ in fitness is u and $v(u + v = 1)$, respectively, the consensus satisfaction as a fitness function is as follows.

$$\text{Fitness} = u\bar{S}(V_i) + vT. \quad (4)$$

In the traditional genetic algorithm, the fitness value is determined by the fitness function. However, the subjective evaluation of each user is different. Therefore, there can be no objective fitness function. Therefore, the adaptation value adopted in this paper should be reflected by user scoring.

This way of extracting the user’s “satisfaction” and “consensus” through user scoring and then obtaining the adaptive value is the full embodiment of the interactive idea.

3.4.3. Algorithm Flow

Step 1. Initializes the population. The population randomly generates effective mathematical expressions in the operator set and operand set as the iterative function of generating fractal patterns. The expression string is represented as a binary tree by structural coding.

Step 2. Generates the fitness value of chromosome in the initial population through interaction with the user. Users can evaluate and score the chromosomes in the population to modify their fitness value, so as to carry out genetic selection of the next generation.

Step 3. Generates new populations according to the fitness of chromosomes.

Step 4. Cross and mutate the population.

Step 5. After multiple rounds of evaluation and elimination. If there is a satisfactory result for users, it will be finished; otherwise, it will be transferred to Step 2.

4. Result Analysis

Taking the escape radius algorithm of generalized $M - J$ set and the escape time algorithm of Newton iterative method to generate fractal patterns as examples to illustrate the application of genetic algorithm in fractal pattern generation in complex dynamic systems.

The performance tracking curve of genetic algorithm is shown in Figure 2 below. After 14 generations, the fitness curve tends to be stable, indicating that the improved genetic algorithm can search for the appropriate weight threshold.

Let us assume that the set of operands given is $(z, z^2, z^3, z^4, z^{-1}, z^{-2}, z^{-3}, z^{-4}, e^z, \sin z, \cos z, \tan z, ctgz, a)$.

Where $z = x + y_i$, a is any constant. The operator set is $B(+, -, *, /)$.

The initial set of operators consists of a set of binary operators and a set of random operators. The steps of building a binary tree are randomly select multiple elements in the operator set as the intermediate node and randomly select multiple elements in the operand set as the end node of the binary tree [21]. Each binary tree represents an iterative function. For example, we select three spanning trees from the initial population generated according to sets A and B: tree A and tree B, and tree C is shown in Figures 3, 4, and 5.

Let 100 users rate and evaluate the pattern generated by the iterative function. Calculate the user's consensus degree through formula (2), calculate the user's satisfaction through formula (3), and finally calculate the fitness value of each fractal design pattern through formula (4). According to the fitness value, excellent chromosomes are selected to produce the next generation.

The selected chromosome lines are crossed and mutated to generate individuals in a new population. Here, it is assumed that tree A and tree B are crossed. Among them, the "-" node of the left subtree of tree A and the "/" node of the left subtree of tree B are randomly selected as intersections. The exchanged part is a subtree rooted at the intersection. The new individuals generated after crossing are tree D and tree e, as shown in Figures 6 and 7.

In the mutation operation, a new subtree is randomly generated by the program, and this subtree is used to replace the subtree below the selected node. Here, we take tree c as an example for mutation operation. Suppose that the selected mutation node is the "cosz" node on the far right of the right subtree of tree C. The randomly generated subtree is tree F, as shown in Figure 8, and the tree generated after the mutation operation of tree c is tree g, as shown in Figure 9.

After the above steps, if a user satisfied art design work is generated, stop the operation, otherwise, return to continue the genetic operation.

Through the above example, we can see that the idea of genetic algorithm is applied to generate fractal art patterns, and new patterns are automatically generated. At the same time, the pattern elements of interest to users are retained for genetic, so as to help designers quickly design fractal art patterns appreciated by users.

5. Conclusion

This paper applies genetic algorithms in computer science to the field of fractal art to create diverse fractal patterns to meet the needs of users. However, due to the problems of single evaluation mechanism, user psychological fatigue, and low convergence efficiency in genetic algorithm, how to reduce the impact on the results of genetic evolution by improving these factors should be the focus of future research.

In this paper, the research on the generation method of fractal art pattern based on genetic algorithm is still in the preliminary stage, and there is still much work to be dis-

cussed and carried out. The further work mainly includes the following aspects: further improve the genetic algorithm and expand the generation method of fractal art pattern based on genetic algorithm. The improvement of fractal pattern drawing system is based on genetic algorithm.

Data Availability

The data used to support the findings of this study are available from the corresponding author upon request.

Conflicts of Interest

The author declares no conflicts of interest.

References

- [1] Y. Wu, "Realization of fractal art pattern composition based on photoshop software," *Computer-Aided Design and Applications*, vol. 17, no. S2, pp. 123–133, 2020.
- [2] T. G. Fawcett, S. Gates-Rector, A. M. Gindhart, M. Rost, and T. N. Blanton, "Total pattern analyses for non-crystalline materials," *Powder Diffraction*, vol. 35, no. 2, pp. 82–88, 2020.
- [3] R. Sampath and K. T. Selvan, "Compact hybrid Sierpinski Koch fractal UWB MIMO antenna with pattern diversity," *International Journal of RF and Microwave Computer-Aided Engineering*, vol. 30, no. 1, pp. e22017.1–e22017.13, 2020.
- [4] S. Ambigapathy and J. Paramasivam, "2.4 GHz and 5.2 GHz frequency bands reconfigurable fractal antenna for wearable devices using ann," *Applied Computational Electromagnetics Society Journal*, vol. 36, no. 3, pp. 354–362, 2021.
- [5] L. Al-Frady and A. Al-Taei, "Wrapper filter approach for accelerometer-based human activity recognition," *Pattern Recognition and Image Analysis*, vol. 30, no. 4, pp. 757–764, 2020.
- [6] X. De, J. Zhang, Y. Yang, J. Du, and Z. Li, "Fractal prediction of frictional force against the interior surface of forming channel coupled with temperature in a ring die pellet machine," *BioResources*, vol. 16, no. 3, pp. 4780–4797, 2021.
- [7] Y. Xie, Y. Ishida, J. Hu, and A. Mochida, "A backpropagation neural network improved by a genetic algorithm for predicting the mean radiant temperature around buildings within the long-term period of the near future," *Building Simulation*, vol. 15, no. 3, pp. 473–492, 2022.
- [8] B. Chen, Y. Niu, and H. Liu, "Input-to-state stabilization of stochastic Markovian jump systems under communication constraints: genetic algorithm-based performance optimization," *IEEE Transactions on Cybernetics*, vol. 99, pp. 1–14, 2021.
- [9] Y. Cao, X. Fan, Y. Guo, S. Li, and H. Huang, "Multi-objective optimization of injection-molded plastic parts using entropy weight, random forest, and genetic algorithm methods," *Journal of Polymer Engineering*, vol. 40, no. 4, pp. 360–371, 2020.
- [10] D. Li, R. Z. Shi, N. Yao, F. Zhu, and K. Wang, "Real-time patient-specific ECG arrhythmia detection by quantum genetic algorithm of least squares twin SVM," *Journal of Beijing Institute of Technology*, vol. 29, no. 1, pp. 29–37, 2020.
- [11] D. Peng, G. Tan, K. Fang, L. Chen, and Y. Zhang, "Multiobjective optimization of an off-road vehicle suspension parameter through a genetic algorithm based on the particle swarm optimization," *Mathematical Problems in Engineering*, vol. 2021, Article ID 9640928, 14 pages, 2021.

Retraction

Retracted: The Study of Virtual Reality Sensing Technology in the Form Design and Perception of Public Buildings

Journal of Sensors

Received 17 October 2023; Accepted 17 October 2023; Published 18 October 2023

Copyright © 2023 Journal of Sensors. This is an open access article distributed under the Creative Commons Attribution License, which permits unrestricted use, distribution, and reproduction in any medium, provided the original work is properly cited.

This article has been retracted by Hindawi following an investigation undertaken by the publisher [1]. This investigation has uncovered evidence of one or more of the following indicators of systematic manipulation of the publication process:

- (1) Discrepancies in scope
- (2) Discrepancies in the description of the research reported
- (3) Discrepancies between the availability of data and the research described
- (4) Inappropriate citations
- (5) Incoherent, meaningless and/or irrelevant content included in the article
- (6) Peer-review manipulation

The presence of these indicators undermines our confidence in the integrity of the article's content and we cannot, therefore, vouch for its reliability. Please note that this notice is intended solely to alert readers that the content of this article is unreliable. We have not investigated whether authors were aware of or involved in the systematic manipulation of the publication process.

Wiley and Hindawi regrets that the usual quality checks did not identify these issues before publication and have since put additional measures in place to safeguard research integrity.

We wish to credit our own Research Integrity and Research Publishing teams and anonymous and named external researchers and research integrity experts for contributing to this investigation.

The corresponding author, as the representative of all authors, has been given the opportunity to register their agreement or disagreement to this retraction. We have kept a record of any response received.

References

- [1] L. Li and X. Zheng, "The Study of Virtual Reality Sensing Technology in the Form Design and Perception of Public Buildings," *Journal of Sensors*, vol. 2022, Article ID 7903386, 9 pages, 2022.

Research Article

The Study of Virtual Reality Sensing Technology in the Form Design and Perception of Public Buildings

Leili Li  and Xinyu Zheng 

Architecture and Urban Planning of Jilin Jianzhu University, Changchun, Jilin 130000, China

Correspondence should be addressed to Leili Li; 15070140224@xs.hnit.edu.cn

Received 21 May 2022; Revised 7 June 2022; Accepted 22 June 2022; Published 25 July 2022

Academic Editor: C. Venkatesan

Copyright © 2022 Leili Li and Xinyu Zheng. This is an open access article distributed under the Creative Commons Attribution License, which permits unrestricted use, distribution, and reproduction in any medium, provided the original work is properly cited.

In order to explore the commercial building design method that meets the needs of contemporary consumer behavior, the author proposes a method of applying virtual reality, behavior simulation, and other technologies to commercial building design. First, through a questionnaire survey of commercial buildings in a city, the influencing factors of consumption behavior are explained with the help of SPSS correlation analysis. Then, applying virtual reality technology on this basis, three-dimensional presentation of the commercial building design scheme, taking the design of commercial space signage system as an example, the preset low-brightness color system, and the color and shape are single, the logo set A and the logo set B using high-brightness color system and changeable form are presented, expand 3D dynamic visual and behavioral simulations. At last, relying on ResNet image recognition technology, it analyzes the user's visual experience and usage effect. Experimental results show: There is a significant correlation between plane layout, spatial identification, familiarity of indoor space, and frequency of use, and visual perception is the main driving factor for choosing commercial buildings; using the comparative analysis of commercial logos, it is found that the average value of the confidence of set B is less than that of set A; in terms of significance, the average time of identifying all categories of logo set A is 0.68 s, and the average identification time of all categories of identification set B is 0.46 s; in terms of discrimination, it takes 0.28 s to correct the misrecognition of all categories of identification set A and 0.11 s to correct the misrecognition of all categories of identification set B, indicating that the design of the identification system uses bright colors and changeable forms, which are easier to use. The results indicate that the elevation, slope, hydrology, transportation conditions, economic indexes and cultural factors are important factors affecting the spatial distribution of traditional villages in a city. The analysis shows that the distribution of traditional villages is affected by natural conditions, social economic conditions, cultural factors and other factors, and the optimal layout of traditional villages can be strengthened from these aspects.

1. Introduction

In recent years, the importance of the home improvement market in the interior design industry has continued to increase, the reason is: The development of the real estate industry has rapidly increased the magnitude of the home improvement market and has a strong driving force for the development of design, building materials, furniture, electrical appliances, and other industries; in turn, it improves the quality of life of ordinary Chinese [1]. With the rise of some luxury houses and villa projects, large-scale, high-investment home improvement projects, it enables designers to display

their creative freedom; in some characteristic homestays and villa renovation projects in the construction of new countryside, it has further expanded the market share [2]. The performance of some home improvement companies has been accumulating to become listed companies, and the home improvement industry has entered the vision of investors, which has further attracted social attention.

In the digital age, the industry change of interior design is no longer partially perfect, but structural and even subversive. The interior designer group has to face the difficulties and move forward bravely. Must be clear: It is unavoidable that artificial intelligence replaces a large number of design

work, which does not follow design logic but industrial logic; Talented and creative designs and designers will be more popular, both because of their rarity and because of society's growing wealth; the group of interior designers is likely to continue to be layered, classified, and even divided [3]. In order to respond to different industrial, commercial, and technological changes, the reform of design education should not be limited to the tinkering of the original system but need to look forward to the future and make a big breakthrough!

2. Literature Review

Matheson, B. et al. proposed a strategic study on the combination of traditional physical buildings and virtual technology [4]. Zhu, Y. et al. have this statement on the interactive design system, "If a designer is needed to have a sense of belonging to the design program and be willing to contribute to the organization and operation of the design program, the most effective way is to let the designer interact with the design program in a way of dialogue, so as to shape the architectural space they want." The history of this interaction can bring new possibilities for designers and design programs to share goals and outcomes [5]. Wei, X. et al. proposed that the transformation of architectural information should be carried out in an orderly manner through the principles of "linking, juxtaposition, metaphor, analogy and socialization" and elaborated on a series of changes brought about by the development of interactive design, such as pan-interface ization, universal connection, and universal media [6]. R Wu et al. proposed and defined the participatory social innovation design method with "participation and collaboration," as the core, and through case analysis summed up the three levels of participatory design and applied them in practice [7]. Li, X. J. et al. proposed the application of virtual reality technology in participatory design, but the article only briefly mentioned the auxiliary role of virtual reality technology in different stages of participatory design, and the application of specific operation methods was not carried out. Details [8]. Phlmann, K. et al. discuss the application of the staged approach to the whole process of participatory design. The addition of digital technology enables participatory design to be refined and concrete, and thus closer to the concept of interactive design [9]. In recent years, the application of virtual reality technology in architectural design has also developed rapidly in China; at the same time, relevant theories and research have also achieved certain progress and results [10].

Existing research results of interactive design mostly focus on interactive multimedia technology and forms of expression, and less research on the interaction between users and design solutions. Therefore, on the basis of drawing on existing research theories, the author constructs an interactive design method for commercial buildings and guides the design from the feedback of users' psychological processes and behaviors [11]. As shown in Figure 1, this method mainly relies on virtual reality technology; in the early stage of design, a commercial building with real size is established to obtain the real scene of the design plan,

and then the virtual model is used for simulation experiments and analysis of the relevant survey data of the subjects to find out the design content in the scheme that does not meet the needs of use and modify and refactor it to form a positive feedback loop, which is also different from the traditional one-way push design process.

3. Research Methods

3.1. Thinking and Method of Interactive Design of Commercial Buildings Based on Virtual Reality Technology. The interactive design using virtual reality technology emphasizes the sense of experience, and the user produces subconscious reactions and related behaviors in a space close to the real world; it can more intuitively and truly record people's activity state and psychological emotions. Compared with the traditional design and communication methods through two-dimensional images and language description, it is more intuitive. Virtual reality technology integrates human-computer interaction technology, sensing technology, human-machine environment synchronization, etc.; it can effectively collect the feedback of the test subjects and carry out data analysis, thereby improving the work efficiency of designers, and at the same time saving costs and ensuring the quality of the design scheme, as shown in Figure 2 [12].

(1) The theoretical basis of interaction design

The interactivity of architectural interactive design is reflected in two aspects; one refers to the participation of the public in architectural design, and the other refers to the intervention of information technology in the architectural space, people, and buildings to form an obvious dynamic system, thus interact. Most of the traditional methods can only realize the one-way expression of the designer's ideas, while the interactive design method is that after the user interacts with the virtual simulation design, a series of behaviors bring about various associated variables, which are fed back to the designer.

Interactive design uses the process of information presentation combining virtual and real, real-time interactive virtual roaming experience, information feedback, scheme optimization, etc. By summarizing the behavior of the subjects in the virtual reality scene, the general rules of the user behavior can be obtained, or by the methods of dynamic images and computer image recognition obtained in the virtual reality model, they can be analyzed and processed, in order to obtain the impact factor or effective data [13]. The designer can, according to the analysis results, and combined with their own experience to optimize the design.

(2) The method and process of interactive design

Research and collection design impact factors: The theoretical basis of the interaction design method comes from the interpenetration theory under environmental behavior; this theory points out that the active role of human beings on the environment includes both material and functional

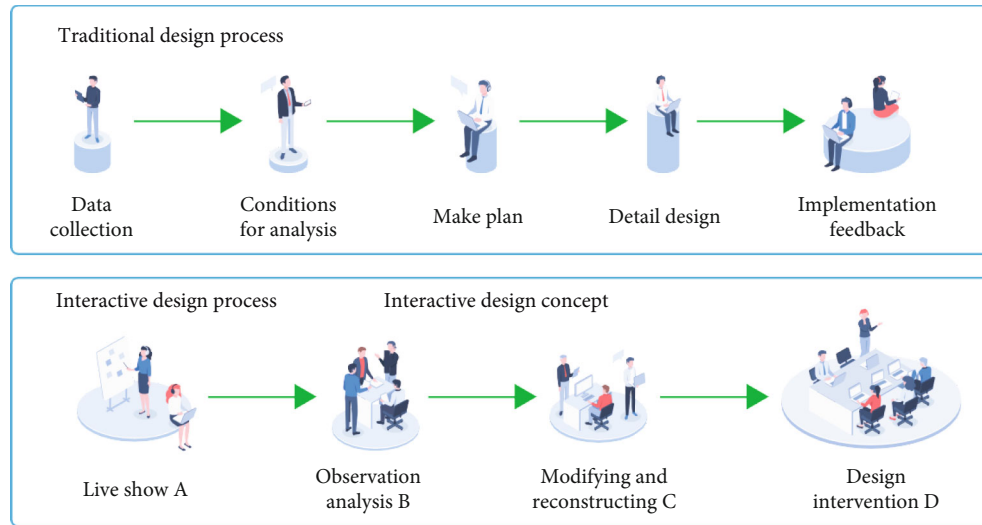


FIGURE 1: Schematic diagram of traditional design process and interactive design process.

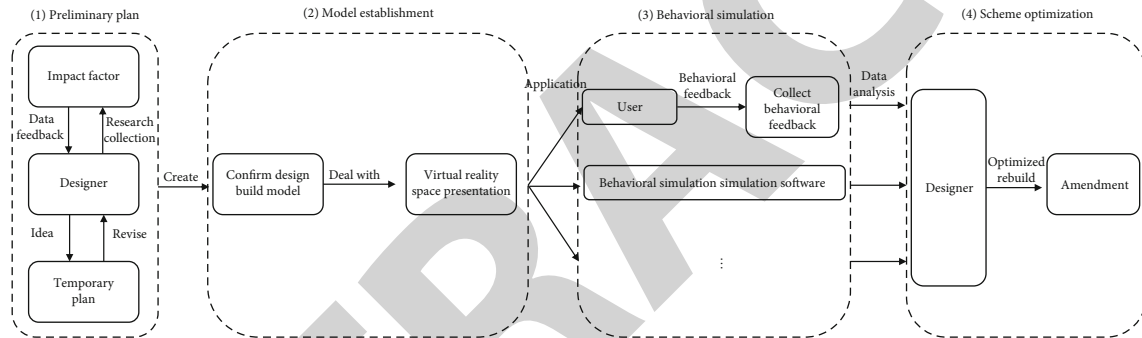


FIGURE 2: Interaction design method flow.

roles, as well as the role of value giving and reinterpretation. The core of the method is user behavior-oriented, analysis of the environment, and design based on this. Through the investigation of commercial space usage, the author summarizes the behavior and psychological characteristics of contemporary consumers, analyzes the factors that affect the use of commercial buildings, and guides the design of commercial buildings.

Realization of virtual scene: The preliminary design scheme is confirmed and modified after consideration, and the scheme is vectorized by traditional modeling software such as AutoCAD. The virtual reality scene construction is carried out on the determined architectural model, and 3DSmax, Revit, Mars, and other software are used for 3D simulation modeling and virtual reality scene rendering. In the modeling process, the interior space of the building should be strictly in accordance with the actual size, proportion, and structure of the model, so as to restore the actual shape of the building space to the greatest extent. At the same time, under the premise of satisfying the correct cognition of the tested person, the model can be optimized by simplifying the secondary components and complicated details to ensure the smooth operation of the hardware device [14].

Spatial experience and behavioral simulation: In the virtual 3D simulation model, the subjects can have a variety of

sensory experiences, and obtain psychological and behavioral information by using physiological data acquisition equipment such as eye trackers or subjective questionnaires; or apply software such as Unity3D and MassMotion3D and conduct various behavioral simulation experiments in the model. Due to the digital nature of virtual space, statistical programs can be present in the working environment, automatically record a large amount of behavioral information such as motion trajectories, in order to analyze the behavioral characteristics of users; it can also use artificial intelligence analysis methods such as image recognition to interface with virtual reality interactive dynamic three-dimensional scenes, simulate behavior, and get quantitative results.

Information feedback and solution optimization: In the virtual scene, the interactive behavior of the user can be fed back in real time, and the efficiency and pertinence of the feedback information can be ensured. Data statistical analysis methods, fuzzy evaluation methods, etc. can be used to analyze it, and accordingly, the internal laws of the data can be scientifically reflected, so that the obtained results are more reasonable. Through the analysis results, the designer can estimate the usage status and user's needs after the completion of the scheme, so as to optimize and modify the original design in a targeted manner.

3.2. Investigation and Analysis of Commercial Building Space Use Behavior. In order to test the validity and feasibility of the method, the author combines the investigation of a city's commercial center and gives an example to introduce the application of the interactive design method of commercial buildings.

(1) Case selection and research

The author conducts research on two popular shopping malls in a city as an example [15]. The two shopping malls selected by the author are typical commercial buildings in a certain city. They have the characteristics of small number of floors, large single-story area, emphasis on environmental shaping of public spaces, and complete public facilities. After visiting 5 large-scale commercial buildings in a city, I chose the shopping center in the suburbs and the urban life shopping area in the center of the city; these two commercial complexes are typical cases of multifunctional complexes and mature operating models. Both the two shopping centers have an area of more than 30,000 m², and the suburban shopping centers, due to their location and opening time, mainly serve the surrounding residents and middle-aged and elderly people [16]; the urban life and shopping area is a representative of modern shopping malls, and its characteristic architectural shape makes it a new landmark of a city; it mainly serves the citizens and tourists living in the city center, especially popular with young people; at the time of the author's research, although the urban life and shopping area has been opened for less than a month, it has already received more than one million passengers, residential, outdoor public activity areas, and supporting facilities in urban life projects; since 2009, it has gradually opened to the public, and it is very popular among tourists and citizens.

The purpose of this survey is to study the behavioral characteristics of users in commercial buildings and to explore the driving factors that affect users' choice of commercial buildings. The research on the driving factors of the interior space of commercial buildings is mainly carried out from the aspects of spatial perception, commercial format distribution, plane and function, architectural and site selection characteristics, and environment and public facilities. The author's pre-research on the needs of consumers in a city's shopping process found that most of the citizens who come to the mall do not care about the time cost, but prefer to have a pleasant shopping process, hoping to obtain information from the mall space, and carry out activities such as shopping, dining, meeting friends, parent-child, walking, enjoying, visiting, and resting. In summary, based on the psychological and behavioral characteristics of consumers in a certain city, the author establishes an index system of the questionnaire, which mainly reflects the users' subjective feelings and behavioral characteristics on the plane and function of commercial space, spatial perception, and external characteristics of buildings.

In February 2018, a survey on the behavior characteristics and satisfaction of commercial buildings was carried out in two shopping malls in a city, 100 questionnaires were randomly distributed in each shopping center, a total of 200

questionnaires were distributed, 192 were valid questionnaires, and the effective recovery rate was 96.0%. The content of the questionnaire includes the basic information of the respondents and the information on the user behavior patterns.

The author mainly studies the wayfinding behavior of users and separately extracts the wayfinding experience data from the questionnaire. The survey options and the proportions of each option regarding the subjective feelings of the wayfinding experience are shown in Table 1, from which it can be seen that users' subjective perceptions of familiarity and orientation perception of the two shopping malls are quite different.

The use frequency data of the two shopping malls will appear as the relevant variable *Y*, which is the judgment standard for the user's preference for the shopping mall. In the survey of suburban shopping malls, 39.58% chose to visit multiple times a month, while in urban life shopping malls, the highest proportion was the first visit, 58.33%. According to the author's on-site interview, it is found that the main reason for the difference in shopping frequency between the two shopping malls is that the suburban shopping malls have long operating hours in a certain city, while the urban life business district has just opened for a month at the time of the author's investigation, and citizens are unfamiliar with it.

(2) Data analysis

According to the questionnaire, the influencing factors were extracted from 3 aspects of users' subjective feelings about the shopping mall, and then they were classified and numbered in turn; a total of 7 main influencing factors were obtained, namely, traffic flow line, functional layout, spatial identification, and interior space, familiarity, environmental satisfaction, architectural features, and traffic accessibility, and used to mark (see Table 2). Using SPSS, each factor *X* and the frequency of use *Y* were used for correlation analysis; it can be found that there is a significant correlation between the spatial plane layout, spatial identification, and spatial familiarity with the frequency of use, and the correlation coefficients are all at a significant level [17]; among the three factors with significant correlation, spatial identification and familiarity both belong to the category of spatial perception; it is inferred from this that spatial perception is a driving factor that has a greater impact on users than spatial functions and building exterior features (see Table 3).

The AHP method is used to determine the weight of factors, the common methods are expert scoring and questionnaire survey, and the author adopts the questionnaire survey method [18]. In the design of the questionnaire content, through a pairwise comparison, the interior design elements of the commercial building of the party with higher demand are scored. The demand degree is divided into 5 levels, one element is "more needed" than the other, 3 points, "more necessary" is 2 points, the demand degree of both elements is "similar", 1 point, and "less necessary" is 1/2 points, "not required" counts as 1/3 point; according to this standard, the demand degree of commercial building interior design

TABLE 1: Survey values of respondents' wayfinding experience.

Store name	Research questions	Options	Proportion/%
Suburban shopping center	Familiarity with the mall	Very familiar	60.42
		A little familiar	31.25
		Unfamiliar	8.33
	When walking in the mall, feel the complexity of the space	Simple plane	43.75
		A little complicated	41.67
		Very complicated	14.58
		Always know	66.67
	Knowledge of the manufacturer's direction	Sometimes I know, sometimes I do not know	29.17
		I do not know since I entered the mall	4.16
	Is the mall guidance system sufficient?	Yes	87.50
No		12.50	
City life shopping district	Familiarity with the mall	Very familiar	12.50
		A little familiar	45.83
		Unfamiliar	41.67
	Consider the complexity of the mall	Simple plane	31.25
		A little complicated	50.00
		Very complicated	18.75
		Always know	31.25
	Knowledge of the manufacturer's direction	Sometimes I know, sometimes I do not know	66.67
		I do not know since I entered the mall	2.08
	Is the mall guidance system sufficient?	Yes	81.25
No		18.75	

TABLE 2: Extraction and classification of questionnaires.

Survey category	Investigation item	Numbering
Space and function	Traffic flow	X_1
	Functional layout	X_2
	Spatial identification	X_3
Spatial perception	Spatial familiarity	X_4
	Environmental satisfaction	X_5
External features	Architectural features	X_6
	Transportation accessibility	X_7

components is converted into equivalent, and finally calculated according to formula (1), the weight of commercial building interior design components at each level is obtained [19].

$$a = \frac{\sum mn}{J}. \quad (1)$$

In the formula, a is the average rating value of element A to element B ; m is the rating value; n is the number of people who marked “√”; J is the number of people surveyed, which is the score of the valid questionnaire.

(3) Research and analysis

According to the survey results of the user behavior of two shopping malls in a city, it is known that spatial percep-

tion is one of the main factors affecting the frequency of shopping malls. People's perception of the atmosphere comes from the relationship between space and environment, the relationship between spaces, etc. The environment becomes the “interface” of space perception, so the relative relationship between the environment and people becomes an important reference for space perception. Vision is the most important sense for humans to obtain external information; visual perception is the most basic way of spatial experience and the basis of emotional experience.

Respondents who were dissatisfied or generally satisfied with their wayfinding experience were interviewed for their satisfaction with their wayfinding experience and suggestions for improvement; most of them suggested improving the navigation system in the mall and the accessibility of some functional spaces.

4. Results Analysis

According to the analysis results obtained from the investigation, the author will take the optimization design of the indoor signage system of commercial buildings as an example and apply the interactive design method of commercial buildings in practice.

4.1. Virtual Simulation of Design Content. From the above survey, it is found that cognitive space is an important factor affecting users' choice of commercial space. Therefore, the author conducts a research on the optimization design of the signage system in the commercial space to improve the

TABLE 3: Correlation analysis between respondents' usage behavior and shopping mall usage frequency.

Place	X_1 Traffic flow line/Y frequency of use	X_2 Functional layout/Y frequency of use	X_3 Spatial identification/Y frequency of use	X_4 Spatial familiarity/Y frequency of use	X_5 Environmental satisfaction/Y frequency of use	X_6 Architectural characteristics/Y frequency of use	X_7 Traffic accessibility/Y frequency of use
Suburban shopping center	0.474**	-0.334*	0.377**	0.511**	-0.326*	0.141	0.172
City life shopping district	0.347**	-0.097	0.297**	0.551**	-0.171	0.339**	-0.121

Note: * and ** are significant correlations; * means $P \leq 0.05$; ** means $P \leq 0.01$.

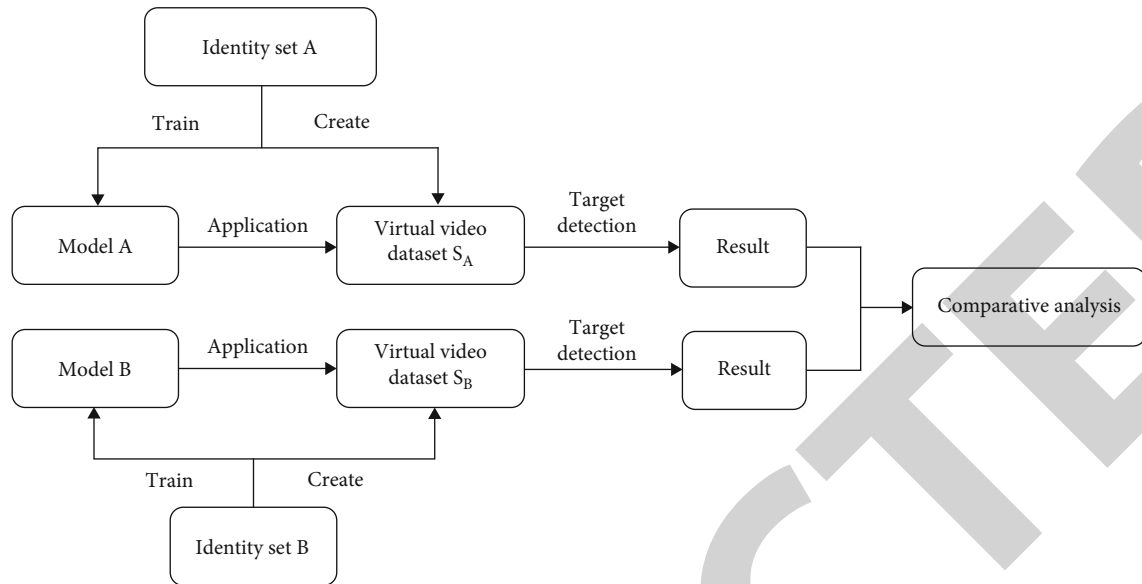


FIGURE 3: The flow of the analysis method based on target detection.

space awareness. The first step of the interactive design method is the virtual construction of the commercial building space model; using the virtual reality three-dimensional software MARS, combined with a commercial space design scheme, the simulation modeling is carried out, and the virtual space S is obtained. In order to optimize the operation experience, in the virtual construction of the building space, only the necessary traffic space and decorative elements in the indoor space are constructed, so as to minimize the number of model rendering surfaces and reduce system operations [20].

Summarize and analyze the logo systems widely used in shopping malls at present, draw on the logo design elements that are widely used, and summarize to obtain two sets of logo sets with different styles and establish models, which are recorded as set A and set B. In each set, it contains 11 logos. Logo set A is mainly gray in color, with 1 to 2 decorative colors, and is dominated by a single rectangle in shape; Collection B is mainly composed of bright colors in color, with a variety of decorative colors, and the shape is mainly geometric or special. Two sets of logo sets are placed in the virtual commercial indoor space S with the same distribution and placement method, respectively, to get virtual spaces S_A and S_B . At last, using virtual reality dynamic vision technology, from the user's perspective, with the same route and travel speed, roaming in S_A and S_B , respectively, and obtain the roaming vision video data in different identification sets for subsequent analysis.

4.2. Interaction and Feedback of Space Scene. According to the visual orientation of the identification system, the target recognition model based on the ResNet neural network structure is selected for analysis in this paper. The model can be docked with dynamic scenes, simulate the visual experience of users roaming in virtual commercial buildings, and make an effective quantitative evaluation of the sign system in the indoor space of commercial buildings.

(1) Behavior simulation recognition analysis method based on target detection

The virtual reality video datasets S_A and S_B simulate the process of users roaming in commercial buildings; on this basis, the visual experience of users can be simulated based on the target detection model, so as to quantitatively evaluate the sign design in commercial buildings, and the specific process is shown in Figure 3 [21, 22].

The above target identification detection model is applied to detect the virtual reality roaming videos constructed by the identification set A and the identification set B, respectively, and the identification results of the entire roaming process are obtained; the results include the identified location of the logo in the current field of view, the category, and a confidence score (the confidence score indicates the probability of the category appearing in the bounding box, and the appropriateness of the size of the bounding box). Example of recognition results for one of the frames [23].

Since each frame in the video represents the user's field of view at the current moment, the sequence between frames corresponds to the dynamic changes of the user when walking and changing the angle of view. Therefore, the detection results of all frames are combined for correlation analysis; it can be effectively analyzed that in this interactive state, the pros and cons of different logo design effects [24].

(2) Quantitative feedback on the recognition degree of behavior simulation

In terms of the significance of the logo, the confidence score is mainly used as the evaluation standard, which represents the confidence level of the detection model for the currently recognized logo, and corresponds to whether the user "sees clearly" the logo [25]. When the marker is farther from the user, the confidence score is usually lower, and the opposite is true when the distance is closer. Therefore, the

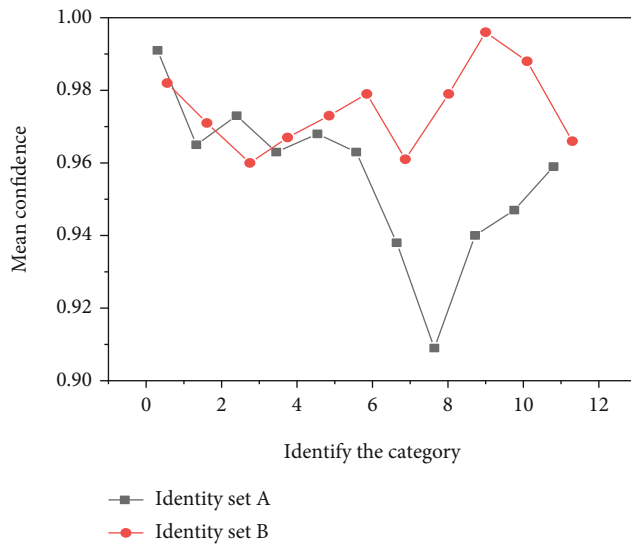


FIGURE 4: Mean confidence level of 11 types of labels in two sets of sets.

confidence score can express the distinctive feature of the logo, that is, whether the logo is easy to identify, easy to find, and so on. In terms of significance of the two schemes, the average identification time of all categories of identification set A is 0.68 s, and the average identification time of identification of all categories of identification set B is 0.46 s; in terms of discrimination, the time of correcting misrecognition of all categories of identification set A is 0.28 s, and it takes 0.11 s to correct the misrecognition of all categories of identification set B. The average confidence level of 11 identification categories of each group of identification sets is shown in Figure 4.

4.3. Data Analysis and Correction of Identification Results.

From the results, the author can find that in terms of significance, the average confidence level and average recognition time of logo set B are both smaller than those of logo set A, indicating that logo set B is more easily recognized by users in the same commercial building environment, and can be easily recognized by users and deliver relevant information more quickly; in terms of discrimination, the time used for correcting the misrecognition of set B is shorter than that of set A, indicating that it is easier to distinguish between different types of logos in set B.

The color, shape, and expression of the signboard have a great impact on the user's ease of identification and distinction, the B-type identification system in the commercial space is more likely to be noticed and accepted by users than the A-type identification system, and it shows that the morphological expression of the B-type logo has higher visual perception. Thus, the use of eye-catching colors and the use of a variety of colors can effectively improve the ease of identification. In the shape design of the sign system, it should break the currently commonly used design method of focusing on the conventional shape and a set of single shape of the sign, and the combination of various shapes or special shapes can effectively improve the distinguishabil-

ity. The combination of pictures and words in the logo system is more effective than pure words.

5. Conclusion

Applying virtual reality technology to interactive design methods provides new ideas for commercial building design. The author aims at the indoor space characteristics of commercial buildings, using virtual reality technology and guided by the interpenetration theory under environmental behavior, and obtains the interactive design method of commercial buildings with the interactive feedback between users and the design scheme as the main process. Taking two commercial centers in a city as an example to conduct a research, analyze the behavior characteristics of users and summarize the main driving forces that affect users' choice of commercial buildings. Correlation analysis was carried out on the survey data of users' shopping behavior, and it was found that the influencing factors significantly related to the frequency of use were layout, spatial identification, and spatial familiarity. From this analysis, spatial perception is a bigger driving factor affecting users' choice of commercial space than spatial functions and external features. According to the thinking of interactive architecture, the thinking process and method of interactive design of commercial buildings are obtained. Using virtual reality technology to simulate the commercial building space, a design plan with a realistic interactive experience is obtained, based on which users can obtain intuitive and effective behavioral feedback and conduct relevant analysis. Taking the optimization design of the sign system in commercial buildings as an example, the method and process of interactive design are shown; this method is universal and popular for the design of sign systems and commercial buildings.

Data Availability

The data used to support the findings of this study are available from the corresponding author upon request.

Conflicts of Interest

The authors declare that they have no conflicts of interest.

Acknowledgments

The study was supported by the Science and Technology Development Plan of Jilin Province. It is a research on 3D virtual reconstruction of traditional villages in Jilin Province based on laser point cloud Big Data. The Project Number is 20210203159 SF.

References

- [1] M. Safari and S. Asadi, "A screening method for lowering customer acquisition cost in small commercial building energy efficiency projects," *Energy Efficiency*, vol. 13, no. 8, pp. 1665–1676, 2020.
- [2] L. Zhang and M. Leach, "Evaluate the impact of sensor accuracy on model performance in data-driven building fault

Retraction

Retracted: Design and Implementation of College Students' Physical Fitness Test Management System Using IoT Smart Sensors

Journal of Sensors

Received 12 December 2023; Accepted 12 December 2023; Published 13 December 2023

Copyright © 2023 Journal of Sensors. This is an open access article distributed under the Creative Commons Attribution License, which permits unrestricted use, distribution, and reproduction in any medium, provided the original work is properly cited.

This article has been retracted by Hindawi, as publisher, following an investigation undertaken by the publisher [1]. This investigation has uncovered evidence of systematic manipulation of the publication and peer-review process. We cannot, therefore, vouch for the reliability or integrity of this article.

Please note that this notice is intended solely to alert readers that the peer-review process of this article has been compromised.

Wiley and Hindawi regret that the usual quality checks did not identify these issues before publication and have since put additional measures in place to safeguard research integrity.

We wish to credit our Research Integrity and Research Publishing teams and anonymous and named external researchers and research integrity experts for contributing to this investigation.

The corresponding author, as the representative of all authors, has been given the opportunity to register their agreement or disagreement to this retraction. We have kept a record of any response received.

References

- [1] J. Xu, Q. Chen, and X. Li, "Design and Implementation of College Students' Physical Fitness Test Management System Using IoT Smart Sensors," *Journal of Sensors*, vol. 2022, Article ID 1481930, 13 pages, 2022.

Research Article

Design and Implementation of College Students' Physical Fitness Test Management System Using IoT Smart Sensors

Jin Xu,¹ Qing Chen ,² and Xinwen Li³

¹School of Sports, Hunan City University, Yiyang, 413000 Hunan, China

²College of Physical Education, Sichuan University, Chengdu, 610065 Sichuan, China

³Department of Physical Education, University of Electronic Science and Technology of China, Chengdu, 610054 Sichuan, China

Correspondence should be addressed to Qing Chen; chen_qing@scu.edu.cn

Received 16 May 2022; Revised 26 June 2022; Accepted 4 July 2022; Published 18 July 2022

Academic Editor: C. Venkatesan

Copyright © 2022 Jin Xu et al. This is an open access article distributed under the Creative Commons Attribution License, which permits unrestricted use, distribution, and reproduction in any medium, provided the original work is properly cited.

As science and technology continue to advance and life standards continue to improve, poor living and study habits are common among today's college students, making their physical health deteriorate. At present, the physical fitness test management system of college students is not perfect. This paper studies the physical fitness test administration system for college students based on IoT smart sensors. It first briefly introduces the design of the physical health test management system and then proposes the IoT smart sensor network algorithm. With the rapid development of IoT, WSN has also grown rapidly as an important technical form of the underlying perception layer of the IoT. Then, this paper tests the data of the college students' physical fitness test management system under the Grey Relational analysis, and finally, it conducts an experimental discussion on the realization and testing of the college students' physical health management system. The experimental results of this paper showed that the college students' physical fitness test management system through the Internet of Things smart sensor can quickly respond to the visits of multiple clients, with relatively high processing efficiency, and the efficiency is increased by 60%. The practical interface designed and implemented by this system has excellent practicality. The system interface uses a light blue background, which has good comfort in application, and the system has complete functions, which can meet the general requirements of university system health management.

1. Introduction

As the successor and mainstay of contemporary socialism, promoting the development of students is the starting and final focus of school work. The State Council further emphasized the importance of the development of physical health of young people, clearly stating that in the physical and mental health of young people, strong physical fitness is a symbol of civilized society, which is a key facet of the country's overall power. It can be seen that there is a close relationship between youth physique and national development. The State Council has also promulgated relevant documents for school sports work, fully demonstrating that school sports work has become a national strategy, and these measures will surely further promote the reform and development of school sports work. Improving the physical

quality of students within the scope of colleges and universities and comprehensively assessing the physical health of college students are conducive to improving students' understanding of their own physical fitness and urging them to participate in physical exercise.

In recent years, research on physical fitness has developed rapidly, but there are few studies on the management of physical fitness testing. It mainly conducts horizontal and vertical research on the related concepts and status quo of students' physical health. On the premise of abundant "research on management mechanism," it is of certain theoretical significance to build a more complete new mechanism of adolescent physical fitness test management by drawing on relevant theoretical knowledge and other disciplines. This paper studies the college students' physical fitness test management system based on the Internet of

Things intelligent sensor, aiming to provide reference for the construction of the college students' physical fitness test management system.

Physical fitness test can detect the quality of a person's physical fitness. In the current era of information networking, people often do not pay attention to their bodies. Especially in young people, lack of exercise also makes the incidence of disease higher and higher. Therefore, physical fitness testing has also become a hot research topic. The traditional health physique test has the characteristics of complicated operation and low efficiency. Lu et al. designed a set of health-related physical fitness testing methods for college students based on smart mobile terminals [1]. Wang and Chen mainly discussed the computer vision-based design of student fitness measurement system and analysis system of test data [2]. Huang et al. proposed that laboratory-based measures of fitness components could be used to predict WTST [3]. The aim of Melchiorri et al. was to describe a combined test to assess physical efficiency in a healthy Italian older cohort and to provide an overview of the physical progression of locomotor skills in various age classes. Due to its simplicity and applicability, test batteries have been proven to be a valuable tool for assessing multiple aspects of physical fitness in older adults [4]. They have done various researches on physical fitness and achieved relatively good results, but they did not focus on young people, which also caused the experimental results to be inconsistent with the current status quo. The study found that the IoT smart sensor-based physical fitness test administration system for college students has good results.

Several scholars have also made corresponding studies on smart sensors for the Internet of Things: Gabriella presents a novel industry compares for the calibration of intelligent grid transducers for conventional and nonconventional voltage and current transducers in the voltage spectrum from DC to several dozen kHz frequencies. Its precision performance allows the calibration of class 0.1 sensors under both sinusoidal and nonsinusoidal conditions [5]. The main contribution of Herrera-Quintero et al. is the development and realization of a prototype of intelligent sensors for ITS (Intelligent Transportation Systems). The prototype integrates and incorporates an IoT approach using serverless and microservice frameworks to help Bus Rapid Transit's (BRT) transportation programming system [6]. Dissanayake et al. concentrated on devising a transducer that measures fluoride and hardly in well water through an auto regime. Here, a simple colorimetric method was employed to develop the proposed optical sensor, using SPADNS reagents and a complexometric titration of the color change procedure [7]. They all explained the application of smart sensors in various fields well and achieved good results, but this paper studies the statistics of smart sensors in physical fitness test data and the establishment of models, which is inconsistent with current research hotspots.

This article investigates the physical performance test management system for college students supported by intelligent sensors based on the IoT. Through experiments, it is known that the college students' physical fitness test management system based on the IoT smart sensor can quickly respond to the visits of multiple clients, which has a very

high processing effect, and its efficiency is increased by 60%. Through systematic analysis and comprehensive evaluation, students can have a more intuitive understanding of their physical health status. At the same time, suitable teaching arrangements can be made for students with different physical conditions to improve the teaching effect.

The innovation of this paper is reflected in the following: (1) it analyzes and introduces the design of the physical health test management system; (2) it expounds the algorithm of the Internet of Things intelligent sensor network and introduces the gray correlation analysis; (3) it conducts experimental analysis on the realization of college students' physical health management system. We provide additional explanations in the introduction section of the paper.

2. Design and Implementation Method of College Students' Physical Fitness Test Management System Based on IoT Smart Sensors

2.1. Design of Physical Fitness Test Management System. In the college students' physical health test system, considering the system convenience and maintenance cost, the B/S structure is mainly used in the system platform architecture, which is also the more popular software architecture at present [8, 9].

The B/S structure includes a browser, a Web server, and a database server, as shown in Figure 1. Among them, part of the transaction logic is completed in the front end, while the server side completes the main transaction logic. The data interaction between the browser and the database is completed by the Web server, so that the system users can use the browser to send their own requests to the server. The server performs query processing on the request and then feeds back the processing result to the system user. In this way, the client only needs to configure simple client software, and the work is simpler. The client only needs to complete simple operations, and the performance requirements for the client are greatly reduced, which also avoids the maintenance personnel from taking too heavy maintenance tasks on the client. The server needs to process all requests sent by the client, access the database, etc., which is a heavier burden than the client [10].

In this architecture, a three-layer browser architecture of data management layer, user interface layer, and middle layer are used. Each layer is independent of each other and does not interfere with each other. The three-tier architecture is gradually developed with the development and maturity of middleware technology [11]. The system uses middleware as the underlying platform to realize the interconnection and communication between the client and the server; it connects the application program and the database; the system develops, runs, deploys, and manages a three-tier browser system [12]. Compared with the C/S structure, the B/S structure has the following characteristics:

- (1) The use cost and technology are simple
- (2) The data security is high

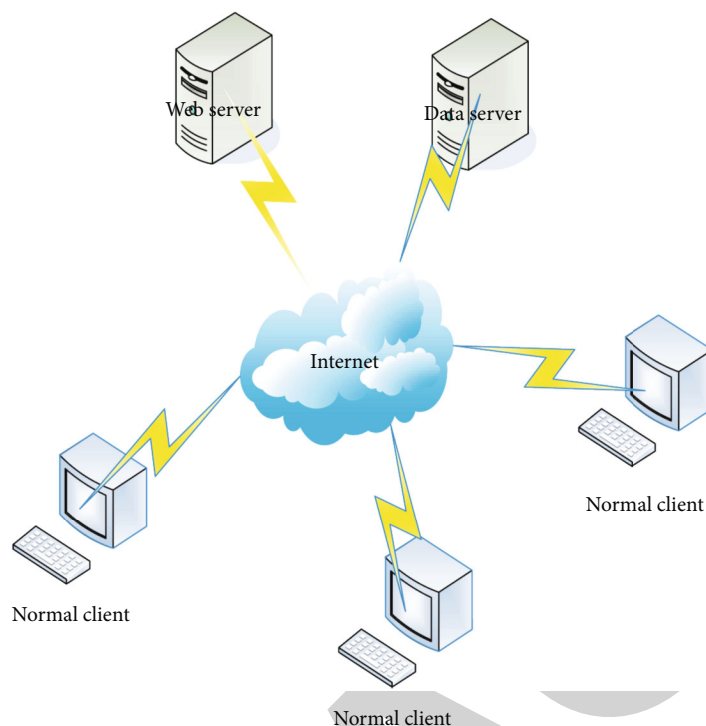


FIGURE 1: B/S frame structure diagram.

Under the B/S architecture, all data are stored on a centralized database server, and clients do not need to store business-related data, nor do they need to store database links [13]. In this way, the security of the data is further guaranteed. Based on the physical fitness test-related request of college students in this paper, the framework diagram of the system design is shown in Figure 2.

The primary subscribers in the structure of this system are students, faculty, and administrators. The application is classified into user interface layer, application service layer, and data layer [14]. The basic structure of the system network hardware is shown in Figure 3.

2.2. IoT Smart Sensor Network Algorithms. With the rapid development of IoT, WSN has also grown rapidly as an important technical form of the underlying perception layer of the IoT. Many sensors form a smart sensor network in a static or dynamic state, which adopts a self-organizing and multihop structure [15]. In the scope it covers, each sensor node senses and collects the information of the sensed object, processes it, transmits it, and finally accepts it by its owner [16]. The network nodes will automatically compress the collected data and periodically send the collected data to the Internet cloud computing platform. At the same time, the data in the cloud is regularly updated, which can reduce the storage and processing requirements of the sensor, reduce the storage capacity of the sensor, and reduce the power consumption of the sensor. Inexpensive, compact, and low power consumption are important features of sensing nodes. Sensor nodes in WSN have functions such as sensor, data processing, and communication [17].

2.2.1. LED Lightweight Encryption Algorithm. The serpent-type S box is used in the LED encryption algorithm. The maximum difference probability and the linear approximation deviation of the algorithm are both 2^{-2} . The row shift is in the form of a circular left shift j nibble, so that 4 of each column can be scattered into 4 different columns. The LED uses a maximum distance-divisionable code matrix based on a single nibble-level linear feedback shift register. In hardware implementation, only one nibble-level LFSR needs to be implemented, so the required area is relatively small [18]. In hardware implementation, only one nibble-level LFSR needs to be implemented, so the required area is relatively small.

The LED encryption algorithm requires almost no key arrangement and uses the master key directly. The encryption of the LED algorithm is to alternately use the round key plus roundAdd and step functions for 64bit data packets. Round key addition is to use the "XOR" method to import the round key into a state, and the step function is used to perform the main transition. After many iterations, packets of encrypted information can be obtained [19]. The algorithm for adding the LED wheel key is as follows:

$$\text{Function roundAdd}(\text{STATE}, R_m) = \text{STATE} + R_m. \quad (1)$$

The step function of LED is composed of 4 round functions, and the round function is composed of Add Constants, SubCells, Shift Row, and Mix Columns Serial operations [20]. LEFR is initialized to a state of all 0s, and an update is completed before the Add Constants

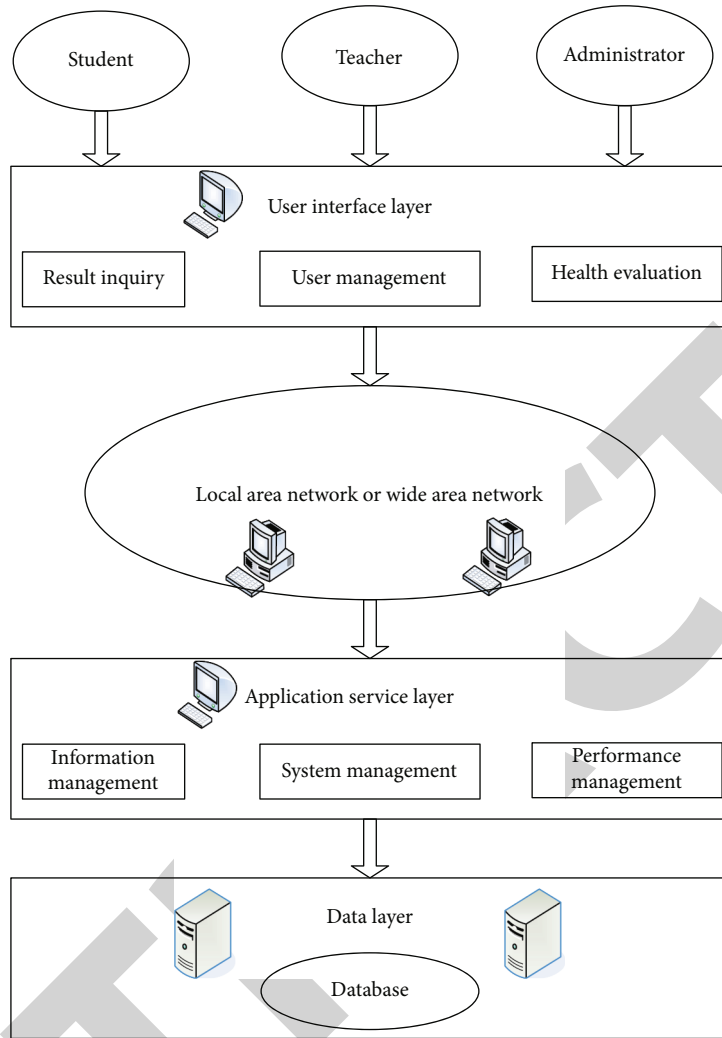


FIGURE 2: System architecture block diagram.

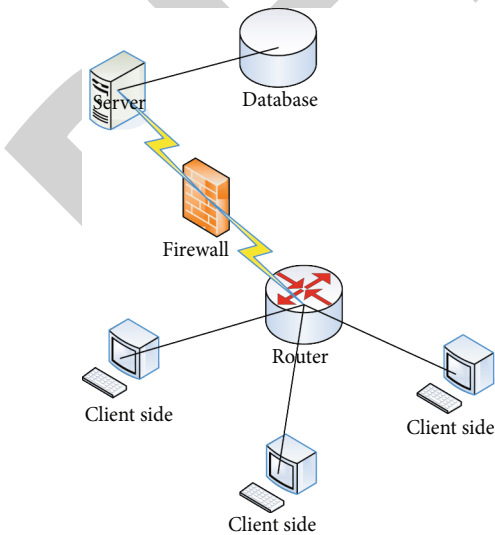


FIGURE 3: Hardware architecture diagram.

operation is performed in each round. SubCells is to replace the value of each nibble m_1 with the value after the 4×4 bitS box $S:P_2^4 \rightarrow P_2^4$ operation, and every time it is $0 \leq j \leq 15$, there are

$$(n_{j*4}, n_{j*4+1}, n_{j*4+2}, n_{j*4+3}) := S(m_j) = S(n_{j*4}, n_{j*4+1}, n_{j*4+2}, n_{j*4+3}). \tag{2}$$

Shift Row treats the intermediate state as a 4×4 matrix:

$$N = \begin{cases} m_0, m_1, m_2, m_3, \\ m_4, m_5, m_6, m_7, \\ m_8, m_9, m_{10}, m_{11}, \\ m_{12}, m_{13}, m_{14}, m_{15}. \end{cases} \tag{3}$$

At that time, the j th of the matrix was shifted to the left j positions: Mix Columns Serial is to continuously

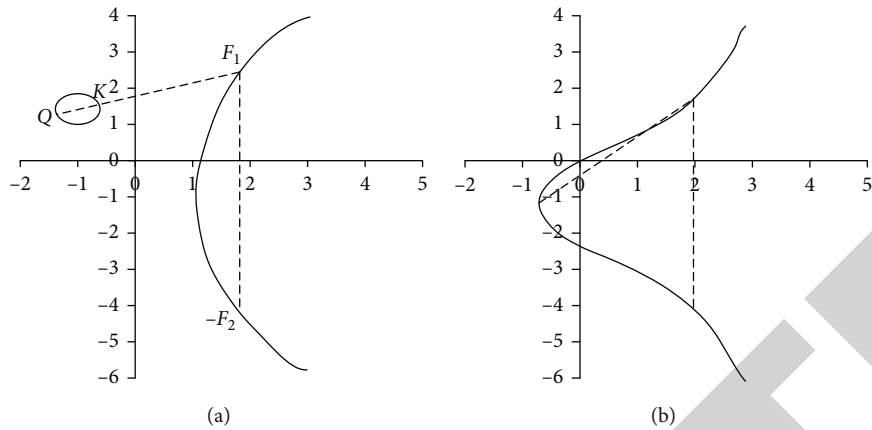


FIGURE 4: Example of an elliptic curve.

multiply the matrix 4 times, and the irreducible polynomial is $A_4 + A + 1$ as follows:

$$S = (X)^4 = \begin{cases} 0, 1, 0, 0, \\ 0, 0, 1, 0, \\ 0, 0, 0, 1, \\ 4, 1, 2, 2, \end{cases} = \begin{cases} 4, 1, 2, 2, \\ 8, 6, 5, 6, \\ B, E, A, 9, \\ 2, 2, F, B. \end{cases} \quad (4)$$

LED-64 is the master key that uses 64bit repeatedly, and the round key is to regard the master key as the sequence P_0, P_1, P_2, P_3 of nibble.

The operation of fetching the key is expressed as

$$PS_i^j = P_{i+j \cdot 16 \bmod l}. \quad (5)$$

2.2.2. SM2 Algorithm and SM4 Algorithm

(1) *SM2 Algorithm.* ECC is an ECC algorithm based on the discrete logarithm problem of point groups on elliptic curves. The elliptic curve equation used by the SM2 algorithm is $b = a^3 + xa + y$. After the coefficients x and y are determined, the unique curve is determined. The advantages of SM2 algorithm are mainly security, low memory size, and quick signal speed. As a kind of public key operator, the SM2 operator can implement signature, signature verification, encryption and decryption, and key negotiation.

To study the SM2 algorithm, first, an elliptic curve should be introduced in a limited area. An elliptic curve is a plane curve determined by the Wellstar equation and can be expressed as

$$Q : b^2 + xab + yb = a^3 + wa^2 + pa + t \quad (6)$$

Among them, w, p, t, x, y all belong to finite fields $GS(q)$. The set of points on the elliptic curve includes the set of all points (a, b) in the above equation and an infinite point O . The infinite point O is a special point on the set of elliptic curve points, which does not exist on the elliptic curve E . If three points belonging to the set of elliptic curve points

lie on a straight line, then the sum of these three points is 0. Figure 4 is an example of two commonly used elliptic curves.

The SM2 algorithm is mainly based on the elliptic curve whose base domain is the prime domain and the binary extended domain. This chapter mainly introduces the SM2 algorithm based on the prime domain elliptic curve. Let p be a prime number consisting of p prime numbers in $\{0, 1, 2, 3, \dots, p-1\}$ to form F_p , and F_p is called the prime field. The prime field used by the SM2 algorithm is fixed, and the elements contained in prime field F_p satisfy the following operation rules:

(i) Addition operation rules: set $x_1, x_2 \in F_p$, then,

$$x_1 + x_2 = (x_1 + x_2) \pmod{p}. \quad (7)$$

(ii) Addition rules: set $x_1, x_2 \in F_p$, then,

$$x_1 \cdot x_2 = (x_1 \cdot x_2) \pmod{p}. \quad (8)$$

(2) *SM4 Algorithm.* The SM4 algorithm is an encryption algorithm based on the same encryption key published by the United States Cryptographic Office, which is mainly used for large-scale data encryption and decryption. The SM4 algorithm is an iterative packet symmetric key encryption algorithm based on a nonequilibrium Festo structure. It mainly includes two algorithms: encryption, decryption, and key expansion. Both the SM4 cryptosystem and the cryptographic expansion mechanism are 32-round nonlinear iterative methods; the difference is that the round keys are used in reverse order. The ciphering procedure of SM4 method is illustrated in Figure 5.

(1) Sm4 encryption and decryption algorithm: assuming that the input plaintext N is $(N_1, N_2, N_3, N_4) \in (Z_2^{32})^4$, the output ciphertext is $(C_1, C_2, C_3, C_4) \in$

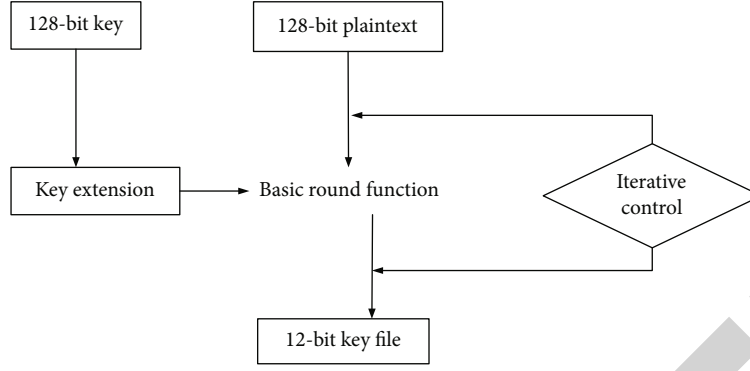


FIGURE 5: SM4 algorithm encryption process.

$(Z_2^{32})^4$, and the round key is $kr_j \in Z_2^{32}$, $j = 1, 2, \dots, 31$, then the encryption process of the SM4 algorithm is

$$\begin{aligned}
 N_{j+4} &= p(N_j, N_{j+1}, N_{j+2}, N_{j+3}, kr_j) = N_j \oplus D(N_{j+1} \oplus N_{j+2} \oplus N_{j+3} \oplus kr_j), \\
 (G_0, G_1, G_2, G_3) &= K(N_{32}, N_{33}, N_{34}, N_{35}) = (N_{35}, N_{34}, N_{33}, N_{32}).
 \end{aligned} \tag{9}$$

- (2) Key expansion algorithm: assuming that the encryption key is NR 1 and the round key is 2, then the algorithm for generating the round key is

$$\begin{aligned}
 (R_0, R_1, R_2, R_3) &= (NR_0 \oplus PR_0, NR_1 \oplus PR_1, NR_2 \oplus PR_2, NR_3 \oplus PR_3), \\
 kr_j = R_{j+4} &= R_j \oplus G'(R_{j+1}, R_{j+2}, R_{j+3}, CR_j).
 \end{aligned} \tag{10}$$

Among them, D' is basically the same as D in the round function in the above SM4 algorithm encryption and decryption algorithm.

Typical application scenarios of smart sensor networks are as follows:

The target parameters observed in the detection range, such as the intelligent sensor network for monitoring and monitoring of grassland, forest, ocean, and other environments, can realize the monitoring of air humidity, temperature, atmospheric pressure, etc. at a specific location or region. On the sensor node, a variety of sensing devices can be installed, and different information can be received at the same time, and the obtained signals can be collected and analyzed according to different sampling speeds.

In the detection of things of interest and estimates of their associated parameters, for example, in WSN applied to traffic, the sign of the trigger event is that the vehicle travels to the monitoring area, and the sensor node records the license plate, running direction, and speed of the vehicle passing through the detection area. The sensing module of the sensor node is set to a working state, and an event-triggered threshold is set. When the acquired data reaches

the preset threshold, other control modules will be triggered, and then the acquired data will be processed.

Classify and identify observations. For example, classification detection of systems with incomplete or incomplete information. In this paper, a data test is made for the management system of college students' physical fitness test under the Grey Relational analysis.

2.3. Grey Association. Grey Relational degree analysis is an important content in the study of Grey system theory. The Grey Relational degree analysis first collects the original evaluation indicators and then uses the dimensionless method. The obtained data are in the $[0,1]$ interval and form a matrix. It obtains the correlation coefficient matrix by solving the correlation coefficients between the indicators in the rows and columns of the matrix. Then, the weight of each indicator is calculated, and it is combined with the correlation coefficient to obtain the correlation between each indicator and comprehensively sort them. Grey correlation analysis is a comprehensive evaluation method that has been widely used in multi-index comprehensive evaluation in recent years. Before the systematic Grey Relational analysis, the features and factors were sorted. The following are some definitions.

2.3.1. Grey Correlation Factor. Assuming that there is a system factor A_j in the system, the observation data at the position of serial number r is $a_j(r)$, $r = 1, 2, \dots, m$; at this time, we call $A_j = \{a_j(1), a_j(2), a_j(3) \dots a_j(m)\}$ is the behavior sequence of the factor. If the serial number r represents a time, an indicator, or an object number, A_j is called a behavior time series, a behavior index series, or a behavior horizontal series. No matter what kind of sequence data, Greyscale correlation analysis can be performed. If the system factor has a dimension, it needs to be dimensionless first, and the negative correlation factor is transformed into a positive correlation factor, and then further processing is carried out.

Supposed that $A_j = \{a_j(1), a_j(2), a_j(3) \dots a_j(m)\}$ is the behavioral A_j sequence of system factors; generally, three transformation methods of initial value, mean value, and interval value can be used to perform dimensionless processing on the sequence, which are as follows:

(i) Initialization:

$$a_j(r)t_1 = \frac{a_j(r)}{a_j(1)}, \quad a_j(1) \neq 0, r = 1, 2, \dots, m. \quad (11)$$

(ii) Average:

$$a_j(r)t_2 = \frac{a_j(r)}{\bar{A}_j}, \quad \bar{A}_j = \frac{1}{m} \sum_{r=1}^m a_j(r), \quad r = 1, 2, 3, \dots, m. \quad (12)$$

(iii) Interval value:

$$a_j(r)t_3 = \frac{a_j(r) - \min_r a_j(r)}{\max_r a_j(r) - \min_r a_j(r)}, \quad r = 1, 2, 3, \dots, m. \quad (13)$$

In these three transformation methods, t_1, t_2, t_3 are called an operator. Corresponding to different methods, they are the initial value operator, mean value operator, and interval value operator. These operators can have dimensionless behavior sequences, but cannot be mixed. Only one of them can be selected for being dimensionless according to the needs of the actual problem. After transformation, these values can be called Grey correlation factors.

2.3.2. Calculation of Grey Relational degree. In the Grey system, we use the concept of Grey correlation degree to reflect the degree of correlation between different system factor sequences and feature sequences. In the Grey system space, the Grey Relational mapping is often not unique. Therefore, the degree of association cannot be simply described by the size of the grey relational degree, but is mainly described by sorting the grey relational degree and using the sorting result. There are several steps to calculate the Grey Relational degree:

First, determine the system sequence.

The systematic sequence mainly includes the characteristic sequence and the related factor sequence. Before analyzing systems and phenomena, the corresponding system behaviors must be screened out from the behavioral characteristics and corresponding sequences of the systems. The feature sequence of the system is expressed as $A_0(r) = \{a_0(1), a_0(2), a_0(3), \dots, a_0(r)\}$. After that, we need to screen out the factors that play a major role in the system behavior and determine the sequence of related factors, which are mainly expressed as follows:

$$\begin{aligned} A_1(r) &= \{a_1(1), a_1(2), a_1(3), \dots, a_1(r)\}, \\ A_m(r) &= \{a_m(1), a_m(2), a_m(3), \dots, a_m(m)\}. \end{aligned} \quad (14)$$

Second, find the difference sequence among the original serial and the sample serial.

Once the above three steps are used to obtain the correlation figures, the Grey Relational degree can be calculated using the equation given below.

$$\gamma_{0j}(r) = \frac{\min_j \max_r |a_0(r) - a_j(r)| + \gamma \max_r \max_r |a_0(r) - a_j(r)|}{\Delta_{0j}(r) + \gamma \max_r \max_r |a_0(r) - a_j(r)|}. \quad (15)$$

Here, γ is taken as 0.5, and then according to the formula,

$$\gamma_{0j} = \frac{1}{m} \sum_{r=1}^m \gamma_{0j}(r) \quad (16)$$

to find the Grey Relational degree γ_{0j} .

3. Experimental Results of the Design and Implementation of College Students' Physical Fitness Test Management System Based on IoT Smart Sensors

3.1. System Database Design. The concept of database is to integrate data information into an independent logical structure and organize and manage data according to the data structure. The database is the "warehouse" of the system, and its design has a great impact on the performance of the software. The system uses SQL Server 2008 as the database on the server side. Combined with the specific application of this subject, the main design data of the database are obtained, as shown in Table 1.

3.1.1. Student Information Sheet. The student information table is mainly used to store the student's login name and password, as well as the student's college, major, and course selection information, as shown in Table 2.

3.1.2. Physical Fitness Test Table. The physical fitness test table is mainly used to store data related to various physical fitness test items, including test number, test name, test content, test standard, test time, result, and description. Its logical structure is shown in Table 3.

3.1.3. Reservation Information Form. Reservation information table, as shown in Table 4.

3.2. Implementation and Testing of Physical Health Management System

3.2.1. Basic Flow of Program Operation. According to the overall functional design of the physical fitness test management system, before entering the system for examination and management, the system will verify and identify the logged in users. Whether it is a candidate exam or a teacher management, identity verification should be carried out first. The main operation flow of the system is shown in Figure 6.

After the student user logs in successfully, enter the exam reservation page, and the teacher will conduct the corresponding physical health test for the student during the

TABLE 1: System overall data sheet.

Serial number	Table name	Alias	Illustrate
1	S-TAB	Student information sheet	Store basic information of student users
2	TEST-TAB	Physical fitness test form	Store physical fitness test related content
3	SA-TAB	Statistical analysis table	Store the relevant results of statistical analysis on student physical data

TABLE 2: Student study sheet.

Field name	Illustration	Data length	Is it empty	Primary key
ID	Numbering	15	No	No
NAME	Student name	50	No	Yes
PASS	Student login password	10	No	No
ROLE	Student category	10	No	No
SEX	Student sex	10	No	No
MAJOR	Student major	50	No	No
INSTITUTE	Affiliated college	100	No	No
COURSE	Selected course	100	No	No

TABLE 3: Physical fitness test table.

Field name	Illustration	Data length	Is it empty	Primary key
ID	Test number	15	No	No
NAME	Test name	50	No	Yes
CONTENT	Test content	600	No	No
STD	Test standard	10	No	No
TIME	Test time	30	No	No
RESULT	Test result	20	No	No
DESCRIPTION	Describe	600	Yes	No

TABLE 4: Appointment information form.

Field name	Illustration	Data length	Is it empty	Primary key
Number	Student ID	15	No	Yes
NAME	Name	50	Yes	No
DATA	Appointment time	60	Yes	No
TYPE	Reservation project	10	Yes	No

reservation time. After the test is completed, the teacher will enter the corresponding test scores into the system, and the system will give a test report according to the test scores. Teachers will also give corresponding fitness guidance according to different students' physical health conditions.

Once the teacher user input his account code, he successfully signed into the system.

According to the actual needs of teachers, it should have management functions, including adding, modifying, deleting users, and managing grades. After the system completes the health evaluation and diagnosis, teachers need to analyze it and give corresponding guidance.

Administrator users can implement basic operations such as adding, deleting, and modifying teacher users and student users. In addition, they can complete the setting and management of system-related information.

3.2.2. Realization of the Main Functional Modules of the System. The main function of the system is to facilitate the physical health management of college students, so that students, teachers, and managers can easily understand the physical health of students, which provides more accurate and detailed theoretical basis for physical exercise and physical education of students and teachers. At the same time, it can also be provided to the relevant functional departments to give qualitative evaluations of students' physical health and provide positive help for the management of students' physical health test scores.

The system mainly consists of modules such as system administration, test appointment, user administration, fitness instruction, communication center, achievement control, message distribution, and fitness evaluation. Among them, user management, performance management, and health assessment are the main contents of the entire system. User management includes user login, user registration, password modification, and permission setting. Score management includes modules such as score query, score analysis, and score statistics. Through the health evaluation module, scientific analysis can be carried out according to the students' sports test results, and the correct physical health report can be obtained, and then according to the report, the exercise methods and sports programs suitable for the students can be formulated.

3.3. Health Evaluation and Diagnosis. At present, various colleges and universities mainly measure the physical health of college students by testing different sports, and then experienced teachers evaluate students' physical health according to the test results. This method is highly subjective, and the importance of the test indicators is determined artificially, which may lead to obvious deviations in the evaluation of students' physical health. Aiming at the shortcomings of the existing physical health evaluation, this study proposes to use the Grey correlation degree to analyze and comprehensively evaluate the results of the students' physical health

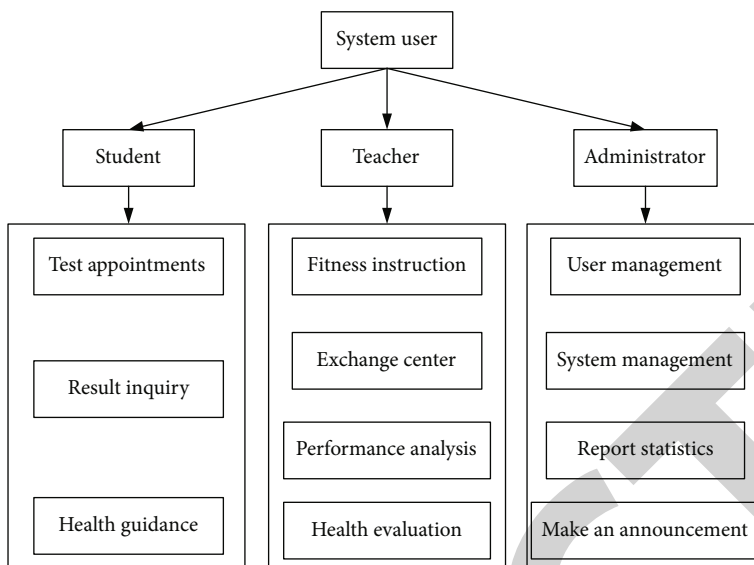


FIGURE 6: Operational flow chart of the system.

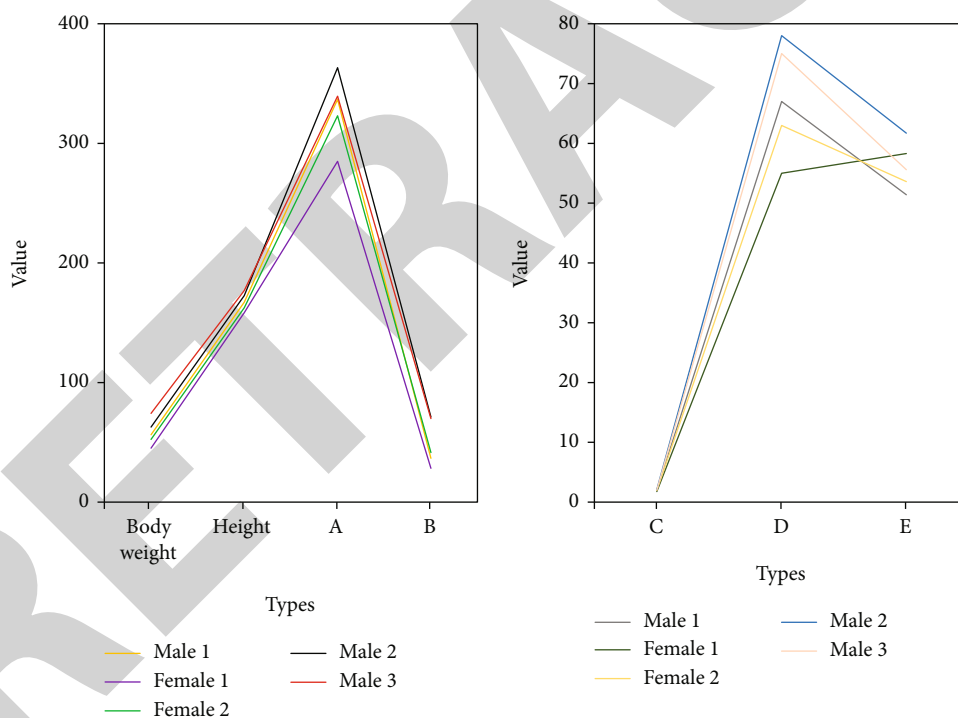


FIGURE 7: The raw data of sports index measurement of 5 college students randomly selected.

test. On the one hand, it is beneficial to reduce the subjectivity of evaluation, and on the other hand, the weight of each indicator on physical health is calculated, which greatly improves the accuracy of evaluation.

This article takes the sports measurement data of 5 college students in 2020 as an example to explain the process of the health evaluation method. The raw data of the test is shown in Figure 7, and the Quetole index is the value obtained by the student's weight (kg) * 1000/height (cm).

For students in grade 20, their standard Quetole index is basically stable. The index can be used to evaluate the body shape of college students. Grip strength BMI and standing long jump can reflect the physical fitness of college students. The larger the value, the better their physical fitness. The ladder test and vital capacity BMI are important indicators to measure the physical fitness of college students. The closer the two are to the limits of their peers, the better their physiological functions. In the figure, the Cetole index is

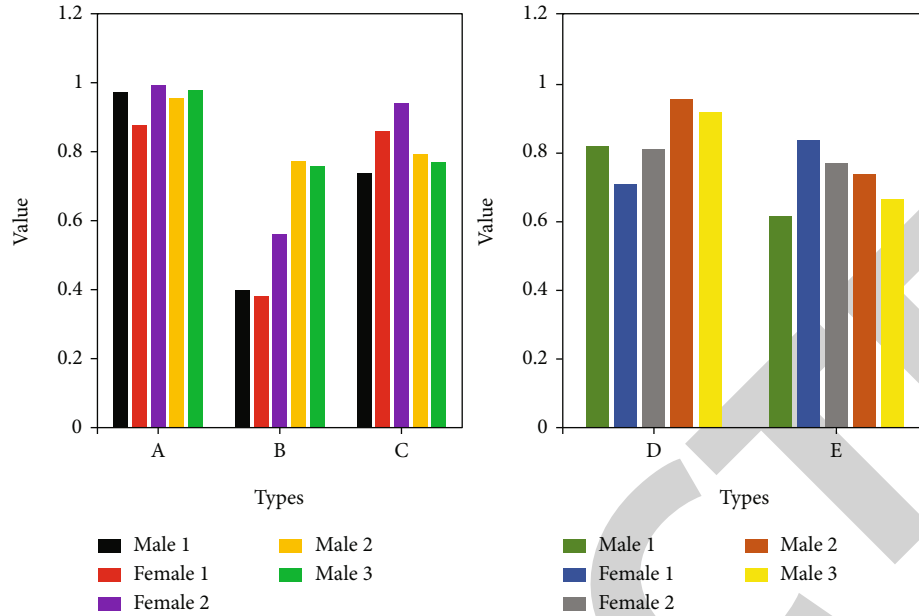


FIGURE 8: The dimensionless results of the measurement data of college students' physical health indicators.

represented by A , the grip strength body mass index is represented by B , the standing long jump (m) is represented by C , the step test index is represented by D , and the vital capacity body mass index is represented by E .

In the figure, taking the test scores of boys and girls of the same age and sex as the standard model value, the Grey correlation analysis was carried out on the index measurement scores of the college students to be tested. Finally, the comprehensive correlation degree of each index is obtained, and the physical health status of college students is determined by its value. The Grey Relational analysis method refers to a method that is affected by a variety of factors and uses the Grey Relational degree of the factor pair to express the influence of the pair. Grey Relational analysis means that r_0 is influenced by multiple factors r_n , and the Grey Relational degree of factors r_n to r_0 is used to express the influence of r_n to r_0 .

Before the Grey Relational analysis, the raw data of the test is preprocessed, the standard mode is $r_0 = (r_{01}, r_{02}, r_{03}, r_{04}, r_{05}) = 347, 92, 2.66, 82, 84$, and $r_{nl} = \min \{r_{nl}, r_{0l}\} / \max \{r_{nl}, r_{0l}\}$ can be obtained by dimensionless processing. r_0 is the reference sequence; r_1, r_2, r_3, r_4, r_5 are the comparison sequence. Subtract the elements corresponding to the comparison sequence and the reference sequence to obtain the absolute value of the difference, denoted by Δ_{nl} . Then, in the comparison sequence r_n , for the reference sequence r_0 , the maximum difference and the minimum difference between the two poles are, respectively, expressed as follows: $Q = \max_n \max_l \Delta_{nl}$. Then the Grey Relational degree at point l can be defined as $w(r_{0l}, r_{nl}) = (q + \beta Q) / (\Delta_{nl} + \beta Q)$. Where $0 \leq \beta \leq 1$ is the resolution constant, the larger the value, the greater the resolution, and vice versa. Normally, set the resolution constant $\beta = 0.5$. Figure 8 can be obtained by dimensionless processing of the above figure, and reference sequence $r_0 = (1, 1, 1, 1, 1)$ at the same time.

Calculate the absolute value difference; you can get Figure 9.

Among them, Q and q can be calculated as: 0.6619 and 0.0059, respectively, and the Grey correlation between the measurement data of college students' physical health index and the standard mode value can be calculated, as shown in Figure 10. Combining the weights of each measurement index obtained above, the correlation between body shape, athletic ability, and physical function can be calculated, and then the comprehensive correlation value of each student can be calculated.

Taking student male 1 as an example, based on the Grey correlation value, its health level can be analyzed. Due to the large Grey correlation value in terms of body shape, the student's body shape is good, but there are deficiencies in athletic ability and physical function. Then, experts can use this table as the basis for students' health judgment, combine their own experience, conduct health assessment for different students, and give corresponding physical exercise advice. Then, experts can use this table as the basis for students' health judgment, combine their own experience, conduct health assessment for different students, and give corresponding physical exercise advice.

Students can learn about their own health status based on the content of the health diagnosis. The health evaluation method in the system is used to obtain the health diagnosis opinions of the students participating in the test, and the teachers give exercise prescriptions according to the health evaluation opinions, which are used to guide the students to carry out corresponding exercise and exercise according to their own physical conditions, so as to enhance the physical health of the students.

3.4. System Test. The purpose of system testing is to check whether the software system implemented by programming

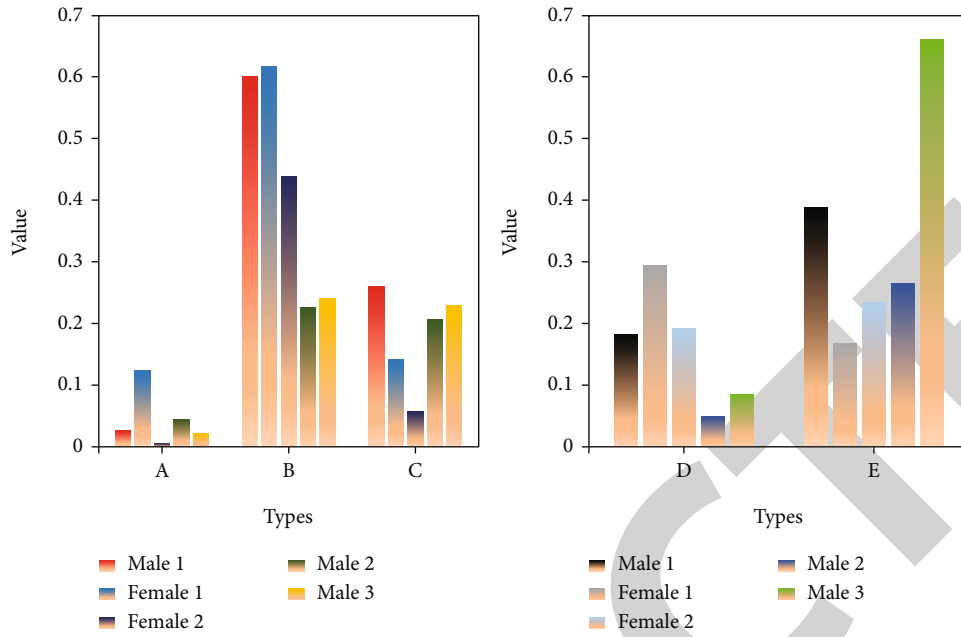


FIGURE 9: The absolute value of the difference between the comparison sequence and the reference sequence.

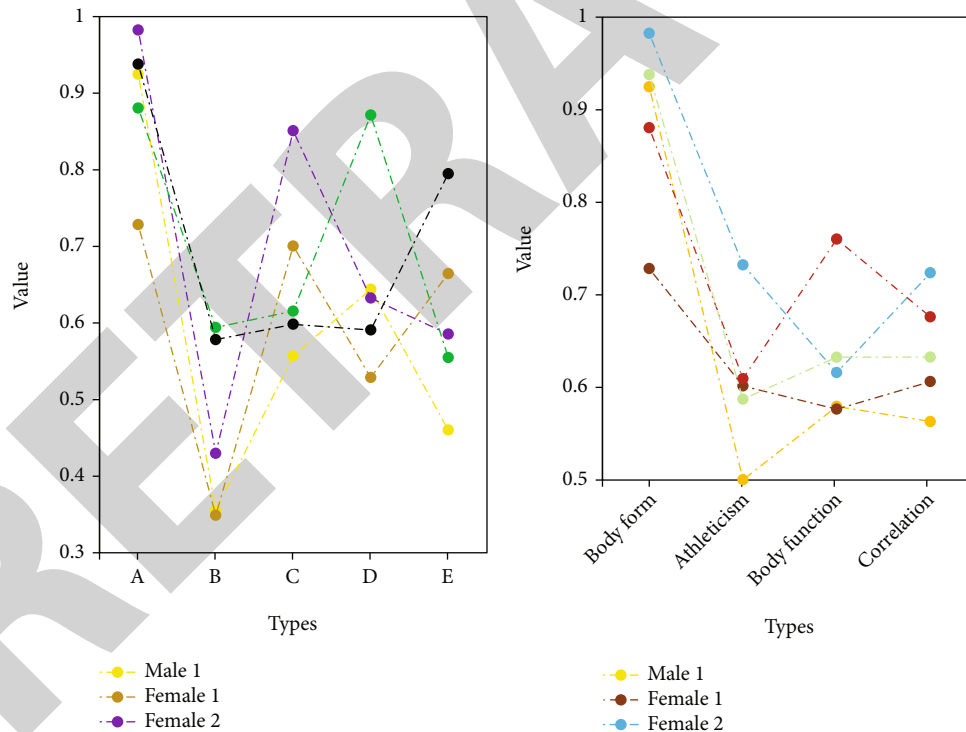


FIGURE 10: The Grey correlation between the measurement data of college students' physical health index and the standard model value.

meets the requirements, and it is the final review and verification of the results of the entire system development stage. In the development process of the system, although all stages of development have been checked, there are inevitably some omissions, and the legacy of these problems may eventually lead to problems or even paralysis of the system during operation. Therefore, after the system development is completed, the final test of the system is required to find

more problems. It can be said that software system testing is to find problems in the software. This paper will introduce and analyze the physical health management system of college students from the aspects of the system's operating environment and functional testing.

3.4.1. *System Function Test.* In this paper, the functional testing of the system mainly includes testing of system

installation/uninstallation, system interface, functional modules, security, and so on. In terms of functional testing, data verification testing and white-box testing are used to test whether each system function meets the requirements.

This article has tested the basic installation and operation of the system. The test situation is as follows: No errors were found during the installation and script running of the system; the server and client programs installed on the Windows 7 operating system, including the code and related content, are correct; the test is installed on computers with different hardware configurations; the system does not find errors and can start and run normally through the configuration. When there is a problem with the system operation, such as insufficient disk space, the system can capture the occurrence of the error, give the user an error prompt, and exit the system normally. From the above test situation, it can be found that the basic operation of the system is normal. Test of system operating interface: The operating interface designed and implemented by the system has good operability. The system interface adopts light blue design, which has better comfort during use. The system has complete functions, which can meet the basic needs of institutional health management in colleges and universities.

3.4.2. System Performance Test. In the aspect of system performance test, it mainly evaluates the security and stability of the system.

In terms of security, the database of the system does not allow direct operations but can only be accessed through the system, including adding, modifying, and deleting database data. The system has done strict authorization control management, and different users have different levels of authority. Only authorized users can perform database operations, and nonauthorized users can only query data, which ensures that the system has good security.

Stability mainly means that the system is not prone to errors during operation or can catch the corresponding errors and handle them appropriately. During the test, the system did not exit abnormally due to errors. In addition, by configuring multiple client programs to access the system server at the same time to test the processing and response speed of the system. The test results showed that the system can quickly respond to the access of multiple clients and has high processing efficiency, which increases its efficiency by 60%.

The performance test results of the system show that the system has good effects in terms of security and stability and can meet the basic functional requirements and performance requirements of college students' physical health test.

This paper starts from the overall goal of physical fitness test management and explains the main functional requirements of the system. It divides the system function modules, gives the detailed system realization, and tests it. Ultimately, this paper will implement a set of high-efficiency college students' physical health management system, comprehensively evaluate and analyze students' physical status through students' physical fitness test results, and provide corresponding decision-making opinions.

4. Conclusions

To address the current problems of physical health of college students, this paper has combined IoT smart sensors and Grey system theory to assess and manage the physical health problems of college students. A set of monitoring and management system for college students' physical health problems has been realized, which can better help the implementation of the national college students' physical health standards and urge students to realize the importance and necessity of physical exercise and physical fitness. The college students' physical health test management system realized in this paper has very important practical significance. It enables students to have a more intuitive understanding of their physical health status through systematic analysis and comprehensive evaluation. In this way, teachers can adjust the teaching content and teaching methods in a more targeted manner, make appropriate teaching arrangements for students with different physical conditions, improve the teaching effect, and truly achieve a purpose. The next work of this paper will further optimize the physiological health assessment method, improve the realization of the program and algorithm, and develop the multiplatform interactive use, so that the system has more generality and practical application significance.

Data Availability

The datasets generated during and/or analyzed during the current study are available from the corresponding author on reasonable request.

Conflicts of Interest

There is no conflict of interest.

Acknowledgments

This work was supported by Hunan Education Department Scientific Research Project: Research on the Development of Public Fitness Informatization O2O Model in Hunan Province (No. 19K015); the Educational Reform Project of University of Electronic Science and Technology of China: Freshman Project Courses: Physical Enhancement and Functional Training (No. 2019PBLF029); and the Ministry of Education, PRC: "Internet +" Era College Physical Education Teachers Professional Development Ability Training (No. 202101275011).

References

- [1] X. Lu, C. Yang, Y. Zhang et al., "Test method for health-related physical fitness of college students in mobile internet environment," *Mathematical biosciences and engineering: MBE*, vol. 16, no. 4, pp. 2189–2201, 2019.
- [2] L. Wang and S. Chen, "Student physical fitness test system and test data analysis system based on computer vision," *Wireless Communications and Mobile Computing*, vol. 2021, no. 1, Article ID 5589065, p. 8, 2021.

Retraction

Retracted: Accurate Detection of Intelligent Running Posture Based on Artificial Intelligence Sensor

Journal of Sensors

Received 12 December 2023; Accepted 12 December 2023; Published 13 December 2023

Copyright © 2023 Journal of Sensors. This is an open access article distributed under the Creative Commons Attribution License, which permits unrestricted use, distribution, and reproduction in any medium, provided the original work is properly cited.

This article has been retracted by Hindawi, as publisher, following an investigation undertaken by the publisher [1]. This investigation has uncovered evidence of systematic manipulation of the publication and peer-review process. We cannot, therefore, vouch for the reliability or integrity of this article.

Please note that this notice is intended solely to alert readers that the peer-review process of this article has been compromised.

Wiley and Hindawi regret that the usual quality checks did not identify these issues before publication and have since put additional measures in place to safeguard research integrity.

We wish to credit our Research Integrity and Research Publishing teams and anonymous and named external researchers and research integrity experts for contributing to this investigation.

The corresponding author, as the representative of all authors, has been given the opportunity to register their agreement or disagreement to this retraction. We have kept a record of any response received.

References

- [1] C. Zhang and K. Cheng, "Accurate Detection of Intelligent Running Posture Based on Artificial Intelligence Sensor," *Journal of Sensors*, vol. 2022, Article ID 6561159, 7 pages, 2022.

Research Article

Accurate Detection of Intelligent Running Posture Based on Artificial Intelligence Sensor

Chenguang Zhang  and Kun Cheng 

Jiyuan Vocational and Technical College, Jiyuan, Henan 459000, China

Correspondence should be addressed to Chenguang Zhang; 201701340208@lzpcc.edu.cn

Received 25 May 2022; Revised 9 June 2022; Accepted 2 July 2022; Published 16 July 2022

Academic Editor: C. Venkatesan

Copyright © 2022 Chenguang Zhang and Kun Cheng. This is an open access article distributed under the Creative Commons Attribution License, which permits unrestricted use, distribution, and reproduction in any medium, provided the original work is properly cited.

In order to solve the problem of low accuracy of human posture recognition during motion, the author proposes a human posture recognition and detection method based on multiple sensors. The method uses acceleration sensor, angular velocity sensor, and single-chip microcomputer to collect data; uses time domain and frequency domain analysis methods to analyze the collected data; and then uses Bayesian classifier to classify and identify the current motion posture of the human body. The obtained results are as follows: in the traditional method, with the increase of subjects, the accuracy of the classification method continues to decline; when the number of subjects reaches 50, the accuracy rate is only 60%; in the experiment, the zero crossing times of the acceleration signal axis are selected, and the axis area of the angular velocity signal is used as the characteristic item to distinguish the two different attitudes of going upstairs and going downstairs; the discrimination can reach about 90%. The authors combine the data collected by the acceleration sensor and the angular velocity sensor to perform feature extraction and classification, and the classification accuracy can reach more than 95%. It is proved that the method proposed by the authors can perform human gesture recognition very quickly and has a high accuracy rate.

1. Introduction

The degree of human health can be reflected by the posture of the human body, so it is more and more popular to judge the degree of physical health by the posture of the human body [1]. In the field of pattern recognition, the recognition of human motion gestures has become a hot research topic [2]. In recent years, with the rapid development of human-computer interaction and other technologies, human motion gesture recognition technology has been widely used in various aspects such as competitive sports, rehabilitation therapy, and somatosensory games [3]. Among these applications, in the field of biomedicine, the typical application is the application dedicated to the detection and evaluation of the daily life of the elderly and this special population undergoing rehabilitation therapy [4].

With the progress of the times and the development of society, the aging of the population is becoming more and more serious, and a new type of family living alone or called

empty-nest family has appeared in the society. This is because in rural areas in my country, most people aged 15-30 leave the countryside to study or work in other places. The elderly in rural areas always live alone with no one taking care of them, and at present, the country cannot provide good social security for these elderly people living alone [5]. Due to the decline of the functions of the elderly in all aspects of the body, the current social focus is more on the physical health of the elderly who live alone without care. In people's daily life, the posture of the human body is closely related to the health of the human body; the injury caused by the fall of the elderly is very serious and even endangers life safety; serious harm caused may include soft tissue injury, muscle tear, collision, cerebral hemorrhage or accidental head injury, and spinal fracture [6, 7].

Collecting the movement data of the elderly in daily life, establishing a large sample movement database, and then estimating and predicting the mobility of the elderly through data mining and analysis of movement information and predicting

the possibility of potential falls and, accidental falls due to various internal and external factors are of great significance.

2. Literature Review

The recognition of human motion poses has received more and more attention from researchers and enterprises. There are already corresponding products on the market. The current human motion gesture recognition technology can be divided into the following two types: the first is to use video technology to detect the motion state of the elderly [8]. The second is monitoring through portable devices [9]. The advantage of using the wearable portable body motion gesture recognition device is that there are no restrictions on the monitoring places of the elderly, the elderly can go anywhere at will and can monitor their movement status, which is superior to video surveillance [10].

The recognition system of human body motion posture based on video device and the monitoring system of human body motion state based on video method are to carry out specific monitoring on the places where the elderly often come and go; in this way, the movement state of the elderly can be monitored with high probability, and since the video technology can intuitively judge the fall posture of the elderly, it will also be of great help to the later treatment [11]. Scientific researchers have also conducted in-depth research on the recognition system of human motion and posture based on video devices and have achieved good results in video surveillance; however, video surveillance can only perform real-time monitoring of fixed places, which affects the travel of the elderly; if the elderly do not appear in frequently occurring areas, video surveillance will not work, and video surveillance will also cause the leakage of the personal privacy of the elderly [12].

Wearable sensor-based attitude monitoring system, a wearable-based portable motion state monitoring method, is not limited by the monitoring area, and because it is a portable device, therefore, it is easy to carry, and the elderly can decide where they want to go according to their own ideas, and at the same time, they can also let medical staff or relatives know their own motion status. When the motion parameters change, the current motion posture of the human body can be judged by algorithms [13, 14].

The disadvantages of the testing equipment currently on the market are as follows:

- (1) The reliability of detection is not high due to the limitation of sensor reliability and software algorithm
- (2) The cost is higher, the volume is larger, and it is not conducive to portability
- (3) Due to the limitation of product technology, the scope of application of the product is greatly limited, and the quality of the product needs to be improved [15]

In the 1950s, some scholars used sensors to judge the motion state of the human body [16]. With the development of MEMS technology, the use of sensor technology to monitor the state of human motion has achieved unprecedented development [17]. In addition, many technologies are borrowed from speech recognition technology and are also used

to judge the motion state of the human body [18]. In terms of human motion gesture recognition, some basic actions of people's daily life, such as walking, jogging, sitting, and standing, can also be successfully recognized [19, 20].

Based on the current research, the authors aim at the motion gesture recognition of wearable sensors, combined with the signals of the acceleration sensor and the angular velocity sensor; the collected data is analyzed using the time domain and frequency domain analysis methods, and then, the Bayesian classifier is used to classify and identify the current motion posture of the human body.

3. Research Methods

3.1. Circuit Planning and Design Production. In the process of recognizing the current motion posture of the human body, the most important step is to collect the data of the current motion posture of the human body; in order to achieve accurate classification and recognition of the current motion posture of the human body, it is necessary to rely on the analysis of these collected data; the accuracy of the collected data is of crucial significance for the subsequent modeling analysis, pose classification, and recognition using Matlab on the host computer; the realization of the device for collecting human motion and attitude information has also become an important issue [21].

The human motion information collection device follows the design guidelines of low cost, low power consumption, easy to wear, and strong environmental adaptability [22]. The human body motion information collection device includes a microprocessor, a three-axis acceleration sensor, a three-axis angular velocity sensor, and a power management module, which is responsible for collecting and storing motion data and information [23]. Among them, each sensor measures the vector data of acceleration and angular velocity, respectively. The microprocessor is responsible for collecting the information of each sensor and storing the collected information in its own Flash; when the human body motion information collecting device is connected to the upper computer, the stored information is read out, and it is sent to the host computer through the UART communication interface. The power management module is responsible for supplying power to the microprocessor, each sensor, and all the electronic components on the circuit board. The specific structural block diagram is shown in Figure 1.

3.2. Experiment Organization and Conduct. In order to obtain the characteristic data of the human body in various states, this subject needs to measure the daily activities of volunteers [24].

We collected data from 37 males and 13 females, for a total of 50 subjects in the specified motion poses. During the experiment, we counted the age, height, and weight of the subjects, mainly because in many previous research works, there have been cases of misclassification and identification due to individual differences of subjects. The mean and variance of subjects' age were 22.2 years and 0.7, respectively; the mean and variance of height were 1.72 meters and 0.006; and the mean and variance of weight were 64.04 kg and 2.93, respectively.

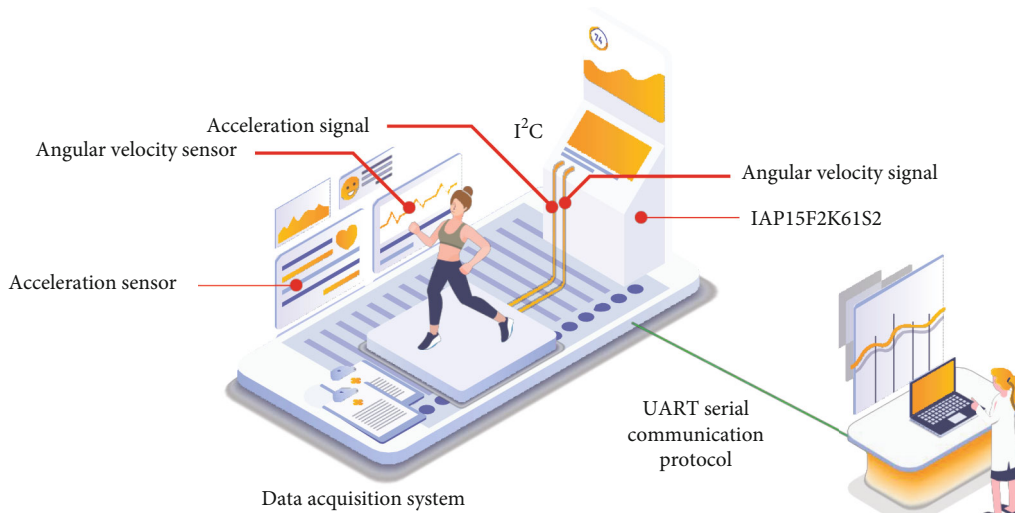


FIGURE 1: Structure block diagram of human motion gesture recognition system.

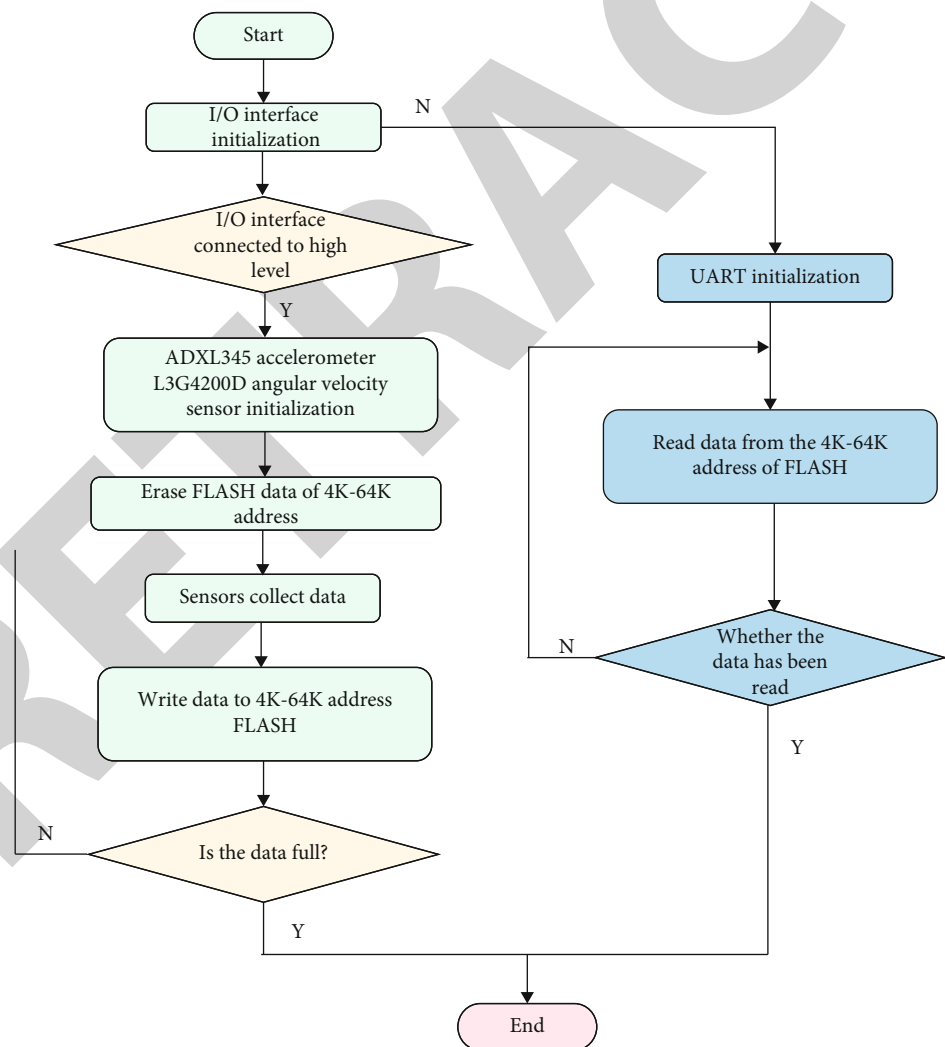


FIGURE 2: The embedded program flow chart of the data acquisition device of the human motion gesture recognition system.

TABLE 1: The traditional classification method of going up and down the stairs.

Classifier	Number of collectors	Number of action categories
Bayesian	1	5
L_1 distance	24	9
Decision trees, support vector machines, naive Bayes	2	8
K-NN	6	8
J48	6	8
MLP	6	4
GMM	50	5

During the experiment, we did not specifically require the subjects to exercise in a specified way [25]. The subjects all followed their usual habitual movement posture for the test. For example, in the process of collecting the movement posture data of going up and down the stairs, the subjects can be allowed to go up two steps at a time, or they can run downstairs. We have not made too many requirements for this.

3.3. Experimental Data Collection and Recording. The experimental data is collected and stored in the built-in 64K Flash of the IAP15F2K6IS2, and then, the data is transmitted to the host computer through the UART serial communication protocol. From the data sheet of the ADXL345 accelerometer, it is known that this accelerometer needs to use 6 bytes to store the collected data each time; these data will be stored in the IAP15F2K6IS2 in the form of two's complement; when using Matlab for time domain, frequency domain, and classification, the decimal data needs to be used; however, the data uploaded to the host computer by the UART serial communication protocol is in hexadecimal, so it is necessary to perform accurate data type conversion many times in this process.

For example, first, the sensor needs to use 6 consecutive bytes of data registers to store the data of a certain time. According to the introduction of the data sheet of the ADXL345 accelerometer, among these 6 consecutive bytes, the first two bytes of data is axis data, the middle two bytes of data is x -axis data, and the last two bytes of data is data for the y -axis. Then, use the IC bus protocol to store these data in the 64K Flash that comes with the microcontroller for temporary storage. Finally, a piece of data stored in the microcontroller is uploaded to the host computer through the UART serial communication protocol and stored in the ".TXT" text, and then, the data is processed by Matlab; these data need to be converted to decimal form before processing. "00FE" converted to decimal form is -1, "0002" converted to decimal form is +2, and "005A" converted to decimal form is +90. Multiply the data of each axis by the currently set resolution 3.9 mg/LSB of the sensor; it is the size of the acceleration we need to measure in the end, that is,

$$\begin{cases} a_x = -3.9g, \\ a_y = +7.8g, \\ a_z = +351g. \end{cases} \quad (1)$$

In the formula, a_x , a_y , and a_z represent the output results of x -, y -, and z -axes; g represents the acceleration of gravity, which is the unit of acceleration.

3.4. Data Collection of Human Motion Gesture Recognition System. The data acquisition device of the human motion gesture recognition system adopted by the authors uses the Keil uVision4 development environment and performs top-down software programming according to the compilation principle of C language; the data acquisition device includes a microcontroller IAP15F2K6IS2 and an acceleration sensor or a microcontroller IAP15F2K6IS2 and an angular velocity sensor.

The main functions of the microcontroller is as follows: determine the current state of collecting data or uploading data; collect sensor data in real time and write the collected data into Flash; and read data from Flash, and transmit it to the host computer through the UART communication interface. Therefore, the software programming in the microcontroller mainly includes the following modules, including microcontroller initialization, sensor initialization, data acquisition, and reading and writing. The steps required for the initialization of the microcontroller mainly include initializing the system clock and setting the timer and initializing the I2C communication interface protocol, the UART communication interface protocol, and various related peripheral I/O interfaces. The configuration required for acceleration and angular velocity sensors mainly includes initialization and zero drift calibration. The data acquisition operation is completed by using the I2C communication interface. The data read and write operation is to write data to the Flash of the microcontroller and read data from the Flash of the microcontroller. The data transmission operation is realized through the UART interface to transfer the data of the microcontroller, one-way transmission function uploaded to the host computer, as shown in Figure 2.

4. Analysis of Results

4.1. Comparison of Traditional Classification Methods for Going Up and Downstairs. When recognizing some basic daily actions, such as standing, walking, running, and falling, it is difficult to accurately identify the posture of the human body going up and down the stairs using the same method, as shown in Table 1. By analyzing Figure 3, it can be known that the researchers did not invite too many subjects during

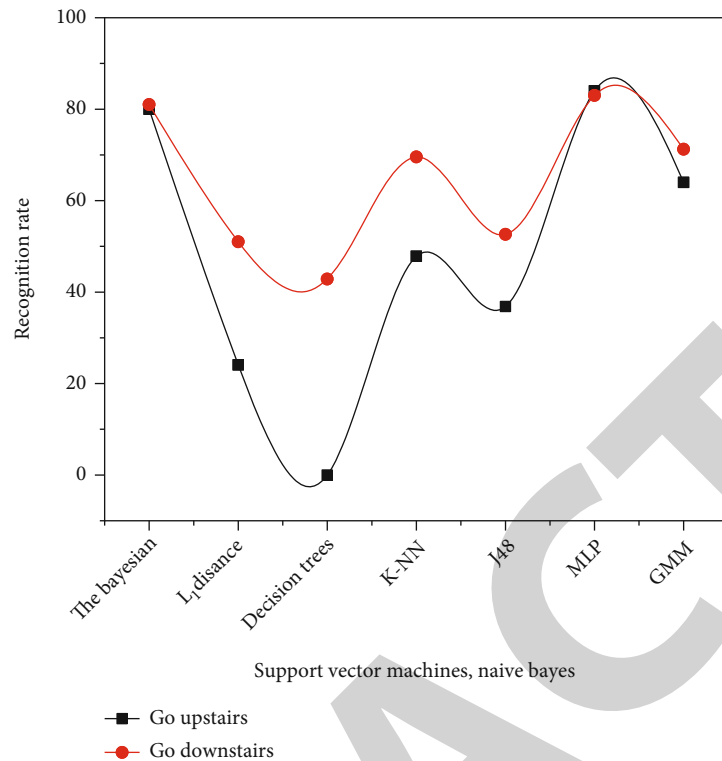


FIGURE 3: Recognition rate of traditional classification going up and downstairs.

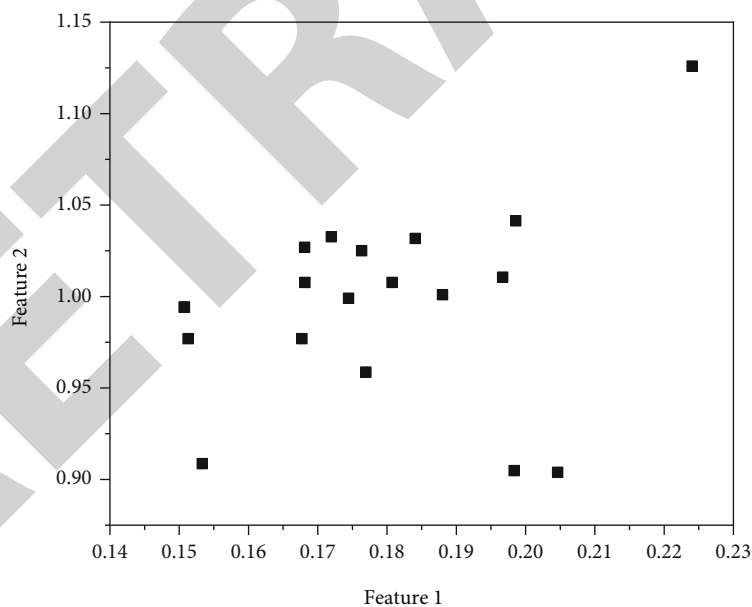


FIGURE 4: Classification results of going downstairs.

the experiment, and the recognition rate obtained was also very low, and with the increase of subjects, the recognition rate decreased significantly.

4.2. Feature Item Selection. In the process of distinguishing human body posture, in order to achieve the effect of accurately distinguishing the posture of the human body

going up and down the stairs, it is necessary to select the most representative features as much as possible, reduce the difficulty of classification, and realize the accurate analysis of the posture of the human body going up and down the stairs.

Feature extraction refers to finding useful information in the data and searching for the most representative features

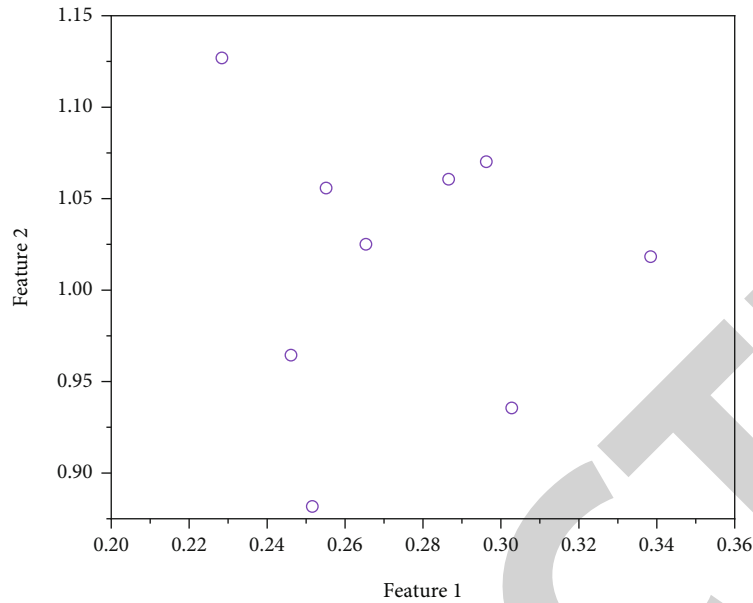


FIGURE 5: Classification results of going upstairs.

from many features, thereby reducing the difficulty of subsequent processing.

The zero crossing times of the x -, y -, and z -axes of the acceleration signal can be selected, combined with the area of the x -, y -, and z -axes of the angular velocity signal, as the characteristic item to distinguish the two different attitudes of going upstairs and going downstairs.

4.3. Classifier Selection. Before classification, the classifier is first trained on samples. Among the 50 sets of experimental data we collected, the feature items of 45 sets of experimental data were extracted for sample training of the classifier. Then, use the trained classifier to classify the features of the remaining 5 sets of experimental data. The classification results are shown in Figures 4 and 5.

As can be seen from the classification results in Figures 4 and 5, the authors combine the data collected by the acceleration sensor and the angular velocity sensor, perform feature extraction and classification to achieve accurate classification of the posture of the human body going up and down the stairs, and can relatively accurately distinguish the different postures of the subject going up and down the stairs.

5. Conclusion

In the field of pattern recognition, the recognition of human motion gestures has become a hot research topic. In recent years, with the rapid development of human-computer interaction and other technologies, human motion gesture recognition technology has been widely used in various aspects such as competitive sports, rehabilitation therapy, and somatosensory games. However, the recognition of human motion posture is still in its infancy, and the distinction of many human motion postures is extremely difficult, and there are many technical problems to be solved. Although sensor-based

human motion gesture recognition technology has developed rapidly in recent years, there have been many studies that can accurately identify the human body in the process of daily life activities; the most basic gestures are shown; the authors study the posture of the human body going upstairs and downstairs. The result obtained is as follows:

- (1) The collection of motion data is the basis of gesture recognition research. The authors' portable human motion information acquisition device is composed of a three-axis acceleration sensor, a three-axis angular velocity sensor, a microprocessor, and a power management module. The collected data is stored in the 64K Flash that comes with the microprocessor, and then, the stored data is uploaded to the host computer through the UART protocol for subsequent data conversion, calculation, and analysis
- (2) Using the time domain, that is, the acceleration modulus algorithm to identify the current motion posture of the human body, can quickly identify the current motion posture of the human body, but if the time domain-based recognition method is simply used, it is easy to cause errors and confusion in posture recognition. In order to improve this recognition error, we combine the frequency domain analysis method to analyze the frequency domain characteristics of the signal to distinguish some basic daily postures of the human body (especially the falling posture of the human body) and improve the accuracy of the recognition of some basic daily postures of the human body
- (3) A Bayesian classifier is applied to solve the confusion problem of upstairs and downstairs movements. First, filter and calculate the data collected by the acceleration sensor and angular velocity sensor.

Retraction

Retracted: Application of Internet of Things Technology in Mobile Education of Smart Campus Culture and Etiquette

Journal of Sensors

Received 17 October 2023; Accepted 17 October 2023; Published 18 October 2023

Copyright © 2023 Journal of Sensors. This is an open access article distributed under the Creative Commons Attribution License, which permits unrestricted use, distribution, and reproduction in any medium, provided the original work is properly cited.

This article has been retracted by Hindawi following an investigation undertaken by the publisher [1]. This investigation has uncovered evidence of one or more of the following indicators of systematic manipulation of the publication process:

- (1) Discrepancies in scope
- (2) Discrepancies in the description of the research reported
- (3) Discrepancies between the availability of data and the research described
- (4) Inappropriate citations
- (5) Incoherent, meaningless and/or irrelevant content included in the article
- (6) Peer-review manipulation

The presence of these indicators undermines our confidence in the integrity of the article's content and we cannot, therefore, vouch for its reliability. Please note that this notice is intended solely to alert readers that the content of this article is unreliable. We have not investigated whether authors were aware of or involved in the systematic manipulation of the publication process.

In addition, our investigation has also shown that one or more of the following human-subject reporting requirements has not been met in this article: ethical approval by an Institutional Review Board (IRB) committee or equivalent, patient/participant consent to participate, and/or agreement to publish patient/participant details (where relevant).

Wiley and Hindawi regrets that the usual quality checks did not identify these issues before publication and have since put additional measures in place to safeguard research integrity.

We wish to credit our own Research Integrity and Research Publishing teams and anonymous and named external researchers and research integrity experts for contributing to this investigation.

The corresponding author, as the representative of all authors, has been given the opportunity to register their agreement or disagreement to this retraction. We have kept a record of any response received.

References

- [1] Y. Guo, "Application of Internet of Things Technology in Mobile Education of Smart Campus Culture and Etiquette," *Journal of Sensors*, vol. 2022, Article ID 6321784, 10 pages, 2022.

Research Article

Application of Internet of Things Technology in Mobile Education of Smart Campus Culture and Etiquette

Yanhui Guo 

Party and Government Office of Huai'an Campus, Nanjing Forestry University, Huai'an, 223001 Jiangsu, China

Correspondence should be addressed to Yanhui Guo; 2016122624@jou.edu.cn

Received 9 May 2022; Revised 28 June 2022; Accepted 5 July 2022; Published 15 July 2022

Academic Editor: C. Venkatesan

Copyright © 2022 Yanhui Guo. This is an open access article distributed under the Creative Commons Attribution License, which permits unrestricted use, distribution, and reproduction in any medium, provided the original work is properly cited.

To address the many uncertainties of technological change in school governance processes, this article offers smart school-based governance based on Internet of Things and Internet access mobile. Regarding the use of technology in cell phones, the system integrates in many ways, interviews staff involved, receives information, and then examines the use of how school governance affects school administration. The results of the experiment were as follows: 91.4% of parents believed that the use of smart home control systems was beneficial to themselves and their children; of the parents, 77.42% were most concerned about their student's school condition, with 41.94% and 38.71% doing homework. In addition, 29.03% and 21.51% of family information and school activities were in the parent's perspective. Parents estimate that in-school communication on WeChat, which is the largest contributor to smart school management, reaches an average of 50%. Smart school management has proven to be able to create a large database of schools and use it to support and streamline school management decisions, especially decisions, decision of the president, improving the whole process of a smart school system.

1. Introduction

As the lower concept of management, school management is also facing unprecedented opportunities and challenges under the influence of modern advanced science and technology [1]. We can all realize that the economic management, government management, enterprise management, and other related management existing in the society have been at the forefront of advanced science and technology, and today's world is in a period of great development, change, and adjustment. If school management can keep up with the trend of science and technology, it will bring great harvest [2]. Therefore, with the progress and development of mobile Internet technology, the society has entered a new mobile Internet era. The home school communication mode of traditional school management will eventually be replaced by the information communication mode. In order to enable school managers and teachers to use mobile phones and other mobile Internet to communicate with parents in real time and to enable parents to use mobile phones and other mobile Internet to grasp students' learning situation and communicate effectively with teachers in time, the

school has introduced a smart campus management system for the management of the school, which to a certain extent enhances the scientific, democratic, efficient, and standardized school management, meets the needs of schools, teachers, parents, and students in school management, and greatly promotes the reform of school management. However, there are many different problems in the practical application of schools, teachers, and parents, which affect the mobile process of school management.

Experts and scholars from a wide range of disciplines have provided different insights into the concept and characteristics of a smart school. Internet experts commented on the good understanding of smart schools, saying that smart schools are Internet applications of products that focus on the interaction of information received or deleted. Technology professionals have focused on innovation in teaching such as smart learning environment and smart classrooms and see smart schools becoming smarter, transforming learning, and learning. Learning environment is based on new communication network technologies. School improvement professionals focus on the use and maintenance of smart schools. They believe that building a smart school is

not just about using Internet technology but also about understanding. We need to pay attention to the quality of the technology and about its use and service. Based on the above ideas, we believe that smart school has become a new stage in the improvement of school information and has returned to the “three-point” form [3, 4]. Smart Campus focuses on the concept of “essential services and management support” such as understanding, service organization, information exchange, thought management, and deduction and makes research. The ultimate goal of a smart school connection is to provide better customer service. Second, smart schools need to reflect on the “deep integration” of school activities. “Deep integration” includes the integration of school work materials and a variety of modern school functions of processes and organizations, integration, integration and use of information platform, the integration of business processes and information, and four stages. Integration of data is based on all activities within the school and the external environment (smart city) [5]. In short, smart school could be defined as “person-centered, deep integration.” One of the unique features of a smart school is that its meaning is clear and descriptive. Its main features are as follows:

- (1) Have the ability to perceive the characteristics and habits of human, material, environment, and other factors in reality and can intelligently predict the general laws and development trends according to the established model
- (2) Support the real-time transmission of all kinds of messages, data, and information with a high-speed multiservice network system to eliminate the space-time constraints to the greatest extent
- (3) Realize the integration and intensive utilization of information platform and reflect the good organization and optimized storage of resources
- (4) Resource mining and resource recommendation based on the concept of “big data” to realize intelligent decision-making, management, and control
- (5) Build an open and multidimensional learning and scientific research space and have a learning and scientific research environment that supports multi-mode, crosstime, space, and context
- (6) Informatization application reflects the personalization, integration, and socialization for end users, and the informatization application is truly integrated with the overall informatization application environment of society

2. Literature Review

Yasmin et al. believe that school management accounts for a large proportion in the application of mobile Internet technology, and many mature mobile Internet technologies have been applied to practice. There have been a large number of convenient mobile technologies for managing schools, such

as campus office platform technology, campus information platform technology, campus microinformation management technology, and smart campus all-in-one card technology [6]. Nagowah et al. believe that mobile Internet technology and development are mainly used in the research of teaching platform, campus security, educational administration management, information management, and other aspects of school management, while there are few articles on the impact of mobile Internet technology on school management as a whole [7].

Celdrán et al. described school administration as “a process in which school leaders use a variety of tools and activities through specialized organizations and procedures to guide educators” and students, utilizing all internal and external resources and improving school performance. “Make sure you use the school’s mission plan as a whole. In the future, he manages school education, training, shipping, and other activities [8].” Gilman et al. believe that school management includes the management of schools by various educational institutions at all levels subordinate to the state and the government and the internal management of schools themselves. We call the discipline studying the management of the former as educational management and the discipline studying the management of the latter as school management [9].

Singh et al. believe that in general, school management includes the management of administration, education and teaching, teachers, students, safety, finance, and other aspects. In this regard, we can further subdivide it: administrative management includes the implementation of educational laws and regulations, the establishment of rules and regulations, the administration of the school according to law, the management of archives and materials, the management of books and periodicals entering the school, and the self-management of principals [10].

Park believes that education and teaching management includes the following: strictly implementing curriculum plans and curriculum standards, standardizing teaching work, implementing teaching inspection, strengthening education and teaching research, improving and perfecting evaluation system, strengthening ideological and moral education, strengthening the connection between school, family and society, and doing a good job in school sports and art work [11].

Stephan and Periera believe that safety management includes the following: establishing safety work institutions and working systems, safety education for teachers and students, safety prevention, accident reporting system management, and strengthening health work [12].

Zhang et al. believes that campus management includes the following: rational allocation of campus facilities, good campus greening, keeping the campus clean and beautiful, paying attention to the construction of campus culture, standardizing indoor layout, and maintaining good order on the campus [13].

Shi et al. believe that financial and asset management includes the following: carefully preparing the annual budget, strictly standardizing the financial management of the school, standardizing the procurement of goods, perfecting

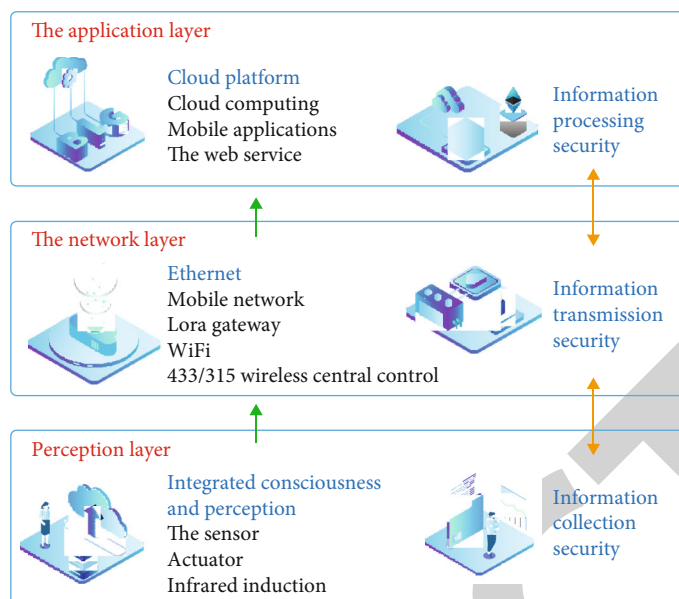


FIGURE 1: Internet of Things platform architecture.

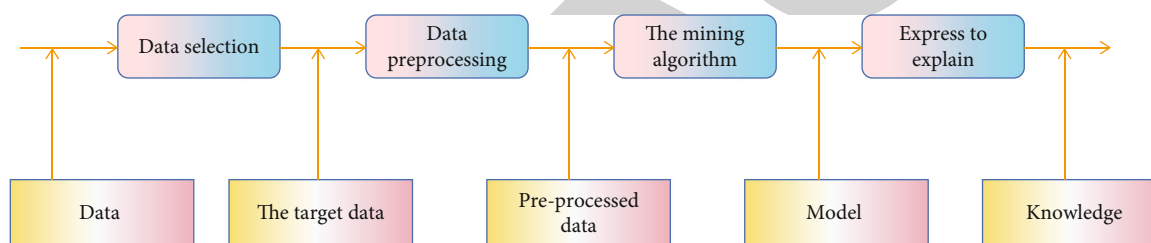


FIGURE 2: Data mining process.

the property registration system, and strengthening the management of equipment and facilities [14].

Kai et al. believe that there are still some deficiencies in the research on school management under the mobile Internet environment, most of which are only aimed at a specific need of the school, such as the design of mobile library management system, the design and implementation of mobile campus information platform, the design and implementation of WeChat campus service official account, and the design and implementation of school visitor management system, but they provide a good idea and reference for this study.

Based on this, the data collected from the school were used after the use of smart school-based monitoring based on this research material. From the point of view of mobile internet technology, this article clearly uses the data mining algorithm on the Internet of Things to obtain and analyze data and then explains the impact of the program: mobile Internet for school management. The Internet of Things is shown in Figure 1.

3. Research Methods

3.1. Data Mining under the Internet of Things

3.1.1. Overview of Data Mining. Data mining is a technology to extract hidden information of use value or interest from a large amount of data. Its emergence and application have a great impact on people's daily life and can guide people's activities. At present, it is widely used in statistics and machine learning. Generally speaking, data mining has the following characteristics: ① the amount of data information that needs to be processed by data mining is very large. ② The valuable rules and information extracted by data mining are potential and implicit, and sometimes, they are not even accurately expressed [15]. ③ Dynamic and rapid update of rules is as follows; that is, data mining can respond quickly to data changes. ④ The variables of information extracted by data mining include both continuous variables and discrete variables.

3.1.2. Data Mining Process. The data mining process is a multistep repeat process of extracting important data from users according to certain characteristics (minimum support, reliability, things) by users. The special process is shown in Figure 2. Generally, it consists of three steps: preparing the data, deleting the data, and presenting and interpreting the results.

Data preparation consists of three steps: data collection, data selection, and predocumentation. Data sharing is the process of sharing and processing data in multiple files or multiple locations, eliminating inaccuracies, resolving inaccuracies, and clean up data. The purpose of data selection is to analyze the data set to identify, narrow down the performance, and improve the quality of the data extraction. Preliminary data mining is about overcoming the limitations of current data mining tools. It only performs functions such as copying data, deleting files, and changing file types. At this stage of data mining, we must first decide what to think, whether the data deletion will automatically determine the user, or whether the user will make assumptions about the experiences that will be included in the case. The first is called discovery data mining, and the second is called validation data mining and then selecting the right tools for real mining operations to find the right rules and regulations. ③ Presentation and interpretation of data analysis information received in accordance with the customer's target decision, identifying the most important information and provided to the customer by decision-making tools. Therefore, the function of these steps is not only to report the results but also to filter the data [16].

3.1.3. Association Rule Mining Algorithm. Rnsactional data is an integral part of government grammar research. Every business usually has small equipment and limited turnaround time. Typically, set $I = \{i_1, i_2, \dots, i_n\}$ is used to represent a subitem, and position t is used to represent a product, for example, $T \in I$. If one of the subsets of i is x and $X \in T$, we can see that t has the status. If it is x , this association rule can be expressed as follows: $X \Rightarrow Y$, which means that event x is true, and event y is also true.

Support is the result that events a and b may occur at the same time. If A and B do not occur frequently at the same time, this indicates that there is no relationship between A and B . If A and B seem to occur simultaneously, then A and B are likely to be affected. Belief is the result of event B in case A . If faith is too low, then event B is almost unaffected by event A . A statement of support and confidence is provided by the model (1) to (2).

$$\text{support}(A \Rightarrow B) = P(A \cup B), \quad (1)$$

$$\text{confidence}(A \Rightarrow B) = P(B|A). \quad (2)$$

3.1.4. Decision Tree Algorithm. The log algorithm is a method of estimating the division of labor that is most often used to determine the value of a data or concept. Specifically, for conflict situations, the distribution of rights is placed in the decision-making tree. The deciduous trees are tree-like structures, such as the main stem, the branches of the branches, and the leaf axils. The nodes of the tree determine the nature of the structure, and the branches represent the value of the property. The core of the tree decides is the most important material of the whole structure, and the branches are the most important material of all the trees. Page value is the value of the sample category. The trees decide to use the top-down recursion. To solve the internal problem of the

tree, first compare the results of the attributes and then filter the results of the lower branches through the nodes according to the different materials. Finally, take into account the leaves of the deciduous tree and the path from the root node to the deciduous tree corresponds to the law, and the tree decides the total for the layers standard instruction [17].

3.1.5. Basic Principle of ID3 Algorithm. When constructing the decision tree, the information gain method is usually used to help determine which attribute is used to generate the following branches. If S is a set containing s samples, the category attribute can take m different values, corresponding to m different categories C and I belong to $\{1, 2, 3, \dots, m\}$. If a is selected as the test attribute, a has V different values $\{a_1, a_2, a_3, \dots, a_v\}$, a has been divided S into v subsets $\{S_1, S_2, S_3, \dots, S_v\}$, and S_{ij} is set as the number of samples belonging to C_i in subset S_j , the information required to divide the current sample set by using A is calculated as shown in formula (3):

$$E(A) = \sum_{j=1}^v \left(\frac{S_{1j} + S_{2j} + \dots + S_{mj}}{S} \right) I(S_{1j} + S_{2j} + \dots + S_{mj}). \quad (3)$$

For a given subset S_j , the information is formula (4):

$$I(S_{1j} + S_{2j} + \dots + S_{mj}) = - \sum_{i=1}^m P_{ij} \log P_{ij}, \quad (4)$$

where $P_{ij} = S_{ij}/|S_j|$ is the probability that the samples in subset S_j belong to category C_i . The information gain obtained by dividing the corresponding sample set of the current branch node with attribute A is formula (5):

$$\text{Gain}(A) = I(S_1, S_2, \dots, S_m) - E(A). \quad (5)$$

By calculating the information of each attribute, and then selecting the attribute with the largest gain as the test attribute of a given set s , the corresponding branch node is generated.

3.1.6. C4.5 Algorithm Principle. Let T be the data set and the category set be $\{C_1, C_2, \dots, C_k\}$. Select an attribute V to divide T into multiple subsets. Let V have n values $\{V_1, V_2, \dots, V_n\}$ that do not coincide with each other, and then t is divided into n subsets $\{T_1, T_2, \dots, T_n\}$, where the values of all instances in T are v . Let $|T|$ be the number of examples of dataset T , $|C_j| = \text{freq}(C_j, T)$ be the number of examples of class C_j , and $|C_{jv}|$ be the number of examples of class C_j in example $V = V_j$, then the occurrence probability of class I C_j is formula (6), and the information entropy of class is formulas (7) and (8).

$$P(C_j) = |C_j|/|T| = \text{freq}(C_j, T)/|T|, \quad (6)$$

$$H(C) = - \sum_{j=1}^k \frac{\text{freq}(C_j, T)}{|T|} \cdot \log_2 \left(\frac{\text{freq}(C_j, T)}{|T|} \right), \quad (7)$$

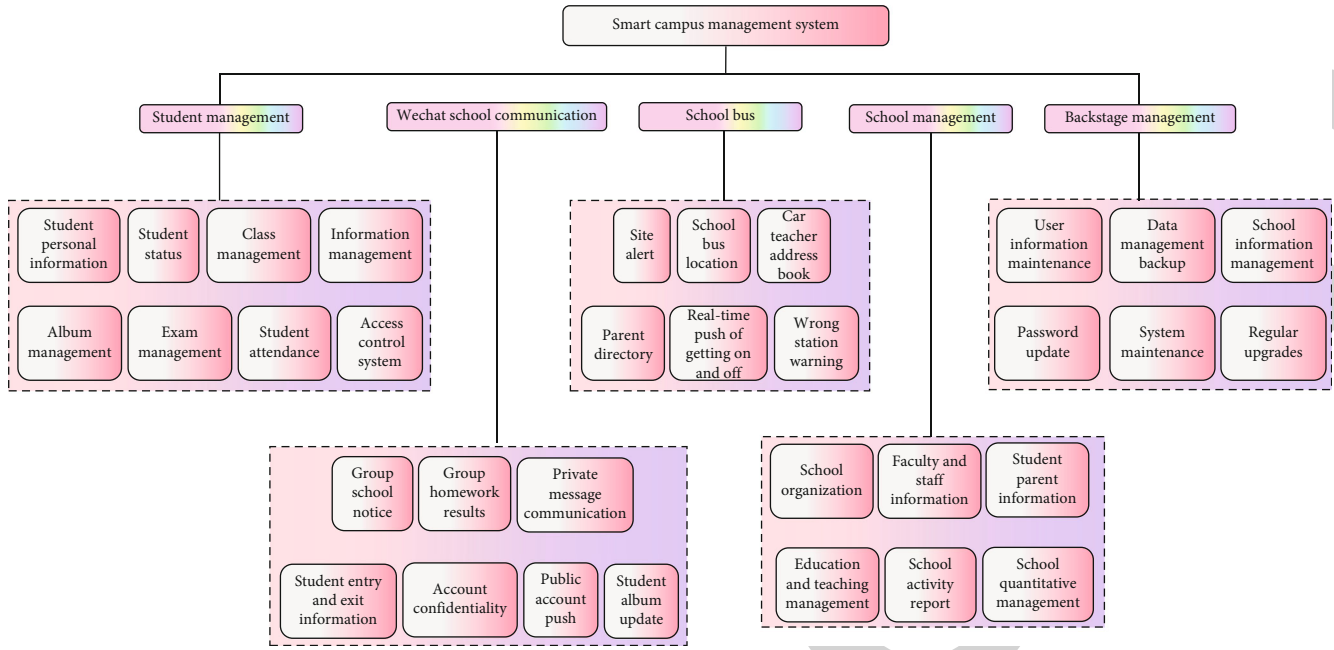


FIGURE 3: Function diagram of the smart campus management system.

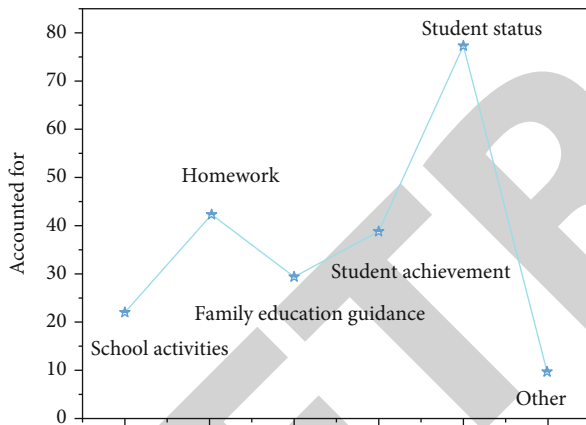


FIGURE 4: Parents' concerns about their children's school through the system.

$$-\sum_{j=1}^k \frac{\text{freq}(C_j, T)}{|T|} \cdot \log_2 \left(\frac{\text{freq}(C_j, T)}{|T|} \right) = \text{inf } o(T). \quad (8)$$

Set $\text{info}(T)$ as the entropy function, then solve the category conditional entropy, and divide the set T according to attribute V , and the segmented category conditional entropy is formulas (9) and (10):

$$H\left(\frac{C}{V}\right) = \sum_I \frac{|T_i|}{|T|} \cdot \text{inf } o(T_i), \quad (9)$$

$$\sum_I \frac{|T_i|}{|T|} \cdot \text{inf } o(T_i) = \text{inf } o(T). \quad (10)$$

3.2. *Comparative Research Method.* The comparative research method is to compare and analyze the different performances of the educated in different periods and under different circumstances, so as to reveal the general laws and special performances of education, so as to summarize the conclusions in line with the objective facts [18]. Through the comparative analysis of the personnel participating in the smart campus management system, this study pays attention to the use feelings of students and parents by using research methods such as observation and interview, so as to provide effective and accurate theoretical data for this study.

3.3. *Smart Campus Management System.* The smart campus management system architecture of the university mainly has three basic levels: infrastructure layer, campus application layer, and network layer [19].

The infrastructure layer mainly includes servers, a large number of hardware resources, wireless campus network, wired campus network, access control system, and network security center. The campus application layer mainly provides schools, teachers, and parents with various contents related to students' campus life, including teacher management edition and parents' ordinary edition [20]. The network layer includes information data center, management and decision-making platform, and network security protection [21].

Generally speaking, in its LAN environment, the school realizes the integrated application of various information of teachers, students, and parents through access control management, school bus transfer management, and teacher-student information management with the help of the mobile jingle campus system [22].

The smart campus management system of the school mainly has five functions: student management function, WeChat home school communication function, school bus

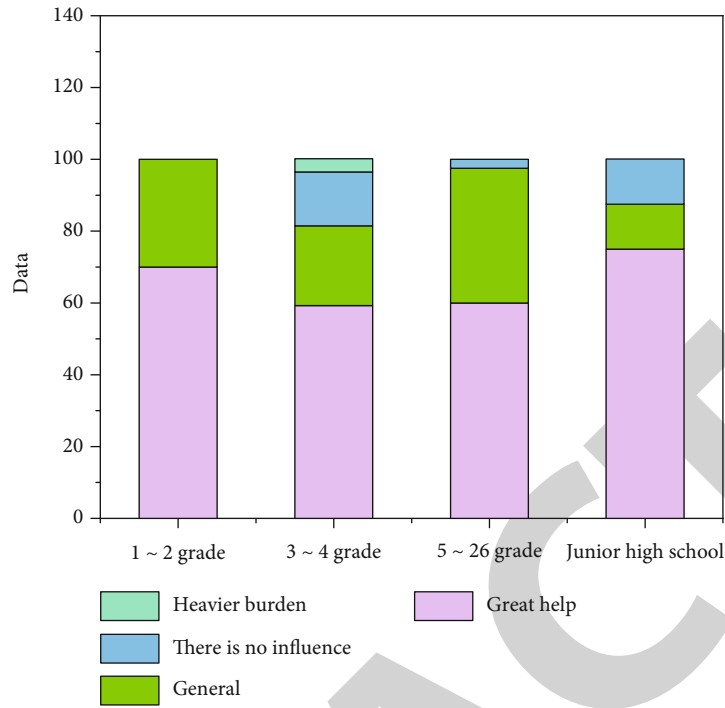


FIGURE 5: Overall experience of the smart campus system on parents of children of different grades.

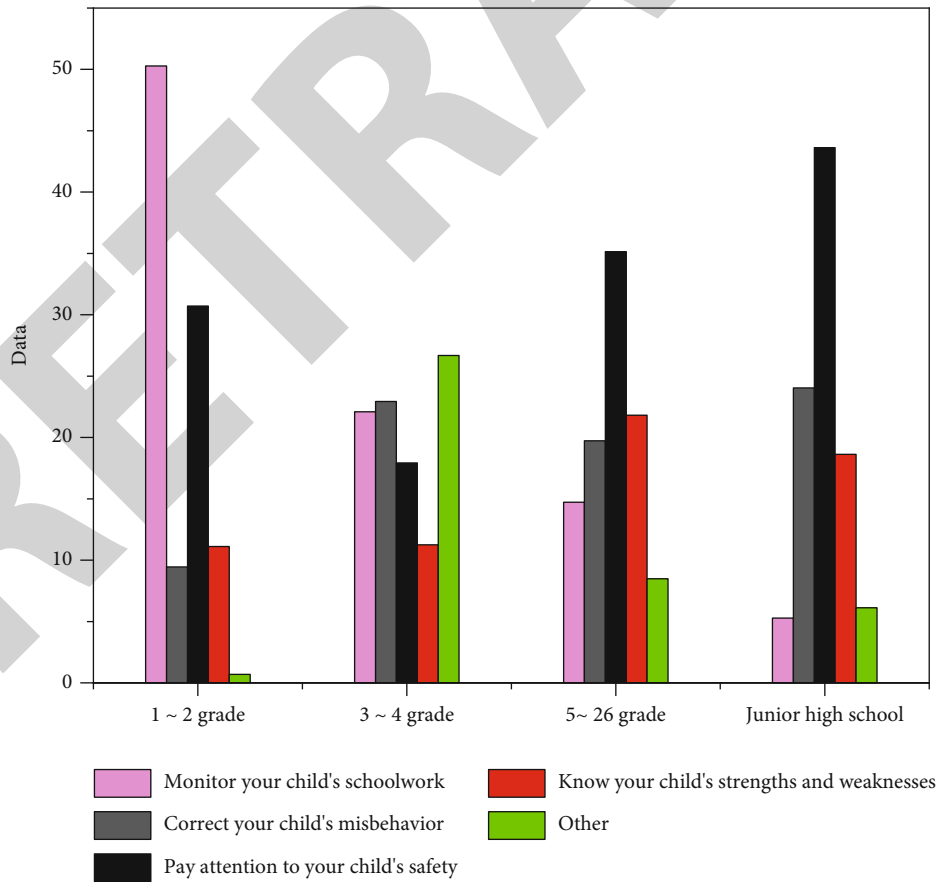


FIGURE 6: Main functions of the smart campus system for parents of children of different grades.

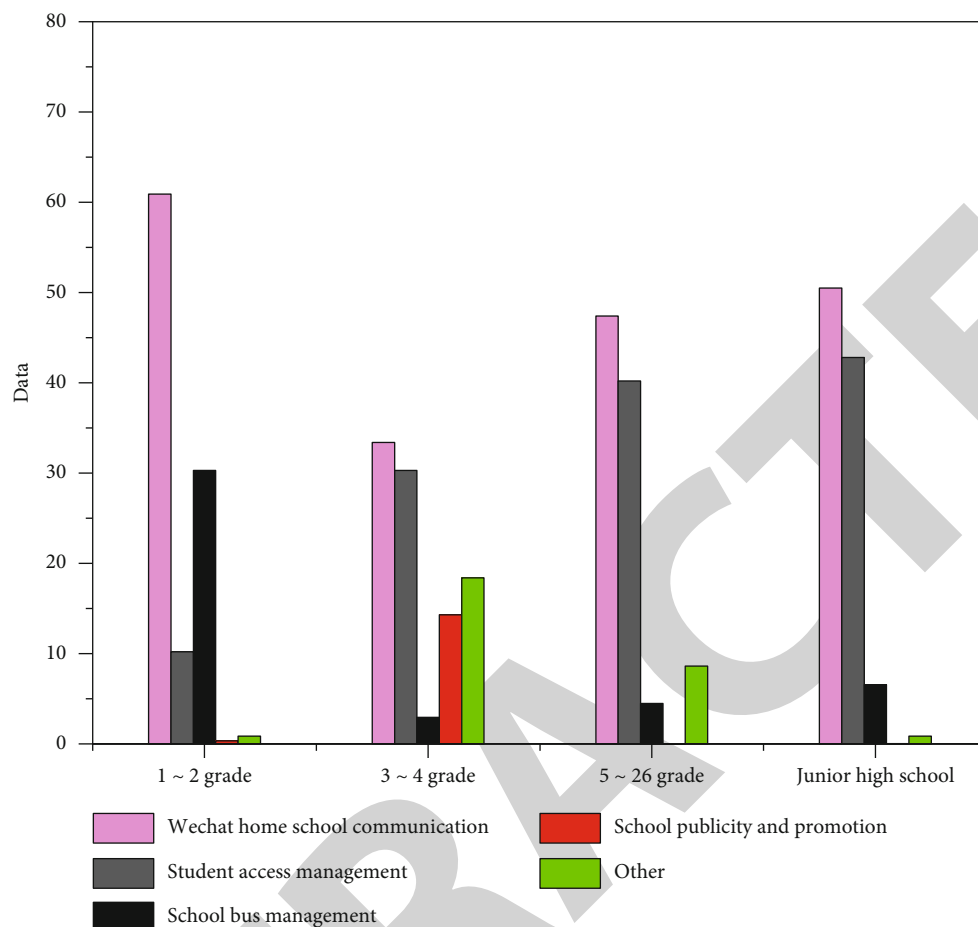


FIGURE 7: Experience of using the smart campus system for parents of children of different grades.

transfer function, school affairs management function, and background management function, as shown in Figure 3.

Student management function is mainly for student personal information, student status, class, information, photo album, examination, attendance, entrance and exit, and management [23].

WeChat home school communication functions include the following: mass sending of school notices, mass sending of homework scores, private message communication, student access information, account confidentiality, official account push, and student photo album update [24].

The services provided by the school bus transfer function include the following: site reminder, school bus location, car following teacher address book, parent address book, real-time push on and off, and wrong station warning [25].

The function of school affairs management includes the management of school organization, faculty information, student parent information, education and teaching activities, school quantitative management, and school activities.

Background management functions include user information maintenance, data management backup, school information management, password update, system maintenance, and regular upgrade.

The functions are complementary, interconnected, and interactive, which together constitute the smart campus

management system of the school and provide a system guarantee for the school.

4. Result Analysis

4.1. Use Feedback of Smart Campus Management System. After the system is used, a questionnaire is sent to students' parents to collect data on their use of the system.

The survey results show that parents generally give full affirmation to the way of school management on the mobile jingle campus of the school. They believe that the system can reasonably set up application functions based on the actual situation of students. Everything is student-oriented, which is convenient for parents to understand their children's school situation and facilitate the communication with schools and teachers, and the overall use is good. The following are the representative results.

- (1) Communication between parents and schools: 91.4% of parents believed that the use of the smart campus management system was of great help to themselves and their children, mainly reflected in that 31.38% of parents thought that they could pay attention to their children's personal safety with the help of the system, 20.43% of parents thought that they could

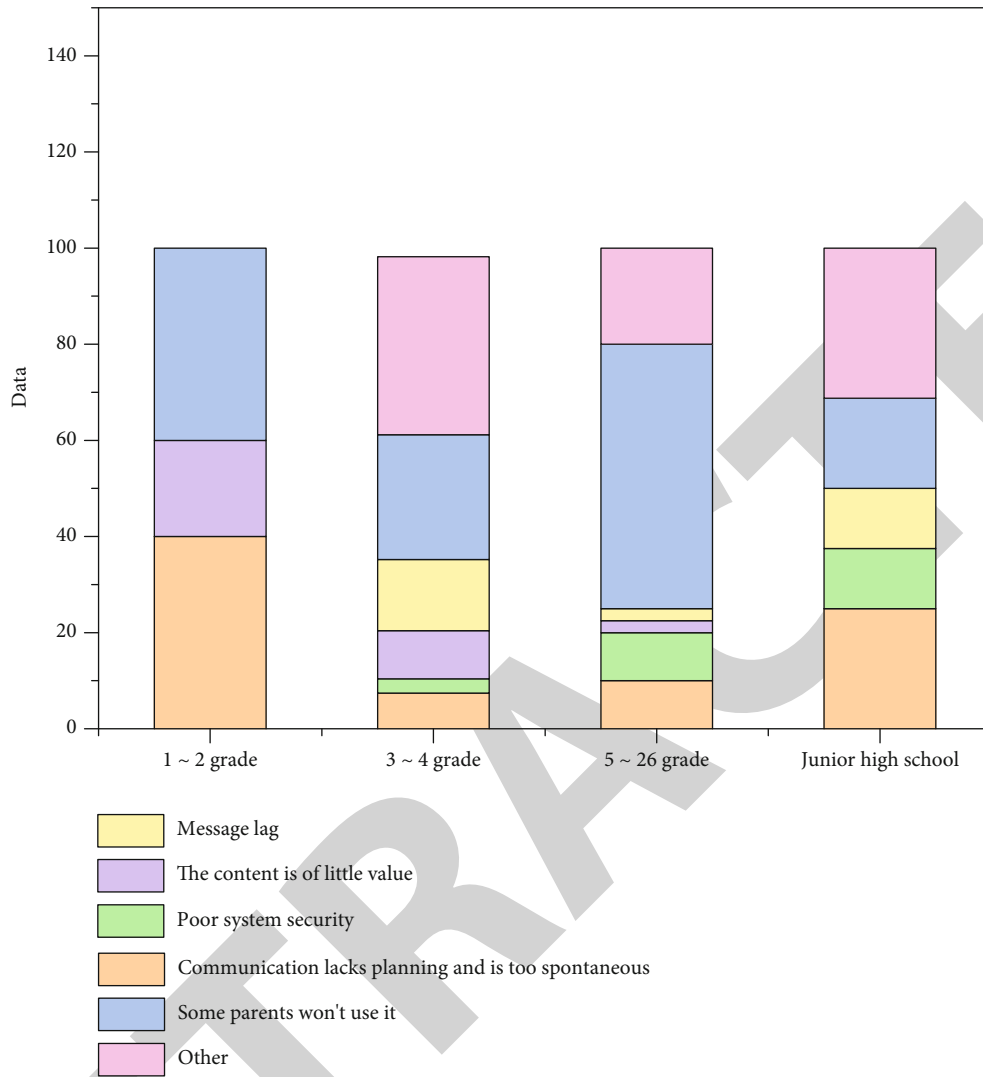


FIGURE 8: Problems pointed out by parents of children of different grades after using the smart campus system.

correct their children’s wrong behavior, 19.35% of parents thought that they could supervise their children’s schoolwork, and 17.12% of parents thought that they could understand their children’s advantages and disadvantages. It shows that the system has become one of the main tools for parents to understand their children’s school situation

As can be seen from Figure 4, parents are most concerned about students’ school situation, accounting for 77.42%. The second is students’ homework and grades, accounting for 41.94% and 38.71%, respectively. Family education guidance and school activity arrangement are also the key points concerned by parents, accounting for 29.03% and 21.51%, respectively.

- (2) The overall feeling of parents of children of different grades on the use of the system: it is learned that there are differences in the physical and psychological development of students in different grades. A crossanalysis is carried out according to the concerns

of parents in different grades. The results are shown in Figure 5

From Figure 5, it can be seen that more than half of the parents in all grades believe that the use of Jingle Bell campus has a great impact on themselves, indicating that the system has indeed brought great improvement to school management, of which more than 70% of the parents in grades 1-2 and junior high school have chosen great help. In junior high school, the students at this stage are in the psychological development stage of self-identity and chaotic roles. The students are generally sensitive, emotional, rebellious, eager for independence, freedom, and inseparable from the care of their parents. Compared with the primary school stage, they are not good at communicating with their parents. Parents can only obtain their children’s school situation through teachers or systems. For grades 3-6 in the middle stage, the students’ psychological development is relatively gentle at this stage, and the parents and teachers have formed a stable communication mode; so, they are less affected by the system.

(3) Function distribution of parents' use of the system in different grades

From Figure 6, it can be seen that parents of lower grade students generally focus on their children's homework and personal safety, while their attention to correcting their children's mistakes and understanding their children's advantages and disadvantages is at a low level. At this time, due to the young age, weak consciousness, imperfect psychological development, and weak self-protection consciousness of lower grade students, the access control system of smart campus and the function of sending homework scores have become the focus of lower grade parents.

(4) Parents of children of different grades' experience of using the system

From Figure 7, it can be concluded that parents believe that the WeChat home school communication function is the most helpful to themselves in the smart campus management system. Student access management also rises with the rise of grades. It is analyzed that the reason for the low level of grades 1-2 may be that some parents have just started to use the system and are not fully familiar with the functions of the system. School bus transfer management helped parents in grades 1-2 the most, reaching 60%. It decreased rapidly from grade 3 and showed a stable trend after grade 4. The reason for the analysis is that for the sake of their children's safety, low-grade parents choose the way of school bus transfer for their children. From grade 3, parents begin to let go to cultivate their children's self-reliance ability. On the other hand, it is also because most students live not far from the school. The overall help of school publicity and promotion to parents is not much. Except for 4% in grades 3-4, parents in other grades think it is not helpful to themselves. The reason may be that the school has not made greater efforts to use the system for school publicity.

(5) Feedback from parents of children of different grades on the use of the system

From Figure 8, it can be seen that the proportion of parents who think that the "smart campus management system" lags behind decreases in the order of grades 1-2, junior middle school, grades 5-6, and grades 3-4. Parents in lower grades of primary school and junior middle school tend to pay attention to their children's personal safety; Parents who think that "the system security is poor and personal information is easy to leak" are the most in grades 1-2, accounting for 20%.

5. Conclusion

Based on the application of mobile Internet technology and the development process of school management and concept, this paper makes an expected research, and the results are as follows:

- (1) This paper makes a systematic research on the school management based on mobile Internet and

reproduces the application platform interface, educational administration management interface, and system setting interface of the smart campus management system

- (2) Through its own observation and analysis, this paper presents the current situation of the use of the mobile Internet system in the school, obtains the basic idea and framework of the questionnaire and interview through the perceptual understanding and rational thinking of the current situation, and implements and analyzes the questionnaire and interview after determining the research questions and research objects
- (3) Combined with the current situation of the campus and the summary and analysis of the data content, this paper finds out some problems encountered in the process of school management mobility: the reasons of the system itself, the reasons of school management, and the constraints of family conditions

Data Availability

The data used to support the findings of this study are available from the corresponding author upon request.

Conflicts of Interest

The author declares no conflicts of interest.

Acknowledgments

This study was supported by the 2022 Scientific Research Project of Jiangsu Institute of Modern Educational Technology and by the research on the path of campus culture construction of colleges and universities running in different places supported by network new media platform.

References

- [1] M. A. Razzaq, J. A. Mahar, M. Ahmad, N. Saher, and G. S. Choi, "Hybrid auto-scaled service-cloud-based predictive workload modeling and analysis for smart campus system," *IEEE Access*, vol. 9, pp. 42081–42089, 2021.
- [2] C. T. Yang, S. T. Chen, J. C. Liu, R. H. Liu, and C. L. Chang, "On construction of an energy monitoring service using big data technology for the smart campus," *Cluster Computing*, vol. 23, no. 1, pp. 265–288, 2020.
- [3] P. S. Chiu, J. W. Chang, M. C. Lee, C. H. Chen, and D. S. Lee, "Enabling intelligent environment by the design of emotionally aware virtual assistant: a case of smart campus," *IEEE Access*, vol. 8, pp. 62032–62041, 2020.
- [4] R. Carli, G. Cavone, S. B. Othman, and M. Dotoli, "Iot based architecture for model predictive control of hvac systems in smart buildings," *Sensors*, vol. 20, no. 3, p. 781, 2020.
- [5] A. Puckdeevongs, N. K. Tripathi, A. Witayangkurn, and P. Saengudomlert, "Classroom attendance systems based on bluetooth low energy indoor positioning technology for smart campus," *Information*, vol. 11, no. 6, p. 329, 2020.

Retraction

Retracted: Research on Data Mining Algorithm of Associated User Network Based on Multi-Information Fusion

Journal of Sensors

Received 13 September 2023; Accepted 13 September 2023; Published 14 September 2023

Copyright © 2023 Journal of Sensors. This is an open access article distributed under the Creative Commons Attribution License, which permits unrestricted use, distribution, and reproduction in any medium, provided the original work is properly cited.

This article has been retracted by Hindawi following an investigation undertaken by the publisher [1]. This investigation has uncovered evidence of one or more of the following indicators of systematic manipulation of the publication process:

- (1) Discrepancies in scope
- (2) Discrepancies in the description of the research reported
- (3) Discrepancies between the availability of data and the research described
- (4) Inappropriate citations
- (5) Incoherent, meaningless and/or irrelevant content included in the article
- (6) Peer-review manipulation

The presence of these indicators undermines our confidence in the integrity of the article's content and we cannot, therefore, vouch for its reliability. Please note that this notice is intended solely to alert readers that the content of this article is unreliable. We have not investigated whether authors were aware of or involved in the systematic manipulation of the publication process.

Wiley and Hindawi regrets that the usual quality checks did not identify these issues before publication and have since put additional measures in place to safeguard research integrity.

We wish to credit our own Research Integrity and Research Publishing teams and anonymous and named external researchers and research integrity experts for contributing to this investigation.

The corresponding author, as the representative of all authors, has been given the opportunity to register their agreement or disagreement to this retraction. We have kept a record of any response received.

References

- [1] X. Kang and C. Hua, "Research on Data Mining Algorithm of Associated User Network Based on Multi-Information Fusion," *Journal of Sensors*, vol. 2022, Article ID 2417826, 8 pages, 2022.

Research Article

Research on Data Mining Algorithm of Associated User Network Based on Multi-Information Fusion

Xiancai Kang ¹ and Chuangli Hua ²

¹School of Information, Zhejiang Guangsha Vocational and Technical University of Construction, Dongyang, Zhejiang 322100, China

²Information Center, Zhejiang Guangsha Vocational and Technical University of Construction, Dongyang, Zhejiang 322100, China

Correspondence should be addressed to Chuangli Hua; 1711011421@hbut.edu.cn

Received 3 June 2022; Revised 16 June 2022; Accepted 28 June 2022; Published 8 July 2022

Academic Editor: C. Venkatesan

Copyright © 2022 Xiancai Kang and Chuangli Hua. This is an open access article distributed under the Creative Commons Attribution License, which permits unrestricted use, distribution, and reproduction in any medium, provided the original work is properly cited.

In order to explore how to realize network mining for associated users, an algorithm of associated user mining based on recommendation system is proposed. This method recommends key technical problems and solutions based on multi-information fusion to explore the research of user network data mining. The data mining algorithm of associated user network based on multi-information fusion is about 35% higher than the previous method. This article is combined with common scoring data to improve the accuracy of algorithm results. The experiment was carried out on the real data set FilmTrust to evaluate the proposed new algorithm, measure the prediction accuracy of the score prediction results, and compare the offline test results to verify the effectiveness of the new algorithm.

1. Introduction

Recommender system (RS) can discover and capture users' preferences and recommend relevant content to users. As a bridge between users and projects, RS plays a key role in many scenes of people's daily life [1]. Today, recommendation system is online shopping, video websites, and search engines, and many other fields have been rapidly developed. Relevant researches in China emerge endlessly and become a hot topic in academia and industry in recent years [2].

In the field of social networks, in recent years, due to the gradual increase of users and the more frequent update rate of information, the explosive growth of network data has led to the problem of information overload [3]. Many efforts have been made in academia and industry to accurately capture users' needs or preferences and filter out useless or uninteresting content for users. Collaborative filtering, as a mainstream method in the field of personalized recommendation, seeks for the similarity between different individuals and selects the most similar individuals to meet the personalized needs of different users. Although collaborative filter-

ing can effectively alleviate the phenomenon of information overload and is widely used, the actual effect of most existing methods based on collaborative filtering is not satisfactory in the face of data sparse and cold start scenarios [4]. In addition, the characteristics of social network make it complicated, and the results of traditional recommendation methods are not ideal when personalized recommendation is carried out for users in social network environment. On the basis of in-depth analysis of common recommendation algorithms, this article tries to combine the idea of multiple information fusion in the personalized collaborative filtering algorithm to help better understand users' interests. In addition, the user item rating data commonly used in collaborative filtering algorithm is combined with the idea of matrix decomposition and the social network trust model to improve the problem of data sparsity and improve the prediction accuracy of recommendation system.

In essence, the recommendation system solves the problem of information overload by pushing new items that users are not familiar with but may need or be interested in [5, 6]. The system usually receives a large number of user requests

at the same time, analyzes the different needs of users based on their real demand environment, and adopts different recommendation mechanisms to respond to users. The system uses the user's personal information, item-related information, and historical purchase records saved in the customized database to help generate recommendation results [7]. After obtaining the recommendation information, users may choose to adopt or reject the generated recommendation content, or they may give various forms of explicit or implicit feedback immediately or after a long time. The system then saves all these user behaviors and feedback information into the log system, so that users can obtain appropriate recommendation information when they use it again in the future [8]. Figures 1 and 2, respectively, describe the basic workflow and ideas of the recommendation system.

Generally, the main data sources of recommendation system include metadata of articles, such as category and keywords; basic user information, such as gender; and users' historical preferences, such as ratings and browsing records [9]. There is no doubt that explicit user feedback can accurately express the actual needs or interests of users, but this kind of feedback data is relatively rare. However, it is relatively easy to obtain the implicit feedback information of users. After analysis and processing, it can also reflect users' preferences from a certain angle, but the accuracy is not high, resulting in the need to spend more on processing data noise. However, if appropriate behavioral characteristics can be accurately selected, implicit feedback information can still obtain good recommendation results [10]. In different scenarios, the selection of behavior characteristics is also different, and the recommendation system will adopt different recommendation mechanisms to select data sources.

2. Literature Review

The recommendation system originated from GroupsLens' exploration of Movielens in the University of Minnesota has a history of more than 20 years. Later, Amazon applied recommendation system technology to e-commerce, analyzing users' purchase records and inferring what they might be interested in. In recent years, recommendation system has been widely applied and extended in academic and enterprise fields. In the academic field, since ACM held the International Conference on Recommendation System in 2019, ACM has also set up a special group to study recommendation system. In the 24th seminar, recommendation system was separately listed as a hot item for discussion by SIGIR group of ACM Society. Amh et al. found that many enterprises also provided open data sets for researchers, among which the most famous was the recommendation system competition organized by Netflix [11]. Some Chinese scholars have also gradually deepened their research on recommendation systems. For example, they elaborate on the key technologies, architecture, and performance evaluation indexes of recommendation systems and analyze the problems to be overcome in recommendation research and the follow-up directions worth exploring. This article describes the core method, effect evaluation, and method practice of mobile recommendation system and prospects its future

application direction. Deep learning is ground-breaking integrated into the recommendation system to study how to integrate massive multisource heterogeneous data to improve user satisfaction and analyze the differences and advantages between it and traditional recommendation system. Based on the classic CNN (convolutional neural network) network structure, a convolutional neural network model of image recognition and word recommendation system under the background of artificial intelligence is proposed to realize image recognition and word recommendation based on deep learning. An implicit feedback matrix decomposition algorithm based on emotion modeling between users and objects is proposed by learning potential factors in videos. Yin et al. focused on personalized recommendation in social networks, summarized the influence of popular social factors on the final results, elaborated the definition of trust and the calculation method of trust, and projected the research dilemma and development trend of trust networks [12]. Combined with all the returned information and the changing trend of social networks, a time-aware recommendation algorithm based on user feedback information is proposed. Weighted social networks are processed by time attenuation function, and the similarity calculation method is improved. The information returned by users is classified into positive feedback information. The other is negative feedback. Then, the influence of these feedback information on the algorithm is summarized, and experiments are carried out to prove that the proposed recommendation algorithm has better performance. Service recommendation in hot topic information physical system (CPS) is studied. In view of the high data sparsity in CPS which may affect the prediction accuracy, the potential similarity between users or services in CPS is mined to improve the prediction accuracy. In addition, Hu et al. constructed a prediction model using random walk and fully verified it on two effective data sets to prove the feasibility of the algorithm when most traditional collaborative filtering methods ignored contextual information such as network location. It is verified that network location is really useful in QoS (quality of service) prediction [13].

In the field of enterprise, recommendation system is also an important technical means of many websites. For example, the very famous Facebook and Twitter use recommendation system to recommend friends to users, and Google use recommendation technology to push information that users may like. Netflix and Youtube use recommendation system technology to recommend content-related videos to users. Tmall, JINGdong and others rely on the recommendation system to provide users with commodity push. Doubanchai pushes fresh and interesting content to users. Percentage Point Group is the leading big data and recommendation engine technology company in China's Internet. The research and development of recommendation engine and analysis engine has been quite mature and has been successfully used in more than 1500 enterprises.

Shi et al. found that mobile Internet not only has the characteristics of open Internet but also has the characteristics of real-time, portable, and positioning interaction of mobile network [14]. The mobile Internet is much more

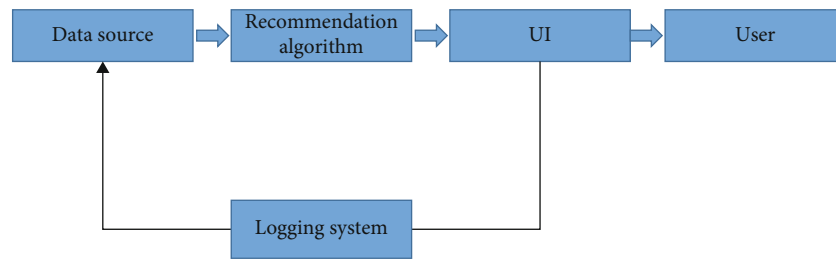


FIGURE 1: Basic workflow of recommendation system.

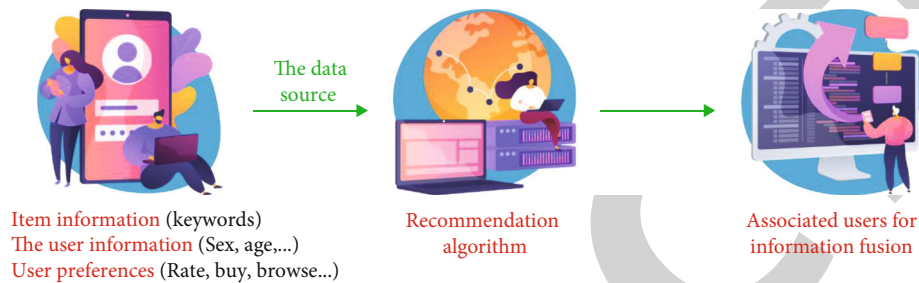


FIGURE 2: Basic idea of recommendation system.

portable for users. For operators, mobile Internet is more open and controllable than traditional Internet. Mobile Internet has penetrated into every field of people's life and work. WAP is one of the most promising services in mobile Internet and the most personalized e-commerce tool. Gupta and Maiti believe that it has three main applications: first, public service, which means providing users with the latest real-time information, such as weather, news, and traffic; second, personal information services, including social networking, information search, email, portal browsing, and information query; the third is commercial economic services, which include basic office applications and the most potential mobile commerce applications, including shopping, payment, and reservation [15]

3. Methods

3.1. Classification and Comparison of Recommendation Systems. Recommendation systems can be classified in different ways according to different analysis perspectives. Through sorting and analysis, the following three recommendation systems based on classification are mainly introduced:

(1) Different recommendation results are divided into:

Based on the recommendation of mass behavior, popular items are pushed to all users by calculating the current popular items. It can push dynamic hot and concerned content to each user in real time, especially for items seeking promotion, which has a good practical effect. Its performance is relatively stable in popular movies, focus news, and other application fields, but the accuracy of recommendation results is not satisfactory [16].

Personalised recommendations are based on user experience, based on data such as historical preferences. It mainly

uses the historical data of users to analyze the habits and characteristics of different individuals or based on the needs of the current environment to achieve targeted services. It is characterized by giving full consideration to the differences of individual preferences of users, making appropriate judgments and pushing the results to users. It has good recommendation accuracy and is an ideal recommendation method. But the cost is high [17] (see Table 1).

Collaborative filter-based recommendation realizes recommendation by analyzing current users' preferences and demands for items and information and calculating the similarity of items or users themselves. As one of the most widely used recommendation methods, it is independent of the characteristics of the item itself and belongs to the domain. In addition, it does not need to conduct modeling for users and products, and the recommendation results are open, which provides good technical support for discovering users' own interests or preferences [18]. The main problem of recommendation based on collaborative filtering lies in its excessive dependence on historical data, which leads to its deficiencies in many related aspects, such as cold start, sparse data, insufficient accuracy, poor flexibility, and other problems. Table 2 compares the characteristics of the three methods, as shown in Table 2.

3.2. User-Based Collaborative Filtering Algorithm. User-based collaborative filtering algorithm (UserCF) was first proposed in 1992, which was used to realize mail filtering function in the early stage and is the most famous collaborative filtering algorithm in the field of recommendation system. The algorithm is mainly divided into two stages: firstly, mining the user set with similar preferences or needs and then looking for the corresponding content that the current user may like but does not know from the set and pushing it to the current user. The selection of algorithm

TABLE 1: Characteristics summary.

	Recommendations based on crowd behavior	Personalized recommendation
Advantages	Hot information recommendation effect is good	Good accuracy
Disadvantages	Accuracy is poor	High input cost

TABLE 2: Characteristics summary.

	Recommendations based on demographics	Content-based recommendations	Recommendations based on collaborative filtering
Advantages	Easy to implement Depend on less No cold start problem	Grasp users' taste accurately	Low modeling requirements No machine understanding required High openness, good reference
Disadvantages	Accuracy is poor Ignoring users' tastes Sensitive information is difficult to obtain	Accuracy depends on modeling comprehensiveness Ignore the user's attitude towards the object cold start problem exists	Sparse matrix affects accuracy Cold start problem It is hard to update in real time

similarity can be considered from different intersection degrees: the similarity between different users can be measured by the preference degree of a certain user for all items, or the similarity between different items can be measured by the preference degree of all users for a certain item [19]. Its basic principle is to use KNN (K -nearest neighbor) algorithm to find the group with similar preferences to the current user, "nearest neighbor," and make recommendations to the current user by using the historical preference data of the nearest neighbor group.

Suppose there are m users and n items in the user-item scoring matrix R . If user u gives a rating for item i , it can be replaced by the updated matrix R . If there is no rating, it can be replaced by empty. Each row in r_{ni} represents the rating vector of all users. Then, as for the similarity between the current user and other users about the scoring vector, cosine similarity is generally used to solve the problem, as shown in

$$\text{sim}(u, v) = \frac{Ru \cdot Rv}{\|Ru\| \|Rv\|} \quad (1)$$

Ru and Rv represent the scoring vectors of user u and user v , respectively. The item that the current user is not interested in before but similar users are interested in is designed as the candidate set, and the predicted score P of the current user u for item i in the candidate set is calculated as shown in

$$P_{u, i} = \frac{\sum \text{sim}(u, v) * r_{vi}}{\sum \text{vesim}(u, v)} \quad (2)$$

The algorithm finds K similar items by giving the items that the current user u has scored, and the current user u gives prediction scores for these similar items, as shown in

$$P_{ui} = \frac{\sum \text{sim}(j, i) * r_{vj}}{\sum \text{vesim}(j, i)} \quad (3)$$

For example, news websites need to focus on the popularity and timeliness of news ontology recommendation. UserCF can push some news contents that are immediately followed by the "near neighbors" who share common interests with the target users, which can not only ensure instant access to hot information but also meet personalized needs in a certain sense. From a technical point of view, UserCF only needs to maintain the similarity table related to users, while ItemCF needs to constantly update the item correlation table, due to the rapid updating of information such as news, which brings some difficulties to technical implementation. Therefore, UserCF is obviously more suitable in this kind of application domain [20].

In areas such as books and movies, ItemCF can maximize its features. Since the user interests of such websites are generally stable, and their main task is to provide and recommend items related to their interests to users, ItemCF algorithm is more suitable for the application and promotion of such websites. From a technical point of view, on the contrary to news websites, books and other websites need ItemCF more to maintain item similarity tables, rather than focusing on user similarity (see Table 3).

Model-based methods not only overcome the technical problem of high computational complexity of memory-based collaborative filtering recommendation by using matrix decomposition but also ensure a significant improvement in service efficiency and strengthen the scalability of the system itself [21]. The recommendation idea based on model is to transform the high-dimensional user-item rating matrix into the product of two different low-dimensional feature vector matrices by dimensionality reduction. The matrix decomposition can be defined as shown in

$$R \cong PQ^T \quad (4)$$

After decomposition, $P \in R$ represents the user eigenmatrix, and f represents the dimension of the vector after dimensionality reduction. Line i in P is the eigenvector for user i . $Q \in R$ represents the feature matrix of the item, and

TABLE 3: Comparison of UserCF and ItemCF.

	UserCF	ItemCF
Performance	Applicable to scenarios with a small number of users. It is very expensive to calculate the user similarity matrix when there are many users.	Applicable to the scenario where the number of items is significantly smaller than the number of users, and it costs a lot to calculate the item similarity matrix when there are many items.
Field	It applies to areas with strong timeliness and less obvious user interest.	It is suitable for the fields with rich long tail items and strong personalized needs of users.
Real-time performance	New user behavior does not necessarily result in immediate changes in recommendation results.	New user behavior is bound to result in real-time changes in recommendation results.
Cold start	New users cannot make personalized recommendations immediately after they have behaviors for a few items.	By acting on an item, a new user can recommend other items related to that item.

the j th row is the feature vector of the j th item. Through modeling and continuous iteration, matrices P and Q with the best learning effect are obtained to achieve the final score prediction. The definition of user u 's score prediction for item i is shown in

$$r_{ui} = p_u q_i. \quad (5)$$

SVD (singular value decomposition) is a typical matrix decomposition technique. SVD was successfully applied in the field of latent semantic indexing in the early stage. Due to its excellent dimensionality reduction ability, Sarwar et al. introduced SVD into the recommendation algorithm to solve the problem of data sparsity and optimize the recommendation quality on the sparse score matrix [22]. In addition to being decomposed into two lower dimensional eigenvector matrices, SVD method can also generate diagonal matrix containing singular values in the recommendation system, which is convenient to find the internal relationship between users and projects. The size and quantity of singular values determine the variation range of dimension.

Before decomposition using SVD. First, the missing term in matrix R is replaced by the average score to obtain a dense matrix. Let the matrix filled with blank items be represented by R' , then SVD decomposition of R' is shown in

$$R' = U \Sigma V^T. \quad (6)$$

Since all singular values in the matrix contain information in the original matrix, SVD uses the sum of singular values to define the concept of information and sets thresholds to ensure the validity of information. If the sum of squares of all singular values is P and the sum of squares of the first f ($f \in Z$) singular values is P_f , then the threshold value of information content is shown in

$$\sigma = \frac{P_f}{P}. \quad (7)$$

In general, $\sigma \geq 99\%$ is required, and f usually takes the minimum integer value that satisfies the premise that $a \geq 99\%$. Therefore, the diagonal matrix is a new diagonal

matrix with only the first f singular values, and the first f singular value vectors are selected from U and V , respectively, to form U_f , V_f and matrix R_f through continuous dimensionality reduction, as shown in

$$R' \cong R_f. \quad (8)$$

The latent factor model (LFM) was proposed in 2004. The main principle of this method lies in the close connection between users' preferences and items by using the latent features. The latent factor model maps all users' information to a dimension f , that is, decompose the rating matrix R into a product of lower-dimensional matrices as shown in

$$\bar{R} = P^T Q. \quad (9)$$

In reality, there will be some inherent attributes of the user and the object that are not directly related to both. To address this problem, a novel improvement strategy is proposed in the Netflix Prize, which adds a bias term on the basis of the original SVD model, known as the BiasSVD model. The prediction formula after adding bias is shown in

$$\bar{r}_{ui} = P \sum_{ui} q_i + b_i + b_u + \mu. \quad (10)$$

3.3. Personalized Collaborative Filtering Algorithm Based on Multientryption Fusion. Recommendation system has always provided users with personalized suggestions based on users' hobbies or needs. In the past ten years, it has received more and more attention and recognition, and now, it is a hot research field in the academic and industrial circles. Generally speaking, the body of recommendation policy-targeted resolution usually includes historical data of users, semantic content, and association between items. The basic idea of collaborative filtering methods commonly used in the field of recommendation systems is to make interest prediction or demand prediction by looking for similar users' preferences or items other than the target users [23]. User rating information for items is the most common information used in collaborative filtering recommendations. Nowadays, social networking sites have become an indispensable part of the Web 2.0 environment. Due to the rapid development of

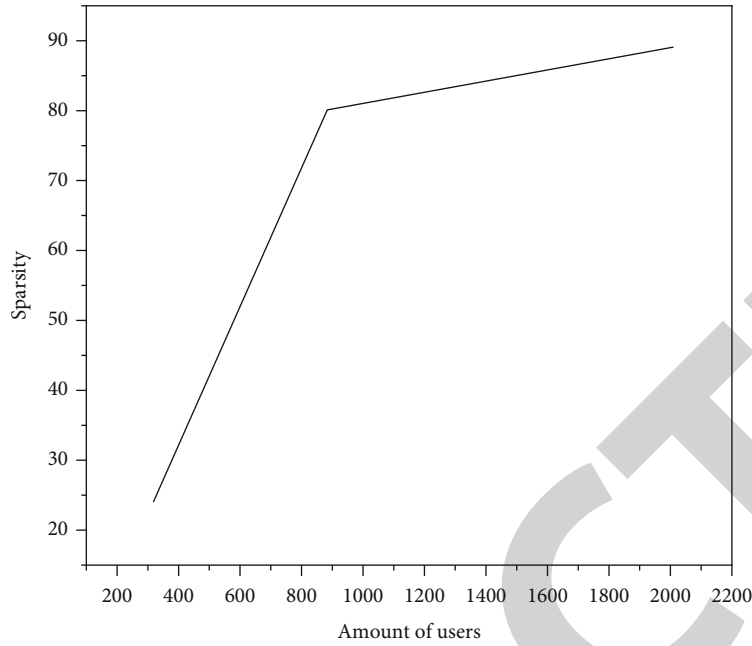


FIGURE 3: Trust data statistics.

social networking, the way people search for information, share resources, and communicate with each other is gradually changing. Social media sites update a huge amount of information every day, making it increasingly difficult for users to find what they really need or are interested in. In this case, rating data alone is not enough to accurately predict users' interests and needs. Users can rate projects on social networking sites, add other users as friends, join online interest groups, and even tag projects. In addition to simple rating information, other available data such as social network data also indicate the preferences of specific users to a certain extent [24]. Therefore, in recent years, more and more scholars and engineers have begun to study whether specific data in the social network environment can help improve the quality of recommendation results. At the same time, it is also helpful to alleviate the problem of cold start.

Although, currently, some researchers have integrated personalized information into recommendation systems and achieved good improvement in accuracy, few researchers have integrated several different types of information into the algorithm. For developers of recommendation systems, diversified information can help them understand users' needs or preferences more accurately and improve the quality of service. Diversified information including basic rating information, social friend information, and tag information is integrated into UserCF algorithm, and two real data sets (Last.fm and Movielens) are used to evaluate the proposed method and then compared with some common collaborative filtering algorithms to test its actual effect.

4. Results and Analysis

Data mining is a process of knowledge discovery [25]. Data mining is a process of knowledge discovery. Specifically,

according to the demand of data mining, the unified preprocessing of data is carried out to obtain a specific and unified data form convenient for mining. Mining potential and useful knowledge from these data is the function of data mining in decision support. Data mining can be simply described as a process of deep analysis of massive data, finding and summarizing potential rules, and transforming them into corresponding models. Data mining is essentially the technical processing of commercial information [26].

Data mining can be divided into four stages: problem definition, data preprocessing, data mining, and pattern evaluation. (1) Problem definition is the process of determining requirements, determining which valuable information is in a large amount of data and how to find interesting data. Problem definition makes data mining more purposeful and meaningful. (2) The preprocessing of data sources is the extraction and purification of data to obtain the data needed for data mining. It can be divided into three steps: the first step is to select the data related to user needs from the mass data; the second step is to remove irrelevant formats in the data, that is, noise. The third step is to convert the extracted and purified data into a unified format suitable for data mining. (3) Data mining is to mine the information in the data that users are interested in through algorithms. According to different needs, the results of data mining are not the same. (4) Mode evaluation is an indispensable stage in the whole system. It can be used to judge whether data mining is valuable or needs to be reminded. If data mining is found to be inconsistent with previously discovered knowledge or inconsistent with user requirements, mining again is required.

In most cases, users are not very clear about their needs, and data mining can find a variety of different knowledge patterns at the same time to help them make

decisions [27]. Data mining in the field of mobile Internet can improve market competitiveness, effectively reduce equipment and labor costs, and improve economic benefits to a large extent under the condition of meeting user needs and quality services. It has become a topic of universal concern for decision-makers.

Most of the time, users have a very clear vision of their needs; data tracking in the area of time can be asked to present a variety of different knowledge models to help the decision. Data mining in the field of mobile Internet can improve market competitiveness, effectively reduce equipment and labor costs, and largely improve economic benefits under the condition of satisfying user needs and providing high-quality services, which has become a topic of general concern for decision-makers [25].

Due to the need to collect trust relationships in social networks, typical data sets containing trust relationships in social networks include Epinions and FilmTrust. Epinions is a consumer rating site that allows users to rate their products and add people they trust to their trust lists. FilmTrust is a website that integrates social trust relationship and user rating, so that users can assign trust values to other users. The data set collected by the website contains user social trust data and user rating data. The offline comparison test adopts FilmTrust data set. According to the weight conversion formula, the traditional binary trust value (0,1) is converted (see Figure 3).

5. Conclusion

With the rapid development and wide application of the Internet, generations of products of the Internet era have been bred. Social networks in the Web2.0 era are attracting the attention of the whole world. Social network has become an open platform and channel for information circulation. It quietly changes the way users use information and share it. The information overload caused by massive amounts of data is becoming a huge barrier to use. Recommendation system provides personalized suggestions based on users' hobbies or behaviors, which has become one of the methods to solve this problem. Combined with the relevant features of social networks, the recommendation algorithm should be improved to improve the accuracy of the recommendation system, so as to provide users with high-quality personalized recommendation services and help solve the problem of information overload.

In view of the information overload problem in the current Internet environment, this article makes some studies on data sparsity and cold start problems in the research of recommendation system and can alleviate them to some extent. Although there has been some improvement in the recommendation results, there are still a lot of work worth further study. Future research will continue to focus on the following issues:

- (1) In real society, social network friend relationships are not necessarily established based on users' interests. How to find user preferences more accurately is still a key issue

- (2) The experiment is based on the data set in the offline environment. Once the algorithm goes online, it is bound to encounter many problems to be solved
- (3) The data set selected in the experiment cannot completely cover the user characteristics in the whole Internet environment. How to obtain good recommendation results in the big data environment needs further study
- (4) Users' preferences in the real environment will change with the influence of objective and subjective factors such as time, so how to dynamically capture users' interests needs further attention

Data Availability

The data used to support the findings of this study are available from the corresponding author upon request.

Conflicts of Interest

The authors declare that they have no conflicts of interest.

References

- [1] C. F. Tsai and Y. H. Hu, "Empirical comparison of supervised learning techniques for missing value imputation," *Knowledge and Information Systems*, vol. 64, no. 4, pp. 1047–1075, 2022.
- [2] M. A. Kumar and A. J. Laxmi, "Machine learning based intentional islanding algorithm for ders in disaster management," *Access*, vol. 9, pp. 85300–85309, 2021.
- [3] A. Sharma and R. Kumar, "A framework for pre-computed multi-constrained quickest QoS path algorithm," *Journal of Telecommunication, Electronic and Computer Engineering (JTEC)*, vol. 9, 2017.
- [4] S. Shalileh and B. Mirkin, "Summable and nonsummable data-driven models for community detection in feature-rich networks," *Social Network Analysis and Mining*, vol. 11, no. 1, pp. 1–23, 2021.
- [5] H. Qin, R. Li, Y. Yuan, G. Wang, and L. Qin, "Periodic communities mining in temporal networks: concepts and algorithms," *IEEE Transactions on Knowledge and Data Engineering*, vol. 9, 2020.
- [6] M. E. Gheche, G. Chierchia, and P. Frossard, "Orthonet: multilayer network data clustering. IEEE transactions on signal and information processing over networks," *IEEE Transactions on Knowledge and Data Engineering*, vol. 1, 2020.
- [7] J. Jayakumar, S. Chacko, and P. Ajay, "Conceptual implementation of artificial intelligent based E-mobility controller in smart city environment," *Wireless Communications and Mobile Computing*, vol. 2021, pp. 1–8, 2021.
- [8] R. A. Vasudev, B. Anitha, G. Manikandan, B. Karthikeyan, and V. Subramaniaswamy, "Heart disease prediction using stacked ensemble technique," *Journal of Intelligent and Fuzzy Systems*, vol. 39, no. 6, pp. 8249–8257, 2020.
- [9] J. Wang, J. Dong, and Y. Tan, "Role mining algorithms satisfied the permission cardinality constraint," *International Journal of Network Security*, vol. 22, no. 3, pp. 373–382, 2020.
- [10] Y. Alagrash, A. Drebee, and N. Zirjawi, "Comparing the area of data mining algorithms in network intrusion detection," *Journal of Information Security*, vol. 11, no. 1, pp. 1–18, 2020.

Retraction

Retracted: Software for Mapping and Extraction of Building Land Remote Sensing Data Based on BIM and Sensor Technology

Journal of Sensors

Received 17 October 2023; Accepted 17 October 2023; Published 18 October 2023

Copyright © 2023 Journal of Sensors. This is an open access article distributed under the Creative Commons Attribution License, which permits unrestricted use, distribution, and reproduction in any medium, provided the original work is properly cited.

This article has been retracted by Hindawi following an investigation undertaken by the publisher [1]. This investigation has uncovered evidence of one or more of the following indicators of systematic manipulation of the publication process:

- (1) Discrepancies in scope
- (2) Discrepancies in the description of the research reported
- (3) Discrepancies between the availability of data and the research described
- (4) Inappropriate citations
- (5) Incoherent, meaningless and/or irrelevant content included in the article
- (6) Peer-review manipulation

The presence of these indicators undermines our confidence in the integrity of the article's content and we cannot, therefore, vouch for its reliability. Please note that this notice is intended solely to alert readers that the content of this article is unreliable. We have not investigated whether authors were aware of or involved in the systematic manipulation of the publication process.

Wiley and Hindawi regrets that the usual quality checks did not identify these issues before publication and have since put additional measures in place to safeguard research integrity.

We wish to credit our own Research Integrity and Research Publishing teams and anonymous and named external researchers and research integrity experts for contributing to this investigation.

The corresponding author, as the representative of all authors, has been given the opportunity to register their agreement or disagreement to this retraction. We have kept a record of any response received.

References

- [1] S. Zhang and Y. Wan, "Software for Mapping and Extraction of Building Land Remote Sensing Data Based on BIM and Sensor Technology," *Journal of Sensors*, vol. 2022, Article ID 1026361, 7 pages, 2022.

Research Article

Software for Mapping and Extraction of Building Land Remote Sensing Data Based on BIM and Sensor Technology

Shaoping Zhang ¹ and Yaqin Wan ²

¹Department of Civil Engineering, Jiangxi Institute of Construction, Nanchang, Jiangxi 330200, China

²Center for Big Data and Smart Campus, Jiangxi Institute of Construction, Nanchang, Jiangxi 330200, China

Correspondence should be addressed to Yaqin Wan; 20120286@stumail.hbu.edu.cn

Received 20 May 2022; Revised 9 June 2022; Accepted 25 June 2022; Published 8 July 2022

Academic Editor: C. Venkatesan

Copyright © 2022 Shaoping Zhang and Yaqin Wan. This is an open access article distributed under the Creative Commons Attribution License, which permits unrestricted use, distribution, and reproduction in any medium, provided the original work is properly cited.

In order to solve the problem of complex extraction caused by large feature dimension of remote sensing data, this paper proposes a dimension compression extraction method of urban building land remote sensing data under BIM Technology. Firstly, the remote sensing data is imported into the BIM model for lightweight processing to obtain the element information required for urban construction land and then analyze the urban construction land data, extract the key elements of BIM Technology through semantic filtering, and use the triangulation method to transform the remote sensing data into the triangulation model that can be processed by GIS model. Finally, the random projection method is used to reduce the dimension and compress the remote sensing data, and the remote sensing data extraction of urban construction land is realized through dictionary learning, vocabulary coding, and feature extraction. The experimental results show that the accuracy of extracting different land use types by this method is more than 99%, while the accuracy of extracting different land use types by depth learning method and PLS method is less than 98.5%. In addition, the signal-to-noise ratio of the image extracted by this method is significantly higher than that by depth learning method and PLS method. *Conclusion.* This method can effectively compress and extract the urban construction land in the remote sensing data, and the extraction accuracy of remote sensing data is high. It provides a technical basis for the approval of urban construction planning. It has the advantages of simple feature extraction and effective differentiation of ground objects.

1. Introduction

Remote sensing is a key technology in the dynamic monitoring of urban construction land. In the process of extracting urban construction land information from satellite images, it fully reflects the systematicness and integrity. Rapid and accurate extraction of urban construction land (residence, industrial land, square road land, municipal land, etc.) and dynamic monitoring of urban construction land are of great significance for scientific planning and balancing the contradiction between economic development and land supply and demand [1]. Compared with the traditional manual statistical survey, the automatic and semiautomatic extraction and change detection methods have strong objectivity and accuracy in the extraction of urban

buildings. Due to the high complexity of remote sensing images, the buildings in urban areas are different from building materials to the overall layout, and many technologies are involved in the recognition and extraction of ground objects, such as digital image processing and intelligent recognition [2]. Using satellites, UAVs, and other aircraft to obtain remote sensing images and detect ground object changes is the research focus of many remote sensing experts and scholars. Gradually reducing the manual intervention in the detection process and realizing the automation of change detection based on remote sensing image is a research hotspot [3]. The rapid and accurate extraction of urban residential construction land information is of great significance to grasp the dynamics of urban development and reasonably plan urban construction.

2. Literature Review

The feature of ground object image is the reflection of the difference of ground object electromagnetic wave reflectivity in remote sensing image. According to its manifestation, it can be divided into color, tone, shape, texture, size, spatial distribution, and so on. For target classification and recognition, image features are one of the basic factors of discrimination. Different image features represent different ground objects. Therefore, the accurate extraction of image features is the key to the extraction of urban construction land information. Spectral information is the most basic feature of remote sensing image. Different ground objects have different components and different reflection characteristics of energy. It is the theoretical basis for distinguishing ground object types by image spectral values. Based on the spectral values of remote sensing images, Yekrangnia and others analyzed the differences between urban construction land and other land types in Landsat TM2, TM3, TM4, TM5, TM7, and other bands; discussed the methods to enhance the information of urban construction land; and analyzed the spectral structure characteristics of various classes. Through a simple closed value method, urban construction land was extracted, with point accuracy of and area accuracy of [4]. The accuracy of extracting information from the urban image by using the method of man-machine interaction is much higher than that by using the method of man-machine interaction, but the reliability of extracting information from the urban image by using the method of man-machine interaction is quite high. Based on the theory of image spectral value, it is a common method to obtain urban construction land information by using the idea of hierarchical classification [5]. Liu and others used Landsat MSS and TM data to study the land cover of cities and suburbs. The study considered that the TM data of suburbs with more uniform land cover was better classified, while the MSS data of regions with complex land cover was better classified, and considered that low-pass filtering was used to improve the separability between land types [6]. Karimi and others proposed a V-I-S (vegetation impervious surface soil) model to study urban ecology and regarded each pixel in the remote sensing image as a linear combination of these three representative land cover types [7].

GIS technology is a spatial database technology, which can store massive three-dimensional spatial data and effectively manage it. At the same time, it can apply visual analysis of massive data, which plays an important role in urban construction land management and analysis. The main information source and core composition of GIS are remote sensing images and data. Using GIS can effectively realize spatial data analysis and management and improve the utilization value of images and data [8]. This paper proposes a method to compress and extract the dimension of remote sensing data of urban construction land under BIM Technology. BIM Technology is used to process a large number of urban construction land, and the processed data is transformed into GIS software. The data dimension compression and extraction method are used to effectively extract the data of urban construction land.

3. Research Methods

3.1. Remote Sensing Data Dimension Compression Extraction Method Based on BIM Technology

3.1.1. Remote Sensing Data Dimension Compression and Extraction Process of BIM Technology. BIM is short for building information model. BIM Technology refers to taking the basic components in the construction project as the design elements, organically organizing the geometric data, physical characteristics, material information, and other relevant information describing the component elements to form a database integrating all aspects of the information of the building system. All parameter information of the component is stored in this database, which constitutes the data model of the construction project. In order to meet the corresponding work needs, all participants insert, extract, edit, and update the information in the model database. The parameter information of various components in the model is not an independent information individual, and they also maintain a certain spatial and logical relationship [9]. As an integral part of BIM model, a virtual digital building, they jointly form a complete and hierarchical building information system. Here, BIM Technology is applied to urban construction land to provide complete and accurate data support for construction planning approval. In this paper, BIM Technology is combined with GIS model. Based on BIM model data, BIM model is used to analyze the collected remote sensing data and compress and extract urban construction land. The specific scheme flow chart of urban construction land compression and extraction [10, 11] is shown in Figure 1.

Import the extracted data to be compressed into the BIM model and lightweight process the BIM model, use lightweight processing to obtain the element information required for urban construction land, extract the key element information of BIM Technology after fully analyzing the urban construction land data, and convert the extracted element data into GIS model [12]. Realize the dimension compression of remote sensing data through random projection dimensionality reduction, and realize the dimension extraction of remote sensing data of urban construction land by using visual vocabulary map.

3.1.2. BIM Key Element Extraction and Data Conversion Method. BIM Technology includes the relevant building settings and spatial interfaces of all links such as architectural design, construction, and management. Simplify the BIM model for different research directions, use the BIM model to process remote sensing data, filter relevant information, and obtain the relevant key elements of urban construction land [13]. The key element extraction and data conversion process of BIM Technology is shown in Figure 2.

In the past, the application of BIM Technology to urban construction land extraction has the disadvantage of data redundancy, which will cause some complexity to urban construction land approval. Before extracting urban construction land, semantic filtering is mainly implemented according to the specific requirements of urban construction land, and different data filters are used to remove the

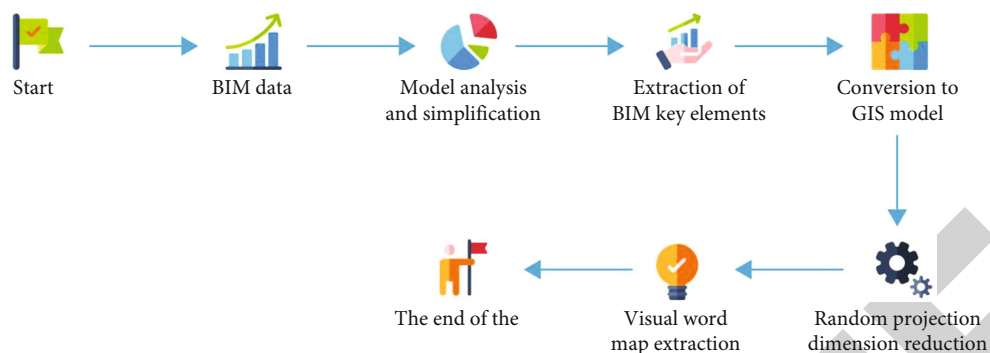


FIGURE 1: Compression and extraction process of remote sensing data dimension of urban construction land.

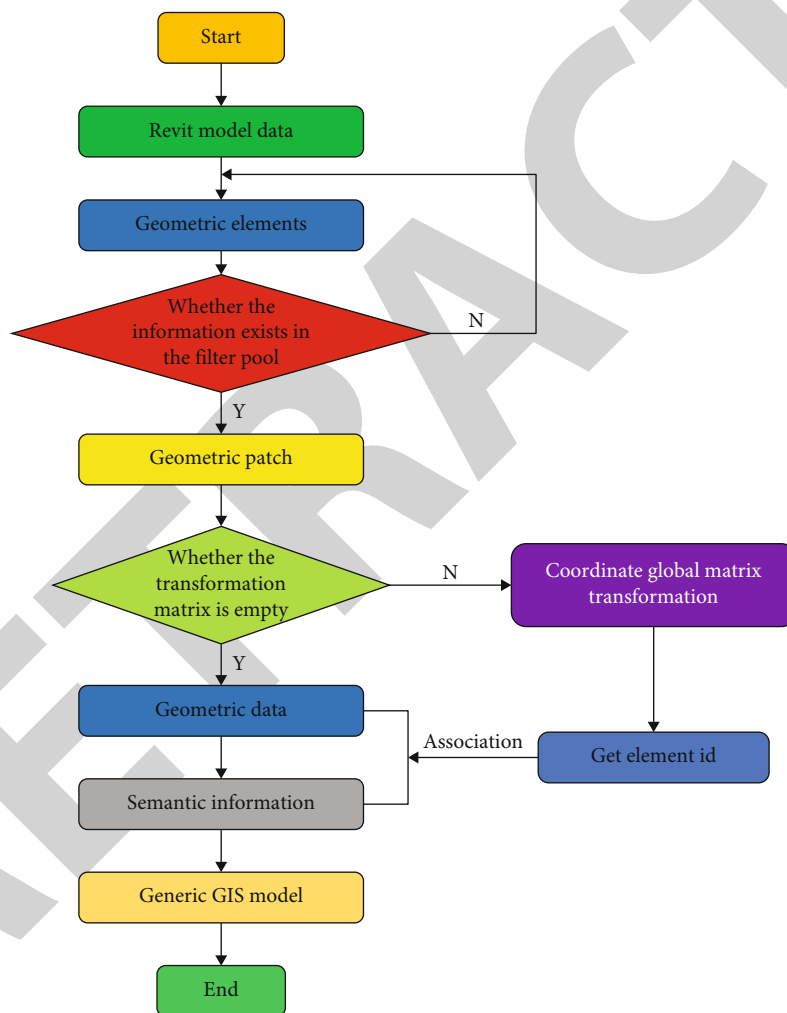


FIGURE 2: Key element extraction and data conversion process.

semantic filtering of urban construction land. In remote sensing images, land use types mainly include high-density construction areas, low-density construction areas, new construction areas, mountains, forests, shrubs, cultivated land, Hubo, oceans, and rivers. According to the type of urban construction land, words unrelated to urban construction land, such as mountain, forest, shrub, cultivated

land, Hubo, ocean, and river, are used as semantic filters. Only words related to urban construction land are retained, and redundant words unrelated to urban construction land are removed.

Combine the internal elements of the BIM model with the constraints of the semantic filter to obtain the important set information of the semantic filter, convert the BIM entity

model into the triangular network model supported by the GIS model by the three network method, obtain the coordinate conversion matrix of the GIS model in the conversion process, and convert the outline of the urban construction land to the global coordinate system of the GIS model [14]. The ID value and the semantic information and geometric information related to urban construction land are used as the management data of GIS model data. The positioning of urban construction land adopts BIM Technology to import massive data into GIS model, and the specific coordinates are determined by one-to-one correspondence between Revit measurement points and actual measurement points, so as to realize the correct positioning of massive remote sensing data after extracting urban construction land by BIM compression technology and transforming it into GIS model coordinate system.

3.1.3. Remote Sensing Data Dimension Compression Extraction Method. The dimension compression extraction method of remote sensing data mainly includes two parts: dimension reduction and dimension selection. The dimension compression of remote sensing data is realized by random projection dimension reduction, and the dimension extraction of remote sensing data of urban construction land is realized by visual vocabulary map.

Feature dimensionality reduction is based on random projection. Set the remote sensing image as I , in which the number of bands is n ; extract the image block from each band of the remote sensing image according to the pixel order; the window size is $b \times b$; and the sorting rule is as follows [15]:

$$z^{S_q} = \left[q_{0,0}, \text{sort}(q_{1,0}, \dots, q_{1,t_1}), \dots, \text{sort}(q_{a,0}, \dots, q_{1,t_a}) \right]^T, \quad (1)$$

where $q_{0,0}$ represents the central pixel and $a = 1, 2, \dots, \text{fix}(b/2)$.

After sorting according to the original sequence $z^{S_q} \in W^{b^2}$, the sequence is formed according to the original sequence (1).

Combining spatial information with spectrum, a new feature vector $z^{S_q} \in W^{nb^2 \times 1}$ is formed by using the feature vector containing the number of bands n .

The high-dimensional feature vector z^{S_q} is mapped to the low-dimensional feature vector Z^{CS} by random projection:

$$Z^{CS} = \Gamma z^{S_q}, \quad (2)$$

where Γ represents the random projection matrix and conforms to $\Gamma \in W^{h \times k}$, $k = nb^2$, $h \ll k$. The compressed feature subspace $\{Z^{CS}\}$ is composed of all compressed feature vectors.

The size parameter of the random projection matrix Γ should conform to the JL introduction, and it should conform to the limited isometric property according to the compressed sensing theory [16].

Feature extraction is based on visual vocabulary map. The visual vocabulary map selects the central word of all

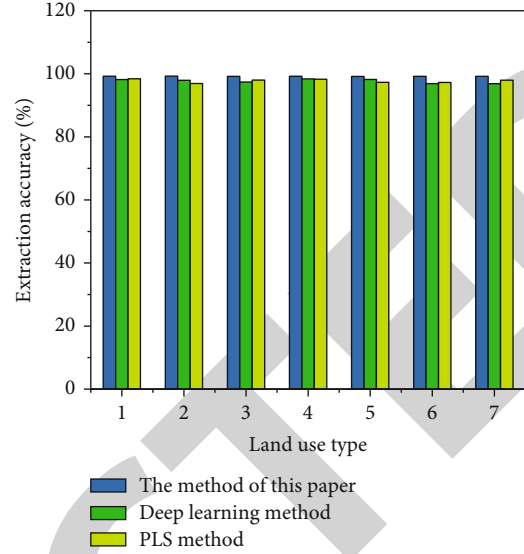


FIGURE 3: Extraction accuracy of different land use types.

pixel positions and the word in the pixel neighborhood $u \times u$ as texture primitives and uses the visual vocabulary map to extract the urban building land in the remote sensing image as the texture feature of the pixel expressing interest. The size of texture primitives containing texture information obtained by this method is $b \times b$, which can reflect the properties of texture primitives with high quality. The words in neighborhood $u \times u$ in the visual vocabulary map can effectively reflect the global spatial information and the spatial information including the category of central pixels. The problem characteristics can be reflected through two windows to describe multiscale remote sensing data. The global texture features of urban construction land are extracted by visual vocabulary map, including dictionary learning, vocabulary coding, and feature extraction [17].

- (1) Dictionary learning. The K-mean algorithm is applied to the compressed feature subspace. The similarity measurement criterion is Euclidean distance, and the center of clustering all kinds of training samples $\{Z_{T_i}^{CS}\}$ is the vocabulary dictionary s_i of this class

Let the number of existing sample categories and the number of clustering centers be C and K , respectively, and use the combination of vocabulary dictionaries of different categories to obtain the final compressed texture vocabulary dictionary $S \in W^{h \times CK} = \{s_1, s_2, \dots, s_C\}$, with the size of CK .

- (2) Vocabulary coding. According to the obtained texture dictionary S , the nearest neighbor algorithm is selected to calculate the Euclidean distance from all words in B to the texture primitive in $\{Z^{CS}\}$, and the texture primitive is coded with the corresponding number of the word with the smallest distance.

TABLE 1: Comparison of extraction accuracy of different methods.

Building type	Actual quantity	Paper method	Deep learning method	PLS method
Multi-storey residential building	584	582	578	581
Factory building	625	623	621	619
Public buildings	715	710	706	708
Single-storey new house	642	640	634	628
Single-storey-old house	584	581	574	564
High-rise residential	602	599	586	589
Total	3752	3735	3699	3689

TABLE 2: Comparison of misjudgment times of different methods (unit: times).

Test area	Paper method		Deep learning method		PLS method	
	Buildings are treated as nonbuildings	Nonbuildings are treated as buildings	Buildings are treated as nonbuildings	Nonbuildings are treated as buildings	Buildings are treated as nonbuildings	Nonbuildings are treated as buildings
1	0	1	3	5	2	4
2	0	2	2	2	5	2
3	0	1	3	4	3	3
4	1	0	1	3	4	5
5	0	1	3	6	2	4
6	0	0	2	4	1	2
7	1	0	3	8	5	3
8	0	1	4	5	0	5
9	0	0	2	1	3	1
10	0	0	3	3	2	3
Total	2	6	26	41	27	32

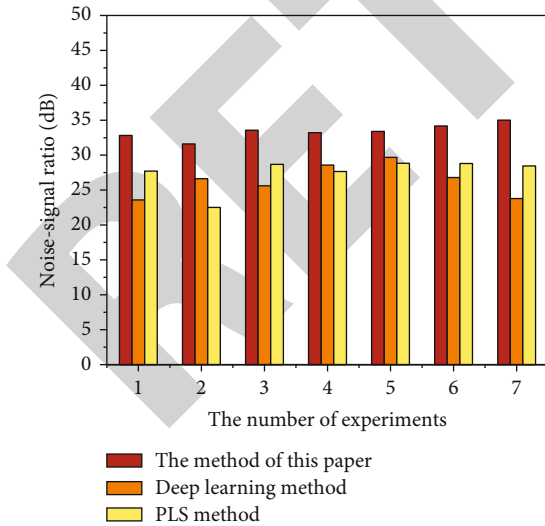


FIGURE 4: Comparison of signal-to-noise ratio of extraction results by different methods.

The visual vocabulary is composed of the word number in the $u \times u$ neighborhood and the central word. The corresponding texture primitive of each word in

the Figure is represented by $l_{i,j}$ and the central pixel is represented by $x_{0,0}$

- (3) Feature extraction. The statistical characteristics of remote sensing data are reflected by the vocabulary histogram $\mathbf{G} = [\eta_1, \eta_2, \dots, \eta_{CK}]^T$ of the visual vocabulary map, and the number of occurrences of word i in the visual vocabulary map is expressed by η_i . The spatial information of words in the visual vocabulary map is added to improve the extraction accuracy. The spatial distribution information in the vocabulary map selects different words, which are reflected by the second-order moment $\mathbf{R} = [\mu_1, \mu_2, \dots, \mu_{CK}]^T$ of the central pixel position, and $\mu_i = (\sum_{j=1}^{\eta_i} (s_{i,j} - \bar{s}_i)^2) / \eta_i$, where $s_{i,j}$ and \bar{s}_i , respectively, represent the distance from the word i to the center point and the average distance

The second-order moment information and histogram information are fused to obtain the final texture measurement $Z \in W^{2CK \times 1}$, which is as follows [18]:

$$Z = (G; R). \quad (3)$$

3.2. Simulation Experiment. In order to test the effectiveness of the system in this paper to compress and extract urban building land, the eastern area of Dazu District in a city was selected as the experimental object, and the method of this paper was programmed in the computer with the operating system of Windows XP using Java language.

4. Result Analysis

This method is used to compress and extract the urban construction land from the remote sensing image. This method can effectively compress and extract the urban construction land in the collected remote sensing images.

The land use types in this area mainly include high-density construction area, low-density construction area, new construction area, mountain, forest, shrub, and cultivated land, including 3 kinds of construction land and 4 kinds of nonconstruction land. Here, the extraction accuracy of this method under different land use types is counted, the compression extraction accuracy of this method is tested, and this method is compared with depth learning method and PLS method [19]. The comparison results are shown in Figure 3. As can be seen from the experimental results in Figure 3, the accuracy of extracting different land use types by this method is more than 99%, while the accuracy of extracting different land use types by deep learning method and PLS method is less than 98.5%, indicating that the extraction accuracy of this method is significantly higher than that of the other two methods.

The buildings in the remote sensing image mainly include 6 kinds of multistorey residential buildings, factory buildings, public buildings, single-storey new houses, single-storey old houses, and high-rise houses. The number of 6 kinds of buildings extracted by three methods is compared with the actual number of buildings. The comparison results are shown in Table 1. It can be seen from the experimental results in Table 1 that the difference between the number of different buildings extracted by this method and the actual number of buildings is small, while the difference between the number of different buildings extracted by depth learning method and PLS method and the actual number of buildings is large [20]. The experimental results verify the extraction accuracy of this method again.

Ten regions are randomly selected from the remote sensing image. Under the method of this paper, the number of two misjudgment indexes of building land as nonbuilding and nonbuilding as building are extracted, and the method of this paper is compared with depth learning method and PLS method [21]. The comparison results are shown in Table 2. It can be seen from the experimental results in Table 2 that the number of misjudgment indexes of using this method to compress and extract urban construction land buildings as nonbuildings and nonbuildings as buildings is significantly lower than that of deep learning method and PLS method, indicating that this method can extract urban construction land more accurately and has high extraction accuracy.

According to the statistics, the signal-to-noise ratio of the final result of urban construction land in the remote

sensing image is extracted seven times by using the method in this paper, and the method in this paper is compared with the depth learning method and PLS method [22]. The comparison results are shown in Figure 4. It can be seen from Figure 4 that the signal-to-noise ratio of the image extracted by this method is significantly higher than that of the deep learning method and PLS method, which shows that this method can effectively maintain the useful information in the image, and the image processed by this method can still maintain a high signal-to-noise ratio, which effectively verifies that this method has good extraction performance.

5. Conclusion

BIM Technology is an information technology widely used in the construction industry. BIM Technology has become the mainstream of the development of the construction industry and provides technical support for the digital management of the construction industry. In this paper, BIM Technology is applied to the dimension compression and extraction method of remote sensing data of urban construction land, the required BIM component information is analyzed, and the information irrelevant to urban construction land is filtered. The method of random projection and visual vocabulary map is used to compress and extract the characteristics of urban construction land. Make full use of the data integrity characteristics of BIM Technology, maximize the accuracy of urban construction land extraction, and provide technical basis for urban construction planning approval. It has the advantages of simple feature extraction and effectively distinguishing features.

Data Availability

The data used to support the findings of this study are available from the corresponding author upon request.

Conflicts of Interest

The authors declare no conflicts of interest regarding the publication of this paper.

Funding

This study is funded by the research on the reconstruction of course system of BIM major of civil engineering under the 1+X"certificate system (JXJG-20-72-3) of teaching reform project of Jiangxi Province colleges and universities and research on the application of BIM technology in the layout of furniture and appliances in hardbound commercial houses (GJJ 191388) under the science and technology research project of Jiangxi Education Department.

References

- [1] Y. Yang, G. Hu, and C. J. Spanos, "Stochastic optimal control of hvac system for energy-efficient buildings," *IEEE Transactions on Control Systems Technology*, vol. 99, pp. 1–8, 2021.
- [2] N. Yu, C. Chen, K. Mahkamov, I. Makhkamova, and J. Ma, "Selection and testing of phase change materials in the physical

Retraction

Retracted: Application of Symmetric Encryption Algorithm Sensor in the Research of College Student Security Management System

Journal of Sensors

Received 17 October 2023; Accepted 17 October 2023; Published 18 October 2023

Copyright © 2023 Journal of Sensors. This is an open access article distributed under the Creative Commons Attribution License, which permits unrestricted use, distribution, and reproduction in any medium, provided the original work is properly cited.

This article has been retracted by Hindawi following an investigation undertaken by the publisher [1]. This investigation has uncovered evidence of one or more of the following indicators of systematic manipulation of the publication process:

- (1) Discrepancies in scope
- (2) Discrepancies in the description of the research reported
- (3) Discrepancies between the availability of data and the research described
- (4) Inappropriate citations
- (5) Incoherent, meaningless and/or irrelevant content included in the article
- (6) Peer-review manipulation

The presence of these indicators undermines our confidence in the integrity of the article's content and we cannot, therefore, vouch for its reliability. Please note that this notice is intended solely to alert readers that the content of this article is unreliable. We have not investigated whether authors were aware of or involved in the systematic manipulation of the publication process.

Wiley and Hindawi regrets that the usual quality checks did not identify these issues before publication and have since put additional measures in place to safeguard research integrity.

We wish to credit our own Research Integrity and Research Publishing teams and anonymous and named external researchers and research integrity experts for contributing to this investigation.

The corresponding author, as the representative of all authors, has been given the opportunity to register their agreement or disagreement to this retraction. We have kept a record of any response received.

References

- [1] K. Wu and C. Li, "Application of Symmetric Encryption Algorithm Sensor in the Research of College Student Security Management System," *Journal of Sensors*, vol. 2022, Article ID 3323547, 7 pages, 2022.

Research Article

Application of Symmetric Encryption Algorithm Sensor in the Research of College Student Security Management System

Kexu Wu ¹ and Chaolin Li ²

¹Smart Radio and Television College, Sichuan Media University, Chengdu, Sichuan 611745, China

²School of Digital Media Creative Design, Sichuan Media University, Chengdu, Sichuan 611745, China

Correspondence should be addressed to Chaolin Li; 31115304@njau.edu.cn

Received 23 May 2022; Revised 1 June 2022; Accepted 21 June 2022; Published 7 July 2022

Academic Editor: C. Venkatesan

Copyright © 2022 Kexu Wu and Chaolin Li. This is an open access article distributed under the Creative Commons Attribution License, which permits unrestricted use, distribution, and reproduction in any medium, provided the original work is properly cited.

In order to solve the problem of information leakage in the process of college students' information security management, this paper proposes a design of college students' security management system based on a symmetric encryption algorithm. The system is based on the principle of the symmetric encryption algorithm and follows the principle of encryption independence to ensure the security and reliability of the system. The general framework of the system is analyzed in detail. Secondly, the security and database of system function modules are designed, and finally, the performance of the system is tested. The results are as follows: the safety management system designed in this paper has obtained satisfactory evaluation in the trial universities, accounting for 93% of the trial population. It is proved that this system has clear authority design, high efficiency, and security. Managers can query students' basic information, students' real-time location, alarm data information, and so on in real time, which can ensure students' safety to the greatest extent.

1. Introduction

At present, people pay more and more attention to the security of computer mass data storage and the antitheft and antitampering of sensitive data [1]. The database system is the core component of the computer information system, and database file is the aggregate of information. Its security will be the top priority of information industry [2].

The core of information security is database security, and database encryption is one of the core issues of database security. Compared with other security means, database encryption is the security means with the highest performance price ratio from the comprehensive consideration of security degree, price, use, and maintenance cost and upgrade cost [3]. Aiming at the security of database, this paper discusses the relevant database security strategy and encryption technology, encryption algorithm and encryption method, and the application of data encryption technology in university archives database.

According to statistics, a computer virus intrusion occurs in an average of 20 seconds around the world. About 1/4 of

the firewalls on the Internet were broken. The incidents of stealing business information increased at an average rate of 260% per month. About 70% of network executives report losses due to disclosure of confidential information [4, 5]. The teaching of many school systems can only be used as a carrier through the Internet, but in this online education system, there are many precious teaching resources facing the risk of disclosure. In addition to taking various preventive measures, there is also a line of defense is the encryption of university archives data base, which starts the discussion of database encryption [6].

The security of university archives database is not isolated, but a complete system. According to the current security needs of university archives database, this paper designs a complete system for university archives information management system, that is, the whole database security system is a three-tier security model: outer defense, middle layer intrusion detection, and inner data security defense, and database encryption is one of the core issues of inner database security defense.

2. Literature Review

Database encryption is to use the existing database encryption technology to study how to encrypt and decrypt the data in the database, so as to improve the security of the database system [7]. Generally speaking, the security control measures provided by the database system can meet the application of general databases, but for the application of some important departments or sensitive fields, such as financial data, military data, and state secrets, naturally including university archives database, only these are difficult to fully ensure the security of data [8]. Therefore, it is necessary to encrypt the important data stored in the database on the basis of access management and security management, so as to strengthen the security protection of data storage.

The basic idea of encryption is to transform the original data (plaintext) into an unrecognizable format (ciphertext) according to a certain algorithm, so that people who do not know the decryption algorithm cannot know the specific content of the data [9]. There are two main encryption methods: one is the replacement method, which uses the key to convert each character in the plaintext into a character in the ciphertext, such as replacing a with F, b with X, c with Q, so lurk may become NMWJ [10]. The other is the rearrangement method, which only rearranges the characters of plaintext in different order. Using either of these two methods alone is not safe enough, but the combination of these two methods can improve the degree of safety.

Since data encryption and decryption are also time-consuming operations, and the higher the degree of data encryption and decryption, the greater the system resources occupied. Therefore, generally, only highly confidential data are encrypted. The traditional encryption takes the message as the unit, and the encryption and decryption are carried out from beginning to end [11]. The use of database data determines that it is impossible to encrypt the whole database file. When the records that meet the search conditions are retrieved, the records must be declassified quickly [12]. However, the record is a random section in the database file, and it cannot be declassified from the middle, unless it is declassified from beginning to end, and then find the corresponding record. Obviously, this is inappropriate. We must solve the problem of random declassification from a certain section of data in the database file. In the traditional cryptosystem, the key is secret, and the fewer people know, the better [13]. Once you get the key and cryptosystem, you can break the password and unlock the ciphertext.

Database encryption is to enhance the security of ordinary relational database management system and effectively protect the contents stored in the database [14, 15]. It realizes the confidentiality and integrity requirements of database data storage through security methods such as database storage encryption, so that the database is stored in ciphertext and works in secret mode, ensuring data security.

The basic process of data encryption includes the translation of plaintext (i.e., read information) into the code form of ciphertext or password. The reverse process of this process is decryption, that is, the process of trans-

forming the encoded information into its original form. Encryption can not only provide confidentiality for data but also provide confidentiality for communication service flow information [16].

Encryption algorithm is some formulas and rules, which stipulates the transformation method between plaintext and ciphertext. Key is the key information to control encryption algorithm and decryption algorithm. Its generation, transmission, and storage are very important.

Database encryption belongs to data encryption, which is just a special data encryption. There is not much fixed data relationship between encrypted data, but there is a certain data relationship between the data in the database [17]. When encrypting the database, we should consider the database system itself. We should first consider the three encryption levels, three encryption methods, and choice of encryption granularity. The three encryption levels of the database are the encryption forms implemented on the OS layer, the DBMS inner layer, and the DBNS outer layer. The three encryption methods are external encryption, internal encryption, and hardware encryption; Encryption granularity refers to the smallest unit of database encryption. The data in the database can be divided into the data table, data record, field, and data item according to the hierarchy, so the encryption granularity of database data encryption usually includes file level, field level, record level, and data item level. For example, the wider the scope of encryption technology for students, the smaller the flexibility of the encryption-based system. In practical application, different encryption granularities are selected according to different security requirements to achieve the goal of ensuring data security and easy operation [18, 19]. Therefore, database encryption is to consider the more complex data encryption of database system, rather than simply considering encryption algorithm and encryption and decryption. Figure 1 is the campus student security management system based on encryption technology.

Based on the current research, through the comparison of various algorithms, this paper selects the CBC mode of 128 bit AES encryption algorithm to encrypt data and adopts the complete database field encryption and decryption mechanism, so as to design a set of practical data encryption system. In this system, the characteristics of demand analysis, analysis design, coding, testing, and deployment of the university archive database encryption project are discussed, with emphasis on the protection provided by the password system for university database, the potential caused by the password system itself, and the preparation for this risk. The key to the security of cryptographic algorithm is how to ensure the confidentiality of the key and how to manage the key to withstand all levels of attacks. Based on the database structure defined by SQL, the coding of each main module of the system is realized.

3. Research Methods

3.1. Establishment of Database Encryption Key Generation Function. Generally speaking, the database system running on a single machine has no data sharing problem, and its

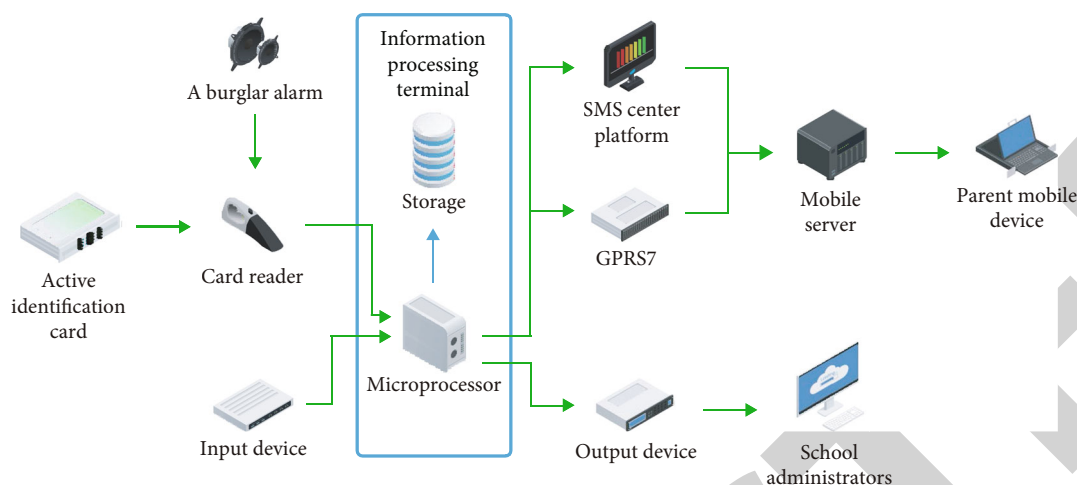


FIGURE 1: Campus student security management system based on encryption technology.

TABLE 1: Comparison of various algorithms.

Password type	Symmetric cryptosystem					Asymmetric cryptosystem	Hash algorithm
Name of comparison item	DES	AES	IDEA	RC5	RC6	RSA	MD5
Development time	1977	2001	1991	1995	1996	1977	1993
Is it protected by patent	No	No	No	No	No	No	No
Key length	56 b (double DES112b, triple DES168b)	128 b or 192 b or 256 b	128 b	Variable length key up to 256 b	Variable length key up to 256 b	512 b is selected, and the longest is 1024 b	238 b
Number of bits of processing block during encryption	64 b	128 b	64 b	128 b	128 b	Most of 110 b	128 b
Encryption speed	Fast	Very fast	Fast	Fast	Fast	Very slow	Slow

confidentiality and authenticity can be guaranteed at the same time. Therefore, the security of the database system can be realized by controlling the access to the database files [20]. For the database system running in the network environment, its remarkable feature is data sharing. Therefore, the function of data encryption technology is to ensure the authenticity of data without affecting data sharing. Its main encryption technology is based on the encryption of records and fields. In order to ensure that the system is not attacked, it is best to use different keys for the same field of different records, so the number of keys is very large [21]. If there are M records in a table and each record has N fields, the number of keys required is $M * N$, and the number of keys of the whole system is more. Obviously, such a large number of keys cannot be stored and managed for a long time and can only be generated dynamically when needed. The key generation function satisfies at least three conditions: first, the probability that the keys of different data items are the same is very small. Second, it is difficult to obtain other data item keys from one data item key. Third, some information of a data item (such as value range and probability distribution) is known, and other information of the data item can-

not be obtained from ciphertext. Then, the key functions that can meet the above three items are shown in

$$k_{ij} = k_i \oplus k_j, \quad (1)$$

$$k_i = E(TK, R_i), \quad (2)$$

$$k_j = E(TK, C_j). \quad (3)$$

In the formula, k_i is the data item key generation function, TK is the table key, R_i is the encrypted field row flag, and C_j is the encrypted field column flag [22]. For the data item key generation function, an effective implementation method is to use an algorithm to encrypt R_i and C_j with table key TK as the key to obtain keys k_i and k_j and then perform logical operation on k_i and k_j to obtain the data item key. Here, TK is the key, R is the row ID, and C is the field ID. Encrypt C_j and R_i , respectively, through key TK , generate field key k_j and record key k_i , and then generate key k_{ij} after XOR operation of k_j and k_i [23].

The comparison of various encryption algorithms is shown in Table 1:

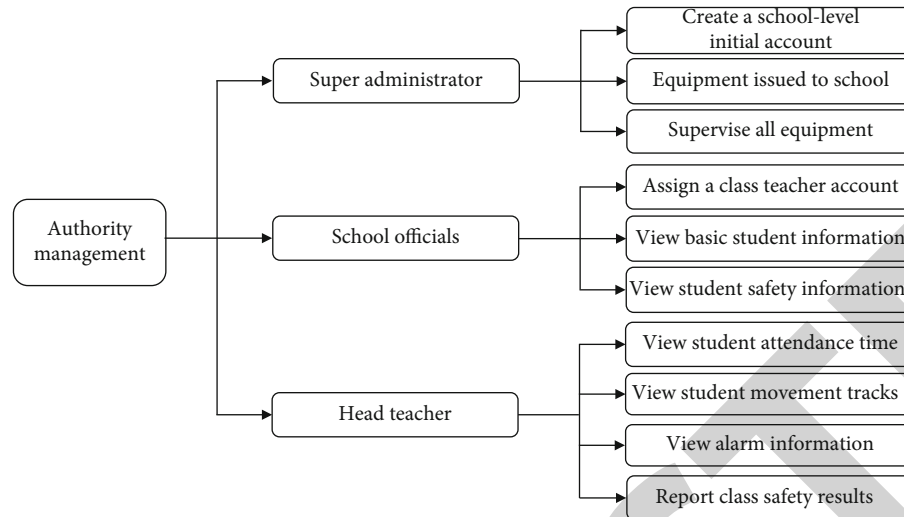


FIGURE 2: Background management platform permissions.

3.2. System General Framework Design. Based on the B/s and C/S frameworks, through comprehensive consideration, the student safety management system is designed in the integration mode of the two [24]. Taking the C/S framework as the carrier, the server receives the data of portable devices and uses the worker man architecture to receive and store the data. With the B/S framework as the carrier, managers monitor students' daily safety in real time through the management platform based on think PHP architecture [25]. This design mode only needs to take the server-side as the auxiliary development system and compile the socket server-side code, which can save the system development cost, and the requirements for the client are relatively low. Students only need to carry portable devices, and managers can monitor students' security in real time through the browser. The combination of worker man architecture and think PHP architecture can not only ensure the data authenticity of student safety management system but also ensure that managers supervise student safety in the whole process.

3.3. Management Platform. The background server management platform selects HTML+CSS+JS to realize the page. The background chooses PHP language to realize development. The PHP language has unique advantages in web development server-side scripting language. It is open source, and the source code can be downloaded and browsed in real time. The use is free, which can effectively save the development cost. It has good platform transfer characteristics and can support Linux, Windows, etc. There are various mainstream frameworks for PHP, that is, Laravel and ThinkPHP. This paper chooses ThinkPHP architecture to design the system.

3.4. Authority and Function. The system is divided into three types of different permissions, corresponding to different functions. When the user logs in to the page, enters the account and password, and verifies that the information is correct, the background will independently evaluate the user authority to jump to different pages and realize different

functions. High-level permissions can manage low-level permissions. Low-level permissions only have basic operation functions. There are three kinds of system design permissions, namely, super manager, college head, and head teacher, as shown in Figure 2.

First, the super administrator and developer manage their account. Their task is to assign the initial account password to the person in charge of the college, manage the person in charge of the school level, add or delete equipment, and monitor the operation status of equipment in real time. Second, the person in charge of the college is responsible for compiling the basic information of the university, assigning the initial account and password to the head teacher, applying for facilities and equipment, and querying the operation status of the equipment, as well as the basic information of students and the student security information transmitted by the person in charge of the class. Third, the head teacher is directly responsible for the safety of students, that is, students are bound with equipment and query students' attendance time, movement track, and alarm information.

3.5. Safety Design

(1) SQL injection attack

SQL injection attack belongs to the form of Web attack. This attack exists because the system background program does not strictly verify the user's input data, resulting in illegal elements to conduct destructive manipulation after obtaining the user's data information in the database in a malicious way. In terms of SQL injection attack, the background system queries statements in the form of array and selects the preprocessing mechanism to filter dangerous data for a few string query conditions.

(2) URL encryption algorithm

Because security problems are easy to occur during data transmission, encryption is a necessary link in the system

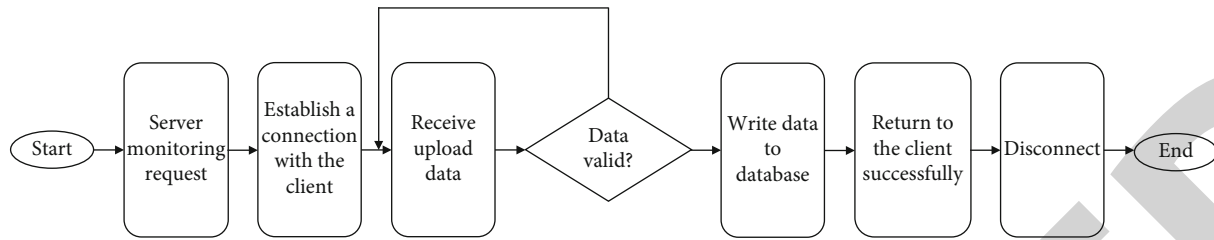


FIGURE 3: Data receiving process.

design. The system design encryption work is mainly carried out based on URL. For important parameters, users are prompted to browse the data information in the encrypted state in the form of encryption. Developers independently compile the encryption algorithm and decryption algorithm.

Commonly used encryption algorithms in PHP include MD5, SHA1 and Base64. MD5 encryption algorithm belongs to one-way hash encryption technology, and Base64 belongs to symmetric encryption algorithm. However, due to its frequent use, it has certain security risks. In addition, in the third-party website, the traditional encryption algorithm can be decoded in the form of payment. In short, the encryption algorithm of this system is independently compiled by the developer, with the best security and economy.

The system design encapsulates encryption and decryption into two functions. The implementation of encryption is to connect the user's character information with a string to obtain a new string; For the new string, Base64 encryption function is used to complete the encryption, and the encrypted string is divided into an array based on the string segmentation function. We splice the elements of the array in the form of array loop to obtain a new array and turn back the string and replace the special characters of the string to obtain the final result after encryption.

The specific effect of encryption is to asynchronously transmit the user form data in the background, strictly encrypt the important parameters in the background, and transmit the encryption results to the foreground. The foreground jumps the encryption parameters and other parameters to the specified interface based on the URL splicing mode, and the background decrypts with the decryption algorithm to recover the data and process the business logic, so as to improve the security and stability of the system.

(3) Socket design

The specific process of socket data receiving of the system is to select JSON format to transmit data, open the port on the server side to receive the client data, and analyze it. Feedback error information to the client for abnormal data and abnormal operation, and stop the operation in time. When the data is correctly programmed into the database, return the normal description to the client, terminate the connection with it, and resupervise in real time. The socket data receiving process is shown in Figure 3.

(4) Database design

The college student safety management system is realized by the entity relational database design. Based on demand analysis, the E-R diagram is used to build a model that can effectively reflect the actual things and relations and explain the data framework of the database which is too abstract. The entity relationship is used to abstract the processing data information, realize the transformation from entity geometry to entity type, and reflect the internal correlation of actual things through entity relationship. We build the local E-R model, integrate the local model into the overall model, and optimize and improve it. The system E-R diagram is shown in Figure 4 (1 and N are interentity relations, that is $1:n$ or $N:1$, one college corresponds to multiple counselors, one counselor corresponds to multiple students, and multiple students correspond to one behavior; 1 represents a single, N represents multiple).

4. Result Analysis

In actual use evaluation of the system, the safety management system designed in this paper is tried in a university, and the students who have used the knowledge sharing system evaluate the system. The evaluation of the system is carried out from six aspects: system resource richness (E), system use convenience (F), system security (G), information transmission speed (H), system fluency (J), and overall evaluation (L). Each aspect is scored in the percentage system. The calculation formula of the overall score (T) is as follows:

$$T = (E * 0.1 + F * 0.1 + G * 0.4 + H * 0.15 + J * 0.15 + L * 0.1) * 100\%. \quad (4)$$

The collected scores are summarized and analyzed, and the results are shown in Figure 5.

As can be seen from Figure 5, the safety management system designed in this paper has obtained satisfactory evaluation in the trial universities, accounting for 93% of the trial population. According to the collected improvement opinions, this paper will focus on the analysis and further improve the system, so as to put it into use on a large scale and improve the management efficiency of university information.

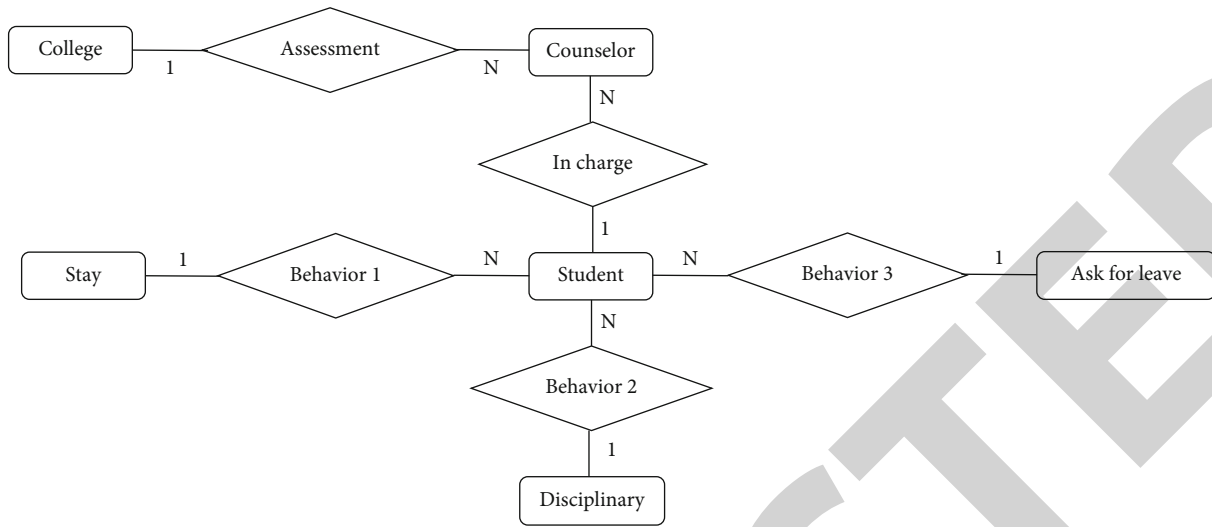


FIGURE 4: E-R diagram.

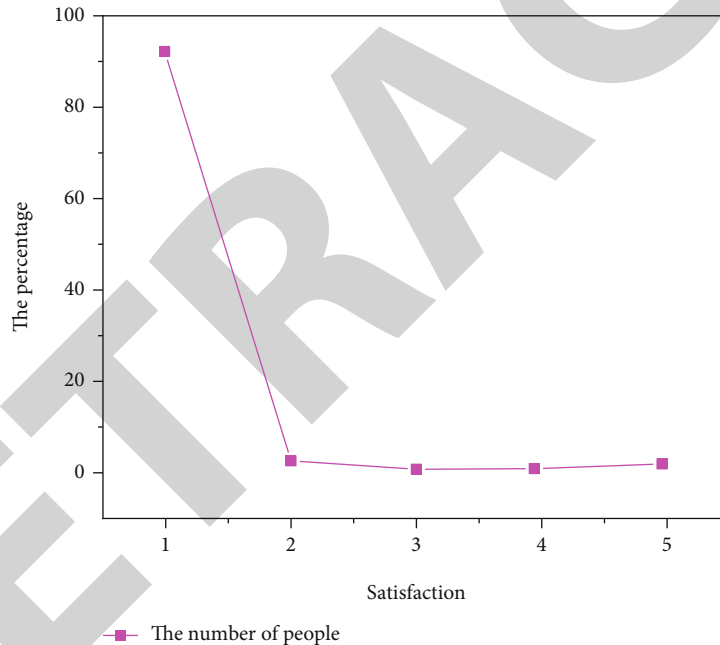


FIGURE 5: System usage evaluation.

5. Conclusion

With the rapid increase of electronic archives data in colleges and universities, the requirements for the authenticity, reliability, and permanence of electronic data are increasing day by day. Based on the discussion of the key technology of database encryption, this paper focuses on the implementation of the method of encryption technology in the management of archives in colleges and universities. According to the security needs of the current university archives database, this paper designs a set of practical system for the university archive information management system to realize the data encryption in the database application system with-

out affecting the ciphertext encryption under the normal operation of the database. The system can also manage the encrypted computer files (including title encryption); realize that all the encrypted data and its derivative parts in the database are encrypted according to the encryption requirements (there is no unclassified channel of ciphertext); realize the requirements of “can’t understand, can’t steal, and it’s useless to steal” in the confidentiality work; and realize the storage, modification, deletion, indexing, printing and retrieval of encrypted data. Combined with the specific requirements of the system and through the comparison of various algorithms, this paper selects the CBC mode of the 128-bit AES encryption algorithm to encrypt the data and

Retraction

Retracted: Slope Shape and Edge Intelligent Recognition Technology Based on Deep Neural Sensing Network

Journal of Sensors

Received 12 December 2023; Accepted 12 December 2023; Published 13 December 2023

Copyright © 2023 Journal of Sensors. This is an open access article distributed under the Creative Commons Attribution License, which permits unrestricted use, distribution, and reproduction in any medium, provided the original work is properly cited.

This article has been retracted by Hindawi, as publisher, following an investigation undertaken by the publisher [1]. This investigation has uncovered evidence of systematic manipulation of the publication and peer-review process. We cannot, therefore, vouch for the reliability or integrity of this article.

Please note that this notice is intended solely to alert readers that the peer-review process of this article has been compromised.

Wiley and Hindawi regret that the usual quality checks did not identify these issues before publication and have since put additional measures in place to safeguard research integrity.

We wish to credit our Research Integrity and Research Publishing teams and anonymous and named external researchers and research integrity experts for contributing to this investigation.

The corresponding author, as the representative of all authors, has been given the opportunity to register their agreement or disagreement to this retraction. We have kept a record of any response received.

References

- [1] Y. Huang, K. Yu, N. Wu, and J. Chang, "Slope Shape and Edge Intelligent Recognition Technology Based on Deep Neural Sensing Network," *Journal of Sensors*, vol. 2022, Article ID 5901803, 7 pages, 2022.

Research Article

Slope Shape and Edge Intelligent Recognition Technology Based on Deep Neural Sensing Network

Yansen Huang ¹, Ke Yu ², Ningbo Wu ², and Juanjuan Chang ²

¹College of Civil Engineering, Guizhou University, Guizhou Provincial Key Laboratory of Rock and Soil Mechanics and Engineering Safety, Guiyang, Guizhou 550025, China

²Guizhou Lianjian Civil Engineering Quality Texting Monitoring Center Co., Ltd., Guiyang, Guizhou 550016, China

Correspondence should be addressed to Yansen Huang; 20160343@ayit.edu.cn

Received 30 May 2022; Revised 7 June 2022; Accepted 24 June 2022; Published 4 July 2022

Academic Editor: C. Venkatesan

Copyright © 2022 Yansen Huang et al. This is an open access article distributed under the Creative Commons Attribution License, which permits unrestricted use, distribution, and reproduction in any medium, provided the original work is properly cited.

In order to solve the problem that the slope surface diseases cannot be accurately identified, which cannot be repaired in time and cause serious slope disasters, a slope intelligent recognition technology based on deep neural network is proposed. Based on convolutional neural network (CNN) theory, the technology adopts the transfer learning method to solve the overfitting problem of slope surface samples, which is difficult to obtain a large number of marked samples, and verifies the proposed model by experiment. The results are as follows: the recognition results of various slope surface diseases by ResNet-18 network are higher than AlexNet and VGG-16, with an average accuracy of 84.1%, and the recognition effect of cracks is the best. Under the same migration strategy, the detection accuracy of ResNet-18 is 96.3%, which is much higher than the other two, and the detection time is reduced by 15% on average. It is proved that the ResNet-18 model proposed can identify slope changes very effectively, so that workers can be timely dispatched for maintenance, reducing the possibility of disaster, which has great significance.

1. Introduction

Expressways play an important role in China's land transportation and meet the basic travel requirements of residents [1]. The continuous acceleration of highway construction is followed by a large number of slope engineering. In remote mountainous areas with large area, highway is still the main transportation choice, and highway slope disaster will lead to casualties and loss of a lot of economic property of people [2].

Due to the slope surface disease that is not timely and effective governance caused by more serious disasters and accidents, endangering people's lives and property losses often occur. Phase of the overall condition of the slope surface detection, so as to targeted, timely, and effective prevention and control of its disease, to avoid causing greater slope disasters is particularly important. In this case, the detection and identification of slope surface disease is an important prerequisite to avoid slope disaster effectively [3, 4].

At present, most people still choose the way of artificial inspection of the slope, focusing on the damage of the slope

(retaining wall, drainage hole). In the environment where the slope is located in complex terrain, the slope angle is too steep, the slope is high, the inspection personnel can only choose to check the slope state on foot, which occupies a lot of manpower, and the work progress is slow but also has the potential of high risk [5]. With the modernization of highway construction, all kinds of signs show that the contradiction between the rapid growth of the demand for the effectiveness and rapidness of slope surface image recognition and the shortage of staff of slope experts and the lag of slope surface disease recognition and detection technology is becoming more and more serious. Therefore, it is urgent to find a new effective and feasible method of slope surface disease identification and detection to solve slope detection and prevention.

2. Literature Review

Conventional slope detection means are displacement monitoring, artificial observation, GPS measurement, and neural network detection [6].

Bao et al. proposed a GA-SVM model for edge prediction of slope stability. The optimization function of the genetic algorithm is used to expand the parameter search of support vector machine. Using the function of support vector machine, very good description of nonlinear, etc., to establish a prediction model, the example proves that the prediction effect is ideal. This is a simple, effective, and easily extended slope stability model [7]. Lin et al. take kinetic energy, resistance, and slope as input and input them to BP neural network. Full display of all the exploration skills of genetic algorithm can optimize the original weight and threshold of its network [8]. At the same time, for the analysis of the principal components, the multiple regression prediction model is constructed. Finally, the two predicted results are compared. BP can predict the movement distance of slope accurately and stably by using the genetic method to expand network optimization [9]. The prediction errors of the maximum horizontal and vertical movement distances less than 10% accounted for 86.67% and 93.33%, respectively. Based on the improved BP neural network, a prediction neural network model for slope stability is constructed for analysis by Kumar and Tiwari and Villaseor-Reyes et al., and the prediction accuracy of the model network is verified. The results show that there is little difference between the expected output and the real output, the constructed BP network can be applied to the stability detection of a mine slope, and excellent results have been achieved [10, 11].

In recent years, with the continuous progress of neural network technology, deep learning has been successfully applied to many applications in computer vision, such as image recognition. This technique has also been applied in the classification, identification, and detection of slope hazards [12].

In order to overcome the problem of handwritten digit recognition in bank check, Nanda et al. applied back propagation in neural network and further constructed LeNet-5 [13]. It includes the input layer and other basic structural layer models [14]. Held et al. used AlexNet to win the photo contest classification [15]. Since then, deep learning has developed rapidly and steadily in the key visual part of the computer. However, increasing the depth of CNN without hindrance is of no use to improving network fitting skills. Instead, it will backfire and cause the dilemma of network degradation. To overcome this dilemma, residual network proposed the identity mapping between modules in 2016, which can deepen the network to more layers and ensure the performance does not degrade [16, 17].

After continuous improvement, the theoretical basis of deep learning becomes more stable. The application of work in every field is very good, and the effect is very good [18]. Poulou et al. proposed the application of a new recursive CNN (RCNN) to face detection and recognition in color images [19]. The use of radial basis function neural network (RBFN) and its feedback application creates a very powerful CNN for facial recognition. The loop CNN first receives the image database as a 3D matrix, and after training, selects the closest faces with acceptable accuracy. In the experimental analysis, the comparison between cyclic CNN and traditional CNN shows the effectiveness of the proposed recur-

sive CNN [20]. Sharma proposed the convolutional nerve with residual connection to perform the task of automatically identifying tree species from the scan image of wood core [21]. In these tasks, the correct recognition rate of the proposed model is 93% and 98.7%, respectively, which is 9% and 3% higher than the most advanced CNN-based model. With the continuous development of transfer learning means, scholars have gradually explored its application in real life scenes. In 2021, research on the correlation between photo identification and land has been continuously produced. Scholars have explored its application in real life scenarios, and there has been considerable research in image recognition, such as advocating a framework based on 50 layers of ResNet-50 for in-depth supervision of the screening of HEP-2 cell photographs. Select two publicly available photo sets and prelearn the ICPR2012 photo set to fine-tune the ICPR2016 photo set in the DSRN model, as the two are similar to the photo set. It proved to be state-of-the-art and superior to the ancient deep CNN (DCNN) method.

On the basis of the current research, this paper takes five common state types of slope surface collected as the research object and uses AlexNet, VGG-16, and ResNet-18 networks to conduct a preliminary study on slope surface image recognition. In order to solve the problem of network overfitting caused by insufficient number of slope surface data sets, transfer learning is used to solve this problem and improve the accuracy of classification recognition, so as to achieve the goal of accurate recognition of slope surface image.

3. The Research Methods

3.1. Image Recognition. Image processing and image recognition are the two most important parts of slope surface image disease recognition, as shown in Figure 1 [22]. The first step is the acquisition of slope surface image, especially for the identification of slope surface disease, which requires comprehensive collection of image data [23]. In order to better identify the images of cracks, water seepage, rockfalls, and landslides, it is necessary to collect the images containing these diseases. On the basis of the original image pretreatment to improve the image quality, so that the original image with representative features more prominent performance, feature extraction of image is the premise of slope surface disease recognition, which is very important for the whole slope surface disease recognition process. Slope surface image classification recognition is the last step, and there are a variety of classification operations, to combine with the actual problems of slope surface image for experimental analysis and selection.

3.2. Convolutional Neural Network. CNN was proposed in the 1990s. It is a kind of feedforward neural network. It not only has strong feature extraction performance but also the neurons only affect some of the surrounding neurons. Local perception and weight sharing are used to reduce the difficulty of CNN operation and improve the operation

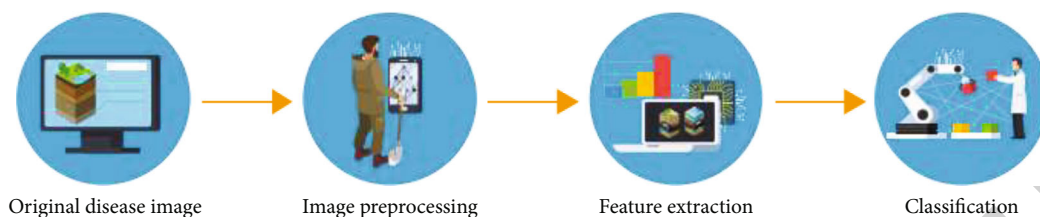


FIGURE 1: Process of image recognition and classification.

speed. CNN is generally composed of the input layer, which is a basic multilayer structural foundation. The initial input (image data) is transmitted layer by layer and finally mapped to the category to which the image data belongs [24].

The two most important operations of CNN are convolution and pooling. The convolutional layer is also the feature extraction layer, which mainly plays a role in feature extraction of a certain part of the input image and is also a key operation of the convolutional network [25]. The process of convolution processing is divided into two parts, one part (initial image) is the input of the network, and the other part (orange area) is the convolution kernel. In the whole process of convolution, according to the preset value of the convolution kernel and the number of moves, the initial coordinate of the convolution kernel is in the upper left corner of the input matrix (the area is marked green), and the weight value in the convolution kernel is the product of the input data. Finally, all the product values are summed, and the set number of steps is moved down or to the right. The above operation process is repeated until all the input data is completed. Finally, a new matrix, called the characteristic matrix, is generated after all the convolution operation process. Equation Formula (1) below is the process of convolution operation:

$$F(z) = \sum_{m=1}^{M_l} C(z+m)L(m). \quad (1)$$

The input and convolution kernel are functions C and L , respectively. The number of elements contained in the convolution domain is represented as M_l , and z is the number of shifts.

3.3. Convolutional Neural Network Construction. Based on the basic theory of deep learning, this paper constructs the multilayer detection structure models of AlexNet, VGG-16, and ResNet-18 networks. Thus, the classification and recognition effects of different types of convolutional neural network structures in the actual scene of slope outer surface image are compared, and the differences between image features extracted by different types of convolutional neural network structural models and slope outer surface disease features are compared. Through the means of continuous practice and detection of network structure, some parameters of model structure (such as the number of implied layers and the size of convolution kernel) are scheduled, so that the model structure can obtain excellent screening and detection results in the external surface conditions of slope.

AlexNet's model is the most classic and basic model in the early stage of CNN. It is a sign that CNN is put into use and opens the door of deep learning in a real sense. The first development of the AlexNet network allowed researchers to see its huge role in artificial intelligence. The birth of VGG network caused the researchers to think whether the deeper the model is, the stronger the screening function of the model is. However, as you continue to expand the depth of the model, the parameters of the model will certainly become more and more. This will lead to low efficiency and slow convergence rate of the network model or even the phenomenon that convergence cannot be achieved at last. Both networks use generic network architecture layers such as the convolutional, pooling, activation, and batch normalization (BN) layers. Therefore, in order to avoid network convergence failure, it is necessary to improve the network structure. In 2015, the deep network residual networks (residual networks) pointed out the development direction for subsequent CNN research.

3.4. Slope Surface Image Recognition Model Framework. Construction of the slope surface disease identification model is as follows: firstly, the ResNet-18 model was pretrained in ImageNet, and the mode of model migration was selected. The shallow image features extracted from the pretrained convolutional neural model were transferred to the image classification and recognition model of the slope surface, which were used as the initial parameters of the slope surface disease recognition. Secondly, the input of the network is to extract the image features of the outer surface of the slope and then train with the image recognition network model of the outer surface of the slope. In this article, the number of categories in the image data set of the outer surface of the slope is set to 5 to replace the number of full-connection classification output at the end of the pretraining network. Finally, the recognition and classification of slope external photos are completed on the slope external surface image data set constructed in this paper. According to the above ideas, the overall frame diagram of slope outer surface image recognition and classification based on ResNet-18 pretraining model and transfer learning is shown in Figure 2.

3.5. Network Model Training Process. Model training adopts K -fold crossvalidation, and K is 6. Figure 3 shows the training process.

- (1) First, the image data set (marked as T) of the outer surface of the slope was randomly divided into 6 equal parts

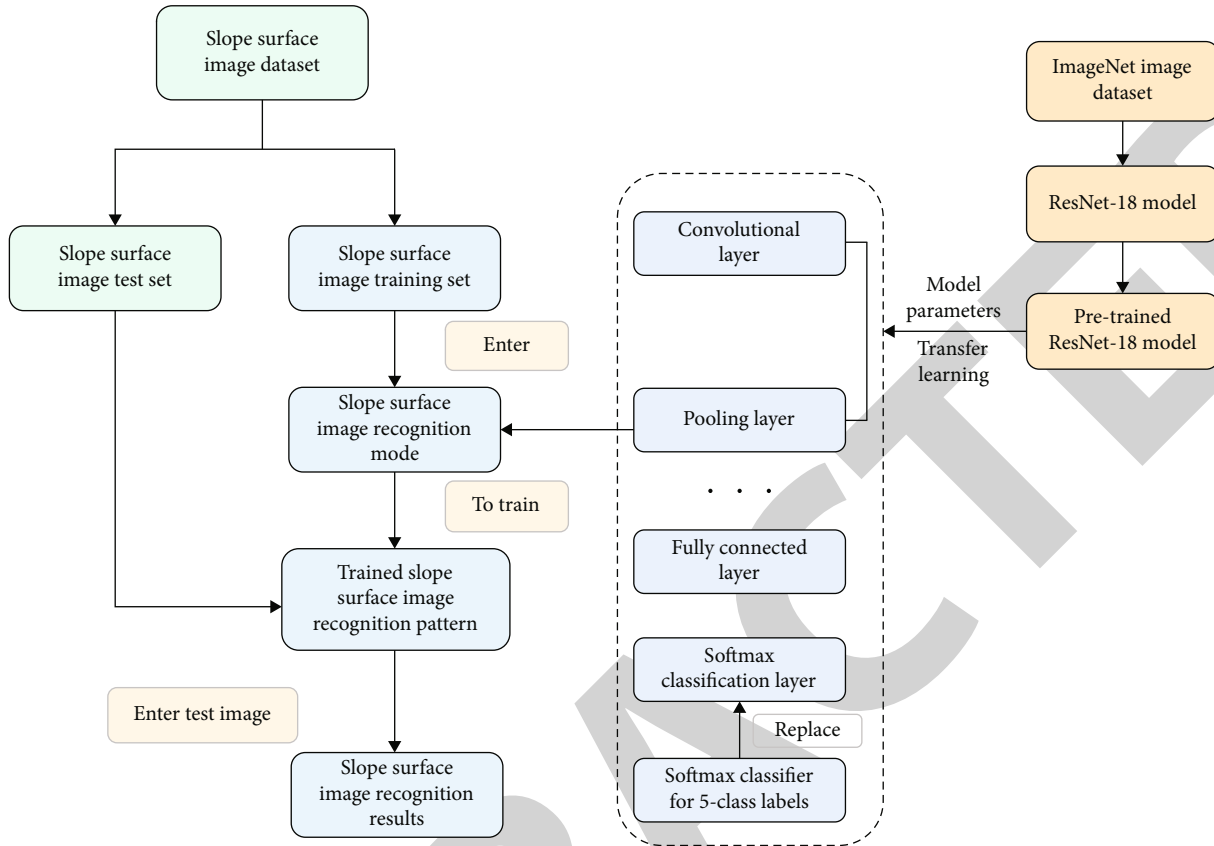


FIGURE 2: Slope surface image recognition based on transfer learning and ResNet-18 pretraining model.

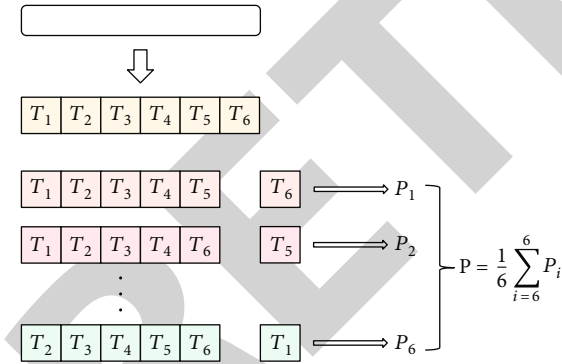


FIGURE 3: K-fold crossvalidation training method.

- (2) Use the 5 subsets included as the training set of the network and save the remaining 1 as the test set
- (3) Training the slope surface recognition model and showing the accuracy of the model test set P_1
- (4) Select different test set data for each training and repeat the above (2) and (3) 5 times
- (5) The values of P_1 - P_6 are obtained in turn to obtain the average value, that is, the correct accuracy of the P model

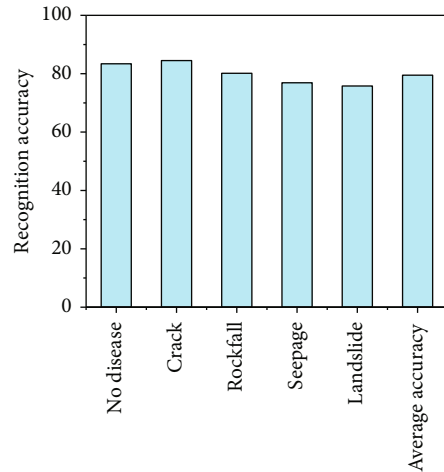


FIGURE 4: Comparison of classification results of AlexNet network structure.

4. Results Analysis

4.1. Image Sets of Slope Surface Are Classified and Compared with Different Network Models. Before the slope surface image is input, the unified resize and padding are used to process the image. The input image of the model is $224 > 224$ GBR size. Adam optimizer was selected for gradient

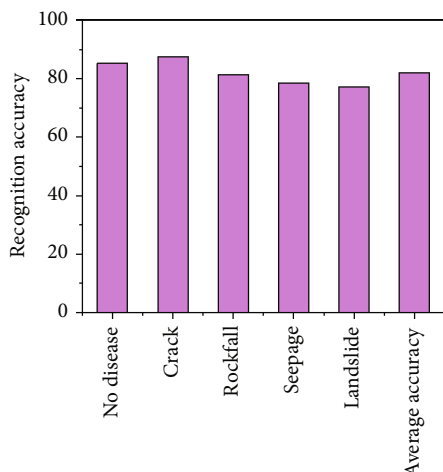


FIGURE 5: Comparison of classification results of VGG-I6 network structure.

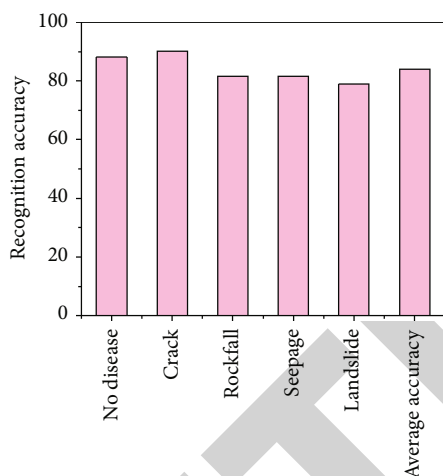


FIGURE 6: Comparison of classification results of ResNet-18 network structure.

descent operation, and then parameters were set. Finally, AlexNet, VGG-16, and ResNet-18 model structures were trained, and the accuracy of the detection model was verified.

Figures 4–6 show the accuracy of slope surface disease detection in all AlexNet, VGG-I6, and ResNet-18 experiments. In this experiment, in the same slope surface disease data set, ResNet-18 network is superior to AlexNet and VGG-16 in identifying all kinds of slope surface diseases. The recognition accuracy of ResNet-18 can reach 84.1% on average, and it has the best recognition effect on cracks, followed by undamaged ones, and the lowest recognition accuracy on landslides. This phenomenon may be caused by the complex background of landslides, which increases the difficulty of network identification. AlexNet VGG-16 network has a weak effect on the identification of various slope surface diseases. It may be that AlexNet and VGG-16 are not suitable for the identification of slope surface diseases, because the model cannot well learn and grasp the deeper characteristics of slope surface training samples.

TABLE 1: Different network models under the same migration strategy.

The network structure	Training time/s	Validation accuracy	Test accuracy
AlexNet	13095	90.5%	88.5%
VGG-I6	22651	93.3%	90.1%
ResNet-18	16245	98.9%	96.3%

4.2. Comparison of Detection Performance of Different Networks. Under the same migration strategy, all network structure layers were selected to participate in the training, and the detection results of AlexNet network, VGG-16 network, and ResNet-18 network were compared. Table 1 illustrates the experimental results of different network models.

It can be seen from Table 1 that the detection accuracy of VGG-16 network is 90.1%, while that of AlexNet network is 88.5%, 1.6% lower than the former. However, the detection accuracy of ResNet-18 is 96.3%, which is far higher than the former two. Furthermore, the accuracy of surface slope surface disease image increases with the increase of network model depth, which indicates that the recognition result of slope surface image disease is affected to a certain extent by the number of layers of CNN.

5. Conclusion

It is very important to study the automatic identification method of slope surface diseases in the actual outdoor environment for intelligent highway slope management and security situation. The disasters caused by highway slope occur frequently, which cause the blockage of the road at least and the death of the masses at the most serious. In order to avoid a series of safety accidents caused by highway slope disaster, it is necessary to test the surface of highway slope quickly and accurately on a regular basis. The existing method of slope surface disease detection is mainly manual, assisted by UAV, which is highly subjective. At present, more and more machine learning techniques are used in slope stability analysis. However, the deep neural network's expertise in image classification and recognition has not been brought into full play, mainly because of the lack of a huge open slope surface image data set, which cannot provide the deep neural network with the image data set required for training. Therefore, there are some limitations in image processing for the recognition of slope surface diseases. In view of the above dilemma, the CNN algorithm is used in this paper to carry out recognition research on slope surface disease. The results are as follows:

- (1) In view of the lack of open and sufficient slope surface image data set, this paper makes slope surface image data set required by deep learning. Therefore, this paper adopts the combination of UAV and camera to complete the slope surface image collection and image processing on the MATLAB platform

- (2) In order to discuss the influence of different network structure types on the accuracy of slope surface disease identification results, AlexNet and ResNet-18 based on slope surface image samples were, respectively, trained in this research. Slope surface images constructed in (1) were used as the input of these two networks, and images were classified according to extracted features
- (3) On the basis of the slope surface disease recognition model, in order to find a better image disease recognition model, a comparative experiment was designed to compare the effects of different training mechanisms, different migration strategies, and different network structure types of neural networks on the slope surface disease recognition structure

Data Availability

The data used to support the findings of this study are available from the corresponding author upon request.

Conflicts of Interest

The authors declare that they have no conflicts of interest.

Acknowledgments

The Central Guiding Local Funding Project of Guizhou Provincial Science and Technology Department [2021]4023 and Guizhou Provincial Scientific Supporting Planning Project (2021) General Category No. 523 (Guiyang Municipal Scientific Planning Project 2021 No. 43-20).

References

- [1] Q. Li, Y. Wang, and K. Zhang, "Failure mechanism of weak rock slopes considering hydrological conditions," *KSCE Journal of Civil Engineering*, vol. 26, no. 2, pp. 685–702, 2022.
- [2] D. Xiao, T. Zhang, X. Zhou, G. Zheng, and H. Song, "Safety monitoring of expressway construction based on multisource data fusion," *Journal of Advanced Transportation*, vol. 2020, Article ID 8856360, 11 pages, 2020.
- [3] L. Xiao, Y. Zhang, T. Ge, C. Wang, and M. Wei, "Analysis, assessment and early warning of mudflow disasters along the Shigatse section of the China–Nepal highway," *Open Geosciences*, vol. 12, no. 1, pp. 44–58, 2020.
- [4] E. S. Hinds, N. Lu, B. B. Mirus, J. W. Godt, and A. Wayllace, "Evaluation of techniques for mitigating snowmelt infiltration-induced landsliding in a highway embankment," *Engineering Geology*, vol. 291, no. 9, p. 106240, 2021.
- [5] T. T. Phi, P. Kulatilake, M. Anka, D. T. Sunkpal, and T. D. Van, "Rock mass statistical homogeneity investigation along a highway corridor in Vietnam," *Engineering Geology*, vol. 289, no. 3, p. 106176, 2021.
- [6] Q. Li, Y. M. Wang, K. B. Zhang, H. Yu, and Z. Y. Tao, "Field investigation and numerical study of a siltstone slope instability induced by excavation and rainfall," *Landslides*, vol. 17, no. 6, pp. 1485–1499, 2020.
- [7] H. Bao, F. Wu, P. Xi et al., "A new method for assessing slope unloading zones based on unloading strain," *Environmental Earth Sciences*, vol. 79, no. 14, pp. 1–13, 2020.
- [8] Y. C. Lin, R. Manish, D. Bullock, and A. Habib, "Comparative analysis of different mobile lidar mapping systems for ditch line characterization," *Remote Sensing*, vol. 13, no. 13, p. 2485, 2021.
- [9] R. Cheng, G. Cheng, Y. Pei, and L. Xu, "Calculation of the roadside clear zone width along highways based on the safe slope," *Journal of Advanced Transportation*, vol. 2021, Article ID 9998503, 12 pages, 2021.
- [10] A. Kumar and G. Tiwari, "Application of re-sampling stochastic framework for rock slopes support design with limited investigation data: slope case studies along an indian highway," *Environmental Earth Sciences*, vol. 81, no. 2, pp. 1–25, 2022.
- [11] C. I. Villaseor-Reyes, P. Dávila-Harris, and O. Delgado-Rodríguez, "Multidisciplinary approach for the characterization of a deep-seated landslide in a semi-arid region (Cañón de yerba buena, San Luis potosí, Mexico)," *Landslides*, vol. 18, no. 1, pp. 367–381, 2021.
- [12] T. L. Gouw, "Case histories on the application of vacuum preloading and geosynthetic-reinforced soil structures in Indonesia," *Indian Geotechnical Journal*, vol. 50, no. 2, pp. 213–237, 2020.
- [13] A. Nanda, Z. U. Hassan, T. A. Kanth, A. Manzoor, and A. Kanth, "Landslide susceptibility assessment of national highway 1d from Sonamarg to Kargil, Jammu and Kashmir, India using frequency ratio method," *Geo Journal*, vol. 85, no. 3, pp. 01–14, 2020.
- [14] Y. He, Y. Song, Y. Pei, B. Ran, and J. Kang, "Theoretical research on longitudinal profile design of superhighways," *Journal of Advanced Transportation*, vol. 2020, Article ID 6680255, 14 pages, 2020.
- [15] M. Held, O. Flrdh, and J. Mrtensson, "Experimental evaluation of a look-ahead controller for a heavy-duty vehicle with varying velocity demands," *Control Engineering Practice*, vol. 108, no. 4, p. 104720, 2021.
- [16] R. Macciotta and M. T. Hendry, "Remote sensing applications for landslide monitoring and investigation in western Canada," *Remote Sensing*, vol. 13, no. 3, p. 366, 2021.
- [17] R. Parthasarathy and R. Bhowmik, "Quantum optical convolutional neural network: a novel image recognition framework for quantum computing," *Access*, vol. 9, pp. 103337–103346, 2021.
- [18] G. Song, Z. Tao, X. Huang, G. Cao, and L. Yang, "Hybrid attention-based prototypical network for unfamiliar restaurant food image few-shot Recognition," *Access*, vol. 8, pp. 14893–14900, 2020.
- [19] A. Poulouse, J. H. Kim, and D. S. Han, "The extensive usage of the facial image threshing machine for facial emotion recognition performance," *Sensors*, vol. 21, no. 6, p. 2026, 2021.
- [20] X. Sun, X. Li, D. Xiao, Y. Chen, and B. Wang, "A method of mining truck loading volume detection based on deep learning and image recognition," *Sensors*, vol. 21, no. 2, p. 635, 2021.
- [21] A. Sharma and R. Kumar, "Risk-energy aware service level agreement assessment for computing quickest path in computer networks," *International Journal of Reliability and Safety*, vol. 13, no. 1/2, p. 96, 2019.
- [22] D. Selva, D. Pelusi, A. Rajendran, and A. Nair, "Intelligent network intrusion prevention feature collection and classification algorithms," *Algorithms*, vol. 14, no. 8, p. 224, 2021.

Retraction

Retracted: Complex Structure of Braid in Fiber Art Creation with Multisensor IoT Technology

Journal of Sensors

Received 12 December 2023; Accepted 12 December 2023; Published 13 December 2023

Copyright © 2023 Journal of Sensors. This is an open access article distributed under the Creative Commons Attribution License, which permits unrestricted use, distribution, and reproduction in any medium, provided the original work is properly cited.

This article has been retracted by Hindawi, as publisher, following an investigation undertaken by the publisher [1]. This investigation has uncovered evidence of systematic manipulation of the publication and peer-review process. We cannot, therefore, vouch for the reliability or integrity of this article.

Please note that this notice is intended solely to alert readers that the peer-review process of this article has been compromised.

Wiley and Hindawi regret that the usual quality checks did not identify these issues before publication and have since put additional measures in place to safeguard research integrity.

We wish to credit our Research Integrity and Research Publishing teams and anonymous and named external researchers and research integrity experts for contributing to this investigation.

The corresponding author, as the representative of all authors, has been given the opportunity to register their agreement or disagreement to this retraction. We have kept a record of any response received.

References

- [1] J. Wang, P. Li, and M. Wang, "Complex Structure of Braid in Fiber Art Creation with Multisensor IoT Technology," *Journal of Sensors*, vol. 2022, Article ID 6358247, 13 pages, 2022.

Research Article

Complex Structure of Braid in Fiber Art Creation with Multisensor IoT Technology

Jingyu Wang,¹ Pengpeng Li,² and Mengyao Wang³ 

¹Institute of Textile&Fashion Design, Lu Xun Academy of Fine Arts, Shenyang 110004, Liaoning, China

²School of Drawing and Painting, Lu Xun Academy of Fine Arts, Shenyang 110004, Liaoning, China

³School of Sino-British Digital Media (Digital Media) Art, Lu Xun Academy of Fine Arts, Dalian, 116650 Liaoning, China

Correspondence should be addressed to Mengyao Wang; wangmengyao@lumei.edu.cn

Received 4 May 2022; Revised 10 June 2022; Accepted 20 June 2022; Published 4 July 2022

Academic Editor: C. Venkatesan

Copyright © 2022 Jingyu Wang et al. This is an open access article distributed under the Creative Commons Attribution License, which permits unrestricted use, distribution, and reproduction in any medium, provided the original work is properly cited.

Fiber-fabric composites have the characteristics of lighter texture, higher strength, higher damage resistance, better toughness, and flexibility than laminated composites, but their complex structures have not been well studied. This paper is aimed at study the complex structure of woven fabrics in fiber art creation based on multisensor Internet of Things technology and at studying the impact of its composite material mechanical properties. In this paper, it is proposed to use glass fibers and carbon fibers to weave the required structural preforms in a two-dimensional braiding machine and then use the obtained preforms and epoxy resin to prepare three-dimensional two-dimensional braided composite materials with different structures through a molding process. The composites were tested in tension, bending, and compression to obtain data and their failure modes, and the data were compared to obtain correlations. The experimental results in this paper showed that through the tensile, bending, and compression tests of the three kinds of hybrid structure braided composites, the tensile properties of the glass fiber braided composites decreased by about 77%; the influence of angle on the bending properties of carbon fiber braided composites has the largest downward trend of 63%. Two-dimensional biaxial and two-dimensional triaxial preforms are made by weaving glass fiber and carbon fiber, and the angle deviation is basically kept within 2.2%.

1. Introduction

The development process of carbon fiber research and production in China is relatively slow. From the late 1990s to the present, it has gone through a long process in recent years. However, China has not yet achieved large-scale industrial production, and the informatization degree of carbon fiber production is relatively low. Therefore, improving the informatization degree of carbon fiber production and applying the Internet of Things technology to the carbon fiber spinning production process are of great significance for improving the output and quality of carbon fiber in China.

With the rapid development of Internet of Things technology, the combination of Internet of Things technology and carbon fiber production can effectively promote the development of China's carbon fiber industry. The monitoring system of carbon fiber production process based on the Internet of Things is a complex system

engineering. Based on the emerging Internet of Things technology, the system covers multiple links of carbon fiber production and realizes the monitoring of the carbon fiber production process. It improves the efficiency of carbon fiber production and the informatization degree of the carbon fiber industry and promotes the development of carbon fiber production to automation and intelligence.

The innovations of this paper are as follows: (1) biaxial glass fiber preforms with different angles, triaxial preforms with different angles, and triaxial carbon fiber preforms with different angles obtained by 64-spindle two-dimensional braiding machine. (2) Two-dimensional braided plate-like composites were prepared by VARI process with three kinds of mixed-braided structural prefabricated parts and epoxy resin, and the fiber content of the composites under different structures and different angles was calculated. (3) Tensile, compressive, and bending tests are carried out on the two-dimensional braided composite materials with different

angles and different number of axes and different fibers; the influence of the two-dimensional braided structure on the mechanical properties of the composites was obtained.

2. Related Work

The mechanical behavior of the nonwoven structure is considered to be represented by the change in fiber orientation according to the orientation angle and the degree of deformation. Stolyarov and Ershov's study found that the fiber orientation in the internal fabric structure corresponds to the applied load direction, and the initial stage of deformation with the maximum material stiffness is not accompanied by a significant change in fiber orientation [1]. Although the fiber deformation mechanism in the internal structure of the nonwoven is explained, the deformation stiffness value is low. Krogh et al. investigated different concepts related to photo frame testing for shear properties of woven prepreg fabrics. Although the sample arm modification was found to have a significant effect on the measured shear load, the uniformity of the shear strain field in the sample was not significantly improved [2]. The effect of the plain weave structure on the cutting mechanism and the mechanism of defect occurrence is rarely studied in detail. Zhang and Li established a three-dimensional finite element model of plain weave carbon fiber cloth, studied the occurrence and expansion of delamination, and found that the plain weave structure can prevent stress transfer and crack growth [3]. There are limitations of further research on the applicability of the optimal design of Kevlar fiber-reinforced polymer (KFRP) composites. Priyanka et al. studied the use of different modeling methods, such as homogeneous isotropic and orthotropic material models, and the effects of different parameters [4]. However, the research on fabric weave pattern, matrix material and composite material manufacturing technology, and working and loading conditions is insufficient.

It becomes particularly important to design a cooperative computing offloading mechanism. Guo et al.'s research shows how to fully utilize the centralized cloud and distributed MEC resources [5]. However, it faces new challenges such as single networking method, time extension, poor reliability, high congestion, and high energy consumption. The features offered by mobile technology are very important when considering the continued aging of the population and the ensuing increase in frailty. Domingues et al. proposed the development of a noninvasive fiber optic sensor (OFS) architecture suitable for shoe soles for remote monitoring of plantar pressure [6]. Although the research on multisensor IoT technology is relatively deep, there is almost no research on the combination of multisensor IoT technology and fiber art weaving technology.

Optical fiber sensors have both communication and sensing functions and have become a bridge connecting people and the world and an important part of accelerating the development of the Internet of Things. Yin et al.'s research showed the basis of fiber optic chemical sensing

or biosensing, including the sensing mechanism of various fiber optic sensors, sensing materials, and new technologies for sensing material deposition [7]. Market forecasts and trends in the use of fiber optic sensors confirm that the demand for them will continue to increase. Senkans et al. focus on fiber Bragg grating (FBG) sensor networks and their applications in IoT and structural health monitoring (SHM), especially their coexistence with existing fiber optic communication system infrastructure [8]. There is emerging infrastructure of the Internet of Things. Given a certain fiber length, there is a trade-off between sensing bandwidth, sensitivity, and spatial resolution. Wang et al. constructed a fully linear system for complete theoretical processing, so that a significant enhancement of the signal-to-noise ratio becomes feasible and the sensing bandwidth remains equal to the quartic average case [9]. Although detailed experiments have been carried out on the fiber art weaving process, the research on its complex structure is still insufficient.

3. Combination Method of Multisensor IoT Technology and Fiber Art Weaving

3.1. Application of Fiber Materials in Fiber Art Creation. In the process of development, fiber art is good at absorbing nutrients from other art types in terms of expression and craftsmanship, which is because fiber materials have inherent advantages, such as linearity, softness, and affinity in their characteristics. The material itself is superior to other materials and has strong plasticity [10].

The weaving method is one of the existing modeling methods of fiber materials in ancient times; that is, various types of fiber materials are used as the basic warp and weft elements, and the interweaving treatment method of mutual floating and sinking is organized according to certain rules. Weaving is the basic means of shaping linear fibers. Linear fibers are the original form of fiber materials and have the most essential characteristics of fibers. The art of fiber weaving is shown in Figure 1.

As shown in Figure 1, the weaving method is one of the traditional fiber material forming techniques. From traditional art forms such as silk, kesi, and tapestries to the changes of modern weaving forms, a weaving method has always been a particularly important process technique. The modern weaving technique breaks the traditional process of copying and translation and turns the artist's creative master to the works and the materials used and then pays attention to the matching and changes of the texture and texture of the materials [11]. This makes weaving break free from traditional concepts and becomes an important turning point in fiber art in the modern sense, and it is also one of the important expressions of fiber materials [12].

3.2. IoT-Based Carbon Fiber Production. The Internet of Things technology is the further development of information technology and an emerging field in the information technology industry. The Internet of Things technology based on wireless sensor network can monitor all aspects of carbon fiber production in real time, help carbon fiber

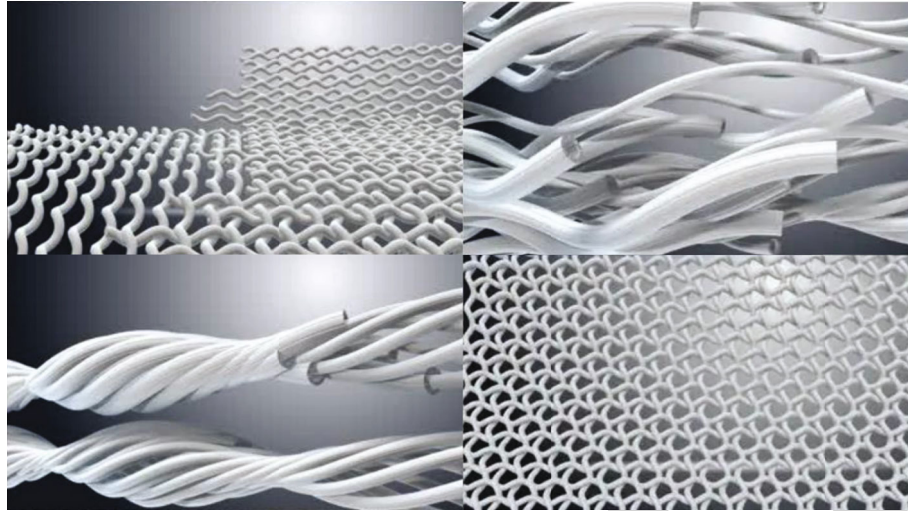


FIGURE 1: The art of fiber weaving.

production enterprises to grasp the production status of the enterprise in real time, and improve the monitoring accuracy and production efficiency [13]. In the short term, carbon fiber manufacturers can reduce operating costs, various resource overheads, and unnecessary losses by applying this technology; in the medium and long term, enterprises can use the Internet of Things technology based on wireless sensor network combined with intelligent optimization control system to improve the intelligence and real-time optimization control ability of carbon fiber production, improve the quality of carbon fiber products, and thus improve the core competitiveness of carbon fiber production enterprises, in order to promote the development of China's carbon fiber industry [14]. In order to ensure the accuracy and effectiveness of information monitoring in all aspects of carbon fiber production, realize intelligent monitoring of carbon fiber production process, and improve carbon fiber production efficiency, this paper designs the following application framework of carbon fiber production process monitoring system based on Internet of Things technology. The overall framework of the carbon fiber production process monitoring system is shown in Figure 2.

As shown in Figure 2, the front-end sensor node includes temperature, pressure and other types of sensors, preprocessing module, A/D conversion module, and embedded microprocessor. It is mainly used to collect on-site ambient temperature, pressure, and other information and convert analog signals into digital signals [15].

3.3. Sensor Fiber Art Weaving Data Fusion. In actual detection, the detection range and reliability of each sensor node are limited. In order to enhance the robustness of the entire network and the accuracy of the collected data, to avoid node failure and interference caused by external factors, multiple identical sensors are often used to measure the same measurement point [16]. The weighting factors of each sensor are W_1, W_2, \dots, W_n ; the relationship

between the fusion value and the weighting factor should satisfy the following two formulas:

$$\hat{X} = \sum_{p=1}^n W_p X_p, \quad (1)$$

$$\sum_{p=1}^n W_p = 1. \quad (2)$$

Since X_1, X_2, \dots, X_n are independent of each other and are unbiased estimates of x , the total mean squared n error is

$$\sigma^2 = E \left[\sum_{p=1}^n W_p (X - X_p)^2 \right] = \sum_{p=1}^n W_p^2 \sigma_p^2. \quad (3)$$

It can be obtained from the above formula that the total mean square error σ^2 is a multivariate quadratic function about the weighting factor, so its minimum value must exist. The weighting factor corresponding to the minimum total mean square error is

$$W_p = \frac{1}{\sigma_p^2 \sum_{i=1}^n 1/\sigma_i^2}, \quad p = 1, 2, \dots, n. \quad (4)$$

Therefore, the weighting coefficient of each sensor is only determined by the measurement variance [17]. The mean square error can be minimized as long as the weights of each sensor conform to formula (3), and at this time,

$$\bar{X} = \sum_{i=1}^n \frac{X_i}{\sigma_i^2} \left(\sum_{i=1}^n \frac{1}{\sigma_i^2} \right)^{-1}. \quad (5)$$

The true value of the measured value is an objective constant, which can be estimated according to the

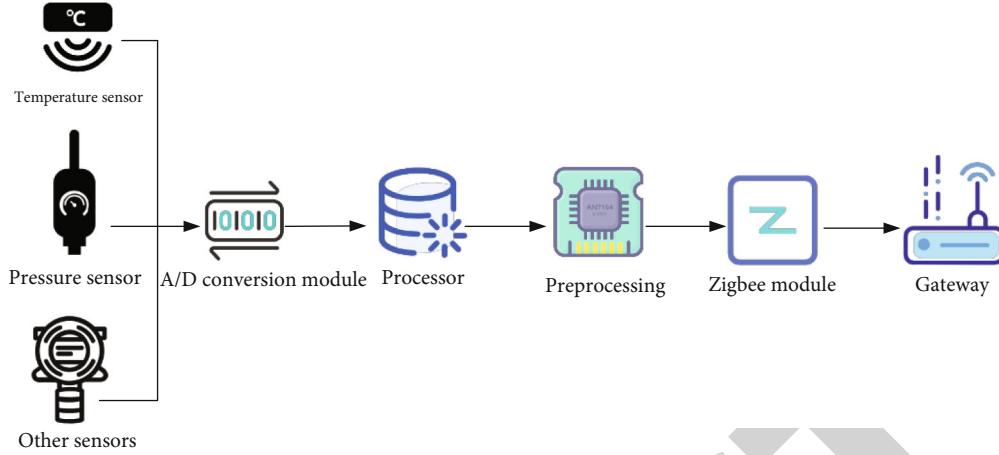


FIGURE 2: The overall framework of the carbon fiber production process monitoring system.

arithmetic mean of the existing measured data. Assume that

$$\bar{X}_i(k) = \frac{1}{k} \sum_{p=1}^k X_p, \quad i = 1, 2, \dots, n. \quad (6)$$

The estimated value at this time is

$$\hat{X} = \sum_{i=1}^n W_i \bar{X}_i(k). \quad (7)$$

The total mean squared error is

$$\bar{\sigma}^2 = \frac{1}{k} \sum_{i=1}^k W_i^2 \sigma_i^2. \quad (8)$$

Using formulas (4), (6), and (7), the estimated value after data fusion can be calculated.

3.4. Improved Adaptive Weighting Algorithm. Assuming that there are two groups of sensors for the same measurement point, the two groups of sensors first use the adaptive weighting method to perform data fusion on their respective measured values. The fused values are \bar{X}_1, \bar{X}_2 , respectively, and the corresponding mean square errors are σ_1, σ_2 [18, 19].

Using the batch estimation algorithm, the measurement equation can be rewritten as

$$X = \begin{bmatrix} \bar{X}_1 \\ \bar{X}_2 \end{bmatrix} = [\mu]^T X_z + [V_1 V_2]^T, \quad (9)$$

$$R = E[VV^T] = \begin{pmatrix} \sigma_1^2 & 0 \\ 0 & \sigma_2^2 \end{pmatrix}. \quad (10)$$

At the same time, consider the above two sets of measurement results \bar{X}_1 and \bar{X}_2 , which are two measurement data at the same monitoring point at the same time, and the influence of the previous measurement of the sensor

on this measurement is negligible [20]. So based on estimated data fusion measurements,

$$X^+ = P^+ H^T R^{-1} X = \frac{\sigma_2^2 \bar{X}_1 + \sigma_1^2 \bar{X}_2}{\sigma_1^2 \sigma_2^2}. \quad (11)$$

3.5. Simplified Anisotropic Hyperelastic Model. Fiber-reinforced braided composite materials are regularly arranged, and this composite material has strong directionality[21, 22]. Therefore, from a macroscopic point of view, fiber-reinforced composites are anisotropic materials. And usually, this anisotropy is very pronounced, and its mechanical properties are highly dependent on the orientation of the fibers. During the large deformation forming process of fiber reinforced woven composite materials, the deformation of the material is mainly realized by the large angle change between the yarns, while the in-plane tensile deformation along the yarn direction of the fiber bundle is relatively small. The schematic diagram of the fabric structure and its deformation before and after is shown in Figure 3.

Figure 3 is a schematic diagram of the deformation of the plain woven fabric containing two reinforcing fibers. There are many ways to express the mechanical properties of the woven material, so the strain energy function can be expressed as

$$W = W(C, a_0, b_0). \quad (12)$$

Similarly, the strain energy function can also be expressed as a function of the invariant I_p , so the strain energy function can be expressed by the following formula:

$$W(C, a_0, b_0) = W(I_i). \quad (13)$$

Carbon fiber woven cloth is called dry carbon fiber woven cloth without matrix material, which is composed of two bundles of reinforcing fibers intertwined[23, 24], and the strain energy can be decomposed into two parts: fiber tensile strain

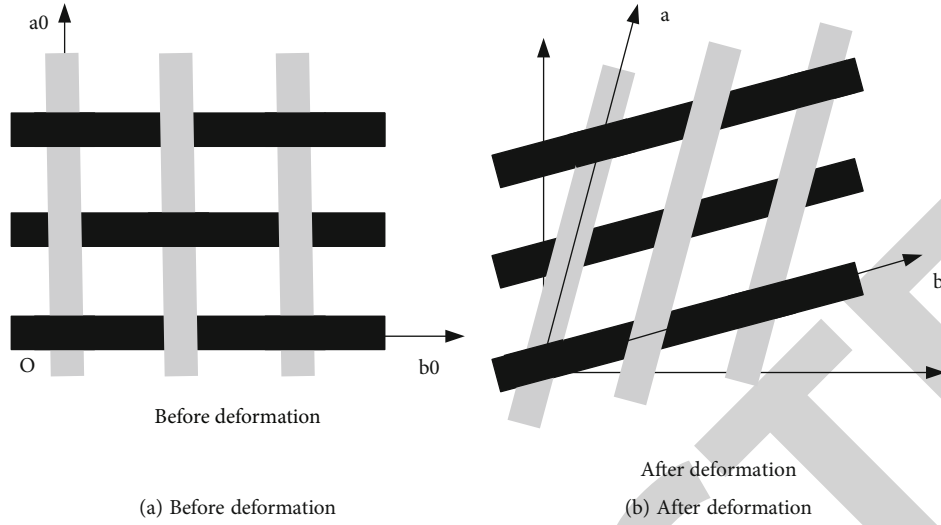


FIGURE 3: Schematic diagram of the fabric structure and its deformation before and after.

energy and fiber shear strain energy in the plane.

$$W = W(C, a_0, b_0) = W^F + W^{FF}, \quad (14)$$

where W^F is the energy contributed by fiber stretching and W^{FF} is the shear energy between the interwoven fibers. The tensile energy W^F of the fiber can be simplified to the expression of the fiber draw ratio, namely,

$$W^F = W^F(C, a_0, b_0) = W_a^F(I_4^a) + W_b^F(I_4^b), \quad (15)$$

where W_a^F and W_b^F represent the tensile energy of the warp and weft fibers, respectively, and I_4^a and I_4^b can be defined by the following formula:

$$I_4^a = a_0 \cdot C \cdot a_0 = (\lambda_a)^2, I_4^b = b_0 \cdot C \cdot b_0 = (\lambda_b)^2. \quad (16)$$

a_0 and b_0 represent the draw ratio of the warp and weft fibers, respectively. Introduce I_{10}^{ab} to represent the shear angle between the two bundles of fibers

$$I_{10}^{ab} = \Delta\varphi = \varphi - \varphi_0 \approx \left(I_4^a I_4^b\right)^{-1/2} a_0 \cdot C \cdot b_0 - a_0 \cdot b_0. \quad (17)$$

The shear strain energy between AFF fiber bundles can be quantified by ground, which is

$$W^{FF} = W_{ab}^{FF} \left(I_{10}^{ab}\right). \quad (18)$$

To obtain the corresponding parameters in the material model, it is necessary to perform uniaxial tensile experiments on the material. The tensile strain energy function of the braided material can be obtained by fitting the material curve using the test results of the material uniaxial tensile test. By changing, the tensile strain energy function of the fiber can be

obtained by the following formula:

$$W_a^F(I_4^a) = k_1(I_4^a - 1)^2 + k_2(I_4^a - 1)^3 + k_3(I_4^a - 1)^2. \quad (19)$$

4. Fabrication Experiment of Two-Dimensional Braided Composite Structure

The preparation of two-dimensional braided composites includes two aspects: the preparation of two-dimensional braided preforms and the preparation of two-dimensional braided composites. The prefabricated parts are made of glass fiber produced by Jushi Group and carbon fiber produced by Zhongfu Shenyang Company. The two-dimensional braided composite material is obtained by compounding the two-dimensional braided preform with the epoxy resin produced by Dongqi Company through the VARI molding process, and the mechanical properties of the prepared two-dimensional braided composite material are tested.

4.1. Preparation of 2D Braided Preforms. Because of the weaving characteristics of two-dimensional weaving, a mandrel needs to be used in the weaving process, so it is necessary to calculate the diameter of the mandrel used for the design of the mandrel according to the width of the yarn. After that, parameters such as weaving pitch and traction speed are determined, and the prefabricated parts are finally woven. The design process is shown in Figure 4.

As shown in Figure 4, preforms with different parameters can be woven by the braiding machine, and the parameters in the preforms include braiding angle, braiding pitch, coverage factor, and the like.

In the experiment, E6D17-1200-380 direct roving produced by Jushi Group Co., Ltd. was used as the braiding yarn, and the linear density was 1200 tex. The width of the yarn is wide, and the yarn width is 2.70 mm when standing still. The yarn of this width is woven on the surface of the mandrel to ensure uniform weaving and a high coverage factor. The shaft yarn is made of A-grade 12K SYT49S

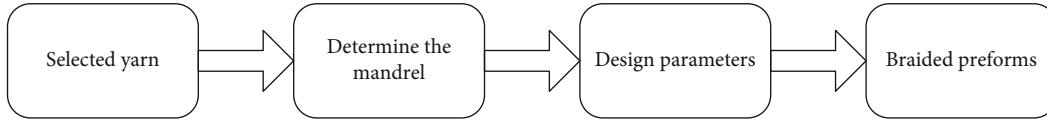


FIGURE 4: Design weaving flowchart.

TABLE 1: Corresponding mandrel diameters for different coverage factors.

Number of spindles (piece)	Weaving yarn width (mm)	Braid angle (°)	Mandrel diameter (mm) when the coverage factor is 0.9	When the coverage factor is 1, the diameter of the core mold (mm)
64	2.70	60	80	55
64	2.70	55	68	47
64	2.70	50	63	43
64	2.70	45	57	39
64	2.70	40	53	36
64	2.70	30	47	32

carbon fiber produced by Zhongfu Shenying Carbon Fiber Co., Ltd., and the fiber width is 2.00 mm when standing. The equipment adopts the high-speed horizontal 64-spindle two-dimensional weaving machine produced by Jiangsu Xuzhou Qixing Ribbon Machinery Co., Ltd. The instrument is simple to operate, has high weaving efficiency and a high degree of automation, and can weave biaxial and triaxial fabrics of 2×2 , 1×1 , and 2×1 specifications. The weave of the samples woven in this subject is 2×2 .

4.2. Core Mold Diameter Design. In the case of weaving the same angle with the same width of yarn, the diameter of the core mold is directly related to the coverage factor of the preform. On the basis that the yarn of the same thickness can be woven, the coverage factor of the preform obtained by using a core mold with a larger diameter is smaller, and vice versa. The size of the coverage factor has a great influence on the mechanical properties of the two-dimensional braided composites. The larger the coverage factor, the tighter the yarn and the higher the strength, and vice versa. The core mold diameters corresponding to different coverage factors are shown in Table 1.

As shown in Table 1, the number of yarns in this test is 64, so $n = 64$. In the case where the width of the knitting yarn is not compressed, the width of the knitting yarn is 2.70 mm, so $br = 2.70$. To avoid low coverage factor, the mechanical properties of composite materials are greatly affected, so the coverage factor of prefabricated parts should reach more than 90% (no obvious voids on the surface). When the braided yarn width is 2.70 mm, the coverage factor is 0.9, the number of yarns is 64, the braiding angle is 60° , and the mandrel diameter is 80 mm. When the coverage factor is 1, the mandrel diameter is 55 mm.

In the experiment, the core molds are all made of PVC round pipes, which are lighter and have stronger hardness, which is convenient for the installation and disassembly of

the core molds. Before the test, sandpaper must be used to polish the surface of the tube and the head and tail to prevent the friction between the tube and the yarn from being too large, causing serious fiber fluff. The PVC round pipe needs to add a fixing clamp at one end to facilitate the mandrel to be fixed on the pulling device. This method helps to give a certain tensile force to the shaft yarn during the weaving process, to ensure that the shaft yarn is parallel to the axial direction, and to prevent the shaft yarn from buckling during the demolding process, which affects the final test result. The parameter table of the two-dimensional braided preform is shown in Table 2.

As shown in Table 2, all organizational structures in the table are 2×2 . The knitting yarn width is 2.70 mm, and the shaft yarn width is 2.00 mm when the coverage factor is calculated, and the knitting speed is 0.191 rad/s. If the weaving speed is too slow, the woven preform will not be formed smoothly; if the weaving speed is too fast, it is easy to cause the yarn to break. After many trials, the weaving speed was chosen to be 0.191 rad/s.

4.3. Prefab Parameters. It takes pictures of the prefab head, middle, and tail. The picture was imported into PS for angle measurement, and the three measured angles were averaged. The fabric is flattened according to half of the corresponding diameter, and the thickness is measured at five points of the preform at random with a thickness measuring instrument, and the average value is obtained. A summary of the parameters of the preform obtained by measurement is shown in Table 3.

As shown in Table 3, the liquid forming process obtains the composite material by laying the fiber fabric in the mold and pouring the resin. The process is simple to form and has high forming efficiency, but it needs to design corresponding molds. The autoclave forming process uses the prepreg to prepare the composite material through high temperature and high pressure, and the cost of this process is relatively high.

In this experiment, the VARTM molding process in the liquid molding process is used; VARTM molding process is one of the liquid molding processes, which has the advantages of low cost, low pollution, and high efficiency, which is widely used in large and complex structures, such as ship hulls, blades, and aviation components. VARTM lays the fiber fabric on a flat plate, then injects resin in a vacuum state, and finally solidifies into a composite material. The VARTM molding process is shown in Figure 5.

As shown in Figure 5, fabrics, guide nets, release cloths, and other materials are laid in the order shown, and a vacuum effect is formed in the gap between the vacuum bag and the glass plate by a vacuum pump. The vacuum pressure makes the fabric and the release cloth guide mesh

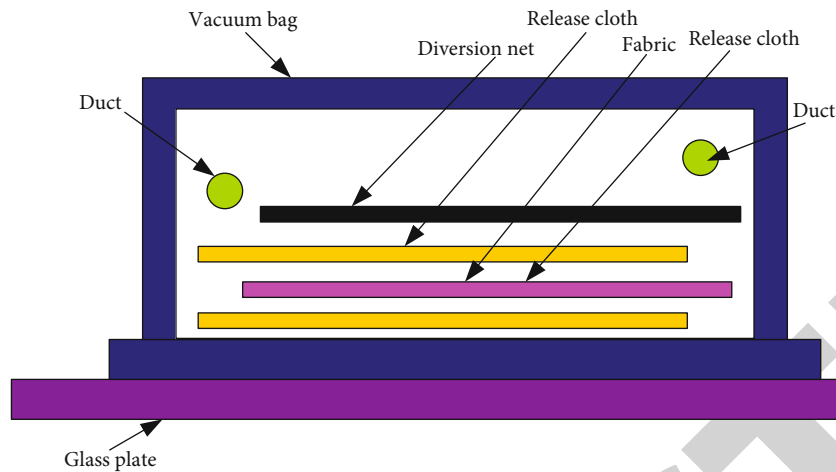


FIGURE 5: VARI schematic.

TABLE 2: Parameter table of 2D braided preforms.

Numbering	Types of weaving yarns	Number of axes	Mandrel diameter (mm)	Braiding pitch/mm	Angle (°)	Traction speed (mm)	Coverage factor (%)
1-1	Glass fiber	Dual axis	60	63	114.3	3.474	98.4
1-2	Glass fiber	Dual axis	55	63	138.6	4.213	94.3
1-3	Glass fiber	Dual axis	50	50	131.8	4.007	97.9
2-1	Glass fiber	Three-axis	60	63	114.3	3.474	99.9
2-2	Glass fiber	Three-axis	55	63	138.6	4.213	99.9
2-3	Glass fiber	Three-axis	50	50	131.8	4.007	99.9
3-1	Carbon fiber	Three-axis	60	63	114.3	3.474	99.9
3-2	Carbon fiber	Three-axis	55	63	138.6	4.213	99.9
3-3	Carbon fiber	Three-axis	50	50	131.8	4.007	99.9

TABLE 3: The actual angle and thickness of each prefab.

Numbering	Types of weaving yarns	Number of axes	Mandrel diameter (mm)	Braiding pitch (mm)
1-1	60	58.8	0.3	1.3
1-2	55	55.8	1.5	1.3
1-3	50	48.9	2.2	1.4
2-1	60	61.0	1.7	2.0
2-2	55	55.2	0.4	1.6
2-3	50	49.6	0.8	1.8
3-1	60	60.2	0.3	1.4
3-2	55	55.6	1.1	1.4
3-3	50	49.8	0.4	1.5

closely fit together, which facilitates the subsequent penetration of epoxy resin.

5. Two-Dimensional Braided Composite Material Performance Test

With the development of industrialization, the application of two-dimensional braided composite materials is gradually widespread. Considering the subsequent use requirements of the material, it is necessary to judge whether the two-dimensional braided composite material in this topic can meet the use requirements, so it is necessary to carry out a mechanical test on the material. The tensile, bending, and compressive properties of two-dimensional braided composites were mainly tested by different angles, different number of axes, and different fiber blends. The influence of angle, number of axes and different fiber blending on the tensile, bending, and compressive properties of composites can be analyzed and compared.

5.1. Influence of Shaft Yarn on Tensile Properties. Two-dimensional triaxial braided composite material compared with the two-dimensional biaxial braided composite

TABLE 4: Tensile strength of three hybrid structural composites.

Numbering	Average tensile strength (MPa)	Dispersion coefficient (%)	Average tensile modulus (GPa)	Dispersion coefficient (%)	Average elongation at break (%)
1-1	315.8	6.27	2.974	5.78	2.73
1-2	166.3	8.77	2.422	7.54	16.75
1-3	159.4	7.98	2.304	6.99	15.09
2-1	431.4	10.13	4.718	9.44	6.72
2-2	390.9	8.85	5.582	7.64	6.05
2-3	368.9	9.65	5.928	8.36	6.61
3-1	576.6	8.33	7.058	7.40	6.88
3-2	542.3	9.50	7.849	9.66	7.01
3-3	526.8	6.63	6.898	7.74	6.54

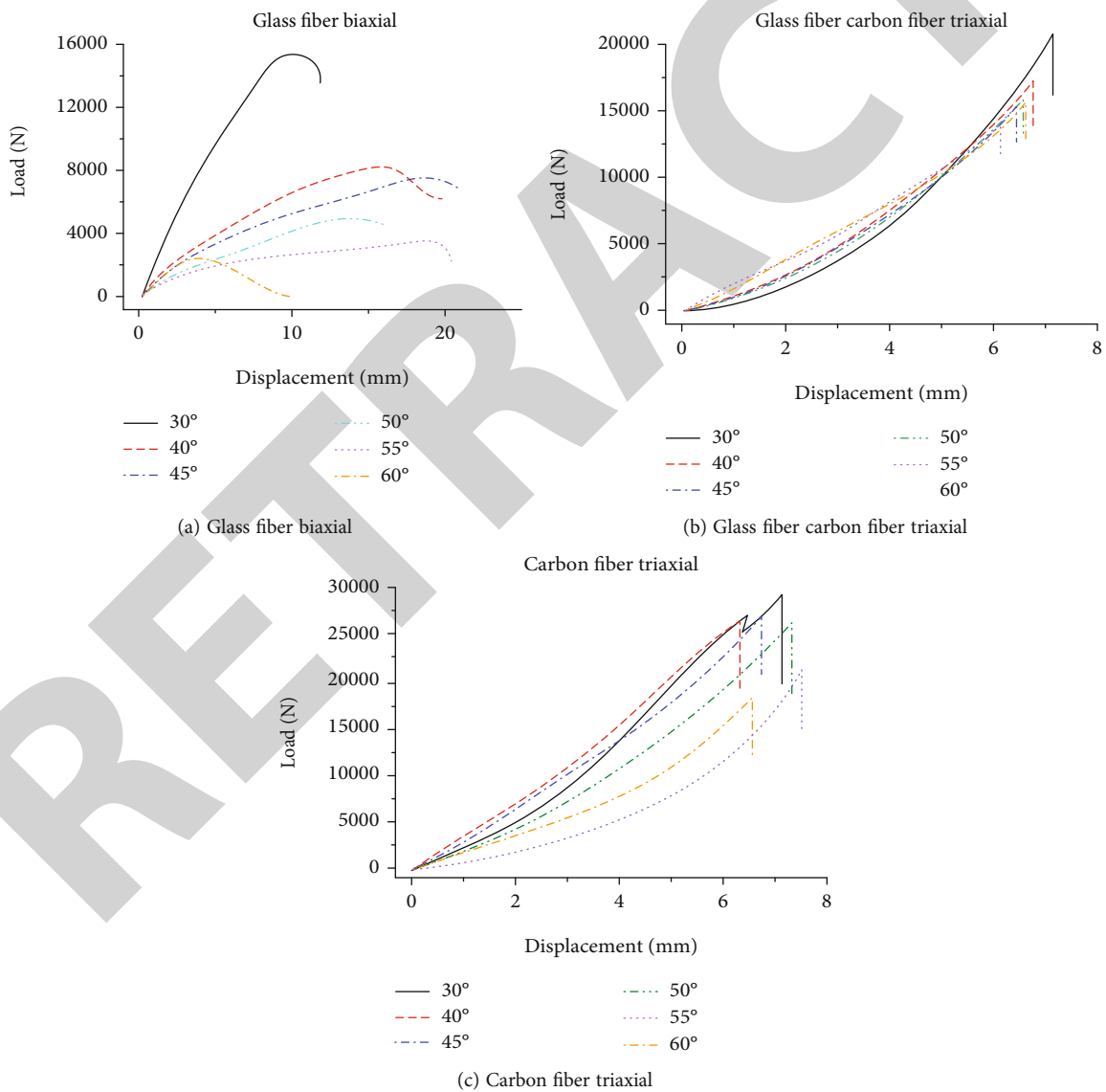


FIGURE 6: Tensile displacement-load curves of three hybrid structures at different angles.

TABLE 5: Flexural strength of three hybrid structural composites.

Numbering	Average yield load (N)	Average flexural strength (MPa)	Dispersion coefficient (%)	Average flexural modulus (GPa)	Dispersion coefficient (%)
1-1	555	444.0	10.32	13.499	9.21
1-2	485	388.0	12.51	11.493	10.02
1-3	477	381.6	11.98	12.327	9.98
2-1	423	338.4	9.88	11.411	8.32
2-2	339	271.2	9.48	7.731	7.69
2-3	258	206.4	11.32	8.287	10.98
3-1	634	507.7	9.32	34.894	9.58
3-2	538	430.9	7.2 I	30.118	8.65
3-3	490	392.5	8.65	21.200	8.39

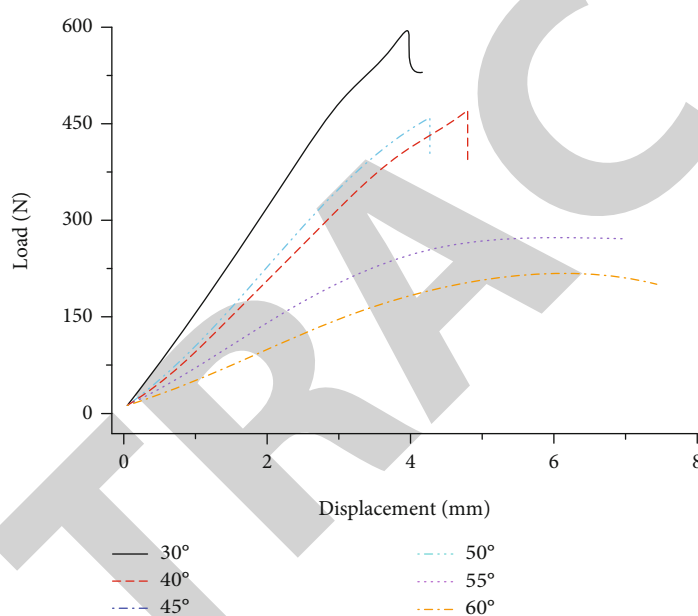


FIGURE 7: Bending displacement load curve of glass fiber braided composites.

material, the two-dimensional triaxial preform is more than the two-dimensional biaxial preform plus a set of shaft yarns composed of carbon fibers. The glassy carbon fiber braided composite material and the carbon fiber braided composite material preform in this paper are all two-dimensional and three-axis, and the three axes are all carbon fibers, and the number of axial yarns is 32 (half of the braided yarns). The addition of carbon fiber axial yarn has two main effects on the tensile strength and elongation at break of the braided composites. The tensile strength of the three kinds of mixed structural composites is shown in Table 4.

It can be seen from Table 4 that the tensile strengths of 2-1 to 2-3 and 3-1 to 3-3 are larger than those of glass fibers (1-1 to 1-3) at the same angle. Compared with glass fiber braided composites, glass carbon fiber braided composites add carbon fiber shaft yarns to their preforms. At 30°, the strength of the glassy carbon fiber braided composite increases by 36%; at 40°, it increases by 135%; at 45°, it increases by 131%; at 50°, it increases by 161%; at 55°, it

increases by 237%; and it increased by 306% at 60°. The data show that basically with the increase of the braiding angle, the reinforcing effect of carbon fiber axial yarn on the two-dimensional braided composite is more obvious. Due to the presence of carbon fiber shaft yarns, the tensile modulus increases and increases with increasing angle. The tensile displacement-load curves of the three hybrid structures at different angles are shown in Figure 6.

As can be seen from Figure 6, the carbon fiber shaft yarn has a relatively obvious effect on the tensile elongation at break of the composite material, which will lead to a decrease in the elongation at break. The displacement of the glass fiber woven composite material during tensile fracture is large, and the elongation at break is large. The displacement of the glassy carbon fiber braided composite material during tensile fracture is small, and the elongation at break is small. It can be seen from the data that the presence of carbon fiber shaft yarn reduces the tensile elongation at break of the composite material. According

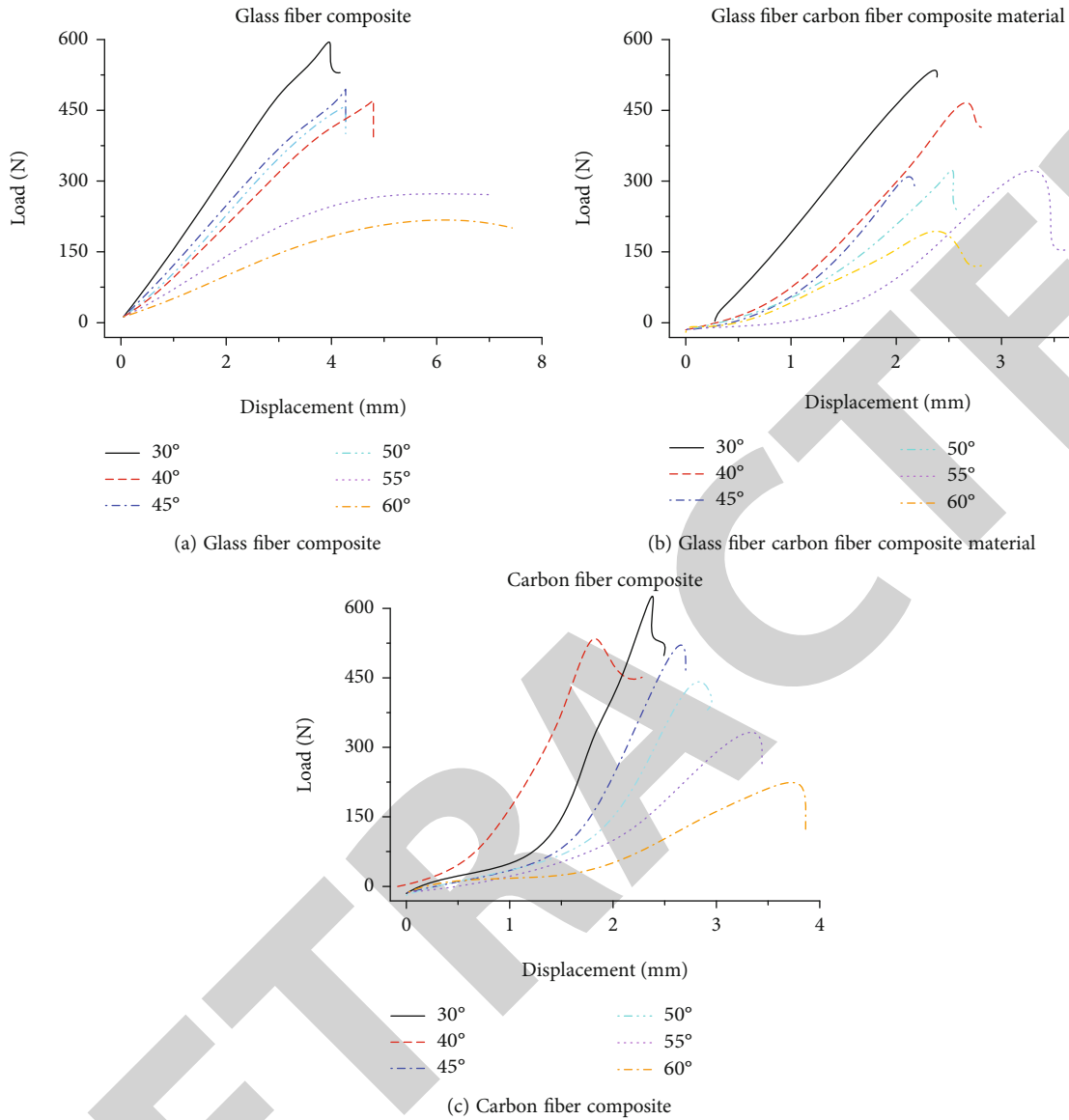


FIGURE 8: Bending displacement-load curves of three hybrid structures at different angles.

to the weaving characteristics of two-dimensional biaxial preforms and two-dimensional triaxial preforms, the axial yarn improves the stability of the preforms to a certain extent. Different from the 2D biaxial preform, the 2D triaxial preform has better overall stability after demoulding from the core mold and does not have the characteristics of good elasticity after demoulding of the 2D biaxial preform, which makes the stability of the composite material formed by the two-dimensional triaxial preform after being compounded with the resin also better. During the stretching process, it is necessary to overcome not only the axial force of the braiding yarn but also the breaking force of all the axial yarns and the stabilizing force of the axial yarn and the braiding yarn after curing, so it finally showed an increase in tensile strength and a decrease in elongation at break.

During the whole process from the beginning of the stretching to the tensile fracture, the stress-strain of the

glassy carbon fiber woven composite with axial yarn and the carbon fiber woven composite at different angles is basically linear, and it is more inclined to the elastic material. Except for 30°, the displacement load curve of the braided composite material corresponding to other braiding angles is divided into two parts, the first part of the displacement load is basically linear, and the slope is large. The second part is similar to linear with a smaller slope, indicating that the presence of carbon fiber shaft yarns makes the braided composite more elastic in the tensile fracture range. When the tensile test was completed, the displacement-load curve showed a very obvious dip and the load no longer increased, indicating that the carbon fiber shaft yarn can make the tensile fracture of the braided composite material instantaneous.

5.2. Influence of Braid Angle on Bending Performance. The flexural properties of three kinds of composites braided with

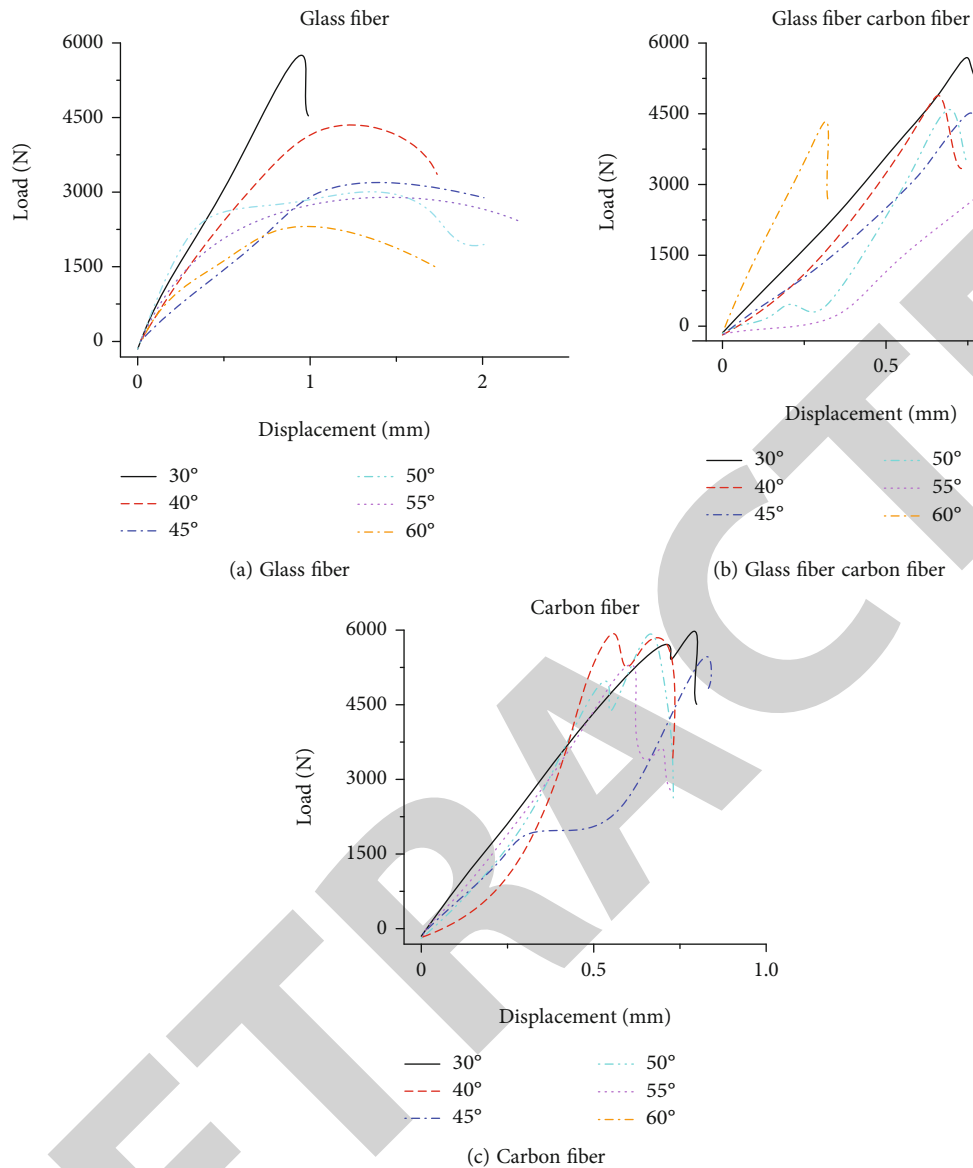


FIGURE 9: Displacement load curves of three hybrid structures at different angles.

different angles of hybrid structure were tested. The test shows that the bending strength is different at different angles and the bending strength is also different at different structures. Table 5 shows the calculation of the bending strength obtained by the bending test of the three kinds of mixed-braided structural braided composites.

As shown in Table 5, when the braiding angle of the glass fiber braided composite material increases from 30° to 60° , the bending strength decreases from 444.0 MPa to 194.4 MPa, with a decrease of about 56%. When the braiding angle of the glassy carbon fiber braided composite material increases from 30° to 60° , the bending strength decreases from 338.4 MPa to 146.4 MPa, with a decrease of about 56%. When the weaving angle of carbon fiber braided composites increased from 30° to 60° , the bending strength decreased from 507.7 MPa to 184.5 MPa, with a decrease of about 63%. In the degree of decline, the carbon fiber woven

composite material is larger than the glassy carbon fiber woven composite material and the glass fiber woven composite material. In the bending test of the glass fiber woven composite at different angles, the bending displacement load curve of the glass fiber woven composite is shown in Figure 7.

It can be seen from Figure 7 that as the braiding angle increases, the displacement corresponding to the maximum bending load is larger. The displacement corresponding to the maximum bending load at 30° , 40° , and 45° is less than 4 mm; the displacement corresponding to the maximum bending load at 50° , 55° , and 60° is greater than 4 mm.

The existence of carbon fiber shaft yarn makes the displacement-load curve in the bending test of the braided composite more linear. The bending displacement-load curves of the three hybrid structures at different angles are shown in Figure 8.

As shown in Figure 8, the displacement-load curves of the glassy carbon fiber braided composite and the carbon fiber braided composite are more linear than the glass fiber biaxial braided composite due to the presence of carbon fiber axial yarns in their preforms. This is because the addition of carbon fiber shaft yarn makes the braided preform more stable, stabilizing the braiding angle, width, length, and other parameters. Braided composites made from 2D triaxial braided preforms also have better stability. Due to the high tensile strength and modulus of carbon fiber itself, it is determined that the triaxial preform braided composite material is more brittle. The maximum bending strength of the glass fiber woven composite material should be relatively large. The smallest displacement is about 4 mm, and the corresponding displacement when the bending strength of the glassy carbon fiber woven composite material is the largest does not exceed 4 mm at different angles. The displacement corresponding to the maximum bending strength of the carbon fiber woven composite material does not exceed 3 mm at different angles. It shows that the carbon fiber shaft yarn can make the woven composite material with smaller bending elongation at break, make the material more elastic, and strengthen the stability of the woven composite material. At the same time, the carbon fiber shaft yarn makes the load of the braided composite material drop in a cliff-like manner when bending and breaking, and the recovery degree of the samples is different after the test is completed. The glass fiber carbon fiber composite material and the carbon fiber composite material are slightly bent, and the glass fiber composite material is more severely bent, indicating that the carbon fiber shaft yarn affects its elastic properties.

5.3. Influence of Shaft Yarn on Compression Properties. The shaft yarn used in this project is 12K SYT49S carbon fiber produced by Zhongfu Shenying Company. Adding a set of axial yarns to the two-dimensional biaxial preform makes the braided preform more stable and also improves the compressive strength of the braided composite material to a certain extent. At the same time, the addition of carbon fiber shaft yarn makes the material more elastic, and as the angle increases, the compressive strength changes less and less. The displacement load curves of the three hybrid structures at different angles are shown in Figure 9.

It can be seen from Figure 9 that the displacement line of the position load of the glass-carbon fiber woven composite material with carbon fiber added to the preform is more linear during the compression process, while the glass fiber woven composite material is 30° apart. The load-displacement curve of the braided composite material corresponding to other angles is basically divided into two parts: two parts with high slope and low slope. However, the load-displacement curve of the glassy carbon fiber woven composite material shows the same slope in the whole process, indicating that the existence of carbon fiber shaft yarn makes the material have better elasticity in compression. Due to the presence of carbon fiber, the compressive strength of the braided composite material decreases gradually with the increase of the angle, indicating that the carbon fiber axial yarn bears most of the compressive force. The

compressive force borne by the braided yarn is smaller than that of the shaft yarn. Therefore, the compressive strength of glassy carbon fiber woven composites and carbon fiber woven composites decreases with the increase of the braiding angle.

6. Conclusion

In this paper, two-dimensional weaving design weaving and mechanical property testing of composite materials are the main research objects, and three kinds of prefabricated hybrid structures are woven by glass fiber and carbon fiber, respectively: glass fiber two-dimensional biaxial preform, glass-carbon fiber braided two-dimensional triaxial preform (glass fiber is braided yarn, carbon fiber is shaft yarn), and carbon fiber braided preform, by measuring the width of glass fiber and carbon fiber, starting from the design of the core mold, and then determining the parameters required for weaving the preform, so as to weave the two-dimensional biaxial and two-dimensional triaxial preforms. The composite material was prepared by VARI process of preform and epoxy resin, and the composite material was tested in tension, bending, and compression. The tensile, flexural, and compressive properties of braided composites with three different structures were tested. It provides some theoretical basis for studying the factors affecting the mechanical properties of two-dimensional braided composites and has a certain theoretical value for simulation research. Due to the limitation of time and cost, the mechanical properties tested in this subject are far from enough, and there is a lack of research on the influence of multiple factors on the braided composite materials, which needs to be further studied in the future.

Data Availability

Data will be available on request.

Conflicts of Interest

There is no conflict of interest.

References

- [1] O. Stolyarov and S. Ershov, "Characterization of change in polypropylene spunbond nonwoven fabric fiber orientation during deformation based on image analysis and Fourier transforms," *Journal of Strain Analysis for Engineering Design*, vol. 52, no. 8, pp. 457–466, 2017.
- [2] C. Krogh, K. D. White, A. Sabato, and J. A. Sherwood, "Picture-frame testing of woven prepreg fabric: an investigation of sample geometry and shear angle acquisition," *International Journal of Material Forming*, vol. 13, no. 3, pp. 341–353, 2020.
- [3] H. Zhang and T. Li, "3D reconstruction method of leather fiber bundle weaving network," *Journal-American Leather Chemists Association*, vol. 113, no. 8, pp. 248–254, 2018.
- [4] P. Priyanka, A. Dixit, and H. S. Mali, "High strength Kevlar fiber reinforced advanced textile composites," *Iranian Polymer Journal*, vol. 28, no. 7, pp. 621–638, 2019.

Retraction

Retracted: Analysis of People Flow Image Detection System Based on Computer Vision Sensor

Journal of Sensors

Received 17 October 2023; Accepted 17 October 2023; Published 18 October 2023

Copyright © 2023 Journal of Sensors. This is an open access article distributed under the Creative Commons Attribution License, which permits unrestricted use, distribution, and reproduction in any medium, provided the original work is properly cited.

This article has been retracted by Hindawi following an investigation undertaken by the publisher [1]. This investigation has uncovered evidence of one or more of the following indicators of systematic manipulation of the publication process:

- (1) Discrepancies in scope
- (2) Discrepancies in the description of the research reported
- (3) Discrepancies between the availability of data and the research described
- (4) Inappropriate citations
- (5) Incoherent, meaningless and/or irrelevant content included in the article
- (6) Peer-review manipulation

The presence of these indicators undermines our confidence in the integrity of the article's content and we cannot, therefore, vouch for its reliability. Please note that this notice is intended solely to alert readers that the content of this article is unreliable. We have not investigated whether authors were aware of or involved in the systematic manipulation of the publication process.

Wiley and Hindawi regrets that the usual quality checks did not identify these issues before publication and have since put additional measures in place to safeguard research integrity.

We wish to credit our own Research Integrity and Research Publishing teams and anonymous and named external researchers and research integrity experts for contributing to this investigation.

The corresponding author, as the representative of all authors, has been given the opportunity to register their agreement or disagreement to this retraction. We have kept a record of any response received.

References

- [1] B. Ou, J. Yang, and W. Wang, "Analysis of People Flow Image Detection System Based on Computer Vision Sensor," *Journal of Sensors*, vol. 2022, Article ID 8099876, 7 pages, 2022.

Research Article

Analysis of People Flow Image Detection System Based on Computer Vision Sensor

Bing Ou ¹, Jingjing Yang ¹ and Wei Wang ²

¹Zhongshan Polytechnic, Zhongshan, Guangdong 528400, China

²Tongji University, Shanghai 200092, China

Correspondence should be addressed to Jingjing Yang; 31115309@njau.edu.cn

Received 30 May 2022; Revised 9 June 2022; Accepted 22 June 2022; Published 4 July 2022

Academic Editor: C. Venkatesan

Copyright © 2022 Bing Ou et al. This is an open access article distributed under the Creative Commons Attribution License, which permits unrestricted use, distribution, and reproduction in any medium, provided the original work is properly cited.

In order to meet the needs of accurately grasping the situation of people in the mall at all times, the author proposes an analysis method based on computer vision for people flow image detection system. This method combines the HOG feature with the SVM classifier, detects pedestrians through dual cameras, and builds an experimental research platform for dual-camera joint detection of pedestrians. The result shows that the error rate of human flow detected by the author's method is the lowest of 0% and the highest of 6.25%. *Conclusion.* This method has a good effect on the statistics of the number of people in the shopping mall and can reduce the workload of the monitoring personnel in the shopping mall.

1. Introduction

Computer vision is an emerging discipline, which is to collect video image data through cameras, apply computer vision to identify, track and measure targets in video images instead of human eyes, further do graphics processing, and make computer processing become more suitable for human eyes to observe or transmit images to instruments for detection [1]. The shape, position, speed, size, and other data of objects in video images can be extracted by computer and can be widely used in finance, justice, military, public security, border inspection, government, aerospace, electricity, factories, education, medical, and other industries. Computer vision is a comprehensive subject and a challenging and important research field, involving computer science and engineering, signal processing, physics, applied mathematics and statistics, neurophysiology, and cognitive science [2].

People flow statistics based on machine vision is an important application field of computer vision technology, with the selection and updating of computer chips and the continuous optimization of image processing algorithms; people counting technology based on machine vision is also changing with each passing day [3]. The video image of the monitored area is collected by the camera, and the collected

video image is processed by relying on the extraordinary data processing capability of the computer. First, the video image is converted into a sequence image, and the sequence image is preprocessed to ensure the accuracy of the collection, extracting the moving objects in the sequence images, identifying whether the moving objects are pedestrians, and establishing and tracking pedestrian trajectories and can not only complete the statistics of people flow but also perform statistical analysis on related information to realize the behavior analysis of pedestrian objects.

With the continuous development of the economy, various large-scale transportation hubs and various public places have appeared, and the passenger flow has caused great pressure on the transportation hubs and public places; if passenger flow statistics are carried out for commercial places, operators can make scientific and effective decisions through the data of passenger flow statistics, thereby increasing the profits of operators. Counting the flow of people in cultural and entertainment places such as scenic spots can count the changes in the flow of people in real time and then get the trend of off-season and peak season, which is convenient to establish a safety warning mechanism [4]. Real-time scheduling and management can be carried out through passenger flow statistics of subway stations, airports, and other

transportation hubs. The passenger flow statistics of mobile vehicles such as buses and subways can be used for early warning management of overload behavior [5].

Therefore, whether it is in the fields of security or business, the technology of people flow statistics based on computer vision is of great significance, and the research on related technologies has important practical value [6].

2. Literature Review

In the early days, people flow statistics adopted manual counting, infrared sensing technology, and gate system; with economic development and scientific progress, the flow of people in various occasions has gradually increased, and traditional passenger flow statistics cannot meet the current needs; at this stage, most of the people flow statistics systems are developed into machine vision-based passenger flow statistics systems. In the field of human flow detection based on computer vision, many research institutions have conducted in-depth research on it in recent years and not only achieved rich results in theory but also introduced a human flow detection system suitable for different scenarios in the application field [7]. As the core technology of pedestrian flow detection, pedestrian detection has been highly concerned by scholars decades ago. The human flow detection system based on computer vision uses digital image processing technology, combined with various gradually updated and improved video image processing algorithms to analyze and process video images, and uses pattern recognition technology and trajectory analysis methods to automatically detect human flow; the detection process includes pedestrian target detection and tracking, pedestrian number statistical analysis, and timely warning of sudden changes in pedestrian flow. The demand for applications has promoted the development of technology, and people flow detection has a great demand in many public places [8].

The interframe difference method proposed by Sun et al. extracts moving objects by the difference between consecutive frame images; this method is the most simple and direct and can quickly detect changes in video images [9]. The optical flow method proposed by Schmidt and Sutton forms the motion field of the whole image by obtaining the velocity vector of each pixel in the image and obtains the position area of the moving target according to the change of the optical flow vector [10]. Li et al. adopted a linear weighting method for foreground ablation and fused this ablation mechanism and background reconstruction into a Gaussian model, but the foreground ablation time of this method was too long, requiring multiple frames to completely ablate [11]. Pei et al. make full use of the neighborhood information of pixels; a foreground detection method based on dynamic background difference is proposed, which ignores the temporal continuity of pixels while considering the spatial information of pixels, resulting in low detection accuracy [12]. Mavredakis et al. proposed a new foreground extraction method, which greatly reduces the computational complexity of the original method, thereby speeding up object detection [13]. Khan et al. implemented the previously pro-

posed HOG feature calculation using the integral graph idea, which greatly improved the detection speed [14].

Based on the analysis of the computer vision human flow image detection system, the author detects and counts pedestrians under the condition of no surveillance and builds an experimental research platform for dual-camera joint detection of pedestrians, which has achieved good results.

3. Research Methods

3.1. Image Preprocessing. Due to the influence of uncertain factors such as lighting and shadows, there will always be noise in the video sequence captured by the camera. The preprocessing of the image can effectively suppress the noise of the image; the process of image preprocessing is to read each frame of image captured by the camera, then grayscale the image, and filter the final grayscale image. Image preprocessing is to filter the edge information of the image to make the image easier to detect, that is, image filtering [15–17].

The main purpose of image filtering is to remove information that is not related to detection, such as illumination; this step occupies the largest proportion in image preprocessing, and the effect of filtering is also an important evaluation of the entire system. There are many filtering methods that are often used; the method used by the author is the Gaussian filtering method, which can be easily implemented in OpenCV; the GaussianBlur function used is as follows: C++: void GaussianBlur (InputArray src, OutputArray dst, Size ksize, double sigmaX, double sigmaY=0, int borderType).

3.2. Detection of Moving Objects. Optical flow method and frame difference method are effective and common methods for moving object detection; these methods are used to detect moving objects; no matter what, it is good to “see” moving objects. The core of these methods is to use the difference between video frames to determine whether there is a moving object. Among these methods, the adjacent frame difference method has strong robustness and is suitable for the system of people flow detection in shopping malls [18]. This method mainly uses the pixels corresponding to the adjacent two frames of sequence images to perform a difference operation; if the obtained difference is greater than a given threshold, it is determined that there is a moving target in the current scene; otherwise, there is no moving target; the formulas of the operation formula (1) and formula (2) are as follows.

$$D_k(x, y) = |H_{k+1}(x, y) - H_k(x, y)|, \quad (1)$$

$$T_k(x, y) = \begin{cases} 1, & D_k(x, y) \geq T, \\ 0, & D_k(x, y) < T, \end{cases} \quad (2)$$

where $H_k(x, y)$ is the pixel of the image sequence and T is a predetermined threshold; if $D_k(x, y) \geq T$, then it is said that there is a moving target. If $D_k(x, y) < T$, then it is said that there is no moving target.

3.3. Pedestrian Detection. The research on pedestrian detection methods is an important and difficult point in the

computer field. Computer vision is a science that studies how to make machines replace human eyes to recognize objects; in pedestrian detection, it is to study how to use a PC to see objects through sensors such as cameras, determine whether it is a pedestrian, and finally make statistics. In general, there are currently three best methods for pedestrian detection. The improved HOG+improved SVM, HOF + CSS + AdaBoost, and HOG+LBP + SVM methods have their own characteristics and are often used in combination. For the actual situation, the author uses the improved HOG + improved SVM method considering the characteristics of the shopping mall.

3.3.1. HOG Features. HOG is a very effective method to mine image information. This image information is called gradient information. By calculating this gradient information, the information is represented by a histogram, which constitutes the HOG feature. The HOG feature detection method was proposed by the French researcher Dalal at the CVPR conference in 2005; after continuous improvement by experts and scholars, the current improved HOG feature was obtained. The usual case is to use the improved HOG feature with the improved SVM classifier to comprehensively detect pedestrians [19].

Since the gradient usually exists at the boundary, it is necessary to use many images as samples to extract the HOG features of pedestrians, which is equivalent to the description of the local area in the image. The main idea of HOG feature is the strategy of dividing the whole into zero, dividing an image whose features are to be extracted into many small regions, counting HOG features in these small regions, and finally combining the small features to obtain the overall HOG feature picture. The extraction of HOG features is an operation in a small local connected area; changes in some areas will not have a great impact on the HOG features of the entire image, so the detection method has strong robustness and is very suitable for pedestrians. Target is detected.

The flow chart of the HOG feature extraction is shown in Figure 1.

The specific process is as follows:

- (1) Since the color information has little effect, grayscale processing is performed on the image to reduce the amount of information processed by the computer
- (2) Use the correction method to correct the pixels of the image, and the method used is the gamma correction method. The formula of this method is shown in formula (3), where $\gamma = 1/2$

$$H(x, y) = H(x, y)\gamma \quad (3)$$

- (3) Calculate the gradient of each pixel in the image, where the gradient calculation method at the pixel point (x, y) is as follows:

$$\begin{aligned} G_x(x, y) &= H(x+1, y) - H(x-1, y), \\ G_y(x, y) &= H(x, y+1) - H(x, y-1). \end{aligned} \quad (4)$$

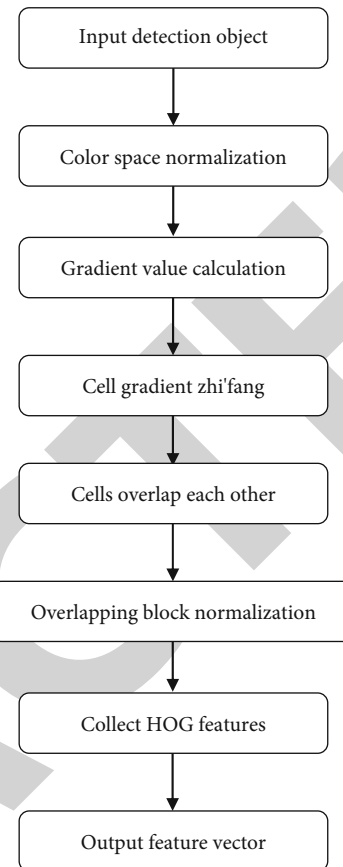


FIGURE 1: HOG feature extraction process.

The gradient magnitude and gradient direction are as follows:

$$\begin{aligned} G(x, y) &= \sqrt{G_x(x, y)^2 + G_y(x, y)^2}, \\ \alpha(x, y) &= \tan^{-1}\left(\frac{G_y(x, y)}{G_x(x, y)}\right) \end{aligned} \quad (5)$$

- (4) Divide the entire image into many small squares called cells. And connect some fixed cells into a block
- (5) Extract the information of the HOG feature of each block, and use 9 bins to count the HOG features of the image; that is, divide $0^\circ \sim 180^\circ$ into 9 parts equally; the gradient direction of each pixel is $\alpha(x, y)$, and which bin it belongs to, the information of the pixel is placed in this bin
- (6) Connect the small ones into large ones, and get all the directional gradient information of the image

3.3.2. SVM Classifier. Pattern recognition technology refers to the recognition technology of various things based on computer technology to realize machine simulation of human beings; it is a branch of artificial intelligence. At present, pattern recognition technology is developing rapidly, and various theories have been proposed and

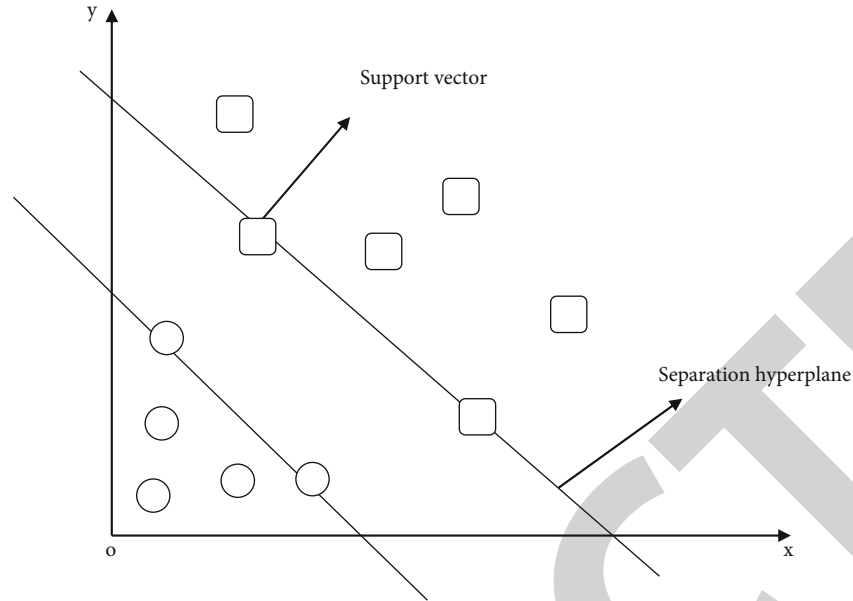


FIGURE 2: SVM classifier.



FIGURE 3: Physical simulation diagram.

continuously improved; at this stage, people's views on pattern recognition are not unified; some people think that pattern recognition technology has inherent deficiencies in simulating people; further development is very limited. The success achieved at this stage is mainly for some simple purposes; for complex operations in complex scenarios, the workload required by pattern recognition technology is not generally large; another part of people believes that with the improvement of hardware technology and the progress of computer processing power, although the software seems to have touched the ceiling, its potential is immeasurable. Although at the theoretical level, pattern recognition technology seems to have entered a bottleneck, but in practical applications, it has achieved good results in many fields, and these results also encourage people to continue to invest in research in this field. In statistical pattern recognition, predecessors have made various attempts and proposed excellent algorithm mechanisms such as Bayesian decision-

making and BP neural network, but they each have obvious shortcomings, so that they often fall into one way or another in practical applications in a vicious circle. The problem of probability density seriously restricts the promotion of the algorithm, because in terms of pattern recognition, the estimation of probability density is often more difficult to solve, and the basis of engineering practice is often less than the development of theory; as a result, some algorithms have obvious strong effects in theoretical experimental environment, but they will encounter unexpected setbacks in specific applications. However, with the breakthrough achievements of statistical theory, especially the establishment of modern statistical theory, the SVM algorithm technology of support vector machine was finally born [20].

SVM, or support vector machine, is a classification method used in the field of computer vision, and it is a classification method defined by the classification hyperplane. The author uses the SVM classifier mainly to classify the

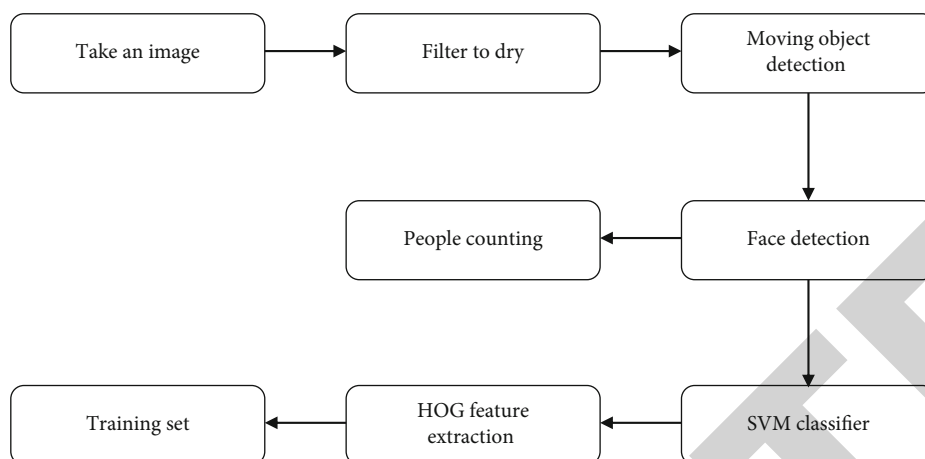


FIGURE 4: Overall block diagram of the system.

TABLE 1: Statistics of people.

	8:00	10:00	12:00	14:00	16:00
Number of people counted by author's method	10	28	15	20	25
The actual number	10	27	16	19	24

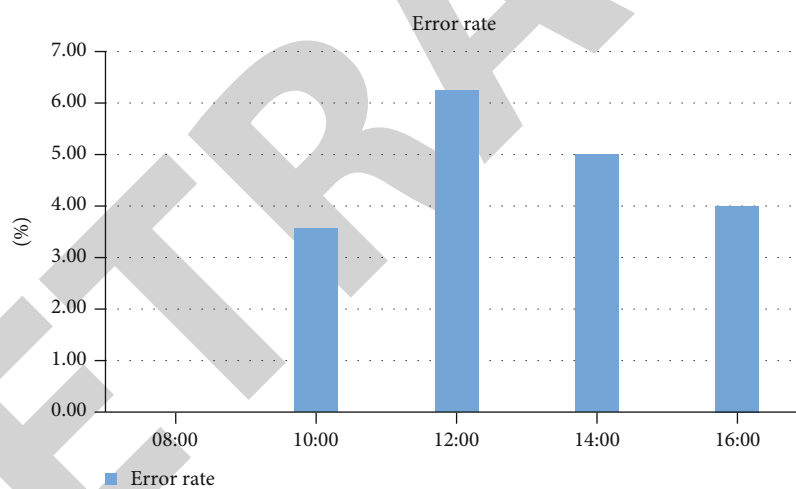


FIGURE 5: Error ratio of each time period.

HOG features of pedestrian faces, that is, after sufficient positive samples (images containing faces) and negative samples (images without faces) are provided, and the HOG features are extracted from these positive and negative samples; the SVM classifier is used for classification and identification. A diagram of the interpretation of the SVM classifier is shown in Figure 2. Find the optimal separating hyperplane from the preorganized positive and negative data sets, and extract the region of interest. The mentioned support vectors are also some data closest to this separating hyperplane.

After using the improved HOG + improved SVM method, for the video frames captured by the camera, we can directly call this method to scan the image continuously, perform template matching, and then determine whether there is a pedestrian.

4. Analysis of Results

The experimental system uses two cameras to capture the faces of pedestrians entering and exiting the mall and transmits the obtained data to the PC, where it is processed and the flow of people in the mall is obtained. Figure 3 is a physical simulation diagram. The processing flow of the PC includes several parts such as calling the camera to take images, filtering processing, moving object detection, face detection, and people counting. The author's overall block diagram is shown in Figure 4.

The idea designed by the author is shown in Figure 4; the pedestrians in the images captured by the two cameras are counted separately, the number of pedestrians collected and counted by camera 1 is the number of people entering

the mall, the number of pedestrians collected and counted by the camera 2 is the number of people leaving the shopping mall, and the difference between these two data is the pedestrian flow in the shopping mall. Through experimental simulation, a certain classroom is used as a place to simulate a shopping mall, and the number of people in the classroom at each time of the day is obtained, as shown in Table 1. The error ratios for each time period are shown in Figure 5. By analyzing and comparing the obtained data, the data obtained by the author's method is not much different from the actual data, which can well replace the responsibilities of the staff.

5. Conclusion

In the response measures of emergency incidents in shopping malls, to minimize casualties, it is necessary to accurately grasp the situation of personnel in shopping malls at all times. In order to reduce casualties, by combining the HOG feature with the SVM classifier, the author uses dual cameras to detect pedestrians, builds an experimental research platform for dual-camera joint detection of pedestrians, and designs a system for detecting people in shopping malls. It has played a very good role in the statistics of the number of people in the shopping mall and can reduce the workload of the personnel responsible for monitoring the shopping mall. There are still some defects in this method, such as the detection effect of occluded pedestrians is not very ideal; there is still a lot of work in this system and the field of human detection and tracking to be further explored. The system is not universal and needs different training samples for different scenarios, especially when the camera angle and height change greatly. Whether it is the human body detection, identification and tracking technology used in video surveillance, or the people flow statistics system, there is a lot of room for development. With the gradual increase in the application of video surveillance and people flow statistics in people's production and life, more and better optimization algorithms will surely be brought, which will promote greater development in this field.

Data Availability

The data used to support the findings of this study are available from the corresponding author upon request.

Conflicts of Interest

The authors declare that they have no conflicts of interest.

References

- [1] C. Alarcon and C. Shene, "Fermentation 4.0, a case study on computer vision, soft sensor, connectivity, and control applied to the fermentation of a thraustochytrid," *Computers in Industry*, vol. 128, no. June 2021, article 103431, 2021.
- [2] J. S. Chou and C. H. Liu, "Automated sensing system for real-time recognition of trucks in river dredging areas using computer vision and convolutional deep learning," *Sensors*, vol. 21, no. 2, p. 555, 2021.
- [3] H. Li, B. F. Spencer, H. Bae, K. Jang, and Y. K. An, "Deep super resolution crack network (SrcNet) for improving computer vision-based automated crack detectability in in situ bridges," *Structural Health Monitoring*, vol. 20, no. 4, pp. 1428–1442, 2021.
- [4] X. Hao, H. Lyu, Z. Wang, S. Fu, and C. Zhang, "Estimating the spatial-temporal distribution of urban street ponding levels from surveillance videos based on computer vision," *Water Resources Management*, vol. 36, no. 6, pp. 1799–1812, 2022.
- [5] G. Li, F. Liu, A. Sharma et al., "Research on the natural language recognition method based on cluster analysis using neural network," *Mathematical Problems in Engineering*, vol. 2021, Article ID 9982305, 13 pages, 2021.
- [6] M. Raj, P. Manimegalai, P. Ajay, and J. Amose, "Lipid data acquisition for devices treatment of coronary diseases health stuff on the Internet of Medical Things," *Journal of Physics: Conference Series*, vol. 1937, article 012038, 2021.
- [7] L. Xin, M. Chengyu, and Y. Chongyang, "Power station flue gas desulfurization system based on automatic online monitoring platform," *Journal of Digital Information Management*, vol. 13, no. 6, pp. 480–488, 2015.
- [8] P. Tumas, A. Nowosielski, and A. Serackis, "Pedestrian detection in severe weather conditions," *Access*, vol. 8, pp. 62775–62784, 2020.
- [9] W. Sun, H. Du, G. Ma, S. Shi, and Y. Wu, "Moving vehicle video detection combining vibe and inter-frame difference," *International Journal of Embedded Systems*, vol. 12, no. 3, p. 371, 2020.
- [10] B. E. Schmidt and J. A. Sutton, "Evaluation of a wavelet-based optical flow method for planar velocimetry using scalar fields," *Experiments in Fluids*, vol. 63, no. 3, pp. 1–16, 2022.
- [11] Y. Li, C. Liu, L. Zhang, and B. Sun, "A partition optimization design method for a regional integrated energy system based on a clustering algorithm," *Energy*, vol. 219, no. 2, article 119562, 2021.
- [12] S. Pei, L. Li, L. Ye, and Y. Dong, "A tensor foreground-background separation algorithm based on dynamic dictionary update and active contour detection," *Access*, vol. 8, pp. 88259–88272, 2020.
- [13] N. Mavredakis, W. Wei, E. Pallecchi et al., "Low-frequency noise parameter extraction method for single layer graphene FETs," *IEEE Transactions on Electron Devices*, vol. 67, no. 5, pp. 2093–2099, 2020.
- [14] M. N. Khan, A. Das, M. M. Ahmed, and S. S. Wulff, "Multilevel weather detection based on images: a machine learning approach with histogram of oriented gradient and local binary pattern-based features," *Journal of Intelligent Transportation Systems*, vol. 25, no. 5, pp. 513–532, 2021.
- [15] S. Zhang, L. Zhang, T. Zhao, and M. M. Selim, "Fault diagnosis of rotating machinery based on time-frequency image feature extraction," *Journal of Intelligent and Fuzzy Systems*, vol. 39, no. 4, pp. 5193–5200, 2020.
- [16] C. Du, M. Lan, M. Gao, Z. Dong, and Z. He, "Real-time object tracking via adaptive correlation filters," *Sensors*, vol. 20, no. 15, p. 4124, 2020.
- [17] R. Huang, S. Zhang, W. Zhang, and X. Yang, "Progress of zinc oxide-based nanocomposites in the textile industry," *IET Collaborative Intelligent Manufacturing*, vol. 3, no. 3, pp. 281–289, 2021.

Retraction

Retracted: Spatial and Temporal Evolution of Urban Green Space Pattern Based on GIS Sensors and Remote Sensing Information: Taking Xi'an as an Example

Journal of Sensors

Received 13 September 2023; Accepted 13 September 2023; Published 14 September 2023

Copyright © 2023 Journal of Sensors. This is an open access article distributed under the Creative Commons Attribution License, which permits unrestricted use, distribution, and reproduction in any medium, provided the original work is properly cited.

This article has been retracted by Hindawi following an investigation undertaken by the publisher [1]. This investigation has uncovered evidence of one or more of the following indicators of systematic manipulation of the publication process:

- (1) Discrepancies in scope
- (2) Discrepancies in the description of the research reported
- (3) Discrepancies between the availability of data and the research described
- (4) Inappropriate citations
- (5) Incoherent, meaningless and/or irrelevant content included in the article
- (6) Peer-review manipulation

The presence of these indicators undermines our confidence in the integrity of the article's content and we cannot, therefore, vouch for its reliability. Please note that this notice is intended solely to alert readers that the content of this article is unreliable. We have not investigated whether authors were aware of or involved in the systematic manipulation of the publication process.

Wiley and Hindawi regrets that the usual quality checks did not identify these issues before publication and have since put additional measures in place to safeguard research integrity.

We wish to credit our own Research Integrity and Research Publishing teams and anonymous and named external researchers and research integrity experts for contributing to this investigation.

The corresponding author, as the representative of all authors, has been given the opportunity to register their agreement or disagreement to this retraction. We have kept a record of any response received.

References

- [1] W. Li, H. Wang, S. Zhang, B. Jiang, and S. Lee, "Spatial and Temporal Evolution of Urban Green Space Pattern Based on GIS Sensors and Remote Sensing Information: Taking Xi'an as an Example," *Journal of Sensors*, vol. 2022, Article ID 3648880, 8 pages, 2022.

Research Article

Spatial and Temporal Evolution of Urban Green Space Pattern Based on GIS Sensors and Remote Sensing Information: Taking Xi'an as an Example

Wei Li ^{1,2}, Hui Wang ², Shaowei Zhang ³, Bingshen Jiang ¹, and Shi-Young Lee ²

¹Huanghuai University, Zhumadian, Henan, China

²Pai Chai University, Daejeon, Republic of Korea

³Shaanxi Geomatics Center of Ministry of Natural Resources, Xi'an, Shaanxi, China

Correspondence should be addressed to Shi-Young Lee; 201999000369@hceb.edu.cn

Received 21 May 2022; Revised 2 June 2022; Accepted 20 June 2022; Published 4 July 2022

Academic Editor: C. Venkatesan

Copyright © 2022 Wei Li et al. This is an open access article distributed under the Creative Commons Attribution License, which permits unrestricted use, distribution, and reproduction in any medium, provided the original work is properly cited.

In order to solve the practical application of the continuously developing remote sensing technology in urban planning, this paper proposes a method of temporal and spatial evolution of urban green spatial pattern based on GIS remote sensing information. Based on the Landsat Image data of the main urban area of Xi'an from 2000 to 2012, different classification methods are used to extract the urban green space information and compare the accuracy. The classification results with high accuracy are selected to analyze the temporal and spatial evolution law of urban green space and the change of landscape pattern in the study area. In this paper, the change of vegetation coverage can be divided into five levels: significant degradation: <-0.006 ; slight degradation: $-0.006\sim-0.002$; stable: $-0.002\sim0.002$; slight improvement: $0.002\sim0.006$; and significant improvement: >0.006 . The results of this paper prove that this method can be used to understand and evaluate the ecological consequences of urbanization and improve our quality of life. At the same time, it can provide basic information for decision-making.

1. Introduction

As a part of urban ecosystem, urban green space plays an important role in urban sustainable development because many ecosystem services and functions are crucial to urban ecological integrity and human well-being [1]. Urban green space is an important part of urban ecosystem. It has important ecological auxiliary function for urban development and progress. It is an important indicator of urban ecological civilization construction and plays an important role in regulating urban ecological environment [2].

With the acceleration of urbanization and urban expansion, the area of urban green space continues to shrink and gradually becomes a scarce resource. However, people's attention to green living standards continues to increase with the growth of economic development level [3]. Urban green space has become the focus of many disciplines [4].

On the one hand, urban green space provides healthy and comfortable rest places for urban residents. On the other

hand, it is also an important measure for the government to reasonably layout the urban spatial structure, and promoting its healthy development has become an important content of urban planning [5]. Urban green space improves the quality of life and air quality, reduces the use of refrigeration and heating energy, purifies the urban environment, regulates the temperature and humidity of the air, and makes the urban environment more aesthetically desirable [6]. With the continuous development of urban economy and the acceleration of urbanization, the environmental problems faced by cities are becoming more and more serious, such as urban heat island effect, air pollution, water resources pollution, ecological environment damage, excessive population expansion, and serious damage to biodiversity. They have seriously affected the physical and mental health of urban residents and are one of the most severe challenges faced by human society in the 21st century. Rational planning of urban green space can effectively solve the severe challenges faced in the process of urban development in China [7, 8].

At the same time, green space plays an important role in enterprise location, local employment rate, and tourism development, as shown in Figure 1.

2. Literature Review

Urban green space is the key to the coupling of urban spatial development and ecological environment, and it is also the key to effectively alleviate the problem of environmental degradation in urbanization areas. As an important living urban infrastructure form attached to urban land resources, urban green space is an important part of urban ecosystem with white and clean function, and it is also an important symbol to measure the level of urban sustainable development and civilization [9]. Due to the differences in the stages of urban development and the focus of ecological and environmental protection research at home and abroad, scholars at home and abroad have different definitions and understandings of green space. Foreign countries mostly refer to urban open space [10]. In 1877, the concept of urban open space was first put forward in London, England [11]. In 1906, urban open space was formally defined as “any enclosed or unclosed land, in which less than 1 / 20 of the land without buildings or buildings, and the rest of the land was used as parks or entertainment, or as waste areas, or unused areas” [12].

Urban open green space emphasizes the openness and greenness of space. All countries in the world are committed to building various forms of urban open green space, such as urban parks, corridors, and green belts. As a kind of urban land, urban green space is distributed in the urban area from the perspective of comprehensive consideration of urban land utilization and has a relatively clear land scope. It pays more attention to the landscape aesthetic benefits, social benefits, and ecological environment benefits of green space. Urban green space is treated from the perspective of city and large region. Its composition and classification have the characteristics of comprehensiveness and integrity. It includes not only the types of green space divided by urban green space but also the agricultural production land, water body, mountain, grassland, wetland, and so on in the whole region. It emphasizes the coordinated development of urban structure and the sustainability and rationality of the development of urban spatial structure, including all land within the city that has a direct or indirect impact on the improvement of urban ecological environment and people's life [13]. According to the classification standard of urban green space issued by the Ministry of Housing and Urban-Rural Development in 2017, urban green space is divided into five categories: park green space, square green space, protective green space, auxiliary green space, and regional green space [14]. The traditional concept of green space in China actually refers to green space in a narrow sense.

Zhu et al. define urban green space as a green network system composed of garden green space, urban forest, three-dimensional space greening, urban farmland, and water wetland [15]. Liu et al. pointed out that urban green space contains at least the following two meanings: first, urban regional space based on natural acquisition, mainly covered

by artificial green vegetation; the second is to provide various social service functions, including ecology, entertainment, and aesthetics [16]. Zhu et al. believe that urban green space refers to the area covered by green plants inside and around the city, including natural or man-made green space such as grassland, forest land, and cultivated land [17]. Wang et al. put forward that urban green space refers to the space covered by living plants in the city, which is the sum of urban forests, crops, shrubs, and other plants. It includes natural vegetation (although the natural vegetation of most cities has disappeared), seminatural vegetation, and artificial vegetation, mainly including the central area of the city and its surrounding areas [18]. Zhang and Shen believe that urban green space can include any vegetation in the urban environment, including parks, open spaces, residential gardens, or street trees. These places provide residents with contact space, opportunities for leisure, and entertainment, as well as habitats of natural species, and maintain biodiversity [19].

Therefore, based on the satellite data with long time series and medium spatial resolution, this paper applies remote sensing and GIS technology to extract the green spatial information of the main urban area of Xi'an and discusses the extraction, composition structure, and temporal and spatial evolution characteristics of the green spatial information in the study area, so as to provide reference for the sustainable development of the city.

3. Research Methods

3.1. Elements of Green Space in Xi'an. Urban green space classification is the basis of green space information extraction, space-time evolution of green space, and landscape pattern analysis [20]. In this paper, according to the classification of land use status, the research of scholars and the actual situation of the main urban area of Xi'an, and according to the contribution of the constituent elements of urban green space to green space, the spatial types of the study area are divided into green space and nongreen space, in which green space includes urban green space cultivated land, and water body, and nongreen space includes construction land and other land, as shown in Table 1.

3.2. Xi'an Green Space Information Extraction Method. Image classification is an integral part of image processing. It extracts topic information by learning the relationship between spectral features and various categories or topics of interest to users. It is a complex process and needs to consider a variety of factors [21]. As an important part of urban ecosystem, urban green space has the function of ecological balance and is closely related to human life. Its integrity, diversity, and systematicness are disturbed by human activities to a great extent, showing dynamic characteristics. Quantitative analysis of the type composition, quantitative characteristics, dynamic evolution, and other characteristics of green space can help understand the development and evolution process of green space and provide crucial basic data and analysis basis for the analysis of the ecological and environmental effects caused by urbanization and human activities [22]. User demand, the scale of the research

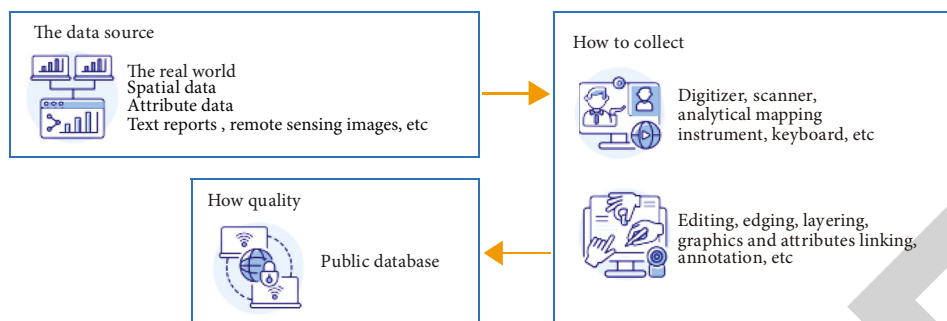


FIGURE 1: Urban green space based on GIS and remote sensing information.

TABLE 1: Classification of urban green space.

Urban space type	Land use type	Types and characteristics of green space
Green space	Cultivated land	Land for planting crops, including paddy field, dry land, and irrigated land
	Urban green space	Forest land mainly refers to the land where trees, bamboos, and shrubs grow Grassland includes natural grassland, swamp grassland, artificial grassland, and other grasslands
	Water body	Including rivers (canals), lakes, reservoirs, pits and ponds, coastal and inland beaches
Nongreen space	Land used for building	Including residential land, commercial land, industrial and mining storage land, public management and public service land, special land, transportation land, hydraulic construction land, etc.
	Other land	Including bare land, sandy land, bare rock gravel land, saline alkali land, etc.

area, economic conditions, and the skills of analysts are important factors affecting the selection of remote sensing data, the design of classification program, and the quality of classification results [23].

3.2.1. Maximum Likelihood Method. Maximum likelihood classification (MLC) is a statistical method of pattern recognition [24]. For each pixel in the image, the probability of belonging to a certain category is calculated and assigned to the category with the highest probability. Generally, assuming that the distribution of each class in the multidimensional space is Gaussian distribution, the mean and covariance matrix of maximum likelihood classification are obtained from the training samples and used to effectively model the class [25]. The basis of this assumption is Bayesian decision rule (BDR), in which different kinds of probabilities need to be specified. Using BDR, we must have a priori knowledge of different kinds of probabilities. Maximum likelihood classification is a common method in supervised classification. It is suitable for most image processing software with high classification accuracy. It is the most commonly used parameter classifier in practice, as shown in

$$g_i(x) = \ln p(\omega_i) - \frac{1}{2 \ln |\Sigma_i|} - \frac{1}{2(x - m_i)^T \Sigma_i^{-1} (x - m_i)}, \quad (1)$$

where i is class i ; x is n -dimensional data, where n is the number of bands; $p(\omega_i)$ is the probability that a certain class i appears in the image, and it is assumed that all classes are the same; $|\Sigma_i|$ is the determinant of the covariance matrix of some type i data; Σ_i^{-1} is the inverse of a class i covariance matrix; m_i is the average vector of some i .

3.2.2. Support Vector Machine Classification. Support vector machine (SVM) was developed in the mid-1990s. This method is a supervised classification method based on statistical learning theory and structural risk minimization (SRM) principle. SVM not only achieves good results in pattern recognition, function estimation, and regression analysis but also shows many unique advantages in solving small sample and nonlinear and high-dimensional pattern recognition. The simplest way to train support vector machines is to use linear classifiers. The formula is expressed as

$$\{X_i, y_i\}, \quad i = 1, 2, \dots, k. \quad (2)$$

In formula (2), k is the number of training samples: X is N -dimensional space, $X \in \mathbb{R}^N$; y is a class label, and $y \in \{-1, +1\}$. If there is a vector W perpendicular to the linear hyperplane (determining the direction of the discrimination plane) and a scalar b showing the offset of the discrimination hyperplane from the origin, these classes are considered to be linearly separable. Two hyperplanes can be used to distinguish data points in various classes. The formula is expressed as

$$\begin{cases} WX_i + b \geq +1, y = +1, \\ WX_i + b \leq -1, y = -1. \end{cases} \quad (3)$$

3.2.3. Random Forest Classification. The basic idea of random forest classification method is as follows: firstly, bootstrap sampling technology is used to extract training samples from the original data set, and each training sample accounts for about two-thirds of the original data set. Then,

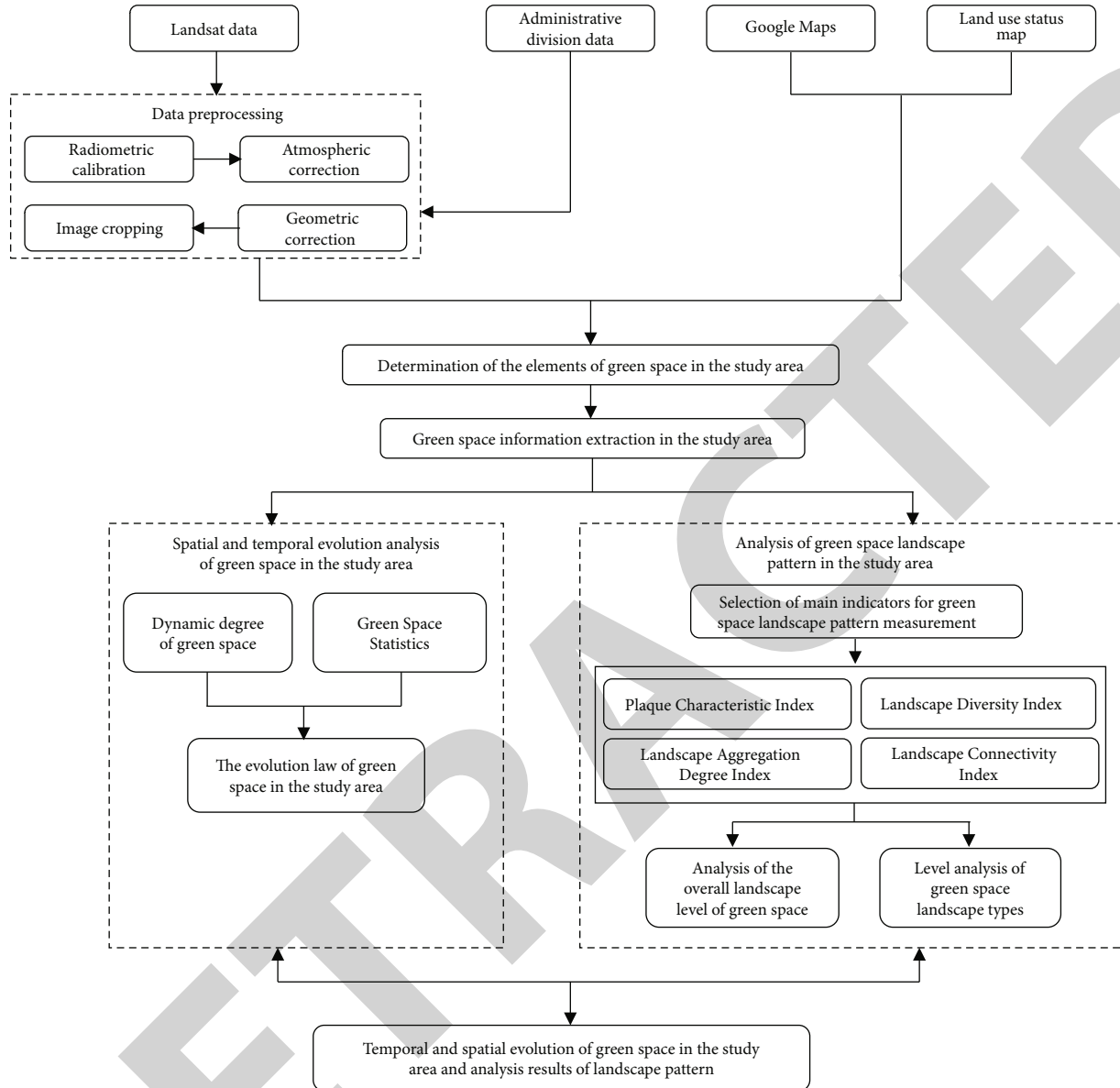


FIGURE 2: Research ideas.

a classification regression tree is established for each training sample to generate a forest composed of $NCART$ decision trees. In the growth process of each tree, m characteristic variables are randomly selected from all M characteristic variables as the input sample of each node, ($m \leq M$). Finally, the classification results of each decision tree are synthesized by voting, and the classification result with the largest number of votes is the final result. The out-of-bag tree is called one-third of the out-of-bag tree. The out-of-bag samples are used as the test data to generate the decision tree. This part of the out-of-bag data is used to estimate the internal error, resulting in OOB error. The random forest classification method uses Gini index as the attribute selection measure. For a given training set T , randomly select a pixel and indicate that it belongs to a class C_i , $f(C_i, T)/|T|$ is the probability that the selected pixel belongs to class C_i . The

Gini index can be expressed as

$$\text{Gini Index} = \sum_{j \neq i} \left(\frac{f(C_i, T)}{|T|} \right) \left(\frac{f(C_j, T)}{|T|} \right). \quad (4)$$

3.3. *Research Ideas.* Based on the five Landsat Image data of 1994, 2000, 2006, 2013, and 2018, taking Xi'an land use map, high-resolution Google map, and administrative division vector data as auxiliary data, this paper carries out a series of preprocessing for Landsat Image data, such as radiometric calibration, atmospheric correction, geometric correction, and image clipping. For the preprocessed data, the maximum likelihood classification method, support vector machine classification method, and random forest classification are used to extract the green space information of the

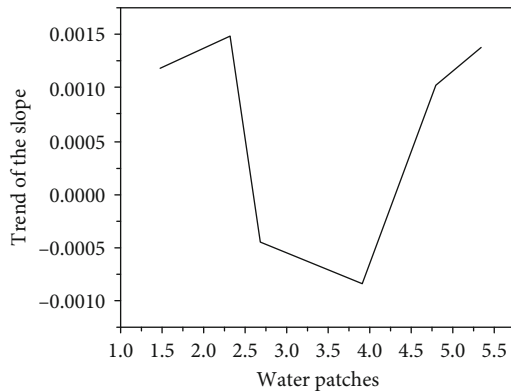


FIGURE 3: Potential slope distribution in the experimental area.

TABLE 2: Statistics of covered mounting categories of each value.

Vegetation cover change category	The measure of area	Proportion
Significant reduction	420	6.23%
Stable	1020	14%
Increase	2300	34%

study area, and the accuracy is verified to obtain the optimal green space extraction method: the random forest classification method and landscape index method are selected for landscape pattern analysis. The research idea of this paper is shown in Figure 2:

4. Result Analysis

Using MODIS NDVI data with stronger timeliness compared with common remote sensing images, this paper analyzes the vegetation cover change and distribution pattern in Xi'an from 2000 to 2012, so as to provide decision-making reference for the evaluation and adjustment of Xi'an industrial pattern and economic layout.

The MODIS NDVI/EVI MOD13Q1 data provided by NASA used in this paper has a spatial resolution of 250 m and a temporal resolution of 16d. Affected by the climatic environment and vegetation growth in Xi'an, and according to the existing research results, July to September of each year is defined as the growth season of plants in this area. This paper selects the relevant data of plant growth season images in Xi'an from 2000 to 2012 for correlation analysis.

In order to eliminate the influence of cloud as far as possible, 117 MODIS NDVI images from 2000 to 2012 were synthesized by maximum value composite in years. In ArcGIS10.0, select the max command to maximize the processing, and then obtain the data related to NDVI-Max in 13 growing seasons from 2000 to 2012.

4.1. Study on Vegetation Cover Change. The interannual linear change trend of NDVI is used to judge the nature and intensity of vegetation cover change. On the basis of each pixel, NDVI-Max is linearly fitted, and the trend slope is

calculated by the least square method, as shown in the following:

$$b = \frac{(x_i - y)}{(x_i - x)}. \quad (5)$$

In the equation, b is the trend of the slope, x and y are the year and the NDVI-Max value of the year respectively, and x and y are the mean value of the year and the NDVI-Max value from 2000 to 2012, respectively. A positive slope indicates the increase of vegetation coverage. The larger the value, the more obvious the trend of vegetation coverage increase. A negative slope indicates a decline in vegetation coverage. The more obvious the value, the more obvious the trend of vegetation coverage reduction.

In order to determine the natural fluctuation range of NDVI-Max in the study area from 2000 to 2012, combine the basic geography.

According to the data, the water body without vegetation cover is extracted in the whole area of Xi'an. Considering that the resolution of remote sensing image is 250 m, 10 patches with an area greater than 1 km² are selected as the experimental area. By analyzing the linear trend slope of the average value of NDVI-Max in the growing season from 2000 to 2012, it is found that almost all tribes are in the range of -0.002~0.002. As shown in Figure 3, set this range as the natural fluctuation amplitude of vegetation cover in Xi'an, and extend the limit of natural fluctuation outward twice to obtain 0.006. Take this value as the limit of slight change and significant change of vegetation cover. Therefore, the change of vegetation coverage can be divided into five levels: significant degradation: <-0.006; slight degradation: -0.006~-0.002; stable: -0.002~0.002; slight improvement: 0.002~0.006; and significant improvement: >0.006.

4.2. Interannual Variation of Vegetation Coverage in Xi'an.

Use ArcGIS10.0 to draw the distribution map of vegetation cover change trend in Xi'an, and count the area of each vegetation cover change category, and calculate the proportion, as shown in Table 2. The results show that the vegetation cover in Xi'an has been mainly stable and increased in recent 13 years, accounting for 81.42%. The vegetation coverage in some areas is seriously reduced and concentrated, mainly distributed in the northeast of Yanbian County, the river area of Miyi County, the west, the area under the jurisdiction of Xi'an city, and the south of Xi'an city. As the distribution is relatively concentrated, it may be caused by the continuous development of industrial land and construction land.

In order to compare the changes of NDVI-Max in different growth seasons, the annual growth season NDVI-Max of two increase types and two decrease types are counted, respectively, and their change trend charts are drawn, as shown in Figures 4(a) and 4(b).

Figures 4(a) and 4(b) show that NDVI-Max increased by an average of 0.01 per year in the growth season of the significantly improved type in the past 13 years (the confidence is 99.9%), the annual average increase rate is 152%, and the

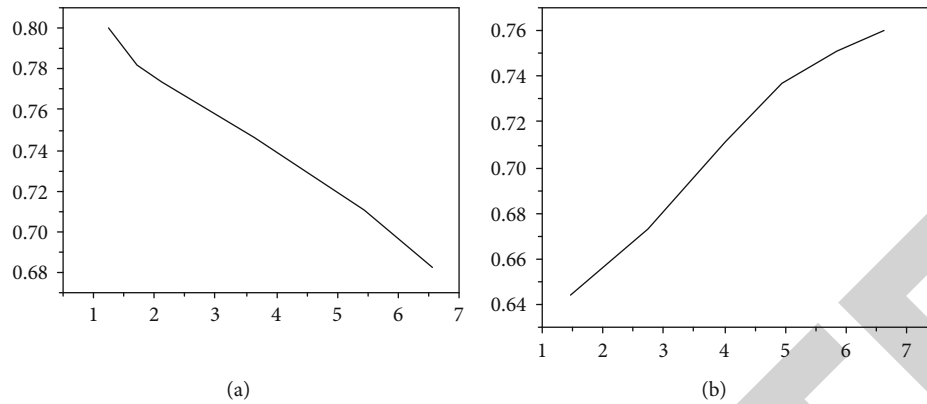


FIGURE 4: Interannual variation of NDVI-Max of four change types (a). Interannual variation of NDVI-Max of four change types (b).

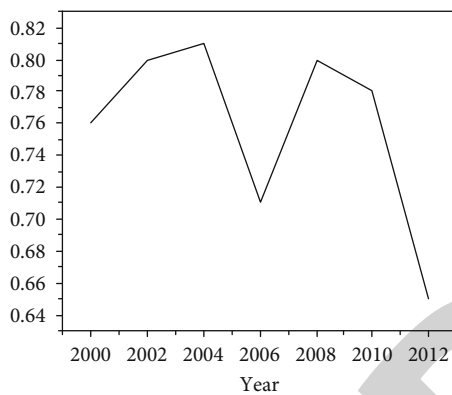


FIGURE 5: Interannual variation of NDVI-Max in growing season.

type of slight improvement is NDVI-Max in the growing season.

The average annual increase is 0.0038 (confidence is 98.0%), and the average annual increase rate is 0.49%. The average annual reduction rate of NDVI-Max in the growth season of significant degradation type is 0.0103 (confidence 99.9%), and the annual average reduction rate is 1.35%. The average annual reduction rate of NDVI-Max in the growth season of slight degradation type is 0.0036 (confidence 99.9%), and the annual average reduction rate is 0.45%.

Make statistics on the changes of the average value of NDVI-Max in the growing season from 2000 to 2012 in the whole Xi'an area, and draw a broken line diagram of the changes. As shown in Figure 5, it can be seen that the overall vegetation coverage in Xi'an is good, and the NDVI changes above 0.76. According to the change trend of NDVI, the vegetation cover change in the past 13 years can be divided into two periods: the fluctuation and rise period from 2000 to 2009 and fluctuation decline period from 2009 to 2012. The reasons for this change also need to be studied in combination with various data.

5. Conclusion

This paper uses ENVI5.3, ArcGIS10.0, and other related software, based on the high-resolution remote sensing image data

of Xi'an, taking Dadukou area as an example, through the splicing, cutting, and extracting green space information of remote sensing images. In a series of steps, the production of thematic map of urban green space landscape types was completed, and the database of urban green space system was established. On this basis, the spatial structure of green space landscape in Dadukou area is analyzed by using statistical analysis software such as Patch Analyst, GS+9.0, and SPSS, mainly from the aspects of urban green space landscape patch composition, urban green space landscape patch scale grade, urban green space landscape patch fragmentation, urban green space landscape overall index, urban green space landscape spatial heterogeneity, and so on. At the same time, based on the MODIS NDVI data of Xi'an, this paper studies the vegetation cover change and distribution pattern in this area from 2000 to 2012. The conclusions are as follows:

- (1) The landscape types of green space in Dadukou area of Xi'an are mainly divided into 9 types: urban park, community park, protective green space, residential green space, public construction green space, road green space, scenic and recreational green space, river green space, and other ecological green space. Through the calculation of the number of various green space types, the number of various green space landscape patches, the area of various green space landscape, the maximum patch index, and other indexes, the composition analysis of green space landscape patches is realized. The results show that the total area of green space in Dadukou area of Xi'an is 219.35 hectares, with a total of 2565 patches, and the overall green space coverage rate of this area reaches 38.3%. Among all types of green space, public construction green space and residential green space account for the absolute advantage in the total area of green space, and the corresponding number of patches is also the largest. The area of road green space is the least, but the number of patches is large, which is mainly due to the fact that there are many intersections on the road and the green space is mostly distributed on both sides of the road, so it is difficult to form continuous green patches. The number of protective green space patches is the least, but the area is large,

mainly because the protective green space is mostly distributed in flakes and the patch area is large. According to the analysis results of the maximum patch index of different green space landscape types, it can be concluded that the maximum patch index of other green spaces is the maximum, indicating that the green space type is uneven in area distribution

- (2) Through the analysis of the scale level of green landscape patches, it is found that the green patches in Dadukou area of Xi'an are mainly small patches, which are scattered. Small patches (area <math>< 0.1 \text{ hm}^2</math>) are mainly residential green space and public construction green space; medium patches (- (3) The results show that the fragmentation degree of road green space is the most serious, while the fragmentation degree of protective green space is the lowest. At the same time, it also verified the relationship between the evaluation patch area, patch density, and the degree of green space fragmentation; that is, the larger the average patch area, the smaller the patch density, and the lower the degree of green space fragmentation

Data Availability

The data used to support the findings of this study are available from the corresponding author upon request.

Conflicts of Interest

The authors declare that they have no conflicts of interest.

References

- [1] J. Jin, S. R. Sheppard, B. Jia, and C. Wang, "Planning to practice: impacts of large-scale and rapid urban afforestation on greenspace patterns in the Beijing plain area," *Forests*, vol. 12, no. 3, p. 316, 2021.
- [2] H. Dang, J. Li, Y. Zhang, and Z. Zhou, "Evaluation of the equity and regional management of some urban green space ecosystem services: a case study of main urban area of Xi'an city," *Forests*, vol. 12, no. 7, p. 813, 2021.
- [3] S. Heo, A. Nori-Sarma, S. Kim, J. T. Lee, and M. L. Bell, "Do persons with low socioeconomic status have less access to greenspace? Application of accessibility index to urban parks in Seoul, South Korea," *Environmental Research Letters*, vol. 16, no. 8, p. 084027, 2021.
- [4] F. Salamone, B. Barozzi, L. Danza, M. Ghellere, and I. Meroni, "Correlation between indoor environmental data and biometric parameters for the impact assessment of a living wall in a ZEB lab," *Sensors*, vol. 20, no. 9, p. 2523, 2020.
- [5] S. Liu, X. Zhang, Y. Feng, H. Xie, and Z. Lei, "Spatiotemporal dynamics of urban green space influenced by rapid urbanization and land use policies in Shanghai," *Forests*, vol. 12, no. 4, p. 476, 2021.
- [6] P. Cheng, M. Min, W. Hu, and A. Zhang, "A framework for fairness evaluation and improvement of urban green space: a case of Wuhan metropolitan area in China," *Forests*, vol. 12, no. 7, p. 890, 2021.
- [7] F. Li, R. Wang, S. Lu, M. Shao, J. Ding, and Q. Sun, "Spatiotemporal simulation of green space by considering socioeconomic impacts based on A SD-CA model," *Forests*, vol. 12, no. 2, p. 202, 2021.
- [8] S. Dinda, N. D. Chatterjee, and S. Ghosh, "An integrated simulation approach to the assessment of urban growth pattern and loss in urban green space in Kolkata, India: a GIS-based analysis," *Ecological Indicators*, vol. 121, no. 2021, pp. 1–22, 2021.
- [9] Y. Zhang, T. Zhang, Y. Zeng, C. Yu, and S. Zheng, "The rising and heterogeneous demand for urban green space by Chinese urban residents: evidence from Beijing," *Journal of Cleaner Production*, vol. 313, no. 3, p. 127781, 2021.
- [10] Y. Sun, X. Wang, J. Zhu, L. Chen, and J. Wu, "Using machine learning to examine street green space types at a high spatial resolution: application in Los Angeles county on socioeconomic disparities in exposure," *Science of the Total Environment*, vol. 787, no. 7, p. 147653, 2021.
- [11] P. Kowe, O. Mutanga, and T. Dube, "Advancements in the remote sensing of landscape pattern of urban green spaces and vegetation fragmentation," *International Journal of Remote Sensing*, vol. 42, no. 10, pp. 3797–3832, 2021.
- [12] Y. Yao, S. Zhang, Y. Shi, M. Xu, and J. Zhao, "Landscape pattern change of impervious surfaces and its driving forces in Shanghai during 1965–2010," *Water*, vol. 13, no. 14, p. 1956, 2021.
- [13] C. C. Nicholson and N. M. Williams, "Cropland heterogeneity drives frequency and intensity of pesticide use," *Environmental Research Letters*, vol. 16, no. 7, p. 074008, 2021.
- [14] R. Wang, J. H. Kim, and M. H. Li, "Predicting stream water quality under different urban development pattern scenarios with an interpretable machine learning approach," *Science of the Total Environment*, vol. 761, no. 4, p. 144057, 2020.
- [15] Z. Zhu, B. Liu, H. Wang, and M. Hu, "Analysis of the spatio-temporal changes in watershed landscape pattern and its influencing factors in rapidly urbanizing areas using satellite data," *Remote Sensing*, vol. 13, no. 6, p. 1168, 2021.
- [16] C. Liu, F. Zhang, V. C. Johnson, P. Duan, and H. T. Kung, "Spatio-temporal variation of oasis landscape pattern in arid area: human or natural driving?," *Ecological Indicators*, vol. 125, no. 1, p. 107495, 2021.
- [17] C. Zhu, X. Zhang, M. Zhou, S. He, and K. Wang, "Impacts of urbanization and landscape pattern on habitat quality using OLS and GWR models in Hangzhou, China," *Ecological Indicators*, vol. 117, no. 3, p. 106654, 2020.
- [18] S. Wang, Y. Zhao, Z. Xu, G. Yang, and N. Ma, "Landscape pattern and economic factors' effect on prediction accuracy of cellular automata-Markov chain model on county scale," *Open Geosciences*, vol. 12, no. 1, pp. 626–636, 2020.
- [19] J. Zhang and H. Shen, "Geo-spatial analysis and optimization strategy of park green space landscape pattern of garden city—a case study of the central district of Mianyang city Sichuan province," *European Journal of Remote Sensing*, vol. 53, no. 1, pp. 309–315, 2020.
- [20] Y. Liu, X. Cao, and T. Li, "Influence of accessibility on land use and landscape pattern based on mapping knowledge domains: review and implications," *Journal of Advanced Transportation*, vol. 2020, no. 3, Article ID 7985719, p. 12, 2020.

Retraction

Retracted: PKPM Architectural Engineering Software System Based on Architectural BIM Technology

Journal of Sensors

Received 17 October 2023; Accepted 17 October 2023; Published 18 October 2023

Copyright © 2023 Journal of Sensors. This is an open access article distributed under the Creative Commons Attribution License, which permits unrestricted use, distribution, and reproduction in any medium, provided the original work is properly cited.

This article has been retracted by Hindawi following an investigation undertaken by the publisher [1]. This investigation has uncovered evidence of one or more of the following indicators of systematic manipulation of the publication process:

- (1) Discrepancies in scope
- (2) Discrepancies in the description of the research reported
- (3) Discrepancies between the availability of data and the research described
- (4) Inappropriate citations
- (5) Incoherent, meaningless and/or irrelevant content included in the article
- (6) Peer-review manipulation

The presence of these indicators undermines our confidence in the integrity of the article's content and we cannot, therefore, vouch for its reliability. Please note that this notice is intended solely to alert readers that the content of this article is unreliable. We have not investigated whether authors were aware of or involved in the systematic manipulation of the publication process.

Wiley and Hindawi regrets that the usual quality checks did not identify these issues before publication and have since put additional measures in place to safeguard research integrity.

We wish to credit our own Research Integrity and Research Publishing teams and anonymous and named external researchers and research integrity experts for contributing to this investigation.

The corresponding author, as the representative of all authors, has been given the opportunity to register their agreement or disagreement to this retraction. We have kept a record of any response received.

References

- [1] Y. Fu, "PKPM Architectural Engineering Software System Based on Architectural BIM Technology," *Journal of Sensors*, vol. 2022, Article ID 5382026, 7 pages, 2022.

Research Article

PKPM Architectural Engineering Software System Based on Architectural BIM Technology

Ying Fu 

Jiangxi Engineering Vocational College, Nanchang, Jiangxi 330025, China

Correspondence should be addressed to Ying Fu; 1411410728@st.usst.edu.cn

Received 24 May 2022; Revised 2 June 2022; Accepted 22 June 2022; Published 4 July 2022

Academic Editor: C. Venkatesan

Copyright © 2022 Ying Fu. This is an open access article distributed under the Creative Commons Attribution License, which permits unrestricted use, distribution, and reproduction in any medium, provided the original work is properly cited.

In order to solve the problems in practical application of Building Information Modeling (BIM) as an innovative tool and production method, the author proposes a method for simulating modern buildings using the Ecotect software. This method establishes a digital BIM parametric model, the digital information technology is directly applied to the whole life cycle of the construction project, and then the effectiveness of the method is verified by examples. The result obtained is as follows: The authors' method is designed with the assumption that Construct III is below the standard limit throughout the year, in order to meet the requirements of energy-saving design; it is recommended to change the type of external window in the engineering design scheme and make the energy consumption of buildings meet the requirements of energy-saving standards. The method proposed by the author saves about 20% of the construction cost compared with the traditional method. It is proved that the author's method can make architectural designers correctly understand the feasibility and applicability of the Ecotect software in building energy conservation and promote BIM technology and software; BIM technology can be widely used in engineering projects, allowing architects to select the right and suitable software for various energy conservation simulations and build energy-saving building solutions.

1. Introduction

Energy is the pillar and driving force of the country's economic development related to community security, traditional employment, national security, sustainable development of ecological environment, and the survival and continuity of future generations [1, 2]. As science and technology improve, communities and businesses around the world develop rapidly, and demand for energy increases.

According to statistics, global electricity demand is growing by two percent annually. This example estimates global demand for electricity, and by the middle of the 21st century, global electricity consumption will be four times the total electricity consumption when the battery life of the 1970s. Since the oil crisis, global energy shortages have made commodity prices heavier, and more and more countries are estimating greater energy savings and consumption [3, 4]. The concept of sustainable development is a viable

answer to environmental and energy issues in the 21st century human development strategy [5]. The concept of the idea of sustainable development is recognized by every country of the world, the problem of energy scarcity should not be ignored, and energy conservation has become a long-term goal of national development [6].

BIM (building information model, for example, building information) technology has been used in the construction industry in many countries around the world according to information releases. New and advanced BIM technology has proven to save development time and reduce construction costs. Rates reach different levels [7, 8]. Developing countries in Europe and the United States have developed and developed BIM research centers. In the future, our country will follow the promotion and use of information of construction companies and make the introduction of new technologies in engineering, such as data center design (BIM).

2. Literature Review

Since the beginning of the global catastrophe in the 1970s, power generation has been gaining traction, and more and more scientists are studying it to reduce energy consumption at home and achieve some achievements [9, 10]. Since the inception of BIM technology, BIM heat wave has appeared in the development of the world, and the use of BIM technology in every cycle of home life has been popular. And scientists have begun to study the use of BIM technology in construction. In energy conservation abroad, BIM research covers the entire life cycle of a home, and the study of energy conservation in the home often includes the following.

Ahmed et al. divide sustainable development into manageable components: Air quality, biodiversity, solid waste, wastewater, etc. In order to solve the problems arising from these parts, this study examines the utilization of drinking water and wastewater according to the requirements of sustainable systems, uses BIM to carry out overall parametric settings such as equipment, systems, and materials to control drinking water, and applies BIM to modeling of urban water use; simulation calculation can utilize wastewater and rainwater collection, design rate roof, calculate water runoff, etc. [11]. Moghadasi et al. explored the interoperability of BIM with the environmental simulation software [12]. Ma et al. used BIM for energy analysis in the conceptual design stage of construction projects and used BIM technology to build a model of a community emergency service station, the model was used to explore the early effects of different building envelopes and components on building design [13]. Nageib et al. used EnergyPlus and virtual environment software IES, respectively, to build the same model to compare their effectiveness and suitability as a BIM-based energy simulation tool [14]. For the further development of the research, the researchers especially focus on the energy consumption caused by different building orientations and window areas and finally summarize how to use BIM-based building energy analysis effectively.

The research time of BIM technology in my country is still short, and it is mostly used in the architectural design stage. In order to achieve building energy conservation, many researchers are actively exploring the application of BIM technology in building energy conservation-related fields. At present, many architectural design and research departments have applied Ecotect's calculation results to practice and research [15].

Billah et al. proposed a method for applying BIM technology to building energy conservation and constructed a building energy conservation work framework based on BIM technology [16]. Bazazzadeh et al., on the basis of analyzing the software requirements of building energy-saving design, carried out the detailed functional design of the building energy-saving design software system, and the system development was carried out [17]. According to Luo and Oyedele, based on the current situation and existing problems of building energy-saving design, this paper introduces the development ideas and key technologies of building energy-saving software based on BIM technology [18]. Chen et al. used the energy consumption results of Ecotect to judge the pros and cons of the inclination angle of the

external windows of the building and finally analyzed the optimal energy-saving angle of the windows to guide the installation of windows in practical buildings [19].

On the basis of the current research, this research is aimed at comprehensively applying BIM technology, using the Ecotect Analysis software to establish an energy consumption simulation information model in the design stage, and conducting energy consumption simulation analysis for a residential building in a certain place. In order to determine how BIM technology has been used in construction compared to the current power generation process in our country, the differences in power consumption analysis of participants, software, process analysis, and electronic data analysis were compared. There are advantages and disadvantages of energy-saving analysis of construction plans compared to conventional electrical inspection procedures.

3. Research Methods

3.1. Application of BIM Technology in PKPM Construction Engineering Software System. BIM or Building Information Technology is made up of three-dimensional digital technology, and the design data engineering that includes information related to the design is digital information on behalf of appropriate documents.

BIM is a product that the whole team works on, and as shown in Figure 1, it can be used by different participants at different angles at each stage to improve performance, quality, and data sharing of all participants. Therefore, the purpose of BIM is to complete the integration of data from various parts of the construction industry, to improve the speed of reuse of data construction, thus reducing construction costs and improving productivity.

All standardized data files for PKPM civil engineering software systems are developed by combining modeling templates, one model for each job, and one model with multiple counts. The design data is all three-dimensional, object-oriented, and parametric, and it is very easy to modify, query, make changes to objects, and modify the view in real time. From simple 3D data modeling, PKPM integrates design ideas, product design, building design, quantity engineering, cost reporting, garden management building, and other links to the construction and implementation of the BIM concept. It is now possible to combine data files, data structures, and design and then apply building materials to the entire life cycle.

Special applications are as follows.

- (1) Three-dimensional housing planning and design software in PKPM can be used for preliminary survey of areas in planning, design, urban planning, design, urban assessment, and planning. 3D modeling technology to ensure the performance of 3D modeling, reconstruction, process and site design, modeling, document design, green space design, counting of materials design, solar analysis, and design of real-life observational models, using experts. The software introduces various technologies such as 3D modeling technology, ground technology, design technology modeling data, index dynamic control technology,

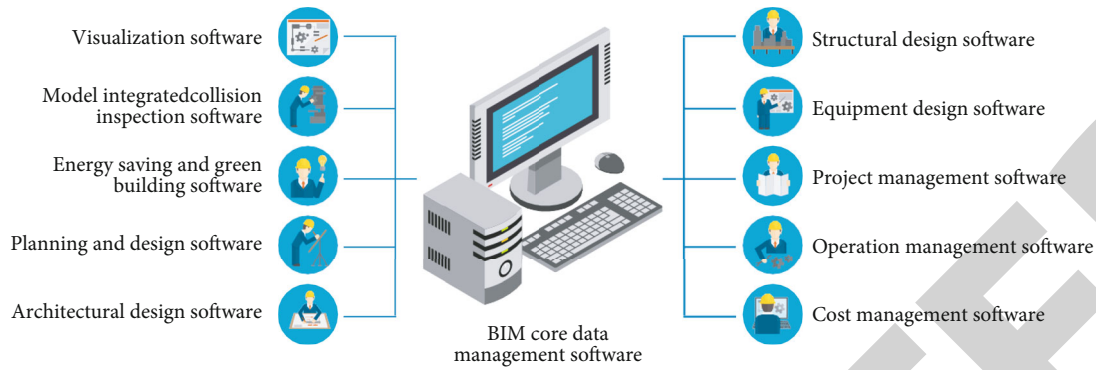


FIGURE 1: Architecture of Building Information Modeling (BIM).

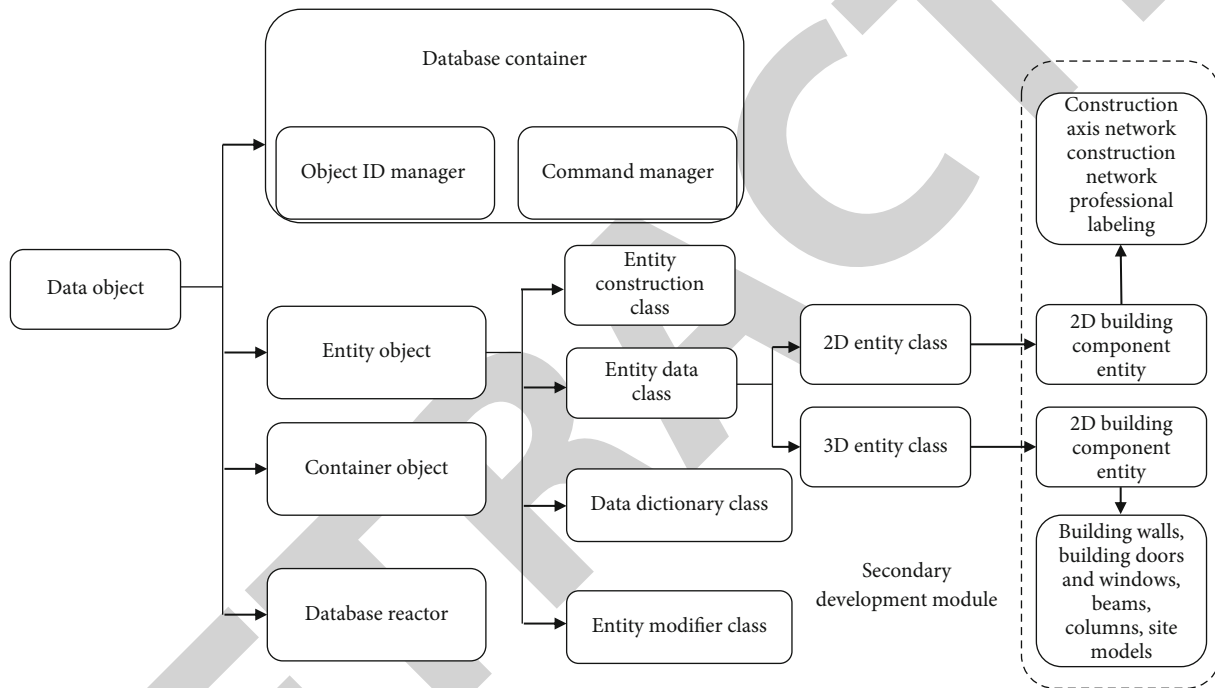


FIGURE 2: Architecture of PKPM 3D graphics platform.

counting, reverse, dynamic shadow simulation technology output, and current image capture and provides design data with good control and sensitivity. 3D photos affect the screen

- (2) PKPM Architectural design software APM is a software architecture based on BIM technology, which starts from the design concept to create simple documentation of the building design, and all the functions are based on simple information. The base file just creates a variety of drawings of the house
- (3) The building information model of the PKPM architectural design link can be reused in the cost (estimated budget) analysis link. The building information model entered in the design process contains the basic information of the building, which is also the concern of the cost engineer. Therefore, the reuse of the building information model can greatly save the workload of the cost

engineer. Of course, this information is not complete and needs to be further supplemented. Based on the architectural structure design model, the PKPM budget software supplements the information required for the budget, such as supplementing the decoration practices of each room and exterior wall, selecting the quota library, and entering the scaffolding information. The program automatically extracts the corresponding quota or list code, completes the calculation of the engineering quantity and reinforcement quantity of each floor and each component, carries out the quantity analysis, and generates various forms and data required by the cost engineer

- (4) CFG, an independent copyright graphic platform that PKPM has long relied on, is mature and stable, various professional software of PKPM have been developed on it, and it has a large user base. Scholars have conducted comprehensive and in-

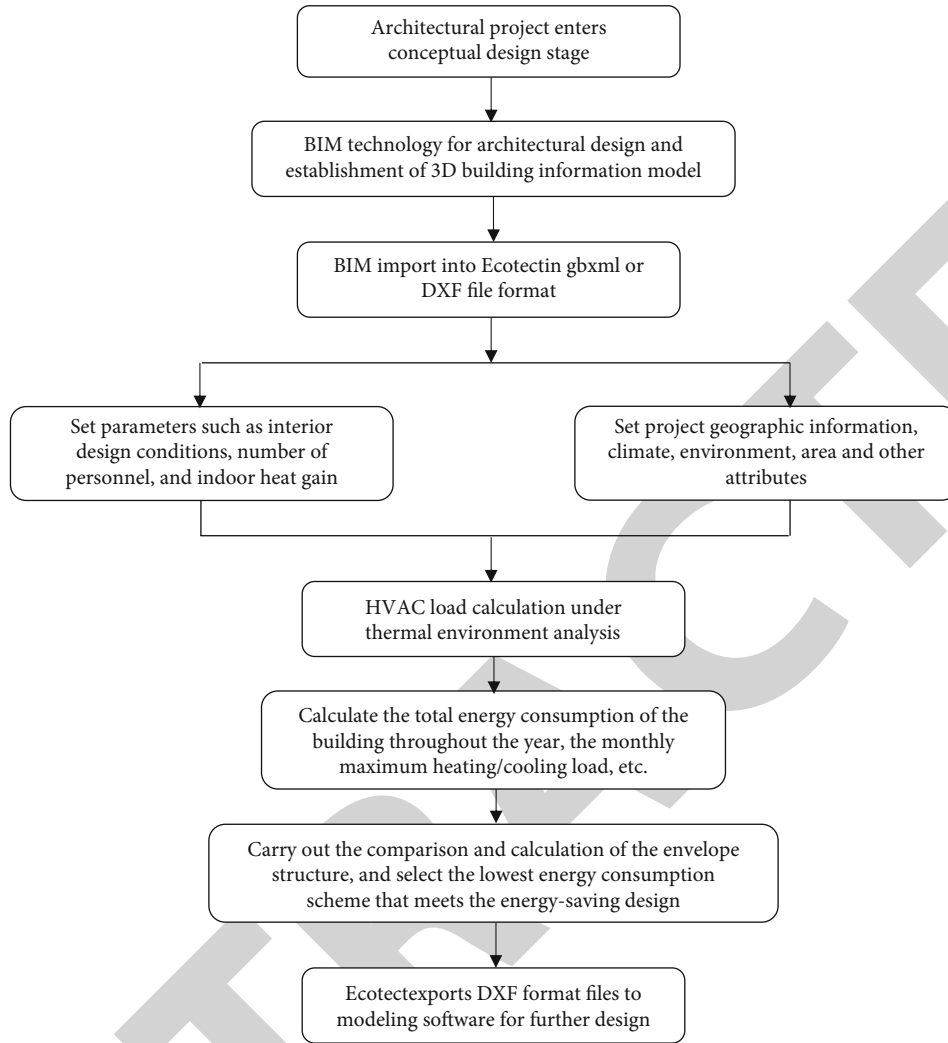


FIGURE 3: BIM technology energy consumption simulation analysis process.

depth research on PKPM in the field of 3D graphics platform and have established a mature system architecture as shown in Figure 2, in object-oriented technology, 3D geometric modeling core system, graphics display technology, parallel computing technology, graphics interaction technology, 3D entity, professional entity modeling technology and related data management, software interactive interface, 3D scene realistic rendering technology, path animation, and key frame animation technology, and other aspects have deep technical accumulation

3.2. Simulation Analysis of Energy Consumption of BIM Technology. BIM technology examines and calculates the electrical applications of the construction, which is a small part of the use of BIM technology throughout the life of the home, and the equipment used to analyze review by the Ecotect Analysis software. Unlike conventional electronic simulation analysis, BIM technology is involved in the entire project life cycle by design phase design, while BIM technology utilizes design software such as Revit Archi-

TABLE 1: Heat transfer coefficient of the building envelope.

	Exterior wall, W/m ² K	Roof, W/m ² K	Exterior window, W/m ² K
Design structure (I)	0.793	0.58	2.665
Standard limit (II)	0.8	0.6	2.5
Hypothetical construction (III)	0.793	0.58	2.5

ecture and Revit during the design phase. Its visual design allows owners to use design ideas by interacting with designers to create 3D data models and to design concepts simultaneously, such as designing and creating project directly into the virtual model, which can be more efficient as the owner needs. Thanks to BIM software integration, gbXML or DXF files can be exported from the Revit Architecture model software at the end of the schematic design phase and imported directly into Ecotect software for various physical models or create a model with the same data files directly from the Ecotect software as a 3D data model and then identify it as stable. The procedure for using

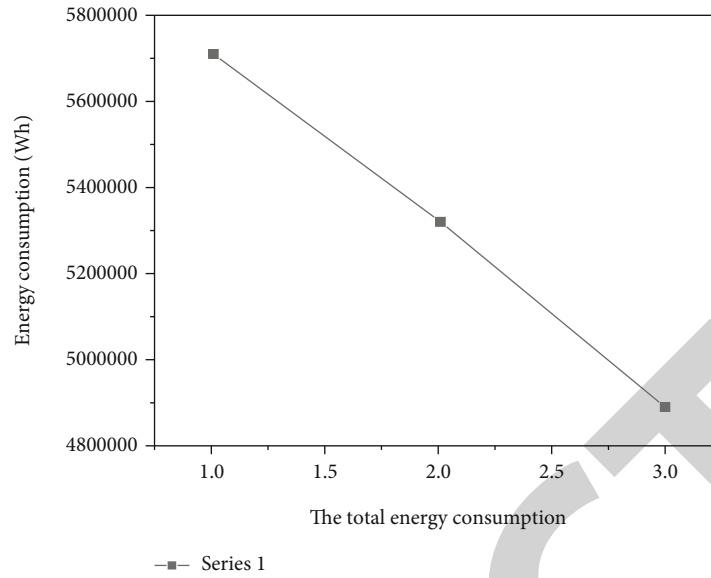


FIGURE 4: Annual total energy consumption.

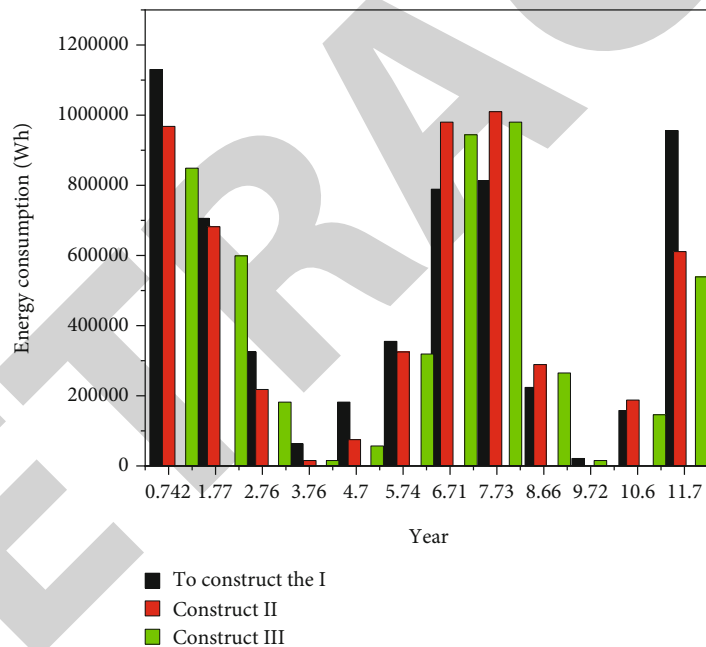


FIGURE 5: Comparison of monthly energy consumption under three structural conditions.

electronic analysis using the Ecotect software to model the electricity is shown in Figure 3.

4. Analysis of Results

4.1. *An Example of Energy Consumption Analysis of Residential Buildings Based on BIM Technology.* The project covers an area of more than 1,800 mu, with a total construction area of 327,158 square meters, a total development volume of more than 1.5 million square meters, a plot ratio of only 1.93, and a green space ratio of 31.23%; after completion, it will have a population of nearly 50,000 people and is currently the largest pure residential project in the area.

The author selects the D9 villa in this residential group as an example to conduct energy simulation analysis; the fire protection height of D9# building is 33 m, with the underground garage floor, the negative floor, and eleven floors above ground, which belongs to the second-class high-rise residential [20]. The outer walls of all enclosures designed in this project are made of 200 mm-thick B5.0 autoclaved aerated concrete blocks. The roof is made of reinforced concrete with a thickness of 20 cm for thermal insulation, 20 mml : 2 cement mortar : 13 mm air layer.

The heat transfer coefficient of engineering design is compared with the limitations specified in “energy save design standard for homes” and is provided in Table 1.

The instructions show that the roof and exterior walls are lower than the maximum height of the structure compared to the thermal conductivity required by the design, which meets the requirements of energy conservation standards. Because the exterior window does not follow the rules of the energy-design model, energy consumption simulation analysis is done to determine the building energy consumption according to the model. In order to create more energy-efficient building materials, Hypothetical Building II is designed to reduce the thermal conductivity of exterior walls, roofs, and exterior windows to a minimum large model [21]. The monthly energy consumption analysis is calculated in turn from cases I to II, and the simulation results are analyzed using Excel charts, as shown in Figures 4 and 5 [22].

As can be seen from Figure 5, the design structure I is not much different from the energy-saving standard limit. However, if the heat transfer coefficient of the external window is reduced to the standard value, the total energy consumption for the whole year is much smaller than that of the design structure [23]. The energy consumption of design structure I in winter is greater than that of standard structure II, and the energy consumption of design structure I is less than that of II in summer. Construct III is assumed to be below the standard limit throughout the year, meeting the energy-efficient design requirements. It is recommended that the engineering design scheme change the type of exterior windows and make the energy consumption of buildings meet the requirements of energy-saving standards [24].

5. Conclusion

Rapid urban growth, increased demand for energy, and energy conservation are future improvements. As BIM technology is developed and promoted in China, BIM has been increasingly used throughout the life of the construction industry, and the role of BIM technology in home design is the importance increases. Designers have used Ecotect to assist with home design because of its versatility, simplicity, design, and seamless integration with SketchUp, CAD, Revit, and more other software. The author compares the usual power simulation techniques with power metrics using BIM technology output models and analyzes the differences. It helps users to understand the differences between the Ecotect software and other electronic simulation analysis software, as well as the differences between participants and processes in the monitoring process. The main conclusions of the author's research are as follows: When the BIM software can be used directly to identify applications using BIM technology to help create building plans, it is very easy to plan, design, and modify the schematics of the software. Its three-dimensional design can be used directly to show the construction of the site, and CAD-format architectural drawings can be directly drawn from the model. Because BIM technology is used to simulate and analyze power consumption in construction, the home data created in BIM software can be used for Ecotect software power simulation, shading system analysis, etc. The performance of the physical environment is used not only in the design phase but also

for various accompanying activities during the construction, operation, and maintenance phase. For example, for construction simulation, collision detection, project planning, etc., the model can also guide construction on site and compare the corresponding degree of project entities and BIM data in real time. The simulation results of Ecotect have a limited scope of use in auxiliary architectural design, and its basic calculation method is not suitable for large changes in the outdoor environment; there are also some errors in the calculation of solar radiation and heat storage, but it is feasible to use Ecotect to judge the pros and cons of building shading system.

Data Availability

The data used to support the findings of this study are available from the corresponding author upon request.

Conflicts of Interest

The author declares no conflicts of interest.

Acknowledgments

This article was financially supported by (1) the Research on Informatization Application Mode of Construction Project Based on BIM Technology (No. gjj205701) of the Science and Technology Project of Jiangxi Provincial Department of Education and (2) the Teaching Reform Project of Jiangxi Provincial Department of Education, "Research on BIM Applied Talent Training Mode in Higher Vocational Education Based on CDIO education concept" (No. jxjg-20-75-3).

References

- [1] X. He, "Research on evaluation of building industrialization level based on bim technology," in *E3S Web of Conferences*, p. 03056, Hangzhou City in China, 2021.
- [2] D. Liu, X. Xia, J. Chen, and S. Li, "Integrating building information model and augmented reality for drone-based building inspection," *Journal of Computing in Civil Engineering*, vol. 35, no. 2, article 04020073, 2021.
- [3] L. H. Yang, L. Xu, W. C. Wang, and S. H. Wang, "Building information model and optimization algorithms for supporting campus facility maintenance management: a case study of maintaining water dispensers," *KSCE Journal of Civil Engineering*, vol. 25, no. 1, pp. 1–16, 2020.
- [4] H. Zheng, X. Zhong, J. Yan, L. Zhao, and X. Wang, "A thermal performance detection method for building envelope based on 3D model generated by UAV thermal imagery," *Energies*, vol. 13, no. 24, p. 6677, 2020.
- [5] L. Kong and B. Ma, "Intelligent manufacturing model of construction industry based on internet of things technology," *The International Journal of Advanced Manufacturing Technology*, vol. 107, no. 3-4, pp. 1025–1037, 2020.
- [6] B. Yang, B. Liu, D. Zhu, B. Zhang, and K. Lei, "Semiautomatic structural BIM-model generation methodology using cad construction drawings," *Journal of Computing in Civil Engineering*, vol. 34, no. 3, p. 04020006, 2020.
- [7] B. Yang, T. Fang, X. Luo, B. Liu, and M. Dong, "A BIM-based approach to automated prefabricated building construction

Retraction

Retracted: Intelligent Campus Resource Sharing System Based on Data Fusion Sensor

Journal of Sensors

Received 12 December 2023; Accepted 12 December 2023; Published 13 December 2023

Copyright © 2023 Journal of Sensors. This is an open access article distributed under the Creative Commons Attribution License, which permits unrestricted use, distribution, and reproduction in any medium, provided the original work is properly cited.

This article has been retracted by Hindawi, as publisher, following an investigation undertaken by the publisher [1]. This investigation has uncovered evidence of systematic manipulation of the publication and peer-review process. We cannot, therefore, vouch for the reliability or integrity of this article.

Please note that this notice is intended solely to alert readers that the peer-review process of this article has been compromised.

Wiley and Hindawi regret that the usual quality checks did not identify these issues before publication and have since put additional measures in place to safeguard research integrity.

We wish to credit our Research Integrity and Research Publishing teams and anonymous and named external researchers and research integrity experts for contributing to this investigation.

The corresponding author, as the representative of all authors, has been given the opportunity to register their agreement or disagreement to this retraction. We have kept a record of any response received.

References

- [1] G. Huang, "Intelligent Campus Resource Sharing System Based on Data Fusion Sensor," *Journal of Sensors*, vol. 2022, Article ID 4814727, 7 pages, 2022.

Research Article

Intelligent Campus Resource Sharing System Based on Data Fusion Sensor

Guangshun Huang 

School of Computer Science, Huainan Normal University, Huainan, Anhui 232038, China

Correspondence should be addressed to Guangshun Huang; 201772497@yangtzeu.edu.cn

Received 18 May 2022; Revised 1 June 2022; Accepted 21 June 2022; Published 4 July 2022

Academic Editor: C. Venkatesan

Copyright © 2022 Guangshun Huang. This is an open access article distributed under the Creative Commons Attribution License, which permits unrestricted use, distribution, and reproduction in any medium, provided the original work is properly cited.

In order to make full use of the large amount of teaching data existing in the data center, the author proposes a mining algorithm using classification technology and association rules in data mining technology; the teaching quality evaluation data and student achievement data were mined. By constructing the C4.5 decision tree algorithm, this method taps the potential links between teachers' professional titles, degrees, ages, and teaching quality evaluation results, through correlation analysis theory; the correlation between professional courses was mined from the student's course achievement database, and some reasonable and reliable course association rules were obtained. Experimental results show that the correct rate of C4.5 decision tree algorithm under different sampling times is above 80%. The conclusions drawn have certain guiding significance for college teaching and personnel training.

1. Introduction

As the foundation of a country's development and innovation, education and scientific research is receiving more and more attention from the whole society. With the continuous progress of information technology, integrating new information technology into the information construction of campus, it not only disseminates advanced educational and scientific research achievements but also improves educational achievements and accelerates the scientific process.

The so-called smart campus is in order to improve the utilization rate of school resources, a campus management method that applies the campus card in the smart campus to access control management, public housing use, and links with scientific research teams [1]. The use of intelligent and informatized campus management can more effectively obtain campus information, campus information sharing, and services and realize an integrated and all-round intelligent corresponding system. It is convenient for the students and the management of the school. First of all, the smart campus can provide teachers and students with a fast and convenient information service platform and can formulate some services based on teachers and students, leaving some space for teachers and students to

play freely [2]. Secondly, the information services relying on cloud computing and the network are integrated into various fields to achieve the purpose of information sharing and, furthermore, from the perspective of information sharing, provide a comprehensive information service platform for the teachers and students of the school to connect and communicate with the outside world. Smart campus is an advanced stage of education informatization; information technology has greatly improved the service level and ability of teaching, scientific research, management, service, and other fields and has unique advantages [3]. At present, the construction of smart campuses in my country is being stepped up, and many educational institutions and campuses are participating in the wave of smart campus construction.

2. Literature Review

In the "Twelfth Five-Year Plan", Zhejiang University constructively put forward a blueprint for a "smart campus," which depicts ubiquitous online learning, convenient and thoughtful campus life, transparent and efficient school governance, integration of innovative online scientific research, and colorful campus culture. The construction of

Nanjing University of Posts and Telecommunications on the “smart campus” is based on the Internet of Things, with various application service systems as the carrier to build a new intelligent work, study, and living environment that integrates teaching, scientific research, management, and campus life. It is believed that “smart campus” should have three core characteristics: (1) provide teachers and students with a full range of intelligent perception environment and comprehensive information service platform, and provide personalized services; (2) integrate network-based information services into various applications and service areas of the campus to achieve interconnection and collaboration; (3) using the intelligent perception of the environment and the comprehensive information service platform, provide an interface for communication and perception between the school and the outside world.

With the evolution of ubiquitous computing, some smart campus prototypes have been developed. For example, Booker and Jabbour proposed that a smart card can be used in the campus to access the services in the campus [4]. Li et al. proposed the ETHOC system, which uses various devices such as mobile phones or PADs to make the system itself support virtual peers with printed documents [5]. Dargan et al. proposed that a “smart campus” should have the following levels: first, sensors can sense, capture, and transmit information about equipment, people, resources, etc.; the second is the perception, capture, and transmission of learners’ individual characteristics such as learning preferences, attention states, learning styles, cognitive characteristics, and learning situations such as learning time, activities, space, and partners [6].

With the advancement of digital campus construction in colleges and universities, application systems of various functions are constantly being built. In order to solve the current situation of the information island between various application systems in the school, in the first phase of digital campus construction, a shared data center was established to realize data sharing and synchronization between various systems [7]. At present, data centers have accumulated rich business data and have grown rapidly. There is a lot of important information hidden behind the proliferating data; if there is no means to discover the relationships and rules existing in the data, it is impossible to predict the future development trend based on the existing data, which will inevitably lead to “data explosion but poor knowledge” phenomenon. How to effectively manage and organize these data and convert data into knowledge to assist university administrators in making the next decision, this is an urgent problem to be solved; it is also how to further analyze and mine the data of various business information systems after the completion of the digital campus, so as to provide decision support for teaching management.

Data mining technology provides a good solution for this [8]. Data mining is to extract from a large number of incomplete, noisy, fuzzy, and random practical application data, which is hidden in it and people do not know in advance, but it is also a process of potentially useful information and knowledge as shown in Figure 1 for the data security management framework [9]. The application of data

mining in digital campus is undoubtedly of practical significance. It will become the trend of college informatization.

3. Research Methods

3.1. Overall Framework of Shared Data Center. Data plays a very important role in the normal development of college teaching. In order to improve the daily office efficiency of the school, various departments have successively built their own information systems. However, information is managed independently, and there is no data interconnection and data sharing, a university officially started the construction of a digital campus in November 2018, and the construction of the shared data center platform began in the first phase of the digital campus. After three years of construction, the function of the shared data center has become more and more complete, and the amount of data has become more and more complete; based on the three main lines of integration of teacher information, student information and asset information, data integration, and information sharing are realized.

All data in the data center has a unique data source; taking teacher information as an example, the source of its generation is the personnel management system; in order to ensure the consistency of the data, other systems have blocked the authority to modify the basic information of teachers; the data center will regularly extract the changed faculty and staff information from the personnel management system and push it to other application systems to achieve data sharing and synchronization. Similarly, the source of student information is the educational administration system, only the educational administration system can maintain student information, and other systems use student information and cannot maintain student information.

The shared data center stores the shared data extracted from various application systems, such as the basic information of personnel extracted from the personnel management system, the teaching workload information, student performance data, teaching evaluation data extracted from the educational administration system, and the thesis results, patents, and reward information extracted from the scientific research system. These data are currently only simple summary and statistics without further analysis and utilization of the data. In view of this, we have selected teachers and students as the theme and discuss the in-depth application of data mining technology in shared data centers.

3.2. Application of Classification Technology in Teaching Quality Evaluation and Analysis. Online evaluation of the teaching quality of teachers is an important means of teaching quality monitoring. At present, the system has accumulated a large amount of evaluation data and uses classification algorithms to construct decision trees [10], it can excavate the relationship between teachers’ educational background, professional title, age and other attributes, and evaluation results and apply the research results to practice to provide more help for teaching managers.

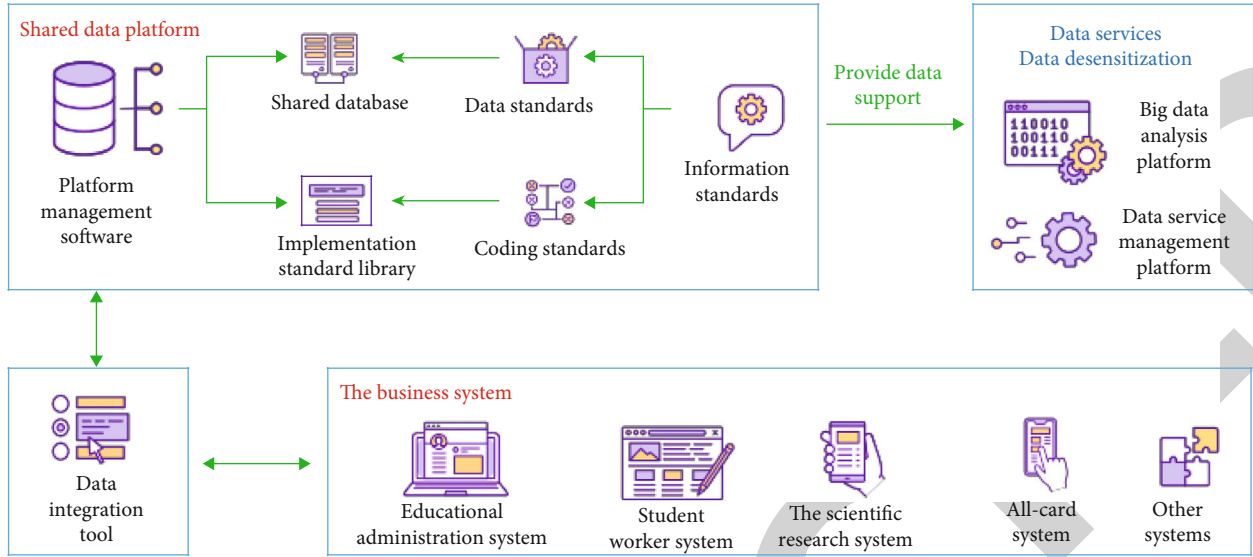


FIGURE 1: Data security management framework.

3.2.1. Overview of Decision Tree Algorithm. Decision tree is an instance-based inductive learning algorithm; it infers classification rules in a decision tree representation from a set of unordered, random tuples [11]. A decision tree consists of three parts: nodes, branches, and leaves; nodes represent attributes, leaf nodes represent categories, and the topmost node of the tree is the root node, a path from the root node to the leaf node forms a classification rule, which is widely used. At present, a variety of decision tree algorithms have been formed, such as CLS, ID3, CHAID, CART, FACT, C4.5, GINI, SEE5, SLIQ, and SPRINT [12]. One of the most famous algorithms is the ID3 algorithm proposed by J.R. Quinlan in the “Induction of Decision Trees” paper in 1986 and the improved C4.5 algorithm in 1993. The C4.5 algorithm is an improved version of the ID3 algorithm; it uses the gain ratio to overcome the insufficiency of selecting attributes with many values when selecting attributes with information gain; during the tree construction process or after the construction is completed, pruning is performed; the discrete processing of continuous attributes can be completed, able to handle incomplete data, and can eventually form production rules [13, 14].

Figure 2 shows a simple decision tree classification model.

3.2.2. Data Acquisition and Preprocessing. This application research mainly analyzes the relationship between teachers’ basic situation and evaluation results and establishes an excellent teacher model, so that schools can have an exact basis for teacher incentives. The research process uses data from two aspects: the basic situation of teachers and the results of teaching evaluation in the second semester of the 2019-2020 school year; the data structure is shown in Tables 1 and 2.

3.2.3. Teaching Quality Evaluation Model Based on C4.5 Decision Tree. Assume that the training dataset contains m

categories, namely, $T = \{t_1, t_2, \dots, t_m\}$. An attribute in the training dataset may have a total of k values of (a_1, a_2, \dots, a_k) , according to the attribute is divided into $T' = \{t'_1, t'_2, \dots, t'_r\}$; other properties are similar to property A. According to the training set, the information of its ideal division can be obtained as follows (1) [15].

$$H(T) = - \sum_{i=1}^m p(t_i) \log_2 p(t_i). \quad (1)$$

Among them, $p(t_i) = |t_i| / \sum_{i=1}^m |t_i|$.

The information entropy obtained by dividing the training set by attributes is as follows (2) [16].

$$\begin{aligned} H_A(T') &= \sum_{i=1}^r p(t'_i) H(t'_i) = - \sum_{i=1}^r \sum_{j=1}^m p(t'_i) p(t_j | t'_i) \log_2 p(t_j | t'_i) \\ &= H(T | T'). \end{aligned} \quad (2)$$

Among them, $p(t'_i) = |t'_i| / \sum_{i=1}^r |t'_i|$; $p(t_j | t'_i) = |t'_i \cap t_j| / |t'_i|$. $p(t_j | t'_i)$ represents the probability that samples belonging to t'_i in partition T' belong to subset t_j in an ideal partition [17]. It can be obtained that the information gain of attribute A for the division of the training set is the following.

$$H_{\text{Gain}}(T') = H(T) - H_A(T'). \quad (3)$$

The segmentation information entropy of attribute A is the following.

$$H(T') = - \sum_{i=1}^m p(t'_i) \log_2 p(t'_i). \quad (4)$$

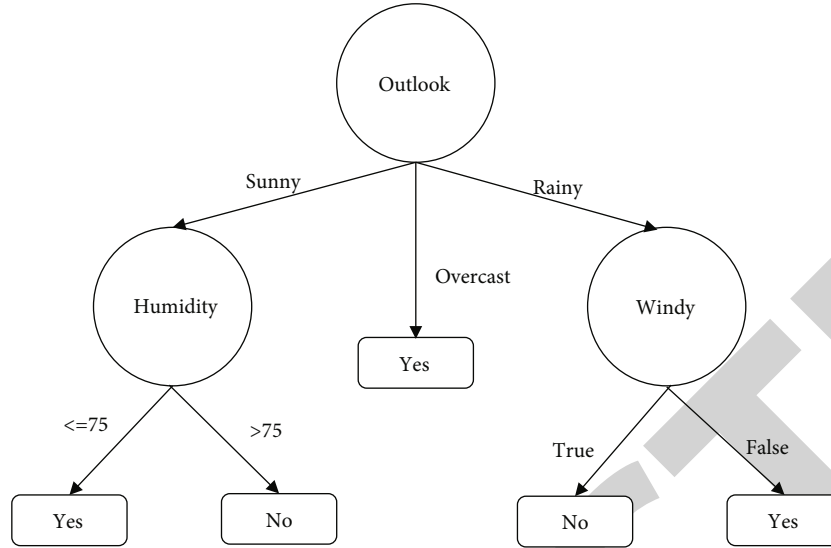


FIGURE 2: Simple decision tree model.

TABLE 1: Basic information of teachers.

Employee number	Gender	Age	Education	Job title	Part
100033	Woman	39	Postgraduate	Associate professor	Business school
100047	Man	48	Postgraduate	Professor	IT academy
100056	Man	41	Undergraduate	Associate professor	Law school
100105	Man	46	PhD student	Professor	Law school
100111	Woman	35	Postgraduate	Lecturer	School of humanities
100116	Woman	48	Undergraduate	Associate professor	School of education
100105	Man	46	PhD student	Associate professor	School of geography
...

TABLE 2: Evaluation results of teachers' classroom teaching quality.

Employee number	School year	Semester	Evaluation of teachers/%	Evaluation level
100033	2019~2020	1	93.864	Excellent
100047	2019~2020	1	94.278	Excellent
100056	2019~2020	1	89.656	Good
100105	2019~2020	1	78.754	Middle
100111	2019~2020	1	89.235	Good
...

From Equations (3) and (4), the information gain rate of attribute A can be expressed as the following.

$$\text{Ratio}(T') = \frac{H_{\text{Gain}}(T')}{H(T')} = \frac{H(T) - H_A(T')}{H(T')}. \quad (5)$$

Similarly, the information gain rate of other attributes can be calculated. By calculating the information gain rate of all attributes, the attribute with the largest information gain rate value is selected as the root node of the decision tree [18]. Then, determine the nodes of each layer of the decision tree

in the same way, and the calculation method is the same as the above steps.

Select the C4.5 decision tree algorithm provided by TipDM data mining platform of Taipu Company, mining 3000 pieces of teaching quality evaluation data in the first semester of the 2019-2020 school year, and extracting some classification rules [19, 20].

Rule 1: IF degree = master student AND professional title = associate professor AND age ≤ 50 , THEN teaching evaluation is "excellent" ratio of 86.3%.

Rule 2: IF academic background = undergraduate AND professional title = associate professor AND age > 37 , THEN proportion of the teaching evaluation is "excellent" which is 79.6%.

Rule 3: IF academic background = doctoral student AND professional title = associate professor AND age ≤ 40 , THEN proportion of teaching evaluation is "excellent" which is 95.6%.

3.2.4. Interpretation and Practical Application of the Rules. From the extracted classification rule 3, it can be seen that the young- and middle-aged teachers with the title of associate professor and doctoral degree are the backbone of the teaching staff. This part of the team should be enriched to

TABLE 3: Original student grade transaction database.

Student ID	C language	Data structure	Database application	Software engineering	Microcomputer principle	Operating system	Introduction to computers	Network principle
0921014101	92	90	79	81	72	88	74	89
0921014102	86	73	66	88	85	75	80	97
0921014103	80	85	86	90	78	79	81	85
0921014104	84	80	79	87	74	81	69	85
0921014105	85	85	74	68	83	87	80	77
0921014106	77	75	80	85	69	85	87	68
...

TABLE 4: Transaction database of student grades after processing.

Student ID	C language	Data structure	Database application	Software engineering	Microcomputer principle	Operating system	Introduction to computers	Network principle
0921014101	K1A	K2A	K3B	K4A	K5B	K6A	K7B	K8A
0921014102	K1A	K2B	K3B	K4A	K5A	K6B	K7B	K8A
0921014103	K1A	K2A	K3A	K4A	K5B	K6B	K7A	K8A
0921014104	K1A	K2A	K3B	K4A	K5B	K6A	K7B	K8A
0921014105	K1A	K2A	K3B	K4B	K5A	K6A	K7A	K8B
0921014106	K1B	K2B	K3A	K4A	K5B	K6A	K7A	K8B
...

the front line of teaching and play a leading and exemplary role in the teaching team; teachers under the age of 50 with the title of associate professor and a master's degree due to the rich teaching experience, the teaching experience, and ability of young teachers can be improved through their help, transmission, and introduction. In the introduction of talents, we mainly focus on highly educated, high professional titles and young doctors to improve the level of the entire teaching staff.

3.3. Application of Association Rules in Student Score Data Analysis. Student achievement is the basis for evaluating the quality of teaching, and it is also an important sign to test whether students have mastered the knowledge they have learned in school, by applying association rule mining technology to a large amount of student achievement data; interesting connections between these data can be found. For example, in the curriculum system, a certain precourse course is excellent, and its follow-up courses are excellent, and the proportion of excellent is also high. For example, students with excellent performance in discrete mathematics have a higher proportion of students with excellent performance in data structure; under the credit system, students can choose courses according to these rules and provide guidance for the revision of the existing curriculum system.

Association analysis is a mining method for discovering hidden relationships between data [21]. In a large database, many similar rules can be analyzed without screening, in order to remove useless association rules, two thresholds are generally set: support and confidence. Support is an

important measure. If the support is very low, it means that this rule only appears by chance, which is basically meaningless [22]. Therefore, support is often used to remove those meaningless rules. Confidence is the reliability of reasoning through rules. The user can define two thresholds, requiring that the support and confidence of the rules mined by the mining system are not less than the given thresholds.

4. Results Analysis

4.1. Data Acquisition and Preprocessing. Now, based on the student achievement data of the shared data center, we select the professional course achievement database of 250 software engineering students from the School of Computer Science, some data are shown in Table 3, each record in the table represents a transaction, the student number attribute can be regarded as an ID number, and the content of the following fields can represent the item set of the transaction, that is, the grades of a certain professional course. The table actually contains a large number of "attribute-value" pairs, such as "C language-85." Curriculum correlation analysis is to study the relationship between multiple "attribute-value" pairs that frequently appear together.

As shown in Table 3, there are very few "attribute-values" in the table that are exactly the same, and if you mine it directly as an item, you will not get the desired result. After the discretization of grades and course coding, the obtained student grade transaction database is shown in Table 4.

The course names are coded with K1, K2, ..., for example, the coding of "C language" is K1, the code of the "data

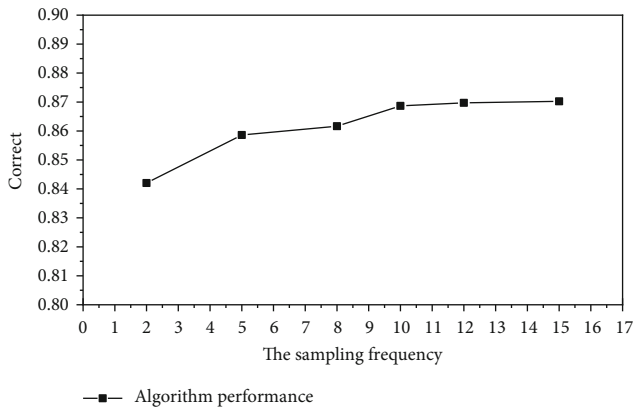


FIGURE 3: Algorithm performance under different sampling times.

structure” is K2; at the same time, the grade data is transformed into three grade data, namely, A: corresponding score 80-100; B: corresponding score 60-79; C: corresponding score 0-59.

Figure 3 shows the accuracy of the dataset at different sampling times. With the increase of sampling times, the correct rate of the algorithm increases, and the correct rate under all sampling times is above 80%, when the sampling times increase to a certain value, the performance of the algorithm also tends to be stable [23, 24]. It can be seen from the figure that when the sampling times are 12 and 15, the difference in algorithm performance is very small, so 12 is selected as the final sampling times.

4.2. Correlation Analysis of Students’ Course Grades. After data preprocessing, the data can be considered to be pure; on this dataset, the classical Apriori algorithm is used to perform association rule analysis on the data, the support degree is set to 0.2, the confidence degree is 0.6, and the maximum number of itemsets is 3, and some association rules are mined [25].

Discrete mathematics by rules, “excellent” → data structure, and “excellent” confidence = 61%, we can find that students who score above 80 in Discrete Mathematics are 61% more likely to score above 80 in “Data Structure.” We can strengthen the teaching of “discrete mathematics” to improve the teaching effect of “data structure”; designed by regular assembly language programming, “excellent” → microcomputer principle and interface technology, and “excellent” confidence = 61%, we can find that students with a score of 80 or more in “Assembly Language Programming,” “microcomputer principle and interface technology” is also 61% likely to score above 80 points; similarly, we can also strengthen the teaching of “Assembly Language Programming” class, in order to improve the teaching effect of “Microcomputer Principle and Interface Technology” course.

5. Conclusion

Based on the shared data center, the application of data mining technology in educational informatization is discussed. Two topics of teaching quality evaluation analysis

and students’ course performance correlation analysis are selected, and decision tree algorithm and association rule mining algorithm are, respectively, applied, which are implemented on two datasets, and some reasonable and effective rules are obtained. According to the analysis results of teaching quality evaluation, it can provide a certain reference for schools in the training, assessment, and talent introduction of teachers. Of course, teachers’ teaching methods, instruments, behaviors, students’ own qualities, and other factors will also affect students’ evaluation of teachers. Through the correlation analysis of students’ performance, it is found that there are correlations between courses of the same major, such as the sequence of courses, the connection of content, and the professional weight of courses. It can provide in-depth analysis of curriculum settings for teaching departments, provide reference for the overall curriculum settings of schools, and provide guidance for students to choose courses under the full credit system. Of course, the applications in the above two directions are just some simple applications of data mining technology in the digital campus system. How to make full use of college resources, it is a practical problem facing colleges and universities to better combine data mining technology and digital campus. The follow-up work will continue to select some topics, such as classification labels to measure the scientific research ability level of teaching and research personnel, cluster analysis, objective and effective description of the current situation of teachers, association rules technical description of teaching, scientific research and social work, and other aspects. Relationship, etc., discusses the in-depth application of data mining technology in digital campus.

Data Availability

The data used to support the findings of this study are available from the corresponding author upon request.

Conflicts of Interest

The author declares that there are no conflicts of interest.

Acknowledgments

This work was supported by the school level scientific research projects of Huainan Normal University: research on enrollment, training, employment and social linkage mechanism based on big data (project no.: 2020xjyb021).

References

- [1] C. T. Yang, S. T. Chen, J. C. Liu, R. H. Liu, and C. L. Chang, “On construction of an energy monitoring service using big data technology for the smart campus,” *Cluster Computing*, vol. 23, no. 1, pp. 265–288, 2020.
- [2] S. D. Nagowah, H. B. Sta, and B. Gobin-Rahimbux, “A systematic literature review on semantic models for iot-enabled smart campus,” *Applied Ontology*, vol. 16, no. 3, pp. 27–53, 2020.
- [3] H. Moayedi, M. M. Abdullahi, H. Nguyen, and A. Rashid, “Comparison of dragonfly algorithm and Harris hawks

Retraction

Retracted: Information Steganography Technology of Optical Communication Sensor Network Based on Virtual Reality Technology

Journal of Sensors

Received 12 December 2023; Accepted 12 December 2023; Published 13 December 2023

Copyright © 2023 Journal of Sensors. This is an open access article distributed under the Creative Commons Attribution License, which permits unrestricted use, distribution, and reproduction in any medium, provided the original work is properly cited.

This article has been retracted by Hindawi, as publisher, following an investigation undertaken by the publisher [1]. This investigation has uncovered evidence of systematic manipulation of the publication and peer-review process. We cannot, therefore, vouch for the reliability or integrity of this article.

Please note that this notice is intended solely to alert readers that the peer-review process of this article has been compromised.

Wiley and Hindawi regret that the usual quality checks did not identify these issues before publication and have since put additional measures in place to safeguard research integrity.

We wish to credit our Research Integrity and Research Publishing teams and anonymous and named external researchers and research integrity experts for contributing to this investigation.

The corresponding author, as the representative of all authors, has been given the opportunity to register their agreement or disagreement to this retraction. We have kept a record of any response received.

References

- [1] Z. Wang, W. Li, and G. Wang, "Information Steganography Technology of Optical Communication Sensor Network Based on Virtual Reality Technology," *Journal of Sensors*, vol. 2022, Article ID 4827306, 7 pages, 2022.

Research Article

Information Steganography Technology of Optical Communication Sensor Network Based on Virtual Reality Technology

ZhongBao Wang ¹, WenMing Li ², and GuoQing Wang ³

¹College of Electronics and Communication Engineering, JiLin Technology College of Electric Information, JiLin 132021, China

²Information Center, State Grid Qinghai Electric Company, Xining, Qinghai 810000, China

³Technology Development Department, State Grid Qinghai Electric Company, Xining, Qinghai 810000, China

Correspondence should be addressed to ZhongBao Wang; b20160503212@stu.ccsu.edu.cn

Received 21 May 2022; Revised 9 June 2022; Accepted 20 June 2022; Published 4 July 2022

Academic Editor: C. Venkatesan

Copyright © 2022 ZhongBao Wang et al. This is an open access article distributed under the Creative Commons Attribution License, which permits unrestricted use, distribution, and reproduction in any medium, provided the original work is properly cited.

In order to solve the problems of narrow object orientation and insufficient visual rendering ability of the optical communication network experimental system, the author proposes a multithreaded scheduling using virtual reality, and the experimental system design method of optical communication network with multichannel serial port design is proposed. The system builds the overall structure model of the optical communication network experimental system in the virtual reality environment, and uses the PCI bus technology to build the transmission channel model of the optical communication network, the basic entity object of the optical communication network experimental system is constructed, and the multithread scheduling method is used to process the local information of the experimental system. The result obtained is as follows: The experimental system of optical communication network designed by the author's method, the optical communication transmission bit error rate is reduced by about 30%, the time overhead is saved by about 60%, and the memory overhead is saved by about 50%, which is superior. Using the author's method, the maximum bit error rate is about 22%, while the maximum bit error rate of traditional method 1 is about 43%, and the maximum bit error rate of traditional method 2 is about 70%. It is proven that the visual simulation effect of the optical communication network experimental system is good, the reliability and stability of the optical communication network are improved, and the communication transmission error is reduced.

1. Introduction

With the development of computer data and graphics devices and the creation of 3D images for various events in virtual reality (VR), screens have the ability to create 3D images and simulations that include virtual reality analysis and interpretation. The phenomenon process was known [1]. Virtual reality technology is an important branch of visual and visual technology, and software development using virtual reality technology will be an integral part of the application environment, such as software design, network communication, and image editing.

Optical communication network technology is the transmission and storage of real-time communication data, and

with the development of optical devices on this platform, it is possible to convert data extensions into packets and red optics and store them in the cloud. Network connections, data storage, and optical communication network connections are prone to external access and theft, leading to data loss and damage. Ensuring the security of customer information [2, 3], therefore, it is necessary to create a secure network protocol that combines the integrity of communication when storing and sending large amounts of communication data to the network using the cloud platform [4].

Because optical data aggregation has a simple structure, optical data aggregation is based on communication, interconnection technology, and the most commonly used digital

experience. Optical data networks are used in an integrated manner to create steganographic data structures that are vulnerable to theft. Software attacks and steganographic performance are poor [5]. Optical network data steganography technology uses only a combination of chaotic encryption, DCT transmission, DNA processing, and know-how of optical network data steganography [6]. The study of optical communication information steganography technology is important to ensure the security of optical communication network and optical communication network, and the study of steganographic technology is of great interest as shown in Figure 1.

2. Literature Review

Optical communication network testing is a network system for modeling communications and communication environments and uses virtual reality technology to create optical communication. The equipment is used to design an experimental platform, which improves the visual performance of optical communication network tests, and the research experimental design process has received considerable attention [7, 8].

Currently, the design of optical communication test system is mainly using external design and remote control functions, and the system receives a single connection. Multi-hop communication is used to describe the application of the whole system, but the visualization and objective-oriented analysis of the communication experimental system is not good. [9]. It is necessary to use three-dimensional virtual reality technology to develop experimental models of optical communication network, and to know about remote access and queries in a network in a virtual reality visual simulation; in doing this, based on design ideas, experimental analysis, and design, some studies have been completed [10, 11]. Among them, Abdul, W. has devised an optical communication network testing method development based on CCD photoelectric parameter testing, which provides a full-duplex communication mechanism in the process of cross-regional optical communication channel transmission, research, and development of optical. Communication network testing is based on CCS2.20 development platform, and test system has high performance reliability; however, the reliability of this method is not high, and interference channel size and the material-orientedness of the optical simulation are negative [12]. Zhu, J. has prepared data transfer and scheduling data model of optical communication test based on PCI bus technology, as a driver design and software development program sell communication network test, and completed a variety of platform communication network developed by the load and network connection; the product-orientedness of the test system is improved, but the portability of the system is not zog [13, 14]. Martins. The overhead of this steganography method is large, and the automatic steganography performance of the optical communication data is poor [15]. Li, J. has developed a data steganography method based on interconnection, using Oracle random selection mechanism for hybrid encryption of optical communication network.

Combined with the semantic security protocol, the risk of deciphered is reduced to zero, and the data steganography of the communication network is known; however, this method has the risk of malfunction to prevent plaintext attack and poor performance of optical communication network data steganography [16, 17].

Based on the current study, the author describes an optical connection test model based on a multichannel serial port model. PCI bus technology and multistream scheduling method are used to generate experimental local data to develop a complete model structure of the optical communication network test system and to develop the transmission channel structure of the optical communication network, and in the implementation of virtual reality phenomenon communication models, multichannel serial ports and host computer communication models, user/design, system software experience, and optical communication network test system development at MATLAB and VC ++ platforms, the test results showed its advantages.

3. Research Methods

3.1. Rendering Process of Virtual Reality Model of Optical Communication Experimental System. To understand the design of an optical communication network that follows virtual reality technology, it is first necessary to observe the process of displaying the virtual reality of optical communication based on an optical communication instruction loop. According to the display list stored in the optical communication experimental system rendering cycle instructions, the information proxy service function of Web-APP browser (Browser), Web-CULI server, and Web-draw Editor (editor) is used to load the program. Optical communication experimental system information data from the control device are read. The current viewpoint and communication transmission information of the experimental system virtual reality simulation are calculated. The state information and rendering instructions of the scene are judged within the current view range, and polygon data is drawn to judge the scene model elements. During the phase of destruction of the graphical characteristic data of the exhibition, a virtual reality model of the optical communication test system was made, and the diagram is shown in Figure 2 [18, 19].

In Figure 2, the angular static viewing point of the optical communication head test system is set as a logical and hierarchical image imaging database, the angular visibility is the same, and the model is sent based on the optical communication information simulation package, and the virtual reality simulation. When the position of the animation model changes, the moving model automatically generates an impression, resulting in a real-time 3D image [20].

When calculating the relative distance visibility of a body motion simulation, the vision automatically moves in the same direction as the body movement and involves three types of interactions and development of a relatively remote static point of view for flow optical communication channels and communication systems [21].

Due to the differences between starting point management and the line of sight, 3D visual simulation is used to manage

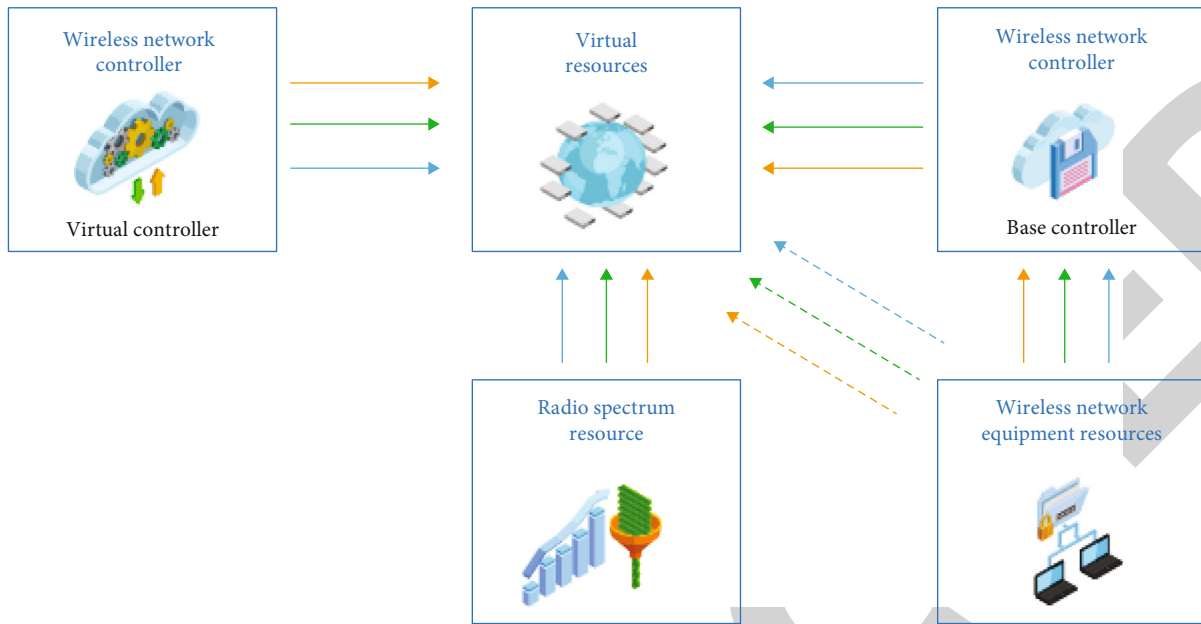


FIGURE 1: Optical communication network of virtual reality technology.

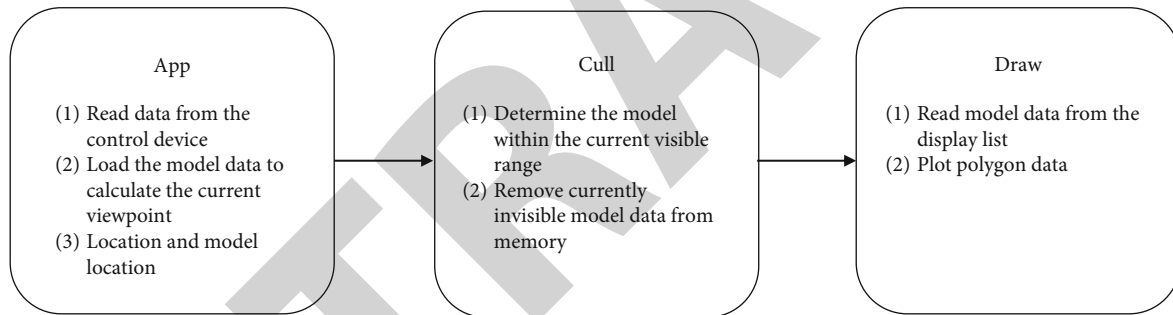


FIGURE 2: The rendering process of the virtual reality model of the optical communication experimental system.

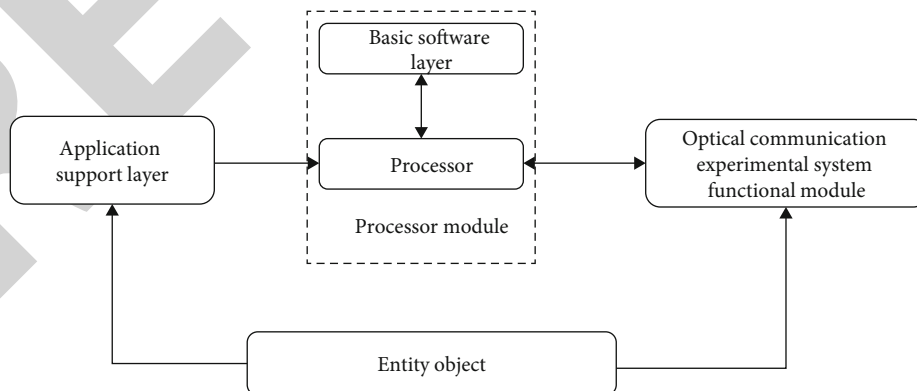


FIGURE 3: Entity object model of the optical communication network experimental system.

Lab-Windows/CVI through high-level integration through multiple filters and filtering processes, and the Android kernel environment is designed to work and to develop a virtual reality model of an optical communication test system [22, 23].

3.2. *Transmission Channel Model of Optical Communication Network.* Based on the above explanation, the optical communication test virtual reality model was developed using the PCI bus technology, and the received optical

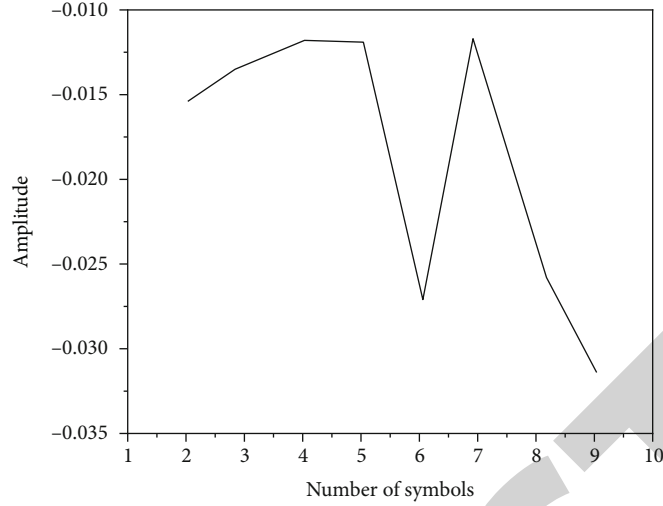


FIGURE 4: Symbol sampling value and partial enlarged view of communication.

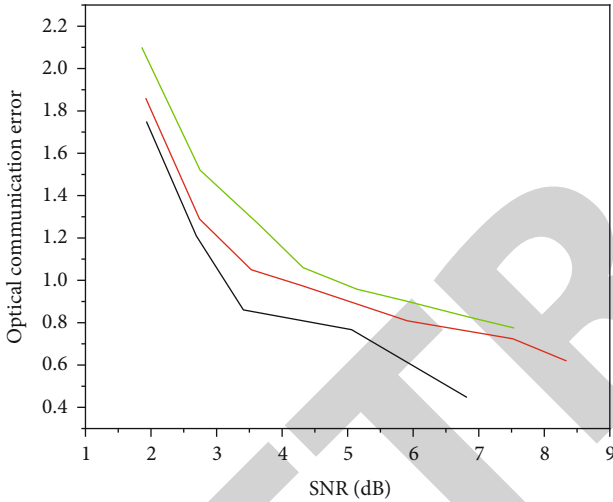


FIGURE 5: Comparison of the bit error rate of the communication experimental system.

TABLE 1: Comparison of time overhead and memory overhead.

Method	Time cost/s	Memory overhead/Gbit
The method of this paper	2.10	0.87
Traditional method 1	6.98	2.33
Traditional method 2	12.87	4.76

communication channel model was developed. According to the EAPSD, the communication mechanism is defined as:

$$Z^k = \bar{w}^k A^T = \sum_{j=1}^n \bar{w}_j^k \cdot a_{ij} (i = 1, \dots, m). \quad (1)$$

Among them, the transmission channel in the bus communication control is the number of nodes of the optical communication channel and the routing matrix of the node

information source. To determine the maximum transmission error in the node and communication group, the transmission speed of the optical communication is based on

$$\rho_{\text{cluster}} = \frac{\sum_{i=1}^L \rho_{\text{lane}-i}}{L} + c_1 \otimes c_2, \quad (2)$$

where if c_1 and c_2 are relatively prime, and the space-time weighting on the communication transmission channel in the cluster is introduced, the impulse response of the optical communication signal transmission is obtained as:

$$R_{cc} \sim (\tau_1, \tau_2, \alpha) = R_{cc} \sim (\tau_1, \alpha) \delta(\tau_1 - \tau_2). \quad (3)$$

A three-dimensional database is constructed to carry out the statistics of the information characteristics of the optical communication network experimental system, and the auto-correlation function recorded by the output master node of the communication network in the WSSUS channel can be expressed as:

$$\text{Time} = \text{abs}[|z(k)|^2 - R_{\text{MDMMA}}(k)] = \min_i \text{abs}[|z(k)|^2 - R_{\text{MDMMA},i}]. \quad (4)$$

The transmission signal A_i of the communication system is obtained through adaptive line spectrum enhancement; the perceived data class Token, based on virtual reality technology, obtains the same frequency interference signal [24].

Calculate the carrier frequency of the transmission channel controlled by the optical communication network bus; at the system application support layer, the estimated time delay of the sink node of the optical communication network experimental system is:

$$\rho(k) = \frac{\beta}{1 + \exp(-\alpha|\hat{e}(k)|)}, \quad (5)$$

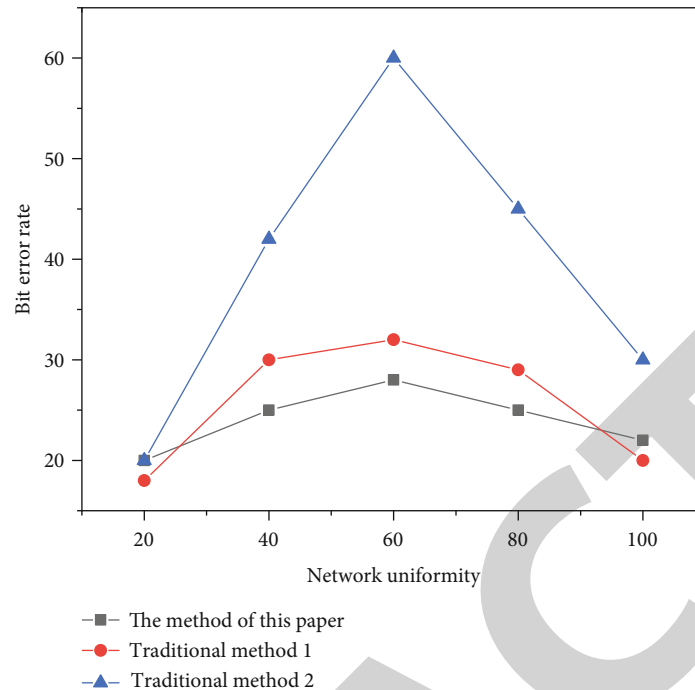


FIGURE 6: Comparative analysis of bit error rates of different methods.

Optical network experimental network application support design was developed for the application development layer and the software layer using the light communication layer to convert the static reality visual image of the optical communication network test. The overall design and construction of the system can be constructed. In virtual reality visual simulation, the smooth transition method of static view point is used to construct the network adaptation layer of optical communication network experimental system. The optical communication network experimental system access service, network generation service will be completed [25].

3.3. Entity Object Design of Optical Communication Network Experimental System. Based on the above virtual reality model rendering and channel model design of optical communication experimental system, the basic entity object of optical communication network experimental system is constructed and the experimental system is improved. This paper presents an experimental system design method of optical communication network based on multi-thread scheduling and multi-channel serial port design. Optical communication network test process is model based on multistream schedule and multipoint model. The components of an optical network test system typically include software support processes, a simple software layer, an application installation layer, an application service layer, and a change layer.

Among them, the use of layer process support includes testing of various midlevel optical communication networks, and intermediate equipment is the basis for public interconnection. The eye network testing platform provides maximum software and flexibility and ease of movement. In the middle of the network, the software provides full access to

the test operation of the optical communication network. The intermediate configuration program completes various configurations of the optical communication network test system, such as routing configuration and topology switches. Intermediate operations complete a wide range of optical network test services that provide interoperability for a variety of virtual monitors. Based on the above observations, design a test product for the optical network as shown in Figure 3.

Figure 3 shows the main test points of the optical network, the virtual reality environment, and the optical network test model equipment. In the virtual reality environment, the entity object of the node model of optical communication network experiment system completes the operation, collection, and storage of network communication nodes. In the above analysis, hierarchical models are used to create a network connection test model, and multiple distributors are used to record the test site and to control the top and face arrangements of the material. Designed a communication test system that allows you to plan the recording process data on a large number of communication lines, obtain a 3D/2D static logic hierarchical database, and complete the optical communication network test product design product.

The OpenFlight hierarchical view generates hierarchical property units with OpenFlight to explain the basic data level (head phase) model ID in a virtual reality environment, the three-dimensional product model of the optical network test system, and the network definition. The control and data are adjusted using the node characteristic data control and closure method, and the completion of the section determines the geometric properties and the location and size of the 3D image model.

3.4. Software Development of the System. Based on the physical design of the virtual reality simulation of the optical communication network test system, the local data processing and optical communication driver configuration are performed using the multiframe scheduling method. The network test system records data during the network-connected API interface on the VISA software interface and configures the external information of each functional subapplication with virtual reality programming.

The ADV656 multimedia schedule software has a built-in CONVST module and a TCPComm class that connects to the client and user/user, creates a virtual reality communication model, and generates the program boot code in the installed Linux kernel environment.

The system receives the serial connection, interprets the communication equipment through the optical communication network test equipment, C code, and performs the multichannel serial port and host computer experience. The system communication design is based on the CCS2.20 development platform, software development knowledge, optical communication network testing, open source and system optical network testing (SystemReg) logs on multiple platforms through open source and ioctl using software, Lynx Prime graphical interface visual simulation system, call acf data design, Configure Lynx Prime, and .acf and system simulation iteration software through a graphical interface and develops an optical network test system.

4. Analysis of Results

4.1. System Performance Test. Simulation tests have been completed to measure optical communication network testing based on the virtual reality technology developed by the author, to improve the quality of optical communication, and to improve product guidance. Attempts to install software on the optical communication network on MATLAB and VC ++ platforms were successful. In the experiment, OpenGL's App (use) and Cull (interrupt) information in the Vega Prime phenomenon are used to retrieve information transmitted by the optical communication channel, and the system automatically dials the number without requiring termination using the PlaySound function for unreliable connections. Converting data using full-screen analysis to mimic the input and output state of large-scale optical communications, the MAC layer process uses the IEEE 802.11 standard, informs the technical use of the interface, and declares content and events. The alarm in the interface, in the main module of the component, directly calls the function declared by the command in the interface, connects to the web server in real time, and connects to the host computer. In this setting, the signal-to-noise ratio of the optical communication system is -12 dB~0 dB, the optical communication sales efficiency is 0-50 m/sec, and the optical communication sample speed is 10 times higher than the carrier frequency. The bandwidth cut-off frequency is 5 kHz. According to the above set of simulation parameters, it is possible to perform a test simulation of an optical communication network test system, first, to make a standard transmission in the communication system and to make a

sample value of the symbol and image part as shown in Figure 4.

Following the above model example for the test equipment and optical network transmission test, Figure 5 shows the optical communication network using the author's method and the usual style, and the results of the bit error comparison are shown in Figure 5.

Comparison of system response time and memory overhead of optical communication network experiments using different methods is shown in Table 1.

The analysis of the above results shows that the optical communication network test developed by the author's method has the advantages of low optical connection error, low time, and low memory load.

4.2. Comparative Analysis of Bit Error Rates of Different Steganography Techniques. To determine the steganographic performance of the author's method, the author's method is compared with standard steganographic techniques used to detect minor errors in optical communication networks. The results of data steganography and analysis can be seen in Figure 6

As shown in Figure 6, in the same situation, the difference between the previous and subsequent errors decreases slightly as the network connection increases. Of these, the maximum bit error rate using the author's method is approximately 22%. The maximum bit error rate of standard 1 is approximately 43%, and the maximum bit error rate of standard 2 is approximately 70%. This shows that the authoring method has more performance and some advantages than the process in the file.

5. Conclusion

The author develops optical communication network experiments in virtual reality and proposes the design of optical communication network experiments based on multistream schedules and other port designs. The overall structure model of optical communication network experiment system is constructed, and the transmission channel model of optical communication network is constructed by PCI bus technology. The basic entity object of optical communication network experimental system is constructed, and the local information processing of the experimental system is carried out by using multithread scheduling method. The virtual reality visual communication transmission model is constructed by client or server model, and the communication design of multichannel serial port and upper computer is carried out. Installation of optical connection test system software on MATLAB and VC ++ platforms is considered. The conclusion is as follows:

- (1) The experimental system of optical communication network designed by this method has the advantages of low optical communication transmission error rate, low time, and memory cost
- (2) In a similar situation, as network integration increases, small errors are observed with the difference between the increase before and after the

Retraction

Retracted: Active Vibration Control of Robot Gear System Based on Adaptive Control Algorithm

Journal of Sensors

Received 17 October 2023; Accepted 17 October 2023; Published 18 October 2023

Copyright © 2023 Journal of Sensors. This is an open access article distributed under the Creative Commons Attribution License, which permits unrestricted use, distribution, and reproduction in any medium, provided the original work is properly cited.

This article has been retracted by Hindawi following an investigation undertaken by the publisher [1]. This investigation has uncovered evidence of one or more of the following indicators of systematic manipulation of the publication process:

- (1) Discrepancies in scope
- (2) Discrepancies in the description of the research reported
- (3) Discrepancies between the availability of data and the research described
- (4) Inappropriate citations
- (5) Incoherent, meaningless and/or irrelevant content included in the article
- (6) Peer-review manipulation

The presence of these indicators undermines our confidence in the integrity of the article's content and we cannot, therefore, vouch for its reliability. Please note that this notice is intended solely to alert readers that the content of this article is unreliable. We have not investigated whether authors were aware of or involved in the systematic manipulation of the publication process.

Wiley and Hindawi regrets that the usual quality checks did not identify these issues before publication and have since put additional measures in place to safeguard research integrity.

We wish to credit our own Research Integrity and Research Publishing teams and anonymous and named external researchers and research integrity experts for contributing to this investigation.

The corresponding author, as the representative of all authors, has been given the opportunity to register their agreement or disagreement to this retraction. We have kept a record of any response received.

References

- [1] D. Zhang and C. Guan, "Active Vibration Control of Robot Gear System Based on Adaptive Control Algorithm," *Journal of Sensors*, vol. 2022, Article ID 4481296, 8 pages, 2022.

Research Article

Active Vibration Control of Robot Gear System Based on Adaptive Control Algorithm

Dayu Zhang ¹ and Cong Guan ²

¹Graduate School of Science and Technology, Gunma University, 1-5-1 Tenjincho, Kiryu 376-8515, Japan

²School of Artificial Intelligence, Nanjing University, Nanjing, Jiangsu 210023, China

Correspondence should be addressed to Cong Guan; 14521209@xzyz.edu.cn

Received 19 May 2022; Revised 4 June 2022; Accepted 20 June 2022; Published 4 July 2022

Academic Editor: C. Venkatesan

Copyright © 2022 Dayu Zhang and Cong Guan. This is an open access article distributed under the Creative Commons Attribution License, which permits unrestricted use, distribution, and reproduction in any medium, provided the original work is properly cited.

With the aim of solving the errors of gear transmission system in the actual manufacturing process, processing and installation, and solving the the vibration and noise of the gear system caused by the deformation brought about by external excitation such as motor load and actuator, which seriously threaten the safety and stability of unit equipment, a novel active vibration suppression structure of multistage gear system with built-in piezoelectric actuator is designed to generate active control force, and it can be used on the shaft. An active controller is designed and established using FxLMS adaptive algorithm. The results of this method show that by measuring the vibration signal system, the base frequency of the high-speed gear pair is 310 Hz, and the basic frequency of the low-speed gear pair is 192 Hz. I had the adaptation snare go for almost 0.5 seconds, with a difference of 0.52%. Adaptive Trap II reached in 1 second, with a difference of 0.96%. In the active vibration suppression test, the basic frequency of the high-speed gear pair is 804 Hz, and the basic frequency of the low-speed gear connector is 500 Hz. Using the FxLMS adaptive algorithm, it is able to effectively suppress the frequency vibrations of the high-speed dual-gear and low-speed dual-gear coupling systems of multispeed gears. After being controlled by FxLMS algorithm at the second frequency of the high-speed gear, the vibration reduction is about 10 dB at the third frequency of the low-speed gear. The vibration reduction is also approximately 7 dB. This has proved that a new experiment of industrial safety can be used to accelerate the movement of gear vibrations using the FxLMS adaptation algorithm.

1. Introduction

As one of the most widely used forms of transmission, gear transmission can achieve constant transmission ratio transmission for its compact structure and the reliable transmission, which is widely used in machinery, automobile, aerospace, metallurgy, mining, robot, and many other fields. It becomes an indispensable part of major rotating machinery and power transmission devices. However, due to the change of system external load and the errors in the process of gear manufacturing and rodent impact, gear transmission in operation may cause vibration and noise in the actual process of gear engagement. It is not only related to the working life of mechanical parts, but also affects people's daily life and work. Therefore, the vibration control problem of gear trans-

mission system has become one of the key technical research hotspots in the field of vibration control [1].

The vibration of the gear transmission system will not only cause noise, but also cause the serious impact on the smooth operation and service life of other transmission parts. It even causes the immeasurable loss. In terms of mechanical equipment, gear failure can cause serious machine failure and the component damage. For example, the main transmission device of the traditional helicopter is generally composed of multistage gear transmission system, which is located at the top of the cabin. The vibration of autonomous transmission system will reduce the comfort of cabin crew, causing fatigue and affecting work safety and efficiency. The precision of the important precision instrument will be affected, reducing reliability and causing a serious threat to flight safety [2].

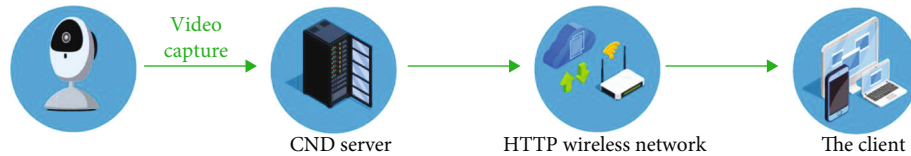


FIGURE 1: Adaptive control algorithm.

Gear transmission is also widely used in cars, such as car gearbox, drive axle, differential, and steering machine. And gear transmission is even also used in many electrical components, such as glass elevator, wiper, and electronic handbrake. The application of gear transmission system in the aviation field is the main transmission system of the US Apache AH-64D attack helicopter. And the application of gear transmission system in the automotive field is the ZF8-speed transmission equipped by the Chrysler 300C. The vibration caused by the gear pair can be transmitted to the supporting structure and the box structure, and then, the noise is transmitted to the outside. Different levels of vibration and noise will be inevitably produced in normal work in the gear system. Therefore, the action of taking effective vibration and noise reduction measures can not only improve the safety and stability of the vehicle, but also meet people's high standards and requirements for car driving safety and comfort.

In the project of "Key Basic Parts and General Parts" of the National Science and Technology Support Plan during the 12th Five-Year Plan, gears and other key transmission basic parts are listed as the key research and support projects. The research on key technologies such as design and manufacturing of science and technology meets the needs of the national development through science and technology. At present, in view of the vibration and noise control problems of the gear transmission system, most researchers are committed to the passive vibration reduction technology research such as improving the processing process and improving the processing precision and wheel tooth repair. The adaptability of the passive vibration control method is poor, and the actual effect of vibration reduction is low. So the limitations of this method are increasingly prominent [3]. With the emergence and application of new multifunctional materials, the rapid development of vibration reduction and noise reduction technology based on active control algorithm is promoted (Figure 1). It can not only achieve a better control effect, but also ensure the controllable stability of the charged system, effectively making up for the insufficient of the passive control method.

Therefore, the vibration control principle of gear transmission system, exploring new methods and designing new schemes, is studied in depth, which is conducive to improving the service life and work stability of mechanical transmission equipment. It has a very critical guiding significance for the development of China's industrial economy.

2. Literature Review

The study of the impact strength of glass has become one of the hot topics of many scientists, because glass plays an important role in the protection of the glass country, industry, and other important applications.

Sun J. was one of the first experts to determine the impact of vibration in transmission gear and introduced a new way to prevent vibrations from spreading through the second gear. The key to this process is the use of a piezoelectric actuator and an analog frequency generator in a vibration control system. Experiments have shown that the vibration reduction can reach 70% [4]. Zhang, J. et al. suppressed the vibration caused by gear engagement by arranging a magnetostrictive actuator acting on the input shaft in the gearbox, which also corrected the dynamic engagement characteristics of the gear. In addition, he used an adaptive feedback controller to output the force that determines the amplitude and phase to drive the actuator on the axis in order to reduce the vibration of the box. And the results showed that the vibration decay at the base frequency was about 20-28 dB [5]. Wang, R. et al. proposed a new control scheme, in which three magnetostrictive actuators are applied directly on the gear body and the actuator generates a circumferential force to suppress the torsional vibration according to the corresponding control strategy. The results of the experiment showed that the vibration decreased by about 7 dB at a base frequency of 250 Hz [6]. Thereafter, Afanas' Ev, V. A., et al. first proposed the idea of lateral vibration control of the gear drive system. The actuator to generate active control force acting on the shaft through additional bearings were adopted, and the active controller based on the LMS method and its improved control algorithm to generate active driving signal was designed. And good control results were obtained [7]. The same approach was used to suppress the vibratory of the rotating machinery by Fukunaga, T.G et al. [8]. Xia et al. fixed the built-in piezoelectric actuator directly on the transmission shaft and also used the FxLMS control algorithm to establish the corresponding active controller. The results of the experiment proved that when the rotation speed was below 180 rpm, the vibration of the plate was reduced by 7 dB [9]. Jiang, S. et al. designed a nonlinear controller which effectively regulates the torque acting on the input shaft gear, which can effectively reduce the impact caused by time-varying engagement stiffness [10]. Major research at home and internationally has found that most studies focus on the theory and process of vibration control at one-phase energy, but there are a few studies on vibration control of secondary and multiphase mechanisms and phase gear transmission system. Thus, this article focuses on modeling, vibration control, and vibration control techniques.

3. Research Methods

3.1. *Dynamic Active Control Algorithm of Gear Transmission System.* The least mean square algorithm, which can modify

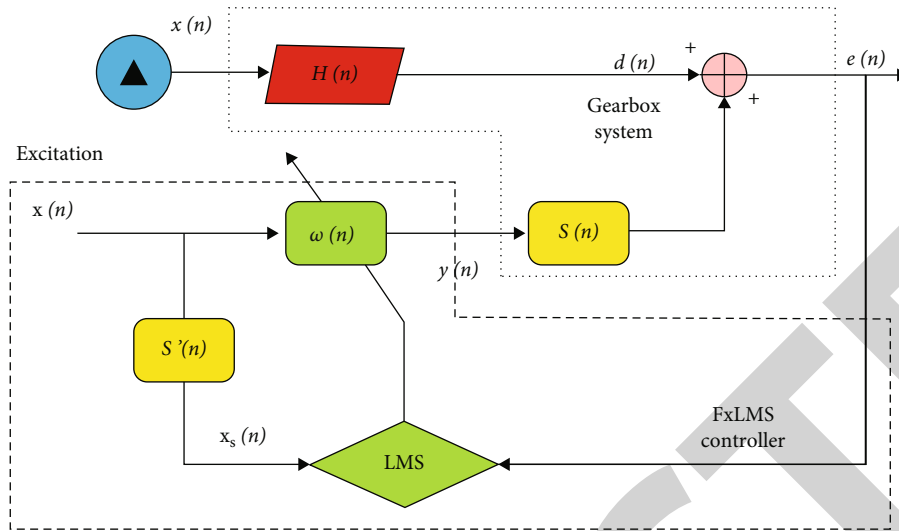


FIGURE 2: Structural diagram of the FxLMS adaptive algorithm.

the objective function to simplify the gradient vector, is one of the most popular algorithms in adaptive filtering theory and active control research and application, with low computing complexity and easy convergence under steady-state conditions [11].

The principle of active vibration control of the adaptive algorithm method is based on the vibration signal received by the sensor, and the signal is equal to the vibration source and antiphase signal to compensate for the problem. Vibration is directly controlled by adaptive law. A signal equal to the size of the vibration source and opposite to the phase of the vibration source is generated to counteract the harmful vibration. The second channel usually represents the channel from the activator to the fault sensor. The second channel includes the D/A converter, the amplifier, the activator, the physical channel, and the error-sensing main [12]. After filtering the signal used by the second channel, the distribution of the individual values on the autocorrelation matrix of the input signal increases and is not diagonalized. In addition, the integration speed of the algorithm is reduced. To improve the control, it is also possible to introduce a model with a second function to change the signal input and integrate the control algorithm into the solution. In order to improve the control effect, a model with the same transfer function as the secondary channel can be introduced to change the input signal $X(n)$ to ensure that the improved control algorithm can still converge to the optimal solution. The filter using the signal can also be involved in calculating the gradient error. The improved control algorithm is called FxLMS adaptation algorithm [13].

The structure of the FxLMS adaptive algorithm being applied to the active vibration suppression of the multistage gear transmission system is shown in Figure 2. $H(n)$ represents the channel between the excitation source input $x(n)$ and the box vibration $d(n)$. The objective existence of the secondary channel is denoted as $S(n)$. $S'(n)$ represents the estimation model of the secondary channel. The weights w of the adaptive filter are mainly affected by the error signal

$e(n)$ and the signal $x(n)$ obtained through the filtering of the secondary channel [14].

The output signal $y(n)$ from the controller actually represents the electrical control signal driving the actuator. And the secondary channel $S(n)$ is modeled with a M step filter (1):

$$S = [S_0, S_1, \dots, S_{M-1}]. \quad (1)$$

The signal $x_s(n)$ filtered by the secondary channel can be expressed as:

$$x_s(n) = \sum_{i=0}^{M-1} S_i x(n). \quad (2)$$

The force or displacement signal $y_s(n)$ used to characterize the actual control output may be expressed as:

$$y_s(n) = y(n)S_i. \quad (3)$$

The error signal $e(n)$ can be expressed as:

$$e(n) = d(n) - y_s(n). \quad (4)$$

Organize the above formula and form:

$$e(n) = d(n) - w(n)^T x_s(n). \quad (5)$$

As the estimate of the error gradient, the product of $e(n)$ and $x_s(n)$ participates in the weight updating of the FxLMS control algorithm. And the following formula is obtained:

$$w(n+1) = w(n) + 2\mu x_s(n)e(n). \quad (6)$$

The calculation process of the FxLMS algorithm is shown in Figure 3.

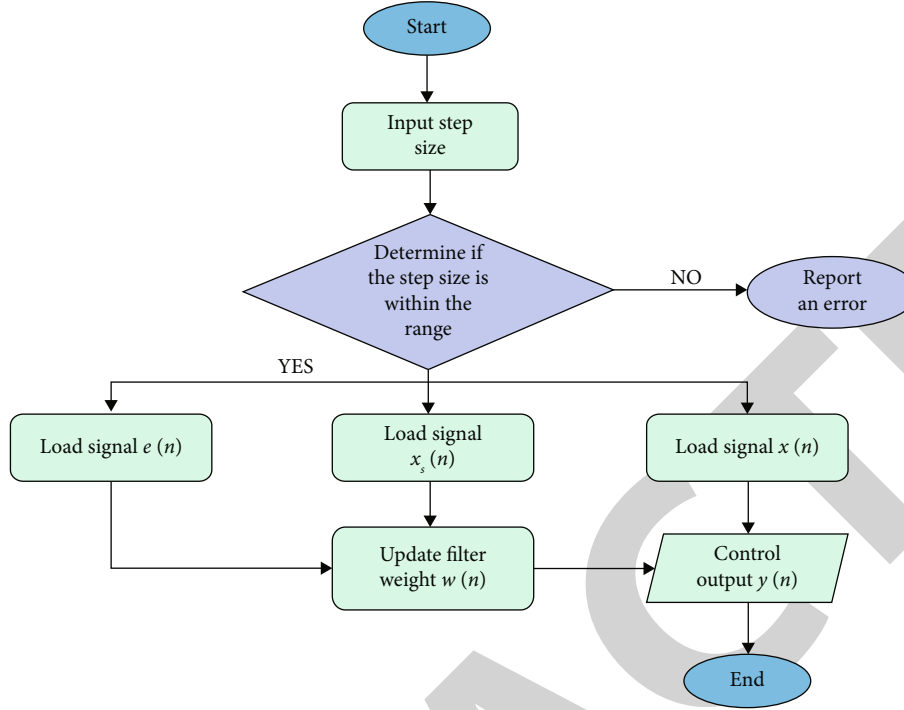


FIGURE 3: Computational flow chart of the FxLMS algorithm.

3.2. Establishment of Vibration Active Control Cooperative Simulation System of Multilevel Gear Transmission System. The PID controller is widely used in the industrial field for its good stability and strong robustness. As a classical control method, it is still one of the basic applied control methods in the manufacturing field. PID control mainly includes three basic parameters: proportion P , integral I , and differential D . The key to PID control is to adjust the three parameters of the PID controller, so that the output is optimal and the control can achieve the desired control effect [15]. In addition, the stability of the system is mainly affected by control factor P . The key of control factor I is to be used to adjust the system steady-state error. And control factor D is used to control the overall stability of the system and suppress overshoot. The control unit output can be expressed by:

$$u(t) = K_p e(t) + K_i \int_{t_1}^{t_2} e(\tau) d\tau + K_d \frac{de(t)}{dt}, \quad (7)$$

$$e(t) = x(t) - y(t), \quad (8)$$

where $e(t)$ is the error signal, $u(t)$ corresponds to the output of the controller, and K_p , K_i , and K_d correspond to the gains of P , I , and D , respectively.

3.3. Design of the Adaptive Controller. As for the experimental research on active vibration suppression of multistage gear transmission system, the actuator received the instruction from the controller, and the active vibration suppression force output real timely controls the transmission shaft of gear transmission system to suppress the complex vibration at the engagement frequency, so as to achieve the purpose of vibration reduction and noise reduction [16].

In the research of active vibration suppression of gear transmission system, obtaining reference signal plays the important role of vibration suppression. The current frequency estimation methods include spectrum analysis, phase-locking technology, and adaptive trap [17, 18]. Adaptive trap is a digital filter with active conditioning characteristics that can actively adjust with the input instruction. A frequency estimator based on the second order infinite impulse response (IIR) adaptive digital trap filter is designed by the LMS algorithm. Due to its simple calculation and strong adaptability, adjusting a single parameter enables frequency estimation. Therefore, it is applied to the acquisition of the reference signal of the secondary gearbox vibration active control system, and then, the two engagement base frequencies are estimated by the vibration acceleration signal.

Set the sinusoidal reference signal as:

$$x(k) = A \cos(\omega_0 k + \theta) + v_0(k), \quad (k = 1, 2, \dots, N), \quad (9)$$

where A is the amplitude of the reference signal, ω is the frequency of the reference signal, θ indicates the signal phase, and $v_0(k)$ is the additive Gaussian white noise.

The transfer function of the adaptive filter is shown in:

$$H(z, a) = \frac{N_{(z,a)}}{D_{(z,a)}} = \frac{1 + az^{-1} + z^{-2}}{1 + \rho az^{-1} + \rho^2 z^{-2}}, \quad (10)$$

where ρ represents the polar radius and determines the width of the notch wave. $a = -2 \cos(\omega)$ is the trap frequency parameter, in which ω is the trap frequency of the trap. In the process of the frequency estimation, ω will gradually

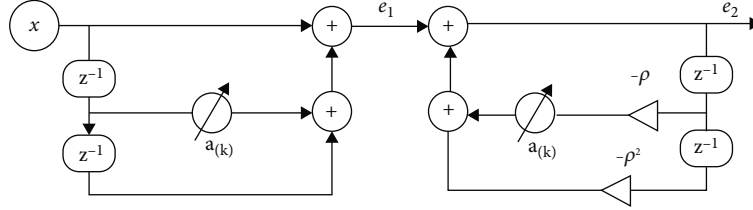


FIGURE 4: The structure of second-order IIR trap.

TABLE 1: Active vibration control effect at the different moving positions of the piezoelectric actuator.

Position controlling means	Position 1	Position 2	Position 3	Position 4
No control	-0.85238 dB	-1.26729 dB	-1.01891 dB	-1.66384 dB
PID	-3.5055 dB	-4.54135 dB	-5.2639 dB	-8.81372 dB
FxLMS	-6.14451 dB	-13.7313 dB	-13.2571 dB	-18.5504 dB

approach w_0 , so w can correspond to the estimated frequency of the estimator. The construction of the secondary trap is shown in Figure 4. From the transmission function, signals $e_{1(k)}$ and $e_{2(k)}$ can be expressed in the following formulas after signal $x_{(k)}$ goes through $N(z, a)$ and $H(z, a)$:

$$e_{1(k)} = x_{(k)} + ax_{(k-1)} + x_{k-2}, \quad (11)$$

$$e_{2(k)} = e_{1(k)} - \rho ae_{2(k-1)} - \rho^2 e_{2(k-2)}, \quad (12)$$

$$e_{2(k)} = e_{1(k)} - \rho ae_{2(k-1)} - \rho^2 e_{2(k-2)}. \quad (13)$$

To obtain the best estimated frequency value, the LMS algorithm is adjusted parameter a and the error function is set to $J_{a(k)} = |e_{2(k)}|^2$. And the updated equation of the trap coefficient is shown in

$$a_{(k+1)} = a_{(k)} - \mu \frac{\partial J_{a(k)}}{\partial a_{(k)}} = a_{(k)} - 2\mu e_{2(k)} s_{2(k)}, \quad (14)$$

$$s_{2(k)} = \frac{\partial e_{2(k)}}{\partial a_{(k)}} = x_{(k-1)} - \rho e_{2(k-1)}, \quad (15)$$

where $s_{2(k)}$ is the gradient of the relative coefficient $a_{(k)}$ of the trap output $e_{2(k)}$.

4. Results Analysis

4.1. Optimization of Piezoelectric Actuator Operation Position. The results of the tests show that a new model in order to generate vibration of various transmission gears is being tested. In other words, the control energy is transmitted through a piezoelectric actuator which acts on the base of the core to break the vibration. At the same time, the location of the piezoelectric activator was examined to find better control [19].

For four different positions of the piezoelectric actuator, the PID control and FxLMS control algorithm can excellently reduce the single frequency vibration of the system

at 4 times the engagement base frequency [20]. For position 1, at the target frequency, the vibration can decrease by about 3 dB by the PID control. By being controlled with the FxLMS algorithm, the vibration can decrease by about 5 dB. For position 2, the vibration can decrease by about 3 dB by the PID control. By being controlled with the FxLMS algorithm, the vibration can decrease by about 12.5 dB. Similarly, for position 3, the vibration can decrease by about 4 dB by the PID control. By being controlled with the FxLMS algorithm, the vibration can decrease by about 12 dB. For position 4, the vibration can decrease by about 7 dB by the PID control. By being controlled with the FxLMS algorithm, the vibration can decrease by about 17 dB. Specific comparative analysis of the data is shown in Table 1.

4.2. Acquisition of the Reference Signal of the Adaptive Controller. In the practical experiment research, it is also a key link in the controller design with the FxLMS algorithm as the core to estimate the target signal accurately.

To verify the real-time frequency estimation capability of the adaptive trap device, the experimental equipment is used for the experiment tests and analysis. The prime motor rotation speed is set to 1000 r/min. And the system vibration signal is measured to obtain the vibration time-frequency domain signal as shown in Figure 5 [21]. It can be seen that the actual engagement base frequency of high-speed gear pair is 310 Hz and that of low-speed gear pair is 192 Hz.

The second-order IIR adaptive notch device based on the LMS adaptive algorithm takes the real-time vibration signal as the input signal to realize the online estimation of the gear engagement frequency by adjusting the notch frequency and changes the trap to update the step to improve the estimation speed and accuracy. The two traps are connected in series to form a cascade adaptive trap group based on the LMS algorithm, and the vibration acceleration signal of the secondary gearbox is estimated online to obtain the two engagement base frequency [22]. According to the experimental test data, the cascade adaptive trap designed in this paper can accurately and effectively estimate the corresponding engagement frequency of the system, which proves

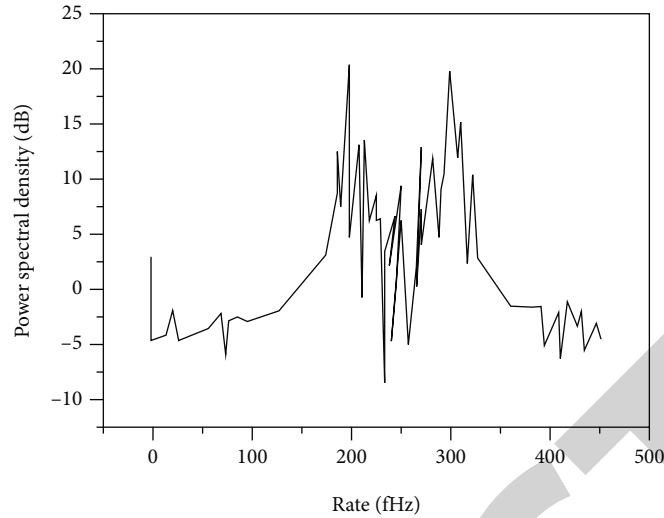


FIGURE 5: Diagram of vibration and acceleration frequency domain of the gearbox.

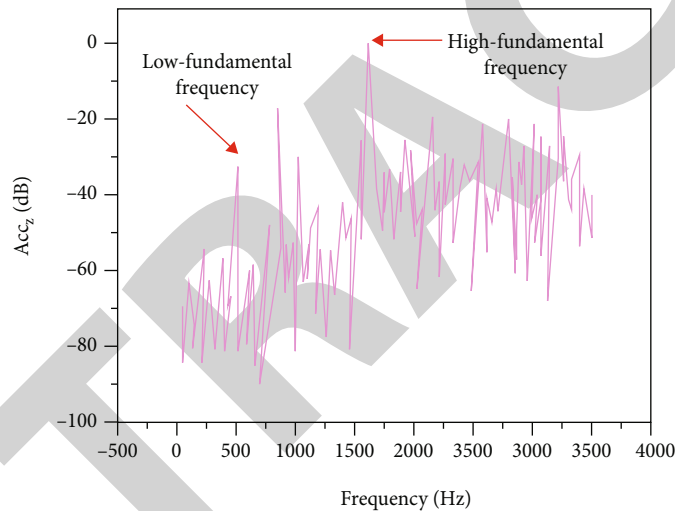


FIGURE 6: Spectrum diagram of wheel box vibration acceleration signal.

that the proposed frequency estimator is effective in the experimental research.

4.3. Analysis of the Experiment Results of Active Vibration Control of Multistage Gear Transmission System. After developing control logic in the Simulink program for active vibration suppression experiments, a new model of active vibration control of a multistage gear system was developed and tested [23]. The engine speed is set to $n = 2540$ r/min, and the dynamometer load is set to $T = 1$ Nm. Vibration acceleration signals are obtained from the multispeed gear system by receiving data, and the signal processing was indeed shown in Figure 6. Joint frequency and the frequencies of the two forces can be clearly seen. The high-speed dual-gear combination is 804 Hz, and the second to fourth sequences are 1608 Hz, 2412 Hz, and 3216 Hz. A common combination of low-frequency gears is 500 Hz.

As shown in Figure 6, the vibration of the high-speed gear pair is the largest of the second-order double coupling, while the maximum for the lower-speed gear pair is at the

third-order double coupling. Therefore, in this paper, the frequency of the gearbox vibration signal is calculated by a two-sequence joint adaptive valve developed by the LMS algorithm, and the frequency signal is provided by the input signal of FxLMS adaptive algorithm and the active vibration control analysis of the corresponding frequency. The benefits of relative vibration control are shown in Figure 6 [24, 25]. The FxLMS adaptive algorithm can handle high-frequency dual and low-speed dual-gear main frequency vibrations in high-speed gear transmission. The frequency of the second phase of the high-speed gear pair is controlled by FxLMS algorithm, and the vibration reduction is approximately 10 dB. At the frequency of the three gears of the lower gear, the vibration reduction using the FxLMS algorithm is approximately 7 dB.

5. Conclusion

In this paper, in order to solve the problem of the complex and time-change vibration caused by the internal engaging

excitation in multiphase gear transmission, piezoelectric actuator has been developed to create an active control force that makes the structure of the new active vibration suppression of multistage gear system. The FxLMS adaptive algorithm is designed and active controller used for active vibration suppression of multistage gear transmission. The main activities and research conclusions of the paper are as follows:

- (1) Analyze the theory and structure of the FxLMS transition control algorithm in order to generate the vibration of multiple gear transmission, and develop a simulation model for functional vibration control simulation based as FxLMS algorithm. The simulation results show that the FxLMS algorithm can control the vibration of the gear and work efficiently
- (2) Obtain a virtual model of a multipower transmission gear developed by ADAMS. After adjusting the functions, the model was sent to Simulink, and the integration for strong vibration suppression was developed using PID and FxLMS algorithms for integration simulation. The benefits of integrated integration have confirmed the functionality of the vibration control model of the new multistage gear. The dynamic position of the internal piezoelectric activator is also optimized. In addition, a comparison and evaluation of the results of multistage gearbox vibration control simulation based on two different control modes of PID and FxLMS algorithms have shown the advantages of control strategy based on FxLMS algorithm

Data Availability

The data used to support the findings of this study are available from the corresponding author upon request.

Conflicts of Interest

The authors declare that they have no conflicts of interest.

References

- [1] M. Kojury-Naftchali, A. Fereidunian, M. Savaghebi, and B. Akhbari, "Change detection in electricity consumption patterns utilizing adaptive information theoretic algorithms," *IEEE Systems Journal*, vol. 15, no. 2, pp. 2369–2377, 2021.
- [2] R. Bendoumia, "New sub-band proportionate forward adaptive algorithm for noise reduction in acoustical dispersive-and-sparse environments," *Applied Acoustics*, vol. 175, no. 107822, pp. 1–12, 2020.
- [3] M. S. Salman, O. Kukrer, and A. Hocanin, "A fast quasi-Newton adaptive algorithm based on approximate inversion of the autocorrelation matrix," *IEEE Access*, vol. 8, pp. 47877–47887, 2020.
- [4] J. Sun, X. Liu, T. Bäck, and Z. Xu, "Learning adaptive differential evolution algorithm from optimization experiences by policy gradient," *IEEE Transactions on Evolutionary Computation*, vol. 25, no. 4, pp. 666–680, 2021.
- [5] J. Zhang, X. Wang, M. Ju, T. Han, and Y. Wang, "An improved sparsity adaptive matching pursuit algorithm and its application in shock wave testing," *Mathematical Problems in Engineering*, vol. 2021, no. 8, 10 pages, 2021.
- [6] R. Wang, Y. Sun, V. Gvozdetzkiy et al., "Theoretical search for possible li–ni–b crystal structures using an adaptive genetic algorithm," *Journal of Applied Physics*, vol. 127, no. 9, article 094902, 2020.
- [7] V. A. Afanas'Ev, A. A. Baloev, G. L. Degtyarev, and A. S. Meshchanov, "Adaptive algorithm for controlling the soft vertical landing of an unmanned return spacecraft. i," *Russian Aeronautics*, vol. 63, no. 4, pp. 604–609, 2020.
- [8] T. Fukunaga, "Adaptive algorithm for finding connected dominating sets in uncertain graphs," *IEEE/ACM Transactions on Networking*, vol. 28, no. 1, pp. 387–398, 2020.
- [9] X. Xia, L. Gui, Y. Zhang et al., "A fitness-based adaptive differential evolution algorithm," *Information Sciences*, vol. 549, no. 9, pp. 116–141, 2021.
- [10] S. Jiang, W. Li, Y. Wang, X. Yang, and S. Xu, "Study on electro-mechanical coupling torsional resonance characteristics of gear system driven by pmsm: a case on shearer semi-direct drive cutting transmission system," *Nonlinear Dynamics*, vol. 104, no. 2, pp. 1205–1225, 2021.
- [11] H. Zhang, X. Wang, Q. Zhao, and T. Li, "Effect of excitation frequency on nonlinear vibration of crack fault in multi-stage gear transmission system," *Journal of Vibroengineering*, vol. 23, no. 3, pp. 603–618, 2021.
- [12] J. H. Xu, C. X. Jiao, D. L. Zou, N. Ta, and Z. S. Rao, "Study on the dynamic behavior of herringbone gear structure of marine propulsion system powered by double-cylinder turbines," *SCIENCE CHINA Technological Sciences*, vol. 65, no. 3, pp. 611–630, 2022.
- [13] K. Tang, S. Dong, C. Zhu, and Y. Song, "Affine arithmetic-based coordinated interval power flow of integrated transmission and distribution networks," *IEEE Transactions on Smart Grid*, vol. 11, no. 5, pp. 4116–4132, 2020.
- [14] X. Lu, Y. Xu, G. Qiao, Q. Gao, and Z. L. Wang, "Triboelectric nanogenerator for entire stroke energy harvesting with bidirectional gear transmission," *Nano Energy*, vol. 72, no. 11, p. 104726, 2020.
- [15] D. Guerra, M. Polastri, M. Battarra, A. Suman, and M. Pinelli, "Design multistage external gear pumps for dry sump systems: methodology and application," *Mathematical Problems in Engineering*, vol. 2021, no. 2, 11 pages, 2021.
- [16] V. Karma, G. Maheshwari, and S. K. Somani, "Analysis of effects of change of gear parameter module on transmission error in spur gear using interference volume method," in *In IOP Conference Series: Materials Science and Engineering*, vol. 1225no. 1, p. 012036, IOP Publishing, 2022, February.
- [17] H. Gao, X. Wang, and X. Zhao, "Coupling fault transfer characteristics of fixed-axis gear crack and planetary gear missing tooth," *Journal of Vibroengineering*, vol. 22, no. 1, pp. 804–816, 2020.
- [18] X. Zhao, J. Ye, M. Chu, L. Dai, and J. Chen, "Automatic scallion seedling feeding mechanism with an asymmetrical high-order transmission gear train," *Chinese Journal of Mechanical Engineering*, vol. 33, no. 1, pp. 148–161, 2020.
- [19] Z. Li, S. Wang, F. Li, Q. Peng, and J. Li, "Research on matching conditions of coaxial six-branch split-torsion herringbone gear transmission system," *Xibei Gongye Daxue Xuebao/Journal*

Retraction

Retracted: Application of Sensor and Fuzzy Clustering Algorithm in Hybrid Recommender System

Journal of Sensors

Received 17 October 2023; Accepted 17 October 2023; Published 18 October 2023

Copyright © 2023 Journal of Sensors. This is an open access article distributed under the Creative Commons Attribution License, which permits unrestricted use, distribution, and reproduction in any medium, provided the original work is properly cited.

This article has been retracted by Hindawi following an investigation undertaken by the publisher [1]. This investigation has uncovered evidence of one or more of the following indicators of systematic manipulation of the publication process:

- (1) Discrepancies in scope
- (2) Discrepancies in the description of the research reported
- (3) Discrepancies between the availability of data and the research described
- (4) Inappropriate citations
- (5) Incoherent, meaningless and/or irrelevant content included in the article
- (6) Peer-review manipulation

The presence of these indicators undermines our confidence in the integrity of the article's content and we cannot, therefore, vouch for its reliability. Please note that this notice is intended solely to alert readers that the content of this article is unreliable. We have not investigated whether authors were aware of or involved in the systematic manipulation of the publication process.

Wiley and Hindawi regrets that the usual quality checks did not identify these issues before publication and have since put additional measures in place to safeguard research integrity.

We wish to credit our own Research Integrity and Research Publishing teams and anonymous and named external researchers and research integrity experts for contributing to this investigation.

The corresponding author, as the representative of all authors, has been given the opportunity to register their agreement or disagreement to this retraction. We have kept a record of any response received.

References

- [1] Z. Xu and J. Zhu, "Application of Sensor and Fuzzy Clustering Algorithm in Hybrid Recommender System," *Journal of Sensors*, vol. 2022, Article ID 4294777, 8 pages, 2022.

Research Article

Application of Sensor and Fuzzy Clustering Algorithm in Hybrid Recommender System

Zihang Xu  and Jiawei Zhu 

Faculty of Data Science, City University of Macau, Macau 999078, China

Correspondence should be addressed to Zihang Xu; 1431307217@post.usts.edu.cn

Received 30 May 2022; Revised 9 June 2022; Accepted 22 June 2022; Published 4 July 2022

Academic Editor: C. Venkatesan

Copyright © 2022 Zihang Xu and Jiawei Zhu. This is an open access article distributed under the Creative Commons Attribution License, which permits unrestricted use, distribution, and reproduction in any medium, provided the original work is properly cited.

In order to solve the problem of topic drift and topic enlargement in hybrid recommendation system, a possibility C clustering algorithm based on fuzzy clustering, namely, IPCM (improved possible clustering method) algorithm, is proposed. This method improves the initial value sensitivity of PCM algorithm and introduces the user interest model into the initial matrix, so that the results obtained by the convergence of IPCM algorithm are closer to the recommended topics required by users. The recommended technology algorithm is also fused by learning from each other to form a fusion recommendation algorithm. The fusion recommendation algorithm and IPCM algorithm are applied to the result sorting, and the accuracy of the applied results is compared with that of the traditional PageRank algorithm, so as to judge the accuracy of the algorithm. The feasibility and superiority of the algorithm are verified by experiments. The experimental results show that IPCM algorithm can speed up the search for useful information and reduce the search time. Moreover, when the query range is reduced, the accuracy of the algorithm is higher than that of the traditional algorithm, which can be improved by 10%~30%. *Conclusion.* This method can effectively make up for the problems of topic drift and topic enlargement in the recommendation system, with faster speed and higher accuracy.

1. Introduction

Since the invention of computer, more and more information resources have been transmitted to the Internet. With the rapid development of Internet technology, the Internet has become the main channel for people to obtain network information resources. The development of the Internet has played a huge role in promoting economic and social development. At the same time, it has also changed the way people used to work and live. Due to the rapid updating of network technology, the application of network is changing with each passing day. Every user can use the Internet to query and publish information, which makes the amount and variety of information on the Internet huge, which makes it difficult to retrieve the useful information that users want to obtain on the Internet. In this case, the search engine was successfully launched. Relying on its powerful and convenient search function, it effectively solves the

problem of how to quickly and effectively obtain Internet information resources [1]. Search engine (web searcher) refers to a system that collects and downloads information resources on the Internet using specific search algorithms and software, stores these information resources after processing them, provides resources for users to retrieve, and finally displays the information resources retrieved by users through the computer interface. The search engine belongs to the active search of users. If users' goals are not clear or there are no keywords, it is obvious that the search engine will lose its role. So in order to solve this problem, a hybrid recommendation system is established on this basis. Hybrid recommendation system and search engine are complementary tools, which do not require users to provide keywords, but provide recommendations for users through the analysis of users' historical behavior information. The recommendation system makes up for the deficiency of search engine [2].

The research of fuzzy clustering algorithm is to fuse the deep learning with the traditional recommendation algorithm. It can optimize the recommendation algorithm through the feature fusion of more auxiliary information, establish a more accurate user interest model, and realize the personalized recommendation to users.

2. Literature Review

For the research of fuzzy clustering algorithm, Lazarini et al. proposed TS PageRank algorithm based on topic similarity model to solve the problem of computational complexity [3]. Aguilera-Alvarez et al. proposed an improved PageRank algorithm based on topic feature and time factor. The algorithm combines the retrieval topic, page relevance, and time compensation to avoid topic drift to a certain extent and effectively reduce the discrimination against new pages [4]. Park et al. proposed PageRank algorithm (link-based web page ranking algorithm) to calculate the ranking of web pages. The algorithm judges the authority of a web page based on the regression relationship that “a web page linked by a large number of authoritative web pages must also be an authoritative web page” [5]. Sheng et al. proposed topic-sensitive PageRank. The algorithm builds a set of PageRank vectors by calculating the PageRank vectors of different topics. When a user queries a topic, the topic-sensitive PageRank algorithm returns the PageRank score of the relevant topic to sort [6]. Quadros et al. used HPR (Hestenes-Powell-Rockafellar) multiplier method to solve and established a new weighted semisupervised FCM algorithm (SSFCM-HPR). The “typicality” of a supervised sample depends on the distance from the cluster center to which it belongs. In this paper, the ratio of the maximum and the second largest membership values of the supervised sample is taken as the weight of the supervised sample. The algorithm not only retains the fuzzy division of FCM algorithm on the supervised samples, so that it can effectively guide the clustering process, but also find out whether they are cross class samples. When the information of supervised samples especially is wrong, the algorithm can effectively reduce the impact of noise supervised samples on the overall classification effect [7].

To solve the above problems, this paper proposes a new search engine result ranking method based on improved fuzzy clustering algorithm, namely, IPCM algorithm. In order to optimize the ranking of retrieval results, this paper adopts the way of learning from each other to fuse the traditional recommendation technologies and obtains the fusion recommendation algorithm. The IPCM algorithm and the fusion recommendation algorithm are combined and applied to the ranking of search engine results. Compared with PageRank algorithm, IPCM algorithm improves the initial matrix of PageRank algorithm. At the same time, the algorithm clusters the web pages through the objective function of IPCM algorithm and gathers the web pages with the same topic, which proves the effectiveness of this method to avoid the phenomenon of topic drift and improve the accuracy of retrieval.

3. Research Methods

3.1. Basic Theory of Recommendation System. Recommendation system is an important means to solve the problem of information overload. On the one hand, it helps users find their favorite items in a small range, and on the other hand, it recommends items to users who need them. Recommendation system and search engine are two different technologies. The former is the development of the latter, and the two are a pair of complementary tools. The working process of the recommendation system is similar to the decision-making process when we face many choices. Taking watching movies as an example, we usually make the final choice in the following ways [8].

- (1) Ask for help. Consult with people you know and get recommendations from others or ask questions on the forum
- (2) We may find all the movies according to our favorite actors or directors, and then select them
- (3) Search the ranking list on the Internet and choose to watch the most popular movies recently. The recommendation system simulates the recommendation process of human society, takes the information of users/items as the input, carries out comprehensive analysis and processing, and then recommends the output results to the target users, thus establishing the relationship between users and items [9]. The online recommendation platform can predict the future behavior of users by analyzing and learning the historical behavior of users, save time for users, and improve user satisfaction and user dependency. There are different connotations in the application of recommendation systems in different fields, and it is difficult to unify the definitions. Recommendation systems mainly work between items and users. When users use the recommendation system, their user information includes user behavior, interest, preference, access, location, and other records of the recommended system. The recommendation system builds a similarity model by extracting the characteristics of users or items and selects the items with the highest similarity to recommend to users through the combination of the two

The focus of the recommendation system is the recommendation algorithm. Different recommendation systems have different recommendation algorithms because different recommendation systems have different requirements. Recommendation algorithm is the decisive factor for the quality of recommendation system [10]. For users, the recommendation system can quickly find the items they want. For items, it is to recommend themselves to users who are looking for such items. Different recommendation systems use different methods, but in essence, they connect users and items in a certain way. Therefore, the general working mode of the recommendation system can be summarized as shown in Figure 1.

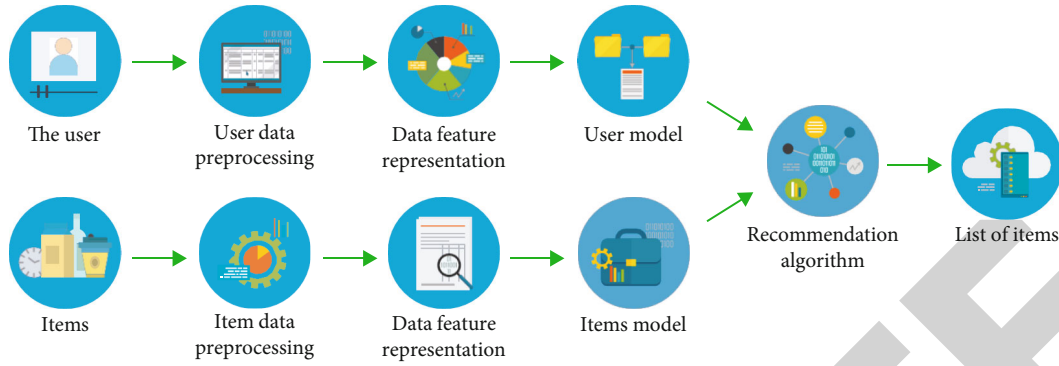


FIGURE 1: General working mode of recommendation system.

3.2. *Traditional PageRank Algorithm.* PageRank algorithm determines its authority based on the citation of documents. A document is often cited by other documents, indicating that this document has high authority. The more citations, the higher the authority. Link the structural characteristics of URLs in web pages with the characteristics of references, and draw on the idea of references to the importance of web pages [11]. That is, the pages are assigned a value (PR value) according to the mutual links between the pages, so as to sort the search results.

The core idea of PageRank algorithm is to determine the importance of web pages based on the regression relationship that “the web pages linked from a large number of important web pages must also be important web pages.” The regression relationship of this important web page of PageRank algorithm is based on two important foundations [12].

- (1) If a web page is linked by multiple other web pages, the web page may be an important web page; If a web page is linked by an important web page even though it is not linked by other web pages, it is more likely that the web page is an important web page. This means that the importance of a single web page is allocated by the web page it links to. This important web page is the authoritative web page [13]
- (2) If a user randomly grabs a web page from the web page collection for access and can only view the URL in the web page forward but not back, the probability of viewing the next web page is the PR value, as shown in Figure 2

PageRank algorithm evaluates the PR value of web pages by defining the following two criteria:

- (1) The more URLs a page is linked to, the more critical the page is and the higher the PR value
- (2) The more critical a page is, the more critical the page is linked to, and the higher the PR value. For the PR value, the higher the PR value, the higher the sorting. These two criteria are to use the network link structure to evaluate the value of a web page. For example, a URL in web page A is linked by web page B, indi-

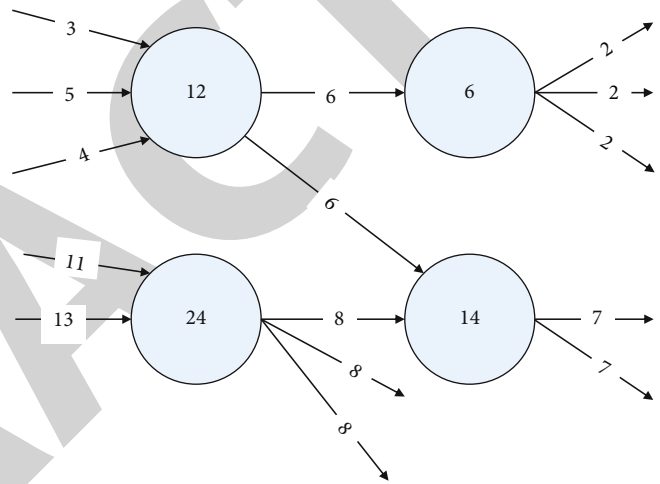


FIGURE 2: PR value of PageRank algorithm.

ating that web page A thinks that web page B has the meaning of linking, so web page B may be a key web page. Then, the PR value of web page B is determined according to the number of URLs linked to web page B and the importance of the corresponding web page. If page A has a high PR value, then page B will also have a certain PR value. In other words, the PR value owned by page A will be evenly distributed by the page it points to. The calculation formula is shown in

$$PR(A) = (1 - d) + d \left[\frac{PR(T_1)}{C(T_1)} + \dots + \frac{PR(T_n)}{C(T_n)} \right], \quad (1)$$

where $PR(A)$ represents the PR value of web page A, $d \in (0, 1)$; generally, the value of d is 0.85, T_1, \dots, T_n is the other web pages linked to web page A, $PR(T_n)$ represents the PR value of web page T_n itself, and $C(T_n)$ represents the number of URLs linked to other web pages by web page T_n

3.3. *Fusion Recommendation Algorithm.* Content-based recommendation is classified according to the feature attributes

contained in the project itself [14]. If the items recommended by the system are in the form of text, the text vocabulary will be recommended as the characteristic attribute of the item, so as to recommend to user pages similar to those that have been viewed. This feature can classify the web content of search engine search results, which is a further division of search results. Moreover, only resources similar to user interests can be mined, but no fresh interest resources can be mined [15].

User-based collaborative filtering recommendation is the earliest and most efficient recommendation algorithm used in various fields [16]. The algorithm is based on the reality that each user has a user group with similar hobbies and behaviors, and the items loved by these similar users can be used as the basis for the user's item recommendation. Therefore, this algorithm is also called the nearest neighbor algorithm. The recommended user is the target user, and the neighbor user has similar hobbies or behaviors with the target user. The most critical step of the algorithm is to find neighbor users, which is conducive to mining users' potential interests. This feature is conducive to the evaluation of search engine search result pages, thus adding a weight to the ranking of search engine results [17].

This paper makes use of the feature that content-based recommendation algorithm classifies items according to their feature attributes and combines with the feature that user-based collaborative filtering recommendation algorithm is good at mining potential user interests to form a fusion recommendation algorithm. Then, it is combined with IPCM algorithm and applied to search engine result sorting. The fusion recommendation algorithm also makes up for the defect that the content-based recommendation algorithm can not mine fresh resources [18].

The steps of merging the recommended algorithm are as follows.

Let R be a matrix of $n \times m$, where n represents the number of users and m represents the number of items. In the R matrix, if the i -th user has user feedback on the j -th item, $R_{i,j}$ represents the score of user feedback; otherwise, it is 0. Set U to represent the collection of items browsed by the target user.

- (1) User items are classified according to the characteristic attributes contained in n user items a
- (2) For a project classification, k users with the highest similarity with the target users are found. Generally, each user is an m -dimensional space vector, and then, the similarity of the two vectors is taken as the similarity of the users. That is, the user set of $a \times k$ users most similar to the target user is found
- (3) Use the user set calculated in (2) to calculate the item set C with high evaluation
- (4) Remove the items browsed by the target user in item set C , assign $C - U$ to C , and then select N items with the highest evaluation from C . The flowchart of the fused recommendation algorithm is shown in Figure 3

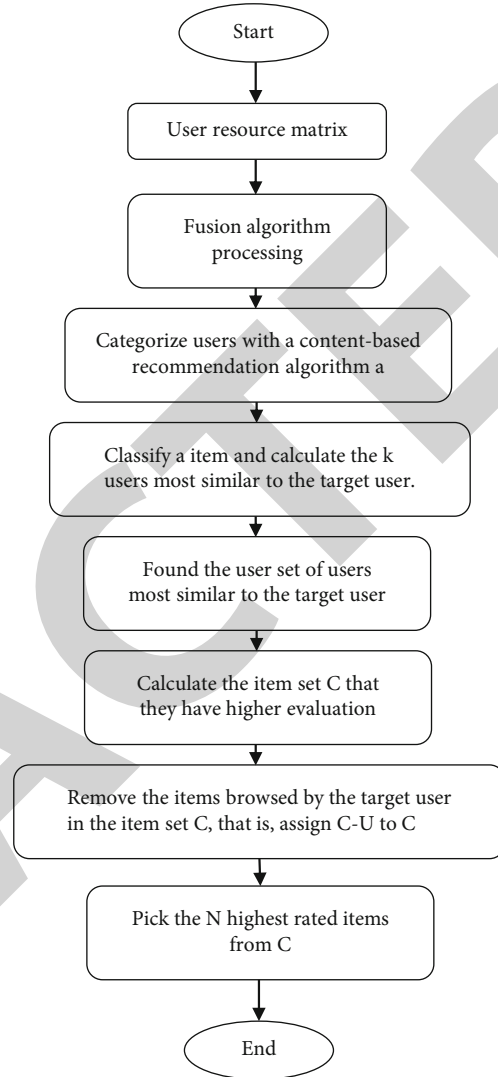


FIGURE 3: Flow chart of fusion recommendation algorithm.

3.4. Structure of IPCM Algorithm. IPCM algorithm is proposed to solve the problem that PCM algorithm is sensitive to initial matrix [19]. The algorithm is very important to the selection of initial matrix. Different selection of initial matrix will lead to different partition and different local optimal values; that is, the results after the objective function of IPCM algorithm converges are different. Choosing a reasonable initial matrix is helpful for good partition results. Otherwise, choosing noise points or outliers as the initial matrix will greatly reduce the clustering accuracy.

The algorithm starts with the selection of the initial matrix [20]. Here, because the IPCM algorithm is applied to the sorting of search engine results, the interests and hobbies of users browsing the web are collected first, and the collected interests and hobbies of users are formed into a user interest model through a mathematical model. After the model is established, the initial classification matrix can be formed [21]. When users input keywords (topics) to collect web pages, the social distance between web pages is calculated through the link relationship between web pages.

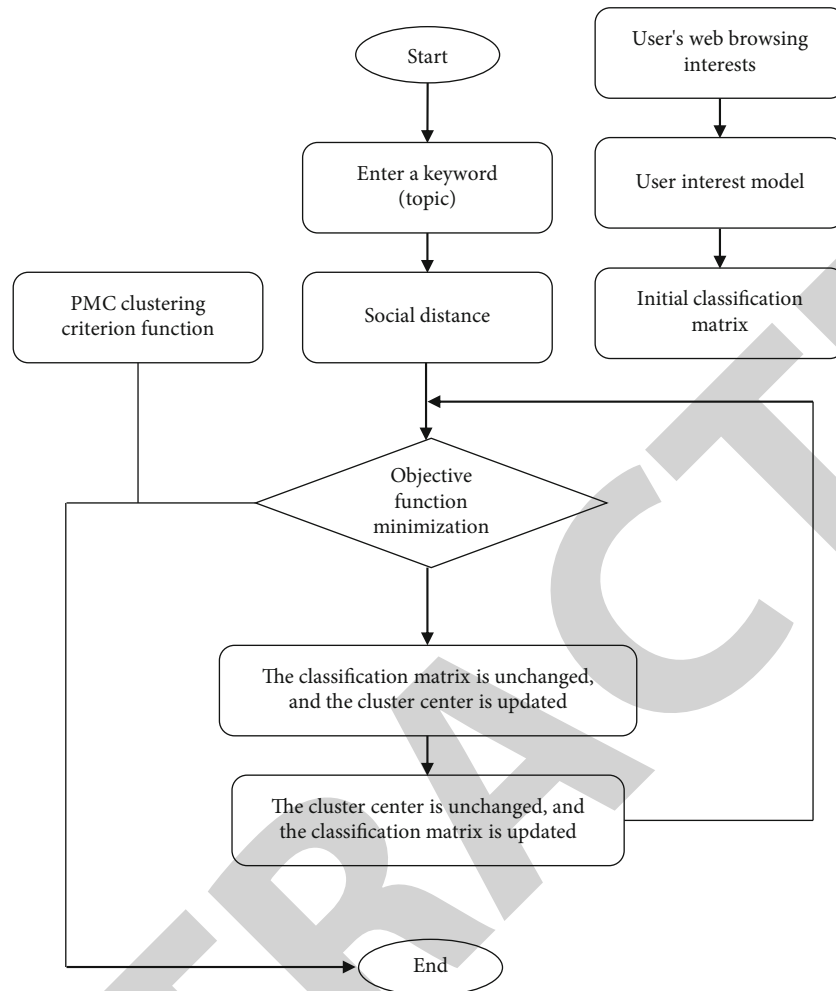


FIGURE 4: Flow chart of IPCM algorithm.

The smaller the social distance, the greater the similarity between web pages. On the contrary, the similarity between web pages is smaller. Calculate the social distance and initial matrix with the IPCM clustering objective function to see whether the objective function converges. If not, update the clustering center and classification matrix of the IPCM algorithm. If it is convergent, the convergent web page clustering is obtained directly. When updating the cluster center, the classification matrix is unchanged. Similarly, when updating the classification matrix, the cluster center is unchanged [22]. The flow chart of IPCM algorithm is shown in Figure 4.

3.5. Algorithm Description and Process. The IPCM algorithm and fusion recommendation algorithm proposed in this paper are applied to the sorting of search engine results. The specific steps are as follows:

- (1) Input the keyword (topic) that the user needs to search, collect the web page set of the topic, and calculate the social distance d_{ij} between the web pages by establishing the connection graph between the web pages and the random walk method
- (2) Acquire users' interests and hobbies and establish a model, which is used as the initial matrix of IPCM clustering algorithm
- (3) Determine the selection of various parameters in IPCM clustering algorithm, including initial classification matrix U^0 , weighted index m , clustering center V^0 , iteration times c , iteration stop threshold ε , and average "width" η_i of category V_i , and the value of η_i is
- (4) If the objective function of IPCM clustering algorithm does not converge to the minimum value, the classification matrix U must be updated. When U is updated, the clustering center V remains unchanged.

$$\eta_i = \frac{\sum_{j=1}^N u_{ij}^m d_{ij}^2}{\sum_{j=1}^N u_{ij}^m} \quad (2)$$

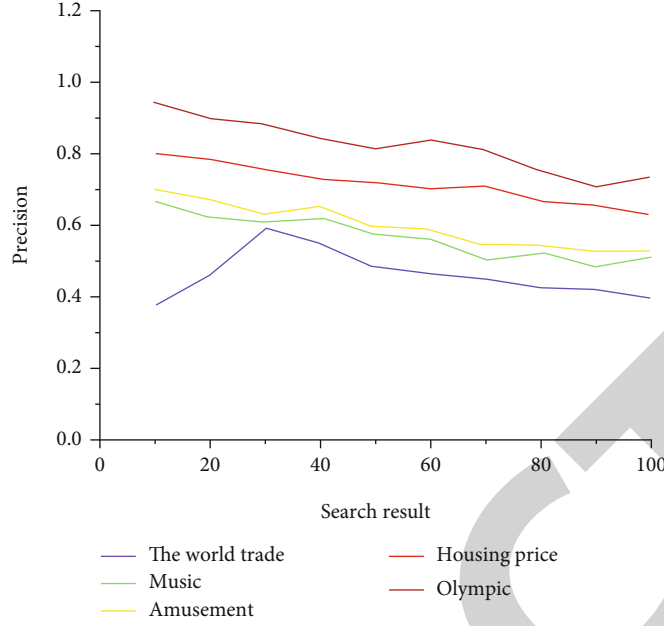


FIGURE 5: Result distribution.

Thus, the probability that point X_j belongs to class V_i is obtained by using

$$u_{ij} = \frac{1}{1 + \left(d_{ij}^2/\eta_i\right)^{1/(m-1)}} \quad (3)$$

(5) Update cluster center V . When V is updated, the classification matrix U remains unchanged. The cluster center has a high probability of being classified into a certain category and a low distance from the members of the category. The cluster center passes the following:

$$v_i = \frac{\sum_{k=1}^n u_{ik}^m x_k}{\sum_{k=1}^n u_{ik}^m} \quad (4)$$

- (6) Reestimate the value of η_i and repeat (4) and (5)
- (7) Decision threshold: according to the stop threshold, if $\|V^{(l+1)} - V^l\| \leq \varepsilon$, the iteration will be stopped
- (8) According to the clustering matrix after the convergence of the objective function, the probability of web pages belonging to the network community is determined
- (9) According to the initial set of web pages collected in (1), use the feature attributes contained in the web pages to classify the web pages a

(10) Classify a web page and calculate the k web pages that are most similar to the query keywords, and then calculate the similarity of the web pages. That is, we found the page set of $a \times k$ pages that are most similar to the query keywords

(11) Use the web page set calculated in (10) to calculate the web page set C with high evaluation

(12) Remove the web pages browsed by the user in the web page set C ; that is, assign $C - U$ to C , and then select N web pages with the highest evaluation from C

4. Result Analysis

Select 50000 web pages crawled by the web crawler as the search database. In the experiment, five keywords in different fields were selected to search. For the retrieved results of each keyword, select the first 100 records, conduct a precision analysis for each 10 records, and finally calculate the average value of precision, as shown in Figure 5. It should be noted that although the value calculated by PageRank is independent of the query conditions, only the pages with query keywords in the page set are extracted for comparison with the page sorting of IPCM algorithm, as shown in Figure 5.

Use PageRank algorithm to search the keywords in the above five different fields, find the average of their precision, and compare them with the results in Figure 5, as shown in Figure 6.

As can be seen from Figure 5, the precision is related to the keywords entered by the user, and the precision of each keyword is different in different search results. For the five keywords in different fields, the accuracy of the top 10 records in the search results is more than 0.6, indicating that

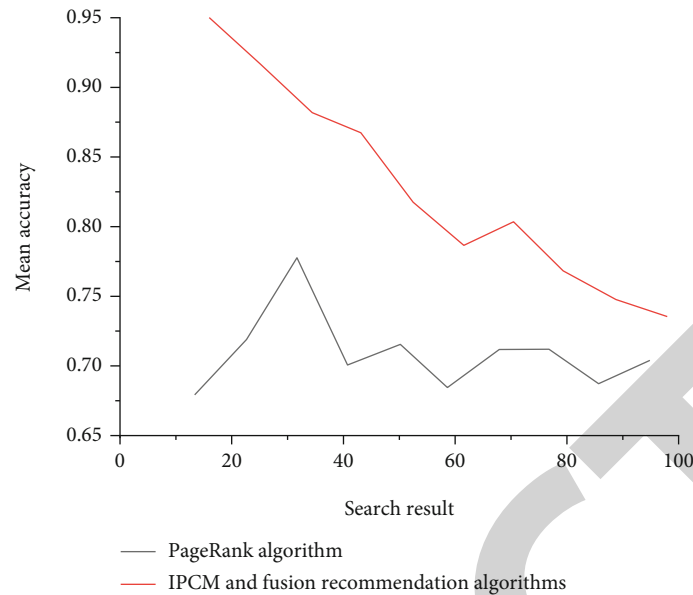


FIGURE 6: Comparison of precision.

the IPCM algorithm and the fusion recommendation algorithm can well divide the web pages into network communities according to the same topics and evaluate the web pages. Thus, the web pages with high similarity to the query keywords are ranked in the front of the search results, which speeds up the speed for users to find useful information in the search results and reduces the user's query time. There are also some special cases in the figure, such as the keyword "WTO." The reason for this phenomenon is that the keyword "world trade" was a hot topic earlier, and users now talk about this topic less often. This shows that the more recent the hot topics, the more consistent the retrieved results will be with the topics queried by users.

It can be seen from Figure 6 that the accuracy of IPCM and fusion recommendation algorithm is higher than that of PageRank algorithm. When the range of search results is smaller, the precision of IPCM and fusion recommendation algorithm is better than PageRank algorithm, and the greater the precision difference between them. When the range of search results is larger, the effect of IPCM and fusion recommendation algorithm is similar to that of PageRank algorithm, and the accuracy difference between them is very small, which is basically the same. The accuracy of IPCM clustering algorithm is improved by 10%~30%, which indicates that the web pages that rank higher in the search results have higher similarity with the keywords to be queried than that of PageRank algorithm.

5. Conclusion

This paper presents a possibility C clustering algorithm based on fuzzy clustering, namely, IPCM algorithm. This experiment verifies the feasibility and superiority of the algorithm. IPCM algorithm will speed up the search for useful information and reduce the search time in the experiment. Moreover, when the query range is reduced, the accuracy

of the algorithm is higher than that of the traditional algorithm. Therefore, in the actual application process, this method can effectively make up for the problems of topic drift and topic enlargement in the recommendation system, with faster speed and higher accuracy.

Data Availability

The data used to support the findings of this study are available from the corresponding author upon request.

Conflicts of Interest

The authors declare that they have no conflicts of interest.

References

- [1] C. M. Thasnimol and R. Rajathy, "An ideal solution for the deployment of photovoltaic generators using agent-based Nash Differential Evolution (NashDE) algorithm," *International Journal of Emerging Electric Power Systems*, vol. 22, no. 6, pp. 705–727, 2021.
- [2] X. Li, K. She, J. Cheng, K. Shi, and S. Zhong, "Dissipativity-based resilient reliable sampled-data asynchronous control for interval-valued fuzzy systems with semi-Markovian hybrid fault coefficients," *Nonlinear Dynamics*, vol. 107, no. 3, pp. 2215–2243, 2022.
- [3] A. Z. Lazarini, M. C. Teixeira, M. D. S. Jean, E. Assunção, R. Cardim, and A. S. Buzetti, "Relaxed stabilization conditions for TS fuzzy systems with optimal upper bounds for the time derivative of fuzzy Lyapunov functions," *IEEE Access*, vol. 9, pp. 64945–64957, 2021.
- [4] J. Aguilera-Alvarez, J. Padilla-Medina, C. Martínez-Nolasco, V. Samano-Ortega, M. Bravo-Sanchez, and J. Martínez-Nolasco, "Development of a didactic educational tool for learning fuzzy control systems," *Mathematical Problems in Engineering*, vol. 2021, Article ID 3158342, 17 pages, 2021.

Retraction

Retracted: Application of 3D Virtual Reality Sensor in Tourist Scenic Navigation System

Journal of Sensors

Received 22 August 2023; Accepted 22 August 2023; Published 23 August 2023

Copyright © 2023 Journal of Sensors. This is an open access article distributed under the Creative Commons Attribution License, which permits unrestricted use, distribution, and reproduction in any medium, provided the original work is properly cited.

This article has been retracted by Hindawi following an investigation undertaken by the publisher [1]. This investigation has uncovered evidence of one or more of the following indicators of systematic manipulation of the publication process:

- (1) Discrepancies in scope
- (2) Discrepancies in the description of the research reported
- (3) Discrepancies between the availability of data and the research described
- (4) Inappropriate citations
- (5) Incoherent, meaningless and/or irrelevant content included in the article
- (6) Peer-review manipulation

The presence of these indicators undermines our confidence in the integrity of the article's content and we cannot, therefore, vouch for its reliability. Please note that this notice is intended solely to alert readers that the content of this article is unreliable. We have not investigated whether authors were aware of or involved in the systematic manipulation of the publication process.

Wiley and Hindawi regrets that the usual quality checks did not identify these issues before publication and have since put additional measures in place to safeguard research integrity.

We wish to credit our own Research Integrity and Research Publishing teams and anonymous and named external researchers and research integrity experts for contributing to this investigation.

The corresponding author, as the representative of all authors, has been given the opportunity to register their agreement or disagreement to this retraction. We have kept a record of any response received.

References

- [1] F. Deng, "Application of 3D Virtual Reality Sensor in Tourist Scenic Navigation System," *Journal of Sensors*, vol. 2022, Article ID 1112261, 7 pages, 2022.

Research Article

Application of 3D Virtual Reality Sensor in Tourist Scenic Navigation System

Fei Deng 

Jiangxi Industry Polytechnic College, College of Economics and Management, Nanchang, Jiangxi 330224, China

Correspondence should be addressed to Fei Deng; 201772455@yangtzeu.edu.cn

Received 22 May 2022; Revised 9 June 2022; Accepted 20 June 2022; Published 1 July 2022

Academic Editor: C. Venkatesan

Copyright © 2022 Fei Deng. This is an open access article distributed under the Creative Commons Attribution License, which permits unrestricted use, distribution, and reproduction in any medium, provided the original work is properly cited.

In order to solve the application of 3D virtual reality technology in the practical development of scenic spot navigation system, this paper proposes a scenic spot navigation system based on multimedia technology and component geographic information system (ComGIS). The system takes Visual Basic 6.0, MapObjectst2.4, and GeoLOD 4.0 as the development platform and develops the tourism navigation system based on component GIS and multimedia technology, which manages nonspatial data with access 2003. The results are as follows: the path length designed by the system in this paper and the three compared navigation apps is 1.56 km, respectively. Although the path designed in this paper is not the shortest, the number of scenic spots passed by this path is up to 6; The accuracy of the navigation system designed in this paper is 97.2%, about 5% higher than that of similar navigation APPs; 55.2% of users felt that the navigation system designed in this paper was excellent. The results show that the system can basically meet the needs of tourists, hoping to promote the information construction of tourism.

1. Introduction

Tourism is an industry that provides tourists with a variety of services. With the in-depth development of tourism and the progress of computer information processing technology, tourism demand is gradually showing a trend of diversification and personalization [1]. The special requirements for the intuitiveness, vividness, and service of tourism information data are gradually improving. In the past, the tourism information obtained through traditional maps and other methods is too single, which not only can not meet the requirements of tourists for the intuitiveness, vividness, and richness of tourism information data, but also lacks the spatial analysis and application of geographic information [2].

Therefore, it is very necessary to explore new ways of tourism information acquisition and transmission. As an industry with strong spatial dependence, the distribution of tourism resources, tourism facilities, and even tourists themselves have important information related to geospatial location. The tourism navigation system should have the ability to effectively manage spatial data, spatial ele-

ment attributes, and multimedia data so that tourists can easily realize the retrieval and query of three kinds of information [3].

The gradual development and maturity of GIS, multimedia, and other related technologies provide theoretical and technical basis and guarantee for the development of tourism navigation system [4]. To develop tourism and realize the successful leap from a large tourism country to a powerful tourism country, we must promote the healthy and rapid development of tourism with advanced information technology, scientific management means, and new expansion ideas [5].

Although the tourism industry has shown a good development momentum in recent years, and its position in the national economy is constantly improving, the tourism industry in this region started late, the overall strength is weak, the advantages of tourism fist products are not obvious, and its own management system and various relevant supporting facilities need to be improved. Once the scientific planning guidance and development, product integration, relevant industrial facilities, and regional integration are completed, and the level of tourism information technology

is improved, the tourism industry is expected to become a new growth point of the national economy and promote the rapid development of the whole local economy.

2. Literature Review

With the gradual development of GIS, computer, and other related technologies, especially the promotion of geographic information system (GIS), high and new technologies have been widely promoted and applied in tourism development, tourism management, tourism marketing, tourism transportation, and tourism services, which has greatly improved the economic benefits, work efficiency, and service quality of tourism and provided a reliable guarantee for the establishment of tourism service system. In the construction of tourism informatization abroad, Denmark, the Netherlands, and other countries have implemented relatively early, among which the more famous ones are Austria Rohr information system and Switzerland appenzer information system. The tourism information system in this period is composed of detailed information databases of tourism resources, tourism facilities, and geographical environment, but there are differences in data organization structure, data coding, information content, information source, and technical level.

At present, many countries have established information systems based on different information technologies. Tourism service information systems for different users and some different information systems have been networked to realize the sharing of tourism resource information [6].

After years of development, great progress has been made in the research of tourism GIS abroad, and GIS technology is combined with encounter technology and GPS (global positioning system) technology. The integration of multidisciplinary and multiprofessional knowledge such as communication technology has greatly promoted the development of tourism industry. The rapid development of modern tourism puts forward higher requirements for tourism information technology. The interactive relationship between information technology and tourism industry has also become a hot spot of great concern to foreign scholars. Many relevant studies have appeared in some academic journals [7]. Khatib and others discussed the application of information technology in various tourism industries [8]. Yang and others further discussed the strategic position of information technology in tourism [9]. Kozorez and others discussed the application of information technology in tourism from the analysis of tourism distribution channels [10].

In China, the research of tourism information system started relatively late, which began in the early 1980s. In order to adapt to the new situation, China's tourism industry has accelerated the application research of GIS and other technologies in tourism information system from two aspects of theory and practice and has made some achievements. Zhao and others research on MapX based tourism information system [11]. Vlacic and others research on the design and implementation of tourism geographic information system [12]. Wang and others studied the tourism scenic spot information system based on GIS [13]. China has initially established a set of "microcomputer national tour-

ism resources information system." Based on the completion of the comprehensive survey of national tourism resources, the system systematically classifies the resources, adopts the method of systematic analysis, and establishes a tourism resource information system composed of geographic information basic database, tourism resource database, tourism service database, tourist statistics database, and database, which provide a foundation for the computerization, data sharing, and exchange of tourism resource information management. However, these studies are still very imperfect. The information construction of China's tourism industry is still in the primary stage. In many aspects of relevant technical research, it is in the initial and exploratory stage. The relevant technical theory is not mature enough, and the research on information collection, processing, and analysis technology is still very weak. Many originally designed functions and schemes cannot be well applied in practice due to various reasons. There are still many problems in the development and application of the system.

Based on this, this paper studies the application and research status of tourism navigation system at home and abroad and expounds the advantages of component GIS technology and multimedia technology in tourism navigation system. This paper introduces GIS and component technology, multimedia technology, spatial data, shortest path algorithm, and other technologies and basic theories related to system development. It sets the system development objectives and analyzes the user needs, feasibility, and data sources of the system. This paper determines the technical route, development method, and implementation environment of the system: The functional module and database of the tourism navigation system are designed.

3. Research Methods

3.1. 3D GIS. Component technology has gradually become the industry standard, which is easy to use, so that non-professional ordinary users can also develop and integrate GIS application system and promote the popularization of GIS. The emergence of component GIS makes GIS not only a professional analysis tool for experts, but also a visual tool for ordinary users to manage geographic related data. The browser of GIS data is much larger than its user and owner (or producer). The three are star pyramid shaped. As shown in Figure 1, ComGIS enables the user and browser of GIS data at the bottom of the pyramid to analyze, browse, and publish the data easily [14].

As we all know, in the decades of development of two-dimensional GIS technology, with the rapid development of computer software and hardware and relational database, two-dimensional GIS technology has become more and more perfect and has incomparable advantages in the analysis function of geographic information.

Three-dimensional GIS is a computer system that inputs, stores, edits, queries, spatially analyzes, and simulates geographic information objects with three-dimensional geographic reference coordinates on the basis of two-dimensional GIS. The biggest advantage of 3D GIS is that it can truly reproduce the geographic information in the real

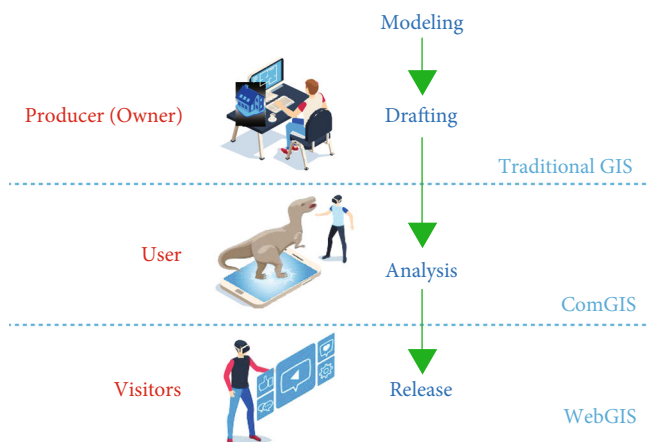


FIGURE 1: Comparison of GIS users.

environment, such as terrain and landform. Using 3D GIS technology, DEM and texture data can realize the generation function of realistic terrain and landform and real-time roaming function. For some functions that can only be realized by 3D GIS technology, they must also be realized by 3D GIS technology. For example, in order to more intuitively understand the results of spatial query and analysis and improve the level of spatial analysis, it is necessary to restore the 3D spatial relationship and carry out perspective display [15].

Combining two-dimensional GIS and three-dimensional GIS, two-dimensional GIS and three-dimensional GIS operate alternately, rather than a single one. Giving full play to the advantages of both is an economic and practical idea, which is the purpose of this study [16].

3.2. System Development Mode. According to its content and function, geographic information system can be divided into two basic types: tool geographic information system and application geographic information system. Tool GIS is a general GIS, that is, GIS tool software package. It has the general functions and characteristics of GIS, such as Arcinfo, MapInfo, MAPGIS, and GEOSTAR. It provides users with a general GIS operation platform or development tool. This kind of GIS generally has no geospatial entity. Users carry out further design and secondary development based on it according to their own needs and certain application purposes, so as to solve practical application problems. The applied geographic information system is a geographic information system designed according to the needs of users to solve one or more kinds of practical problems, including thematic geographic information system and regional integrated geographic information system [17].

With the expansion of GIS application field, the development of application-oriented GIS is becoming more and more important. How to develop an economic, practical, and needed application-oriented GIS system is a very concerned problem for GIS developers. There are three modes: independent development mode, host secondary development mode, and secondary development mode based on GIS.

To sum up, the independent development is too difficult. The host secondary development is limited by the script language provided by the GIS platform, and the GIS component development mode combines the advantages of the component development mode of GIS platform software and visual development platform and has become the mainstream direction of GIS application development.

3.3. Technical Route of the System. The system adopts the technology of taking Visual Basic 6.0 as the front-end development tool and integrating MapObjects and realizes the application of the system by using the access of Visual Basic 6.0 to the database, the support of SQL (structured query language), and the support of Geo-dataset of map objects to the integrated development environment and SQL. The overall architecture of the system is shown in Figure 2.

3.4. System Database. Data organization and management is the basic core of system construction, the data basis for the realization of various functions of the system, and the key factor for the success of system construction [18], which directly affects the practicability and efficiency of the system. In this tourism navigation system, the design of system database includes the design of spatial database, attribute database, and multimedia database. The design and establishment of database is a very important and arduous task in the construction of tourism navigation system. In the organization and management of system database, how to organize, store, and manage all kinds of data according to a certain structure in order to improve the efficiency of system information query and processing is the key of system database design. In this system, the GIS data management method of mixed management mode of file and database system is adopted, that is, the entity vector data structure is used to express the spatial entity data, the spatial entity (graphics) data is managed by the serialized file, and the attribute data adopts the relational database to connect the data to associate the graphics and attribute data. The data flow chart of tourism navigation system based on component GIS and multimedia technology is shown in Figure 3.

The spatial database is mainly used to store the spatial graphic data of the salt pond. MapObjects uses the concept of map layer. Each map layer is composed of geographical objects of the same nature, and a layer as a theme corresponds to a layer entity table. Each layer is represented by specific symbols and corresponds to different data sources. A map layer corresponds to a DBF database, and several map layers are superimposed to form a complete map [19].

Attribute data is an important feature of GIS, which is mainly used to describe the characteristics of spatial entities, such as the name, category, quality, and quantity of entities. Attribute data itself belongs to nonspatial data, but it is an important data component in spatial data. Attribute data is also called statistical data or thematic data. The attribute database of this system mainly includes attribute data of tourism resources, tourism services, and tourism facilities [20, 21].

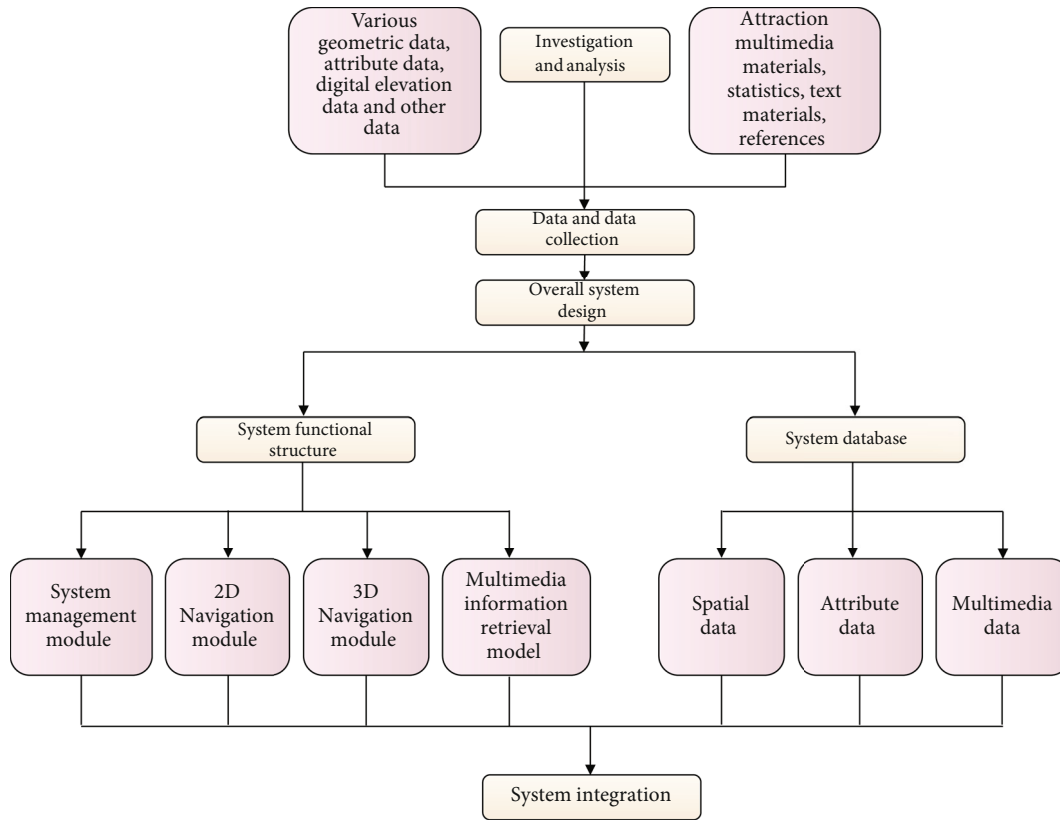


FIGURE 2: Overall system architecture.

Multimedia data is a kind of special thematic data; what methods should be adopted to organize and manage multimedia data effectively and how to combine it with attribute database are very important links. Establishing effective association between spatial databases is the key to the application of multimedia technology in GIS. The multimedia data in the tourism navigation system is mainly used for information query, so as to increase the expressiveness of the most scenic spots, more vividly and intuitively reflect the content of scenic spots, and strengthen the publicity of tourism industry. Multimedia data need not be stored directly in spatial database.

Spatial database, attribute database, and multimedia database are independent of each other, but in the process of use, spatial data and nonspatial data are inseparable, and their association must be realized [22]. When designing the data structure, the method of adding public key fields is adopted, that is, each spatial entity in the spatial database has a unique identification number, and there is also an attribute corresponding to the identification number in the relational data table structure. The two correspond with the public key ID and finally realize the two-way query and retrieval of graphic data and attribute data [23].

4. Result Analysis

4.1. Route Avoidance of Navigation System. In order to test the performance of the navigation system designed in this

paper, this paper uses several similar products to compare with this system. For the same starting point and end point, the optimal route design is carried out, and the results are shown in Figure 4.

As shown in Figure 4, the designed path lengths of the system in this paper and the three compared navigation apps are 1.56 km, 1.33 km, 1.74 km, and 1.22 km, respectively. Although the path designed in this paper is not the shortest, the number of scenic spots passed by this path is 6, which is the largest among the comparison systems, proving the superiority of the navigation system designed in this paper [24, 25].

4.2. Accuracy of Navigation System. This paper also uses several similar products to compare with this system. For the same starting point and ending point, route design and check the accuracy of navigation. The results are shown in Figure 5.

As shown in Figure 5, the accuracy of the navigation system designed in this paper is 97.2%, and the accuracy of similar comparison navigation apps are 92.6%, 86.7%, and 85.2%, respectively.

4.3. Overall Evaluation of Navigation System. The navigation system designed in this paper is given to the experimenters for trial. The navigation system is scored from five aspects: interface simplicity (I), operation convenience (C), navigation accuracy (D), three-dimensional scene authenticity

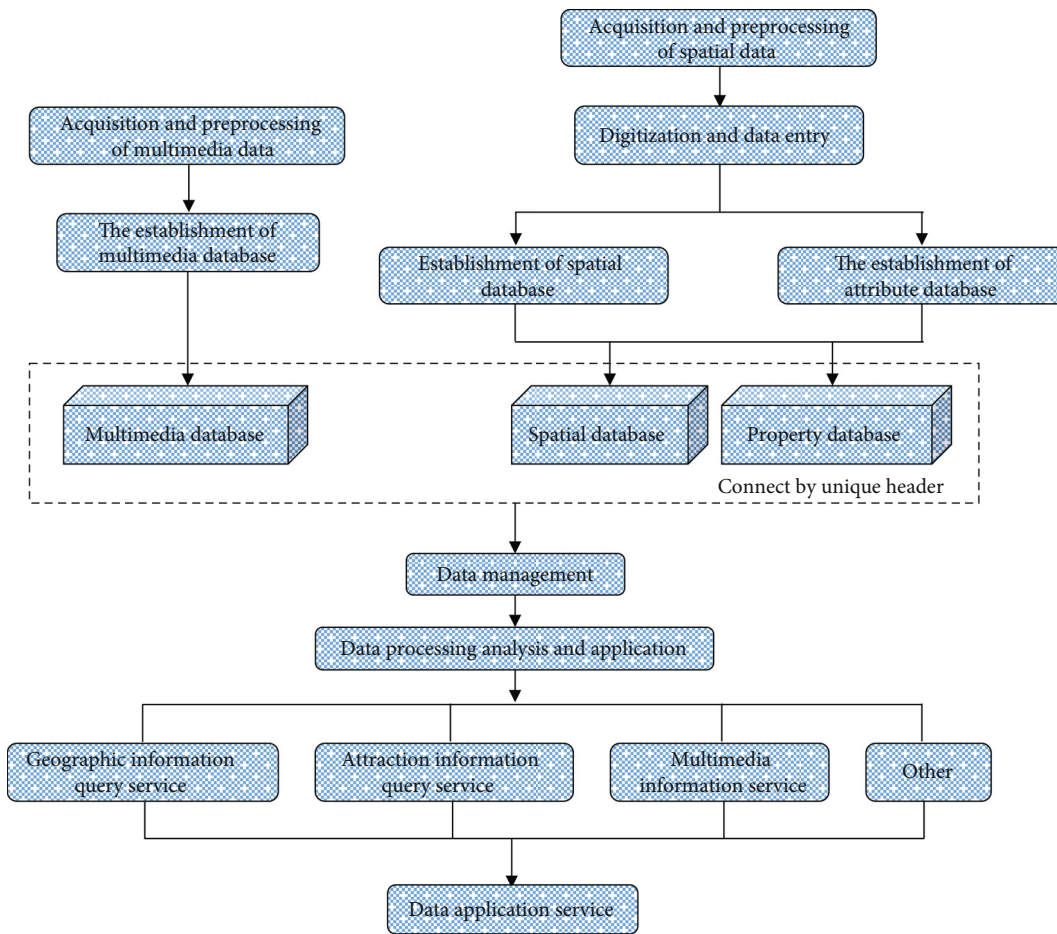


FIGURE 3: System database flow chart.

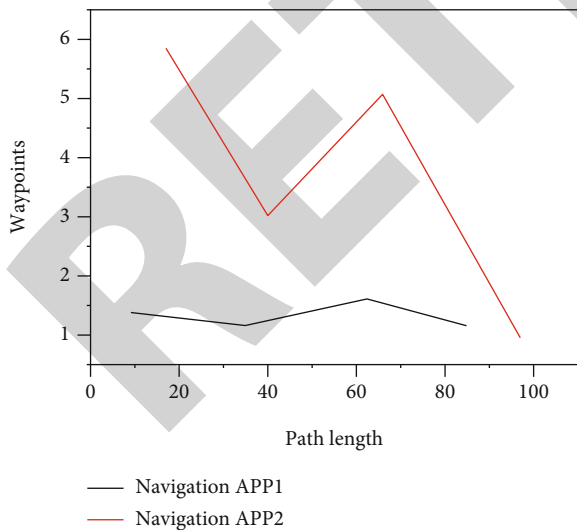


FIGURE 4: Comparison of optimal path design.

(S), and use feeling (G). After collecting the data, the overall score (T) is obtained. The calculation formula is as follows:

$$T = (J * 0.15 + C * 0.1 + D * 0.3 + S * 0.25 + G * 0.2) * 100%. \quad (1)$$

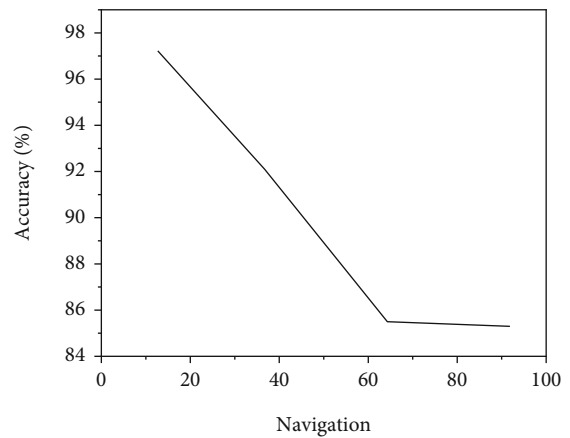


FIGURE 5: Navigation accuracy.

A score of 85-100 is excellent, 70-85 is good, 55-70 is average, and less than 55 is poor. The results are shown in Figure 6.

As shown in Figure 6, 55.2% of users felt that the navigation system designed in this paper was excellent, 28.4% felt good, 12% felt average, and 4.4% felt poor.

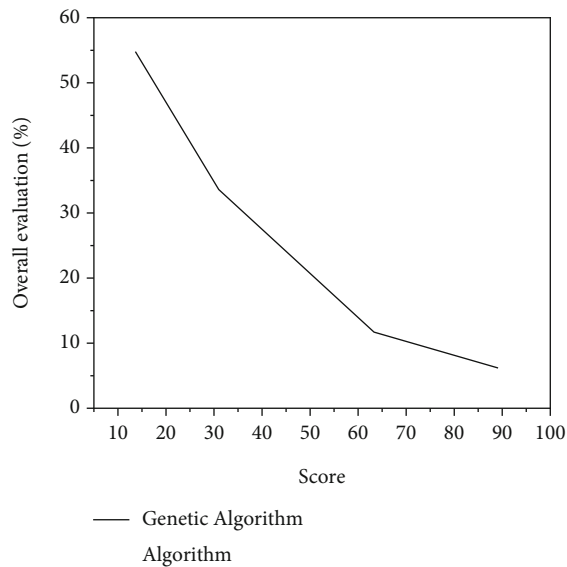


FIGURE 6: Overall evaluation of use.

5. Conclusion

With the continuous improvement of people's material and cultural living standards, returning to nature has increasingly become an ideal, and tourism is facing new development opportunities. For the development of tourism, unique tourism resources are very important, but tourism publicity and related high-quality services are also one of the essential conditions.

With the popularization and application of multimedia technology and GIS technology, the perfect combination of multimedia technology and GIS is applied to tourism, which opens up a new way for the development of tourism navigation system and has become a new research hot spot in tourism. It overcomes the defects of the traditional tourism navigation system, such as the lack of visual and intuitive expression ability of query results.

The results are as follows: Through in-depth investigation and analysis, serious damage and exploration, and feasibility study, overall system design, database design, program compilation and debugging, a tourism navigation system based on component GIS and multimedia technology is established. The system function is basically realized, and the interface is friendly and concise. Users who know a little about basic computer knowledge can operate the system.

Data Availability

The data used to support the findings of this study are available from the corresponding author upon request.

Conflicts of Interest

The author declares that there are no conflicts of interest.

References

- [1] J. Slavík, M. Dolej, and K. Rybová, "Mixed-method approach incorporating geographic information system (GIS) tools for optimizing collection costs and convenience of the biowaste separate collection," *Waste Management*, vol. 134, no. 9, pp. 177–186, 2021.
- [2] P. Shan and W. Sun, "Research on 3d urban landscape design and evaluation based on geographic information system," *Environmental Earth Sciences*, vol. 80, no. 17, pp. 1–15, 2021.
- [3] Z. Zhou, Z. Qingshan, L. Dongyi, and T. Weihong, "Three-dimensional reconstruction of Huizhou landscape combined with multimedia technology and geographic information system," *Mobile Information Systems*, vol. 2021, Article ID 9930692, 13 pages, 2021.
- [4] J. Yang, F. Wu, E. Lai, M. Liu, and Y. Zhao, "Analysis of visualization technology of 3d spatial geographic information system," *Mobile Information Systems*, vol. 2021, Article ID 9173281, 9 pages, 2021.
- [5] O. Sonmez and H. Bizimana, "Flood hazard risk evaluation using fuzzy logic and weightage based combination method in geographic information system," *Scientia Iranica*, vol. 27, no. 2, pp. 517–528, 2020.
- [6] A. W. Azeze, "Modeling of landslide susceptibility in a part of Abay basin, northwestern Ethiopia," *Open Geosciences*, vol. 12, no. 1, pp. 1440–1467, 2020.
- [7] J. Xu, G. Yang, Y. Sun, and S. Picek, "A multi-sensor information fusion method based on factor graph for integrated navigation system," *Access*, vol. 9, pp. 12044–12054, 2021.
- [8] E. Khatib, M. Jaradat, and M. F. Abdel-Hafez, "Low-cost reduced navigation system for mobile robot in indoor/outdoor environments," *Access*, vol. 8, pp. 25014–25026, 2020.
- [9] B. Yang, X. Yang, G. Qu, and J. Wang, "Accurate integrated navigation method based on medium precision strapdown inertial navigation system," *Mathematical Problems in Engineering*, vol. 2020, Article ID 1420393, 10 pages, 2020.
- [10] D. A. Kozorez and D. M. Kruzhkov, "Selecting the beacon locations in a radio navigation system for lunar missions," *Russian Engineering Research*, vol. 41, no. 8, pp. 756–758, 2021.
- [11] D. Zhao, H. Yu, X. Fang, L. Tian, and P. Han, "A path planning method based on multi-objective cauchy mutation cat swarm optimization algorithm for navigation system of intelligent patrol car," *IEEE Access*, vol. 8, pp. 151788–151803, 2020.
- [12] L. Vlacic, "On global navigation satellite system-assisted intelligent transportation systems [editor's column]," *IEEE Intelligent Transportation Systems Magazine*, vol. 12, no. 3, pp. 4–9, 2020.
- [13] D. Wang, N. Ding, Y. Zhang, L. Li, X. Yang, and Q. Zhao, "A new approach of the global navigation satellite system tomography for any size of GNSS network," *Remote Sensing*, vol. 12, no. 4, p. 617, 2020.
- [14] D. Li, X. Jia, and J. Zhao, "A novel hybrid fusion algorithm for low-cost gps/ins integrated navigation system during GPS outages," *Access*, vol. 8, pp. 53984–53996, 2020.
- [15] Q. Wang, C. S. Yang, and S. Wu, "RFID aided sins integrated navigation system for lane applications," *International Journal of Embedded Systems*, vol. 13, no. 1, p. 113, 2020.
- [16] Y. Zhao, G. Yan, Y. Qin, and Q. Fu, "Information fusion based on complementary filter for SINS/CNS/GPS integrated navigation system of aerospace plane," *Sensors*, vol. 20, no. 24, p. 7193, 2020.

Retraction

Retracted: Digital Library Information Integration System Based on Big Data and Deep Learning

Journal of Sensors

Received 17 October 2023; Accepted 17 October 2023; Published 18 October 2023

Copyright © 2023 Journal of Sensors. This is an open access article distributed under the Creative Commons Attribution License, which permits unrestricted use, distribution, and reproduction in any medium, provided the original work is properly cited.

This article has been retracted by Hindawi following an investigation undertaken by the publisher [1]. This investigation has uncovered evidence of one or more of the following indicators of systematic manipulation of the publication process:

- (1) Discrepancies in scope
- (2) Discrepancies in the description of the research reported
- (3) Discrepancies between the availability of data and the research described
- (4) Inappropriate citations
- (5) Incoherent, meaningless and/or irrelevant content included in the article
- (6) Peer-review manipulation

The presence of these indicators undermines our confidence in the integrity of the article's content and we cannot, therefore, vouch for its reliability. Please note that this notice is intended solely to alert readers that the content of this article is unreliable. We have not investigated whether authors were aware of or involved in the systematic manipulation of the publication process.

Wiley and Hindawi regrets that the usual quality checks did not identify these issues before publication and have since put additional measures in place to safeguard research integrity.

We wish to credit our own Research Integrity and Research Publishing teams and anonymous and named external researchers and research integrity experts for contributing to this investigation.

The corresponding author, as the representative of all authors, has been given the opportunity to register their agreement or disagreement to this retraction. We have kept a record of any response received.

References

- [1] X. Lin, Y. Zhang, and J. Wang, "Digital Library Information Integration System Based on Big Data and Deep Learning," *Journal of Sensors*, vol. 2022, Article ID 9953787, 8 pages, 2022.

Research Article

Digital Library Information Integration System Based on Big Data and Deep Learning

Xiao Lin , Ying Zhang, and Jianguo Wang

The Minjiang University Library, Fuzhou, Fujian 350000, China

Correspondence should be addressed to Xiao Lin; 1401040237@xs.hnit.edu.cn

Received 19 May 2022; Revised 4 June 2022; Accepted 15 June 2022; Published 1 July 2022

Academic Editor: C. Venkatesan

Copyright © 2022 Xiao Lin et al. This is an open access article distributed under the Creative Commons Attribution License, which permits unrestricted use, distribution, and reproduction in any medium, provided the original work is properly cited.

In order to solve the defects of traditional text classification in digital library, the author proposes a method based on deep learning in the field of big data and artificial intelligence, which is applied to the digital library information integration system. On the basis of systematically sorting out the traditional text classification of digital library of this method, this paper proposes a digital library text classification model based on deep learning and uses the word vector method to represent text features, the convolutional neural network in the deep learning model is used to extract the essential features of text information, and experimental verification is carried out. Experimental results show that deep learning-based text classification model can effectively improve the accuracy (average 94.8%) and recall (average 94.5%) of text classification in digital libraries; compared with the traditional text classification method, the text classification method based on deep learning improves the average F1 value by about 11.6%. *Conclusion.* This method can not only improve the intelligence of the internal business of the digital library, but also improve the efficiency and quality of the information service of the digital library.

1. Introduction

With the rapid and organic integration of computer, network technology, communication technology, and other technologies, digital information has been widely used in the human environment. Digital and other forms of information have a life cycle and play a role in that life cycle [1]. Its life cycle includes production, storage, analysis, distribution, change, innovation, and reproduction. The digital library has rich digital information resources, such as e-books, images, audio and video materials, CD-ROMs, and other media. It has a technology platform that can provide advanced simple and fast information services such as intelligent messaging, data transfer, and mobile services.

The emergence of the digital library is inseparable from the popularization of the Internet. The digital library is the crystallization of human wisdom. It has changed the way people obtain information. Make it easier and more colorful for people to acquire knowledge. The digital library is not only a new development in science, but also a new branch of public electronics [2]. Computer technology, network storage technology, communication technology, and many

other technologies have developed rapidly in the past ten years. Their development and expansion have expanded a lot of digital information, and now people are moving around digital information. In fact, due to the widespread use of digital information, the way people receive information has changed dramatically, and people no longer want to receive information through text, but transmit electronic data through the Internet [3]. Due to the huge amount of Internet data, how to obtain more, better, more accurate, timely, and useful information from it has become a problem that people care about.

2. Literature Review

Wang, J. et al. discussed the application prospects of expert systems in libraries [4]. Shi, M. et al. describe how a knowledge-based librarian system, UMLS, can be used to search the MEDLINE bibliographic database [5]. *Wu, Y. et al.'s research on AI technology in digital libraries, specifically discussed how to use Daubechey wavelet transform for image indexing; An extension of the Stone Li algorithm for handling occlusions in images; Fault-tolerant structure

extraction strategies for semistructured text documents, etc. [6]. According to Kim, Y. et al., the structure of each department responsible for data retrieval in the digital library is described. Ontology is used to present problems, avoid ambiguous information as much as possible, and also use ontology to identify relevant information [7]. The formation of these agents is based on the Gaia method. According to Wang, D. et al., some applications of fuzzy light theory in retrieving data are reported, as well as final research in the field [8]. Lu, L. et al. show how to better answer example questions posed using static electronics such as blinking and gazing [9]. Yus, Y. et al. explore the development and use of international conferences while focusing on the availability of Canadian libraries [10].

At present, for the in-depth research of library data service users, data recovery, and intelligent question answering robot, there are also some researches on intelligent research of digital library business information distribution. At the same time, some scholars from many countries discussed the application of in-depth research in the field of psychology, but most of them focus on using deep learning for entity extraction, information extraction, cross-language retrieval, and sentiment analysis; however, there are few related researches on the application of deep learning in library text classification, automatic summarization, and topic extraction.

This paper summarizes the traditional text classification methods from two aspects: text feature representation and text feature selection. He researches and writes about text distribution patterns. Traditional text categories do not have high-dimensional sparse data or semantics, so text classification is recommended. The library model first converts the data files in the digital library, and then uses the word vector method to represent the text as two-dimensional network data, which can solve the traditional text representation method. Latent problem, sparse data, no semantics, with word vector as the concept, in-depth study of recurrent neural network model. Through the special design of the convolutional neural network, the basic feature is that it can delete the text and finally complete the text to achieve the purpose of improving the text quality of the digital library.

3. Research Methods

3.1. Overview of Traditional Text Classification. Text classification in digital library refers to the classification of text according to the subject, content, or attribute of text information under the premise of a given classification standard and the process of classifying massive text information resources into single or multiple categories. As an important basis for information management and organization in digital libraries, text classification can help users find and locate the required information quickly and accurately, and it is a very effective method to manage textual information resources with huge amount of data [11].

The text classification process in a traditional digital library includes four parts, namely, text preprocessing, feature representation, feature selection, and classifier, of which the most important are text feature representation and text

feature selection, which play a decisive role in the results of text classification [12]. The main process of text classification is shown in Figure 1.

3.1.1. Text Feature Representation. Special representation is the basis of text distribution in digital library and an important function of information organization and management in digital library, and a good text feature representation plays a decisive role in the performance of text classification tasks in digital libraries. Currently, scientists have proposed a variety of esthetic models: Boolean models, probabilistic models, vector space models, and various hybrid models [13]. Among them, vector space modeling has been widely used in recent years and is one of the most effective methods to describe text features.

The vector space model is a text feature representation method based on statistical theory, this representation method is simple and direct, compared with other models, the text feature representation method of the vector space model is also more standardized, and the use effect is also ideal. Therefore, the vector space model has always been the focus of scholars. Although the vector space model can reduce the complexity of text processing and improve processing efficiency to a certain extent, however, it leads to the high dimensionality of text feature vectors and the consequent data sparse phenomenon. In response to this problem, the first thing is to find a method that can reduce the dimension of text features without affecting the effect of text classification, and this is the dimensionality reduction process that people need to perform before classifying.

3.1.2. Text Feature Selection. Reducing the dimension of text functions is a key factor affecting the accuracy and efficiency of text classification in digital libraries. Currently, there are two main ways to reduce script size: select specific and remove features. Feature selection is the basis for ignoring the first feature. From the initial text settings, select some features that best represent the text content and then reduce the size of the text features. Improve the accuracy and efficiency of text distribution in digital libraries. The most common options include data frequency, chi-square statistics, and data gain [14].

Compared to optional features, feature extraction takes a more efficient way, shifting the importance of the text source from the art to creating a new feature source of shorter length, longer duration, and more freedom to improve the text and dimensionality reduction. However, since the subtractive features are very close to identifying semantic scripts and the technology involved in this is immature, the impact size is not good. Compared with feature extraction methods, script features for selection feature selection are a subset of the original source features and have the advantages of semantic context, easy understanding, simple structure, and ease of use. Therefore, it has attracted the attention of many scientists and has become an important means of reducing the size.

3.2. Text Classification Based on Deep Learning. After analyzing the characteristics of traditional text classification

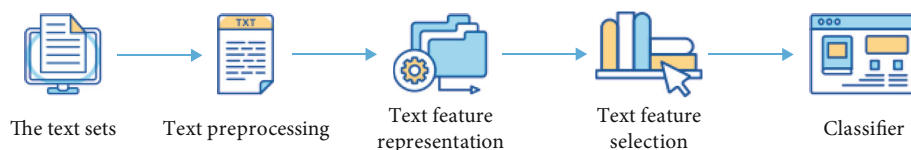


FIGURE 1: Text classification process.

methods, it will be found that when dealing with the problem of digital library text classification in the big data environment, there are many difficult problems to solve. In the process of feature extraction, manual participation is required, and it will affect the accuracy of the final extracted text features. The use of vector space models in text representation ignores the semantic and semantic information in the text, which affects text features; in the case of high-dimensional and sparse data, although attribute selection methods can be used to reduce dimensionality, it increases feature and data loss risks, making text processing more complex overall [15]. There are few features that do not affect the distribution of the text distribution process, Joachims said, and a good text distribution standard should take advantage of all features. Therefore, in order to complete the text work of the digital library in the era of big data, it is necessary to make the text more efficient, high quality, and higher in text design.

The authors' in-depth courses based on classification models for digital libraries include pre-written scripts, vector-based word representations, pamphlets, and classification using convolutional neural networks [16]. Text preprocessing uses word vectors to represent text, and the convolutional neural network in the deep learning model is used to extract text features and complete the final classification. The main process of deep learning-based digital library text classification is shown in Figure 2.

3.2.1. Text Preprocessing. Therefore, before the text classification, the original text information needs to be preprocessed; in this way, the subsequent text classification tasks can be carried out. The quality of text preprocessing has a great influence on the accuracy of text classification results. Text preprocessing mainly includes text segmentation and stop word removal.

- (1) *Participants:* Characters, words, and phrases in Chinese appear in sequence without specific segmentation. A word is the basic unit of meaning. When sorting text, a word is needed to describe the characteristics of the text. Therefore, Chinese word segmentation is a relatively basic and important link in text classification. At present, the word segmentation technology is relatively advanced, and word segmentation tools such as jieba word segmentation, Baoding analyzer, and ICTCLAS of the Chinese Academy of Sciences are widely used [17]
- (2) *Go to the station:* Delete words that are meaningless but frequently appear in the text. These words are not helpful for segmenting text, as they do not repre-

sent text, but increase the size of the text vector. This will affect the final effect of text classification; therefore, it needs to be removed so that the remaining text information can better express text features

3.2.2. Text Feature Representation: Word Vectors. When using deep learning to perform text classification tasks in digital libraries, it is first necessary to use text representation methods and convert semistructured or unstructured text into vector representations that computers can understand and process. In view of the problem of high latitude of vectors, data is scarce, there is no semantics in the traditional text distribution process, and the benefits of digital libraries are not good; the author uses the word vector method to represent the text content, which can effectively solve these problems.

The traditional text representation model represents the text features, which will make the text feature space very high, and the deep learning model cannot exert its powerful feature extraction ability when classifying it. With the proposal of word vector method, the text feature representation based on word vector provides a prerequisite for deep learning to be used for text classification tasks in digital libraries.

A word vector is a combination of each word in the text by plotting each word in the text as a constant of small dimension in real space. Instead of expressing multiple real spaces by separating vector space models, high-dimensional sparse vectors can be transformed into low-dimensional, dense real vectors.

Compared with the usual representation card, after the word vector is mapped in the new low-dimensional text feature position, the relationship between the word vector relative to words with different letters represents the relationship between texts, and it can provide richer textual semantic information. At the same time, the word vector method can overcome the problems of high vector dimension and data sparseness in grammar models. This is a big advantage that text representation does not have, so using word vector method to represent text can improve the quality and accuracy of distributed literature in digital libraries [18].

Word2vec is a tool for training and designing word vectors launched by Google in 2013 based on in-depth research. It can train a large amount of corpus conveniently, and through training, it can effectively map the feature words in the text into dense vector at low latitude.

3.2.3. Text Feature Extraction. In the context of the previous section, the use of word vectors to represent text solves the problem of text representation. This demonstrates the use of convolutional neural networks in deep learning standards to solve the problem of automatic subtraction of text distributions in digital libraries. As one of the most deeply researched

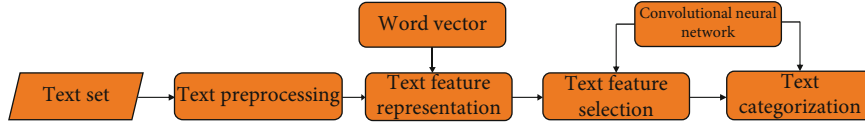


FIGURE 2: Text classification process based on deep learning.

models, neural communication has been used by many scientists to solve problems in natural language processing, and writers have attempted to use these connected neural languages to enable the distribution of text in digital libraries.

The basic structure of the convolutional neural network is shown in Figure 3. The first half consists of the input layer, and the middle part consists of the multirecurrent layer and the consolidation layer; i.e., an additional recurrent layer is added. The second half consists of a generic connection layer and an output layer, where one layer is connected first and then to the recurrent layer [19].

The training of convolutional neural networks can be thought of as a healing problem, and the functional objective should be designed to be maximized or reduced according to the healing objective. In in-depth research, job cost is often used as a job objective by proper terminology, and job cost is the error in measuring the distribution of objects. Calculate the result and the actual value; the operating cost is usually used in the division function and is the average value of the cross-entropy loss function of each model. Cross-entropy is a measure of the similarity of two probability distributions, and the target distribution is expressed as $p(x)$, the distribution obtained by prediction estimation is denoted as $q(x)$, and the cross-entropy between them is defined as the following formula (1) [20]:

$$H(p, q) = -\sum_x p(x) \log q(x). \quad (1)$$

If the label value is represented by a one-hot vector, that is, the label value for k -category classification is represented as a target vector of length k : $[p^1, \dots, p^j, \dots, p^k]$; if the target class is $y_i = c$, then let $p^c = 1$, all other items are 0, and then, the final objective function can be expressed as formula (2). The expression $1\{c = y_i\}$ indicates that the condition in the parentheses is satisfied, and then take 1; otherwise, it is 0.

$$L = -\frac{1}{m} \sum_{i=1}^m \sum_{c=1}^k 1\{c = y_i\} \cdot \log \frac{e^{z_c}}{\sum_{j=1}^k e^{z_j}}. \quad (2)$$

The convolution process can eliminate the different local features of the text, and the lower-level convolution process can eliminate the lower-level features of the text such as words, phrases, sentences, lines, and words, and the high-level convolution process can be omitted. High-level features of text, such as sentences, phrases, semantics, etc. The background of the convolutional layer is the pooling layer, which can give semantically similar text features and play the role of secondary feature extraction. The combination of convolution process and layer pooling process is based on the whole ensemble process, and the role of the whole connection pro-

cess is to identify and assign various local concepts. The function of the full connection layer is to summarize and classify various local text features extracted from the convolutional layer and the pooling layer. Similar to the function of classifiers in traditional text classification, classification information is finally obtained through the output layer.

The special network structure of convolutional neural network makes it have the following characteristics: ① The special structure of the convolutional neural network makes it good at processing grid-type data. Convolutional neural networks can prove their ability to eliminate images and speech, which is why image and speech data are meshed. Data is the difference between images and speech, data is the solution, and the text represented by the model is written as a representation of the negated text using a convolutional neural network. By using the word vector method to represent the text features, the text features can be converted into continuous and dense two-dimensional grid data similar to images and speech, which can be well-processed by the convolutional neural network. ② The combination of convolutional process and layer pooling specially built for convolutional neural networks can exclude locally unreliable features at various levels in the text. Compared with the design structure in the traditional text, the convolutional neural network can learn the characteristics of the data file, which not only saves time and effort, but also avoids the negative impact of the accumulation of errors caused by manual feature extraction. The extracted features are stronger than discrimination ability. ③ When using convolutional neural network to classify text, the feature extraction and classification of text are taken as a whole. In traditional text classification methods, the feature extraction part of text and the classifier are two independent parts. In the convolutional neural network, the feature extraction and classification of text are carried out in the convolutional neural network; as the input of the convolutional neural network, the word vector will be continuously optimized with the training of the network; and therefore, the performance of the joint collaboration of feature extraction and classification as a whole can be maximized, thereby further improving the effect of text classification.

Convolutional neural networks can simplify the process by the aggregation and stacking of layers and layers, which can extract higher-level and more complex solutions, which can render text more intensely, affecting the main features. Convolutional neural network can deepen the number of layers through the accumulation and superposition of convolutional layer and pooling layer, so as to extract higher-level and more abstract text features, so that text features have stronger expression ability and more accurately reflect the essential features

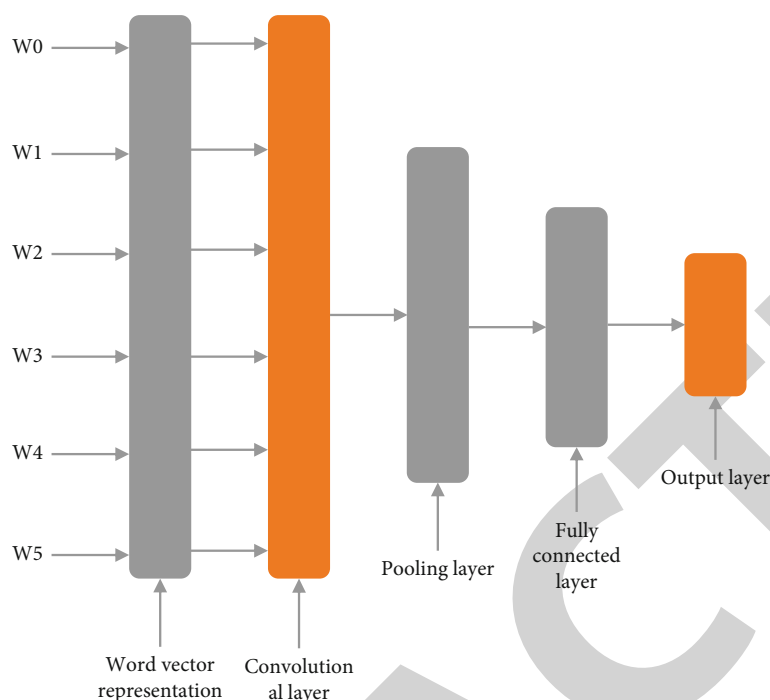


FIGURE 3: Structure diagram of text classification based on convolutional neural network.

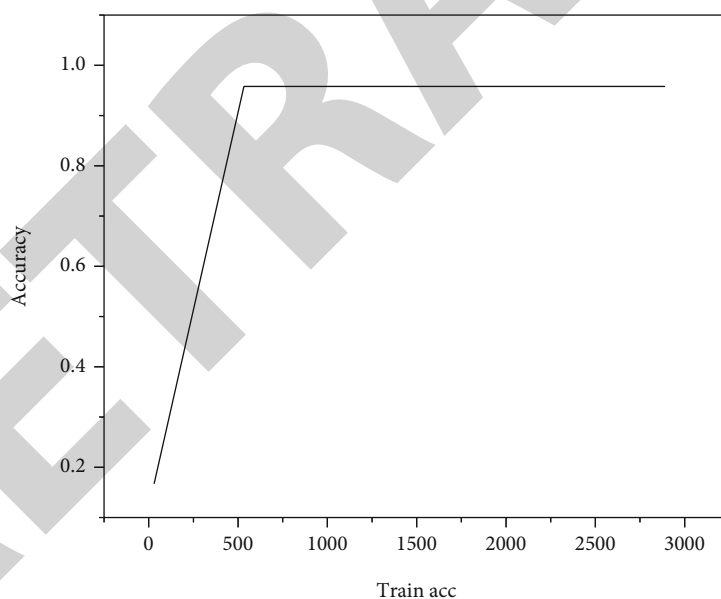


FIGURE 4: Error rate and accuracy rate of model training set.

of text. While the depth of the layers can be more complex and time-consuming, this can be compensated by increasing hardware performance. Therefore, convolutional neural networks are used to solve the text features of digital libraries, which can improve the performance and accuracy of distribution.

4. Analysis of Results

The authors conducted experiments to determine the distributional advantages of a depth-based digital library. Using

convolutional neural network, the experiment of Chinese distribution is carried out through Google's open source deep learning TensorFlow [21]. The most common measures we use in text distribution are to measure the benefits of text distribution: precision, recall, and F1 value.

The experimental data is selected by the author from a set of public records set up by a school's natural language laboratory. The experimental data consists of 10 categories: sports, finance, real estate, real estate, education, technology, fashion, current affairs, sports, and entertainment. There are 6500 pieces of information in the category, and the

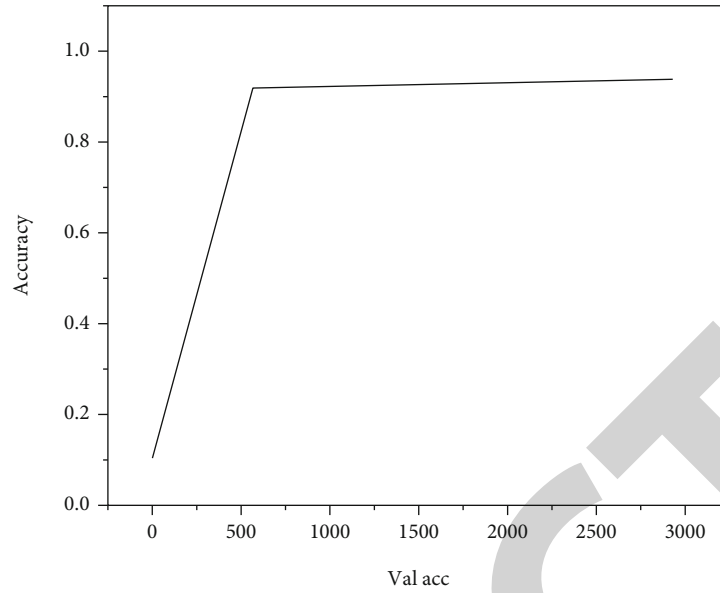


FIGURE 5: Error rate and accuracy rate of model validation set.

TABLE 1: Statistics of experimental results of text classification.

Category	Traditional text classification methods			Deep learning-based text classification		
	Accuracy (P)	Recall (R)	F1	Accuracy (P)	Recall (R)	F1
Entertainment	0.78	0.79	0.78	0.94	0.96	0.95
Game	0.83	0.83	0.83	0.96	0.94	0.95
Current affairs	0.86	0.81	0.84	0.96	0.91	0.93
Fashion	0.86	0.87	0.87	0.93	0.96	0.94
Technology	0.86	0.85	0.85	0.95	0.96	0.96
Educate	0.77	0.76	0.76	0.9	0.92	0.91
Furniture	0.87	0.82	0.85	0.95	0.9	0.93
Real estate	0.87	0.89	0.88	0.98	0.96	0.97
Finance	0.82	0.84	0.83	0.94	0.97	0.96
Physical education	0.81	0.83	0.82	0.97	0.97	0.97
Average value	0.833	0.829	0.831	0.948	0.945	0.947

information layers are divided as follows: 5000 * 10 for training process, 500 * 10 for usability, and 1000 * 10 for testing process.

In the preliminary data set, the data experiments were segmented using the ICTCLAS term segmentation system of the Chinese Academy of Sciences. In the process of text representation, the word2vec tool is used to identify the vector representation of text data, and the convolutional neural network model and the convolutional neural network model are studied with the text receiving vector content as the input. And complete the TensorFlow platform test.

Before using the training process and the verification process to train the convolutional neural network, after the training process accuracy rate is stable, it is above 95%, as shown in Figure 4, and the verification process accuracy rate is stable at about 94%, as shown in Figure 5; the text distribution and the performance on training and implementation are very good.

Finally, the distribution results of the convolutional neural network distribution model are identified by a test procedure not included in the training. And vector format is always available for text feature representation, and text selection using TF-IDF is used to compare distributions. The comparative experimental results are shown in Table 1, and the F1 values of the two text distribution methods are compared, as shown in Figure 6. An in-depth study of the average accuracy and average return is shown in Table 1 and Figure 6. According to the text distribution about 94.8% and 94.5%, respectively, the average accuracy and average return of the text distribution process are usually between 83.1% and 82.9%, especially for the deep learning-based text distribution, and the accuracy and the return of the distribution results are very good.

The F1 value of entertainment, games, technology, education, finance, and sports has increased by a large margin, while the F1 value of current affairs, fashion, furniture, and real estate

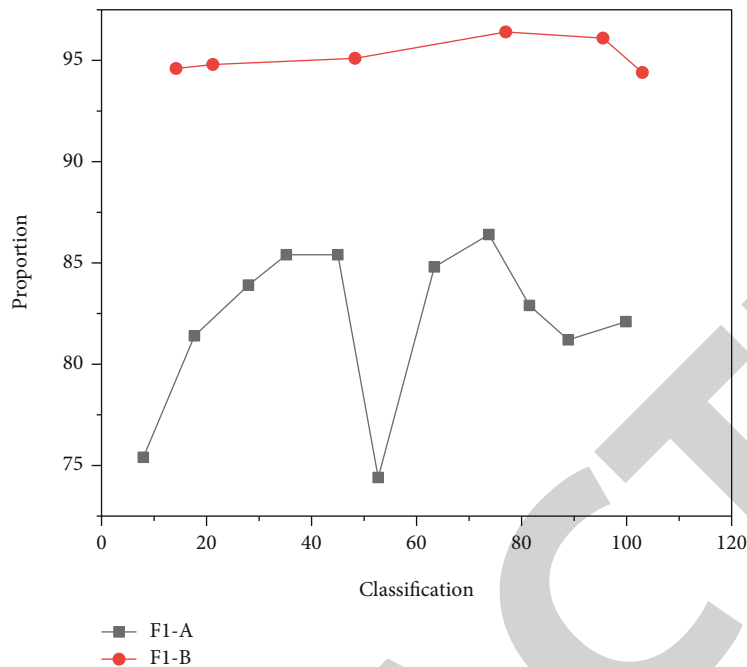


FIGURE 6: Comparison of F1 values.

has increased relatively little; compared with the traditional text classification method, the text classification method based on deep learning improves the average F1 value by about 11.6%. Therefore, in general, according to the well-studied text distribution used in this paper, it can improve the results of text distribution compared to the text distribution model. This shows that text is represented by word vectors, and then, the neural network connections in the deep learning model are used to extract and segment the text, which can help improve the efficiency of book distribution in digital libraries.

5. Conclusion

On the basis of analyzing the text distribution model of digital library, a text distribution model of digital library based on depth and text model is proposed, while word vectors can carry the syntactic and semantic text of the text, a special hierarchical model connected by a neural network of deep learning models, and features at the syntactic and semantic levels, such as words, phrases, phrases, and sentences. Texts can be taught by themselves. Combining texts with word vectors and convolutional neural networks can work together on the text distribution of digital libraries, which can solve the problems that have always existed in texts. The experimental results show that, compared with the standard text distribution model based on the vector space model, the depth-based digital library text distribution model can meet the author's requirements, and the distribution effect is better.

Data Availability

The data used to support the findings of this study are available from the corresponding author upon request.

Conflicts of Interest

The authors declare that they have no conflicts of interest.

Acknowledgments

The second batch of science and technology projects of Fuzhou Science and Technology Bureau: digital library knowledge service platform based on WeChat official account's open source big data (project number: 2021-SG-039).

References

- [1] L. Gu, "Integration and optimization of ancient literature information resources based on big data technology," *Mobile Information Systems*, vol. 2021, no. 3, Article ID 6452418, 8 pages, 2021.
- [2] Q. Jia, "Research on mobile learning in a teaching information service system based on a big data driven environment," *Education and Information Technologies*, vol. 26, no. 5, pp. 6183–6201, 2021.
- [3] X. Lv and M. Li, "Application and research of the intelligent management system based on internet of things technology in the era of big data," *Mobile Information Systems*, vol. 2021, no. 16, Article ID 6515792, 6 pages, 2021.
- [4] J. Wang, "Massive information management system of digital library based on deep learning algorithm in the background of big data," *Behaviour and Information Technology*, vol. 5, pp. 1–9, 2020.
- [5] M. Shi, "Knowledge graph question and answer system for mechanical intelligent manufacturing based on deep learning," *Mathematical Problems in Engineering*, vol. 2021, no. 2, Article ID 6627114, 8 pages, 2021.

Retraction

Retracted: Energy Efficiency Improvement of Composite Energy Building Energy Supply System Based on Multiobjective Network Sensor Optimization

Journal of Sensors

Received 17 October 2023; Accepted 17 October 2023; Published 18 October 2023

Copyright © 2023 Journal of Sensors. This is an open access article distributed under the Creative Commons Attribution License, which permits unrestricted use, distribution, and reproduction in any medium, provided the original work is properly cited.

This article has been retracted by Hindawi following an investigation undertaken by the publisher [1]. This investigation has uncovered evidence of one or more of the following indicators of systematic manipulation of the publication process:

- (1) Discrepancies in scope
- (2) Discrepancies in the description of the research reported
- (3) Discrepancies between the availability of data and the research described
- (4) Inappropriate citations
- (5) Incoherent, meaningless and/or irrelevant content included in the article
- (6) Peer-review manipulation

The presence of these indicators undermines our confidence in the integrity of the article's content and we cannot, therefore, vouch for its reliability. Please note that this notice is intended solely to alert readers that the content of this article is unreliable. We have not investigated whether authors were aware of or involved in the systematic manipulation of the publication process.

Wiley and Hindawi regrets that the usual quality checks did not identify these issues before publication and have since put additional measures in place to safeguard research integrity.

We wish to credit our own Research Integrity and Research Publishing teams and anonymous and named external researchers and research integrity experts for contributing to this investigation.

The corresponding author, as the representative of all authors, has been given the opportunity to register their agreement or disagreement to this retraction. We have kept a record of any response received.

References

- [1] J. Huang, "Energy Efficiency Improvement of Composite Energy Building Energy Supply System Based on Multiobjective Network Sensor Optimization," *Journal of Sensors*, vol. 2022, Article ID 6935830, 11 pages, 2022.

Research Article

Energy Efficiency Improvement of Composite Energy Building Energy Supply System Based on Multiobjective Network Sensor Optimization

Jingyun Huang 

Building Environment and Energy Application Engineering, School of Energy and Security Engineering, Tianjin Urban Construction University, Tianjin 300384, China

Correspondence should be addressed to Jingyun Huang; 631418020207@mails.cqjtu.edu.cn

Received 21 May 2022; Revised 7 June 2022; Accepted 20 June 2022; Published 1 July 2022

Academic Editor: C. Venkatesan

Copyright © 2022 Jingyun Huang. This is an open access article distributed under the Creative Commons Attribution License, which permits unrestricted use, distribution, and reproduction in any medium, provided the original work is properly cited.

In order to solve the problem of improving the energy efficiency of the energy supply system, the author proposes a method for improving the energy efficiency of the energy supply system of composite energy buildings based on multiobjective grid optimization, the method solves the energy efficiency improvement of the grid-optimized composite energy building energy supply system, with the increasing material needs of people, the traditional fossil energy consumption is increasing, and the environmental pollution problem is also becoming more and more serious, and people will face serious energy crisis. Due to the high proportion of coal in China's energy, most thermal power plants use coal as fuel to generate electricity. In the process of coal combustion power generation, a large amount of air pollutants such as CO_2 , SO_2 , and NO_x are produced, which destroys the ecological environment. In order to alleviate the energy crisis and reduce the emission of polluting gases, the development of renewable energy sources such as wind energy and solar energy is extremely important. Electricity supply and heat supply account for the main part of China's energy consumption, 40% of China's energy consumption is used for electricity supply, and 25% is used for heat supply. In terms of electricity supply, 12% of electricity is used for residential use, about 74% is used for industrial production, and 14% is used for commercial development.

1. Introduction

The microgrid unifies the distributed power generation units into an organic whole, the original microgrid can only provide electricity for users, with the development of multi-energy interconnection, the combined heat and power system is connected to the microgrid, so that the microgrid can provide electricity to users, which can also provide thermal energy, and it realizes the transformation from microgrid to microenergy grid. Adding the energy storage system to the cogeneration microgrid, it can better realize the combined electric and heat dispatching of the system, making the system more flexible and controllable. Due to the joint supply of electric energy and heat energy to users at the same time, the distributed power sources in the cogeneration microgrid are becoming more and more diverse and complex, which also makes the flexible scheduling of each

unit in the microgrid more difficult; therefore, it is better to study the synthesis of various energy microgrids. Reducing energy and environmental energy impacts, making total energy use renewable and reducing emissions, are the best goals of many economic and environmental decisions, worth looking into around cost. Study the combined electric and heat dispatching of CHP-type microgrid; it is beneficial to the unified management of energy and the coordinated operation of the system. By optimizing the output of each unit of the microgrid, the energy flow of the multienergy interconnected microgrid system is efficiently optimized. The combined optimization of electricity and heat for the microgrid can improve the peak shaving capacity of the unit. In the microgrid system, the cogeneration unit mostly works in the working mode of "heat-based electricity," in this mode, due to the constraints of the unit's electric-heat coupling; the unit's electrical output follows the thermal output,

which makes the unit inflexible operation, reducing the effect of the unit on load peak shaving and valley filling. The author adds electric energy storage and thermal energy storage devices to the combined electric and heat system of the microgrid and installs an electric boiler for electric-heat conversion, which will greatly decouple the electric-heat coupling characteristics of the CHP unit. The microgrid studied by the author not only operates in connection with the large power grid but also operates in connection with the thermal grid; in this operating mode, the microgrid can exchange electrical energy with the grid and thermal energy with the thermal grid, which not only improves the flexibility of the system control, the comprehensive utilization of energy is realized, and the operating cost of the whole system is reduced.

2. Literature Review

Bhattarai et al. said that, in recent years, China has experienced multiple severe storms, and the habitat has persisted, facing the dual efforts of energy conservation and emission reduction and environmental constraints [1]. Kalkan et al.'s power industry is the key to emission reduction. In the face of energy saving and emission reduction, only improving the power generation capacity of equipment can no longer adapt to the construction of low-carbon industries under the new situation [2]. Brahim and Abderafi said that the "13th Five-Year Plan" period is to continue to deepen China's energy revolution; it is an important period for the comprehensive realization of energy transformation and development [3]. Dan et al. said that in the context of structural reforms on the energy supply side, the decentralized form of clean energy utilization will develop rapidly, and the power market reform will also drive the power industry, from supply-side management to both demand-side and supply-side management [4]. Yu and Song said that with the promotion of smart grid and energy Internet technologies, a large number of distributed power sources and demand-side resources will participate in the optimal scheduling of power systems [5]. Li et al. said that distributed renewable power, demand response, electric vehicles, and other demand-side resources have been paid attention to because of their advantages of low maturity, fast response, and low pollution emissions [6]. Storodubtseva et al. said that users reduce electricity load by using energy-efficient terminal equipment or responding to electricity price signals, use demand-side resources to partially replace the output of units with high power supply costs, reduce pollutant emissions, and realize comprehensive and optimal allocation of power resources; the power system has the characteristics of simultaneous completion of power generation, power supply, and power consumption, and electrical energy cannot be economically stored on a large scale [7]. Punsawat and Makcharoen said that this requires that the entire power system dispatching must be balanced in real time; in order to cope with the pressure on resources and the environment, China will develop and utilize renewable energy on a large scale and increase the proportion of clean energy, and by 2020 and 2030, the proportion of nonfossil energy in China

will reach 15% and 20%, respectively [8]. Berawi and others believe that in the future, a large number of wind power, photovoltaic power generation, and other renewable energy power generation with random fluctuation characteristics will be connected to the grid, which will seriously threaten the quality of power transmission and the safe operation of the power system [9]. Among them, the distributed power generation resources with scattered layout, because of their small installed capacity, as a result, is difficult to fully participate in the competition in the electricity market. Serale et al. said that in order to alleviate the above negative effects, stabilize the volatility of renewable energy power generation output, give full play to the positive effect of clean energy power generation, and promote the development of distributed energy, virtual power plants have received increasing attention [10]. A virtual machine is an integrated power plant that combines the control of energy and small electronic devices through technologies such as data, control, respect, and communication. Power distribution is usually the distribution of electrical equipment, the required capacity, and the distribution of electrical equipment that can be connected to the grid. With the development of Internet energy technology, virtual machine owners can directly participate in the equipment and demand balance in electrical energy, optimize the power load curve, and promote the utilization of renewable energy. At present, China's economy has entered a new normal, and its development mode will also change from relying on excessive consumption of energy resources, turn to pursue the quality of economic growth, and optimize the economic structure. The goal of future power industry development will not only support economic development but also improve the quality of power consumption and the sustainable development of the ecological environment. The deepening of China's power system reform is driving the power industry to shift from single supply-side resource planning to comprehensive power resource planning and from supply-side management to demand-side and supply-side comprehensive management, and virtual power plants are also developing in the direction of marketization, as shown in Figure 1.

3. Methods

In the power business environment, two types of on-site application of virtual power plants can establish a relationship. Price-based demand-responsive virtual power plants focus on different applications, combine multiple pricing strategies, and interact with different levels of the virtual power industry. Incentive-based application fields' virtual power plants can bring together a variety of ideas to participate in medium- and long-term power markets, daily markets, and real-time markets [11], the time period in which two types of demand response virtual power plants participate in the electricity market. As a result, power operators need to integrate multiple demand response options, adjusting the need for capital participation in market value and timing accordingly. As different industries, formulate strategies to participate in the power industry, as shown in Figure 2.

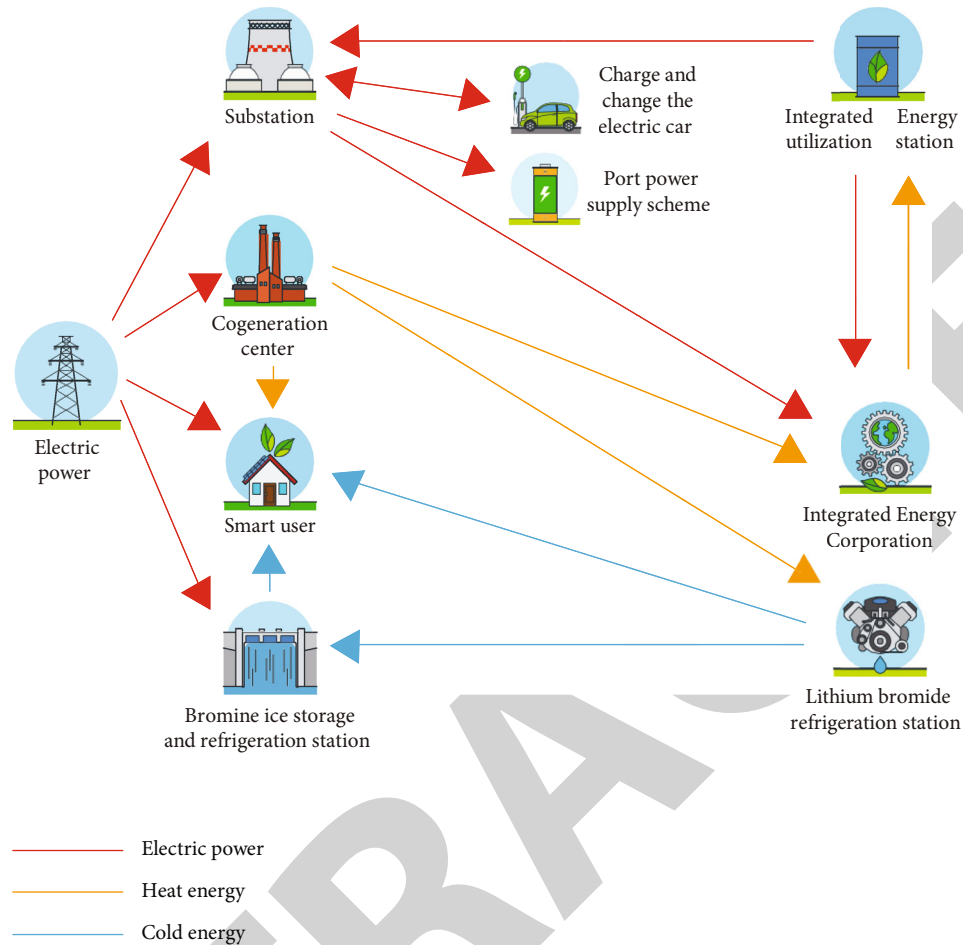


FIGURE 1: The energy efficiency improvement of the energy supply system of composite energy buildings based on multiobjective network optimization.

During system dispatch, the demand response virtual power plant can be regarded as the generation output and compete with traditional generator sets in the power market [12, 13]. Therefore, the authors compare the similarities and differences between traditional generator sets and demand response virtual power plants. The output of the two types of power plants is similar in that there are upper and lower output constraints, system ramp rate constraints, and operating cost constraints. But they have many differences in minimum downtime, number of system calls, and startup cost, as shown in Table 1.

This section will consider market operation strategies based on price-based demand response projects; it acts as a price taker to purchase electricity in a multilevel market to meet the electricity demand of users. In the electricity market environment, the transaction and scheduling process of virtual power plant operators is shown in Figure 3.

From a transaction point of view, as the main body of electricity sales of virtual power plant operators, a reasonable time-of-use price strategy is formulated downward to attract users to participate in the response to load reduction and upward through the power dispatch trading center and power generation entities to carry out medium- and long-term transactions and spot transactions, in order to purchase

electricity to meet the needs of users and obtain the income from the purchase and sale of electricity. E-commerce companies transmit the changes in electricity prices in the store to consumers through electricity consumption time and encourage users to adjust the power consumption and reduce the maximum voltage. After assembly, the “negative” motor unit can generate peak hours [14]. Therefore, through the time-of-use electricity price, the virtual power plant operator can save electricity purchase cost and system operation cost. From the perspective of dispatching, the main body of electricity sales collects the electricity price response information of users downward, summarizes the overall load reduction, and uploads it to the dispatch center, which adjusts the power generation dispatch plan during peak, flat, and valley periods [15, 16]. Based on the maximization of its own interests and the requirements of system energy-saving scheduling, the main power generation entity will readjust the operation combination of the units. In a commercial environment, the demand for virtual power plants by electricity sellers needs to purchase electricity from the electricity market, medium- and long-term electricity, and retailers to meet the needs of consumers. Electricity will be sold to consumer. This chapter will consider the changes in the electricity sales revenue of e-commerce after using the peak-

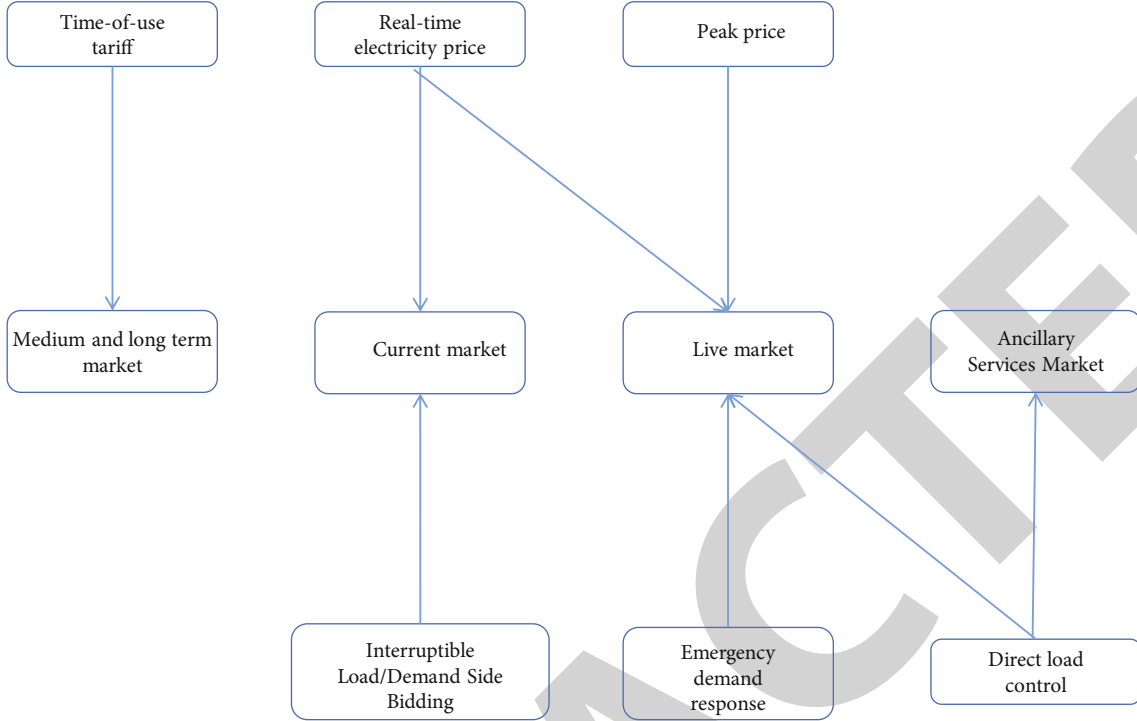


FIGURE 2: Schematic diagram of the time period when virtual power plants participate in the electricity market.

TABLE 1: Differences between traditional power plants and demand response virtual power plants.

Project	Traditional power plant	Price-based demand response VPP	Incentive demand response VPP
Minimum start and stop time	√	×	√
System call limit	×	×	√
Unit start-up cost	√	×	×

valley electricity price and explain the impact of the peak-valley time-sharing rate of virtual power plants. Based on the cost, the power equipment must be sourced and retailed in the medium- and long-term market. In the medium- and long-term market, based on the game of consumer electronic transportation, a part of electricity is purchased at a certain cost with the energy generated by both parties or the virtual consumer electricity market that competes in the middle [17]. In the current electricity market environment, power generation companies finally sell power generation loads for multiple periods of time to users at one price. Therefore, in the medium- and long-term market, the author does not consider the impact of the peak-valley time-of-use electricity price on the power generation side on the main body of electricity sales. Before the implementation of peak and valley electricity prices, the electricity purchase cost of electricity sellers in the medium- and long-term electricity market is shown in

$$C_{ml}^0 = \rho^{ml} \bullet L^{ml0}. \quad (1)$$

Among them, ρ^{ml} is the transaction price of electricity sellers in the medium- and long-term electricity market,

L^{ml0} is the electricity purchase volume of electricity sellers in the medium- and long-term electricity market, it is obtained by predicting the electricity consumption of the user side in the previous transaction period. Among them, $L^{ml0} = \sum_{t=1}^t \theta L_t^0$ and θ are the proportion of electricity purchased by electricity sellers in the medium- and long-term electricity market. L_t^0 is the load demand at time t before the implementation of the peak-valley electricity price. The electricity purchase cost C_{sp} of the electricity seller in the spot market before the implementation of the peak-valley electricity price is shown in

$$C_{sp} = \sum_{t=1}^T \rho_t^{sp} L_t^{sp0}. \quad (2)$$

Among them, ρ_t^{sp} is the electricity purchase price of the electricity seller at time t in the spot market, ρ_t^{sp} is the electricity purchased in the spot market at time t , and $\sum_{t=1}^T L_t^{sp0} = (1-0) \sum_{t=1}^T L_t^0$. In the spot market, the electricity purchase price of the electricity sellers in each period will fluctuate with the market price, and there is uncertainty. The author uses expectation theory to deal

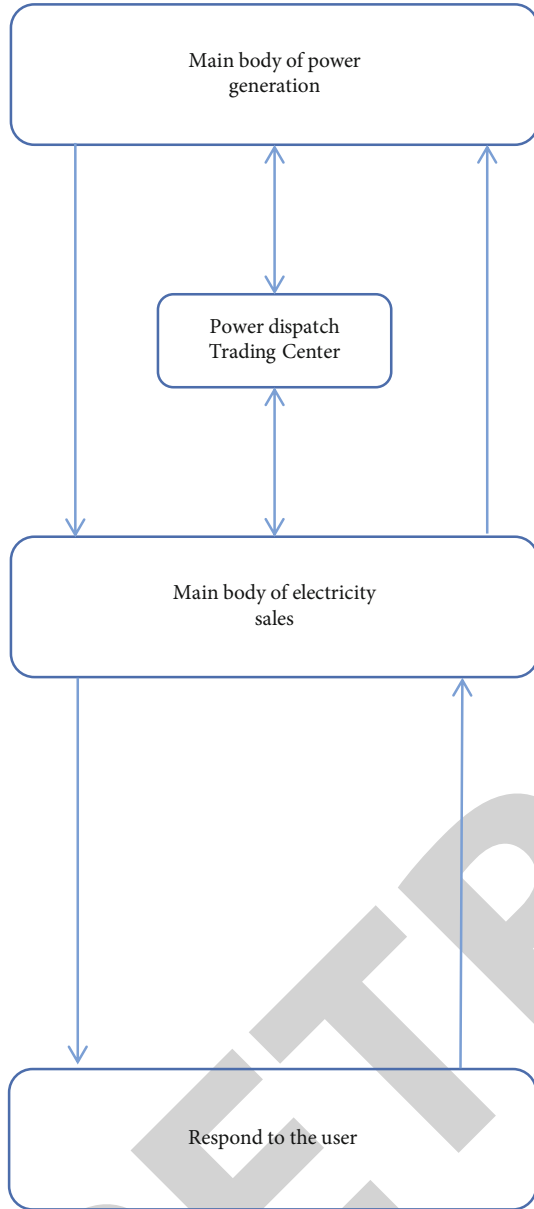


FIGURE 3: Market operation mechanism of price-based demand response virtual power plants.

with market price fluctuations, and the main body of electricity sales is affected by the fluctuations of spot market electricity prices. Assuming that there are s scenarios of electricity price fluctuations in the spot market at time t , the electricity price in each scenario is $\rho_{s,t}^{sp}$, and λ_s^{sp} represents the probability of occurrence of each scenario, then the expected electricity purchase cost C_{sp}^0 faced by the electricity seller is represented, as shown in

$$C_{sp}^0 = \sum_{t=1}^T \sum_{s=1}^S \lambda_s^{sp} \rho_{s,t}^{sp} L_t^{sp0}. \quad (3)$$

After using the maximum power consumption, the user's power consumption will change at any time. It is

assumed that the concept of e-commerce purchasing power in the medium- and long-term market and retail market remains unchanged, that is, the proportion of electricity purchases remains unchanged, then the electricity sellers are in the mid-to-long-term and spot markets, and the electricity purchase cost in the long-term market is shown in

$$C_{ml}^{PB} = \rho^{ml} \cdot L^{mlPB}. \quad (4)$$

Among them, $L^{mlPB} = \sum_{t=1}^r \theta L_t^{PB}$ and L_t^{PB} are the load demand at time t after the implementation of the peak-valley electricity price. The electricity purchase cost C_{sp}^{PB} of the electricity seller in the spot market is shown in

$$C_{sp}^{PB} = \sum_{t=1}^T \rho_t^{sp} L_t^{spPB}. \quad (5)$$

Based on price uncertainty, the electricity purchase cost of electricity sellers in the spot market after the implementation of peak and valley electricity prices is shown in

$$C_{sp}^{PB} = \sum_{i=1}^T \sum_{s=1}^S \lambda_s^{sp} \rho_{s,t}^{sp} L_t^{spPB}. \quad (6)$$

Before the implementation of the peak-valley time-of-use electricity price, the revenue of the electricity sales company is the electricity sales revenue based on the fixed selling price, as shown in

$$I_{sell}^0 = \rho_0 \sum_{i=1}^{N_c} \sum_{t=1}^T L_{i,t}^0. \quad (7)$$

Among them, N_c is the number of users, $L_{i,t}^0$ is the electricity load of user i at time t , and ρ_0 is the fixed sales price. After the implementation of the peak-valley electricity price, the income of the electricity sales company becomes as shown in

$$I_{sell}^{PB} = \rho_p \sum_{i=1}^{N_c} \sum_{t=1}^{T_p} L_{i,t}^{PB} + \rho_f \sum_{i=1}^{N_c} \sum_{t=1}^{T_f} L_{i,t}^{PB} + \rho_v \sum_{i=1}^{N_c} \sum_{t=1}^{T_v} L_{i,t}^{PB}. \quad (8)$$

Among them, ρ_p , ρ_f , and ρ_v are the electricity sales prices during peak, normal, and valley periods, respectively. T_p , T_f , and T_v represent the peak period, the valley period, and the peace period, respectively.

Therefore, the profit TR^0 of the virtual power plant operator before the peak and valley electricity price is shown in

$$TR^0 = I_{sell}^0 - C_{sp}^0 - C_{sml}^0. \quad (9)$$

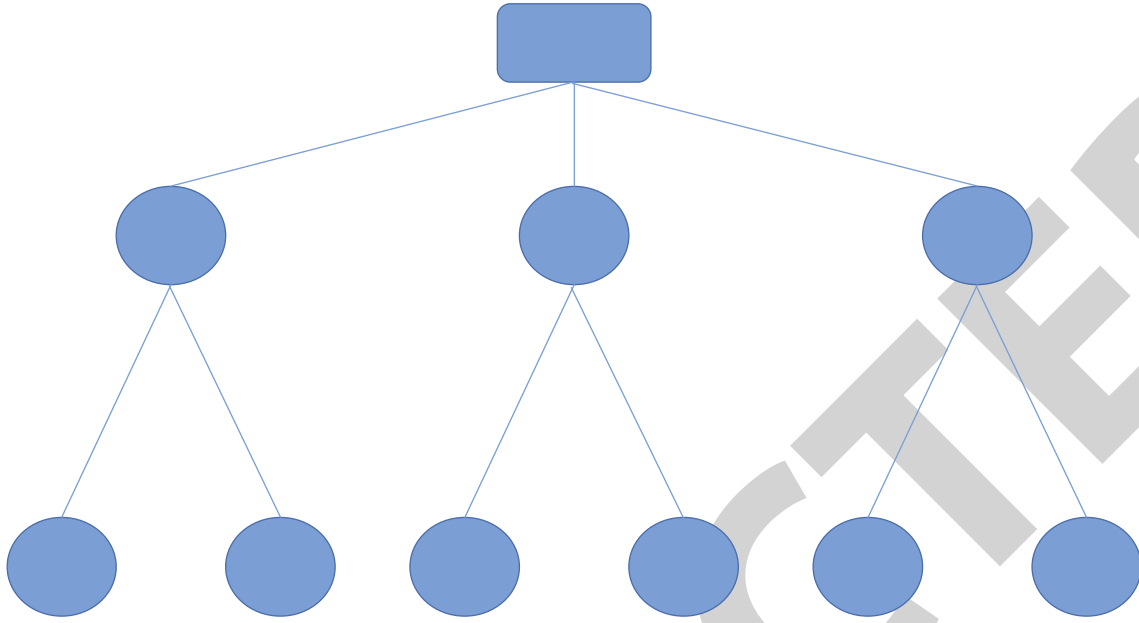


FIGURE 4: Hierarchical structure diagram of AHP.

It is arranged as shown in

$$TR^0 = \rho_0 \sum_{i=1}^{N_c} \sum_{t=1}^{T_p} L_{i,t}^0 + \sum_{i=1}^T \sum_{s=1}^S \lambda_s^{sp} \rho_{s,t}^{sp} L_t^{sp0} - \rho^{ml} \bullet L^{ml0}. \quad (10)$$

The steps of fuzzy AHP decision-making based on the concept of horizontal triangle number are as follows, establishing the AHP hierarchical structure of indicators. Based on this hierarchical structure, the decision problem can be divided into three levels, namely, the target decision level, the criterion level, and the element level, as shown in Figure 4.

Judgment matrix is established by pairwise comparison between indicators. First, the pairwise comparison results of the importance of each indicator are collected by experts in the form of a questionnaire [18]. Due to the ambiguity of expert decision-making, the pairwise comparison results of indicator importance are represented by linguistic variables such as extremely important, very important, obviously important, slightly important, and equally important [19]. To determine the feasibility and performance of the various peak turnaround time cost-benefit models used in this chapter, the area considered by the S Electricity Marketing Company was used as an example to evaluate, for example, the typical load in this area before using peak-valley electricity; the peak-valley load is 1532 MW, and the valley load is 687 MW [20]. The author formulates the peak-valley electricity price strategy based on the original load data of this typical day, as shown in Figure 5.

Based on the market transaction model of demand response VPP in the VPP business model, the author discusses the operation mechanism of demand response VPP participating in the power system based on China's electricity market environment; the pricing decision model of price-based demand response VPP is established. Firstly,

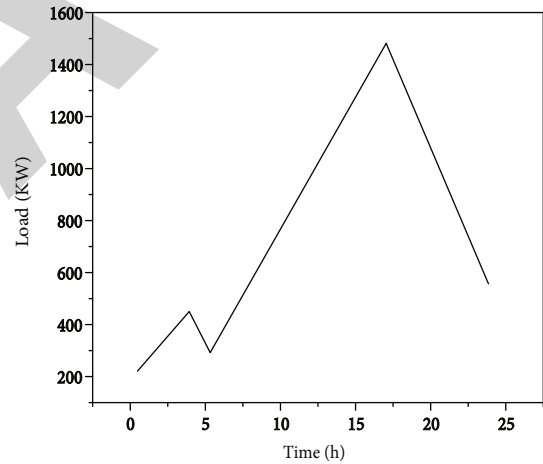


FIGURE 5: Typical daily load in the area under the jurisdiction of the electricity sales company.

based on the characteristics of demand response, the demand response VPP is classified, and its operating characteristics are described, and from the perspective of participating in the market, it analyzes the relationship between price-based demand response VPP and incentive-based demand response VPP. Then, it focuses on the market share strategy of price-based demand response VPP with electricity sales companies as the main body and analyzes the impact of using peak-valley time-sharing from the perspective of price tariff and evaluated the use of VPP. The revised VPP response will focus on analysis in Chapter 4. Finally, the rate is calculated based on the peak-to-valley time period divided by the K-means path and the user's response to the electricity consumption peak-to-valley time. A cost-benefit model determination based on VPP response request is established with public utility companies as the main body

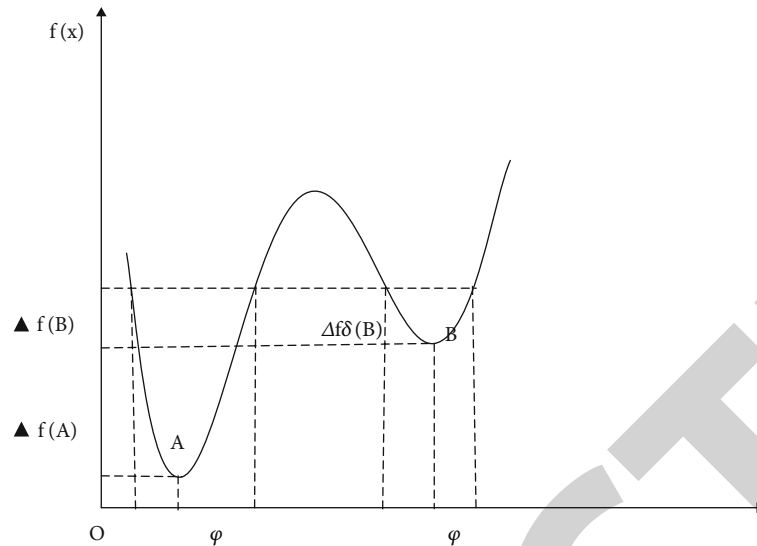


FIGURE 6: Schematic diagram of the robustness of the solution.

and peak and valley time utilization as the basis. Among them, the optimization objective selects the minimum coal consumption of the system, the minimum peak-to-valley load difference, and the minimum user electricity expenditure, and based on the fuzzy AHP method, the multiobjective optimization problem is transformed into a single-objective optimization problem. The results of the case analysis show that the implementation of the peak-valley electricity price can reduce the coal consumption of the system, reduce the peak-valley load difference, and reduce the user's electricity bill.

4. Analysis of Results

Due to the controllability of the output of traditional conventional generator sets, the power generation can be stable without fluctuation, while the power generation of wind turbines has fluctuations, and the random change of wind power will affect the balance of power generation of the entire system. Due to the influence of my country's climate, the output of wind power is usually larger at night and smaller during the day, and there is no load at night, and the day is the maximum load time, if the maximum shaving power is capable. Not enough, some air will be blocked. When wind power is connected to the grid, the uncertainty of wind power will affect the voltage and frequency of the system, the system voltage will exceed the limit or change, the air volume change rate at the point close to the wind turbine is larger, and the additional point is less affected [21]. When the wind speed is unstable, sometimes, it is greater than the cut-in wind speed, and sometimes, it is less than the cut-in wind speed, causing the fan to start and stop continuously, thereby increasing the frequency of system instability. As the compression power of the wind turbine increases, in order to reduce the impact of the wind turbine, the storage capacity of the wind turbine is further increased. RDES are distributed to end users as a combination of cooling, heating, and power systems, combined with local renew-

able and nonrenewable energy sources, and operate in a network with large projects and power pipelines to provide air conditioning, heating, and electricity, users in the same region at the same time, and other electrical services. Design, inspection, and refinement are important steps in understanding the R&D process, and China has done extensive R&D. In order to improve the quality of power distribution, China has done a lot of research on the development and improvement of power distribution. Model (building 233234) is based on a model that focuses on different applications and uses different tools and procedures to improve the model. However, most of the existing models start with a distributed power solution and provide other power sources in the area to optimize the solution from standard designs. Compared to traditional air conditioning and heating systems in the region, more power input and more power output of RDES data can lead to safety, performance-quality and high-quality electronics, integration of operations, and data flow, as well as communication, control technology, and information technology have been used to improve efficiency, improve energy efficiency, and provide feedback for the stable and efficient operation of RDES. Based on the consensus on the transmission of electricity and the main force in the network, Internet power will definitely take the main force as the "history," "network," and use distributed systems, microgrids, and other sites in a large-scale Regional Energy Internet Network. RDES with the characteristics of Internet energy is not a simple superposition of multiple energy sources. It has multiple connectivity such as power generation, power conversion, energy storage, and electricity consumption, as well as the interaction and connection of various energy sources. The flow of air conditioning, heating, and electricity in the system, through the integration of information fusion technology, realizes the extensive use and integration of energy at different levels and realizes the integration and exchange efficiency of various energy integrations, an energy system [22]. With the increasing dependence of various scheduling

and control functions of the physical system on the information system, this puts forward higher requirements for the integrity, accuracy, and timeliness of information quality, that is to say, in the energy Internet, information systems are as important as physical systems. The basis for the research on the interaction between information and physical systems in the energy Internet is the unified modeling of information systems and physical systems, referred to as cyber-physical modeling. Cyber-physical systems with cyber-physical modeling and optimal control as the core are considered to be the future development direction of power systems; there have been some discussions on the cyber-physical modeling of power systems, but the research on cyber-physical modeling in the field of energy Internet has just begun. On the basis of the general structure of the regional distributed energy system, the author proposes a multiagent system- (MAS-) based regional energy Internet architecture model under the combined cooling, heating, and power supply, and on this basis, it has further constructed to meet the user's demand for cooling, heating, and electric energy and comprehensively consider the constraints of nature, environment, social development level, energy policy, system reliability, and operability, etc., a system optimization model to maximize economic and environmental goals. Caregivers are an important concept in the field of intelligence. It generally refers to an organization that has the intelligence to actively begin to achieve its goals by creating activities based on its own state and modifying its own internal data as the environment changes [23]. It is generally believed that the agent has several basic characteristics of autonomy, reactivity, initiative, sociality, and evolution; these characteristics are concentrated in that the agent can respond to external stimuli and actively adjust its own behavior according to changes in the external environment and state to adapt to changes and accumulate learning experience and knowledge. Multiagent system (MAS) consists of multiple loosely coupled agents (agents), each of which is a physical or abstract entity with incomplete information and problem-solving capabilities, the data is scattered and distributed, and the system can adapt to changes in the environment and the corresponding self-adjustment ability, focusing on solving complex distributed tasks and problems through interaction and cooperation between independent agents. Multiagent technology is an important realization of distributed artificial intelligence technology; the rise and development of complexity science have promoted the development and wide application of MAS; this is because there are a large number of complex systems with complex relationships, complex structures, interrelated, mutual constraints, and interactions in nature, such as economic, social, natural ecology and other objective environments; these systems are abstracted into MAS, the essential properties of complex systems [24, 25]. Multiagent technology and its ideas have been widely studied in power system, and robust optimization has always been one of the focuses of current research. How to define robustness has also been carefully considered by experts. At present, many experts have agreed to define the anti-interference ability of the solution as the robustness of the solution. There is a certain difference

between the robustness of the solution and the optimality of the solution, the solution with good robustness is not necessarily the optimal solution, and the robustness of the optimal solution is not necessarily the best. In practical applications, the decision maker should choose the optimal solution or the solution with better robustness according to specific needs. Of course, there may be situations where the optimal solution is the solution with the best robustness. A comparative analysis of the robustness and optimality of the solution is shown in Figure 6.

There are many devices in the RDES system, and there is a certain degree of interconnection between the devices. The integration is difficult. The configuration and capability of the devices have a significant impact on the value economy, environmental benefits, and energy efficiency of the device system. Improper installation of equipment and excess capacity can result in wasted operations and low-energy consumption; if the capacity is too small to meet the needs of the region, it will result in power consumption that is greater than the reduction. It can be seen that to make the regional layout plan more suitable, feasible, and efficient, which is the basis for meeting the regional load demand, it is necessary to comprehensively consider the social development foundation, environmental conditions, system resource allocation, energy policy status, and physical properties of key equipment in the entire region. Characteristics know how to set the efficiency of the distribution area [26]. A decision-based and system-based RDES bilevel optimization is proposed, and a general RDES multiobjective optimization configuration model is constructed; the nondominated sorting genetic algorithm based on elite strategy (NSGA-II) is used to find the global optimal solution. The growth of power distribution is reflected in the widespread use of carbon monoxide triple power distribution. Driven by the further increase in oil resources and construction, China's natural gas-powered pipelines and RDES have developed well. However, as people's health requirements are getting higher and higher, the proportion of renewable energy in the total power generation is increasing, and its application in the power distribution system will be done more. Especially under the development concept of the energy Internet, as an open energy system, the complementarity between energy resources is brought into play; the distributed energy system will show the application trend of multiple energy types. Regional differences in natural gas resource ownership and pipeline network coverage affect the use of natural gas distributed energy systems, and various regions in China also have innate endowments in renewable energy such as wind energy, solar energy, geothermal energy, and biomass energy; the endowment difference of this energy resource constrains the choice of multienergy body types in the distributed energy system. Under the long-term development trend of climate change and energy transformation, building an environment-friendly energy system is the focus of regional distributed energy system planning; therefore, in the configuration decision of regional distributed energy system, it is necessary to fully consider and determine the variety and

abundance of energy resources in the region, subject to conditions, and maximize the utilization of renewable energy, in order to improve the reverse distribution characteristics between China's energy resource endowment and energy demand. China's natural gas resources, pipeline network distribution, solar energy, wind energy, geothermal energy, biomass energy, and other renewable energy distribution and zoning research results, in order to determine the RDES allocation decision-making level of resource factors. The biggest advantage of the regional distributed energy system is the improvement of energy efficiency and the corresponding reduction of pollutant emissions; therefore, the realization of low-carbon development of energy conservation and emission reduction is one of the important forces to promote the development of RDES [27, 28]. At the same time, we see that under the trend of global climate change, more developed countries and regions have increased the use of distributed energy systems to replace traditional high-carbon energy consumption patterns, at present, China's environmental pollution problem is severe, and air quality is poor in most areas, large-scale and long-term smog has become the most difficult environmental problem, the current situation of carbon emissions and air quality in China is analyzed in detail. Heterogeneous economic development among regions is also reflected in regional environmental quality, with marked differences in carbon emission levels, energy efficiency, and air quality; this difference will inevitably lead to different degrees of awareness of energy conservation and emission reduction in different regions, different understandings of environment-friendly energy consumption, different concepts of energy planning, and different action forces for the energy consumption revolution. Therefore, the current situation of the regional environment should be taken into consideration at the RDES planning decision-making level, the environmental value of the distributed energy system should be highlighted, and the environmental benefits of the RDES planning should be comprehensively judged from the current situation of the regional environment and the environmental pressures faced. At the same time, environmental decision factors also help to optimize the configuration and operation of RDES. The energy Internet establishes a new energy system by coupling energy flow and information flow and uses computer technology and other means to coordinate resources and their utilization to improve energy efficiency. On the basis of the general structure of the regional distributed energy system, the author constructs a regional energy Internet model based on the multi-agent system (MAS), that is, the MAS-based RDES model architecture. The model is closely coupled with four complex network systems, including power network, heating network, cooling network, and information network; by introducing MAS and its powerful energy management function, it can ensure that the energy supply equipment in the RDES and the equipment are connected to each other, the coordination, reliability, safety, and effectiveness of the control operation with the load. The energy management agent and routing agent are set in the model,

and the future scheduling and operation of RDES are undertaken by the energy management agent; the coordinated control of physical devices such as energy supply, energy conversion, and energy storage in RDES is realized through the information network with routing agent as the core device. A decision- and system-based RDES two-layer optimization structure is proposed for the planning stage of regional distributed energy system. The decision optimization layer is composed of social development factors, environmental factors, resource factors, policy factors, and equipment factors and optimizes RDES planning decisions. The system optimization layer is composed of objective factors, constraint factors, and algorithm factors; the objective factors are composed of economic and environmental objectives, and the constraint factors are determined based on equipment performance and regional energy flow balance conditions, NSGA-II multiobjective genetic algorithm is used to solve multiobjective problems, the Pareto optimal solution is obtained, and the corresponding realization program is written. Using the RDES double-layer optimization structure, combined with the island operation mode and the grid-connected operation mode, the system optimization analysis of the simulation example is carried out, and the feasibility of the double-layer optimization structure is verified and realizes the operability of the program and the efficiency and reliability of the optimization algorithm. By comparing the optimization results of the calculation example under the two operating modes, reasonable planning suggestions are obtained, that is, under the development of the energy Internet, the regional distributed energy system should actively strive for grid-connected and online operation.

5. Conclusion

There are historical energy technologies, power management, and power consumption processes such as power generation, substation, distribution, and health. The past of the energy Internet, in the context of the energy Internet, is evolving into a diversified, clean, and cost-effective practice, to study the compilation of China's regional power distribution system, which is not only conducive to the construction of a stable power grid in China, but also to increase the energy consumption of electricity in the region, reduce carbon emissions, and improve air quality. The author studies the regional power distribution system planning under the background of Internet power development, formulates a regional power distribution system planning scheme, and provides a general structural framework and optimization algorithm technology for key planning problems and through the design and implementation of decision support, to provide decision support for regional planning and power distribution systems. The main conclusions of the paper are as follows: the definition of the regional distribution system and the definition of regional indicators are discussed. The regional distribution system in the development of the energy Internet is a low-carbon and flexible energy system that is widely used. The key to flexible and powerful online behavior is to

realize the integration and integrity of site-network-load storage. System planning is in a certain spatial structure, under certain constraints, based on the realization of environmental protection, economic, and other goals, through the planning links of energy demand, system construction, configuration optimization, and pipe network optimization, in order to implement the system's production capacity, energy use, energy transmission, energy storage, and energy saving processes, and through the design of energy transmission network, energy information transmission network, and the Internet of Things for energy equipment, the framework of the regional energy Internet is realized. The regional distributed energy system under the development of the energy Internet has multiple and comprehensive characteristics, and it has sorted out the climate, resources, environment, architecture, social development, regional functions, and comprehensive system value that affect the system planning. Through cluster analysis, the regional distributed energy system climate adaptability zoning and solar energy availability zoning are obtained; combined with China's various clean energy resource endowment conditions, the energy complementary planning of distributed energy system is proposed; in terms of carbon emissions and air environmental pressure, therefore, regional distributed energy system planning needs to highlight environmental friendliness; macroeconomics, urbanization level, energy preferential policies, etc. determine the economic acceptability of regional distributed energy system planning; the profitability, technology, and environmental protection of the system also affect the planning of the regional distributed energy system. The change of building load is determined by internal and external disturbance factors, and there are obvious differences in the building load of different functions. After sorting out various load forecasting methods and comparing the existing dynamic load simulation software in China and abroad, it is proposed to combine SketchUp Pro, EnergyPlus, and Openstudio to realize the hourly load forecasting of cooling, heating, and electricity of individual buildings in the area; at the same time, the coefficient is calculated to obtain the overall load of the area, so as to avoid the problem of excessive load prediction error caused by simple superposition.

Data Availability

The data used to support the findings of this study are available from the corresponding author upon request.

Conflicts of Interest

The author declares that there are no conflicts of interest.

References

- [1] B. H. Bhattarai, B. R. Pahari, and S. Maharjan, "Comparison of energy efficiency of traditional brick wall and inco-panel wall: a case study of hotel sarowar in Pokhara," *Journal of the Institute of Engineering*, vol. 15, no. 3, pp. 57–61, 2020.
- [2] E. O. Kalkan, L. Gündüz, and A. M. Sker, "A comparative analysis on the effects of pumice, tuff and conventional aggregates on energy efficiency performance in new generation composite mortars," *Arabian Journal of Geosciences*, vol. 14, no. 11, pp. 1–8, 2021.
- [3] A. O. Brahim and S. Abderafi, "Energy efficiency improvement of debutanizer column, for ngl separation," *International Journal of Environmental Science and Development*, vol. 12, no. 9, pp. 255–260, 2021.
- [4] Z. Dan, W. Ren, M. Guo, Z. Shen, and Y. Shen, "Structure design boosts concomitant enhancement of permittivity, breakdown strength, discharged energy density and efficiency in all-organic dielectrics," *IET Nanodielectrics*, vol. 3, no. 4, pp. 147–155, 2020.
- [5] C. Yu and Y. S. Song, "Modification of graphene aerogel embedded form-stable phase change materials for high energy harvesting efficiency," *Macromolecular Research*, vol. 30, no. 3, pp. 198–204, 2022.
- [6] P. Li, N. Xu, and C. Gao, "A multi-mechanisms composite frequency up-conversion energy harvester," *International Journal of Precision Engineering and Manufacturing*, vol. 21, no. 9, pp. 1781–1788, 2020.
- [7] T. Storodubtseva, B. Bondarev, and K. Pyaduhova, "Waste of wood and glass fiber in composite materials for products transport construction," *Actual Directions Of Scientific Researches Of The Xxi Century Theory And Practice*, vol. 8, no. 1, pp. 156–160, 2020.
- [8] W. Punsawat and W. Makcharoen, "Development of a ternary composite of pu resin/carbon black/pzt for mechanical energy harvesting application," *Materials Today: Proceedings*, vol. 43, no. 10, pp. 2599–2604, 2021.
- [9] M. A. Berawi, A. A. Kim, F. Naomi, V. Basten, and M. Sari, "Designing a smart integrated workspace to improve building energy efficiency: an Indonesian case study," *International Journal of Construction Management*, vol. 1, pp. 1–24, 2021.
- [10] G. Serale, M. Fiorentini, and M. Noussan, "Development of algorithms for building energy efficiency," in *In Start-Up Creation (Second Edition)*, pp. 267–290, Woodhead Publishing, 2020.
- [11] S. Copiello and IUAV University of Venice, Department of Architecture, Dorsoduro 2206, 30123 Venice, Italy, "Economic viability of building energy efficiency measures: a review on the discount rate," *AIMS Energy*, vol. 9, no. 2, pp. 257–285, 2021.
- [12] E. Pealvo-López, J. Cárcel-Carrasco, D. Alfonso-Solar, I. Valencia-Salazar, and E. Hurtado-Pérez, "Study of the improvement on energy efficiency for a building in the Mediterranean area by the installation of a green roof system," *Energies*, vol. 13, no. 5, p. 1246, 2020.
- [13] K. Sharma and B. K. Chaurasia, "Trust based location finding mechanism in VANET using DST," in *Fifth International Conference on Communication Systems & Network Technologies*, pp. 763–766, Chongqing city in China, 2015.
- [14] A. E. Kele, E. Nen, and J. Górecki, "Make saving crucial again: building energy efficiency awareness of people living in urban areas," *Advances in Building Energy Research*, vol. 1, pp. 1–14, 2021.
- [15] M. Bradha, N. Balakrishnan, A. Suvitha et al., "Experimental, computational analysis of Butein and Lanceoletin for natural dye-sensitized solar cells and stabilizing efficiency by IoT," *Environment, Development and Sustainability*, vol. 24, no. 6, pp. 8807–8822, 2021.

Retraction

Retracted: Test of Ultimate Bearing Capacity of Building Concrete Structures in Earthquake Area Based on Virtual Reality

Journal of Sensors

Received 17 October 2023; Accepted 17 October 2023; Published 18 October 2023

Copyright © 2023 Journal of Sensors. This is an open access article distributed under the Creative Commons Attribution License, which permits unrestricted use, distribution, and reproduction in any medium, provided the original work is properly cited.

This article has been retracted by Hindawi following an investigation undertaken by the publisher [1]. This investigation has uncovered evidence of one or more of the following indicators of systematic manipulation of the publication process:

- (1) Discrepancies in scope
- (2) Discrepancies in the description of the research reported
- (3) Discrepancies between the availability of data and the research described
- (4) Inappropriate citations
- (5) Incoherent, meaningless and/or irrelevant content included in the article
- (6) Peer-review manipulation

The presence of these indicators undermines our confidence in the integrity of the article's content and we cannot, therefore, vouch for its reliability. Please note that this notice is intended solely to alert readers that the content of this article is unreliable. We have not investigated whether authors were aware of or involved in the systematic manipulation of the publication process.

Wiley and Hindawi regrets that the usual quality checks did not identify these issues before publication and have since put additional measures in place to safeguard research integrity.

We wish to credit our own Research Integrity and Research Publishing teams and anonymous and named external researchers and research integrity experts for contributing to this investigation.

The corresponding author, as the representative of all authors, has been given the opportunity to register their agreement or disagreement to this retraction. We have kept a record of any response received.

References

- [1] H. Liu, X. Yang, and L. Dou, "Test of Ultimate Bearing Capacity of Building Concrete Structures in Earthquake Area Based on Virtual Reality," *Journal of Sensors*, vol. 2022, Article ID 6049308, 7 pages, 2022.

Research Article

Test of Ultimate Bearing Capacity of Building Concrete Structures in Earthquake Area Based on Virtual Reality

Hui Liu ^{1,2}, Xintian Yang ², and Lijun Dou ²

¹Shenyang Jianzhu University, Shenyang, Liaoning 110168, China

²Changchun Institute of Technology, Changchun, Jilin 130103, China

Correspondence should be addressed to Lijun Dou; 1522020208@st.usst.edu.cn

Received 19 May 2022; Revised 1 June 2022; Accepted 15 June 2022; Published 1 July 2022

Academic Editor: C. Venkatesan

Copyright © 2022 Hui Liu et al. This is an open access article distributed under the Creative Commons Attribution License, which permits unrestricted use, distribution, and reproduction in any medium, provided the original work is properly cited.

In order to solve the poor matching ability between concrete structures of traditional architectural space optimization design methods, it leads to the problem of low space optimization ratio, so based on virtual reality technology, the author proposes a new method for optimizing the space of concrete structure buildings. Using virtual reality technology to improve the basic structure of building space, reorganize the form through the design space, and optimize the design of the concrete structure building space function; based on the test model of virtual reality technology, design the matching method of concrete structure, increase the proportion of building space optimization, and adopt linear buckling method, geometric nonlinear method, and double nonlinear analysis method; the ultimate bearing capacity of steel structures of residential buildings in earthquake areas is tested. Experimental results show that for the simple structure building space, the average optimization ratios are 97.17% and 96.71%, respectively; for the complex structure building space, under the proposed optimization design, the average optimization ratio is maintained at 94.34%, and the error between the stress prediction value of the finite element model and the axial stress obtained by testing is less than 6%. Compared with the traditional space optimization design, in the proposed space optimization design method, the proportion of building space optimization is higher; it can be seen that the virtual reality technology has a better matching effect on the concrete structure, and the accuracy of the ultimate bearing capacity value obtained by prediction is high.

1. Introduction

In the current concrete structure construction methods, there are mainly cast-in-place and prefabricated [1], the difference between cast-in-place and fabricated is the former is to complete the entire steps at the construction site, while the latter is mainly prefabricated first, and then transported to the site for hoisting; the specific difference [2] is shown in Figure 1.

In the existing building system in my country, the cast-in-place system is widely used in engineering; whether it is the previous multilayered structure or the high-rise reinforced concrete structure, the construction of the concrete structure part of the building basically adopts the cast-in-place system. The reason why this system is widely recog-

nized and used is because the cast-in-place system is relatively inexpensive, and the construction personnel are also very experienced, and the technology has matured. However, the cast-in-place structure has some obvious defects in engineering application, for example, there are a series of problems such as high labor intensity of workers, excessive manual operation, long construction period, cumbersome procedures, low production efficiency, and difficulty in guaranteeing project quality [3]. Our country is in a period of accelerating urbanization process, and a large number of houses need to be built every year. With the reduction of the labor force, the rise of labor costs is an inevitable trend; at the same time, the owners have higher and higher requirements for quality and quality, and the advantages of prefabricated houses are then reflected.

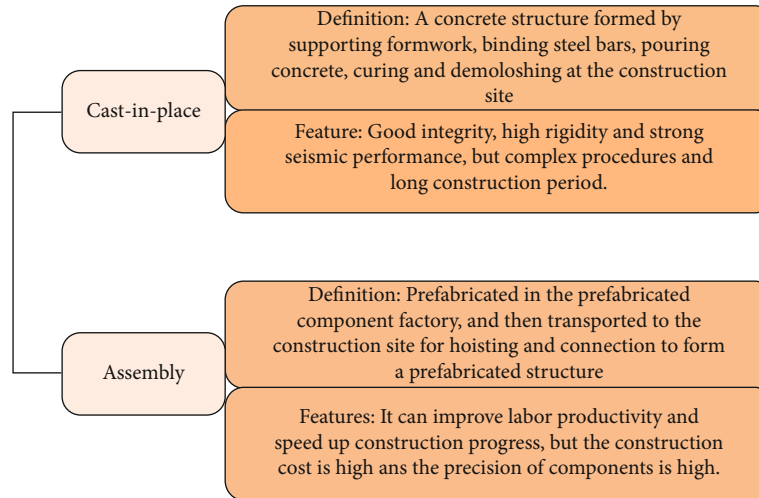


FIGURE 1: Construction method of concrete structure.

2. Literature Review

Johnston et al. designed the test of composite CFST short column under the action of axial compressive load, and the test included 26 different shapes [4]. Na and Shen completed the experimental study of the composite CFST members under the action of axial compressive load and applied the superposition principle to deduce the bearing capacity of the members [5]. Aravind and Abdulrehman carried out an experimental study on the axial compressive performance of composite CFST with different stiffening and composition types and studied the influence of the arrangement of stiffeners at the end of the steel tube wall on the axial compressive performance of the composite CFST column [6]. By arranging tie bars in duplex concrete-filled steel tubular columns, the strengthening and restraint effect of tie bars on the axial compression performance of column members is studied [7]. Using the finite element analysis method, the numerical analysis model of the axial compression of the composite concrete filled steel tube was established [8]. Guo and Jiang proposed a reinforced ring-shaped rectangular crosssection CFST beam-column joint after the diaphragm is penetrated; through conducting experimental research, it was found that the arrangement of the stiffener plate on the steel beam can improve the seismic performance of the joint and improve the flexural bearing capacity of the joint [9]. Xue et al. believed that the two-way horizontal load has a great influence on the performance of CFST beam-column space joints; therefore, a quasistatic test is carried out for the square section column-combined section beam joint of the inner diaphragm type, the effect of bidirectional horizontal loads on the failure form, and seismic performance of such joints was studied [10].

With the development of technical level and the continuous improvement of people's aesthetic vision, the architectural space structure of the design tends to be diversified and complicated. On the basis of ensuring the beauty of the architectural space structure, in order to ensure that the

space can exert its maximum effect, the author proposes to use virtual reality (VR) technology to test the ultimate bearing capacity of building concrete structures in earthquake areas.

3. Research Methods

3.1. VR Technology Improves the Basic Structure of Building Space. At present, the building space is divided into multiple levels and regions, and the functions of each floor or region are also different; Table 1 details the basic functions of conventional building space [11].

Architectural space morphological features include the following: it integrates the characteristics of openness to the outside world, flexible structure of space with blurred boundaries, and strong sense of modular partition; therefore, according to the above characteristics, the basic structure of the building space is improved by using the similarity principle of VR technology.

The similarity principle refers to a set of physical processes; there is a fixed proportional relationship between its parameters, including its geometric similarity. In the process of similarity virtual improvement, the proportional constant of the known physical quantity is called the similarity constant, and its expression is the following formula (1) [12]:

$$P_A = \frac{x_1}{x_2}. \quad (1)$$

In the formula, P_A is the similarity constant of the building structure; x_1 is the improved characteristic quantity; and x_2 is the original characteristic quantity of the building structure. Using the above formula, the improvement of the architectural space morphological characteristics is completed.

At the same time, the characteristics of the building environment are investigated, and by understanding the purpose of the building, the overall atmosphere of the building, the

TABLE 1: Basic functional composition of conventional building space.

Space type	Regional function	Features
Entrance area	Building space entrance	Access control, signage, information desks, entry and waiting areas
Rest area	Staff rest area	Spread out resting positions
Office area	Workspace	Mainly on working hardware
Entertainment area	Provide leisure area	Placement of recreational facilities
Shared space	Common use area	High flow of people and loud noise
Expand space	Areas used for tasks other than work	Other auxiliary equipment installation and manual activities, etc.
Public space	Space accessible to all personnel	Large area, large flow of people, more frequent use
Independent space	For one person only	Quiet and small
Other	Other uses	—

humanized characteristics of local details, and the nodes of intelligent technology equipment are clarified [13]. Integrate the above features with architectural morphological features, use VR technology to set the spatial structure and geometric dimensions of the building, and attach the color and pattern corresponding to the architectural purpose on the building structure, and guarantee the original properties of the building space.

Assuming that the similarity criterion between the physical quantities obtained through VR technology is $\pi_1, \pi_2, \dots, \pi_n$, then according to the functional relationship between the criteria, combined with formula (1), set the improved building space model generation function, through which a new building space structure is automatically generated [14]:

$$f(\pi_1, \pi_2, \dots, \pi_n) = P_A \times f(\pi). \quad (2)$$

In the formula, $f(\pi)$ is the calculation function of the building space structure before improvement [15].

According to the basic spatial morphological characteristics and environmental characteristics of the building, the spatial structure of the building is improved, and part of the results are improved. Use VR technology to establish an improved basic structure of building space, and split and adjust the inappropriate or mismatched connection positions at any time; according to the above operation, the improvement of the basic structure of the building space is realized.

3.2. Optimal Design of Concrete Structure Building Space Function. Improve the concrete building space of the basic structure; it is necessary to optimize the function of the concrete structure building space and then perform structural matching through VR technology [16]; finally, a complete, ready-to-use building space model is generated. According to the architectural space model, reoptimize the design of the use functions of different spaces, give each area new use functions, and cater to the trends and design purposes of the times. Figure 2 is a schematic diagram of the basic strategy of spatial function optimization design [17].

There are two main forms of division of building space: splitting vertically and splitting horizontally [18]. The splitting in the horizontal direction is relatively simple, and more

independent space can be obtained only by adding a partition wall and satisfy the requirement to increase the amount of space used. This split will not change the basic structure of the improved building space and can be achieved through nonstructural processing. The splitting of vertical space is suitable for buildings with high height inside the building space; by dividing the vertical direction, the amount of space used and the utilization rate of space are increased. At this time, it is easy to cause the problem that the old and new structures of the vertical split do not match; therefore, the VR technology uses formula (3) to set the split ratio:

$$k_2 = k_1 \times c. \quad (3)$$

In the formula, k_2 is the size of the virtual model after splitting and adjustment; k_1 is the space size of the actual concrete structure building; and c is the scale.

The use of formula (3) can realize the splitting of building space. Reorganization according to the split virtual model mainly includes three forms: completely independent reorganization, mutually inclusive reorganization, and fully inclusive reorganization.

Complete independence is to completely separate the two split spaces, while mutual accommodation is that one space contains another subspace; full containment is a larger space, and it accommodates spaces with completely inconsistent structural forms. According to the form of space reorganization, optimize the design of the space function of the concrete structure building, and enhance the use function of the building space by establishing a new arrangement order. Combining formulas (2) and (3), the sorted virtual building space size is obtained [19]:

$$s_0 = k_2 \times f(\pi_1, \pi_2, \dots, \pi_n) - \Delta s. \quad (4)$$

In the formula, Δs is the spatial reorganization error; s_0 is the virtual building space size.

When the ratio between s_0 and the actual concrete building space size S is in line with reality, it proves that the optimized space function design is achievable.

3.3. VR Technology Design Concrete Structure Matching Method. When the optimized building space function meets

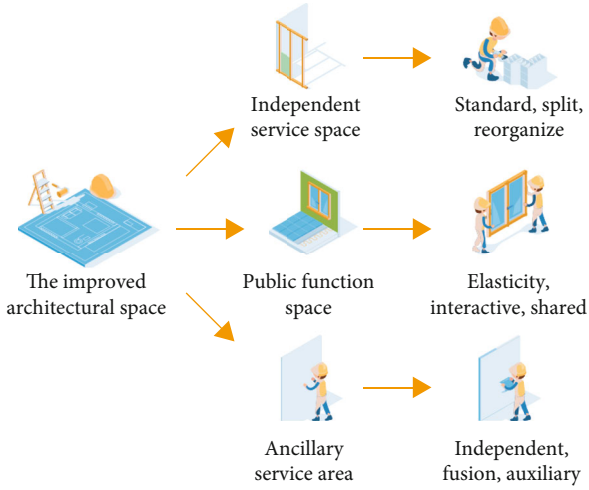


FIGURE 2: Basic strategy of functional optimization design.

the requirements of architectural geometric design, the VR technology is used to design the concrete structure matching method, and the space optimization of the concrete structure building is realized through the interactive integration and matching between concretes. In interactive integration under VR technology, according to the relationship between buildings and exhibitions, buildings and structures, and buildings and equipment, through morphological contrast and streamline composition, the matching between the concrete structures of the building space is realized.

The three components of VR technology are temporal component X , spatial component Y , and attribute component Z . Among them, the temporal component describes the dynamics of the spatial design [20]; when the value of the spatial component is 0, 1, 2, and 3, it corresponds to the point, line, surface, and volume of the real building space and the virtual building model, which fully describes the spatiality of the building; the attribute component corresponds to the architectural attributes of a specific time and space. The virtual model is used to detect the matching degree between concrete models; Equation (5) is the basic algorithm to control the model.

$$\begin{cases} F_X(A_1, A_2) = \sqrt{\frac{\sum_{i=1}^n w_i \times (x_{i1} - x_{i2})^2 \times s_0}{s}}, \\ F_Y(A_1, A_2) = \sqrt{\frac{\sum_{i=1}^n w_i \times (y_{i1} - y_{i2})^2 \times s_0}{s}}, \\ F_Z(A_1, A_2) = \sqrt{\frac{\sum_{i=1}^n w_i \times (z_{i1} - z_{i2})^2 \times s_0}{s}}. \end{cases} \quad (5)$$

In the formula: F_X , F_Y , and F_Z are the matching values of virtual space A_1 and actual building space, respectively; x_{i1} , x_{i2} , y_{i1} , y_{i2} , z_{i1} , and z_{i2} are, respectively, in two spaces, the time, space, and attribute factors of the i th concrete structure; w_i is the architectural space matching weight.

According to formula (5), the matching degree test result is obtained as the following:

$$F = \begin{cases} \sqrt{\frac{F_X \times (A_1, A_2)}{N}}, \\ \sqrt{\frac{F_Y \times (A_1, A_2)}{N}}, \\ \sqrt{\frac{F_Z \times (A_1, A_2)}{N}}. \end{cases} \quad (6)$$

In the formula, F is the matching value; N is the weighting coefficient participating in the matching test.

According to the calculation results of F , it can be judged whether the dimensions of the model components match. When $F \geq 0.97$, it means a high degree of fit between model components; when $0.95 < F < 0.97$, it means a regular fit between model components, and the setting parameters of some components need to be adjusted; when $F \leq 0.95$, the architectural model design parameters need to be readjusted.

3.4. Analysis Method of Ultimate Bearing Capacity. Based on the finite element model of the steel structure of residential buildings in the earthquake area, the linear buckling, geometric nonlinearity, and double nonlinearity are studied; evaluate its ultimate bearing capacity. Linear buckling is an eigenvalue solution process, which is usually processed by inverse vector iteration and subspace iteration.

The linear buckling method is a general method for testing the ultimate bearing capacity of bearing steel structures [21]. If the structure and material are both linear, the structural failure factor λ is obtained by using the form of the solution eigenvalue, and the ultimate bearing capacity of the building steel structure is obtained; the geometric nonlinear analysis method regards the material as linear, and for the structural beam-column effect and large displacement effect, use incremental and iterative methods to deal with the ultimate bearing capacity of the structure; the structure and data of the geometric and material nonlinear research method have nonlinear properties, and the ultimate bearing capacity of the building steel structure is obtained by means of incremental and iterative measures.

(1) Linear buckling method

Under the influence of the critical load, the linear balance equation of the steel structure of residential buildings in the earthquake area is as follows (7) [22]:

$$(K_0 + \lambda K_\sigma) \cdot \{\Delta u\} = 0. \quad (7)$$

In the formula, K_0 represents the elastic stiffness matrix of the building steel structure; K_σ represents the geometric stiffness matrix under the reference load; $\{\Delta u\}$ and λ represent the node displacement increment and the load stability factor, respectively. The eigenvalue problem presented by Equation (7) is dealt with by the inverse vector iteration

TABLE 2: Concrete structure parameters.

Concrete structural system	Spatial scale variability	Space expansion flexibility	Facade retrofit flexibility
Framework	Good variability of bay and depth	Removal of interior walls or partial columns	Flexible
Shear wall structure	Poor bay and depth variability	Difficult to carry out space expansion renovation	Facade windows are restricted
Frame shear structure	Good variability of bay and depth	Removal of nonload bearing walls or columns	Flexible

method and the subspace iteration method [23]. Structural critical loads are shown as $F = \lambda_{\min} \cdot F_0$.

(2) Geometric nonlinear method

The geometric nonlinear incremental balance equation of the steel structure of residential buildings in the earthquake area is as follows (8) [24]:

$$(K_0 + \lambda K_\sigma) \cdot \{\Delta u\} = \Delta F, \quad (8)$$

where ΔF is the external load increment.

By the incremental Newton Raphson iteration method, the nonlinear incremental balance equation in Equation (8) is solved.

(3) Double nonlinear analysis method

Considering geometric nonlinearity and material nonlinearity, the incremental balance equation is as follows:

$$(K_{ep} + \lambda K_\sigma) \cdot \{\Delta u\} = \Delta F, \quad (9)$$

where K_{ep} is the elastic-plastic stiffness matrix of the structure. Through incremental Newton Raphson iteration and arc length method, the nonlinear incremental equilibrium equation of Equation (9) is solved [25].

4. Analysis of Results

The architectural space optimization design method was proposed and compared with the traditional architectural space optimization design method, analysis of different building technologies, and optimization effect of concrete structure building space.

Two buildings are randomly selected as experimental test objects, among which object A is a simple structure building space, and object B is a complex structure building space. The concrete structure parameters of the known buildings are shown in Table 2. On the premise of changing the parameters of the concrete structure by using two methods, complete the structural optimization of the building space.

According to the parameters in Table 2, two optimization design methods are used, respectively; space optimization was performed on 2 groups of experimental test objects. The optimal design method proposed this time was used as the

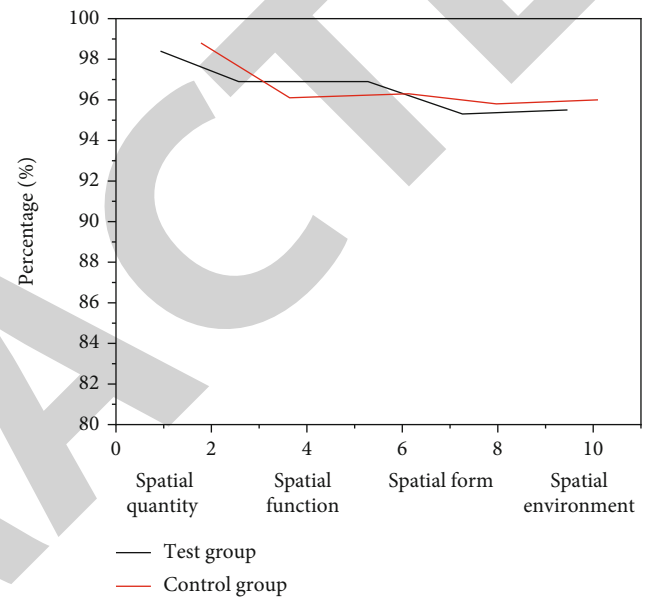


FIGURE 3: Test results of space optimization design of simple structure buildings.

experimental group, and the traditional spatial optimal design method was used as the control group. Figure 3 is the optimal design test result of the simple structure building A.

It can be seen from Figure 3 that the two optimal design methods, for the simple structure building space, and the average optimization ratios are 97.17% and 96.71%, respectively, both of which have high optimization ratios. The different members of the steel structure of residential buildings in the experimental earthquake area were converted into beam elements for discrete finite element analysis, with a total of 127 nodes and 246 elements. The accuracy of the finite element model of the steel structure of the residential building is related to the error of the model structure, the error of the model order, and the error of the model parameters. If model parameter error is the key contributing factor, it is caused by rough material, geometric parameters and joints, and boundary specification predictions. In the author's method, in the process of revising the parameters of the finite element model, the material parameters are set accurately, and the joint parts are welded, if it is a rigid connection, during the research process of the finite element model, the lifting guide rails of the deployed steel

TABLE 3: Initial frequency and correction results.

Natural frequency	Initial frequency/Hz	Target frequency/Hz	Correction frequency/Hz	Frequency error before correction/%	Frequency error after correction/%
f_1	0.795	0.614	0.597	27.85	2.62
f_2	1.005	0.749	0.737	47.42	0.26
f_3	1.599	1.327	1.446	10.23	1.21

TABLE 4: Comparison of tested stress values and predicted stress values.

Axial stress	Second-story platform column number				Middle and lower column number			
	①	②	③	④	①	②	③	④
Test value/MPa	-11.82	-12.86	-10.97	-8.69	-10.44	-11.38	-10.51	-9.91
Predicted value/MPa	-11.91	-12.83	-10.23	-8.84	-10.11	-10.83	-10.95	-8.39
Relative error/%	-0.076	0.19	2.24	2.46	2.75	4.39	3.85	5.98

structure pillars and the fixed equipment at the top of the steel structure are not analyzed. Therefore, the section parameters of the main bearing members of the experimental residential building steel structure are the design variables. In the first second-order natural frequency obtained by vibration detection, the finite element model is adjusted, and the third-order natural frequency of the adjusted finite element model is compared with the third-order natural frequency obtained by the modal experiment; then, the validity of the correction process of the method in this paper is tested. The original frequencies and the adjustment results are listed in Table 3. It can be seen, through the finite element model adjusted by the method in this paper, that the modal parameters of the experimental residential building steel structure are accurately described; it also inverts the parameters outside the objective function, which has strong prediction performance.

Using the modified finite element model of the method in this paper, the mechanical performance of the experimental residential building steel structure was analyzed, the hook load is set to 458 kN, and the test axial stress, operational stress, and relative error between the two key members of the steel structure are listed in Table 4. By analyzing this table, it can be obtained that the predicted stress value of the finite element model modified by the method in this paper is the axial stress error obtained from the same test is less than 6%, indicating that the method in this paper can accurately describe the real bearing performance of the steel structure of residential buildings in the earthquake area; the predicted ultimate bearing capacity has high accuracy.

5. Conclusion

Using VR technology to optimize the concrete structure building space, by increasing the fit between the component models, enhance the matching degree between virtual building structures, realize more comprehensive building space optimization, and solve the traditional space optimization design method due to poor building structure matching and the problem that leads to the low optimization ratio.

Also proposed based on vibration parameters, as well as dynamic models, is the revised method for predicting and analyzing the ultimate bearing capacity of steel structures of residential buildings in earthquake areas and through the method for evaluating the ultimate bearing capacity based on the revision of the dynamic model and accurate prediction of ultimate bearing capacity of building steel structures. However, the spatial optimization design method proposed this time does not consider environmental factors such as geographic location information; in the future research design, this point can be optimized and analyzed.

Data Availability

The data used to support the findings of this study are available from the corresponding author upon request.

Conflicts of Interest

The authors declare that they have no conflicts of interest

References

- [1] A. Vukadinović, J. Radosavljević, A. Đorđević, M. Protić, and N. Petrović, "Multi-objective optimization of energy performance for a detached residential building with a sunspace using the nsga-ii genetic algorithm," *Solar Energy*, vol. 224, pp. 1426–1444, 2021.
- [2] H. H. Saber, W. Maref, and A. E. Hajiah, "Effective r-value of enclosed reflective space for different building applications," *Journal of Building Physics*, vol. 43, no. 5, pp. 398–427, 2020.
- [3] H. Mohammadi and F. Samadzadegan, "An object based framework for building change analysis using 2D and 3D information of high resolution satellite images," *Advances in Space Research*, vol. 66, no. 6, pp. 1386–1404, 2020.
- [4] D. Johnston, M. Siddall, O. Ottinger, S. Peper, and W. Feist, "Are the energy savings of the passive house standard reliable? A review of the as-built thermal and space heating performance of passive house dwellings from 1990 to 2018," *Energy Efficiency*, vol. 13, no. 8, pp. 1605–1631, 2020.

Retraction

Retracted: Application of Image Processing Sensor and Pattern Recognition in Detection of Bearing Surface Defects

Journal of Sensors

Received 17 October 2023; Accepted 17 October 2023; Published 18 October 2023

Copyright © 2023 Journal of Sensors. This is an open access article distributed under the Creative Commons Attribution License, which permits unrestricted use, distribution, and reproduction in any medium, provided the original work is properly cited.

This article has been retracted by Hindawi following an investigation undertaken by the publisher [1]. This investigation has uncovered evidence of one or more of the following indicators of systematic manipulation of the publication process:

- (1) Discrepancies in scope
- (2) Discrepancies in the description of the research reported
- (3) Discrepancies between the availability of data and the research described
- (4) Inappropriate citations
- (5) Incoherent, meaningless and/or irrelevant content included in the article
- (6) Peer-review manipulation

The presence of these indicators undermines our confidence in the integrity of the article's content and we cannot, therefore, vouch for its reliability. Please note that this notice is intended solely to alert readers that the content of this article is unreliable. We have not investigated whether authors were aware of or involved in the systematic manipulation of the publication process.

Wiley and Hindawi regrets that the usual quality checks did not identify these issues before publication and have since put additional measures in place to safeguard research integrity.

We wish to credit our own Research Integrity and Research Publishing teams and anonymous and named external researchers and research integrity experts for contributing to this investigation.

The corresponding author, as the representative of all authors, has been given the opportunity to register their agreement or disagreement to this retraction. We have kept a record of any response received.

References

- [1] Q. Wu and M. Zhu, "Application of Image Processing Sensor and Pattern Recognition in Detection of Bearing Surface Defects," *Journal of Sensors*, vol. 2022, Article ID 7924982, 7 pages, 2022.

Research Article

Application of Image Processing Sensor and Pattern Recognition in Detection of Bearing Surface Defects

Qinghong Wu  and Minghui Zhu 

School of Electronic and Information Engineering, University of Science and Technology Liaoning, 114051 Anshan, Liaoning, China

Correspondence should be addressed to Qinghong Wu; 1330117238@cjlu.edu.cn

Received 22 May 2022; Revised 2 June 2022; Accepted 20 June 2022; Published 1 July 2022

Academic Editor: C. Venkatesan

Copyright © 2022 Qinghong Wu and Minghui Zhu. This is an open access article distributed under the Creative Commons Attribution License, which permits unrestricted use, distribution, and reproduction in any medium, provided the original work is properly cited.

In order to solve the problem that the traditional detection technology can not meet the requirements of online detection, a visual detection device for bearing inner ring defects based on image processing and pattern recognition is proposed in this paper. The device systematically designs an image acquisition device of bearing inner ring based on CCD. In the hardware scheme, the appropriate lens, camera, light source, and other related hardware are selected according to the actual needs, a complete image acquisition platform of bearing inner ring is built, and the software function design is completed. The simulation results show that the qualified rate of machine detection is 98.6%, the missed detection rate is 0, and the false detection rate is 1.4%, which are better than manual detection. *Conclusion.* The test results show that the bearing inner ring defect detection system can detect the surface defects of bearing inner ring quickly, stably, and reliably, and the detection efficiency and accuracy are higher than the original manual detection method, so it has a good application prospect.

1. Introduction

Bearing is the basic component of modern industry and known as the “joint” of mechanical equipment. It is widely used in automobile, household appliances, agricultural machinery, engineering machinery, heavy machinery, electric power, railway, machine tool, and other industries. Its main function is to support the rotating shaft or other moving bodies. It plays the role of fixing the rotating shaft and reducing the load friction coefficient in the process of mechanical transmission. Its accuracy, performance, service life, and reliability play a decisive role in the service performance and reliability of the main engine. Bearing industry is a national basic and strategic industry. Its development level and industrial scale reflect a country's comprehensive industrial strength and play an important role in national economy and national defense construction [1].

With the improvement of production automation level and the continuous improvement of product quality requirements and production efficiency, machine vision image processing and pattern recognition technology have

received more and more attention. At present, the application field of machine vision is deep and wide, with strong practicability and real time. It is widely used in many fields such as industry, agriculture, medical treatment, and transportation [2]. In recent decades, with the continuous acceleration of industrialization and the transfer of manufacturing centers in various countries and regions to China, bearings usually need mass production with high speed and accuracy requirements. In order to comply with the development of modern bearing production mode, machine vision image processing and pattern recognition technology have important application prospects and research value in bearing detection [3]. In addition, benefiting from the continuous improvement of supporting infrastructure, the continuous expansion of the overall scale of manufacturing industry, and the continuous improvement of intelligent level, favorable policies, and other factors, the demand of China's machine vision image processing market is growing. With the improvement of industry technology and wider product application fields, the machine vision market will further expand in the future [4].

2. Literature Review

In foreign countries, the monitoring and diagnosis of bearings have been started in the 1960s. After about half a world's development, it has basically reached the period of marketization and commercialization. Boeing company in the USA uses resonance demodulation technology for fault analysis. This technology improves the signal-to-noise ratio and can well detect the fault. Resonance demodulation method is similar to impulse method, but it can also judge the existence of the fault, the location, and damage degree of the fault. Therefore, this method has been widely used [5]. Later, due to the progress of science and technology, after the 1980s, companies in some industrial developed countries began to use computers to monitor and diagnose the state of rolling bearings. For example, the USA and Russia developed ReBAM system and dream automatic diagnosis system, respectively. These systems use the combination of nonlinear signal and signal processing of rolling bearing and build an information database according to the characteristics. In this database, there is huge bearing information, which can realize intelligent classification and fault judgment and monitor the condition of bearing.

At present, there are many research institutes engaged in bearing fault diagnosis, but there are relatively few research on the bearing of relevant railway freight cars, and the application is even less. In terms of image detection, Nikiforova, Z. S. and others designed the detection system according to some characteristics of brake valve surface defects, processed the corresponding defect images, and judged the corresponding level of the workpiece. In actual operation, it has some advantages of long time, good stability, and high accuracy, completely avoiding the false detection caused by manual long-time labor [6]. Urazghildiiev, I. R. and others studied the defects on the surface of steel cord by using image processing technology. In order to remove the interference of noise to the follow-up research, they denoised the collected steel curtain wire image in the first step. Secondly, the moving edge algorithm is used to extract the target area and perimeter, the gray level co-occurrence matrix is used to process the texture features of the wire, and a variety of features are used to judge the defects of the detected objects. The results show that the algorithm for feature extraction has certain value and plays a certain role in promoting the self-energy of detection [7]. Li, Z. and others have conducted preliminary discussion and research on online bearing size detection based on machine vision and designed a detection system on the flow production line [8]. The system requires the bearing to move on the conveyor belt according to a certain beat, the image capture is synchronized with the production line, and the images are captured at the same time. The collected images are processed in order, such as graying, median filtering, Laplace sharpening, threshold segmentation, and contour extraction; finally, the actual size of the bearing is obtained through calculation, and whether the bearing size is qualified is judged. Although this system replaces manual detection and reduces the detection cost, the whole system has not been completed, and there are still some problems to be solved, such as online

dynamic image acquisition. This system also lays a foundation for future research. He, J. and others designed the bearing inner and outer diameter detection system [9]. When the system collects images, the CCD optical axis is collinear with the central axis of the bearing, and the ideal image can be obtained. Then, the required information can be obtained, and the bearing size can be calculated through the operations of median filter, Laplace sharpening, smoothing filter, threshold segmentation, and contour extraction. A standard sample bearing is used for system calibration, and the bearing outer diameter measurement test is carried out. The standard deviation can reach 0.015 mm, and the accuracy meets the design requirements.

In this paper, combined with the quality inspection standards specified by the bearing manufacturer, a set of visual detection device for bearing inner ring defects is designed and implemented. In the hardware scheme, the appropriate lens, camera, light source, and other related hardware are selected according to the actual needs, a complete set of bearing inner ring image acquisition platform is built, and the software function design is completed to realize the test of bearing surface defect detection.

3. Research Methods

3.1. Overall Design of Detection System Scheme. In order to meet the actual needs of the bearing manufacturer, the online visual inspection system for the appearance defects of the bearing inner ring designed and developed in this paper needs to meet the following basic requirements:

- (1) The system is fully automated: It can realize 100% detection of the bearings on the production line and screen the bearings according to the detection accuracy. Instead of the original manual detection method, the whole detection process is controlled by computer
- (2) Accurate classification: It can correctly identify and classify defects, and the repeated detection rate is high [10, 11].
- (3) High reliability: The system can operate safely and stably for a long time and ensure the corresponding accuracy. For bearings with various defects, it can also ensure reliable operation

The bearing inner ring defect visual inspection system is mainly composed of four modules: mechanical module, software module, electrical control module, and image acquisition. As shown in Figure 1, the module division of the whole system and the relationship between each module are shown.

3.2. Hardware Design of Bearing Inner Ring Defect Detection System. The hardware part of the visual inspection system for bearing inner ring defects mainly consists of mechanical transmission module, optical lighting module, image acquisition module, computer image processing module, and electrical PLC control module [12]. The defect detection system

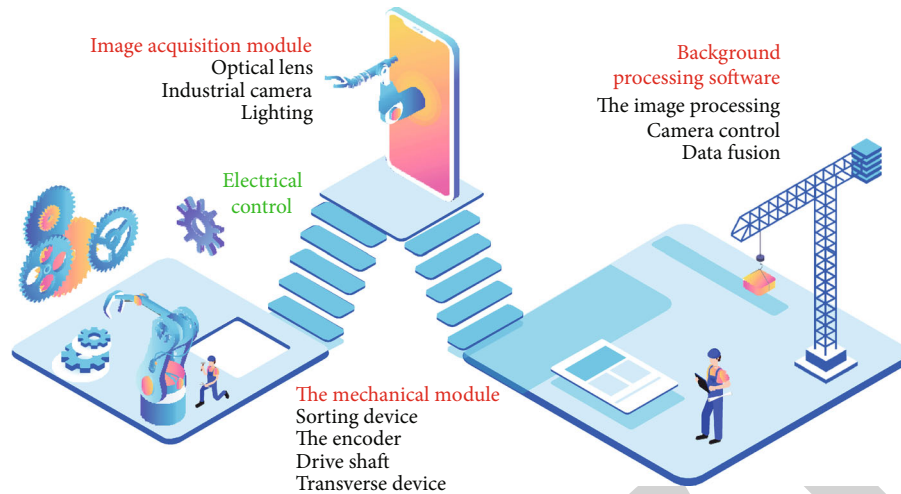


FIGURE 1: Module structure diagram of bearing inner ring detection system.

of bearing inner ring is controlled by an industrial computer. Four high-speed CCD cameras collect images in parallel and process them in real time. The processing results are fed back to the electrical control unit, and finally, the bearings are sorted.

3.2.1. Mechanical Transmission Module. The main function of the mechanical transmission system is to pass the bearing test samples through each image acquisition station one by one at a certain rate to complete the image shooting. The uniform speed and stability of the transmission module are related to the quality of image shooting [13]. The module is mainly composed of motor, frequency converter, and encoder. While rotating, it sends pulse trigger signal to the camera.

3.2.2. Optical Lighting Module. The main responsibilities of this part are to supplement the light and shield the influence of ambient light on the bearings on the production line, highlight the surface defects of the bearings, make them compare with the background, and facilitate subsequent image processing. A good lighting system can not only assist the camera to collect high-quality images, but also simplify the subsequent image processing algorithm and improve the operation efficiency of the system [14].

3.2.3. Image Acquisition Module. Four industrial cameras assume that the real-time image acquisition of the bearing on the mechanical transmission device is carried out on the bearing production line, and the collected image data is transmitted to the industrial computer software system [15].

3.2.4. Computer Image Processing Module. The core part of the module is the software system running on the computer, mainly including multicamera parallel control, image processing algorithm, and multistation data fusion [16].

3.2.5. Electrical Control Module. The electrical control is mainly controlled by PLC to the solenoid valve. According to the results of image processing by the computer, the result data is sent by the computer to the electrical control unit,

which drives the mechanical device to make corresponding actions to sort the bearings [17].

In the machine vision system, the lens is an essential part. The optical lens can image the long-distance target on the CCD target surface of the camera. The appropriate lens selection will give full play to the camera. The parameters of the lens mainly consider four parameters related to the lens: focal length, field of view, working distance, and depth of field. When the size of the subject and the distance from the object to the lens are known, the focal length of the selected matching lens can be estimated according to the following formulas:

$$f = h \times \frac{WD}{H}, \quad (1)$$

$$f = v \times \frac{WD}{V}, \quad (2)$$

where WD is the distance from the lens center to the subject; H and V are the horizontal and vertical dimensions of the subject, respectively; v is the imaging height of the target surface; and h is the horizontal width of target imaging. That is, focal length = object distance \times CCD chip size (width or height)/field of view size (width or height).

3.3. Bearing Inner Ring Surface Defect Detection Algorithm. The image processing generally starts from extracting the region of interest (ROI). Region of interest (ROI) is an image region selected from images, which is the focus of image analysis. Delineate the area for further processing. Using ROI to delineate the area where the target to be detected is located can reduce the processing time and increase the accuracy [18].

Then, locate the target to be detected in the ROI area and segment it from the image; that is, accurately locate the target on the basis of the ROI area. Through this operation, the interference of noise and the design complexity of defect identification algorithm can be greatly reduced.

The defect recognition algorithm is used in the accurately located target area to segment the defect area. However, in the actual segmentation results, there are usually other nondefect regions that meet the defect characteristics. Therefore, screening links should be added to select defects and meet different testing standards [19]. The flowchart is shown in Figure 2.

3.4. Software Design of Bearing Inner Ring Defect Detection System. The bearing inner ring defect detection software is developed under Windows system based on visual studio compilation environment. The main functions of the software include camera parameter configuration of linear array camera and area array camera, camera image acquisition, image display, bearing inner ring defect detection algorithm, multistation camera parallel control, multistation processing result fusion, lower computer communication control, and other basic functions. The function is shown in Figure 3.

When the bearing enters the detection station from the feeding port, the sensor switch is triggered, and the two long rolling shafts take the bearing to rotate. At this time, the camera collects the image of the bearing and processes it in real time. When the outer ring of the tested bearing turns around for one week, the mechanical arm moves the tested bearing to the next station. Each bearing needs to go through the program flow as shown in Figure 4: image acquisition, image display, image processing, and data fusion to the final sorting process. The overall detailed steps of the program are as follows:

4. Result Analysis

4.1. Experimental Description. This test is a complete machine test on site. According to the needs of the project, the initial construction of a complete set of detection system is completed to form a complete set of bearing inner ring defect detection system. The detection object is the bearing inner ring sleeve of model IM-BBQ-3155D. The end face diameter of the bearing inner ring of this model is 39.78 mm, the width of the outer circumferential surface is 21.25 mm, and the alarm is given if there are black skin defects on the inner surface, side, and outer surface, or the size of collision defects is greater than 1 mm. Randomly select the bearing inner ring samples that have not been manually tested on site for testing [20].

4.2. Testing Process. Aiming at the existing detection methods of bearing inner ring defects, combined with the requirements of automatic transformation of factory production line, this paper proposes a detection method based on machine vision. The main detection process is as follows:

- (1) Initialization power on: After the user opens the software system, initialize and return the whole system, confirm whether the camera is connected normally and relevant parameters of the camera, and power on the PLC to return the mechanical device to the initialization position and wait for feeding

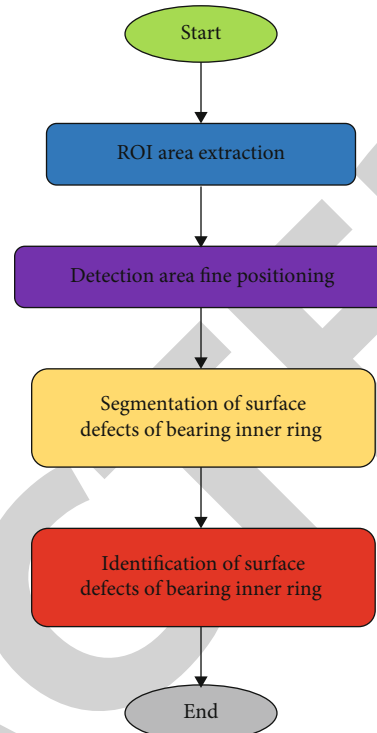


FIGURE 2: Flow chart of bearing inner ring defect detection algorithm.

- (2) Feeding: Since the system is an initial commissioning prototype and is not combined with the production line, the inner ring of the bearing is manually placed in the feeding groove, the bearing is placed in the feeding groove, and the feeding of the inner ring of the bearing is controlled by PLC and sensor to enter the detection station
- (3) Collection and detection: Run the software system. The bearing inner ring enters the detection station 1 from the feed inlet. Collect the image, and call the algorithm in the background to calculate the image and identify the defects. When the bearing inner ring rotates to a circle, it is moved horizontally to the next station. The feed from the feed inlet flows into station 1. The bearing is detected in the way of flow waterline. The bearing inner ring goes through the detection links of station 1, station 2, station 3, and station 4, respectively
- (4) Sorting: When the bearing enters station 4, collect images and identify defects. After processing, fuse the results of the first three stations for sorting

4.3. Result Analysis. Combined with the above testing process, 1000 sets of bearing inner ring samples were selected, including 800 qualified bearings and 200 unqualified products through manual testing. The appearance of bearing inner ring is tested, and the test results are shown in Table 1.

According to the analysis of the test results of 1000 sets of bearing inner rings, the whole system runs smoothly, and there will be false detection. After checking the test

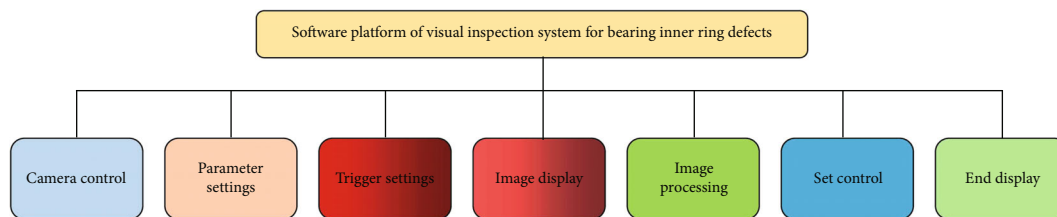


FIGURE 3: Software system structure.

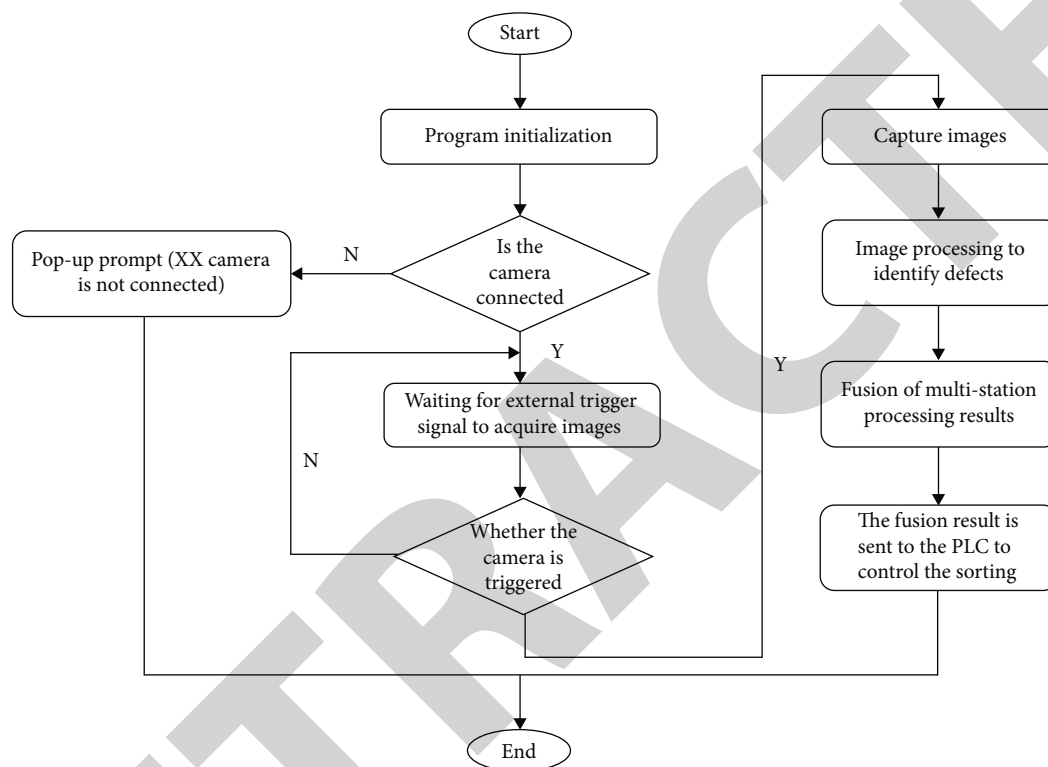


FIGURE 4: Overall flow chart of program framework.

TABLE 1: Sample test results.

	Inspected quantity	Correct detection quantity	False check quantity	Accuracy
Qualified bearing inner race	800	781	19	97.6%
Defective bearing inner race	200	200	0	100%
Total	1000	981	19	98.1%

results, it is found that there are fine scratches on the bearing surface, and the scratches are intertwined too densely, which will show a shape similar to black skin defects in the image. When the algorithm is determined, it will be mistakenly detected as black skin defects, and the qualified bearing will be determined as unqualified. However, in this case, it will not be detected as defective bearing in the process of manual detection. There are also a small number of false inspections of bearings because the manual inspection standards are not well integrated with the machine vision inspection standards. The manual inspection is subjective, and the inspection standards cannot be consistent at all times because the

staff will have visual fatigue after working for a long time. When using machine vision detection, the length and width of the initial standard defect are 1 mm. This standard is very small for human eyes in manual detection. After the image is collected by the camera, the details of the bearing surface are very clear, and the 1 mm appears very large. Therefore, some qualified bearing inner rings will be incorrectly detected as unqualified. Compared with the unqualified bearing inner ring, there is no false inspection in the inspection process, and the defects can be correctly detected without being wrongly identified as qualified products. In the process of the above experiment, the qualified products of the bearing

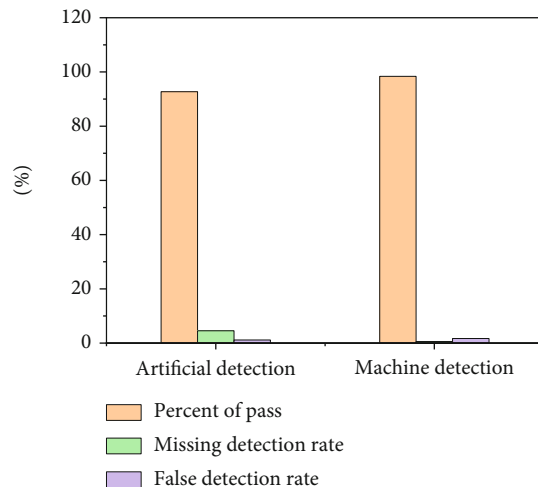


FIGURE 5: Comparison of detection methods.

inner ring will be falsely detected as unqualified due to the problem of detection scale. Next, 1000 bearing samples are randomly selected to compare the original manual detection method of the factory with the machine vision detection method. The two detection methods are carried out according to the unified standard; that is, if the defect size length exceeds 1 mm, it is unqualified. The comparison of detection results is shown in Figure 5.

Comparing the two detection methods, the qualified rate of machine vision is higher than that of manual detection, and the time is faster than that of manual detection. Manual detection takes 58 minutes, and machine detection takes 26 minutes. In the actual test, when the manual detection standard is the same as the machine detection standard, the manual detection method will produce visual fatigue with the increase of working time, resulting in the decline of detection efficiency and detection accuracy. However, for the machine vision detection method, it is always the same, and the image processing speed is between 100 ms and 150 ms for each image. It takes about 1-2 seconds for a bearing inner ring to go through four detection stations. In terms of the accuracy of detection results, there will be missed detection in manual detection, which does not exist in machine vision detection. The reason is that in the manual detection process, people will have fatigue and subjectivity problems, which will cause inconsistency between the detection accuracy and the detection results, but the detection standard is consistent in the machine detection process. And the false detection rate of machine vision detection method is also lower than the original manual detection [21]. It is concluded that using machine vision to detect the defects of bearing inner ring is a detection method with higher efficiency and accuracy than traditional manual detection, and the test results also lay a foundation for subsequent field application.

5. Conclusion

As an important part of machinery, the quality of bearing is related to the reliability of mechanical operation. For a long

time, bearing manufacturers mostly use manual visual inspection to detect the appearance of bearing. Due to human subjectivity and visual fatigue caused by long-term work, this detection method is not only inefficient, but also has a high rate of missed detection. Aiming at the problems of manual detection, this paper designs and implements a set of bearing inner ring defect detection system based on machine vision. In the hardware scheme, based on the actual needs, this paper selects the appropriate lens, camera, light source, and other related hardware; designs the lighting system according to the characteristics of bearing inner ring defects; and builds a complete set of bearing inner ring image acquisition platform. In the software scheme, this paper mainly includes two aspects: one is the design and implementation of software functions, and the other is the design and implementation of bearing inner ring image processing algorithm.

The actual test shows that the bearing inner ring defect detection system realized in this paper has the characteristics of good real time and high detection accuracy, and can meet the requirements of industrial detection, but there are still deficiencies.

- (1) Due to the complexity of the production environment, when the angle of the light source and the camera cannot be strictly aligned, the camera will collect the image and process the image, and the gray distribution of the image will be uniform, so that the recognition is inaccurate in the subsequent inspection process. Therefore, in the future optimization process, the algorithm needs to be optimized to reduce the impact of the angle of the light source and camera
- (2) The detection efficiency of the system needs to be further improved. In the actual test, the detection accuracy of the system is more accurate than that of manual detection, but the running speed has not been greatly improved. Therefore, in view of this problem, the whole system needs to be further optimized in terms of machinery and algorithm, compress time, and improve the detection efficiency

Data Availability

The data used to support the findings of this study are available from the corresponding author upon request.

Conflicts of Interest

The authors declare that they have no conflicts of interest.

References

- [1] K. Yang, L. Yang, P. Gong, L. Zhang, Y. Yue, and Q. Li, "Experiment and analysis of mechanical properties of carbon fiber composite laminates under impact compression," *E-Polymers*, vol. 22, no. 1, pp. 309–317, 2022.
- [2] S. Bonardd, C. Saldías, N. Leiva, D. D. Díaz, and G. Kortaberria, "Molecular weight enables fine-tuning the

Retraction

Retracted: A Wood Quality Defect Detection System Based on Deep Learning and Multicriterion Framework

Journal of Sensors

Received 22 August 2023; Accepted 22 August 2023; Published 23 August 2023

Copyright © 2023 Journal of Sensors. This is an open access article distributed under the Creative Commons Attribution License, which permits unrestricted use, distribution, and reproduction in any medium, provided the original work is properly cited.

This article has been retracted by Hindawi following an investigation undertaken by the publisher [1]. This investigation has uncovered evidence of one or more of the following indicators of systematic manipulation of the publication process:

- (1) Discrepancies in scope
- (2) Discrepancies in the description of the research reported
- (3) Discrepancies between the availability of data and the research described
- (4) Inappropriate citations
- (5) Incoherent, meaningless and/or irrelevant content included in the article
- (6) Peer-review manipulation

The presence of these indicators undermines our confidence in the integrity of the article's content and we cannot, therefore, vouch for its reliability. Please note that this notice is intended solely to alert readers that the content of this article is unreliable. We have not investigated whether authors were aware of or involved in the systematic manipulation of the publication process.

Wiley and Hindawi regrets that the usual quality checks did not identify these issues before publication and have since put additional measures in place to safeguard research integrity.

We wish to credit our own Research Integrity and Research Publishing teams and anonymous and named external researchers and research integrity experts for contributing to this investigation.

The corresponding author, as the representative of all authors, has been given the opportunity to register their agreement or disagreement to this retraction. We have kept a record of any response received.

References

- [1] P. Sun, "A Wood Quality Defect Detection System Based on Deep Learning and Multicriterion Framework," *Journal of Sensors*, vol. 2022, Article ID 3234148, 8 pages, 2022.

Research Article

A Wood Quality Defect Detection System Based on Deep Learning and Multicriterion Framework

Pingan Sun ^{1,2}

¹College of Chemistry and Materials Engineering, Zhejiang A&F University, Hangzhou, Zhejiang 311300, China

²School of Mathematics and Computer Science, Wuyi University, Wuyishan 354300, China

Correspondence should be addressed to Pingan Sun; 1522020204@st.usst.edu.cn

Received 22 May 2022; Revised 6 June 2022; Accepted 20 June 2022; Published 1 July 2022

Academic Editor: C. Venkatesan

Copyright © 2022 Pingan Sun. This is an open access article distributed under the Creative Commons Attribution License, which permits unrestricted use, distribution, and reproduction in any medium, provided the original work is properly cited.

In order to solve the problems of image perception and quality decision-making of wood defects with typical bionic intelligent algorithms, the existence of multidimensional degradation factors causes serious real problems of image distortion; the author proposes a wood defect image reconstruction and quality evaluation model based on deep reinforcement learning. The model introduced the deep learning mechanism and realized real-time and efficient reconstruction of multidimensional defect images of different wood by using the deep residual network for iterative training. In this model, a panoramic autonomous perception model was constructed for the fine segmentation and feature extraction of multidimensional defects of different wood and a shared resource pool of wood defect features of the magnitude of big data was constructed. Introduce the reinforcement learning mechanism, use the deep deterministic policy gradient algorithm, and establish a high-dimensional decision mapping between the iterative update of defect features, autonomous decision-making, panoramic visualization, depth prediction, and wood quality evaluation; it realizes the horizontal sharing integration of multidimensional difference wood defect image reconstruction and quality evaluation. The results obtained are as follows: in a typical environment, systematic wood quality evaluation, and autonomous intelligent decision-making performance, the coincidence rate with artificial defect recognition and evaluation efficiency can reach 90% and the loss of the training set can be controlled below 0.2%. Compared with the traditional wood quality grading system, the wood defect image reconstruction, and quality evaluation model system designed by the author, the quality evaluation decision-making efficiency rate was 90.19%, an increase of about 20%, and the system decision-making operation and maintenance loss was 2.23%, a decrease of about 10%. It is proved that the system designed by the author can realize the timely detection of wood quality defects very effectively and save a lot of manpower and material resources.

1. Introduction

Wood is one of the most precious natural resources in basic building materials, and at the same time, it is also one of the longest-used materials in human history [1]. Wood, cement, steel, and plastic are the four basic building materials today, of which only wood is a renewable resource [2]. At present, China is faced with the shortage of forest resources and the low quality of wood, which are not conducive to the development of forestry; as a country with relatively poor forest resources, the limited forest resources should be cherished and protected and the wood resources should be used fully

and rationally. How to improve the utilization rate of wood and make full use of forest resources is an important issue that Chinese forestry scientists need to face seriously [3].

In the process of wood processing and production, wood quality inspection and classification are an important link, the so-called wood quality inspection and classification, that is, based on the standards in the national standards of the People's Republic of China, the quality of wood is tested and graded, the detection is essentially the detection of wood defects, and the grading standard is based on national standards, for example, GB/T4822-2015 is the national standard for sawn timber inspection, which describes in detail the

material judgment of sawn timber to determine the grade of wood. At present, there are different standards for wood testing, which leads to an increase in the misjudgment of defects and affects the quality judgment of wood.

Due to the high intensity and long time of manual work, it is easy to cause visual fatigue and affect the final detection accuracy. Research on the digital transformation of traditional wood surface defect detection and quality grading based on artificial intelligence will greatly liberate manual labor, guide the conversion of original manual labor to mental labor, change the production mode of traditional wood screening, and improve industrial efficiency and automation level [4, 5].

2. Literature Review

Before the 1950s, the detection of wood defects, basically, manual identification is used to classify and calibrate defects. However, with the development of society and industrial production, the requirements for testing speed and testing quality have been continuously improved and the shortage of manual testing has gradually emerged; the problems of different judgment standards, misjudgment, and omission of judgment restrict the development of wood processing technology. Therefore, manual detection technology has been gradually abandoned by enterprises and other relatively commercial new detection technologies have begun to emerge [6].

With the rapid improvement of the level of modern industrial technology, since the 1950s, researchers have applied emerging technologies such as lasers, rays, and nuclear magnetic resonance to the field of wood defect detection, which has improved the automation level of wood defect detection. Western developed countries were the first to apply these emerging technologies to the study of wood defect identification; they used X-ray and ultrasonic to identify defects earlier, which improved the shortcomings of inconsistent manual inspection standards. But these techniques still have some other shortcomings: X-ray identification takes a lot of time, the diameter of the logs to be tested needs to be less than 600 mm, and the cost of testing equipment and maintenance costs are high. These detection techniques are affected by multiple factors such as wood structure texture, material, and the cost of detection equipment, which make these techniques not universally applicable. In modern wood processing enterprises, these emerging technologies have not been adopted on a large scale for the detection of wood defects.

With the rapid improvement of the level of information technology and the continuous enhancement of computer computing capabilities, artificial intelligence, computer vision, and other image-specific technologies have developed rapidly. At present, researchers in the field of wood defect detection have focused their research on the detection of surface images of wood defects and defect detection has entered the stage of informatization development. In recent years, more and more researchers have applied computer image processing and other technologies to the field of wood defect detection, forming a series of new feature detection methods [7]. In the 1980s, Gao et al. used a specific thresh-

old to divide the grayscale image of wood into rectangular blocks and realized the detection of wood defects based on texture analysis and spatial correlation of the image [8]. Then, Wu et al. applied this method to the color image of wood defects; first, the two-dimensional histogram of the R, G, and B channel maps of the image was subjected to double-threshold segmentation, and then, the low-frequency points were eliminated from the obtained results, the resulting area of the largest 2D histogram sum, that is, the defect background area [9]. In the 1990s, Hu et al. combined the self-organizing feature structure with the neural network for defect detection and achieved an accuracy of 85% [10]. Esteves et al. obtained the conclusion that the RGB space is the best color space in wood defect detection [11]. After entering the 21st century, related research has advanced by leaps and bounds. Some people combine the clustering method with the district-city growth method to obtain a better scoring effect. Lopes et al. proposed an algorithm to estimate the score by calculating the curvature from the shape structure of wood defects [12].

On the basis of the current research, this paper proposes a wood defect image reconstruction and quality evaluation model based on deep reinforcement learning. Deep learning mechanism is used to realize real-time and efficient reconstruction of multidimensional defect images of different wood. A panoramic autonomous perception model oriented to the fine segmentation and feature extraction of multidimensional defects of different wood was constructed, and a shared resource pool of wood defect features of the magnitude of big data was constructed. Also, through the reinforcement learning mechanism, a high-dimensional decision mapping between defect feature iterative update, autonomous decision-making, panoramic visualization, depth prediction, and wood quality evaluation is established for the deep deterministic strategy gradient algorithm; it realizes the horizontal sharing integration of multidimensional difference wood defect image reconstruction and quality evaluation [13].

3. Research Methods

3.1. Model Architecture of Wood Defect Image Reconstruction and Quality Evaluation. Based on the wood defect image reconstruction and quality evaluation model system with deep reinforcement learning, the architecture has real-time panoramic perception of wood defect images to be inspected. Multithreading transmission of heterogeneous defect image data in the format of fast reconstruction and temporary storage is constructed. The whole life cycle system of three-dimensional visual inspection of the wood production quality, such as quality grading evaluation and independent intelligent decision making, was constructed. A full-chain mechanism with real-time panoramic perception of wood defect images, image reconstruction quality evaluation, defect recurrence, and independent decision-making is also established. As shown in Figure 1, a special framework of wood defect image reconstruction and the quality evaluation model system is designed [14].

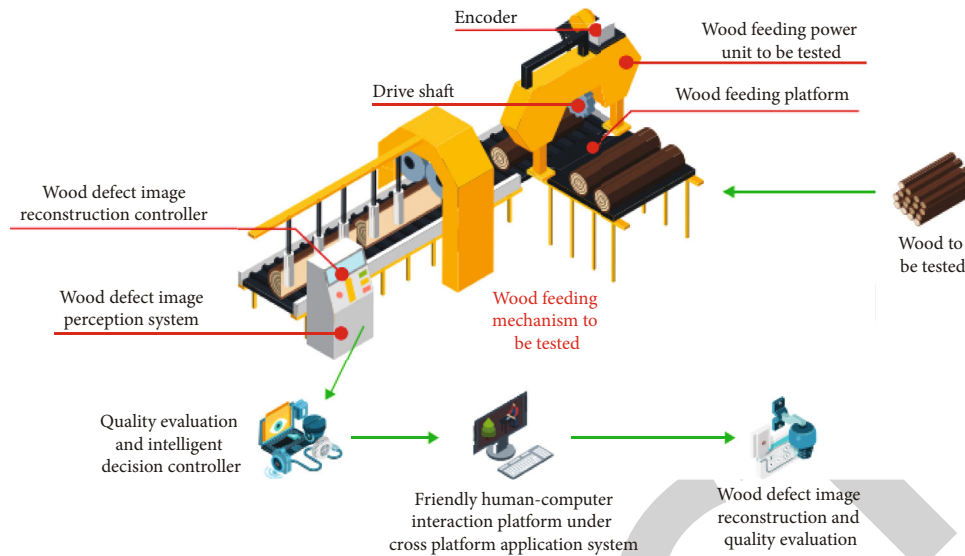


FIGURE 1: Architecture of wood defect image reconstruction and quality evaluation model.

Guided by the operation and maintenance requirements of the whole life cycle system efficiency of wood production quality visual inspection, the system architecture of the wood defect image reconstruction and quality evaluation model based on deep reinforcement learning is divided into wood defect image perception submodule, wood defect image reconstruction [15]. Construct submodule, quality evaluation, intelligent decision-making submodule, human-computer interaction submodule, etc.; among them, the wood defect image perception submodule uses a high-speed linear CCD camera to efficiently collect and accurately locate and identify wood defect images such as joints, dead joints, insect eyes, and cracks; The wood defect image perception submodule uses a high-speed linear CCD camera to efficiently collect and accurately identify wood defect images such as live segment, dead segment, and bug eye crack. The wood defect image reconstruction submodule introduces the deep learning mechanism. The deep residual network was used for iterative training to realize real-time and efficient reconstruction of multidimensional defect images of different wood. A panoramic autonomous perception model for multidimensional defect segmentation and feature extraction was constructed [16]. Quality evaluation and the intelligent decision submodule enhance the learning mechanism. The depth deterministic strategy gradient algorithm was used to establish a high-dimensional decision mapping between defect feature iteration and autonomous decision panoramic visual depth prediction and wood quality evaluation. The horizontal sharing integration of multidimensional and different wood defect image reconstruction and quality evaluation can be realized. The human-computer interaction submodule realizes the human-computer friendly interaction under the crossplatform application system.

Taking the wood defect image reconstruction and quality evaluation model architecture as the top-level design guidance of the state flow, the control flow logic of the wood defect image reconstruction and quality evaluation model based on deep reinforcement learning is designed; obtaining

large-scale normal wood images through linear CCD, a training sample dataset is formed and these normal sample datasets are input into the deep residual network based on a convolutional autoencoder for training, which can learn the data distribution characteristics of normal wood, but not the data distribution characteristics of defects. In the inference stage, input the image to be tested to the network for reconstruction, take the sliding area as the reconstruction object, make a residual with the original image, calculate the residual value, and compare it with the threshold to obtain the binary image classification result, which can show the defects of your region. The wood image is input into the classifier to distinguish and obtain the corresponding wood quality grade, after the detection of the abovementioned algorithm is completed; the image of the defective area is input into the wood quality classification system based on the image classifier for quality classification. The hardware part collects the normal wood image and the wood image to be detected by the image acquisition device (linear CCD); input the image into the computer and store it as a sample dataset and a dataset to be detected, and train the sample dataset through the embedded computer to obtain a model with parameters; input the image data to be detected into the model of the embedded computer for inference, and get the detection result; the classification instruction is given to classify the quality of the wood image, and then, it is handed over to the next-level execution equipment for processing; the control flow logic of the wood defect image reconstruction and quality evaluation model based on deep reinforcement learning is shown in Figure 2.

3.2. Wood Defect Image Reconstruction and Quality Evaluation Model Modeling. Based on the model architecture of wood defect image reconstruction and quality evaluation, the wood defect image perception submodule uses a high-speed linear CCD camera to efficiently collect and accurately locate and identify wood defect images such as joints, dead joints, insect eyes, and cracks; it is a standardized

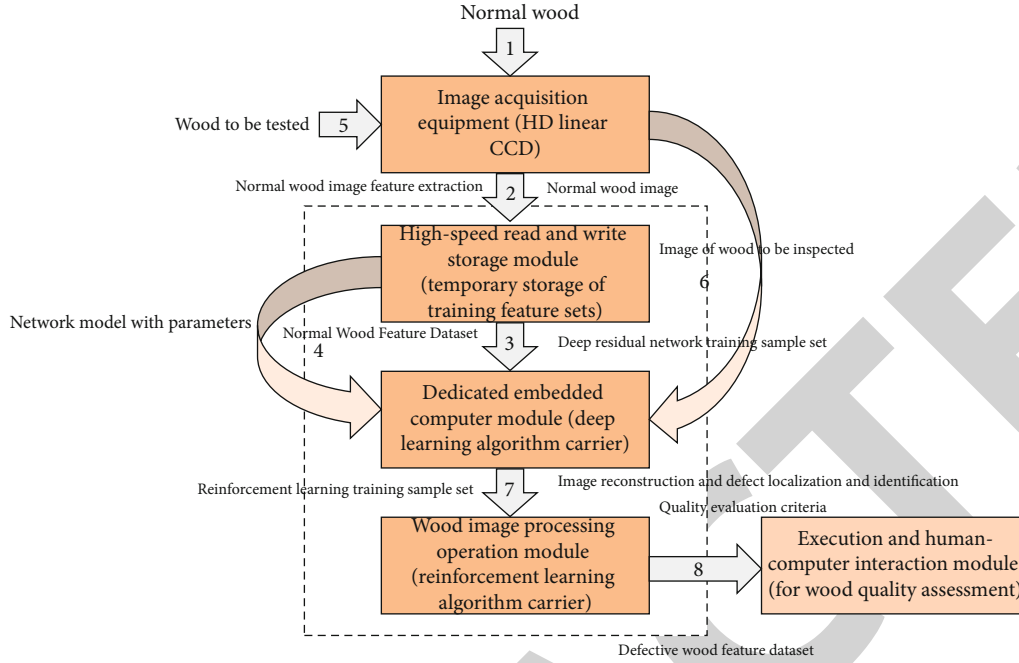


FIGURE 2: Control flow logic of wood defect image reconstruction and quality evaluation model.

engineering implementation method, and it is enough to follow the corresponding engineering standards of linear CCD: innovative design of wood defect image reconstruction submodule, quality evaluation, and intelligent decision-making submodule [17]. When focusing on improving typical bionic intelligent algorithms to deal with wood defect image perception and quality decision-making, under the action of the existing multidimensional degradation factors, the defect image is seriously distorted, the variance of the prior feature extraction of the defect image fluctuates frequently, the texture of the defect image is uneven, and the grayscale segmentation of the defect image fails; the optimal convergence rate varies hysteresis with defect dimension and other congenital deficiency. The deep learning mechanism was introduced to realize real-time and efficient reconstruction of multidimensional defect images of different wood by iterative training using the deep residual network. A panoramic autonomous perception model oriented to the fine segmentation and feature extraction of multidimensional defects of different wood was constructed, and a shared resource pool of wood defect features of the magnitude of big data was constructed. The reinforcement learning mechanism is introduced, and the deep deterministic strategy gradient algorithm is used to establish a high-dimensional decision mapping between the iterative update of defect features, autonomous decision-making, panoramic visualization, depth prediction, and wood quality evaluation; the horizontal sharing integration of multidimensional differential wood defect image reconstruction and quality evaluation is realized [18]. Based on the abovementioned analysis, the quantitative realization process of wood defect image reconstruction and quality evaluation model is given, which provides quantitative guarantee for engineering efficiency analysis.

3.2.1. Introduce the Deep Residual Network Mechanism. Wood defect image perception has high requirements on learning efficiency and real-time performance, introduces the deep residual network mechanism to improve the decision-making performance of deep learning, and uses the residual learning network to realize the identity mapping between stacked layers and input features; specifically, $Q(s, a, \theta_i)$ represents the output of the current residual network Eval.net, used to evaluate new features perceived by current learning; $Q(s, a, \theta_{-i})$ represents the output of the residual unit, and the optimal perceptual feature set is obtained from the identity mapping between the stacked layer and the input feature. After the introduction of Target-net, the residual unit remains unchanged for a period of time, which reduces the correlation between the unit mapping and the identity mapping to a certain extent, and improves the stability of the algorithm. After introducing the deep residual network mechanism, the parameters in the residual network are defined as θ^Q , $Q^\mu[s, \mu(s)]$ which represents the expected return value obtained by using the μ strategy to select an action in the s state, and because it is in a continuous space [19], it is expected that it can be calculated by integral; then, formula (1) can be used to express the quality of strategy μ .

$$J_\beta(\mu) = \int_{S_e}^{S_s} \rho^\beta(s) Q^\mu[s, \mu(s)] ds = E_{s \sim \rho^\beta} \{Q^\mu[s, \mu(s)]\}. \quad (1)$$

The residual unit establishes a direct correlation channel between the input and output through the identity mapping component, and through the probability distribution function, the optimal perception strategy is determined, and at each step, the best action in the current state is obtained according to the probability distribution and the random strategy $a_t \sim$

$\pi_\theta(s_t|\theta^\pi)$ is adopted to generate the action and the objective gradient function is shown in formula (2) as follows:

$$\begin{aligned} \nabla_\theta J(\pi_\theta) &= \int_{S_c} \rho^\pi(s) \int_{A_t} \nabla_\theta \pi_\theta(s, a) Q^\pi(s, a) da ds \\ &= E_{s \sim \rho^\pi, a \sim \pi_\theta} [\nabla_\theta \log \pi_\theta(a|s) Q^\pi(s, a)]. \end{aligned} \quad (2)$$

3.2.2. Introduce the Mechanism of the Deep Deterministic Policy Gradient Algorithm. Using the deep residual network panorama perception normal wood image feature set, provide a training sample set for reinforcement learning; use the powerful self-perception ability of the DDPG algorithm, real-time perception, and reconstruction of wood defect images, using the powerful self-decision ability of DDPG algorithm; realize the feature extraction and sharing calculation of multidimensional difference wood defect image parameters; and provide a positive feedback mechanism to correct the errors in the sharing process, building a quality evaluation mechanism under the global collaborative control [20]. Based on formula (2), the deterministic strategy formula (3) is given and an action is directly determined by the function μ according to the behavior; μ can be understood as an optimal behavior strategy $a_t = \mu(s_t|\theta^\pi)$; then, the quantitative wood defect image perception and reconstruction system can be represented as formula (3).

$$J(\mu_\theta) = \int_{S_c} \rho^\mu(s) r[s, \mu_\theta(s)] ds = E_{s \sim \rho^\mu} \{r[s, \mu_\theta(s)]\}. \quad (3)$$

Considering the instability of equation (3) in a competitive environment, the first-order derivation of equation (3) is carried out and the deterministic policy gradient can be expressed as equation (4), which has strong compatibility; through self-learning, real-time and efficient reconstruction of differential wood multidimensional defect images can be achieved and a panoramic autonomous perception model for fine segmentation and feature extraction of differential wood multidimensional defects can be constructed.

$$\nabla_\theta J(\mu_\theta) = \int_{S_c} \rho^\mu(s) \nabla_\theta \mu_\theta(s) Q^\mu(s, a) \Big|_{a=\mu_\theta} ds = E_{s \sim \rho^\mu} [\nabla_\theta \mu_\theta(s) Q^\mu(s, a)|_{a=\mu_\theta}]. \quad (4)$$

According to the wide variety of wood and the complex and changeable characteristics of wood defect images, use the policy network μ to act as an actor and use the value network to fit the (s, a) function; acting as the critical role, it realizes the horizontal sharing integration of multidimensional difference wood defect image reconstruction and quality evaluation, so the objective function of DDPG can be defined as formula (5).

$$J(\theta^\mu) = E\theta^\mu [r_1 + \gamma r_2 + \gamma^2 r_3 + \dots]. \quad (5)$$

Based on equations (3) and (4), efficient and orderly

reconstruction of wood defect images can be achieved; by storing the characteristics of wood defect images in the memory playback pool, the fusion quality evaluation function is solved by the substrategy parameters for information fusion and sharing; it fundamentally realizes the panoramic visualization of wood defect image recognition, reconstruction, and quality classification and realizes the horizontal sharing and integration of multidimensional difference wood defect image reconstruction and quality evaluation.

4. Analysis of Results

4.1. Simulation Verification under the Typical Environment of the Model. In order to multidimensionally verify the wood defect image reconstruction based on deep reinforcement learning and the actual working efficiency of the quality evaluation model, analyze the actual synergistic effect of automatic real-time perception and fusion of wood defect characteristics to be tested: autonomous and accurate reconstruction of wood defect images, global optimal quality evaluation, and autonomous intelligent decision-making mechanism; set the initial training wood defect feature sample size as N , the initial network input size is $128 * 256 * 16$; the discount factor γ is 0.96; the learning rate a is 0.001; the absolute value of the reward value of the decision policy is limited within $[-1, 1]$, because the negative reward is sparse; the standard action reward value is set to -1 , and the selection of parameters is guided by practical problems to ensure that there is still strong evolutionary vitality in the later stage of model training. And guide the training evolution towards a better direction. Develop [21]. Based on Google's Tensorflow 1.2.1 and OpenAI's Gym 0.9.2 environment, the verification environment was developed and the model was empirically analyzed; set the initial loss function, from the global optimal wood quality evaluation in a typical environment, with the performance simulation of autonomous intelligent decision-making, image perception, and reconstruction efficiency of wood defects in typical environments; the algorithm is verified by simulation and multidimensional simulation of model training loss performance under the control of the perception decision system; in the Gym 0.9.2 environment, the graphical schematic simulation is carried out and the comparison curve is given in the simulation diagram by using the significant difference mark; the final simulation results are shown in Figures 3–5.

It can be seen in Figures 3–5, that the wood defect image reconstruction and quality evaluation model based on deep reinforcement learning can better solve the following problems: when typical bionic intelligent algorithm deals with wood defect image perception and quality decision, the defect image distortion is serious under the action of multidimensional degradation factors; the variance of the defect image prior feature extraction fluctuates frequently, showing uneven texture defect image gray segmentation failure and other congenital defects [22]; under the action of the existing multidimensional degradation factors, the defect image is seriously distorted, the variance of the prior feature extraction of the defect image fluctuates frequently, and the grayscale segmentation of the uneven texture defect image fails; it has good perception and

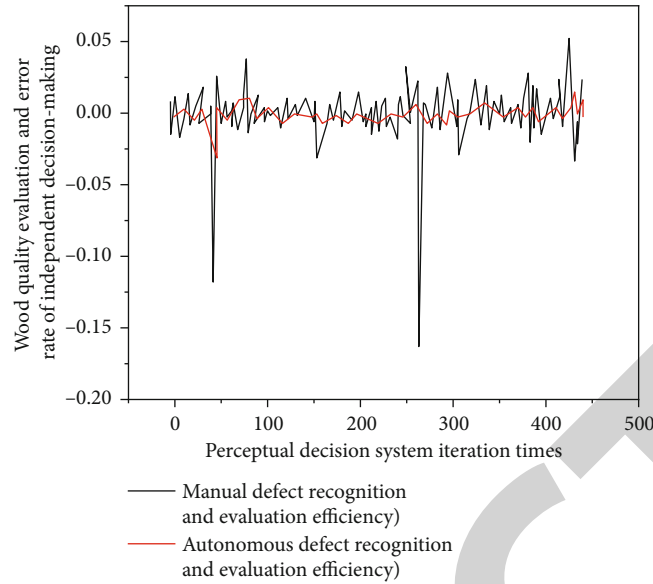


FIGURE 3: Simulation of global optimal wood quality evaluation and autonomous intelligent decision-making performance in a typical environment.

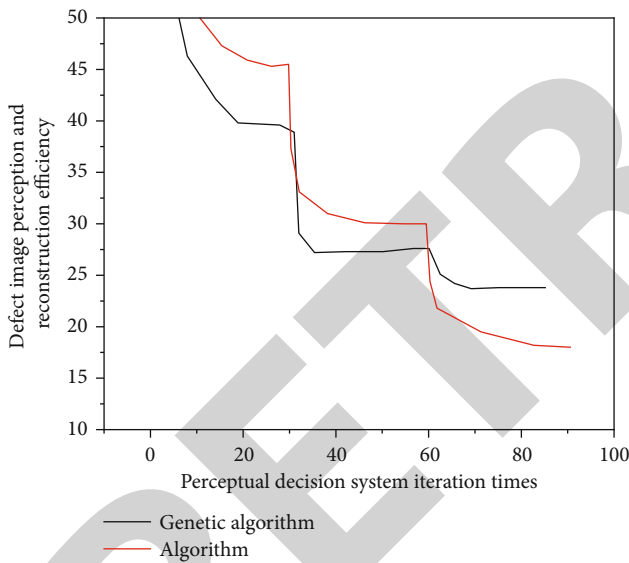


FIGURE 4: Comparison and simulation of wood defect image perception and reconstruction efficiency under typical environment.

reconstruction autonomy, can achieve global optimal quality evaluation and decision-making, and has the advantages of high stability, strong anti-interference, and strong model generalization ability.

4.2. Effectiveness Verification of Engineering Application of the Wood Defect Image Reconstruction and Quality Evaluation Model. In order to verify the reconstruction of wood defect images based on deep reinforcement learning and the actual engineering application efficiency of the quality evaluation model in the first-line operation and maintenance environment, select the economic forest in a certain place as the efficiency evaluation carrier. Ignoring the imbal-

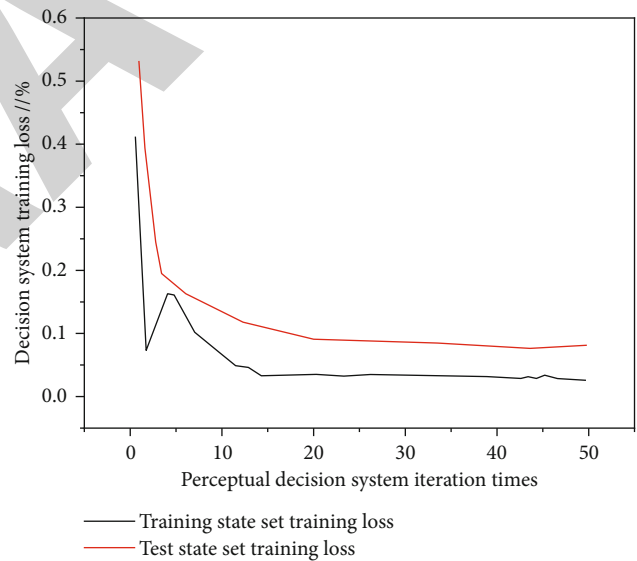


FIGURE 5: Simulation of model training loss performance under the control of perceptual decision-making system.

ance interference of the generalization ability and learning ability of the dissimilar wood texture itself, the engineering application analysis of the model was carried out, the normal images of wood are used as the training parameter set, and the images of wood defects are used as the test training set. Based on economic considerations, the wood quality comprehensive classification system of a wood processing line in this area was adaptively modified by using the microapplication expansion mode. In addition, real-time panoramic perception of heterogeneous defect image data of wood defect images for inspection is added to the software processing process of the full life cycle of three-dimensional visual inspection of the wood production quality, such as

TABLE 1: Comparison of engineering application efficiency of wood defect image reconstruction and quality evaluation model.

Compare items	Traditional wood quality grading system	Wood defect image reconstruction and quality evaluation model system based on deep reinforcement learning
Quality evaluation decision-making efficiency (%)	71.72	90.19
Image perception and reconstruction efficiency (s)	3.74	2.11
Decision system operation and maintenance loss performance (%)	12.14	2.23
Human-computer interaction friendliness of the system	Better	Very good
Defective image reconstruction effectiveness	Poor	Better
Internet push of quality evaluation information	Generally	Very good

rapid reconstruction of multithread transmission quality grading evaluation and independent intelligent decision-making under the temporary-normalized format. Independent memory resources are allocated to periodically interact with service data on the Intranet. Data panorama sharing and model engineering efficiency are realized [23].

The defect images of live nodes, dead nodes, and bug eye cracks in an economic forest with significant heterogeneity were selected as the performance verification carrier. Quantitative analysis was carried out from the aspects of global optimal wood quality evaluation and autonomous intelligent decision-making performance under a typical environment [24], wood defect image perception and reconstruction efficiency under a typical environment, and model training loss performance under the control of perceptual decision-making system. Qualitative analysis is carried out around the engineering application of the sensing decision system in human-computer interaction friendly defect image reconstruction, real-time effectiveness quality evaluation, and information interconnection push (Table 1).

Table 1 shows the wood defect image reconstruction based on deep reinforcement learning and quality evaluation model; it can effectively deal with the problem of perceptual reconstruction of wood defect images in a relatively short period of time and has obvious advantages in perceptual autonomy, panoramic reconstruction, independent evaluation, and model generalization ability [25].

5. Conclusion

When the author focuses on improving typical bionic intelligent algorithms to deal with wood defect image perception and quality decision-making, under the action of the existing multidimensional degradation factors, the defect image is seriously distorted, the variance of the prior feature extraction of the defect image fluctuates frequently, and the gray-scale segmentation of the defect image with uneven texture fails: the inherent disadvantages of dissimilar wood, such as the imbalance between the generalization ability and learning ability of the texture itself and the hysteresis of the optimal convergence speed with the defect dimension; the author

proposes a new wood defect image reconstruction and quality evaluation model and selects a certain economic forest in a certain place as the performance evaluation carrier and analyzes the engineering application of the model; the first-line operation and maintenance verification results show that the prototype system has real-time panoramic perception of wood defect images to be inspected: rapid reconstruction and temporary storage of heterogeneous defect image data, multithreaded transmission in normalized format, quality grading evaluation, and autonomous intelligent decision-making; The prototype system also has quality grading evaluation and autonomous intelligent decision making and other full-life cycle system efficiency of three-dimensional visual inspection of the wood production quality, it has good perception and reconstruction autonomy, can achieve global optimal quality evaluation and decision-making, and has the advantages of high stability, strong anti-interference, and strong model generalization ability.

Data Availability

The data used to support the findings of this study are available from the corresponding author upon request.

Conflicts of Interest

The authors declare that they have no conflicts of interest.

References

- [1] J. Shi, Z. Li, T. Zhu, D. Wang, and C. Ni, "Defect detection of industry wood veneer based on nas and multi-channel mask r-cnn," *Sensors*, vol. 20, no. 16, p. 4398, 2020.
- [2] M. Kryl, L. Danys, R. Jaros, R. Martinek, and P. Bilik, "Wood recognition and quality imaging inspection systems," *Journal of Sensors*, vol. 2020, Article ID 3217126, 19 pages, 2020.
- [3] J. Sandak, A. Sandak, A. Zitek, B. Hintestoisser, and G. Picchi, "Development of low-cost portable spectrometers for detection of wood defects," *Sensors*, vol. 20, no. 2, 2020.
- [4] A. Sardet, B. Perot, C. Carasco, G. Sannie, and F. Pino, "Performances of c-bord's tagged neutron inspection system for explosives and illicit drugs detection in cargo containers,"

Retraction

Retracted: Gymnastics Action Recognition and Training Posture Analysis Based on Artificial Intelligence Sensor

Journal of Sensors

Received 12 December 2023; Accepted 12 December 2023; Published 13 December 2023

Copyright © 2023 Journal of Sensors. This is an open access article distributed under the Creative Commons Attribution License, which permits unrestricted use, distribution, and reproduction in any medium, provided the original work is properly cited.

This article has been retracted by Hindawi, as publisher, following an investigation undertaken by the publisher [1]. This investigation has uncovered evidence of systematic manipulation of the publication and peer-review process. We cannot, therefore, vouch for the reliability or integrity of this article.

Please note that this notice is intended solely to alert readers that the peer-review process of this article has been compromised.

Wiley and Hindawi regret that the usual quality checks did not identify these issues before publication and have since put additional measures in place to safeguard research integrity.

We wish to credit our Research Integrity and Research Publishing teams and anonymous and named external researchers and research integrity experts for contributing to this investigation.

The corresponding author, as the representative of all authors, has been given the opportunity to register their agreement or disagreement to this retraction. We have kept a record of any response received.

References

- [1] Y. Chen and Q. Chen, "Gymnastics Action Recognition and Training Posture Analysis Based on Artificial Intelligence Sensor," *Journal of Sensors*, vol. 2022, Article ID 1605529, 7 pages, 2022.

Research Article

Gymnastics Action Recognition and Training Posture Analysis Based on Artificial Intelligence Sensor

Yuanxiang Chen ¹ and Qiao Chen ²

¹*Xi'an Peihua University, Xi'an, Shanxi 710061, China*

²*Department of Sports, Chengdu University of Technology, Chengdu, Sichuan 610059, China*

Correspondence should be addressed to Yuanxiang Chen; 2016122631@jou.edu.cn

Received 19 May 2022; Revised 2 June 2022; Accepted 20 June 2022; Published 1 July 2022

Academic Editor: C. Venkatesan

Copyright © 2022 Yuanxiang Chen and Qiao Chen. This is an open access article distributed under the Creative Commons Attribution License, which permits unrestricted use, distribution, and reproduction in any medium, provided the original work is properly cited.

In order to solve the problems that the gymnastics action recognition system cannot select gymnastics training items and difficulty modes, the calculation matching degree and its threshold angle are inaccurate, the effect and efficiency of action learning are low, and this research proposes a gymnastics action recognition and training pose analysis methods based on artificial intelligence sensors. This method completes the performance improvement of the traditional human action recognition algorithm and uses the skeletal features of the Kinect sensor to discriminate sports actions. Clustering based on static *K*-means algorithm increases the accuracy of pose selection, and each pose is recognized by human action using artificial neural network (ANN) and hidden Markov model (HMM). The obtained results are as follows: comparison of nonstatic and proposed static *K*-means algorithm on the training set and the overall accuracy of the proposed method is much better than the previous method. Among the four movements, the accuracy rate of “sitting” and “standing” movements is significantly higher, reaching 100%. In the gymnastics action recognition experiment, the average recognition rate of the system in this research is 93.6%, the false rejection rate is 5%, and the false acceptance rate is only 1.4%. It is proved that the system interface designed in this research can prompt the part that needs to be corrected, display the error on the output device, more efficiently assist the user to perform targeted training on the action to be learned, and improve the effect and efficiency of action learning.

1. Introduction

With the successful commercial use of somatosensory games by Microsoft in recent years, it has brought a brand new gaming experience to players, and with the rapid popularization and application of computer technology, many researchers and businesses have completely subversive and innovative ways of somatosensory games based on connection. Into the equipment has seen a very broad application and promotion prospects in the field of rehabilitation training [1, 2]. The main problem obtained on the basis of applied research is how to use it for human action recognition and processing equipment. Kinect, as a data scanning device based on somatosensory technology under Microsoft, has been widely used in human motion detection. Its constantly improved motion capture technology and speech rec-

ognition technology make it easy for people to talk to machines with only body movements or sounds [3, 4].

The somatosensory data scanning equipment based on virtual reality also provides a new training guidance idea for gymnastics training: sports data collection is used in many professional gymnastics training and national training to assist researchers to observe coaches' movements from multiple perspectives, obtain training data of multiple movement parameters and physiological indicators, and provide a reliable data source for scientific training [5, 6]. The coach can customize a scientific training plan for each trainer through various training data, guide the training in a targeted manner, and accurately grasp the trainer's body contour and body position. The user's body movements are wrong, thereby reducing the difficulty of the students' movement and improving the training efficiency [7].

2. Literature Review

Kinect devices were born at the stage of booming virtual reality technology, more and more consumers favor its immersive experience, and the consumer market is also expanding, not only for games, education, and rehabilitation services [8]. Therefore, the application of virtual reality technology in virtual training has attracted widespread attention [9]. In order to reduce training costs and improve training effects, various industries such as military and fire protection are trying to develop virtual training simulators [10]. In order to provide an interactive, immersive environment for the trainee, the virtual training simulator must be able to recognize the movements performed by the trainee [11]. For this reason, the human action recognition method was introduced into the virtual training simulation based on the Kinect-based somatosensory device [12]. So far, most of the research on virtual training simulators is based on human motion recognition of wearable motion capture suits to obtain precise information of human motions, thereby synchronizing the training content according to the motions.

Recognition of palm bones through Kinect, Wang et al. have designed a set of dynamic gesture recognition based on Kinect. Through the Kinect device connected to the Internet of Things, Liu et al. have developed a smart home that can simplify life style system. Zhang et al. developed a learning assistance system to assist users in learning Tai chi movements and moves: auxiliary exercises. Zhao et al. applied Kinect to medical treatment and designed an auxiliary system for diagnosis and recovery of movement disorders based on gait analysis. Xu and others follow the trend of the times and combine the preferences of contemporary people to design and research somatosensory educational games. Zhang and Jia and Li have used Kinect in swimming, which has been well used to guide athletes to contact swimming styles [13, 14].

A major feature of the Kinect device is to capture the data of moving objects or moving human bodies when they make actions, record the motion trajectory data of moving objects, process these data with machine learning algorithms, and then convert them into digital motion data. Taking advantage of this feature of Kinect, it is widely used in somatosensory games, medical human detection, and even in the film industry. For the research of Kinect, many research institutes and universities, including the Institute of Artificial Intelligence, have used the feature of Kinect data capture [15, 16]. The artificial intelligence research institute of a university manually marked the feature points of the human body in the first frame and used monocular vision to capture and track the movement of the unobstructed parts of the human body without retaining the lost depth data stream. The data acquisition of the position information of the occluded parts becomes difficult to achieve.

From the above, the system in this research combines the static initial centroid of the first estimate of K -means and an artificial neural network, which is effectively evaluated on the public data-set UTKinect. In this system, a human action recognition system in Kinect skeletal joints is proposed.

3. Research Methods

3.1. Skeletal Skinning Animation for Gymnastics Movements.

The algorithm principle of skinned mesh technology is to divide the character's body structure into animations of multiple skeletal joints and add a layer of skin to the outside of the skeletal model. The essence of the skin is a mesh model animation. A mesh point set is commonly used in modeling software. The principle is bone skinning and bone joints are bound and paired one by one. According to the reason why a vertex is affected by multiple surrounding joint points, the position of the bone nodes of the human model is formed into a whole, and the bone and skin vertices determine its weight, to calculate the position of the bones, only need to weight the bones with different weights and their corresponding skin vertices. Through the interpolation of two adjacent key frames, through linear calculation, the vector data of the key frame, including the position and direction, can be determined, and its weight can be obtained through grid model calculation, and then the changed position can be calculated. The characteristic of skeletal skinning animation is to make the animation look more complete and more delicate in expression on the basis of skinning. The feature of the skeleton skinning algorithm is that by putting a "coat" on the bones, it drives the movement of the entire human body structure, making the whole look smoother. Skeletal skinning animation saves production costs and cycles because it reduces computational storage while representing skeletal motion. Since the mesh structure of the skeletal model is mostly composed of adjacent quadrilaterals or polygons, it is necessary to add a set of bones to the human body mesh model and their positions in order to connect the skin vertices of the bones to cooperate with the action and better reflect the smooth changes of the human body model [17].

The principle of the skinning algorithm is that since the parent vertices of the skin at the skeleton node are affected by multiple surrounding child skeletons, there is no need to predefine the position of the skin vertices. It is only necessary to use the interpolation of the joint positions of the skin mesh to calculate the skin through the linear calculation method. Vertex and bone weights, then get the updated positions of skin vertices to quickly update the skin joint positions during the movement, and finally deduce the positions of all skin mesh vertices. The specific algorithm formula is as follows:

$$v' = \sum_{i=1}^n w_i M_i D_i^{-1} v \quad \sum_{i=1}^n w_i = 1. \quad (1)$$

The algorithm can effectively update the position information. w_i indicates the weights of its skin vertices, v indicates the position coordinates of the bone joints before the skin update, v' indicates the updated position coordinates, and M_i and $D_i^{-1}v$ indicate the v segment of the bone of global coordinate system and the local coordinate system.

The principle of the dual quaternion linear blending (DLB) algorithm is to maintain the skin volume of the animation model before and after the transformation, that is, a rigid body transformation, which is formed based on the invariance of the coordinate system. It can avoid the

unnatural phenomenon of skin knotting, which not only avoids the shortcomings of the rotation center offset in the spherical hybrid skinning algorithm but also sets the interpolation of the shortest path in the transformation, so that the skin behaves better nature.

The formula form of the dual quaternion linear blending (DLB) algorithm representing the spatial rotation transformation is as follows:

$$q = \left[\cos \left(\frac{\theta}{2} \right), n \sin \left(\frac{\theta}{2} \right), ny \sin \left(\frac{\theta}{2} \right), nz \sin \left(\frac{\theta}{2} \right) \right]. \quad (2)$$

$[nx, ny, nz]$ and θ represent the rotation axis and angle through the origin. The formula is in the form of $z = r - d\epsilon$, where $\epsilon^2 = 0$, the dual quaternion is the real part, r and the dual part d are the dual numbers of the quaternion, and ϵ represents the dual operator. Through this formula, the positional relationship of rotation and translation in the space can be expressed. The dual quaternion formula is as follows:

$$q = q_r + q_d\epsilon. \quad (3)$$

The dual quaternion linear blending (DLB) algorithm has the characteristics of rigid transformation between it and the matrix. In addition, due to the invariance of the coordinate system of the algorithm, the position of the bones before and after the update of the human body model can be kept inconvenient, avoiding the shortcoming of the rotation center offset in the spherical hybrid skinning algorithm.

BVH data is a motion manipulation data format, which is converted after the Kinect device collects real-time motion data. This data can be driven in real time under the user's operation, and the model can change in real time according to the user's actions. The sequence of BVH data is also in accordance with the sequence of motion data collected in real time, matching with the three-dimensional character model, and is widely used.

The production steps in skeletal animation are shown in Figure 1.

3.2. Introduction to Algorithm Model. Hidden Markov model (HMM, hidden Markov model) is a statistical model that randomly generates observation sequences. Hidden Markov models have strong dynamic modeling capabilities in the fields of natural language and biological information processing, as well as action recognition. For input human model samples, new training can be constructed without resetting model parameters. For input human model samples, a new training template library can be constructed without resetting model parameters. The emergence of HMM has played a huge role in the expansion of the field of somatosensory recognition [18].

The structure of ANN artificial neural network (artificial neuron network) is similar to the neuron structure of the human brain. Its operation and processing methods are parallel and distributed, and it has the ability of classification, comparison, and machine learning in pattern recognition, which vividly imitates the neurons of the brain. It is widely used in processing network information. ANN is composed of neurons with input and output functions and has strong classification ability, which is embodied in the parallel con-

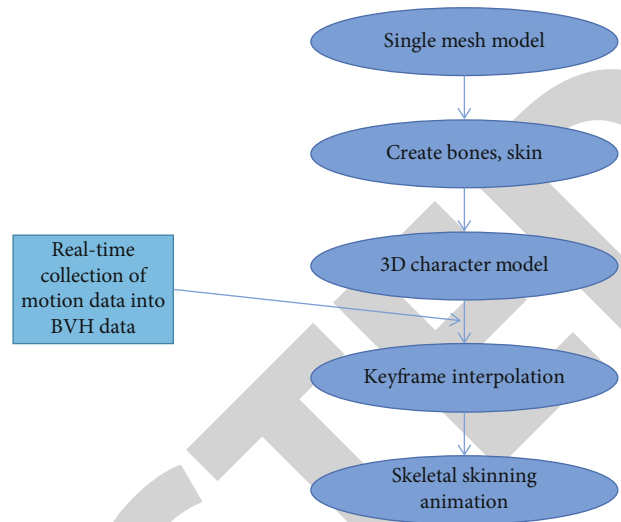


FIGURE 1: Steps for creating 3D character animation with bone skinning.

nection between each processing neural unit, and information processing and calculation are performed through the connection of neurons or skeletal joints. ANN has a pattern response to the input information for the weights between different joints in the system [19].

The main purpose of the system designed in this research focuses on the development of efficient skeletal joint feature representations to recognize gymnastic movements. The structure of the human action recognition system is shown in Figure 2.

In this system, 3D skeletal joint data is used as the input of the Kinect sensor, and joint distance features are used for feature extraction. Clustering of such features is developed based on static K -means starting from a static initial centroid at the first estimate of the K -centroid to improve performance in pose selection for ergonomic gymnastics, and in contrast to nonstatic initial K -means starting from the static initial K -means, the static K -means difference is always a random centroid of K centroids. The class label for each gymnastics pose is determined by using an artificial neural network (ANN), which makes the system more intelligent. Finally, gymnastics action recognition is performed using a hidden Markov model (HMM) based on a set of known gymnastic action poses to improve performance and accuracy.

3.3. Design of Gymnastics Action Recognition Method. The system architecture of this system includes data processing, motion capture, mannequin driving, motion analysis and feedback, and system scoring. The system architecture of this system includes data processing, motion capture, mannequin driving, motion analysis and feedback, and system scoring. Each module is linked together, and the most primitive Ren Xi motion data is finally presented on the screen in the form of mannequin animation.

The system architecture is shown in Table 1.

Data processing process of each module:

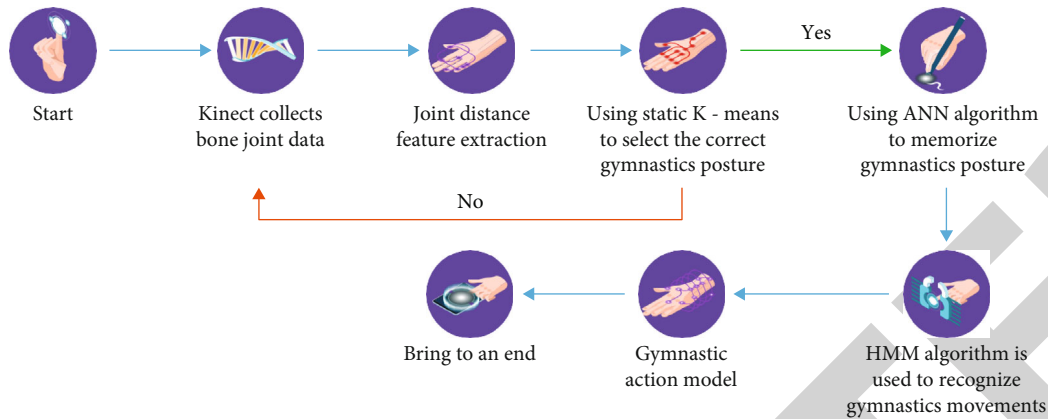


FIGURE 2: Flowchart of gymnastics action recognition system.

- (1) *Data Processing.* Convert the raw data captured by Kinect. Including color data and depth data, plus time vector programming ordered frame data sequence, easy to input into the next module
- (2) *Motion Data Capture.* Through the data stream after data processing, the machine learning algorithm is used to analyze the 20 bone positions of the human body and their joint points, and then the improved human motion recognition algorithm is used for optimization processing, and the updated bone joint positions are output
- (3) *Human Body Model Drive.* The real-time position information of the joints output by the motion capture module is bound to the joints of the human body model of the modeling software in a one-to-one correspondence, so as to achieve the effect of synchronous movement between the model and the user, and then input it into the Unity platform for rendering
- (4) *Action Analysis and Feedback.* The collected exercise data of the trainer is combined with the real-time data of data processing, motion capture, and human body model drive module, and the standard sports action is compared with the exercise data of the trainer, and the wrong action information is displayed on the screen
- (5) *System Scoring Module.* The comparison between the user's motion data and the standard motion data, and the user's real-time score when learning the action is calculated according to the harshness of the action (i.e., the threshold angle) set before the user enters the system
- (6) Compare the angle data of the trainer's human skeleton model with the angle of the standard gymnastics training items, determine the threshold range, and evaluate the degree of movement standard in the form of scores [20]

The relationship between the modules is shown in Figure 3.

4. Analysis of Results

4.1. UTKinect Public Dataset Test. Experiments on the dataset are in this research. The proposed method is tested on the public dataset UTKinect-Action3D recorded by the Kinect sensor.

There are three channels in this dataset, which are bone joint position, color, and depth channels [21]. This dataset contains ten movements (stretching, chest expansion, body rotation, jumping, walking, sitting, standing, picking up, throwing, pushing, pulling, waving, and clapping) for ten objects, where it contains two instances, each object performs each action twice, using some of the activities corresponding to the system (stretching, chest expansion, body rotation, and jumping). The joint distance features of these movements are extracted and grouped together by similar gymnastic movement poses based on k -means (nonstatic and static) with five cluster identifiers. The labels of each gymnastic action pose are determined by ANN, and a corresponding HMM is built to recognize the sequence of gymnastics action poses [22].

The method proposed in this research is static K -means, which statically adopts the initially defined centroid mass when estimating the K -shaped centroid for the first time, in order to improve the accuracy and correctly classify human gymnastics action poses. Experiments using this method are tested on the training set and compared with the nonstatic K -means method [23]. Table 2 also shows a comparison of the nonstatic and static K -means algorithms on the training set. The overall accuracy of the proposed method is much better than previous methods.

The experimental results show that the accuracy of these four actions is relatively high, especially the accuracy of "sitting" and "standing" actions is significantly higher and can reach 100%.

4.2. Gymnastics Action Recognition Experiment and Analysis. The daily gymnastics movements are complex and changeable. In order to refine this identification process, the system should set several gymnastics movements and name them according to the actual situation and then identify them [24].

TABLE 1: Architecture of each system.

Module name	Input stream	Output stream
Data processing	Raw data stream	Frame data sequence
Motion data capture	Frame data sequence	The real-time position of the user's skeletal joints
Mannequin driven	Joint real-time position information sequence	Real-time 3D character animation
Action analysis and feedback	User motion data and standard motion	Misplacement reminder message
System score	User motion data and standard motion	Real-time comparison results (scores)

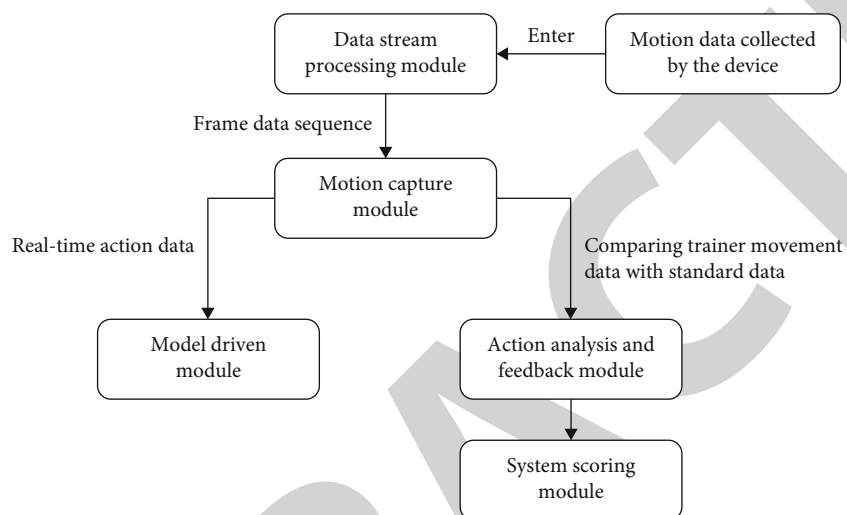


FIGURE 3: The relationship between the information processing modules in the system.

TABLE 2: Comparison of nonstatic and static K -means on UTKinect dataset.

Action type	Accuracy (%)	
	Nonstatic K -means	Static K -means
Stretching exercises	92	100
Chest expansion	54	100
Body rotation	37	95
Jumping motion	82	95

This research defines 6 simple gymnastics movements for the purpose of interaction, including stretching, chest expansion, body rotation, jumping, whole-body movement, and finishing. Human-computer interaction with the computer can be performed by recognizing these kinds of gymnastics action commands.

In the experiment, the person to be tested first recorded each gymnastics movement through Kinect and then saved the recorded gymnastics movements into the reference template. Each gymnastics movement was recorded 20 times, divided into 6 times, and a total of 120 pieces of sample data were recorded. A total of 720 experimental data were obtained by 6 experimenters. Record the recognition results of each gymnastics action and calculate the recognition rate, as shown in Figure 4.

It can be seen from the figure that the test recognition rate is high, the average recognition rate is 93.6%, the rejection rate is 5%, and the misrecognition rate is only 1.4%. Before the experiment, because the subjects to be tested received the guidance of pictures and texts of gymnastics movements, the similarity between gymnastics movements and postures was not large, and the difficulty of distinguishing them was small, so the recognition rate was high [25].

Therefore, the recognition ability of the system in this research is good and meets the requirements of daily training, but the recognition complexity should be considered when selecting gymnastics action features, and the gymnastics action recognition system is designed for the purpose of practical application.

5. Conclusion

With the increasingly vigorous development of somatosensory technology, more and more somatosensory technology platforms and recognition systems are widely used in our daily life, while traditional gymnastics training will always have unsatisfactory conditions, including relatively high costs and risks. Relatively existing problems, nowadays, relying on somatosensory technology, you can train the gymnastics items you want to learn, such as stretching, chest expansion, and jumping. This allows many ordinary people to experience another world through the somatosensory system, and the practicality and convenience brought by somatosensory technology are more

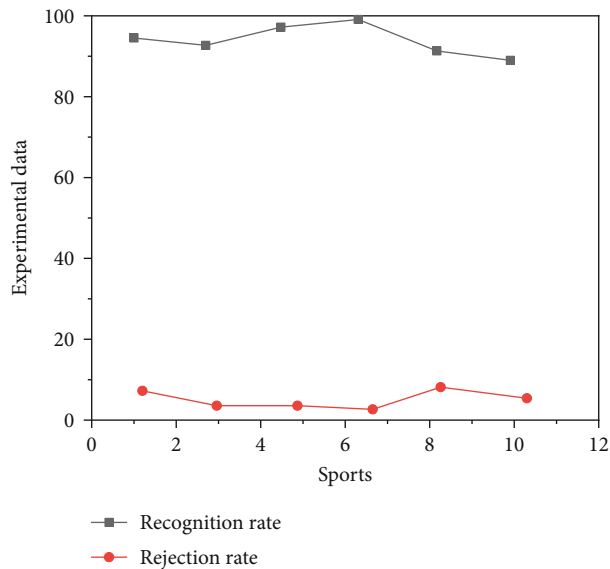


FIGURE 4: Identification results (%).

and more popular among people. Therefore, this system aims to simplify the gymnastics training process, so as to research and implement a gymnastics action recognition system based on Kinect, so that trainers can efficiently learn various gymnastics items at home and understand their own deficiencies.

The performance improvement of the traditional human action recognition algorithm is completed. Sports action is discriminated by utilizing the skeletal features of the Kinect sensor. Clustering based on the static K -means algorithm increases the accuracy of pose selection. Each pose is recognized by human action using artificial neural network (ANN) and hidden Markov model (HMM), which makes the system more intelligent and improves system performance and accuracy. Finally, it is evaluated on the public dataset UTKinectAction3D.

The developed gymnastics action recognition system can relatively meet the needs of users' gymnastics training. Users can choose gymnastics training items and difficulty modes according to their needs, calculate the matching degree and its threshold angle, prompt the part that needs to be corrected in the interface, and display the error. On the output device, it can more efficiently assist users to perform targeted training on the actions to be learned and improve the effect and efficiency of action learning.

Data Availability

The data used to support the findings of this study are available from the corresponding author upon request.

Conflicts of Interest

The authors declare that they have no conflicts of interest.

References

- [1] H. Mohammadzade, S. Hosseini, M. Dastjerdehei, and M. Tab Amaat, "Dynamic time warping-based features with class-specific joint importance maps for action recognition using kinect depth sensor," *IEEE Sensors Journal*, vol. 21, no. 7, pp. 9300–9313, 2021.
- [2] P. Wang, "Research on sports training action recognition based on deep learning," *Scientific Programming*, vol. 2021, 8 pages, 2021.
- [3] J. Dogra, S. Jain, A. Sharma, R. Kumar, and M. Sood, "Brain tumor detection from MR images employing fuzzy graph cut technique," *Recent Advances in Computer Science and Communications*, vol. 13, no. 3, pp. 362–369, 2020.
- [4] C. Li and J. Cui, "Intelligent sports training system based on artificial intelligence and big data," *Mobile Information Systems*, vol. 2021, 11 pages, 2021.
- [5] U. Sugumlu, "An action research on the improvement of writing skill in teacher training," *Educational Policy Analysis and Strategic Research*, vol. 15, no. 1, pp. 137–162, 2020.
- [6] X. Chen and V. Dinavahi, "Group behavior pattern recognition algorithm based on spatio-temporal graph convolutional networks," *Scientific Programming*, vol. 2021, 8 pages, 2021.
- [7] J. Dan, Y. Zheng, and J. Hu, "Research on sports training model based on intelligent data aggregation processing in internet of things," *Cluster Computing*, vol. 25, no. 1, pp. 727–734, 2022.
- [8] J. Tan, D. Xia, S. Dong, H. Zhu, and B. Xu, "Research on pre-training method and generalization ability of big data recognition model of the internet of things," *ACM Transactions on Asian and Low-Resource Language Information Processing*, vol. 20, no. 5, pp. 1–15, 2021.
- [9] Z. Liu, "Analysis of physical expansion training based on edge computing and artificial intelligence," *Mobile Information Systems*, vol. 2021, 9 pages, 2021.
- [10] S. Shriram, J. Jaya, S. Shankar, and P. Ajay, "Deep learning-based real-time AI virtual mouse system using computer vision to avoid COVID-19 spread," *Journal of healthcare engineering*, vol. 2021, 8 pages, 2021.
- [11] Y. Bai and Y. Chen, "Human motion analysis and action scoring technology for sports training based on computer vision features," *Journal of Intelligent and Fuzzy Systems*, vol. 34, pp. 1–9, 2021.
- [12] N. Suyoto and T. Sidodadi, "P3t (training, guidance and integrated assistance) model-based on assesment necesiity to create ptk (class action research) article results for elementary school teachers," *European Journal of Humanities and Social Sciences*, vol. 6, pp. 54–65, 2020.
- [13] L. Zhang, "Evaluation and simulation of sports balance training and testing equipment based on medical video image analysis," *IEEE Sensors Journal*, vol. 20, no. 20, pp. 12005–12012, 2020.
- [14] L. Jia and L. Li, "Research on core strength training of aerobics based on artificial intelligence and sensor network," *EURASIP Journal on Wireless Communications and Networking*, vol. 2020, 16 pages, 2020.
- [15] M. Bradha, N. Balakrishnan, A. Suvitha et al., "Experimental, computational analysis of butein and lanceoletin for natural dye-sensitized solar cells and stabilizing efficiency by IoT," *Environment, Development and Sustainability*, vol. 24, 2021.

Retraction

Retracted: Data Management Platform of Forest Ecological Station Based on Internet of Things and Big Data Sensor

Journal of Sensors

Received 17 October 2023; Accepted 17 October 2023; Published 18 October 2023

Copyright © 2023 Journal of Sensors. This is an open access article distributed under the Creative Commons Attribution License, which permits unrestricted use, distribution, and reproduction in any medium, provided the original work is properly cited.

This article has been retracted by Hindawi following an investigation undertaken by the publisher [1]. This investigation has uncovered evidence of one or more of the following indicators of systematic manipulation of the publication process:

- (1) Discrepancies in scope
- (2) Discrepancies in the description of the research reported
- (3) Discrepancies between the availability of data and the research described
- (4) Inappropriate citations
- (5) Incoherent, meaningless and/or irrelevant content included in the article
- (6) Peer-review manipulation

The presence of these indicators undermines our confidence in the integrity of the article's content and we cannot, therefore, vouch for its reliability. Please note that this notice is intended solely to alert readers that the content of this article is unreliable. We have not investigated whether authors were aware of or involved in the systematic manipulation of the publication process.

Wiley and Hindawi regrets that the usual quality checks did not identify these issues before publication and have since put additional measures in place to safeguard research integrity.

We wish to credit our own Research Integrity and Research Publishing teams and anonymous and named external researchers and research integrity experts for contributing to this investigation.

The corresponding author, as the representative of all authors, has been given the opportunity to register their agreement or disagreement to this retraction. We have kept a record of any response received.

References

- [1] P. Sun, "Data Management Platform of Forest Ecological Station Based on Internet of Things and Big Data Sensor," *Journal of Sensors*, vol. 2022, Article ID 1207745, 8 pages, 2022.

Research Article

Data Management Platform of Forest Ecological Station Based on Internet of Things and Big Data Sensor

Ping'an Sun ^{1,2}

¹College of Chemistry and Materials Engineering, Zhejiang A&F University, Hangzhou, Zhejiang 311300, China

²School of Mathematics and Computer Science, Wuyi University, Wuyishan, Fujian 354300, China

Correspondence should be addressed to Ping'an Sun; 2016122630@jou.edu.cn

Received 18 May 2022; Revised 4 June 2022; Accepted 15 June 2022; Published 29 June 2022

Academic Editor: C. Venkatesan

Copyright © 2022 Ping'an Sun. This is an open access article distributed under the Creative Commons Attribution License, which permits unrestricted use, distribution, and reproduction in any medium, provided the original work is properly cited.

In order to solve the problems of low data storage efficiency and poor retrieval performance in forest ecological station, a method of a forest ecological station data management platform based on Internet of Things and big data sensor is proposed. The framework method designs the prepartition algorithm to ensure the uniform distribution of data in the cluster. According to the characteristics of ecological data, the RowKey is scientifically designed to realize the rapid retrieval of ecological data. The Elasticsearch index fragment placement strategy based on index data and server performance evaluation is designed, and the packaging and merging strategy based on data site and time correlation is proposed to improve the storage efficiency. The results are as follows: when the scale of structured data is 10^8 , the retrieval time of the system is 1.045 s, which is 3.99 times faster than that of the original HBase. When the scale of unstructured data is 10^7 , the packaging small image strategy based on data site and time correlation is 1.15 times higher than that of the sequence file and 1.79 times higher than that of the original HBase. In the case of 10^4 concurrent users, the number of queries per second after optimization is 1.88 times higher than the original, the throughput per second is 1.74 times higher than that before optimization, and the system response time is 69.5% lower than that before optimization. The results show that the proposed scheme has significantly improved the performance in the aspects of cluster load balancing and massive structured and unstructured data retrieval efficiency and system throughput, and provide the necessary theoretical basis and technical implementation for the storage and management of forest ecological data.

1. Introduction

In recent years, the rapid development of forests in China has caused a large number of ecological and environmental problems. Soil change, land occupation, climate change, air pollution, and water pollution are becoming more and more serious, resulting in forest ecosystems being affected by human activities, frequent urban disasters, and more serious environmental pollution [1]. The overall balance of the forest ecosystem is broken, which will affect the development of cities and reduce the ability to resist external interference, which will directly affect the sustainable development of urban society and economy. With the emergence of ecological and environmental problems, people began to pay attention to and

monitor the change and development of the environment. Ecological environment monitoring is a trade-off measurement method based on time and space. This measurement method can use the professional methods in the field of forest ecology to study the overall structure and function of the system at different levels [2]. Connect the monitored data and information with modern technology, measure and judge, and analyze the feedback effect of different levels and types of objects in the forest ecosystem on the changes of ecology, nature itself, and human activities. By synthesizing different types of feedback information, we can analyze and measure the impact and harm of these interferences from different factors on the environment. At the same time, we can also summarize the trend of their development and change, which

provides a strong basis for evaluating environmental quality and measuring ecological services.

In order to better evaluate the service function of the forest ecosystem, China has established a large number of forest ecological positioning observation stations around the country and conducted long-term continuous positioning observation for typical ecosystem types. So far, China has more than 180 national forest ecological positioning and observation stations (hereinafter referred to as ecological stations), which are distributed in different climatic regions and cover different types of ecosystems. The ecological observation station can carry out long-term and continuous observation and automatically perceive and obtain the ecological factor data of water, soil, gas, and biomass in the observation area. The accumulated data is massive and diverse. However, using a single site to store and manage ecological data cannot meet the storage and management needs of massive heterogeneous ecological data. Each ecological site is independent of each other and gradually forms an information island, which cannot meet the needs of multistation joint analysis, data mining, real-time retrieval, and highly concurrent access for ecological service function evaluation. Moreover, the massive ecological data is diverse and complex and cannot be reconstructed. It is easy to have problems such as heavy computing burden and slow retrieval time in the process of ecological data processing [3]. Therefore, it is very necessary to study the storage and index model of forest ecological big data and establish a massive ecological data management platform based on it. Figure 1 shows a data processing system of Forest Ecological Station Based on Internet of Things technology.

At present, the storage architecture of most ecological stations is mainly a relational database represented by MySQL. Some scholars proposed to realize the application of a digital forest ecological station through MySQL Server Replication Technology and then call the Rest Service API provided by the cloud platform to realize the construction of the data management system of the West Tianshan forest ecological station, which can ensure the consistency of transactions, but it cannot meet the storage and management of massive heterogeneous data in terms of expansibility, fault tolerance, and availability [4]. Aiming at the disadvantages of a traditional relational database, the Hadoop distributed platform and HBase distributed NoSQL database are adopted, which have great advantages in scalability, fault tolerance, and availability. In order to solve the massive GIS data, the researchers designed a Hadoop-based GIS platform and built a forest resource information platform through Hadoop to provide more effective, scientific, and accurate data reference for departments at all levels [5]. The birth of Hadoop and HBase technology has laid an important technical foundation for solving the problem of efficient storage and rapid indexing of ecological big data. However, native Hadoop cannot handle the problem of small files well, and native HBase only supports primary indexing by default [6]. There are two main problems in the above platforms: (1) In terms of storage, native Hadoop does not solve the storage problem of massive small images and does not partition massive data. (2) Native HBase does not provide a good

fast retrieval scheme in the face of a massive data multidimensional query [7, 8].

A large number of small files generated by the ecological station will lead to memory bottleneck and low retrieval performance of NameNode. Hardballing technology is proposed to package small files into large files through a packaging technology, but the preprocessing takes a long time [9]. It was also proposed to merge small files of the same type into large files and establish the index relationship from small files to merged large files. The index relationship is stored in HashMap. If this method fails to hit the cache, the reading performance is not high. The SequenceFile technology is used to realize the massive Internet of Things image packaging and merging strategy. This method can solve the problem of excessive memory in NameNode but does not consider the relationship between images, which is not conducive to association query. For GIS data, some researchers try to use the traditional relational database to store, but this architecture will have the problems of poor expansibility and low access efficiency when facing the massive GIS data of an ecological station. In addition, for the application scenario of massive ecological data, if the reasonable prepartition is not achieved, the data will be tilted. In extreme cases, the distributed storage will become a single node storage [10].

Based on this research, this paper proposes a data management method of the forest ecological station platform based on the Internet of Things and big data sensor. In view of the urgent needs of ecological big data storage and fast index, as well as the disadvantages of the existing forest ecological data schemes, this paper scientifically designs RowKey in storage and then designs a prepartition algorithm to ensure consistent data distribution. For the processing of massive small files, a Redis-based station time cooperation (RBSTC) storage method based on data site and time correlation is proposed. Aiming at the problem of GIS data storage, HBase and GeoTools storage methods are proposed. In terms of index, RowKey is designed according to the characteristics of ecological sites, and the Elasticsearch fragmentation algorithm based on index data and server performance evaluation is designed to optimize the secondary index failure of multicondition retrieval, in order to meet the storage and efficient retrieval of massive heterogeneous ecological data and provide technical support for efficient storage, management, and analysis of ecological monitoring data.

2. Research Methods

2.1. Overall Architecture of Forest Ecological Big Data Platform. Starting from the characteristics of forest ecological data, a forest ecological big data platform based on Hadoop is proposed, which can be used for data management of ecological stations distributed all over the country [11]. The platform deeply integrates big data, Internet of Things, artificial intelligence, and other technologies to provide users with rapid retrieval, processing, and visual analysis of forest ecological data [12]. Its overall architecture is

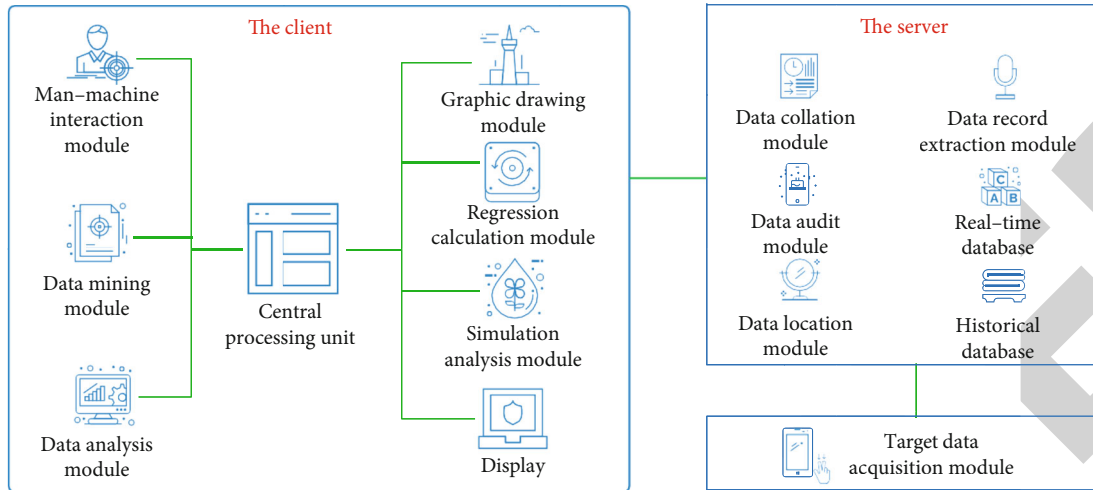


FIGURE 1: A data processing system of Forest Ecological Station Based on Internet of Things technology.

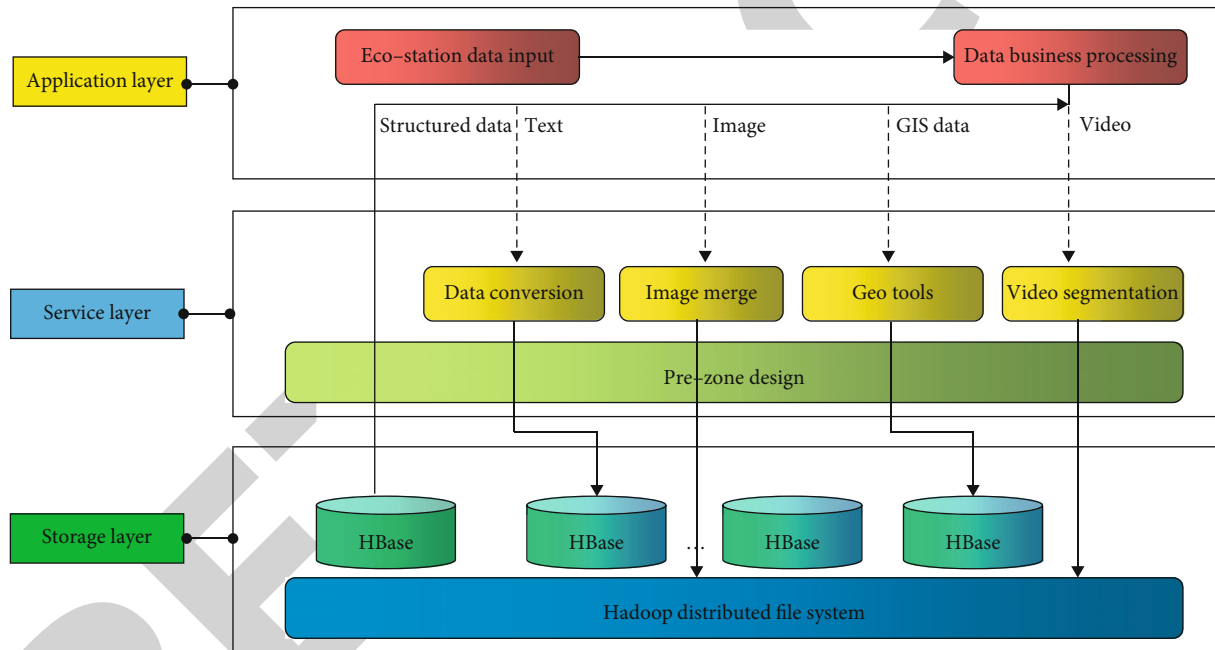


FIGURE 2: Overall architecture.

shown in Figure 2, mainly including the application layer, service layer, and storage layer.

The storage layer is the most important part of the big data model of forest ecology, and its main function is to use it for persistent storage. This layer includes distributed HDFS and the column-oriented HBase database. HDFS stores video, image, and other unstructured data in forest ecological data; the HBase database is used to store structured data generated in forest ecology [13, 14].

The service layer mainly includes data conversion, image merging, GeoTools, video segmentation, prepartition design, and HBase secondary index [15]. Data conversion is mainly because the access data is complex and massive. At the same time, the models and types of sensors are different, and the

data transmission format is not unified. Using the data conversion module to continue to unify the data is conducive to the later expansion and performance enhancement of the system. The image merging module mainly solves the problem of insufficient performance when Hadoop processes massive small files. Small files are merged based on data site and time correlation algorithm and stored on HDFS after reaching the threshold. GeoTools mainly analyzes GIS data and stores it into the HBase database. Video segmentation is to segment large files according to the size of the HDFS data block and store them directly on HDFS. the HBase secondary index module mainly solves the problem of failure of the HBase data index outside the query primary key and can realize efficient data retrieval [16].

The application layer is mainly for all kinds of users to conduct unified data processing for various businesses in the forest ecological big data platform. Users can query, analyze, manage, and download forest ecological data.

2.2. Platform Business Design Process. At present, the data collected by forest ecological sites are mainly divided into five categories: image, video, GIS data, unstructured data of text data, and structured data. Text data mainly includes Excel files and txt files. The business processing module needs a unified data access interface to judge the data types to be stored and adopts different storage strategies for different data types.

When storing images, the images in ecological monitoring are mainly massive small files (each image is usually within a few megabytes), while the default capacity of the HDFS data block is 128 MB. When an image is stored in a data block, although it will not occupy the whole data block, and a large number of small files will not put pressure on the hard disk storage, it will increase the memory consumption of the NameNode in HDFS, and reading small-size images will waste a lot of time [17]. In general, the metadata capacity of NameNode is 250 B. by default, the metadata capacity of two new replicas is 368 B. When a small image is stored in three copies on HDFS, NameNode's memory consumption M increases as n increases, as shown in the following equation.

$$M = a + 250n + (368 + b) \sum \frac{F}{B}, \quad (1)$$

where a is the memory capacity occupied by the NameNode when there is no data in HDFS, b is the memory consumption of each data block in the NameNode, B is the capacity of the HDFS data block, and F is the memory capacity of n images stored in HDFS.

Therefore, when the data is an image, the strategy of merging and storing the image based on data site and time correlation is adopted; that is, first write the image to an image queue, judge whether the value of the image queue is greater than the capacity of a block, and continue to write if it is not enough. If it is larger than the capacity of a block, it will be directly stored in HDFS and indexed, and the image meta information will be stored in HBase. When the written data is a video, first judge whether it exceeds the capacity of a block. If not, it will be processed directly according to the capacity of a block. If it is greater than the capacity of a block, it will be segmented directly according to the HDFS blocking strategy, an index will be established, and the video metadata information will be stored in HBase [18]. When the written data is GIS data, it is analyzed via GeoTools tool and stored in the HBase database. When the written data is text data, the text data is transformed into structured data through corresponding service layer analysis and stored in the HBase database. When the written data is structured data, the data is directly stored in the HBase database.

2.3. Prezoning Design. By default, when HBase creates a data table, it will create a region without start and end, and the

TABLE 1: Server configuration.

Equipment	Parameter
CPU	Inter (R) Xeon (R) Silver 4110 CPU @ 2.10 GHz
Memory capacity (CB)	32 (server configuration)
Hard disk capacity (CB)	500
Network type	Gigabit LAN
Operating system	Centos Linux server 7.4
Hadoop	3.1.2
HBase	2.1.0
Elasticsearch	6.7.0
Zookeeper	3.4.10
Solr	6.0.0
Phoenix	5.0.0

data will be written to the region in ascending order according to the dictionary of key value pairs. If the region of HBase reaches the threshold, it will frequently trigger split operation, which will cause hot spot tilt, and the value range is 0-60. Assuming that it is to be divided into k partitions (k is an integer), start the data SplitKey in the range of 0-60 from 1 and preliminarily prepartition according to the HBase prepartition algorithm. Finally, the SplitKey is obtained according to the prepartition algorithm, and the prepartition table is created to avoid hot spot tilt [19, 20].

2.4. RowKey Design. The HBase database is mainly composed of a row key, column family, column family qualifier, and timestamp. On the premise of meeting the length principle, hash principle, and uniqueness principle, the line key can improve memory utilization. Due to the frequent use of an ecological site query, this field is added in the design. At the same time, in order to record the data generation time and data version control, the time is also placed in the primary key RowKey. Therefore, the RowKey format designed by this system is as follows: site + time.

Forest ecological structured data is divided into 4 column families according to its characteristics, which are divided into the soil column family, meteorological column family, biodiversity column family, and hydrological column family, including 742 elements, such as temperature, relative humidity, wind speed, and precipitation. The identification ID of a site at a specific time stores a RowKey. Each RowKey will have multiple column qualifiers, representing the element values at different times [21].

2.5. Image Merging Index Algorithm. Since most of the images stored in the ecological station are small images, there will be a NameNode bottleneck and low retrieval performance. The existing algorithms are generally used to solve the problem of high memory occupation by merging small files into large files and then storing them into large files but do not take into account the problems between images. For example, taking an ecological feature data image may be scattered in different large files, resulting in low storage efficiency. Therefore, this paper proposes a consolidated

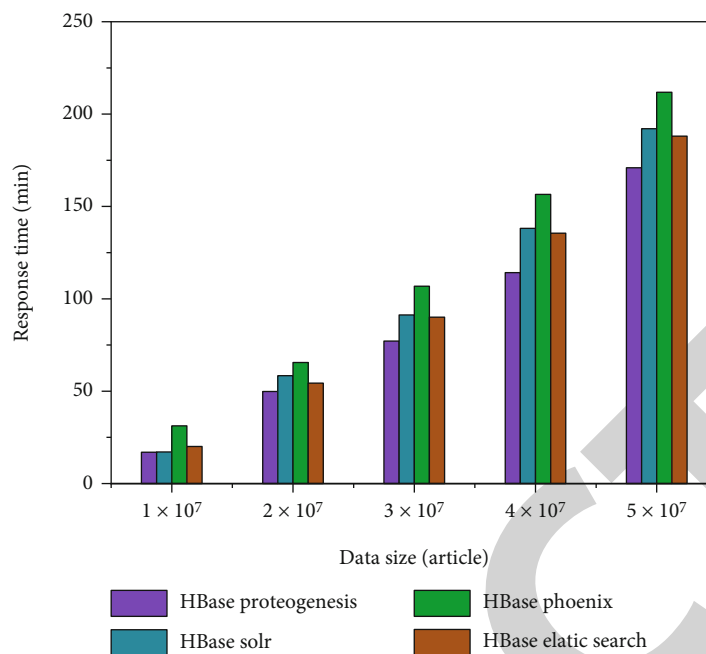


FIGURE 3: Comparison of response time for inserting data.

storage method RBSTC based on data site and time correlation. First, create a temporary queue and store the initial image. Then, judge whether the images to be stored come from the same site and on the same day. If so, merge the stored images into the temporary queue. Otherwise, create a new queue, and the images to be stored will be used as the initial images in the new queue. Repeat the above operations until all images to be uploaded are transmitted to HDFS.

2.6. GIS Data Storage Design. GeoTools is a GIS toolkit developed in Java language. Based on the standard GIS interface, it supports the access of multiple GIS data sources. GIS data is generally composed of coordinate data, attribute data, and topological relationship data. According to the characteristics of vector data, a vector data storage model suitable for HBase is designed. In the design of GIS data RowKey, RowKey is site + timestamp, which is divided into three column families: the spatial information column family, attribute information column family, and topological information column family [22, 23].

3. Result Analysis

3.1. System Insertion Performance Comparison. In order to evaluate the performance of the technical scheme in this paper, the performance of the storage model, prepartition, RowKey design, secondary retrieval scheme, and image merging strategy is tested based on the data of different data levels. This paper configures the server-related environment and builds the Hadoop cluster, HBase cluster, and Zookeeper cluster. In order to conduct the secondary index comparison experiment, the Elasticsearch cluster, Solr cluster,

and Phoenix cluster are also built. The server configuration is shown in Table 1.

In the experiment, four clients simultaneously insert data into the HBase table, and we count the put time of each 107 data on the four clients. After repeating the experiment for 10 times, take the average value and test the put time of the HBase native, Elasticsearch-based index, Solr index, and Phoenix index under the same conditions. The results are shown in Figure 3.

It can be seen from Figure 3 that put is the most efficient way to build indexes without additional resource allocation. It can be seen that when the same 10 pieces of data are added, the insertion time is longer and longer, because with the increase of the amount of data, there are more and more index data, making it difficult to insert the index. At the same time, because the Phoenix bottom layer needs to build an appropriate storage index structure in the coprocessor, it consumes additional computing resources. Based on Elasticsearch and Solr, you only need to build indexes in your own cluster without additional computing resources. Therefore, the Phoenix secondary index has the greatest loss on insertion performance [24, 25].

3.2. Comparison of Single Condition Query Performance of Different Secondary Indexes. The retrieval data still adopts the above data, and its retrieval performance comparison is shown in Figure 4.

It can be seen from Figure 4 that the response speed of the native HBase decreases obviously. When the amount of data reaches 1×10^8 , the response time is greater than 5 s. Theoretically, HBase is a column-oriented database. Its bottom layer is to establish a B+ tree index based on RowKey, which can retrieve data efficiently, but the system will scan the whole table corresponding to the index of the nonrow

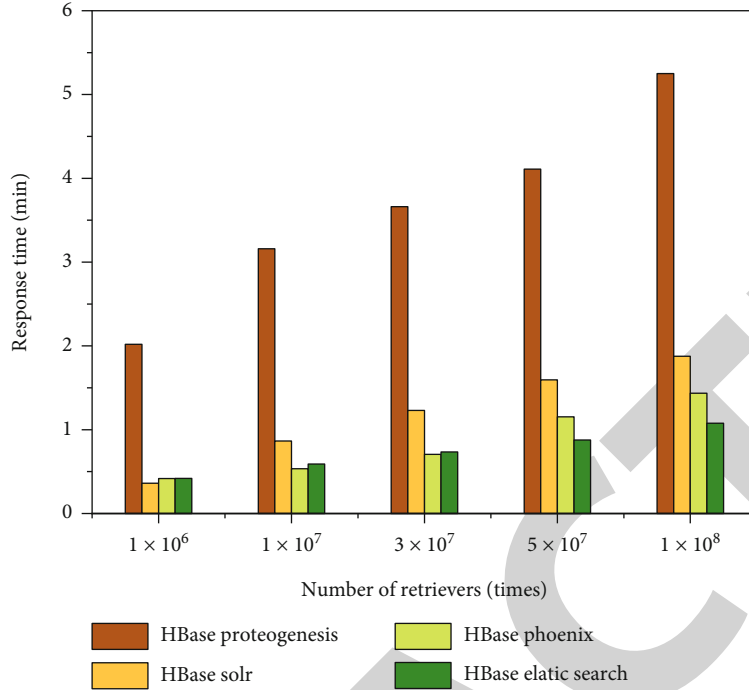


FIGURE 4: Comparison of retrieval performance.

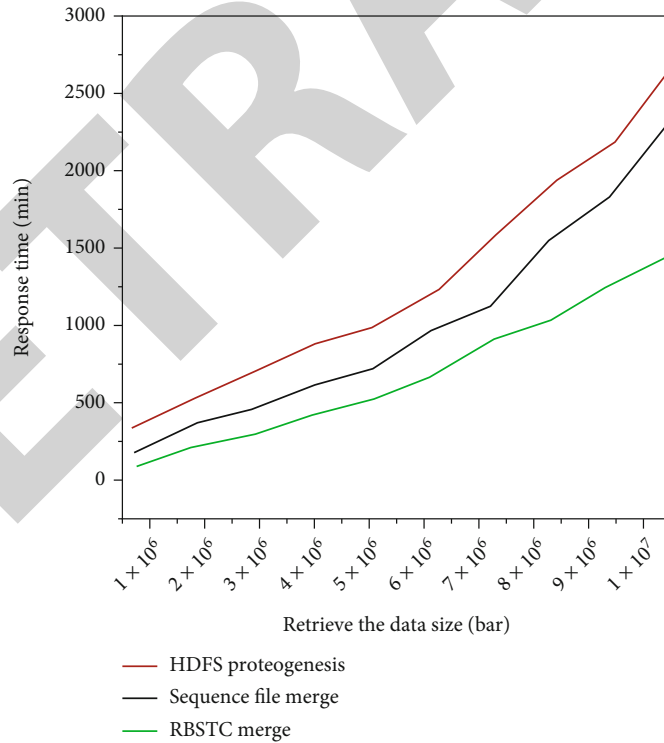


FIGURE 5: Comparison of reading and writing performance.

key, resulting in low efficiency of overall data retrieval. For the comparison of secondary indexes, the bottom layers of Solr and Elasticsearch are based on Lucene, but the framework design of Elasticsearch is further optimized, and the data retrieval efficiency also has better performance. There-

fore, when the amount of data reaches 1 × 10⁸, the efficiency of Elasticsearch is 1.72 times that of Solr. The retrieval efficiency of Phoenix is close to that of Elasticsearch, but Phoenix has strong coupling, so Elasticsearch is finally selected as the secondary index.

TABLE 2: Concurrent stress test.

Parameter	HBase	HBase secondary index
Queries per second	3475	6520
Throughput per second (MB)	42	73
Response time (ms)	852	260

3.3. Performance Verification of Unstructured Data Storage Scheme. In the data storage verification part, the performance of the image merging strategy is verified; that is, the default sequence file merging of HDFS is verified and compared with the RBSTC algorithm used in this experiment. A total of 10^7 images in the eco station system are used, occupying 100~500 kb of storage space. The images are tested, respectively, via HDFS default sequence file merging and RBSTC merging index. 10 read-write experiments are carried out, and the average value of 10 reads and writes is taken as the final time consumption. The average read-write verification is shown in Figure 5.

As can be seen from Figure 5, with the increasing scale of image data, the advantages of the merging method based on data site and time correlation become more and more obvious. When the number of images is 10^7 , the merging of small files based on data site and time correlation is 1.79 times that of original reading and writing and 1.15 times that of the sequence file. Therefore, the merging strategy based on data site and time correlation is more suitable for the storage scenario of massive images in ecological stations.

3.4. System Pressure Test. In order to verify the stability of the system, the postman tool is used to conduct pressure test on the big data platform. The query rate per second (QPS), throughput (TPS), and response time (RT) are selected as the main parameters. The concurrency is 1×10^4 times and the test time is 3 min. The average value of 10 experiments is taken. The concurrency test is shown in Table 2.

Through the test results, it can be found that in the case of 10^4 concurrent users, the number of queries per second after optimization is 1.88 times that of the original, the throughput per second is 1.74 times that of before optimization, and the system response time is 69.5% lower than that before optimization, indicating that the system can also operate stably under the condition of high concurrency.

4. Conclusion

The subject of this study involves relevant knowledge in the fields of forestry and ecology. In the process of understanding and studying this subject, I have carefully studied the basic knowledge in relevant fields. In the process of developing the data management platform of forest ecological monitoring network, it not only deepened the understanding of ecology but also had a certain research conclusion on the significance of building a forest ecological monitoring network. This paper designs the big data storage framework of the Forest Ecological Station Based on Hadoop and HBase. The results are as follows:

- (1) Facing the demand of massive ecological data storage and rapid retrieval, the traditional model architecture cannot guarantee the data processing performance of the ecological data platform. The distributed big data technology is used to build the ecological big data platform. Through the scientific design of RowKey, Hadoop and HBase are used as the data storage layer to realize the storage of massive data. A prepartition algorithm is proposed and designed to ensure consistent data distribution and avoid the problem of hot data skew
- (2) According to the storage requirements of massive image data, an association merging storage method based on data site and time correlation is proposed. When the unstructured data is 10^7 , the packaging small image strategy based on data site and time correlation is 1.15 times the merging efficiency based on SequenceFile and 1.79 times that of native HBase

The research and development of the forest ecological monitoring network data management platform is still in its infancy. Although the analysis and processing of forest ecological data is currently written, there are still many areas that need to be improved and further studied. In terms of data cleaning, although outliers have been removed from the granularity of months and years, the cleaning efforts are still not enough. It is still necessary to learn more about the field of forest ecology and be able to determine different types of indicators for different ecosystems. For its numerical range, we optimize the calculation method proposed for outliers; in terms of data filling, it is necessary to understand more models and methods in the field, and through the comparison of different filling methods, the data can be filled more accurately.

Data Availability

The data used to support the findings of this study are available from the corresponding author upon request.

Conflicts of Interest

The author declares that they have no conflicts of interest.

References

- [1] M. E. Spicer, H. Radhamoni, M. C. Duguid, S. A. Queenborough, and L. S. Comita, "Herbaceous plant diversity in forest ecosystems: patterns, mechanisms, and threats," *Plant Ecology*, vol. 223, no. 2, pp. 117–129, 2022.
- [2] A. Reuber, C. Flávio, L. Maurice, and D. Wesley, "Discovery-defense strategy as a mechanism of social foraging of ants in tropical rainforest canopies," *Behavioral Ecology*, vol. 91, no. 5, pp. 5–11, 2021.
- [3] S. Estrada-Villegas, J. S. Hall, M. Breugel, and S. A. Schnitzer, "Lianas reduce biomass accumulation in early successional tropical forests," *Ecology*, vol. 101, no. 5, pp. 7–10, 2020.
- [4] X. Tong, M. Brandt, Y. Yue, P. Ciaias, and R. Fensholt, "Forest management in southern China generates short term extensive

Retraction

Retracted: Application of Internet of Things Based on Wireless Sensor in Tunnel Construction Monitoring

Journal of Sensors

Received 12 December 2023; Accepted 12 December 2023; Published 13 December 2023

Copyright © 2023 Journal of Sensors. This is an open access article distributed under the Creative Commons Attribution License, which permits unrestricted use, distribution, and reproduction in any medium, provided the original work is properly cited.

This article has been retracted by Hindawi, as publisher, following an investigation undertaken by the publisher [1]. This investigation has uncovered evidence of systematic manipulation of the publication and peer-review process. We cannot, therefore, vouch for the reliability or integrity of this article.

Please note that this notice is intended solely to alert readers that the peer-review process of this article has been compromised.

Wiley and Hindawi regret that the usual quality checks did not identify these issues before publication and have since put additional measures in place to safeguard research integrity.

We wish to credit our Research Integrity and Research Publishing teams and anonymous and named external researchers and research integrity experts for contributing to this investigation.

The corresponding author, as the representative of all authors, has been given the opportunity to register their agreement or disagreement to this retraction. We have kept a record of any response received.

References

- [1] J. Cao, R. Zhao, L. Hu, Q. Liang, and Z. Tang, "Application of Internet of Things Based on Wireless Sensor in Tunnel Construction Monitoring," *Journal of Sensors*, vol. 2022, Article ID 5302754, 8 pages, 2022.

Research Article

Application of Internet of Things Based on Wireless Sensor in Tunnel Construction Monitoring

Jianfeng Cao ¹, Ruichuan Zhao ², Liqiang Hu ¹, Qing Liang ³, and Zhenhua Tang ³

¹Guangxi Xinfazhan Communications Group Co., Ltd., Nanning, Guangxi 530000, China

²CCCC Highway Planning, Design and Research Institute Co., Ltd., Beijing 100088, China

³Guangxi Road Construction Engineering Group Co., Ltd., Nanning, Guangxi 530000, China

Correspondence should be addressed to Liqiang Hu; 1400440530@xs.hnit.edu.cn

Received 18 May 2022; Revised 29 May 2022; Accepted 14 June 2022; Published 28 June 2022

Academic Editor: C. Venkatesan

Copyright © 2022 Jianfeng Cao et al. This is an open access article distributed under the Creative Commons Attribution License, which permits unrestricted use, distribution, and reproduction in any medium, provided the original work is properly cited.

In order to solve the problems of insufficient frequency, time-consuming, and labor-consuming of monitoring and measurement in the process of tunnel construction, a tunnel construction monitoring and measurement technology based on Internet of Things is proposed in this paper. This method adopts the basic theory and technology of Internet of Things, analyzes the fit relationship between Internet of Things technology and tunnel construction, uses the comprehensive perception, reliable transmission, and intelligent auxiliary technology possessed by the existing Internet of Things technology system, and has been successfully applied to tunnel engineering. The experimental results show that the contact pressure between the surrounding rock and the initial support on the monitoring and measurement section in the tunnel is zero after the initial support shotcrete is applied. The contact pressure between the surrounding rock and the shotcrete layer at the right arch waist of the left tunnel is the smallest, and the stress in the whole change process is less than 10 kPa. The contact pressure between surrounding rock and shotcrete layer after excavation is divided into three stages. *Conclusion.* the tunnel construction monitoring and measurement technology based on Internet of Things technology fully realizes the intellectualization and informatization of the construction process, plays a scientific and effective monitoring and early warning role, and reduces the project cost of the whole project, which has a certain engineering value.

1. Introduction

At present, in the aspect of tunnel construction, dynamic construction monitoring has become an urgently needed supporting technology. With the progress of technology, the construction technology for tunnel construction is also improving. Automatic mechanical equipment is mostly used in the process of tunnel excavation. The geological conditions of the tunnel are related to the selection of construction methods. Therefore, it is very important to obtain and reasonably deal with geological information in the process of construction. With the continuous improvement of the collection automation of various multisource information, the wireless data transmission, the safety early warning, and the relevant technical methods of the construction management system,

the construction monitoring system can basically realize the detection of relevant environmental parameters (including vulnerable harmful gases) and the tracking and positioning of construction personnel. Moreover, in case of safety accidents during tunnel construction, the system can give corresponding safety warnings and relevant reminder information according to the monitoring data and wireless communication, so as to facilitate the construction management personnel to start early warning and corresponding emergency plan, which plays a good guiding role in the evacuation and rescue of construction personnel, and ensure the safety of tunnel construction and the property safety of units and individuals [1]. These have important practical significance for the normal progress of tunnel construction, efficient dispatching management on the construction site, and ensuring safe construction [2].

2. Literature Review

Kirpichenkova and others used a Jikang static leveling system, Campbell data acquisition system, wireless transmission module, and automatic acquisition software to form an automatic real-time monitoring system and applied the automatic real-time monitoring technology to the crossing project of a rail transit line. The system can realize data acquisition and transmission once a minute, process and analyze data in real time, realize data alarm and chart analysis, enable the construction party to adjust the speed and direction of shield propulsion in time during crossing construction, and facilitate analysis and summary after construction [3]. Ootani and others combined the static level and displacement meter to establish an omnidirectional displacement (deformation) real-time monitoring system. The remote real-time monitoring system of dangerous road displacement (deformation) based on sensor is mainly composed of on-site monitoring and data acquisition system, main control computer system, and application terminal system. Through the remote real-time monitoring system, we can timely and accurately grasp the changes of the geometric shape and position of the subway dangerous road structure and judge the safety of the subway dangerous road structure in time [4]. Liu and others applied the automatic real-time monitoring system to the Yanda section of the east extension section of Shenzhen Metro Line 2 crossing the Dake section of Metro Line 1, carried out the dynamic monitoring of the subway, implemented the information construction, continuously optimized the design, improved the construction technology, effectively prevented or reduced the occurrence of various accidents, and promoted the smooth progress of the project [5]. Marco and others developed a set of "information management system during tunnel construction" based on the geographic information system (GIS). The system uses electronic total station to conduct noncontact monitoring and data processing on the three-dimensional convergence deformation of the surrounding rock surface of the tunnel. It realizes the functions of real-time data acquisition and real-time transmission, analysis and processing, query, and visual output of monitoring data [6].

Limited by geological conditions and technical factors, at present, the application scope of Internet of Things in China is more applied in intelligent transportation than in engineering monitoring. The application of Internet of Things in tunnel engineering focuses on personnel positioning and intelligent management, and its application in the field of tunnel construction monitoring still needs to be developed. According to the basic principle and structure of Internet of Things technology, this paper analyzes the fit between Internet of Things technology and tunnel construction monitoring and measurement, puts forward the tunnel construction monitoring and measurement system based on Internet of Things technology, applies it in practical engineering, and evaluates the guidance and feedback function of the tunnel construction monitoring system based on Internet of Things. The results show that the tunnel construction monitoring and measurement system based on the Internet of Things can provide real-time and accurate information for the design and construction parties in the actual project, so as to ensure the requirements of project progress and safety.

3. Research Methods

3.1. Technical Composition of Tunnel Internet of Things

3.1.1. Constituent Elements of Internet of Things Technology. Internet of Things technology is a new network technology that connects various entities with various networks such as the Internet and widely obtains all kinds of information through strip QR code, radio frequency identification technology (RFID), sensor technology equipment, global positioning system, and wireless transmission technology, so as to realize comprehensive intelligence such as positioning, tracking, and monitoring and realize good communication between people and things [7, 8].

Structurally, it can be divided into three layers: perception layer, transmission layer, and intelligent processing layer, as shown in Figure 1.

The sensing layer is the bottom layer of Internet of Things technology, including radio frequency identification (RFID), telemetry and remote sensing (RS), sensors, and sensor networks. The transmission layer includes Internet technology, wireless transmission technology, and satellite communication technology. Intelligent processing layer refers to the data processing and application technology in the Internet of Things, including cloud computing, data processing and fusion technology, computer vision technology, and communication technology [9, 10].

3.1.2. Key Technologies of Tunnel Internet of Things

(1) Key Technologies of Perception Layer. In the sensing layer of the Internet of Things, sensor technology and RFID technology play a key role: generally speaking, sensors are devices that convert other physical information (such as pressure, speed, humidity, displacement, and deformation) into electrical signals or other required forms of information according to certain laws and output, process, store, display, and control data. Radio frequency identification (RFID) is a noncontact automatic identification technology. It can automatically identify objects to obtain relevant data through RF signals without manual intervention. It is a wireless version of bar code [11, 12].

(2) Key Technologies of Transport Layer. Electromagnetic wave signals can propagate freely in space without the help of media. The transmission mode of information reception or transmission using this characteristic is wireless transmission. It mainly includes the following: Wi Fi technology, ZigBee technology, and the third generation mobile communication technology (3G Technology).

(3) Computer Vision Technology. Computer vision technology is the key technology of the Internet of Things in the intelligent processing layer. Instead of the visual processing of the brain, the three-dimensional image processing is used to complete the corresponding image processing by the computer instead of the visual processing of the brain. Computer vision technology includes image processing technology, pattern recognition technology, and image understanding technology.

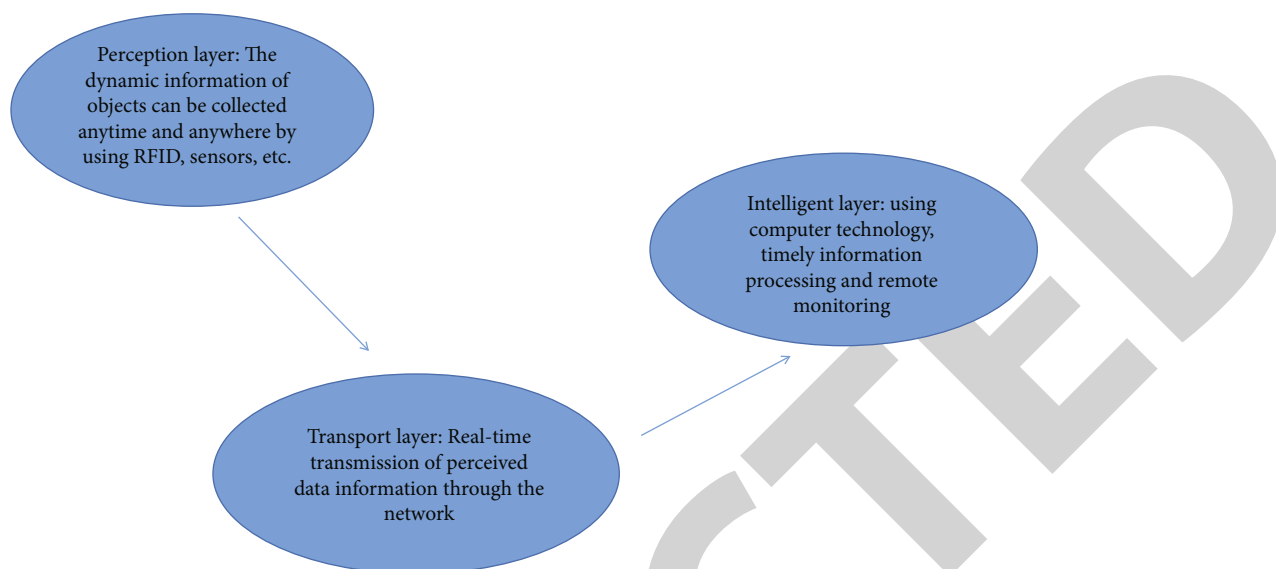


FIGURE 1: Schematic diagram of technical structure of Internet of Things.

3.2. Technical Scheme Design of Tunnel Internet of Things

3.2.1. Design of Tunnel Monitoring System. In the traditional tunnel monitoring system, the observation and data measurement of measurement items rely on manual measurement and paper records. It needs to spend a lot of human and material resources for real-time measurement during the construction period and operation period, and the economy and safety are low. The use of Internet of Things system for construction monitoring overcomes the shortcomings of insufficient manual measurement frequency and time-consuming in the past, provides accurate and timely changes of enclosure structure, so as to better modify construction parameters and construction technology, and provides technical support for dynamic construction [13, 14]. At the same time, the monitoring results provide information for judging the stability of surrounding rock and the reliability of primary support and secondary lining and provide basis for adjusting the grade of surrounding rock, modifying the design of support system, providing reasonable construction time of secondary lining, and changing the construction method during construction.

3.2.2. Hardware Design of Monitoring System. According to the definitions of perception layer, network layer, and application layer in the basic theory of the Internet of Things, the equipment required for monitoring and measurement can correspond to these three structural levels of the Internet of Things in function [15, 16]. Taking the monitoring and measurement system based on the Internet of Things of dugong expressway tunnel as an example, the equipment required by the monitoring and measurement system mainly includes the following: sensors, data collectors, transmission networks, terminal equipment, and software. According to the definitions of perception layer, network layer, and application layer in the basic theory of the Internet of Things, the equipment required for monitoring and measurement corresponds to the three structural levels of the Internet of Things.

- (1) **Sensors:** sensor is an important component and basic equipment of the sensing layer of the Internet of Things, and it is the basis of the monitoring system. In terms of the structural system of the Internet of Things, the corresponding equipment belonging to the sensing layer of the Internet of things plays the function of sensing the changes of the physical and mechanical properties of the measured object and recording the change data in the whole monitoring system. The sensors used in this study mainly include vibrating wire reinforcement stress gauge, vibrating wire surface strain gauge, vibrating wire concrete strain gauge, and vibrating wire earth pressure gauge
- (2) **Collector:** the collector in the tunnel monitoring system plays the task of collecting, saving, processing, and transmitting the data collected by the sensor. From the structural system of the Internet of Things, it belongs to the corresponding equipment including the sensing layer and the transmission layer in the Internet of Things

The preprocessing methods of monitoring data include the following: data interpolation, averaging and extension. Data smoothing is to adjust the unreasonable amount of data in the monitoring data section. When the monitoring data is greatly affected by accidental factors and fluctuates irregularly, this group of data can be smoothed by simple moving average (or moving average), exponential smoothing, and wavelet denoising to eliminate the influence of accidental factors. Exponential smoothing refers to the weighted exponential decreasing smoothing of all past data over time. According to this definition, a simple recursive expression of exponential smoothing can be deduced as follows (1):

$$\overline{A}_t = aA_t + (1 - a)\overline{A}_{t-1}, \quad (1)$$

TABLE 1: Main technical indexes of MCU-32 distributed modular automatic measurement unit.

Model	MCU-32
Overall dimension	400 mm × 300 mm × 185 mm
Working power supply	220 V AC or 16.5 V solar power
Transmission distance	About 1000 m (485 transmission), other transmission modes are determined by external transmission equipment
Working temperature and humidity	Temperature: -30~70°C, relative humidity 90%
Stored data	About 7000 × 32
Data retention time	>10 a
Access sensor	32/set
Networking quantity	64 sets
Design life	>10 a

where $\overline{A_{t-1}}$ represents the data after smoothing the weighted index of each previous time period, A_t indicates that there is no monitoring data for leveling, and a is the weighted exponential smoothing coefficient, taking 0.2 ~ 0.3 according to the calculation accuracy.

According to the research requirements, MCU-32 distributed modular automatic measurement unit is selected to automatically collect the data of various sensors. This type of collector can automatically collect the data of each sensor, with high measurement accuracy, reliable system stability, and flexible data collection mode; good adaptability to the site, waterproof; lightning protection; and anti-interference. It has a variety of data transmission modes and supports wired and wireless data transmission, which comprehensively considers the ability of information collection, transmission diversity, and anti-interference.

Each MCU-32 distributed modular automatic measurement unit includes four modules: measurement module, main control and communication module, power supply module, and wiring port module. These four modules can work together, see Table 1 for its main technical indicators.

MCU-32 distributed modular automatic measurement unit has the following basic characteristics: open structure, high measurement accuracy, and strong system stability. Each MCU-32 is a modular combination, which is convenient for repair and maintenance; MCU-32 does not need additional lightning arrester and has perfect lightning protection function and complete system self-inspection function; there are many data transmission modes: RS485 transmission, TCP/IP network transmission, optical cable transmission, GPRS/CDMA transmission, etc. The stored data can be transmitted through the serial port or copied to the computer with USB flash disk, and the data transfer is flexible.

- (3) Transmission network: the transmission network of tunnel construction monitoring system needs to summarize the data and transmit the data to the database and data processing system. From the structural system of the Internet of Things, it belongs to the corresponding equipment in the transmission layer of the Internet of Things [17, 18]

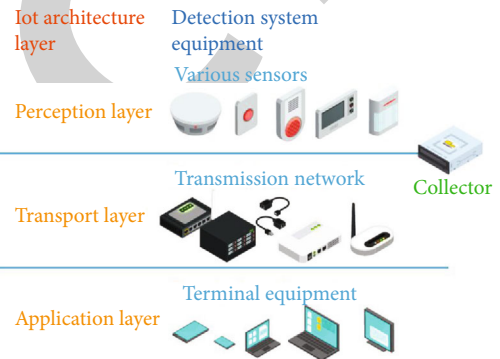


FIGURE 2: Corresponding relationship between tunnel construction monitoring system equipment and IOT structure layer.

TABLE 2: Pressure test frequency.

Excavation time	Frequency
1 ~ 15 d	1 ~ 2times/d
16~30 d	1/2 d
1 ~ 3 m	1 ~ 2 times/w
>3 m	1 ~ 3 times/m

The transmission network needs to support more flexible data transmission and transfer modes, which can be completed with the help of MCU-32 main control and communication module and wiring port. The wired transmission modes of the collector include RS485 transmission, TCP/IP network transmission, and optical cable transmission, and the wireless transmission modes include wireless data transmission, radio transmission, and GPRS/CDMA transmission. In terms of data transfer mode, it can be transmitted through serial port or copied by USB flash disk.

- (4) Terminal equipment: terminal equipment is the equipment for the operation of database and data

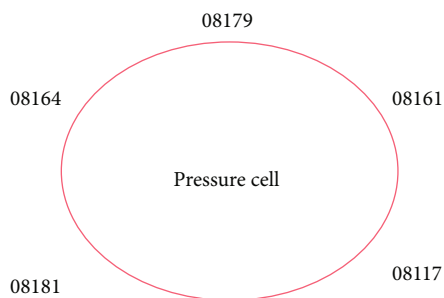


FIGURE 3: Layout of section measuring points.

analysis and processing software. It mainly completes the reception, storage, analysis, and processing of the data transmitted by the collector. From the structural system of the Internet of Things, it belongs to the corresponding equipment in the application layer of the Internet of Things. The corresponding relationship between tunnel construction monitoring system and IOT structure layer can be used as shown in Figure 2

3.2.3. *Software Scheme of Monitoring System.* The software scheme of the monitoring system can be divided into two parts.

- (1) The collector control program can manage the data transmission of each monitoring section and the data collection of each sensor
- (2) The monitoring and analysis program can connect with the control software of the collector, analyze and process the monitoring and measurement data collected by the collector, draw the displacement time curve according to the data, form the data chart and analysis report, and more intuitively display the changes of tunnel structure

3.3. Application of Tunnel IOT Monitoring System

3.3.1. *Monitoring Scheme.* Taking the contact pressure between surrounding rock and initial support as an example, this paper illustrates the specific application of Internet of Things technology in tunnel monitoring and measurement. The monitoring method is to embed various pressure boxes and other sensors between surrounding rock and support, combined with MCU 32 collector. The monitoring frequency is shown in Table 2. The main technical points are as follows.

- (1) Five measuring points are arranged on each section, as shown in Figure 3. The number on the side of the pressure box is the number of the pressure box
- (2) The sensor is arranged at the interface between surrounding rock and primary lining for surrounding rock pressure measurement
- (3) Before embedding, the initial frequency of the pressure box sensor shall be recorded, the sensor shall be numbered, and the corresponding connector shall be marked. Pay attention to the conductor protection during embedding

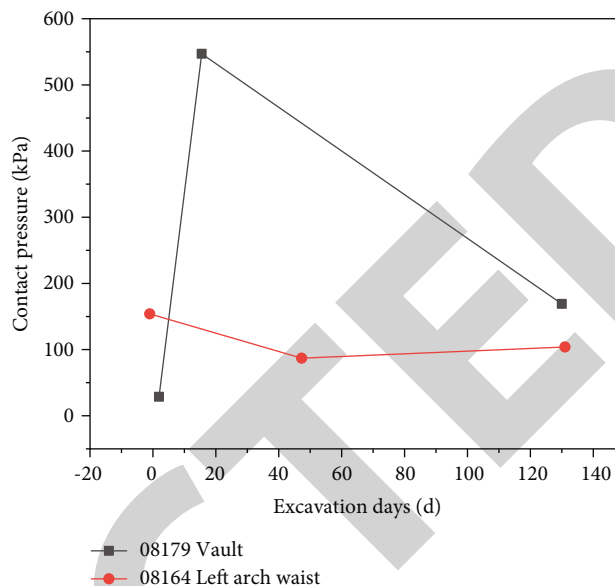


FIGURE 4: Contact pressure time curve of left tunnel K47+487.

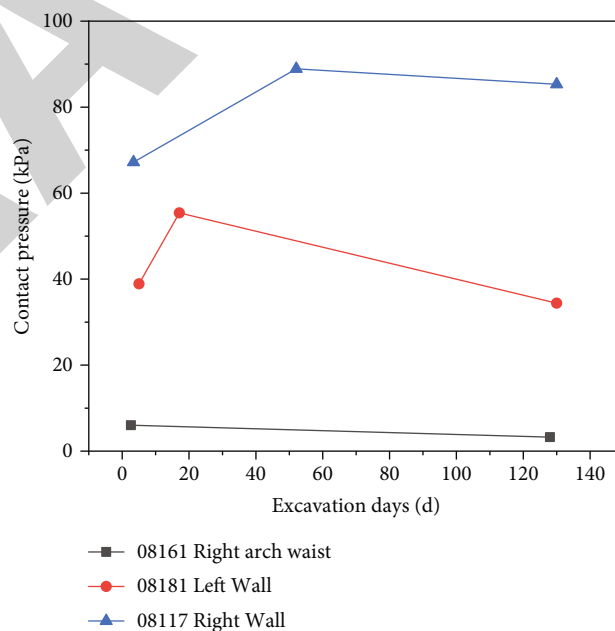


FIGURE 5: Contact pressure time curve of left tunnel K47+487.

- (4) Connect the pressure box to the MCU 32 collector and convert the frequency into the corresponding contact stress according to the calibration coefficient

4. Result Analysis

4.1. *Measurement Data and Results of Monitoring System.* At K47+487 of the tunnel left tunnel face, in order to dynamically grasp the change of surrounding rock pressure and provide effective data and information for the smooth

TABLE 3: Stress changes at monitoring points of tunnel monitoring section.

Deformation stage	Deformation parameters	Location of monitoring section				
		Vault	Left arched waist	Right arch waist	Left wall	Right wall
Phase I	Duration/d	16	6	2	16	10
	Contact stress growth/(kPa d-1)	34.03	24.82	3.15	3.44	6.98
Phase II	Duration/d	84	24	4	64	45
	Contact stress growth/(kPa d-1)	-4.48	-2.08	-1.18	-0.23	0.42
Phase III	Duration/d	30	100	124	50	75
	Contact stress growth/(kPa d-1)	-0.43	-0.11	0.02	-0.11	0.05
Whole deformation process	Peak stress/kPa	544.6	148.9	6.3	55.0	88.8
	Pressure range after stabilization/kPa	100~200	40~100	0~10	30~40	80~90
	Time required for stabilization/d	100	30	6	80	55

progress of construction, the pressure box is installed in time after the excavation of the face, the contact pressure is monitored and measured, the data of surrounding rock pressure changing with time is obtained, and the data curve is preliminarily analyzed [8, 19]. The monitoring and measurement frequency shall be implemented according to Table 2 above. The variation curve of surrounding rock pressure along time is shown in Figures 4 and 5.

4.2. Analysis of Monitoring Measurement Results

- (1) It can be seen from Figures 4 and 5 that after the construction of the initial support shotcrete, the shotcrete layer can adapt to the deformation of the surrounding rock and deform accordingly because the concrete has not been consolidated. Therefore, the contact pressure between the surrounding rock and the initial support on the monitoring and measurement section in the tunnel is zero. When the shotcrete layer is consolidated to form effective strength, the shotcrete layer will prevent the further deformation of the surrounding rock, which is still in the stress release stage, resulting in stress between the shotcrete layer and the surrounding rock. With the passage of time, the stress of the shotcrete layer at each monitoring point gradually increases, and then the deformation tends to be stable [20, 21]
- (2) According to the statistics, the contact stress between the left and right sections of the tunnel is less than 10 kPa. According to the statistics, the contact stress between the left and right sections of the tunnel is the smallest, and the contact stress between the left and right sections of the tunnel is less than 10 kPa. The contact pressure between the surrounding rock of the left arch waist and the shotcrete layer increased rapidly in the first 6 days and began to drop after reaching the peak stress of 148.9 kPa in the sixth day and stabilized between 80~90 kPa. At the initial stage of excavation, the contact pressure of the left wall rises rapidly, and the rising speed decreases after the 7th day of excavation. After the

16th day of excavation, the peak pressure reaches 55 kPa, and then at the 16th day (about 2 weeks), the contact pressure begins to decline and tends to be stable. The change of the right wall is similar to that of the left wall. The contact pressure increases rapidly with time within one week of excavation and then increases slowly. It does not increase at the 55th day (about 2 months) but decreases slightly and tends to be stable. The contact pressure between the surrounding rock of the arch crown and the shotcrete layer is the largest, and the stress is the largest. The peak stress reaches 544.6 kPa when excavating for 16 days (about 2 weeks), then the contact pressure begins to decrease, but the value is still large, and the deformation tends to be stable for a long time. It gradually tends to be stable after excavating for 90 days (3 months) [22, 23]

- (3) According to the results reflected in the contact pressure time statistical diagram, the contact pressure between surrounding rock and shotcrete layer after excavation can be roughly divided into three stages: the first stage is from just excavation (0 d) to 1~2 weeks after excavation, the stress is released rapidly in this stage, and the contact pressure between surrounding rock and shotcrete layer rises rapidly. The second stage is from 1~2 weeks after excavation to 1 month after excavation. In this stage, the contact pressure between surrounding rock and shotcrete layer is still in the rising stage, but the rising speed is significantly lower than that in the first stage. There is no significant change in the contact pressure between surrounding rock and shotcrete layer at some measuring points, and it is in the slow growth or stable stage. The third stage is one month after excavation. At this time, the contact pressure between surrounding rock and shotcrete begins to stabilize without great change. It can be considered that the surrounding rock is in a stable state. The deformation of each monitoring point of the tunnel is summarized in Table 3

4.3. Guiding Role for Construction

- (1) According to the results reflected in the contact pressure time statistical diagram, the contact pressure at the vault of the left tunnel of Dabaoshan tunnel is significantly higher than that at the rest of the tunnel face. Moreover, there is a tensile stress zone in the vault, which is easy to produce local damage such as relaxation, falling blocks, and falling stones. In addition, during the construction of the shotcrete layer at the arch crown, the thickness of the shotcrete layer is often insufficient due to the construction process and construction period, or the shotcrete layer is not in close contact with the surrounding rock, resulting in a large cavity after the shotcrete layer, which will affect the construction progress and endanger the safety of construction personnel. Therefore, during construction, due to paying special attention to the thickness and compactness of the shotcrete layer at the arch crown, grouting treatment shall be carried out in time at the poor surrounding rock to prevent local damage
- (2) One to two weeks after tunnel excavation is a period of rapid growth of contact pressure and deformation. In this stage, the construction principle of NATM shall be strictly followed, monitoring and measurement shall be strengthened, shotcrete shall be applied as soon as possible, surrounding rock shall be closed, and bearing ring shall be formed. At the same time, grouting shall be carried out in time for the parts with cavities between the shotcrete layer and the surrounding rock to fill the cracks in the surrounding rock and improve the self-supporting capacity of the surrounding rock

5. Conclusion

- (1) Through the core technology of Internet of Things, this paper provides technical support for the tunnel construction monitoring system, which makes the construction more efficient and ensures the safe and efficient progress of tunnel engineering. It provides technical support for intelligent and information construction
- (2) The internal construction environment of the tunnel is bad, and a variety of technologies and equipment are affected by the tunnel construction environment, which cannot ensure the normal application of technologies and equipment. Therefore, corresponding data sensing and acquisition modules and wireless communication modules are required to maintain good operation status in poor environment
- (3) Reducing the cost of the application of Internet of Things technology can not only reduce the project cost but also reduce the exclusion of owners and construction parties from the Internet of Things monitoring platform. To solve this problem, the

key lies in the maturity of technology application. Mature technology can ensure the rapid and large-scale development of the Internet of Things and promote the virtuous cycle of Internet of things related industries, so as to reduce the cost of each link

- (4) There are a large number of wireless transmission networks in the Internet of Things environment. The network signals in public places are not encrypted; so, the network is easy to be invaded, and data information is easy to be stolen. This not only affects the safety of tunnel engineering data but also affects the normal operation of the emergency command system. Therefore, it is necessary to strengthen the security of the underlying sensor network and ensure the normal operation of the equipment through technical means
- (5) Nowadays, the application of Internet of Things technology in various fields has its own system, which makes the application of Internet of Things technology in the field of tunnel engineering personnel detection and emergency command have obstacles. Therefore, cooperation in various fields is needed to establish a standardized standard system to truly realize the unity of tunnel engineering safety monitoring and intelligent emergency command

Data Availability

The data used to support the findings of this study are available from the corresponding author upon request.

Conflicts of Interest

The authors declare that they have no conflicts of interest.

Acknowledgments

This study was supported by the (1) Ningbo Transportation Technology Plan (202110) and (2) Science and Technology Program of Zhejiang Provincial Communications Department (No. 2019040).

References

- [1] K. Sharma and B. K. Chaurasia, "Trust based location finding mechanism in VANET using DST," in *Fifth International Conference on Communication Systems & Network Technologies*, pp. 763–766, Gwalior, India, 2015.
- [2] J. Jayakumar, B. Nagaraj, S. Chacko, and P. Ajay, "Conceptual implementation of artificial intelligent based E-mobility controller in smart city environment," *Wireless Communications and Mobile Computing*, vol. 2021, Article ID 5325116, 8 pages, 2021.
- [3] N. V. Kirpichenkova, O. I. Lozin, and A. A. Kosach, "Numerical modeling of the anomalous low-temperature dependence of the tunneling conductance of a "dirty" n-i-n junction," *Solid State Phenomena*, vol. 316, pp. 1004–1010, 2021.
- [4] Y. Ootani, A. Satoh, H. Yu, and T. Taketsugu, "Trajectory on-the-fly molecular dynamics approach to tunneling splitting in the electronic excited state: a case of tropolone," *Journal of*

Retraction

Retracted: Application of Industrial Big Data Cloud Control Platform Based on Fusion Transmission Sensor

Journal of Sensors

Received 17 October 2023; Accepted 17 October 2023; Published 18 October 2023

Copyright © 2023 Journal of Sensors. This is an open access article distributed under the Creative Commons Attribution License, which permits unrestricted use, distribution, and reproduction in any medium, provided the original work is properly cited.

This article has been retracted by Hindawi following an investigation undertaken by the publisher [1]. This investigation has uncovered evidence of one or more of the following indicators of systematic manipulation of the publication process:

- (1) Discrepancies in scope
- (2) Discrepancies in the description of the research reported
- (3) Discrepancies between the availability of data and the research described
- (4) Inappropriate citations
- (5) Incoherent, meaningless and/or irrelevant content included in the article
- (6) Peer-review manipulation

The presence of these indicators undermines our confidence in the integrity of the article's content and we cannot, therefore, vouch for its reliability. Please note that this notice is intended solely to alert readers that the content of this article is unreliable. We have not investigated whether authors were aware of or involved in the systematic manipulation of the publication process.

Wiley and Hindawi regrets that the usual quality checks did not identify these issues before publication and have since put additional measures in place to safeguard research integrity.

We wish to credit our own Research Integrity and Research Publishing teams and anonymous and named external researchers and research integrity experts for contributing to this investigation.

The corresponding author, as the representative of all authors, has been given the opportunity to register their agreement or disagreement to this retraction. We have kept a record of any response received.

References

- [1] W. Meng and W. Shao, "Application of Industrial Big Data Cloud Control Platform Based on Fusion Transmission Sensor," *Journal of Sensors*, vol. 2022, Article ID 6955028, 8 pages, 2022.

Research Article

Application of Industrial Big Data Cloud Control Platform Based on Fusion Transmission Sensor

Weiping Meng  and Wenxin Shao 

School of Intelligent Science and Information Engineering, Xi'an Peihua University, Xi'an, Shaanxi 710125, China

Correspondence should be addressed to Weiping Meng; 2016122635@jou.edu.cn

Received 19 May 2022; Revised 29 May 2022; Accepted 15 June 2022; Published 28 June 2022

Academic Editor: C. Venkatesan

Copyright © 2022 Weiping Meng and Wenxin Shao. This is an open access article distributed under the Creative Commons Attribution License, which permits unrestricted use, distribution, and reproduction in any medium, provided the original work is properly cited.

In order to solve the problem that the traditional operation and maintenance system of photovoltaic operation and power station is mainly based on statistical analysis and multisite and multilevel deployment mode, which wastes software and hardware resources, is not easy to expand and has extremely low efficiency, which cannot meet the urgent needs of users to reduce costs and increase efficiency. This research proposes a methodology for integrating big data, cloud computing, and photovoltaic operation and maintenance. This method constructs the business model, data model, application model, and technical model of the photovoltaic power station operation and maintenance cloud platform. The results obtained are as follows: the system provides diagnostic services for the application system of a 30 MWp photovoltaic power station in a certain place, and a total of 87 defects are found, the defect elimination rate is 88.51%, and the monthly power generation of the power station is increased by 122,529 kWh; the use effect of the system in this research after it goes online. The evaluation is 93.04 points, ranging from very satisfactory (A) to satisfactory (B) and biased towards A, indicating that the use effect is good. It is proved that the successful research and promotion of the system in this research will be of great significance to improve the intelligent operation and maintenance level of photovoltaic power plants and improve the operation and maintenance efficiency of photovoltaic power plants.

1. Introduction

In recent years, in the field of new energy photovoltaic power generation, with the strong support of national policies and a relatively open and favorable market environment, the number of enterprise groups investing in photovoltaic power generation and the number and scale of new photovoltaic power plants under the group have increased year by year [1]. However, in the context of the thriving development of the photovoltaic power generation industry, there are many problems, especially, the operation and maintenance management of photovoltaic power plants under the jurisdiction of power generation groups. The operation and maintenance management level or means of most photovoltaic power generation groups are far from matching their power plants [2]. The speed of construction, coupled with the scattered geographical location of photovoltaic power stations, large power station area, and relative

scarcity of professionals and other characteristics and status quo, has led to the insufficient production and management capabilities of photovoltaic power plants in photovoltaic power generation enterprise groups and the low power generation efficiency of photovoltaic power plants; corporate profits cannot be reliably guaranteed. With the continuous improvement of China's industrial automation level, the computer-centered ICT (Information and Communication Technology, ICT) technology has developed rapidly through the network and penetrated into all fields of social life [3]. Figure 1 is based on fusion transmission sensor data fusion technology and application research. With the development of Internet of Things technology, cloud computing technology, big data technology, and mobile communication technology, the traditional operation and maintenance software of photovoltaic power plants, which is mainly based on statistical analysis and multilevel deployment, can no longer meet the actual needs. The operation and maintenance of

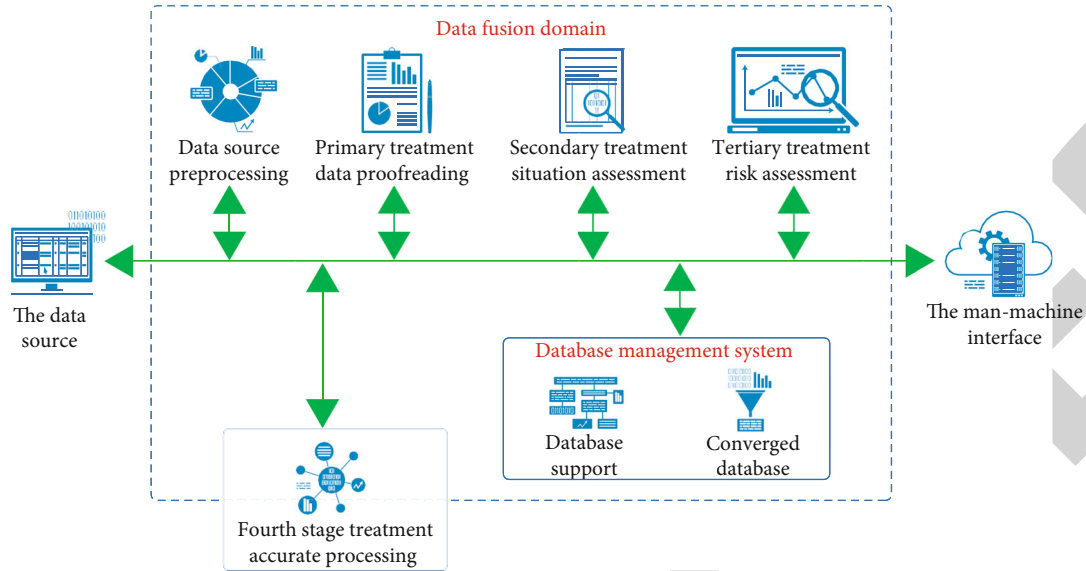


FIGURE 1: Research on sensor data fusion technology and application based on fusion transmission.

intelligent centralized power station has become an inevitable trend of development [4]. Therefore, building a photovoltaic power plant operation and maintenance cloud platform that integrates real-time collection of photovoltaic power station data, automatic calculation of power station operation and maintenance indicators, equipment status early warning, fault location, intelligent analysis, remote monitoring, and big data improvement conforms to the technological development trend of photovoltaic industry. It is an inevitable trend for power generation enterprises to realize intensive, refined, specialized, and intelligent operation and maintenance management [5]. It is also the core issue that photovoltaic power generation enterprises and operation and maintenance enterprises pay attention to in terms of operation and maintenance [6].

2. Literature Review

For the utilization of solar energy, Germany is the country that mainly utilizes solar energy. In 2007, its installed solar energy capacity reached more than 1300 MW, accounting for nearly half of the global newly added capacity. It is currently the largest solar power generation market in the world. Japan and the U.S. are second only. The U.S. market grew by 57% year-on-year in 2007, while the Japanese market began to decline after the government canceled certain policy subsidies, dropping by 22% in 2007 [7]. Spain has a fast growth rate. In 2007, the newly installed solar capacity increased by 480% year-on-year, becoming the new second largest market in the world. The rapid growth of the construction scale of photovoltaic power plants will inevitably lead to the development of corresponding technologies [8]. In terms of power station evaluation and monitoring system, Germany's TUV Süddeutsche Group is already a very experienced evaluation organization in the world. In terms of power station operation and maintenance, Meteo Control, the world's largest solar power station operation and maintenance

company from Germany, is second to none among the global photovoltaic operation and maintenance service providers. With more than 40 years of power station operation and maintenance experience, it has developed software and hardware products suitable for various installed capacities around the world and the overall solution. Its products have been used in more than 3,000 power stations in the world, with a total installed capacity of more than 8 GW and a power station investment of more than 10 billion euros. With the world's largest power station operation database, the independent third-party operation and maintenance model created by it has been relatively mature in Europe [9]. Meteo Control's photovoltaic power station operation and maintenance products have also used big data technology in meteorological data, solar energy forecast, technical operation and maintenance management, power generation report, system rating, and other functions [10].

China's renewable energy started relatively late. From the "Golden Sun Demonstration Project," which was implemented by the state in 2009 to support the technological progress of the photovoltaic power generation industry, to the large-scale development of photovoltaic power plants in 2012, and then, to the current full-scale outbreak of distributed photovoltaic power plants. The photovoltaic power station operation and maintenance system is also gradually developed from scratch. The early photovoltaic power station operation and maintenance system focused on management and was generally deployed in the existing formation, belonging to the MIS management system of the power station. With the intelligentization of photovoltaic power station-related equipment and the development of ICT technology, the photovoltaic power station operation and maintenance system has gradually turned to focus on monitoring, monitoring the status of equipment, and alarming. With the development of cloud computing technology, each enterprise has built its own private cloud platform, and the photovoltaic power station operation and maintenance system

has turned to centralized management. From 2014 to 2016, with the development of big data technology and Internet of Things technology, the operation and maintenance of photovoltaic power plants took the lead in entering the era of remote monitoring. At this stage, the photovoltaic power station operation and maintenance platform realizes basic management and control such as report statistics, power generation upload, fault work order management, and real-time display of equipment data. However, in 2017, with the increase of the number of power stations, the data volume has become a reality, and the current power station operation and maintenance platform has been unable to meet the deep-level needs such as in-depth analysis and refined management and control of trend warning [11, 12]. On the basis of remote monitoring and operation, photovoltaic power plant operation and maintenance has entered the era of big data operation platform, that is, using big data technology to analyze, give early warning, and propose solutions. With the development of mobile Internet, photovoltaic power plants have entered the era of “no entry, less the centralized and intelligent era of human operation and maintenance, remote monitoring, and big data improvement.”

Based on these foundations, this topic combines cloud computing, big data, and mobile communication technology with the actual business needs of photovoltaic power plant operation and maintenance and uses the massive data generated by photovoltaic power plants in the daily operation process to predict the power generation of equipment and to predict the power generation of the equipment that may be generated. Early warning of faults, accurate positioning of actual faults, health inspection, and benchmarking of photovoltaic power plants achieve standardized, intelligent, and professional operation and maintenance of photovoltaic power plants. The success and promotion of the system research will be of great significance to improve the intelligent operation and maintenance level of photovoltaic power plants and improve the operation and maintenance efficiency of photovoltaic power plants.

3. Research Methods

3.1. Effective Integration of Big Data, Cloud Computing, and Photovoltaic Power Plant Operation and Maintenance. Google published three technical researches on MapReduce (distributed computing framework), Google File System (GFS, distributed file system), and BigTable (GFS-based distributed database system), proposing a new set of distributed computing theory. Subsequently, various scientific research institutions and large IT companies began to implement their own distributed computing systems based on Google's new theory. The distributed computing framework MapReduce, distributed file system GFS, and distributed database system BigTable have therefore become the mainstays of the era of big data development technical foundation [13].

From the emergence of the concept of big data to the rapid development of big data today, through the analysis of actual application, Hadoop, Spark, and Storm are the three most widely used and popular platforms in the current

big data field. It is only analyzed from the perspective of big data processing, and the comparison results of the three platforms are shown in Table 1.

There is a loose relationship between the three services of SaaS, PaaS, and IaaS in cloud computing, that is, the three service modes can have dependencies or no dependencies on each other. For example, SaaS can run on PaaS or not on PaaS. In the same way, PaaS can run on IaaS or not. In terms of service objects, SaaS provides application system services, and the users are mainly the actual users of the business system. PaaS is to provide platform development and other services, and the general users are mainly application system developers. IaaS provides the underlying IT infrastructure as a service and is mainly used to deploy applications, so the users are generally IT resource users and managers [14]. Although the three models are at different levels, any one of the services can be independently provided externally and provide corresponding cloud services. Its relationship is shown in Figure 2.

In the field of photovoltaic power station informatization, the construction goal of the photovoltaic power station management and control platform is to “reduce costs and increase power generation.” Therefore, the IaaS and PaaS service models are mainly used when the photovoltaic power station management and control platform realizes cloud computing integration. In the IaaS layer, the hardware resources of the centralized control center are used, and virtualization technology is used to realize the deployment and operation of multiple application platforms; in the PaaS layer, a unified operating platform is used to meet the needs of the company for running multiple applications.

Big data and cloud computing are mutually influenced and developed together. From the perspective of practical application, the purpose of cloud computing is to better call, expand, and manage computing and storage resources and capabilities through resource sharing to reduce the IT cost of enterprises; the purpose of big data is to fully exploit massive information in data to discover value in data. Cloud computing saves users' IT resource costs, big data helps users discover the value in data, and the integration of the two from the application level can bring great benefits to users. From a technical point of view, cloud computing provides a basic support environment for the storage and processing of big data, and big data also broadens the technical application of cloud computing. Cloud computing and big data learn from each other's technical ideas and integrate with each other. By establishing a unified and shared infrastructure resource pool, on-demand allocation, unified scheduling, and mutual coordination of resources for different business application systems can be achieved, to achieve the purpose of intensive and efficient utilization of resources. Based on a unified infrastructure, big data can be stored, processed, and analyzed more conveniently, thereby maximizing the value of data mining [15, 16].

3.2. Data Process Analysis of PV Operation and Maintenance Cloud Platform. The entire data flow of the system is shown in Figure 3.

TABLE 1: Comparison of distributed computing platforms.

Platform	Types of big data processing	Remark
Hadoop	Offline, complex	With data collection and storage capabilities
Spark	Offline, fast	With data collection and storage capabilities
Storm	Online, real-time	No data collection and storage capabilities

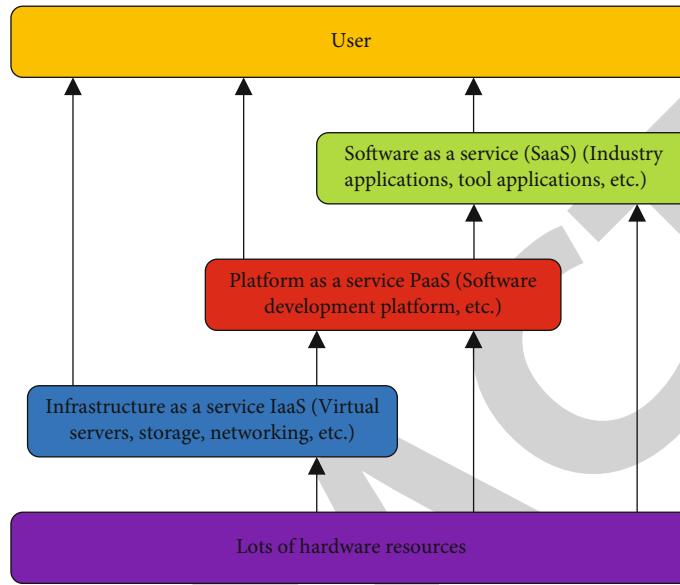


FIGURE 2: Cloud service hierarchy diagram.

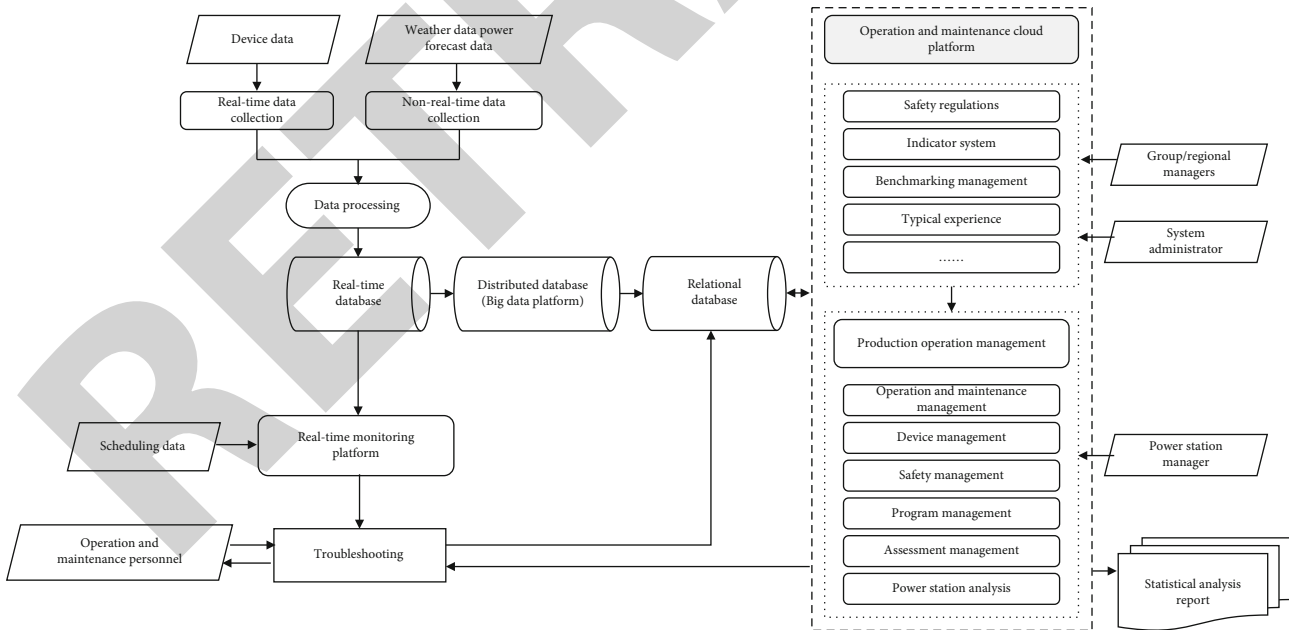


FIGURE 3: System data analysis flow chart.

The acquisition software collects real-time data (photovoltaic power station acquisition equipment related data) and nonreal-time data (meteorological data, electrical energy data, and optical power prediction data) and stores them in the real-time database. Whether to alert or control the real-

time monitoring platform also accepts the instructions sent from the scheduling and performs corresponding control according to the instructions. The big data platform reads data from the real-time database for processing and visual analysis and writes the resulting data into the structured

database for subsequent statistical analysis by the operation and maintenance cloud platform. The intelligent operation and maintenance cloud platform obtains relevant data from the structured database for statistical analysis and early warning. Management data is written into the structured database through the intelligent operation and maintenance cloud platform for subsequent query and analysis [17].

3.3. *System Functional Architecture.* System functions mainly include the following aspects:

(1) Big data collection and transmission

Big data acquisition and transmission mainly includes software/hardware equipment and related supporting facilities required for data acquisition, data uploading, and communication management at each power station and solves the problem of communication interface protocol between each system of the centralized control center and the equipment of various local intelligent monitoring system manufacturers. All the collected data is encrypted and uploaded to the centralized control center through the intermediate transmission link layer, which is unified into the data platform integrated with the centralized control center system, and the dispatching channel is opened to realize the remote monitoring function of all power stations.

The station side of the power station mainly collects real-time operating data such as photovoltaic equipment (including photovoltaic arrays, combiner boxes, inverters, booster stations, energy metering devices, and box-type transformers) and nonreal-time data such as power prediction. Upload it to the centralized control center of the headquarters, and send it to the big data processing platform through the program [18, 19].

(2) Real-time monitoring platform

Set up a centralized control center at the company's headquarters, which is the company's operation and maintenance management center, display center, and evaluation and decision-making center. The real-time monitoring platform and operation and maintenance cloud platform are deployed in the centralized control center. The real-time monitoring platform receives the real-time data and nonreal-time data uploaded by the subordinate power plants and remotely and centrally monitors the operation of the main equipment of the subordinate photovoltaic power plants. Realize the integration of on-site operation monitoring, and realize remote control and monitoring of station equipment.

(3) Intelligent operation and maintenance cloud platform

The operation and maintenance cloud platform is the core platform for the operation and maintenance management of photovoltaic power plants, which realizes the remote management and control of the subordinate photovoltaic power plants, including the regional/group management and the local operation and maintenance management of each power station.

(4) Mobile platform

The mobile platform adopts a lightweight design, which can be accessed directly by scanning the QR code or integrated into the group's official account. Users do not need to download additional APP programs and do not occupy mobile phone memory [20].

The system functional architecture is shown in Figure 4.

4. Analysis of Results

4.1. *Evaluation of Economic Effects of System Application.* After the system was launched, during the one-month experiment period, a diagnostic service was performed on the application system of a 30 MWp photovoltaic power station in a certain place. A total of 87 defects were found, and the defect elimination rate was 88.51%. The monthly power generation of the power station was increased by 122,529 kWh. The specific defect statistics are shown in Table 2.

4.2. *Evaluation of System Application Use Effect.* The basic idea of analytic hierarchy process (AHP) is to first determine the main factors affecting the evaluation object, form a hierarchical structure, and establish an index system according to the affiliation of each factor, and then, judge the relative importance of each factor by experts. And assign values to get the judgment matrix M and check its consistency: finally, calculate the combined weight of each layer factor to the system. The following uses the analytic hierarchy process to evaluate the actual use effect of the system [21–23].

(1) Construction of evaluation index system

After analysis, the evaluation index system of this system is divided into two levels: the first level analyzes the evaluation indexes from the user's point of view (B1 is the management personnel, B2 is the on-site operation and maintenance personnel, and B3 is the system's own status); the second level is based on different users build different indicators, B1 includes C11, C12, and C13, B2 includes C21, C22, and C23, and B3 includes C31, C32, and C33.

(2) Construct judgment matrix

When determining the weights between the factors at each level, the consistent matrix method is used, that is, all factors are not compared together, but compared with each other. To improve accuracy, relative scales are used when comparing with each other. The scaling method of the judgment matrix element a_{ij} is shown in Table 3.

The judgment matrix element a_{ji} can be obtained by:

$$a_{ji} = \frac{1}{a_{ij}}. \quad (1)$$

(3) Calculate the weight vector and do the consistency check

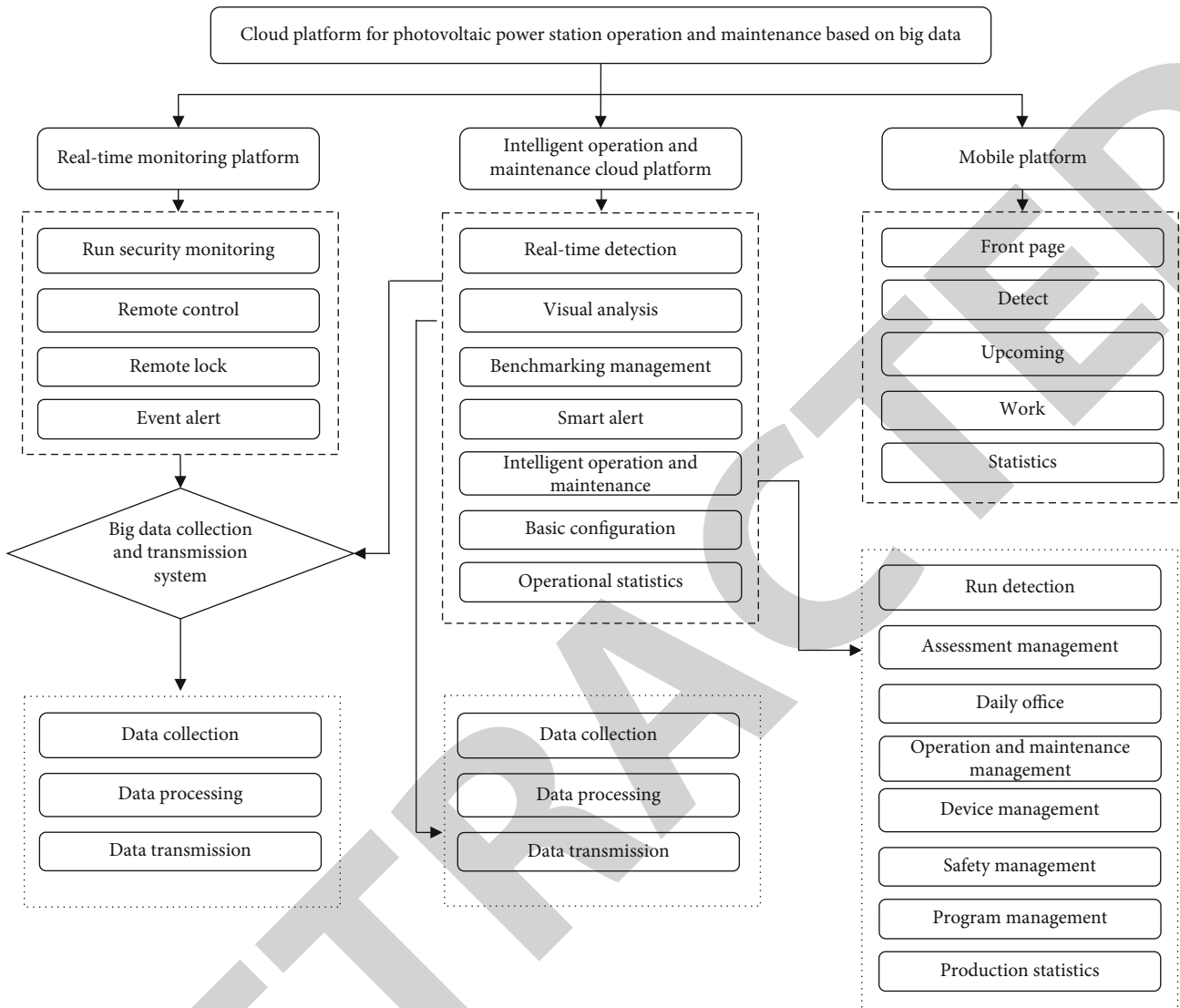


FIGURE 4: System functional architecture diagram.

TABLE 2: Defect statistics.

Serial number	Defect classification	Total number of defects (bars)	Missing (articles)	Elimination rate (%)
1	Branch circuit fuse burnt	62	62	100
2	Component power is abnormally attenuated	3	3	100
3	Cable failure	9	1	11.11
4	Inverter conversion efficiency is low	1	0	0
5	Abnormal data acquisition module	2	2	100
6	The communication of the combiner box is abnormal	5	5	100
8	Environmental monitor	2	2	100
9	Other	3	2	66.67
Total		87	77	88.51

TABLE 3: Proportional scale table.

Factor i is better than factor j	Quantized value
Equally important	1
Slightly important	3
Strong and important	5
Strongly important	7
Extremely important	9

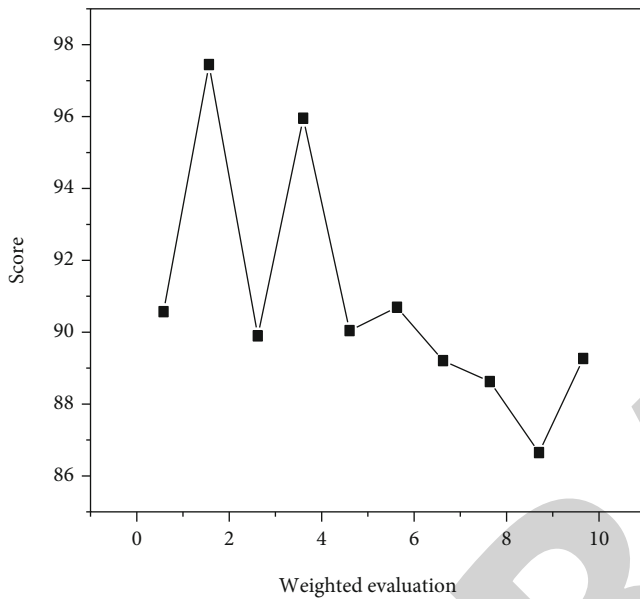


FIGURE 5: System review score table.

The calculation steps are as follows:

- (1) Calculate the maximum eigenvalue λ_{\max} and eigenvector of the judgment matrix
- (2) Judging the consistency of the matrix

The so-called consistency refers to the logical consistency of judgment thinking. The consistency index CI is obtained by:

$$CI = \frac{\lambda_{\max} - n}{n - 1}, \quad (2)$$

where λ_{\max} is the maximum eigenvalue of the matrix; n is the order of the matrix.

When $CI = 0$, the judgment matrix is consistent; the larger the CI, the more serious the inconsistency of the judgment matrix.

Taking a group in Gansu Province that has used the photovoltaic power station operation and maintenance cloud platform as the object, the weight value calculation is carried out. The steps are: construct the index questionnaire → questionnaire survey → weighted evaluation to obtain the application effect value.

The questionnaire is designed according to the constructed first- and second-level index system, and four options of “very satisfied (A), satisfied (B), relatively satisfied (C), and dissatisfied (D)” are set for each indicator to facilitate users’ selection. The “A” level corresponds to 100 points, the “B” level corresponds to 85 points, the “C” level corresponds to 75 points, and the “D” level corresponds to 60 points [24, 25].

The index system questionnaire was collected, analyzed, and weighted for evaluation. The final calculation result is shown in Figure 5.

According to the analysis in Figure 5, the evaluation of the use effect after the system goes online is 93.04 points, ranging from very satisfied (A) to satisfied (B) and biased towards A, indicating that the use effect is good.

5. Conclusion

Aiming at the problems existing in the current photovoltaic power plant operation and maintenance management process, this research analyzes the new requirements, new business processes, management modes, and management goals of photovoltaic power plant operation and maintenance. The business model, data model, application model, and technical model of the photovoltaic power station operation and maintenance cloud platform are constructed; the construction method of the overall model of the photovoltaic power station operation and maintenance cloud platform is deeply studied; in the process of platform construction, the process of reducing enterprise costs, the thinking method of improving system efficiency and intelligent operation and maintenance, adhering to the construction concept of compatible, easy-to-use, robust, and safe information system, and demonstrating its practical application effect based on individual cases.

The main work and research results of the research are summarized as follows:

- (1) Combined with big data technology, cloud computing service model, and deployment model, the cloud platform architecture, business architecture, application architecture, network architecture, data architecture, functional architecture, and information security architecture of photovoltaic power plant operation and maintenance based on big data are designed. The functional modules of photovoltaic big data are designed and described in detail
- (2) Discussed the Hadoop big data processing framework and MongoDB storage technology used in the realization of the photovoltaic power station operation and maintenance cloud platform, briefly described the hardware environment, software environment requirements and system development and configuration environment of the platform operation; demonstrated the core functions of the system interface; and the application effect of the system is evaluated from the economic and usage perspectives with actual cases

Retraction

Retracted: Life Prediction of Dry Reactor Sensor Based on Deep Neural Network

Journal of Sensors

Received 17 October 2023; Accepted 17 October 2023; Published 18 October 2023

Copyright © 2023 Journal of Sensors. This is an open access article distributed under the Creative Commons Attribution License, which permits unrestricted use, distribution, and reproduction in any medium, provided the original work is properly cited.

This article has been retracted by Hindawi following an investigation undertaken by the publisher [1]. This investigation has uncovered evidence of one or more of the following indicators of systematic manipulation of the publication process:

- (1) Discrepancies in scope
- (2) Discrepancies in the description of the research reported
- (3) Discrepancies between the availability of data and the research described
- (4) Inappropriate citations
- (5) Incoherent, meaningless and/or irrelevant content included in the article
- (6) Peer-review manipulation

The presence of these indicators undermines our confidence in the integrity of the article's content and we cannot, therefore, vouch for its reliability. Please note that this notice is intended solely to alert readers that the content of this article is unreliable. We have not investigated whether authors were aware of or involved in the systematic manipulation of the publication process.

Wiley and Hindawi regrets that the usual quality checks did not identify these issues before publication and have since put additional measures in place to safeguard research integrity.

We wish to credit our own Research Integrity and Research Publishing teams and anonymous and named external researchers and research integrity experts for contributing to this investigation.

The corresponding author, as the representative of all authors, has been given the opportunity to register their agreement or disagreement to this retraction. We have kept a record of any response received.

References

- [1] H. Guo, J. Meng, Y. Yang, L. Zheng, X. Liu, and M. Tan, "Life Prediction of Dry Reactor Sensor Based on Deep Neural Network," *Journal of Sensors*, vol. 2022, Article ID 6982950, 7 pages, 2022.

Research Article

Life Prediction of Dry Reactor Sensor Based on Deep Neural Network

Hongbing Guo ^{1,2}, Jianying Meng ³, Yue Yang ^{1,2}, Lu Zheng ^{1,2}, Xuan Liu ^{1,2}, and Ming Tan ⁴

¹Inner Mongolia Power (Group) Co., Ltd., Inner Mongolia Power Research Institute Branch, Hohhot 010020, China

²Inner Mongolia Enterprise Key Laboratory of High Voltage and Insulation Technology, Hohhot 010020, China

³Inner Mongolia University of Technology, Hohhot 010051, China

⁴Nanjing Unitech Electric Power Co., Ltd., Jiangsu, Nanjing 210000, China

Correspondence should be addressed to Hongbing Guo; 201772511@yangtzeu.edu.cn

Received 19 May 2022; Revised 31 May 2022; Accepted 15 June 2022; Published 25 June 2022

Academic Editor: C. Venkatesan

Copyright © 2022 Hongbing Guo et al. This is an open access article distributed under the Creative Commons Attribution License, which permits unrestricted use, distribution, and reproduction in any medium, provided the original work is properly cited.

In order to solve the problem of increasing the number and service life of a dry-type air core reactor and frequent interturn insulation faults, this paper proposes a life prediction method of a dry-type reactor sensor based on the deep neural network. On the basis of summarizing the research status of turn-to-turn insulation-related problems, this method studies the switching overvoltage generated in the process of breaking the dry-type air core reactor, the deterioration law of turn-to-turn insulation under the cumulative action of switching overvoltage, the influence of thermal aging on the Switching Overvoltage Withstand characteristics of turn-to-turn insulation, and the electrical aging life of turn-to-turn insulation under the power frequency overvoltage. Based on the deep neural network, the electrical aging life model of turn-to-turn insulation of the dry-type air core reactor under power frequency overvoltage is obtained. The results are as follows: with the increase of the applied voltage amplitude, the deterioration speed of the turn-to-turn insulation of the model sample accelerates. When the applied voltage amplitude reaches a certain value, the maximum discharge amount and pulse discharge power of the partial discharge pulse increase rapidly, and the image coincidence degree reaches 85%. The electric aging life curve of the modified interturn insulation model sample of the dry-type air core reactor has a high correlation with the measured aging life data, and the performance is more than 95%. The research results of this paper lay a practical foundation for further research on the deterioration mechanism of interturn insulation under the combined action of multiple factors and provide theoretical support for the risk and life assessment of the dry-type air core reactor.

1. Introduction

As a basic industry related to the national economy and the people's livelihood, the power industry is related to the overall situation of economic and social development. The economically developed load center is concentrated in the eastern coast, which is far away from the large-capacity hydropower units in the southwest and the large-capacity thermal power units in the north [1]. Objective conditions require the power system to have higher transmission effi-

ciency and capacity, so as to realize economic, reasonable, safe, and reliable high-capacity and long-distance power transmission. Reactors are mainly divided into iron core reactors and dry-type air core reactors. Dry-type air core reactors have technical advantages such as unsaturated, high strength, light weight, low noise, and simple structure and are widely used in power systems (as shown in Figure 1). In the power system with a voltage level of 66 kV and below, the dry-type air core reactor accounts for more than 80%. By 2016, the market capacity of the dry-type air core reactor has

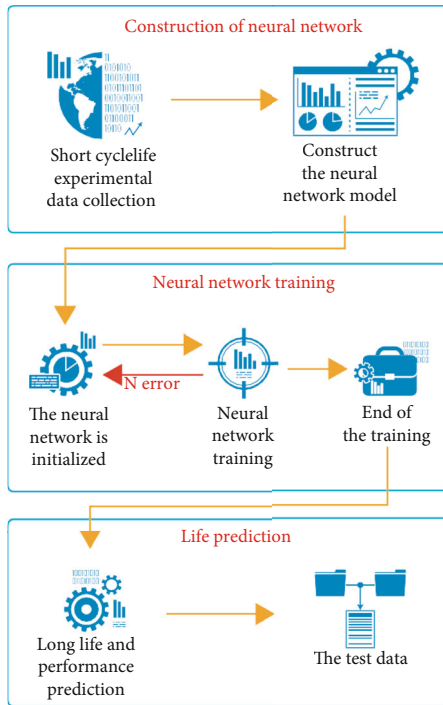


FIGURE 1: A life prediction method and process of dry reactor sensor based on deep neural network.

reached 30 billion yuan. With the increase of the number of dry-type air core reactors put into operation and operation life, the failure rate also gradually increases [2, 3].

In the early fault analysis, the researchers believed that rain invasion caused the moisture on the outer surface of the encapsulated insulation of the dry-type air core reactor and surface discharge, resulting in uneven distribution of the electric field inside the insulation, partial discharge, continuous corrosion of insulation, and finally interturn insulation fault. According to the research results, relevant departments have taken a variety of preventive measures for outdoor dry-type air core reactors. The actual operation experience of the air core reactor shows that there are still frequent interturn insulation accidents. Studying the causes of the operating overvoltage of the dry-type air core reactor and the laws followed and the causes and development process of the interturn insulation fault under the conditions of operating overvoltage and power frequency overvoltage and understanding the failure mechanism of interturn insulation of the dry-type air core reactor can provide a theoretical basis for manufacturing enterprises to optimize the interturn insulation design of the dry-type air core reactor and improve the production process. It can also provide reference for the power operation department to improve the operation mode of the dry-type air core reactor, study various protective measures, and develop corresponding protective devices.

2. Literature Review

In the late 1950s, dry-type air core reactors were used to limit various kinds of overcurrent in the power system. At

that time, most of the dry-type air core reactors produced by power equipment manufacturing enterprises used cable conductors as windings, cable insulation as turn-to-turn insulation, and cement castings as support. The mechanical strength of the cement reactor is large, but it has the disadvantages of low insulation level, poor heat dissipation, easy moisture absorption, and inconvenient installation and use, so it is not widely used [4]. With the continuous application of new materials and the progress of technology, some changes have taken place in the structure of the dry-type air core reactor in the early 1960s. In the 1970s, the Canadian Trend Electric Company (hereinafter referred to as the TE company) first developed a new type of dry-type air core power reactor which is now widely used. This new type of dry-type air core power reactor is quickly recognized by power system users for its unique structure and excellent electrical performance and gradually replaces the traditional oil-immersed iron core power reactor and the old air core power reactor in the power system and its power users. At present, the manufacturers of dry-type air core reactors mainly include the TE company in Canada, ABB company in Germany, Spezieketa company in Austria, and Haefly company in Switzerland. Among them, the TE company has the highest market share and the widest coverage. After years of development, although the design idea and structure of the dry-type air core reactor manufactured by the TE company have not been greatly improved, the application field of its products has been continuously expanded, and the voltage level of the products has been increasing. The maximum voltage level of the current limiting reactor has reached 765 kV, the maximum voltage level of the shunt reactor has reached 115 kV, and the maximum voltage level of the smoothing reactor has reached 500 kV [5, 6]. In the late 1970s, the power sector began to try to purchase new dry-type air core reactors produced by foreign power equipment manufacturing enterprises and apply them to the power system. Compared with the old domestic reactor at that time, the imported new dry-type air core reactor has obvious technical advantages. In 1985, the Beijing Power Equipment Group Company of the former Ministry of Water Resources and Electric Power signed a special technology transfer agreement on a line wave arrester (a new type of small dry air core power reactor) and its manufacturing equipment with the TE company of Canada. The power equipment manufacturing department began the production of this new type of dry air core power reactor. In the early 1990s, some reactor manufacturers began the localization of new dry-type air core reactors by cooperating with colleges and universities. The mid-1990s have been able to produce some different types of new dry-type air core power reactors with small capacity. At the beginning of the 21st century, with the vigorous construction of the power grid, the research and development of new dry-type air core reactors has made great progress [7].

Based on the above background, aiming at the practical problem of the high turn-to-turn insulation failure rate of the dry-type air core reactor in the power grid, this study studies the operating overvoltage generated in the process of breaking the dry-type air core reactor via the circuit breaker,

the failure mechanism of turn-to-turn insulation of the dry-type air core reactor under the cumulative action of operating overvoltage, the influence law and micromechanism of thermal aging on the Switching Overvoltage Withstand capacity of turn-to-turn insulation, and the deterioration mechanism of turn-to-turn insulation under power frequency overvoltage and electric aging life equation.

3. Research Methods

3.1. Simulation of Starting Overvoltage System of Dry-Type Air Core Reactor. Different from other types of power equipment in the power system, the dry-type air core reactor, as a compensation device, needs to be switched frequently according to the change of the system reactive power. Due to the parameter characteristics of the dry-type air core reactor, high-frequency and high-amplitude exponential attenuation oscillation overvoltage occurs at both ends of the reactor during the switching operation. On the basis of summarizing the current research status of breaking the overvoltage simulation of the dry-type air core reactor and the theoretical analysis of the single-phase circuit, taking the 66 kV dry-type air core shunt reactor in an actual power grid as the prototype, the overvoltage generated in the process of breaking the reactor via the three-phase circuit breaker is studied. According to the rated parameters and structural parameters of the reactor and the rated parameters and working characteristics of the SF6 circuit breaker, the simulation model of the reactor and circuit breaker is established, and the three-phase simulation circuit is built according to the actual wiring. Combined with the typical waveform of on-off overvoltage, the influence law of random parameters such as cut-off value and action time difference on overvoltage is analyzed. The theoretical analysis model of the three-phase circuit breaker breaking the shunt reactor is built [8–10].

The actual circuit breaker model involved in this study is LTB72.5/D1. Its working characteristics mainly include current cut-off value, high-frequency arc extinguishing capacity, and dielectric recovery characteristics. The current chopping is caused by the instability of arc combustion. If the circuit breaker can inhibit the arc discharge ionization, the unstable plasma will be interrupted and form a nonzero chopping. This current value is called the cut-off value. The cut-off value of the circuit breaker is determined by its own characteristics and external circuit parameters. There are differences and great dispersion during each disconnection. An SF6 circuit breaker with a rated voltage of 300 kV was used in the laboratory to disconnect a 275 kV-150 mVa reactor. It was detected that the chopping current of the circuit breaker was between 0 and ~30 A. Considering that the voltage level of the circuit breaker and reactor in this paper is small, the cut-off value is 0~13 A. When the current frequency is greater than a certain value, the circuit breaker cannot successfully extinguish the arc regardless of whether other conditions are met. The upper frequency limit of the current that can be extinguished by the circuit breaker is called the high-frequency arc extinguishing capacity of the circuit breaker. The high-frequency arc extinguishing capacity of the LTB72.5/D1 SF6 circuit breaker

is between 50 and ~300 A/ μ s, and 100 A/ μ s is taken in this paper [11].

According to the actual action characteristics of the circuit breaker in the process of disconnecting the reactor, the model module is programmed. In the program, given the action time t_s of the circuit breaker, the chopper current value I_0 and the specific value of the high-frequency arc-extinguishing capacity, the initial state of SW_TACS is closed, the time range of each simulation is 0, the value is 30 ms, and it is calculated every 10 ns. In the simulation, the model module automatically measures the source side voltage U_1 , load side voltage U_2 , and loop current i and outputs the switching state of the control SW_TACS. The workflow of the model module is shown in Figure 2.

The reactor model is BKK-20000/66, and its rated parameters and structural parameters are shown in Table 1.

This paper studies the overvoltage of the reactor as a whole, and the overvoltage frequency is very high. The equivalent circuit represented by centralized parameters is shown in Figure 3.

In Figure 3, L is the inductance of the reactor, R_L is the equivalent parallel resistance representing the loss of the reactor, C_Z is the equivalent capacitance of the interturn capacitance network, and C_{g1} and C_{g2} are the values of the stray capacitance of the reactor to the ground equivalent to the first and last ends, respectively [12, 13].

3.2. Electrical Aging Life Evaluation System of Turn-to-Turn Insulation under Power Frequency Overvoltage. Under the action of a single electric field, when the applied voltage is lower than the initial partial discharge voltage, the solid insulating material can work for decades without electrical aging, which mainly occurs after partial discharge. It is difficult to make solid insulating materials uniform and dense with their processing technology. Air gap or impurities lead to electric field distortion. When the applied voltage meets the conditions, it will lead to partial discharge. Under normal working conditions, the turn-to-turn insulation voltage of the dry-type air core reactor is very low, which is not enough to induce partial discharge. However, in the whole life cycle, the turn-to-turn insulation of the reactor bears a variety of overvoltages, such as switching overvoltage and local turn-to-turn power frequency voltage rise caused by moisture on the envelope surface, which may lead to partial discharge. In this paper, the electrical aging life equation of turn-to-turn insulation of the dry-type air core reactor under power frequency overvoltage is studied. The initial partial discharge voltage and power frequency breakdown voltage of the interturn insulation model sample of the nonaged dry air core reactor are measured to provide a reference for the determination of the aging voltage value. The constant power frequency voltage method and stepped power frequency voltage method are used to carry out the accelerated electrical aging test of model samples under power frequency overvoltage [14].

The electric aging test platform is composed of the console, regulated power supply, voltage regulator, protective resistor, and capacitor voltage divider. The experimental circuit adds a regulated power supply on the basis of the

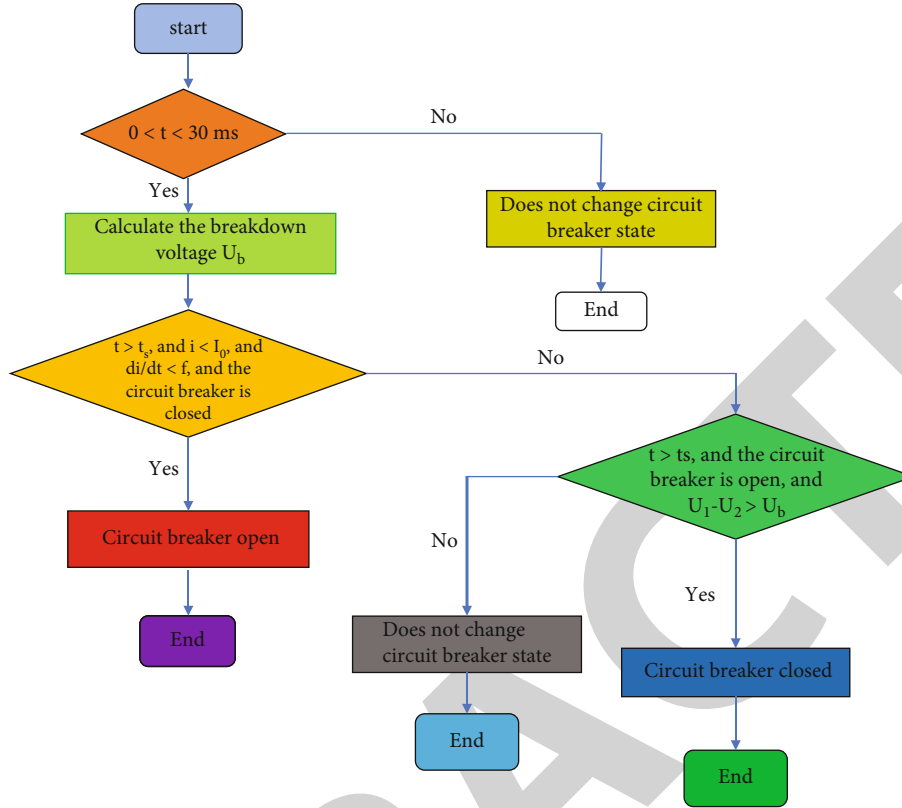


FIGURE 2: Workflow of model module.

TABLE 1: Rated parameters of BKK-20000/66 dry-type air core reactor.

Rated voltage (kV)	Rated capacity (kVA)	Rated reactance (Ω)	Installation height (m)
38.11	20000	72.6	4.13

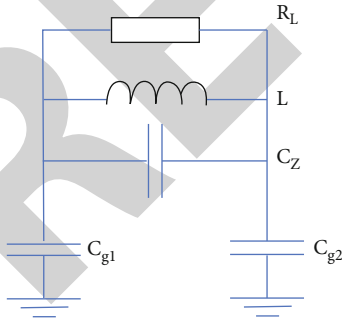


FIGURE 3: Concentrated parameter equivalent circuit of reactor.

traditional power frequency high-voltage test power supply to eliminate the influence of the power grid voltage fluctuation in the aging process to the greatest extent. The rated voltage of the test transformer is 100 kV and the rated capacity is 10 kVA.

Common accelerated electrical aging methods include the constant voltage method, step voltage method, and sequential voltage method. The constant voltage method is the earliest and most widely used. In recent years, some scholars have

used the step voltage method to carry out the electrical aging test of XLPE, polypropylene, and polyimide films and achieved good test results. In this paper, the step voltage method and constant voltage method are used for the accelerated electrical aging test. The test results of the two methods can confirm each other. The application process of the two voltages is shown in Figure 4: Figure 4(a) is the step voltage method, $U_1 \sim U_m$ is the voltage of each stage, $\Delta u_k (k = 1 \sim m - 1)$ is the boost value, $t_{rk} (k = 1 \sim m - 1)$ is the boost time, $T_1 \sim T_{m-1}$ is the duration of the previous stage of withstand voltage, T_m is the duration of the last stage of withstand voltage, and m is the step-up stage; Figure 4(b) is the constant voltage method, which is continuously boosted to the test voltage and maintained until the test object breaks down [15, 16].

4. Result Analysis

4.1. Effective Power Frequency Constant Voltage Electrical Aging Test. Conduct electrical aging test under 6 kV~13 kV constant power frequency voltage. For 12 samples under each voltage, remove the maximum and minimum values of the test data to obtain 80 effective data. The variation trend of pulse maximum discharge and pulse discharge power with voltage was measured. The application mode of voltage is the step-by-step boost, and the duration of the step-by-step voltage is 720 s. The specific step-by-step boost mode is consistent with the step-by-step boost process [17, 18]. The partial discharge parameters of 12 model samples were measured, and the maximum and minimum values of the test data were removed to obtain 10 effective test data.

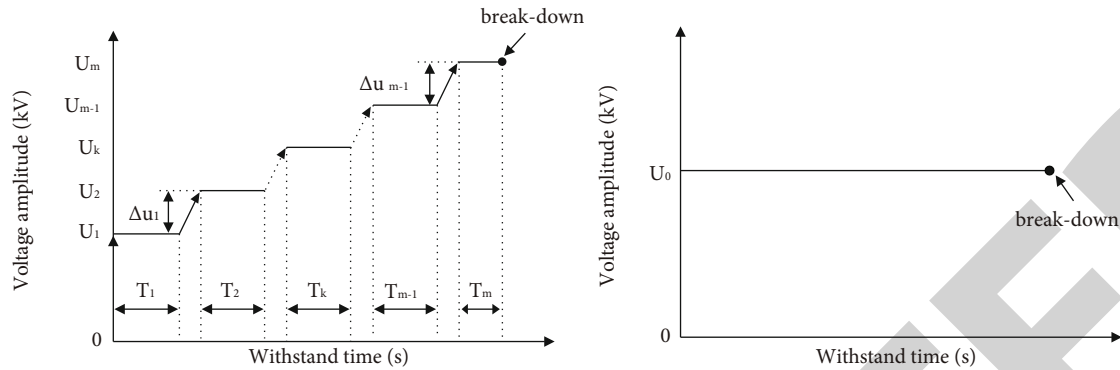


FIGURE 4: Electric aging pressurization method.

In order to prevent the current overshoot caused by accidental breakdown from damaging the partial discharge measuring instrument in the process of partial discharge parameter measurement, only the partial discharge parameters with a voltage amplitude less than 4.5 kV are measured.

The electrical aging test data of 140 effective power frequency constant voltage at 14 voltage levels are obtained. Based on the differential idea, when the voltage amplitude changes little, the electric aging life equation should follow the inverse power formula. In order to determine that the aging voltage amplitude will affect the value of the withstand voltage life index N , the constant voltage electrical aging test data in different voltage amplitude ranges are analyzed, and the values of index N and constant C are shown in Table 2.

It can be seen from Table 2 that no matter whether the number of aging life data increases or decreases, as long as the electrical aging life data obtained under the high-amplitude voltage used for parameter estimation of inverse power life model increases, the parameter estimation values of the withstand voltage life index n and constant C increase [19].

Calculate the average value of 10 effective data of the maximum partial discharge pulse and pulse discharge power of the model sample under each aging voltage amplitude and obtain the variation law of the partial discharge parameters of the interturn insulation model sample with the aging voltage amplitude, as shown in Figure 5.

As can be seen from Figure 5, when the applied voltage amplitude is low, the maximum pulse discharge amount and pulse discharge power amplitude of partial discharge of the model sample are very small. After the applied voltage amplitude reaches a certain value, the maximum pulse discharge amount and pulse discharge power of the partial discharge pulse increase rapidly. The maximum pulse discharge generally represents the partial discharge of large-scale defects in the insulation. Therefore, the variation trend of the maximum pulse discharge with the applied voltage amplitude proves that the size of air gap defects with partial discharge increases with the increase of the applied voltage amplitude. The pulse discharge power of partial discharge comprehensively represents the instantaneous value of the pulse discharge frequency, pulse discharge quantity, and applied voltage amplitude and represents the amount of energy released in the process of partial discharge. The

greater the energy, the faster the insulation deterioration rate. Therefore, the variation trend of the partial discharge pulse power with the applied voltage amplitude shows that the deterioration rate of the turn-to-turn insulation of the model sample increases with the increase of the applied voltage amplitude [20–23].

4.2. Modification of Electric Aging Inverse Power Life Model.

Under the condition of partial discharge, the electrical aging life data of the turn-to-turn insulation model sample of the dry-type air core reactor does not follow the inverse power life model. With the increase of the aging voltage amplitude, the values of parameters N and C in the inverse power model increase, in order to obtain a more accurate empirical formula of electrical aging life under the partial discharge condition, so as to estimate the electrical aging life of the turn-to-turn insulation of dry-type air core reactor under lower voltage. Take the voltage amplitude corresponding to the estimated values of each group of N and C parameters in Table 2 as the average value of the voltage within the range and obtain the effective data of 15 groups of unknown parameters N and C varying with the voltage amplitude. The empirical formulas of N and C affected by the voltage amplitude u are formulas (1) and (2), respectively:

$$N = -10.1 + 8.51e^{0.0518U}, \quad (1)$$

$$\ln C = 13.9 + 0.017U^{2.54}. \quad (2)$$

Substituting equations (1) and (2) into their logarithmic form, the modified empirical formula of electric aging life is the following equation:

$$\ln L = 13.9 + 0.017U^{2.54} + (10.1 - 8.51e^{0.0518U}) \ln U. \quad (3)$$

The curve corresponding to equation (3) and the measured electric aging life data points (average value of 5 samples) of model samples under electric aging voltage amplitudes of 4.5 kV, 6.5 kV, 8.5 kV, 10.5 kV, 12.5 kV, 14.5 kV, and 16.5 kV are drawn in Figure 6.

It can be seen that the electrical aging life curve of the modified interturn insulation model sample of the dry-type air core reactor has a high correlation with the measured aging life data, which can reach more than 95%. Therefore,

TABLE 2: N and C values calculated from constant piezoelectric aging data corresponding to different voltage ranges.

Voltage range (kV)	6~10	6~11	6~12	6~13	6~14
N value	2.73	3.04	3.43	4	4.21
C value	2.74E7	4.92E7	1.02E8	2.94E8	4.32E8
Voltage range (kV)	6~15	7~16	8~17	9~18	10~19
N value	4.38	5.34	6.31	7.15	7.94
C value	5.89E8	5.4E9	5.57E10	5.48E11	4.67E12
Voltage range (kV)	11~19	12~19	13~19	14~19	15~19
N value	8.35	8.66	8.96	10.19	10.56
C value	1.62E13	4.09E13	1.02E14	3.66E15	1.26E16

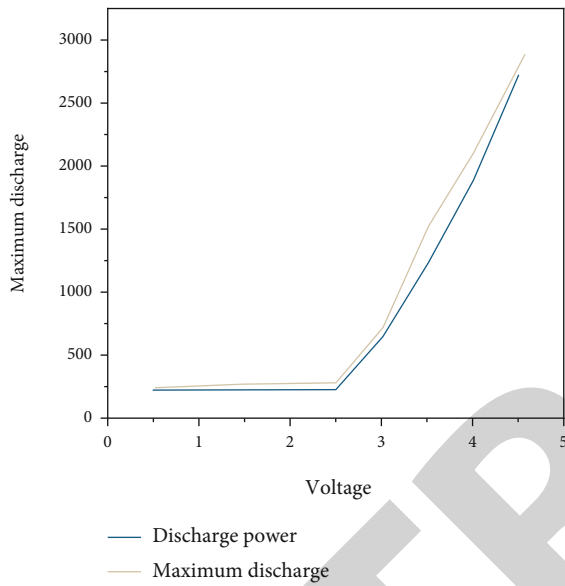


FIGURE 5: Variation trend of partial discharge parameters with voltage.

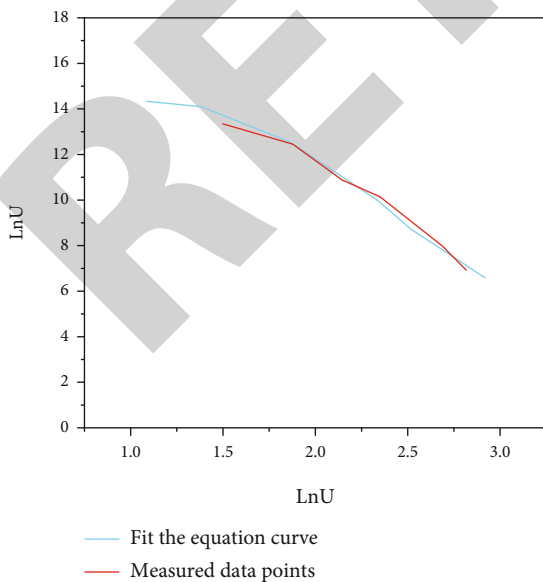


FIGURE 6: Comparison between electric aging life curve and measured data.

the new empirical formula of electrical aging life can accurately reflect the electrical aging law of the turn-to-turn insulation model sample of the dry-type air core reactor under the action of power frequency overvoltage [24, 25].

5. Conclusion

With the increase of the number and service life of the dry-type air core reactor, turn-to-turn insulation faults occur frequently. This paper summarizes the research status of turn-to-turn insulation. Focusing on the failure mechanism of turn-to-turn insulation of the dry-type air core reactor under overvoltage, this paper mainly studies the switching overvoltage generated in the process of disconnecting the dry-type air core reactor, the deterioration law of turn-to-turn insulation under the cumulative action of switching overvoltage, the influence of thermal aging on the Switching Overvoltage Withstand characteristics of turn-to-turn insulation, and the electrical aging life of turn-to-turn insulation under power frequency overvoltage. The main work and conclusions of this paper are as follows:

- (1) This paper studies the influence of thermal aging on the Switching Overvoltage Withstand characteristics of turn-to-turn insulation of the dry-type air core reactor. The results show that thermal aging will not reduce the breakdown voltage, partial discharge, and other parameters of the dry-type air core reactor. With the deepening of thermal aging, the mechanical properties of the polyester film decrease, which leads to the exponential decline of the cumulative action times of the model sample to withstand the operating overvoltage
- (2) This paper carried out the accelerated electrical aging life test of interturn insulation model samples and established the mathematical model of the electrical aging life. The results show that when there is partial discharge under power frequency overvoltage, the electrical aging life of turn-to-turn insulation of the dry-type air core reactor does not follow the inverse power model, and the withstand voltage life index n and constant C increase with the increase of the test voltage. The modified electric aging life equation can more accurately predict the interturn insulation life of the dry-type air core reactor under the condition of partial discharge

Retraction

Retracted: Tennis Technology Recognition and Training Attitude Analysis Based on Artificial Intelligence Sensor

Journal of Sensors

Received 17 October 2023; Accepted 17 October 2023; Published 18 October 2023

Copyright © 2023 Journal of Sensors. This is an open access article distributed under the Creative Commons Attribution License, which permits unrestricted use, distribution, and reproduction in any medium, provided the original work is properly cited.

This article has been retracted by Hindawi following an investigation undertaken by the publisher [1]. This investigation has uncovered evidence of one or more of the following indicators of systematic manipulation of the publication process:

- (1) Discrepancies in scope
- (2) Discrepancies in the description of the research reported
- (3) Discrepancies between the availability of data and the research described
- (4) Inappropriate citations
- (5) Incoherent, meaningless and/or irrelevant content included in the article
- (6) Peer-review manipulation

The presence of these indicators undermines our confidence in the integrity of the article's content and we cannot, therefore, vouch for its reliability. Please note that this notice is intended solely to alert readers that the content of this article is unreliable. We have not investigated whether authors were aware of or involved in the systematic manipulation of the publication process.

In addition, our investigation has also shown that one or more of the following human-subject reporting requirements has not been met in this article: ethical approval by an Institutional Review Board (IRB) committee or equivalent, patient/participant consent to participate, and/or agreement to publish patient/participant details (where relevant).

Wiley and Hindawi regrets that the usual quality checks did not identify these issues before publication and have since put additional measures in place to safeguard research integrity.

We wish to credit our own Research Integrity and Research Publishing teams and anonymous and named external researchers and research integrity experts for contributing to this investigation.

The corresponding author, as the representative of all authors, has been given the opportunity to register their agreement or disagreement to this retraction. We have kept a record of any response received.

References

- [1] K. Li, "Tennis Technology Recognition and Training Attitude Analysis Based on Artificial Intelligence Sensor," *Journal of Sensors*, vol. 2022, Article ID 6594701, 7 pages, 2022.

Research Article

Tennis Technology Recognition and Training Attitude Analysis Based on Artificial Intelligence Sensor

Ke Li 

College of Physical Education, Henan University of Technology, Henan, Zhengzhou 450001, China

Correspondence should be addressed to Ke Li; 20148863@stu.sicau.edu.cn

Received 18 May 2022; Revised 29 May 2022; Accepted 14 June 2022; Published 24 June 2022

Academic Editor: C. Venkatesan

Copyright © 2022 Ke Li. This is an open access article distributed under the Creative Commons Attribution License, which permits unrestricted use, distribution, and reproduction in any medium, provided the original work is properly cited.

In order to solve the problem of traditional tennis serving technique teaching, subjective, and experience-based teaching methods, the author proposes a method to extract tennis training movements based on artificial intelligence sensor video analysis. This method requires the use of ordinary cameras and computer technology; video analysis technology is used to guide tennis teaching and training. The result obtained is as follows: in the experimental group and the control group, at the end of the teaching stage, the movement characteristics of each link of the body are quite different, which can reach 15%-20%; when the experimental group and the control group did the “scratching back” movement during the teaching period, at the end of teaching, the students in the experimental group were close to high-level tennis players in their movement skills, and the movement gap was only about 5%. It is proved that the method proposed by the author provides an objective and scientific basis for measuring the referee’s penalty level. In the grass-roots tennis teaching and training, it has important value and significance and has a great promotion prospect.

1. Introduction

Video images obtained by humans use a variety of images and devices to observe the world from a different perspective, which directly and indirectly affect the human eye and create visual acuity, for example, static images or dynamic videos [1]. According to research and statistics, about 75 percent of the information that a person receives from the outside world is from vision. With the rapid development of science and technology, sports technology has played an important role in national leadership and sports [2]. With the introduction of the use of technology in sports training and the emergence of new research to make a difference in the study of physical education, training teaching training has not been completed previously. With the improvement of sports competitive level, the training method which only relies on the coach’s intuition in the past has been unable to improve the competitive level [3]. The development of computer and video technology makes it a new tool for trainers, because the machine’s vision is more real than the human eye, it has memory, it can hold the target fast, and

it can record various moves of the target and allows the performance of the athlete to be clearly expressed [4].

Video image processing technology is more and more widely used in athletes’ sports training and sports competitions [5]. It has become a research hotspot, in foreign countries, such as the United States; the “Eagle Eye” test system has been applied to tennis competitions; it is mainly used to monitor the game; when the player disagrees with the landing position of the tennis ball, the three-dimensional image of the landing position of the ball can be retrieved [6]. In China, the Institute of Computing Technology of the Chinese Academy of Sciences has developed DVCoach software, which applies video analysis to sports training and teaching. The prices of these systems are very high (hundreds of thousands or even millions of RMB) [7]. In general physical education and training, such a huge investment cannot be afforded. And these systems have certain pertinence to a certain sports activity. The hardware composition of tennis video analysis system is shown in Figure 1.

In addition, the video data is analyzed, and the corresponding court and tennis recognition algorithms are

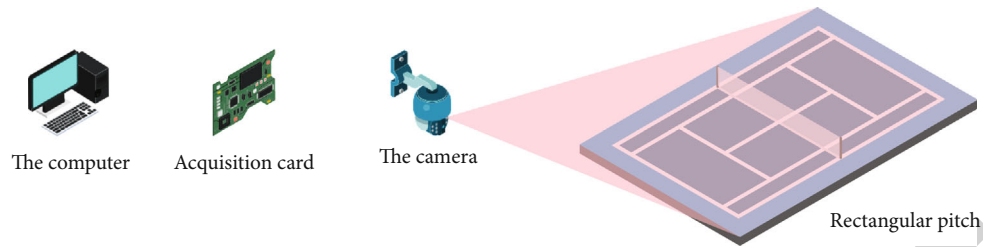


FIGURE 1: Tennis video analysis system hardware composition.

designed; it can automatically judge whether the tennis is out of bounds, automatically measure the running speed of the tennis space, and deal with it accordingly, so as to provide a scientific basis for the development of tennis teaching and training effect evaluation system.

2. Literature Review

The tennis video analysis system consists of hardware and software. The main research tools used include optical lenses, CCD cameras, image acquisition, and research and design of processing cards [8]. With the help of video professionals, the video analysis algorithm is designed and implemented on the computer, so as to meet the requirements for the use of video data in the author's research [9].

According to the image processing recognition algorithm and the characteristics of the court, the characteristics of the high speed of tennis properly select the resolution of the CCD camera and the sampling rate of the frame grabber, in order to form a high-quality image information acquisition system, ensure reliable image sampling and digitization, and provide correct and reliable raw data for subsequent image signal processing [10]. In terms of software, DirectShow acquisition technology is used to realize digital video acquisition [11]. Features are as follows: (1) high-quality digital video capture is achieved through intelligent deinterlacing technology and deinterlacing technology and (2) support multicamera head acquisition.

Cheng et al. studied the application of traditional teaching methods and information technology teaching methods in the teaching of tennis serve technique, the video technology is mainly used in the teaching of information technology, and the experimental research shows that the teaching of information technology is more superior than the traditional teaching method; it is the same trend of teaching technology development in the future [12]. Gao et al. use video technology to analyze the action structure of tennis players' serve technique; no further research was carried out in the application analysis of video technology of tennis speed and landing point [13]. Sun et al. conducted a research on the application of video technology in the production of tennis multimedia CAI courseware and did not conduct further analysis and research on the data of video technology [14]. Srivastava et al. conducted an experimental study on improving tennis forehand stroke technique using computer-aided teaching methods [15]. Chen et al. proposed a motion vector field transformation algorithm for tennis video analysis [16]. The above research results mainly show

the research on teaching methods and how video technology is used in tennis sports, the main purpose of the research is the use of video technology and the video technology itself, few special researches are carried out on the data obtained by video analysis technology, the instruments and software used are relatively professional, and the hardware facilities are very expensive, which is difficult for most researchers to accept and access, and it is very difficult to promote in reality [17].

In addition, there are other applications of this technology in the field of sports, such as the application of video technology in the analysis of techniques and tactics of table tennis, research on the application of video technology in aerobics teaching, diving technique training video analysis and quick feedback system, talking about the application of video technology in swimming teaching and training, the development of video image technology and its application in track and field training, and 3D human motion simulation and video analysis system for sports training. The above research results show that video technology, as a high-tech means, has achieved good teaching and training effects in table tennis, aerobics, diving, and other projects, and the research angles are different [18, 19]. From the perspective of video technology, some analyze which video technology is used or how to improve the existing video technology for analysis and research. Some conduct research from analytical feedback systems. Some conduct research from images [20, 21].

Based on current research, the author proposes the application of video analysis to tennis teaching training and competition, it can quickly provide coaches and athletes with data such as the technical action structure diagram of the athlete's serve, the speed of the serve, and the landing point; it can not only reduce the cost of using expensive equipment but also provide scientifically quantified index data for the tennis evaluation system. Video technology can provide a reference for referees to accurately determine the placement of tennis balls in the game, effectively avoid the embarrassment of using "hawk-eye" technology in small and medium-sized tennis events, and obtain maximum returns with less investment.

3. Research Methods

3.1. Research Objects. Select high-level tennis players (higher than level 2), and show real-time combat videos of the game based on statistics equipment. Select 40 boys from the specialized tennis college according to the educational goals.

The median age of the test students was 20.4, average height 173.25 cm, and average weight 65.63 kg. The average length of the arm was 73.16 cm.

The average age of the students in the control room was 20.5, average height 172.87 cm, and average weight 64.72 kg. The average length of the arm was 72.69 cm.

3.2. Adoption Method

3.2.1. Document Law. The author carefully read the relevant information about tennis and systematically reviewed the articles about tennis published in recent years, keep abreast of the new achievements in the research and application of video technology in sports, study and analyze the problems of video technology in tennis teaching and training, and provide reference for the research of this topic [22].

3.2.2. Interview Method. The author conducts interviews with tennis coaches, experts, and administrators to hear their detailed descriptions of tennis teaching and training. They also conducted interviews with experts engaged in video technology and computer technology, helping to conduct research on video technology and design of video software, thereby summarizing, researching, and analyzing. The main contents of the interview are as follows: the status quo of tennis teaching and training, the application of video technology and software programming involved in tennis teaching and training, etc. [23].

3.2.3. Experimental Method. During the experiment, the training items, training intensity, training time, and teachers of the two groups were the same.

The 06 special-grade tennis students selected were divided into control and experimental groups, and the procedures for the student groups did not vary by age, height, weight, or arm length.

The board uses the usual procedures of the instructor to explain, demonstrate, and practice. Experimental teams combine video analysis, feedback, and routines to teach the experimental team and the board a video of the process to be used in the first place phase and late, and special instructions must be used in the end. The inspection and control teams were compared and evaluated.

3.2.4. Comparative Method. The technical movements of the high-level tennis players were compared with those of the students in the control group and the experimental group; for students in the experimental group and the control group, a comparative analysis is made based on the technical characteristics of serving at the end of teaching and so on [24].

3.2.5. Mathematical Statistics. The obtained statistical data were subjected to routine statistical analysis. Using a variety of mathematical methods and SPSS and EXCEL software systems, a database was established to conduct statistics on the data [25].

3.3. Application of Video Analysis in the Technical Action Structure of Tennis Serve. The application of tennis serving skills is often carried out at a relatively high speed, it is diffi-

TABLE 1: The time difference between the throwing and hitting of the students in the experimental class (unit: second) ($n = 10$).

	Average value at the beginning of teaching	End-of-teaching average
B0	4.04	2.72
B1	4.32	2.96
B2	4.48	2.32
B3	3.92	2.48
B4	3.84	2.52
B5	3.90	2.44
B6	4.08	2.64
B7	4.28	2.32
B8	4.24	2.44
B9	4.32	2.52

cult for the naked eye to observe every detail of the athlete's skills, and it is impossible to form a deep "action impression" in the brain, and it is impossible to store this kind of "action" for long-time action impressions." It is also difficult for the coaches to guide and evaluate the technical details of the athletes. Through video analysis, each technical detail of the athlete can be clearly obtained, and through feedback, it can be observed and compared intuitively, so as to further improve the technical movement level of the athlete.

Through video analysis, every detail in the technical link of the athletes can be obtained, and static pictures of the structural details of the students' serving actions can be collected; coaches can guide athletes through pictures and can also compare and analyze the same technical details of different athletes; it is also possible to compare the technical details of student-athletes with the technical details of high-level tennis players, in order to identify gaps. High-level tennis players may have individual differences and characteristics in the use of technical details; by analyzing their different technical details and characteristics through video technology, it is also possible to find out the common and regular technical details of technical details.

3.4. Application of Video Analysis in Tennis Serve Speed Test. In the evaluation of tennis technical level, coaches usually can only use subjective qualitative evaluation to evaluate the movement posture of the players, the landing point of the ball, and the speed of the serve. However, a correspondingly accurate quantitative assessment cannot be given. Through video analysis, we can use the acquired tennis flight image and then perform programming and calculation through image recognition software and can quickly measure the speed of the player's serving over the net.

Use video technology to obtain static images between two adjacent frames (0.04 seconds) when the tennis passes the net. From the logo on the background (the black and white interval is 0.1 meters), we can roughly calculate that the running distance of the tennis ball between these 0.04 seconds is 1.7 meters. From the formula (1), it can be calculated that the speed of the serve before the net reaches

TABLE 2: The time difference between the throwing and hitting of the students in the control class (unit: second) ($n = 10$).

	Average value at the beginning of teaching	End-of-teaching average
Co	4.48	3.64
CI	4.32	3.72
C2	4.32	3.76
C3	4.04	3.52
C4	4.44	3.44
C5	4.24	3.52
C6	4.52	3.36
C7	4.00	3.52
C8	3.84	3.24
C9	3.92	3.20

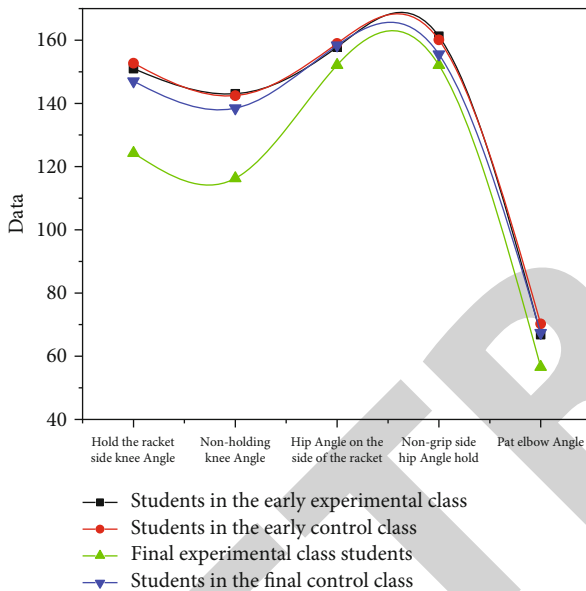


FIGURE 2: Comparison of the action structure of students before and after the experiment when they bend their knees, raise their rackets, and prepare to hit the ball (unit: degree) ($n = 10$).

42.5 meters per second (153 km/h).

$$V = \frac{S}{T}. \quad (1)$$

Although there will be a large error between the results obtained by this calculation method and the actual results, the error can be ignored when comparing the serving speed between players. The error value of this calculation method can also be calculated through correction, so as to achieve the purpose of simply testing the serving speed.

4. Analysis of Results

4.1. Statistical Analysis of the Time Difference between Toss and Hits in the Serve of the Research Object. Serving tech-

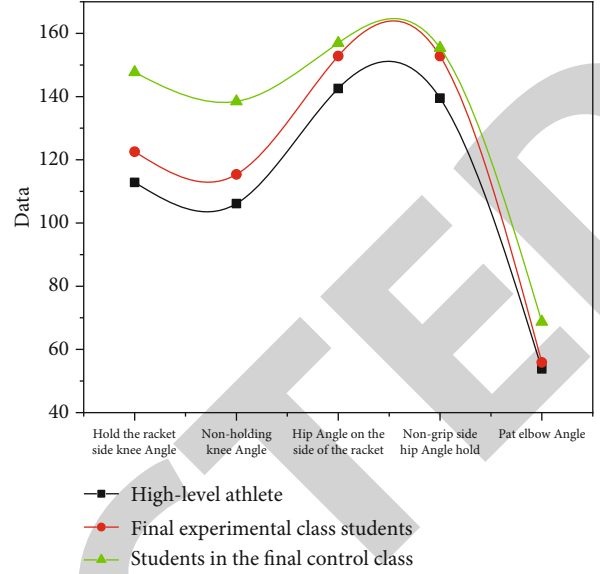


FIGURE 3: Comparison of action structure between students and high-level athletes when they bend their knees, raise their rackets, and prepare to hit the ball after throwing the ball (unit: degree) ($n = 10$).

nique is a difficult point in tennis teaching, and the rhythm of throwing and hitting is one of the more difficult links in serving technique. The route and height of the toss will directly affect the difficulty and accuracy of the serve. The author made statistics on the time difference between tossing and hitting in 10 consecutive servings at the beginning and end of teaching, record the athlete's serve action with a video recorder, store it in the computer, and drag it frame by frame with the Photo 9 software; the number of frames used is multiplied by 1/25 second, which is the time difference between the player's throwing and hitting the ball, which greatly reduces the amount of time spent and error in manual stopwatch timing (see Tables 1 and 2).

All the measured data, using SPSS, conducted a T test on the time difference between throwing and hitting in 10 consecutive servings at the beginning and end of teaching. The result shows the following: the average value of the time difference between throwing and hitting the ball in the experimental class and the control class is basically the same in the early stage of teaching, and there is no significant difference ($P > 0.05$).

The average value of the time difference between throwing and hitting the ball in the experimental class was between 3.84 and 4.48 in the early stage of teaching, and the average value of the time difference between tossing and hitting the ball in the control class was between 3.84 and 4.52. However, the average time difference between the experimental class and the control class at the end of teaching is significantly different ($P < 0.05$).

The average value of the time difference between tossing and hitting the ball at the end of teaching in the experimental class is between 2.32 and 2.96, and the average value of the time difference between tossing and hitting the ball in the control class at the end of teaching is between 3.20 and

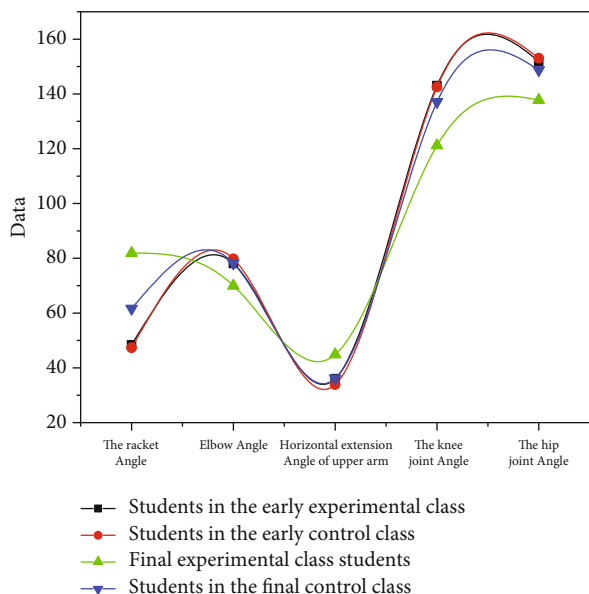


FIGURE 4: Comparison of the posture characteristics of each link of the body when students scratch their backs before and after the experiment (unit: degree) ($n = 10$).

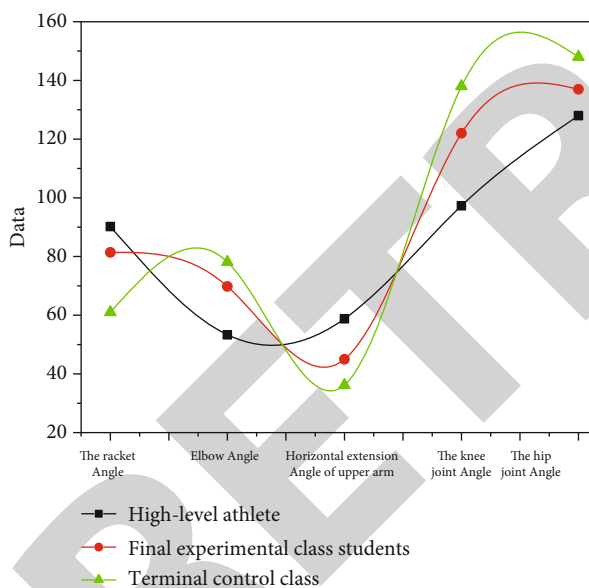


FIGURE 5: Comparison of the posture characteristics of each link of the body when students and high-level athletes scratch their backs (unit: degree) ($n = 10$).

3.76. Although there is difference between the throwing and hitting times at the end of the teaching period between the experimental class and the control class, it is shorter than the initial stage of teaching, but through the above data test results, it can be seen that the subjects in the experimental class performed much better than those in the control class.

4.2. Analysis of the Movement Structure of the Research Subjects when They Bend Their Knees, Raise Their Rackets, and Prepare to Hit the Ball after Throwing the Ball. In the stage of throwing the ball and raising the racket, make an

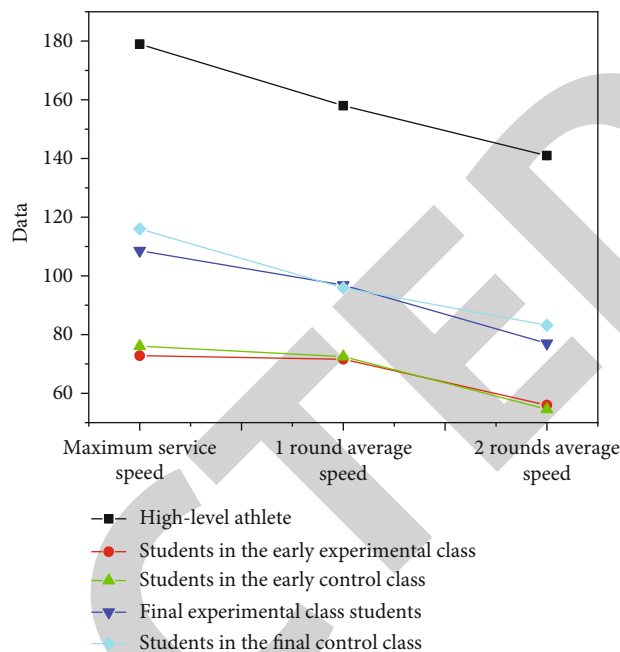


FIGURE 6: Statistical summary table of students' serving speed at the end of the video test (unit: KM/H) ($n = 10$).

obvious knee squatting action, this is an important part of the technical action structure of the serve, and its purpose is to provide good body support and a state of force for the “back-scratching” action.

In the specific throwing racket, the posture characteristics of each link of the body when preparing to hit the ball are shown in Figures 2 and 3.

According to the above data analysis, the experimental group and the control group have a large difference in the movement characteristics of each link of the body at the end of the teaching stage, which can reach 15%-20%; compared with the students in the control group, there was little change in the beginning of teaching and the end of teaching. Compared with the students in the experimental group at the beginning and end of teaching, there were obvious changes, the students in the experimental group were in the final stage of teaching the movement techniques, and it is closer to a high-level tennis player than the initial movement technique.

4.3. Structural Analysis of the Object's Back-Scratching Action while Serving. At the end of throwing the ball and raising the racket, the athlete will quickly kick the knee and push the hip and at the same time bend the elbow and rotate the upper arm externally, keep the tennis racket away from the hitting point, and keep it behind; the head is almost vertically downward, and the body is in a “back arch” posture. There is a movement to tickle the back, which we call a “back-scratching” movement. It is also a very important key technical action in the technical link of tennis serving. Through video collection, we analyzed the movement characteristics of the “scratching back” technique of the research subjects. The results are shown in Figures 4 and 5.

According to the above data analysis, when the experimental group and the control group did the “scratching back” movement stage during the teaching period, the movement characteristics of each link of the body were quite different. Compared with the students in the experimental group at the beginning and end of teaching, there were significant changes, the students in the experimental group were in the final stage of teaching the movement techniques, and it is closer to a high-level tennis player than the initial movement technique.

To sum up, in the teaching of tennis serving skills, the use of video analysis technology can eliminate the interference of human factors and more quickly, objectively, and directly evaluate the players’ serving skills. Because the shooting speed of the camera is 25 seconds/frame and the video data can be stored, compared, etc., these functions cannot be achieved by the human eye. Athletes can see their own serving skills before the experiment, and they can also see the movements after the experiment; they can not only compare and analyze with others horizontally but also realize vertical analysis, thereby greatly improving the enthusiasm and initiative of students to learn tennis skills. It can be seen that in the teaching of tennis serve technology, the application of video analysis technology is of great significance.

4.4. Comparison of Effective Rates of Urinary Incontinence Treatment among Three Treatment Options. Video test speed data, research speed in tennis serve technical action analysis, is an important evaluation standard for tennis serve quality; a high-quality serve must have a high speed. The related research results show that the more standard and reasonable the technical action of serving is, the faster the serving speed will be; the two are positively correlated. The author uses an ordinary camera as a test instrument for serving speed; it is easy to measure the serving speed of tennis players, although there will be certain errors between the data and the objective real data, but it is feasible as a comparison tool, and it can be as close to the real objective value as possible through constant revision. At the same time, as a speed test instrument, ordinary cameras can reduce the test cost and have great promotion value.

The authors tested high-level tennis players, experimental tennis players, and control tennis players; the speed of 10 1 s and 10 2 s served by each athlete was randomly selected for the study. The experimental class and the control class were also researched on the serving speed at the beginning and end of the teaching, and the results are shown in Figure 6.

In summary, using video analysis technology for the teaching of serve technical movements, from the measured speed data, it can be clearly seen that the improvement space of the athlete’s serving speed is better than the traditional teaching method, serve speed has been significantly improved, and the improvement of the quality of the athlete’s serve is explained. In data measured using video data, it can provide a meaningful reference for coaches to objectively evaluate tennis players’ serving skills; at the same time, the athletes can see their own serving skills before the exper-

iment, and they can also see the movements after the experiment and not only can horizontally compare and analyze with others but also can realize vertical ratio analysis, thereby greatly improving the enthusiasm and subjective initiative of the students to learn the tennis serve technique.

5. Conclusion

The author applies video analysis technology to tennis teaching and training, and through a period of teaching experiments, the results are as follows:

- (1) The technical movement characteristic parameters of the students in the experimental group are higher than those of the students in the control group, closer to the technical characteristics of high-level tennis players. It is proved that the video analysis technology is used in the teaching of tennis serve technique, it is more conducive to students’ mastery of technical movements and can test and judge athletes’ serving speed and landing point, and it is beneficial to improve the serve speed and serve control ability of tennis players. Video analysis technology is of great significance and value to the reform of tennis serving technique teaching and serving method
- (2) The traditional teaching model is the comments of the coach and the athlete’s own feeling of completing the action. In the tennis training process, the video analysis feedback training method is applied; that is, after the athlete completes the action, the athlete immediately watches video recordings of his/her own actions and various analysis results, which is equivalent to adding a video feedback loop to the system. For sports training, the effect will be that athletes can improve their training level more quickly and effectively and shorten the time to learn and master technical movements. Tennis is a typical skill sport

Data Availability

The data used to support the findings of this study are available from the corresponding author upon request.

Conflicts of Interest

The author declares that there are no conflicts of interest.

Acknowledgments

This paper is the periodical achievement of Philosophy and Social Science Planning Project of Henan Province. Project number is 2021BTY004.

References

- [1] S. Gomez-Gonzalez, G. Neumann, B. Schölkopf, and J. Peters, “Adaptation and robust learning of probabilistic movement

Retraction

Retracted: Abnormal Data Monitoring and Analysis Based on Data Mining and Neural Network

Journal of Sensors

Received 13 September 2023; Accepted 13 September 2023; Published 14 September 2023

Copyright © 2023 Journal of Sensors. This is an open access article distributed under the Creative Commons Attribution License, which permits unrestricted use, distribution, and reproduction in any medium, provided the original work is properly cited.

This article has been retracted by Hindawi following an investigation undertaken by the publisher [1]. This investigation has uncovered evidence of one or more of the following indicators of systematic manipulation of the publication process:

- (1) Discrepancies in scope
- (2) Discrepancies in the description of the research reported
- (3) Discrepancies between the availability of data and the research described
- (4) Inappropriate citations
- (5) Incoherent, meaningless and/or irrelevant content included in the article
- (6) Peer-review manipulation

The presence of these indicators undermines our confidence in the integrity of the article's content and we cannot, therefore, vouch for its reliability. Please note that this notice is intended solely to alert readers that the content of this article is unreliable. We have not investigated whether authors were aware of or involved in the systematic manipulation of the publication process.

Wiley and Hindawi regrets that the usual quality checks did not identify these issues before publication and have since put additional measures in place to safeguard research integrity.

We wish to credit our own Research Integrity and Research Publishing teams and anonymous and named external researchers and research integrity experts for contributing to this investigation.

The corresponding author, as the representative of all authors, has been given the opportunity to register their agreement or disagreement to this retraction. We have kept a record of any response received.

References

- [1] Y. Chen, "Abnormal Data Monitoring and Analysis Based on Data Mining and Neural Network," *Journal of Sensors*, vol. 2022, Article ID 2635819, 7 pages, 2022.

Research Article

Abnormal Data Monitoring and Analysis Based on Data Mining and Neural Network

Yanyan Chen 

Zhejiang Financial College, Hangzhou, Zhejiang 310018, China

Correspondence should be addressed to Yanyan Chen; 185101029@xzy.edu.cn

Received 18 May 2022; Revised 1 June 2022; Accepted 14 June 2022; Published 24 June 2022

Academic Editor: C. Venkatesan

Copyright © 2022 Yanyan Chen. This is an open access article distributed under the Creative Commons Attribution License, which permits unrestricted use, distribution, and reproduction in any medium, provided the original work is properly cited.

In order to solve the problems of low efficiency, high consumption of human and time resources, and low degree of intelligence in the current financial abnormal data detection system in computerized accounting, this paper proposes a financial abnormal data monitoring and analysis algorithm based on data mining and neural network. The analysis algorithm uses the method of data mining to process the original financial data, remove invalid information, retain valuable information, and standardize the data to solve the problem of large labor and time consumption. Then, neural network-related algorithms are used to identify the anomalies of standardized data, so as to realize the intelligent early warning of financial abnormal data. Compared with the financial audit algorithm in traditional accounting computerization, this algorithm has the advantages of high efficiency, low energy consumption, and high intelligence. The test results show that the classification accuracy of the proposed algorithm for abnormal data can reach more than 90%. It is proved that the algorithm is effective and improves the efficiency at the same time. The classification error rate of the classifier designed in this paper is 22.5%, and the accuracy rate is 77.5%. Both estimated and actual values represent the number of times, and there is no physical unit. The experiment shows that the main reason for the error rate is the delay of the inspection results of financial abnormalities. Through the example analysis, it can be concluded that the proposed intelligent analysis method of financial abnormal data based on deep learning has good effectiveness and accuracy and has a certain practical value.

1. Introduction

The 129 financial data in the financial statements of Chinese listed companies and the financial ratios derived from these financial data can be called financial indicators [1]. If the financial indicators reflecting debt repayment, operation, profit, growth, and cash flow are abnormal, there is no doubt that the enterprise has problems in internal operation, external marketing, or finance. Through data mining of these abnormal financial indicators, find one or several abnormal transmission paths connecting them. If there are economically meaningful items on the abnormal transmission path, this abnormal transmission path is of great significance to enterprises [2, 3].

From a macro perspective, since the establishment of the Shanghai Stock Exchange and Shenzhen Stock Exchange in 1990, China's stock market has developed rapidly following the pace of national economic growth. It is very important

for securities regulators to formulate the supervision system for listed companies. At present, in the regulatory environment where China's regulatory mechanism is not perfect enough, the risk of fraud in the listed companies increases. Fraud is reflected in the financial statements, and a series of abnormal financial indicators are bound to appear. Microscopically speaking, for mature listed companies, due to the poor management of normal business activities, some financial indicators will be abnormal. For newly listed companies, due to the strict listing conditions (especially on the main board), the company may whitewash the financial statements before listing in order to achieve the purpose of listing [4]. Once the company is listed, some financial indicators are bound to decline or rise, resulting in abnormalities.

With the rapid development of the economy, the market is more and more prosperous, and the competition among enterprises is becoming increasingly fierce. The authenticity of financial data has attracted more and more attention.

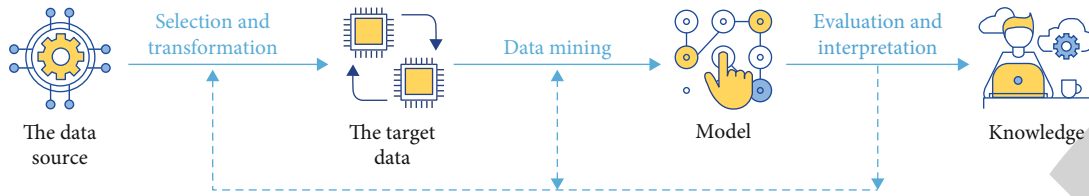


FIGURE 1: Workflow of data mining.

Academia has also taken a variety of measures and methods to analyze the abnormal situation of enterprise financial data and achieved corresponding results.

2. Literature Review

The research on the identification of financial anomaly characteristics of listed companies appeared earlier. Jiang and others believe that there is a certain relationship between company size and financial fraud, and the size of the company may directly affect the possibility of financial information fraud [5]. According to the research of Kim et al., there is a large correlation between financial information fraud and companies in financial distress. When the company is in financial difficulties, the management of the company is more likely to commit fraud in order to cover up its temporary financial difficulties [6]. Aydemir and others found that the company's abnormal financial information or even fraud has a great relationship with the company's industry. His experiments have proved that compared with other industries, the computer industry and manufacturing industry are more likely to have financial fraud, which needs special attention [7]. According to the research of Ali and others, according to the analysis of the financial report, we can find the signs of abnormal financial information, such as some unexplained changes in the financial report, some obviously different large transactions, and sudden increase of profits. In addition, frequent changes in management and faster growth of expenses than income may also be signs of financial fraud [8]. Asami and others conducted an empirical study on the relationship between insider trading and financial fraud of listed companies and established a cascaded logit regression model. The research points out that insider trading is a signal to reveal the potential possibility of financial fraud. Whether the company has financial fraud can be identified according to the analysis of insider trading variables and the specific financial characteristics of the company [9]. Moayedi and others proposed a new financial fraud identification model—fuzzy neural network (FNN) model. This model combines fuzzy logic, neural networks, and other methods to simulate the uncertainty in human rationality. The empirical results show that this model can effectively make up for the shortcomings of auditors or reduce their bias. Later research mainly uses artificial neural network (ANN) [10]. Xiang and others collected 164 fraudulent and nonfraudulent company data to verify the effectiveness of using machine learning technology to identify financial information fraud [11].

Most of these studies focus on the theoretical analysis of finance and accounting, only give the financial model analysis, but do not give the specific implementation scheme, resulting in poor realizability. Aiming at this problem, this paper focuses on the implementation scheme and puts forward the financial abnormal data monitoring and analysis algorithm based on data mining and neural network. For the problem of financial abnormal data, the specific identification model and implementation method are given, as shown in Figure 1.

Based on the current research, in order to solve the problems of low efficiency, high consumption of human and time resources, and low degree of intelligence in the current financial abnormal data detection system in computerized accounting, this paper proposes a financial abnormal data monitoring and analysis algorithm based on data mining and neural network. The analysis algorithm uses the method of data mining to process the original financial data, remove invalid information, retain valuable information, and standardize the data to solve the problem of large labor and time consumption.

3. Research Methods

3.1. System Framework. The overall frame structure of the system is shown in Figure 2. As can be seen from the figure, the system is mainly divided into four parts: identification object part, data processing part, identification process part, and result and early warning part. Among them, the identification object is the traditional financial system. This paper takes the data in the traditional financial system as the data set, takes it as the data acquisition channel, and carries out intelligent data monitoring [12]. Next is the data processing part, which processes the obtained original data through data mining technology. It is mainly divided into three modules: data acquisition, data preprocessing, and data coding. Among them, the data acquisition module is responsible for using the programming language to obtain the relevant original data required for abnormal data monitoring from the traditional financial database. The data preprocessing module mainly includes removing unique attributes, integrating related attributes, processing missing values, and data standardization so that the original data can become effective data. The data coding module is mainly responsible for coding the standardized data so that all data can be directly input into the intelligent algorithm to lay the foundation for the subsequent intelligent identification part. Next is the identification process part, which uses the processed financial data to train the intelligent algorithm through the artificial intelligence algorithm. The last part is the result

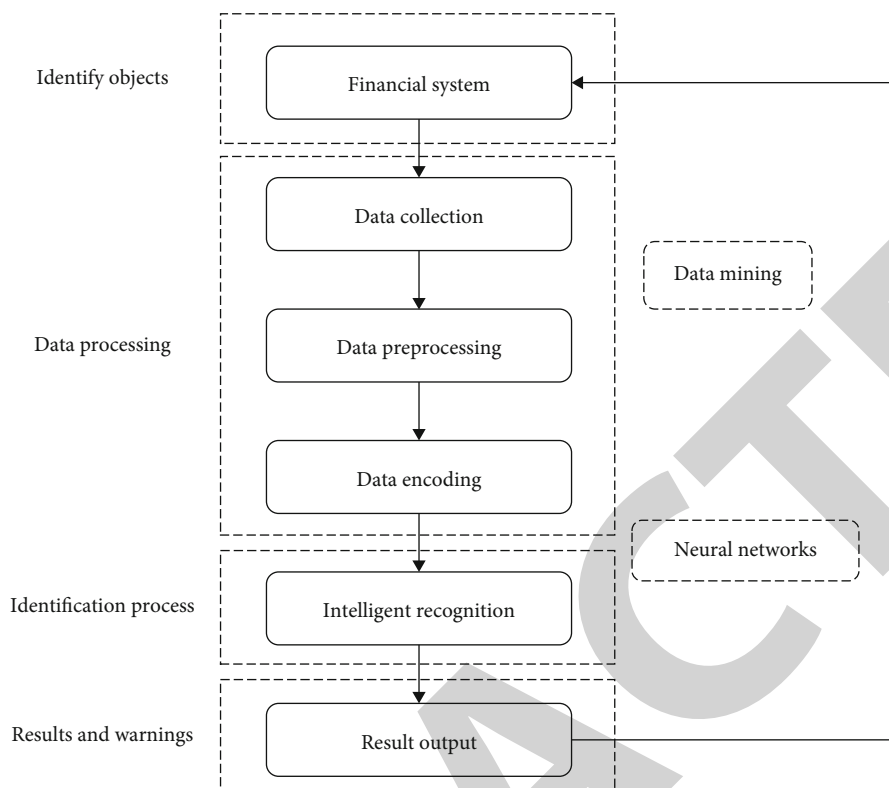


FIGURE 2: Overall framework of the system.

and early warning part, which uses the trained model to identify the financial data, mark and early warning the abnormal data, and feedback the early warning system to the financial system to form a closed loop.

Due to the infinite approximation ability of intelligent algorithm to nonlinear relationship, all kinds of abnormal identification methods of financial data are similar. This paper only takes the abnormal identification of employee travel invoice reimbursement as an example to illustrate the implementation process of the system.

3.2. Data Acquisition and Data Processing. In this system, the acquisition method of basic financial data is similar to that of traditional financial system data. It is mainly obtained through the statistics of financial department or personal report, and then, the original data is converted into standard data that can be directly input into intelligent control algorithm through corresponding data preprocessing methods [13]. The system is mainly divided into two parts: data acquisition and data processing.

3.2.1. Realization of Data Acquisition. The data required by this system usually consists of three types: personal information, including name, gender, age, department, length of service, professional title, position, basic salary, and other data. This kind of data can be obtained directly from the human resource department and the financial department through the internal network of the company. The second category is the bonus category, including the data of

quarterly bonus, year-end bonus, various honor bonuses, and subsidy bonuses of corresponding employees. This kind of data is usually distributed by their department according to their work performance, so it can be obtained directly through the department database. The third category is personal reimbursement data, mainly including travel location, travel duration, travel type, vehicle time, and various invoices and amounts. This kind of data is mainly reported by individuals and verified by department heads. With the development of network technology, the collection method of such data has also been greatly affected.

3.2.2. Realization of Data Processing. Data processing can be divided into two parts: data preprocessing and data coding. The implementation process of these two parts is described in the following two parts [14].

(1) Implementation of Data Preprocessing. The main process of data preprocessing is shown in Figure 3.

Figure 3 shows the problems to be solved in data preprocessing and the corresponding solutions. The following implementation scheme is given by taking Python language as an example:

- (1) Unique attribute processing: the unique attribute refers to the name, job number, and other features that can uniquely identify the sample to be identified, but have no effect on the identification of abnormal data

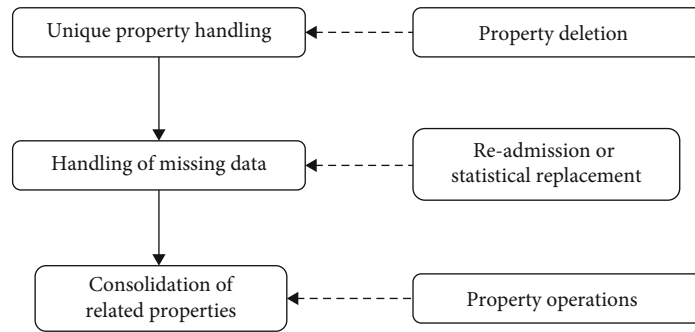


FIGURE 3: Data preprocessing.

and can be deleted directly. The instructions deleted in Python are as follows: use this command to delete the entire row or column data of the `feature_name` attribute, where `axis = 1` means to delete the column and `axis = 0` means to delete the row

- (2) Processing of missing data: the processing steps of missing value are as follows: ① find the location of missing value; ② padding of missing values. Using Python language, the specific processing methods are as follows: the index information of the missing value of a characteristic data can be quickly obtained by using Pandas scientific calculation library. The function returns the location logical index of the missing value in the `feature_name` attribute. The missing value can be processed by using the location logical index
- (3) Related attribute merging: for the characteristic data with obvious correlation, the operation of data can be used to merge the relevant data into one data and delete other data, so as to achieve the purpose of data merging and reducing the amount of calculation. The addition of two attribute columns `feature 1` and `feature 2` in data is realized, and the deletion operation after attribute merging is realized. For example, length of service and year of employment, such data can be consolidated

So far, the preprocessing of the original data has been completed, making the original data set into a data set without missing data and containing only effective features.

3.2.3. Realization of Data Coding. Data coding mainly realizes the transformation of feature data from semantic data convenient for human understanding to digital data convenient for machine processing. Data coding can be divided into discrete data and continuous data for processing, respectively. The specific processing methods are as follows:

- (1) For discrete data: among the corresponding attributes, one or more discrete attributes can be classified into one class, and each class can be coded separately by `One_Hot` coding method. In Python language, Pandas scientific computing library can be used to realize this function conveniently

- (2) For continuous data: for the coding of continuous data, in order to facilitate processing, the continuous data can be discretized in the form of segments and then encoded in sequence by `One_Hot` [15]. In the Python language, you can use custom operations to discretize continuous data. Next, take the binary classification as an example to illustrate the implementation method of continuous data discretization. It realizes the operation of separating and dispersing the feature data feature of continuous feature `feature_name` according to the threshold. Then, the discrete coding method can be used to encode the data

3.3. Realization of Identification Process and Result Output.

The identification of abnormal data can be understood as the classification of data; that is, all data are divided into normal data and abnormal data or into normal data, doubtful data, and abnormal data. At present, the main classification algorithms are support vector machine (SVM). For example, SVM is used to build a prediction and classification system for the spread range of microblog rumors and the order volume of e-commerce. SVM is used to evaluate and classify the network system risk, personal credit, and daily stress state, and the application of gesture state classification and fault diagnosis is realized by the method of support vector machine. At present, SVM algorithm is widely used in classification applications, but it is still difficult to implement large-scale training samples.

Decision tree algorithm uses the decision tree algorithm to realize the classification of network loans, ECG signals, and financial crisis prediction models, but the decision tree algorithm has the problems of pruning and overfitting under large data samples [16]. *K*-means algorithm uses *K*-means to realize the classification of text and plants, but the algorithm has the problem that the *K* value has a great impact on the classification effect but cannot be obtained accurately [17].

Considering the application environment of financial abnormal data monitoring and analysis, the system adopts BP neural network with mature technology, ideal adaptability, and realization as the identification algorithm [18, 19]. The implementation method is as follows.

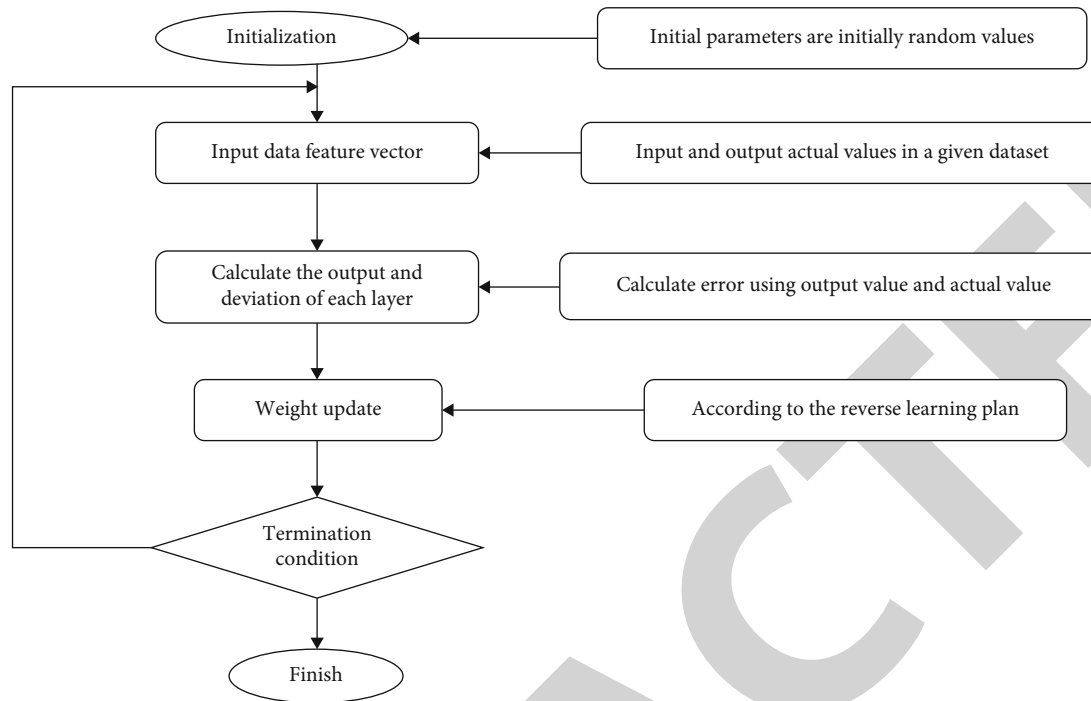


FIGURE 4: Training process of BP neural network.

(1) The number of input features and the number of coding bits of each feature determine the number of neurons in the input layer of the neural network

$$N_{\text{in}} = \sum_{i=1}^N n_i. \quad (1)$$

The calculation method is shown in formula (1), where N is the feature tree, n_i is the coding digit of the i -th feature, and N_{in} is the number of neurons in the input layer.

(2) Determination of intermediate layer: according to experience, the middle layer is usually 1 layer, and the number of neurons in the middle layer is $2 * N_{\text{in}}$, which can be adjusted according to the actual situation. The neuron correlation function is generally conventional.

(3) Output layer design: the number of neurons in the output layer is equal to the number of demand classification. One_Hot coding method is used to encode the demand state, and the output neuron function is selected as Logsig function.

The hidden layer in this paper is mainly used for feature learning and extraction through convolution and pooling. Different layers will extract different features. In order to ensure the optimal classification performance of the hidden layer, the training data and test data in the experimental data are divided according to the ratio of 4:1 and input into the convolutional neural network for solution optimization [20].

So far, the neural network has been designed and trained by using the processed data. The training method is shown in Figure 4 [21].

Finally, the monitoring and analysis of abnormal financial data can be realized by using the trained neural network. Give the identification results of normal and abnormal financial data, and feedback the abnormal financial data to the financial system.

4. Result Analysis

The BP neural network classifier in this paper is realized by MATLAB programming. In this section, the financial data of traditional indicators are processed by the timing construction method proposed above and then input into the classifier. After running, the classification effects of traditional models and various forms of models can be obtained. The operation results of each model are shown in Figure 5.

As can be seen from Figure 5, the recall rate of the time series index model in the ratio form and the first relative value form is the highest. In terms of precision, the time series index model in the form of difference is the best. It can also be seen from Figure 5 that the recall rate and precision rate show the law of one ebb and flow [22]. The comparison of classification accuracy under different hidden layer structures is shown in Table 1.

It can be seen from Table 1 that hidden levels 1, 2, 3, and 4 show good classification accuracy, all reaching more than 91%. After 400 iterations, the classification accuracy of the second level reaches 99.21%, which is the maximum of the classification accuracy. Therefore, it can be concluded that the convolutional neural network model with 4-layer hidden layer structure has good classification accuracy.

It can be seen from Table 2 that the classification and recognition error rate of the classifier designed in this paper is 22.5% and the accuracy rate is 77.5%. The estimated and

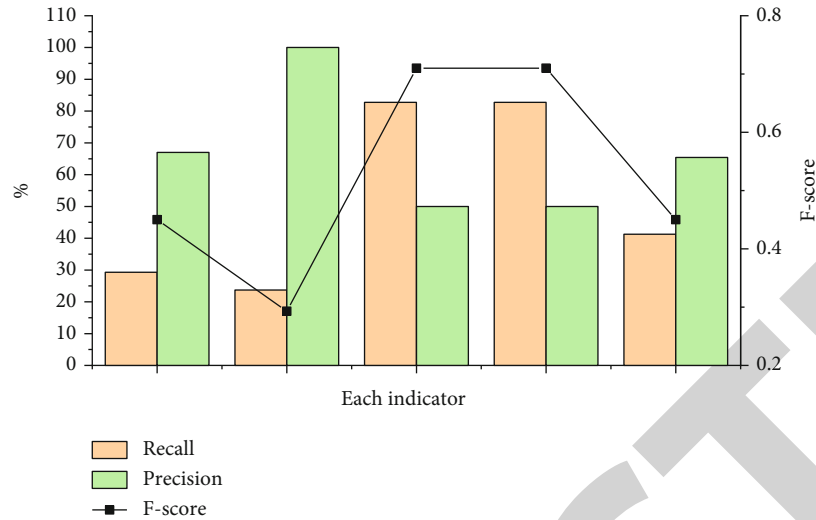


FIGURE 5: Comparison results of recognition effects of various forms of models.

TABLE 1: Comparison of classification accuracy under different hidden layer structures.

Number of iterations	Accuracy			
	Level 1	Level 2	Level 3	Level 4
100	0.9614	0.9637	0.9268	0.9177
200	0.9742	0.9763	0.9503	0.9315
300	0.9847	0.9873	0.9689	0.9655
400	0.9898	0.9921	0.9841	0.9678
500	0.9898	0.9922	0.9841	0.9678
600	0.9898	0.9921	0.9919	0.9738
700	0.9898	0.9892	0.9919	0.9794
800	0.9874	0.9897	0.9919	0.9851
900	0.9844	0.9897	0.9895	0.9875
1000	0.9819	0.9843	0.9895	0.9903

TABLE 2: Error rate of neural network classification.

	Abnormal	No abnormality
Estimated value	55	25
Actual value	64	16
Error rate	16.36%	36.00%
Total error rate	22.5%	

actual values in Table 2 represent the number of times without physical units. The experiment shows that the main reason for the error rate is the delay of the inspection results of financial abnormalities [23]. Through the example analysis, it can be concluded that the proposed intelligent analysis method of financial abnormal data based on deep learning has good effectiveness and accuracy and has certain practical value [24].

5. Conclusion

This paper presents a detailed analysis of the current financial anomaly monitoring algorithm based on the combination of neural network and artificial intelligence and solves the problem of abnormal data mining. Taking the abnormal recognition of business trip invoice reimbursement as an example, this paper expounds the implementation process of data analysis and early warning and verifies the effectiveness of the system. The BP neural network classifier in this paper is realized by MATLAB programming. In this section, the financial data of traditional indicators are processed by the timing construction method proposed above and then input into the classifier. After running, the classification effects of traditional models and various forms of models can be obtained. At the same time, there are still some deficiencies in the system, which are mainly reflected in the long training time of neural network and the lack of guiding opinions on the selection of initial value of network. The optimization of network initial value and the adaptation of network parameters in the system will be the further research direction.

Data Availability

The data used to support the findings of this study are available from the corresponding author upon request.

Conflicts of Interest

The author declares that there are no conflicts of interest.

References

- [1] W. Silva, F. Nascimento, and M. Bourguignon, "A change-point model for the r -largest order statistics with applications to environmental and financial data," *Applied Mathematical Modelling*, vol. 82, pp. 666–679, 2020.